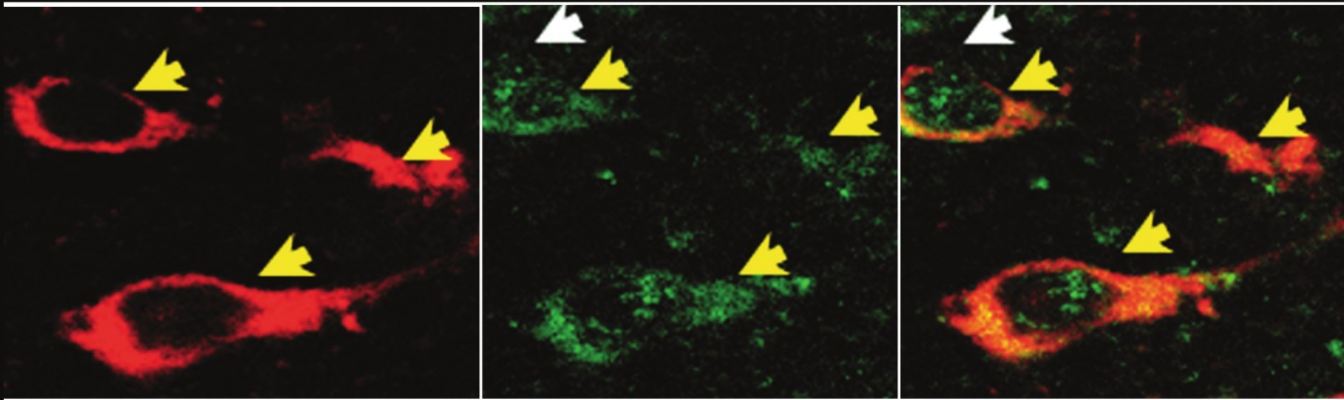


SECOND EDITION

Brain Control of Wakefulness and Sleep



Mircea Steriade and Robert W. McCarley

Brain Control of
Wakefulness and
Sleep
Second Edition

Brain Control of Wakefulness and Sleep

Second Edition

Mircea Steriade

*Université Laval
Quebec, Canada*

and

Robert W. McCarley

*VA Boston Healthcare System and
Harvard Medical School
Brockton and Boston, MA*



Springer

ISBN-10: 0-306-48714-4

ISBN-13: 978-0306-48714-9

© 2005 by Kluwer Academic/Plenum Publishers, New York
233 Spring Street, New York, New York 10013

<http://www.kluweronline.com>

10 9 8 7 6 5 4 3 2 1

A C.I.P. record for this book is available from the Library of Congress.

All rights reserved

No part of this book may be reproduced, stored in a retrieval system, or transmitted in any form or by any means, electronic, mechanical, photocopying, microfilming, recording, or otherwise, without written permission from the Publisher, with the exception of any material supplied specifically for the purpose of being entered and executed on a computer system, for exclusive use by the purchaser of the work.

Permissions for books published in Europe: permissions@wkap.nl

Permissions for books published in the United States of America: permissions@wkap.com

Printed in the United States of America

Preface

We regard this book as part of an ongoing history of efforts to understand the nature of waking and sleeping states from a biological point of view, and are convinced that the current moment is especially propitious because of the recent technological revolutions in anatomy and physiology. In planning such a book we had the choices of producing an edited volume with invited chapter authors or of writing the book ourselves. Edited volumes offer the opportunity for expression of expertise in each chapter, but, we felt, would not allow the development of our ideas on the potential and actual unity of the field, and would not allow the expression of coherence which can be obtained only with one or two voices, but is quite difficult with a chorus assembled and performing together for the first time. (Unlike musical works, there is very little precedent for rehearsals and repeated performances for authors of edited volumes, or even for the existence of conductors able to induce a single rhythm and vision of the composition.)

We thus decided on a monograph. The primary goal was to communicate the current realities and the future possibilities of unifying basic studies on anatomy and cellular physiology with investigations of the behavioral and physiological events of waking and sleep. In keeping with this goal we cross-reference the basic cellular physiology and anatomy in the first chapters with the systems of waking and sleeping physiology in the latter chapters, and we take up possible links to relevant clinical phenomenology. We are well aware of the limitations of our knowledge, and have thus chosen to write about what we know best or, in any case, what strikes us as most interesting and relevant for what we do know. We make no claim for encyclopedic knowledge in all aspects of sleep and waking and the relevant basic studies, and similarly do not apologize for including that which we do know best, namely our own work, and for omitting some areas that have been recently reviewed elsewhere. While the reference list indicates we do not ignore the field as a whole, many of the detailed expositions are drawn from our own studies. Our wish is that the reader finds the field as exciting and promising as we, and we welcome comments.

MS thanks his colleagues, post-doctoral fellows and Ph.D. students D. Paré, R. Curró Dossi, A. Nuñez, F. Amzica, D. Contreras, I. Timofeev, and F. Grenier for their collaboration in his projects over the past 15 years that elapsed since the first edition of this monograph, and all his collaborators and students since he established the Laboratory of Neurophysiology at Laval University in 1968. MS also thanks T.J. Sejnowski, M. Bazhenov, A. Destexhe, and W. Lytton for their collaboration in combined experimental and computational studies. MS's work is supported by the

Medical Research Council of Canada (now Canadian Institutes for Health Research), National Science and Engineering Research of Canada, Human Frontier Science Program, and National Institute of Health of the United States.

RWM thanks his colleagues and members of his Laboratory of Neuroscience in the Harvard Medical School Department of Psychiatry and the VA Boston Healthcare System. These include: for the *in vivo* physiological and anatomical studies, K. Ito, R. Strecker, R. Tao, M. Thakkar, and post-doctoral fellows L. Chen, S. Higo, H. Imon, T. McKenna, A. Mitani, J. Tatar, and C. Ward; for the molecular biological studies, R. Basheer and R. Vijay; for the *in vitro* studies, E. Arrigoni, R. Brown, U. Gerber, R. Greene, H. Grunze, and D. Stevens; and for the mathematical modeling, S. Massequoi. RWM's work has been made possible by grant support and a Medical Investigator award from the Medical Research Service of the Department of Veterans Affairs and by grant support from the National Institute of Mental Health.

MS dedicates this book to his two daughters, Donca and Claude, and to his wife Jacqueline. RWM dedicates this book to his wife Alice and to his sons, Rob and Scott.

Mircea Steriade
Robert W. McCarley

Contents

Chapter 1

Changing Concepts of Mechanisms of Waking and Sleep States.	1
1.1. Pioneering Steps	2
1.2. Definition of States of Vigilance and Activation.	11
1.3. Concepts of Passive and Active Mechanisms Promoting Sleep	20
1.3.1. Theories of Passive Sleep	20
1.3.2. Theories of Active Sleep	24
1.4. “Centers” and Distributed Systems.	30

Chapter 2

Methodology of Morphological and Physiological Substrates	
Underlying States of Vigilance	35
2.1. Morphological Tools	35
2.1.1. Nissl and Golgi Staining, and Some Recent Developments. . .	35
2.1.2. Anterograde and Retrograde Tracing Techniques.	39
2.1.3. Immunohistochemical Identification of Various Cell-Groups and their Projections	44
2.2. Electrophysiological Methods.	48
2.3. Noninvasive Techniques	54

Chapter 3

Afferent and Efferent Connections of Brainstem and	
Forebrain Modulatory Systems	55
3.1. Afferents to Brainstem Cholinergic Nuclei and Classical Reticular Formation Fields	56
3.1.1. Systematization of Cholinergic Nuclei and Nuclei with Unidentified Neurotransmitters	56

3.1.1.1.	Brainstem Cholinergic Nuclei	56
3.1.1.2.	Brainstem Reticular Nuclei With Unidentified Transmitters	61
3.1.2.	Afferents from Spinal Cord and Sensory Cranial Nerves	63
3.1.3.	Afferents from Diencephalon and Telencephalon.	68
3.1.3.1.	Thalamic Nuclei	68
3.1.3.2.	Hypothalamic Areas	72
3.1.3.3.	Basal Forebrain and Related Systems	73
3.1.3.4.	Neocortical Areas	76
3.1.3.5.	Convergent Inputs Onto Single Brainstem Reticular Neurons	76
3.1.4.	Afferents from Intrabrainstem Sources	78
3.1.4.1.	Afferents to the Pontine Reticular Formation	78
3.1.4.2.	Afferents to the Midbrain and Bulbar Reticular Formation	82
3.2.	Afferents to Brainstem Monoaminergic Nuclei	85
3.2.1.	Locus Coeruleus	85
3.2.2.	Raphe Nuclei	87
3.2.3.	Ventral Tegmental Area	87
3.2.4.	Tuberomammillary Area	88
3.3.	Afferents to Basal Forebrain Cholinergic Nuclei	88
3.3.1.	Systematization of Basal Forebrain Cholinergic Nuclei.	88
3.3.2.	Afferents to Basal Forebrain Modulatory Systems	89
3.4.	Efferent Connections of Brainstem Cholinergic Nuclei and Classical Reticular Fields	90
3.4.1.	Rostral Projections of Cholinergic and Noncholinergic Reticular Neurons	91
3.4.1.1.	Are There Direct Cortical Projections?	91
3.4.1.2.	Thalamic Projections	92
3.4.2.	Brainstem and Spinal Cord Projections of Mesopontine Cholinergic and Pontobulbar Nuclei	106
3.4.2.1.	Cholinergic Projections to Pontine FTG	106
3.4.2.2.	Bulbar and Spinal Cord Cholinergic Projections.	110
3.4.2.3.	Brainstem and Spinal Cord Projections of the Noncholinergic Pontobulbar Reticular Formation	112
3.4.3.	Intrinsic Cellular Morphology and Projections of Pontine and Bulbar Gigantocellular Fields	117
3.4.3.1.	Cell Size Distribution Within the Pontine and Bulbar FTG.	118
3.4.3.2.	Morphology of Pontine FTG Neurons	118
3.4.3.3.	Pontine FTG Neurons Sending Axons in the Ipsilateral MLF.	119
3.4.3.4.	Pontine FTG Neurons Sending Axons Directly to Bulbar Reticular Formation	119
3.4.3.5.	Dendrites	123
3.4.3.6.	Morphology of Bulbar FTG Neurons	124
3.4.3.7.	Bulbar FTG Neurons Sending Axons into the Ipsilateral Bulbar Reticular Core	125
3.4.3.8.	General Comments on Morphology.	127
3.4.3.9.	Organization of Bifurcating Axonal Collaterals	128

3.5. Efferent Connections of Monoamine-Containing Neurons	128
3.5.1. Norepinephrinergic Systems	128
3.5.2. Serotonergic Systems	130
3.5.3. Dopaminergic Systems	132
3.5.4. Histaminergic Systems	133
3.6. Efferent Connections of Basal Forebrain Nuclei	133
3.6.1. Cortical Projections	133
3.6.2. Thalamic Projections	134
3.6.3. Posterior Hypothalamic Projections	137

Chapter 4

Neuronal Circuits in the Thalamus, Neocortex, and Hippocampus, Targets of Diffuse Modulatory Systems.	139
4.1. Thalamus	141
4.2. Neocortex.	145
4.3. Hippocampus and Related Systems	153

Chapter 5

Intrinsic Electrophysiological Properties of Brainstem and Forebrain Neurons	155
5.1. Medial Pontine Reticular Formation Neurons	156
5.1.1. Neuronal Classes of the Medial PRF: Overview.	156
5.1.2. Low- and High-Threshold Ca^{2+} Spikes	159
5.1.3. Role of mPRF Neuron Membrane Potential in Controlling Repetitive Firing Properties and Implications for Behavior.	167
5.2. Pedunculopontine and Laterodorsal Tegmental Nuclei.	167
5.3. Neurons of the Locus Coeruleus and the Dorsal Raphe Nucleus	171
5.3.1. Locus Coeruleus Neurons	171
5.3.2. Dorsal Raphe Neurons	175
5.4. Basal Forebrain and Medial Septum Neurons	179
5.5. Thalamic Neurons	179
5.5.1. Thalamocortical Neurons.	181
5.5.1.1. The Low-Threshold Ca^{2+} Current	181
5.5.1.2. High-Voltage Ca^{2+} Currents.	185
5.5.1.3. Hyperpolarization-Activated Cation Current	187
5.5.1.4. Persistent (Noninactivating) Na^{+} Current	189
5.5.1.5. Voltage- and Ca^{2+} -Dependent K^{+} Conductances	189
5.5.1.6. Effects of Synaptic Activities on Some Intrinsic Properties.	191
5.5.2. Local-Circuit Inhibitory Cells.	191
5.5.3. Thalamic Reticular GABAergic Neurons.	194

5.6.	Neocortical Neurons	197
5.6.1.	Characteristics of Firing Patterns in Four Neuronal Types and Underlying Ionic Currents	197
5.6.2.	Changes in Firing Patterns During Synaptic Activities and Shifts in Behavioral State	199
5.7.	Entorhinal Cortex, Amygdala, and Hippocampal Neurons	208
5.7.1.	Entorhinal Cortex Neurons	208
5.7.2.	Amygdala Neurons	208
5.7.3.	Hippocampal Neurons	209

Chapter 6

Neurotransmitter-Modulated Currents of Brainstem Neurons and Some of Their Forebrain Targets		211
6.1.	Acetylcholine	212
6.1.1.	Brainstem	212
6.1.1.1.	Medial Pontine Reticular Formation	212
6.1.1.2.	Pedunculopontine Tegmental Cholinergic Neurons	219
6.1.1.3.	Locus Coeruleus	219
6.1.2.	Basal Forebrain	223
6.1.3.	Thalamus	223
6.1.3.1.	Thalamocortical Neurons	223
6.1.3.2.	Thalamic Reticular Neurons	226
6.1.3.3.	Local Interneurons	229
6.1.4.	Neocortex	231
6.1.5.	Hippocampus	234
6.2.	Norepinephrine	236
6.2.1.	Brainstem	236
6.2.1.1.	Locus Coeruleus	236
6.2.1.2.	Dorsal Raphe	243
6.2.1.3.	Pontine Reticular Formation	243
6.2.2.	Basal Forebrain	244
6.2.3.	Thalamus	245
6.2.4.	Neocortex and Hippocampus	245
6.3.	Serotonin	246
6.3.1.	Brainstem	247
6.3.1.1.	Dorsal Raphe	247
6.3.1.2.	Pontine Reticular Formation and Facial Motoneurons	248
6.3.1.3.	Mesopontine Cholinergic Nuclei	249
6.3.2.	Thalamus and Cerebral Cortex	250
6.4.	Excitatory Amino Acids	250
6.4.1.	Summary of Excitatory Amino Acid Receptor Types	250
6.4.2.	Brainstem	253
6.4.2.1.	Mesopontine and Bulbar Reticular Formation	253
6.4.2.2.	Locus Coeruleus	254
6.4.3.	Thalamus and Neocortex	254

Synchronized Brain Oscillations Leading to Neuronal Plasticity during Waking and Sleep States	255	CONTENTS
7.1. Rhythms during Brain-Active States of Waking and REM Sleep.	256	
7.1.1. Alpha.	256	
7.1.2. Oscillations during Waking Immobility: The Sensorimotor Rhythm.	257	
7.1.3. Theta.	259	
7.1.4. Fast (Beta/Gamma) and Ultrafast (Ripple) Rhythms	262	
7.2. Low-Frequency Rhythms during Non-REM Sleep	276	
7.2.1. Spindles.	277	
7.2.1.1. Chronology of Spindles and Other NREM Sleep Rhythms	277	
7.2.1.2. Cellular Basis of Spindles.	279	
7.2.1.3. The Pacemaking Role of Thalamic Reticular Neurons in Spindle Genesis.	284	
7.2.1.4. The Role of Neocortex in Synchronizing and Terminating Spindle Sequences.	290	
7.2.1.5. Blockage of Spindles by Brainstem Activating Influxes	295	
7.2.2. Two (Thalamic and Neocortical) Components of Delta Waves.	300	
7.2.2.1. Clock-like Thalamic Delta Rhythm: Generation, Synchronization, and Suppression	300	
7.2.2.2. Cortical Delta Waves	304	
7.2.3. The Neocortical Slow Oscillation: Its Role in Grouping NREM Sleep and Fast Rhythms.	305	
7.2.3.1. Cellular Basis of the Slow Oscillation	306	
7.2.3.2. Intracellular Recording of the Slow Oscillation during Natural NREM Sleep	310	
7.2.3.3. Intracortical Synchronization of Slow Oscillation	311	
7.2.3.4. Synaptic Reflection of the Slow Oscillation in Thalamus and Other Structures.	314	
7.2.3.5. Grouping of Delta, Spindles, and Fast Oscillations by the Slow Oscillation	318	
7.3. Abnormal Oscillations during Non-REM Sleep	325	
7.3.1. Electrical Seizures Developing from NREM Sleep Oscillations	325	
7.3.2. Burst-Suppression	327	
7.4. Plastic Changes in Thalamocortical Systems during Sleep and Waking Oscillations	329	
7.4.1. Augmenting or Incremental Responses.	330	
7.4.2. Plasticity Following Spindles and Their Experimental Model, Augmenting Responses	335	
7.4.3. Potentiation of Cortical Responses Following Fast Oscillations	343	
7.4.4. Concluding Remarks.	343	

CONTENTS

Brainstem and State dependency of Thalamocortical Systems	345
8.1. Thalamocortical Neurons	346
8.1.1. Two Modes of Spontaneous Firing During NREM Sleep and Brain-Active States	346
8.1.2. Evoked Potential Studies	347
8.1.3. Extracellular Recordings	351
8.1.4. Intracellular Studies	352
8.1.4.1. Excitatory Responses	352
8.1.4.2. Differential Brainstem Reticular Effects on Three Phases of Inhibitory Responses	361
8.2. Thalamic Reticular Neurons: Dual Types of Responses	363
8.3. Selective Increase in Cortical Excitability During Attentional Tasks	371
8.3.1. Event-Related Potentials in Humans	373
8.3.2. Neuronal Recordings During Set-Dependent Tasks in Monkeys	375
8.3.3. Differential Alterations in Two Phases of Inhibitory Responses During Brain Activation	378

Chapter 9

Neuronal Activities in Brainstem and Basal Forebrain Structures	
Controlling Waking and Sleep States	381
9.1. Brainstem–Thalamic Neurons Implicated in Tonic Electrical Activation of the Cerebrum	382
9.1.1. Midbrain Reticular Noncholinergic Neurons	384
9.1.2. Bulbar Reticular Noncholinergic Neurons	384
9.1.3. Mesopontine Cholinergic Neurons	388
9.2. Basal Forebrain Neurons Implicated in Tonic Cortical Activation ..	391
9.3. Brainstem Neurons and the Genesis of Pontogeniculo(thalamo)cortical Potentials	394
9.3.1. Brainstem Genesis of PGO Waves	395
9.3.2. Cellular Mechanisms of Thalamic PGO Waves	402
9.3.3. PGO-Related Thalamic Neuronal Activities During Natural Sleep	409

Chapter 10

Motor Systems	417
10.1. Saccadic Eye Movements	417
10.1.1. Physiological Properties of Oculomotor Neurons	418
10.1.2. Afferents to Oculomotor Neurons: Lesion Studies	419
10.1.3. Efferent Projections of Abducens Neurons	420

10.2.	Burst Neurons	420
10.2.1.	Burst Neuron Physiology	420
10.2.2.	Anatomical Connectivity of Burst Neurons	424
10.2.2.1.	Anatomy of Pontobulbar Reticular Projections to Abducens	424
10.2.2.2.	Nonreticular Brainstem Projections to Abducens.	424
10.2.2.3.	Superior Colliculus and Frontal Eye Field Projections to Reticular Formation	426
10.3.	Omnipause Neurons	426
10.4.	Tonic Neurons	429
10.5.	Saccade Generation: Interaction of Neurons in the Circuit	432
10.5.1.	Role of Superior Colliculus in Saccades	433
10.5.2.	Saccade Trajectories: Mutable or Immutable?	434
10.5.3.	Models of the Saccade Generator	435
10.6.	Gaze Control	437
10.7.	State-Dependent Alterations in Oculomotor System Function	439
10.7.1.	Waking to Synchronized Sleep Transitions	439
10.7.2.	Activity During REM Sleep	441
10.8.	Mechanisms of the Muscle Atonia of REM Sleep: Motoneurons ...	444
10.8.1.	Inhibition and Diminished Excitability of Trigeminal Jaw-Closer Motoneurons During REM Sleep.	444
10.8.2.	Spinal Alpha Motoneurons During the Sleep–Wake Cycle.	446
10.8.2.1.	Changes in Membrane Potential of Alpha Lumbar Motoneurons During Waking and Sleep	446
10.8.2.2.	Hyperpolarizing PSPs in Alpha Lumbar Motoneurons During Waking and Sleep	447
10.8.2.3.	Excitatory Activity in Alpha Lumbar Motoneurons During Waking and Sleep	450
10.8.2.4.	Sources of REM Sleep IPSPs and EPSPs	451
10.9.	Central Mechanisms of REM-Sleep Muscle Atonia	452
10.9.1.	Lesion Data and REM Without Atonia	452
10.9.2.	Electrophysiological Data and REM-Muscle Atonia	454
10.9.3.	Role of Other Pontine Structures and the Pharmacology of REM-Sleep Muscle Atonia	458

Chapter 11

Neuronal Control of REM Sleep.	461
11.1. Introduction and Overview	461
11.2. Brainstem Reticular Neuronal Activity over the REM Sleep Cycle.	462
11.2.1. The View from Extracellular Recordings	464
11.2.2. The View from Intracellular Recordings.	467
11.2.2.1. Synchronized Sleep	467

11.2.2.2.	Pre-REM Sleep Changes: The Transition Period to REM Sleep, T	468
11.2.2.3.	REM Sleep	469
11.2.2.4.	Wakefulness: The REM <i>Sleep–Wake</i> Transition, and Motor Activity in Wakefulness	469
11.2.2.5.	State-Dependent Alterations in Reticular Excitability	470
11.2.2.6.	Summary of Behavioral State Alterations in the mPRF	470
11.2.3.	Sleep–Wake Control as Resulting from Modulation of Excitability in Neuronal Pools	470
11.2.3.1.	The Concept.	470
11.2.3.2.	Experimental Evidence for Modulation of Excitability in Neuronal Pools.	473
11.2.3.2.1.	Brainstem Reticular Formation	473
11.2.3.2.2.	Peripheral Motoneurons	474
11.2.3.2.3.	Sensory System Neurons	474
11.2.3.3.	Summary of Orchestration of REM Sleep Components	475
11.2.3.3.1.	Rapid Eye Movements	475
11.2.3.3.2.	Muscle Atonia	475
11.2.3.3.3.	EEG Desynchronization.	476
11.2.3.3.4.	PGO Waves.	476
11.2.3.3.5.	Other Components of REM Sleep	476
11.2.3.4.	Approach to Factors Producing Modulations of Excitability	478
11.2.3.5.	Recruitment through Reticuloreticular Excitatory Connections	478
11.2.3.5.1.	Intracellular Evidence on Recruitment Within the Reticular Pool	480
11.3.	Criteria for Neuromodulation in REM Sleep.	480
11.4.	Cholinergic Influences on REM Sleep	482
11.4.1.	Cholinergic Induction of REM Sleep-Like Phenomena	482
11.4.2.	Cholinergic LDT Stimulation Produces Scopolamine-Sensitive EPSPs in mPRF Neurons	485
11.4.3.	Cholinergic Unit Activity During Sleep and Wakefulness	485
11.5.	Monoaminergic Influences—REM-Off Neurons	488
11.5.1.	Raphe Nuclei.	488
11.5.2.	Locus Coeruleus.	490
11.5.3.	Do REM-Off Neurons Play a Permissive, Disinhibitory Role in REM Sleep Genesis?	490
11.5.3.1.	Dorsal Raphe Discharge and REM Events: An Inverse Association	490
11.5.3.1.1.	Raphe System REM-Off Neurons and PGO Waves.	491

11.5.3.2.	Suppressing Dorsal Raphe Activity Increases REM Sleep	495
11.5.3.3.	LDT/PPT REM-On Neurons are Inhibited by a 5-HT1A Agonist.	497
11.5.3.4.	Locus Coeruleus Lesions and Cooling Increase REM Sleep	498
11.5.3.4.1.	Locus Coeruleus Cooling Induces REM Sleep	499
11.5.3.4.2.	Site(s) of REM-Off and REM-On interaction.	501
11.6.	GABAergic Influences and REM Sleep	501
11.6.1.	Dorsal Raphe Nucleus	502
11.6.1.1.	Microdialysis	502
11.6.1.2.	Microiontophoresis	503
11.6.2.	Locus Coeruleus	505
11.6.2.1.	Microdialysis	505
11.6.2.2.	Microiontophoresis	506
11.6.3.	Source of State-Related GABAergic Input to DRN and LC	506
11.6.3.1.	Periaqueductal Gray?	506
11.6.3.2.	Ventrolateral Preoptic Area (VLPO)	507
11.6.4.	GABA and the Pontine Reticular Formation: Disinhibition and REM Sleep	507
11.6.4.1.	Pharmacological Studies in Cats on the Behavioral State Effects of GABA Agents ...	507
11.6.4.2.	Pharmacological Studies in Rats on the Behavioral State Effects of GABA Agents	508
11.6.4.3.	Microdialysis Measurements of GABA in the Pontine Reticular Formation	509
11.6.5.	The Pedunculopontine Tegmental (PPT) Nucleus	509

Chapter 12

REM Sleep as a Biological Rhythm: The Phenomenology and a Structural and Mathematical Model with Application to Depression		513
12.1.	Introduction and Overview	513
12.2.	A Structural Model of REM Sleep Organization	513
12.2.1.	REM-On Neurons and Interaction with Other Elements in the Model	514
12.2.1.1.	REM-On Neurons and the Postulate of Self-Excitation (Positive Feedback) and Exponential Growth—Term “a” in Fig. 12.1 ...	514
12.2.1.2.	Reticular Formation and GABAergic Influences	516
12.2.2.	Excitation of REM-Off Neurons by REM-On Neurons (Fig. 12.1 term “d”)	517
12.2.3.	Inhibition of REM-On Neurons by REM-Off Neurons (Fig. 12.1 term “b”)	517

12.2.4.	Inhibitory Feedback of REM-Off Neurons (Fig. 12.1 term “c”)	518
12.2.4.1.	GABAergic Influences in the LC and DRN during REM Sleep	518
12.2.4.2.	Source of GABAergic Inputs to LC and DRN	519
12.3.	Characteristics of the REM Sleep Rhythm	520
12.3.1.	Phenomenology of the REM Sleep Rhythm	520
12.3.2.	Mathematical Characterization of Oscillators	522
12.4.	The Reciprocal Interaction Model and the Lotka–Volterra Equations	526
12.4.1.	Postulated Steps in Production of a REM Sleep Episode	526
12.4.2.	Simple Lotka–Volterra Equations	528
12.4.3.	Limitations of the Simple Lotka–Volterra System	530
12.5.	The Limit Cycle Model	531
12.5.1.	Summary of Changes from the Simple Lotka–Volterra Model	531
12.5.2.	Modeling Events at Sleep Onset, Human Sleep Patterns, and Circadian Variation	532
12.5.2.1.	Events at the Onset of Sleep	532
12.5.2.2.	Modeling Human Sleep Patterns	532
12.5.2.3.	Circadian Variation in the REM Cycle	533
12.6.	Details of Simple Lotka–Volterra Model	537
12.6.1.	Significance of the Terms in the Equations	537
12.6.2.	Phase Plane Representation	538
12.7.	Details of Limit Cycle Model	539
12.7.1.	Use of $a(X)$	539
12.7.2.	Limitations on Growth of Firing Rates, $S_1(X)$, $S_2(Y)$	540
12.7.3.	Use of $b(X)$ and c	543
12.7.4.	Circadian Variation, $d(\text{circ})$ and Entry into the Limit Cycle	543
12.7.5.	Phase Plane Representation of Entry into the Limit Cycle	545
12.8.	Sleep Abnormalities in Depression and Quantitative Modeling	546
12.8.1.	Monoaminergic–Cholinergic Factors in Mood Disorders and Associated Sleep Abnormalities	550
12.8.1.1.	Monoamines	550
12.8.1.2.	Cholinergic Abnormalities and the Sleep of Depressives	552
12.8.2.	Quantitative Modeling of the REM Sleep Abnormalities in Depression	552
12.8.2.1.	Modeling the Bimodal Distribution of REM Sleep Latencies in Depression	555
12.8.2.2.	Earlier Quantitative Models of REM Sleep Latency in Depression	557
12.8.2.3.	Modeling the Cholinergically Induced Hastened Onset of REM Sleep	557
12.8.2.4.	Circadian Rhythms in Depression: Decreased Amplitude Instead of a Phase Advance?	559
12.8.3.	Deficient Process S and Sleep Abnormalities in Depression	560

12.8.3.1. REM Sleep	560
12.8.3.2. Non-REM Sleep	560

Chapter 13

The Role of Active Forebrain and Humoral Systems in Sleep Control	561
13.1. Adenosine	562
13.1.1. Adenosine as a Mediator of the Sleepiness Following Prolonged Wakefulness (Homoeostatic Control of Sleep)	562
13.1.2. Site Specificity and Sources of Adenosine Increases with Prolonged Wakefulness	565
13.1.3. Neurophysiological Mechanisms of Adenosine Effects ...	570
13.1.4. Receptor Mediation of Adenosine Effects: A1 and A2A Subtypes.	571
13.1.4.1. Receptor Mediation of Adenosine Effects: The A1 Subtype.	571
13.1.4.2. Receptor Mediation of Adenosine Effects: The A2A Subtype and the Prostaglandin D2 System	574
13.1.5. Adenosine A1 Receptor-Coupled Intracellular Signal Transduction Cascade and Transcriptional Modulation	576
13.1.6. Sleep-Mediated Alterations in Behavior: Possible Relationship to Adenosine-Induced Changes in the Basal Forebrain Cholinergic System.	583
13.2. Cytokines and Other Humoral Factors.	584
13.2.1. Introduction and Overview of the Cytokines: Interleukin-1 Beta and Tumor Necrosis Factor Alpha (IL-1 Beta and TNF Alpha)	585
13.2.2. Interleukin-1 Beta (IL-1 Beta)	587
13.2.3. Tumor Necrosis Factor Alpha (TNF Alpha)	589
13.2.4. Other Humoral Systems	590
13.2.4.1. Growth Hormone Releasing Hormone (GHRH)	590
13.2.4.2. Somatostatin	592
13.3. The Ventrolateral Preoptic Area (VLPO) and Active Control of Sleep	592
13.3.1. Identification of Sleep-Active Neurons in the VLPO.	592
13.3.2. Lesions of VLPO and the Extended VLPO and Effects on Sleep	596
13.3.3. Relationship of VLPO to Other Preoptic Regions and the Suprachiasmatic Nucleus	598
13.3.4. VLPO and Adenosine	598
13.3.5. Modeling the VLPO Control of Sleep	600
13.4. Orexin/Hypocretin, Narcolepsy, and the Control of Sleep and Wakefulness	600

13.4.1.	Background and Identification of Orexin/Hypocretin	600
13.4.2.	Orexin Neuronal Projections and Orexin Receptors	602
13.4.3.	Actions of Orexin at the Cellular Level.....	603
13.4.4.	Orexin and the Control of REM-Related Phenomena and Wakefulness	606
13.4.5.	Orexin Release: Linked to Circadian Cycle and/or to Behavioral State?	606
References.....		611
Index		691

**Brain Control of
Wakefulness and
Sleep**
Second Edition

Changing Concepts of Mechanisms of Waking and Sleep States

[1] Moruzzi (1964, 1972).

[2] Jouvet (1967, 1972).

[3] Steriade and McCarley (1990).

The comprehensive reviews on the historical development of ideas on waking and sleep states written by Moruzzi [1] and Jouvet [2] dealt with experiments using electrical stimulation and electrolytic lesion techniques. Newer, more powerful tools have been introduced in recent years for activating and destroying cellular aggregates. However, the concepts of the location of various brain “centers” involved in the genesis of waking and sleep states have not significantly changed since the late 1960s although, since the first edition of our monograph [3], the increasing tendency of conducting experiments in extremely simplified preparations has further contributed to pinpointing circumscribed brain circuits as implicated in the generation of global states of vigilance and/or their electrographic correlates. What has basically changed since the epoch when brain lesions and stimulation prevailed, is the view of neuronal mechanisms and interactions between different parts of the brain, mostly due to the introduction of new techniques allowing the recording of single cells in the behaving animal and, since 1980, the analysis of ionic conductances underlying intrinsic electroresponsive properties of neurons. We shall, of course, refer to earlier concepts, and we shall try to resurrect some of them from unjustified oblivion, especially when they have withstood experimental testing. But our main goal in this historical perspective and throughout this monograph is to examine critically the conclusions of older studies, couched in terms of large black boxes, with the more precise data gained by looking inside single cells and neuronal networks, and by defining connectivity and transmitters. Our basic tenet is that the cellular approach furnishes the ultimate criterion to test hypotheses from studies conducted at more global levels.

We begin by pointing out four major discoveries that belong to Frédéric Bremer, Giuseppe Moruzzi, Nathaniel Kleitman, and Michel Jouvet, which set the scene for more recent developments.

Since his stay at the Salpêtrière in Paris during the 1910s, the Belgian neurophysiologist Frédéric Bremer (1892–1982) was involved in the clinical–pathological sleep studies related to the lethargic encephalitis [4]. He discovered the quite different electrographic and ocular syndromes of the *encéphale isolé* and *cerveau isolé* preparations during the 1930s [5]. Bremer found that a high spinal transection at C1 that disconnected the whole encephalon from the spinal cord is compatible with fluctuations between EEG patterns of waking and sleep states. The *encéphale isolé* preparation should be used in conjunction with ablation of Gasser ganglion to prevent pain impulses through the trigeminal nerve. In contrast, a mesencephalic transection caudal to the third nerves was associated with extremely fissurated pupils, as in normal sleep, and uninterrupted sequences of waxing and waning EEG spindle waves, much the same as during barbiturate narcosis (Fig. 1.1). Bremer modified the ordinary decerebrate preparation by leaving the forebrain *in situ* after midbrain transection, instead of destroying it, with the hope of demonstrating “the existence of a continuous facilitation of functional innervation of the forebrain resulting from the steady flow of ascending inputs from the spinal neuraxis and the brainstem” [6]. Bremer also demonstrated that the cerebral cortex contributes to self-awakening through projections to the brainstem reticular formation [7] that re-afferent the thalamocortical systems.

The idea that, indeed, the structures located between the bulbospinal transection and the rostral midbrain are crucially involved in the maintenance of waking, and that a sudden fall in the cerebral “tone” follows the withdrawal of the steady flow of impulses impinging upon the cerebrum, was extended in the studies conducted by Bremer’s disciple, Moruzzi. The Italian physiologist Giuseppe Moruzzi (1910–1986) was a visiting fellow in Bremer’s laboratory during the late 1930s, thereafter worked with Adrian, and eventually went to collaborate with Magoun at the Institute of Neurology of the Northwestern University Medical School in Chicago. Initially, Moruzzi intended to continue his analysis of paleocerebellar inhibition upon the hyperexcitable state of motor cortex. To this end, Moruzzi and Magoun placed stimulating electrodes in the cerebellum and the bulbar reticular formation that was thought to

[4] Trétiakoff and Bremer (1920).

[5] Bremer (1935, 1937, 1938).

[6] Bremer (1975, pp. 267–268).

[7] Bremer and Terzuolo (1954). Besides the cortical projections to the brainstem reticular core, the neo-cortical projections to thalamic intralaminar nuclei as well as other thalamic nuclei with widespread projections to cortex, such as the ventromedial nucleus, are also implicated in the process of self-awakening of the cerebral cortex.

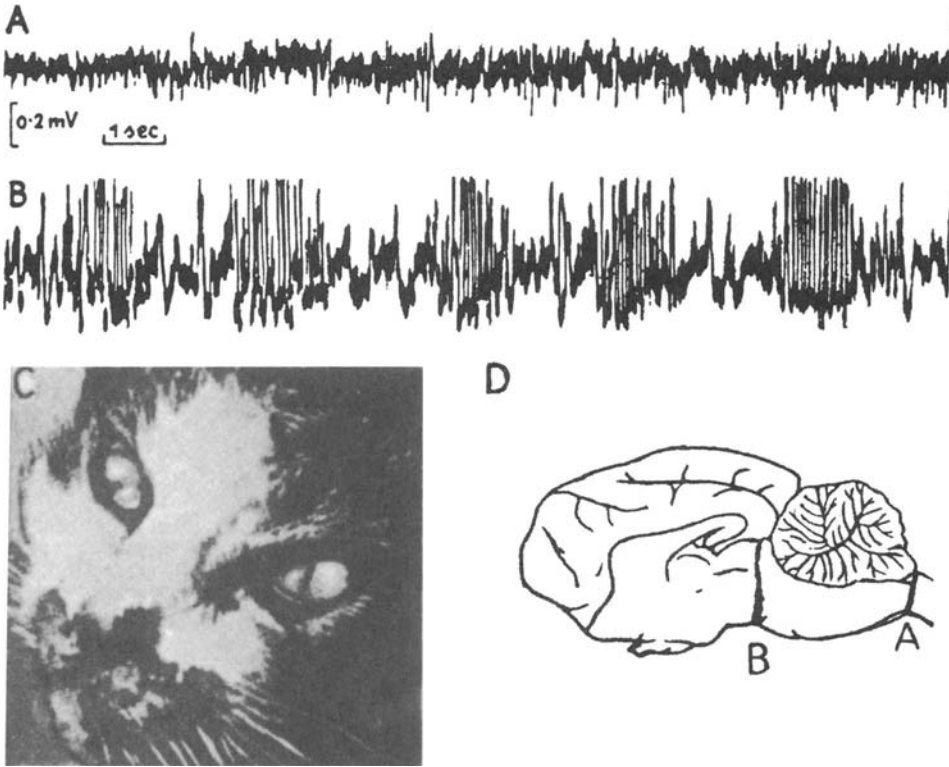


Figure 1.1. EEG and ocular behavior in the acute *encéphale isolé* (isolated encephalon; EEG trace in A and bulbospinal section in D) and *cerveau isolé* cat (isolated forebrain; EEG trace in B and transection at the collicular level in D). A, activity typical for the waking state. B, spindling activity interrupted by interspindle lulls, as in the sleeping brain (see also fissured myosis in C). From Bremer (1937).

relay cerebellar impulses in their route to the cerebral cortex. To their surprise, the electrical stimulation of the brainstem reticular formation suppressed the high-amplitude slow EEG waves displayed by their chloralose-anesthetized preparations [8]. They were surprised by the complete flattening of cortical electrical activity recorded from motor cortex during reticular stimulation and believed “the experiments had stumbled upon some perplexing type of ascending inhibition ... Only after some delay, and quite by chance, was the gain finally turned up, and it was then possible to see the large waves give way during reticular stimulation to the low voltage, fast activity of EEG” [9]. In those experiments, many of them conducted under chloralose anesthesia, Moruzzi also used the unanesthetized *encéphale isolé* cat, a preparation that he learned during his stage in Bremer’s laboratory. The suppressing effect of brainstem stimulation upon synchronized EEG waves resembled the alpha-wave blockage during attention or visual stimulation, known from Berger’s [10] and Adrian’s [11] studies. While the chloralose-anesthetized

[8] Moruzzi and Magoun (1949).

[9] Magoun (1975, p. 524).

[10] Berger (1930). Berger’s series of papers on the electroencephalogram, from 1929 to 1938, have been translated in English by Gloor (1969).

[11] Adrian (1936).

animal was obviously not the best experimental preparations for studying arousal and activation processes, Moruzzi and Magoun decided to go far beyond observed facts and used the term *activation*. This was in spite of the fact that only spontaneous EEG waves were recorded and no sign of real cerebral activation was documented. Indeed, suppression of high-amplitude slow EEG waves may be seen in a variety of conditions that do not necessarily imply a heightened cerebral excitability. The actual demonstration of cortical facilitation during brainstem reticular stimulation came a decade later, in independent studies of thalamocortical evoked potentials conducted during the late 1950s in Bremer's and Dell's laboratories (see Chapter 9). Anyway, the choice of the term *activation* in Moruzzi and Magoun's 1949 paper was better than Berger's [12] choice to explain the blockage of alpha waves as a secondary diffuse *inhibition* of the cortex from a highly localized and hardly detectable enhancement of cortical activity produced by a sensory arousing stimulus. Berger's interpretation was under the influence of Pavlov's notion of negative induction. As to the term *activation*, it is certainly better than the commonly used term EEG "desynchronization," employed by most epigones of Moruzzi and Magoun, because slow waves are obliterated upon brain arousal, whereas fast waves in the beta and gamma frequency bands (20–60 Hz) are synchronized over restricted cortical territories and well defined corticothalamic systems [13]. It should be emphasized that the first mention of synchronized fast spontaneous oscillations upon brainstem reticular appeared in a paper by Bremer [14] describing the effect of arousal on cortical field potentials and qualifying this response as an "*accélération synchronisatrice*" (synchronizing acceleration), which was uncommon in the 1960s and even more recently when desynchronization was the usual term.

The discovery by Moruzzi and Magoun [8] of an ascending brainstem reticular system with energizing actions upon the forebrain is an important step forward in the physiology of states of vigilance. The progress relates to the localization of an executive system for cortical activation. On the conceptual side, the notion of *nonspecificity* in the activating process was introduced. Conceptually, the notion of a role played by specific sensory impulses (relayed in the spinal cord or brainstem and hypothesized by Bremer to maintain the tone of the cerebrum) was replaced after Moruzzi and Magoun's experiments by the idea of a nonspecific ascending reticular system, a site of collateralization of heterogeneous sensory impulses, in a vein similar to the concept of *sensorium commune* that was localized by Jiri Prohaska, around 1750, in a region

[12] Berger (1933).

[13] Steriade *et al.* (1996a, b).

[14] Bremer *et al.* (1960). See legend of fig. 5 in that article in which Bremer mentions the synchronization of fast rhythms, as reflected in field potential recordings, induced by mid-brain reticular stimulation.

[15] See the history of concepts in the central nervous system by Soury (1899).

[16] Lindsley *et al.* (1949, 1950).

[17] Claes (1939) worked in Bremer's laboratory and she reported the occurrence of sleep spindle oscillations after section of the optic nerves. For the role of other cranial nerves in the maintenance of the vigil state in the *encéphale isolé* preparation, see Roger *et al.* (1956).

[18] Steriade and Glenn (1982); Steriade *et al.* (1982a).

between the medulla and the diencephalon [15]. The nonspecific nature of the activating system was supported by lesion experiments showing that the interruption of lemniscal (specific sensory) pathways did not produce the sleep or comatose syndrome of the *cerveau isolé* preparation, whereas lesions of the medial brainstem reticular formation, sparing lemniscal projections, produced such a syndrome [16]. However, a sharp distinction between Bremer's idea of a role played by ascending specific projections in maintaining the state of waking and, on the other hand, Moruzzi and Magoun's concept of nonspecific brainstem reticular pathways is not necessary because forebrain activation is maintained by both these systems. Indeed, sleep EEG patterns are not only produced by interruption of ascending reticular activating systems but also appear following transections of sensory nerves [17].

Since the study by Moruzzi and Magoun was the first that attempted to localize the brainstem substrate of cortical activation, we discuss below some of the data and speculations in the 1949 paper, and we relate them to the modern findings and concepts. Although EEG activation responses were elicited from a variety of loci in the whole brainstem tegmentum, Moruzzi and Magoun depicted the most effective area in the midbrain (see fig. 3 in their paper, [8]). With minimal stimulation intensity, the EEG response could be localized in the sensory-motor cortex of the ipsilateral hemisphere. The cortical effect was thought to be mediated, in part at least, by the diffuse thalamic projection system [8]. All these findings have been confirmed and expanded in more recent cellular studies. Indeed, neurons recorded from the midbrain reticular formation increase their firing rates during transition from sleep to arousal, reliably preceding EEG desynchronization, and they directly excite thalamic neurons with diffuse projections toward the cerebral cortex, but prevalently to the sensory-motor areas [18]. These data are analyzed in Chapters 4 and 10. The elicitation of EEG activation by stimulating a series of foci from the medulla to the midbrain is due to lower brainstem projections to the most effective sites in the upper brainstem core (see Chapter 3).

The notion of nonspecificity and the schemes with heavy arrows depicting pathways of unknown origins, acting diffusely by means of unknown transmitters upon unknown targets, betrayed the state of a primitive knowledge of the reticular core that persisted for three decades since the late 1940s. Spectacular advances have been achieved in this direction since 1980, and they are mainly due to modern tracing techniques combined with immunohistochemistry that helped to define the transmitter agents used by brainstem intrinsic, ascending and

descending projections. During the 1950s, Golgi studies and experiments with axonal degeneration following massive electrolytic lesions in the brainstem tegmentum showed axons of reticular origin that projected almost everywhere in the thalamus, without obvious differentiation between various brainstem sites of axonal origin. The same reticular neuron seemed to send bifurcating axonal branches to the spinal cord and the cerebral cortex [19]. More recent retrograde tracing studies with double-labeling techniques and experiments with antidromic identification of brainstem reticular neurons from multiple stimulated sites have altered this viewpoint (see Chapter 3). Such pontifical reticular neurons, with ascending and descending projections controlling both cortical and spinal cord operations, are the exception rather than the rule.

Absence of data supporting the idea of such hypothetically ubiquitous projections, as well as the uncertain transmitters and actions of brainstem reticular neurons, caused a temporary desuetude of the ascending reticular concept. Con-fronted with morphological and physiological studies employing lesion and stimulation techniques that could not dissociate cell bodies from passing fibers, the reaction of some anatomists was even to deny, until quite recently, the existence of brainstem reticular projections to major thalamic nuclei. The accumulating evidence of the past few years on the existence of these projections and their chemical codes are discussed in Chapter 3.

The notion of a monolithic reticular core, with global and undifferentiated energizing actions upon the fore-brain, was challenged by Moruzzi himself, after crucial experiments with his team in Pisa during the late 1950s. The midpontine pretrigeminal brainstem transection is only a few millimeters behind the low collicular transection that induces the comatose syndrome of the *cerveau isolé* preparation. However, the midpontine trigeminal animal exhibits persistent EEG and ocular signs of alertness (Fig. 1.2), and its eye movements follow the objects passing across the visual field. In the acute conditions of these two close transections (*cerveau isolé* and midpontine pretrigeminal), only the neurons lying between the two sections are the likely candidates for explaining the critical differences in both the EEG and ocular behavior [20]. Spectacular differences between the two (rostral mesencephalic and midpontine) transections, separated by just a few millimeters (Fig. 1.3), have also been observed using measures of cortical metabolism [21]. We shall discuss in Section 1.3.1 the experimental evidence that, in chronic conditions, structures lying in the isolated cerebrum, above the mesencephalon, may be effective in maintaining wakefulness. But the demonstration of the dramatic differences displayed by the *cerveau isolé* preparation and the animal with a

[19] Scheibel and Scheibel (1958).

[20] Reviewed in Moruzzi (1972).

[21] Steriade *et al.* (1969b).

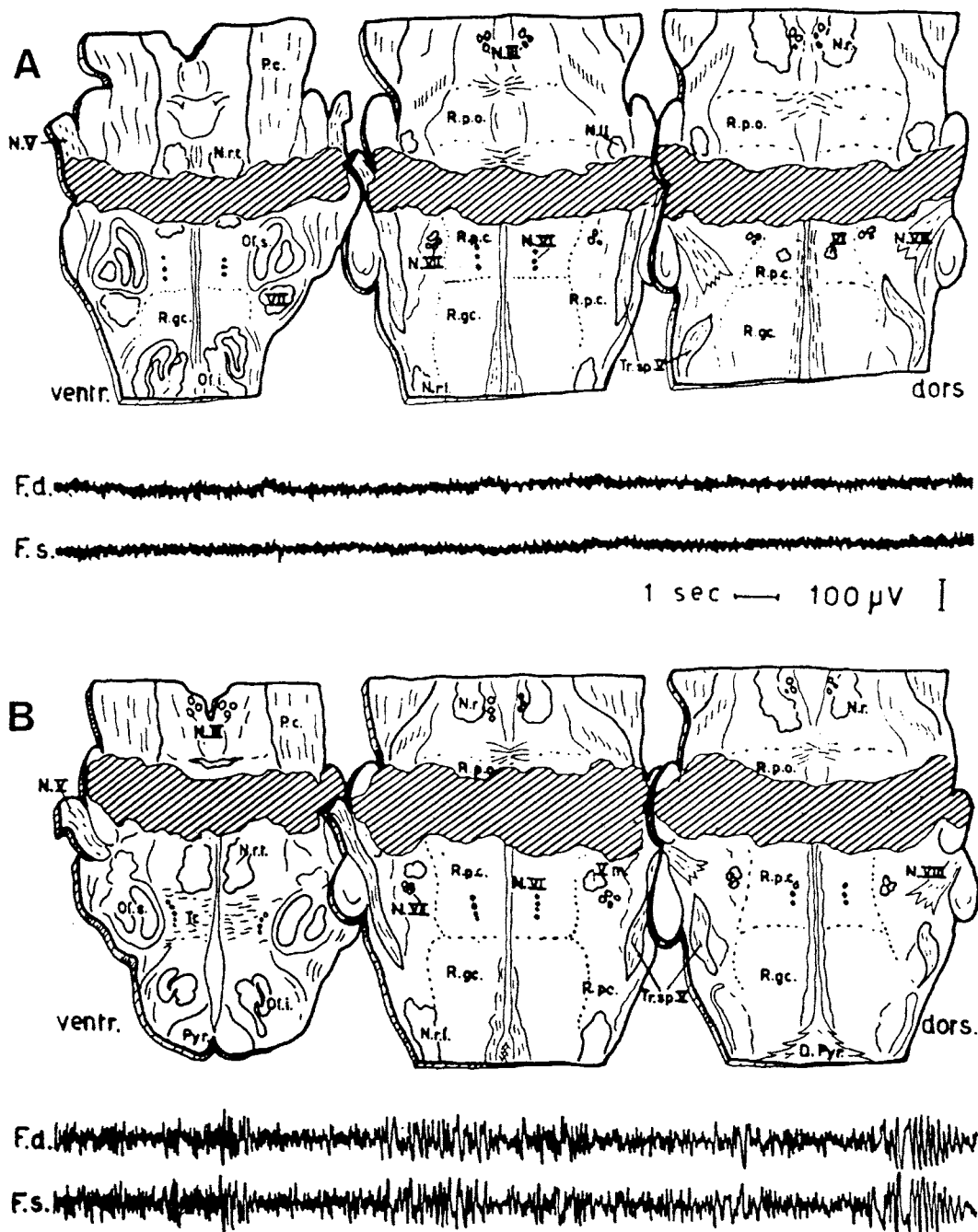


Figure 1.2. EEG patterns following midpontine and rostrpontine transections. Drawings of horizontal sections of the cat's brainstem. Cross-hatched areas indicate level and extent of brainstem lesions in the midpontine pretrigeminal (A) and rostrpontine (B) preparations. EEG patterns typical for each preparation, as recorded from right (F.d.) and left (F.l.) frontal areas, are reproduced below each set of anatomical drawings. It can be noticed that both types of transection result in the complete interruption of ascending trigeminal influences. Abbreviations: D.Pyr., decussatio pyramidum;

N.II, nucleus lemnisci lateralis; N.r., nucleus ruber; N.r.l., nucleus reticularis lateralis; N.r.t., nucleus reticularis tegmenti pontis; N.III, V, VI, VII, VIII, root fibers of cranial nerves; O.l.i., nucleus olivaris inferior; O.l.s., nucleus olivaris superior; P.C., pes pedunculi cerebri; Pyr., pyramis; R.g.c., nucleus reticularis gigantocellularis; R.p.c., nucleus reticularis parvocellularis; R.p.o., nucleus reticularis pontis oralis; Tr., corpus trapezoidum; Tr.sp. V, tractus spinalis nervi trigemini; Vm, VI, VII, motor nuclei of cranial nerves. From Batini *et al.* (1959).

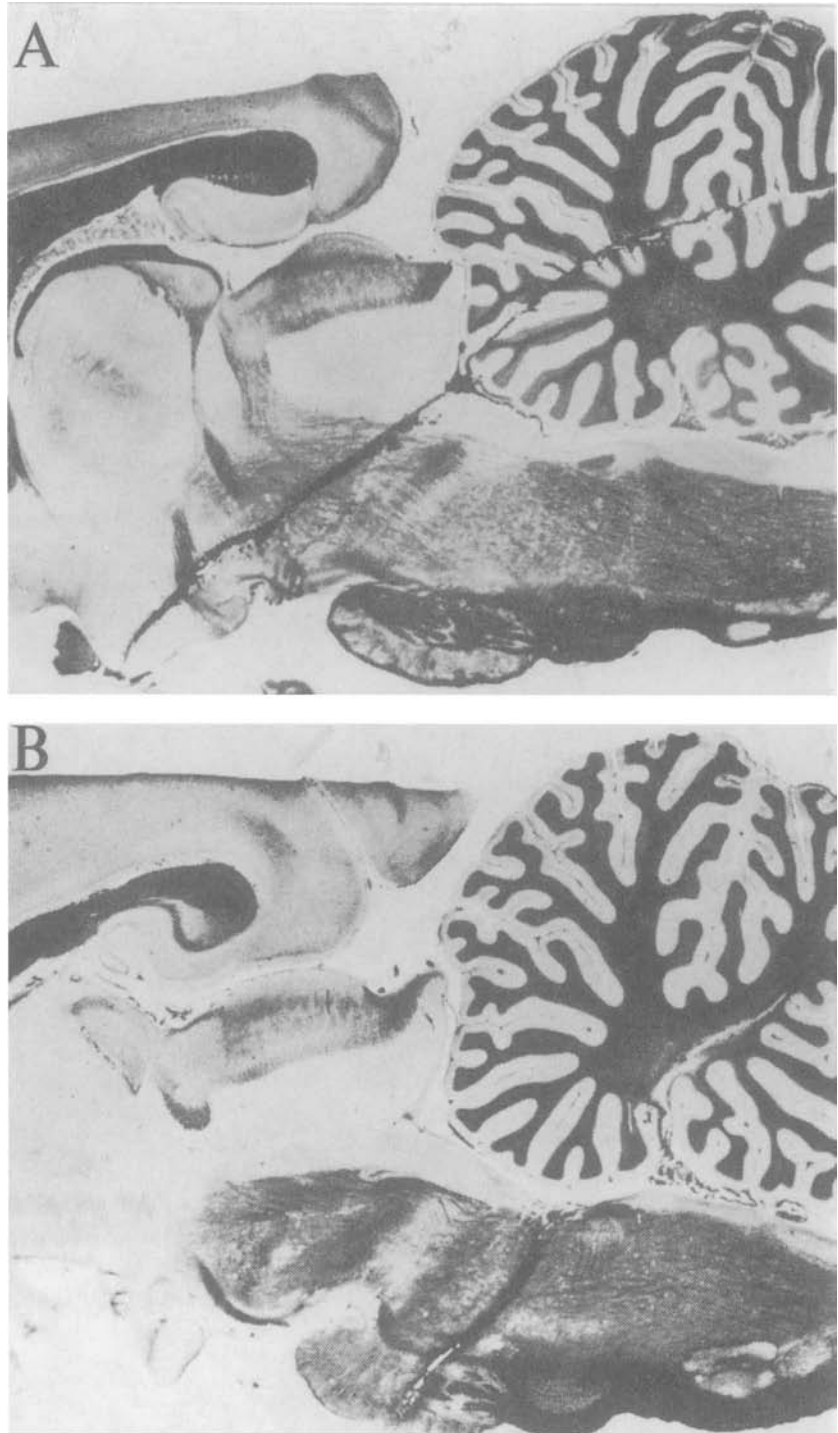


Figure 1.3. Two brainstem transections and their different effects on cortical metabolism. A, cut at the collicular level that also disconnects the forebrain from the posterior hypothalamus (at the extreme ventral part of the transection), leading to deep coma. B, midpontine pretrigeminal transection, a fully alert preparation. Cortical aspartate transaminase (AspT) activity increased following the transection at the collicular level, whereas it significantly decreased in midpontine pretrigeminal preparations. Modified from Steriade *et al.* (1969b).

midpontine transection was prescient in anticipating recent findings on the brainstem substrate of ascending activation. Data presented in Chapters 3 and 9–10 show that brainstem cholinergic neurons with thalamic and basal forebrain projections and activating properties are concentrated in two cellular aggregates at the midbrain–pontine junction. This is precisely the region predicted by the experiments of Moruzzi and his pupils. The enduring alert state of the midpontine pretrigeminal preparation was ascribed to the removal of inhibitory influences arising in the lower brainstem. These more disputable data, related to the concept of active inhibitory influences promoting sleep, are discussed in Section 1.3.2, together with other hypotheses of hypnogenic structures.

Nathaniel Kleitman (1895–1999) was a leading proponent of the passive theory of sleep, as he emphasized that there is not a single fact that supports the theory of active sleep (see Section 1.3.2) and that what needs to be explained is not sleep, but wakefulness [22]. Kleitman performed experiments on prolonged sleep deprivation but found his data incompatible with the notion of a continual buildup of hypnotoxin (see Section 1.3.2). The major discovery of Kleitman pertains to the sleep stage with rapid eye movements (REMs) that he reported in seminal papers, with his students, Aserinsky and Dement [23]. Periodic REM-sleep episodes with low voltage, fast EEG patterns, associated with limb and vibrissae twitches, have been described since antique times, were termed *sonno profondo* (deep sleep) by Fontana around 1765, and again described as *Tiefen Schlaf* with low voltage and fast EEG waves by Klaue in the late 1930s [24]. The notion of “deep sleep” in those earlier descriptions did not imply a qualitative difference between the REM-sleep state and that of sleep with EEG synchronization. In fact, the dual nature of sleep is a recent concept. At the Lyon’s 1965 Symposium, some participants thought of sleep as a unitary phenomenon, emphasizing the similarities, rather than the differences, between EEG-synchronized sleep and REM sleep. After the description by Dement and Jouvett of major dissimilarities between the two states of sleep, Dement commented that EEG-synchronized sleep and REM (or paradoxical) sleep “are as far as night and day. It is difficult to point to a single attribute that is commonly shared ... In terms of definition, it would seem more appropriate to regard slow-wave sleep and paradoxical sleep as entirely different states with their own specific mechanism or mechanisms. I would even go so far as to suggest that there may be some validity in questioning whether they should be subsumed under the general heading of sleep” [25]. The dual nature of sleep is emphasized by recent

[22] Kleitman (1929, 1963).

[23] Aserinsky and Kleitman (1953, 1955); Dement and Kleitman (1957a, b). See also Dement (1958).

[24] Cited by Moruzzi (1963) and Jouvett (1967).

[25] See Jouvett (1965b, pp. 628–629).

investigations at the cellular level, including intracellular recordings during natural waking and sleep states in chronically implanted animals (see details in Section 1.2 and Chapters 2, 7, and 9–10). In essence, the so-called quiet sleep state is characterized by EEG synchronization associated with decreased transfer function of incoming messages from the external world, but with preserved corticocortical and corticothalamic dialog as well as with plastic neuronal properties that may lead to consolidation of memory traces acquired during the state of wakefulness [26], whereas the brain-active REM-sleep state is characterized by EEG activation and enhanced excitability of central networks.

Michel Jouvét discovered that the oscillator for the state of sleep with rapid eye movements (REM sleep) is located in the pontobulbar brainstem [27]. Jouvét and his colleagues discovered the presence of muscular atonia and spiky pontine waves, thus establishing the signs that differentiate REM sleep from the other states of the sleep–waking cycle [28]. In more recent years, the mechanisms of muscular atonia were first described by Pompeiano and his colleagues who showed that both tonic and phasic inhibition of spinal reflexes occur during REM sleep in unrestrained cats [29]. Later on, this disclosure was substantiated by intracellular recordings of spinal motoneurons in naturally sleeping cats [30]. As to the spiky waves recorded in the mesopontine tegmentum, lateral geniculate, and occipital cortex (termed PGO waves), their progenitors have been discovered in a region at the midbrain–pontine junction [31]. These data, the cellular evidence of the involvement in PGO-wave genesis of several cell-classes recorded from the pedunculopontine and laterodorsal tegmental cholinergic nuclei and identified antidromically as projecting to different thalamic nuclei [32], the role played by the pontine reticular formation [33], the neuronal mechanisms of thalamic PGO waves [34], and the progressive synchronization of PGO waves during REM sleep throughout thalamocortical systems [35], are discussed in Chapter 9.

Probably the most important discovery of Jouvét came from his now classical experiments using rostrpontine transections in acute and chronic cats [36]. These studies led to the current hypotheses of REM-sleep genesis by showing that periodic episodes of muscular atonia (especially antigravity muscles), saccadic eye movements, the pontine component of PGO waves, and phasic muscle twitches, occur in the prepontine preparation with a rhythmicity that is similar to that of REM sleep in the intact animal. The discovery of a brainstem sleep oscillator that operates in the absence of the forebrain has generated a series of models of REM-sleep genesis, based upon the

[26] Steriade (2001b).

[27] Jouvét (1962).

[28] Jouvét and Michel (1959); Jouvét *et al.* (1959).

[29] Pompeiano (1967a, b).

[30] Morales and Chase (1978); Chase and Morales (1983); Glenn and Dement (1981). See details on these intracellular investigations in chapter 11.

[31] McCarley *et al.* (1978); Sakai and Jouvét (1980); Nelson *et al.* (1983); Sakai (1985).

[32] Steriade *et al.* (1990c).

[33] McCarley and Ito (1983).

[34] Deschênes and Steriade (1988); Hu *et al.* (1988, 1989c); Steriade *et al.* (1989).

[35] Amzica and Steriade (1996).

[36] Jouvét (1962, 1965a).

[37] McCarley and Hobson (1975b); Pompeiano and Valentinuzzi (1976b); McCarley and Massaquoi (1986a, b); Sakai *et al.* (2001).

interaction of different cell-groups located between the midbrain–pontine junction and the bulbar reticular formation [37]. The models of oscillatory sleep–waking states and the supportive experimental data are discussed in Chapter 12.

In the next sections of this chapter, we describe the physiological correlates of various behavioral states of vigilance and define the notion of activation; we analyze the validity of data supporting the concepts of passive and active sleep; and we survey the ideas on waking and sleep centers, as opposed to the more encompassing concept of distributed systems.

1.2. Definition of States of Vigilance and Activation

[38] Rosen (1970).

[39] See chapters 7 and 11 in Bartee *et al.* (1962).

State means the values assumed by the (potentially infinite) set of variables describing the system or organism [38]. This definition is easily understood by a computer analogy wherein the “machine state” at any point in time is completely defined by the presence of ones or zeros in the binary logic elements [39]. Appealing as this logical simplicity is, it suffers the practical complexity of requiring a specification of all the current values of the very large number of elements in the biological organism. Even the computer software engineer finds little use in the precise definition of machine state as used by his counterparts in machine design. Although complete machine state is theoretically and operationally specifiable, this description is much too detailed and complex. Instead, the software engineer abstracts certain features and uses these more global definitions of state; his “machine state” refers to global characteristics of the machine, such as whether it is operating in “foreground” or “background” mode, or whether it is servicing an interrupt request.

The definition of behavioral state that will follow is offered as one that is in this practical spirit, and one that is in accord with general usage. We first briefly discuss the terms of the definition and the rationale for including them. We use the term *indicator variable* to mean a variable that, when in a particular range of values, indicates with a high probability that *other* variables will have a particular range of values. Use of indicator variables reduces the dimensionality (number of variables) necessary to specify state. We further will objectively define state as a particular *range of values of the indicator variables*. Our definition of behavioral state also includes the criteria of recurrence

and temporal persistence of the state; a one-time, one-millisecond condition is not a useful object for scientific study, nor is it in accord with everyday usage of state.

The definition thus becomes: *A state is a recurring, temporally enduring constellation of values of a set of indicator variables of the organism.*

The use of the term “indicator variable” makes explicit that the variables used in state definition are not themselves the state but rather are used because they efficiently imply the presence of other measures.

The three main states of vigilance (waking, slow-wave sleep with EEG synchronization, and REM sleep with EEG activation) can be objectified by a set of three physiological signs that include EEG rhythms, muscular tone, and eye movements associated with sharp waves in brainstem–thalamocortical systems. (1) The tonic EEG activation in waking is undistinguishable from that in REM sleep. This led Jouvet and his colleagues [40] to coin the term *paradoxical* sleep for a state with the highest threshold for motoric arousal, but an EEG pattern that suggested a highly active brain state. The EEG-synchronized rhythms (consisting of spindle oscillation at 7–14 Hz, slow oscillation at 0.5–1 Hz, and delta waves at 1–4 Hz) distinguish the state of slow-wave sleep from both waking and REM sleep. (2) The other tonic aspect, muscular atonia, specifically distinguishes REM sleep from the other two states. (3) Phasic eye movements are voluntary during waking and occur as involuntary ocular saccades without relation to the visual field in REM sleep. The eye movements are accompanied by spiky PGO potentials, which originate in the mesopontine tegmentum; the neurons of the final common path for transmitting PGO waves to various thalamocortical systems are located at junction between the midbrain and pons (see Chapter 10). The PGO waves herald REM sleep and continue throughout this state. During waking, eye movement potentials (EMPs) are similar to, but much less ample than, PGO waves during REM sleep.

[40] Jouvet *et al.* (1959).

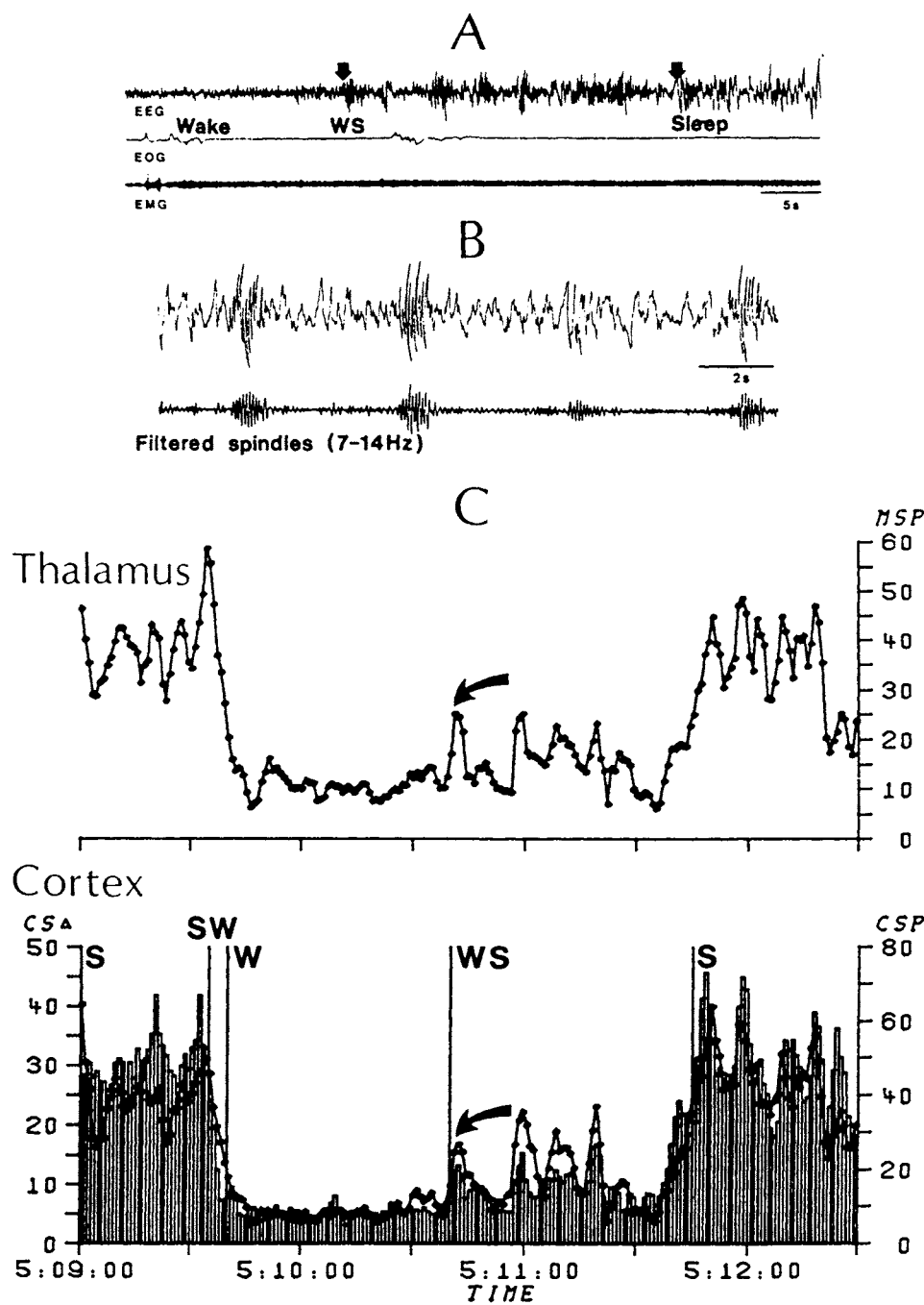
Note that the above three cardinal signs can be used as an easy way for objective identification of behavioral states with various degrees of vigilance. These electrographic events, however, merely represent the physiological correlates of behavioral states and they say nothing about the psychology of the three states of vigilance. Since this monograph is mainly concerned with the brain structural and physiological bases of waking and sleep states, we only refer *en passage* to the role of slow-wave sleep in memory consolidation in Chapters 7–8 but discuss at length the neuronal bases of dreaming activity in Chapter 14.

The above electrographic characterization applies only to steady, fully developed states of vigilance. More

subtle features have to be used for the transitional epochs between waking and slow-wave sleep and vice versa, and between slow-wave (or non-REM) sleep and REM sleep, when most dramatic neuronal changes are expected to occur. Such neuronal activities may shed light on the mechanisms of various physiological aspects of awakening, falling asleep, and entering REM sleep. The electrographic criteria of these transitional epochs between the main states of the waking–sleep cycle are briefly presented below, while cellular investigations related to mechanisms of arousal, sleep onset, and REM-sleep genesis are treated in detail in Chapters 7 through 12. Since the data discussed in all subsequent chapters mostly derive from animal studies, we shall also mention the similarities and some differences between the main electrical signs of waking and sleep states in humans and cats, the species of choice for the study of sleep mechanisms.

The transition from EEG-synchronized sleep to arousal is usually short in duration. It may last for a few seconds and consists of decreased amplitude and increased frequency of EEG waves that precede the abruptly increased muscular tone and eye movements, which occur with arousal. By contrast, the reverse transition, from waking to EEG-synchronized sleep, does not display a clear-cut picture of uninterrupted EEG synchronization. In humans, sleep onset is characterized at the EEG level by a change from alpha waves to a mixed-frequency pattern of low-voltage waves (termed stage 1 sleep). Since this initial sleep stage may or may not coincide with perceived sleep onset in humans, many investigators recognize the clear-cut onset of sleep by the EEG correlates of stage 2 sleep, that is, spindle oscillations and K-complexes [41]. In cats, the transition from waking to sleep is marked by episodic appearance of spindle waves that precede overt postural signs of sleep (Fig. 1.4C). Spindle waves are high-amplitude, waxing and waning waves at 7–14 Hz. They are grouped in sequences that last for 1.5–2 s and recur periodically every 5–10 s (Fig. 1.4B). In some instances, slow waves appear usually one or several minutes after the occurrence of spindles, when sleep is completely installed and when transient EEG desynchronizing reactions no longer appear (Fig. 1.4C). However, the slow oscillation (0.5–1 Hz) can also be observed since the earliest stage of natural EEG-synchronized sleep, in association with spindles. As discussed in Chapter 7, the association of slow and spindle oscillations results in K-complexes. This EEG picture in cats resembles that occurring in stage 2 of human sleep. While the slow oscillation dominates brain electrical activity throughout slow-wave sleep, spindles appearing early sleep stages, are overwhelmed by delta waves

[41] Carskadon and Dement (2000).



[42] See the chronology of EEG correlates of slow-wave sleep in fig. 3 of Steriade and Amzica (1998).

(1–4 Hz) during late stages of EEG-synchronized sleep, and reappear toward the end of this sleep stage, just before REM sleep [42]. These changes that occur throughout slow-wave sleep, from prevalent spindles to prevalent delta and back to spindles, are attributable to changes in the membrane potential of thalamocortical neurons (see Chapter 7).

[43] Moruzzi (1969).

Some authors include drowsiness within the final stage of relaxed wakefulness, while other consider it within the initial stage of sleep. For example, Moruzzi depicts drowsiness in the lower part of wakefulness, before sleep, and hypothesizes that an animal's behavior during drowsiness corresponds to the appetitive phase, while sleep itself should be regarded as the consummatory action of a special instinctive behavior [20]. In another review article, Moruzzi [43] analyzes the typical manifestations of the appetitive behavior and points to the period immediately preceding sleep as a stage when the animals strive for a situation, a "home" for sleep, which will facilitate sleep onset. These ethological observations and hypotheses leave little doubt that, in the natural conditions of animals' life, sleep is preceded by a set of stereotyped or less stereotyped movements toward the search of a place to sleep. However, in the conditions of cellular investigations in an experimental animal which is sure of our good intentions and does not have to look at safer places to sleep, the period of drowsiness that precedes sleep (with transient closing and reopening the eyes) is typical associated with EEG spindle (and slow) oscillations and, in the absence of unwanted stimuli, this period inevitably leads to genuine manifestations of sleep.

The transition from EEG-synchronized to REM sleep is marked by a short (1–2 min) period during which the EEG is still fully synchronized, there is yet no sign of muscular atonia, but high-amplitude, singly, sharp pontogeniculo

Figure 1.4. Electrographic criteria of waking and EEG-synchronized sleep. A, behaving cat with chronically implanted electrodes. EEG from the motor (precruciate) cortex, electrooculogram (EOG), and electromyogram (EMG) of neck muscles. Spindle oscillations appear during the transitional period between waking and sleep (WS). B, thalamic spindles in a cat with a high brainstem transection. Top trace shows the field electrical activity recorded by a microelectrode in rostral intralaminar thalamic nuclei; bottom trace shows the same period, with spindle waves filtered from 7 to 14 Hz. Note that spindle sequences recur periodically. C, normalized amplitudes (ordinates) of simultaneously recorded focal spindle waves in the thalamus (top MSP trace) and in the cortex (bottom CSP line–circle trace depicts spindles; and bottom CS bar-graph trace depicts slow waves) in a behaving cat. Spindles filtered between 7 and 14 Hz; slow waves filtered between 0.5 and 4 Hz (they include both slow and delta frequency bands). Abscissa indicates real time (hr, min, s). S: EEG-synchronized sleep; W: waking; SW and WS: transitional periods from S to W, and from W to S, respectively. Note EEG activation with decreased wave amplitudes on awakening (SW and W); rhythmic sequences of spindles, recurring with a period of 8–10 s in both thalamic and cortical recordings, beginning with drowsiness (WS, oblique arrows); and increased amplitudes of both spindles and slow waves beginning with S. A and C, modified from Steriade *et al.* (1986); B, modified from Paré *et al.* (1987).

occipital (PGO) waves can be recorded in the brainstem, thalamus, and cortical areas (Fig. 1.5). Later on, when REM sleep is fully developed, PGO waves appear as either single potentials or clusters of smaller amplitude potentials with a frequency of about 6 Hz. This phasic activity announcing REM sleep has been described in a number of mammals, but the bulk of data on cellular mechanisms of PGO waves derive from experiments on cats.

Since PGO waves related to saccadic eye movements are thought to represent the substrate of oneiric behavior during REM sleep, the question is usually raised about the similarities between REM sleep in humans and cats as well

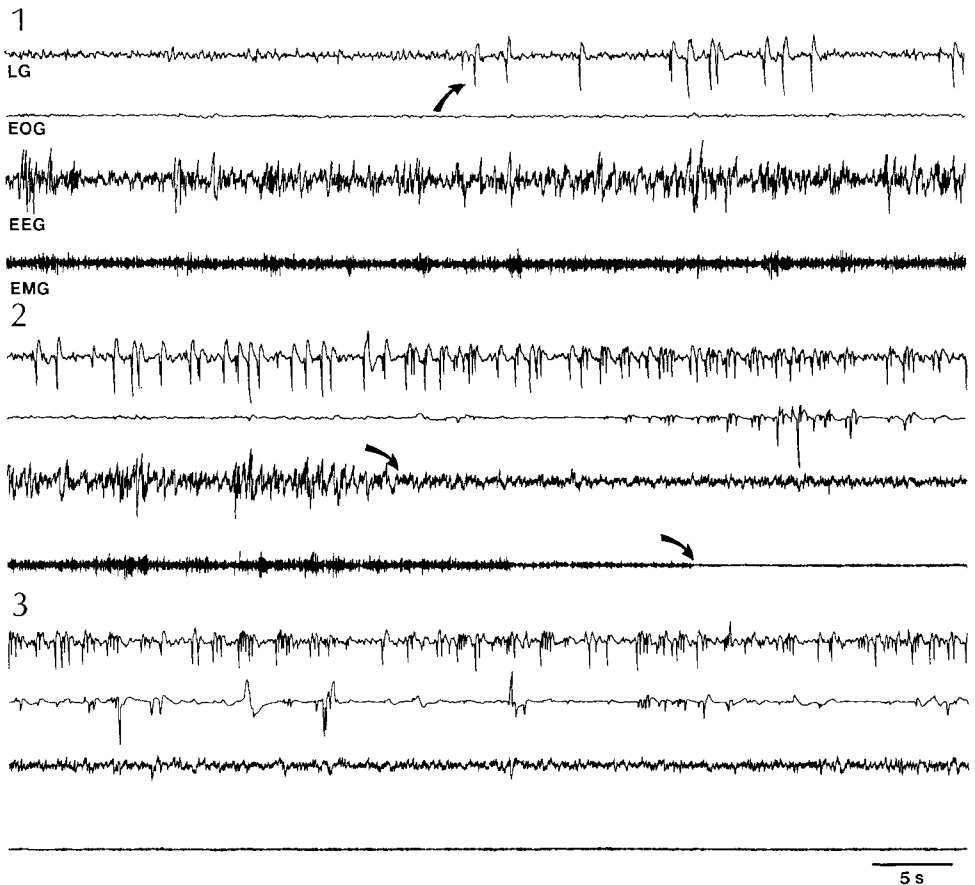


Figure 1.5. Electrographic criteria of transition between slow-wave sleep and REM sleep. Chronically implanted, behaving cat. The four traces in 1 (LG, field potentials in the lateral geniculate (LG) thalamic nucleus; EOG; EEG recorded from the anterior suprasylvian gyrus; and EMG) are repeated in 2 and 3. Parts 1-to-3 are in continuation. Parts 1 and 2 represent the transition from EEG-synchronized sleep to REM sleep (in 1, oblique arrow indicates the occurrence of PGO waves; in 2, first oblique arrow points to EEG activation and second arrow points to complete muscular atonia). Part 3 depicts fully installed REM sleep. Note singly PGO waves with high amplitudes during the transitional period 1, and clusters of PGO waves (at about 6 Hz) with smaller amplitudes during a later stage of REM-sleep (in 3). Modified from Steriade *et al.* (1989).

as whether animals have dreams. The low voltage and fast EEG rhythms during the REM sleep of the adult cat are strikingly similar to the EEG rhythms directly recorded from the cerebral cortex in humans. In scalp recordings from humans, rhythms at 6–8 Hz appear in occipital areas. The origin of these waves in the higher range of the theta band is unknown, especially since the theta rhythm is not evident in primates and humans. As to dreaming in animals, the usual remark is made that, since dreams are verbal reports of subjective experiences, the question must remain unanswered. However, some of the REM dreams features may apply to nonhuman mammals since dreaming is a perceptual experience that does not necessarily depends on abstract thought and language. As discussed in Chapters 11 and 14, the overt behavior during REM sleep in cats with lesions in the dorsolateral part of the pontine tegmentum, which suppress muscular atonia, strikingly suggests oneiric behavior. The cat seems to fight with imaginary enemies or to play with an absent mouse, and exhibits fear reactions associated with autonomous phenomena, episodes during which the pupils are extremely myotic and nictitating membranes are relaxed [44]. This pattern resembles that of hallucinatory oneiric-like behavior that can be elicited during the waking state by chemical stimulation of the same region at the mid-brain–pontine junction [45] where internal signals for brain activation are generated during both REM sleep and arousal (see Chapters 9–10).

Under most conditions the states of waking, slow-wave sleep, and REM sleep can be specified using only three indicator variables: the voltage amplitude of the cortical EEG, the frequency of rapid eye movements, and the record of antigravity muscle activity. Figure 1.6 illustrates this point and the use of these three indicator variables that are the most frequently used, with animal studies utilizing PGO waves as the next most important indicator variable. The presence of hippocampal theta rhythm is often used as an important REM sleep indicator in recordings in rodents, who have much less visual system activity than primates. Finally we point out that the frequently used modifier “behavioral” indicates that the state is related to the external comportment of the organism, and also implies an internal pervasiveness, since it usually refers to global states such as sleep and waking.

The use of indicator variables to define state, as schematized in Fig. 1.6 [46], has been concretized and implemented as a method for display of actual data and of state diagnosis [47]. In general, accurate and reliable use of waking, EEG-synchronized sleep, and REM-sleep state definitions is straightforward in studies of normal,

[44] Jouvet and Delorme (1965).

[45] Kitsikis and Steriade (1981).

[46] McCarley (1980).

[47] Friedman and Jones (1984). Ursin and Sterman (1981) have provided a manual of criteria for sleep state definition in the adult cat.

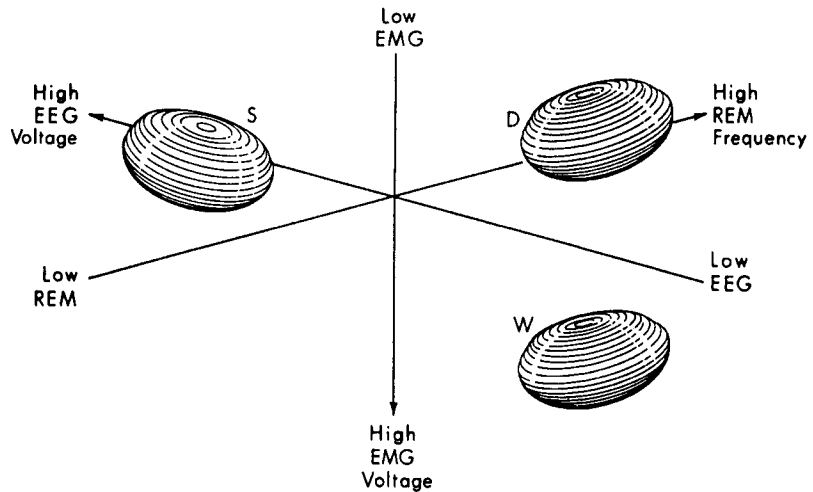


Figure 1.6. Three-dimensional indicator space illustrating the definition of waking (W), EEG-synchronized sleep (S), and REM sleep (labeled D, for the synonym EEG-desynchronized sleep), with the use of three indicator variables. The range of values taken on each state is indicated by an ellipsoid. This includes variability between occurrence of the state and within-state moment-to-moment variability. Modified from McCarley (1980).

sufficiently mature, nondiseased, and nonlesioned animals. One simply looks for the presence of the three major indicator variables and, when jointly present, the organism is deemed to be in the behavioral state of REM sleep. Problems arise when the central nervous system (CNS) is not intact or when a pharmacological agent is used to alter state; it is then that the presence or absence of REM sleep becomes a matter of definition of whether sufficient indicator variables are present and have the proper range of values. For our part, we see little point in hermeneutics of state diagnosis. We take the viewpoint that REM sleep involves many component systems and that lesions and pharmacological agents may selectively and/or partially suppress or activate a number of these systems. Following experimental questions, the question often arises as to the definition of the ensuing state, as, for example, whether it is REM sleep or not. We think the obvious procedure to follow with such altered states is the set of indicator variables useful in normals must be enlarged so that the "organism state" can be specified with more precision; ideally one would measure the activity (EEG and cellular) in each component system of REM sleep. If this is not done, and it is often technically impossible to do so completely, then some uncertainty must remain about how close the match is to normal REM, with the degree of uncertainty inversely correlated with the thoroughness of the match. The reason for going into this apparently simple, straightforward line of argument in detail will become

clear as lesion and REM-induction studies are presented. We suggest that many disagreements arise from whether the investigator thinks the criteria for "true REM" have been satisfied, and from the fact that, not surprisingly, individual definitions of "true REM" vary widely. Our reason for using "indicator variables" is to move the argument away from the hermeneutics of "true REM" and employ the descriptive, operational notation of the values of certain indicator variables after an experimental manipulation. These objectively describe the closeness of the match and suggest what other variables should be recorded.

The paradox that REM sleep, a state with a motoric arousal threshold higher than in EEG-synchronized sleep [48], is a time when the electrical activity suggests that the cerebrum is in a highly excitable state, leads us to define *activation* and *vigilance*.

Activation has to be used at the physiological, not behavioral, level. Moruzzi and Magoun [8] referred to the activation of the EEG, but they did not equate this EEG response with arousal or waking. Activation was defined [49] as a tonic readiness in cerebral networks that brings neuronal circuits closer to threshold, thus insuring secure synaptic transmission and quick cellular responses, a response readiness to either messages from the outside world (as during the waking state) or to internally generated drives (as during REM sleep), whether or not a motor reaction is generated. This definition is based on data showing similar enhanced excitability of thalamic and cortical neurons to monosynaptic and antidromic volleys during both EEG-activated states of waking and REM sleep (see Chapter 9). The definition does not refer, however, to inhibitory processes that insure a behavioral state with adequate, selective responsiveness. While inhibitory processes have not yet been investigated at the intracellular level during REM sleep, extracellular recordings of neocortical neurons show that inhibitory processes are overwhelmed by excitatory activity during REM sleep [50]. Also, the bizarre imagery during REM sleep would indicate that many sensory channels are simultaneously activated and, correlatively, fine sculpturing inhibitory processes would probably be much less effective during this sleep state as compared to waking (see Chapter 9). The inclusion of inhibitory processes in the activating process leads to the notion of vigilance.

Vigilance was defined by Head [51] as a state with an increased reaction but with highly adapted responses, similarly to Dell's [52] notion of a readiness to receive only some stimuli to the exclusion of others, in order to perform efficiently. Both these definitions implicate the presence of inhibitory processes during the active and adaptive

[48] Only one study found that the arousal threshold to auditory stimulation is higher in stage 4 of non-REM sleep than in REM sleep (see Dement, in Jouvet, 1965b).

[49] Steriade (1984, 1991).

[50] Steriade *et al.* (1979a).

[51] Head (1923).

[52] Dell (1958).

behavioral state of wakefulness. Considering the requirement of a differential organization of cerebral networks for conscious integrative functions, Jasper [53] concluded that, for such high processes, ascending activation should include inhibition and that “some activated cells may have an inhibitory function.” While cellular studies in the two decades that followed Jasper’s prediction (1960s–1970s) rather claimed that a global blockage of inhibitory circuits occurs upon arousal, current concepts fully agree with Jasper’s assumption that some inhibitory neurons that underlie discriminatory functions are activated upon natural arousal, brainstem reticular stimulation, or iontophoretic application of brainstem reticular transmitter agents. These data are fully discussed in Chapter 9.

[53] Jasper (1958, p. 341).

1.3. Concepts of Passive and Active Mechanisms Promoting Sleep

Theories of passive sleep view sleep as a cessation of wakefulness, resulting from forebrain deafferentation by decreased or interrupted activity in specific sensory channels or in generalized activating systems. These theories appeared since Lucretius’ *De Rerum Natura* and were elaborated in the last century by Bremer, Moruzzi and Magoun, and Kleitman [5, 8, 22]. Theories of active sleep view sleep as promoted by increased activity in systems with presumed inhibitory actions upon cerebral structures maintaining the state of wakefulness. They stemmed from the following lines of evidences: sleep induced by thalamic stimulation [54], insomnia following anterior hypothalamic lesions [55], brainstem transection experiments [20], and experimental manipulations leading to the serotonergic hypothesis of sleep [56]. In this section we review the roots and the current state of the passive and active hypotheses of sleep.

[54] Hess (1944).

[55] Nauta (1946).

[56] Jouvet (1972).

1.3.1. Theories of Passive Sleep

The idea that falling asleep is the simple result of negation of the active waking state is based on experiments with stimulation inducing arousal and EEG activation, and on clinical and animal studies with midbrain and thalamic lesions followed by lethargy or coma.

The experiments with brainstem reticular stimulation by Moruzzi and Magoun [8] led to the precise formulation of their theoretical concept of active waking and passive sleep: “The presence of a steady background of ... activity within this cephalically directed brainstem system,

contributed to either by liminal inflows from peripheral receptors or preserved intrinsically, may be an important factor to the maintenance of the waking state, and absence of such activity may predispose to sleep" (p. 470). This statement indicates that Moruzzi and Magoun did not express a clear choice between the two parts of the proposed alternative: (1) an intrinsic property of the brainstem core maintains the waking state; or (2) wakefulness requires the contribution of sensory pathways that collateralize in the reticular formation.

In fact, there is no incompatibility between the idea of a cerebral tone maintained by activities in sensory pathways and the brainstem reticular activating concept. Both factors should be considered as acting in concert. Experiments conducted in Speranski's laboratory have shown that the interruption of olfactory, visual, and auditory pathways at the peripheral level is followed in dog by a prolonged state of lethargy. This led Pavlov [57] to emphasize the role of sensory impulses in the activated state of the cerebrum. Bremer's [5] claim of a role played by sensory projections in maintaining the cerebral tone was undoubtedly strengthened by the experiments performed in his laboratory by Claes (1939). The locally activated electrical activity in various neocortical areas by setting into motion specific sensory projections may become a generalized EEG activation by the action of corticofugal pathways impinging upon the brainstem reticular formation [58]. These pathways, that use excitatory amino acids as transmitter agents, are discussed in Chapters 3–4. Suffice it to mention the role of the corticoreticular feedback for the maintenance of the alert condition [7] and the depression of cell responsiveness in the upper brainstem reticular formation after a reversible cryogenic blockade of cortical sensory–motor areas [59].

The emphasis on the role of brainstem structures in the diffuse cerebral activation of the waking state was the result of acute experiments. Subsequent studies on chronic *cerveau isolé* preparations [60] have shown that, after a period of 7–10 days, the animals recover from the comatose state that appears immediately after a precollicular transection. Such chronic preparations display oscillations between EEG patterns and ocular behavior of wakefulness and sleep, with the conclusion that a genuine state of wakefulness may be maintained in the isolated cerebrum [20]. The recovery of wakefulness in chronic *cerveau isolé* preparations deserves some comments concerning the activating role of supramesencephalic structures, namely, the thalamus, the posterior hypothalamus, the amygdala nuclear complex, and the basal forebrain.

A bilateral symmetrical vascular lesion that mainly affected some medial and especially intralaminar thalamic

[57] Pavlov (1928).

[58] Bremer (1975).

[59] Buser *et al.* (1969).

[60] Batsel (1960);
Villablanca (1965).

nuclei, due to a thrombosis at the bifurcation of the basilar artery, was followed by a state of lethargy lasting for more than 2 years [61]. In those studies, the thalamic lesions were associated with small vascular lesions in the midbrain periaqueductal gray. Generally, pure thalamic lesions are possible only experimentally. During the first 10 postoperative days after bilateral thalamectomy, with a midline approach that minimized cortical damage, “although the cat behaviorally awoke... the EEG remained synchronized” and, 3 months after thalamectomy, there was a delay of 10–20 s between behavioral arousal and EEG desynchronization [62]. Thus, while an enduring lethargic syndrome may occur after medial–intralaminar thalamic lesions combined with smaller midbrain tegmental lesions, behavioral arousal is not severely impaired after pure, total thalamic lesions. However, the EEG desynchronization ordinarily accompanying arousal is absent or greatly delayed even at late postoperative stages.

Clinical–anatomical observations point to the posterior hypothalamus as a cerebral site whose lesions are followed by somnolence or coma [63]. More localized lesions than those resulting from the natural experiments created by the encephalitis letargica became possible with the introduction of the Horsley–Clarke stereotaxic instrument and its use through the 1930s. In experiments on macaque monkeys, Ranson [64] observed that bilateral lesions of the lateral parts of the posterior hypothalamus, which did not significantly encroach upon the thalamus and the midbrain, produce a state of continuous lethargy, followed in later stages by a prevailing state of drowsiness and lack of motor initiative. Ranson did not decide whether the lethargic syndrome, presumably produced by elimination of excitatory activity arising in the hypothalamus, was mediated by downward projections to the brainstem and spinal cord or by upward projections toward the cerebral cortex. The results of Ranson’s experiments and the idea of a waking “center” located in the posterior hypothalamus have been revived during recent years by studies performed in Jouvet’s laboratory and postulating the maintenance of the waking state by histaminergic, cortically projecting neurons in the ventrolateral part of the posterior hypothalamus [65].

Related to the syndrome with loss of motor initiative described in monkeys by Ranson (see above), the clinical syndrome of akynetic mutism was first described in a patient with an epidermoid cyst of the third ventricle [66]. It can be described as a vigil coma, since the patients can be easily roused, but they lie inert and make no sound. Their eyes may follow moving objects or regard the observer steadily. Similar clinical cases have been subsequently

[61] Façon *et al.* (1958). Our 1958 clinical–anatomical data have been confirmed by French neurologists at the Salpêtrière hospital (Castaigne *et al.*, 1962).

[62] Villablanca (1974, p. 72; see fig. 4.16 in that chapter).

[63] Von Economo (1929).

[64] Ranson (1939).

[65] Vanni-Mercier *et al.* (1984); Lin *et al.* (1986).

[66] Cairns *et al.* (1941).

[67] Klee (1961); Steriade
et al. (1961); Lhermitte
et al. (1963).

[68] See discussion of this
clinical syndrome in
Steriade (1997b).

[69] Szerb (1967); Jasper
and Tessier (1971).

[70] Meynert (1872).

[71] Buzsáki *et al.* (1988a).

[72] Coben *et al.* (1983).

[73] Wickler (1952).

[74] Steriade *et al.*
(1987b).

described following hypothalamic and brainstem tegmental lesions [67]. We stressed the point that this nosological entity should be confined to cases where there is a pathological interruption of ascending activating systems, excluding those cases where the lesion is diffuse and interrupts the effector pathways. In conditions without interruption of corticospinal or corticobrainstem pathways (as ascertained by precise motoric answers to the examiner's questions, by moving one or two fingers according to given codes and verbal instructions), the akynesia and mutism were interpreted as *Antriebsmangel*, an abolishment of incitation to action, due to the interruption of ascending activating impulses [68].

The history of cortical activating processes induced by basal forebrain structures is more recent and it is related to the long-standing concept that ascending activation processes are largely cholinergic in nature. This concept was based on data showing that midbrain reticular stimulation or EEG-activated behavioral states of waking and REM sleep are associated with a large increase in cortical release of acetylcholine (ACh), as compared with EEG-synchronized states [69]. While described a long time ago by Meynert [70], the nucleus basalis and the adjacent basal forebrain structures of the same family were implicated in cortical cholinergic activation only since the 1980s, when immunohistochemical studies showed that thalamocortical neurons, the final link in the ascending brainstem reticular system, do not use ACh as a transmitter agent. In some early kainate-induced lesion studies of the basal forebrain, there was a loss of cortical EEG activation, but those results are not interpretable because there was also extensive damage to the thalamus. More precise chemical lesions of basal forebrain cell bodies in the rat, with consequent reduction in acetylcholinesterase (AChE) staining in the ipsilateral cortex, produced a large increase in slow and delta EEG waves during all behaviors [71]. Similarly, EEG alterations with an increased tendency toward slow waves are seen in Alzheimer's patients [72]. These data, that are reminiscent of results obtained by means of cholinergic blockers, such as atropine [73], substantiate a direct cholinergic effect exerted by cortically projecting basal forebrain neurons in inducing cortical low voltage and fast activity. An indirect activating effect on the EEG is mediated by nucleus basalis cholinergic (and GABAergic) projections to the thalamic reticular nucleus [74] that effectively block synchronous spindle oscillations at their very site of genesis (see Chapters 7 and 9).

The point should be emphasized that the most powerful drive of all activating supramesencephalic structures arises in the upper brainstem reticular core. This is true

for ventromedial and intralaminar thalamic nuclei with diffuse cortical projections, the posterior and lateral hypothalamic areas, and the basal forebrain cellular aggregates. In the intact animal, these diencephalic and forebrain neurons integrate ascending reticular impulses in their route to the cerebral cortex. The question arises as to the source of excitatory input to supramesencephalic structures in the chronic precollicular-transected preparation. This preparation displays EEG and ocular signs indicating a waking condition in the isolated cerebrum [60]. It is known that basal forebrain nuclei receive a projection from the amygdala [75] and stimulation of amygdala nuclei induces EEG activation even after complete disconnection from the midbrain reticular formation [76]. We suggest that, in a precollicular preparation, intrinsic or sensory (olfactory and visual)-induced activities of thalamic, posterior hypothalamic, and basal forebrain nuclei are effective in providing excitatory inputs for activation processes. It is also possible that denervation hypersensitivity [77] occurs in supramesencephalic structures after precollicular transection. Indeed, following excitotoxic lesions of midbrain reticular neurons, there is a strikingly decreased duration of the waking state but, 7 to 10 days after, an increased duration of wakefulness occurred [78], likely due to the denervation hypersensitivity of target structures located more rostrally, in the diencephalon. Studies of cellular activity in supramesencephalic areas, hypothetically endowed with activating properties in the chronic stages of a *cerveau isolé* preparation, are still lacking. Such studies would provide information on the activity of neuronal networks in the isolated cerebrum.

The main reasons accounting for an active theory of sleep is that sleep can be induced by stimulation of sensory receptors or central structures. Some of these experiments are discussed below.

1.3.2. Theories of Active Sleep

We shall not review data with EEG synchronization promoted by low frequency (6–14/s) peripheral or central stimulation [20] because such frequency parameters induce synchronized waves over the cortex even when applied to structures known to have activating properties. The variety of sites implicated in “sleep” simply because their stimulation led to EEG synchrony extends from the neo- and allocortex down to the medulla. Thus, if we accept this criterion, we would be forced to conclude, as remarked by Jouvet [2], that the whole encephalon has hypnogenic properties. Moreover, while rhythmic waves

[75] Price and Amaral (1981).

[76] Kreindler and Steriade (1964).

[77] Cannon and Rosenblueth (1949).

[78] Steriade (1983).

within the low frequency range may outlast the stimulation period, they are probably due to resonant activities in reciprocal thalamocortical loops (see Chapters 7–8) and are not necessarily related to the state of falling asleep.

We shall therefore discuss only the evidence *pro* and *contra* three cerebral sites that were postulated as having active hypnogenic properties: the region of the solitary tract nucleus in the medulla, some medial thalamic nuclei, and the preoptic area in basal forebrain. We consider that lesion studies inducing insomnia are more convincing for hypotheses of active hypnogenic structures than data obtained with electrical stimulation. While the latter technique should be used for the analytical purposes of identifying the input–output organization of a neuron or for studying state-dependent excitatory–inhibitory events in a cell, such synchronous stimuli are nonsensical for normal brain activity since they disturb natural patterns of neuronal discharges, and thus can hardly be used to mimic natural states of sleep.

The active inhibitory role of the lower brainstem reticular formation upon the rostral reticular core was hypothesized by Moruzzi and his group after the results of the midpontine pretectal transection [20]. Those experiments showed that the midpontine-transected animal displays a state of enduring alertness, about 70–90% of the total time of recording, a true experimental insomnia [79]. Among the numerous arguments brought by the Pisa group in favor of the synchronizing or possibly sleep-inducing influence of the lower brainstem reticular core, we mention the EEG-activated state following inactivation of the lower brainstem core by intravertebral injections of barbiturates [80] or by cooling the medullary floor of the fourth ventricle [81]. At the cellular level, however, the projections from the lower to the upper brainstem reticular formation are usually described in excitatory terms, with both extra- and intracellular recordings in unanesthetized preparations (see Chapter 3). Moreover, recordings of bulbar reticular units during the waking–sleep cycle have revealed neurons with physiologically identified projections to the midbrain and/or thalamus that displayed an increased activity related to EEG activation in both waking and REM sleep (see Chapter 10), but no evidence was found for neurons with increased activity during drowsiness or slow-wave sleep.

Sleep was also induced in cat by electrical stimulation of a medial thalamic area, just lateral to nucleus reuniens, by Hess [54] who claimed that sleep occurred after low-rate (8–10 Hz) stimulation. Besides the long latencies of the observed effects (tens of seconds or even a few minutes), the difficulties in interpreting Hess' studies [82] also come from the fact that cat is a good sleeper and the

[79] Batini *et al.* (1958).
See Fig. 1.2 in the present chapter.

[80] Magni *et al.* (1959).

[81] Berlucchi *et al.*
(1964).

[82] See Bremer (1954).

described effects may well have been due to the animal's natural propensity toward sleep. Hess' data can be related to more recent clinical investigations reporting "fatal insomnia" after "selective degeneration" of medial thalamic nuclei [83]. However, those thalamic lesions were not selective as they also included lesions of at least seven or eight other major thalamic nuclei and they were also associated with brainstem and forebrain lesions [84]. In fact, in "fatal insomnia" severe neuronal loss is found in "most thalamic nuclei" and a series of brainstem structures [85]. The "fatal" characteristic of this disease can be explained by hypothalamic and other lesions leading to autonomic disturbances. Therefore, there is no thalamic sleep "center." Contrariwise, lesions in some thalamic nuclei are associated with hypersomnia [61, 86].

Jouvet's theory of the role played by raphe nuclei and their major transmitter, serotonin (5-hydroxytryptamine, 5-HT), in sleep generation was based, among other experimental findings, on sleeplessness after destruction of raphe nuclei, EEG synchronization after ventricular infusions of 5-HT or local application of 5-HT at the level of critical brain structures implicated in sleep generation by other evidence, insomnia after administration of *p*-chlorophenylalanine (PCPA), an inhibitor of 5-HT biosynthesis, and sleep recovery after a small dose of a direct precursor of 5-HT [2]. The raphe theory did not apparently resist the advent of results based on cellular recordings from dorsal raphe neurons, which showed that their activity decreases when the animal passes from wakefulness to EEG-synchronized sleep [87]. Although Jouvet's claims seem unfounded in the light of these data at the single-cell level and also by experiments of his own group [88], more recent results show that 5-HT may be a factor that, in addition to other mechanisms, may contribute to generation of slow-wave sleep. Thus, 5-HT hyperpolarizes and increases the membrane conductance of thalamic relay neurons of many dorsal thalamic nuclei [89] but depolarizes reticular neurons [90] and may thus contribute to the generation of sleep spindles in these pacemaker GABAergic neurons [91]. As discussed in Chapter 7, sleep spindles are associated with rhythmic inhibitory postsynaptic potentials (IPSPs) in thalamocortical neurons, which obliterate synaptic transmission through the thalamus and disconnect the cerebral cortex from the outside world.

Electrical stimulation of the lateral preoptic region and diagonal band nuclei led to EEG synchronization and behavioral sleep in the behaving cat, even when high frequency (150 Hz) stimuli were used [92]. The usual criticism of those experiments is that the latency of the hypnogenic effect was quite long (average time about 30 s)

[83] Lugaresi and Parmeggiani (1997).

[84] Manetto *et al.* (1992).

[85] Macchi *et al.* (1997); Rossi *et al.* (1998).

[86] Segarra (1970); Plum (1991); Steriade (1994, 1997b).

[87] McGinty and Harper (1976); Trulson and Jacobs (1979); Lydic *et al.* (1983, 1987a, b).

[88] Cespuglio *et al.* (1979, 1984).

[89] Monckton and McCormick (2002).

[90] McCormick and Wang (1991).

[91] Destexhe *et al.* (1994b).

[92] Stermann and Clemente (1962).

and might well have represented “spontaneous” drowsy periods of the cat, a naturally very good sleeper. The other criticism is that, with electrical stimuli, one cannot distinguish between activation of cell bodies and terminal or passing fibers. In this respect, Jouvet [2] argued that fibers from the serotonergic raphe nuclei terminating in the basal forebrain were implicated in the sleep syndrome produced by stimulating the basal forebrain areas. In fact, pretreatment with PCPA, a depletor of serotonergic terminals, suppresses the sleep effect of basal forebrain stimulation [93], although the nonspecificity of PCPA effects renders the significance of this result uncertain.

The hypothesis implicating the hypnogenic nature of the preoptic area in the anterior hypothalamus can be traced back to Nauta’s [55] experiments showing that insomnia follows lesions of that area. Nauta’s results have been confirmed by experiments with basal forebrain lesions leading to insomnia, appearing after a quite long delay [94]. The long-latency appearance of insomnia and the fact that alterations of temperature regulation could appear after basal forebrain lesions led Jouvet [2] to cast doubt on this phenomenon and to term it a secondary insomnia due to unknown factors, but not directly induced by suppressing a sleep-promoting structure. However, a long-lasting insomnia, mostly affecting the deep stage of EEG-synchronized sleep and REM sleep, was induced in experiments performed by Jouvet’s group using ibotenic-induced lesions of perikarya in the lateral part of the preoptic area, without secondary signs of temperature disturbances [95]. These results led to the hypothesis that the insomnia after preoptic lesions is due to enhanced excitability of the posterior hypothalamic implicated in awakening, attributed to inhibitory (GABAergic) projections from the anterior hypothalamus to the posterior hypothalamus, which have subsequently been demonstrated [96]. This hypothesis is congruent with the transient recovery of sleep following inactivation of awakening posterior hypothalamic neurons by muscimol infusion into that area [97]. The integrity of preoptic areas in the anterior hypothalamus seemed then not a necessary condition for sleep onset, as sleep could be restored by inhibition of posterior hypothalamic activating neurons.

Nonetheless, these experiments with insomnia produced by excitotoxic lesions of preoptic perikarya raised again the possibility that this region plays a hypnogenic role. However, recordings of basal forebrain neurons showed that more than 70% were waking-active or state-indifferent and that only a relatively small proportion exhibit higher discharge rates during EEG-synchronized sleep than in waking or REM sleep [98]. Other studies

[93] Wada and Terao (1970).

[94] McGinty and Serman (1968).

[95] Sallanon *et al.* (1989).

[96] Gritti *et al.* (1994).

[97] Lin *et al.* (1988, 1989).

[98] Szymusiak and McGinty (1986).

have demonstrated even a more clear-cut relationship exists between the increased firing rates of basal forebrain neurons and EEG-activated behavioral states [71, 99]. Adenosine, the most likely hypnogenic factor, inhibits basal forebrain neurons [100], similarly to the action exerted on mesopontine cholinergic neurons [101]; see details on adenosine in Chapters 6 and 13.

More recent studies tested the hypothesis of a hypnogenic role played by ventrolateral preoptic neurons through their GABAergic projection to the posterior hypothalamus. Immunohistochemical studies identified the *fos* protein accumulated in a group of preoptic neurons that were activated during the state of slow-wave sleep [102] and unit recordings from the ventrolateral preoptic area confirmed that a minority of neurons in that region discharged at higher rates during slow-wave sleep than during wakefulness, a pattern that was reciprocally related with that of posterior hypothalamic (putative histaminergic) neurons [103].

The active theory of sleep was also tested with the method of 2-deoxyglucose autoradiography, which was used to investigate more than a dozen brain structures postulated as “hypnogenic,” including the preoptic area of the basal forebrain. No region was found to increase the metabolic rate during quiet sleep [104]. It is notable that, with the same method, a significant increase in metabolic activity was found in the intralaminar thalamic nuclei after stimulation of the midbrain reticular formation [105]. However, the 2-deoxyglucose autoradiography method may not detect small groups of neurons, dispersed within the preoptic region.

We conclude that the idea of an active hypnogenic focus still awaits consistent data at the cellular level. The neurons hypothetically endowed with such sleep-promoting functions should be recorded and physiologically identified as projecting toward, and exerting inhibitory actions upon, the most likely candidates of activation processes, such as the brainstem cholinergic and noradrenergic neurons and posterior hypothalamus histaminergic neurons. While the concept of a hypnogenic focus in the basal forebrain may be disputable in the light of the evidence discussed above, it is our opinion that *it is in the ventrolateral part of the preoptic area, or more generally in the basal forebrain, that actively hypnogenic neurons should be searched*. The reasons are that basal forebrain neurons projecting to the brainstem core and posterior hypothalamus [96, 106] are cholinergic [107] and GABAergic [108] and that the presumed inhibition of waking-active brainstem neurons would be ascribable not only to GABA but also to ACh that exerts hyperpolarizing actions upon brainstem peribrachial [109] and pedunculopontine cholinergic [110]

[99] Detári *et al.* (1987).

[100] Portas *et al.* (1997).

[101] Rainnie *et al.* (1994).

[102] Sherin *et al.* (1996).

[103] Szymusiak *et al.* (2001).

[104] Kennedy (1983).

[105] Gonzalez-Lima and Scheich (1985).

[106] Swanson *et al.* (1987).

[107] Mesulam *et al.* (1983, 1984).

[108] Nagai *et al.* (1983); Brashear *et al.* (1986).

[109] Egan and North (1986a).

[110] Leonard and Llinás (1990).

neurons. The latter elements are known to project widely to the thalamus and to exert activating influences at that level (see Chapters 4 and 9).

Finally we note that passive and active theories of sleep need not be mutually exclusive, but may be regarded as complementary mechanisms. Thus, the high-frequency spike-bursts of thalamic and cortical neurons that result from deafferentation during drowsiness may be effective in triggering structures hypothesized to have active hypnogenic properties. Indeed, the production of high-frequency bursts in thalamocortical neurons can be partly ascribed to disfacilitation processes in brainstem–thalamic excitatory pathways, as indicated by a period of neuronal silence preceding the appearance of spike bursts [111]. At sleep onset, a period of neuronal silence lasting about 0.5–1 s reliably precedes the spike bursts of antidromically identified corticospinal and corticobrainstem neurons, associated with rhythmic focal oscillations within the spindle frequency (Fig. 1.7). The spike bursts in the axons of pyramidal tract or other types of corticofugal neurons are coincident, during sleep induction by vagoaortic stimulation, with phasically increased neuronal activity in the area surrounding the nucleus of the solitary tract [112], one of the structures postulated to cause active induction of EEG synchronization

[111] Steriade *et al.*
(1971); Steriade (1978).

[112] Puizillout and
Ternaux (1974).

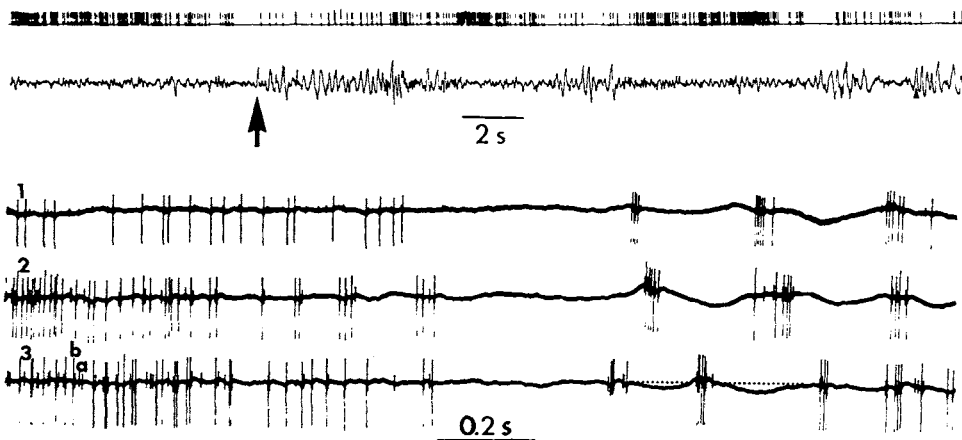


Figure 1.7. Changes in neuronal firing of corticofugal neurons with transition from waking (W) to sleep (S) in behaving cats. The top part (ink-written record) depicts a cortical neuron from parietal association area 5, antidromically identified from the lateral posterior thalamic nucleus. Note diminished firing rate of the neuron (first trace) prior and during a focal spindle sequence recorded by the same microelectrode (second trace; arrow marks the onset of the first focal spindles). The bottom part depicts the original spikes of two neurons (a and b in 3) recorded from cortical area 5; both were antidromically identified from the thalamic centromedian nucleus. Traces 1-to-3 represent three W-to-S transitions during three successive wake-sleep cycles; increased amplitudes of both a and b discharges from periods 1 to 3, separated by about 70 min. Note that the appearance of focal spindles (dotted line in 3 tentatively indicates the baseline) is preceded by silent firing, thereafter followed by rhythmic burst discharges. Modified from Steriade (1978).

and sleep. Similar sequences may exist in other connected brain structures that initially undergo passive deafferentation effects, display postinhibitory rebound excitation, and eventually trigger active hypnogenic areas.

1.4. “Centers” and Distributed Systems

The whole path of research on behavioral states is paved with laudable attempts to find centers for waking and sleep. Centers may be defined in a number of different ways, and anatomical, physiological, and pharmacological criteria may be used, or some combination of these. We begin by suggesting a narrow definition of a center using each of these criteria. Using this concept, it will be seen that no sleep or wake state *in toto* can be said to have a center and even that few, if any, components of waking-sleep states have a “center.”

Functionally, a neural center may be thought of as subserving one function and not any other. A behavioral state center would imply a group of neurons, homogenous in their input-output organization and chemical code(s), and having the required pathways to project the generated activity to the final effectors of the events involved in that state. Furthermore, additional criteria in our restrictive definition are: (1) stimulation of perikarya in the center induces increased incidence of a given behavioral state or, at least, some of the crucial electrographic correlates of that state; (2) destruction of the center is necessarily followed by suppression of the implicated state; (3) the center, when deafferented from its major inputs, should continue to generate the state or to exhibit some of the defining electrographic signs of the state; and (4) neurons recorded in the center must display changes in activity in advance of the overt electrographic and behavioral aspects of the given state of vigilance. As we shall see, such rigid criteria are difficult for sleep-wake states to fulfill. They even have difficulty meeting a weaker definition of a center that uses the functional-anatomical criterion that a “center is an anatomically defined and localized set of neurons serving one function and no other.”

To begin with, homogenous cell-groups are difficult to find in the mammalian brain. A few happy examples are the thalamic reticular nucleus that consists of a single type of GABAergic cells or the locus coeruleus of rat that is a homogenous collection of noradrenergic neurons; however, the same does not apply to cat, a species in which locus coeruleus contains a certain proportion of cholinergic cells. On the other hand, the heterogeneity of the so-called giant

[113] Steriade (1981).

[114] Mitani *et al.* (1988b).

[115] Jones (2000).

field of the pontine reticular formation, a structure that has strongly been implicated in the genesis of REM sleep, is manifold. Conventional staining showed that pontine giant cells are intermingled with even more numerous medium-size and small neurons [113]; and intracellular staining with horseradish peroxidase have revealed the existence of at least two cell populations with descending projections [114], not to mention pontine reticular neurons with ascending projections that, as yet, have not been morphologically identified (see details in Chapter 3). As to the transmitter agent(s) used by pontine reticular neurons, they have not yet been completely defined, although many large-size brainstem reticular neurons are thought to be glutamatergic [115]. Other brain structures implicated in tonic and/or phasic events of EEG-desynchronized states were initially considered as purely cholinergic centers. However, it is now known, for example, that the pedunculopontine tegmental nucleus also contains catecholaminergic neurons and that nucleus basalis has a significant proportion of GABAergic neurons (see Chapter 4).

It is then difficult to conceive that such “centers” would exert functions that are sometimes depicted simply as pluses or minuses in models’ diagrams, when the different transmitters of their neurons may exert various (even opposite) effects. The situation is made more complicated by the fact that two or more transmitters are colocalized in the same brainstem neuron [116]. The nature of this coexistence (synergism or competition) is not generally understood at the present time [117].

[116] Vincent *et al.* (1986);

Lavoie and Parent (1994).

[117] Hökfelt (1987).

Until now, very few cerebral structures have been found that fulfill the above criteria defining a center, and this is true for any function or state, not only states of vigilance. In a much looser sense, the pons may be thought to be the center of REM sleep since the prepontine cat displays major aspects of this state, whereas the animal with a caudopontine transection does not (see Section 1.1). In addition, studies employing all (stimulation, lesioning, and cellular recording) techniques have consistently revealed that the major events of REM sleep originate within or close to this brainstem sector (see Chapters 11–12). But the heterogeneity of the pontine tegmentum defies the notion of a center in a restrictive sense. It is, in fact, this heterogeneity, with interacting cellular groups having different input–output organizations and using different transmitters, which probably underlies the genesis of REM sleep. The interaction of heterogeneous elements must be understood by an intensive analysis at the cellular level, taking into account the connectivity, the intrinsic neuronal properties, and the neurotransmitters, an approach we seek to further in this book.

It is similarly difficult to establish a “center” for EEG activation since, as yet, all lesions in many structures have failed to abolish it for a long time during waking and, even more problematically, during REM sleep.

Confronted with the difficulties in fulfilling the rigid criteria of centers for states of vigilance or their peculiar physiological correlates, some investigators have begun to use the notion of distributed systems. This has the danger that the flexibility of this notion means a retreat into vagueness so that hypotheses concerning the role of multiple interrelated structures in the genesis of a given behavioral state cannot be proved wrong.

The GABAergic thalamic reticular nucleus does appear to meet the above-mentioned criteria of stimulation, lesion, isolation, and cellular recording, for a pacemaker of spindle oscillations, a defining electrographic feature of sleep onset. Indeed, spindles are abolished in thalamocortical systems after disconnection from reticular nucleus, the deafferented reticular neurons continue to oscillate *in vivo* within spindle frequencies, intracellular recordings *in vivo* demonstrate inverse images in GABAergic reticular cells and their inhibited targets (the thalamocortical neurons), and stimulation of reticular nucleus (with the same frequencies as those of reticular spike barrages during sleep spindles) induces oscillations within spindle frequencies in thalamocortical neurons *in vitro* (see details in Chapter 7). Still, the widespread synchronization of sleep spindles requires the intactness of the cerebral cortex [118] and the transfer of spindles to cortex require interactions between reticular and thalamocortical cells [119]. This indicates that even such homogeneous structures, like the thalamic reticular nucleus, displaying pacemaker properties for the generation of an electrographic correlate of sleep, needs extensive relations with other structures for the generation of a given function. Further light on the complex pacemaking properties of reticular thalamic neurons, intrathalamic spread of spindle oscillations, and brainstem–thalamic mechanisms of spindle disruption, will obviously be possible by using the isolated whole-brain preparation in which spindle sequences have been recorded [120], resembling very much those observed in the intact animal. Similarly, the knowledge of REM sleep mechanisms will be greatly advanced by using the technique of the *in vitro* perfused brainstem, whose viability was assessed by comparing the electrophysiological properties of inferior olive and pontine neurons, among others, to those observed *in vivo* [121].

These new techniques provide the possibility of studying both the intrinsic properties of neurons (that are commonly investigated in brain slices) and the interactions between the cell and the entire sets of neuronal circuits

[118] Contreras *et al.* (1996a, 1997a).

[119] Steriade *et al.* (1993d).

[120] Serafin and Mühlethaler (1988).

[121] Llinás and Mühlethaler (1988).

that are preserved in the isolated whole-brain or brainstem preparation. One can predict that the next decade will see a true renaissance of brain studies based on the combination of the isolated whole-brain, in parallel with *in vivo* investigations. Indeed, while the properties of neuronal networks are engraved to a minor extent in the intrinsic properties of their constituent single neurons, the full understanding of network characteristics depends on the knowledge of driving forces and connections between the elements of neuronal ensembles, so that different networks would generate dissimilar functional states despite the fact that their individual components have similar or identical intrinsic properties [122].

[122] Steriade and Llinás (1988); Steriade (2001a, b).

Finally, an important consideration for behavioral state control is that brain-activated states, such as REM sleep, may result from modulation of excitability in sets of neurons subserving its many component functions, such as the phenomena of saccades, muscle atonia, EEG activation, and PGO waves, which define this state [123]. Thus, behavioral state physiology may, to a large part, rest on increased knowledge of the effect of changing excitatory and inhibitory bias on defined neuronal networks, a physiology readily amenable to, and even demanding, quantitative modeling.

[123] McCarley and Ito (1985).

Methodology of Morphological and Physiological Substrates Underlying States of Vigilance

2.1. Morphological Tools

2.1.1. Nissl and Golgi Staining, and Some Recent Developments

Until the 1970s, the Nissl, Golgi, and degeneration techniques were the most important tools for the knowledge of brainstem morphology and hodology.

The differentiation of the brainstem reticular core into nuclei was based on Nissl-stained sections in human, cat and rat [1]. The classical study by Olszewski and Baxter [1] was the most important of the early signs reflecting the interest aroused among the anatomists by the discovery of Moruzzi and Magoun [2]. Olszewski and Baxter believed in a difference in functional organization of different areas in the brainstem reticular core that justified the delineation and classification of such regions as nuclei. They considered, however, that the anatomical designation of reticular formation might be abandoned altogether (possibly because of the “reticularistic” flavor of the term, implying continuity between neurons) and, instead, proposed the use of the term “nuclei of unknown connections” for the newly described regions belonging to the reticular formation. In those early times and even more recently, many physiologists felt that there was no need for so many reticular nuclei, differentiated on the basis of cytological differences. Ironically, when Nissl and Golgi techniques were more recently used to define the neuronal morphology in regions where retrograde labeling was observed after horseradish peroxidase (HRP) injections into the spinal cord, at least 13 brainstem nuclei were

- [1] Olszewski and Baxter (1954); Brodal (1957); Taber (1961); Berman (1968); Petrovicky (1980).
- [2] Moruzzi and Magoun (1949).

found just in the pons and mesencephalon and these were limited to cell-groups giving rise to reticulospinal projections [3].

At variance with the tendency toward analytic dissection of brainstem nuclei by means of Nissl staining, Golgi studies emphasized the uniform morphology of reticular neurons and suggested a cellular archetype based on dendroarchitectonics. The brainstem reticular neuron was defined by its radiate, relatively long and rectilinear dendrites that transcend the limits of the nucleus in which the soma lies and that overlap with dendrites of other reticular cells [4]. The term *isodendritic* was introduced for its topognostic value, the dendritic configuration allowing not only the identification of Golgi-stained cells as belonging to the brainstem reticular formation, but also permitting the recognition of similar neurons in distant (thalamic, subthalamic, and hypothalamic) territories that are connectionally and functionally related to the brainstem core (Fig. 2.1). Obviously, the considerable degree of dendritic overlap in the brainstem core suggests that reticular neurons are not likely to receive specialized inputs and that they offer a substrate for integration of afferents from heterogeneous sources.

The typical radiating dendritic pattern of brainstem reticular cells was first seen in newborn animals. In some brainstem nuclei of the medullary reticular formation, this pattern is rearranged during maturation, eventually

[3] Newman (1985a,b).

[4] Scheibel and Scheibel (1958); Leontovich and Zhukova (1963); Ramón-Moliner and Nauta (1966).

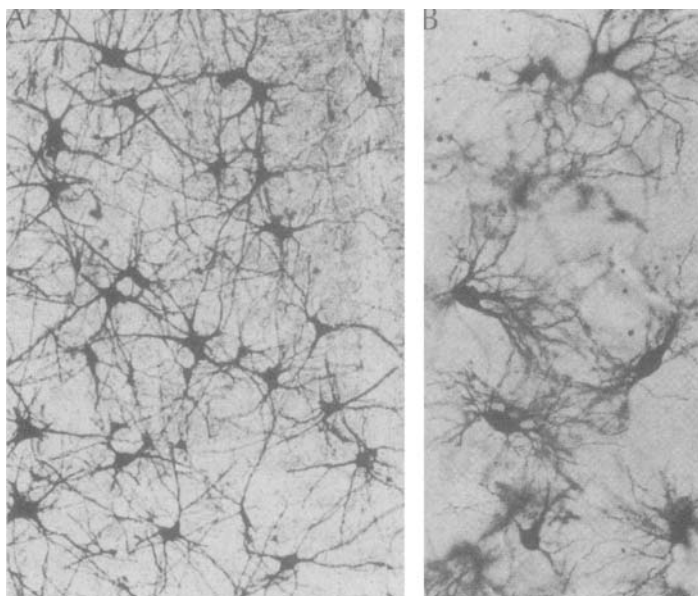


Figure 2.1. Different dendritic patterns of brainstem reticular neurons and thalamic relay neurons in Golgi impregnations. A, gigantocellular field of pontine reticular formation in kitten, $\times 180$. B, lateral geniculate thalamic nucleus in kitten, $\times 240$. Courtesy of Dr. E. Ramón-Moliner.

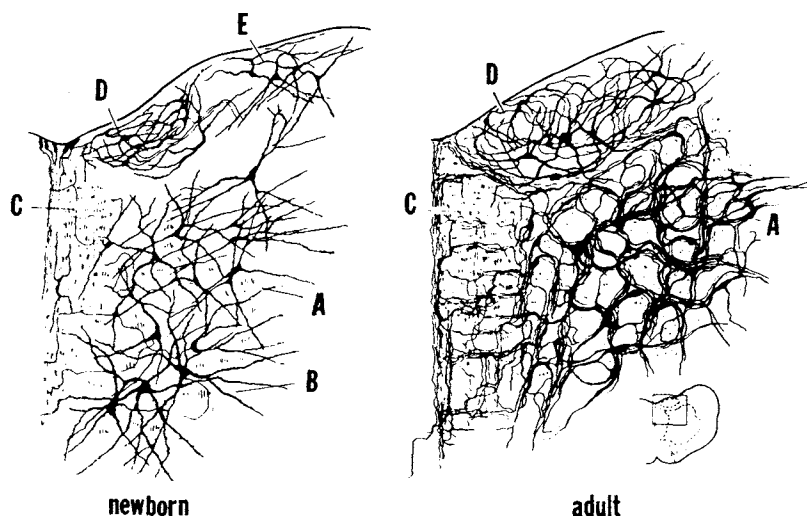


Figure 2.2. Cross-sections through the dorsal half of the lower medulla oblongata in newborn and adult cats to show the difference in dendrite patterns of reticular neurons. Neurons of the rostral part of the nucleus reticularis parvocellularis (A) and of the nucleus reticularis magnocellularis (B) show familiar radiating dendrites bearing many excrescences in the newborn. In the adult, the dendrites have been “resculpted” to form characteristic bundles that surround the rostrocaudal running fascicles of myelinated fibers. Other abbreviations include: C, medial longitudinal fasciculus; D, nucleus prepositus hypoglossi; E, medial vestibular nucleus. Drawn at $\times 103$ from cat brainstem material stained by variants of the rapid Golgi method. From Scheibel and Scheibel (1975).

[5] Scheibel and Scheibel (1975).

[6] Melker and Purpura (1972); Hammer *et al.* (1981).

forming complexes of dendritic bundles that surround running fascicles of myelinated fibers [5] (Fig. 2.2). While the protospines of dendrites increase in number during the course of early development and peak near 11 days of age, later on they decline and eventually many are resorbed onto the dendritic surface [6].

In the Scheibels’ 1958 study [4], the Golgi method also helped to rule out the earlier hypothesis that the brainstem reticular core essentially consists of chains of short-axoned cells. Their stainings revealed, on the contrary, that “no short-axoned Golgi type II cells exist in the brainstem core” (p. 37) and that “bulbar magnocellular elements usually emit axons which course dorsomedially toward the region of the MLF (medial longitudinal bundle) ... , and bifurcate into caudad- and rostrad-running fibers which may reach the spinal cord and the mesencephalon or diencephalon, respectively” (p. 38–39). As yet, there are no systematic data from studies with more powerful tools (such as intracellular HRP staining) indicating the presence of short-axoned neurons in the brainstem core. As to the second statement, concerning the long conductors branching both rostrally and caudally, this feature may characterize the brainstem reticular projections in the newborn (up to 7–10 days old) animals from which Scheibels’ material

derived, but it is certainly not valid in adult animals in which neurons with ascending or descending projections are rather segregated (see Chapter 3). Nonetheless, Scheibels' studies were the first to emphasize the projections of single brainstem reticular neurons to distant sites and, thus, to provide data on the substratum of brainstem core control upon spinal cord and diencephalic operations.

The capriciousness of Golgi method and the lack of quantitative data in earlier studies were compensated by attempts at determining the real shape and the actual dimension of the neuronal soma and dendrites of Golgi-stained elements by photogrammetric representations using different stages of illumination in serial sections [7] and by tridimensional reconstruction using computer analyses [8]. Such studies have been performed on various cellular types in the cerebellum, hippocampus, and neocortex, but detailed analyses of the brainstem core have not so far been undertaken.

That Golgi technique can be combined with many other, more recent methods, including electron-microscopy (EM), retrograde transport of HRP, and immunocytochemistry, was demonstrated in a series of elegant studies by Somogyi and his colleagues, performed on visual cortex and striatonigral neurons [9]. A neuronal circuit was identified by Golgi staining and anterograde degeneration under EM analysis, as involving three successive links: from geniculostriate degenerated axons to two Golgi-stained cortical targets in layer IV (a small pyramidal cell and a spiny stellate); in turn, some of the axonal arborizations of these two types of Golgi-stained neurons were found to establish asymmetrical contacts on large nonspiny stellate cells [9]. There are limitations of the above method of tracing neuronal chains since the Golgi technique does not usually stain myelinated axons and little information is obtained about the local-circuit or long-axon character of the third neuron in the circuit. This led to staining, with the Golgi method, of neurons that had been retrogradely labeled by HRP transport; then EM was used to identify the type of synapses on the efferent neuron. Thus, Golgi-staining is used to identify the soma shape and dendritic patterns of a neuron (say X) whose projections were identified by means of retrograde HRP transport from a distant site, and the input to cell X is studied by EM-identified synapses of degenerating boutons after a lesion in a given structure [10]. The immunohistochemical localization of glutamate decarboxylase (GAD) in neurons that have also been processed with the Golgi procedures and the EM identification of synaptic contacts made by GAD-positive boutons on Golgi-impregnated neurons have also been used. It has demonstrated that

[7] Mannen (1975).

[8] Glaser and van der Loos (1965); Llinás and Hillman (1975); Cowan *et al.* (1975).

[9] Somogyi (1978); Somogyi *et al.* (1983).

[10] Somogyi *et al.* (1979).

[11] Kisvárdy *et al.*
(1993).

GABAergic short-axoned cortical neurons receive powerful excitatory inputs and that some of them are contacted by other GABAergic neurons, a presumed basis for disinhibition in target pyramidal cells [9, 11]. These methods of tracing neuronal networks should now be applied to brainstem circuits between cholinergic and monoaminergic neurons with identified (ascending and descending) projections, which have been hypothesized to play a role in the genesis of behavioral states of vigilance and in the regulation of state-dependent neuronal activities in the cerebral cortex, thalamus, and spinal cord.

[12] Kelly and Van Essen
(1974).

During the past two decades, the more powerful tool of intracellular or intraaxonal staining technique was added to the Golgi method for the characterization of soma shape, dendritic domains, and axonal collateralization. In addition to details gained for the knowledge of cellular morphology, this method allows the knowledge of neuronal structure in physiologically identified elements. First employed in the visual cortex of cat, using the fluorescent dye Procion yellow as the marker [12], the method was greatly developed with the use of intracellular HRP, Neurobiotin and Biocytin injections in a great variety of central structures, from the cerebral cortex to the spinal cord [13]. Within the brainstem, the intracellular HRP staining helped to demonstrate autapses, that is, a synapse between a neuron and a collateral of its own axon [14], in thalamically projecting neurons in substantia nigra pars reticulata [15], the soma-dendritic (SD) profile and axonal trajectory and branching of tectobulbosplinal neurons [16], and the soma size, orientation of dendrites and axonal collateralization in two distinct classes of pontine and bulbar reticulospinal neurons [17]. In the cerebral cortex, intracellular staining showed the presence of many more dendritic spines in small-sized pyramidal neurons than in large-sized ones [18], which may be a basis for the higher discharge rates, with tonic firing, in monkey's slow-conducting corticothalamic and corticospinal pyramidal neurons during natural state of wakefulness, compared to fast-conducting pyramidal neurons [19].

[13] After electrophysiological characterization of the neuron through a glass micropipette filled with different staining substances, the marker is injected by using direct current for several minutes, while continuously monitoring cell's responses to assure that the pipette remained intracellular.

[14] Van der Loos and Glaser (1972).

[15] Karabelas and Purpura (1980).

[16] Grantyn and Grantyn (1982).

[17] Mitani *et al.*
(1988b,c).

[18] Deschênes *et al.*
(1979).

[19] Steriade *et al.*
(1974a,b).

[20] Lasek *et al.* (1968);
Cowan *et al.* (1972).

[21] Rogers (1979).

2.1.2. Anterograde and Retrograde Tracing Techniques

The autoradiographic tracing technique, introduced around 1970 [20], is based on the anterograde axonal transport of macromolecules that have incorporated radiolabeled amino acids injected in the vicinity of projection neurons. The radioactive label is transported up to the axonal terminals (see technical procedures in [21]).

This method was amply used to reveal descending and ascending projections of brainstem reticular neurons. The anterograde transport technique is still the only tracing technique that unequivocally avoids the fiber-of-passage problem. Thus, the exact termination in the spinal gray matter of axons originating in various nuclei of the brainstem (including direct projections to the motoneuronal cell-groups) was determined by means of radioactive amino-acids tracers that avoided the possible uptake of the retrograde HRP tracer by damaged axonal terminals (see below) and that proved to be much more sensitive than the anterograde degeneration technique [22].

However, when the ascending brainstem reticular projections were studied, the anterograde autoradiographic technique proved to be less powerful than the retrograde transport techniques. Indeed, autoradiographic experiments revealed that midbrain and pontine reticular neurons project to medial, intralaminar, and reticular thalamic nuclei, but major sensory and motor relay thalamic nuclear groups remained unlabeled, such as the medial and lateral geniculate, ventrobasal and ventrolateral nuclei [23]. Since clear signs of facilitated synaptic transmission were seen in these relay thalamic nuclei following stimulation of the upper brainstem reticular formation, the pathways underlying the potentiating effect remained to be elucidated. The disclosure of brainstem reticular projections to virtually all relay and associational thalamic nuclei was made possible by using injections of retrograde tracers strictly confined within the limits of those thalamic nuclei (see Chapter 3).

Since 1984, the *Phaseolus vulgaris* leucoagglutinin (PHA-L) has been employed as an anterograde axonal tracer to reveal the axonal trajectory and terminals, and has sometimes been combined with the EM analysis of synaptic profiles [24]. The PHA-L method was used to trace efferent projections from the upper brainstem cholinergic nuclei [25] and it can be combined with immunohistochemical labels on the same brain section [26].

The retrograde tracers consist of the enzyme HRP, a series of fluorescent dyes, and labeled transmitter-related compounds. These three categories of retrograde markers are briefly presented below.

The demonstration of the retrograde transport from the intramuscularly injected HRP to spinal cord motoneurons [27] and the retrograde transport in the centrifugal control pathway from the isthmooptic nucleus to the chick's retina [28] was shown during the 1970s. Since then, the sensitivity of this method has been greatly improved with the introduction of tetramethylbenzidine (TMB) as the chromogen; this proved to be superior to all other

[22] Holstege and Kuypers (1988).

[23] Edwards and DeOlmos (1976); Graybiel (1977); Robertson and Feiner (1982); Jones and Yang (1985).

[24] Gerfen and Sawchenko (1984); Wouterlood and Groenewegen (1984).

[25] Satoh and Fibiger (1986); Mitani *et al.* (1988d).

[26] Woolf *et al.* (1986).

[27] Kristensson and Olsson (1971).

[28] LaVail and LaVail (1972).

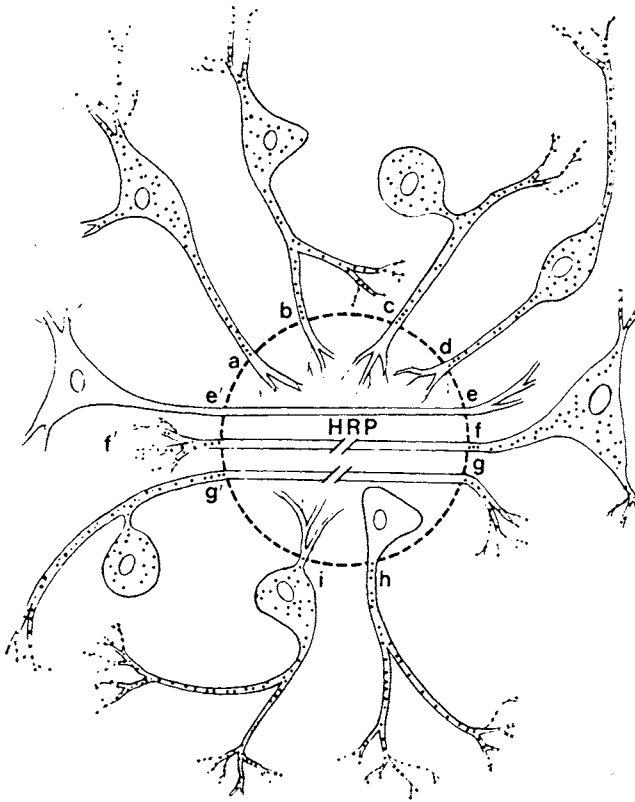


Figure 2.3. Types of horseradish peroxidase (HRP) transport. The broken line contains the injection site. a: uptake into intact terminals results in retrograde transport to the perikaryon and dendrites. b: the same type of uptake also results in labeling of axonal collaterals. c: uptake into intact peripheral sensory terminals results in labeling of the ganglion cell as well as in transganglionic labeling of central sensory terminals. d: a similar complex transport occurs along bipolar neurons. e and e': there is virtually no uptake or transport by intact axons passing through the injection site. f and f': there is entry of HRP into severed axons; entry into the proximal stump results in retrograde labeling; the labeling is granular and occurs within membrane-delimited organelles if the perikaryon is at a distance from the point of injury or if the survival time is sufficiently long; labeling of the distal axonal stump is mostly by cytoplasmic diffusion. g and g': entry into an injured peripheral sensory axon results in retrograde, anterograde, and transganglionic labeling; the resulting transganglionic labeling almost always occurs as a consequence of active vesicular transport. h: uptake into an intact perikaryon results in anterograde transport into terminal fields. i: uptake into intact dendrites may result in labeling of the perikaryon and its axonal branches. From Mesulam (1982).

[29] Mesulam (1978);
Mesulam and Rosene
(1979).

[30] Mesulam (1982).

methods in tracing projections at the light-microscopic level [29]. The conjugation of HRP with the lectine wheat-germ-agglutinin (WGA) has the advantage of a much more potent tracing for neuronal connections, especially when minute amounts of tracer have to be injected [30].

The problems involved in studies with HRP injections mainly concern the uptake by passing fibers and the precise delineation of the injected territory. While there is virtually no uptake or transport by intact axons coursing through the injection site, there is entry of HRP into

severed axons (axons e and f, respectively, in Fig. 2.3). The absence of uptake by intact axons was documented in a study that showed lack of retrogradely labeled cells in habenular nuclei, in spite of the fact that the HRP injection into the center median-parafascicular thalamic complex also covered the passing retroflex bundle [31]. A precaution to avoid HRP entry into severed axons is a delayed injection through a previously implanted cannula, allowing about 24–36 hr for axonal cicatrization or degeneration, to preclude the HRP transport. As to the site of the HRP injections, its size is greater (and probably overestimated) when using the TMB procedure, as compared to the diaminobenzidine (DAB) procedure. It is generally believed that only the center of the injection corresponds to the region of effective uptake.

[31] Steriade *et al.* (1988).

One of the most difficult assessments as to the critical localization of HRP injections concerns the various thalamic nuclear groups (Fig. 2.4, A–B), quite closely located on the thalamic map, each of them being interposed within distinct sensory and motor modalities or systems with general regulatory functions. In those cases, in addition to the histological examination of HRP injection sites on counterstained sections to facilitate the recognition of nuclear boundaries, the evidence that the injection was strictly localized within a given nucleus comes from the differential patterns of retrograde and anterograde labeling

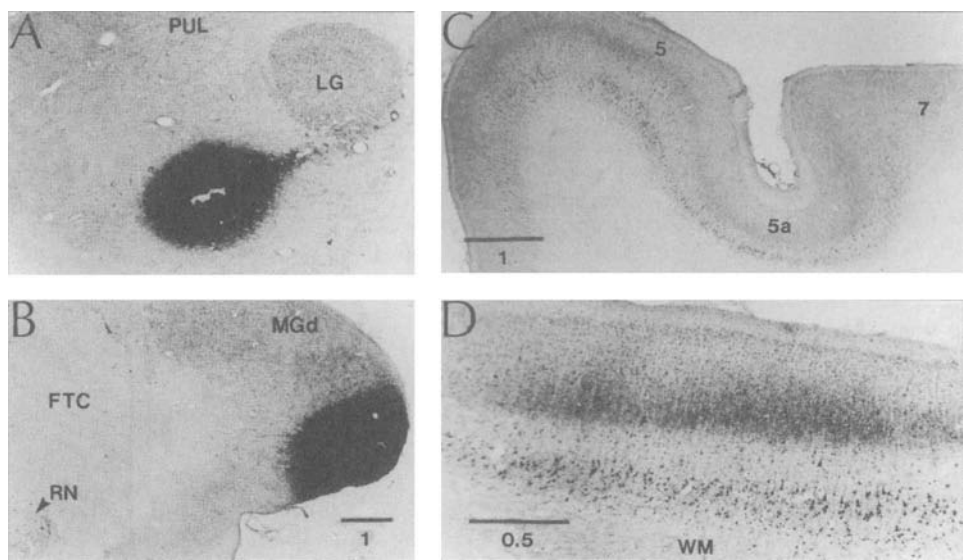


Figure 2.4. Localization of WGA–HRP injections in various thalamic relay nuclei of cat. A and B, oblique injections in the ventroposterior and medial geniculate nuclei, respectively. C and D, anterograde and retrograde labeling in suprasylvian gyrus (C) and coronal gyrus (D) after WGA–HRP injections in the thalamic lateral posterior and ventroposterior nuclei, respectively. Horizontal bars indicate mm. Modified from Steriade *et al.* (1988).

in various cortical areas, known to have reciprocal connections with the injected thalamic nucleus (Fig. 2.4, C–D). Thus, for example, after an injection in anterior nuclei, massive retrograde cell labeling occurs in the retrosplenial gyrus, but not in the pericruciate cortex, indicating that the injection did not encroach upon the adjacent centrolateral and ventromedial thalamic nuclei. The localization of HRP injections within the limits of various sensory thalamic nuclei was necessary because very great percentages (70–90%) of retrogradely labeled brainstem reticular cholinergic neurons were uniformly distributed in a circumscribed region at the midbrain–pontine junction, regardless of the thalamic location of HRP injection [31].

In addition to the retrograde tracing, HRP is comparable to the amino-acid autoradiographic technique for anterograde tracing [32]. The validity of HRP histochemistry for both retrograde and anterograde tracing is especially fruitful for the disclosure of reciprocal connections between two structures. For example, when WGA–HRP is injected in a thalamic relay or association nucleus, retrograde labeling is found in neurons of cortical layer VI, while the fine-grained extraperikaryal product reflecting the anterograde HRP transport is mainly seen in middle layers IV and supervening part of layer III (see above, Fig. 2.4, C–D). The anterograde transport of HRP was also used to reveal a superficial diffuse cortical projection of the cat ventromedial thalamic nucleus to the outer third of layer I [33], in line with data obtained by means of autoradiographic experiments in the rat [34]. In some cases, the HRP method proved to be more sensitive than the autoradiographic one. With injections of ^3H -proline into the intralaminar centrolateral nucleus, anterograde labeling was found in layers V and VI of visual cortical areas 17 and 18 in the cat, whereas the use of the anterograde transport of WGA–HRP led, in addition, to a distinct band of terminal labeling in layer I as well as, occasionally, the labeling of a thalamocortical axon traversing the cortical layers vertically [35].

The fluorescent dyes were introduced by Kuypers and his colleagues [36] and are especially suited for the demonstration of axonal collateralization to different structures by means of multiple-labeling methods. The most employed compounds are Fast Blue and Nuclear Yellow that are useful for retrograde transport in long pathways. This method was applied to test the hypothesis of ascending and descending projections of the same brainstem reticular neuron. One fluorescent dye was injected in the spinal cord and another dye in the cerebellum or in the diencephalon; the results showed that very few reticulospinal cells of the pontine gigantocellular field also provide collaterals to the cerebellum or to the

[32] Mesulam and Mufson (1980).

[33] Glenn *et al.* (1982).

[34] Herkenham (1979).

[35] Cunningham and LeVay (1986).

[36] Kuypers *et al.* (1980); Van der Kooy *et al.* (1978).

diencephalon [37]. The same method was recently used to demonstrate that a significant number of monkey's basal forebrain neurons send axon collaterals to both the thalamic reticular nucleus and the cholinergic peribrachial area in the upper brainstem core, while no basal forebrain neurons were disclosed to send branching axons to the brainstem core and the cerebral cortex [38].

Lastly, retrograde tracing can be obtained by using some transmitters or related molecules that, after having been selectively taken by the axon terminals, migrate toward the perikaryon where they are accumulated. By contrast with HRP or other retrograde tracers that label nonselectively all neurons with terminals within the injected area, only neurons with an affinity uptake mechanism for a given transmitter or precursor will be retrogradely labeled after the injection of the tritiated transmitter marker into the projection area. The first experiments with this method have been performed in the 1970s on the pigeon optic tectum [39]. Since then, a series of studies succeeded in demonstrating the retrograde transport of tritiated serotonin (5-HT) in the pathways between the nucleus raphe dorsalis and substantia nigra or caudoputamen [40], glutamate/aspartate in corticothalamic pathway [41], and choline in the pigeon's thalamo-Wulst projection [42] and in the pathway between the brainstem core and the basal forebrain [43].

[37] Waltzer and Martin (1984).

[38] Parent *et al.* (1988).

[39] Hunt *et al.* (1976).

[40] Streit (1980).

[41] Baughman and Gilbert (1980, 1981); Rustioni *et al.* (1983).

[42] Bagnoli *et al.* (1981).

[43] Jones and Beaudet (1987b).

2.1.3. Immunohistochemical Identification of Various Cell-Groups and their Projections

The history of research on the chemical code of neurons in various groups of the brainstem core began in the 1960s with the use of formaldehyde histofluorescence method [44] and continued with the introduction of the glyoxylic acid fluorescence method [45]. Both these methods were successful in identifying monoamine-containing neurons and their projections. However, the catecholaminergic system was better visualized than the 5-HT-containing system, and, among catecholaminergic systems, the noradrenergic component could not be clearly distinguished from the dopaminergic one.

During the 1980s, immunohistochemical methods were introduced by using antisera raised against synthesizing enzymes of catecholamines [46] and, finally, directly against each of monoamine transmitters: serotonin (5-HT), noradrenaline (NA), and dopamine (DA) [47]. In the past decade or so, chemically identified projections of monoaminergic systems have been studied by combining the retrograde transport of HRP with immunohistochemical

[44] Dahlström and Fuxe (1964).

[45] Lindvall and Björklund (1974); Lindvall *et al.* (1974).

[46] Hökfelt *et al.* (1984).

[47] Steinbusch (1981); Geffard *et al.* (1986); Onteniente *et al.* (1984).

methods using, for example, the synthesizing enzyme of catecholamines, the tyrosine hydroxylase (TH). These data are reported in Chapter 3.

The cholinergic systems could be formally identified during the 1980s with the production of monoclonal antibodies reactive to choline acetyltransferase, the synthetic enzyme of acetylcholine (ACh), a highly specific marker for cholinergic neurons and fibers. The ascending projections of the brainstem reticular formation have long been hypothesized to be cholinergic on the basis of the trajectories of fibers containing AChE [48], the degradative enzyme of ACh. Since the documentation of AChE-stained projections was usually based on diagrams or on coronal sections that preclude a satisfactory evaluation of ascending brainstem pathways, a new perspective was recently provided by employing a three-dimensional photographic characterization of the dorsal tegmental pathway that originates in the midbrain and pontine reticular core [49].

There is a specificity problem related with the use of AChE histochemistry as a marker of cholinergic elements. For example, the ventral tegmental component of the ascending brainstem pathway, originally described as cholinergic, is now known to arise mainly from dopaminergic neurons [50]. Nonetheless, studies in different brain regions emphasize the similarities between the results obtained by means of AChE histochemistry and those employing monoclonal antibodies to ChAT. Thus, studies comparing AChE histochemistry with ChAT immunohistochemistry revealed that intense AChE staining of neurons in some cerebral structures, such as the neostriatum and the basal forebrain, can be reliably used for identifying cholinergic elements [51]. Also, the pattern of AChE-staining in the thalamus [31, 52] (Fig. 2.5) is generally similar to the distribution of ChAT-immunoreactive fibers [53]. Despite these similarities, it is accepted that the correspondence between the two methods is not complete.

The most reliable results concerning the identification of basal forebrain and brainstem cholinergic cell-groups have been obtained with ChAT immunohistochemistry [54]. The various brainstem reticular cholinergic cell-groups and their efferent connections to the thalamus and the basal forebrain have been investigated by combining the retrograde transport of HRP or fluorescent tracers with ChAT immunohistochemistry. The combined ChAT + HRP technique reveals three types of elements: simple HRP-positive cells with small blue HRP granules in both perikarya and dendrites; simple ChAT-positive cells displaying a diffuse light-brown immunostaining throughout the cell body and its processes; and double-labeled neurons containing both retrogradely transported HRP and ChAT (Fig. 2.6). The first

[48] Shute and Lewis (1967a-b).

[49] Wilson (1985).

[50] Butcher *et al.* (1975); Moore and Bloom (1978).

[51] Levey *et al.* (1983b).

[52] Olivier *et al.* (1970); Jones (1985).

[53] Levey *et al.* (1987).

[54] The first description of ChAT immunohistochemistry (Kimura *et al.*, 1981) used an antiserum raised in rabbit against human ChAT. Since then, monoclonal antibodies to ChAT have been introduced (Eckenstein *et al.*, 1981; Levey *et al.*, 1983a) and used to map brain cholinergic neurons in rat (Armstrong *et al.*, 1983), cat (Vincent *et al.*, 1987) and macaque monkey (Mesulam *et al.* 1984).

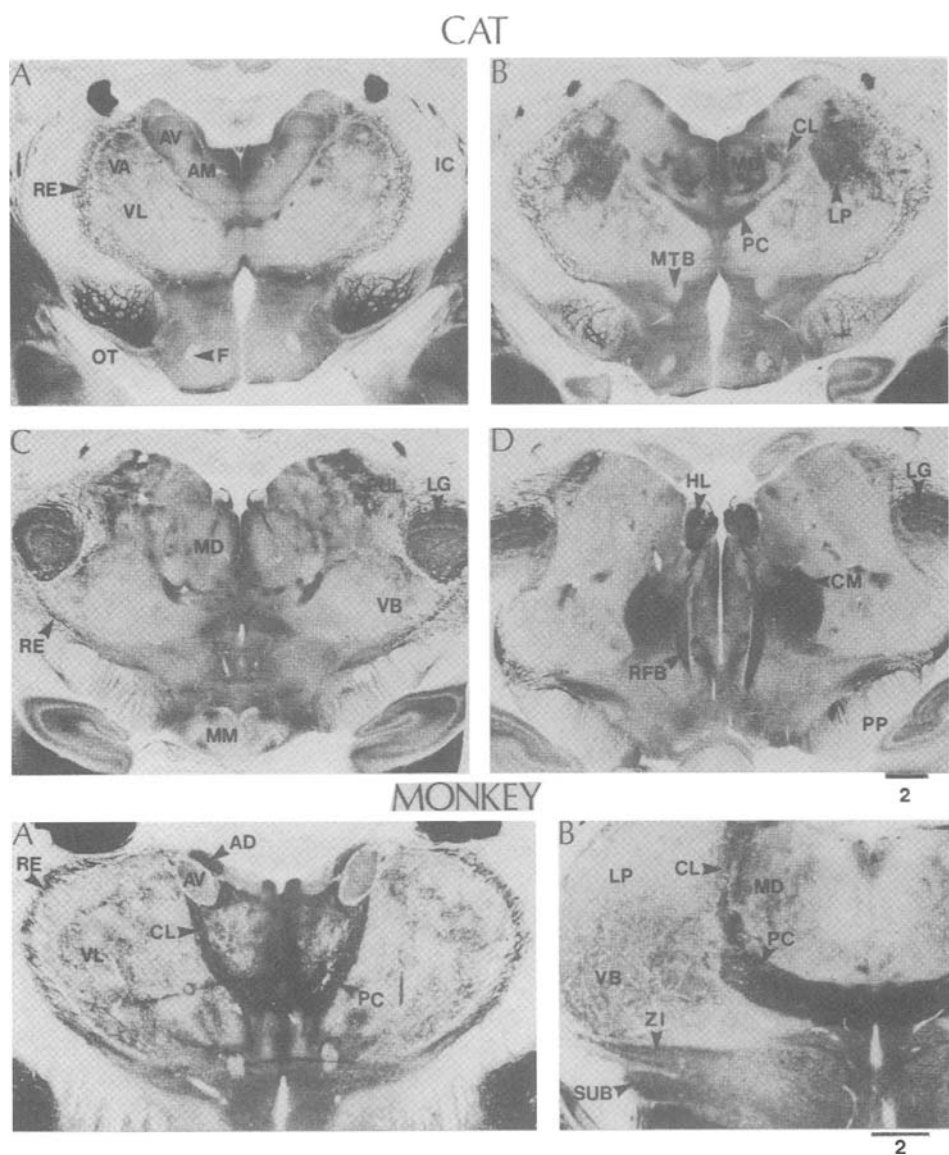


Figure 2.5. Distribution of acetylcholinesterase (AChE) activity in thalamic nuclei in the cat and macaque monkey. Staining according to Gomori's technique. Four levels rostral to caudal (A–D) in cat and two levels (A and B) in monkey. Horizontal bar indicates mm. AD–AM–AV, anterodorsal–anteromedial–anteroventral thalamic nuclei; CL and CM, central lateral and centrum medianum thalamic nuclei; IC, internal capsule; F, fornix; HL, LG, LP, lateral habenula, lateral geniculate, lateral posterior thalamic nuclei; MM, medial mammillary nucleus; MTB, mammillothalamic bundle; OT, optic tract; PC, paracentral thalamic nucleus; PP, pes pedunculi; RE, reticular thalamic nucleus; RFB, retroflex bundle; SUB, subthalamic nucleus; VA, VB, VL, ZI, ventroanterior, ventrobasal, ventrolateral, zona incerta thalamic nuclei. From Steriade *et al.* (1988).

study used large injections of HRP in the thalamus of rat [55]. Two subsequent studies on rat used more localized injections of fluorescent [56] or HRP [57] tracers into various thalamic nuclei. Finally, ChAT immunoreactivity

[55] Sofroniew *et al.* (1985).
[56] Woolf and Butcher (1986).
[57] Hallanger *et al.* (1987).

[58] Paré *et al.* (1988).

[59] Mitani *et al.* (1988d).

[60] Smith *et al.* (1988).

[61] DeLima and Singer
(1987).

combined with WGA–HRP retrograde transport has been used to demonstrate that brainstem cholinergic neurons project to virtually all sensory and motor, associational, intralaminar, and reticular [58] thalamic nuclei of cat, and to major associational thalamic nuclei of macaque monkey [31], as well as to the pontine reticular formation [59]. Two studies have been focused on the visual thalamus of cat, one of them dealing with all (lateral geniculate, lateral posterior, and perigeniculate) sectors [60], the other one providing the first detailed comparative analysis of brainstem cholinergic and monoaminergic projections to the lateral geniculate nucleus [61]. The results of these studies are reported in Chapter 3.

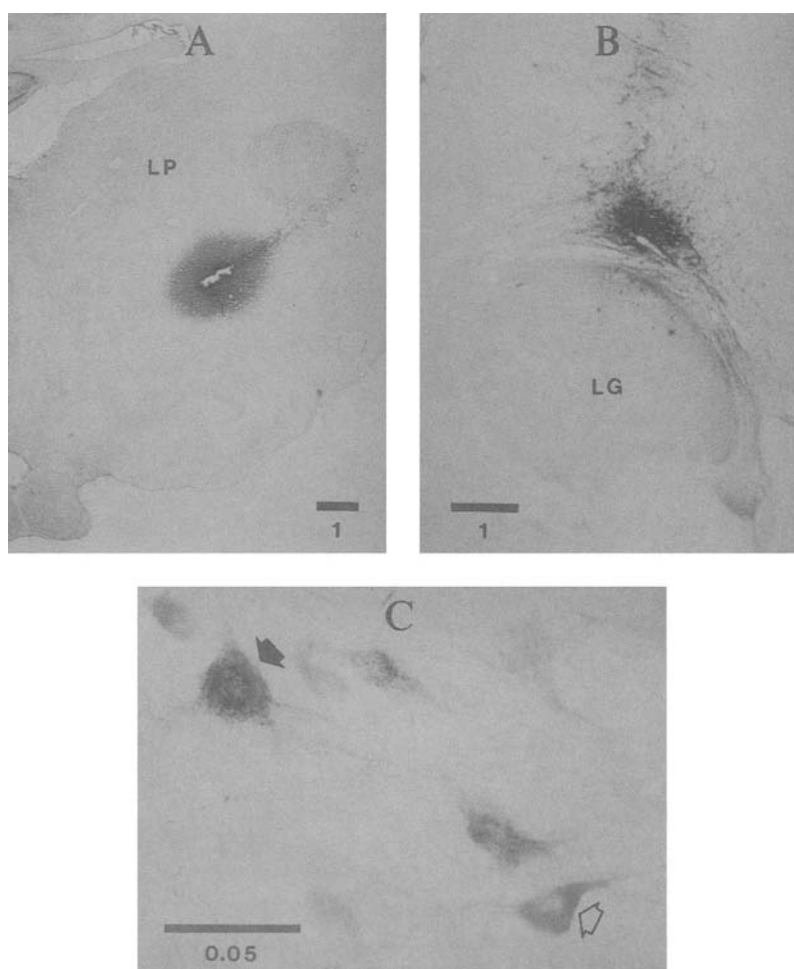


Figure 2.6. Retrograde labeling of cholinergic and noncholinergic neurons in mesopontine nuclei after injections of wheat-germ-agglutinin (WGA)—horseradish peroxidase (HRP) in thalamic nuclei. A, injections of WGA–HRP in thalamic ventroposterior (left) and perigeniculate (reticular) (right) nuclei. B, examples of three types of cells labeled after thalamic injection of WGA–HRP. C, choline-acetyltransferase (ChAT)-positive cell (open arrow); and double-labeled neurons (\rightarrow); horizontal bar, mm. Modified after Steriade *et al.* (1988) and Smith *et al.* (1988). See also color plate 1.

Immunoreactivity for somatostatin, substance P, cholecystikinin, and other peptides was demonstrated in a series of brain structures, from the spinal cord up to the cerebral cortex [62]. The presence of substance P and other peptides was also described in brainstem cholinergic neurons with ascending projections [63]. In the thalamus, the somatostatin-like immunoreactivity was first shown in reticular neurons [64], colocalized with GAD immunoreactivity in the same elements [65]. Immunoreactivity for all above mentioned peptides was recently demonstrated especially in the intralaminar and reticular thalamic nuclei [66]. The combination of staining for cytochrome oxidase and immunostaining for calcium-binding proteins was used to group various thalamic nuclei [67].

Immunohistochemical studies also demonstrated the heterogeneity of brainstem reticular and thalamic nuclei as well as cellular populations in the cerebral cortex. For example, the dorsal raphe nucleus of monkey contains, in addition to 5-HT neurons, cells displaying immunoreactivity for GABA, TH, substance P, and different calcium-binding proteins [68]. Differential distribution of calcium-binding proteins has been found in the human thalamus [69, 70].

2.2. Electrophysiological Methods

As discussed in the previous chapter, EEG patterns reliably distinguish slow-wave sleep from both brain-active states, waking and REM sleep. The global EEG activity is constantly used in animal experiments and human studies to ascertain the level of vigilance. The pioneering descriptions of variation in brain electrical activity when animals passed from a state of vigilance to another, which have been made in the second half of the 19th century by the British physician and physiologist Richard Caton and by a series of Polish and Russian physiologists, as well as Hans Berger's observations, during the 1930s, on alpha and beta waves recorded from the human scalp, have been reviewed elsewhere [71]. The neuronal substrates of the EEG began to be investigated intracellularly in the 1960s [72]. During the past 15 years, the EEG correlates of sleep rhythms during waking and sleep states have been studied by combining single and dual intracellular recordings with multisite extracellular recordings from cortex and thalamus *in vivo*. The ionic conductances and receptors implicated in the synaptic mechanisms of different oscillatory types have been explored *in vitro*. The results of these recent studies are dealt with extensively in Chapter 7.

[62] Björklund and Hökfelt (1986).
[63] Vincent *et al.* (1983a, 1986).

[64] Graybiel and Elde (1983).
[65] Oertel *et al.* (1983).

[66] Molinari *et al.* (1987).

[67] Rausell *et al.* (1992).

[68] Charara and Parent (1998).
[69] Fortin *et al.* (1998).
[70] Staining for parvalbumin and calbindin-D_{28k} can be a more useful guide to identify neuronal populations within different thalamic nuclei than for the delineation of nuclear borders (see Jones' unpublished data in fig. 2.17 of Steriade *et al.*, 1997a). In the cerebral cortex, a variety of local-circuit cells subserving different functions (see Jones, 1988; Gupta *et al.*, 2000) have been identified as GABAergic and peptidergic (Kawaguchi and Kubota, 1997).

[71] Brazier (1961); Niedermeyer (1993); Marshall and Magoun (1998).

[72] Purpura and Cohen (1962); Purpura *et al.* (1964, 1966); Creutzfeldt *et al.* (1966); Andersen and Andersson (1968).

[73] Ribary *et al.* (1991);
Lu *et al.* (1992); Llinás and
Ribary (1993).

[74] Reviewed in Hari
(1993).

[75] Steriade (1970).

[76] Paré *et al.* (2002).

[77] Steriade *et al.* (1969).

Magnetoencephalography (MEG) was introduced in the late 1960s and is now used to investigate spontaneous and evoked activities during wake and different sleep stages in humans [73]. MEG is reference-free and picks up the magnetic fields without direct contact of the sensor with the scalp, thus being less distorted than scalp-recorded potentials [74].

Local field potentials, occurring spontaneously or evoked by stimuli applied to afferent pathways, can be recorded in all central relay stations as well as in bulk of axons. In closed fields, such as dorsal thalamic nuclei or nuclei of the amygdala complex, the negative field waves reflect summated excitation of neighboring neurons. Central stimuli are abnormally synchronous but have the advantage of avoiding multiple intercalated synaptic relays. Thus, with stimuli applied to the white matter, just beneath the explored cortical area, alterations undergone by peripheral stimuli at the thalamic level are avoided [75]. Also, with pulses applied to the cerebellothalamic pathway, the magnitude of the afferent volley to the thalamus, reflected in the presynaptic deflection of the evoked potential, is monitored and it is possible to determine the fluctuations of the postsynaptic component, generated within the thalamus, during waking and sleep states in chronically implanted animals. Figure 2.7A shows that, during the transition between the wake and sleep states, in drowsiness, when spindle waves already appear in the EEG, the postsynaptic negative component of field potentials recorded from the motor thalamus (termed relayed, r), is selectively diminished and later, during full-blown slow-wave sleep, completely obliterated, whereas the positive presynaptic deflection (termed tract, t) is not changed. This demonstrates *that the first relay station where significant changes appear with transition from waking to sleep is the thalamus*. That the negativities of field potentials reflect excitation in a group of neurons is shown by the presence of superimposed action potentials of single cells or multiple units recorded in conjunction with the focal waves (Fig. 2.7B) [76]. Different components of pyramidal tract responses generated by thalamus or direct stimulation of motor cortex, and their alterations during brainstem reticular-induced arousal, can also be recorded using field potentials recorded from the bulk of corticospinal axons (Fig. 2.7C) [77].

Event-related potentials (ERPs) are field potentials evoked by different types of sensory stimuli, consisting of a series of waves, and usually recorded from scalp in humans. Because of their very small amplitudes, ERPs are usually averaged. The early components of ERPs in the somatosensory and other systems are stable under a variety

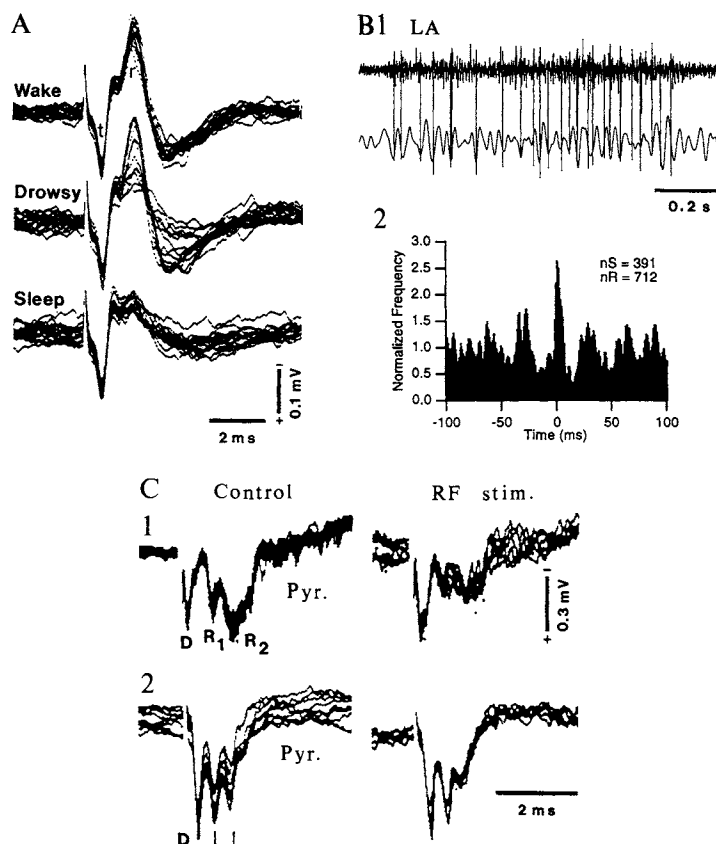


Figure 2.7. Local field potentials from central relay stations and fiber tracts, and their alterations during natural states of vigilance or arousal elicited by stimulation of midbrain reticular formation. A, blockade of synaptic transmission through the thalamus from the very onset of sleep (drowsiness). Field potentials (superimposed traces) were recorded from the thalamic ventrolateral (VL) nucleus and were evoked by stimulation of cerebellothalamic axons. Note progressively diminished amplitude of monosynaptically relayed (r) wave during drowsiness, up to complete disappearance during sleep, in spite of lack of changes in the amplitude of the afferent (presynaptic) volley monitored by the tract (t) component. B, relationship between unit discharges and fast focal oscillations in lateral amygdaloid nucleus of cat. Peri-event histogram of neuronal discharges (1-ms bin) using the negative peak of fast (gamma) waves as time zero. C, field potential recordings from pyramidal tract (PT) in the medulla of *encéphale isolé* cat. Direct (D) and relayed (R) or indirect (I) waves in PT are obtained by stimulating the thalamic VL nucleus (C1) or motor cortex (C2). Note suppression or reduction of synaptically relayed waves in the motor cortex under stimulation of midbrain reticular formation (RF) eliciting EEG activation. Modified from Steriade (1991, A), Paré *et al.* (2002, B) and Steriade *et al.* (1969, C).

of manipulations. The late components, especially P100 (positive at the scalp, with a latency of 100 ms) and P300 are modified by attention [78].

Extracellular recordings of single neurons during sleep, conditioning, motor performances and attentive fixation have been used since the 1960s [79]. More recently, the neuronal mechanisms of natural waking and sleep states have been explored using intracellular recordings from spinal cord motoneurons [80], pontine reticular

[78] Galambos and Hillyard (1981); Desmedt *et al.* (1983).

[79] Jasper *et al.* (1957, 1960); Evarts (1964, 1965); Mountcastle *et al.* (1975, 1981).

[80] Morales and Chase (1978); Glenn and Dement (1981); Chase and Morales (1983).

- [81] Ito and McCarley (1984); Ito *et al.* (2002).
 [82] Hirsch *et al.* (1983).
 In that study of thalamic lateral geniculate neurons, "slow spikes" superimposed by burst of action potentials were reported for the first time in chronically implanted cats, during natural slow-wave sleep when thalamic neurons are hyperpolarized. Those "slow spikes" represented low-threshold spikes (LTSs) described during the same epoch (1982–1984) both *in vitro* (Llinás and Jahnsen, 1982; Jahnsen and Llinás, 1984a) and *in vivo* under barbiturate anesthesia (Deschênes *et al.*, 1982, 1984; Steriade and Deschênes, 1984).
 [83] Steriade *et al.* (2001a); Timofeev *et al.* (2001b).
 [84] Coombs *et al.* (1955); Llinás and Terzuolo (1964).
 [85] Steriade *et al.* (1974a).

neurons [81], thalamocortical neurons [82], and pyramidal and local-circuit neurons in neocortex [83].

Several criteria should be met by any cellular study on states of vigilance. One of the most important, even in those cases in which intracellular staining is possible, is the identification of input–output organization of recorded neurons by antidromic and orthodromic responses. This is important in studies conducted on forebrain neurons, but especially in investigations on brainstem reticular neurons that behave differently when they project to oculomotor nuclei and spinal cord, or to rostral structures as part of ascending activating systems. In an extracellular position, antidromic responses are differentiated from synaptic ones by fixed latency, collision with spontaneous and/or evoked action potentials at proper time intervals, and faithful following of high-frequency stimuli. With intracellular recordings, antidromic responses start directly from the baseline and are abolished by hyperpolarization (Fig. 2.8). Changes in probability and pattern of antidromic responses during waking and sleep states can be studied even in the absence of intracellular recordings. In particular, the delay between the initial segment (IS) and SD spikes of these response and the appearance of IS spikes in isolation are indicative of neuronal hyperpolarization [84], appear during slow-wave sleep and disappear with neuronal depolarization upon awakening [85] (see Chapter 9). It is very useful that, contrary to the habit

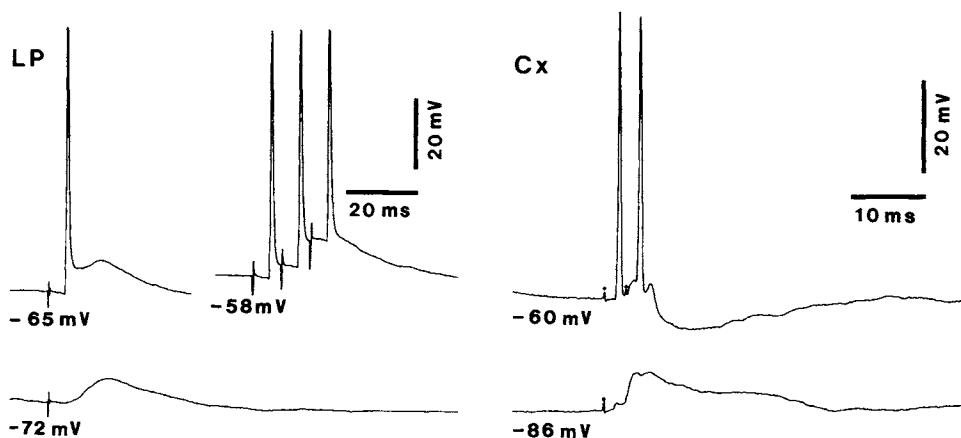


Figure 2.8. Antidromic and orthodromic responses of neocortical neurons. Intracellular recordings from area 7 in cat under urethane anesthesia. Left, cell recorded at 1.3 mm, antidromically activated at a membrane potential of -65 mV from thalamic lateroposterior nucleus (latency, 4.3 ms), using one or three stimuli. Under steady hyperpolarization (-72 mV), absence of antidromic response and appearance of excitatory postsynaptic potential (EPSP). Right, cell recorded at 0.5 mm in area 7, backfired from the contralateral cortex (latency 1.5 ms) at a membrane potential of -60 mV; absence of antidromic responses and appearance of EPSP at a more negative membrane potential (-86 mV). Modified from Steriade *et al.* (1993e).

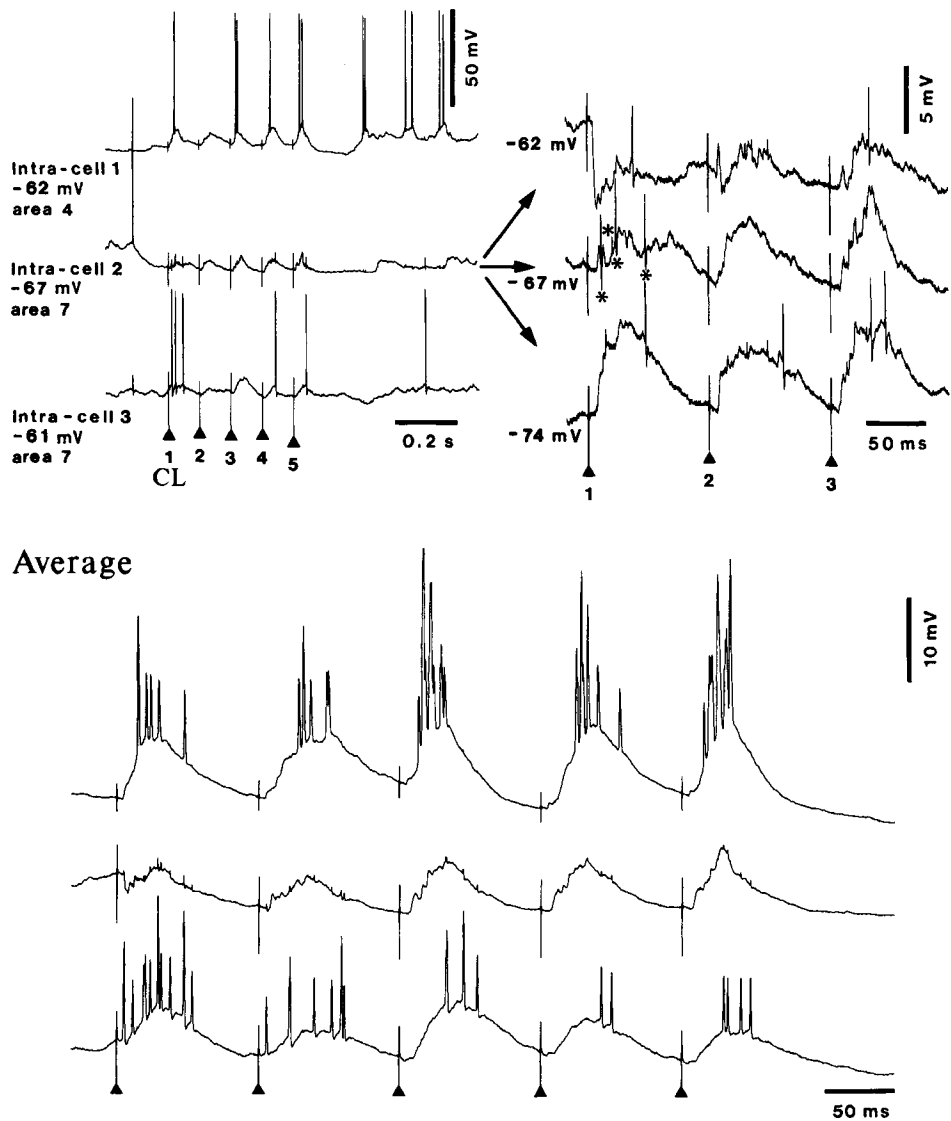


Figure 2.9. Specific features of augmenting responses in different cortical areas. Cat under ketamine–xylazine anesthesia. Triple (simultaneous) intracellular recording from area 4 (cell 1, upper trace) and area 7 (cells 2 and 3, middle and bottom traces). Stimulation of rostral intralaminar centrolateral (CL) thalamic nucleus with a pulse-train at 10 Hz (stimuli marked by arrowheads). Responses of cell 2 were investigated at three levels of membrane potential (upper right; asterisks indicate the artifacts of capacitive coupling among the three neurons). Average responses ($n = 5$) show that clear-cut augmenting responses only in cell 1. Discrete augmentation in cell 2 occurred largely under hyperpolarization. Cell 3 displayed a decremental response. Note early IPSP in cell 2, under slight depolarization (upper right panel). From Steriade and Timofeev (2001).

of filtering slow waves, extracellular recordings contain together unit discharges and focal field potentials, which provide information regarding the correspondence between the activity of single neurons and those of neighboring neuronal pools (see Fig. 2.7B). Extracellular unit

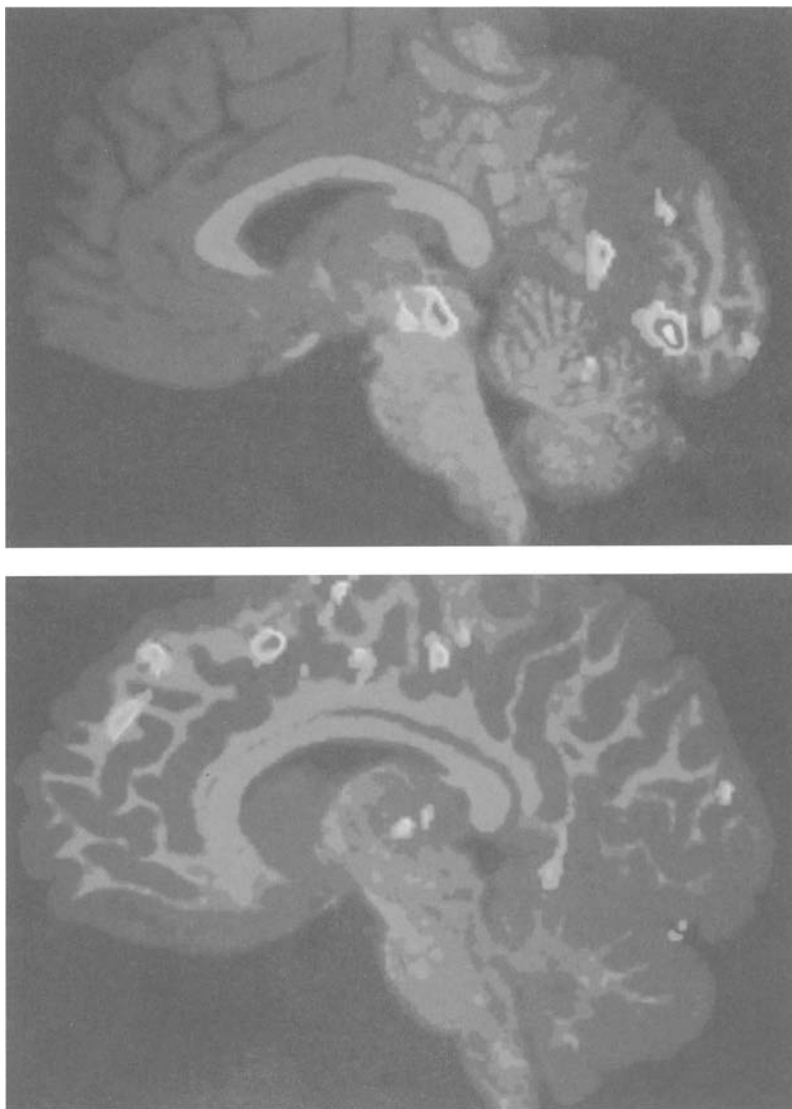


Figure 2.10. Activation of the human midbrain reticular formation and (upper panel) and thalamic intralaminar nuclei (bottom panel) by increased attentional demands in reaction-time tasks. The regional cerebral blood was measured by PET in 10 normal volunteers at rest and when they were engaged in two difficult and attention-demanding somatosensory and visual reaction-time tasks. The yellow and red colors indicate the areas of overlap between significant activation in the different conditions. Modified from Kinomura *et al.* (1996). See also color plate 2.

[86] Thakkar *et al.* (1998).

recordings can be combined with microdialysis in behaving animals to investigate the role of various neurotransmitters during states of vigilance [86].

During the past decade, dual intracellular recordings *in vivo*, from neocortical neurons, from related neocortical and thalamic neurons, and from neocortical neurons and glial cells, in conjunction with multisite recordings of extracellular unit activities and field potentials, have been

used in anesthetized animals to investigate brain rhythms during EEG-synchronized states, mimicking natural slow-wave sleep, as well as plasticity processes occurring during, and outlasting, sleep spindles and other oscillatory types [87] (see Chapters 7–8). Triple intracellular recordings have been used to analyze the propagation of evoked activities in cortical slabs *in vivo* and to study different patterns of augmenting responses, which constitute an experimental model of sleep spindles [88] (Fig. 2.9). Hopefully, dual and triple intracellular recordings will be attempted in the future in naturally awake and sleeping animals. For analysis of single-axon excitatory postsynaptic potentials (EPSPs) and inhibitory postsynaptic potentials (IPSPs), connections onto various neuronal classes and their synaptic strength, and different receptor types, dual, triple and quadruple intracellular recordings have been obtained in slices maintained *in vitro* [89].

2.3. Noninvasive Techniques

Noninvasive mapping of brain structures, such as positron emission tomography (PET) to image the 2-deoxyglucose metabolism and magnetic resonance imaging (MRI), are used in humans and nonhuman primates to localize regions of increased activity during waking–sleep cycle, sensory processing, and cognitive tasks [90]. PET studies have reported that, contrary to the common assumption that slow-wave sleep is accompanied by a global reduction in brain metabolism, the regional cerebral blood flow (rCBF) is lowest during this sleep stage in the brainstem core, medial thalamus, and orbitofrontal, prefrontal, and anterior cingulate cortical areas [91]. Also, a PET study showed activation of upper mesencephalic reticular formation and rostral intralaminar thalamic nuclei in attentive processes of humans [92] (Fig. 2.10). As attention processes are impaired after inactivation of thalamic pulvinar nucleus, it is thought that the attention deficits occurring after thalamic inactivation is due to the removal of thalamocortical excitatory inputs [93]. MRI can be combined in humans with MEG and ERPs.

[87] Steriade *et al.* (1994b; 1998b); Amzica and Steriade (1995a); Contreras and Steriade (1995); Timofeev and Steriade (1996; 2001a); Amzica and Steriade (2000).

[88] Timofeev *et al.* (2000a); Steriade and Timofeev (2001).

[89] Thomson *et al.* (1995, 1996); Markram *et al.* (1998); Gupta *et al.* (2000).

[90] Reviewed in Posner and Raichle (1994); Ledberg *et al.* (1998); London *et al.* (2000).

[91] Braun *et al.* (1997); Hofle *et al.* (1997); Maquet *et al.* (1997); Maquet (2000).

[92] Kinomura *et al.* (1996). This study supported the crucial role played by this midbrain–intralaminar–cortical circuit in ascending activation processes (Steriade and Glenn, 1982; Glenn and Steriade, 1982; see Chapter 9).

[93] Desimone and Duncan (1995).

Afferent and Efferent Connections of Brainstem and Forebrain Modulatory Systems

We now discuss the inputs and outputs of brainstem reticular (RE) and forebrain modulatory systems, as revealed by morphological and electrophysiological studies. Since neurons in the classical brainstem reticular fields (either identified immunohistochemically as cholinergic, or using different monoamines) have morphological and functional characteristics, these two groups of elements will be dealt with separately. Cholinergic nuclei of various species also contain a minority of monoaminergic cells and some monoaminergic nuclei possess a certain amount of cholinergic cells. For example, the parabrachial nucleus (i.e., the caudal part of the neuronal group that surrounds the brachium conjunctivum) contains both cholinergic and aminergic neurons. Moreover, although the emphasis was placed since the 1980s on cholinergic or monoamine-containing neurons, in order to specify systems within a structure prior viewed as “nonspecific,” noncholinergic neurons are much more numerous than cholinergic ones in the brainstem reticular core and most of them, especially large-sized ones, are glutamatergic. In the upper midbrain reticular formation, where there are virtually no cholinergic neurons, cells with antidromically identified projections to the thalamus display precursor signs of increased activity with shifts from slow-wave sleep to either wakefulness or REM sleep (see Chapter 10) and are regarded as crucial for changing the state of vigilance toward brain activation. Some of glutamate-induced excitatory actions consist in depolarization and increased input resistance of thalamocortical neurons, similarly to the effects exerted by acetylcholine (ACh), as both these neurotransmitters block a “leak” K^+ current (see Chapter 6). The role of glutamatergic midbrain and medullary neurons is also important in

maintaining mesopontine cholinergic pedunculopontine and laterodorsal tegmental (PPT/LDT) neurons in a sustained excitatory state even during waking, when monoaminergic neurons are active and exert an inhibitory tone upon them (see Chapters 6 and 10).

Section 3.1 will discuss extrabrainstem and intrabrainstem (reticuloreticular) sources of cholinergic nuclei as well as classical reticular formation fields (noncholinergic, presumably glutamatergic), which are treated together in view of the functional considerations exposed above. Sections 3.2 and 3.3 will discuss the afferents of brainstem and posterior hypothalamic monoaminergic nuclei, and the afferents to the basal forebrain cholinergic nuclei. The last sections in this chapter (Sections 3.4 to 3.6) will discuss the projections of different brainstem and basal forebrain cellular aggregates.

3.1. Afferents to Brainstem Cholinergic Nuclei and Classical Reticular Formation Fields

3.1.1. Systematization of Cholinergic Nuclei and Nuclei With Unidentified Neurotransmitters

We first analyze the cholinergic cell-groups in the brainstem reticular formation. The nuclear groups of choline acetyltransferase (ChAT)—positive neurons in the upper brainstem core. The brainstem (as well as basal forebrain; see Section 3.3) nuclear systematization and cytoarchitecture described below derives from studies using ChAT immunoreactivity in rat, cat, and macaque monkey [1]. Other studies have studied the interdigitation of cholinergic with catecholamine neurons in rat and cat [2].

The nomenclature proposed by Mesulam and his colleagues [1], with subsequent additions made by the same group [3], is adopted here to designate brainstem core cholinergic nuclei. We describe in more detail cholinergic groups whose neurons are implicated in the genesis of wake–sleep states and in the regulation of state-dependent processes of sensory–motor integration.

[1] Mesulam *et al.* (1983a), 1984; Vincent and Reiner (1987).

[2] Jones and Beaudet (1987a); Rye *et al.* (1987).

[3] Mufson *et al.* (1986).

3.1.1.1. Brainstem Cholinergic Nuclei

The two brainstem cholinergic cell-groups, Ch5 and Ch6, extend from the caudal part of the midbrain to the rostral pons. The Ch5 group is located within the central

tegmental field (FTC) of the caudal midbrain. In rat, many authors include it within, or simply term it, pedunculo-pontine tegmental nucleus (PPT). The PPT was first described in human material, and thereafter in other primates. It consists of medium- to large-sized, darkly stained neurons that appear from the decussation of brachii conjunctivi rostrally to the level of locus coeruleus (LC) and subcoeruleus caudally. The PPT is not a cytoarchitecturally distinct cell-group in the cat [4] and its close association with the brachium conjunctivum should be emphasized. We will use interchangeably the term PPT or the descriptive term of peribrachial (PB) area, part of the PPT nucleus, for the cat Ch5 group. The PB area should not be confused with the *parabrachial* nucleus that is an elongated nuclear mass located more caudally in the brainstem and characteristically aligned lateral to the caudal portion of brachium conjunctivum. These distinctions should be kept in mind in our discussion of the cytoarchitecture and cytochemistry of PPT. While the PPT is one of the major sources of generalized projections to virtually all (specific relay, associational, intralaminar, and reticular) thalamic nuclei (see Section 3.4) and to pontine and bulbar reticular formation, the parabrachial nucleus is mainly specialized in relaying taste and visceral information to the forebrain.

In cat, PPT neurons are medium-sized (soma surface 400–600 μm^2), fusiform or polygonal in shape. A detailed analysis in rat [5] showed that, in Nissl-stained sections, the rostral third of the PPT nucleus consists of medium- to large-sized neurons, the middle third consists of smaller neurons, and the caudal third has a dense cell-group that corresponds to the PPT-pars compacta described in several investigations on rat [6]. The comparative analysis of Nissl-stained and ChAT-positive neurons reached the conclusion that the large multipolar neurons in the rat PPT nucleus, as they appear on Nissl-stained sections, are entirely cholinergic neurons [5]. In fact, immunoreactive cholinergic neurons are larger than immunonegative neurons by an average of 40% [7]. Intracellular staining neurons in the cholinergic laterodorsal tegmental (LDT) nucleus of guinea pig revealed that the somata of these neurons is relatively large ($\sim 25\text{--}30\ \mu\text{m}$) and gives rise to an average of ~ 5 dendrites [8]. The average number of cholinergic cells in the PPT/LDT nuclei of humans is $\sim 20,000$, with 30% of cells in the pars compacta of the PPT nucleus [9]. In addition to the population of medium- to large-sized cholinergic neurons, the rat PPT contains smaller noncholinergic perikarya, some of them GABAergic [10], intermingled with the cholinergic ones.

The admixture of cholinergic, noradrenergic, and serotonergic neurons in the PPT/LDT nuclei was investigated

[4] Moon-Edley and Graybiel (1983).

[5] Rye *et al.* (1987).

[6] The medium- and large-sized neurons in the rostral third of the pedunculo-pontine tegmental (PPT) rat nucleus have a mean perikaryal longest axis of 20 μm , the middle part of the nucleus has neurons with rounder shape (16 μm), and the most posterior part consists of neurons with soma size around 19 μm . The ChAT⁺ neurons have angular to pyramidal somata, 3–5 primary radiating dendrites that divide into 2–3 secondary dendrites with irregularly spaced swellings resembling varicosities. The axon usually originates from a proximal dendrite.

[7] Honda and Semba (1995).

[8] Surkis *et al.* (1996).

[9] Manaye *et al.* (1999).

[10] Ford *et al.* (1995).

in cat, rat, and guinea pig, using ChAT, tyrosine hydroxylase (TH), and 5-HT immunohistochemical techniques on the same or adjacent sections [2, 5, 11]. In cat, ChAT⁺ and TH⁺ cells in the PPT area are morphologically similar and both are medium in size. At rostral PPT levels (frontal planes anterior 2 to 0), there are very few TH⁺ neurons. Significant percentages of TH⁺ neurons appear at more caudal levels of the PPT (Fig. 3.1). Within the *parabrachial* nucleus, TH⁺ neurons are as numerous as ChAT⁺ neurons. In rat, the rostral pole of the PPT cell-group is distinct from the TH⁺ cells belonging to the substantia nigra (SN) and retrorubral field (RRF) (respectively A9 and A8 groups of monoamine-containing neurons), but the dendritic arbors of PPT neurons overlap with those of the most caudal SN cells. In the middle part of the PPT, its medial aspect is traversed by TH⁺ ascending axons. And in the caudal third of the PPT, ChAT⁺ neurons are admixed with TH⁺ perikarya extending from the rostral pole of the LC [5]. Thus, it seems that both in cat and rat a significant population of TH⁺ neurons only appears within the caudal third of PPT.

In both cat and rat, the caudal part of the PPT merges dorsomedially into the Ch6 group (LDT), embedded in the periaqueductal—periventricular gray (Fig. 3.2). In cat, the cholinergic LDT neurons are similar in size to PPT neurons, but more roundish in shape. As in the rostral part of the PPT area, the number of ChAT⁺ positive neurons by far exceeds that of TH⁺ neurons in the LDT nucleus [2].

Approximately 15% to 30% of rat PPT and LDT cholinergic neurons also display substance P, corticotropin-releasing factor (CRF), bombesine/gastrin-releasing peptide, and atriopeptin-like immunoreactivity [12]. Many of PPT and LDT cholinergic cells also display intense nicotinamide-adenine-dinucleotide-phosphate (NADPH)-diaphorase activity in double-staining experiments. The functional significance of ChAT and neuropeptides colocalizations is still obscure. As cholinergic neurons in Ch5–Ch6 cell-groups are strongly implicated in processes of thalamocortical activation (see Chapter 9), it may be of interest to mention that bombesine and CRF can produce EEG and/or behavioral signs of arousal [13].

In addition to Ch5–Ch6 groups, virtually all neurons in the parabigeminal (PBG) nucleus, located at the extreme lateral part of the midbrain tegmentum, are cholinergic. The PBG nucleus was designated as Ch8 in experiments on mouse [3] and was also identified as a cholinergic nucleus in the cat [14]. PBG projects to the superior colliculus (SC) and to lamina C of the lateral geniculate (LG) thalamic nucleus [15]. WGA-HRP

[11] Leonard *et al.* (1995a).

[12] Vincent *et al.* (1983, 1986); Saper *et al.* (1985); Standaert *et al.* (1986).

[13] Sutton *et al.* (1982); Ehlers *et al.* (1983); Rasler (1984).

[14] Smith *et al.* (1988).

[15] Graybiel (1978b); Hughes and Mullikin (1984).

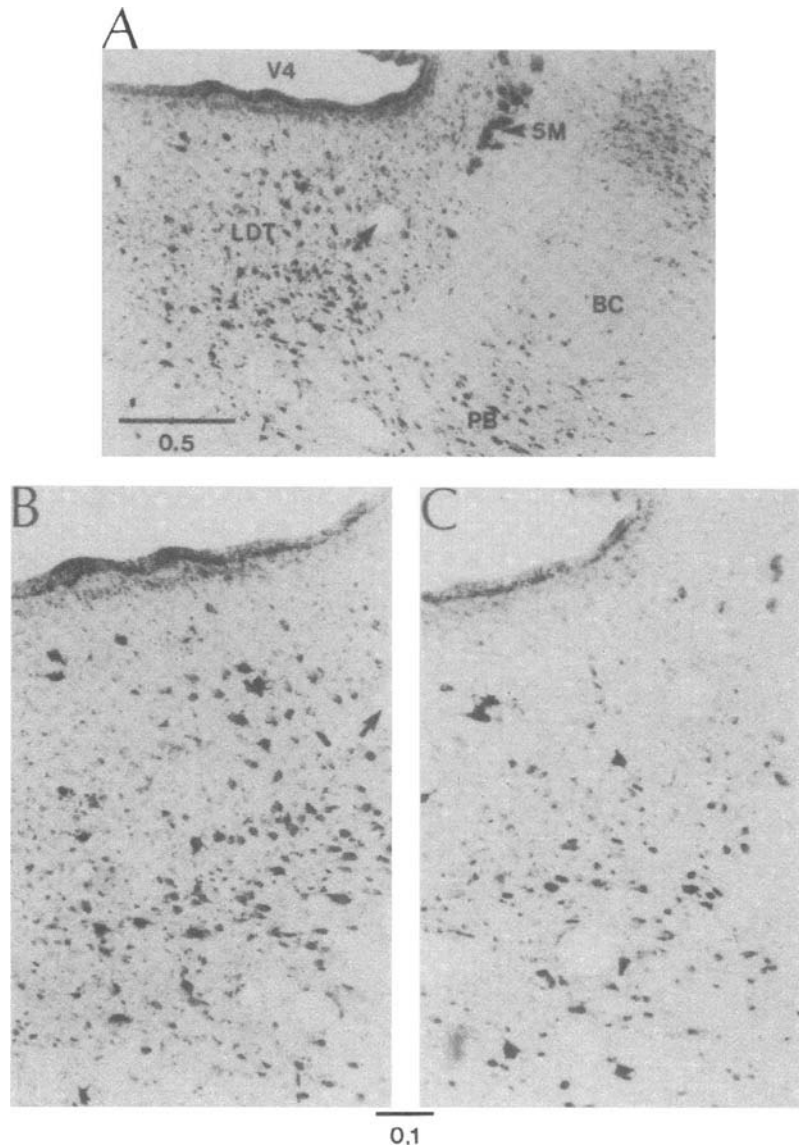


Figure 3.2. Features of retrograde cell labeling in brainstem peribrachial (PB) area of the PPT nucleus and laterodorsal tegmental (LDT) nucleus after a WGA–HRP injection into the mediodorsal (MD) thalamic nucleus in the cat. Arrow in A points to the same blood vessel as indicated in the enlarged photograph in B. C is an adjacent more posterior section. Abbreviations: BC, brachium conjunctivum; 5M, mesencephalic nucleus of the 5th nerve; V4, fourth ventricle. From Steriade *et al.* (1988).

retrograde tracing combined with ChAT immunoreactivity revealed that cholinergic neurons are the sources of the PBG-tectal [3] and PBG-geniculate [14] projections.

The complex arrangements of neurons and fibers in the mesopontine reticular core challenge prior views that assumed that the effects induced upon thalamocortical systems are simply cholinergic in nature. First, in most electrophysiological experiments conducted during the

1960s–1970s, stimulation was applied in the rostral midbrain core where there are virtually no cholinergic perikarya. In those cases, stimulation was applied, at best, to the axons arising in cholinergic neurons located more caudally, at the mesopontine junction. While substance P-containing and histaminergic neurons have been identified in some territories of the rostral mesencephalon, the transmitter(s) of most upper midbrain reticular neurons remain largely unknown, although glutamate is the most probable candidate. Second, even when stimuli are applied in more recent studies within the PB (or PPT) area, it must be acknowledged that this cholinergic territory also contains a certain amount of TH⁺ neurons and that it is traversed by catecholaminergic axons issuing from LC. As discussed in Chapter 6, ACh and norepinephrine (NE) similarly exert depolarizing actions on some thalamic neurons studied *in vitro*. Muscarinic and nicotinic blockers can ascertain the cholinergic nature of the phenomena, but, with some happy exceptions (see Chapter 9), the synaptic effects elicited by rostral brainstem reticular stimulation *in vivo* are rarely entirely blocked by one or the other of cholinergic blockers. In those cases, the colocalization of peptides in cholinergic neurons may be the factor that accounts for the observed failure of blockage. The physiological actions of various peptides whose colocalization was described in immunohistochemical studies of brainstem cholinergic neurons are almost completely unknown. Lastly, in any study conducted on the deep layer C of the cat's LG neurons, the cholinergic effects elicited by PPT stimulation may be due to costimulation of fibers arising in the PBG (Ch8) nucleus.

3.1.1.2. Brainstem Reticular Nuclei With Unidentified Transmitters

The principal nuclei of the midbrain, pontine, and bulbar reticular formation, other than the recently identified cholinergic groups at the midbrain–pontine junction, have been described since the 1950s on the basis of Nissl-stained preparations (see Chapter 2). Some terminological differences arose from various authors' preferences to use nuclear designations according to neuronal size (parvo-(PC), magno-(MC), and gigantocellular (GC)) or to their position on the brainstem map (dorsal, ventral, rostral, caudal).

At rostral (perirubral) levels, the midbrain reticular core is termed the FTC [16]. The FTC is a large territory extending between the SN and the deep layers of the SC. Many authors consider the large neurons of the deep SC layers as more closely related to the reticular formation

than to the SC, because of their isodendritic patterns and heterogeneity of sensory inputs [17]. The FTC cells of the cat are prevalently small-sized (soma surface 200–400 μm^2). This fits in with their slow axonal conduction velocities, as determined by antidromic invasion of FTC neurons from intralaminar thalamic nuclei and zona incerta (ZI) [18]. Caudally to the red nucleus, the ventral border of FTC is contiguous with the RRF, occupied in part by the catecholamine group A8. It should be emphasized that, at least in the cat, the FTC territory, located dorsally to the RRF, does not contain catecholaminergic neurons [19]. The distinction between FTC and RRF also results from their different connections. The rostral part of the FTC essentially projects to the thalamus (mediodorsal (MD), intralaminar, and ZI nuclei), while RRF projections are directed to the head of the caudate nucleus [20]. More caudally, at the level of the trochlear nucleus, the cholinergic PB (PPT) nucleus appears in the lateral part of the FTC, around the brachium conjunctivum. The cuneiform nucleus can be regarded as a dorsal extension of the FTC. It appears at the caudal pole of the trochlear nucleus and its relations are the inferior colliculus dorsally, the nucleus sagulum and dorsal nucleus of the lateral lemniscus laterally, and the PPT area ventrally.

The transmitter(s) of FTC neurons are largely unknown. Some studies report a number of substance P-containing neurons in nucleus cuneiformis [21] and histaminergic neurons located more ventrally in the midbrain reticular formation [22]. The elucidation of transmitter(s) used by the great number of neurons in the huge territory of the rostral mesencephalic reticular formation is a matter of future investigations. It may be predicted that the major transmitter of thalamically projecting rostral midbrain reticular neurons will be found to be an excitatory substance since, as discussed in Section 3.4 and Chapter 9, the effect of stimulating that midbrain region (after chronic degeneration of passing fibers) is a monosynaptic excitation of thalamocortical neurons.

The continuation of the midbrain FTC in the pontine tegmentum was termed paralemniscal tegmental field (FTP) in the atlas on cat brainstem [16]. The FTP might be differentiated from the Pc FTC by the presence of scattered medium-sized, and very few large-sized, neurons. The FTP occupies the largest part of the rostral pontine tegmentum and it is replaced more caudally (posterior planes 3–4) by a lateral tegmental field (FTL) and a paramedian gigantocellular tegmental field (FTG). The FTL contains cells of all sizes, well below those of FTG neurons. But FTG is also heterogenous, with giant neurons (soma large diameter around 60 μm) interspersed with

[17] Grofova *et al.* (1978); Edwards (1980).

[18] Steriade (1981).

[19] Parent (1984).

[20] Paré *et al.* (1988).

[21] Ljungdahl *et al.* (1978).

[22] Brownstein (1975); Schwartz *et al.* (1980).

[23] Mitani *et al.* (1988b).

[24] Fuller (1975).

[25] Newman (1985b). The medial part of reticularis pontis oralis (RPO) nucleus contains neurons with triangular or polygonal somata usually ranging between 30 μm and 50 μm in length, and medially directed dendrites that occasionally enter the nucleus raphe centralis superior. The lateral part of RPO contains neurons with somata between 20 μm and 80 μm , and dendrites coursing laterally and frequently intersecting with the axons of the lateral lemniscus.

[26] Steriade *et al.* (1984b).

medium-sized neurons (30–40 μm) and small neurons (around 20 μm) [18]. Intracellular HRP staining revealed that giant cells of the paramedian pons prevalently project to the spinal cord, whereas medium-sized neurons are reticuloreticular elements [23]. While not yet formally identified, evidence based on antidromic invasion suggests that the smaller pontine neurons are those with ascending projections to the thalamus [24].

The heterogeneity of pontine reticular neurons is the reason why some prefer to use the topographical terms reticularis pontis oralis (RPO) and reticularis pontis caudalis (RPC) to designate the nuclei of the pontine reticular core. The RPO extends from the caudal pole of the inferior colliculus to the trigeminal motor nucleus. A Golgi analysis of rat RPO distinguished a medial and a lateral part of this nucleus [25]. As to the RPC, it extends caudally to the rostral pole of facial nucleus where it merges with the bulbar reticular core. Whereas the large and giant cells of the Mc and Gc medullary field are clustered within the medial part of the bulbar reticular formation, the same type of neurons are fewer in number in the RPC and widely scattered throughout this pontine nucleus.

The bulbar reticular formation consists of three main territories: the Gc nucleus in the dorsal paramedian region, the Mc nucleus in the ventral paramedian zone, and the Pc nucleus in the dorsolateral area. These nuclei are synonymous with FTG, FTM, and FTL fields [16]. The sizes of neurons in various bulbar reticular regions fit in with their axonal conduction velocities, the antidromically identified Gc neurons having significantly higher conduction velocities than Mc neurons [26].

3.1.2. Afferents from Spinal Cord and Sensory Cranial Nerves

Since the first decade of the last century there was evidence, based on axonal degeneration and Golgi impregnation, that fibers originating in the spinal cord end exclusively in the brainstem reticular formation or collateralize within it, while the parent axon ascends further to the thalamus. These afferents are probably involved in alerting responses to noxious stimuli. We shall discuss only data accumulated during the past two decades or so [27].

There are interspecies differences as to the origin of spinoreticular pathways. Electrophysiological studies show that, in cat, the spinoreticular tract is mostly crossed and originates in laminae VII and VII, that is, in the ventral part of the spinal cord [28]. Most of these data resulted from antidromic activation of cat spinal neurons

[27] The early literature on this topic was comprehensively reviewed by Pompeiano (1973).

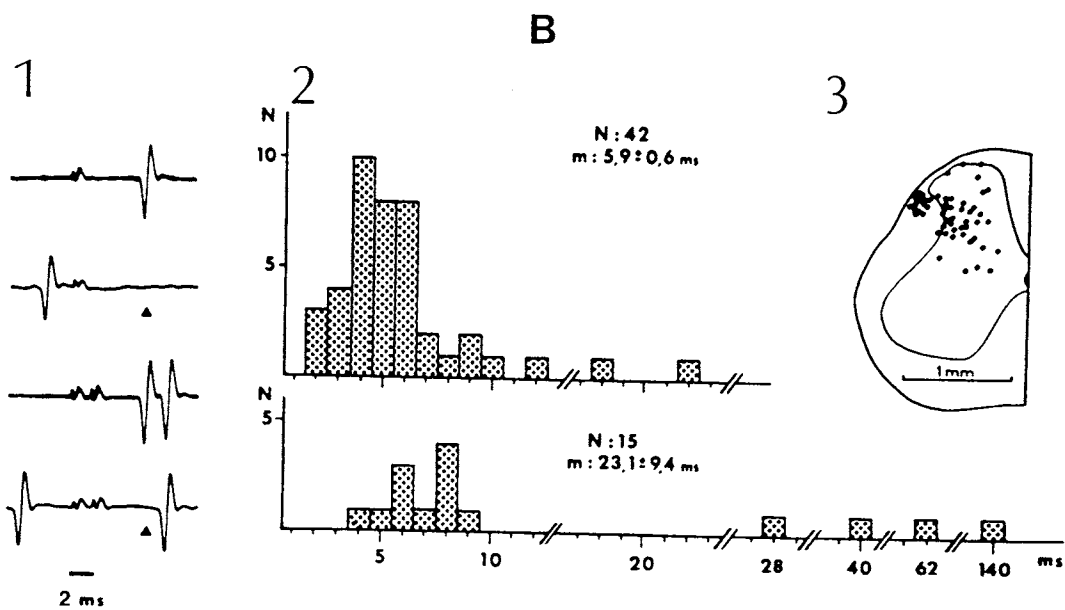
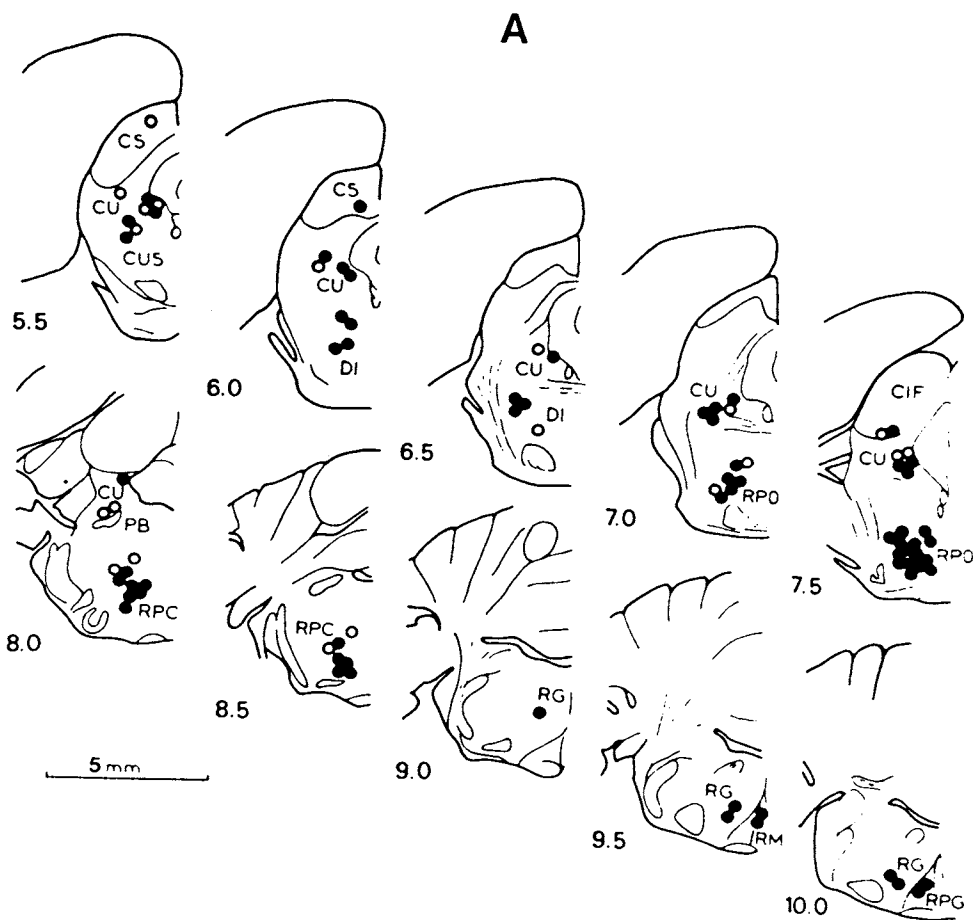
[28] Albe-Fessard *et al.* (1974); Maunz *et al.* (1978).

by stimulating the bulbar Gc field and the nucleus RPC. The median of axonal conduction velocities is around 45 m/s. Stringent limitations on stimulus intensity and failure to activate spinal neurons from more rostral (midbrain–diencephalic) sites indicated that the axons of those neurons probably end in the lower brainstem reticular formation and do not ascend to more rostral levels [28].

At variance with cat, the spinoreticular axons of rat originate in two neuronal groups in the dorsal half of the cord: the dorsolateral funiculus nucleus (DLF) and the dorsal horn, within or around the nucleus proprius and within lamina I [29]. Those neurons were antidromically activated mostly from both nuclei RPC and oralis, and from the rostral (peribrachial) and caudal (parabrachial) regions around the brachium conjunctivum in the midbrain reticular formation and at the midbrain–pontine junction (Fig. 3.3). These projection sites were corroborated by the same authors using retrograde tracing experiments following localized HRP injections. The monkey spinoreticular projections are more similar to those of rat than to those of cat. This similarity also concerns the collateral projections of spinothalamic axons to the brainstem reticular core. Indeed, both electrophysiological and HRP tracing experiments show that the lumbar spinothalamic tract of rat and monkey originates in the dorsal horn [30], whereas the source of the same tract of cat is mainly found in neurons of the ventral horn, with only some additional cells in lamina I [31]. In monkey, the collateralization of spinothalamic axons toward the brainstem core was estimated by multiple stimulation sites and differences in antidromic response latencies, and it seems to take place in the medullary reticular formation where the branch crosses the midline and terminates in the reticular core ipsilateral to the soma [32].

- [29] Menetrey *et al.* (1980). The rat spinoreticular neurons are heterogeneous. The dorsolateral funiculus nucleus (DLF) cells project to the midbrain or the midbrain–pontine junction with slow conduction velocities (mean around 3.5 m/s) and are driven by stimulation of subcutaneous or deep structures. The dorsal horn cells project to both pontine and midbrain levels with higher conduction velocities (mean around 13 m/s), are driven by both innocuous and noxious stimulation, and are submitted to descending inhibitory influences from the bulbar reticular formation and the nucleus raphe magnus.
- [30] Giesler *et al.* (1979).
- [31] Carstens and Trevino (1978).
- [32] Giesler *et al.* (1981).

Figure 3.3. Spinoreticular neurons in rat. A, locations of the active brainstem reticular (RE) sites for antidromic activation of spinal neurons. Each dot corresponds to an activated unit. Contralateral (filled circles) and ipsilateral (open circles) activations have been separated. The stereotaxic levels of various coronal sections are indicated by figures. From rostral to caudal, abbreviations correspond to: colliculus superior (CS), colliculus inferior (CIF), cuneiformis area (CU), subcuneiformis area (CUS), subnucleus dissipatus (DI), nucleus reticularis pontis oralis (RPO), nucleus reticularis pontis caudalis (RPC), nucleus parabrachialis (PB), nucleus reticularis gigantocellularis (RG), nucleus raphe magnus (RM), and nucleus paragigantocellularis (RPG). B, criteria for demonstrating antidromic activation (1), antidromic latencies (2), and location of spinoreticular neurons (3). The demonstration of antidromic activation is shown in 1. This cell responded to a single reticular shock with a constant latency (upper line, 10 superimposed responses) and followed 2 pulses (600 Hz) without any change in latency (3rd line, 10 superimposed sweeps). Antidromic spikes were occluded by the presence of orthodromic spikes in the critical period (equal to twice the antidromic latency plus one refractory period). Occlusion indicated by arrowheads on 2nd and 4th lines. In 2, top histograms correspond to dorsal horn neurons, bottom histogram to the dorsolateral funiculus cells. In 3, location of 55 spinoreticular cells. Modified from Menetrey *et al.* (1980).



The response decrement in brainstem reticular neurons to stimuli applied on the body surface at frequencies higher than 0.25–0.5 Hz indicates the inability of these neurons to relay efficiently rapidly recurring peripheral volleys and was interpreted as a sign of behavioral habituation [33].

In addition to transmitting impulses from noxious and some nonnoxious receptors to brainstem reticular neurons with ascending projections and alerting functions, spinal afferents arising in lamina I innervate the brainstem parabrachial nucleus and thus contribute to a series of vegetative processes mediated by this nucleus in response to nociceptive stimuli. The role of parabrachial nucleus in cardiovascular and respiratory reactions has been revealed in both rat and cat [34]. Anterograde and retrograde HRP tracing showed that neurons of spinal cord lamina I project to a series of parabrachial subnuclei [35]. So far it is not precisely determined whether lamina I cells that give rise to the spinothalamic tract [36] collateralize to the brainstem parabrachial nucleus or if there are two distinct populations of lamina I neurons with thalamic or brainstem projections, as double-labeling experiments with fluorescent dyes on cat would suggest [37]. Anyway, many spinoparabrachial neurons, that receive afferent terminals immunoreactive to substance P [35], are probably the afferent source of cardiovascular and pulmonary reactions mediated by the parabrachial nucleus in response to nociceptive stimuli.

The termination of spinal afferents at the level of the medullary and pontine reticular neurons of Gc fields was studied at the electron microscopic level [38]. Degenerating presynaptic terminals are in contact with both soma and dendrites. Some calculations estimated that only one in 1,000 of presynaptic endings on polydendritic reticular neurons is of spinal origin.

Brainstem reticular neurons are also the targets of axons collaterals of sensory cranial (mainly trigeminal, vestibular, acoustic, and optic) nerves [39]. One of the interposed relay stations through which the optic afferents reach the brainstem reticular neurons is the SC from which tectoreticular projections originate. Intracellular HRP injections have been made in neurons located in the intermediate and deep SC layers, with antidromically identified projections to the rhombencephalon and the spinal cord (tectobulbosplinal neurons, TBSNs) [40] (Fig. 3.4). SC projections to brainstem reticular formation are also discussed in conjunction with the oculomotor system in Chapter 11. Those studies [40] revealed that TBSNs send axonal collaterals to the midbrain reticular territory and an ascending branch that could be traced up to the caudal diencephalon, in the field of Forel.

[33] Peterson *et al.* (1976).

[34] Fulwiler and Saper (1984).

[35] Cechetto *et al.* (1985).

[36] Willis *et al.* (1979).

[37] Panneton and Burton (1985).

[38] Bowsher and Westman (1970); Westman and Bowsher (1971).

[39] See Brodal (1957).

[40] Grantyn and Grantyn (1982).

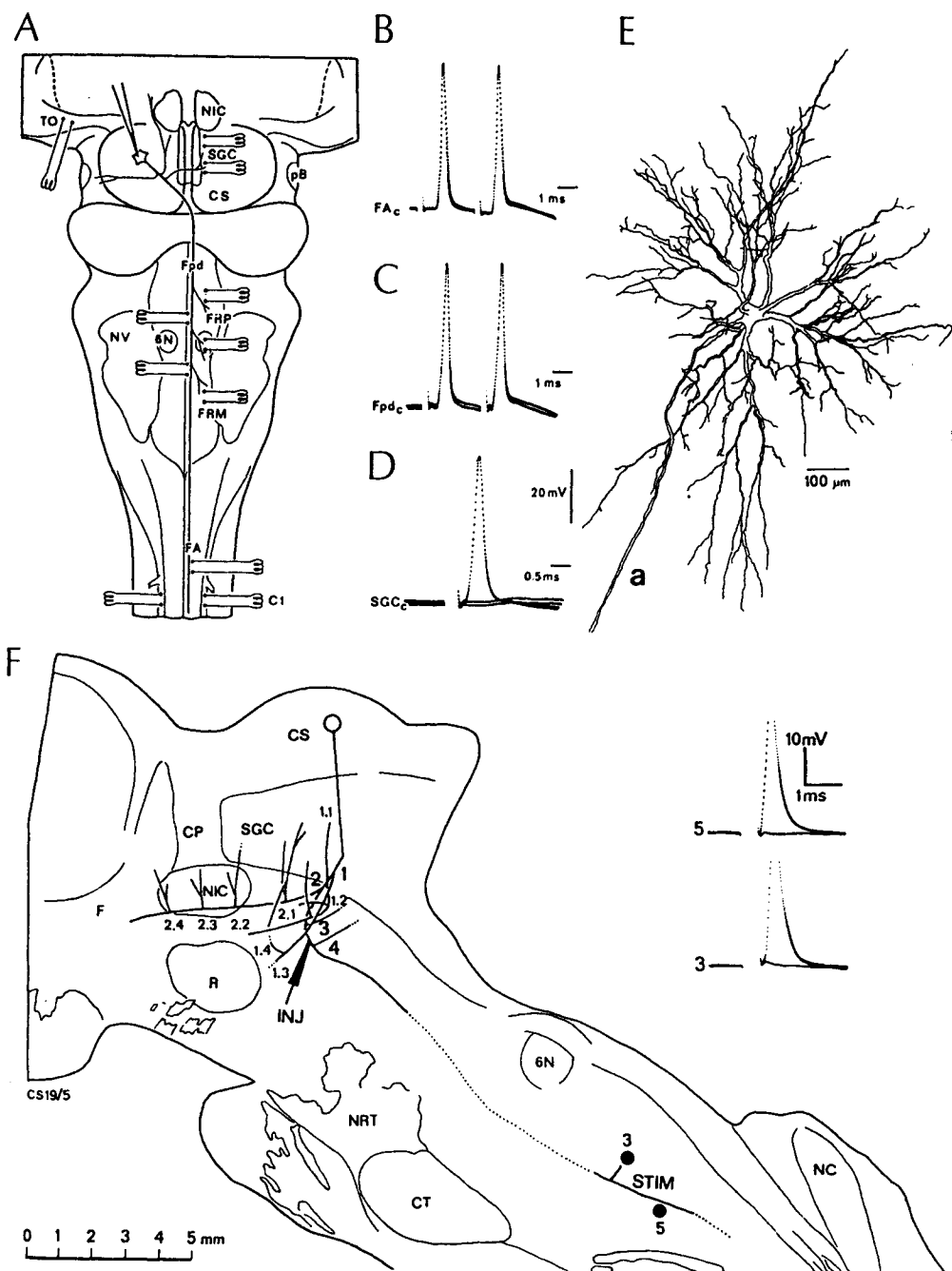


Figure 3.4. Electrophysiological identification, somadendritic profile, and axonal trajectory of tectobulbospinal neurons (TBSNs) in the cat. A, schematic diagram of experimental arrangement for antidromic activation of TBSNs. B to D, specimen recordings of antidromic spikes to show identification of axonal projection into the contralateral predorsal bundle (Fpd_c), anterior funiculus (FA_c), and collaterals to periculo-motor zone of the central gray (SGC_c). E, soma, dendrites, and axon (a) of a representative TBSN. Complete reconstruction from serial sections after intrasomatic HRP injection. F, axonal pattern of TBSN labeled by HRP injection into the main axon

near the dorsal tegmental decussation. Schematic drawing in parasagittal plane. INJ, injection site. Solid lines: part of axonal tree reconstructed on the basis of HRP staining. Dotted line: extension of the main axon into the medulla as demonstrated by antidromic response to contralateral predorsal bundle stimulation at point 5 (record 5). Presence of collaterals in the bulbar tegmentum proved by antidromic response to stimulation at point 3 located 1.7 mm from midline (record 3, threshold 50 μ A). 1, 3, 4: first order collaterals of the main axon within the mesencephalic reticular (RE) formation. 2: the main ascending branch. Modified from Grantyn and Grantyn (1982).

Another structure that relays visual and auditory impulses in their collateralization to the brainstem reticular core is the cerebellum. The observations by that impulses of retinal and acoustic origin reach certain cerebellar areas challenge the Sherringtonian concept that the cerebellum is solely the headganglion of the proprioceptive system. The distribution of teleceptive responses in the cerebellar vermis and the hodology of cerebellopetal impulses of visual and auditory origin were reviewed in detail [41]. The cerebellofugal projections from vermal areas that receive auditory afferents (lobules VI and VII) do not reach the secondary areas of the cat auditory cortex through the medial geniculate (MG) thalamic nucleus, but through a relay in the upper brainstem reticular formation [42] that probably transmits further the information through the intralaminar thalamic nuclei. In those early studies, the projections from the vermal cerebellar surface to the upper brainstem reticular formation were studied by the evoked potential method and the intermediate relay in deep cerebellar nuclei was not investigated. There is now morphological evidence that the fastigial nuclei, which are the obvious candidates for relaying impulses from the auditory-visual vermal areas, project to the midbrain reticular formation [43]. In addition, deep cerebellar nuclei modulate the activity of the deep layers of the SC through topographically organized projections [44].

[41] Fadiga and Pupilli (1964).

[42] Steriade and Stoupe (1960).

[43] Kievit and Kuypers (1972).

[44] Roldan and Reinoso-Suarez (1981).

3.1.3. Afferents from Diencephalon and Telencephalon

The following sources of descending inputs to the rostral brainstem reticular core will be considered, as they may be involved in behavioral state control: thalamic nuclei, posterior and anterior hypothalamic areas, basal forebrain and related structures, and cerebral cortex.

3.1.3.1. Thalamic Nuclei

The thalamic projections to the midbrain reticular formation essentially originate in the intralaminar, reticular thalamic, and ZI nuclei. These descending projections have been revealed by both morphological and antidromic invasion techniques.

Horseradish Peroxidase or WGA-HRP injections in the rostral midbrain reticular core or within the limits of the cholinergic PPT nucleus led to retrograde labeling of neurons in the centromedian-parafascicular (CM-Pf) and centrolateral-paracentral (CL-Pc) intralaminar nuclei [45]. Neurons in those caudal and rostral components of

[45] Parent and Steriade (1981); Steriade *et al.* (1982b).

[46] Ropert and Steriade (1981).

[47] Steriade *et al.* (1980). Another possibility is that such thalamobrainstem responses merely represent axon-reflex activation of spinothalamic projections, or superior colliculus (sc) projections, to intralaminar thalamic nuclei. These axons may branch and collateralize into the midbrain reticular core. Longer-latency (>10 ms) synaptic responses of brainstem reticular neurons to thalamic stimulation may be ascribed to circuitous pathways, including thalamocortical and corticoreticular projections.

the thalamic intralaminar complex can be antidromically activated from the midbrain reticular formation, with response latencies usually ranging between 1 and 3 ms (Fig. 3.5), suggesting axonal conduction velocities around 3–4 m/s. Such conduction velocities are similar to those found in the reciprocal pathway from the midbrain core to intralaminar thalamic nuclei [46]. These thalamobrainstem pathways may account for the monosynaptic responses elicited in midbrain reticular neurons by stimulation of intralaminar or other thalamic territories, responses that can faithfully follow 100-Hz volleys [47].

Until recently, the projection from the thalamic reticular nucleus to the upper brainstem core was a matter of controversy. In cat and squirrel monkey, this projection was described by means of the retrograde transport of HRP and fluorescent tracers, and was further substantiated in the same study with antidromic responses of reticular neurons

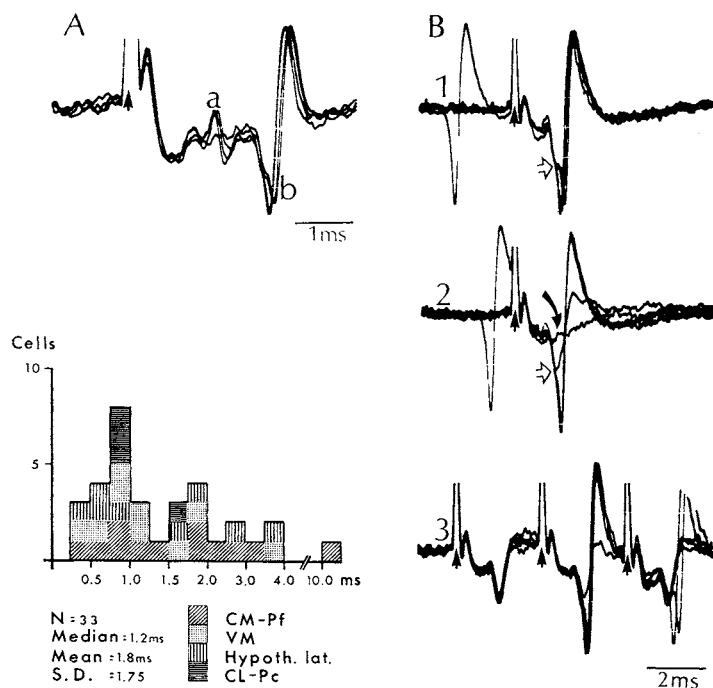


Figure 3.5. Antidromic identification of neurons in the lateral area of the posterior hypothalamus, centromedian–parafascicular (CM–Pf), centrolateral–paracentral (CL–Pc) and ventromedial (VM) thalamic neurons projecting to the midbrain central tegmental field (FTC). Stimulation applied to the peribrachial (PB) and more rostral areas in FTC, ipsilateral to the recorded diencephalic neurons. Specimen recordings of antidromic responses shown in A (neurons a and b recorded from CM–Pf) and B (neuron recorded from VM). Stimuli artifacts indicated by arrows. Histogram of response latencies for antidromic responses to various sites of stimulation, as indicated by symbols. Open arrows in B point to break between initial segment (IS) and somadendritic (SD) spikes of antidromic responses. Oblique arrow in B2 shows collision of antidromic response with a preceding spontaneous discharge. From Paré *et al.* (1989).

to midbrain reticular stimulation [48] (Fig. 3.6). The very long latencies of antidromic responses (median around 12 ms) suggest that the conduction velocity of reticular axons to the midbrain core is about 1 m/s.

A major diencephalic input to the upper brainstem reticular core originates in ZI, a lens-shaped nuclear field that continues laterally with the reticular thalamic nucleus, with which it shares a common origin from the ventral thalamus [49]. The input–output relationships of the ZI place it as an integrator of heterogeneous messages transmitted by spinothalamic, deep cerebellar, brainstem RE, hypothalamic, and corticofugal projections. Retrograde transport experiments showed that ZI projects to the Sc and periaqueductal gray [50] and to the FTC of the midbrain reticular core [51]. The projections from ZI to the midbrain reticular formation exceed those from the reticular thalamic nucleus. The morphological demonstration of ZI projections to the midbrain reticular formation was corroborated by the antidromic invasion of ZI cells, the axonal conduction velocities being around 11 m/s [51], twice as high as the values found in the reciprocal pathway from the midbrain core to the ZI [46].

The caudally directed ZI axons may eventually synapse with colliculopontine neurons [52] involved in eye movement commands, with brainstem reticular neurons projecting to the anterior or lateral funiculi of the spinal cord [53] that are involved in phasic and/or postural events of axial and limb musculature, but also with brainstem reticular neurons with ascending axons and arousing properties. The probable involvement of these projections in motor operations was shown by significantly increased firing rates of antidromically identified ZI–brainstem neurons during epochs with waking movements, as compared with periods without movements [51]. And a large proportion of ZI neurons of monkey were found to be activated when the animal reached for objects of interest [54]. The speculation may then be advanced that the reciprocal pathway between ZI and the upper brainstem reticular

[48] Parent and Steriade (1984). This study was conducted in cat. In rat, this descending projection was disclaimed on the basis of negative results of retrograde labeling after HRP injections in the midbrain reticular formation, with the conclusion that interspecies differences mark the organization of reticular projections to the brainstem core (Berry *et al.*, 1986). The same study in the rat also reported that ascending brainstem RE projections to the reticular nucleus are extremely sparse or even absent (Berry *et al.*, 1986). It is now demonstrated that, in both cat (Paré *et al.*, 1988) and rat (Hallanger *et al.*, 1987), cholinergic and non-cholinergic brainstem reticular projections innervate the reticular nucleus (see Section 3.4).

[49] Jones (1985).

[50] Grofova *et al.* (1978).

[51] Steriade *et al.* (1982b).

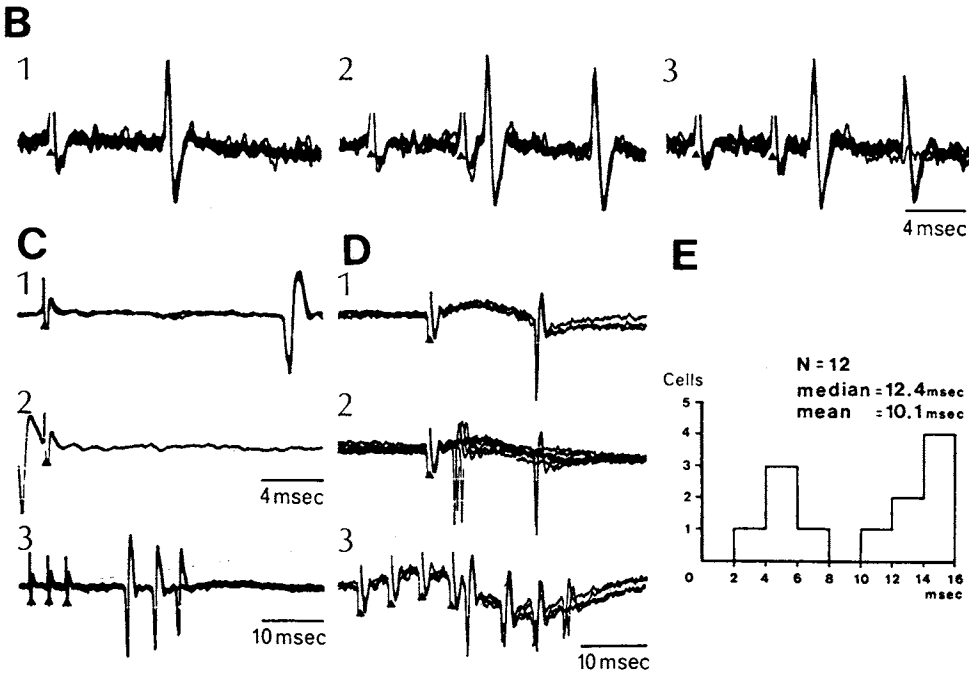
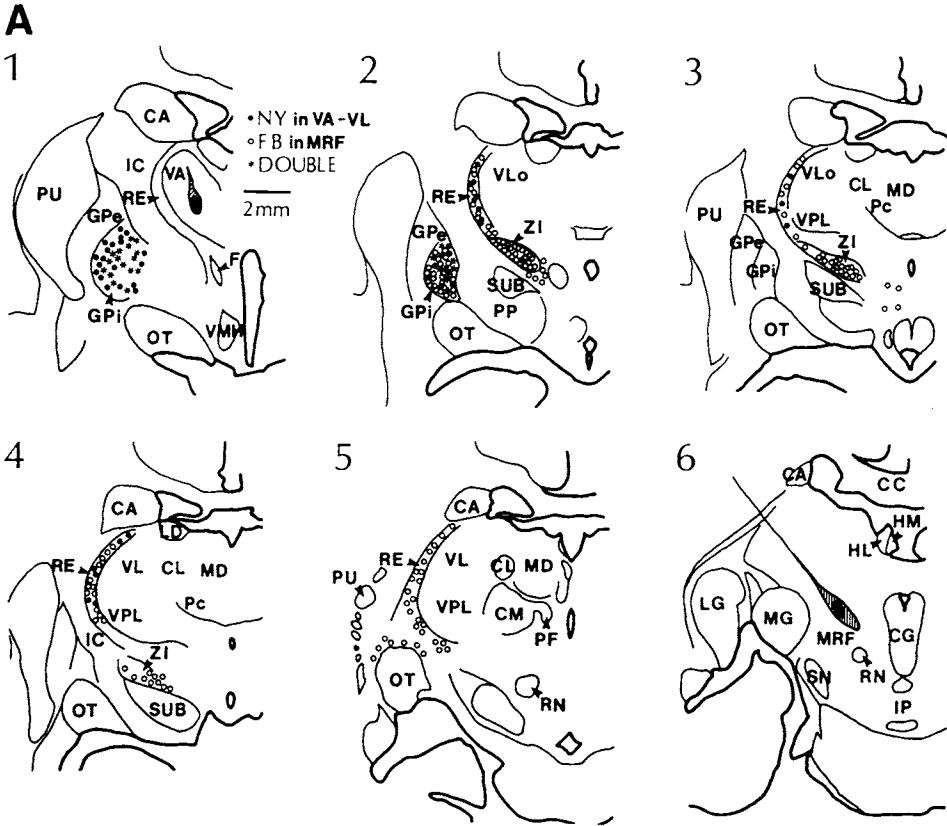
[52] Edwards (1975).

[53] Tohyama *et al.* (1979a).

[54] Crutcher *et al.* (1980).

Figure 3.6. Midbrain reticular (RE) projections of thalamic reticular neurons in squirrel monkey and cat. A, schematic drawings illustrating retrograde labeling after injections of fluorescent tracers in squirrel monkey. Nuclear Yellow (NY) was injected in ventroanterior–ventrolateral (VA–VL) thalamic complex (panel 1) and Fast Blue (FB) was injected in the peribrachial (PB) area of the midbrain reticular formation (MRF; panel 6). Various symbols are indicated in 1. Retrograde labeling of reticular neurons projecting to MRF is shown in panels 2 to 5. Note lack of double-labeled neurons in reticular nucleus, as compared to a large number of double-labeled neurons in internal part of globus pallidum (GPI; panels 1–2). B to D, antidromic identification of three different reticular thalamic neurons projecting to MRF in the cat. Note fixed latencies, collision with spontaneously occurring (C2) or orthodromically evoked (D2) discharges, and faithful following of fast stimuli (B2, C3, and D3). Median and mean of antidromic response latencies in a sample of 12 reticular neurons are shown in E. Latencies were measured from the middle of the initial phase of stimulus artifact (arrowheads) and initiation of discharge. Modified from Parent and Steriade (1984).

AFFERENT AND
EFFERENT
CONNECTIONS OF
BRAINSTEM

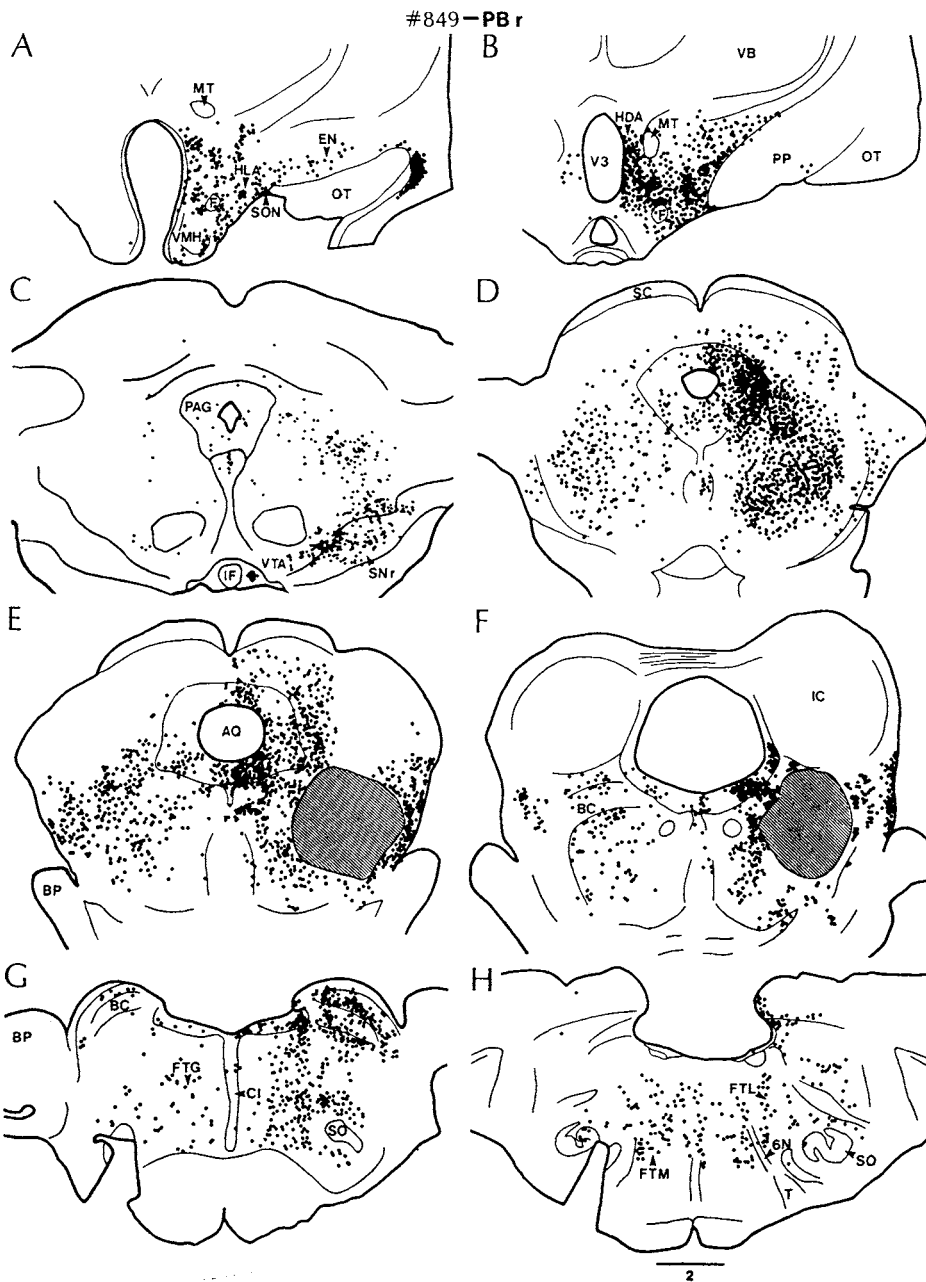


core is one of the elements that contribute to the attendance to relevant stimuli and thus prepare the motor commands.

3.1.3.2. Hypothalamic Areas

Massive retrograde labeling is observed in the ventro-medial (VM) and ventrolateral (VL) parts of the posterior hypothalamus of the cat after HRP injections in the rostral midbrain reticular formation or, more caudally, in the PB area at the midbrain–pontine junction [51, 55] (Fig. 3.7).

[55] Paré and Steriade (1990).



[56] Holstege (1987).

[57] Milner and Pickel
(1986).

[58] Chi and Flynn (1971).

[59] Mizuno *et al.* (1969);
Morrell *et al.* (1981);
Swanson *et al.* (1987).

[60] Kucera and Favrod
(1979); Stephan *et al.*
(1981).

[61] Inouye and
Kawamura (1979).

[62] Ibuka *et al.* (1977);
Yamoaka (1978).

The paraventricular hypothalamic nucleus has even more widely distributed projections, extending to a series of brainstem core nuclei, as well as to the spinal cord [56]. The descending projections from the paraventricular and lateral hypothalamic nuclei were also traced to the rat parabrachial nucleus, and related to the presence of substance P-like immunoreactivity in axon terminals that form asymmetrical synapses with dendrites of parabrachial neurons [57]. The projections from the posterior hypothalamus, an area that has been strongly implicated in alertness (see Chapter 1), may be related to defense–aggression instinctive behavior elicited from the hypothalamus [58] and are a possible source of tonic impingement upon midbrain reticular neurons involved in the maintenance of thalamocortical activation processes (see Chapters 9–10).

The projections from the anterior hypothalamus to the midbrain reticular core arise in the medial and lateral parts of the preoptic area [59]. The preoptic area is hypothesized to be an active sleep-promoting structure and to exert this role by an inhibitory influence upon activating structures located in the posterior hypothalamus and the rostral brainstem reticular neurons (see Chapter 1). Recordings of midbrain neuronal responses to preoptic stimuli in the nonanesthetized animal showed direct excitatory actions [46], much the same as with the other inputs onto brainstem reticular cells. Other afferents originate in the suprachiasmatic nuclei [60]. Suprachiasmatic nuclei display circadian periodicity in action potential generation [61] and lesions of these hypothalamic nuclei are followed by disruption of normally occurring oscillation between slow-wave-sleep and REM-sleep states [62]. The link between suprachiasmatic nuclei and the brainstem oscillator of sleep states is so far not elucidated.

3.1.3.3. Basal Forebrain and Related Systems

The basal forebrain consists of a series of structures, such as substantia innominata (SI) whose Mc elements constitute the nucleus basalis (NB) of Meynert, the vertical and horizontal branch of diagonal band nuclei (DBv and

Figure 3.7. Posterior hypothalamic and brainstem core afferents to the peribrachial (PB) area in the cat. A to H, eight frontal sections, rostral to caudal. The site of WGA–HRP injection shown in panels E and F. Each dot represents one retrogradely labeled neuron. Note, in A–B, retrograde labeling in dorsomedial, ventromedial, and lateral areas of the posterior hypothalamus (HDA, VMH, HLA, respectively). Retrograde labeling in substantia nigra pars reticulata (SNr) shown in C. Note massive retrograde labeling in deep layers of the superior colliculus (SC) and the midbrain central gray and central tegmental field, both ipsilaterally and contralaterally to the injection site (D and E). Retrograde labeling also seen in the caudal pontine gigantocellular tegmental field (pontine FTG), magnocellular field (FTM), and lateral tegmental field (FTL), ipsilaterally and contralaterally (G and H). Horizontal bar indicates mm. Modified from Paré *et al.* (1989).

DBh, respectively), and the medial septum (see Section 3.3). These nuclei contain cholinergic and noncholinergic (among them GABAergic) neurons. Recent morphological and electrophysiological studies have disclosed reciprocal projections between the basal forebrain and the rostral brainstem reticular formation as well as monoaminergic nuclei. We discuss here the basal forebrain inputs to the upper reticular core. As the amygdala nuclear complex receives projections from cholinergic and GABAergic basal forebrain neurons [63] and, in turn, sends back axons to this input source [64], we also mention the projections from the amygdala to the rostral reticular core, because such connections may be involved in the organization of some phasic events which are characteristic of REM-sleep state.

The projection from the basal forebrain to the brainstem reticular core was disclosed by means of retrograde HRP tracing in rat and squirrel monkey [65]. Experiments in cat and monkey, combining ChAT immunohistochemistry with the retrograde transport of WHA-HRP and retrograde double-labeling method by means of fluorescent tracers, determined the amount of cholinergic basal forebrain neurons with brainstem projections and the degree of collateralization of basal forebrain axons directed to the brainstem, thalamus, and cerebral cortex [66]. After WGA-HRP injections in the brainstem PB area, numerous retrogradely labeled cells were found in the preoptic area, a moderate number in SI, and a small number in the VL part of the DBh, but only 10% of HRP-positive cells in NB of SI were identified as cholinergic. The candidate transmitter of the remaining, large majority of basal forebrain neurons with brainstem projections is probably GABA, since numerous GABAergic elements are found intermingled with cholinergic cells in DB nuclei and in SI of rat and squirrel monkey [67]. Electrophysiological studies show that both excitatory and inhibitory responses are recorded in pedunculo-pontine (or PB) neurons after stimulation of the SI [68]. The probable transmitter for inhibition is GABA, but excitatory responses are not necessarily due to ACh since *in vitro* studies revealed that ACh exerts hyperpolarizing actions upon neurons surrounding the brachium conjunctivum, most of them cholinergic in nature [69].

After simultaneous injections of the fluorescent dyes Fast Blue (FB) in the brainstem PB area and Nuclear Yellow (NY) in the rostralateral part of the thalamic reticular nucleus, about 10% of all retrogradely labeled neurons in the SI and adjacent structures of the same family contained both FB and NY tracers (Fig. 3.8). Double labeling was not however obtained when FB was injected in the PB area and NY was injected either in other thalamic territories or in the cerebral cortex.

[63] Zaborski *et al.* (1986); Kitt *et al.* (1987).

[64] Russchen *et al.* (1985).

[65] Divac (1975). The projection from the basal forebrain to the brainstem reticular core was confirmed in rat with the safe method of anterogradely transported lectin PHA-L, and was found to terminate in and around the peribrachial (PB) area of the pedunculo-pontine nucleus (Swanson *et al.*, 1984) and in the latero-dorsal tegmental (LDT) nucleus (Satoh and Fibiger, 1986). The PB and LDT nuclei mainly consist of cholinergic neurons and are termed Ch5 and Ch6 groups in the nomenclature introduced by Mesulam *et al.* (1983).

[66] Parent *et al.* (1988).

[67] Nagai *et al.* (1983); Brashear *et al.* (1986); Smith *et al.* (1987).

[68] Swanson *et al.* (1984).

[69] Egan and North (1986); Leonard and Llinás (1990, 1994).



Figure 3.8. Basal forebrain neurons with branching axons to the thalamic reticular (RE) nucleus and brainstem peribrachial (PB) cholinergic area in the squirrel monkey. Drawings of four transverse sections through the basal forebrain (1–3) and upper brainstem (4) showing the injection sites and the distribution of retrogradely labeled cells after injection of the fluorescent tracers Fast Blue (FB) in the PB area and Nuclear Yellow (NY) in the rostrolateral sector of the reticular nucleus. The symbols are explained in the upper left portion of the figure and the injection sites are illustrated by dark and hatched areas. From Parent *et al.* (1988).

[70] Hopkins and Holstege (1978); Takeuchi *et al.* (1982).

Reciprocal connections also exist between the upper brainstem reticular areas (such as the PB, parabrachial, and LDT nuclei) and amygdala nuclei [70]. The bulk of amygdaloid projections to those areas at the midbrain–pontine

junction arise in the central nuclei of the amygdala (CNA). During REM sleep of cat, CNA stimulation significantly increases the number of PGO waves and their cluster density [71]. It is known that the final common path for transmission of PGO waves to the thalamus originates in and around the PB area (see Chapter 10). The amygdala-induced facilitation of this phasic component of REM sleep in cat may be related to the elicitation of dreaming by electrical stimulation of amygdala and other limbic structures in man [72].

[71] Calvo *et al.* (1987).

[72] Halgren *et al.* (1978).

3.1.3.4. Neocortical Areas

Golgi studies, anterograde degeneration, and retrograde tracing techniques showed that the projections of neocortical neurons to the brainstem core mainly arise in motor-sensory and somato-sensory areas and terminate in the midbrain reticular formation and in pontomedullary reticular fields [73]. The sign of this projection is excitatory, as all 20% of midbrain reticular formation that responded to cortical stimulation were directly excited, the great majority being activated at latencies shorter than 5 ms [46]. The corticoreticular feedback projections have been implicated in the maintenance of the alert condition (see Chapter 1).

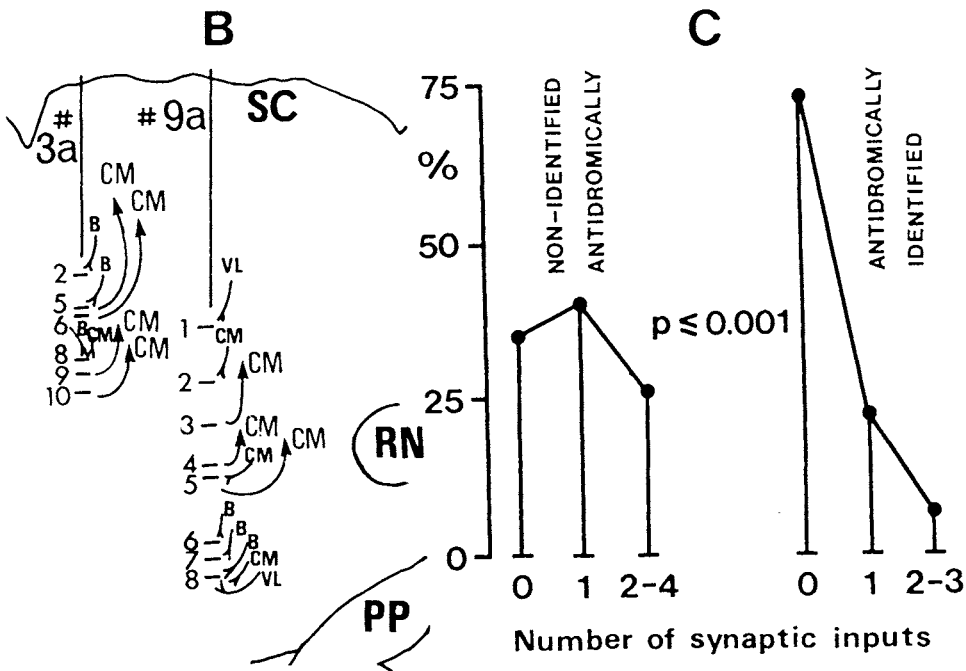
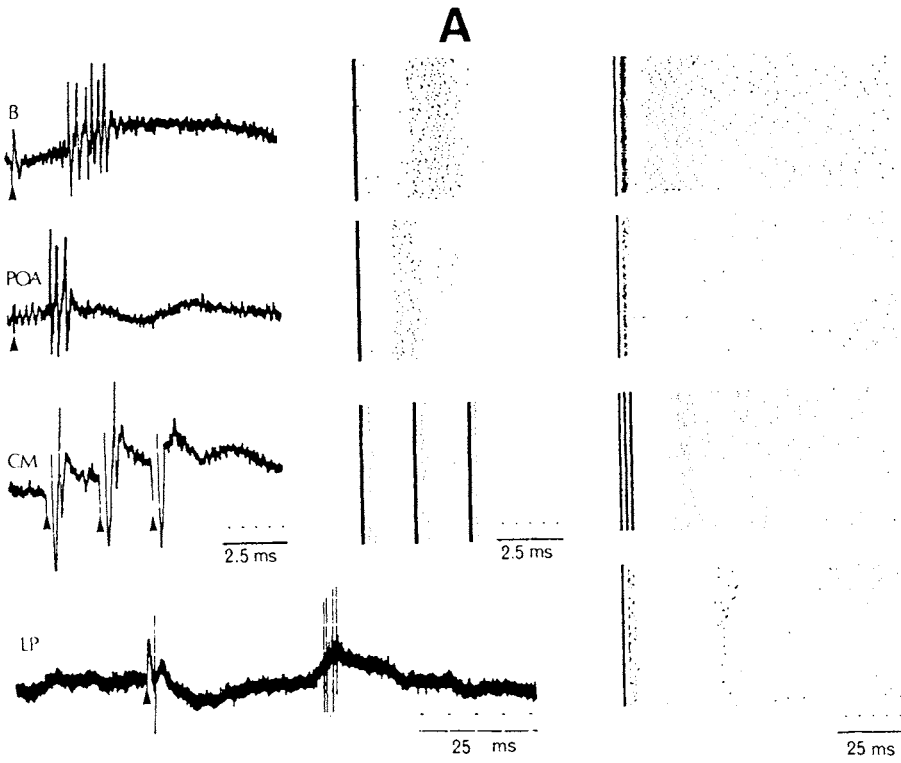
[73] Rossi and Brodal (1956); Kuypers (1958); Valverde (1961); Catsman-Berrepoets and Kuypers (1975, 1981).

3.1.3.5. Convergent Inputs Onto Single Brainstem Reticular Neurons

The convergence of various types of inputs from sensory pathways and central structures onto lower brainstem reticular neurons has been demonstrated [74]. Those rhombencephalic reticular cells may periodically function as part of one network and then of another network, as they display cyclic variations in responsiveness to multiple volleys of somatic and visceral origin. The midbrain reticular neurons are the site of convergences between inputs arising in the cerebral cortex, preoptic area, some thalamic nuclei, and bulbar reticular formation [18]. Figure 3.9 shows that the

[74] Scheibel *et al.* (1955).

Figure 3.9. Convergent synaptic excitation of midbrain reticular (RE) neurons in cat. A, a neuron in nucleus cuneiformis was excited synaptically following stimulation of the bulbar reticular formation (B), preoptic area (POA), center median (CM), and lateral posterior (LP) thalamic nuclei. Original spikes (left) and 50-sweeps dotgrams at fast (middle) and slow speed (right) to show dissimilar latencies, discharge patterns and suppressed firing-rebound sequences following stimulation of different sites; 3-pulse-train to the CM. B, two descents (3a and 9a) in the midbrain reticular core drawn from sagittal sections (lateral plane 3). Target structures (oblique arrows) were identified by antidromic invasion, while excitatory inputs (forked symbols) were recognized from synaptically elicited discharges at short latencies. PP, pes pedunculi; RN, red nucleus; SC, superior colliculus; VL, ventrolateral thalamic nucleus. The graph in C depicts the percentage (ordinate) of cells with various degrees of synaptic convergence in two neuronal populations (which could not be or have been antidromically identified from structures outside the midbrain reticular formation). 0 indicates neurons that have not been synaptically excited, and 1–4 indicate the number of stimulated sites which induced synaptic excitation. Modified from Steriade *et al.* (1980), Ropert and Steriade (1981), and Steriade (1981).



responses of midbrain reticular neurons display very slight latency dispersion and may follow high-rate volleys. More importantly, the common feature of midbrain reticular neurons receiving multiple converging inputs is the dissimilar discharge patterns and temporal evolution of the excitatory-inhibitory sequence evoked in the same neuron by several testing stimuli (Fig. 3.9A). This suggests that each of those inputs reaches different parts of the somadendritic membrane and differentially sets into motion various sources of inhibition acting on midbrain neurons. Synaptic convergences from multiple sites were more often seen in midbrain reticular neurons that remained unidentified by antidromic invasion than in midbrain reticular neurons with antidromically identified projections to distant sites (Fig. 3.9, B–C).

3.1.4. Afferents from Intrabrainstem Sources

3.1.4.1. Afferents to the Pontine Reticular Formation

In examining the afferents to the pontine reticular formation (PRF), it is helpful to provide an overview by describing a recent HRP/WGA–HRP study which systematically tabulated the relative percentage of retrogradely labeled neurons in the different regions sending projections to PRF in the rat [75]. In looking at these data, it must be kept in mind that the “relative percentage of projecting neurons,” while an essential measure, is only one way of measuring importance of connections to PRF. Other chapters in this monograph make clear the importance of neuronal groups with particular chemical codings that may powerfully modulate excitability and be of consequent importance for behavioral state changes, although the number of projecting neurons is relatively few; the cholinergic neurons are excellent examples. In that study [75], neurons were retrogradely labeled from “the medial magnocellular pontine reticular formation,” which includes a rostral non-giant cell portion (FTP) termed nucleus RPO, and the caudal nucleus RPC, corresponding to the giant-cell field (FTG) [16]. In our illustration of the results we will follow the use of the terms RPO and RPC. The major finding was that almost one half of the labeled neurons come from regions within the brainstem reticular core, including the midbrain, intrapontine connections, and bulbar reticular formation. These data provide a strong anatomical basis for the recent physiological data (discussed below) indicating dense reticuloreticular connections, and point to dense reticuloreticular connectivity as a major feature of reticular formation. Crossed, contralateral, and homotopic reticuloreticular input is important for

[75] Shammah-Lagnado *et al.* (1987).

both caudal and rostral PRF; this input constitutes 7–13% of the labeled neurons. There is also a dense interconnectivity between rostral and caudal PRF (8–14% of labeled neurons). Midbrain input is predominantly ipsilateral and from the area designated as FTC, with some input from nucleus cuneiformis. Bulbar input is predominantly from the giant cell field (BFTG), with some input from ventralis, parvocellularis, paragigantocellularis (PGCL), and magnocellularis areas.

With respect to nonbrainstem input, the diencephalic ZI and field of Forel provide the most important rostral input (14%) to RPO and 4% to RPC. This diencephalic zone may be regarded as a rostral extension of the brainstem reticular core.

Corticoreticular connections, primarily from frontal lobe, account for 5% of the labeled neurons. The Sc is the source of 15% of neurons with input to both rostral (ipsilateral predominance) and caudal portions of PRF (contralateral predominance). The central gray of midbrain, predominantly periaqueductal gray (including what was termed the midbrain extrapyramidal area [76]) contains 10% of neurons with projections to RPO and 4% of neurons with projections to RPC. Cerebellum contributes 2%. The spinal cord is the source of 13% of neurons with input to RPC, but very few projecting to RPO. With respect to projections from nuclei suspected of playing roles in modulating reticular excitability, retrogradely labeled neurons were found in dorsal raphe (DR), raphe magnus, LC, LDT nucleus, and peri/parabrachial complex. The main findings were essentially paralleled in a study in the cat [77].

Electrophysiological studies of inputs from other brainstem reticular formation areas to the pontine gigantocellular tegmental field (PFTG) [78, 79] addressed the nature of input to pontine FTG by means of intracellular recording in PFTG in the unanesthetized animal, using microstimulation of other brainstem reticular areas. The monosynaptic responses of PFTG neurons to microstimulation of bulbar [78] or contralateral pontine and midbrain [79] reticular formation are initially depolarizing excitatory postsynaptic potentials (EPSPs) in proportions from 75% to 90%. The percentage of initial PSPs that were inhibitory postsynaptic potentials (IPSPs) evoked by midbrain or contralateral pontine stimulation represented only about 4% of responses, statistically significant less than the IPSPs in response to stimulation of the bulbar Gc or Mc tegmental fields (about 12%). The shape of the EPSPs varied as a function of the stimulated sites: the EPSPs from the contralateral pontine and the bulbar reticular fields had a rapid rise time and a relatively constant latency, whereas those evoked by midbrain reticular stimulation had a less rapid rise time and a

[76] Rye *et al.* (1988)

[77] Leichnetz *et al.* (1987).

[78] Ito and McCarley (1987).

[79] McCarley *et al.* (1987).

longer plateau (Fig. 3.10). These results were collected from pontine neurons that, in a subsample with intracellular HRP labeling, proved to have in their great majority (80%) a soma diameter greater than 40 μm [79].

At variance with data on midbrain reticular neurons that suggested a relative segregation between receivers of multiple inputs and projection neurons [46] (see Fig. 3.9), the intracellular studies of pontine reticular neurons suggest an identity of input and output pontine reticular neurons with respect to synaptic response properties [78, 79]. The type and latency of initial PSPs in pontine reticular neurons are diagrammatically indicated in Fig. 3.11.

The anatomical data described above indicate the presence of dense and reciprocal pontobulbar interconnections, but do not of course indicate whether these are excitatory or inhibitory, nor whether there is any input differentiation for neurons with different projection pathways, such as those with and without axons in medial longitudinal fasciculus (MLF), the ventral funiculus (VF) or the medial reticulospinal projection pathway. Electrophysiological studies performed on the same neurons, morphologically characterized with intracellular HRP injections, have answered these questions. Pontine FTG neurons uniformly respond to stimulation of the bulbar FTG (BFTG) with an initial, short-latency EPSP response that has the short latency, rapid rise time, and faithful following indicative of monosynaptic connections. This is true of PFTG neurons identified by intracellular HRP injection as sending axons in MLF (Fig. 3.12) and also of those sending axons into bulbar

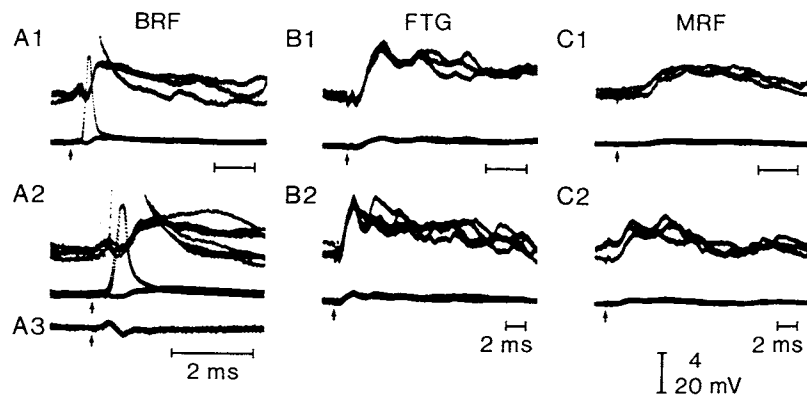


Figure 3.10. Typical responses of an intracellularly recorded medial pontine reticular formation (PRF) neuron to microstimulation of bulbar reticular formation (BRF, column A), contralateral pontine giant cell field (cFTG, column B), and mesencephalic reticular formation (MRF, column C) in cats. Part A3 shows the extracellular field response following BRF stimulation (4 mV calibration); note, in particular, the presence of an antidromic field potential temporally coincident with the antidromic responses shown in A1 and A2 (A2 has same time base as A3). Antidromic field potentials are also seen in the intracellular potential records with cFTG stimulation (column B) but not with MRF stimulation (column C). Note the presence of short latency EPSPs in all records; stimulation of BRF and cFTG produced EPSPs with a faster rise time than with stimulation of MRF. Modified from McCarley *et al.* (1987).

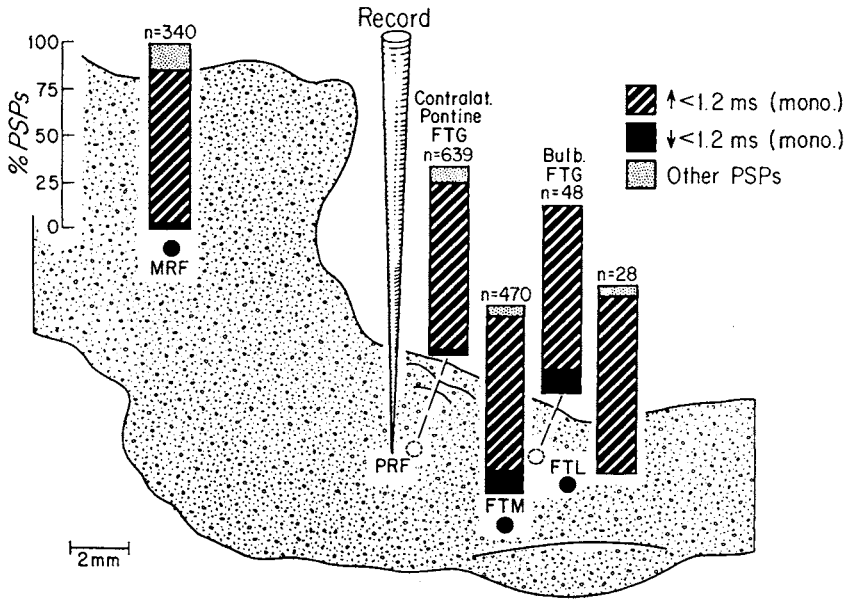


Figure 3.11. Summary of type and latency of initial PSPs produced in mPRF neurons by stimulation of various brainstem reticular (RE) regions in cats. Note: (1) the presence of dense monosynaptic excitatory input from almost all reticular regions; and (2) the maximum percentages of monosynaptic inhibitory PSPs occur with stimulation of bulbar FTM and FTG. Adapted from McCarley *et al.* (1987).

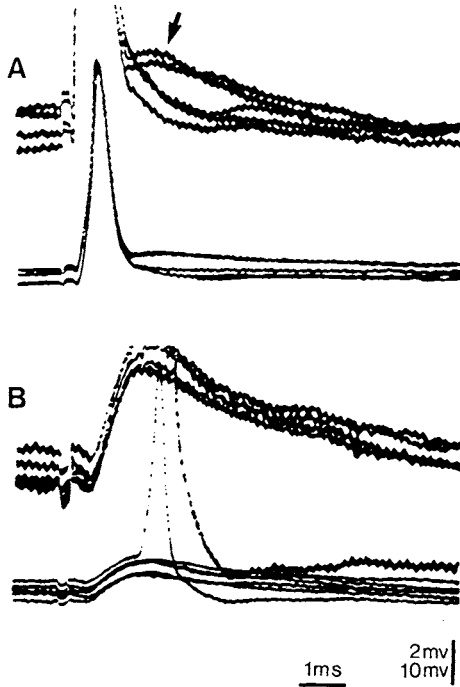


Figure 3.12. Intracellular recording of a pontine gigantocellular (Gc) field neuron with axon descending in MLF (intracellular HRP labeling). A, antidromic spike potentials with a latency of 0.3 ms were elicited by MLF stimulation; EPSPs (solid arrow) were also produced. B, EPSPs with a monosynaptic latency of 0.7 ms were evoked by microstimulation of BRF. AC-coupled recordings in upper traces in A and B (calibration bar = 2 mV) and DC-coupled recordings in lower traces (calibration bar = 10 mV). Resting membrane potential was -58 mV. Adapted from Mitani *et al.* (1988b).

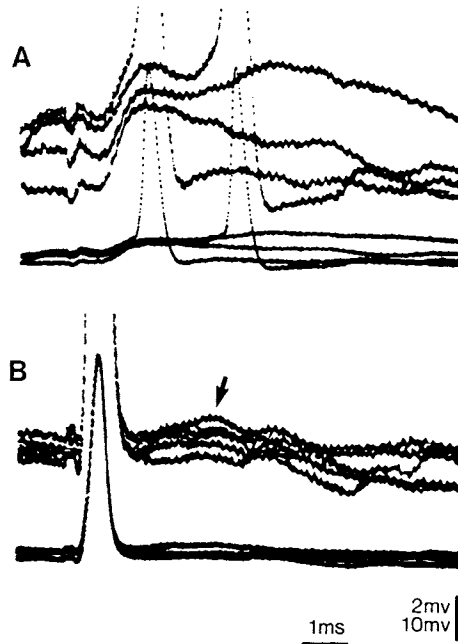


Figure 3.13. Intracellular recording of a pontine gigantocellular (Gc) field neuron with axon descending in BRF (intracellular HRP labeling). A, EPSPs with a latency of 0.8 ms were evoked by MLF stimulation; antidromic spike potentials were not present. B, antidromic spike potentials with a latency of 0.35 ms were evoked by stimulation of BRF; EPSPs (solid arrow) were also produced. Calibration and AC- and DC-coupling as in Fig. 3.12. Adapted from Mitani *et al.* (1988b).

reticular formation, when no antidromic response was present (Fig. 3.13).

Similarly, BFTG neurons respond to microstimulation of the ipsilateral pontine FTG with initial EPSPs that also have the characteristic of monosynaptic responses. This monosynaptic EPSP response to PFTG microstimulation is seen in all types of BFTG neurons identified by intracellular HRP injection, including those sending axons to MLF and those with axons descending in the bulbar reticular formation (Fig. 3.14). Longer-latency hyperpolarizing responses frequently followed these initial EPSPs in both bulbar and pontine neurons.

3.1.4.2. Afferents to the Midbrain and Bulbar Reticular Formation

After the demonstration, based on Golgi staining, of long-axoned neurons coursing from the lower to the upper brainstem reticular core [80], autoradiographic studies have shown projections from rhombencephalic reticular nuclei to the upper brainstem core [81] and from the midbrain reticular formation to the rostral pons and, less substantially, to the bulbar reticular formation [52]. An autoradiographic and

[80] Scheibel and Scheibel (1958).

[81] Graybiel (1977a).

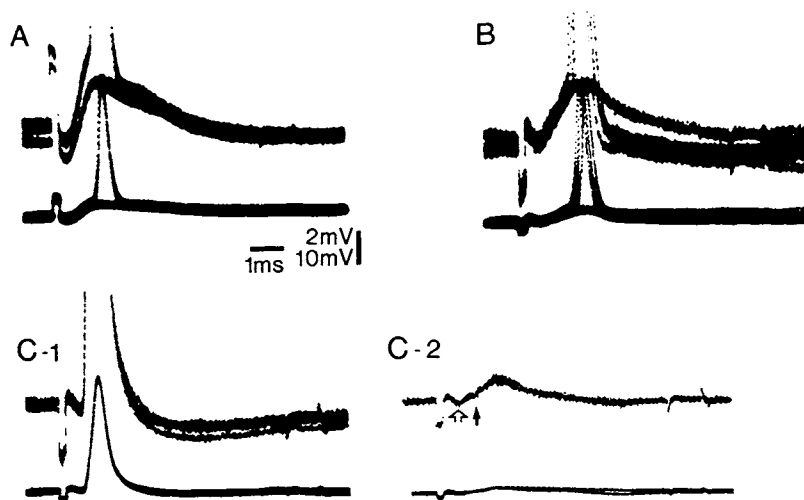


Figure 3.14. Intracellular recordings of bulbar gigantocellular (Gc) reticular (RE) formation neurons labeled by intracellular HRP injections. Part A is from a neuron sending its axon in contralateral MLF (cMLF neuron), part B from a neuron with axon coursing in ipsilateral MLF (iMLF neuron), and part C from a neuron with an axon coursing in ipsilateral bulbar reticular formation (iBRF neuron) and a bifurcating axonal branch to ipsilateral pontine gigantocellular reticular formation (PFTG). In A and B, EPSPs with latencies of 0.5 ms (A) and 0.6 ms (B) were evoked by PFTG stimulation. C-1, in this iBRF neuron PFTG stimulation (0.10 mA) elicited antidromic spike potentials with a latency of 0.6 ms. C-2, at a lower stimulus amplitude (0.04 mA) EPSPs were elicited (solid arrow, 1.1 ms latency); open arrow shows the antidromic field component. Calibration and AC- and DC-coupling as in Figure 3.12. Adapted from Mitani *et al.* (1988c).

retrograde transport study that focused on the bulbopontine reticular projections of the rat indicated that the bulbar Mc tegmental field projects ipsilaterally to the VM part of the PRF (FTG zone), with a decreasing density of projections toward more rostral pontine sites, while the rostral portions of the bulbar Gc field send bilateral projections throughout the pons and, further, to the forebrain [82]. Reticuloreticular projections from pontine sites to BFTG have recently been quantified [83] and found to be most dense from pontine FTG, which accounts for 70% of the percentage of retrogradely labeled neurons, with an approximately equal ipsi- and contralateral distribution. Projections from FTP, primarily contralateral, accounted for 24%, while predominantly ipsilateral projections from FTL and the parabrachial regions accounted for about 2% each.

Antidromic identification studies on bulbar reticular neurons of cat revealed that the afferents to midbrain reticular projections mainly arise in Mc field, while both Mc and Gc bulbar neurons project to medial and intralaminar thalamic nuclei [26].

Massive retrograde labeling occurs in rostral midbrain, paramedian PRF and Gc as well as Mc bulbar reticular fields after WGA-HRP injections localized within the limits of the cholinergic PPT nucleus at the midbrain-pontine junction (see Fig. 3.7).

[82] Zemlan *et al.* (1984).

[83] Mitani *et al.* (1988a).

In earlier electrophysiological studies, some controversial data resulted from the attempts at characterizing the nature of these reticuloreticular projections. The IPSPs described in lower brainstem reticular neurons as responses to midbrain stimulation [84] were contrary to the midbrain-evoked short-latency (1–3 ms) depolarizing potentials in bulbar reticular neurons [85]. The IPSPs could well be due to collaterals in the ascending pathway (toward unidentified inhibitory sources) since the antidromic invasion of medullary neurons from the midbrain occurred before the IPSP [84]. On the other hand, the IPSPs produced in midbrain reticular cells by bulbar stimulation [85], and interpreted in the light of a hypothesized inhibitory linkage from the lower to the upper brainstem reticular core, may be ascribed to costimulation of medullary monoaminergic neurons. Indeed, immunohistochemically identified adrenergic neurons project to rostral sites at the midbrain–pontine junction [86]. Studies conducted in chronically implanted, behaving cats reported monosynaptic excitatory responses of midbrain reticular neurons to pontine or bulbar reticular stimulation [46].

The connections between substantia nigra pars reticulata (SNr) and brainstem reticular nuclei, in particular the PPT cholinergic nucleus, are direct or through an intermediate relay in the SC. These connections play a key role in some physiological correlates of behavioral states of vigilance. The reciprocal connections between SNr and PPT result from anterograde and retrograde tracing techniques [4, 87] as well as by intracellular analysis [88]. The reciprocal connections are reflected electrophysiologically by antidromic activation of midbrain–pontine neurons surrounding the brachium conjunctivum (PB—area in the PPT nucleus) after SN stimulation, suppression of PB-cells' discharge by SN stimulation (as SNr cells are GABAergic), and prevalently excitatory effects in SN neurons by PB stimulation [89]. The latter study was conducted in chronically decorticated rats to preclude axon-reflex activation of descending corticofugal fibers giving off collaterals to both SN and PB.

The indirect connections between SNr and PB are mediated by a relay of SNr axons in the SC. The nigrotectal pathway was studied by retrograde tracing methods [90]. A comparative analysis showed that, in the rat, the SNr–SC projection arises in a ventral stratum of SNr and is almost exclusively ipsilateral, while crossed SNr–SC projections are visible in the cat and even more substantially in the monkey [91]. The GABAergic nature of SNr–tectal pathway was revealed by combined retrograde tracing and histochemical techniques [92] and the inhibitory effects upon SC neurons were assessed by SNr stimulation and GABA iontophoresis [93]. In turn, the cells in intermediate and

[84] Ito *et al.* (1970).

[85] Mancina *et al.* (1974).

[86] Guyenet and Young (1987).

[87] Jackson and Crossman (1981); Beckstead and Frankfurter (1982); Saper and Loewy (1982); Beckstead (1983); Sugimoto and Hattori (1984). Small HRP injections localized in the lateral and dorsal parts of the PPT nucleus led to retrograde labeling mostly in substantia nigra (SN) pars reticulata, with only occasional cells lying in the pars compacta of SN (Moon-Edley and Graybiel, 1983).

[88] Noda and Oka (1984).

[89] Scarnati *et al.* (1987).

[90] Rinvik *et al.* (1976); Graybiel (1978a, b); May and Hall (1986).

[91] Beckstead *et al.* (1981).

[92] Childs and Gale (1983); Araki *et al.* (1984).

[93] Chevalier *et al.* (1981a, b).

deep SC layers send axons caudally that give off collaterals to the PB area [40] (see Fig. 3.4).

The SNr–SC connection is involved in orienting reactions. Novel sensory stimuli are accompanied by a decrease in the firing rates of SNr cells, that releases from inhibition the target SC neurons, and eventually leads (through SC projections to premotor pontine reticular neurons) to eye movements toward the signal [94]. On the other hand, the inhibitory projections from SNr neurons to PPT neurons may be one of the decisive factors for hyperpolarizing some PPT elements during REM sleep. The consequence would be postinhibitory rebound bursts that are indeed the characteristic discharge patterns of some elements recorded from the cholinergic PPT/LDT nuclei, known as PGO-on burst neurons, other neuronal types firing tonically during PGO waves or even displaying suppression of their discharges time-locked with PGO waves (see Chapter 10).

[94] Hikosaka and Wurtz (1983a, b).

3.2. Afferents to Brainstem Monoaminergic Nuclei

3.2.1. Locus Coeruleus

The locus coeruleus (LC) was previously described as a site of convergence from a great variety of pathways. Retrograde HRP transport experiments have been performed in rat [95], a species in which LC is well defined and is homogenously composed of elements using NE as neurotransmitter. That study reported that afferents to LC arise in the marginal zones of the dorsal horn of the spinal cord, fastigial nuclei of the cerebellum, various brainstem nuclei (the solitary tract nuclei, medullary areas that correspond to A1–A2 catecholamine groups, several cell-groups located dorsal and lateral to the superior olive, the DR nucleus, and parts of classical reticular formation fields), paraventricular and lateral hypothalamic areas, medial and lateral preoptic areas, the central nucleus of amygdala, and a highly restricted band of cerebral cortex containing areas 13 and 14 around and dorsal to the rhinal sulcus. In cat, similar afferents from medullary (presumed catecholaminergic) cell-groups and hypothalamus reach the VL part of the LC, while the dorsomedial or principal part of the LC receives afferents from the contralateral LC, fastigial nuclei, DR nucleus, and mesencephalic central gray, but not from the bulbar reticular formation or the pontine Gc field [96]; however, other data using WGA–HRP methods indicate projections from these bulbar and

[95] Cederbaum and Aghajanian (1978). In that study, a series of manipulations were undertaken to ascertain the accurate placement of the HRP deposit, such as: recording of single cells with discharges (fairly regular, with a rate of 0.5–5 Hz) known to characterize LC neurons; and control injections in adjacent structures, including the parabrachial nucleus.

[96] Sakai *et al.* (1977b).

pontine reticular zones (A. Mitani and R.W. McCarley, unpublished data). The projection from the midbrain reticular formation to the LC of cat was also documented with the anterograde labeling method [52].

The projection from the DR is one of the sources of immunocytochemically identified serotonergic fibers that surround the perikarya and dendrites of NEergic LC neurons [97]. The sources of other inputs, among them those originating in various hypothalamic areas and/or the brainstem medullary core, are neurons containing enkephalin and substance P, beta-endorphin, or neurophysin [98].

After these reports of afferents to LC from so many sources, from the spinal cord up to the cerebral cortex, it was reported that the rat LC has a restricted afferent control, mainly consisting of two rostral medullary nuclei, paragigantocellularis (termed PGCL, [99]) and prepositus hypoglossi (PH), the connection being predominantly ipsilateral [100].

The nucleus PGCL is located in the VL part of the medulla, is involved in processes of autonomic integration, and contains the somata of bulbospinal neurons that provide the excitatory drive to the vasoconstrictor preganglionic neurons [101]. It is a pleomorphic nucleus and has neurons that contain serotonin, NE, enkephalin, as well as more typically reticular neurons; a major input is the pontine and BFTG and there is also strong connectivity with regions associated with the autonomic nervous system and nociception [99, 102]. As to the nucleus PH, it is involved in oculomotor system control (see Chapter 10) and is a site of afferents from quite diverse sources. In addition to massive retrograde labeling in PGCL and PH nuclei after WGA-HRP injections in the LC, much weaker retrograde labeling was found in the paraventricular hypothalamic nucleus and intermediate gray of the spinal cord.

These somewhat controversial results [100] were attributed to a more precise localization of the tracer injection into the LC, while the previous results were ascribed to diffusion of the tracer outside the LC limits, particularly in the parabrachial nucleus. Some comments can be made with regard to these data [100]: (1) the criteria used for retrograde labeling ("at least ten TMB reaction granules," p. 234) may dismiss elements with axonal collaterals, which usually display very few reaction granules (the so-called diluting collateral effect); (2) the parabrachial nucleus was injected in a control experiment [95] and, while retrograde labeling was found in preoptic area, ventromedial-dorsomedial hypothalamic areas and DR nucleus after LC injections, the same areas remained unlabeled after parabrachial injections (see Table 2 in that paper); (3) this restrictive view of LC input has also been criticized on the grounds that input to the large LC dendritic extensions outside the compact nuclear zone of the

[97] Pickel *et al.* (1977).

[98] Swanson (1977); Bloom *et al.* (1978); Pickel *et al.* (1979).

[99] Andrezik *et al.* (1981a, b).

[100] Aston-Jones *et al.* (1986).

[101] Guyenet and Brown (1986).

[102] Satoh *et al.* (1980); Khachaturian *et al.* (1983); Ross *et al.* (1985); Gray and Dostrovsky (1985); Ruggiero *et al.* (1985).

somata was neglected and that the extracellular techniques used to cross-validate input physiologically were insensitive compared with intracellular recordings which detect PSPs as well as action potentials.

The short-latency, robust excitatory responses of LC neurons (73%) to PGCL stimulation [100] have been characterized as subject to blocking by the excitatory amino acid (EAA) antagonists kynurenic acid and gamma-D-glutamylglycine, but not by the more specific NMDA EAA antagonist 1-amino-7-phosphonoheptanoic acid (AP7) and the preferential quisqualate receptor antagonist glutamate diethyl ester (GDEE) [103]. The nonexcitatory, suppressive responses to PGCL stimulation may result from a PGCL-LC projection originating from phenylethanolamine-*N*-methyltransferase-immunoreactive cells (the C1 adrenergic cluster). The effect of NE on LC cells is a powerful hyperpolarization mediated by alpha-2-receptors (Cederbaum and Aghajanian, 1978). In fact, the effects exerted by PGCL upon LC neurons are not simply inhibitory or excitatory because of the complexity of transmitters used by the heterogenous PGCL neurons. After the pharmacological blockade of PGCL-evoked excitation, LC neurons display purely inhibitory responses to PGCL stimulation [103] that may also be attributable to the adrenergic hyperpolarization of LC cells.

[103] Ennis and Aston-Jones (1988).

3.2.2. Raphe Nuclei

The serotonergic raphe nuclei that are mainly involved in the control of the sleep-waking cycle are raphe dorsalis and raphe medianus. Their major afferents seem to arise in the rostral part of the nucleus of the solitary tract, LC, SN, lateral part of the posterior hypothalamus, preoptic area, lateral habenula, hippocampus, and prefrontal cortex [104]. The pathway from the lateral habenula to the DR is inhibitory, probably GABAergic, as the effect induced by electrical stimulation of the habenula can be blocked by picrotoxin [105].

[104] Nauta (1958); Aghajanian and Wang (1977); Sakai *et al.* (1977a).

[105] Wang and Aghajanian (1977).

[106] Steinbush (1981).

[107] Mosko *et al.* (1977).

[108] Baraban and Aghajanian (1981).

As to the transmitter-specified afferents to the nucleus raphe dorsalis, disclosed by means of immunocytochemistry, the serotonin-immunoreactive fibers [106] originate partly in the DR itself [107] and in other raphe nuclei. The noradrenergic fibers that make synaptic contacts with DR neurons [108] probably originate in the LC.

3.2.3. Ventral Tegmental Area

Dopamine (DA)-containing neurons with connections to widespread areas of the cerebral cortex are located in the ventral tegmental area (VTA), while DA-containing neurons

projecting to the striatum are located in substantia nigra pars compacta (SNc). Since we shall deal in other chapters with the dopaminergic modulation of the cerebral cortex, we refer here to the afferent connections of VTA.

In rat, they originate in LC, parabrachial nucleus, various raphe nuclei (mainly dorsalis and magnus), posterodorsal hypothalamus and preoptic area, SI and diagonal band nuclei, amygdala, nucleus accumbens, and various cortical areas, especially the dorsal bank of the rhinal sulcus, and the prefrontal cortex [109]. Antidromic invasion studies in rat indicate that, in addition to innervate the VTA, prefrontal cortical neurons send axon collaterals to the MD thalamus, SN, and central gray [110]. In cat, VTA afferents arise in the spinal cord, deep cerebellar nuclei, several raphe nuclei, LC, mammillary nuclei, basal forebrain structures, and some cortical areas, such as the medial sigmoid gyrus [111]. These sources of inputs point to the VTA as a site of convergences from a variety of brain structures. In addition to the more conventional projections and transmitters, there are probably seven amines and at least ten peptides that modulate VTA neurons [112].

[109] Phillipson (1979).

[110] Thierry *et al.* (1983).

[111] Tork *et al.* (1984).

[112] Reviewed in Oades and Halliday (1987).

3.2.4. Tuberomammillary Area

The tuberomammillary area in the posterior hypothalamus contains the majority of histamine (HA) neurons, but some HAergic cells are also found in the brainstem and the preoptic area [113]. The main afferents to the tuberomammillary area arise in various brainstem structures, notably in nuclei located at the mesopontine junction, periaqueductal gray, amygdala, septum, and diagonal band nuclei [114]. A GABAergic as well as galaninergic projection to these HAergic neurons arises in the preoptic area [115]. This projection probably plays a major role in deactivating HA neurons and in promoting sleep (see Section 1.3.2 in Chapter 1).

[113] Schwartz *et al.* (1986).

[114] Parent *et al.* (1981); Vertes and Martin (1988); Sakai *et al.* (1990).

[115] Gritti *et al.* (1994); Sherin *et al.* (1998); Steininger *et al.* (2001); Chou *et al.* (2002).

3.3. Afferents to Basal Forebrain Cholinergic Nuclei

3.3.1. Systematization of Basal Forebrain Cholinergic Nuclei

The cholinergic nuclei of the basal forebrain are designated Ch1 to Ch4, according to Mesulam's [1] nomenclature.

The Ch1 sector consists of small-sized ChAT-positive neurons grouped in the medial septum. In both rat and monkey, the medial septum also contains a sizable proportion of noncholinergic neurons, at least a half of the total neuronal population. The noncholinergic cells are probably GABAergic elements [116]. Scattered single ChAT-positive neurons are also found in the lateral septum of cat.

The Ch2 and Ch3 sectors consist of ChAT-positive cells within, respectively, DBv and DBh. These neurons are multipolar and of larger size than Ch1 neurons. Here also, cholinergic neurons are intermingled, at least in rat, with GABAergic elements [117]. There are no definite boundaries between Ch2 and Ch1, or between Ch3 and the following basal forebrain sector, Ch4.

The Ch4 group mostly corresponds to NB of Meynert, but cholinergic cells are also found in the larger region known as SI that forms a neuronal band located ventrally to the anterior commissure, with extensions that surround the internal part of the globus pallidus (termed entopeduncular nucleus in cat). The Ch4 neurons are larger and hyperchromic, as compared to Ch1-to-Ch3 neurons, and 90% of NB cells are cholinergic in rat and monkey [1]. Caudally, SI neurons extend into the anterior part of the preoptic area and the amygdaloid complex, with few cholinergic cells within the central nucleus of amygdala in cat [1].

3.3.2. Afferents to Basal Forebrain Modulatory Systems

The activity of NB (Ch4) neurons is under the influence of the brainstem, hypothalamus, amygdala, and the cerebral cortex. Changes in NB cellular activities during states of vigilance are mainly controlled by brainstem, posterior hypothalamus, and amygdala neurons.

The projections from the upper brainstem core to NB were first revealed in primates [118]. The majority of brainstem core inputs to NB cholinergic cells appear to arise from neurons other than the mesopontine cholinergic ones as only <1 % of cholinergic PPT/LDT neurons project to NB [119]. Transport techniques, immunohistochemistry, and electron microscopical analysis [120] revealed that anterogradely labeled PPT/LDT axons do not contact NB cholinergic cells with cortical projections and cholinergic NB cells receive inputs from noncholinergic terminals. Thus, the main source of afferents to NB cells is not the aggregate of mesopontine cholinergic neurons. In macaques, NB (Ch4) neurons receive synaptic inputs from catecholaminergic, GABAergic, and cholinergic axons that

[116] Onteniente *et al.*
(1987).

[117] Brashear *et al.*
(1986).

[118] Jones *et al.* (1976).

[119] Jones and Cuello
(1989).

[120] Hallanger *et al.*
(1988).

usually form asymmetric synapses on ChAT⁺ neurons [121]. Even if direct brainstem–NB, cholinergic-to-cholinergic projections were to be eventually demonstrated, ACh elicits a muscarinic-mediated hyperpolarization of NB cells [122]. Extracellular recordings showed that stimulation of PPT nucleus exerts ambiguous, excitatory or inhibitory, effects upon cortical-projecting NB cells [123]. As to the monoamine-containing cells in the DR and LC, they make synaptic contacts with cholinergic as well as noncholinergic cells in the NB nucleus [124].

The most likely candidates for the brainstem drive reaching NB neurons during activated states are brainstem glutamatergic neurons, within the limits of, or outside, the PPT/LDT nuclei or even colocalized with ACh in the same cholinergic mesopontine cells [125]. The hypothesis that PPT-induced activating actions on neocortical cells are attributable to the glutamatergic activation of NB cholinergic cells [126] was supported by a study in which the ACh release from cortex was collected using microdialysis, while stimulating PPT nucleus and exposing NB to different blockers [127].

The hypothalamic afferents to the NB [128] make synapses with both cholinergic and noncholinergic neurons. The histaminergic tuberomammillary cells also project to NB neurons and are implicated their activation [129].

The origin of amygdaloid complex projections to the basal forebrain are excitatory neurons located in the basolateral and central nuclei, which may underlie the response of reinforcement-related neurons in the primate basal forebrain [130] and inhibitory neurons in the GABAergic intercalated cell masses [131], the latter terminating in NB and the horizontal limb of the diagonal band nuclei [132].

3.4. Efferent Connections of Brainstem Cholinergic Nuclei and Classical Reticular Fields

In this section, we describe the projections of both immunohistochemically identified brainstem cholinergic and nonidentified neuronal aggregates.

We first analyze (Section 3.4.1) the rostral (thalamus and basal forebrain) projections of brainstem reticular nuclei that consist of quite circumscribed populations of cholinergic neurons at the midbrain–pontine junction and a series of nuclei whose chemical transmitter(s) remain(s) largely unidentified. Brainstem and spinal cord efferents of the cholinergic mesopontine and noncholinergic

[121] Smiley and Mesulam (1999).

[122] Khateb *et al.* (1997).

[123] Semba *et al.* (1988). In that study, only one fifth of sampled neurons were responsive, half of them with initial excitation followed by inhibition of spontaneous firing, the other half with initial suppression of discharge.

[124] Záborski *et al.* (1991).

[125] Lavoie and Parent (1994).

[126] Steriade *et al.* (1993a).

[127] Rasmusson *et al.* (1994, 1996).

[128] Cullinan and Záborsky (1991).

[129] Khateb *et al.* (1995).

[130] Wilson and Rolls (1990).

[131] McDonald and Augustine (1993); Paré and Smith (1993).

[132] Paré and Smith (1994).

pontobulbar reticular formation are discussed in Section 3.4.2. The intrinsic morphology of pontobulbar reticular formation neurons and the correlations with anatomical projections are discussed in Section 3.4.3.

The actions of various transmitters of brainstem neurons upon thalamic, cortical, and spinal cord neurons, and the synaptic influences exerted on those distant targets by stimulating brainstem projection pathways, are examined together with the intra-brainstem transmitter actions in Chapter 6. The hypothesized interactions between brainstem cholinergic and monoaminergic neurons that may underlie oscillations in states of vigilance are discussed in Chapter 12.

3.4.1. Rostral Projections of Cholinergic and Noncholinergic Reticular Neurons

The projections of brainstem reticular neurons are described as a function of rostral (diencephalic and telencephalic) targets. In many instances, the same target area is afferented from both cholinergic and noncholinergic, upper and lower, brainstem reticular neurons.

As originally described by fiber degeneration techniques [133] and Golgi studies [80] and subsequently confirmed and elaborated by autoradiography [134], long ascending projections from the giant cell fields of the bulb and pons, as well as from FTP and FTC areas, ascend as Forel's tegmental fascicles into the diencephalon where this diffuse band of fibers splits into a dorsal and ventral leaf. The dorsal system supplies the intralaminar and midline nuclei of the thalamus while the ventral division distributes fibers to subthalamus (mainly nucleus of the field of Forel) and (mainly lateral) hypothalamus, and beyond to basal forebrain.

[133] Nauta and Kuypers (1958).

[134] Jones and Yang (1985).

3.4.1.1. Are There Direct Cortical Projections?

The ascending axons of cholinergic neurons at the midbrain–pontine junction (Ch5–Ch6 groups) and noncholinergic reticular neurons of midbrain, pontine, and medullary fields are overwhelmingly relayed in the thalamus. This stands in contrast to the direct cortical projections of monoaminergic brainstem nuclei (see Section 3.4). The absence of direct cortical projections of non-monoaminergic brainstem neurons (using ACh or other, as yet nonidentified, transmitters) was especially reported in studies conducted in cat, but the scarcity of such projections also results from studies in rat and squirrel monkey. The only species that seems to have a significant brainstem

reticular projection to the visual cortex is the chimpanzee. This should be emphasized because reports continue to accumulate in the literature referring to direct reticulocortical projections, without qualifications about their importance and their widespread or localized character, and without dissociating the classical reticular (cholinergic and noncholinergic) fields from the monoaminergic systems.

After large injections of retrograde tracers in cat visual cortex, no nonmonoaminergic neurons were labeled in the brainstem reticular formation, but a significant number of 5-HT⁺ or TH⁺ neurons were also HRP⁺ in the DR or LC [135]. The absence of retrogradely labeled brainstem reticular neurons was also reported in other experiments using retrograde tracer injections in cat visual cortex [136] as well as large HRP injections in motor (pericruciate), parietal associational (suprasylvian) neocortical areas, and posteroventral hippocampus of cat [137]. In rat, after ³H-proline injections in the upper brainstem reticular formation, the projections to the cerebral cortex were sparse and difficult to visualize [134]. Only isolated fibers were anterogradely labeled in the cortex, and confined to the infralimbic area, after WGA-HRP and *phaseolus vulgaris*-leucoagglutinin (PHA-L) injections in the cholinergic LDT nucleus [138]. A study dealt in detail with rat "reticulocortical" systems, as disclosed by retrograde transport of fluorescent tracers or WGA-HRP, but the notion of reticular formation was extended to include monoaminergic nuclei [139].

In squirrel monkey, brainstem core neurons were labeled after HRP injections into different visual cortical areas, but they were found in "the medial portion of the formatio reticularis pontis oralis (RF) which adjoins the nucleus raphe centralis superior.... This region of the RF corresponds to that described as containing the serotonergic cell group S9..." [140]. In the chimpanzee, a similar arrangement of retrogradely labeled neurons was found in the pontine tegmentum after HRP injections in the occipital lobe (namely, coextensive with labeled neurons in the nucleus raphe centralis superior (CS)) but, in addition, HRP⁺ cells were described within the ventral midbrain reticular formation, in the triangular region between the red nucleus, SN nigra and the rootlets of the oculomotor nerve [141].

3.4.1.2. Thalamic Projections

There is a general consensus that the great majority of ascending brainstem reticular axons are synaptically relayed in the thalamus. The other, less massive, contingent is directed to the basal forebrain nuclei (see below). The thalamic projections have been investigated by using anterograde and retrograde tracing techniques, corroborated by antidromic identification experiments that provided

[135] Sakai (1985a).

[136] Tigges and Tigges (1985).

[137] Steriade *et al.* (1988).

[138] Satoh and Fibiger (1986).

[139] Newman and Liu (1987). Table 2 in that study shows that: (1) no cell, or occasionally one, was labeled in midbrain and pontine reticular cholinergic or noncholinergic nuclei (PPT pars compacta or Ch5, and both RPO and RPC nuclei; LDT nucleus was not mentioned) after retrograde tracer injections in somatosensory or visual cortices, which was in sharp contrast with about 50 to 100 labeled cells in various raphe and locus coeruleus nuclei; (2) after tracer injections in motor, premotor or cingulate cortices, the approximate ratios between labeled cells in the cholinergic or noncholinergic mesopontine reticular nuclei and those found in monoaminergic nuclei were 1/10 to 1/30; and (3) only after prefrontal injections, significant numbers of labeled cells were found in the Ch5 group (about one fifth with respect to those found in monoaminergic nuclei). [140] Tigges *et al.* (1982, p. 31). [141] Tigges *et al.* (1983).

information about axonal conduction velocities, and the cholinergic sources of these projections have been disclosed by retrograde transport techniques combined with ChAT immunoreactivity of brainstem reticular neurons.

Generally, the rostral targets of brainstem reticular neurons were thought in earlier studies to be limited to some medial, intralaminar, RE, and ZI thalamic nuclei, while major sensory and motor relay thalamic nuclei remained unlabeled in autoradiographic experiments on the pontine and mesencephalic reticular formation [142]. And, despite some indications that the brainstem PB area of the PPT nucleus projects to LG and lateral posterior (LP) nuclei of the cat visual thalamus [4, 143], the same thalamic nuclei remained unlabeled after similar midbrain injections with tritiated amino acids in the rat [134]. Since the mid-1980s there was no certain morphological evidence for brainstem reticular projections to thalamic relay nuclei [49]. Then, the facilitatory and presumed cholinergic effects induced by stimulating the midbrain reticular formation upon neurons recorded from the LG, LP, ventroposterior (VP), VL, and other thalamic relay and associational nuclei remained something of a mystery and awaited the clarification of the underlying pathways as well as their chemical signature.

We now know that: (1) cholinergic nuclei at the midbrain–pontine junction (Ch5–Ch6 groups) project to virtually all thalamic nuclei; (2) in addition to Ch5–Ch6 projections, some associational and especially intralaminar nuclei receive a massive projection from the noncholinergic (presumably glutamatergic) neurons located in the rostral midbrain FTC territory and in the rostral PRF; and (3) medullary reticular neurons also project to some medial and intralaminar thalamic nuclei.

We analyze in some detail the brainstem reticular projections to the sensory and motor relay nuclei: MG, dorsal part of the LG, VP, VM, and ventroanterior–ventrolateral (VA–VL); and to the associational pulvinar–lateroposterior (PUL–LP) and MD thalamic nuclei. The analysis of brainstem projections to some or all these nuclei was performed in studies on rat [144], cat, and macaque monkey [137]. Other studies focused on the visual thalamic nuclei of cat [14], with comparisons between cholinergic and monoaminergic projections to the LG nucleus [145].

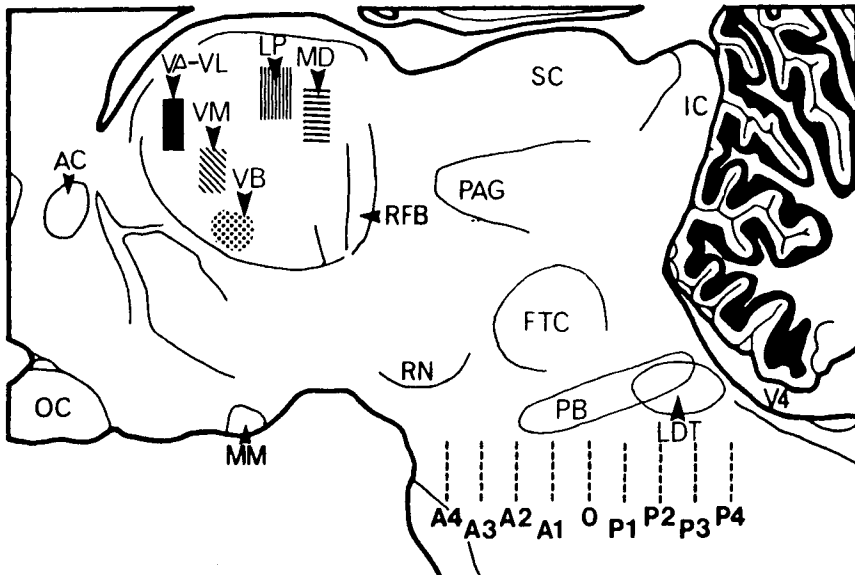
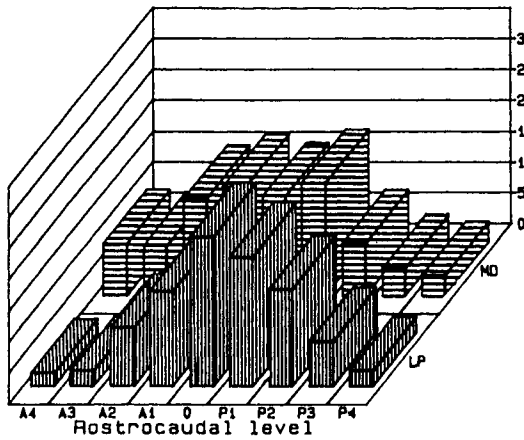
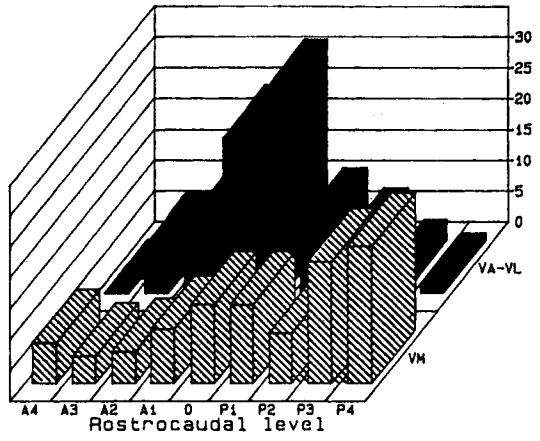
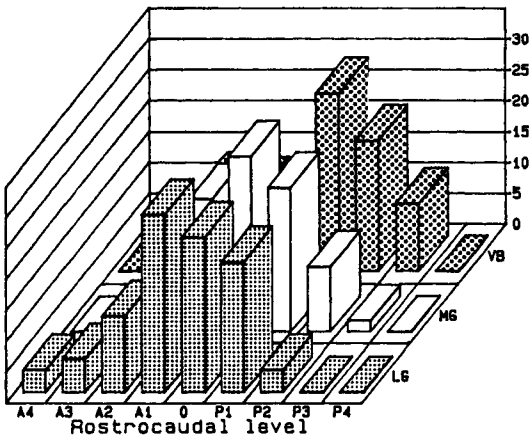
Specific relay sensory and motor (MG, LG, VP, VA–VL, VM) nuclei receive less than 10% of their brainstem reticular afferents from noncholinergic neurons located at rostral midbrain (perirubral) levels (frontal levels A4–A3 in the cat). Instead, they receive 85–95% of their brainstem afferents from a region concentrated around 3 mm, between A1 and P1, where cholinergic PPT and LDT (Ch5–Ch6) nuclei are maximally developed (Fig. 3.15; see the localization of WGA–HRP injections strictly confined

[142] Edwards and DeOlmos (1975); Robertson and Feiner (1982).

[143] Graybiel (1977a, b).

[144] Hallanger *et al.* (1987).

[145] DeLima and Singer (1987). This study used the retrograde transport of rhodamine-labeled latex spheres injected in the LG thalamic nucleus, combined with immunohistochemistry techniques for ChAT, 5-HT, and TH. These data thus provide quantitative data not only for projections arising in cholinergic nuclei, but also for projections of monoaminergic systems to the LG nucleus of cat, thus allowing a comparison between the power of these distinct brainstem systems impinging upon the principal thalamic visual relay station. There are species differences concerning these relative proportions of cholinergic and monoaminergic brainstem neurons projecting to the LG, since in rat the number of dorsal raphe neurons are at least 40% of those found in Ch5–Ch6 groups (see Table 1 in Hallanger *et al.*, 1987). At any rate, these data indicate that the thalamic projections of cholinergic nuclei by far exceed those of monoaminergic nuclei.



within the limits of relay thalamic nuclei in Fig. 2.4). The only exception to this peaked localization between A1 and P1 is the VM nucleus that receives approximately 40% of its brainstem innervation from posterior levels P3–P4. Double-staining (ChAT + HRP) in cat material revealed that the percentages of retrogradely labeled cholinergic brainstem neurons from the total number of simply HRP⁺ elements were between 73% and 87% in the case of sensory (MG, LG, VP) nuclei, and around 60% after injections in VA–VL and VM motor nuclei. The ratios between the number of double-labeled neurons in PPT (Ch5) and those in LDT (Ch6) were much higher for sensory thalamic nuclei (LG: 40; MG: 15; VP: 8) than in motor VA–VL (2) and VM (4) nuclei. And, while the afferent projections arise predominantly from the ipsilateral brainstem reticular nuclei, the contralateral projections are surprisingly high, from 20% to 40% of the ipsilateral projection [137]. Compared to the total number of retrogradely labeled ChAT⁺ cells found between stereotaxic planes A3 and P5, 5-HT⁺ neurons in the DR represent only about 10%, and TH⁺ neurons in the LC cells about 20% [145] (Fig. 3.16).

Antidromic identification studies by threshold mapping at closely spaced foci in the LG laminae also indicated that brainstem neurons with LG projections are located around the brachium conjunctivum, in the region of the Ch5 group, and the conduction velocities from the stimulated sites of the parent axons to the PPT cell bodies were estimated to be around 1–3 m/s [146].

The ChAT⁺ fibers form dense networks within the main LG laminae [147]. Since the basal forebrain does not participate to the cholinergic innervation of the LG nucleus, these cholinergic fibers probably arise in the brainstem Ch5 group (see above). In lamina A, ChAT⁺ terminals participate in synaptic contacts with the dendrites of LG relay cells in the extraglomerular neuropil, but also in the complex synaptic arrangements of glomeruli where they have access to presynaptic dendrites of local-circuit LG cells [148].

The brainstem reticular projections to thalamic associational nuclei are more massive than those to the specific

[146] Ahlsén (1984).

[147] Stichel and Singer (1985).

[148] DeLima *et al.* (1985).

Figure 3.15. Brainstem reticular (RE) projections to relay and associational thalamic nuclei in the cat. The parasagittal section shows some of the thalamic nuclei where WGA–HRP was injected and the main brainstem reticular territories where retrogradely labeled neurons were found (FTC, PB, and LDT nuclei). Frontal stereotaxic planes are indicated (A4–P4). The three computer-generated graphs show the percentage (ordinate) of HRP-positive cells at various rostrocaudal levels (abscissa) from the total number of labeled neurons in the upper brainstem reticular core. For abbreviations of thalamic nuclei, see text. Other abbreviations: AC, anterior commissure; IC, inferior colliculus; MM, medial mammillary nucleus; OC, optic chiasm; PAG, periaqueductal gray; RFB, retroflex bundle; RN, red nucleus; SC, superior colliculus. From Steriade *et al.* (1988).

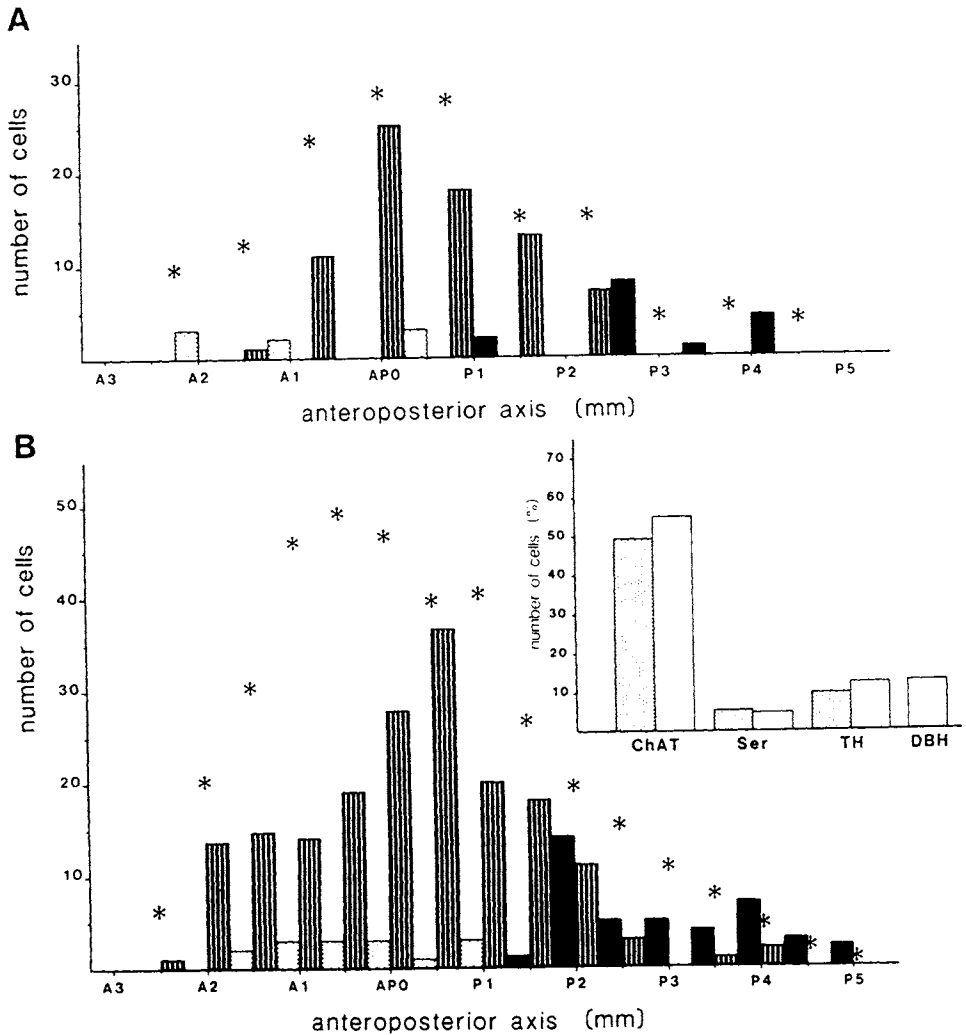


Figure 3.16. Brainstem cholinergic and monoaminergic projections to the lateral geniculate (LG) thalamic nucleus in the cat. A, histogram quantitatively representing the distribution of all double-labeled cells in the anteroposterior axis. Each bar corresponds to the number of cells in one section. Punctuated bars correspond to serotonergic double-labeled cells; black bars correspond to noradrenergic (TH⁺) cells; and black-and-white bars correspond to cholinergic (ChAT⁺) cells. The crosses indicate the mean of the total retrogradely labeled cells in the immunostained adjacent sections. B, histograms indicating the proportion of double-labeled cells in each series of immunostained sections relative to the total retrogradely labeled cells in the respective series. Punctuated and white bars represent the results of two experiments. ChAT, choline acetyltransferase; Ser, serotonin; TH, tyrosine hydroxylase; DBH, dopamine-beta-hydroxylase. TH and DBH probably labeled the same population of cells. Modified from DeLima and Singer (1987).

relay nuclei. WGA-HRP injections in the PUL-LP or MD nuclei of cat led to 3 to 8 times more retrograde cell labeling in the brainstem core than the injections into the relay nuclei. By contrast to the LG projection that arises almost exclusively in the Ch5 group, the LP nucleus receives an important projection from both Ch5 and Ch6 groups [14] (Fig. 3.17). The ratio between retrogradely labeled cells in

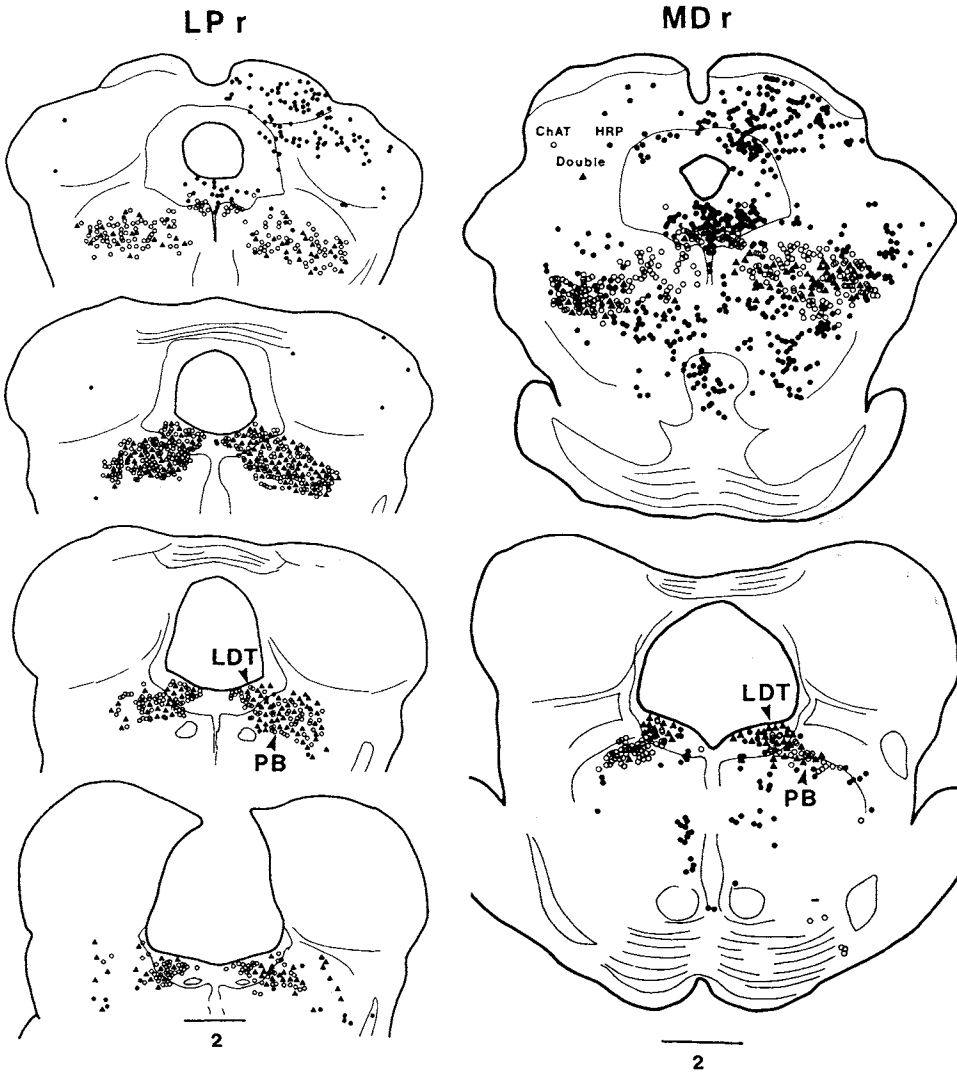


Figure 3.17. Cholinergic and noncholinergic brainstem reticular (RE) projections to the right latero-posterior (LP) and mediodorsal (MD) nuclei in the cat. In the LP case, four levels at stereotaxic planes A1, P0.5, P1, and P2.5. Three types of neurons are represented (ChAT⁺, HRP⁺, and double labeled; see symbols in top section of the MD case), as found on one section after combining the TMB procedure for retrogradely labeled WGA–HRP with ChAT immunohistochemistry. In the MD case, same type of graph as for LP nucleus, but each of the two drawings represents labeled cells found on two sections. Camera lucida localization. LP, modified from Smith *et al.* (1988). MD, modified after Steriade *et al.* (1988).

the Ch5 and Ch6 groups was 40 in the case of LG, while it was 2 in the case of the LP injection. In monkey too, the projection to the PUL–LP thalamic complex arises in cholinergic neurons of the medial part of Ch5 and the adjacent Ch6 group [137]. As to the brainstem–MD massive projection, it is not accounted for by a greater contribution from PPT and LDT cholinergic nuclei, but by the massive labeling in noncholinergic parts of the midbrain

and rostral PRF (Fig. 3.17). Moreover, numerous cells in the periaqueductal gray project to MD in both cat and monkey. Note that the rich innervation of MD with ChAT⁺ fibers [149] does not exclusively originate in the brainstem, since MD as well as a limited number of other thalamic nuclei receive a cholinergic innervation from the basal forebrain [150, 151] (see below).

While brainstem reticular projections to relay thalamic nuclei modulate the synaptic transmission of impulses from various sensory and motor modalities, the projections to intralaminar and reticular nuclei are involved in generalized processes of activation and oscillation in thalamocortical systems. The caudal intralaminar (CM–PF) nuclei are essentially related to the striatum. In addition to their efferent connections to the caudate nucleus, the rostral intralaminar (CL–PC) neurons project over widespread cortical territories where they exert depolarizing actions and thus represent an important link in the activating circuit from the brainstem reticular formation to the cerebral cortex. The reticular thalamic nucleus is a pacemaker of spindle oscillations and the main source of long-range inhibition of thalamocortical neurons during slow-wave sleep (see Chapter 7). The brainstem cholinergic projections to the reticular nucleus are an important factor in the disruption of synchronized spindle oscillations upon arousal. ZI, which is sometime included in the subthalamic region, has the same developmental history as the reticular nucleus, both originating from the ventral thalamus. The anterior (anterodorsal–anteroventral–anteromedial, AD–AV–AM) nuclei project over the whole limbic cortex (anterior and posterior cingulate gyri, retrosplenial gyrus, pre- and parasubiculum) and are part of a basically different network than most dorsal thalamic nuclei, as they are interposed in the circuit between the hippocampus, mammillary nuclei, and the cingulate cortex.

All brainstem reticular fields, from the medulla to the rostral midbrain, send projections to the CM–PF and CL–PC intralaminar nuclei. This is quite different from the brainstem reticular innervation of most specific relay nuclei that receive afferents almost exclusively from the circumscribed brainstem region of Ch5–Ch6 groups (see Fig. 3.15). The contribution of the whole brainstem reticular formation to the afferentation of intralaminar thalamic nuclei, already indicated in axonal degeneration studies and in early autoradiographic experiments, was repeatedly confirmed. Thus, in anterograde and retrograde transport experiments, the source of afferents to CM–PF and CL–PC nuclei was found not only in the upper brainstem reticular core, but also in rostral and caudal pontine reticular nuclei, and in medullary reticular Gc and Mc fields. By

[149] Levey *et al.* (1987a).

[150] Steriade *et al.* (1987b).

[151] Parent *et al.* (1988).

[152] Vertes *et al.* (1986).

contrast, few of the projections from the medullary Pc nucleus ascend beyond the mid-pons [82, 134, 152]. Antidromic identification experiments revealed that: (1) the midbrain-to-intralaminar axons conduct between 3.5 and 4.6 m/s [46], in keeping with the small-sized neurons in the mesencephalic FTC; (2) the larger pontine reticular neurons project to intralaminar nuclei with conduction velocities around 7 m/s [24]; and (3) Gc and Mc bulbar reticular neurons project to intralaminar nuclei with conduction velocities of 20 m/s and 7–14 m/s, respectively, also as a function of the larger size of Gc, compared to Mc, neurons [26].

[153] Wiklund and Cuénod (1984).

The cholinergic nature of brainstem reticular projections from the PPT and LDT nuclei to intralaminar nuclei was revealed by a series of methods. Transmitter specific labeling was used to investigate the retrograde transport of ^3H -choline from CM–PF nuclei mainly to PPT and LDT nuclei of rat [153]. In the opposite sense, the anterograde labeling of LDT projections to PF and more rostral (CL–PC) intralaminar nuclei was shown after injections of WGA–HRP and PHA-L [138]. The demonstration of brainstem cholinergic projections to both (caudal and rostral) components of the intralaminar nuclei was achieved by combining the retrograde transport of HRP or fluorescent tracers with ChAT immunohistochemistry in rat [144, 154], cat [20], and dog [155].

[154] Woolf and Butcher (1986).

[155] Isaacson and Tanaka (1986).

The considerably more numerous brainstem reticular neurons labeled after WHA–HRP injections into the cat CM–PF nuclei or CL–PC nuclei, as compared to the number of brainstem reticular cells labeled after injections in relay sensory and motor thalamic nuclei, result from a dissimilar distribution of retrogradely labeled neurons. In addition to massive projections from the Ch5–Ch6 groups, the intralaminar nuclei receive a substantial proportion of afferents from noncholinergic neurons in the rostral mid-brain (planes A4–A3) and in the paramedian rostral PRF [20] (Figs. 3.18 and 3.19). In rat too, there were 2 or 3 times more numerous cells labeled in midbrain FTC and PRF, than in Ch5–Ch6 groups, after WGA–HRP injections in CM or CL thalamic nuclei [144]. The noncholinergic neurons labeled in the periaqueductal gray after the CM injection (Fig. 3.19) may use aspartate as synaptic transmitter, since injections of ^3H -aspartate into the CM–PF nuclear complex leads to retrograde labeling in the small-sized cells of the midbrain periaqueductal gray [153]. The axons of Ch5 cells form asymmetrical synaptic contacts with dendrites of CM–PF and CL neurons [156].

[156] Sugimoto and Hattori (1984).

The distribution and amount of retrogradely labeled brainstem reticular neurons after WGA–HRP injections in the rostral pole or rostromedial districts of cat reticular thalamic nucleus are similar to those found after tracer injections

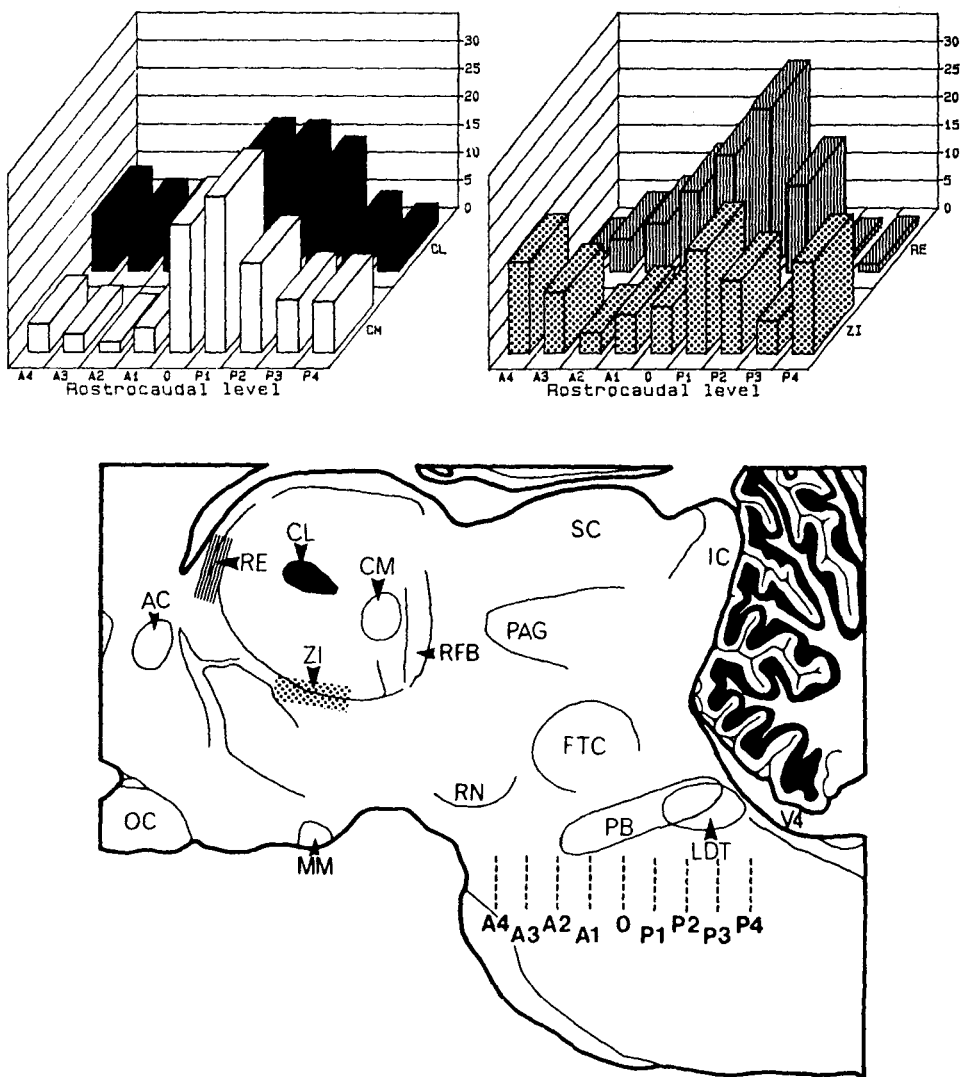


Figure 3.18. Brainstem reticular projections to intralaminar, reticular (RE), and ZI thalamic nuclei of cat. The parasagittal section shows the thalamic nuclei where WGA-HRP was injected (CM-PF, CL-PC, rostral pole of RE, and ZI) and the main brainstem territories where retrogradely labeled neurons were found (FTC, PB, and LDT). Frontal stereotaxic planes are indicated (A4–P4). The two computer-generated graphs at top show the percentage (ordinate) of HRP⁺ cells at various rostrocaudal levels (abscissa) from the total number of retrogradely labeled elements in the brainstem core. Note that the peak of retrogradely neurons is at A0–P2 for the CM–PF and reticular injections, that a significant proportion of cells was found at most rostral level (A4) of the midbrain in the case of the CL–PC injection, and that three peaks were found after the ZI injection (at A4–A3, P1–P2, and P4). For abbreviations, see legend of Fig. 3.15. From Paré *et al.* (1988).

in relay nuclei (Fig. 3.18). Of all retrogradely labeled neurons in the brainstem reticular core, 50% were also ChAT⁺. The demonstration of a substantial brainstem cholinergic and noncholinergic projection to the rostral reticular nucleus in both rat [144, 154] and cat [20] settles the controversial issue of interspecies differences between rat and cat

819—CM

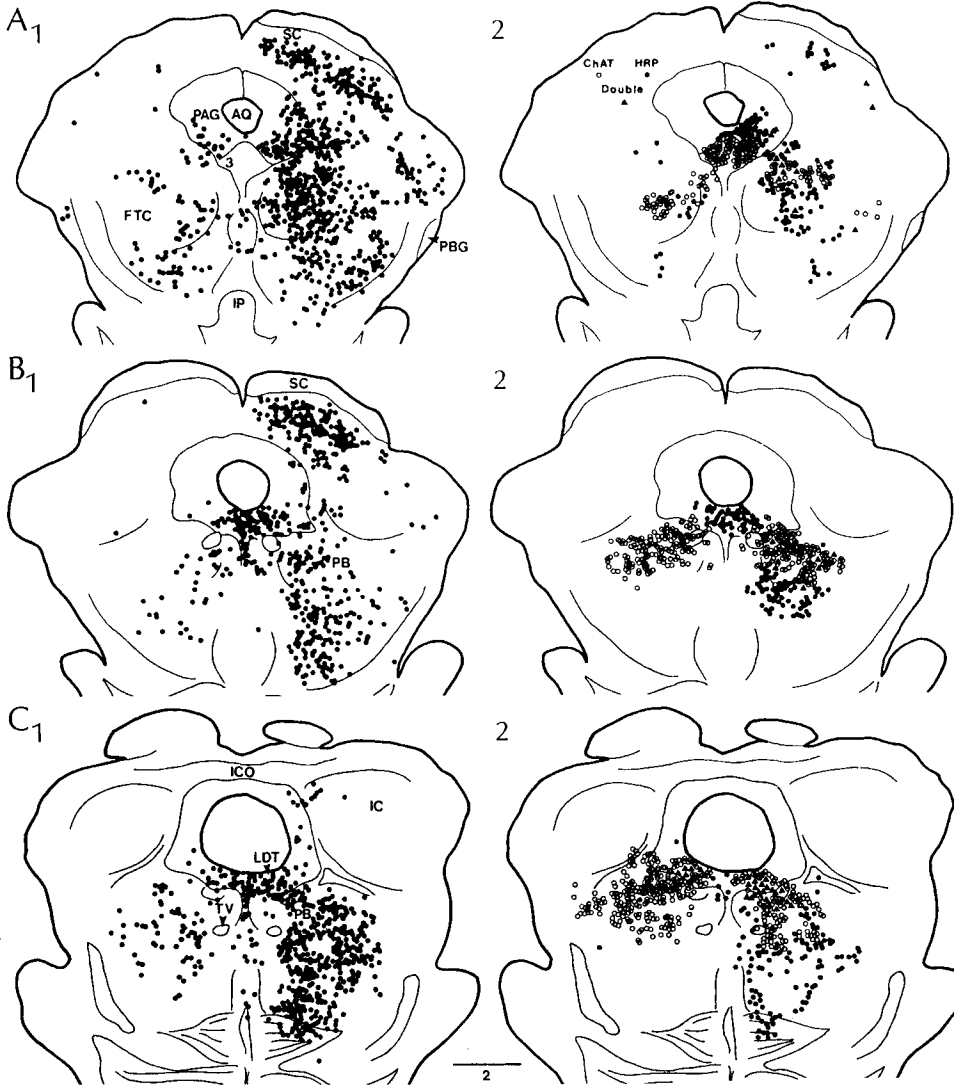


Figure 3.19. Cholinergic and noncholinergic brainstem core neurons projections to the right CM–PF thalamic nuclei of cat. A, B, and C, three levels, from rostral to caudal. At each level, left column depicts the total number of retrogradely labeled neurons as found in five successive sections after TMB procedure counterstained with Neutral Red. Right column depicts the same levels, with the three types of cells (ChAT^+ , HRP^+ , and double labeled; see symbols in A2), as found in two sections after TMB procedure combined with ChAT immunohistochemistry. Right part in brainstem drawings ipsilateral to thalamic injection. From Paré *et al.* (1988).

related to the reticular thalamic nucleus (see Section 3.1.3.1). In addition, WGA–HRP injections confined within the limits of the perigeniculate (PG) part of the reticular nucleus result in retrograde labeling in PPT and LDT nuclei, with 73% of PPT neurons being also ChAT^+ [14] (Fig. 3.20). Antidromic identification studies [146] revealed that, of three PPT cell types encountered, one

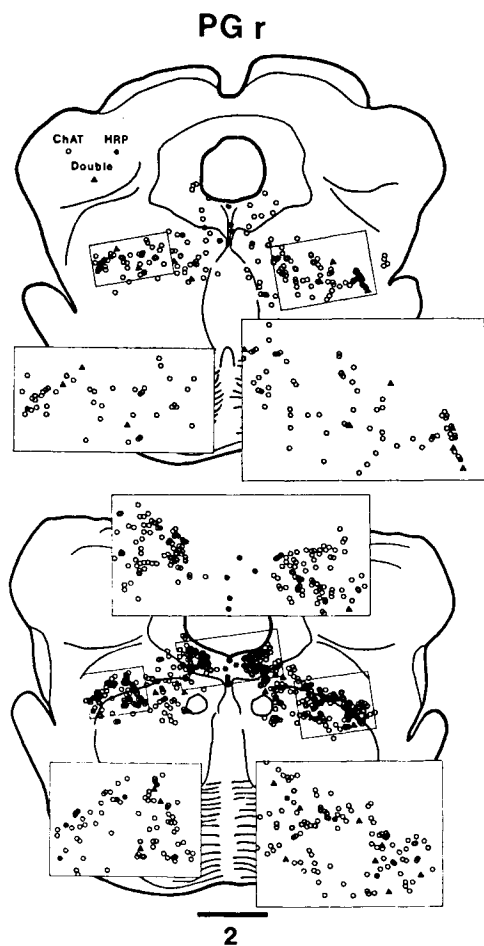


Figure 3.20. Cholinergic and noncholinergic brainstem reticular (RE) cells projecting to the right perigeniculate (PG) sector of the reticular nuclear complex of cat. Localization of WGA–HRP injection in PG is depicted in the microphotograph of Fig. 2.4 in Chapter 2. LG, lateral geniculate nucleus; OT, optic tract. Two levels (A1 and P0.5) with the three cell types (ChAT⁺, HRP⁺, and double labeled; symbols in top drawing) as found on one section (WGA–HRP procedure combined with ChAT immunohistochemistry). Localization of cells by means of a computer-assisted microscope. The areas delimited by rectangles are shown at higher magnification. Modified after Smith *et al.* (1988).

sends axons exclusively to the LG nucleus, another to the PG nucleus (and/or to the overlying reticular sector subserving the PUL-LP thalamic nuclei), while a third group projects to both LG and PG nuclei, being then probably involved in the control of intrinsic LG inhibitory processes as well as the control of the recurrent inhibitory loop between PG and LG (Fig. 3.21).

The upper brainstem core projections to ZI have been shown with anterograde [142] and retrograde [157] transport techniques and in electrophysiological experiments [158]. The territory of origin for brainstem–ZI axons extends up to the PRF, but this projection exclusively arises from small- and medium-sized pontine reticular cells;

[157] Shammah-Lagnado *et al.* (1985).

[158] Steriade *et al.* (1982b).

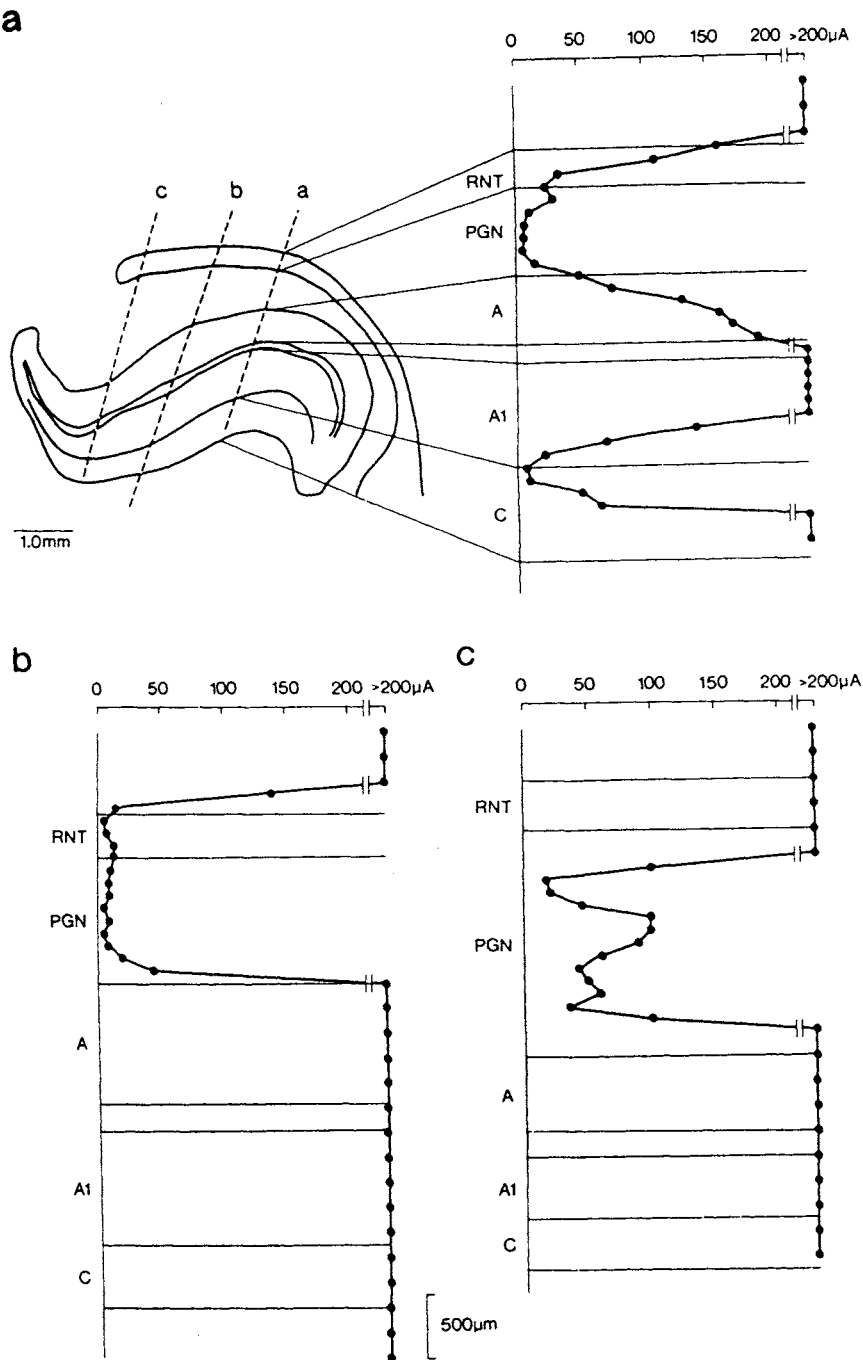


Figure 3.21. Antidromic identification of a brainstem peribrachial (PB) neuron with projections to the laminae A1 and C of the lateral geniculate (LG) nucleus, the perigeniculate nucleus (PGN) and the sector of the reticular thalamic nucleus (RNT) located dorsally to the PGN. Threshold mapping; stimulus intensities indicated at top, in each of the three microelectrode penetrations (a, b, and c). Note different types of axonal termination in three microelectrode tracks: in RNT, PGN, and A1/C interlaminar plexus (a); in RNT and PGN (b); and only in PGN (c). From Ahlsén (1984).

no giant cell was found retrogradely labeled after tracer injections in ZI, much the same as after injections in intralaminar thalamic nuclei [20].

The AD–AV–AM nuclear group receives projections from cholinergic and noncholinergic neurons of the upper brainstem reticular core. The anterior thalamic complex in cat is heavily afferented from the Ch6 group [137]. Indeed, the ratio between Ch5- and Ch6-labeled neurons after a WGA–HRP injection into AV–AM nuclei is 1, while for all other thalamic nuclei such ratios range from 2 to 40. Moreover, in rat the number of labeled Ch6 cells outnumbers that in the Ch5 group [144, 154].

The final corticopetal link of brainstem–thalamic projections was demonstrated by antidromic activation of thalamic intralaminar (CL–PC) neurons from cortex and their orthodromic, monosynaptic excitation from the brainstem reticular core. This has been achieved in unanesthetized animals in which the pontine tegmentum was chronically lesioned to allow degeneration of passing fibers through the stimulated PPT region [159] (Fig. 3.22).

Such circuits probably exist for all cortically projecting neurons in the dorsal thalamus since there are brainstem reticular projections from Ch5–Ch6 groups to virtually all thalamic nuclei and, for many nuclei, additional projections arise from the noncholinergic FTC, rostral pontine, medullary Gc and Mc fields. These ascending fibers must have access to cortically projecting thalamic neurons because they represent at least 70% of thalamic neurons in cat, and reach much higher proportions in the rat.

While specific relay thalamic nuclei project over relatively circumscribed cortical territories, especially to mid-layers IV–III or with a trilaminar pattern (including minor projections to layer VI or I), two groups of nuclei project diffusely over the neocortex: the intralaminar CL–PC over layer I and VI, and the VM nucleus to the outer third of layer I [160].

The cortical projections of CL–PC and VM nuclei represent the required substratum for the generalized activation of cortical processes by stimulating the rostral reticular core, since both rostral intralaminar and VM thalamocortical nuclei receive massive projections from

[159] Steriade and Glenn (1982).

[160] Herkenham (1979); Glenn *et al.* (1982); Cunningham and LeVay (1986).

Abbreviations: CeM, Rh, VM, and VPM, central medial, rhomboidal, ventromedial, and ventroposteromedial thalamic nuclei. F, electrophysiological identification of CL–PC thalamic cells. 1 and 2, two different neurons, antidromically activated from the internal capsule (IC), motor cortex (MC), or parietal cortex (PC), and synaptically driven from MRF. Stimulus artifacts marked by arrowheads. In 2, only first stimulus of MC 3-shock train at 250/s is marked; arrow indicates fractionation of antidromically elicited discharges to last stimulus in MC train. Collision between cortically elicited antidromic spikes and MRF-evoked synaptic discharges shown in right superimposition (1) and in 10-sweep sequence (in 2). Modified from Steriade and Glenn (1982) and Glenn and Steriade (1982).

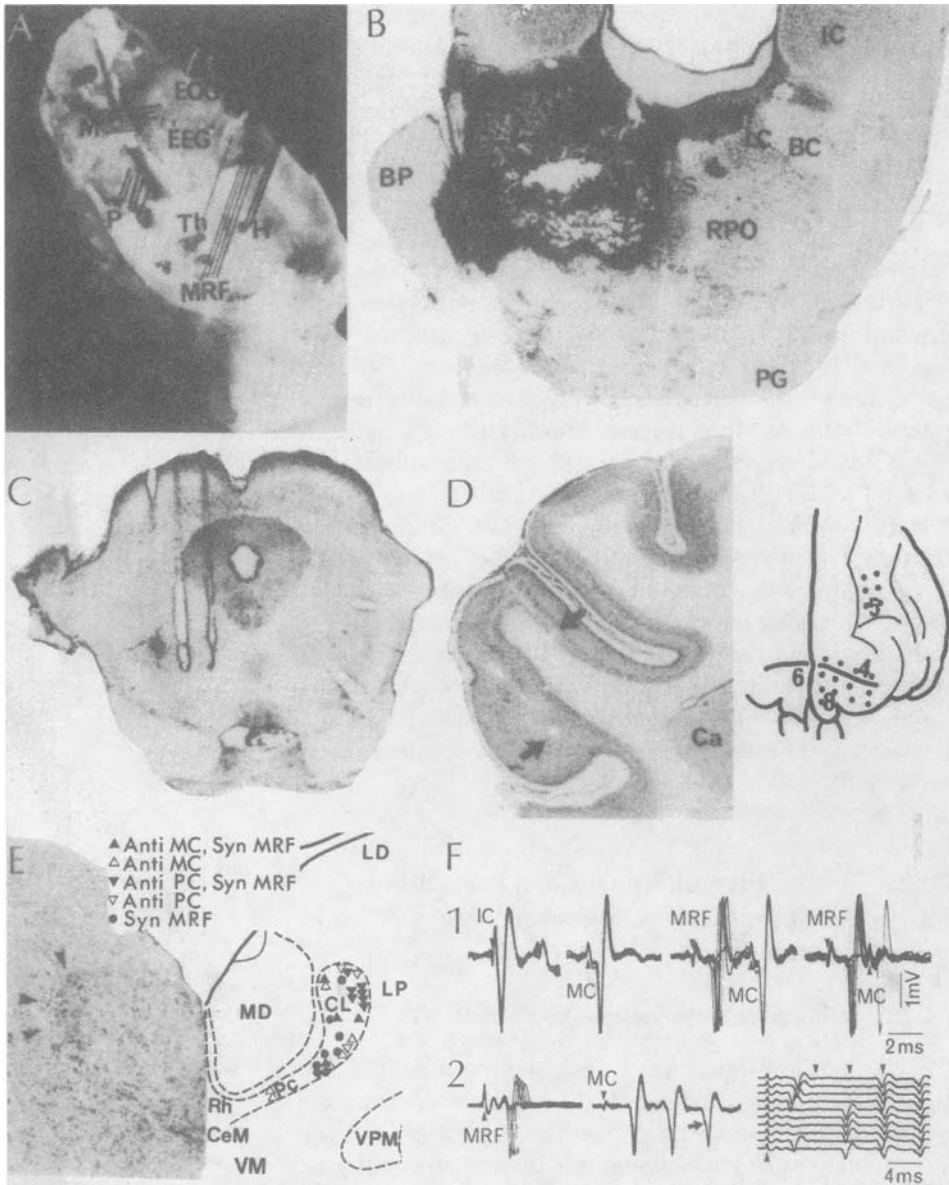


Figure 3.22. Neocortical projections of intralaminar thalamic neurons and their monosynaptic excitation from upper brainstem reticular (RE) core in cat. A, calvarium with last recording thalamic microelectrode (Th) and chronically implanted stimulating electrodes in pericruciate motor cortex (M), parietal association cortex (P), and midbrain reticular formation (MRF). EOG and EEG, silver balls for recording eye movements and EEG rhythms; H, electrodes for recording hippocampal rhythms. B, lesion of the ipsilateral pontine tegmentum for chronic degeneration of ascending systems coursing through MRF. Abbreviations: BC, brachium conjunctivum; BP, brachium pontis; CS, nucleus raphe centralis superior; IC, inferior colliculus; LC, locus coeruleus; PG, pontine gray; RPO, nucleus reticularis pontis oralis. C, array of stimulating electrodes in the caudal part of the MRF, within the peribrachial (PB) area of the pedunculopontine nucleus; the most lateral electrode track was found in an anterior section. D, location of precruciate stimulating electrodes within deep layers of medial parts of areas 8 and 6. In the diagram, black dots indicate the whole territory of pericruciate and anterior suprasylvian gyri (various cytoarchitectonic areas are indicated). E, location of a sample of CL-PC thalamic neurons. *Anti* and *Syn*, antidromic and synaptic responses to stimulation of motor cortex, parietal cortex, and MRF.

the brainstem reticular core, their neurons make asymmetrical synaptic contact with dendritic shafts and spines of cortical neurons, and exert depolarizing actions upon their targets [161]. The excitatory nature of thalamocortical neurons is also ascertained by retrograde labeling with transmitter-related compounds indicating that they use aspartate as synaptic transmitter [162].

As to the diffuseness of the intralaminar–cortical projection, it concerns the rostral intralaminar CL–PC nuclei as a whole. By contrast, double-labeling experiments [163] and antidromic identification studies [159] indicate that a very small proportion of individual CL or PC neurons project to more than one cortical region, or to both the caudate and the cerebral cortex. About 20% of single VM neurons that project to the insular (anterior sylvian) cortex send axon collaterals to the precruciate (motor) fields, but very few branched cells were found in other combinations of cortical areas examined [164].

Finally, a series of studies have demonstrated that the axon of the same mesopontine cholinergic neuron innervates more than one thalamic target [165], some neurons innervate both thalamic reticular neurons and related thalamocortical cells [166], and some brainstem cholinergic neurons have dual projections to the thalamus and the basal forebrain [167].

[161] Donoghue and Ebner (1981); Endo *et al.* (1977).

[162] Streit (1980); Ottersen *et al.* (1983).

[163] Bentivoglio *et al.* (1981); Macchi *et al.* (1984).

[164] Minciacchi *et al.* (1986).

[165] Shiromani *et al.* (1990).

[166] Spreafico *et al.* (1993).

[167] Losier and Semba (1993).

3.4.2. Brainstem and Spinal Cord Projections of Mesopontine Cholinergic and Pontobulbar Nuclei

3.4.2.1. Cholinergic Projections to Pontine FTG

The natural source of cholinergic input to PRF is of interest for the physiology of REM sleep because microinjection of cholinergic drugs into the PRF of the cat activates a state that has, depending on the injection site, either all or some of the components of natural REM sleep, which include rapid eye movements, PGO waves, and a suppression of postural muscle tone with superimposed distal muscle twitches (see Chapters 10–11).

The LDT and PPT both provide cholinergic projections to the cat PFTG [168]. Neurons of the LDT and PPT were double labeled utilizing ChAT immunohistochemistry combined with retrograde transport of horseradish peroxidase conjugated with wheat germ agglutinin (WGA–HRP; Fig. 3.23). In LDT the percentage of cholinergic neurons retrogradely labeled from PFTG was 10.2% ipsilaterally and 3.7% contralaterally, while in PPT the percentages were 5.2% ipsilaterally and 1.3% contralaterally

[168] Mitani *et al.* (1988c)

(Fig. 3.24). Double-labeled neurons were observed throughout the rostral-caudal extent of the LDT and PPT, and no apparent preferential topographic localization was observed in those nuclei. These projections and their relative density have been recently confirmed in a double-labeling study [169].

The above study [168] also used (PHA-L) antero-grade transport technique to show that PHA-L-positive fibers projecting from LDT into the PFTG spread ventrally

[169] Shiromani *et al.*
(1988a).

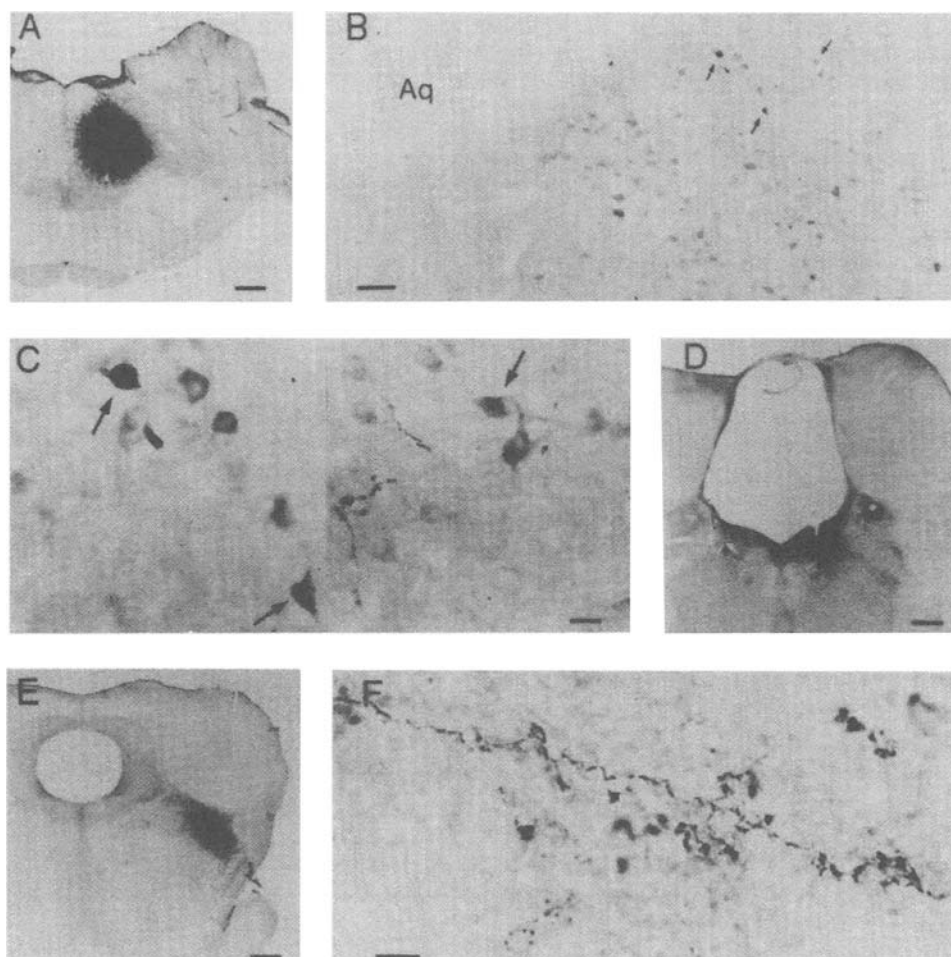


Figure 3.23. Projections of mesopontine cholinergic nuclei to the gigantocellular (Gc) field of the PRF. A, site of WGA-HRP injection in the pontine gigantocellular tegmental field (PFTG) of the cat. B, double-labeled neurons (solid arrows) with both ChAT immunoreactivity and retrogradely transported WGA-HRP were found in the LDT together with neurons stained only for ChAT. C, higher magnification of three double-labeled neurons shown in upper part of B. Note the black granular HRP reaction product in the double-labeled ChAT-positive neurons (solid arrows), but not in the single-labeled ChAT-positive neurons near them. D, photograph of PHA-L injection site in the laterodorsal tegmental nucleus. E, PHA-L injection site in the pedunculopontine nucleus (pars compacta). F, labeled fine axons and bouton-like varicosities in the ipsilateral PFTG after PHA-L injection into the laterodorsal tegmental (LDT) field. Calibration bars: A, D, E = 1 mm. B = 0.1 mm. C = 0.02 mm. F = 0.01 mm. Abbreviation: Aq, cerebral aqueduct. From Mitani *et al.* (1988d).

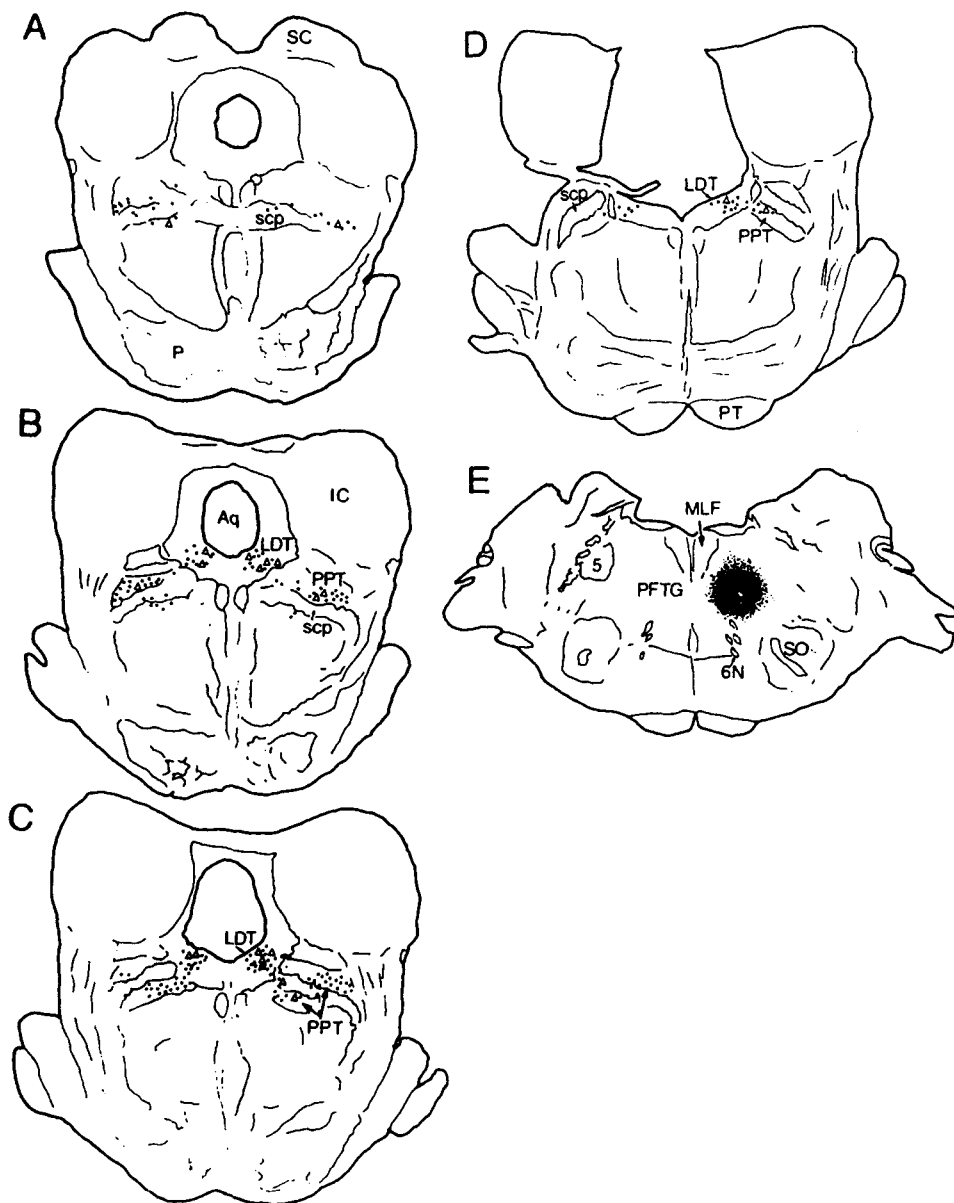


Figure 3.24. The distribution of LDT and PPT neurons double labeled with both retrogradely transported WGA-HRP and ChAT immunocytochemistry (open triangles), and single-labeled with ChAT immunocytochemistry (black dots) after PFTG injection of WGA-HRP (A to D). E, representation of the PFTG injection site of WGA-HRP. Abbreviations: IC, inferior colliculus; LDT, laterodorsal tegmental nucleus; MLF, medial longitudinal fasciculus; P, pontine nuclei; PFTG, pontine gigantocellular tegmental field; PPT, pedunculopontine tegmental nucleus; PT, pyramidal tract; SC, superior colliculus; scp, superior cerebellar peduncle; SO, superior olive; 5, trigeminal nucleus; 6N, abducens nerve. From Mitani *et al.* (1988d).

from the injection site and enter the ipsilateral PFTG, while some crossed the midline and entered the contralateral PFTG (Fig. 3.25, part 1). PHA-L-positive fibers and varicosities were also observed in the raphe nucleus and

contralateral LDT. The PHA-L positive fibers from PPT injections course ventromedially from the injection site and enter the ipsilateral PFTG, while some cross the mid-line and enter the contralateral PFTG (Fig. 3.25, part 2). On both sides of the PFTG, the PHA-L-positive fibers from both LDT and PPT give rise to bouton-like varicosities (see Fig. 3.23 F), suggestive of termination within the PFTG.

As measured by the percentage of double-labeled cholinergic neurons, the density of cholinergic LDT to PFTG projections observed appears to approximate that of cholinergic LDT to thalamus projections in rat [144] where, ipsilaterally, a mean of 10% of ChAT-positive LDT neurons were double labeled after WGA-HRP injections

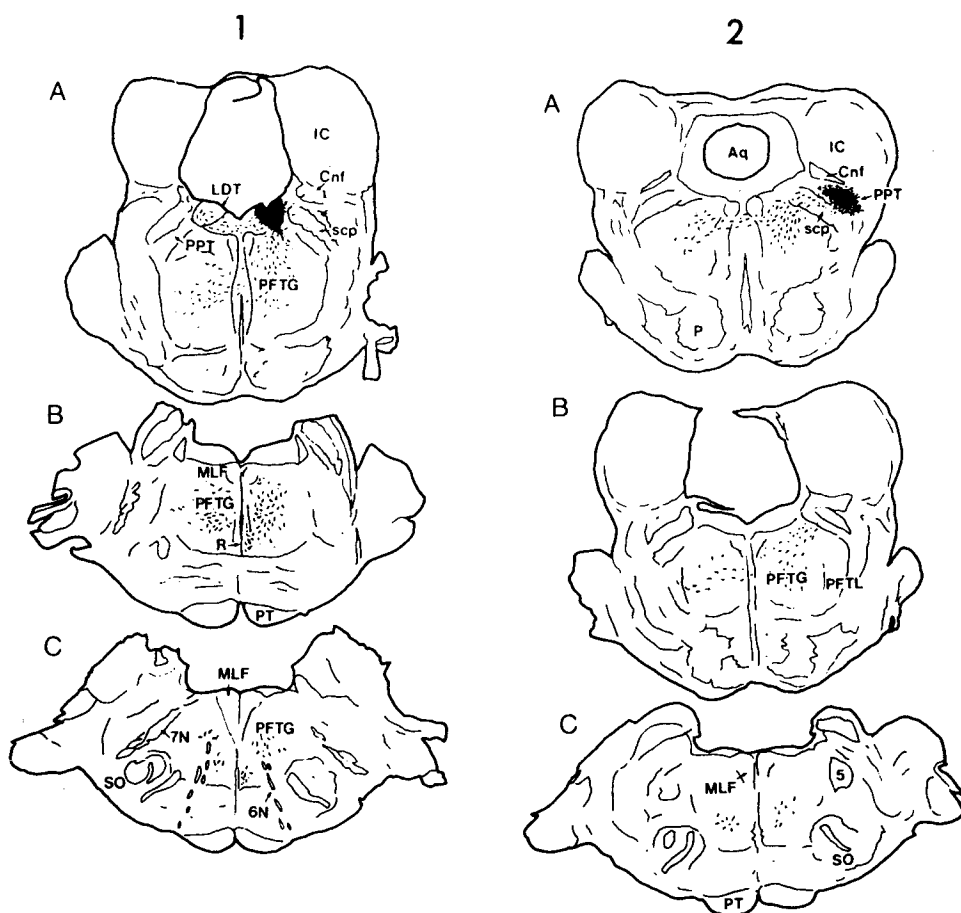


Figure 3.25. Part 1 (left column): distribution of labeled fibers and terminals (broken lines) after an iontophoretic injection of PHA-L into the laterodorsal tegmental (LDT) nucleus in the cat. Injection site is represented in A. Abbreviations: Cnf, cuneiform nucleus; R, raphe nucleus; 7N, facial nerve. Part 2 (right column): distribution of labeled fibers and terminals (broken lines) after an iontophoretic injection of PHA-L into the pars compacta of the pedunculopontine tegmental nucleus (PPT). Injection site is represented in A. Abbreviation: PFTL, pontine lateral tegmental field. From Mitani *et al.* (1988d).

of comparably small size in thalamus, as compared with the ipsilateral percentage of about 10% in the LDT–PFTG study in cat [168]. Cholinergic PPT to PFTG projections appear to be somewhat less dense than described for PPT to thalamus in rat, where ipsilateral double-labeling averaged 22% of PPT neurons (range 3–47%) [144]. While the basic techniques of injection, processing, and counting were similar in the cat and rat studies, the percentages should, of course, be taken only as approximate comparisons of projection strengths, since the species were different and the size of WGA–HRP injections in the zones of interest varied.

These cholinergic inputs to PFTG are likely form the basis of induction of REM sleep by PFTG neostigmine injections [170] that presumably act through the ACh released by these inputs. Pathology of these projections may be responsible for the abnormalities of muscarinic receptor binding in PFTG observed in canine narcolepsy [171] (see Chapter 13). As will be discussed later, these LDT/PPT projections may be important in the induction and maintenance of various components of normal REM sleep and of other behavioral states. The presence of LDT/PPT projections to other pontine reticular nuclei remains to be determined.

[170] Baghdoyan *et al.* (1985).

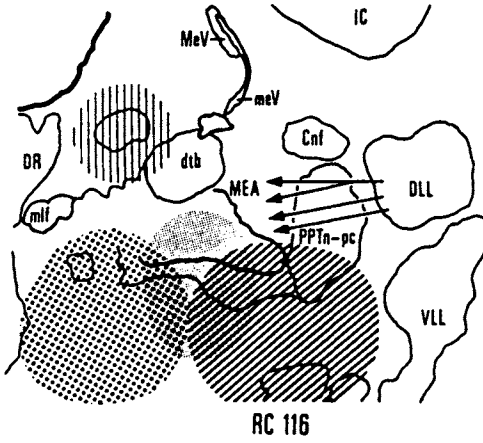
[171] Boehme *et al.* (1984).

3.4.2.2. Bulbar and Spinal Cord Cholinergic Projections

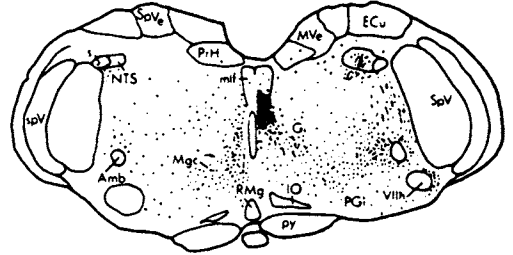
Utilizing autoradiographic anterograde tracing and retrograde HRP/WGA–HRP techniques in conjunction with ChAT immunohistochemistry, a study in the rat has characterized the bulbar and spinal efferents from the mesopontine junctional region that includes the cholinergic PPT nucleus and the noncholinergic mesopontine tegmentum [76]. Figure 3.26 summarizes the anatomy of this region and the major descending pathway. The major

Figure 3.26. Five major descending pathways of the dorsolateral tegmentum in the rat. Part A shows anatomy at tritiated amino acid injection site of RC116 as indicated by heavy oblique lines; other shadings in inset correspond to other injection sites. Note the position of the pedunculopontine tegmental nucleus-pars compacta (PPTn-pc) and midbrain extrapyramidal area (MEA); arrows indicate fascicles of the commissure of the lateral lemniscus (DLL). Parts B–H show the five major descending pathways: (1) Probst's tract descending in the dorsolateral reticular (RE) formation in close relation to the nucleus of the solitary tract (NTS, D–G). (2) A ventrolateral (VL) branch of Probst's tract that extends ventrolaterally alongside the spinal trigeminal nucleus (SpV, C–G). (3) A ventromedial (VM) branch of Probst's tract that extends ventromedially throughout the gigantocellular field of the medulla (Gi) (C–G). This Ventromedial (VM) branch is often termed the "lateral tegmentoreticular tract" and contains fibers thought to be important in the muscle atonia of REM sleep (see Chapter 11). (4) The medial reticulospinal tract which descends in parallel with the medial longitudinal fasciculus (MLF) (C–E), and turns ventrolaterally along the dorsal surface of the inferior olive (F–G) to enter the VL funiculus of the spinal cord. (This pathway arises primarily from pontine tegmental fields, including the gigantocellular field (GC)). (5) A crossed VM pathway which descends in a ventral paramedian position through the magnocellular (Mc) field of the medulla (Mgc) (B–E). All except the crossed VM pathway were labeled bilaterally with a strong ipsilateral predominance. Calibration bar = 0.5 mm for A and 1 mm for B–H. Modified from Rye *et al.* (1988).

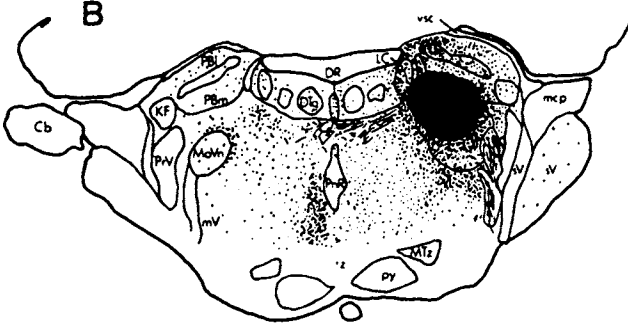
A



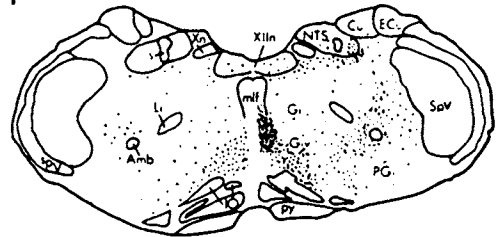
E



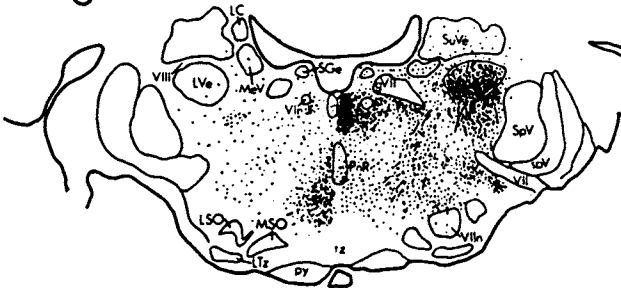
B



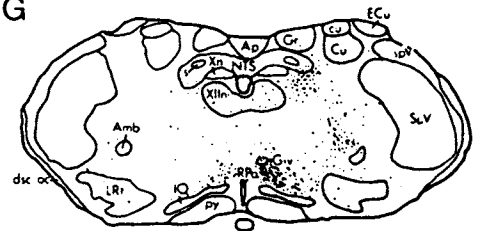
F



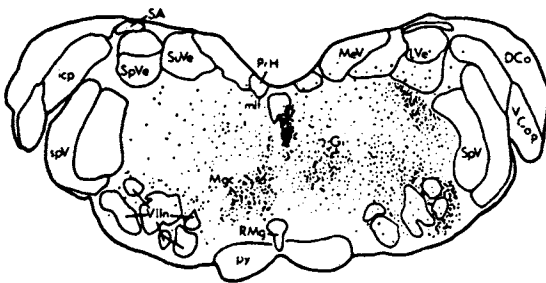
C



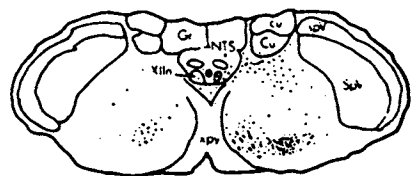
G



D



H



descending pathway is termed as Probst's tract [172]. The VM branch of this tract courses through the pons to bulb where its fibers distribute to the ipsilateral bulbar Gc field. This VM branch closely corresponds to the "lateral tegmentoreticular tract" [173] and is physiologically important because of its role in the postural atonia in sleep [174]. Intracellular studies [175] have characterized a portion of the BFTG as involved in muscle atonia during REM sleep. A VM pathway crosses the midline shortly after origin and descends in a ventral paramedian position through the contralateral bulbar Mc field, but this crossing cholinergic pathway is apparently not critical for REM atonia [76]. Most of the spinal projections of this mesopontine zone arise from the noncholinergic midbrain extrapyramidal area, but no cholinergic neurons project to spinal cord. Retrograde HRP studies suggest the spinal fibers arising from this zone course in the lateral funiculus (LF) [176].

The PPT cholinergic projection to bulbar reticular formation to be dense, with 18% of the cholinergic PPT neurons double labeled after a BFTG injection of WGA-HRP, with an ipsilateral:contralateral ratio of about 2:1 [76]. Although those authors did not describe LDT as a significant source of projections to bulbar reticular formation, their Fig. 12 indicates that at least 12 LTD neurons were double labeled after an injection centered in BFTG, approximately 10% of the PPT double labeling on the same sections. The crossed cholinergic PPT projection to the MC bulbar nucleus was about one fourth as dense as that of the ipsilateral PPT to BFTG projection. This study did not evaluate the density of cholinergic projections to other bulbar reticular nuclei.

3.4.2.3. Brainstem and Spinal Cord Projections of the Noncholinergic Pontobulbar Reticular Formation

Anatomical advances have clearly characterized the descending pathways from the giant-cell field portion of the pons (PFTG) and bulb (BFTG), and have made it apparent that particular pathways arise preferentially from reticular elements of different size. It is consequently useful to follow this division in discussion of the pathways, for which we will present only the major projections, which are epitomized in Fig. 3.27.

Before going into a more detailed description, we believe it is useful to provide the following overview. Large and giant neurons form the predominant source of the descending projections in the MLF in both the pontine

[172] Probst's tract descends in the dorsolateral reticular formation in close apposition to the nucleus of the solitary tract (Fig. 3.26) and has several branches.

(1) A ventrolateral branch of Probst's tract courses alongside the spinal trigeminal nucleus and is the primary projection pathway of the parabrachial nucleus, particular the Kölliker-Fuse nucleus. (2) A ventromedial branch of Probst's tract contains fibers from PPT, the subcoeruleus region as well as an adjacent portion of FTC that has reciprocal connections with entopeduncular nucleus and substantia nigra (SN) and afferents from globus pallidus, and was termed the midbrain extrapyramidal area by Rye *et al.* (1987).

[173] The lateral tegmentoreticular tract was described by Russell (1955) and Sakai *et al.* (1979) as descending from the subcoeruleus region.

[174] Both Sakai's [173] and Rye's [172] papers indicate the presence of a projection of the ventromedial branch to the reticular zone just dorsal to the caudal two-thirds of the inferior olive, termed the "magnocellular tegmental field" by Sakai and his colleagues. However, Rye and coworkers suggest that the designation of this area as "magnocellular tegmental field" is not in accord with Berman (1968) and Kalia and Fuxe (1985), who indicate this is a ventral portion of the gigantocellular tegmental field. While this may seem a trivial point, it is in fact not, since the pathway and its projection zone are important for muscle inhibition in sleep. [175] Chase *et al.* (1986). [176] Tohyama *et al.* (1979b); Mitani *et al.* (1988a).

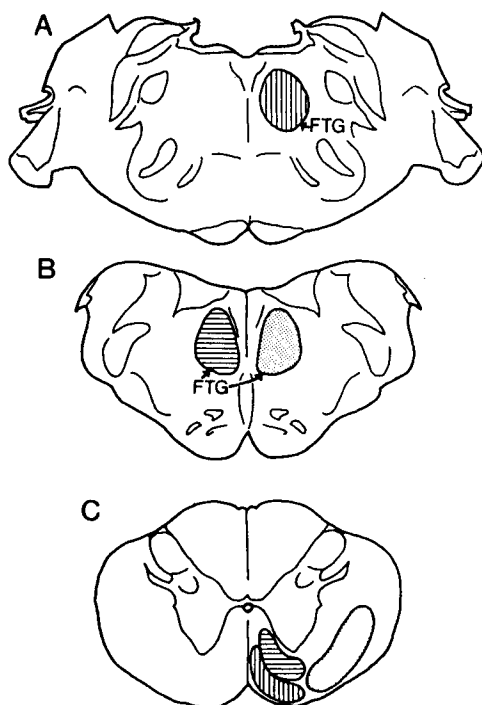


Figure 3.27. Summary diagram of the course of the major reticulospinal pathways from the pontine FTG (A) and bulbar FTG (BFTG) (B). C, approximate location of the reticulospinal pathways at the C1 level. Pontine reticulospinal fibers (vertical lines) descend in the ipsilateral ventromedial (VM) part of the ventral funiculus (VF). Crossed bulbar reticulospinal fibers (horizontal lines) descend in the contralateral dorsolateral part of the VF. Uncrossed bulbar reticulospinal fibers (stipples) descend in the ventral part of the ipsilateral lateral funiculus. See text for description of the sizes of the cells of origin of each pathway. From Mitani *et al.* (1988a).

and the bulbar reticular formation and these projections descend in the spinal cord in the VF. In contrast, neurons of medium and small size in PFTG project primarily and densely to ipsi- and contralateral bulbar reticular formation, especially the BFTG. Neurons of small and medium size in BFTG send descending axons in the LF.

Because of the possibility of terminological confusion, it is also useful at this point to review the terminology associated with the midline fiber tracts of the pons and bulb, the trajectory taken by many reticulospinal fibers. The dorsal-most portion is consistently termed the medial longitudinal fascicle MLF and is comprised of caudally and rostrally coursing fibers associated with the oculomotor and vestibular systems (see Chapter 11). Traveling more ventrally in the same central white matter area are fiber bundles that have been termed the tectospinal tract and the medial reticulospinal tract, after their presumed site of origin, a terminology based on earlier studies and followed

by classic anatomical texts [177]. However, anterograde tracing studies (Figs. 3.28 and 3.29) and intracellular HRP injections (illustrated below) have refined our conception of the course taken by pontine and bulbar reticulospinal fibers. This book, in agreement with terminological conventions [178], has taken the course of using the MLF as a convenient terminological reference point for the pontine

[177] Ranson and Clark (1953, Fig. 153); Crosby *et al.* (1962, Figs. 140 and 145); Elliott (1969, Plates XXI–XXIII).

[178] Holstege and Kuypers (1982).

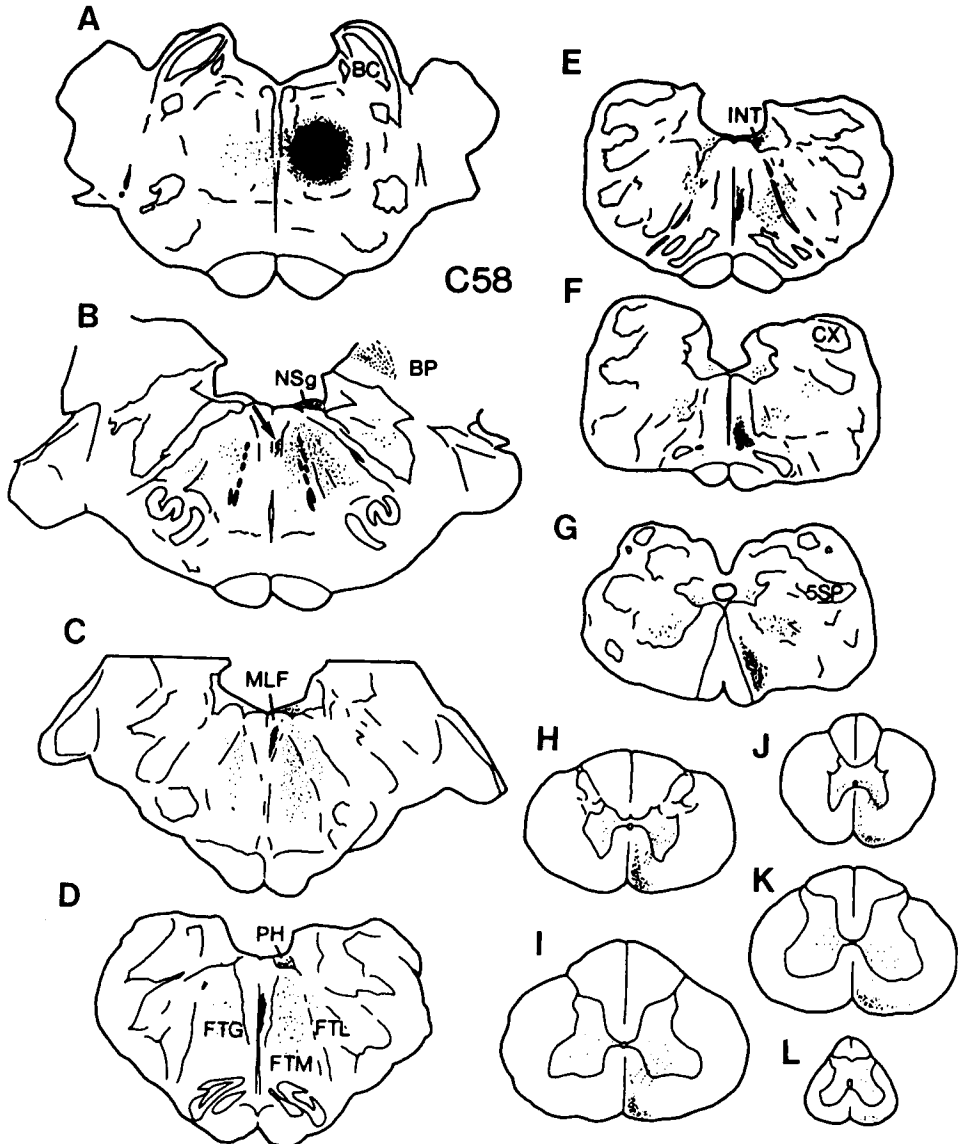


Figure 3.28. Anterogradely labeled descending fiber course for pontine FTG WGA-HRP injection. Sections H, I, J, K, and L are at spinal cord C1, C7, T5, L4, and S3, respectively. Note fibers descending ipsilaterally in the medial longitudinal fasciculus (MLF)—ventral funiculus (VF)—and bilaterally to the bulbar reticular (RE) formation. 5SP, spinal trigeminal nucleus; 7G, genu of the facial nerve; BC, brachium conjunctivum; BP, brachium pontis; CX, external cuneate nucleus; INT, nucleus intercalatus; NSg, n. supragenualis; PH, n. prepositus hypoglossi. From Mitani *et al.* (1988a).

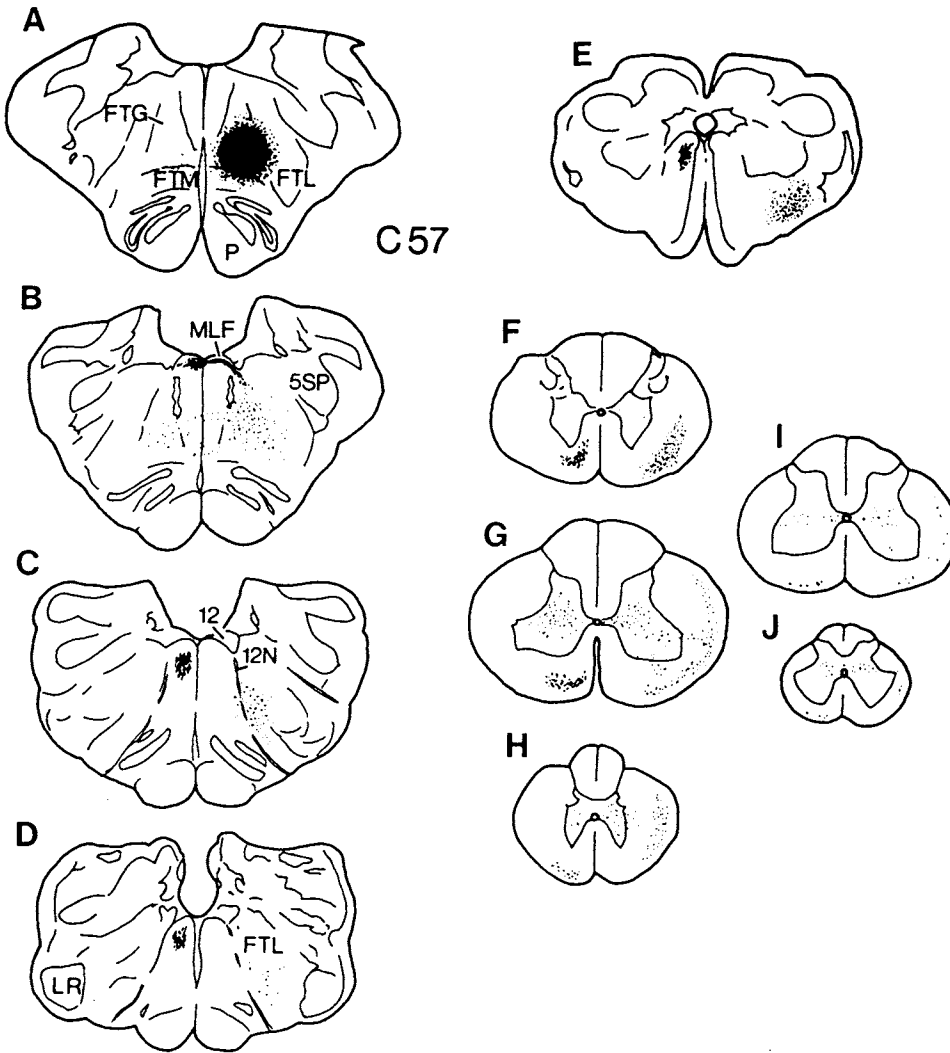


Figure 3.29. Anterogradely labeled descending fiber course for injection in bulbar FTG (BFTG). Sections F, G, H, I, and J are at C1, C7, T5, L4, and S2, respectively. Note fibers descending both in the contralateral medial longitudinal fasciculus—ventral funiculus (VF)—and the ipsilateral bulbar reticular (RE) formation—lateral funiculus (LF). 12, hypoglossal nucleus; 12N, hypoglossal nerve; LR, lateral reticular nucleus. From Mitani *et al.* (1988a).

and bulbar central white matter, while letting the data speak for themselves about the exact reticulospinal fiber course within this midline substantia alba.

In the pons, ipsilateral VF pathways have been indicated by autoradiographic studies in the cat [178], opossum [179], and rat [134], and a retrograde HRP study in the cat [53]. Recent anterograde WGA–HRP and intracellular HRP injection studies in the cat [83] have provided a more detailed description of the fiber trajectory: PFTG reticulospinal fibers enter the ipsilateral MLF, descend

[179] Martin *et al.* (1979).

through the ventral part of the MLF in the bulb and the VM part of the VF in the upper cervical cord, and continue in the VF to all spinal levels. All studies suggest distribution to laminae V–X, with a main distribution to laminae VII and VIII. In rat, reticulospinal fibers from the PFTG descend not only into the ipsilateral VF but also into the contralateral VF; the contralateral descending fibers cross over dorsally to enter the contralateral MLF after leaving the injection site [134]. However, in an anterograde WGA–HRP study on cat [83], reticulospinal fibers descending into the contralateral MLF–VF from the PFTG in the cat were only observed when the WGA–HRP deposit extended into levels caudal to the abducens nerve, as described below for BFTG.

The initial autoradiographic study in the cat [180], as well as subsequent autoradiographic studies in the cat [178] and rat [82, 134], indicate that bulbar reticulospinal neurons send axons bilaterally in MLF–VF with a contralateral predominance. The course of BFTG reticulospinal fibers in the contralateral MLF–VF has been detailed with anterograde WHA–HRP and intracellular HRP studies [83] and is congruent with the findings of the previous studies, namely: fibers course dorsomedially to the floor of the fourth ventricle, cross the midline, turn caudally, descend in the dorsal part of the contralateral MLF, and then continue in the contralateral VF. Reticulospinal fibers in the contralateral MLF–VF descend to all spinal levels although they are diminished in number at lumbosacral levels [180]. Distribution is principally to laminae VII–VIII.

In contrast to the large and giant neurons sending axons in MLF–VF, the dense PFTG-to-BFTG projections arose from small and medium neurons [23, 83]. The density of this projection has also been seen in autoradiographic studies in the cat [134]. The HRP studies indicate that there is a slight contralateral preference and that the density of PRF retrograde labeling after HRP injections into the BFTG is approximately 3-fold greater in PFTG compared with other pontine reticular nuclei (FTP>FTL) and with the midbrain FTC [83]. A non-VF descending fiber system has been described in the cat [178, 180] and rat [82, 134] and consists of fibers descending in the ipsilateral LF of the spinal cord [181].

The relative preponderance of reticulospinal projections onto motoneurons as opposed to other spinal cord neurons is unknown. However, an autoradiographic/EM study in rat with injection zones including BFTG and magnocellularis (as well as other ventral reticular structures) reported evidence that more than 50% of medial reticular formation synaptic terminals studied in lumbar spinal cord contact motoneurons, and preferentially their proximal

[180] Basbaum *et al.* (1978).

[181] While Basbaum *et al.* (1978) suggested there was an initial course of fibers in MLF, Mitani *et al.* (1988a) observed that the relatively small diameter fibers directly descended in BRF, while those descending in the ipsilateral MLF were mainly of relatively large diameter, findings directly confirmed with intracellular HRP injections (Mitani *et al.*, 1988c).

dendrites; the motoneurons had been retrogradely labeled by HRP injected in the muscle [178]. Electrophysiological mapping of reticular projections to spinal motoneurons has shown the presence of several different projection zones within the pontobulbar reticular formation [182].

[182] Peterson (1977).

3.4.3. Intrinsic Cellular Morphology and Projections of Pontine and Bulbar Gigantocellular Fields

The neuronal morphology of brainstem reticular neurons has been examined by the Golgi method [80, 183]. Scheibel and Scheibel [80], using the Golgi method in young mammals, described neurons in the pontobulbar FTG region with axons that bifurcated into ascending and descending branches, and also gave off richly branching collaterals to the cranial nerve nuclei and reticular formation. For many years their camera lucida drawing (Fig. 3.30) was often used to represent “the canonical reticular formation neuron,” until studies in adult animals found less of the exuberant axonal branching and a relative paucity of neurons with both ascending and descending branching. The Scheibels further suggested that the dendritic fields of PFTG neurons had a characteristic flattening in the anterior–posterior direction, which was described as a “poker chip” configuration.

[183] Valverde (1961);
 Ramón-Moliner and Nauta
 (1966).

Morphology is of special interest in FTG because the giant cells are among the largest in the brain and also from the standpoint of whether any functional or projection specialization might be indicated by size. As an example, after



Figure 3.30. Extent of reticular neuron as depicted by the Scheibels (1958). Golgi preparation.

the discovery of REM-sleep related activity in this region, an initial speculation was that the “giant cells” served to convey this excitation to many regions, presupposing that it was the giant cells of the FTG that had the effulgent branching represented by the Scheibels “canonical reticular neuron.” Evaluations by McCarley and coworkers of pontobulbar reticular neurons in the giant cell field, using the technique of electrophysiological recording and stimulation techniques combined with intracellular HRP injection, have begun to allow more definitive answers about FTG morphology and its functional linkage, and we here sketch this information (unless otherwise stated, data described below are from Mitani *et al.* [23, 83, 181]).

3.4.3.1. Cell Size Distribution Within the Pontine and Bulbar FTG

The discussion in this section will make clear that the large and giant neurons in PFTG and BFTG apparently tend to have different functional connections (to MLF-VF) and an absence of collaterals. In this regard and for future studies, it is important to have quantitative data on the cell sizes in the pontobulbar FTG and the cytoarchitectural observations of a recent study in cats are of interest [184]. FTG neuronal cell bodies were classified as: (1) small, average diameters $<20\text{ }\mu\text{m}$; (2) medium, $<40\text{ }\mu\text{m}$; (3) large, $<60\text{ }\mu\text{m}$; and (4) giant, $>60\text{ }\mu\text{m}$. The percentage of each size was then calculated in each of the ten 1 mm square areas of each brain stem. The average percentages were: small (57%), medium (35%), large (6%), and giant (2%). Thus, in general, the giant cell field has a few large and giant neurons that are scattered among many small and medium neurons (for the prevalence of small- and medium-sized cells in the conventionally termed pontine giant cellular field, see also [18]). While the absolute values of the soma sizes will vary somewhat (perhaps 10–20%) with differences in anatomical and measurement technique, and hence the boundary values listed here should not be taken as rigid absolutes, it is likely true that the relative proportions of neurons of different sizes is accurate, and should be taken into account in modeling function and interpreting results. For example, because of the sampling bias of microelectrodes for medium-to-large neurons, we know much more about the physiology of medium-to-giant neurons than the numerous small neurons in FTG.

[184] On Nissl-stained sections, 1 mm square areas of FTG were randomly selected at every 1 mm distance from posterior 2.0 mm to posterior 11.0 mm, and the diameters of all FTG neuronal cell bodies with a nucleolus were measured.

3.4.3.2. Morphology of Pontine FTG Neurons

The morphology of reticuloreticular pontine neurons (antidromically identified from the bulbar reticular

formation) and of reticulospinal pontine neurons was recently studied by means of intracellular HRP injections. The pontine reticular neurons projecting to bulbar reticular fields have soma diameters (mean, 40 μm) smaller than reticulospinal neurons ($\sim 60 \mu\text{m}$), thinner axons, and smaller, slightly oblate dendritic fields. Quantitative data indicated that, by contrast to previous Golgi studies on young mammals [80, 183] who assumed that the reticular dendritic field is flattened in the anteroposterior plane, the mean anteroposterior extent of the dendritic field of intracellularly stained pontine reticular cells in the adult cat is at least 16% less than the dorsoventral and mediolateral extents. While no reticulospinal cell has axon collaterals, 36% of pontobulbar reticular neurons have axon collaterals projecting to the ipsilateral abducens nucleus or the adjacent pontine GC field. The collaterals to the abducens nucleus may be involved in the generation of horizontal saccades [185], while the collaterals to the adjacent pontine reticular fields and the bulbar reticular formation may subserve the spread and maintenance of membrane depolarization in the reticular population during the REM-sleep state [186].

[185] Igusa *et al.* (1980);
 Sasaki and Shimazu (1981).

[186] Ito and McCarley
 (1984).

3.4.3.3. Pontine FTG Neurons Sending Axons in the Ipsilateral MLF

Figure 3.31 is a composite photomicrograph of an intracellularly HRP-labeled giant cell neuron in PFTG. The ellipsoid–polygonal soma measures $100 \times 50 \mu\text{m}$ (long \times short axis) with an average soma diameter of 75 μm ; even in the photograph, dendritic field diameter is seen to extend some 2 mm in the dorsoventral and mediolateral directions. Such HRP-stained neurons are clearly visible in sections viewed without the aid of a microscope. Figure 3.32 shows a camera lucida reproduction of another giant cell with soma measurements of $103 \times 41 \mu\text{m}$ (mean = 72 μm) and a dendritic field diameter of about 2 mm with the axonal course in ipsilateral MLF labeled in part B. [187]. No neurons sending axons in MLF were observed to have axon collaterals.

[187] Both neurons illustrated in Figs. 3.31 and 3.32 were antidromically activated from stimulating electrodes placed in ipsilateral bulbar MLF. Most PFTG neurons sending axons in iMLF have large ellipsoid–polygonal somata (mean: 60 μm) and thick axons (average diameter, 3 μm). Slightly oblate, large dendritic fields are also typical, with mean anteroposterior extent of 1,500 μm , a mean mediolateral extent of 1,800 μm and a mean dorsoventral extent of 1,600 μm .

3.4.3.4. Pontine FTG Neurons Sending Axons Directly to Bulbar Reticular Formation

Figure 3.33 is a camera lucida drawing of horizontal section with a PFTG neuron whose axon projects directly to BRF and does not collateralize. The neuron was of medium size (mean soma diameter 38 μm), with an axon diameter of 1.6 μm . The dendritic field, although large, is only 10% reduced in the anteroposterior direction (1,400 μm) as

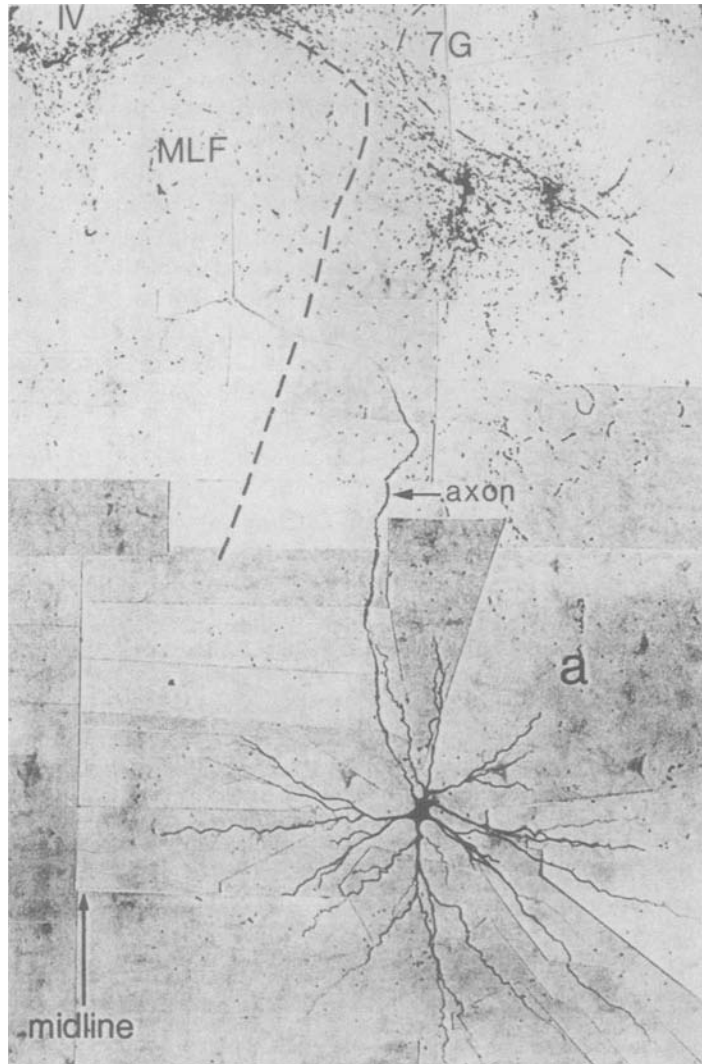


Figure 3.31. Composite photomicrograph of brain stem (frontal section) showing an intracellularly stained large PFTG neuron (a) with axon entering MLF. Note the axon courses caudodorsomedially in the PFTG and enters the ipsilateral MLF at a level near the genu of the facial nerve (7G). Note the large extent of the dendritic field, over 2 mm. IV, fourth ventricle. From Mitani *et al.* (1988b).

compared with the mediolateral direction (1,500 μm), and hence does not resemble a “poker chip.” Figure 3.34 shows another PFTG neuron whose axon courses directly into BRF; this axon like that of 36% of the BRF neurons, was collateralized, in this case with projections to abducens nucleus. Overall PFTG neurons whose axons projected directly to BRF had, in comparison to those with axons in MLF, smaller ellipsoid–polygonal somata (mean, 40 μm), thinner axons (average diameter, 2.3 μm), and slightly smaller dendritic fields, with a mean anteroposterior extent of 1,300 μm , a mean mediolateral extent of 1,500 μm and a mean dorsoventral extent of 1,200 μm . All of these neurons were antidromically activated from BFTG, but not from MLF.

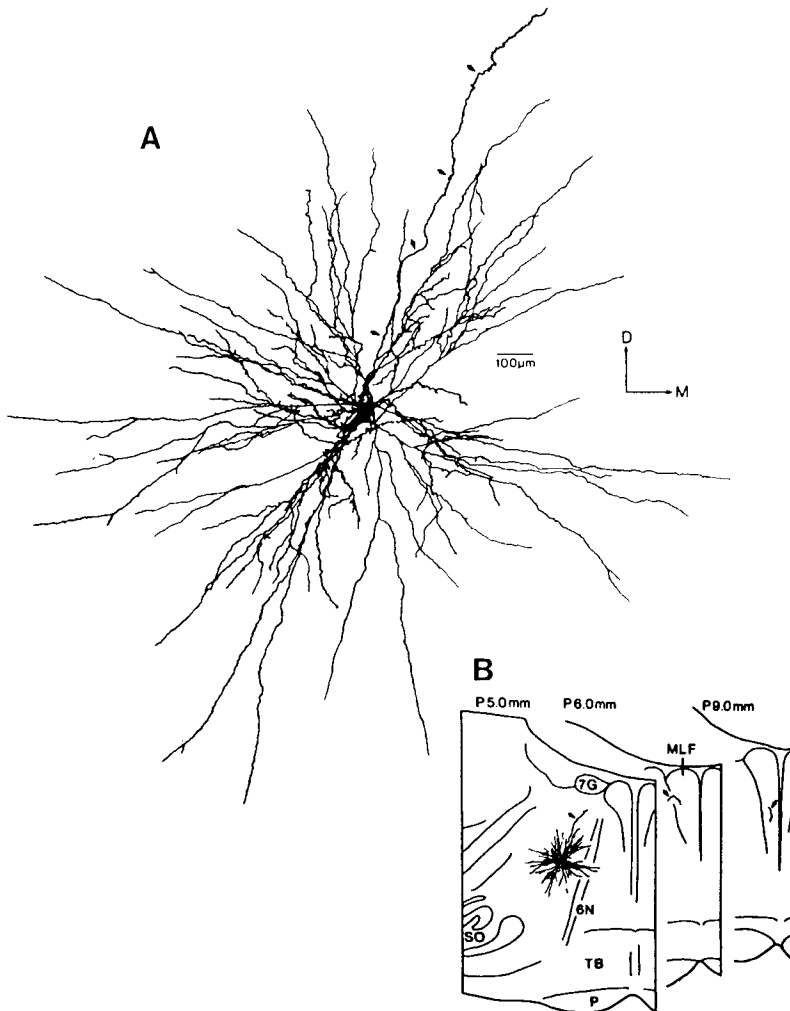


Figure 3.32. Camera lucida drawing of pontine FTG neuron sending its axon in ipsilateral MLF (frontal sections); the cell body, dendrites, and proximal axon shown in (A) and neuronal location and axon course in (B). Note the large ellipsoid–polygonal cell body (major axis, 103 μm and minor axis, 41 μm with average diameter, 72 μm) with the major axis slanted from dorsomedial to ventrolateral. The dendrites were nonspiny and had extensive branching. The dendritic field was large, extending 2,100 μm in the M–L direction and 2,030 μm in the D–V direction; the axis of the dendritic field was tilted from dorsomedial to ventrolateral (VL). The axon (solid arrows in A and B) originated from the cell body, ran dorsomedially, then turned caudally into the ipsilateral MLF and descended toward the spinal cord (B). No axon collaterals were observed. The average axon diameter was 3.3 μm . Abbreviations: P (posterior) 5.0 mm, 6.0 mm, and 9.0 mm are frontal coordinates of labeled neuron and axons in Berman's atlas (the plane of this section ran 40° caudal to the Berman perpendicular plane). SO, superior olivary nucleus. From Mitani *et al.* (1988b).

The trajectories of axon collaterals of the above two PFTG-to-BRF neurons which projected to the ipsilateral abducens nucleus resembled those of HRP-stained reticular neurons in the cat [188], HRP-intraxonally-stained reticular neurons in the monkey [189], and Golgi-impregnated neurons in young mice (see Fig. 31, neuron b, in [80]). However, intracellularly labeled PFTG neurons with

[188] Grantyn *et al.* (1980, 1988).

[189] Strassman *et al.* (1986).

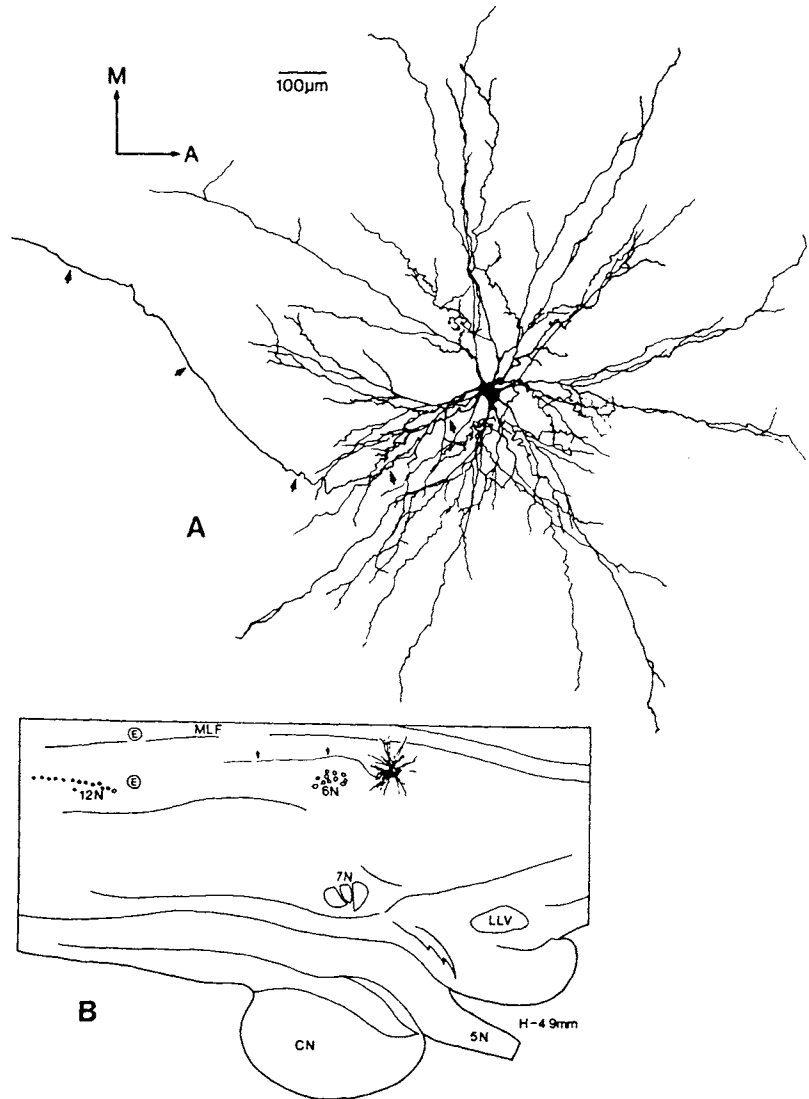


Figure 3.33. Camera lucida drawing of pontine FTG neuron with axon descending in BRF but not in MLF (horizontal section). This neuron had an ellipsoid-polygonal cell body of medium size (major axis, $45\ \mu\text{m}$ and minor axis, $31\ \mu\text{m}$ with average diameter, $38\ \mu\text{m}$). The dendrites were nonspiny. The dendritic field extended $1,360\ \mu\text{m}$ in the A-P direction and $1,520\ \mu\text{m}$ in the M-L direction. The axis of the longest extent was tilted from medial to lateral. The axon (solid arrows in A and B) originated from the dendritic trunk, and after curving laterally for a short distance coursed caudally and entered the BRF. No axon collaterals were observed. The average axon diameter was $1.6\ \mu\text{m}$. H -4.9 mm is the horizontal coordinate of labeled neuron in Berman's atlas (this horizontal plane of section approximately parallel to floor of IVth ventricle). From Mitani *et al.* (1988b).

projections to both the abducens nucleus and the spinal cord [188] were not observed. As described in Chapter 11, the Grantyn's data [188] were from a physiologically selected and specialized population. Since the anterograde WGA-HRP study by Mitani *et al.* [83] also found that fibers of PFTG neurons descending in the BRF could not be traced as far as the spinal cord, it is likely that the neurons described by Grantyn and colleagues may be relatively few.

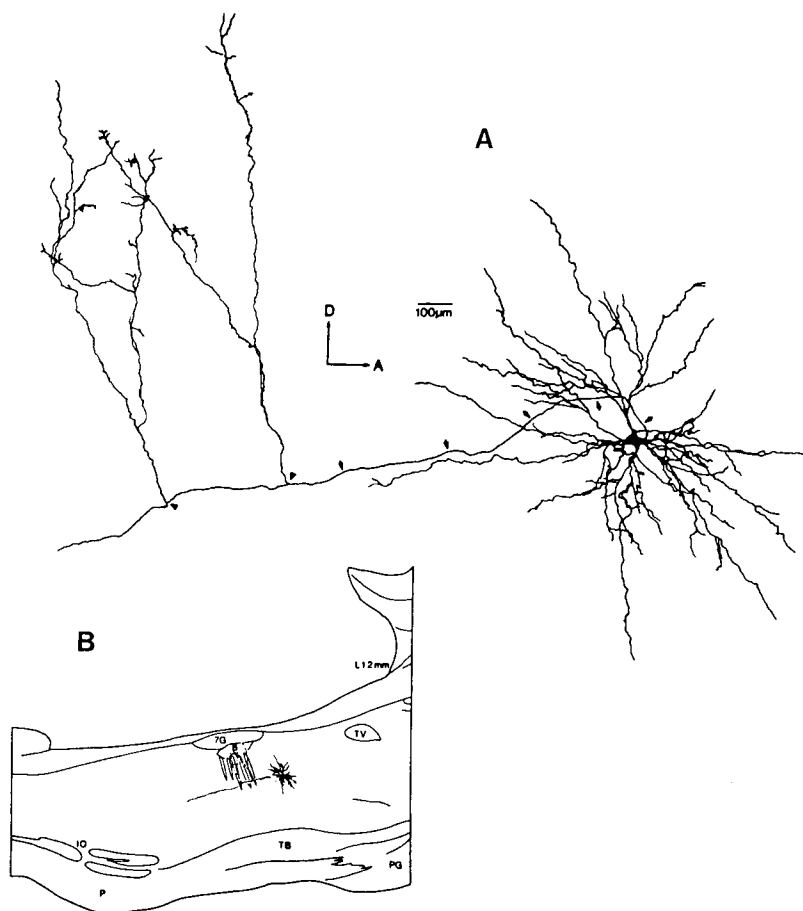


Figure 3.34. Camera lucida drawing of a pontine FTG neuron with axon descending in BRF but not MLF (parasagittal section). This neuron had an ellipsoid–polygonal cell body of medium size (major axis, 55 μm and minor axis, 39 μm with average diameter, 47 μm). The dendrites were nonspiny. The dendritic field extended 1,350 μm in the A–P direction and 1,470 μm in the D–V direction, and the axis of the longest extent was tilted slightly from dorsocaudal to ventrorostral. The axon (solid arrows) originated from the dendritic trunk, and coursed dorsally for a short distance, then turned caudally and entered the BRF. Axon collaterals originated from the main axon (solid triangles in A) and projected into the ipsilateral abducens nucleus (B). Average main axon diameter was 1.7 μm and average axon collateral diameter was less than 1.0 μm . L1.2 mm is parasagittal coordinate of labeled neuron (Berman's atlas coordinate). TV, ventral tegmental nucleus. From Mitani *et al.* (1988b).

[190] The major axis of those neurons was angled from dorsomedial to ventrolateral in frontal sections (67%), from dorsocaudal to ventrorostral in parasagittal sections (76%), and from medial to lateral in horizontal sections (91%). The finding in frontal sections agrees with previous work by Newman (1985), while preferences in parasagittal and horizontal sections had not previously been studied.

[191] Edwards *et al.* (1987).

A specific orientation preference of the major soma axis was present only in PFTG-to-iMLF neurons [23, 190].

3.4.3.5. Dendrites

The findings that PFTG dendrites repeatedly gave off two or three branches and extended for long distances are in agreement with data from Golgi studies [25, 80, 183]. The “dendritic index” is defined by dividing the total number of terminal branches by the total number of trunks [191] and, when high, indicates a high degree of branching. The dendritic indices were high for both PFTG-to-iMLF neurons (mean = 16) and for PFTG-to-BRF neurons

(mean = 14) and did not significantly differ, but were higher than for some bulbar reticular neurons (see below).

3.4.3.6. Morphology of Bulbar FTG Neurons

As was true for PFTG neurons, it was found that BFTG neurons with axons traveling in MLF had somata that were predominantly in the large-giant size range, and, also like the PFTG, had axons that did not collateralize [192]. The BFTG-to-iMLF neurons closely resembled the PFTG-to-iMLF neurons with large ellipsoid-polygonal somata (mean, 60 μm), thick axons (average diameter, 3 μm), mostly nonspiny dendrites and dendritic fields that were only slightly flattened in the anteroposterior direction. The BFTG-to-cMLF neurons were similar in somata size (mean, 57 μm), and in having thick axons (average diameter, 3 μm) and mostly nonspiny dendrites (Fig. 3.35 and 3.36) [193].

[192] Mitani *et al.* (1988c).

[193] The BFTG-to-cMLF neurons were however different from both pontine and bulbar neurons sending axons in iMLF in that BFTG-to-cMLF neurons had dendritic fields flattened in the anteroposterior direction, where mean extent was 1,100 μm , compared with 1,700 μm in the mediolateral direction, and 1,400 μm in the dorsoventral direction. The mean anteroposterior extent was thus 32% and 20% less than the mean mediolateral and dorsoventral extents, respectively.

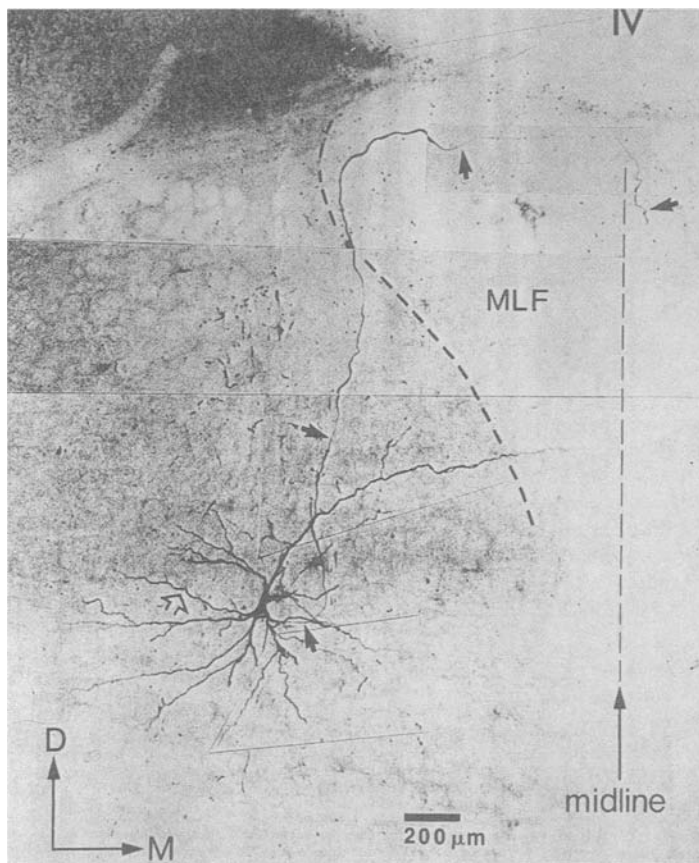


Figure 3.35. Composite photomicrograph showing an intracellularly stained bulbar FTG (BFTG) neuron with axon descending in cMLF. This frontal section shows a neuron whose axon (solid arrows) coursed dorsally and entered the ipsilateral MLF, then turned medially and crossed the midline to descend in the dorsomedial part of the contralateral MLF. IV, fourth ventricle; M, medial; MLF, medial longitudinal fasciculus. From Mitani *et al.* (1988c).

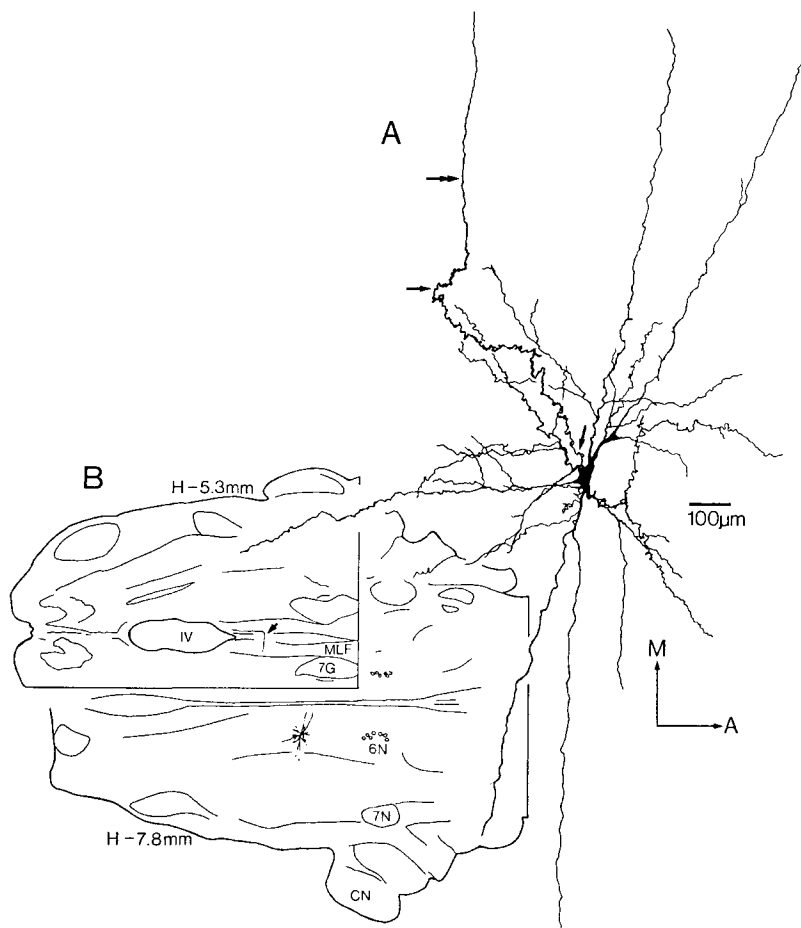


Figure 3.36. Camera lucida drawing of bulbar FTG (BFTG) neuron with axon descending in cMLF (horizontal section). Note the ellipsoid–polygonal soma (major axis, $62\text{ }\mu\text{m}$ and minor axis, $38\text{ }\mu\text{m}$ with average diameter $48\text{ }\mu\text{m}$) and slant of the major axis from medial to lateral. The dendritic field extended $1,330\text{ }\mu\text{m}$ in the A–P direction and $2,230\text{ }\mu\text{m}$ in the M–L direction; the longest extent of the dendritic field was mediolateral. The axon originated from the soma and coursed dorsally while curving (corresponding to the part between the two solid arrows in A), then turned medially (double-headed arrow in A), entered the ipsilateral MLF (arrow), crossed the midline (solid arrow in B) and descended in the medial part of the contralateral MLF toward the spinal cord. No axon collaterals were observed. The average axon diameter was $3.1\text{ }\mu\text{m}$. Abbreviations: H(horizontal) -5.3 mm and -7.3 mm are horizontal coordinates of labeled neuron and axon in Berman's atlas (horizontal plane of section approximately parallel to floor of fourth ventricle). 7N, facial nerve; CN, cochlear nerve. From Mitani *et al.* (1988c).

3.4.3.7. Bulbar FTG Neurons Sending Axons into the Ipsilateral Bulbar Reticular Core

Compared with bulbar and pontine iMLF and cMLF neurons, most BFTG-to-iBRF neurons had smaller ellipsoid–polygonal somata (mean, $39\text{ }\mu\text{m}$) and thinner axons (average diameter, $1.8\text{ }\mu\text{m}$) and dendritic fields that were flattened in the anteroposterior direction, where mean extent was $1,200\text{ }\mu\text{m}$, 35% and 30% less than the mediolateral

mean extent of 1,900 μm , and the mean extent of 1,800 μm in the dorsoventral direction, respectively.

In contrast to neurons sending axons in cMLF and iMLF, axon collaterals were present in BFTG-to-iBRF neurons, and were much more frequent than in PFTG-to-BFTG neurons. 73% of BFTG-to-iBRF neurons have axon collaterals. Bifurcated axon collaterals with both anterior and posterior projections were also common in the BFTG-to-iBRF neuronal population, being present in about half of BFTG-to-iBRF neurons (Fig. 3.37). In these neurons antidromic spike potentials were elicited by stimulation of the ipsilateral PFTG.

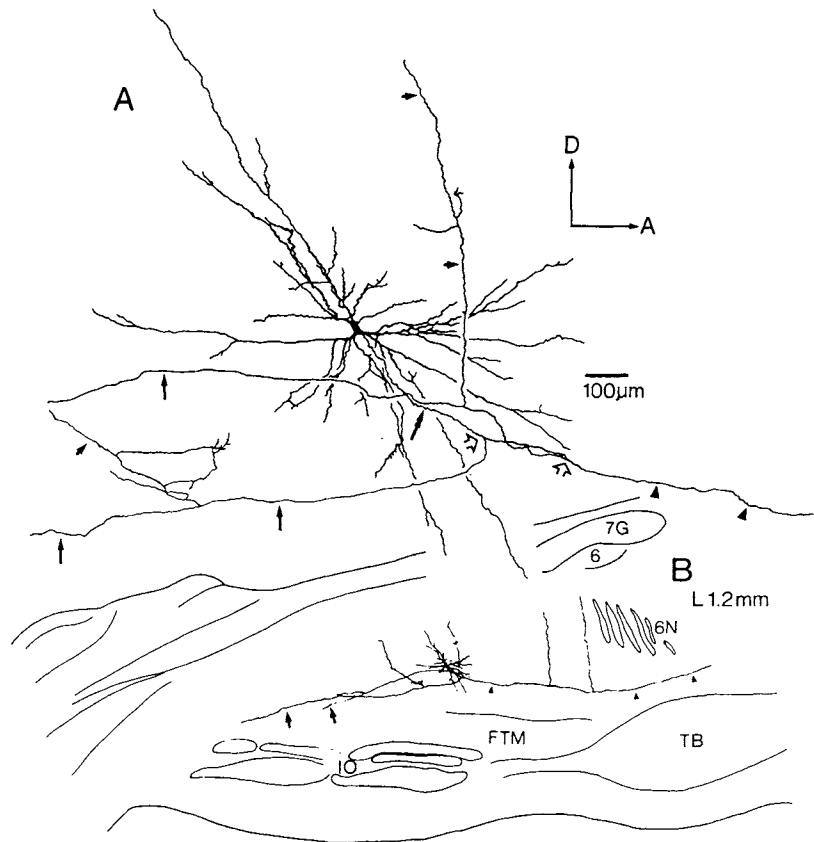


Figure 3.37. Camera lucida drawing of a bulbar FTG (BFTG) neuron with axon descending in iBRF and with extensive collaterals (parasagittal section). This neuron had an ellipsoid-polygonal soma of medium size (major axis, 39 μm and minor axis, 20 μm with average diameter, 30 μm). The dendrites were nonspiny. The dendritic field extended 1,170 μm in the A-P direction and 1,610 μm in the D-V direction, and the axis of the longest extent was tilted slightly from dorsocaudal to ventrorostral. The axon originated from the dendritic trunk, and coursed anteriorly for a short distance (double headed arrow in A), then bifurcated (open arrows) into an ascending branch (solid triangles in A and B) and two descending branches (solid arrows in A and B); the ascending axon entered the pons and the descending axons descended in the bulbar reticular (RE) formation. Both ascending and descending axonal branches gave off dorsally coursing axon collaterals (B) (some of them are indicated by small arrows in A). From Mitani *et al.* (1988c).

The “dendritic index” (defined above) was smaller in BFTG neurons (means of cMLF, iMLF, and iBRF neurons = 8, 7, and 9, respectively) than in PFTG neurons (means of two types of PFTG neurons = 16 and 14). These results indicated that BFTG neurons had fewer branching dendrites, and were similar to those reported for bulbar reticular neurons near the raphe magnus [191].

3.4.3.8. General Comments on Morphology

The large neurons with large and noncollateralized axons coursing in the MLF and the VF would seem ideally suited for rapid, secure transmission of information. The phylogenetic homology is of course with the Mauthner neurons and other giant reticulospinal neurons of fish and other lower vertebrates. These large neurons with axons in VF may be involved in locomotion. A study of bulbar medial reticular formation neurons (most within FTG) in alert cats during treadmill walking showed that it was the neurons antidromically identified as reticulospinal by stimulation of ventral cord at L2 that showed predominance of EMG- and locomotor-related discharge; those neurons had high conduction velocities (approximately 100 m/s), compatible with a large soma size [194]. In contrast, neurons of smaller and medium size neurons in both PFTG and BFTG appear to be the carriers of reticuloreticular information, in addition to their other targets. It should be emphasized that there is some overlap of soma size of PFTG- and BFTG-to-MLF neurons with neurons sending axons in BRF; in the studies cited this was about 10% and thus the size distinctions are not absolute.

Although Golgi studies of young mammals indicate that the reticular dendritic field was flattened in the anteroposterior plane, and assumed a nearly two-dimensional configuration described as resembling “poker chips” [80], the quantitative data of the HRP intracellular study in adult cats, described above, modify these conclusions. In PFTG, there is only a tendency to a “poker chip” configuration in a few neurons. The mean anteroposterior (A–P) extent of the population of PFTG neurons was only 16% less than the mean dorsoventral (D–V) and 3% less than the mean mediolateral extent. Furthermore, only 15% of PFTG neurons showed a flattening of the anteroposterior dendritic fields that was between 30–39%, a degree of flattening much less than shown in Figure 3 in [80]. In fact, the dendritic field extent of 19% of PFTG neurons was slightly longer in the A–P direction than in the mediolateral or D–V direction [195].

[194] Drew *et al.* (1986).

[195] However, a tendency toward A–P flattening, although not quite as strong as in the Scheibels’ material [80], was present in the BFTG-to-cMLF and BFTG-to-iBRF neuronal classes of BFTG neurons. The mean anteroposterior extent of the BFTG-to-cMLF and BFTG-to-iBRF neurons is 31% and 35% less than their respective mean mediolateral extent and 20% and 30% less than their respective mean dorsoventral extent. In contrast, dendrites of BFTG-to-iMLF neurons showed only a small trend to anteroposterior flattening, less than 16% and thus less than half of that seen in cMLF and iBRF neurons and similar to that of PFTG neurons.

3.4.3.9. Organization of Bifurcating Axonal Collaterals

With respect to the extent of collateralization of FTG neurons, it is of interest that double-labeling experiments have shown that only relatively few (<4%) BFTG neurons project both to spinal cord and cerebellum, or both to cerebellum and diencephalon, or both to spinal cord and diencephalon [196]. This is also in accord with the older physiological studies [197]. This paucity is, however, in marked contrast to the 55% of non-MLF projecting BFTG axons that had bifurcating collaterals, and suggests that, in the adult, the neurons with bifurcating collaterals have one branch that is shortened, that is, terminates before arrival in diencephalon or spinal cord. Our supposition from the intracellular HRP data is that it is the rostral branch that ascends only a relatively short distance. Given the strong tendency of bulbar neurons to project to the spinal cord, the observation of “frequent” double labeling of BFTG neurons from midbrain and spinal cord is of interest [134]. The actual axonal BFTG-to-PFTG tracings with bouton-like terminations, the presence of antidromic activation of BFTG neurons from PFTG, and the 100% monosynaptic excitatory responsiveness of PFTG neurons to BFTG microstimulation [23, 192] lead to the inference that pontine FTG neurons are heavily innervated by the class of BFTG neurons with ascending collaterals.

- [196] Martin and Waltzer (1984a, b); Waltzer and Martin (1984).
- [197] Magni and Willis (1963); Eccles *et al.* (1975).

3.5. Efferent Connections of Monoamine-Containing Neurons

3.5.1. Norepinephrinergic Systems

Norepinephrine(NE)-containing neurons are located in the pons and medulla, with about 60% of them in the LC-subcoeruleus complex. In rat, the LC almost exclusively consists of NE elements, contains about 1,500 neurons, and is divided into a ventral part with multipolar neurons and a dorsal part with smaller-size, densely packed fusiform cells [198]. Colocalization of TH immunoreactivity with neuropeptide Y-immunoreactivity was recently found in approximately 23% of rat's LC neurons [199]. In cat, the LC is more loosely arranged, with an LC proper (corresponding to the dorsal compact part of the rat LC, and containing about 5,300 NE cells on each side), and more scattered NE cells extending into the parabrachial nucleus and the subcoeruleus and Kölliker-Fuse nuclei [200].

The rostral projections of NEergic cells ascend mostly ipsilaterally via the dorsal tegmental bundle, with a minor

- [198] Swanson (1976); Grzanna and Molliver (1980).
- [199] Holets *et al.* (1988).

- [200] Wiklund *et al.* (1981); Bjorklund and Lindvall (1986).

projection taking a ventral course. In the midbrain, the bundle gives off collaterals to the ventral tegmental area, dorsal regions of the FTC, and inferior and SC. Most of the ascending NE fibers enter the medial forebrain bundle at the caudal diencephalic level and enter the thalamus via the retroflex bundle or the mammillothalamic tract, while other fibers ascend along the ZI and radiate within the internal and external medullary laminae. NE fibers distribute to various hypothalamic areas, thalamic nuclei, septum, amygdala, hippocampus and pyriform cortex, and neocortical areas [201].

In contrast with the congruent results on the cholinergic innervation of different thalamic nuclei in rat, cat, and monkey (see Section 3.4.1), the density of NE projections to the thalamus greatly varies from nucleus to nucleus and from species to species. While the LG thalamic nucleus of rats is one of the most important targets of LC nucleus, the associative visual thalamic nuclei (pulvinar and LP) only receive a sparse to moderate NE input [202]. A reverse picture is seen in some primates (squirrel monkey and cynomolgus monkey) that display a striking paucity of NE fibers in the LG nucleus, while pulvinar and LP thalamic nuclei are densely innervated; the thalamic reticular nucleus is very densely innervated throughout its extent [203].

The corticopetal NE fibers have been found to leave the main bundle at rostral hypothalamic levels, to continue their course up to the frontal lobe, and to distribute caudally for the entire length of the hemisphere [204]. Earlier autoradiographic studies [205] and antidromic identification experiments [206] indicate, however, that some fibers originating in the LC nucleus reach the occipital lobe without coursing through the frontal lobe. The interspecies differences that characterize NE projections to the thalamus are also observed in the cerebral cortex, and the degree of regional and laminar variation increases with the phylogenetic development. Thus, while the NE innervation of rat's neocortex is quite constant throughout the cortex and the axons seem to ramify in all layers [207], marked laminar variations are seen in striate and extrastriate cortices of primates [208]. In particular, sudden changes in the density and laminar profiles of NE fibers are seen by passing from area 17 to area 18: in area 18, a distinct lamination pattern emerges, with the highest density of NE axons in layers III and V, and the lowest density in layers I and IV [203]. Antidromic activation of rat's LC neurons can be elicited from many target cortical areas and most LC-cortical axons conduct with wide range and very low (<0.6 m/s) velocities [209], suggesting thin non-myelinated fibers, but a significant population of monkey's

[201] Lindvall and Bjorklund (1974); Pickel *et al.* (1974); Foote *et al.* (1983).

[202] Swanson and Hartman (1975).

[203] Morrison and Foote (1986).

[204] Morrison *et al.* (1981).

[205] Jones and Moore (1977).

[206] Sakaguchi and Nakamura (1987).

[207] Levitt and Moore (1978); Lindvall *et al.* (1978).

[208] Morrison *et al.* (1982).

[209] Aston-Jones *et al.* (1980); Nakazato (1987).

LC neurons was found to exhibit conduction velocities greater than 1 m/s [210].

A very low proportion of NE axons were seen to be engaged in genuine synaptic relations and it was postulated that NE is released in a neurohumoral type, over great distances, like in the peripheral nervous system [211]. Similar findings were reported for distribution of cholinergic axons in neocortex [212]. Probably, synaptic and nonsynaptic release coexist [213].

The descending projections of LC neurons run dorso-medially in the pontine tegmentum and varicosities are present in PRF, including giant cell field. A lateral group enters the cerebellum through the brachium conjunctivum and the fibers terminate in the molecular layer as well as around the Purkinje cells [214]. In the pons and medulla, the prime targets of LC axons are sensory nuclei, namely, the pontine gray nuclei, the cochlear nuclei, and the principal sensory trigeminal nucleus [215]. The projections to the spinal cord originate in the ventral part of the LC and in nucleus subcoeruleus, descend in the ventral and VL funiculi, and distribute bilaterally to the ventral horn, intermediate gray, and ventral part of the dorsal horn [216].

A significant proportion of LC cells give rise to axons that collateralize to different structures. About 10% to 30% of LC neurons are double labeled when one fluorescent tracer is injected in the spinal cord and the other one into the cerebellum, cortex, or thalamus [217].

3.5.2. Serotonergic Systems

The serotonergic (5-HT) neurons are located in the brainstem raphe system that consists, at midbrain–pontine levels, of the CS (or medianus), linearis, and dorsalis nuclei; at pontobulbar levels, it comprises the magnus, obscurus, and pallidus nuclei [218].

The heterogeneity of raphe nuclei, with both 5-HT and non-5-HT neurons, was repeatedly emphasized [219]. The heterogeneity of the DR nucleus is reflected in the different firing patterns, electrophysiological properties, and morphology of its constituent neurons. Aghajanian and coworkers [219] have initially distinguished three types of DR neurons: type I are medium-sized 5-HT cells (disappearing in animals treated with the selective toxin 5,7-dihydroxytryptamine, 5,7-DHT), with spontaneous firing rates of 0.5–1.5 Hz; type II cells (almost silent) and type III (rapidly firing) are still recordable in experiments after lesions produced by 5,7-DHT, and are probably non-5-HT neurons. Rapidly firing neurons (100–130 Hz) have been

[210] Aston-Jones, *et al.* (1985).

[211] Descarries *et al.* (1977); Beaudet and Descarries (1978).

[212] Umbriaco *et al.* (1994); Descarries and Umbriaco (1995); Descarries *et al.* (1997). See also Mrzljak *et al.* (1995).

[213] Olschowska *et al.* (1981); Freund *et al.* (1984). For further details and methodological issues concerning junctional vs nonjunctional relations of NE terminals in the cortex, see Beaudet and Descarries (1984).

[214] Pickel *et al.* (1974).

[215] Levitt and Moore (1979).

[216] Bjorklund and Lindvall (1986).

[217] Nagai *et al.* (1981); Room *et al.* (1981).

[218] See details on systematization and cytoarchitectonics of serotonergic nuclei in Steinbusch and Nieuwenhuys (1983).

[219] Aghajanian *et al.* (1978); Belin *et al.* (1979); Steinbusch *et al.* (1980). Among non-5-HT raphe cells, there are GABAergic (Belin *et al.*, 1979) and dopaminergic (Descarries *et al.*, 1986) elements.

- [220] Park (1987). recently recorded intracellularly, stained with HRP, and compared to slowly firing neurons [220]. The action potentials of rapidly firing cells have a repolarization that is about five times faster than that in slowly firing 5-HT cells. Intracellular labeling revealed that type III fast-discharging DR neurons have small (10–15 μm) somata [220], similar to GABAergic neurons of the DR nucleus [221].
- [221] Belin *et al.* (1979).

The ascending projections originate in DR and CS nuclei. The major organizational features of the ascending raphe projections to the hypothalamus, diencephalic periventricular gray, striatum, globus pallidus, diagonal band nuclei, septum, hippocampus, and glomerular layer of the olfactory bulb, have been revealed in the rat by light-microscope autoradiography after intraventricular administration of tritiated 5-HT [222]. The CS raphe projections to septum and hippocampus of rat have also been identified by antidromic invasion, and the results showed conduction velocities of 0.8 m/s as well as branching axons to both the fornix and the medial septum [223]. An autoradiographic study of efferent raphe projections in cat disclosed some differences between DR and CS nuclei, with preferential DR projections to striatum, amygdala, pyriform lobe, and olfactory bulb, while CS nucleus was found to project rather selectively to the mammillary body and hippocampus [224].

- [222] Parent *et al.* (1981).

- [223] Crunelli and Segal (1985).

- [224] Bobillier *et al.* (1976).

The axons issuing from DR and CS nuclei ascend to the thalamus mostly along the retroflex bundle, the mamillothalamic tract, and stria terminalis. The 5-HT projections to the rat thalamus have been demonstrated by combining retrograde transport techniques with 5-HT immunohistochemistry [225]. The thalamically projecting neurons are confined within the lateral DR wing. The highest density of the 5-HT innervation is found in the ventral part of the LG nucleus and the intrageniculate leaflet, while other thalamic nuclei display low to moderate density of 5-HT fibers [226]. The low density of 5-HT fibers in the rat thalamus is paralleled by low levels of the two types of 5-HT receptors [227]. In cat, DR cells with projections to the LG nucleus are not restricted to a particular sector of the DR nucleus [14, 145], and the density of 5-HT fibers is moderate to high in the ventral part of the LG and intralaminar nuclei, but rather low in A and C laminae of the LG nucleus [228]. In primates, it was found a relatively uniform distribution of 5-HT fibers in various visual thalamic nuclei, which was at variance with the marked nuclear variations of NE fibers [203].

- [225] Consolazione *et al.* (1984).

- [226] Cropper *et al.* (1985).

- [227] Pazos and Palacios (1985); Pazos *et al.* (1985).

- [228] Mize and Payne (1987).

The 5-HT fibers that reach the cortex traverse the septum, sweep around the genu of the corpus callosum, and continue in the cingulum. In rat, the 5-HT innervation does

not display regional differences or laminar preferences [229], whereas in primates 5-HT fibers are concentrated in layer IV of striate area 17 and are homogeneously distributed in area 18 [203, 208]. In both rat and monkey, 5-HT innervation of the cerebral cortex is denser than the NE input. At this time, the innervation of cat cerebral cortex has not been systematically studied with immunohistochemistry. Biochemical investigations indicate that the highest concentration of 5-HT is in the pyriform cortex and the lowest in the visual cortex of cat [230].

The descending projections of DR and CS are mostly directed to pontine and bulbar core structures, while the 5-HT projections to the spinal cord derive from magnus, obscurus, and pallidus raphe nuclei [231].

3.5.3. Dopaminergic Systems

The DA-containing brainstem neurons are grouped in the substantia nigra pars compacta (SNc) or A9 group, the ventral tegmental area (VTA) or A10 group, the retrorubral (RR) area corresponding to group A8, and the periaqueductal gray (PAG) thought to be a caudal extension of group A11 [232]. Extensive interconnections are established between SNc, VTA, and RR cell-groups [233] that may integrate the forebrain projections of the DA aggregates.

The use of a polyclonal antibody raised against DA-glutaraldehyde-lysyl-protein conjugate [234] helped to describe the distribution and fine morphological features of the SNc, VTA, RR, and PAG cell-groups in the squirrel monkey and to study the rostral projections of immunocytochemically identified DA neurons in the rat [235].

The thalamus is largely bypassed by DA axons. As classically known, axons from SNc project to the striatum. Retrograde double-labeling studies in squirrel monkeys point to a complex mosaic pattern of SNc cell-clusters that project either to the caudate or to the putamen [236]. The VTA efferent connections distribute caudally to various districts of the brainstem core and to the spinal cord, while rostrally they are mostly directed toward the septohippocampal complex, amygdala, accumbens, bed nucleus of stria terminalis, and prefrontal (pregenual) and insular (suprarhinal) cortices [112]. Distinctly from SNc single axons that are highly collateralized to telencephalic target structures, VTA neurons are predominantly single labeled after injections of three retrograde tracers into the caudate-putamen, septum, and frontal cortex [237]. Finally, the RR group contributes to the dorsal mesostriatal pathway in rodents [238] and cat [20].

[229] Lidov *et al.* (1980).

[230] Gaudin-Chazal *et al.* (1979); Reader *et al.* (1979).

[231] Steinbusch and Nieuwenhuys (1983).

[232] Dahlström and Fuxe (1964). In addition, DA cells are found in the dorsal raphe nucleus of both cat (Wiklund *et al.*, 1981) and rat (Descarries *et al.*, 1986).

[233] Deutch *et al.* (1986).

[234] Geffard *et al.* (1984).

[235] Voorn *et al.* (1986); Arsénault *et al.* (1988); Séguéla *et al.* (1988).

[236] Carter and Fibiger (1977); Parent *et al.* (1983).

[237] Fallon (1981).

[238] Björklund and Lindvall (1984).

3.5.4. Histaminergic Systems

The cerebral cortex is innervated by tuberomammillary, presumably histaminergic (HA), neurons [239], but only a small proportion (5%) of such cells project to widely separated cortical areas [240]. Varicose HA fibers innervate layer I in human frontal and temporal cortices [241]. The tuberomammillary neurons projecting to cortex are probably unmyelinated as antidromic identification of presumptive HA neurons showed that these cells have conduction velocities at 0.3–0.5 m/s [242]. Cortically projecting GABAergic neurons are also found within the tuberomammillary nuclei and 5-HT cells within the same region project bilaterally to neocortex [239].

Posterior hypothalamic neurons project to the MD thalamic nucleus [137, 243] and immunocytochemical mapping studies showed HA fibers in dorsal thalamic nuclei, including the LG [244] where they innervate most densely the ventral LG, while A laminae are sparsely labeled and C laminae as well as the PG (RE) nucleus display intermediate amounts of label [245]. Very few, if any, conventional synapses are found in other structures where numerous HA profiles were examined [246].

The descending projections from the posterior hypothalamus to the LC, rostral midbrain reticular formation, and mesopontine cholinergic neurons [247] provide linkages between major supramesencephalic and brainstem activating systems. HA excites neurons in the mesopontine cholinergic neurons [248], an action mediated by HA₁ receptors that promotes thalamocortical activation during wakefulness [249].

[239] Sakai *et al.* (1983a); Vincent *et al.* (1983b).
[240] Saper (1987).
[241] Panula *et al.* (1990).
[242] Takagi *et al.* (1986); Reiner and McGeer (1987).
[243] Le Gros Clark and Boggon (1933).
[244] Airaksinen and Panula (1988).
[245] Uhlrich *et al.* (1993).
[246] Hayashi *et al.* (1984); Takagi *et al.* (1986). In view of these data, it was hypothesized that HA achieves its action in a nonsynaptic (volume transmission) fashion, similarly to the monoamines and ACh in the cerebral cortex (Descarries *et al.*, 1977, 1997; Beaudet and Descarries, 1978, 1984; Umbriaco *et al.*, 1994).
[247] Saper *et al.* (1976); Parent and Steriade (1984).
[248] Khateb *et al.* (1995).
[249] Lin *et al.* (1996).

3.6. Efferent Connections of Basal Forebrain Nuclei

3.6.1. Cortical Projections

Anterograde tracing and immunohistochemical methods have revealed that the cholinergic projections from the NB and diagonal band nuclei distribute to the frontal, parietal, temporal, occipital, cingulate, and entorhinal areas [250], with a topographical organization similar in nonhuman primates and humans [251]. There are widely divergent axonal collaterals of NB cells in cortex [252], but also evidence for a certain degree of topographical arrangements in this pathway [253]. In the cerebral cortex of different species, the distribution of ChAT⁺ axons displays interareal differences, with concentration

[250] (Carey and Rieck, 1987; Kitt *et al.*, 1987) Mesulam *et al.* (1983b); Saper (1984); Woolf *et al.* (1986); Eckenstein *et al.* (1988); Wainer and Mesulam (1990).
[251] Mesulam and Geula (1988).
[252] Rye *et al.* (1984).
[253] Carey and Rieck (1987); Kitt *et al.* (1987).

in laminae that mainly characterize each area, such as deep layers V–VI in motor cortex, mid-layers III–IV in primary sensory cortices, and supragranular layers II–III in associational areas [254]. The majority of cholinergic synapses in cortex are of symmetric type and they contact apical and basal dendrites of pyramidal-shaped cells as well as local interneurons [255].

In addition to cholinergic cells, NB also possesses GABAergic neurons that were found to terminate in an overwhelming proportion on dendritic shafts of cortical GABAergic local-circuit neurons [256]. Thus, the NB-elicited activation of neocortex implicates a direct cholinergic excitation of pyramidal neurons [257] and their disinhibition through GABAergic inhibition of inhibitory interneurons.

Ultrastructural studies have characterized the morphology of cortical cholinergic terminals in serial sections of large number of axonal varicosities in the rat parietal cortex and reached the conclusion that more than 85% of cholinergic varicosities are nonjunctional [212]. Synaptic membrane differentiations are usually symmetric and occupy a small portion (<3%) of the surface varicosities. These studies are in line with the demonstration that some monoamines may also act in a volume transmission mode (see Section 3.5).

3.6.2. Thalamic Projections

Some thalamic nuclei receive cholinergic and non-cholinergic projections from both brainstem and basal forebrain. Basal forebrain nuclei contribute to the cholinergic innervation of a limited number of nuclei in the medial and rostral thalamus. While the rostral pole of thalamic reticular nucleus, MD, and AM nuclei of cat and macaque monkey receive projections from cholinergic and noncholinergic neurons of different basal forebrain cell-groups [150, 151], only the reticular nucleus is afferented from the basal forebrain in the rat [258]. Asanuma [259] demonstrated that basal forebrain neurons project to reticular nucleus by using PHA-L anterograde labeling of single axons from basal forebrain neurons and intracellular staining of reticular thalamic cells. The basal forebrain projection to the reticular thalamic nucleus is crucial in EEG activation processes since, in addition to the brainstem–RE projection, it is a source for disruption of synchronized spindle oscillations at their very site of genesis, the reticular nucleus (see Chapter 7). As to the basal forebrain projection to the MD nucleus, it can be involved in the modulation of memory and learning processes.

- [254] Lykasowski *et al.* (1989); Mesulam *et al.* (1992); Mrzljak and Goldman-Rakic (1993).
- [255] Houser *et al.* (1985).

- [256] Freund and Meskenaite (1992).

- [257] Krnjević *et al.* (1971); McCormick and Prince (1986a).

- [258] Levey *et al.* (1987b).
- [259] Asanuma (1989).

After WGA–HRP injections in the rostral pole of cat reticular nucleus, retrograde labeling mostly occurs in the horizontal branch of diagonal nuclei (DBh) and in SI where 16–18% of HRP⁺ cells were also ChAT⁺ (Fig. 3.38) [150]. A similar distribution of labeled basal forebrain neurons was found after MD injections in cat. After the MD injection in the macaque monkey (Fig. 3.39), the vast

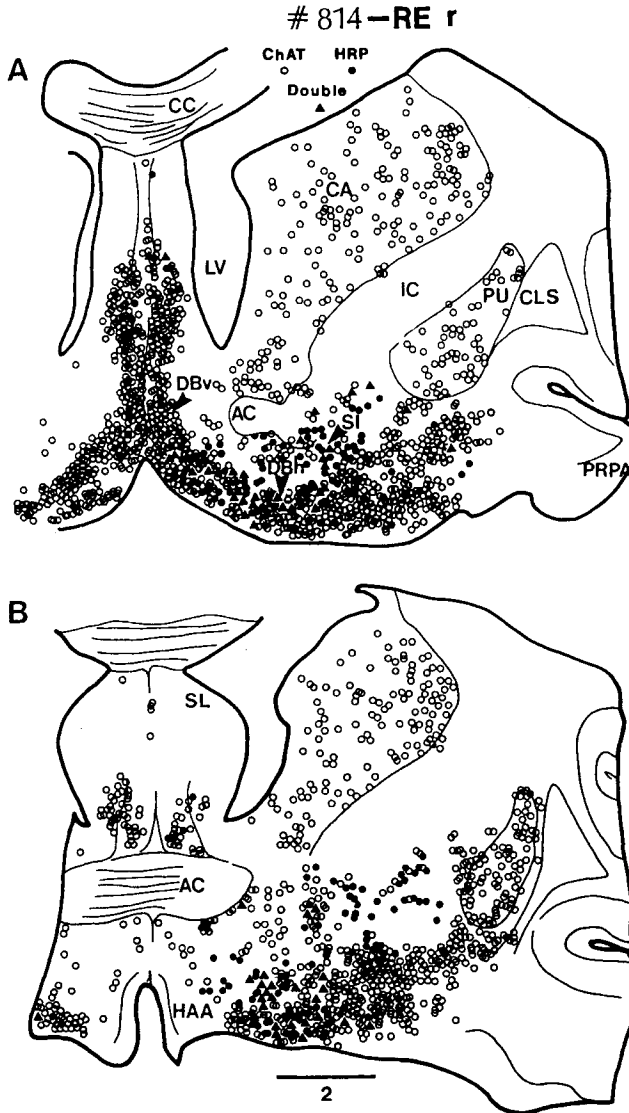


Figure 3.38. Distribution of cholinergic and noncholinergic basal forebrain neurons projecting to the rostral pole of the right thalamic reticular (RE) nucleus in the cat. Symbols of the three types of cells (ChAT⁺, HRP⁺, and double-labeled) indicated in A. Two basal forebrain levels (A16 in A, and A14.5 in B). Abbreviations of DBh, DBv, and SI, explained in text. Other abbreviations: AC, anterior commissure; CA, caudate nucleus; CC, corpus callosum; CLS, claustrum; HAA, anterior hypothalamic area; IC, internal capsule; LV, lateral ventricle; PRPA, anterior prepyriform area; PU, putamen. Bar indicates mm. From Steriade *et al.* (1987b).



Figure 3.39. Distribution of cholinergic and noncholinergic basal forebrain neurons projecting to the right mediodorsal (MD) thalamic nucleus of the *Macaca sylvana* monkey. Two frontal sections (A more anterior than B). Symbols of the three types of cells (ChAT⁺, HRP⁺, and double-labeled) indicated in A. GPe and GPi, external and internal segments of globus pallidus. From Parent *et al.* (1988).

majority of HRP⁺ cells occur medially in the vertical branch of the diagonal band nuclei (DBv), ventrally in DBh, and dorsolaterally in the SI, with double-labeled (HRP + ChAT) cells ranging from 11% to 23% [151]. The projection from basal forebrain to thalamic MD nucleus was also observed with the PHA-L transport in rat [260] and both cholinergic and GABAergic preoptic neurons in the basal forebrain neurons project to the cat MD nucleus [261].

The salient finding after AV-AM injections was that the number of labeled cells was much higher in DBv (compared to those found after reticular or MD injections),

[260] Ray and Price (1987).
[261] Gritti *et al.* (1998).

where neurons displaying also ChAT immunoreactivity reached 27% of the total number of retrogradely labeled elements [151]. Finally, after VM injections, HRP⁺ cells were observed in SI and lateral part of the preoptic area, but no double-labeled (HRP + ChAT) cell was detected.

The low-affinity nerve growth factor receptor (NGFr) is expressed by basal forebrain cholinergic neurons [262]. The colocalization of ChAT and NGFr in NB neurons that project to the thalamic reticular nucleus was investigated and 10–20% of NB cholinergic neurons were also found to be NGFr-immunoreactive [263].

The majority of noncholinergic basal forebrain neurons with thalamic projections are GABAergic cells intermingled with the cholinergic ones (see Section 3.3.1). The differential termination of cholinergic and GABAergic terminals on rostral thalamic reticular neurons was demonstrated by EM analyses. Cholinergic terminals are very small ($< 0.25 \mu\text{m}$), with spherical vesicles and asymmetrical synaptic contacts onto distal dendrites of thalamic reticular neurons, and do not form axoaxonic contacts, thus precluding a presynaptic cholinergic effect upon axonal terminals arising in the dorsal thalamus or cerebral cortex [264]. By contrast, axons originating in the NB terminate perisomatically onto reticular neurons [259, 265]. The GABAergic NB projection to the reticular nucleus was demonstrated by combining retrograde labeling and GABA immunoreactivity [266]. A GABAergic projection from basal forebrain structures was also found to terminate in the MD thalamic nucleus [267]. The inhibitory effect of GABA on thalamic reticular neurons is associated with a marked increase in Cl^- conductance (see Chapter 6). These data, combined with the ACh-induced hyperpolarization and increased K^+ conductance of thalamic reticular neurons, support the idea of a permissive role played by NB (in conjunction with brainstem cholinergic cells) in spindle genesis, with the appearance of spindle oscillations immediately after the reduction in firing rates of NB neurons [268].

3.6.3. Posterior Hypothalamic Projections

A neuronal circuit, which may explain the transition from waking to sleep, is the descending projection from the basal forebrain to the histaminergic neurons located in the tuberoinfundibular region of the posterior hypothalamus that are regarded as a cellular group with activating properties (see Section 1.3.2). Morphological/immunohistochemical data support the idea of a descending inhibitory circuit from the preoptic area in the basal forebrain to the posterior hypothalamus. The descending pathway from NB,

[262] Bachelor *et al.* (1989); Woolf *et al.* (1989).

[263] Chen and Bentivoglio (1993).

[264] Hallanger and Wainer (1988).
 [265] Asanuma (1997).

[266] Asanuma and Porter (1990).

[267] Kuroda and Price (1991).

[268] Buzsáki *et al.* (1988); Steriade and Buzsáki (1990). See Chapters 7–10).

diagonal band nuclei, and Mc preoptic nucleus of the anterior hypothalamus, to the posterolateral hypothalamus was revealed by combining retrograde tracing techniques with GAD immunohistochemical staining [115]. Other experiments have demonstrated the selective firing, during sleep, of preoptic cells with identified projections to the posterior hypothalamus [269].

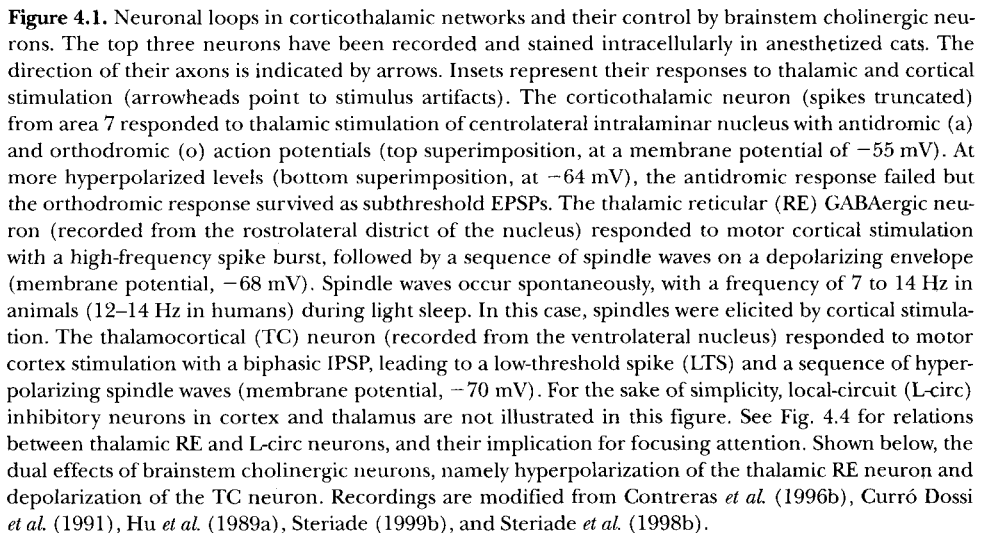
[269] Sherin *et al.* (1996).

Neuronal Circuits in the Thalamus, Neocortex, and Hippocampus, Targets of Diffuse Modulatory Systems

As discussed in the previous chapter, brainstem cholinergic and noncholinergic, most likely glutamatergic, neurons project overwhelmingly to the thalamus and have negligible direct projections to neocortex, whereas monoamine-containing neurons of the locus coeruleus and dorsal raphe nucleus have less prominent projections to the thalamus but have direct access to the cerebral cortex. The basal forebrain cholinergic and GABAergic neurons project to neocortex, archicortex, and related structures, and also impact on the activity of thalamic reticular (RE) GABAergic neurons and, to a lesser extent, some medial nuclei of the dorsal thalamus.

The aim of this chapter is to briefly present the main cellular types and synaptic articulations in neuronal networks that operate under the influence of brainstem and basal forebrain modulatory systems. Full accounts on thalamic and cortical connectivity, neuronal properties, and networks are found in previous monographs [1]. The intrinsic properties of neurons, which are participating in the circuits presented here, are dealt with in Chapter 5. Needless to say, the complexity of forebrain neuronal circuits and their dependency on brainstem and other modulatory systems require investigations in intact-brain preparations. Figure 4.1 illustrates the basic cellular phenomena in intrathalamic, thalamocorticothalamic, and brainstem–thalamic networks. In essence, although corticothalamic projections are excitatory on both reticular and thalamocortical (TC) neurons, the actions are inhibitory on TC cells when reticular neurons are in the burst mode, because of prevalent excitation of reticular neurons; and, the brainstem cholinergic actions on TC

[1] Jones (1985); Steriade *et al.* (1990b, 1997a); Steriade (2001b, 2003a).



neurons are both direct depolarization and indirect disinhibition because of hyperpolarization of GABAergic reticular neurons (see Section 4.1).

4.1. Thalamus

There are three types of thalamic neurons: thalamic neurons with cortical projections (TC) that are glutamatergic (excitatory); reticular neurons that are GABAergic (inhibitory) and represent an interface between the thalamus and neocortical outputs; and local-circuit (L-circ) GABAergic neurons whose axons remain within the limits of the dorsal thalamic nucleus where somata are located.

Thalamocortical neurons are bushy and their variations are linked mainly to soma size, large neurons projecting to deep and middle cortical layers, whereas small neurons project preferentially to superficial layers [1]. TC neurons in relay nuclei receive ascending afferents from sensory and motor pathways. The highest degree of specificity and organization characterizes sensory nuclei, in particular the lateral geniculate, medial geniculate, and ventroposterior nuclei. Motor relay nuclei, ventrolateral and ventromedial, receive afferents from the cerebellum and other structures related to motor functions. Other thalamic nuclei, such as pulvinar and lateroposterior, project to wider cortical areas and are implicated in association processes. Intralaminar nuclei lie within a narrow lamina that separates medial from lateral thalamic nuclei. Distinctly from relay nuclei that receive specific information from sensory or motor pathways, intralaminar nuclei receive afferents from a variety of heterogeneous sources, including fibers from pain pathways, motor centers, and brainstem systems implicated in the control of states of vigilance. The lack of specific afferentation to these nuclei matches their less circumscribed projections to the forebrain. The posterior intralaminar nuclei (center median and parafascicular) project mainly to the striatum. The anterior intralaminar (central lateral and paracentral) nuclei project not only to the striatum, but also to superficial as well as deep layers of widespread cortical areas. This diffuse projection to cortex characterizes anterior intralaminar nuclei as a whole, but the overwhelming majority of their individual neurons project to quite restricted neocortical areas, either sensory, motor, or association.

Reticular neurons have axons that collateralize within the nucleus and also project to dorsal thalamic nuclei, but not to cortex; they have long dendrites, whose secondary and tertiary branches possess vesicle-containing appendages

that form synapses on the dendrites of other reticular neurons [2]. Thus, contrary to TC neurons, that can communicate only through intermediary reticular or neocortical neurons (Fig. 4.1), reticular neurons form an interconnected network which is particularly well suited for the generation of some sleep oscillatory types which can occur even in the deafferented reticular nucleus [3, 4]. There is a reciprocal excitatory circuit between glutamatergic neocortical and TC neurons and a recurrent inhibitory loop between TC neurons and GABAergic reticular neurons (Fig. 4.1).

Local-circuit GABAergic thalamic interneurons constitute 25–30% of neurons in all thalamic nuclei of cats and primates, as well as in the dorsal lateral geniculate nucleus of rats, but they are virtually absent in other nuclei of rodents [1]. The relations between TC neurons and interneurons occur in thalamic synaptic islands encapsulated by glial sheets (called glomeruli) as well as outside these islands. The glomeruli contain two presynaptic and two postsynaptic elements (Fig. 4.2). The first presynaptic element consists of axon terminals of ascending afferent fibers that have round and large vesicles and excite the dendrites of both relay and L-circ cells. The second presynaptic elements are the dendrites of local interneurons. These dendrites are postsynaptic to afferent terminals and make inhibitory synaptic contacts on dendrites of TC cells as well as on dendrites of other local interneurons. The basic synaptic arrangements and the excitatory or inhibitory influences at different synaptic contacts account for the sequence of events that follow the arrival of an afferent impulse in the thalamus (see bottom panel in Fig. 4.2). The bisynaptic inhibition of relay cells (following their initial excitation) consists of an early IPSP (IPSP_a), followed by a prolonged IPSP that consists of two phases, IPSP_A and IPSP_B. The α -IPSP is generated within the glomerulus by presynaptic dendrites of local interneurons [5], while A- and B-IPSPs are generated by axons of interneurons as well as, in the case of those nuclei that receive afferents from the thalamic reticular nucleus, from the latter. As shown in Fig. 4.2, the cause of inhibition produced by local interneurons onto TC neurons can be quickly removed because of excitation from afferent axons to other interneurons (I₂d) and inhibition from I₂d to I₁d, thus disinhibiting relay neurons. These effects explain the short (a few milliseconds) duration of the EPSP in TC neurons, which is immediately cut off by the subsequent IPSP, which is in turn removed, thus allowing the relay cell to transfer with high fidelity signals recurring at very fast rates (even 200 to 300 Hz). As discussed in Chapter 8, section 8.1.4.2), the earliest IPSP (GABA_A) undergoes completely different effects under brainstem reticular stimulation mimicking arousal,

[2] Deschênes *et al.* (1985); Yen *et al.* (1985).

[3] Steriade *et al.* (1987a).

[4] Bazhenov *et al.* (1999).

[5] Paré *et al.* (1991); Curró Dossi *et al.* (1992b).

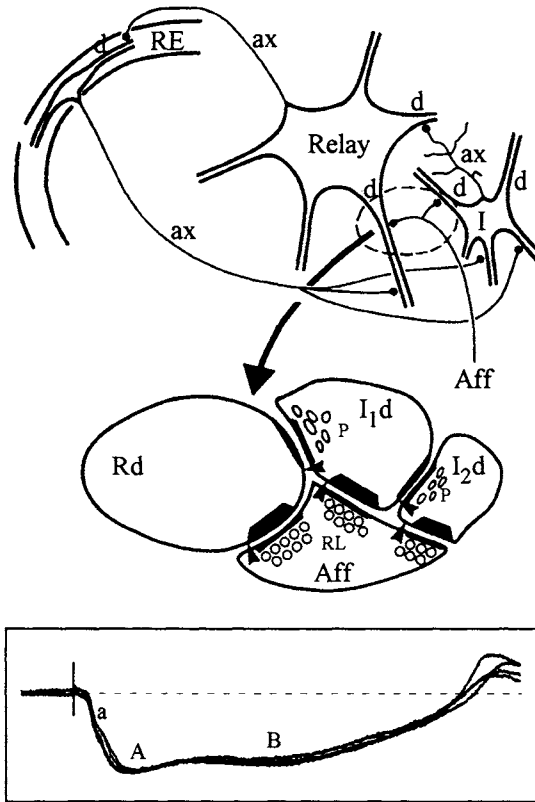


Figure 4.2. Thalamic glomeruli and three types of inhibitory postsynaptic potentials (IPSPs) in thalamocortical (TC) neurons. Synaptic contacts between thalamic reticular (RE), TC (relay), and local interneurons (I) are indicated by dots at the end of axons (ax). Note that RE axons contact not only relay cells but also local interneurons. Afferent (Aff) fibers to the thalamus contact dendrites (d) of relay cells and local interneurons. Territory delineated by dashed line, representing a thalamic glomerulus, is expanded below (arrow). The first presynaptic element consists of ascending afferent axons that have round and large (RL) vesicles and make asymmetrical synaptic contacts with dendrite of relay cell (Rd) as well as dendrites of local interneurons. The second presynaptic element is the dendrite of interneuron which is postsynaptic to afferent axon, contains pleomorphic (P) vesicles, and makes symmetrical synaptic contacts on dendrites of relay cell as well as on dendrites of other local interneurons (I_1d and I_2d are dendrites of two interneurons). In the latter case, contacts may be reciprocal. Bottom, superimposition of intracellularly recorded traces in thalamic relay neuron showing three types of IPSPs: *a*, *A*, and *B*. See also text. Modified from Steriade (1999c) and Paré *et al.* (1991).

[6] Timofeev and Steriade (1996). The relations between thalamic RE and TC cells have also been investigated in slices from the perigeniculate nucleus, the visual sector of RE nucleus (Bal *et al.*, 1995a, b). In those *in vitro* studies, the spike-burst of RE neurons lasted for about 30 ms, while the IPSP generated in TC neurons by burst discharges

compared to the following biphasic sequence of $GABA_{A-B}$ IPSPs [5]. This difference accounts for the blockage of low-frequency sleep oscillations upon awakening, but preservation or even enhancement of a short IPSP in TC neurons, which is required for inhibitory sculpturing of incoming messages during the adaptive state of waking.

The interactions between reticular and TC neurons during spontaneously occurring spindles are depicted in Fig. 4.3, using dual intracellular recordings *in vivo* [6]. Such recordings demonstrate a close correlation between the depolarizing envelope and spike-bursts during spindle waves in

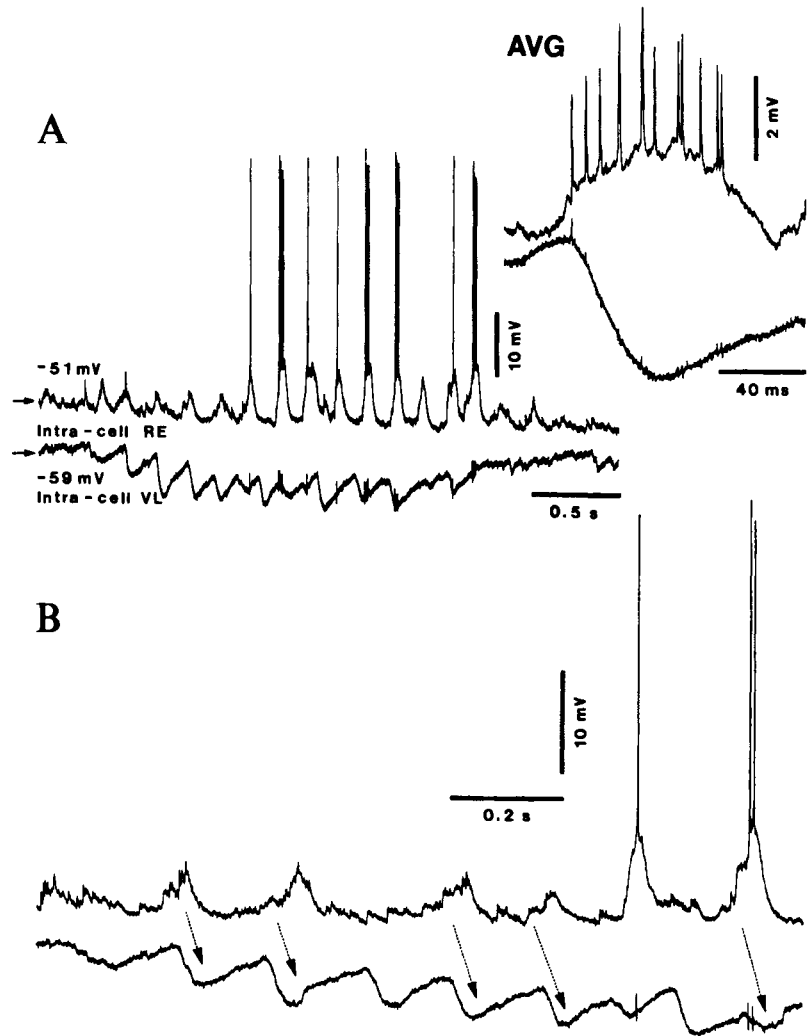


Figure 4.3. Relations between simultaneously recorded depolarizing spindle waves in rostralateral thalamic reticular (RE) cell and hyperpolarizing IPSPs in thalamocortical (TC) cell from ventrolateral (VL) nucleus. Decorticated cat under ketamine–xylazine anesthesia. A, spindle sequence. Inset: averaged ($n = 15$) activity triggered by the onset of IPSPs in VL neuron. B, another spindle sequence showing the close time relation between the depolarizing waves in RE cell and IPSPs in VL cell. Small deflections in the trace from VL cell are capacitive coupling artifacts from RE-cell's action potentials. From Timofeev and Steriade (1996).

reticular neurons and, on the other hand, IPSPs in the simultaneously recorded TC cell. The requirement of synaptic inputs from reticular to TC neurons in the generation of sleep spindles is underlined by the absence of spindles in those thalamic nuclei that lack these connections. Anterior thalamic neurons display LTS-generated spike-bursts with the same characteristics as those found in other thalamic neurons [7]. As anterior thalamic neurons do not receive synaptic inputs from the reticular nucleus of cats [8] and the reticular nucleus is the spindle pacemaker (see Chapter 7),

in reticular neurons was about 130 ms in duration if it was followed by a rebound LTS, and about 150 ms in duration if it was not. The spike-burst in TC cells was about 10 ms in duration. These differences between spike-bursts crowning low-threshold spikes (LTSs) in RE and TC cells, displaying much longer

duration in RE cells, corroborate data from *in vivo* recordings during natural sleep (Domich *et al.*, 1986; Steriade *et al.*, 1986).
 [7] Mulle *et al.* (1985); Paré *et al.* (1987).
 [8] Steriade *et al.* (1984a); Velayos *et al.* (1989).
 [9] Wilcox *et al.* (1988).

spindles are absent in anterior thalamic nuclei as well as in limbic cortical areas where these nuclei project [7]. The fact that the lateral habenular neurons do not receive inputs from the reticular nucleus [8] also explains the absence of spindles in those neurons that have similar intrinsic properties and ionic conductances as other thalamic neurons [9]. Instead of spindles, lateral habenular neurons display other oscillatory activities in their membrane potential, within the frequency range of the theta rhythm that is imposed from hippocampus and related structures. These data emphasize the role played by synaptic operations within the thalamus in the generation of sleep spindles, rather than the intrinsic properties of TC cells.

Eight to ten percent of reticular neurons project, in addition to TC neurons, to L-circ GABAergic neurons [10]. The synaptic weight of this projection is not known and this GABA-to-GABA projection may produce significant effects on the ultimate targets, TC neurons. Indeed, an increased probability of IPSPs in TC neurons was found after excitotoxic lesions of reticular neurons [11], as if GABAergic local interneurons were released from the inhibition that arises in reticular neurons. The circuitry between RE, L-circ, and TC neurons was implicated in processes of focusing attention [12]. Thus, the top Th-cx (TC) neuron in Fig. 4.4 receives prevalent excitation from the afferent fiber (Aff.) while the bottom Th-cx receive less collaterals from the Aff. axon. The reticular neurons which are directly connected to the top Th-cx neuron (the top reticular neuron is part of this pool) contribute to further enhancing the relevant activity by inhibiting the pool of L-circ elements (the top L-circ neuron is part of this pool). Simultaneously, the activity in adjacent reticular areas (bottom reticular neuron in Fig. 4.4) is suppressed by axonal collateralization and dendrodendritic synapses within the reticular nucleus. The consequence would be the released activity of target L-circ neurons (bottom L-circ cell) and inhibition of weakly excited Th-cx neurons (bottom Th-cx neurons) in areas adjacent to the active focus [13].

[10] Liu *et al.* (1995).

[11] Steriade *et al.* (1985).

[12] Steriade (1999b).

[13] This hypothesis derived from a study on the activity of RE neurons during the natural waking-sleep cycle (Steriade *et al.*, 1986). The circuit illustrated in Fig. 4.4 was proposed in Steriade (1991) and was redrawn by E.G. Jones.

4.2. Neocortex

The four cell classes of neocortical neurons, defined by their responses to depolarizing current pulses, are described in Chapter 5. Basically, these neurons are pyramidal-shaped long-axoned (excitatory) neurons and aspiny or sparsely stellate L-circ (inhibitory) neurons. There is a great variety within each group of these two major neuronal types, regarding their target domains,

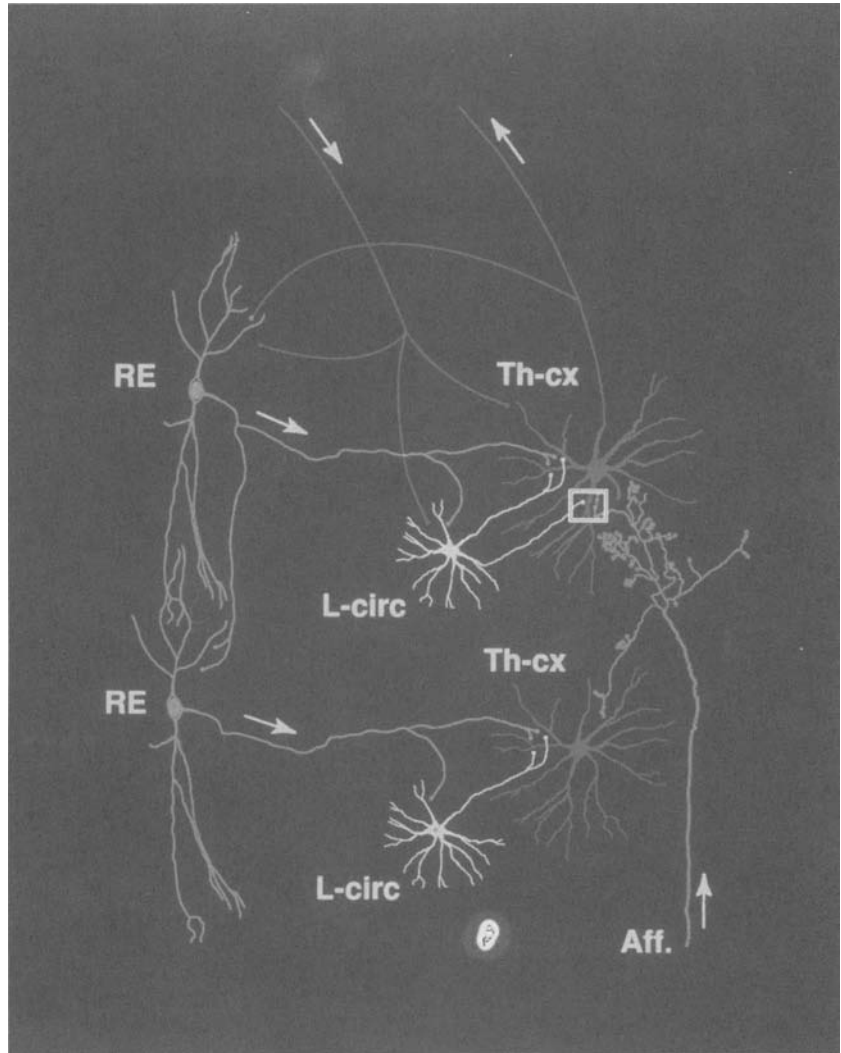


Figure 4.4. Relations between GABAergic thalamic reticular (RE) and local-circuit (L-circ) neurons, and their effects on thalamocortical (Th-cx) neurons. See main text for full explanation and hypothesis of focusing attention based on these connections. This hypothesis derived from a study on the activity of RE neurons during the natural waking-sleep cycle of chronically implanted cats (Steriade *et al.* 1986). The circuit was proposed in Steriade (1991) and was redrawn by E.G. Jones. See also color plate 3.

chemical codes, electrophysiological characteristics, and dependency on behavioral state of vigilance.

The targets of axons from pyramidal neurons located in layers II–III are ipsi- and contralateral cortical areas; layer V neurons project to basal ganglia, intralaminar thalamic nuclei, superior colliculus, and spinal cord; and layer VI pyramidal neurons project to specific thalamic nuclei and claustrum. The neurotransmitter of pyramidal-shaped neurons is glutamate or aspartate. The different firing patterns

(regular-spiking, intrinsically-bursting, and fast-rhythmic-bursting) of pyramidal neurons recorded from different cortical layers are presented in Chapter 5 (Section 5.6.1). As to their state-dependent fluctuations in firing rates, one of the most dramatic difference among two classes of antidromically identified corticospinal neurons upon the short period of awakening from sleep in behaving monkeys is the tonically increased firing rates of slow-conducting (below 40 m/s) pyramidal neurons, whereas fast-conducting (above 40 m/s) pyramidal neurons stopped firing on arousal [14] (see also Chapter 10).

Probably, the greatest variety is found in the group of local inhibitory interneurons that form about 20–25% of all cortical neurons. This was described in morphological studies long ago [15] and was recently substantiated by studying the chemical codes of different L-circ cells and their electrophysiology. Thus, inhibitory interneurons release GABA as transmitter and some also express parvalbumin, somatostatin, cholecystokinin, and vasointestinal peptides [16]. Various types of inhibitory neurons target various parts of the somadendritic membrane of pyramidal cells or other inhibitory neurons. (1) Basket cells are located in all layers, mainly III and V/VI, their axons contact the soma and proximal dendrites of pyramidal neurons, and they innervate themselves through autapses. (2) Chandelier neurons are mainly located in layers II/III and their main target is the initial segment of pyramidal cell axons, thus having a strategic location for preventing the latter to communicate with other neurons. (3) Double bouquet dendritic neurons are concentrated in layers II/III and their vertical axons contact pyramidal and local interneurons. (4) Neurogliaform cells, the smallest interneurons (soma diameter, 10–12 μm), are found in superficial layers, mainly layer I, and have a very dense axonal arbor. And (5) Martinotti cells are found in deep layers, mainly layer VI.

Local-circuit operations in neocortex implicate excitatory connections among pyramidal neurons as well as inhibitory contacts among GABAergic interneurons and between the latter and pyramidal cells (Fig. 4.5). The short-lasting, presumably GABA_A-receptor-mediated, IPSPs in pyramidal neurons, result from firing of local inhibitory interneurons (Fig. 4.6). Although *in vitro* recordings showed that cortical IPSPs are made of two distinct phases, mediated by GABA_A and GABA_B receptors [17], the amplitude of the GABA_B-mediated IPSP is much smaller *in vivo* or not visible at all, and neocortical IPSPs are reversed almost completely by Cl[−] [18]. *In vivo*, a condition in which spontaneous activity of neurons is rich, the evoked GABA_A IPSP shuts off cellular activity and leads to a generalized

[14] Fast-conducting pyramidal neurons of *Macaca mulatta* stopped firing upon arousal for periods ranging from 4 to 33 s in different units (Steriade *et al.*, 1974a).
[15] Jones (1975b).

[16] Somogyi *et al.* (1983, 1985); Somogyi (1989); DeFelipe and Jones (1992); DeFelipe (1993); Kawaguchi and Kubota (1997).

[17] Connors *et al.* (1988).

[18] Pollen and Lux (1966); Renaud *et al.* (1974); Contreras *et al.* (1997c).

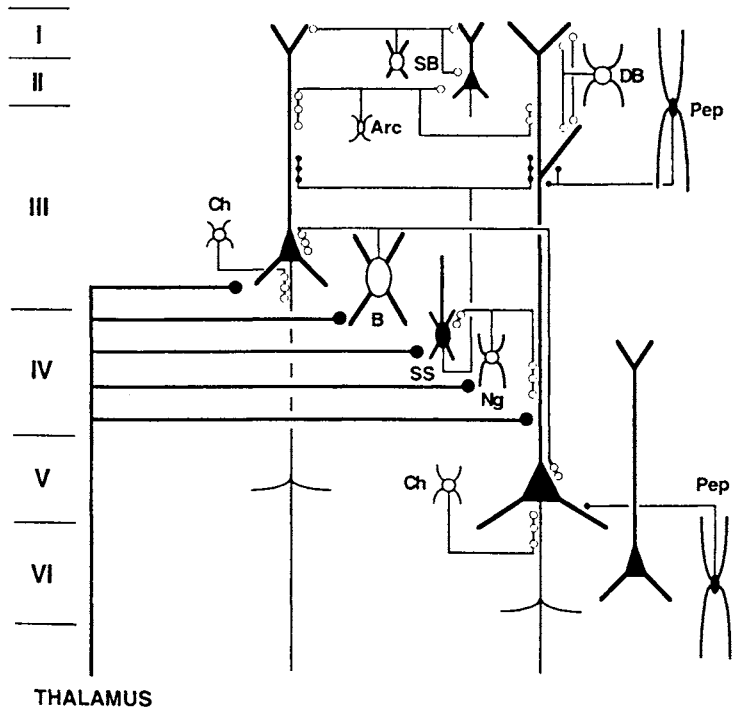


Figure 4.5. Excitatory and inhibitory neuronal circuits in cat primate somatosensory cortex. Solid dots are excitatory terminals; open circles, inhibitory terminals; solid cells, excitatory; shaded cells, inhibitory. Cell designations are: Arc, arcade; B, large basket; Ch, chandelier; DB, double bouquet; Ng, neurogliaform; Pep, peptide cell; SB, small basket. SS, spiny stellate. Modified from Jones (1991) and Mountcastle (1998).

phenomenon of disfacilitation during which “leak” K^+ currents dominate the membrane behavior. The inhibitory actions of L-circ GABAergic cells are exerted on the soma and initial segment of pyramidal cells’ axons, but also on dendrites where they are able to delay or block spiking in dendrites [19].

The synaptic transmission is differentially exerted by the same pyramidal cell’s axon innervating pyramidal cells and local inhibitory interneurons. Thus, a pyramid produces synaptic depression on nearby pyramids, whereas facilitation is produced on interneurons (Fig. 4.7) [20]. These differential effects are useful for understanding the rules underlying frequency-dependent plasticity.

The long-range connections of the neocortex include ipsilateral corticocortical and callosal pathways, as well as corticofugal projections to many subcortical structures. The intrinsic cortical circuitry is abundant in the association cortex, but such connections also exist in sensory and motor cortical areas, as demonstrated by both morphological and electrophysiological studies [21]. Although monosynaptic excitatory connections in cat’s motor cortex seem

[19] Kim *et al.* (1995).

[20] Markram *et al.* (1998).

[21] Jones *et al.* (1978); Avendaño *et al.* (1988); Keller (1993); Matsumara *et al.* (1996).

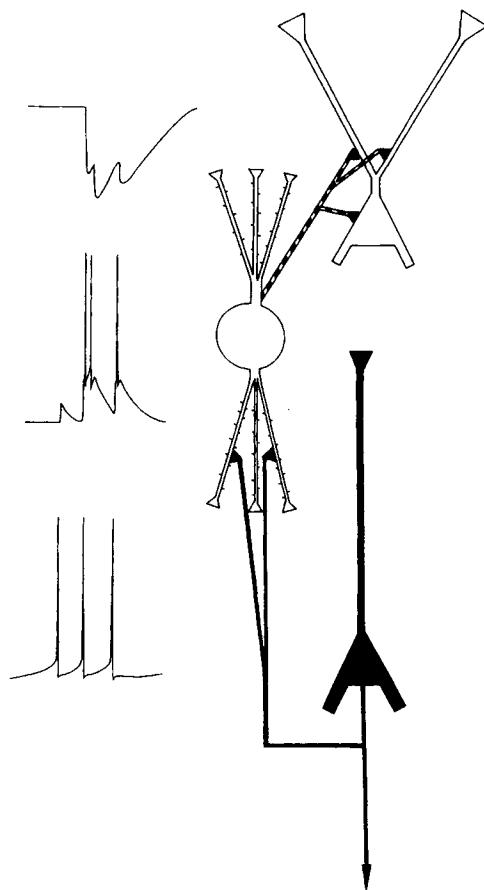


Figure 4.6. Connections made by neurons identified anatomically and physiologically as spiny, burst firing interneurons. Trains of action potentials in the presynaptic pyramid (bottom trace at left) elicit EPSPs in burst firing interneuron that displays paired-pulse facilitation and can drive the interneuron to fire action potentials (middle trace); in turn, the interneuron elicits trains of fast (presumably GABA_A) IPSPs in the postsynaptic pyramid (top trace). From Deuchars and Thomson (1995).

[22] Asanuma and Rosen (1973).

[23] Amzica and Steriade (1995a).

[24] Gilbert and Wiesel (1983); Gilbert (1992).

to be limited to a distance of less than 1 mm [22], short- and fixed-latency, presumably monosynaptic responses between caudal and rostral sites in the association cat's suprasylvian gyrus, separated by 7–10 mm, have been demonstrated by means of dual intracellular recordings from areas 7 and 5 [23] (Fig. 4.8). These pathways may underlie the intra- and intercolumnar operations necessary for the cortical synchronization of slow and fast rhythms that characterize different states of vigilance. In the visual cortex too, intracortical horizontal connections may span up to 8 mm, allowing communication between neuronal assemblies that have widely separate receptive fields [24]. While most horizontal intracortical connections are provided by pyramidal-shaped neurons and are excitatory in nature, a similar excitatory outcome (through

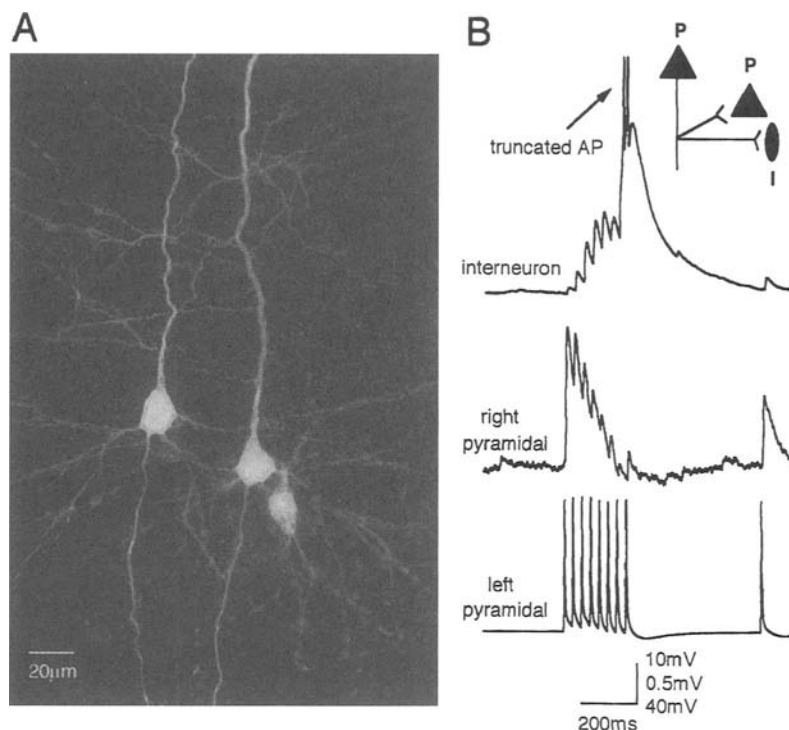


Figure 4.7. Differential synaptic facilitation and depression via the same axon innervating two different targets, *in vitro*. Sagittal slice from rat somatosensory cortex. A, a light microscopic image of three biocytin-filled neurons. The pyramidal neuron on the left innervated the pyramidal neuron on the right and the bipolar interneuron on the right (see also scheme at top in B). B, single trial responses (30 Hz) to the same train of action potentials (APs). Failure rate for first EPSP: interneuron, 24%; pyramidal neuron, 0% (60 sweeps). Coefficient of variation for first EPSP: interneuron, 1.12; pyramidal neuron, 0.15. Coefficient of variation for 6th EPSP: interneuron, 0.32; pyramidal neuron, 0.68. From Markram *et al.* (1998).

disinhibition) may result from interactions between large inhibitory basket cells and other GABAergic L-circ neurons [25].

The longest-range intracortical connections generally link association neocortical areas in cats [26] and primates [27]. In macaque monkeys, areas 46 and 7a project over a dozen target cortical areas (Fig. 4.9).

The callosal projection plays a crucial role in integrative functions of the two hemispheres [28] and the inter-hemispheric coherent activity of low- and fast-frequency oscillations during slow-wave sleep [29] and brain-activated states of waking or REM sleep [30], respectively. The location of corpus callosum neurons is mainly in cortical layers II/III but also in infragranular layers [31]. Callosal neurons have significantly greater spine density and more complex apical and basal dendritic arbors than neurons with ipsilateral cortical projections [32]. Callosal neurons contribute not only to the coherent activity between cortical areas but

[25] Kisvárdy *et al.* (1993); Gupta *et al.* (2000).

[26] Bignall *et al.* (1966).

[27] Goldman-Rakic (1987, 1988).

[28] Reviewed in Seymour *et al.* (1994) and Berlucchi *et al.* (1995).

[29] Steriade *et al.* (2001a).

[30] Engel *et al.* (1991); Nuñez *et al.* (1992b); Kiper *et al.* (1999); Knyazeva *et al.* (1999).

[31] Barbaresi *et al.* (1994);

Milleret *et al.* (1994);

Matsubara *et al.* (1996).

[32] Soloway *et al.* (2002).

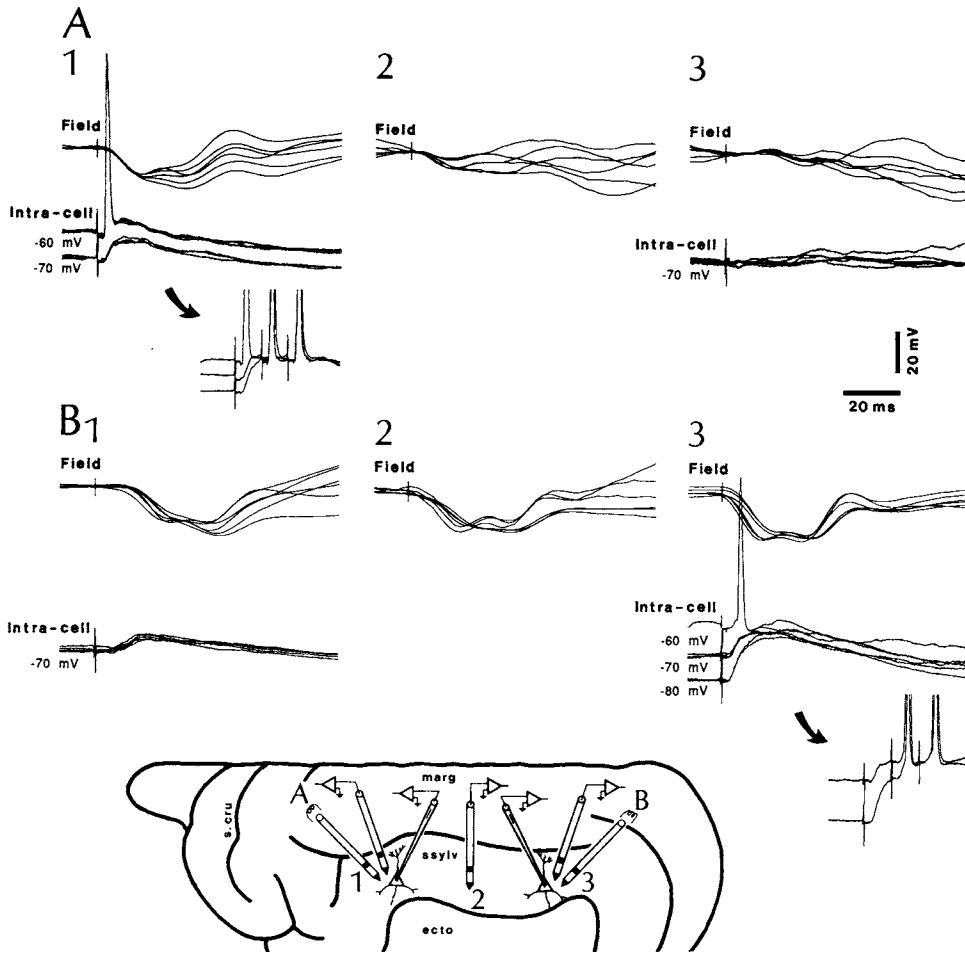


Figure 4.8. Electrophysiological identification of intracortical pathways in suprasylvian gyrus of cat. Ketamine–xylazine anesthesia. Two simultaneous intracellular recordings at sites 1 and 3 in the rostral and caudal suprasylvian gyrus (see bottom scheme). Close (1 mm) to each intracellular micropipette there were two coaxial electrodes, one for bipolar recording of field potentials (FPs), the other for stimulation. An additional FP was recorded in the middle suprasylvian gyrus (site 2). Stimulation through the anterior electrode (A) elicited in the closely recorded cell (A1) an antidromic action potential, with a latency of 3 ms, at the resting membrane potential (−60 mV). An EPSP was revealed by hyperpolarizing the membrane at −70 mV. The same stimulation evoked a biphasic depth-negative FP. The inset in A1 shows three responses of this neuron, at different membrane potentials, to a three-shock train at 100 Hz. The anterior stimulation was less effective toward the caudal recording sites, as shown by the progressively reduced amplitude of FPs and absence of overt EPSPs in the posterior intracellular recording (A2–3). By contrast, stimuli delivered at the posterior site (B) induced EPSPs in both (posterior and anterior) cells, with shorter latencies in the posterior neuron. The inset in B3 displays the temporal summation of EPSPs to 100 Hz stimulation. From Amzica and Steriade (1995a).

also ensures that cortical activity on one side is reflected on the contralateral thalamus, as the same neocortical neuron in the monkey's precentral gyrus and cat's association cortex receives monosynaptic excitation from homotopic sites in the contralateral cortex and is antidromically activated from the related thalamic nuclei [33].

[33] Steriade *et al.* (1974b); Cissé *et al.* (2003).

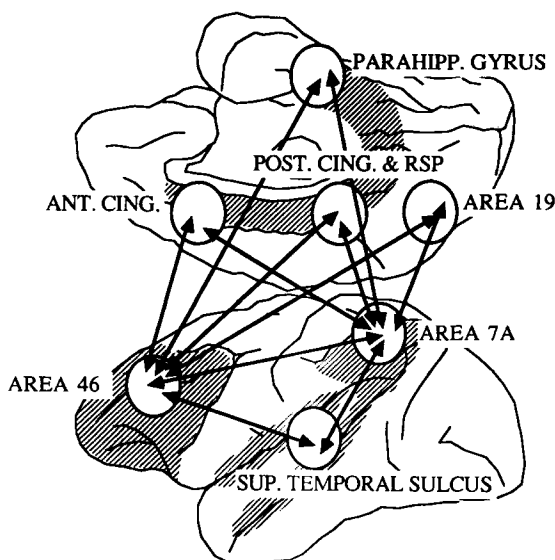


Figure 4.9. The results of a double-labeling study in macaques in which WGA–HRP (or 3-H leucine and proline) was placed in area 7a and tritiated amino acids (or WGA–HRP) were placed in area 46 in the same hemisphere of the same animal. Paired sections were superimposed and analyzed. Cross-hatched regions represent areas that have been reported to receive afferents from the thalamic medial pulvinar nucleus. See also main text. From Goldman-Rakic (1988).

The corticothalamic projections originate in layers VI or V and they outnumber the TC axons by almost one order of magnitude. Thin corticothalamic axons originate in layer VI, whereas thick fibers arise from layer V. In addition to ipsilateral corticothalamic projections, contralateral projections terminate in medial thalamic nuclei of monkeys [34]. Although the corticothalamic projection to all three major types of thalamic neurons (relay TC neurons as well as GABAergic thalamic reticular and L-circ neurons) is glutamatergic, therefore excitatory, synchronous volleys occurring naturally during cortical sleep oscillations or elicited by electrical stimuli, produce powerful depolarizing actions on both types of thalamic GABAergic (RE and L-circ) neurons and hyperpolarizing actions on TC neurons (see Fig. 4.1). In contrast to these direct excitatory effects on both types of thalamic inhibitory neurons, the cortical action on TC neurons is a long-lasting hyperpolarization, consisting of a biphasic (GABA_{A-B}) IPSP (Fig. 4.1) mediated by thalamic reticular or local interneurons. Indeed, following excitotoxic lesions of reticular neurons, the prolonged IPSPs disappear in TC neurons but they receive numerous, short-lasting IPSPs from local interneurons [11; see Section 4.1]. Thus, when reticular neurons are in the burst mode, as during slow-wave sleep or different forms of seizures, the prevalent corticothalamic actions are inhibitory on TC cells [35]. Direct

[34] Preuss and Goldman-Rakic (1987).

[35] These electrophysiological data, from experiments on the slow sleep oscillation (Steriade *et al.*, 1993b) and paroxysmal discharges (Steriade and Contreras, 1995; Timofeev *et al.*, 1998), are supported by recent studies showing that the numbers of glutamate receptor subunits GluR4 are 3.7 times higher at corticothalamic synapses in RE neurons, compared to TC neurons, and the mean peak amplitude of corticothalamic excitatory postsynaptic currents (EPSCs) is about 2.5 higher in RE, than in TC, neurons (Golshani *et al.*, 2001).

excitatory cortical influences on TC cells may be seen either after lesioning reticular neurons or during behavioral states, such as waking or REM sleep, in which these thalamic GABAergic neurons fire tonically, in the single-spike mode [36]. In the latter condition, the cortically elicited excitation of TC cells may overcome the inhibition mediated via reticular neurons.

[36] Steriade *et al.* (1986).

4.3. Hippocampus and Related Systems

The hippocampus, entorhinal cortex, and nuclear complex of amygdala have been intensively studied because of their role in learning and memory, the presence of a neuronal type involved in spatial coordinates of the environment, the generation of theta oscillation during active wakefulness and REM sleep, and their high susceptibility to develop epileptic activity.

[37] Amaral and Witter (1989); Lopes da Silva *et al.* (1990); Freund and Buzsáki (1996).

[38] Andersen *et al.* (1964, 1969); Ben-Ari *et al.* (1981a).

[39] Somogyi *et al.* (1983, 1985). The importance of chandelier (axoaxonic) cells in controlling the excitability of hippocampal pyramidal neurons is demonstrated by the loss of axons of chandelier neurons in rat's hippocampal transplants that display paroxysmal discharges (Freund and Buzsáki, 1988). There is also a decrease in chandelier neurons in entorhinal cortex and subiculum of epileptic patients (DeFelipe, 1999).

[40] Alonso and Klink (1993). Layer II neurons receive cholinergic innervation from the septum (Alonso and Köhler, 1984) and a muscarinic agonist, carbachol, produces membrane depolarization of stellate cells associated with oscillations in the theta frequency range.

[41] Paré *et al.* (2002).

[42] Kreindler and Steriade (1964).

The trisynaptic loop in the dentate gyrus and CA1–CA3 fields of hippocampus proper was extensively reviewed elsewhere [37]. The perforant path axons, arising in layers II–III of the entorhinal cortex, produce EPSPs on granule cells' dendrites in neurons of the dentate gyrus, which project to the pyramidal cells in CA3 field; and the pyramidal cells in the CA1 field receive excitatory inputs from Schaffer fibers (collaterals of CA3 pyramidal cells' axons) as well as from axons originating in the entorhinal cortex that terminate on more distal parts of their apical dendrites. The initial EPSPs produced in the pyramids of CA1–CA3 fields are followed by large IPSPs that may lead to a postinhibitory rebounds [38]. The IPSPs are produced by different types of interneurons, such as chandelier (or axoaxonic) cells [39], basket cells, inhibitory neurons that target the dendritic trees of granule and pyramidal cells, and interneuron-selective GABAergic cells that are specialized in innervating other inhibitory interneurons.

The entorhinal cortex receives direct inputs from association neocortical areas and has direct access to the hippocampus via the perforant path (see above). The stellate cells in layer II, which give rise to the perforant path, generate depolarization-dependent rhythmic oscillations within theta frequency range (see Chapter 7), whereas pyramidal-like cells do not oscillate [40].

The neuronal circuits in the amygdala nuclear complex implicated in oscillatory activities were recently reviewed [41]. The central lateral nucleus of amygdala, which is the major output station of this nuclear complex, induces electrographic activation of neocortical areas, even in the absence of the brainstem reticular formation [42].

Intrinsic Electrophysiological Properties of Brainstem and Forebrain Neurons

The properties of neuronal circuits controlling behavior are determined not only by their anatomical connectivity but also by the intrinsic properties of the constituent neurons, including voltage- and transmitter-sensitive membrane currents. Only during the past decade we witnessed some “cross-talk” between physiologists interested in analysis of behavior from a macropotential or even cellular perspective in the behaving mammal and those physiologists exploring cellular properties in *in vitro* preparations, including slices and dissociated neuronal cultures. One of the purposes of our book is to facilitate and promote information transfer between these still largely separate domains of work by emphasizing areas of potential and demonstrated commonality of interest. We believe the future course of brainstem investigation will be toward increasing joint use of both techniques to understand mechanisms of behavior. This chapter will also present data from basal forebrain, thalamic, and cortical neurons since these are important targets of brainstem influences and also furnish some contrasts with properties of brainstem neurons.

We begin with a discussion of the properties of cholinceptive and cholinergic brainstem reticular core neurons (Sections 5.1 and 5.2), we summarize *in vitro* data on monoaminergic neurons (Section 5.3), and we compare the intrinsic properties of brainstem neurons with those of basal forebrain (Section 5.4), thalamic (Section 5.5), and cortical (Sections 5.6).

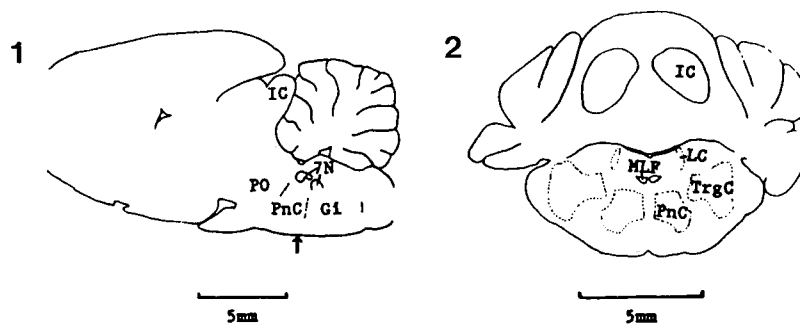


Figure 5.1. Schematic representation of the *in vitro* recording zone in the medial pontine reticular formation (nucleus reticularis pontis caudalis, PnC) in sagittal and coronal sections, with the latter having the same orientation as the slices used for recording. Other abbreviations: Gi, bulbar nucleus reticularis gigantocellularis; IC, inferior colliculus; LC, locus coeruleus; MLF, medial longitudinal fasciculus; PO, nucleus reticularis pontis oralis; TrgC, trigeminal complex; 7N, 7th nerve. From Gerber *et al.* (1989a).

5.1. Medial Pontine Reticular Formation Neurons

Figure 5.1 illustrates the plane of section of the pontine reticular formation (PRF) slice preparation [1, 2]. Unless otherwise stated, these references apply to the data of this section.

5.1.1. Neuronal Classes of the Medial PRF: Overview

Our classification of mPRF neurons will be based on the presence of different kinds of firing pattern as influenced by the presence of different voltage-sensitive membrane currents. Two main neuronal classes have thus far been defined by the presence of two types of firing pattern in response to current injection (Fig. 5.2 and Table 5.1). We will first summarize data on these main types before proceeding with more detailed descriptions. Later sections will also include brief primers of terminology and technical aspects of cellular physiology for the reader not working in this field.

Low-threshold burst neurons (LTBNs) generated a low-threshold burst (LTB) that was caused by the presence of a low-threshold Ca^{2+} spike (LTS). The LTS was visible as a slow potential on which rode a burst of fast (Na^{+} -dependent) action potentials (APs) (Fig. 5.2A). LTBNs also produced a nonburst (NB) firing pattern, consisting of a relatively regular series of APs (Fig. 5.2A, column 3). Production of the LTB pattern was dependent upon a sufficiently hyperpolarized baseline membrane potential that de-inactivated the LTS, as described in detail below.

[1] Greene *et al.* (1986).
 [2] Gerber *et al.* (1989a).
 The PRF slice preparation utilized 500- μm -thick transversely cut brainstem slices from young Sprague Dawley rats; slices were totally submerged in perfusate in a modified recording chamber (Haas *et al.*, 1979). When the preparation was viewed under a binocular dissecting microscope, identifying anatomical landmarks were readily observable; these were primarily white matter tracts and include VI nerve rootlets, the VII nerve, and the medial longitudinal fasciculus. Use of young, 7–13 day old animals facilitated tissue viability (slices remained viable throughout the 8–16 hr recording sessions), and was also appropriate in that the behavior of principal interest, REM sleep, is some 4–5 times more abundant in young than in adult animals (Jouvet *et al.*, 1968). Recordings of medial pontine reticular formation neurons described in this section were made in the giant cell field zone (FTG).

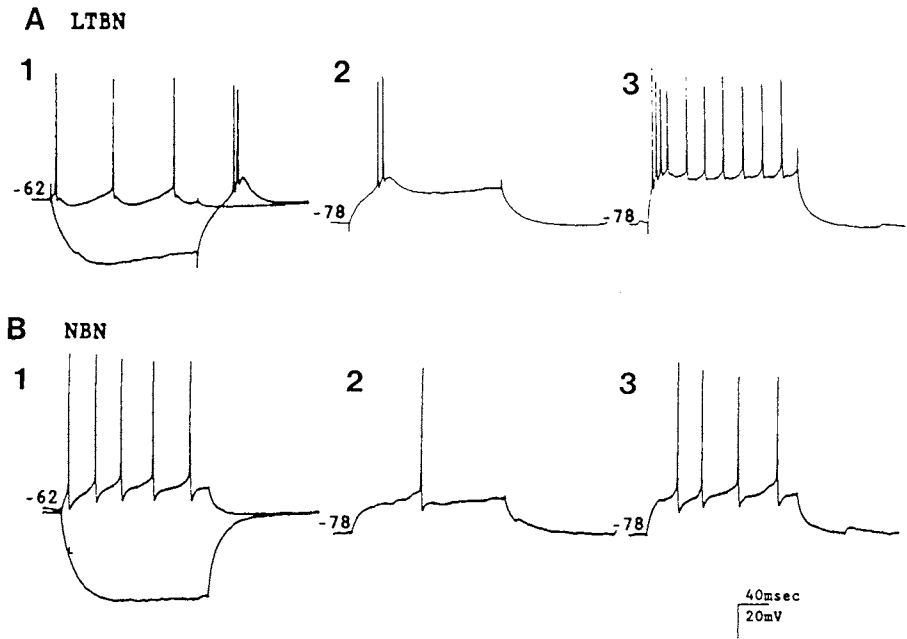


Figure 5.2. Two patterns of repetitive firing in the two main classes of mPRF neurons recorded *in vitro*. Part A shows voltage traces from a low-threshold burst neuron (LTBN) illustrating the presence of a low-threshold burst (LTB) and nonburst (NB) patterns. A1, a depolarizing current pulse of 200 pA amplitude and 200 ms duration (same duration throughout figure) evokes an NB repetitive firing pattern. A hyperpolarizing current pulse of 400 pA amplitude evokes a rebound LTB. A2–A3, with a hyperpolarized membrane potential (–78 mV) depolarizing current pulses of 300 pA and 500 pA evoke LTB, which with 500 pA current injection, is followed by an NB pattern. Part B shows voltage traces from an NB neuron evincing an NB pattern but no LTB pattern: there is no rebound LTB seen in B1 even with the same amplitude hyperpolarizing pulse as in A1, and no LTB results from depolarizing pulses in B2 and B3 of the same magnitude and from the same hyperpolarized membrane potential in A2 and A3. Note, however, the delay in depolarization evident in B2–3 compared with B1; evidence indicating this delay is due to A current as described in the text. Modified from Gerber *et al.* (1989a).

Table 5.1. Characteristics of Medial Pontine Reticular Formation Low-Threshold Burst Neurons (LTBN) and Nonburst Neurons (NBN)

	NBN	LTBN
Firing pattern		
Low-threshold burst	0	+
Nonburst	+	+
Calcium action potentials		
Low-threshold	0	+
High-threshold		
in control media	0	0
with K(Ca) antagonists	+	+
Outward potassium currents		
Early transient, A-current	+	+
Delayed, calcium-dependent	+	+

In addition to the LTS, LTBNs also showed a high-threshold Ca^{2+} spike (HTS); this HTS was dependent upon a Ca^{2+} current with a higher threshold for activation than the LTS. Both the LTS and HTS were visualized in the presence of tetrodotoxin (TTX), a blocker of Na^+ APs, and the HTS also required the presence of K^+ current blockers. We note that, while the LTS is not so common in neuronal populations, the HTS is quite common and the Ca^{2+} current associated with it is often triggered by the depolarization associated with the Na^+ AP. LTBNs constituted about 45% of the recorded neurons.

Nonburst neurons (NBNs) showed only an NB firing pattern (Fig. 5.2B) and a HTS. They did not show an LTS and the associated spike-burst. The AP frequency of the NB pattern was principally controlled by a Ca^{2+} -dependent K^+ conductance and the latency to occurrence of the first spike by A-current, an early outward (hyperpolarizing) current that opposed the depolarization leading to the initial spike. NBNs constituted about one-half of the neurons recorded.

These two neuronal classes did not show statistically significant differences in input resistances or resting membrane potentials. Resting membrane potentials averaged -65 mV and input resistances (measured by the change in membrane potential resulting from a 200 ms hyperpolarizing current pulse) were about $65\text{ M}\Omega$. The observed lack of correlation between input resistance and the neuronal type as identified by firing pattern suggests that the two patterns resulted from recordings in different neurons rather than from recordings obtained from different zones of the same neuron (e.g., patterns characteristic of an LTN might be elicited from the soma and patterns characteristic of an NBN from the dendrites). There was also no association of age of preparation and the frequency of occurrence of the different classes. Use of recording site marker lesions and Nissl staining showed the different classes were not preferentially localized to any particular portion of the pontine FTG.

Carboxyfluorescein injected intracellularly into mPRF neurons enabled computation of mean soma diameters as the average of long and short axes (see Chapter 3). Diameters ranged from $20\text{--}50\text{ }\mu\text{m}$, and there was a tendency ($p < 0.1$) for LTBNs to have larger somata (mean diameter = $37\text{ }\mu\text{m}$) than NBNs ($30\text{ }\mu\text{m}$). For comparison of the soma sizes of the sample of intracellularly recorded neurons with all mPRF neurons, and to compare young (10-day-old) with adult animals, soma size measurements were performed on neurons on Nissl stained sections from young and adult rats. Average soma diameters were not statistically different for young ($25\text{ }\mu\text{m}$) and adult ($28\text{ }\mu\text{m}$)

[3] Mitani *et al.* (1988a–b).

[4] Neurons in the upper 8% had diameters larger than 40 μm in cat and 39 μm in young rats, while the next 35% had diameters of 20–40 μm in cat and 24–39 μm in rat, and the smallest 57% of the sampled neurons had diameters less than 20 μm in cat and 24 μm in rat.

[5] Fatt and Ginsborg (1958).

[6] Reviewed in Llinás (1988).

[7] Reviewed in Hille (1984).

rats. In terms of comparability of results to those obtained in the adult cat [3], the soma size percentile distributions, based on three subdivisions (large, medium, and small neurons), were remarkably similar [4]. The majority of cat mPRF neurons with soma sizes greater than 45 μm project to the spinal cord without collaterals [3]; if a similar association of size and efferent projection pattern exist in the rat, then these data suggest that the LTB pattern predominates in the class of noncollateralized reticulospinal neurons.

5.1.2. Low- and High-Threshold Ca^{2+} Spikes

For those readers not familiar with Ca^{2+} APs, a brief review may be useful. Soon after the Na^+ AP was described, Fatt and Ginsborg [5] found that muscle fibers in crab legs utilized a Ca^{2+} spike, an AP based on the inflow of Ca^{2+} rather than Na^+ ion, during the depolarization of the upstroke. Llinás and colleagues have described LTSs and associated LTB firing patterns in mammalian neurons [6]. Neurophysiological studies have shown that, in general, Ca^{2+} channels activate (open) with membrane depolarization and also show inactivation (e.g., closing of channels) with time courses slower than for the Na^+ channels involved in fast AP production [7]. Of particular importance for the LTS is the concept of *de-inactivation*, a process leading to removal of inactivation so that the current may be activated under the proper conditions, such as membrane depolarization. De-inactivation or removal of inactivation may be analogized to the “cocking of a gun”; the process itself does not cause a dramatic change but, with depolarization, *permits* activation of the currents causing the Ca^{2+} spike or, in the analogy used, permits pressing the trigger to be effective.

In mPRF neurons (Fig. 5.2A), the slow potential seen as a rebound after a hyperpolarization (A1) or elicited by a depolarizing pulse from a hyperpolarized baseline potential (A2) will be shown to represent a Ca^{2+} spike while the burst of fast (Na^+ -dependent) APs riding on the Ca^{2+} spike (LTB) occurs because the Ca^{2+} spike depolarizes the membrane past the threshold for generation of Na^+ spikes. The subsequent discussion will further dissect the various factors involved in production of Ca^{2+} spikes. The Ca^{2+} spike associated with the LTB pattern is termed a low-threshold spike because of the low-threshold for activation of this Ca^{2+} current and spike, and is to be contrasted with the higher threshold Ca^{2+} spike to be described later.

It is to be noted that the LTB pattern is characterized by sensitivity to baseline membrane potential (Fig. 5.2A). A depolarizing current pulse from a baseline membrane

potential more negative than -75 mV activates an LTS, with a burst of 2–5 fast APs superimposed upon it. Larger amplitude current pulses (5.2A3) evoke similar bursts of APs, but they are followed by an NB firing pattern. LTB patterns could not be activated with depolarizing current injection from a baseline membrane potential more positive than -65 mV (Fig. 5.2A1); they instead elicited only an NB pattern. Note further (Fig. 5.2A1) that a rebound LTB is evoked following current pulses that hyperpolarize the membrane to potentials more negative than -75 mV.

The number of APs generated during an LTB, the intensity of a burst, was strongly controlled by different factors. Increasing the amplitude of depolarizing current (amplitude of activation) (Fig. 5.3A) produced an LTB with more APs. The threshold for activation of the LTB, obtained by a visual estimation of the inflection point on the membrane potential charging trajectory, was about -60 mV. Another important factor in the intensity of an LTB was the degree of de-inactivation, dependent on the degree and time duration of hyperpolarization (Figs. 5.3B and C) prior

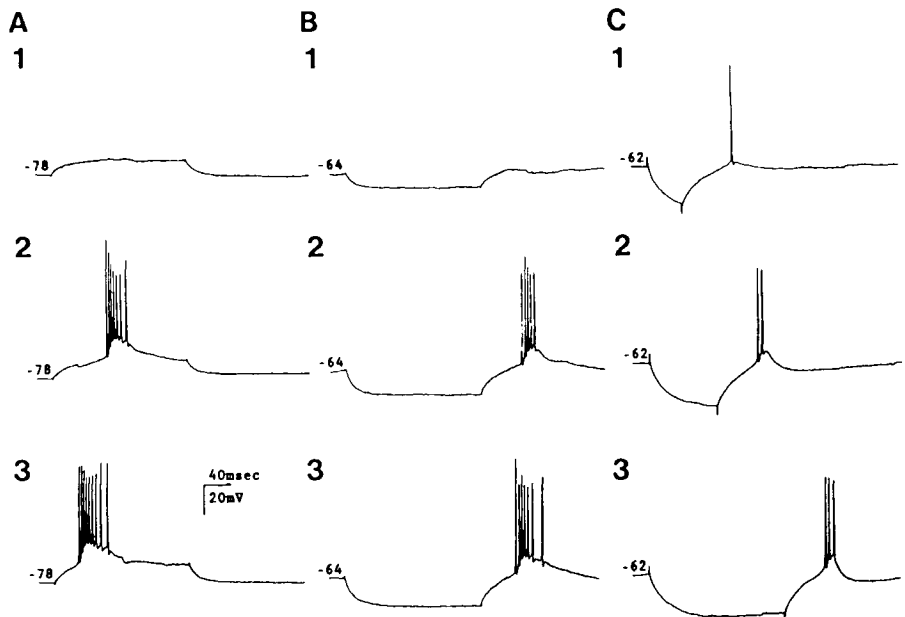


Figure 5.3. Activation and the removal of inactivation of the low-threshold burst response of mPRF neurons recorded *in vitro*. Column A illustrates graded activation of the LTB with voltage traces of responses to depolarizing current pulses of 200 ms duration and 200 (A1), 250 (A2), and 300 (A3) pA amplitude, all applied from a hyperpolarized membrane potential of -78 mV. Column B illustrates the voltage sensitivity of the removal of inactivation with the responses to hyperpolarizing pulses of 200 ms duration and 300 (B1), 500 (B2), and 600 (B3) pA amplitude applied on a baseline membrane potential of -64 mV. Note the increased number of action potentials with greater hyperpolarization. Column C illustrates the time dependence of the removal of inactivation with the responses to hyperpolarizing pulses of the same amplitude (300 pA) but of increasing duration: 100 ms in C1, 200 ms in C2, and 400 ms in C3. Modified from Gerber *et al.* (1989a).

to a rebound LTB. Maximal LTBs averaged about five APs per burst.

The Ca^{2+} dependence of the LTS and associated LTB firing pattern is shown in Fig. 5.4. Addition of TTX, a blocker of Na^+ -dependent APs, led to the abolition of the burst of Na^+ spikes and clearly revealed the time course of the Ca^{2+} spikes resulting from a rebound hyperpolarization (Fig. 5.5A1) or depolarization from a hyperpolarized membrane potential (Fig. 5.5A2). The slow Ca^{2+} spikes were abolished in perfusate containing no Ca^{2+} (Fig. 5.5A3). The LTS amplitude increased and its latency to peak decreased in direct relationship to the magnitude of the preceding hyperpolarization (Fig. 5.5A1). The graded increase of the LTS produced by increasing hyperpolarization of the membrane potential was similar to the graded increase in the number of APs observed in the rebound LTB.

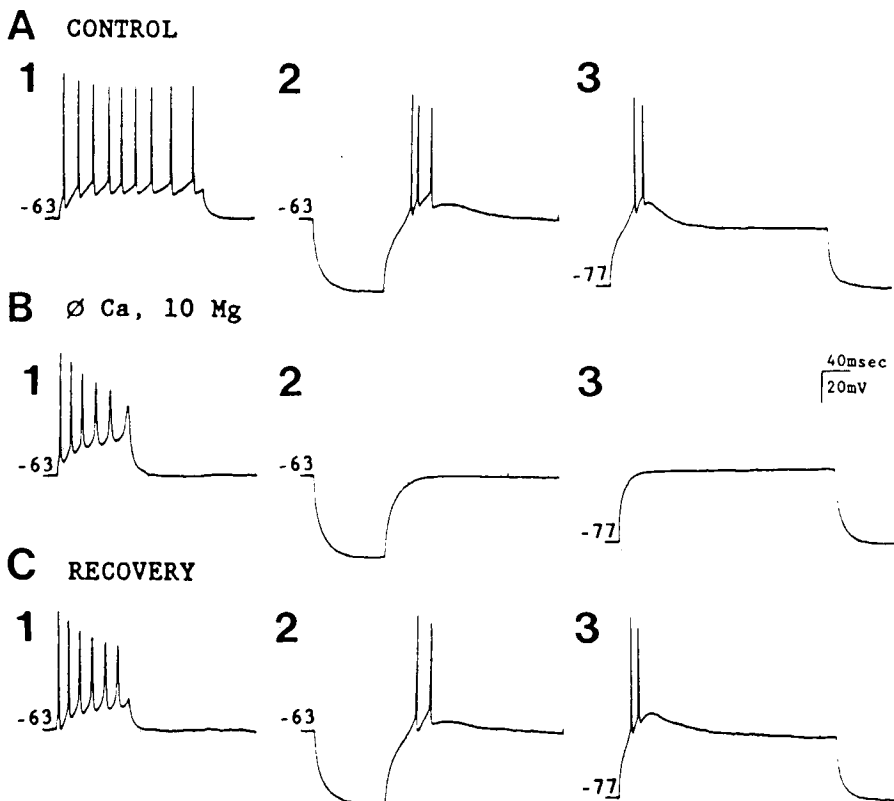


Figure 5.4. Ca^{2+} -dependence of repetitive firing patterns of a low-threshold burst (LTB) mPRF neuron recorded *in vitro*. Row A is during perfusion with control medium. In A, column 1, there is a nonburst response to a depolarizing current pulse of 300 pA amplitude from a baseline membrane potential of -63 mV. In A, column 2, a rebound LTB response follows a hyperpolarizing pulse of 500 pA amplitude. In A, column 3, there is an LTB response to a depolarizing pulse of 400 pA amplitude delivered from a hyperpolarized baseline. Row B, during perfusion with medium containing 10 mM magnesium and no calcium, shows the absence of the LTB response in B2-3. Row C shows partial recovery 5 min after returning to perfusion with control media. Modified from Gerber *et al.* (1989a).

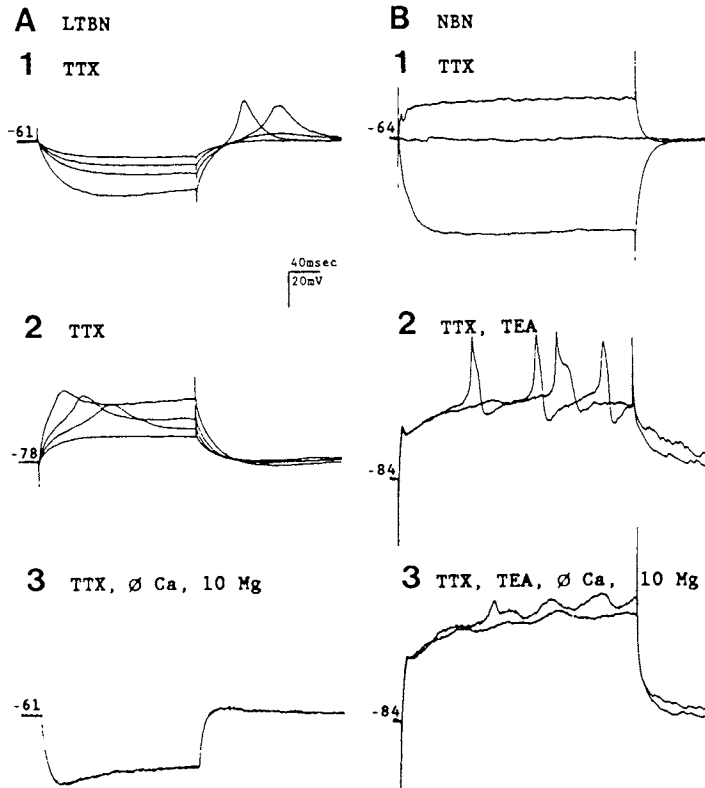


Figure 5.5. Tetrodotoxin (TTX) resistant, Ca²⁺-dependent action potentials of mPRF neurons recorded *in vitro*. Voltage traces from a low-threshold burst neuron (LTBN) are shown in column A and from a nonburst neuron (NBN) in column B. A1, in the presence of TTX, increasingly greater hyperpolarization of the membrane potential (current amplitudes of 100, 200, 300, and 500 pA) results in increasingly greater amplitude rebound low-threshold calcium spikes (LTSs). A2, from a baseline potential of -78 mV, increasingly greater depolarization (current pulse amplitudes of 200, 400, 600, and 800 pA amplitude) also evoked increasingly greater amplitude LTSs. A3, the LTS is abolished in the presence of 10 mM magnesium and no calcium. B1, in the NBN no Ca²⁺ spikes were evoked even by large amplitude current pulses (+600 pA and -600 pA) in the presence of TTX. B2, with the addition of tetraethylammonium (10 mM), depolarizing current pulses (+1000 and 1200 pA) evoke high threshold Ca²⁺ spikes (HTSs). B3, HTSs are abolished when calcium is replaced by 10 mM magnesium (B3) and identical current pulses are applied. Calibration bar is 80 ms for A3. Modified from Gerber *et al.* (1989a).

The LTS was not “an island unto itself” but interacted with other currents to shape firing pattern; one of these currents appeared to be similar to the A-current first described in gastropod mollusks [8] and present in mammalian central nervous system neurons from many different regions [9]. The A-current (I_A) is so named because of its sensitivity to blockage by 4-AP [10], and is also known as the transient outward current. The A-current is activated when a neuron is depolarized after a period of hyperpolarization; since it is an outward K⁺ current, it tends to counteract depolarizing, inward currents, such as the Ca²⁺ current associated with the LTS. Figure 5.6B shows how the threshold and size of an LTS in LTBNs was influenced by interaction with a 4-AP

[8] Neher (1971); Connor and Stevens (1971).

[9] Gustafsson *et al.* (1982); Williams *et al.* (1984); Yarom *et al.* (1985); Champagnat *et al.* (1986).

[10] Thompson (1977).

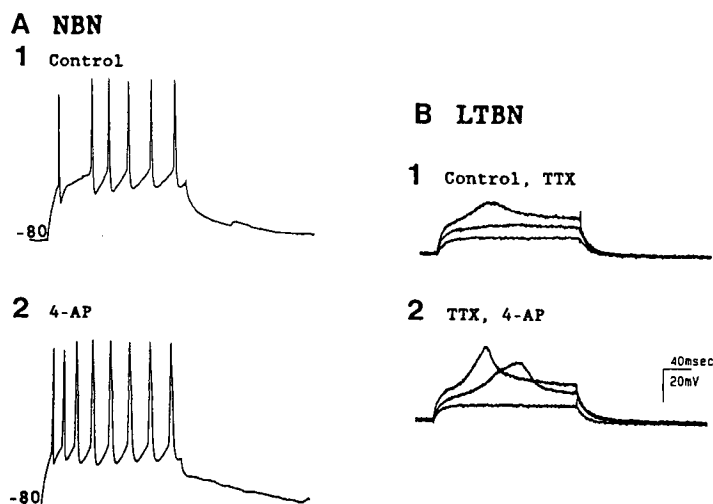


Figure 5.6. In mPRF neurons recorded *in vitro*, 4-AP reduces the latency to the first action potential, shortens the interspike interval between the first and second actions and reduces the threshold and increases the amplitude of the low-threshold calcium spike. A, voltage traces of responses to depolarizing pulses of 400 pA in a nonburst neuron before (A1) and during (A2) application of 4-AP (0.5 mM). B, responses of a low-threshold burst neuron to depolarizing current pulses of 200, 400, and 600 pA amplitude applied before (B1) and during (B2) 4-AP exposure (0.5 mM) in the presence of tetrodotoxin (TTX) and from a baseline membrane potential of -79 mV. Note that, in all cases, the subthreshold responses to the current pulses were not affected by the 4-AP. Calibration: 20 mV and 40 ms. Modified from Gerber *et al.* (1989a).

sensitive conductance. Blocking the 4-AP sensitive current by perfusion with 4-AP increased the peak amplitude of the LTS by at least 30% compared with no 4-AP control conditions. Further, in the presence of 4-AP and starting with a baseline membrane potential of -76 mV (A-current inactivation removed), depolarizing currents elicited a more rapid LTS rise than the no-4-AP control.

Since the putative I_A and the current responsible for the LTB had similar voltage sensitivities for both activation and inactivation, this interaction may be especially important in the control of the LTB. Depending on the relative amplitudes of these two currents, depolarization from a hyperpolarized membrane potential may produce either a state of decreased excitability when I_A predominates or increased excitability with a burst response when low-threshold Ca^{2+} current predominates.

Not only was an LTS present in LTBNs, there was also a higher threshold Ca^{2+} spike that was revealed with the addition to the perfusate of 5–10 mM tetraethylammonium (TEA), an antagonist of a number of outward K^+ currents, including both the Ca^{2+} -dependent K^+ channel [11] as well as the Ca^{2+} -independent delayed rectifier [12]. Column B of Fig. 5.5 shows the presence of HTS in response to depolarizing pulses in the presence of TEA

[11] Hermann and Gorman (1981).

[12] Stanfield (1983).

(TTX was added to eliminate fast Na^+ APs); these HTSs (B2) were Ca^{2+} -dependent since they disappeared when Ca^{2+} was replaced by 10 mM Mg^{2+} (B3). The threshold for the TTX-resistant HTS was -33 mV for LTBNs, easily distinguishable from the LTS threshold that was approximately 30 mV more hyperpolarized (Fig. 5.5A). The HTS and LTS were also distinguished by the selective antagonism of the LTS by Mg^{2+} ; in the presence of 10 mM Mg^{2+} and an antagonist of the outward K^+ current, the LTS was reversibly abolished but the HTS was still readily evoked by depolarizing current pulses. This was directly analogous to the effects of these treatments on the LTB and NB firing patterns.

The most likely explanation for the differences between the LTS and HTS is that two distinct types of Ca^{2+} channels control the Ca^{2+} fluxes on which they depend. The voltage sensitivity of the LTS and HTS were similar to those of Ca^{2+} channels described as low-voltage-activated [13] or T-type [14], and high-voltage-activated or L-type, respectively.

The amplitude and duration of the LTS, and hence the number of APs in the LTB, was controlled not only by the depolarizing Ca^{2+} -dependent conductance but also by an interaction with delayed hyperpolarizing (outward) K^+ conductances. In the presence of TTX, application of blockers of delayed outward K^+ currents, including TEA or intracellular Cs^+ , resulted in an LTS of sufficient amplitude to surpass threshold for the HTS; in this case, these TTX-resistant APs reached membrane potentials more positive than $+5$ mV, a level never reached without TEA or intracellular Cs^+ . However, the inability to elicit the LTS from depolarized membrane potentials without a preceding hyperpolarization was not affected by these antagonists. Cs^+ in the presence of TTX had the additional effect of eliciting a rebound LTS followed by repetitive HTSs; these continued until hyperpolarizing current was applied.

As noted in the previous section, both NBNs and LTBNs generated an NB pattern, and the discussion here pertains to the NB pattern in both types of neurons. The NB pattern was characterized by a relatively constant interspike interval during depolarizing current injection (Figs. 5.2, A1, B1, B3, C1, which are to be compared to Figs. 5.2, A2, A3, C2, C3). With increased amplitude of current injection, some accommodation was apparent but never to the extent of complete cessation of AP firing, nor was there any evidence of an associated long duration (greater than 0.5 s) afterhyperpolarization (AHP). This was in marked contrast to the accommodation and associated

- [13] Carbone and Lux (1984); Yaari *et al.* (1987).
- [14] Nowycky *et al.* (1985).

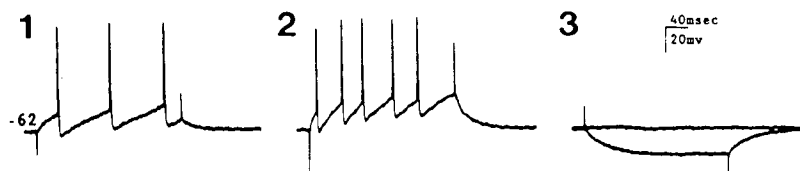
[15] Hotson and Prince (1980); Schwartzkroin and Stafstrom (1980); Madison and Nicoll (1984).

long duration AHP observed in hippocampal CA1 and CA3 neurons [15].

As shown in Fig. 5.5B, NBNs had no LTS, but large amplitude depolarizing pulses in the presence of TEA and TTX demonstrated the presence of an HTS whose threshold was similar to the HTS in LTBNs.

In contrast to the direct dependence of the LTB pattern on a Ca^{2+} spike, the NB pattern was indirectly controlled by a high-threshold, inward Ca^{2+} conductance that, in turn, activated an inhibitory (outward) $I_{\text{K}(\text{Ca})}$. Thus, Ca^{2+} -free media altered the NB pattern in both NBNs (Fig. 5.4) and LTBNs [2] in that the spike frequency was increased and the AHP reduced. The Ca^{2+} conductance mediating these effects was shown to be different than for the LTS conductance because neither NB firing frequency nor the AHP was altered by high Mg^{2+} in control concentrations of Ca^{2+} while this treatment antagonized the LTB/LTS (Fig. 5.5A). The effects of addition of 5 mM TEA (Fig. 5.7), an antagonist of Ca^{2+} -dependent K^{+} currents, were similar to those following exposure to Ca^{2+} -free media suggesting an $I_{\text{K}(\text{Ca})}$ mediated both effects. The presence of a Ca^{2+} -dependent outward current was also indicated by the fact that large current pulses in the presence of TTX did not depolarize the membrane potential positive to -38 mV (Fig. 5.5B1); the removal of Ca^{2+} from the perfusate resulted abolished this effect.

A CONTROL



B TEA

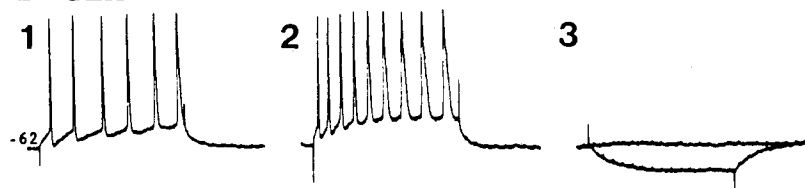


Figure 5.7. A tetraethylammonium (TEA)-sensitive outward current modulates the excitability of the (NB) firing mode of mPRF neurons recorded *in vitro*. Responses of an NB neuron to depolarizing current pulses of 300 pA (column 1) and 500 pA (column 2) and to a hyperpolarizing pulse of 300 pA (column 3). After the addition of TEA (10 mM in row B), the frequency and number of action potentials evoked is increased compared to control condition (row A) despite an unaltered input resistance as measured in column 3. Note also that action potential amplitude is increased and that with successive firing action potential duration is also increased. From Gerber *et al.* (1989a).

The high-threshold Ca^{2+} current may indirectly control the repetitive firing of the NB pattern by the following sequence of events: under physiological conditions, the TTX-sensitive Na^+ currents of the fast AP elicit sufficient membrane depolarization to exceed the threshold of the high-threshold Ca^{2+} current. In turn, the influx of Ca^{2+} leads to Ca^{2+} -dependent K^+ current, which then contributes to AP repolarization and the AHP. Similar effects of Ca^{2+} -dependent K^+ current have been observed in the vertebrate peripheral nervous system [16] and in hippocampal neurons [17]. Other factors controlling the NB pattern, not yet directly examined in mPRF neurons, may include the Ca^{2+} -independent delayed outward rectifier and the removal of Na^+ inactivation [18].

There may be more than one $I_{\text{K}(\text{Ca})}$, as has been demonstrated in other neurons. In hippocampal neurons, repolarization of the AP and fast AHP (<10 ms duration) has been attributed to a TEA and charybdotoxin sensitive $I_{\text{K}(\text{Ca})}$ [17], but a medium AHP (<200 ms) is Ca^{2+} insensitive. In contrast, in neurons of the sensorimotor cortex [19] and spinal cord [20] AP repolarization is not dependent on Ca^{2+} flux across the membrane (although it is antagonized by TEA in both cases) but the medium duration AHP is Ca^{2+} -dependent. In mPRF neurons, repolarization of AP, the medium duration AHP, and restriction of the LTS are all mediated to some extent by one or more $I_{\text{K}(\text{Ca})}$. However, additional investigation of the voltage and pharmacological sensitivities of these phenomena is needed before more precise statements can be made.

When NBNs were hyperpolarized to membrane potentials negative to -65 mV and then depolarized, there was a delay in reaching AP threshold in association with a (outwardly rectifying) deviation from the membrane charging trajectory seen with current pulses applied from more depolarized baselines (compare Figs. 5.2, B1–B3). Since this is consistent with an activation of I_{A} (see above), the effects of 4-AP, an antagonist of I_{A} , was tested using the same experimental procedures (Fig. 5.7). Compared with control conditions, exposure of NBNs to 4-AP (200–500 μM) reduced the delay to threshold of the first AP and the first interspike interval when baseline membrane potential was maintained at levels negative to -65 mV but, when examined from a membrane potential of -60 mV, 4-AP had no effect. These effects are consistent with the known characteristics of I_{A} : inactivation at membrane potentials of -60 mV and more positive, removal of inactivation of more hyperpolarized potentials, and activation at potentials more positive than -60 mV [8]. Further, the 4-AP antagonism affected only the early part (<150 ms) of the firing pattern and did not alter input resistance, again arguing for a specific blocking of I_{A} .

[16] Adams *et al.* (1982).

[17] Lancaster and Nicoll (1987); Storm (1987)

[18] Adams *et al.* (1980).

[19] Schwindt *et al.* (1988a).

[20] Barrett and Barrett (1976); Walton and Fulton (1986).

5.1.3. Role of mPRF Neuron Membrane Potential in Controlling Repetitive Firing Properties and Implications for Behavior

Identical inputs to LTBNs and NBNs can result in markedly different responses when the membrane potential is sufficiently hyperpolarized. An excitatory input can evoke an LTB response in LTBNs and, if the excitatory input continues, the LTB will be followed by an NB pattern. However, in NB neurons at the same baseline membrane potential, the same excitatory input may fail to elicit even a single AP due to an unopposed I_A ; if input continues, I_A will finally inactivate and an NB pattern will emerge. This heterogeneity and specialization of response may be important to the physiological organization of the mPRF in waking for both oculomotor and somatomotor systems. In particular, the reader's attention is directed to the examples given in Chapter 11 of quick activation of oculomotor system neurons from a baseline of absence of firing and presumed membrane hyperpolarization. The presence of an LTS may be functionally advantageous in permitting a quick recruitment of AP discharge from a hyperpolarized membrane potential level.

Furthermore, the change of baseline membrane potential during behavioral state changes may have important consequences for firing patterns in these states. In passage from waking and slow-wave sleep to REM sleep, neurons of the mPRF depolarize 7–10 mV [21]. This depolarization may inactivate both the LTS and I_A . Under such conditions, LTB and NB neurons will respond similarly to excitatory input with an NB firing pattern. Overall, excitability may be increased as membrane potential depolarizes toward AP threshold, but the specificity of response to excitatory input that distinguishes NB from LTBNs in waking may be decreased, and burst firing may be absent. Consistent with this, analysis of the firing pattern of mPRF neurons *in vivo* indicates an increased firing frequency in association with an absence of burst discharges during REM sleep [22].

[21] Ito and McCarley (1984).

[22] McCarley and Hobson (1975a).

5.2. Pedunculopontine and Laterodorsal Tegmental Nuclei

The location of these mesopontine cholinergic neurons and their thalamic projections are discussed in Chapter 3. Those data, obtained by combining retrograde tracing with ChAT immunohistochemistry in cat [23] and rat [24], have been confirmed in guinea pig slices containing

[23] Paré *et al.* (1988); Steriade *et al.* (1988).

[24] Hallanger *et al.* (1987).

the pedunclopontine tegmental (PPT) nucleus [25]. Intracellular injection of Lucifer Yellow in retrogradely labeled PPT cells showed that their shape and soma-dendritic size is similar to cholinergic PPT neurons described in rodents [26]. The results of experiments dealing with the intrinsic properties of thalamically projecting PPT cells [25] are described below. Three major neuronal classes have been observed.

One class of PPT neurons did not spontaneously fire APs after impalement, but they fired a spike-train under depolarizing current pulses (Fig. 5.8A). If the membrane was hyperpolarized sufficiently, the same depolarizing pulse elicited an LTS crowned by a burst of 2-to-5 fast APs

[25] Leonard and Llinás (1990, 1994). PPT or laterodorsal tegmental (LDT) neurons were retrogradely labeled after injections of rhodamine labeled microspheres into thalamic latero-posterior and lateral geniculate nuclei, prior to the preparing of the slice. The cholinergic nature of PPT/LDT neurons was determined by NADPH-diaphorase, a reliable marker of brainstem cholinergic neurons. [26] Rye *et al.* (1987).

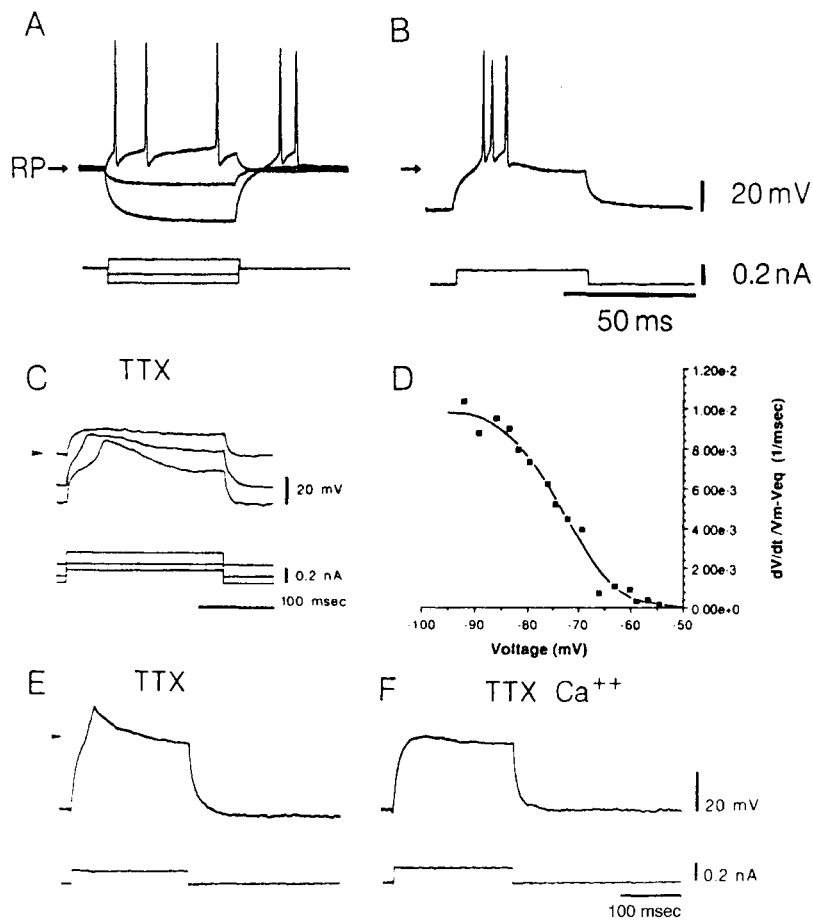


Figure 5.8. Low-threshold spiking (LTS) neuron recorded from the pedunclopontine tegmental (PPT) nucleus of guinea pig *in vitro*. A, top trace: neuron fires repetitively during depolarization from resting potential. Following hyperpolarizing current pulses (bottom trace) of sufficient magnitude, the neuron demonstrates rebound bursts of action potentials. B, hyperpolarization from resting potential elicits for subsequent depolarizing steps a burst-mode firing. C, spike burst is mediated by an LTS, is insensitive to tetrodotoxin (TTX), and is inactive at resting potential (arrow), but becomes progressively de-inactivated as the membrane potential is hyperpolarized. D, maximum rate of rise of the LTS is plotted as a function of membrane potential. The spike is half maximally active at -75 mV membrane potential. E-F, Ca^{2+} -dependency of the LTS (E) is demonstrated by its blockage with 500 mM CdCl (F). Modified from Leonard and Llinás (1990).

[27] Wilcox *et al.* (1989).

(Fig. 5.8B). The conductance underlying this burst was TTX-insensitive (Fig. 5.8C) but was blocked by Co^{2+} and Cd^{2+} , thus indicating that it is Ca^{2+} -mediated. This neuronal type was designated as generating purely LTS responses. Similar LTS-generating neurons have been found in the other brainstem cholinergic group, the lateral dorsal tegmental nucleus [27].

The second neuronal type in the PPT nucleus also displayed an LTS but, unlike the first type, did fire spontaneously upon impalement and, at the resting membrane potential, did not show a rebound excitation at the break of a hyperpolarizing pulse [25]. At rest, these cells had a transient outward current, I_A , which delayed the return to baseline of the voltage trace after the termination of a hyperpolarizing pulse. This cellular class was then designated as LTS + A.

The third cellular type did not display LTS responses but had the outward K^+ current, I_A . Such neurons were regarded as particularly suited to the relatively slow, tonic repetitive firing observed in some PPT neurons explored *in vivo*. Upon intracellular current injection, these neurons fired repetitively (Fig. 5.9A). Following a hyperpolarizing

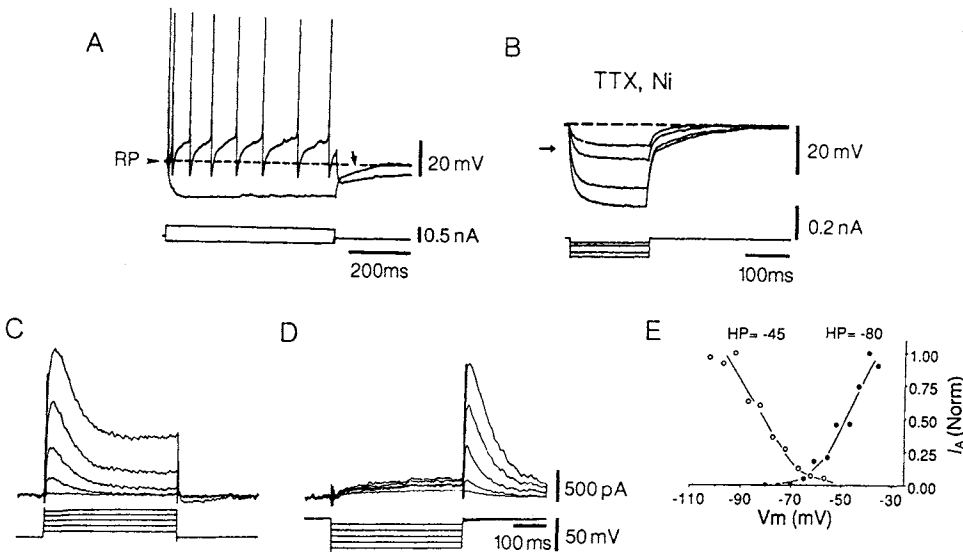


Figure 5.9. I_A -type neuron in the guinea pig pedunclopontine tegmental nucleus *in vitro*. A, repetitive firing elicited by depolarizing current pulses. The delay in the return of the membrane potential to rest following hyperpolarizing current pulses characterizes the presence of I_A . B, the I_A is not blocked by tetrodotoxin (TTX) and nickel, is inactive at resting potential, and increases with membrane hyperpolarization. C, single electrode voltage-clamp recording of A-current activation in TTX from other neuron of this class. Progressively larger depolarizing steps produce larger fast transient outward currents of increasing amplitude (-80 mV holding potential). D, hyperpolarizing voltage steps from a holding potential of -45 mV rapidly reactivate I_A . E, peak I_A plotted as a function of membrane potential. From a holding potential of -80 mV, this current is half maximally activated by voltage steps to about -50 mV. From a holding potential of -45 mV, this current is half maximally reactivated by a voltage step to about -75 mV. Modified from Leonard and Llinás (1990).

current pulse from resting potential, the membrane potential displayed a delay in the return to baseline, typical for I_A . This current was inactivated at resting membrane potentials and was progressively de-inactivated by brief hyperpolarizing prepulses (Fig. 5.9B). Single electrode voltage-clamp records (Figs. 5.9C and D) showed that the outward current peaked rapidly (within 6 ms) and decayed more slowly (about 200 ms). I_A was normally inactivated at resting membrane potentials (Fig. 5.9E) and was de-inactivated during the AHP of the AP. Thus, this conductance leads to an increased duration of the AHP and consequently to a lengthening of the interspike interval.

The first two cell-classes (LTS and LTS + I_A) may be related to the burst firing of PPT neurons whose activity underlies the thalamic component of the phasic pontogeniculo-occipital (PGO) waves of REM sleep (see Chapter 10), while the third cellular type (I_A) probably corresponds to the tonically firing neurons in PPT that may be involved in the tonic aspect of EEG activation during both waking and REM sleep [28]. As to the PGO-wave production in some brainstem PPT bursting neurons, it is of interest that octanol, a high molecular weight alcohol that specifically blocks the LTS of inferior olive neurons [29], was also found to block the PGO-like waves induced in the LG thalamic nucleus by brainstem peribrachial (PB) stimulation [30] (Fig. 5.10). The suppressing effect of octanol on PGO waves may be related to the fact that REM sleep is partially suppressed by acute doses of alcohol and that it continues to be suppressed for longer periods if the dosage is increased.

Another group, working in PPT/LDT slices, described three types of neurons. Type I cells were characterized by Ca^{2+} -mediated LTS; type II displayed I_A ; and type III cells had neither LTS nor I_A [31]. The ionic mechanisms of these cellular classes were also investigated more recently [32] and, using combined intracellular recordings with immunohistochemistry, it was found that none of the type I (LTS) neurons were immunopositive to choline acetyltransferase (ChAT), whereas 60% of type II (I_A) cells were immunopositive.

Thus, only a negligible proportion or none of PPT/LDT cholinergic neurons display spike-bursts in adult guinea pig and rat investigated in slices [25, 31, 32]. This finding is similar to data from studies of cat cholinergic PPT/LDT neurons during natural states of vigilance showing that very short (<5 ms) interspike intervals, reflecting high-frequency spike-bursts, represent less than 7% of intervals during all states of vigilance, wakefulness, slow-wave sleep, and REM sleep [28]. However, *in vitro* studies in slices from young rats (9–15 days old) showed

[28] Steriade *et al.* (1990a).

[29] Llinás and Yarom (1986).

[30] Llinás *et al.* (1987). In those *in vivo* experiments, octanol was injected systemically and, therefore, the blockage of the all-or-none PGO-like component of the peribrachial (PB)-LG response (appearing at a latency of about 50–80 ms after the PB stimulation) could well be due to the blockage of brainstem or thalamic LTS.

[31] Kang and Kitai (1990).

[32] Takakusaki and Kitai (1997). In a companion paper, Takakusaki *et al.* (1997) described the synaptic inputs, morphologies, and axonal projections of two subgroups of type II (I_A) neurons and two subgroups of type I (LTS) neurons divided according to the duration of their action potentials.

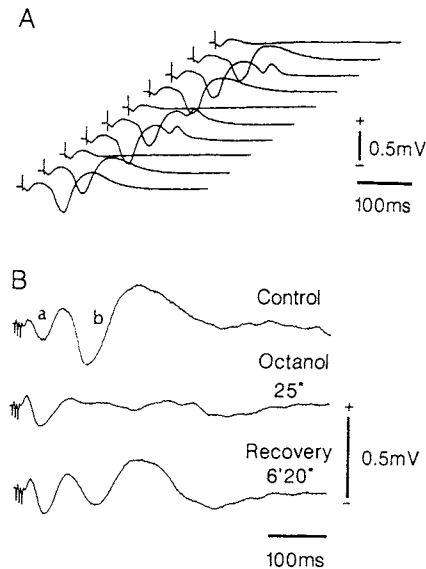


Figure 5.10. Octanol-induced blockage of all-or-none (ponto-geniculo-occipital [PGO]-like) component of field potential evoked in the lateral geniculate (LG) thalamic nucleus by stimulation of the brainstem peribrachial (PB) area in cat. A, 10-sweep sequence showing the all-or-none character of the 2nd component of PB-evoked LG field potential. B, effect of octanol on 2nd component of LG field potential evoked by midbrain reticular stimulation (3-shock train). Reserpine-treated (2 mg/kg) *encéphale isolé* preparation with deafferentation of trigeminothalamic pain pathways. Second component (b) disappeared 25 s after octanol administration (despite no alteration in a component) and recovered 6 min and 20 s later. Unpublished data by R. Llinás, D. Paré, M. Deschênes, and M. Steriade.

[33] Kamondi *et al.* (1992); Luebke *et al.* (1992).

that the majority of LTS-bursting brainstem LDT neurons were cholinergic [33]. It is possible that the membrane properties of LDT neurons change with maturity.

5.3. Neurons of the Locus Coeruleus and the Dorsal Raphe Nucleus

5.3.1. Locus Coeruleus Neurons

Locus coeruleus (LC) neurons slow and virtually arrest discharges with the approach and advent of REM sleep (see Chapter 9). A further striking characteristic of extracellular recordings *in vivo* of LC neurons is their slow, regular discharge pattern, which has suggested the possibility of pacemaker-like activity determined by intrinsic membrane properties. Thus, intracellular *in vitro* recordings are of great importance for determining the mechanisms of this pacemaker-like discharge pattern, and the existence of modulatory mechanisms that would account for its dramatic alteration with change in behavioral state. This section will present data supportive of the hypothesis

that LC neurons have intrinsic pacemaker activity at certain membrane potential levels, and that Ca^{2+} -dependent currents play a key role in this pacemaker activity. The data also are supportive of the general hypothesis that behavioral state changes may alter discharge pattern and discharge rate through the modulation of membrane potential and consequent changes in voltage-sensitive membrane currents [1, 34]. Certain K^+ conductances of LC neurons will be discussed in Chapter 6, together with ligand-activated K^+ conductances.

In the *in vitro* preparation [35], almost all LC neurons were found to be spontaneously active, with a firing threshold of about -55 mV and membrane potentials otherwise ranging from -55 mV to -65 mV. As can be seen in Fig. 5.11, APs arose from a slowly depolarizing membrane potential (rate of change, 7 mV/s). There were two components of the rising phase of the AP: an initial Ca^{2+} -dependent slow depolarization followed by a rapid depolarization of the Na^+ -dependent AP proper. The falling phase showed an initial slow repolarization of membrane potential, a Ca^{2+} -dependent shoulder, followed by a more rapid repolarization. Mean duration of the AP measured at threshold was 1.4 ms. The AP was followed by an AHP that carried the membrane potential 15 – 20 mV negative to the AP threshold. The AHP had an initial period of rapid decay (e.g., depolarization) followed by a slower

[34] McCarley and Ito (1985); McCarley and Massequoi (1986a).

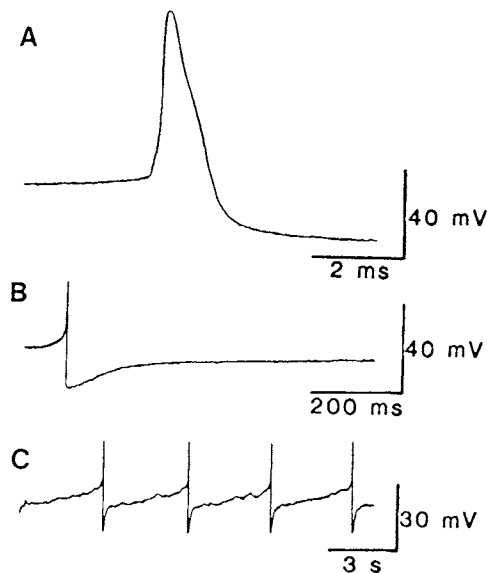


Figure 5.11. Spontaneous action potentials (APs) of locus coeruleus neurons recorded *in vitro*. A, in control perfusate a change in slope on the rising phase is visible, as well as a shoulder on the falling phase. B, the spontaneous AP (full height not shown) was followed by an afterhyperpolarization, which merged into the interspike depolarization, seen more clearly at the slower recording speed of C. Modified from Williams *et al.* (1984).

depolarization phase that merged into the interspike depolarization.

Of interest with respect to the *in vivo* recording data showing virtual arrest of spontaneous LC neuronal discharges in REM sleep was the finding that, *in vitro*, hyperpolarization to ~ 60 mV arrested LC spontaneous firing, suggesting a strong voltage dependence of the spontaneous activity. The presence of intrinsic pacemaker activity was further suggested by the absence of any evidence for spontaneous synaptic potentials driving the depolarization and repetitive discharges. In a few neurons ($<10\%$) small spike-like depolarizations were evident upon hyperpolarization; these occasionally reached AP threshold, and vanished in Ca^{2+} -free, high Mg^{2+} solutions, suggesting they were spontaneously occurring dendritic Ca^{2+} spikes. The frequency of spontaneous discharge activity did not change with the addition of TTX to the perfusate, indicating both the lack of significance of synaptic input from Na^+ -dependent APs for driving the depolarization and regular discharge of LC neurons and also demonstrating the importance of ion(s) other than Na^+ in the generation of one component of the LC APs. The APs after TTX were of lesser amplitude (46 mV) and had a slower maximal rate of rise, and interference with Ca^{2+} currents eliminated these TTX-resistant smaller, slower spikes: they were not present in perfusates containing either the Ca^{2+} channel blockers Co^{2+} or Mg^{2+} , or containing no Ca^{2+} (Fig. 5.12), data agreeing with the formulation that the initial component of the LC AP was a Ca^{2+} spike.

Analysis of membrane properties with single electrode voltage clamp techniques showed a steady state slope conductance that was relatively constant at membrane potentials from -90 mV to -70 mV, then progressively less with depolarization and negative at about -55 mV (Fig. 5.13). The negative slope conductance at -55 mV was analyzed further as to the nature of the current responsible for the change. Blockade of inward Ca^{2+} currents by Co^{2+} and Mg^{2+} abolished the negative slope conductance (Fig. 5.14). The negative slope conductance at ~ 55 mV was also abolished by Ca^{2+} -free, high- Mg^{2+} solutions. Other data indicated a later outward current (associated with the AHP) was an $I_{\text{K}(\text{Ca})}$.

It was concluded that LC neurons have a Ca^{2+} current flowing into the cell at membrane potentials close to threshold for AP generation. This inward current is voltage dependent, being small at -75 mV and increasing with depolarization; it activates and deactivates rapidly when the membrane is depolarized or hyperpolarized.

Other experiments indicated the presence of K^+ currents contributing to spike repolarization; these included

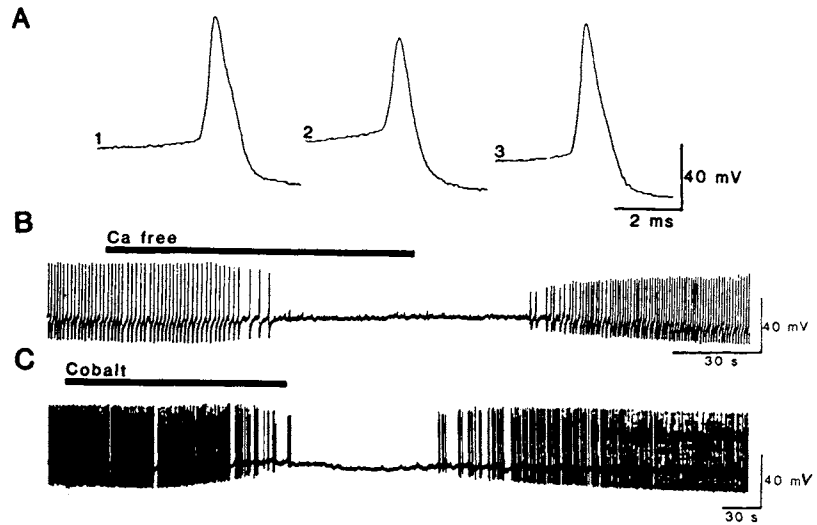


Figure 5.12. The locus coeruleus action potential (AP) recorded *in vitro* is composed of Ca^{2+} and Na^{+} spikes. A, part 1 shows a control spontaneous AP. Part 2 is after addition of 2 mM cobalt; note the persistence of a smaller spike. Part 3 is recovery after wash-out of cobalt. B and C, in TTX ($1 \mu\text{M}$), spontaneous action potentials persist but are reversibly abolished by Ca^{2+} -free solutions (B, with 10 mM magnesium) or by cobalt (2 mM). Modified from Williams *et al.* (1984).

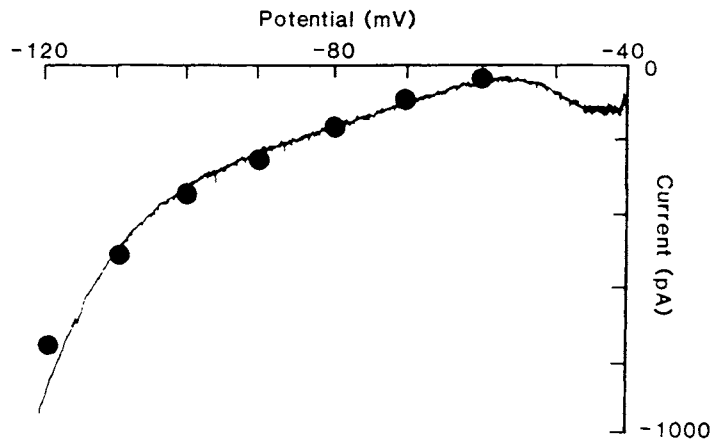


Figure 5.13. Steady state I/V characteristics of a locus coeruleus neuron recorded *in vitro*. The continuous line was plotted directly on an $X-Y$ plotter using a ramp depolarization from -120 mV to -40 mV. The filled circles indicate the currents evoked by hyperpolarizations from a holding potential of -60 mV. Modified from Williams *et al.* (1988a).

a fast, 4-AP sensitive component, the $I_{K(\text{Ca})}$, and perhaps other “delayed rectifier” currents.

The following unifying hypothesis about the mechanisms involved in generation of the pacemaker-like activity of LC neurons was proposed [35]. We begin the description of a cycle at the peak of the AP, a point with a high Ca^{2+} conductance and a consequent rapid increase in internal Ca^{2+} concentration. AP repolarization is dependent on

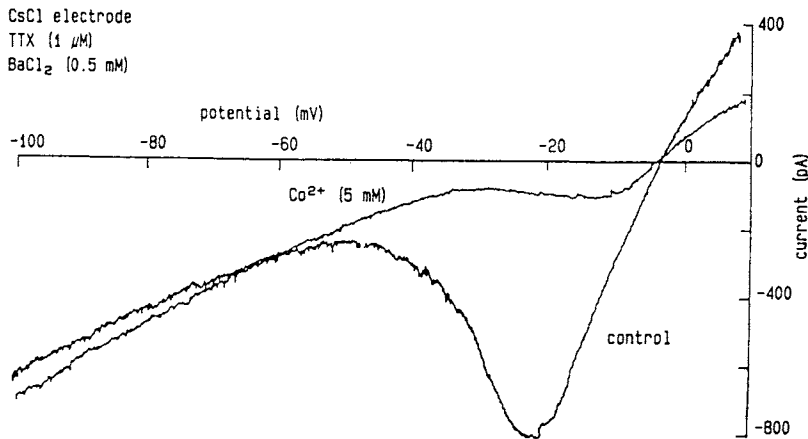


Figure 5.14. Blockade of Ca^{2+} current by cobalt abolishes the negative slope conductance in the I/V plot of a locus coeruleus neuron recorded *in vitro*. Graph constructed from ramp depolarizations of a neuron impaled with a CsCl-filled recording electrode. Control I/V plot is in medium with $1 \mu\text{M}$ tetrodotoxin and 0.5 mM BaCl_2 . Note strong negative slope conductance beginning at about -50 mV that is almost totally abolished by addition of cobalt. This Ca^{2+} current was also sensitive to dihydropyridines. Figure courtesy of J.T. Williams and R.A. North.

[35] The slice preparation and the data in this section, except where otherwise indicated, are described in detail by Williams *et al.* (1984). Adult rat brainstem slices were cut in the transverse (coronal) plane, and the slice with the maximum lateral extent of the LC was used for recording. The zone of the LC was identified as a translucent area using transmitted light in the slice in the recording chamber, and the identity of this area with the anatomically defined LC was confirmed both by Nissl staining and by intracellular injections of sample neurons in the presumptive LC zone with Lucifer Yellow; the morphological characteristics of the injected neurons were the same as previously described for noradrenergic LC neurons. [36] Smith *et al.* (1975); Gorman *et al.* (1982); Smith and Thompson (1987).

voltage-dependent currents and $I_{\text{K}a}$; these outward currents bring the membrane potential to -75 mV at which level the Ca^{2+} and Na^{+} conductances are near zero. The slow depolarization that follows may be primarily due to a progressive reduction in the outward current due to a reduction in free intracellular Ca^{2+} . As the membrane potential moves from -75 mV to less negative values, the 4-AP sensitive outward current may slow the return to the AP threshold potential. Then, as the membrane potential approaches -55 mV , the slow inward Ca^{2+} current develops with increasing magnitude. This leads to the initial slow rising phase of the AP. At about -45 mV , there is a large increase in the TTX-sensitive Na^{+} channels leading to the AP proper. The cycle then repeats itself.

This hypothesis [35] offers a plausible explanation for the pacemaker activity observed in LC neurons and agrees with data on the origin of spontaneous activity in invertebrate neurons [36]. It is useful also to underline the distinction between the slowly or noninactivating Ca^{2+} conductance important in pacemaker activity and the transient, inactivating Ca^{2+} conductance of the LTS, whose rapid inactivation would not make it a reasonable mechanism to generate the LC pacemaker cycle.

5.3.2. Dorsal Raphe Neurons

There is ample evidence indicating serotonergic dorsal raphe (DR) neurons have widespread projections

and a role in modulating the excitability of the large numbers of postsynaptic neurons (see Chapter 4). Serotonergic neurons, like LC neurons, show a dramatic state-related modulation of discharge *in vivo*; they join the LC population in slowing and virtually ceasing discharge with the advent of REM sleep, and, as discussed in Chapter 10, the arrest of their discharges appears to be closely correlated with the onset of the PGO waves of REM sleep. Thus, the intrinsic membrane properties contributing to their discharge pattern are of considerable interest to physiologists interested in control of behavioral state alterations and in general features of control of excitability in target neurons. We will discuss two intrinsic, inwardly rectifying K^+ conductances of DR neurons in Chapter 6, together with the serotonin-controlled, inwardly rectifying K^+ conductance.

The intracellular *in vitro* data on DR neurons described in this section is from the work of Aghajanian and collaborators [37]; work that followed the initial *in vitro* extracellular DR recordings [38]. Input resistances of presumptive serotonergic neurons recorded *in vitro* ranged between 40 and 230 M Ω . These input resistances were higher than those recorded *in vivo* [39], as is typical for *in vivo* vs *in vitro* input resistance measurements, but other characteristics of the neurons were the same as the *in vivo* sample.

Extracellular and intracellular recordings of neurons in the slice showed the presence of a spontaneous slow, regular discharge rhythm also characteristic of *in vivo* recordings of these neurons. As shown in Fig. 5.15, the AP was followed by an AHP, then a rapid phase of depolarization followed by a long plateau of very slow depolarization, then the rapidly rising phase of a spike that, in most instances, had a "shoulder" during the repolarization phase. The cycle then repeated; of particular note was the absence of evidence for PSPs that might drive the depolarization, both in the *in vivo* and in the *in vitro* recordings, thus suggesting a true pacemaker organization. These neurons showed an early transient outward current with the characteristics of I_A . Single electrode voltage clamp studies revealed the presence of a transient outward current when depolarizations were made from holding potentials of -70 mV in TTX-containing perfusate, but not when holding potentials of -60 mV were used for the same depolarizing pulse. Perfusion with 1 mM 4-AP also greatly reduced this transient outward current.

Activation of this presumptive I_A from a holding potential of -80 mV first occurred with a voltage step to -60 mV, with progressive increases in current up to a voltage step to -40 mV. At a holding potential of -40 mV,

- [37] VanderMaelen and Aghajanian (1983); Aghajanian and Lakosi (1984); Aghajanian (1985); Burlhis and Aghajanian (1987); Freedman and Aghajanian (1987). Aghajanian and coworkers utilized 300–450 μ m thick frontal (coronal) slices from albino rats that were mounted in a modified Haas chamber (not submerged in perfusate). Viewed through a binocular microscope, the DR nucleus was easily visualized, lying ventral to the central aqueduct and dorsal to the medial longitudinal fasciculus and decussation of the brachium conjunctivum. Neurons were classified as serotonergic on the basis of long-duration action potentials (2 ms), large AHPs, and pacemaker potentials; these were characteristic of neurons identified as serotonergic by an *in vivo* double-labeling technique (Aghajanian and VanderMaelen, 1982b). [38] Mosko and Jacobs (1976); Trulson *et al.* (1982). [39] Griffith (1988).

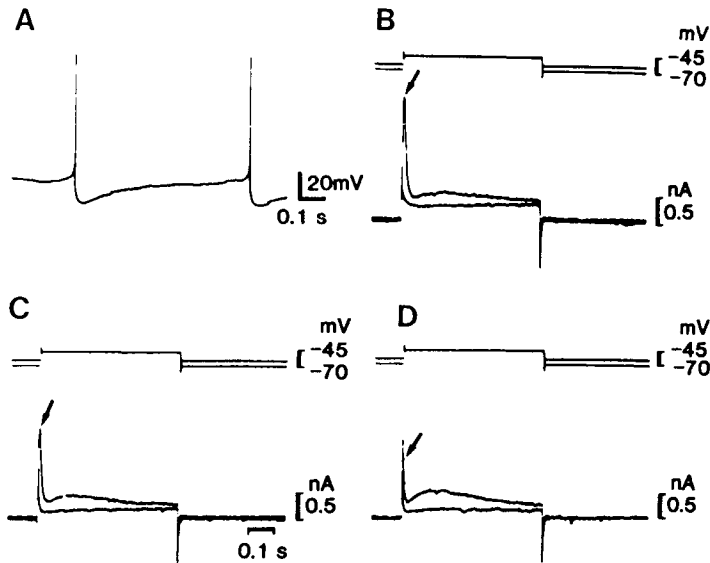


Figure 5.15. *In vitro* recordings of dorsal raphe (DR) serotonergic neurons. Presence of a transient outward current suppressed by 4-AP. A, spontaneous pikes of a typical serotonergic neuron in the DR slice preparation. Note the large AHPs, followed by a rapid phase of depolarization, and then a plateau period before the subsequent spike. B, voltage clamp at -70 mV in 1 M tetrodotoxin to eliminate Na^+ spikes; top traces are voltage; bottom are current; outward currents are upward going. A step depolarization to -45 mV elicits a transient outward current (arrow) which peaks 8 ms after the depolarizing step; superimposed traces show the virtual absence of a transient outward current when the holding potential is -60 mV rather than -70 mV. C, 10 min after the addition of 1 mM 4-AP, the transient outward current (arrow) is reduced by about 30% . D, 12 min after the 4-AP has been increased to 2.5 mM the transient outward current is reduced by more than 60% . Modified from Aghajanian (1985).

the current was inactivated; de-inactivation occurred only with hyperpolarizations below -60 mV and was maximal at about -90 mV.

Burlhis and Aghajanian [37] demonstrated the presence of an LTS conductance in the serotonergic DR neurons. This conductance was blocked in the presence of Ni^{2+} and other divalent cations known to block Ca^{2+} conductances (Fig. 5.16), was de-inactivated at low voltages in a time- and voltage-dependent manner, and was differentiated from a HTS conductance by the failure of the latter to be blocked by Ni^{2+} . Single electrode voltage clamp studies using electrodes filled with Cs^+ (to suppress I_A and other K^+ conductances) showed a negative slope conductance from -60 to -50 mV, indicating the presence of an inward current (the LTS current) in this voltage range. The LTS conductance was not directly altered by phenylephrine or serotonin.

These workers suggested the following hypothesis for the sequence of events underlying generation of rhythmic activity in DR serotonergic neurons. With the occurrence of a fast Na^+ spike, there is entry of Ca^{2+} through HTS channels. This activates $I_{\text{K}(\text{Ca})}$ (the AHP current), which

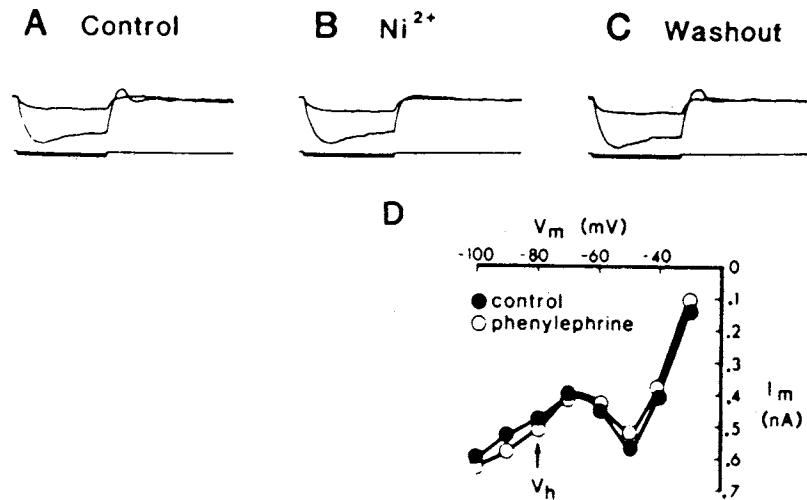


Figure 5.16. *In vitro* recordings of serotonergic dorsal raphe neurons. Upper panel block by nickel of low-threshold current following hyperpolarizing pulse. A, control, in 1 M tetrodotoxin. B, current is abolished by 100 M nickel. C, current returns upon wash-out. Lower panel D, single electrode voltage clamp data on I/V relationship, showing region of negative slope conductance. Modified from Burlhis and Aghajanian (1987).

hyperpolarizes the neuron to the region of de-inactivation for I_A and for the LTS current (I_T). As the internal free Ca^{2+} concentration decreases, the membrane potential depolarizes to the voltage (about -60 mV) where the LTS current is activated, and this current acts to bring the membrane potential to the threshold for the fast Na^+ spike and the cycle is repeated.

It will be noted that the inward, depolarizing I_T is counteracted by I_A , and the relative strength of these two currents may determine the presence and frequency of rhythmic discharge in serotonergic neurons. The pacemaker plateau period occurs between -60 mV and -50 mV, precisely the range in which both the LTS and I_A become activated. When activated, the outward (hyperpolarizing) I_A may thus diminish the frequency of discharge and be responsible for the long plateau period. As will be discussed in Chapter 6, I_A is also important because it is decreased by norepinephrine α 1-agonists, and is thus an important pacemaker system component that may be modulated by input from other neurons.

In commenting on this model of the DR rhythmic activity, we underline the fact that both I_A and I_T are transient in the sense of rapidly inactivating. Data presented indicate they both should be inactivated within 200 ms and thus seem not kinetically suitable conductances for modeling the rhythmic activity of DR neurons. The plateau potential typically lasts several-fold longer than the inactivation time for these conductances and thus could not be

caused by them. Voltage clamp studies of persisting rather than transient conductances, and of their kinetics and voltage sensitivity, appear to be needed.

5.4. Basal Forebrain and Medial Septum Neurons

The intrinsic membrane properties of acetylcholinesterase-positive, presumably cholinergic basal forebrain neurons recorded from the diagonal band (DB) nuclei and ventral part of the medial septum (MS) of guinea pig have been first studied *in vitro* by Griffith [39]. Three types of neurons were described as displaying slow AHP (duration of about 600 ms) or fast AHP (5–50 ms) of smaller amplitudes; a small proportion (7%) of cells fired in a burst pattern. The slow AHP neurons have been tentatively regarded as corresponding to some slowly firing cholinergic basal forebrain projection neurons, while the characteristics of fast AHP elements resembled those of fast-spiking (FS) cortical local-circuit cells.

Subsequently, a series of studies have defined the intrinsic properties and oscillations displayed by cholinergic and noncholinergic nucleus basalis (NB) neurons. In addition to the tonic firing pattern shown *in vivo*, magnocellular NB neurons display rhythmic bursting activity mediated by a Ca^{2+} -mediated LTS [40]. The rhythmic firing of cholinergic NB cells can be generated and prolonged by NMDA application [41]. A comparative study of cholinergic and noncholinergic NB neurons revealed that the former fire rhythmic spike-bursts at low frequencies (<10 Hz) riding on LTSs and tonic firing (10–15 Hz) when depolarized. Noncholinergic neurons discharge in a unique mode, with clusters of spikes interspersed with rhythmic subthreshold membrane potential oscillations when depolarized from levels less negative than -55 mV [42].

In the MS, noncholinergic (presumably GABAergic) neurons discharge in rhythmic clusters of APs at frequencies ranging from 1–8 Hz as well as 20–60 Hz [43], that is, the frequencies of theta and beta/gamma oscillations. The subthreshold oscillations are eliminated by TTX.

5.5. Thalamic Neurons

The intrinsic properties of thalamic neurons allow them to function in two different modes in two distinct

[40] Khateb *et al.* (1992). In this study, NB neurons were investigated in guinea pig slices, filled with biocytin and immunohistochemically identified to be ChAT+.

[41] Khateb *et al.* (1995a).

[42] Alonso *et al.* (1996).

[43] Serafin *et al.* (1996).

types of behavioral states: a *tonic* discharge pattern during both EEG-activated states (wakefulness and REM sleep), accompanied by enhanced and accurate synaptic transmission of incoming information from the outside world during the adaptive waking state; and a *bursting* mode, associated with depressed transfer function during EEG-synchronized sleep (Fig. 5.17; see details in Chapter 7). While the study of electrical responsiveness of thalamic LG neurons in slices has been attempted since the mid-1970s [44] and postsynaptic potentials (PSPs) in rat and cat LG neurons have been investigated *in vitro* during the late 1970s [45], the discovery of major intrinsic properties of thalamic neurons and of their ionic conductances started in 1982 [46]. In the same years, intracellular studies *in vivo* disclosed that thalamic relay and intralaminar neurons possess intrinsic properties similar to those investigated *in vitro* and put them in the context of the oscillatory and

[44] Yamamoto (1974).

[45] Kelly *et al.* (1979).

[46] Llinás and Jahnsen (1982); Jahnsen and Llinás (1984a–b).

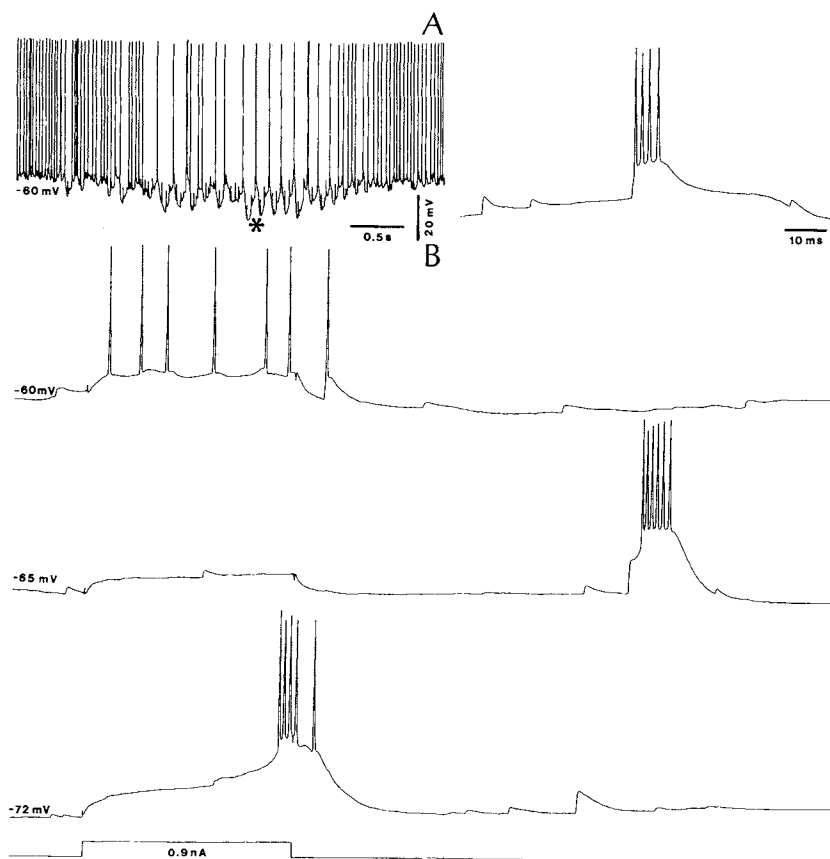


Figure 5.17. Two firing modes of thalamocortical cell. Intracellular recording in centrolateral intralaminar nucleus of cat under urethane anesthesia. Top trace, tonic firing at resting membrane potential ($V_m = -60$ mV) and rhythmic (~ 8 Hz) high-frequency spike bursts during episode with spontaneous hyperpolarization. Burst indicated by asterisk is expanded at right. Bottom, responses to depolarizing current pulses (identical parameters) at different V_m by applying DC hyperpolarizing current. Note tonic firing at resting V_m (-60 mV), silent zone at -65 mV, and high-frequency burst at -72 mV. From Steriade (1999a).

- [47] Deschênes *et al.* (1982, 1984); Steriade and Deschênes (1984).
 [48] Roy *et al.* (1984).
 [49] Crunelli *et al.* (1987a–c, 1988); Hirsch and Burnod (1987).
 [50] Steriade and Llinás (1988); Huguenard (1996); Chapter 5 in Steriade *et al.* (1997a).

relay modes that typically characterize behavioral states of light sleep and wakefulness [47, 48]. A new series of *in vitro* added a series of data related to the various components of the long-lasting hyperpolarization in LG thalamic neurons [49]. The complex series of Na^+ , Ca^{2+} , and K^+ conductances of thalamic neurons, other than the conventional currents that generate the fast AP, are reviewed elsewhere [6, 50]. *In vitro* studies mainly related to transmitter actions are discussed in Chapter 6.

Here, we briefly discuss some currents, mainly those that appear to be critical in the patterning of spindle and delta oscillations, the peculiar features of thalamic neurons during EEG-synchronized sleep. We emphasize that, while the intrinsic properties of thalamic neurons endow them with the ability to oscillate, the synchronized oscillations in thalamocortical (TC) neurons, as they appear during natural sleep, require a synaptic network with a driving force for the coordination of individual oscillations. The importance of synaptic networks including the thalamic reticular (RE) GABAergic nucleus, the pacemaker of spindling, in synchronizing thalamic rhythmicity becomes evident when considering the absence of spindle rhythms in TC neurons deprived of inputs from reticular nucleus, despite their having identical intrinsic properties as RE-connected TC cells (see details in Chapter 7). We will also show that major intrinsic properties of TC cells are drastically changed by synaptic activities, as seen in *in vivo* experiments [51].

- [51] Steriade (2001a–b).

5.5.1. Thalamocortical Neurons

The intrinsic electrophysiological properties of TC neurons recorded from different dorsal thalamic nuclei are similar. They consist mainly of (a) a transient Ca^{2+} current (I_T) de-inactivated by hyperpolarization and underlying low-threshold spikes (LTSs) crowned by rebound spike-bursts [6, 46, 47, 50]; (b) high-voltage Ca^{2+} currents [52]; (c) a hyperpolarization-activated cation current (I_H) that produces a depolarizing sag [53]; (d) a persistent Na^+ current ($I_{\text{Na(p)}}$) [46]; and (e) different types of K^+ currents [46, 54]. These intrinsic properties are important in the generation and synchronization of thalamic oscillations (see Chapter 7). Below, we discuss some of these intrinsic properties in TC neurons.

- [52] Hernández-Cruz and Pape (1989); Kammermeier and Jones (1997).
 [53] McCormick and Pape (1990a–b); Leresche *et al.* (1991); Soltesz *et al.* (1991)
 [54] McCormick (1991a); Budde *et al.* (1992).

5.5.1.1. The Low-Threshold Ca^{2+} Current

The Ca^{2+} -dependent LTS was first described in inferior olive neurons [55] and was thereafter found in

- [55] Llinás and Yarom (1981).

guinea pig thalamic neurons *in vitro* [46] and cat thalamic neurons *in vivo* [47]. As discussed in the first section of this chapter, the LTS is inactive at rest and is de-inactivated with membrane hyperpolarization (Fig. 5.18A). On the average, de-inactivation to allow the necessary level of regenerative response is attained at about -65 mV. The LTS is prevented by Ca^{2+} blockers, such as Co^{2+} or Cd^{2+} , and it underlies a burst of fast Na^+ -dependent APs, that can be blocked by TTX (Fig. 5.18B).

At the normal resting membrane potential, the thalamic-cell's response to a depolarizing pulse is tonic repetitive firing and the response to an excitatory synaptic input is an EPSP that may trigger single spikes, whereas each of these stimuli applied to the hyperpolarized cell by a few millivolt from the rest elicits an LTS crowned by a burst of fast APs. The LTS and the superimposed burst may also be triggered at the break of a hyperpolarizing current pulse (Fig. 5.19). These intracellular data indicate that the LTS is the basis of the high-frequency bursts that characterize the activity of TC neurons during EEG-synchronized

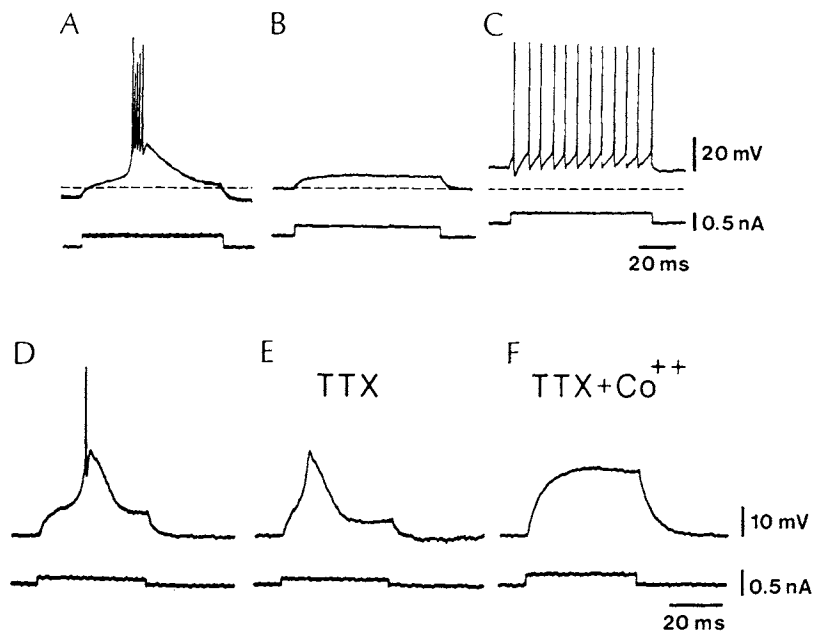


Figure 5.18. Two firing levels in thalamic neurons and ionic basis for low-threshold spike (LTS) in *in vitro* studies of guinea pig thalamus. A, cell was directly excited while being hyperpolarized by a constant current injection. Outward current pulse induces an LTS that triggers a burst of fast action potentials. B, same current pulse produces a subthreshold depolarization if superimposed on a slightly depolarized membrane potential level. C, after further depolarization by a direct current, pulse produces a train of action potentials. D, LTS generated by direct stimulation from a slightly hyperpolarized neuron. E, blockage of I_{Na} by tetrodotoxin removes fast spike but leaves LTS unmodified. F, addition of Co^{2+} to the bath abolishes LTS even when current pulse is increased in amplitude by 2.5 times, demonstrating that LTS is generated by low-threshold I_{Ca} . Modified from Llinás and Jahnsen (1982).

[56] Steriade *et al.* (1985).

[57] Paré *et al.* (1991).

[58] Although some authors have hypothesized that spike-bursts of thalamic relay neurons from lateral geniculate nucleus are also present during the waking state (Guido *et al.*, 1992), those data came from anesthetized animals. Subsequently, the same group worked in chronically implanted cats and realized that spike-bursts are quite rare during wakefulness (Guido and Weyand, 1995) and, more recently, the same authors (Weyand *et al.*, 2001) reported that “during wakefulness, <1% of action potentials are associated with bursting” (p. 1107) and found a “negative relationships between

sleep when they become hyperpolarized (see details in Chapter 7).

As shown both *in vitro* and *in vivo*, the de-inactivation of the LTS is not only voltage-dependent, but also time-dependent. Indeed, hyperpolarizing pulses of increasing duration produce graded de-inactivation and short-lasting hyperpolarizing current pulses subthreshold for rebound excitation can sum and trigger overt LTSs (Fig. 5.19) [56]. When periodic hyperpolarizing current ramps are injected at a frequency of 12.5 Hz, rhythmic burst discharges are observed at a frequency of about 2.5 Hz (Fig. 5.20). This frequency transformation suggests that temporal integration of short hyperpolarizations in normal conditions could lead to production of rhythmic LTSs in thalamic neurons [56, 57].

The refractory period of LTS in virtually all TC neurons (but see exception below) is quite long, both *in vitro* and *in vivo*, that is, 150–200 ms [46, 47]. This feature and the fact that LTS is dependent on hyperpolarization of TC cells explain why spike-bursts are seen during slow-wave sleep, when these neurons are hyperpolarized by ~7–10 mV [58]. It is also known that spike-bursts of TC

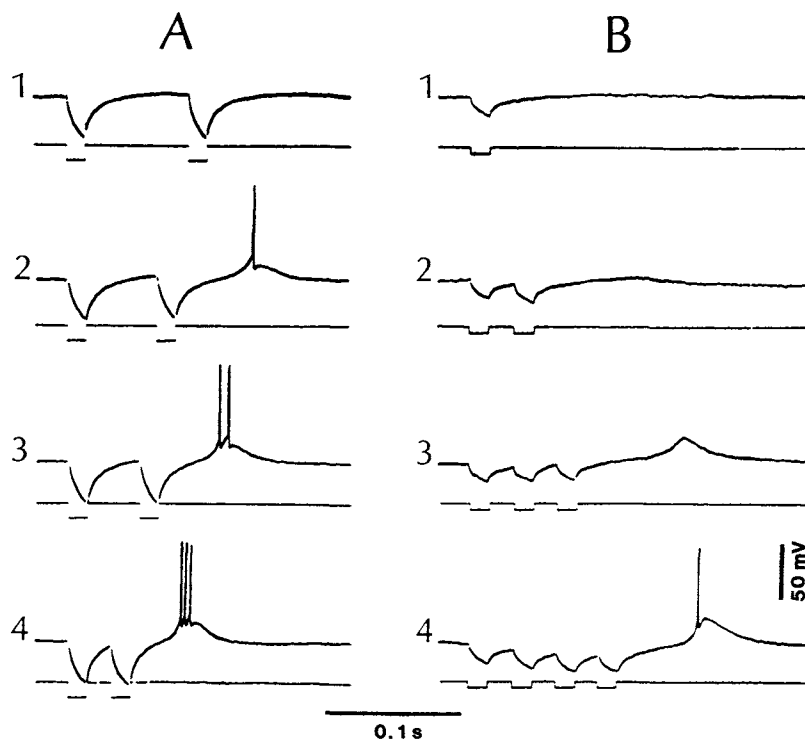


Figure 5.19. Time-dependency of low-threshold conductance in thalamocortical neuron from ventrolateral nucleus. Intracellular recording in cat under barbiturate anesthesia. Pairing of two (A) or one-to-four (B) hyperpolarizing current pulses with 2 nA (A) and 1 nA (B). Further explanations in text. Modified from Steriade *et al.* (1985).

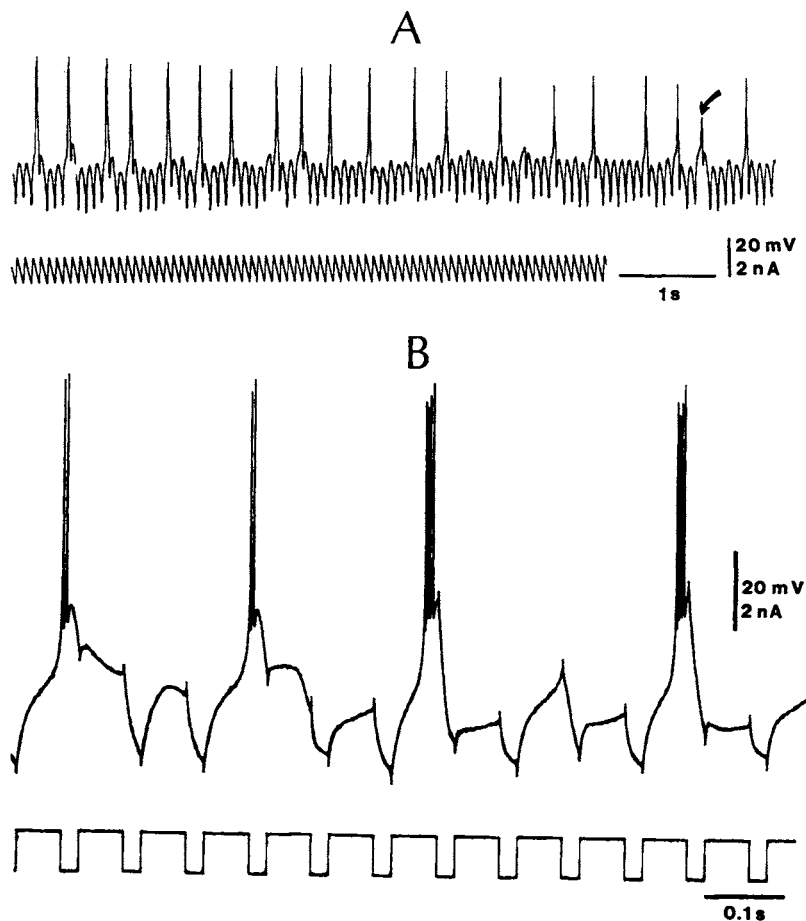


Figure 5.20. Frequency transformation of rhythmic hyperpolarizations by thalamocortical neurons. A, polygraphic recording showing how repetitive injection of subthreshold hyperpolarizing ramps at a frequency of 12.5 Hz is transformed in rhythmic bursting at 2.5 Hz. The amplitude of fast spikes is truncated. The arrow points to an isolated LTS. B, response of a thalamic ventrolateral neuron to a train of hyperpolarizing pulses at 12 Hz. Note the rhythmic occurrence of LTSs at 4 Hz. Modified from Steriade *et al.* (1985) and Paré *et al.* (1990a).

neurons cannot follow frequencies above 6 Hz [59]. Thus, spike-bursts would not be able to follow rapidly recurring signals during wakefulness.

A special class of TC neurons, recorded from the large-cell part of rostral intralaminar nuclei and antidromically activated from cortex at latencies indicating very fast conduction velocities ($40\text{--}50\text{ m s}^{-1}$), generate unusually high-frequency (900–1000 Hz), rhythmic (20–60 Hz) spike-bursts at relatively depolarized levels (Fig. 5.21). The LTSs of these rostral intralaminar neurons have a shorter refractory phase (60–70 ms) than other TC neurons (150–200 ms), which allows them to rebound following each IPSP during sleep spindles [60].

attention and bursting” (p. 1113). For the incidence of spontaneous spike-bursts fired by TC neurons during waking and sleep, *see also* Steriade (2001c). [59] McCormick and Feese (1990).

[60] Steriade *et al.* (1993c).

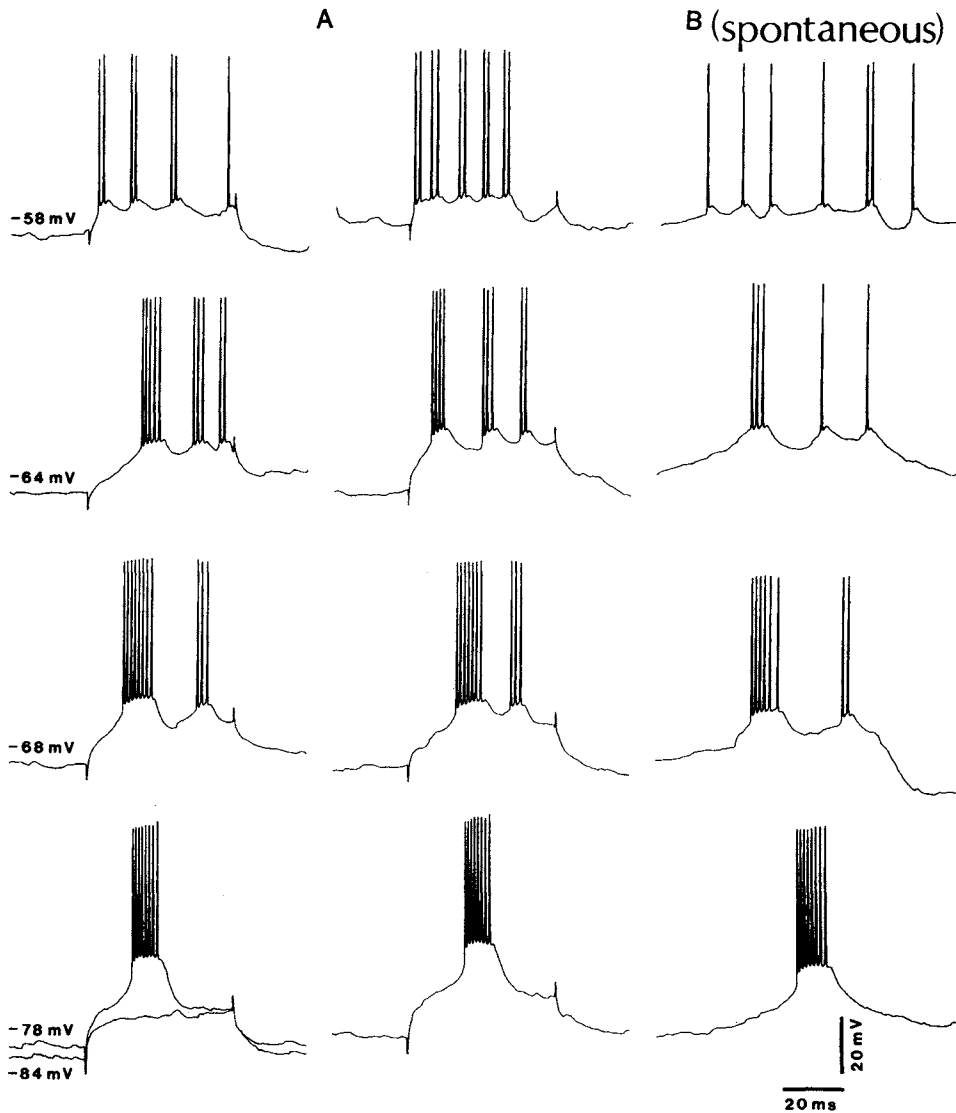


Figure 5.21. Fast oscillatory patterns of a thalamocortical neuron recorded from the dorsolateral part of the thalamic centrolateral (rostral intralaminar) nucleus of cat. Bursting patterns were induced by depolarizing current pulses at different V_m s and also occurred spontaneously. A, activities triggered by a depolarizing current pulse (+1.2 nA, 50 ms) at different V_m s (indicated at left). Two examples are illustrated for each V_m . At bottom, the presence of an LTS leading to high-frequency (800 Hz) spike-burst at -78 mV and its absence at -84 mV. B, oscillatory patterns similar to those elicited by current injection occurred spontaneously at similar V_m s (from top to bottom, -58 mV, -64 mV, and -78 mV). From Steriade *et al.* (1993c).

5.5.1.2. High-Voltage Ca^{2+} Currents

Presumed intradendritic recordings in thalamic cells studied *in vitro* [46] and *in vivo* [48] revealed a voltage-dependent, high-threshold Ca^{2+} conductance that triggers depolarizing responses followed by the activation of a Ca^{2+} -dependent K^+ conductance, $g_{\text{K}(\text{Ca})}$. In cortically

evoked responses of TC neurons *in vivo*, the disclosure of this high-threshold conductance requires an increase in stimulus strength (as compared to the primary EPSP) or the facilitatory action of 2–3 stimuli. This conductance is reflected in the depth of the early IPSP as repetitive fast-rising depolarizations with or without superimposed spike discharges (Fig. 5.22) [61] and it corresponds to component c in Fig. 5.23. This high-threshold secondary excitation was identified *in vivo* as a dendritic Ca^{2+} conductance on the basis of intracellular injections of ethyleneglycol-tetracetic acid (EGTA), a substance that binds free calcium. This treatment prevents the development of the subsequent $g_{\text{K}(\text{Ca})}$. Consequently, the EGTA injections in presumed dendrites of thalamic neurons lead to the appearance of long-lasting plateaus and prolonged spike discharges [48].

[61] Steriade (1984).

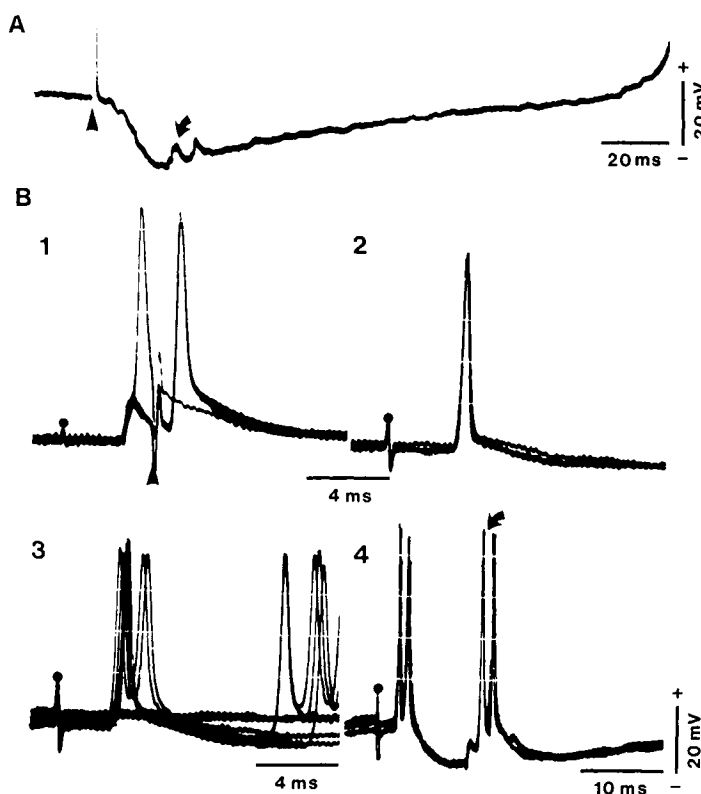


Figure 5.22. Secondary excitation (see component c in Fig. 5.23) in cat thalamocortical (TC) neurons. Intracellular recordings under barbiturate anesthesia. A, response of a ventrolateral TC cell to cortical precruciate area 4 stimulation (arrowhead); the secondary excitation appears as two rapidly rising depolarizing events (arrow) with a latency of about 25 ms in the deep portion of the early IPSP. B, response of a ventrobasal TC cell to stimulation of the medial lemniscus in the medulla (dot) and antidromic response to stimulation of the primary somatosensory cortex (arrowhead in 1); note collision of cortically evoked antidromic spike with a preceding orthodromic discharge in 1. In 1–4, increasing stimulation intensities to medial lemniscus; note appearance of secondary excitation in 3 and 4 during the early IPSP (arrow in 4). Modified from Roy *et al.* (1984) and Steriade (1984).

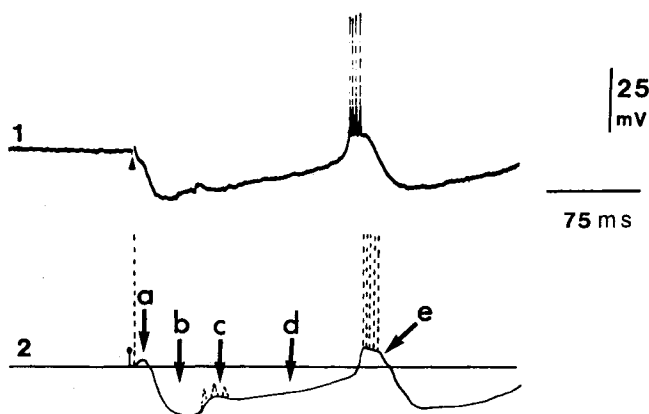


Figure 5.23. The archetypal response sequence of a thalamocortical (TC) cell to cortical stimulation. Intracellular recording of a cat ventrolateral TC neuron under barbiturate anesthesia (1) and diagrammatic representation of five components in the excitatory–inhibitory response sequence (2) Components are: a, primary EPSP associated or not with antidromic spike (dotted line); b, early Cl⁻-dependent IPSP; c, secondary excitation; d, late part of the long-lasting hyperpolarization; and e, postinhibitory rebound. See further explanations in text. Modified from Roy *et al.* (1984).

[62] Maekawa and
Purpura (1967a).

[63] Paré *et al.* (1990b).

[64] Mulle *et al.* (1985).

[65] Steriade and
Timofeev (1997).

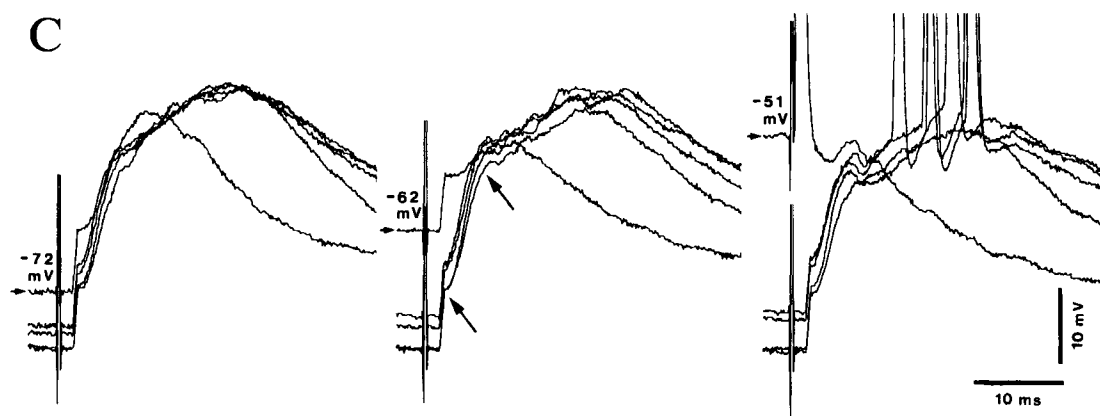
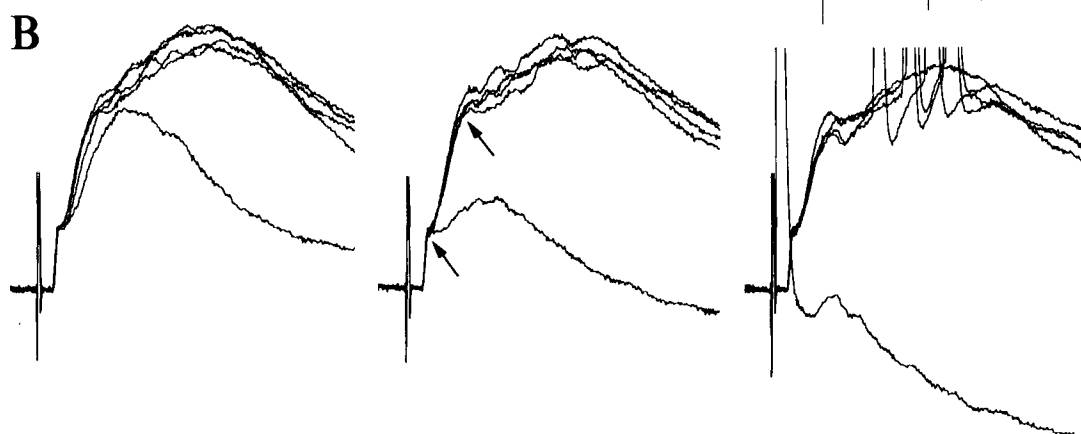
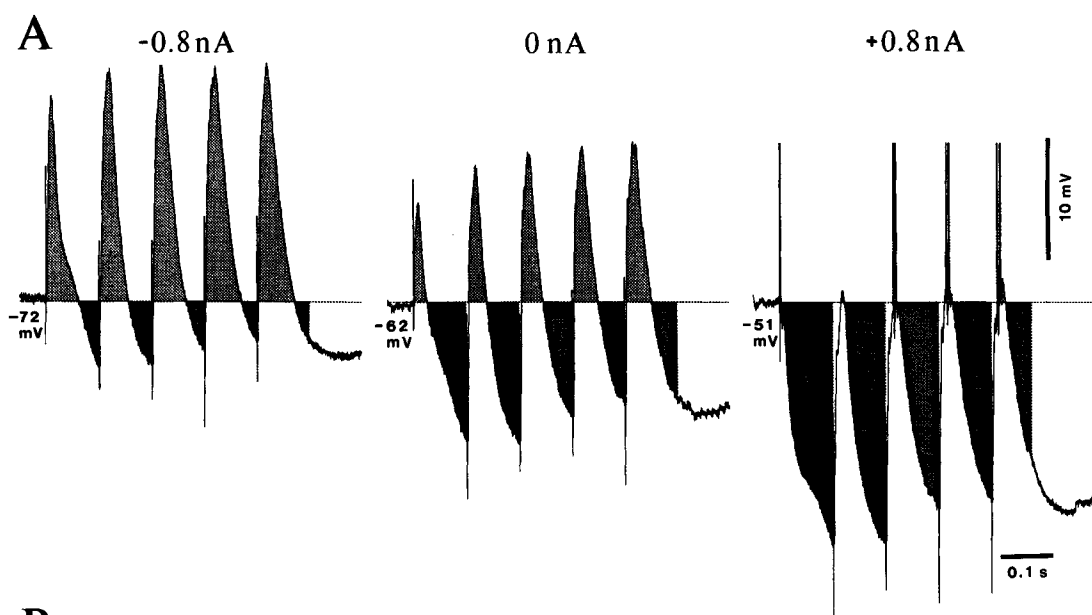
Some of the fast prepotentials (FPPs) seen in thalamic cells [47, 62, 63] probably represent dendritic spiking since they can be blocked in an all-or-none manner by hyperpolarizing currents. Intracellular injections of QX314 in thalamic neurons lead to the appearance of very numerous FPPs, because the dendritic conductance dominates the cell's behavior when somatic Na⁺ channels are blocked [64]. The main role of dendritic spiking is to assist the neuron in the transfer of EPSPs from distal portions of dendrites toward the somatic spike trigger zone.

High-threshold spikes also appear during augmenting responses in TC neurons of decorticated animals [65]. Rhythmic thalamic stimuli within the frequency range of sleep spindles produce decreased amplitudes of IPSPs and augmented responses to the second and following stimuli. This augmentation consists of a progressive increase in the number of synaptically elicited APs, associated with a progressive neuronal depolarization. The above-described type of augmentation is termed high-threshold [65] because it occurs at depolarized levels (Fig. 5.24) (see details in Chapter 8).

5.5.1.3. Hyperpolarization-Activated Cation Current

This current (I_H), described *in vitro* [53] and *in vivo* [66], is implicated, together with the Ca²⁺-dependent T-current, in the generation of pacemaker oscillations in TC cells within the frequency range of 1–4 Hz (Fig. 5.25). Such oscillations represent the thalamic, clock-like component of sleep delta waves, while the cortical component of

[66] Steriade *et al.*
(1991a); Curró Dossi *et al.*
(1992a).



delta waves is generated in neocortex, even after thalamectomy (see Chapter 7).

5.5.1.4. Persistent (Noninactivating) Na^+ Current

The voltage-dependent, noninactivating (or very slowly inactivating) Na^+ current is also termed persistent and is referred to as $I_{\text{Na(p)}}$. It was first described in cerebellar Purkinje cells where it generates a slow TTX-sensitive depolarizing response [67] (Fig. 5.26A). It is located at the soma and has a lower activation threshold and slower kinetics than those generating the fast AP. In the thalamus, $g_{\text{Na(p)}}$ was demonstrated *in vitro* [46] (Fig. 5.26B) and was found to be important in cell oscillation, as it counterbalances I_{K} to generate a rebound excitation. *In vivo* studies have shown the crucial role of $I_{\text{Na(p)}}$ in the patterning of sleep spindles by means of inactivation of Na^+ channels through intracellular injection of quaternary derivatives of local anesthetics, such as QX314 [64]. After QX314 injection in TC neurons, the spontaneous and evoked hyperpolarizations become exceedingly long-lasting (due to the dominance K^+ currents unopposed by the slow Na^+ conductance) and rhythmic postinhibitory rebounds disappear (Fig. 5.27).

[67] Llinás and Sugimori (1980).

5.5.1.5. Voltage- and Ca^{2+} -Dependent K^+ Conductances

There are at least four different voltage-dependent K^+ currents that are activated by depolarization and inactivated with time. The most quickly inactivating is I_{A} [8] that inactivates over a period of tens of milliseconds [54, 68]. Two more slowly inactivating K^+ currents are termed I_{Km} and I_{Ks} [54]. Among $I_{\text{K(Ca)}}$, the AHP potential is a rate-limiting factor. This is demonstrated by the different duration of AHPs in two distinct classes of thalamic

[68] Huguenard *et al.* (1991).

Figure 5.24. Intrathalamic high-threshold augmenting potentials developing in parallel with progressively decreased hyperpolarizations. Intracellular recordings in decorticated cat, under ketamine-xylazine anesthesia. A, Thalamocortical neuron from the ventrolateral nucleus was tested with trains of five stimuli at 10 Hz under steady hyperpolarizing current (-0.8 nA) (left), at rest (0 nA) (middle), and under steady depolarizing current ($+0.8 \text{ nA}$) (right). Superimposed responses were offset at the initial V_{m} (see real V_{m} s in C). B, superimposed and expanded early responses (at the same V_{m} as in A). The bottom arrow in the middle column tentatively indicates the level where the initial excitatory postsynaptic potential gave rise to a low-threshold response, whereas the top arrow marks the inflection

where high-threshold augmenting responses were initiated at a more depolarized level. Note action potentials triggered by the augmented response under $+0.8 \text{ nA}$ (right column). C, the early responses were superimposed and expanded but shown at the real V_{m} . In all superimpositions, the response to the first stimulus in the train is at the indicated V_{m} (-72 mV under -0.8 nA , -62 mV without current, and -51 mV under $+0.8 \text{ nA}$). The next two traces illustrate the responses to the fifth and fourth stimuli, and the last traces represent responses to the second and third stimuli. Note, under $+0.8 \text{ nA}$, the antidromic spike immediately after the first stimulus in the train at -51 mV but its blockage at more hyperpolarized levels. From Steriade and Timofeev (1997).

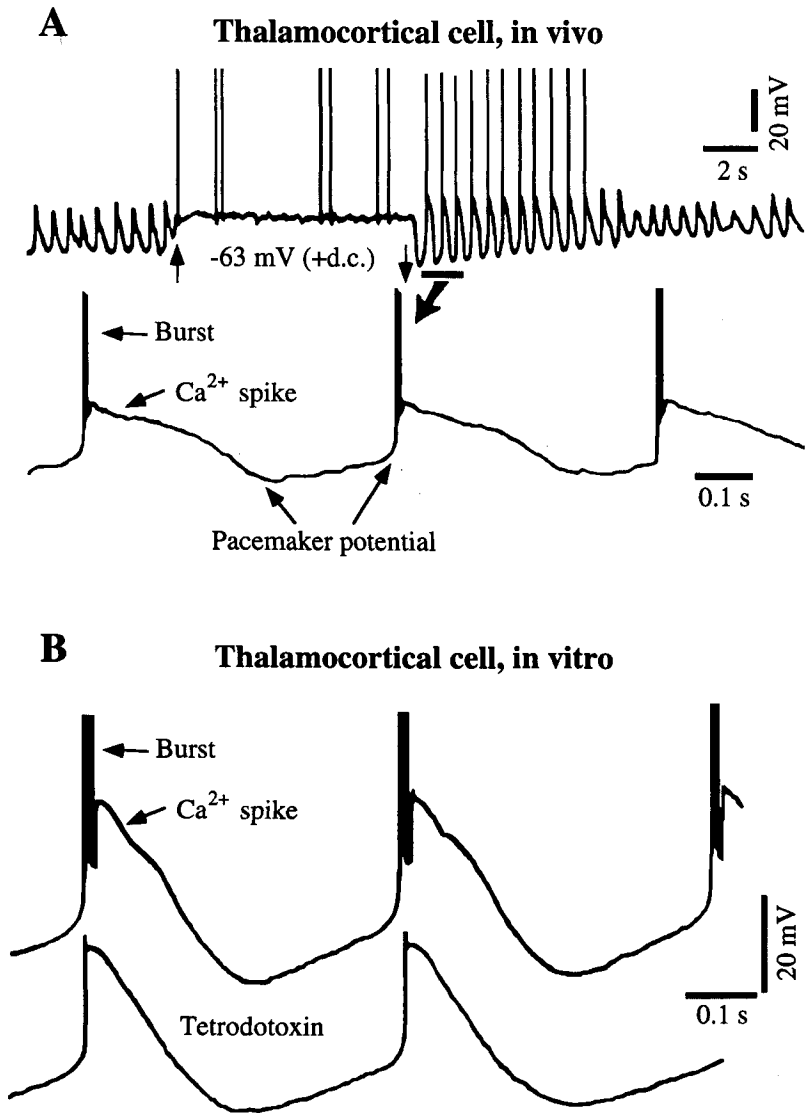


Figure 5.25. Intrinsic cellular mechanisms of thalamic clock-like delta oscillation. A, voltage-dependency of delta oscillation. Shown is the intracellular recording *in vivo* of a lateroposterior thalamocortical neuron after decortication of areas projecting to that nucleus in an anesthetized cat. The cell oscillated spontaneously at 1.7 Hz. A 0.5-nA depolarizing current (+DC) pulse (between arrows), bringing the membrane potential to -63 mV, prevented the oscillation, and its removal set the cell back into the oscillatory mode. Three cycles marked by the horizontal bar in the upper trace are expanded below. B, spontaneous rhythmic burst firing in a cat lateral geniculate relay cell recorded *in vitro* before and after block of voltage-dependent Na⁺ conductance with application of the Na⁺ channel blocker tetrodotoxin. Modified from Steriade *et al.* (1993d).

neurons: TC cells have AHPs of about 70 ms, whereas in reticular neurons the AHP terminates after 8–10 ms [69]. Accordingly, the firing rates of TC neurons in behaving animals do not generally exceed 7–10 Hz during EEG-synchronized sleep, whereas reticular neurons display during the same behavioral state, discharge frequencies of about 20 Hz; and, on arousal, reticular neurons may reach

[69] Mulle *et al.* (1986).

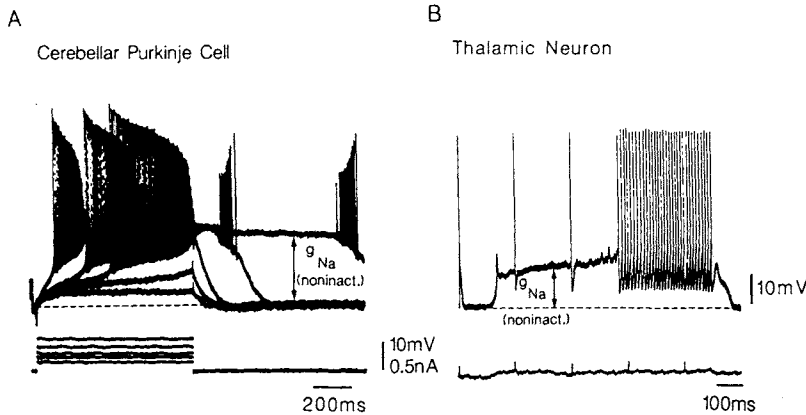


Figure 5.26. Plateau depolarization generated by persistent Na^+ current, $I_{\text{Na(p)}}$. A, direct activation of an intracellularly recorded cerebellar Purkinje cell *in vitro*. Voltage-dependent Ca^{2+} conductance was blocked by addition of CdCl_2 to the bathing solution. Transmembrane current steps (lower trace) depolarized cell to threshold for spike initiation. Activation consisted of action potentials firing repetitively on a slowly rising depolarizing response that terminates on a plateau potential and spike inactivation. Higher two stimuli generate plateaus that outlast stimulus duration. A fast burst of spikes is seen as plateau depolarization returns to resting membrane potential. This plateau is generated by an equilibrium state between I_K and $I_{\text{Na(p)}}$. B, similar set of responses as in A but for a thalamic neuron. A very small depolarizing current step is given, which triggers a rapid depolarization of the thalamic cell and a plateau that lasts for several seconds. This plateau is partly produced by $I_{\text{Na(p)}}$, and part of voltage is produced by outward current pulse. However, latter component is small and $I_{\text{Na(p)}}$ is responsible for much of plateau amplitude. Superimposed on this plateau are short-lasting depolarizing pulses that generate single spikes and, as plateau reaches a steady level, generate repetitive firing. For thalamic neurons, $I_{\text{Na(p)}}$ is powerful enough to generate a plateau response without blockage of voltage-dependent Ca^{2+} conductances. A, unpublished data from R. Llinás and M. Sugimori. B, modified from Jahnsen and Llinás (1984a).

firing rates between 50 and 100 Hz that are not seen in TC neurons [70].

[70] Steriade *et al.* (1986).

5.5.1.6. Effects of Synaptic Activities on Some Intrinsic Properties

Like in cortical neurons (see Section 5.6), the intrinsic properties of thalamic neurons are subject to significant changes due to impact of synaptic activities arising in afferent networks. Thus, fast oscillations, consisting of EPSPs generated in deep cerebellar nuclei, greatly reduce and even abolish the LTS of TC neurons in ventrolateral nucleus [71] (Fig. 5.28). Also, $\text{GABA}_{\text{A-B}}$ -mediated IPSPs have a shunting influence on LTSs by delaying the generation of rebound LTSs (Fig. 5.29). Other effects of network activities on intrinsic properties of TC neurons are discussed elsewhere [72].

[71] Timofeev and Steriade (1997).

[72] Steriade (2001a–b).

5.5.2. Local-Circuit Inhibitory Cells

Intracellular studies of local-circuit GABAergic neurons have been performed in thalamic slices from LG

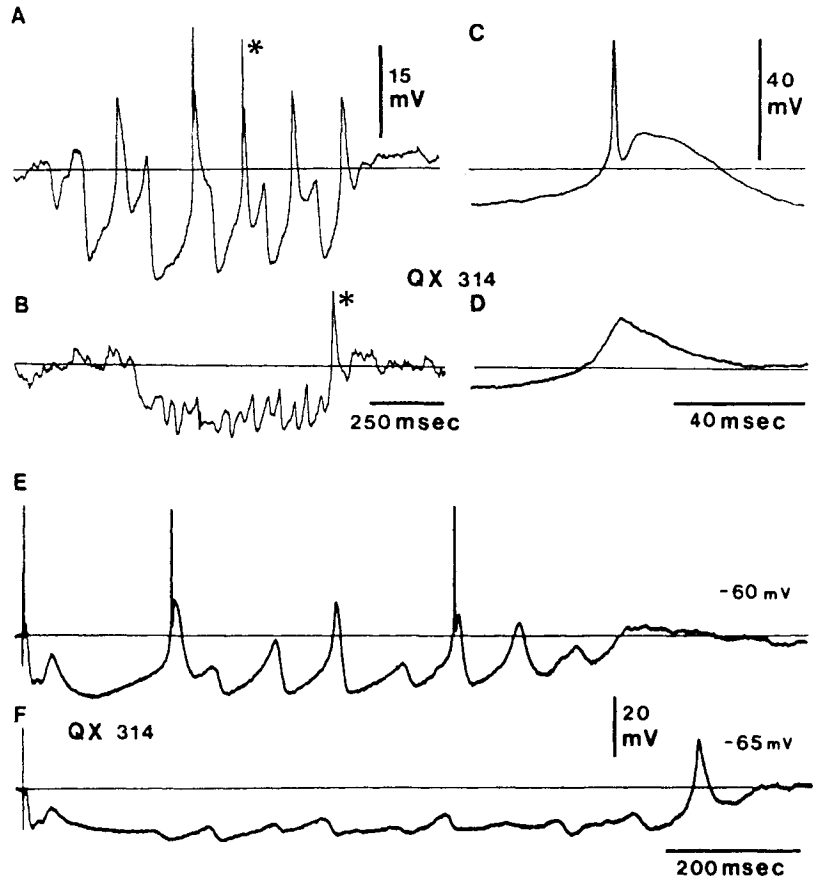


Figure 5.27. Effect of intracellular injection of QX314, a quaternary derivative of lidocaine that blocks Na^+ spike electrogenesis and $I_{\text{Na(p)}}$, on thalamic spindle oscillations. Intracellular recording of a ventrolateral TC cell in cat under barbiturate anesthesia. A and B, polygraphic recordings of spontaneous spindle oscillations 2 min (A) and 12 min (B) after impalement with a pipette containing 0.1 M QX314. Spikes are truncated. Asterisks in A and B indicate LTSs that are expanded in C and D, respectively. The LTS in C triggers a Na^+ action potential. Note, in B, the effect of QX314; abolition of spindle-related rhythmic LTS rebounds and production of a single LTS at the end of the long-lasting hyperpolarization. E and F, same cell, with spindle oscillations triggered by stimulation of the motor cortex (in E, 2 min after impalement), and the abolition of cortically evoked spindles as an effect of QX314 (in F, 15 min after impalement). Modified from Mulle *et al.* (1985).

nucleus of rats and cats. Initially, the emphasis was placed on the balance between two opposing currents (I_T and I_A) in promoting spike-bursts, with the conclusion that I_A opposes the burst [73].

Recent studies using whole-cell patch recording of formally identified local-circuit interneurons in the LG nucleus showed that these cells are more electrotonically compact than previously believed. Robust burst firing was obtained in all interneurons when a depolarizing step was imposed at a slightly hyperpolarized membrane potential [74] (Fig. 5.30). The bursts of local interneurons have longer duration and lower intraburst frequency than the

[73] Pape *et al.* (1994); Pape and McCormick (1995); McCormick *et al.* (1997).

[74] Zhu *et al.* (1999a–b).

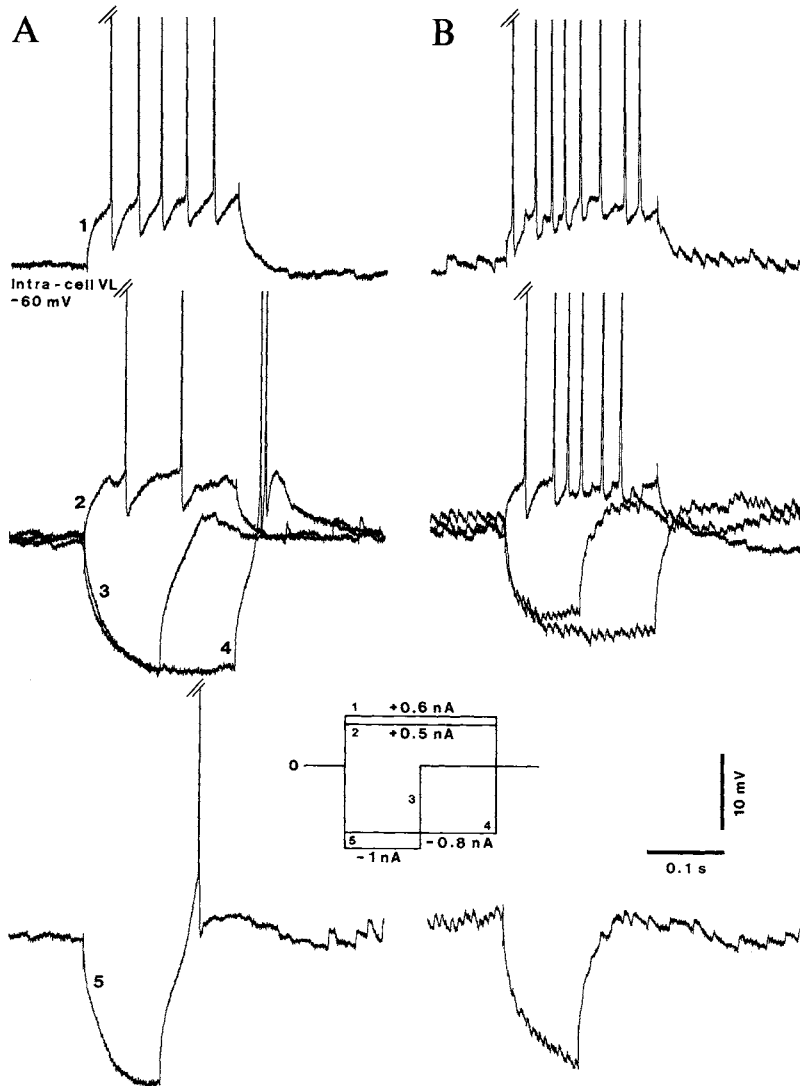


Figure 5.28. Alterations in basic electrophysiological properties of thalamocortical neurons during the fast oscillations in cerebello-thalamic pathway. Intracellular recording in cat under ketamine-xylozine anesthesia. Amplitude and duration of depolarizing (1 and 2) and hyperpolarizing (3–5) current pulses as indicated by numbers on the traces that correspond to the protocol diagram (inset), in the absence (A) and presence (B) of spontaneously occurring fast oscillations. Resting V_m , -60 mV. Action potentials are truncated. Note in B the diminution of voltage deflections (3–4) triggered by hyperpolarizing current pulses and abolition of low-threshold spike during the fast oscillation (3–5). From Timofeev and Steriade (1997).

bursts of TC neurons. Moreover, LG interneurons display an oscillatory property within a frequency range of 5–15 Hz, similar to that previously reported *in vivo* at the level of other thalamic nuclei [75], and the burst oscillation could be initiated by stimulation of optic tract fibers, suggesting that it may occur in natural conditions [74].

[75] Steriade *et al.* (1972).

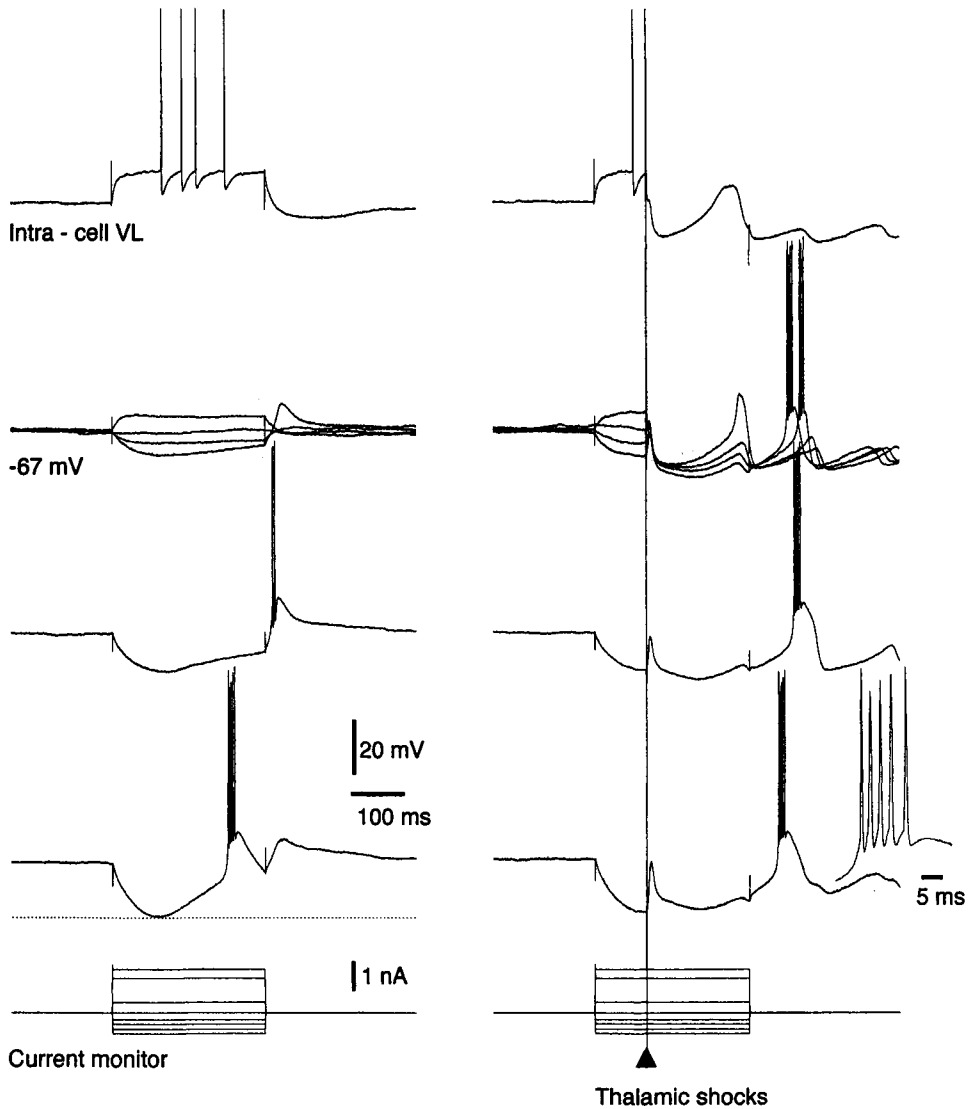


Figure 5.29. The low-threshold spike (LTS) and its interaction with synaptic responses in thalamocortical neurons. Intracellular recordings from ventrolateral nucleus in cat under barbiturate anesthesia. Left column shows responses to intracellularly applied current pulses (depolarizing and hyperpolarizing) during periods largely free of synaptic events (interspike lulls). In the right column, local thalamic stimuli (marked by triangle) were applied during the current pulses. Note the delays in generation of rebound LTSs. From Timofeev *et al.* (2001a).

5.5.3. Thalamic Reticular GABAergic Neurons

Reticular neurons operate in two functional modes, similar to TC neurons: tonic discharges during brain-active states and rhythmic spike-bursts during natural slow-wave sleep. The spike-bursts are much longer (30–80 ms, but up to 1 s when followed by a tonic tail) than in TC neurons (5–15 ms), and RE-cells' bursts display an *accelerando-decelerando* pattern, different from the progressively

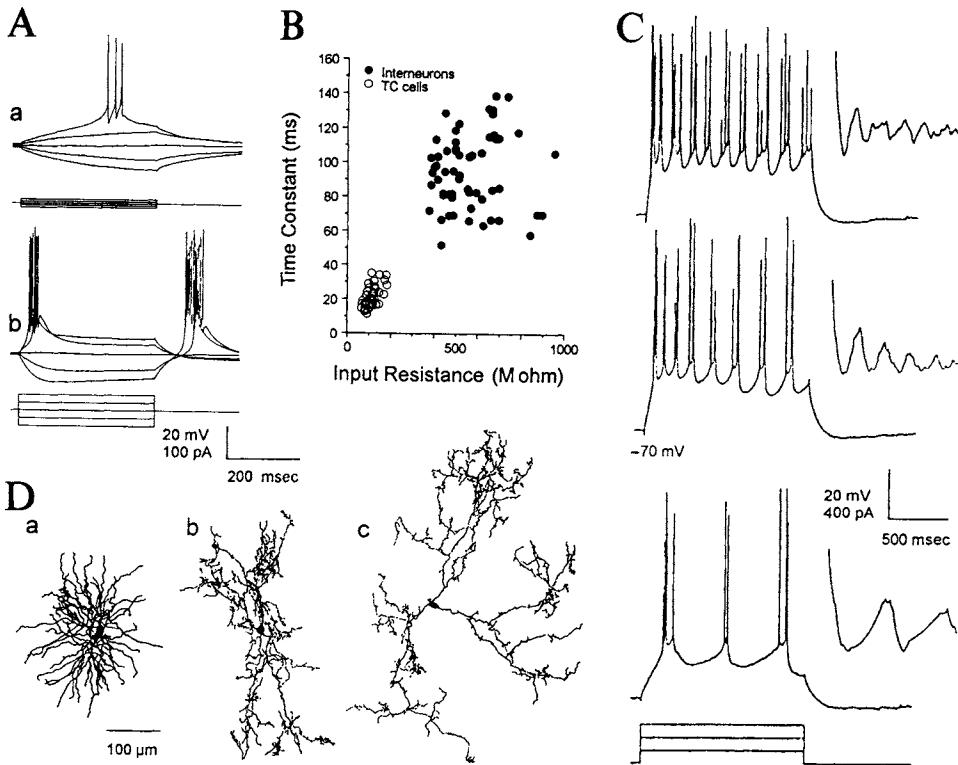


Figure 5.30. Physiological and morphological characteristics of bursting and oscillatory behavior of rat lateral geniculate (LG) local interneurons *in vitro*. Whole-cell patch recordings. A, responses to a series of current pulses of an interneuron (Aa) and a thalamocortical (TC) neuron (Ab). The resting membrane potentials were -66 mV (Aa) and -71 mV (Ab). Spike height was truncated artificially due to digital sampling. B, the interneuron has a higher input resistance and longer membrane time constant than the TC neuron. C, varying burst oscillation with increasing current injection in LG interneuron. Right, autocorrelation function for each trace. D, camera lucida reconstructions of a physiologically identified TC neuron (a) and two interneurons (b-c). Modified from Zhu *et al.* (1999a).

[76] Domich *et al.* (1986).

increasing interspike intervals in TC neurons [70, 76]. These studies on naturally awake and sleeping cats (Fig. 5.31) were followed by intracellular recordings in acute experiments, both *in vivo* and *in vitro*, which showed that the LTSs of reticular neurons are located in dendrites [69, 77]. Presumed dendritic recordings from reticular neurons *in vivo* revealed spike-bursts and the graded nature of dendritic LTSs (Fig. 5.32) [78]. The prolonged burst responses of reticular neurons (see Fig. 5.31), which is modulated by the level of membrane hyperpolarization and the intensity of depolarizing inputs (Fig. 5.33), indicate that reticular neurons exhibit a bursting behavior with a broad range of integrative properties.

[77] Huguenard and Prince (1992).

[78] Contreras *et al.* (1993).

The graded bursting behavior of reticular neurons support their role as generator and synchronizer of spindle rhythmicity *in vivo* [56]. Intracellular recordings *in vivo* combined with computational studies showed that in contrast to reticular cells with intact dendritic arborizations in which there is a high density of low-threshold transient Ca^{2+}

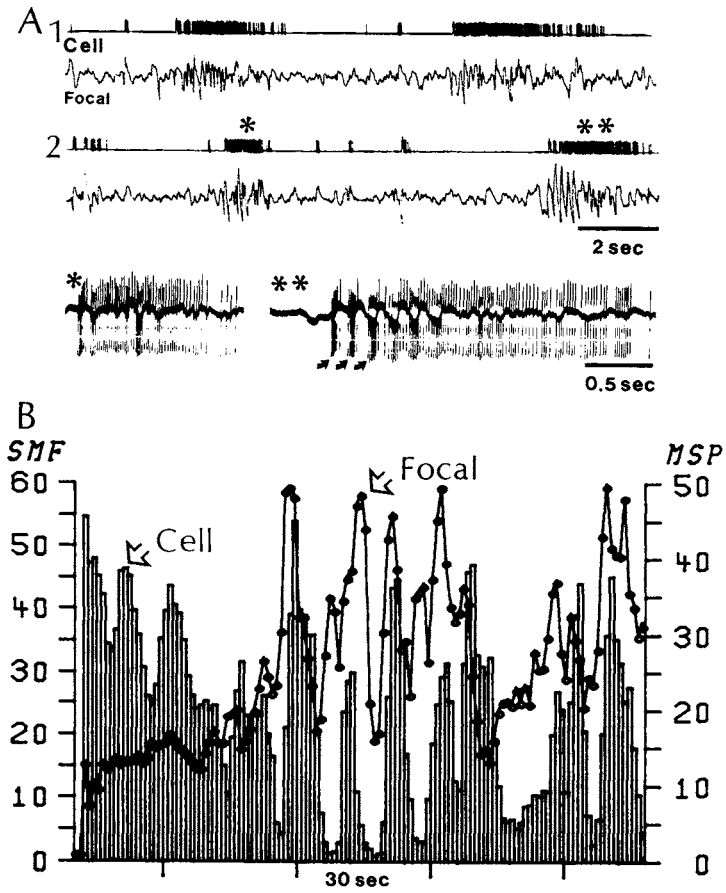


Figure 5.31. Characteristics of spike-bursts of rostral thalamic reticular neurons during natural slow-wave sleep. Chronically implanted cat. A, two ink-written traces are unit discharges and focal waves within the reticular nucleus recorded simultaneously through the same microelectrode. The oscilloscopic traces, shown below, depict two spike-barrages, indicated by one and two asterisks (corresponding to those on the above ink-written trace). Note, in double-asterisk barrage, initial, repetitive spike-bursts (arrows) in close relation with focal spindle waves at 7.5 Hz. B, sequential RE-cell's firing and reticular focal spindle waves during transition from waking to slow-wave sleep. SMF, sequential mean frequency; MSP, amplitudes of simultaneously recorded field potentials, filtered to frequency range of sleep spindles (7–15 Hz). Modified from Steriade *et al.* (1986).

currents (I_{Ts}), reticular cells in which most of the dendritic arborizations were removed have a much lower density of I_{Ts} [79]. With normal (high density) I_{Ts} in dendrites, the spike-bursts show *accelerando-decelerando* patterns, as is the case during natural slow-wave sleep [70, 76]. The long dendrites of reticular neurons, up to 1.5–2 mm along the curved axis of the nucleus [80] are probably impaired when thalamic slices are prepared. This may explain why spindles occur in the deafferented reticular neurons *in vivo* [81] and not in slices maintained *in vitro* [82] (see details in Chapter 7).

The tonic discharges that follow low-threshold spike-bursts of GABAergic reticular neurons (see Fig. 5.31) are due to a Ca^{2+} -activated nonselective cation current, I_{CAN} [83] (see details concerning modulatory actions in Chapter 6).

[79] Destexhe *et al.* (1996).
[80] Yen and Jones (1983); Steriade and Deschênes (1984).
[81] Steriade *et al.* (1987a).
[82] Von Krosigk *et al.* (1993).
[83] Bal and McCormick (1993).

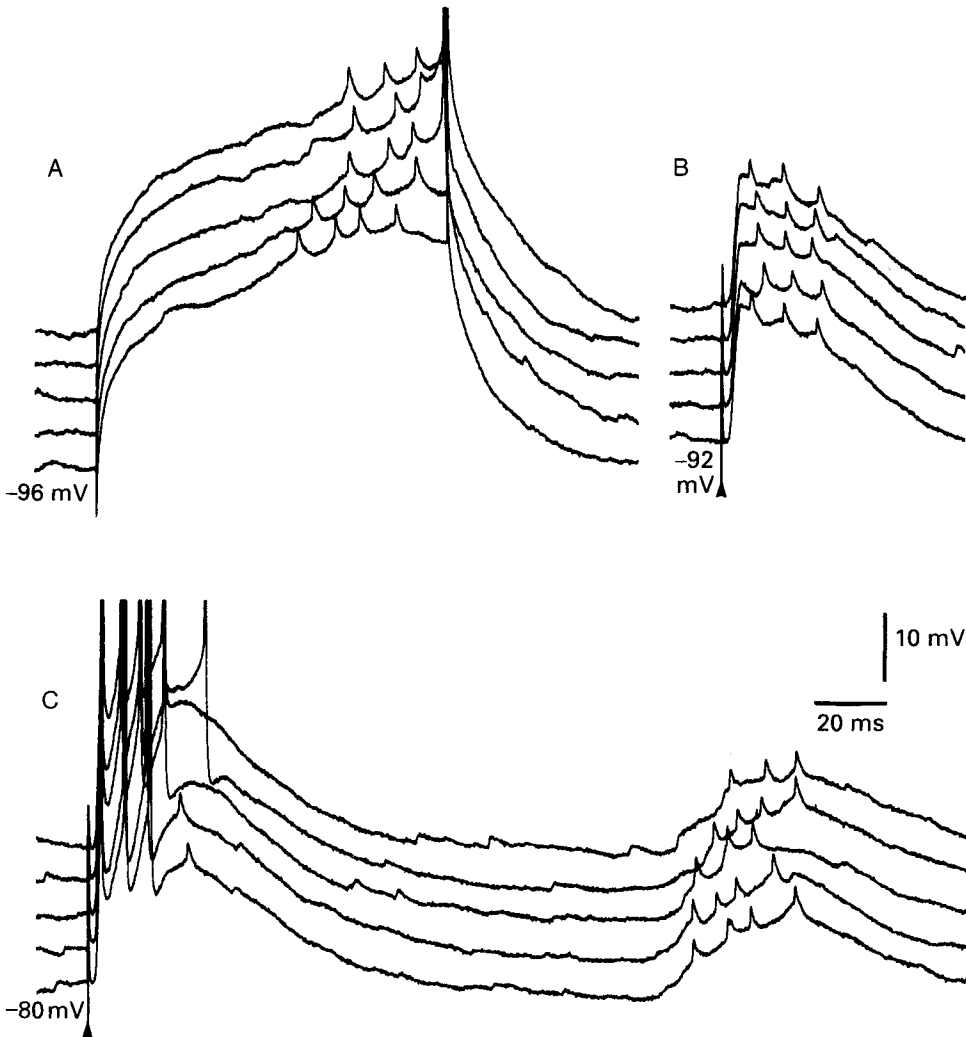


Figure 5.32. Presumed dendritic recordings reveal dendritic spikes elicited by depolarization of a cat thalamic reticular neuron. Intracellular recording *in vivo*, under urethane anesthesia. A, constant-amplitude depolarizing pulses were applied at the same membrane potential (V_m). B, the excitatory postsynaptic potential triggered by internal capsule stimulation consistently triggered a burst of three dendritic spikes. C, the depolarizing waves of cortically evoked spindles were also capable of triggering dendritic spikes. Action potentials constituting the early burst response to cortical stimulation are truncated. Traces are displayed vertically for clarity. From Contreras *et al.* (1993).

5.6. Neocortical Neurons

5.6.1. Characteristics of Firing Patterns in Four Neuronal Types and Underlying Ionic Currents

[84] Connors *et al.* (1982);
McCormick *et al.* (1985);
Connors and Gutnick
(1990).

Four different types of firing patterns are usually described in intracellularly recorded neocortical neurons by applying depolarizing current pulses *in vitro* [84] and

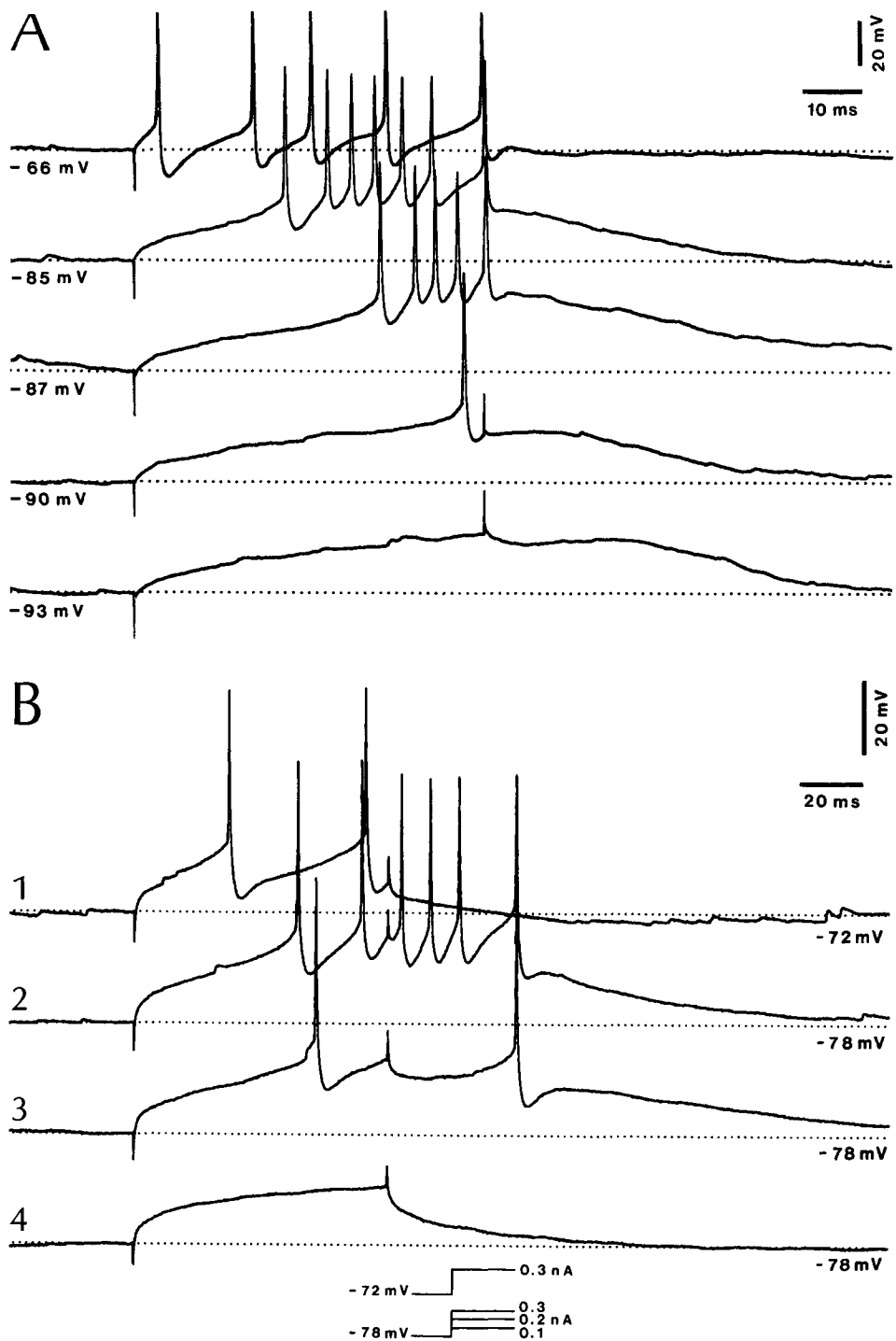


Figure 5.33. Gradual nature of the burst response in cat reticular neurons, recorded from the rostralateral sector of the nucleus. Urethane anesthesia. A, a depolarizing pulse of constant amplitude was applied while the cell was progressively hyperpolarized by direct current. B, a depolarizing pulse of 0.3 nA was applied at rest (trace 1) and at a hyperpolarized V_m (trace 2). The V_m was then kept constant and the pulse was reduced in amplitude. The burst response diminished in parallel. From Contreras *et al.* (1993).

[85] Nuñez *et al.* (1993);
Gray and McCormick
(1996).
[86] Steriade *et al.*
(2001a).

[87] Steriade *et al.*
(1998a).

[88] Nishimura *et al.*
(2001).
[89] Rudy and McBain
(2001).
[90] Solomon *et al.* (1993).
[91] Kawaguchi (1993);
de la Peña and Geijo-
Barrientos (1996);
Destexhe *et al.* (2001).
[92] Brown *et al.* (1993).
[93] Schwindt *et al.*
(1988a–b, 1989).

in vivo under anesthesia [85] as well as in chronically implanted, naturally awake and sleeping animals [86]. These four neuronal types, recorded intracellularly in the awake cat, are illustrated in panel A of Fig. 5.34. (a) Regular-spiking (RS) neurons constitute the majority of cortical pyramidal neurons. They display trains of single spikes that adapt quickly or, more often, slowly to direct stimulation. (b) Fast-rhythmic-bursting (FRB) neurons give rise to high-frequency (300–600 Hz) spike-bursts recurring at fast rates (30–50 Hz). Some of these neurons are found in deep layers and are antidromically activated from the thalamus (Fig. 5.35); others are local-circuit neurons [87]. FRB neurons display spontaneously occurring, compound EPSPs consisting of fast (~30–40 Hz) depolarizing wavelets (see panel C in Fig. 5.35), suggesting that these FRB neurons are the target of another excitatory FRB cell. (c) Intrinsically bursting (IB) neurons generate clusters of APs, with spike inactivation. (d) FS neurons fire thin APs and sustain tonically very high firing rates without frequency adaptation. The duration of intracellularly recorded APs is between 0.6 and 1 ms in RS neurons, with slightly longer spikes fired by IB neurons. In contrast, both FRB and FS neurons fire much shorter APs, with modes at about 0.3 ms [86].

The spike-bursts in IB neurons develop from a depolarizing afterpotential (DAP), as is also the case for FRB neurons (see arrows in Figs. 5.35B and 5.36B). The DAPs of IB neurons are due to the activation of the persistent Na^+ current, $I_{\text{Na(p)}}$, as they are sensitive to TTX and QX314 [88]. As to the high-frequency spike-bursts and very brief duration of spikes fired by FRB neurons, they are probably due to voltage-gated K^+ currents of the Kv3 subfamily, which are characterized by very fast deactivation rates—a property that underlies fast repolarization of APs [89].

Other currents of cortical pyramidal neurons are a hyperpolarization-activated cation current, I_{H} [90]; a low-threshold Ca^{2+} current de-inactivated by hyperpolarization [91]; high-threshold Ca^{2+} currents [92]; and a series of K^+ currents [93].

5.6.2. Changes in Firing Patterns During Synaptic Activities and Shifts in Behavioral State

In contrast with the invariable responses of neocortical cells obtained in slices, which lack spontaneously occurring changes in neuronal activity and display no or negligible background synaptic activities, the four classes of neocortical neurons described above are subject to alterations of their firing patterns with changes in

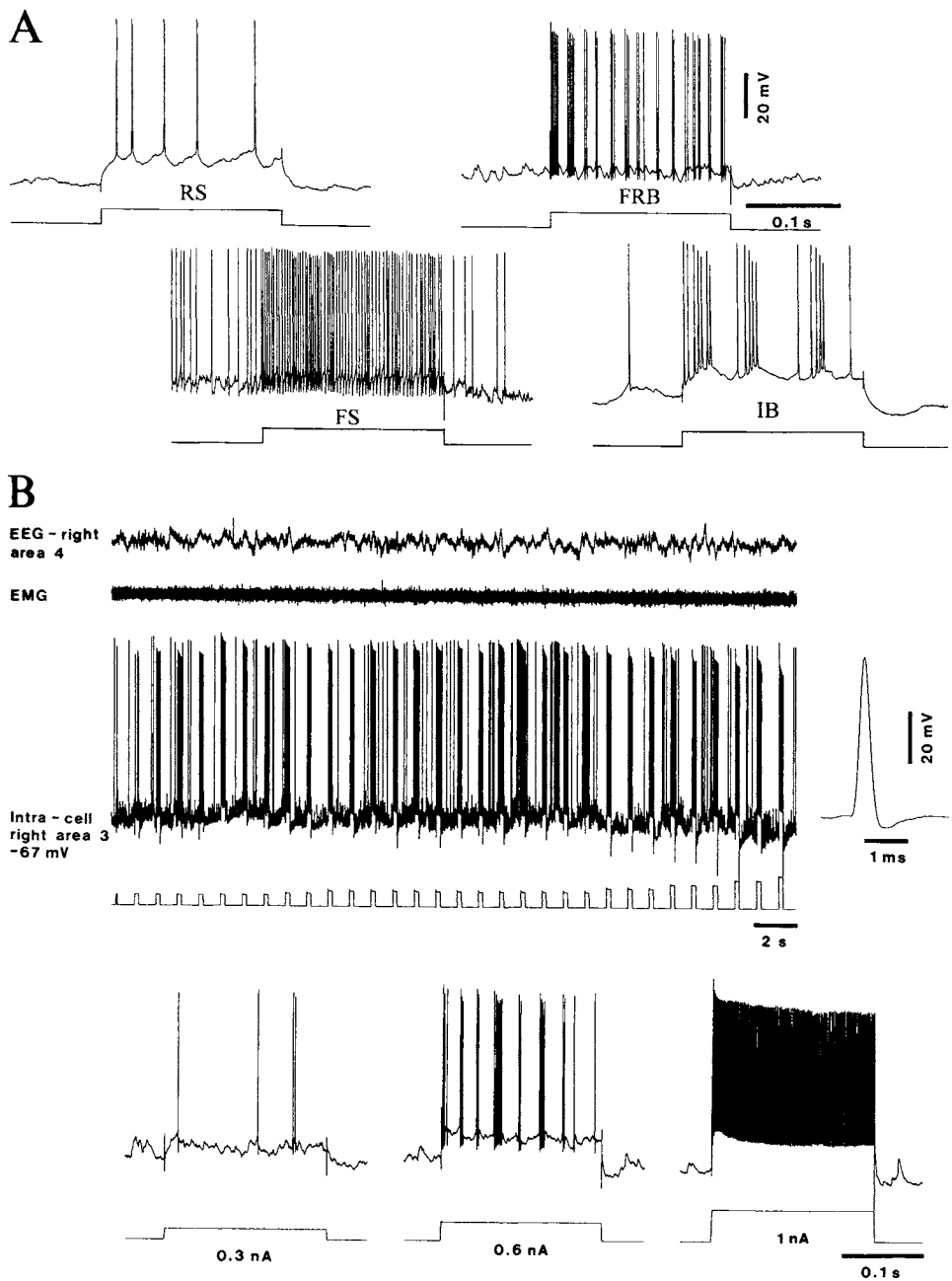


Figure 5.34. Electrophysiological identification of four different cell-classes in neocortex. Chronically implanted, awake cats. A, responses of regular-spiking (RS), fast-rhythmic-bursting (FRB), fast-spiking (FS), and intrinsically bursting (IB) neurons from area 4 to depolarizing current pulses (0.2 s, 0.8 nA). B, changing firing patterns in the same cortical FRB neuron by increasing the strength of direct depolarization. Recording from area 3 (somatosensory) neuron, together with EEG from area 4 and electromyogram (EMG). Depolarizing current pulses (0.2 s in duration) with different intensities evoked different firing patterns: RS (0.3 nA), FRB (0.6 nA), and FS (1 nA). From Steriade *et al.* (2001a, A) and unpublished data by M. Steriade, I. Timofeev, and F. Grenier (B).

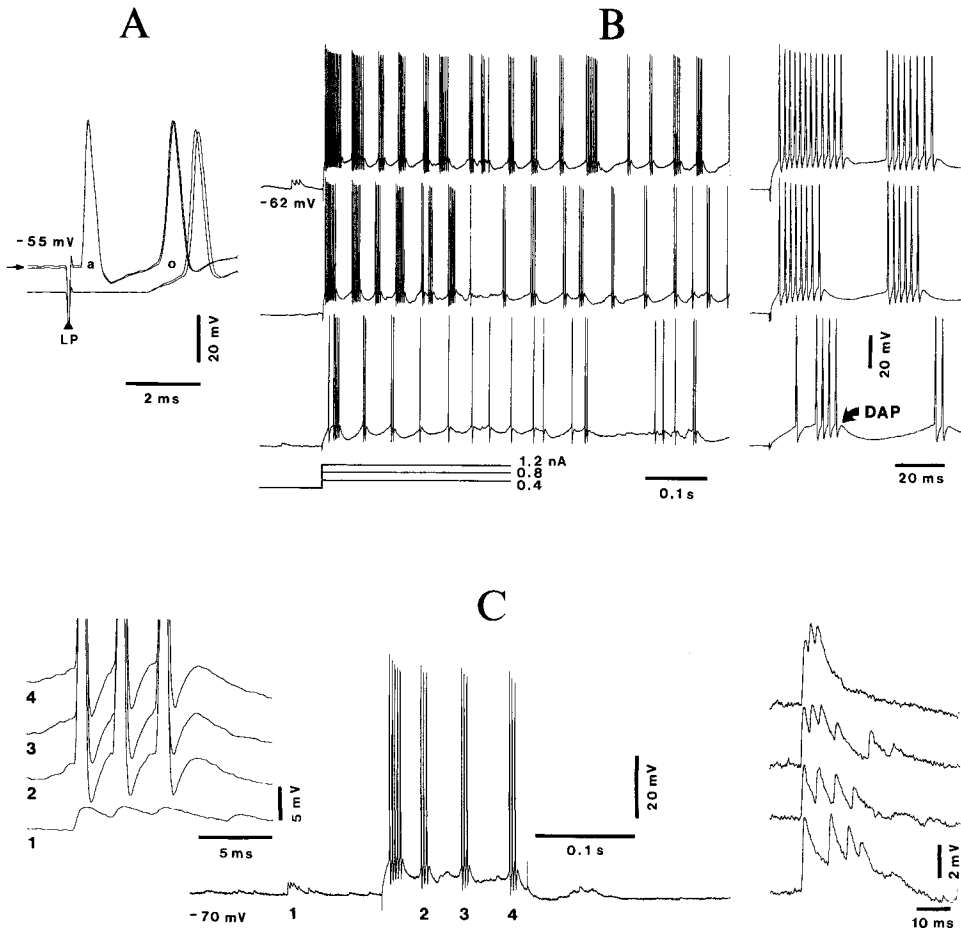


Figure 5.35. Fast-rhythmic-bursting corticothalamic neurons. Cats under ketamine-xylazine anesthesia. A, physiological identification of a corticothalamic cell from layer VI in area 5. Stimulus (arrowhead) to thalamic lateral posterior nucleus elicited an antidromic (a) spike followed by orthodromic (o) response (upper trace, resting membrane potential -55 mV). At a hyperpolarized level (lower trace), the antidromic response failed but the orthodromic response survived. This neuron is an example of a cell interposed in a corticothalamocortical loop. B, fast rhythmic bursts in an identified corticothalamic neuron from area 5, elicited by direct depolarization of the cell. Responses to three depolarizing steps (0.4, 0.8, and 1.2 nA) are illustrated. The initial part of each response is expanded on the right (arrow indicates depolarizing afterpotentials, DAPs). Note progressive increase in the number of action potentials within bursts (up to 500 Hz) and in the number of rhythmic bursts (from 20 to 30 Hz) by increasing the direct depolarization. C, a corticothalamic neuron fired high-frequency spike-bursts in response to a depolarizing current pulse (0.8 nA) and also displayed spontaneously occurring, compound excitatory postsynaptic potentials consisting of fast (~ 30 – 40 Hz) depolarizing wavelets (see text). From Steriade *et al.* (1998a).

[94] These changes, observed *in vivo*, are due to intact brain connectivity under this experimental condition. Indeed, *in vitro* studies on sensorimotor neocortex showed that by increasing the slice from

membrane potential, during brain activation elicited by modulatory systems, and during shifts in the state of vigilance of behaving animals [94]. Such changes indicate that far from being inflexible, one type discharge may develop into another one. Besides, the location of various neuronal types is far from being exclusively confined to distinct cortical layers, as suggested in earlier slice studies.

Initially, FRB neurons, also termed “chattering,” were found in the visual cortex only as pyramidal-shaped cells located in superficial layers, but they were subsequently recorded at all investigated depths, from 0.25 to 1.5 mm, in motor and association cortical areas [87]. The deep location of FRB neurons was demonstrated by antidromic invasion from appropriate thalamic nuclei (see panel A in Fig. 5.35) and the fact that the same type of firing pattern belongs to local-circuit aspiny or sparsely spiny neurons was demonstrated by intracellular staining (Fig. 5.36). Similarly, IB neurons recorded from sensorimotor cortical slices were found at a narrow range of depths, comprising layer IV and the more superficial parts of layer V [95] but subsequent studies *in vivo* found such cells also in layer III and *in vitro* investigators found that IB neurons are also located “in all layers below layer I,” with apical dendrites densely coated with dendritic spines [95].

The first difficulty in maintaining a strict classification in four distinctly separate cortical cell classes, partly based on the duration of APs, is that neurons with brief (0.3–0.4 ms) APs are not just FS-firing neurons, conventionally regarded as local-circuit GABAergic neurons, but also long-axoned, corticothalamic (glutamatergic, thus excitatory) FRB cells (Fig. 5.35A). Also, in chronically implanted animals, RS neurons, which are overwhelmingly pyramidal-shaped neurons, fire surprisingly thin APs (<0.5 ms), not far from the duration of FS-cells’ spikes.

An adding factor against this strict classification is the transformation of firing patterns in the same cortical neuron. Thus, corticothalamic neurons, as well as local-circuit sparsely spiny basket (presumably inhibitory) interneurons, may pass from an RS to an FRB and eventually an FS firing pattern by increasing the strength of the depolarizing current pulse (Fig. 5.36). This transformation in discharge patterns, by increasing the intensity of direct depolarization, also occurs in chronically implanted, naturally awake animals (see panel B in Fig. 5.34). Synaptic activity generated in corticocortical and TC networks during various functional states also modifies the firing patterns of FRB neurons. Thus, FRB patterns evoked during the silent background activity of silent periods between spindle wave sequences (these silent epochs may mimic the absence of background activity in slices maintained *in vitro*), develop into patterns resembling FS-type firing during epochs with spindle sequences, with rich synaptic activity produced by TC volleys (Fig. 5.37).

A reorganization of firing patterns may also occur in IB-firing neurons by changes in the membrane potential and during shifts in the behavioral state of vigilance from deafferented to activated states. The bursts of IB neurons

0.4 mm to 0.5 mm, the probability of connections rose about three times and spontaneous activity increased significantly (Thomson *et al.*, 1996; Thomson, 1997). The increase in connectivity and background activity on increasing the slice thickness by just 0.1 mm may explain many differences between some results from slices and those from the intact brain.

[95] Chagnac-Amitai *et al.* (1990); Chen *et al.* (1996). See also Nishimura *et al.* (1996).

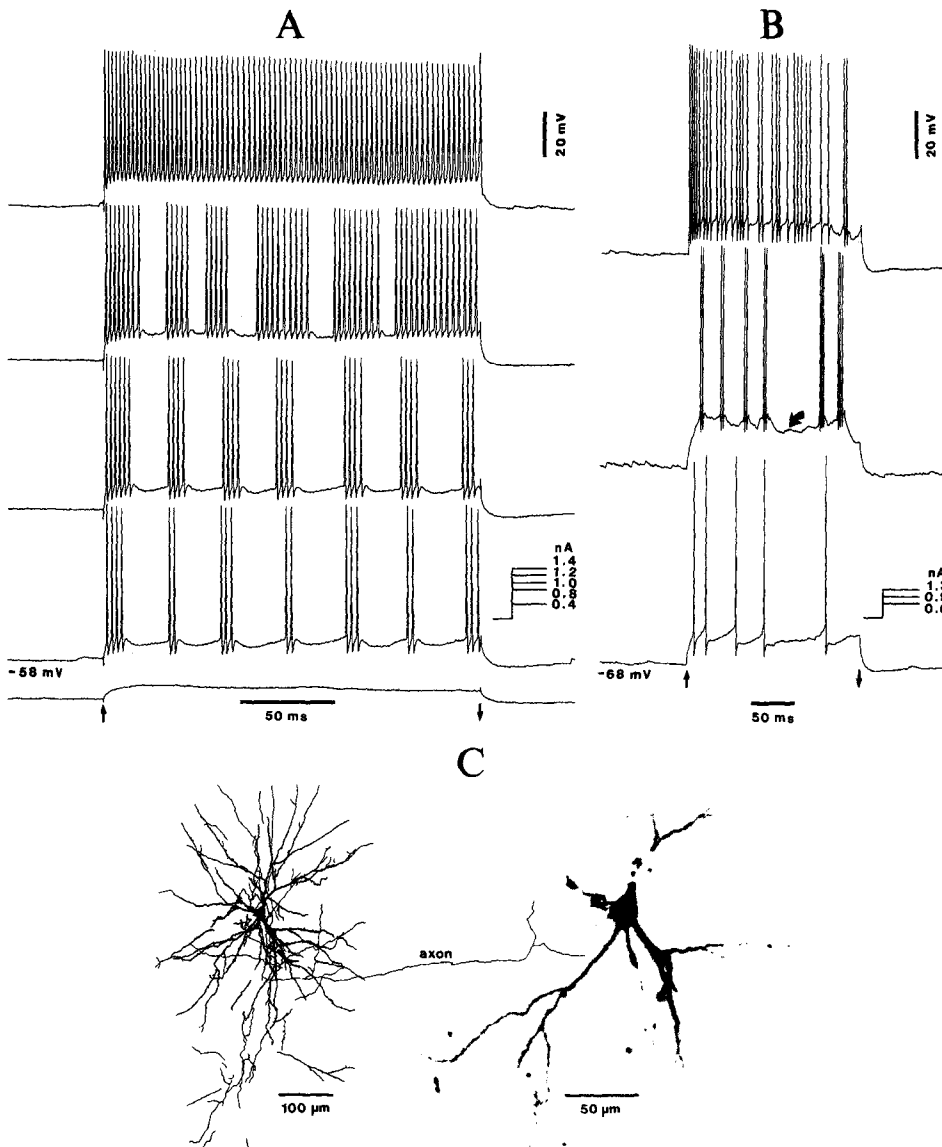
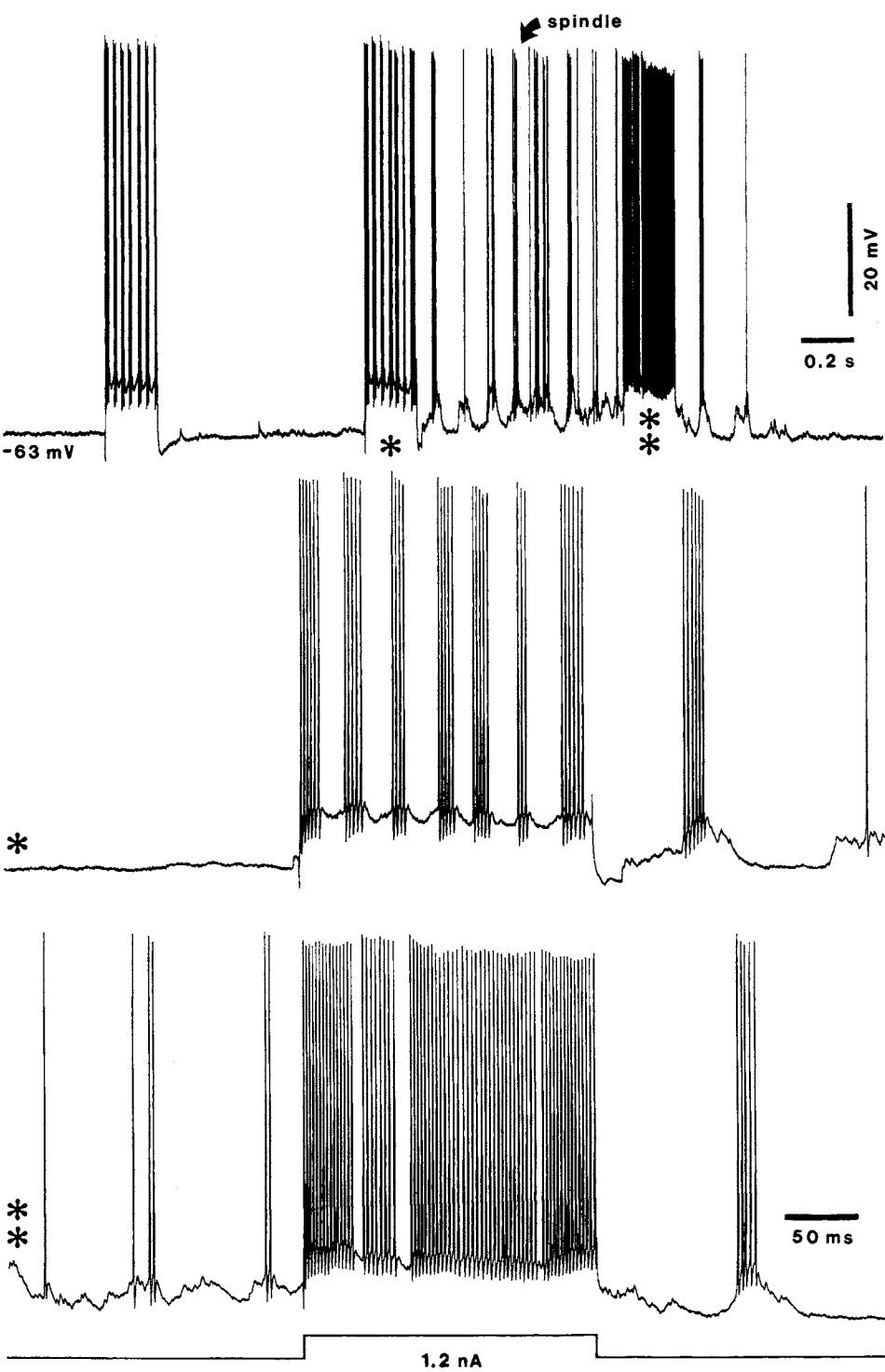


Figure 5.36. Changes in discharge patterns of fast-rhythmic-burst (FRB) neurons by increasing the intensity of direct depolarization (200-ms pulses in both A–B neurons). Ketamine–xylazine anesthesia. A shows an identified corticothalamic neuron in area 7 that, upon subthreshold depolarization (0.4 nA), displayed a passive response; pulses of 0.8, 1, and 1.2 nA elicited high-frequency spike-bursts with increasing repetition rates (from 30 to 40 Hz) and number of action potentials within each burst; and, finally, fired tonically at 450 Hz, without frequency adaptation (1.4 nA). Intracellular staining showed its pyramidal shape and location in layer VI (not shown). B shows a similar transformation, from single spikes to rhythmic spike-bursts (~40 Hz), and finally to tonic firing by increasing the intensity of direct depolarization in a morphologically identified local-circuit, sparsely spiny neuron located in layer 3 of area 7 (see C). Spontaneous action potentials showed their very brief duration (0.3 ms at half amplitude; not depicted). C is the camera-lucida reconstruction of a local-circuit cell and a photomicrograph of the same neuron (same as in B). From Steriade *et al.* (1998a).



[96] Mason and Larkman
(1990); Timofeev *et al.*
(2000a).

[97] Steriade *et al.*
(1993a).

are inactivated and they develop into RS firing patterns during maintained depolarization of these neurons [96] or during brain activation elicited by stimulation of the brainstem cholinergic nuclei [97] (Fig. 5.38). Then, neocortical neurons could operate in two modes, switching between bursts (IB pattern) and tonic discharges (RS pattern), as a function of modulatory neurotransmitters. A similar transformation occurs during shifts from the natural state of slow-wave sleep to either REM sleep or wakefulness when the membrane potential of cortical neurons is slightly depolarized [86]. Different (IB and RS) firing patterns of the same neuron may be evoked by depolarizing current pulses (with the same parameters) applied during slow-wave sleep and REM sleep, respectively, and the mode of interspike intervals during the spontaneous activity in slow-wave sleep (3–3.5 ms) reflects the presence of spike-bursts, while this mode was absent in REM sleep and many more longer intervals (20–100 ms) during REM sleep reflecting the single spike firing in the latter activated state (Fig. 5.39).

The above-described reorganization in firing patterns, generated by intrinsic cellular properties under the modulatory influences of synaptic activities in complex neuronal networks, may explain different proportions of various neuronal classes under different experimental conditions. Comparing a sample of neurons that were selected because depolarizing current pulses could be applied in chronically implanted animals—during the steady state of quiet waking without phasic motor events with more than 1,000 intracellularly recorded neurons recorded from intact cortex under anesthesia or from small isolated cortical slabs *in vivo*—revealed the following differences in the incidence of some neuronal classes. Neurons displaying the firing patterns of FS neurons (conventionally regarded as local-circuit inhibitory cells) are much more numerous in experiments on naturally alert animals (24%) than in previous experiments on the intact cortex of anesthetized animals (10%) or in small isolated cortical slabs *in vivo* (4%) [86]. The increased proportion of FS-firing neurons may be due to the transformation of other firing patterns into that of FS cells, such as depicted

Figure 5.37. Changing in firing patterns of cortical fast-rhythmic-bursting neuron by synaptic activity in thalamocortical systems. Intracellular recording of corticothalamic area 21 neuron in cat under barbiturate anesthesia. Top, 3 depolarizing current pulses (+1.2 nA) were applied every second in period with poor synaptic activity (first two pulses, before spindle sequence) and during spindle. Below, expanded responses to the second pulse (asterisk) and the third pulse (two asterisks). Note that the pattern of fast (~35 Hz) rhythmic spike-bursts during period with poor synaptic activity (as in slices) changed into a pattern close to that of a fast-spiking cell when the pulse was applied during the spindle sequence. Unpublished data by M. Steriade, I. Timofeev, and F. Grenier. See also Steriade *et al.* (1998a).

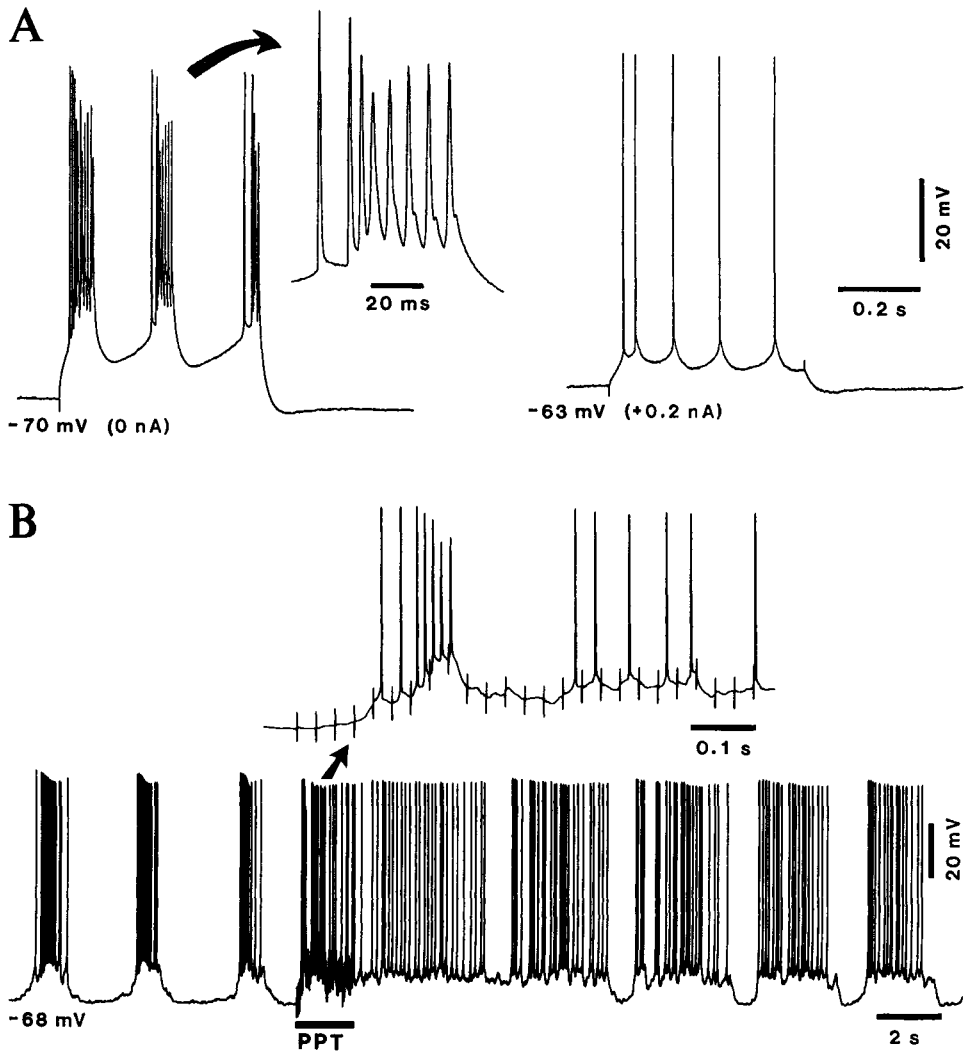


Figure 5.38. Transformation of bursting to tonic firing patterns in neocortical neurons by changing the membrane potential (V_m) and synaptic activity. **A**, responses of intrinsically-bursting neuron in isolated cortical slab from suprasylvian gyrus *in vivo* (cat under ketamine-xylazine anesthesia) to the same intensity of depolarizing current pulse (0.5 nA) at the resting V_m (−70 mV) and under slight depolarization (+0.2 nA, −63 mV). A typical burst is expanded at right (arrow). **B**, area 7 neuron in cat under urethane anesthesia, recorded *in vivo*. An IB cell (as identified by depolarizing current pulses) fired spike-bursts during the slow-sleep oscillation and transformed this burst firing into tonic, single action potentials following brain activation produced by stimulation (horizontal bar, 1.8 s, 30 Hz) of the pedunculopontine tegmental (PPT) nucleus. Arrow points to an expanded detail showing a spike-burst followed by single spikes. **A**, modified from Timofeev *et al.* (2000a). **B**, modified from Steriade *et al.* (1993a).

in Figs. 5.36–5.37. On the contrary, neurons displaying IB firing patterns are found in only 4% of neurons of awake animals [86], whereas they represent 15% of neurons in anesthetized animals and reach 40% of neurons in isolated cortical slabs. These differences are highly significant statistically. The strikingly diminished proportion of IB

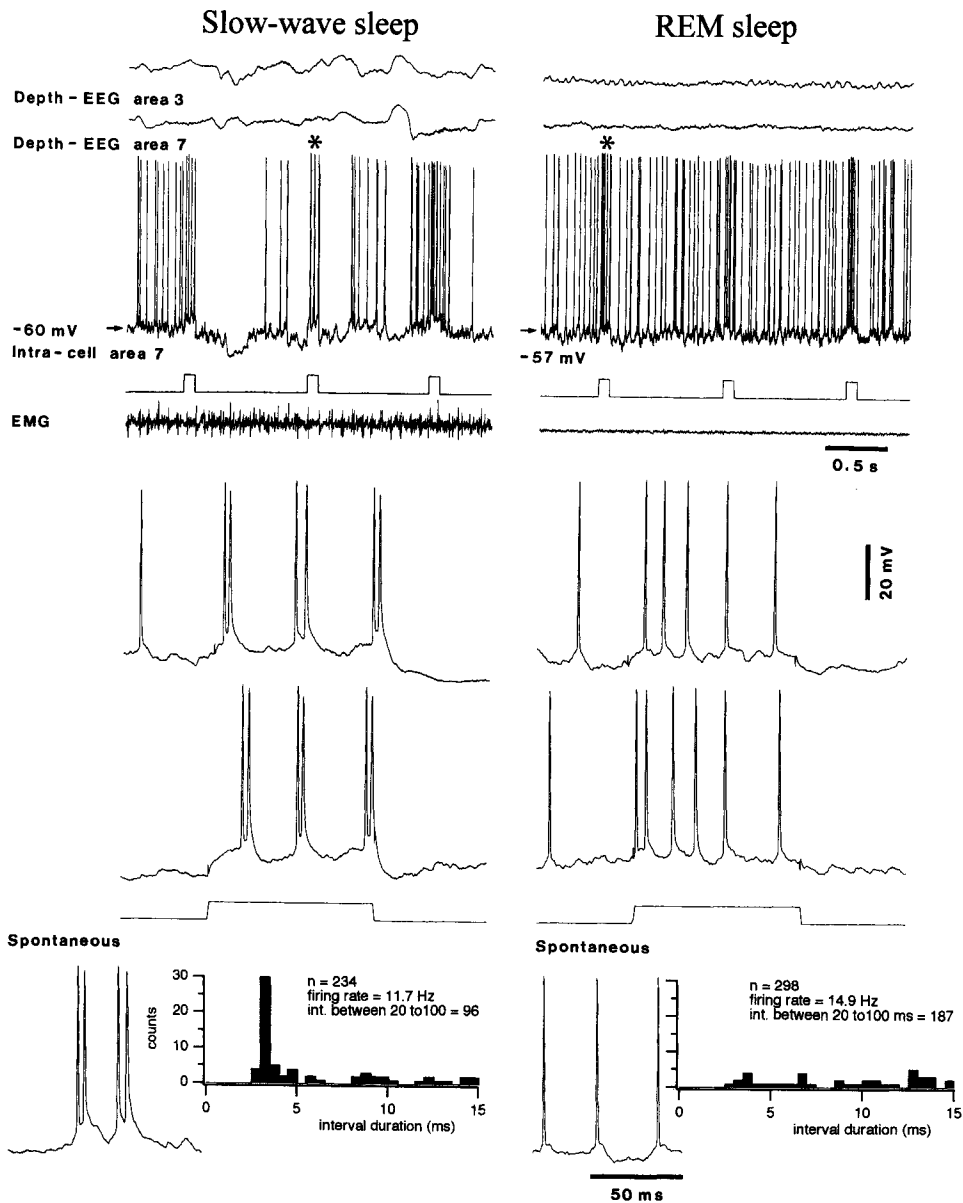


Figure 5.39. Changes in firing patterns of an intrinsically bursting (IB) cortical neuron from area 7 during slow-wave sleep (SWS) and REM sleep in chronically implanted cat. Top panels show EEG and EMG patterns characterizing the two states, as well as intracellular recording of this neuron together with three depolarizing current pulses (indicated by current monitor). Below, responses to depolarizing current pulses (the first response is indicated by asterisk in the top panel). Note spike doublets in SWS and single spiking in REM sleep. At the bottom, examples of spontaneous firing of this neuron during SWS and REM sleep. The interspike interval histograms in each state show a mode at 3–3.5 ms in SWS (reflecting bursting activity), absence of this mode in REM sleep, and many more longer intervals (20–100 ms) in REM sleep, reflecting single spike firing. Modified from Steriade *et al.* (2001a).

firing patterns in the alert condition is likely due to the relatively depolarized membrane potential, enhanced synaptic activity, and increased release of some modulatory neurotransmitters, all conditions that may transform IB into RS firing patterns. Such transformations suggest that a high degree of synaptic activity in the intact brain, which is lacking in brain slices or in isolated cortical slabs *in vivo*, decisively modulates and may even overwhelm the intrinsic neuronal properties expressed by responses to direct depolarization.

5.7. Entorhinal Cortex, Amygdala, and Hippocampal Neurons

The functional properties of entorhinal, amygdala, and hippocampal neurons have been intensively explored because the entorhinal cortex is a gate between neocortical operations and processes elaborated within the hippocampus and related systems; amygdala complex is implicated in coloring memory with affectivity; and hippocampus plays a key role in learning and memory, and also generates (in conjunction with other structures) an oscillation, theta rhythm that characterizes certain types of alert behavior in rodents and both brain-activated states of wakefulness and REM sleep in other species.

5.7.1. Entorhinal Cortex Neurons

Stellate neurons in layer II of the entorhinal cortex produce depolarization-dependent rhythmic subthreshold oscillations in the theta frequency range, $\sim 8\text{--}9\text{ Hz}$, which depends on the activation of $I_{\text{Na(p)}}$ [98]. The neuronal population activity that generates theta-like activity is due to recurrent axonal collaterals of stellate cells [99] and is also modulated by cholinergic innervation from the septum [100]. Pyramidal neurons in layer III of entorhinal cortex do not display subthreshold oscillations, but fire tonically at relatively low frequencies [101].

5.7.2. Amygdala Neurons

The intrinsic properties of amygdala neurons have only recently been investigated *in vitro*. A group of GABAergic neurons, called intercalated cell masses (ICMs), which is interposed between basolateral and central nuclei of the amygdaloid complex, express a voltage-dependent

- [98] Alonso and Klink (1993). This *in vitro* study also showed that stellate cells in layer II of the entorhinal cortex also display, upon direct depolarization, subthreshold oscillations in the beta frequency range ($\sim 22\text{ Hz}$). The theta rhythm generated by layer II entorhinal cells was also shown *in vivo* (Mitchell and Ranck, 1980; Dickson *et al.*, 1995).
- [99] Alonso and Llinás (1989).
- [100] Alonso and Köhler (1984). The cholinergic pathway from septum to entorhinal cortex is the morphological substratum of the muscarinic depolarization of stellate cells, associated with oscillations in the theta waves (Klink and Alonso, 1997a–b).
- [101] Dickson *et al.* (1997).

[102] Royer *et al.* (2000b).

K^+ current, termed I_{SD} , for slowly de-inactivating; this activates in the subthreshold regime, inactivates in response to suprathreshold depolarizations, and slowly de-inactivates upon the return to rest [102]. This current provides ICM neurons with a state of increased excitability, which makes these amygdala neurons to display a higher probability of responses to excitatory inputs, with effects on emotional reactivity, particularly during fear.

5.7.3. Hippocampal Neurons

[103] Andersen *et al.* (1980).

The neuronal loops and some synaptic operations in the circuits between the entorhinal cortex, dentate gyrus, and CA3–CA1 fields are dealt with in Chapter 4. The EPSPs produced at the distal dendritic level of CA1 pyramidal neurons are quite effective because of the compact electrotonic structure of these neurons [103]. It was predicted that the fast pre-potentials of CA1 neurons arise from Na^+ -dependent dendritic hot spots and that alterations in CA1-cells' Ca^{2+} electroresponsiveness may lead to bursting behavior [104]. Electrotonic coupling among hippocampal pyramidal cells may facilitate or disrupt the synchronous firing induced through chemical synapses [105].

[104] Traub and Llinás (1979).

[105] MacVicar and Dudek (1981, 1982); Traub and Wong (1981).

Neurotransmitter-Modulated Currents of Brainstem Neurons and Some of Their Forebrain Targets

This chapter discusses the actions on target neurons of projections from chemically identified neurons within the brainstem. The actions of brainstem chemical transmitters are discussed primarily on the basis of intracellular investigations *in vitro*, although some intracellular and extracellular *in vivo* data are included. Needless to say, data from *in vitro* experiments are the most reliable since they can be obtained after blockage of synaptic transmission and the concentrations of agents can be precisely specified, in addition to the greater stability of recording conditions. One should, however, also emphasize the necessity of reproducing the effects of agent application by stimulation of the appropriate pathway. It is also unlikely that the complex conditions of behavioral states, and even the mechanisms underlying just one physiological correlate of states of vigilance, will be found to be attributable to one synaptic transmitter. Many data obtained in extremely simplified preparations, such as brain slices and cultures, have been challenged by the results obtained in the intact brain [1]. Thus, the data presented here should be considered as a prologue to future studies that will explore the effect of neurotransmitters in the context of operations in brains with intact connectivity, will investigate transmitter interactions, including synergetic or competitive actions of colocalized transmitters, and will more deeply probe second messenger actions.

[1] Steriade (2001b).

A general discussion of the criteria to be met in assigning any substance a role as a neurotransmitter, the methods of drug application, the synaptic mechanisms of action, presynaptic and postsynaptic receptors, and

correspondences or mismatches between transmitters and receptor localizations, may be found in previous monographs and reviews [2]. The synaptic effects exerted upon the same central neurons by stimulating the nuclei giving rise to chemically coded projections are discussed in some sections to allow comparisons between the pure actions of the neurotransmitter and those induced by stimulating the synaptic pathway.

Each section concerning a given transmitter is organized according to projection targets, save for the hippocampus, which has been reviewed elsewhere [3] and hence will be compared and contrasted *en passant* in some sections. For many neurotransmitters, a very common theme appears to be mediation of agonist-induced effects by changes in K^+ conductances. For many hyperpolarizing effects, the K^+ conductances are inwardly rectifying, that is, there is increased conductance at more hyperpolarized membrane potential levels. Because of the prevalence of ligand-induced alteration of K^+ currents, we also will discuss certain intrinsic K^+ currents in this chapter, in addition to those discussed in Chapter 5.

6.1. Acetylcholine

6.1.1. Brainstem

6.1.1.1. Medial Pontine Reticular Formation

The importance of brainstem cholinergic systems for control of neuronal excitability during the waking-sleep cycle has been the subject of recent intense investigation and their role in the control of thalamocortical (TC) systems during brain-activated states of wakefulness and REM sleep as well as in the sleep cycle will be discussed in detail in Chapters 8–9 and 11–12. From the standpoint of REM sleep, it has been known for several years that *in vivo* microinjections of cholinergic compounds into the pontine reticular formation furnish the only phenomenologically adequate pharmacological model of this state. Depending on the injection site, these compounds can reproduce all of the phenomena of REM sleep [4], even extending to the membrane potential alterations found in spinal motoneurons [5].

In Chapter 3, we have described anatomical results that have greatly strengthened the argument that cholinergic compounds may play a role in the natural induction and/or maintenance of REM sleep. There are projections from the cholinergic laterodorsal and pedunculo-pontine tegmental (PPT) nuclei to the pontine reticular

[2] Phillis (1970); Krnjević (1974); North (1986a, b); Siggins and Gruol (1986); Herkenham (1987); McCormick (1992); Chapter 8 in Steriade *et al.* (1997a).

[3] Mongeau *et al.* (1997); Vizi and Kiss (1998); Malenka and Nicoll (1999).

[4] Amatruda *et al.* (1975); Baghdoyan *et al.* (1985, 1987).

[5] Morales *et al.* (1987).

formation, the site of cholinergic REM induction. An additional essential component of cholinergic hypotheses of REM sleep control is the demonstration that cholinergic compounds directly excite medial pontine reticular formation (mPRF) neurons, an investigation necessitating the synaptic isolation and control of bathing media feasible only with an *in vitro* preparation. Further, it is essential to demonstrate that the direct cholinergic actions on mPRF include those known to occur in natural REM sleep.

This section outlines data indicating cholinergic agonists applied to synaptically isolated mPRF neurons produce powerful muscarinic, excitatory effects that parallel the electrophysiological membrane changes seen in natural REM sleep. Unless otherwise specified, the data in this section are taken from an *in vitro* study [6]. Sixty percent of mPRF neurons responded to carbachol with a depolarization of 16 mV associated with a 20% increase in input resistance (Fig. 6.1A). Carbachol evoked a hyperpolarization associated with a decrease in input resistance in 20% of the neurons (Fig. 6.3A), and a biphasic response of a shorter duration hyperpolarization followed by depolarization was present in 15% of neurons. Only 5% of neurons did not respond to carbachol. These were direct, nonsynaptically mediated effects, as indicated by their presence during bath application of tetrodotoxin (TTX), which prevents Na^+ action-potential-dependent synaptic activity. The carbachol effects were seen on each of the two main types of mPRF neuron, the low-threshold burst (LTB) neurons and the nonburst (NB) neurons (see Chapter 5) and the percentages of the types of carbachol responses did not differ in NB and LTB neurons.

We first discuss the depolarizing responses. The addition of atropine to the perfusate resulted in complete blockade of the carbachol-evoked depolarization (Fig. 6.1B), indicating its muscarinic nature. This response, studied under voltage clamp control, was associated with a reduced outward current (a net inward current) and a decrease in membrane conductance (Fig. 6.1C). The inward current evoked by carbachol was voltage insensitive, having a constant I/V plot slope (Fig. 6.1D). The reversal potential was -98 ($[\text{K}^+]_0 = 3.25$ mM), compatible with a reduction primarily in K^+ permeability, although ion substitution studies would be required for a proof of K^+ conductance changes.

The depolarization response evoked by carbachol was accompanied by an increase in neuronal excitability, since identical amplitude and duration depolarizing current pulses (Figs. 6.2A–B) elicited from 1.3- to 4-fold as many action potentials during carbachol application as compared with control. To determine if the steady-state reduction in outward current elicited by carbachol was alone

[6] Greene *et al.* (1989a); reviewed in Greene and McCarley (1990). The *in vitro* preparation and methods for mPRF recordings were the same as described in Chapter 5. Drugs were usually bath applied except for a few experiments in which carbachol was applied by a puffer pipette with tip submerged in media but above the surface of the slice. All neurons maintained robust and stable electrophysiological properties throughout the wash-in (2–5 min) and wash-out (10 min) periods. Neurons in the giant cell field portion of mPRF were exposed to carbachol at concentrations of 0.5–1.0 μM in the bath or 1–10 mM in puffer electrodes.

sufficient to account for the increased excitability, carbachol application was combined with intracellular injection of a hyperpolarizing DC current to return the membrane potential to control level. In this condition, excitability was not increased (Fig. 6.2C).

The effects of carbachol on postsynaptic potentials (PSPs) elicited by stimulation of the contralateral pontine reticular formation were also examined, since it is known that reticular (RE) stimulation during REM sleep produces

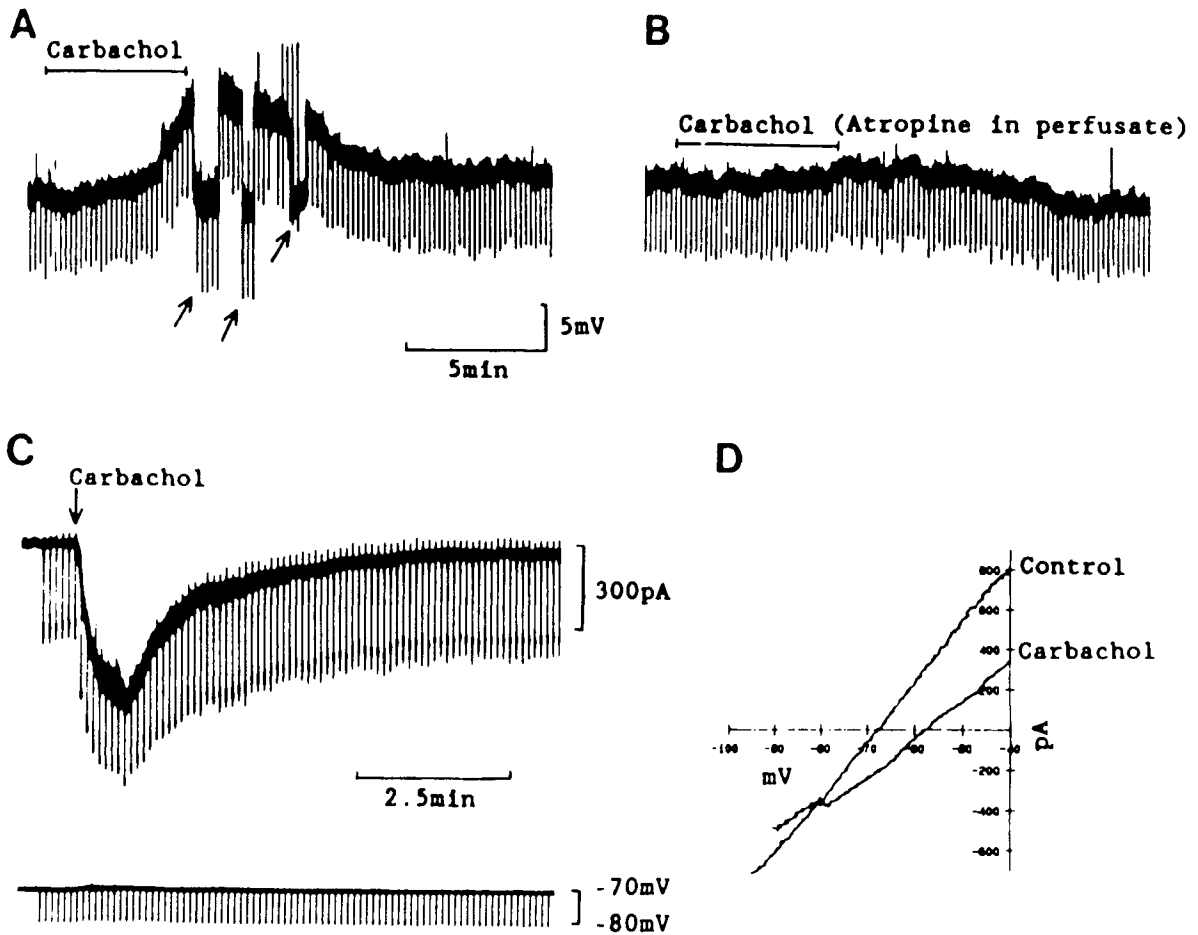


Figure 6.1. Carbachol-evoked depolarization response of mPRF neurons *in vitro* is mediated by a decrease in a voltage insensitive conductance and is blocked by atropine. A, chart record of a typical depolarizing response of an mPRF neuron to bath application of carbachol ($0.5 \mu\text{M}$ during time indicated). Downward deflections are due to intracellular current pulses (400 ms, 200 pA) applied to assess input resistance. At arrows, membrane potential was returned to the baseline potential of -74 mV by DC hyperpolarizing current to avoid voltage sensitive changes of the membrane resistance not specific to carbachol. B, atropine ($0.5 \mu\text{M}$) blocks the depolarizing response to

carbachol (same neuron as in A). C, decreased membrane conductance during puffer application (arrow, 1 s, 3 psi) of carbachol (1 mM) is indicated by the decreased amplitude of downward deflections in the upper current record in response to 10 mV, 400 ms membrane potential shift commands (lower record) in a neuron under voltage clamp control. D, I/V plot generated by a constant depolarization of the membrane potential ($1 \text{ mV}/200 \text{ ms}$) from -100 mV to -50 mV during control conditions and during exposure to $0.5 \mu\text{M}$ carbachol in the perfusate. Note the voltage insensitivity of the carbachol current. Modified from Greene *et al.* (1989a).

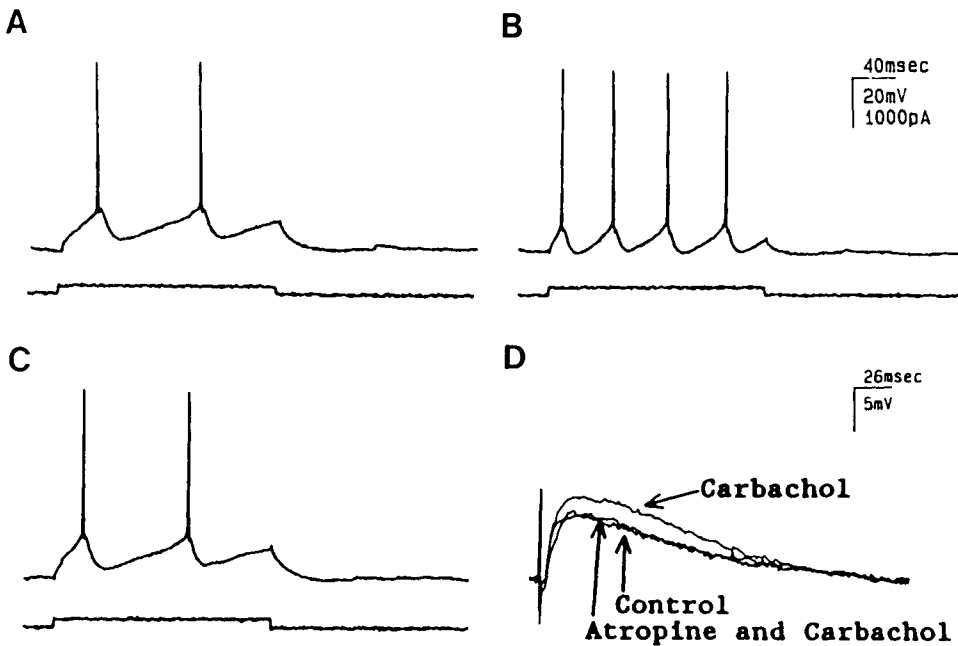


Figure 6.2. Carbachol elicits an increase in medial pontine reticular formation (mPRF) neuronal excitability *in vitro* and in the amplitude of excitatory postsynaptic potentials (PSPs). A, control conditions. Two oscilloscope traces of neuronal membrane potential response (upper) to intracellular depolarizing current injection of 400 ms duration and 150 pA (lower). Baseline membrane potential is -65 mV. B, same stimulus conditions and neuron as in A but with puffer application of carbachol (10 mM, 0.5 s, 1.5 psi). The membrane potential depolarized 6 mV and the number of spikes increased. C, same neuron with same stimulus and carbachol application parameters as in B, but with DC hyperpolarizing current injection to return the membrane potential to the control level. Note the number of action potentials is the same as in A. D, three superimposed oscilloscope traces from an mPRF neuron of a PSP elicited by stimulation of the contralateral mPRF (stimulation artifact is the first biphasic positive-negative deflection). Topmost trace is during bath perfusion with carbachol (0.5 μ M), and bottom traces are during the control condition and during bath perfusion with both carbachol and atropine (0.5 μ M). Note the 20% increase of PSP amplitude in the presence of carbachol compared to control and carbachol/atropine conditions. Modified from Greene *et al.* (1989a).

[7] McCarley and Ito (1984).

[8] Madison *et al.* (1987).

[9] McCormick and Prince (1987d).

[10] Spinal cord motoneurons also exhibit a slow depolarizing response to ACh, probably due to a reduction in K^+ conductance; the slow depolarization is associated with an increase or no change in input resistance and is mediated by muscarinic receptors

enhanced PSPs as contrasted with stimulation in EEG-synchronized sleep [7]. Stimulation of the contralateral mPRF, with bipolar double barrel glass electrodes filled with perfusate, evoked depolarizing PSPs (Fig. 6.2D). These evoked PSPs were enhanced in the presence of carbachol-elicited depolarization, and this enhancement was blocked by atropine.

With respect to the mechanism of depolarization, it should be noted that a similar depolarizing response to muscarinic activation has been reported in neurons of the hippocampus [8] and the medial and lateral geniculate (LG) thalamic nuclei [9], and in both cases this was mediated via reduction of a K^+ conductance active at all membrane potentials, with an apparent lack of inactivation and a reversal potential more negative than -90 mV [10].

The hyperpolarizing response to carbachol was blocked by atropine, and was associated with increased outward current and decreased input resistance (Fig. 6.3). There was a nonlinear current-voltage relationship (examined between -100 and -50 mV) of this carbachol-evoked current in the presence of $1 \mu\text{M}$ TTX (Fig. 6.3). Inward rectification was present, that is, slope conductance was greater at membrane potential levels negative to the reversal potential, a feature reported to be characteristic of the

(Zieglängsberger and Reiter, 1974). The motoneuronal synapse on inhibitory Renshaw cell involves a rapid and quickly reversible nicotinic excitation (Curtis and Eccles, 1958; Curtis and Ryall, 1966a) but Renshaw cells also possess muscarinic receptors acting slowly

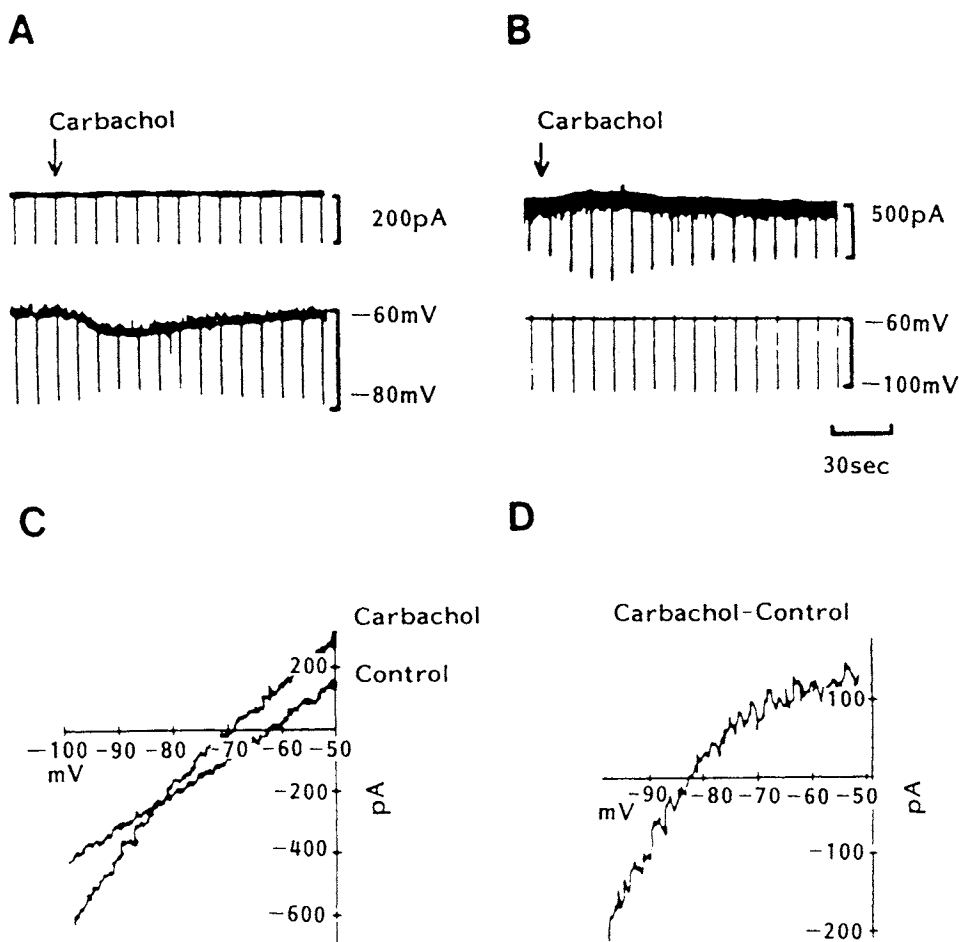


Figure 6.3. The hyperpolarization elicited by carbachol in medial pontine reticular formation (mPRF) neurons *in vitro* is mediated by an increase in an inwardly rectifying conductance. A–B, records of current (upper record) and membrane potential (lower record) obtained in current clamp (A) and voltage clamp (B) conditions during puffer application of carbachol at arrow (1.0 mM carbachol, 10 s , 5 psi). In A, downward deflections result from current injection (400 ms) and in B from a membrane potential shift command (400 ms). Following carbachol ejection there is an increase in chord conductance observable in A and B. In C, I/V plot from another neuron generated by a constant depolarization of the membrane potential from -100 to -50 mV ($1 \text{ mV}/400 \text{ ms}$) before and during exposure to carbachol ($[\text{K}^+]_0 = 5.0 \text{ mM}$). D, I/V plot of the current elicited by carbachol constructed by subtraction of the control plot from the carbachol plot. Note that the slope conductance of the outward (positive) current is less than that of the inward current indicative of inward rectification. Modified from Greene *et al.* (1989a).

- (Curtis and Ryall, 1966b). The K^+ conductance observed in mammalian neurons and reduced by ACh is similar to the S-current, modulated by neurotransmitters in invertebrate neurons (Siegelbaum *et al.*, 1982; Pollock *et al.*, 1985; Brezina *et al.*, 1987).
- [11] Katz (1949); Hagiwara and Takahashi (1974).
- [12] Egan and North (1986a).
- [13] McCormick and Prince (1986b).
- [14] North *et al.* (1987); see also Section 6.2 in this chapter.
- [15] Trussell and Jackson (1985).
- [16] Yakel *et al.* (1988).
- [17] Noma and Trautwein (1978); Sakmann *et al.* (1983).
- [18] Hartzell *et al.* (1977).
- [19] Breitwieser and Szabo (1985); Pfaffinger *et al.* (1985); Andrade *et al.* (1986); North *et al.* (1987); Trussell and Jackson (1987).
- [20] Drummond *et al.* (1980).
- [21] Gerber *et al.* (1989b).

[22] See Mash and Potter (1986) who also provide a review of earlier autoradiographic studies.

anomalous rectifier current [11]. At membrane potentials between -65 and -50 mV, the slope conductance was less than 2.5 ns, so that the outward current evoked by carbachol was nearly constant over this range. This was, in contrast, a slope conductance of 12 ns over the range of -100 to -80 mV.

As will be discussed later in this chapter, cholinergically evoked hyperpolarizations have been observed in both the brainstem [12] and the thalamic reticular nucleus [13], although voltage sensitivity has not been analyzed. Hyperpolarizations resulting from an enhancement of an inwardly rectifying K^+ conductance have been reported in locus coeruleus (LC) and submucosal neurons in response to opioid agonists [14], and in cultured striatal and hippocampal neurons in response to adenosine [15] or serotonin [16]. In cardiac cells, muscarinic cholinergic agonists elicit an increase in K^+ conductance [17], similar in its inwardly rectifying voltage sensitivity to the responses observed in mPRF neurons, and also in amphibian parasympathetic neurons [18]. In vertebrate cells, the inwardly rectifying K^+ conductance was coupled by GTP-binding proteins [19], and in invertebrate neurons, cAMP has been reported to mediate this transmitter-evoked effect [20].

Other data [21] have suggested that neither the hyperpolarizing or depolarizing responses of mPRF neurons to cholinergic agonists have the characteristics of M_1 receptor mediation since, as shown in Fig. 6.4, the pirenzepine sensitivity expected in M_1 receptors was not present. Further work is required to define whether the receptor characteristics are those of an M_2 or another muscarinic receptor type.

The pharmacological *in vitro* identification of non- M_1 receptors in the reticular formation is in accord with *in vitro* autoradiographic data that indicated almost exclusive presence of M_2 receptors in the brainstem, including those in the pedunculo pontine and laterodorsal tegmental (PPT/LDT) cholinergic nuclei, in the reticular formation, in LC and in cranial nerve nuclei [22]. M_1 receptors were largely confined to telencephalic and diencephalic structures.

In summary, two-thirds of mPRF neurons respond to carbachol with a strong depolarizing response that is associated with an increase in input resistance. There is an increase in excitability as measured by increased number of spikes to the same depolarizing current and enhancement of PSPs elicited by electrical stimulation of the contralateral pontine reticular formation. Atropine blockade of carbachol effects suggests mediation by a muscarinic receptor. The remaining one-third of neurons respond

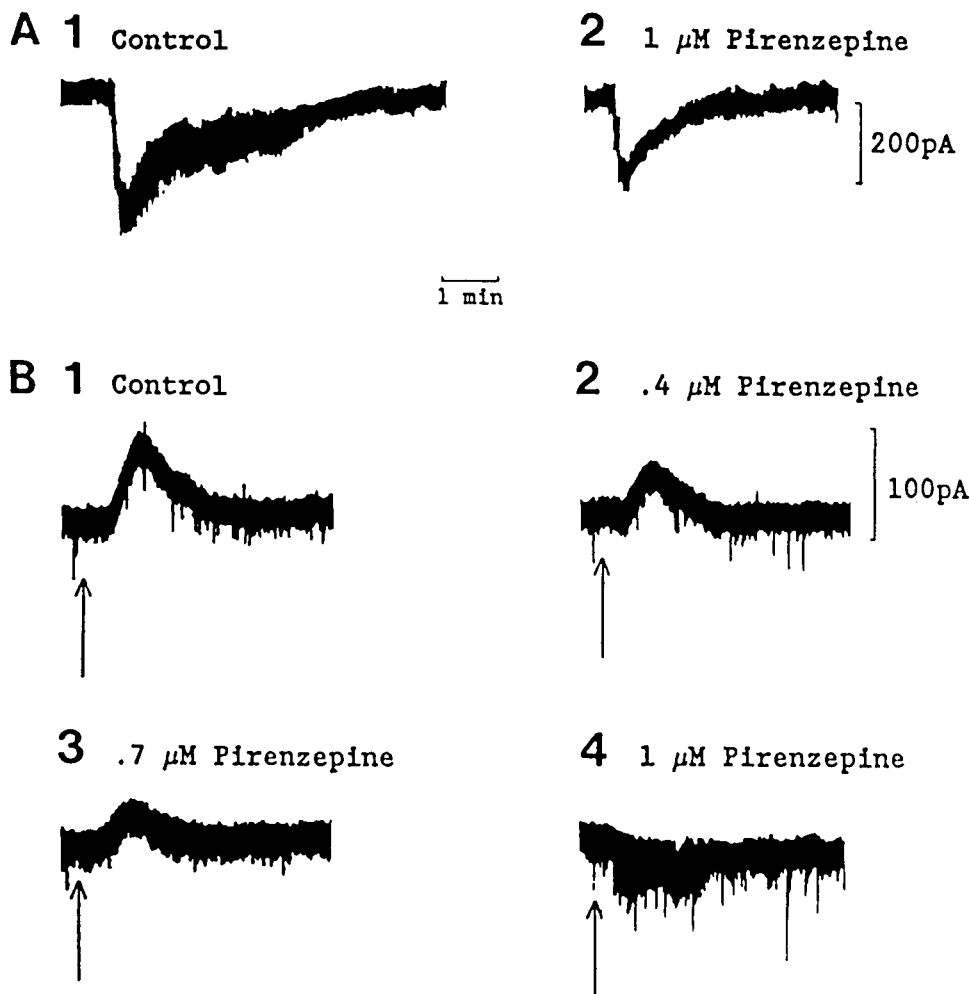


Figure 6.4. Non- M_1 nature of the muscarinic response of medial pontine reticular formation neurons *in vitro*. A, voltage clamp recording of the current associated with the depolarizing response elicited by puffer application of carbachol. Note the inward current increase (downward deflection, equivalent to an outward current decrease) in control conditions. Even 1 μM concentrations of pirenzepine did not fully block this response. B, outward current increase (upward deflection) associated with the hyperpolarizing response; note the failure to block by 400 μM or even 700 μM pirenzepine, although there was blockage at 1 μM . Thus, both the depolarizing and hyperpolarizing responses to carbachol were not blocked by the 200 μM pirenzepine concentration that would have been expected for an M_1 receptor, given the K_d s of carbachol and pirenzepine for the M_1 receptor (cf. Mash and Potter, 1986). Modified from Gerber *et al.* (1989b).

with either a biphasic hyperpolarization–depolarization or hyperpolarization alone, consistent with microiontophoretic studies of ACh effects on spike rates of identified reticulospinal mPRF neurons [23].

The depolarizing effects of carbachol nicely parallel the phenomenology of naturally occurring REM sleep in medial pontine reticular neurons, that is, a membrane depolarization of 7–10 mV and enhancement of excitatory PSPs elicited by reticular stimulation [24]. Furthermore, the

[23] Greene and Carpenter (1985).

[24] Ito and McCarley (1984); see Chapter 10.

[25] McCarley and
Hobson (1975a).

effects on firing pattern of a carbachol-induced depolarization also parallel those occurring during natural REM sleep [25] in that no bursting discharge pattern is present in REM sleep, a finding that is also compatible with the presence of depolarization-dependent inactivation of the low-threshold Ca^{2+} spike responsible for the burst discharge pattern.

Thus, the direct effects of cholinergic muscarinic activation of mPRF neurons *in vitro* are consistent with the presence of cholinergic activation of this zone during naturally occurring REM sleep. At the single-cell level, these results provide a mechanism for the action of microinjected muscarinic cholinergic agents in pharmacological production of a REM-sleep-like state.

6.1.1.2. Pedunculopontine Tegmental Cholinergic Neurons

[26] Leonard and Llinás
(1990, 1994).

The ACh actions on thalamically projecting PPT neurons, thought to be cholinergic, have been studied in guinea pig slices [26]. Figure 6.5A shows the inhibition of spontaneous firing of a PPT cell associated with hyperpolarization of the membrane by pressure injection of bethanechol from a micropipette positioned above the slice. Superfusion with 20 μM ACh and 20 μM eserine produced a rapid and reversible suppression of neuronal firing and a marked increase in membrane conductance (Fig. 6.5B). This conductance was probably K^+ -dependent since it decreased and was reversed by membrane hyperpolarization between -85 and -90 mV (Figs. 6.5D–E), corresponding closely to the K^+ equilibrium potential. That this action was direct was demonstrated by blocking spontaneous synaptic potentials by a 0 mM Ca^{2+} and 2 mM Co^{2+} superfusate (Figs. 6.6A–B). The hyperpolarizing action of bethanechol was unaffected by this blockage (Figs. 6.6C–D). The bethanechol-induced hyperpolarization was blocked by the muscarinic antagonist atropine (Fig. 6.6F). The muscarinic receptor mediating the hyperpolarization of PPT neurons is not M_1 since high concentrations of pirenzepine are required to block the response [26].

[27] Albanese and Butcher
(1980).

[28] Mash and Potter
(1986).

[29] M.T. Shipley
(personal communication). Unpublished data of A. Mitani, S. Higo, and R.W. McCarley also indicate the presence of anterograde LC labeling from PHA-L or WGA-HRP injected in the PPT/LDT cholinergic nuclei.

6.1.1.3. Locus Coeruleus

The presence of cholinergic receptors in LC has been suggested by both acetylcholinesterase staining [27] and *in vitro* autoradiographic techniques [28], with the latter study indicating the presence of M_2 , but not M_1 , receptors. In addition, choline acetyltransferase (ChAT) immunohistochemical studies indicate the presence of cholinergic fibers in LC [29].

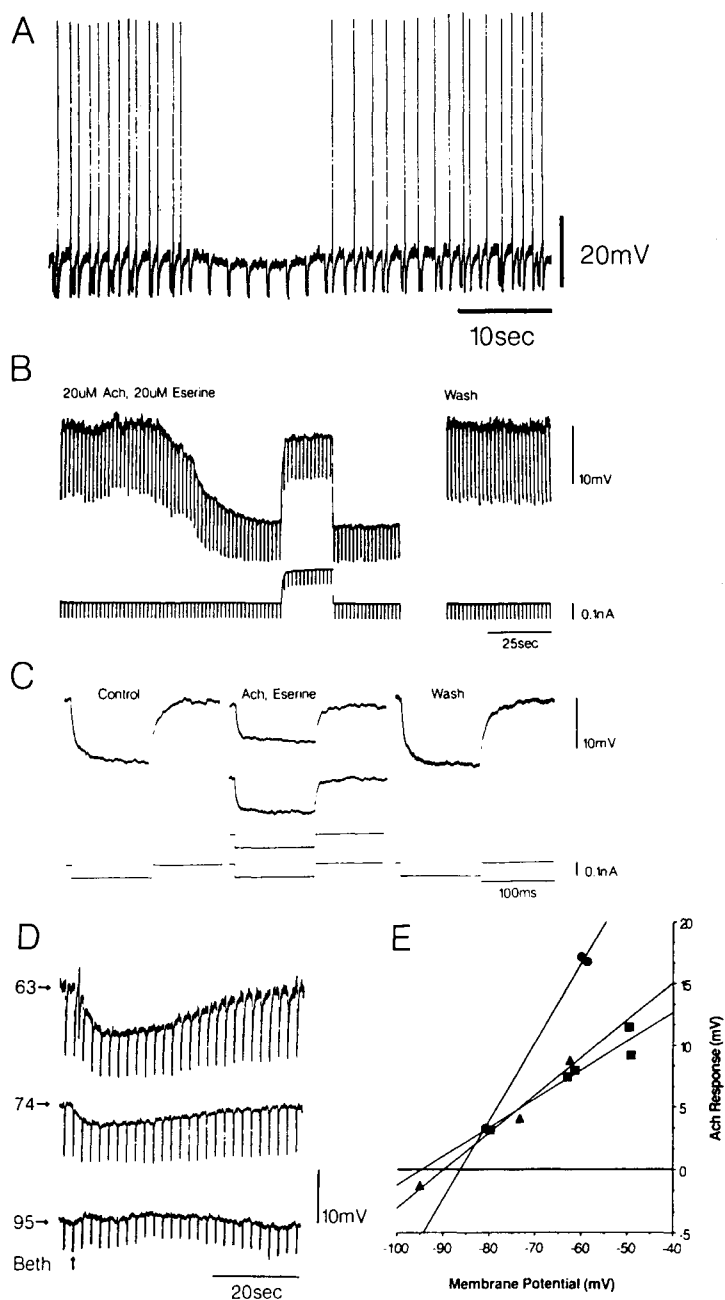


Figure 6.5. Actions of ACh on guinea pig pedunculo pontine tegmental cholinergic neurons *in vitro*. A, spontaneous firing is inhibited by pressure ejection of bethanechol from a micropipette positioned above the slice. B, superfusion with 20 μ M ACh and 20 μ M eserine in normal Ringer produces a steady, reversible hyperpolarization accompanied by a 50% decrease in input resistance. C, representative traces from each condition in B displayed at higher sweep speed. D, bethanechol hyperpolarization elicited by pressure ejection at different membrane potentials. Response is reversed at -95 mV. E, response amplitude plotted against membrane potential for 3 neurons. The extrapolated reversal potential is between -85 and -95 mV. Unpublished data by C. Leonard and R. Llinás.

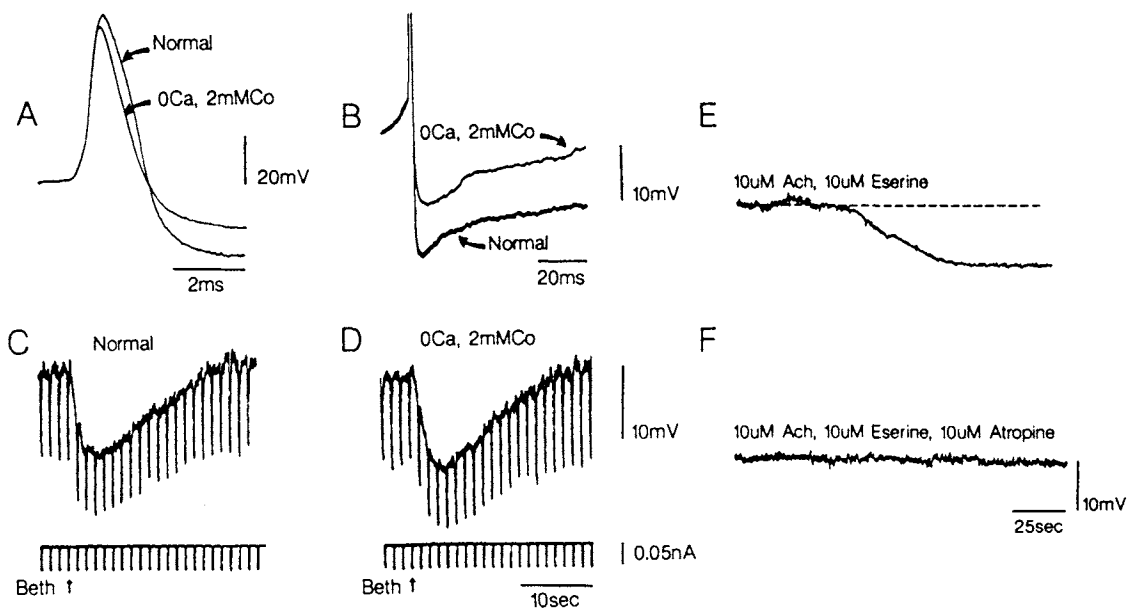


Figure 6.6. ACh has a direct, muscarinic action on guinea pig pedunculo-pontine tegmental cholinergic neurons *in vitro*. A, action potential (AP) before and after g_{Ca} blocked by superfusion with 0 mM Ca^{2+} and 2 mM Co^{2+} . Note the blockade of the Ca^{2+} -dependent component of the AP. B, same as A at a slower sweep speed to show the blockade of the calcium-dependent after hyperpolarization. C, hyperpolarization of neuron from A and B in normal Ringer produced by pressure

ejection of bethanechol. D, hyperpolarization on neuron from A–C after blockade of Ca^{2+} conductances (and synaptic transmission). Note that the action of bethanechol is unaffected by Ca^{2+} conductance blockade. E, membrane hyperpolarization (another neuron) produced by superfusing 10 μ M ACh and 10 μ M eserine. F, membrane hyperpolarization is completely blocked by 10 μ M atropine. Unpublished data by C. Leonard and R. Llinás.

[30] Egan and North (1985).

[31] Egan and North (1986b).

Intracellular recordings in the *in vitro* rat LC showed that superfusion of ACh (in the presence of neostigmine to prevent degradation) increased the firing rate of LC neurons by depolarizing the membrane [30]. This effect was reduced by antagonists of both nicotinic (hexamethonium) and muscarinic (atropine) type. In this intracellular study defining muscarinic receptor type in single central neurons, the authors found that the muscarinic action was relatively pirenzepine insensitive, with a mean dissociation constant (K_d) of 233 nM, a value typical of M_2 receptors (Fig. 6.7). Subsequent experiments [31] showed that both the nicotinic and muscarinic actions were direct since they persisted in the presence of a zero Ca^{2+} /high Mg^{2+} superfusate or in superfusates containing TTX, that is, solutions blocking synaptic potentials. They further demonstrated that pressure injections of ACh from microelectrodes (puffer electrodes) produced a biphasic depolarization in about half of the neurons; there was a hexamethonium-sensitive (hence nicotinic) initial, rapid component (Fig. 6.8) and a slower component that decayed slowly over about 30 s. This late slow component was abolished by atropine. Nearly half the neurons showed only a slow

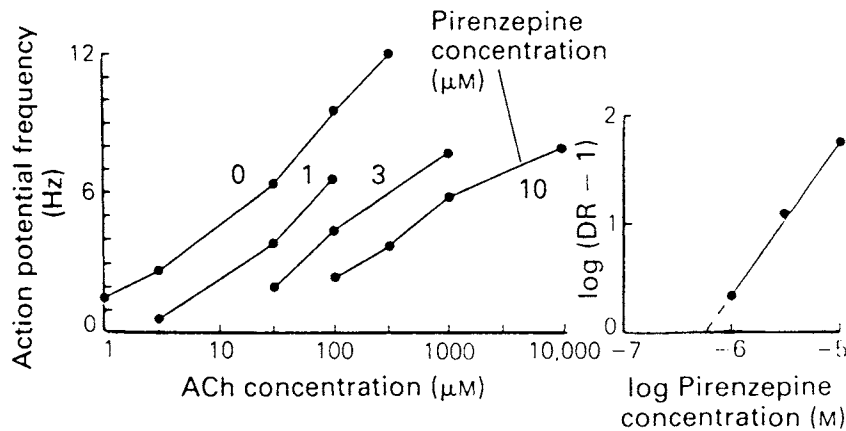


Figure 6.7. An M_2 receptor mediates muscarinic depolarization of locus coeruleus (LC) neurons *in vitro*. Left panel shows dose–response curve for acetylcholine in terms of LC action potential frequency increase at various concentrations of pirenzepine. The right panel shows a Schild plot of these results. The least squares line has a slope of 1.1 and the pirenzepine K_d is 288 nM. Modified from Egan and North (1985).

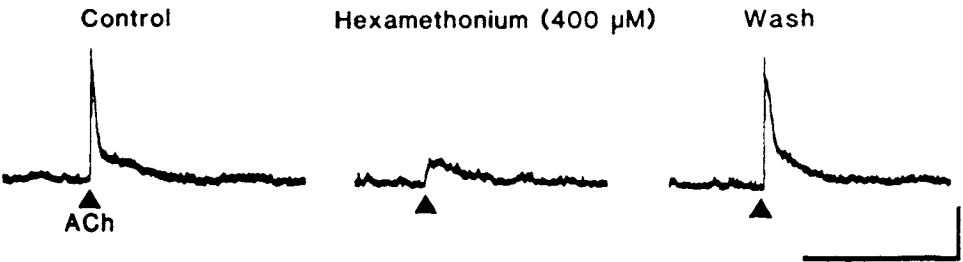


Figure 6.8. Acetylcholine depolarization of locus coeruleus neurons has a fast and slow component. Records are of membrane potential; neurons were held at -75 mV to prevent spontaneous firing. Triangles indicate time of application of a few nanoliters of ACh by pressure injection. Note the presence of a rapid and slow component of the depolarization, with the rapid component being blocked by the nicotinic antagonist hexamethonium (center). The slow component was blocked by muscarinic antagonists (not shown). Modified from Egan and North (1986b).

depolarization, requiring 10–20 s to peak, and decaying over 30 s. Fewer than 10% of the neurons showed only the fast nicotinic response. Voltage clamp studies indicated the presence of an inward current whose time course paralleled that of the voltage changes. In all types of nicotinic response, there was a striking desensitization to nicotine, with a half time of 30 min for recovery. A practical experimental point is that with superfusion or iontophoresis with ACh the nicotinic response may be masked by desensitization [32]. It was also of interest that alpha-bungarotoxin did not block the nicotinic response, suggesting that the LC nicotinic receptor was more like that in sympathetic ganglia than at the neuromuscular junction.

A final point with respect to ACh and LC is the presence of short-latency excitatory postsynaptic potentials

[32] This was what perhaps occurred in Svensson and Engberg’s study (1980).

(EPSPs) elicited by electrical stimulation of the slice surface in the LC region (Fig. 6.8). These PSPs were graded with stimulus intensity and abolished by Ca^{2+} -free solutions, and thus likely synaptic, but not blocked by nicotinic antagonists hexamethonium or dihydro-beta-erythroidine, arguing against a nicotinic origin of this EPSP. Section 6.4.2 will indicate that this EPSP is mediated by an excitatory amino-acid neurotransmitter.

6.1.2. Basal Forebrain

Carbachol produces a hyperpolarization, associated with increased membrane conductance, in cholinergic nucleus basalis neurons [33]. Muscarine mimics this hyperpolarizing effect. Applied in conjunction with *N*-methyl-D-aspartate (NMDA), carbachol promotes bursting firing in half of cholinergic cells recorded from the basal forebrain. In this condition, however, the duration of spike-bursts is markedly increased, compared with that of bursts elicited by NMDA alone. This is due to the fact that ACh reduces the afterhyperpolarization (AHP) of nucleus basalis cholinergic neurons [33].

6.1.3. Thalamus

The sources of cholinergic pathways acting upon neurons in all thalamic nuclei are in the Ch5 and Ch6 cell-groups of the midbrain-pontine reticular formation. For the rostral parts of reticular (RE), mediodorsal (MD), and anteroventral–anteromedial (AV–AM) nuclei, the brainstem cholinergic innervation is supplemented by projections arising in cholinergic neurons in Ch2, Ch3, and Ch4 cell-groups of the basal forebrain (see Chapter 3). The understanding of ACh actions on thalamic neurons is of fundamental importance for the concept of ascending reticular activation. While brainstem cholinergic neurons directly excite TC neurons, both brainstem and basal forebrain cholinergic neurons hyperpolarize thalamic reticular GABAergic neurons, with consequent disinhibition in TC cells. We discuss the effects of ACh on the three major cell classes in thalamus: TC, RE, and local-circuit GABAergic neurons.

6.1.3.1. Thalamocortical Neurons

Beginning with the mid-1960s, the excitatory postsynaptic action of ACh has been demonstrated on dorsal thalamic (mainly ventrobasal—VB and lateral geniculate—LG) single neurons recorded extracellularly, some of them

[33] Khateb *et al.* (1997). The same authors (Khateb *et al.*, 1998) reported that nucleus basalis cholinergic cells are depolarized by application of GABA in basal forebrain slices. The depolarization was associated with a decrease in input resistance and diminished firing rate, suggesting that the GABA-evoked depolarization exerts predominantly inhibitory actions on these neurons.

identified antidromically as TC cells [34]. Cholinergic facilitation was also selectively observed upon the postsynaptic components of evoked mass field potentials in ventroanterior–ventrolateral (VA–VL), VB, and LG nuclei [35]. The excitatory action of ACh was blocked by both muscarinic (atropine, scopolamine) and nicotinic (hexamethonium, mecamylamine) antagonists [36]. The ACh action is considerably more evident in animals anesthetized with gas than under barbiturate anesthesia [37].

The ACh-induced excitation of VL and ventromedial (VM) thalamic neurons is accompanied by the conversion of the burst response to stimulation of cerebellar afferent pathways into a single-spike response [38]. This is similar to the action of a sustained depolarization (see Chapter 5) and much the same as the state-dependent change by passing from EEG-synchronized sleep to wakefulness (see Chapter 9). In fact, ACh-induced excitatory responses of muscarinic type are mainly observed when the recorded cell is discharging in the single-spike mode associated with EEG activation. The dependency of ACh excitatory action upon activated brain electrical activity was observed in VM neurons of acutely prepared animals [38] and in LG neurons recorded in chronic experiments [39]. In the latter condition, the ACh-elicited facilitation of LG-cell discharges (an action antagonized by scopolamine) was only observed in waking and REM sleep. All these results are congruent with the established fact that barbiturate anesthesia abolishes the excitation by ACh iontophoresis [40] and with the direct excitation of TC neurons by stimulating the brainstem–thalamic cholinergic pathways [41].

In vitro studies of medial geniculate (MG) and LG thalamic neurons showed the presence of species differences in ACh effects [42]. (a) In the guinea pig, ACh causes a hyperpolarization associated with an increased K^+ conductance, followed by a slow depolarization associated with a decreased potassium conductance (Fig. 6.9). Both these components persist after blockade of synaptic transmission and are mediated by muscarinic receptors. (b) In the albino rat, ACh results in the slow depolarization only. (c) In cat, MG neurons and LG neurons recorded from laminae A–A1, some of them formally identified as TC cells, ACh induces a rapid (nicotinic) depolarization followed by a slow hyperpolarization and a slow depolarization caused by activation of muscarinic receptors (Fig. 6.10). The nicotinic excitation of LG cells resembles the ACh action upon peripheral ganglion cells; corroboratively, the nicotinic receptors in the LG nucleus seem to be of ganglionic type [43]. As to the hyperpolarization, it prevails in MG neurons in keeping with previous extracellular data *in vivo* [44]. The slow depolarization

[34] Andersen and Curtis (1964a, b); McCance *et al.* (1968a); Phillis (1971); Duggan and Hall (1975).
[35] Marshall and Murray (1980).
[36] Phillis and Tebecis (1967); Satinski (1967); Godfraind (1978).
[37] McCance *et al.* (1968b).

[38] Marshall and McLennan (1972); MacLeod *et al.* (1984).
[39] Marks and Roffwarg (1987).
[40] Eysel *et al.* (1986). Extracellular recordings from the visual thalamic LG nucleus showed that microiontophoretically applied ACh increases firing rates of these neurons and that the excitatory ACh-induced effect is completely blocked by barbiturate (Pape and Eysel, 1988).
[41] Hu *et al.* (1989b).
[42] McCormick and Prince (1987a); McCormick (1992).

[43] Clarke *et al.* (1985).

[44] Tebecis (1972).

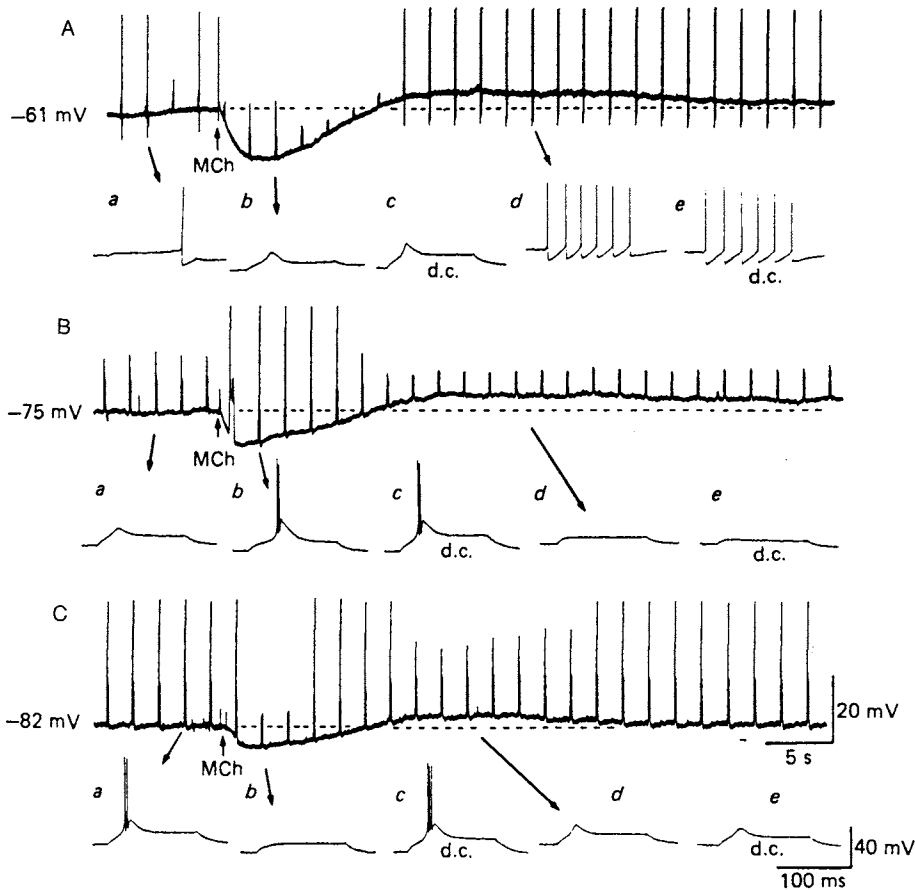


Figure 6.9. Effect of muscarinic hyperpolarization and slow depolarization on the response of a guinea pig LG thalamic neuron to a depolarizing current pulse. *In vitro* recordings. Responses to three applications of acetyl-methylcholine (MCh) are illustrated when the membrane potential was held with DC at levels indicated to the left of each segment. The cell was in the, A, single-spike firing mode, B, the burst firing mode, and C, in between. Sample traces are expanded for detail, as indicated. The effect of mimicking the MCh-induced change in V_m with the intracellular injection of current is indicated by DC. This particular neuron was in the burst firing mode when the membrane potential was around -80 mV. A more typical membrane potential for this type of activity would be between -70 mV and -75 mV. From McCormick and Prince (1987a).

occurs with equal frequency in MG and LG nuclei. While the fast nicotinic depolarization is associated with an increase in membrane conductance, the slow hyper- and depolarizing events are associated with conductance changes similar to those found in guinea pig (see above). The slow depolarization inhibits the occurrence of burst discharges and promotes single-spike firing, opposite to the action of the hyperpolarization, and very similar to the picture seen in transition from sleep to arousal. The fast nicotinic excitation by ACh was also found in medial habenular neurons maintained *in vitro* [45].

Intracellular recordings of TC cells *in vivo* showed that stimulation of brainstem-thalamic cholinergic pathways

[45] McCormick and Prince (1987b).

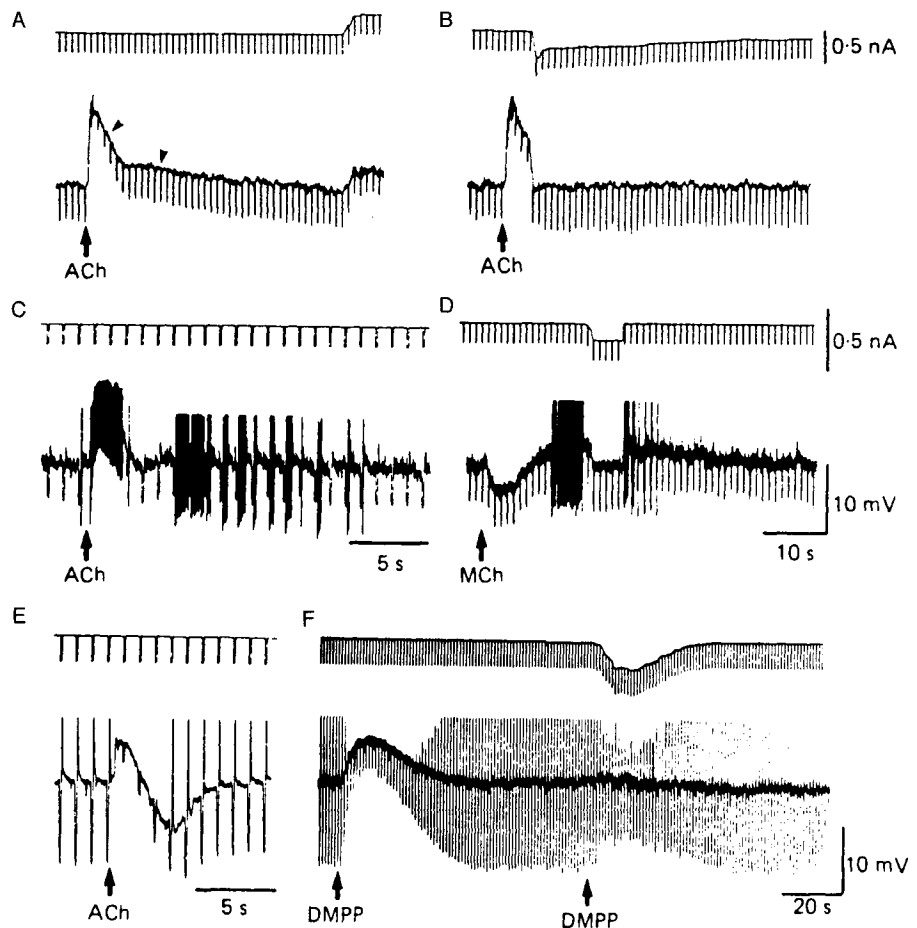


Figure 6.10. Actions of ACh in the cat LG and MG thalamic neurons *in vitro*. A, application of ACh to an LG cell in lamina A (resting potential -64 mV). B, manual voltage clamp of the slow depolarizing component (second arrow head) of the response to ACh in the neuron in A. C, application of ACh to another LG neuron in lamina A, depolarized with intracellular injection of DC to near firing threshold (-60 mV). D, application of the muscarinic agonist acetyl-methylcholine (MCh) to the neuron of C. E, application of ACh to an MG neuron. F, application of the nicotinic agonist DMPP to the MG neuron of E. In all pairs, the top trace is the injected current and the bottom trace is the membrane potential. Current calibration in E–F as in D. From McCormick and Prince (1987a).

gives rise to a short-latency depolarizing response, associated with increased membrane conductance and abolished by the nicotinic receptor antagonist mecamylamine (Fig. 6.11), and a long-latency depolarizing response, associated with increase in the apparent input resistance and abolished by the muscarinic receptor antagonist scopolamine (Fig. 6.12) [46].

6.1.3.2. Thalamic Reticular Neurons

Extracellular recordings in acute experiments on anesthetized animals showed that ACh application depresses

[46] Curró Dossi *et al.* (1991). The latency of the nicotinic-mediated depolarization induced by stimulation of brainstem cholinergic nuclei *in vivo* is approximately 140 ms and its duration is approximately 1.3 s, while the latency of the muscarinic-mediated depolarization is approximately 1.2 s and its duration is approximately 20 ms. The amplitude of the late depolarization is

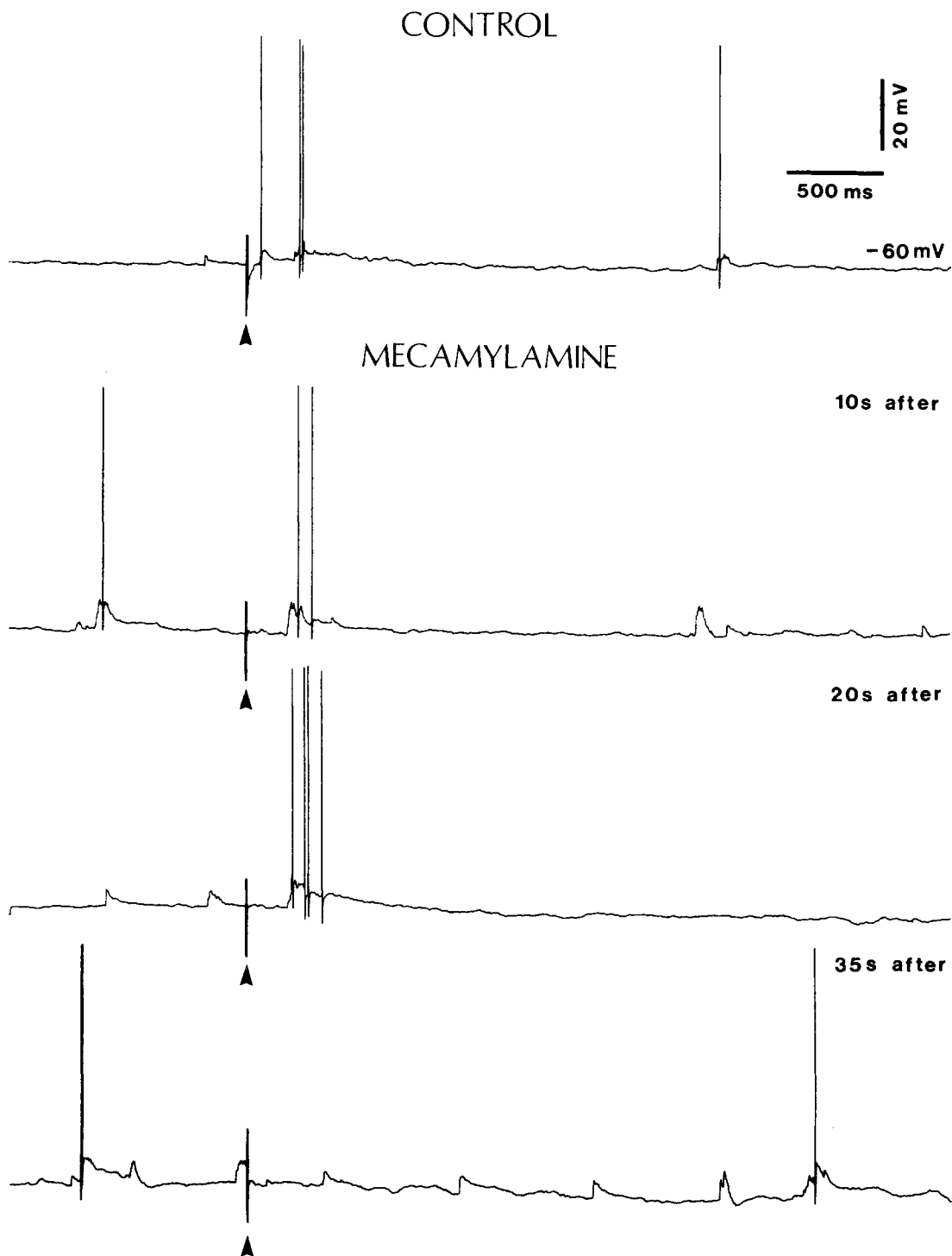
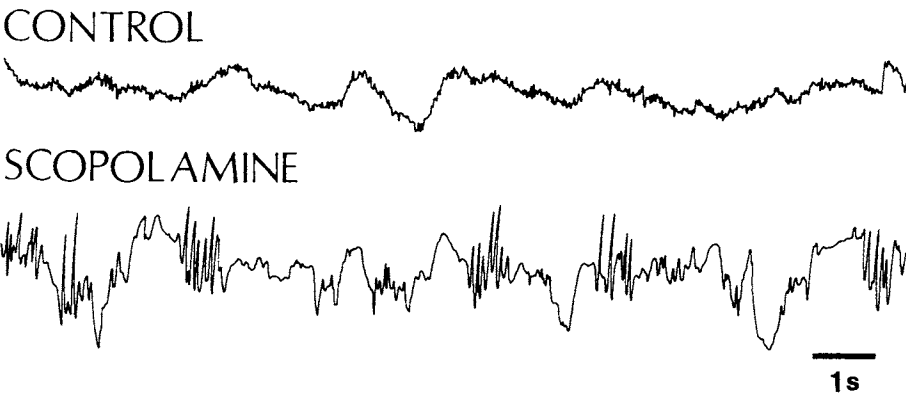
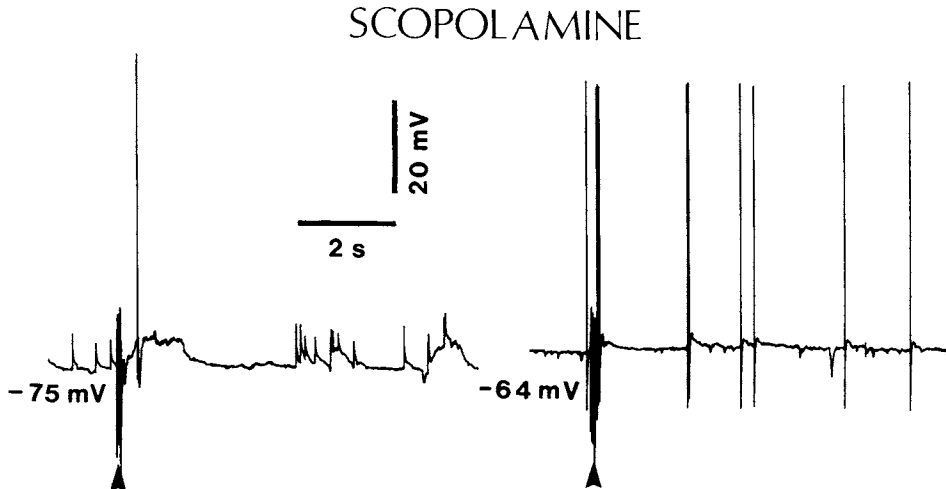
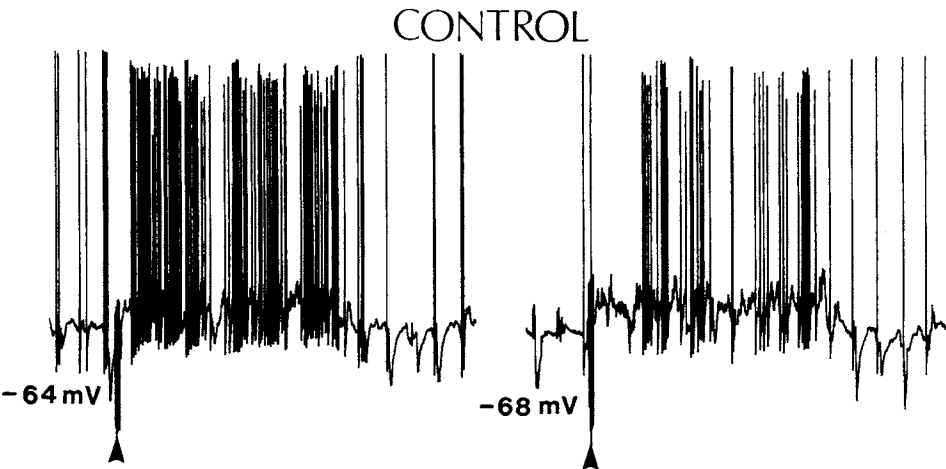


Figure 6.11. Mecamylamine, a nicotinic antagonist, abolishes the short-lasting depolarization elicited in anterior thalamic (AT) relay cell by stimulation of laterodorsal tegmental (LDT) cholinergic nucleus in cat. *In vivo* recordings under urethane

anesthesia. LDT stimulation with pulse-train (3 stimuli at 300 Hz). Indicated by arrowhead. On the top right of each trace, the time after the injection is indicated. From Curró Dossi *et al.* (1991).



voltage-dependent, increasing under depolarizing current. [47] Ben-Ari *et al.* (1976); Dingledine and Kelly (1977); Godfraind (1978); Sillito *et al.* (1983); Eysel *et al.* (1986); Sillito (1987).

the spontaneous and evoked discharges of neurons recorded from the peri-VB, peri-pulvinar (PUL) or peri-LG (perigeniculate—PG) sectors of the reticular nuclear complex [47]. The ACh-evoked inhibition of reticular neurons is blocked by atropine. As opposed to the ACh-induced excitation of TC neurons, the ACh-inhibition of reticular neurons is not abolished by systemic injections of barbiturates [40]. This is congruent with the barbiturate-sensitivity of brainstem-induced excitation of LG cells, as opposed to the persistence, under barbiturates, of the brainstem-induced depolarizing–hyperpolarizing sequence in PG neurons [41] (see Chapter 9).

Application of ACh on reticular neurons *in vitro* results in a hyperpolarization and increase in membrane conductance, an effect probably mediated by the M_2 subclass of muscarinic receptors [48]. Varying extracellular K^+ concentration changes the reversal potential of the ACh-induced hyperpolarization, thus indicating that it is due to an increased K^+ conductance. On the other hand, intracellular iontophoresis of Cl^- fails to alter the RE-cell response to ACh, while dramatically altering the response of the same neurons to GABA (Fig. 6.13).

[48] McCormick and Prince (1986b).

6.1.3.3. Local Interneurons

As yet, there are no available data on formally identified local-circuit cells in thalamic nuclei *in vivo*. The ACh effects on these elements have been inferred by investigating the stimulus-specific (or short-range) inhibitions on thalamic relay cells in the LG nucleus [47]. These studies report that the center-surround antagonism is enhanced by ACh application and conclude on an excitatory influence of ACh upon GABAergic local-circuit cells intrinsic to the LG nucleus. The ACh action seems to be similar to the enhanced discrimination in LG relay neurons upon awakening from sleep [49]. However, these data are far from definitive because the short-axoned cells should be identified by intracellular staining and their inhibitory nature has to be demonstrated by immunohistochemistry.

[49] Livingstone and Hubel (1981; see Chapter 9)

Figure 6.12. Scopolamine, a muscarinic antagonist, abolishes the long-lasting depolarization elicited in anterior thalamic (AT) relay cell by stimulation of laterodorsal tegmental (LDT) cholinergic nucleus. *In vivo* recording under urethane anesthesia. LDT stimulation with a pulse-train (30 stimuli at 300 Hz). Control trace at rest (top left) and under hyperpolarizing current (top right). After intravenous administration of scopolamine (0.5 mg/kg), the cell hyperpolarized by 11 mV, and only an early depolarizing component was detected as response to LDT stimulation (middle left). This early depolarization was subsequently abolished by mecamylamine (not depicted; see Fig. 6.11). The disappearance of the long-lasting depolarization persisted after compensation of the membrane potential by injection of depolarizing current (middle right). After scopolamine, the cortical EEG showed slow-waves with increased amplitudes as well as occurrence of sequences of spindle waves. From Curró Dossi *et al.* (1991).

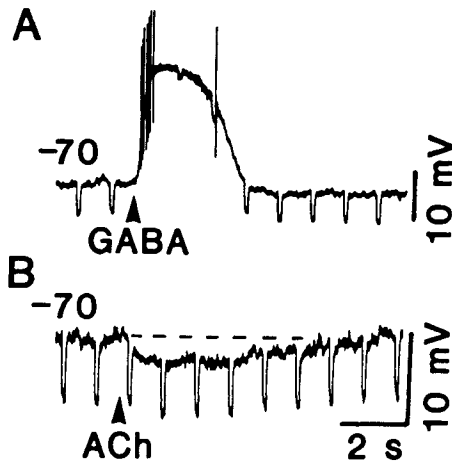


Figure 6.13. Intracellular injection of KCl dramatically alters the response of a guinea pig thalamic reticular neuron to GABA but not to ACh. *In vitro* recordings. A, the fast excitatory depolarizing response of this neuron to GABA after intracellular iontophoresis of Cl^- . B, application of ACh to the same neuron as in A results in the typical hyperpolarizing response to ACh, which was subsequently found to reverse at -90 mV. From McCormick and Prince (1987c).

Presumed local-circuit neurons in cat LG slices have been recognized by their short-lasting action potential, lack of a low-threshold calcium spike (LTS; see Chapter 5), and intracellular staining showing a somadendritic morphology resembling that of putative local interneurons or type 3 LG cells [50], as defined in Golgi studies [51]. ACh was found to hyperpolarize those presumed GABAergic local-circuit cells through an increase in membrane K^+ conductance, an action mediated by the M_2 class subclass of muscarinic receptors. The locally ramifying axon and the GABAergic nature of those presumed local inhibitory interneurons remain to be demonstrated. The inhibitory action of ACh is difficult to understand in the light of iontophoretic studies demonstrating ACh-induced enhancement of stimulus-specific inhibitory responses of LG relay cells [47] and the fact that a long series of experimental data demonstrated the ACh-induced inhibition of the other class of thalamic inhibitory neurons, the reticular cells. Thus, both types of progenitors of inhibitory processes in the thalamus seem to be inhibited by ACh, in spite of the same transmitter enhancing inhibitory processes in TC neurons. Probably, however, the ACh-inhibition of somatic activity of local interneurons (what can easily be seen by an intracellular impalement) is not accompanied by an inhibition of intraglomerular dendrodendritic synapses between local-circuit and relay cells, the contacts that are presumably involved in shunting inhibitory processes related to discriminatory functions. Indeed, stimulation of brainstem cholinergic nuclei *in vivo*

[50] McCormick and Pape (1988). However, more recent studies demonstrated that robust burst firing occurs in local-circuit GABAergic cells when a depolarizing step is imposed at a slightly hyperpolarized membrane potential (Zhu *et al.*, 1999a, b; see Chapter 5, Section 5.5.2).

[51] Guillery (1966).

leads to suppression of prolonged hyperpolarizations in TC cells (due to the biphasic sequence of GABA_{A-B} IPSPs), but preservation or even enhancement of the earliest IPSPs, termed GABA_A IPSP and attributed to the activity of intraglomerular presynaptic dendrites of local interneurons [52] (see Chapter 9).

[52] Curró Dossi *et al.* (1992b).

6.1.4. Neocortex

It was initially reported that ACh exerts excitatory actions on neurons of the sensorimotor cortex, that the effects are most clearly seen in cells located relatively deep (below layers II–III), and that they are unambiguously muscarinic in nature [53]. The deep cortical location of ACh-excited neurons was confirmed by antidromic identification of pyramidal tract and corticothalamic neurons in layers Vb and VI of rat somatosensory cortex [54]. While more than 50% of corticothalamic or pyramidal tract neurons are cholinceptive, only 16% of callosally-projecting cells are sensitive to ACh [54]. The latter investigations on rat showed that the ACh effects on long-axonated cortical cells are most frequently mediated by muscarinic receptors; however, partial suppression of ACh effects by mecamylamine, a nicotinic antagonist, was also observed [55]. Subsequent studies have identified the ACh-induced excitatory effects on neurons recorded from both superficial (layer II–III) and deep layers in the visual, cingulate, and somatosensory cortices [56].

[53] Krnjević and Phillis (1963a, b); Crawford and Curtis (1966).

[54] Lamour *et al.* (1982, 1983).

[55] See also McLennan and Hicks (1978) for nicotinic excitation of cortical cells.

[56] Sillito and Kemp (1983); Donoghue and Carroll (1987).

[57] Krnjević *et al.* (1971).

The ACh-induced muscarinic excitation of cortical neurons is slow in onset and may outlast the ACh application by tens of seconds [57]. The ACh-induced depolarization is due to a reduction in K⁺ conductance and is associated with a rise in membrane resistance (Fig. 6.14). As is the case of TC neurons (see Section 6.1.3.1), the ACh excitatory effect is particularly susceptible to depression by barbiturates.

[58] McCormick and Prince (1985, 1986a); reviewed in McCormick (1990, 1992).

In vitro studies [58] on cingulate, sensorimotor, and visual neurons of guinea pig revealed that before the muscarinic excitation of pyramidal-shaped neurons, those elements display a short-latency inhibition associated with a decrease in input resistance. The initial inhibition of pyramidal cells appears to be mediated by a rapid muscarinic excitation of local GABAergic interneurons, since it has a reversal potential similar to the hyperpolarizing response produced by GABA; and ACh application on elements identified by intracellular staining as aspiny or sparsely spiny interneurons results in a short-latency excitation associated with a large decrease in input resistance, an excitatory response whose duration is similar to the ACh-induced initial inhibition in pyramidal neurons (Fig. 6.15).

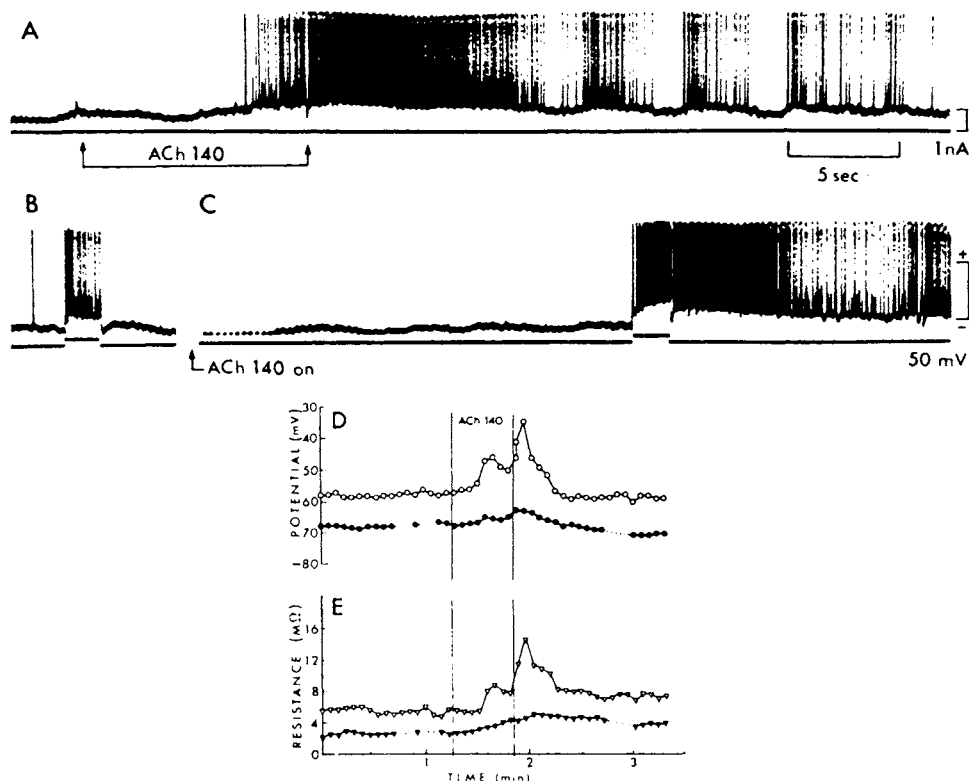


Figure 6.14. Facilitatory action of ACh in cat cerebral cortex. *In vivo* recordings. A, intracellular recording from neuron in motor cortical area shows delayed depolarizing effect and prolonged firing evoked by iontophoretic application of ACh (140 nA). B, brief and instantly reversible depolarization and strong firing of the same neuron caused by short intracellular current injection (monitored on lower trace). C, same neuron depressed after treatment with dinitrophenol no longer fired in response to application of ACh (as in A). However, during continued ACh application, identical intracellular current injection (see B) now induced particularly powerful and prolonged discharges. The ACh thus greatly facilitates and prolongs any depolarizing input received by the same cell. D–E, magnitude and time course of changes in potential and resistance induced by ACh. Open circles: resting potential; note slow and prolonged depolarizing effect. Open triangles: resting resistance; note marked increase in resistance synchronous with depolarization. Closed symbols: corresponding data recorded during IPSPs; they show relatively little change, except some possible reduction of inhibitory effect. Modified from Krnjević *et al.* (1971).

The ACh-excitation on cortical interneurons is partially congruent with extracellular data on visual cortex neurons [56]. In addition to its facilitatory effect, ACh strikingly increases the stimulus-specificity of the response without any loss in the selectivity. This suggested that inhibitory interneurons outside the III–IV layers are facilitated by ACh. It was postulated that another class of cortical interneurons, located in layers III–IV, might be inhibited by ACh, with disinhibitory consequences on pyramidal cells.

As to the slow muscarinic excitation of pyramidal neurons, it is mainly due to a decrease in a voltage-dependent K^+ current, M-current [59], and is associated with a rise in

[59] Brown and Adams (1980).

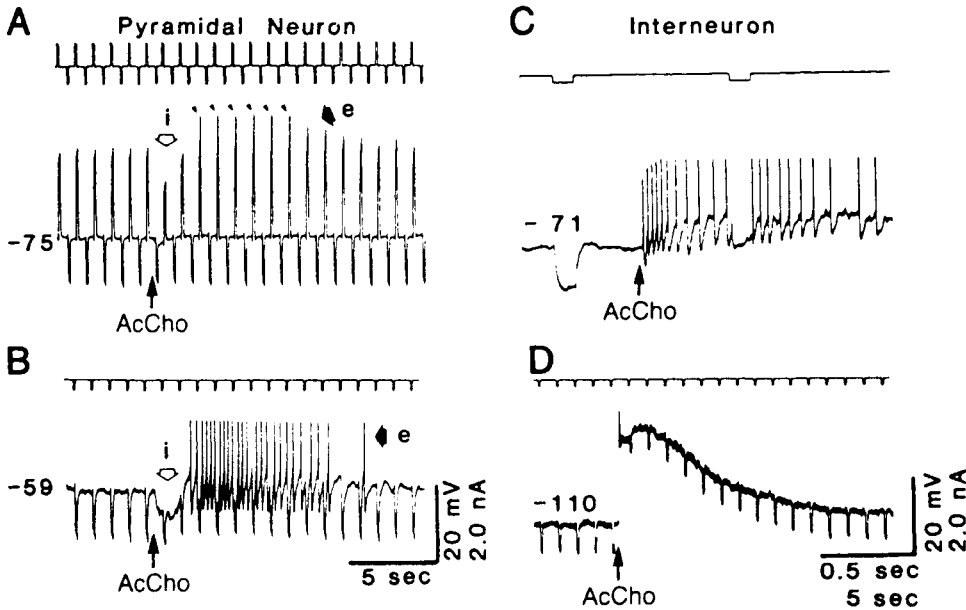


Figure 6.15. Effects of ACh on physiologically identified pyramidal cells and interneurons in guinea pig cerebral cortex. *In vitro* recordings. A, application of ACh to a typical pyramidal cell at resting membrane potential (-75 mV) initially caused a decrease in the response to the current pulse (i) followed by a selective potentiation of the depolarizing responses without affecting resting membrane potential or the response to the hyperpolarizing pulses (e). The potentiated depolarizing pulses reached firing threshold and evoked action potentials (APs) (downward arrowheads). B, application of ACh to the neuron from A after depolarization to near firing threshold (-59 mV) caused inhibition at a short latency (i) and was followed by a slow depolarization and AP generation (e). C, application of ACh to an interneuron at resting membrane potential (-71 mV) caused robust excitation at short latency. D, application of ACh to the interneuron from C after hyperpolarization to -110 mV evoked a large depolarization with short onset latency. The top trace in each set is the current monitor. The intracellular current pulses were 120 ms in duration and were applied at 1 Hz. AP amplitudes are truncated. Time calibration is 0.5 s for C and 5 s for other parts. From McCormick and Prince (1985).

input resistance [58] in keeping with the earlier *in vivo* studies [57]. The ACh-induced slow depolarization of cortical pyramidal neurons is very effectively blocked by pirenzepine, a muscarinic antagonist with a selectivity for M_1 receptors [60]. It was hypothesized that cyclic guanosine 3',5'-monophosphate (cGMP) may play a second messenger role in the muscarinic actions of ACh on pyramidal tract and some unidentified neurons in rat and cat cerebral cortex [61].

The ACh-induced dramatic facilitation and prolongation of any depolarizing input received by the same cortical cell [57] (see Fig. 6.14) underlies the potentiating effects produced by the modulatory agent ACh released by basal forebrain neurons upon phasic specific inputs of thalamic origin received by cortical neurons. This ACh action may be one of the bases of long-term enhancement in cortical responsiveness, such as that involved in the acquisition of responses during some forms of learning

[60] Cf. Bradshaw *et al.* (1987).

[61] Stone *et al.* (1975); Stone and Taylor (1977); Woody *et al.* (1978, 1986); but see Krnjević *et al.* (1976) and Benardo and Prince (1982b).

and memory. Studies on cat visual cortex neurons show that while ACh produces an increase of background firing in only 20% of tested cells, it alters the responses to visual stimuli in more than 90% of neurons [56]. ACh permits long-term (from several minutes to over 1 hr) enhancement of somatosensory cortical responses to tactile stimulation of the receptive field or to glutamate application [62]. The somatosensory cortical cholinceptive cells are more likely than noncholinceptive cells to be driven by ventroposterolateral (VPL) thalamic stimulation, and ACh selectively alters certain properties of the neuron rather than acting as a general excitant [63]. For example, while glutamate application results in an uniform decrease of the threshold for activation throughout the receptive field, the ACh effect is more selective and decreases the threshold of activation in only a limited part of the receptive field. Often, the ACh-induced alterations in cellular excitability last for prolonged periods of time. When somatic stimuli are used, about a third of the ACh-induced increases in excitability last more than 5 min [64].

The enhancement in cortical cell excitability is state-dependent, as the ACh release from the cerebral cortex is dependent on activated behavioral states [65]. Indeed, the same cortical somatosensory neuron, which is unresponsive to passive touch of the digits, displays clear receptive fields on the digit when the monkey grasps food [66]. This state-dependency of neuronal responsiveness may be related to similar motivational changes in basal forebrain neurons [67] that provide the bulk of cholinergic innervation of the cortex.

6.1.5. Hippocampus

In many respects, the ACh effects on hippocampal neurons are similar to those observed in neocortical cells. Most *in vitro* studies have investigated pyramidal cells in the CA1 field of guinea pig and rat [68]. ACh depolarizes CA1 pyramidal neurons with an associated increase in input resistance, blocks a Ca^{2+} -activated K^+ conductance, and blocks accommodation of action potential discharges. These actions are mimicked by stimulation of sites in the slice known to contain cholinergic fibers and are reversed by the muscarinic antagonist atropine (Fig. 6.16). A voltage-clamp analysis showed that cholinergic agents (carbachol, muscarine, bethanecol) turn off the M-conductance in CA1 pyramidal cells [69]. The overt effect of the ACh-induced reduction of M-current is a tendency to discharge repetitively in response to other depolarizing inputs, without necessarily causing significant cell depolarization.

[62] Metherate *et al.* (1987).

[63] Metherate *et al.* (1988a).

[64] Metherate *et al.* (1988b).

[65] Celesia and Jasper (1966); Collier and Mitchell (1967).

[66] Iwamura *et al.* (1985).

[67] Rolls *et al.* (1986).

[68] Dodd *et al.* (1981); Benardo and Prince (1982); Cole and Nicoll (1983).

[69] Halliwell and Adams (1982). The voltage-dependent K^+ current termed M-current undergoes a reciprocal regulation by ACh and the somatostatin-derived peptides. The former reduces this current, but somatostatin augments it, as shown by voltage-clamp studies on CA1 pyramidal cells in the slice preparation of rat hippocampus (Moore *et al.*, 1988). A similarly increased M-current by somatostatin was observed in the solitary tract nuclear complex (Siggins *et al.*, 1987).

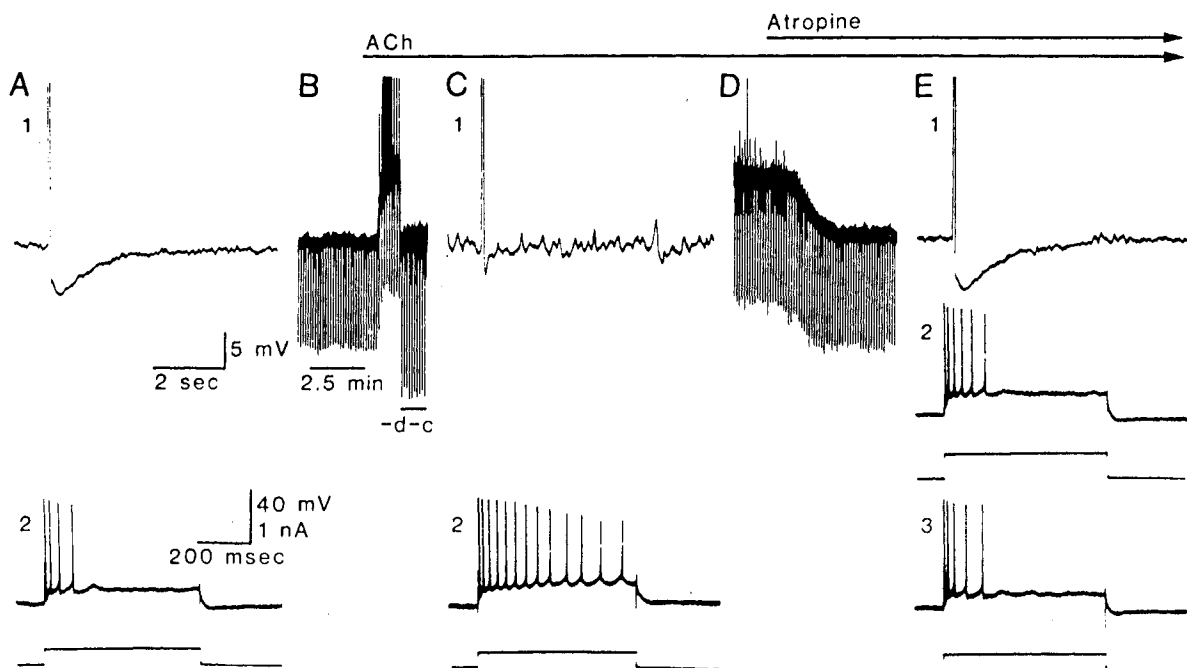


Figure 6.16. Effects of ACh on rat CA1 pyramidal neurons in hippocampal slice preparation. All responses from the same neuron. A, chart record of control afterhyperpolarizing potential (AHP) after a 60-ms direct depolarizing current pulse (trace 1) and film record of response to a 600-ms pulse (trace 2). The current record is positioned below the voltage record. B, ACh (200 μ M) superfusion depolarized the membrane and increased the cell's input resistance. C, blockade of the AHP (trace 1) and accommodation (trace 2) in the presence of ACh. D, the addition of atropine (0.5 μ M) in the presence of ACh reversed the effects of ACh. E, atropine also reversed the

effects of ACh on the AHP (trace 1) and on accommodation (traces 2 and 3). The current pulse in trace 3 was identical to those in trace 2 in A and C. In trace 2 the current pulse was increased to match the depolarization evoked in the presence of ACh (trace 2 in C). The gain in trace 1 in A applies to all of the chart records. The time calibration for trace 1 in A also applies to trace 1 in C and E, and the time calibration in D is the same as that in B. The calibration for trace 2 in A applies to all the film records. Resting membrane potential: -57 mV. From Cole and Nicoll (1983).

[70] Krnjević and Ropert (1981).

[71] Krnjević *et al.* (1988).

[72] Ben-Ari *et al.* (1981).

[73] Haas (1982).

[74] Benardo and Prince (1981, 1982a, b).

Such effects have been indeed elicited *in vivo* by septal stimulation upon CA1 and CA3 hippocampal neurons [70].

In addition to direct excitatory effects on pyramidal hippocampal cells, ACh reduces the inhibitory input that normally prevents or limits pyramidal cell discharges [71]. Intracellular recordings from CA1 and CA3 neurons indicate that ACh reduces by about 60% the conductance increase associated with IPSPs evoked by entorhinal or fimbrial stimulation [72]. The ACh-elicited reduction in the size of IPSPs suggested either an ACh-induced inhibition of GABAergic interneurons or a depression of transmitter release from inhibitory terminals. These data from *in vivo* experiments are congruent with data obtained *in vitro* [73]. However, an ACh-induced initial short-lasting hyperpolarization of pyramidal cells, with a conductance increase, has also been observed [74], thus suggesting that direct ACh-excitation of some inhibitory interneurons may also be postulated.

6.2. Norepinephrine

Norepinephrine (NE) is recognized as one of the most important neurotransmitters and neuromodulators arising from the brainstem. The anatomical distribution of afferents and efferents of NE-containing neurons has been described in Chapter 4. NE is of great importance to behavior, as an important rôle for NE has been postulated in almost every behavioral system, including sleep-waking, feeding, thermoregulation, sensory processing, motor activity, and growth and development [75].

[75] Reviewed in Foote *et al.* (1983).

The early literature on *in vivo* microiontophoresis and systemic injections of NE agonists and antagonists is truly vast. Unfortunately, the absence of control over concentrations, the lack of synaptic isolation, and the inability to manipulate the recorded neuron by injections of current and by voltage clamping, renders data from this literature less than definitive with respect to receptor type and action. We, thus, will rely on *in vitro* data when available and cite *in vivo* work only where other data are not available or are incomplete. We note also that we will not attempt to cover in any systematic way the large recent literature on second messenger mediation of NE effects.

Electrophysiological responses to NE have been observed following activation of receptors classified as β , α_1 , α_2 , and also unclassified α receptors in central nervous system (CNS) vertebrate neurons. (We here describe an α receptor as unclassified with respect to subtype when the agonist/antagonist response pattern does not follow that of peripheral receptors; it is an obvious but important point that CNS receptors may not exactly parallel peripheral receptors in structure and sensitivity, and thus the peripheral classification may incompletely describe CNS receptors.) NE responses in various CNS neurons have been reported to be mediated by alterations in at least five different types of Ca^{2+} and K^+ conductances (see summary in Table 6.1 below). We begin our review with a brief summary of data from brainstem.

6.2.1. Brainstem

6.2.1.1. Locus Coeruleus

One major effect of NE on LC neurons is an α_2 -mediated membrane hyperpolarization accompanied by a decrease in membrane resistance similar to the α response observed in the hippocampus. All LC neurons tested showed a hyperpolarization to puffer electrode or

[76] Egan *et al.* (1983).

bath application of NE; no depolarizations were observed [76]. The hyperpolarization was attributed to an increase in K⁺ conductance, and will be discussed below in detail.

Of great interest in terms of synaptic effects between LC neurons was the response to focal electrical stimulation of the slice in the region of the LC [76]. As shown in Fig. 6.17, there was an initial short-duration depolarization followed by a long-lasting hyperpolarization. It was inferred that the depolarization and hyperpolarization were synaptically mediated since they were reversibly blocked in zero Ca²⁺/high Mg²⁺ superfusates. Both the stimulation- and NE-induced hyperpolarizations showed the same characteristics, namely a reversal potential of about 110 mV (left panel, Fig. 6.17), antagonism by bath application of the same concentrations of the α₂ antagonists yohimbine (right panel, Fig. 6.17) and phentolamine, and potentiation by the NE reuptake blocker desmethyylimipramine (DMI). The authors [76] concluded that their data supported the hypothesis that LC neurons can release NE onto the somadendritic membrane of other LC neurons and thereby provide local feedback inhibition. These *in vitro* data support the earlier conclusions from *in vivo* data [77] on the presence of α₂-mediated LC–LC feedback inhibition.

[77] Aghajanian *et al.* (1977).

Table 6.1. Adrenergic Receptor Type^a

	β	α (unclassified)	α ₁	α ₂
Location	CA1 (β ₁), graunle cell, in hippocampus; Sensorimotor neocortex (β ₁)	Locus coeruleus, PNS, cerebellum	1. Dorsal raphe 2. LC, mPRF neurons, dorsal mtr. vagus, supraoptic nuc.	CA1 (presumptive), locus coeruleus, mPRF neurons, dorsal mtr. vagus, Sub. gelatinosa, sympathetic pregang. neurons
Effects on: Membrane potential	↓ AHP (slow), ↓ accommodation	↓ Ca ²⁺ -dependent action pots. (LC)	1. ↓ Early transient outward rect. 2. Depolarize, ↑ resistance	Hyperpolarization, ↓ resistance
Current	↓ Ca ²⁺ -dependent K ⁺ current	↓ Low- and high-threshold Ca ²⁺ current	1. ↓ I _A 1. ↓ K ⁺ current	↑ Anomalous rectification (K ⁺ current)
Typical agents				
Agonist	Isoproterenol		Phenylephrine	Clonidine
Antagonist	Propranolol		Prazosin	Yohimbine

^a PNS, peripheral nervous system; mPRF, medical pontine reticular formation; AHP, afterhyperpolarization; rect., rectification. References for antagonists are: yohimbine (Williams *et al.*, 1985; Crepel *et al.*, 1987), prazosin (Aghajanian, 1985; Crepel *et al.*, 1987), propranolol (Madison and Nicoll, 1986a,b). Other references in text, except: sensorimotor cortex (Foehring *et al.*, 1989, who also report a β₁ reduction in a Na⁺-dependent K⁺ current); dorsal motor vagus (Fukuda *et al.*, 1987); supraoptic nuc. (Yamashita *et al.*, 1987); and sympathetic preganglionic neurons (Yoshimura *et al.*, 1987). Note the presence of two types of α₁ effects; the α₁ excitatory effects are developmentally transient in the LC.

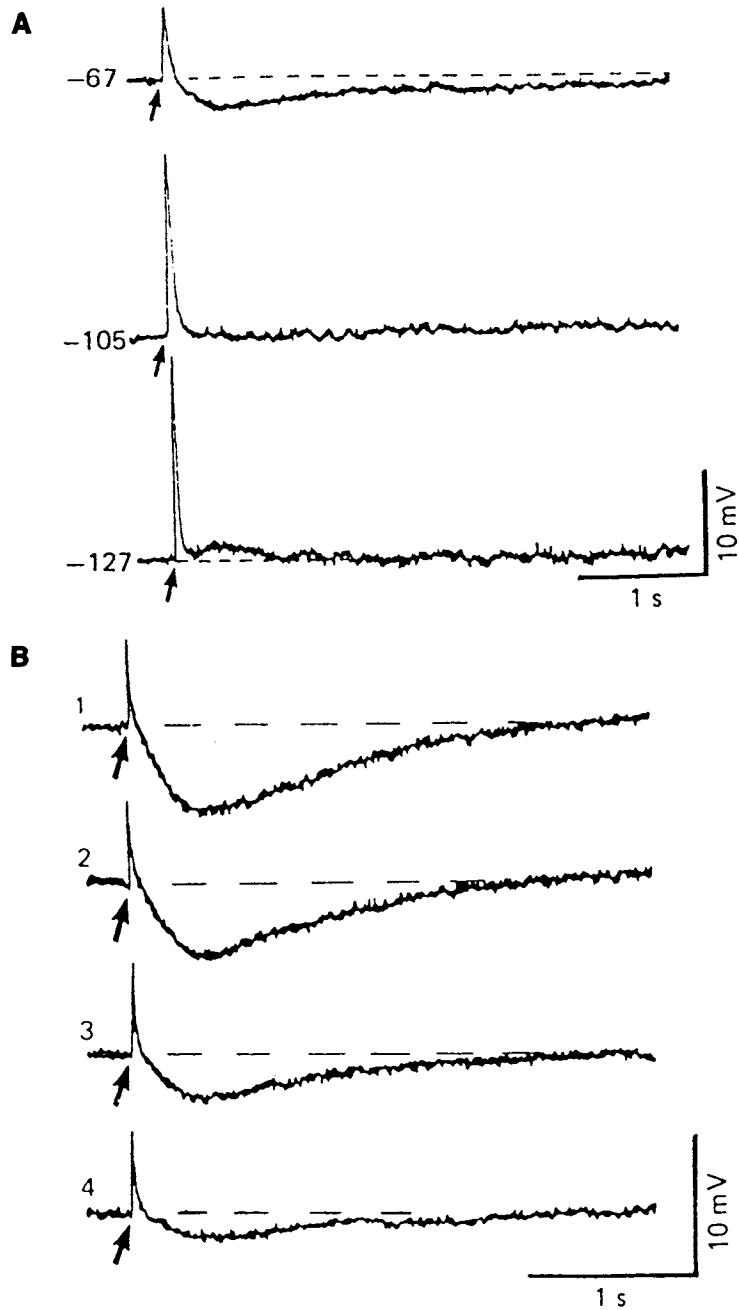


Figure 6.17. Reversal potential and yohimbine antagonism of IPSPs in locus coeruleus (LC) neurons elicited by focal electrical stimulation within the LC zone in the rat LC slice preparation. A, top trace is control condition, showing the stimulation-induced short-duration excitatory postsynaptic potential (EPSP) and long-duration IPSP. At -105 mV membrane potential, the IPSP is nulled and is reversed at -127 mV. The reduction in duration of both the EPSP and IPSP at -105 and -127 mV is likely due to membrane rectification at these hyperpolarized potentials. B, top trace is control condition, subsequent traces show progressive reduction of the IPSP but not EPSP by progressively greater superfusate concentrations of the α_2 antagonist, yohimbine at (2) 10 nM, (3) 30 nM, and (4) 100 nM. Modified from Egan *et al.* (1983).

[78] Williams *et al.* (1985).

Subsequent work has more precisely characterized the receptor type and NE effects [78]. NE was found to produce only hyperpolarizations (no depolarizations) in all LC neurons examined. That the mediating receptor was α_2 was supported by reproduction of the effect by the α_2 agonist clonidine, but not by the α_1 agonist phenylephrine or β agonist isoproterenol, which at $10 \mu\text{M}$ had no effects, although higher concentrations ($30\text{--}100 \mu\text{M}$) produced a slight hyperpolarization. The concentration response curves for clonidine and NE were shifted rightward in a parallel manner by the α_2 antagonists RX 781094, yohimbine, phentolamine, and piperoxan. Fig. 6.18 illustrates the concentration-dependent hyperpolarization of NE and the competitive antagonism of phentolamine.

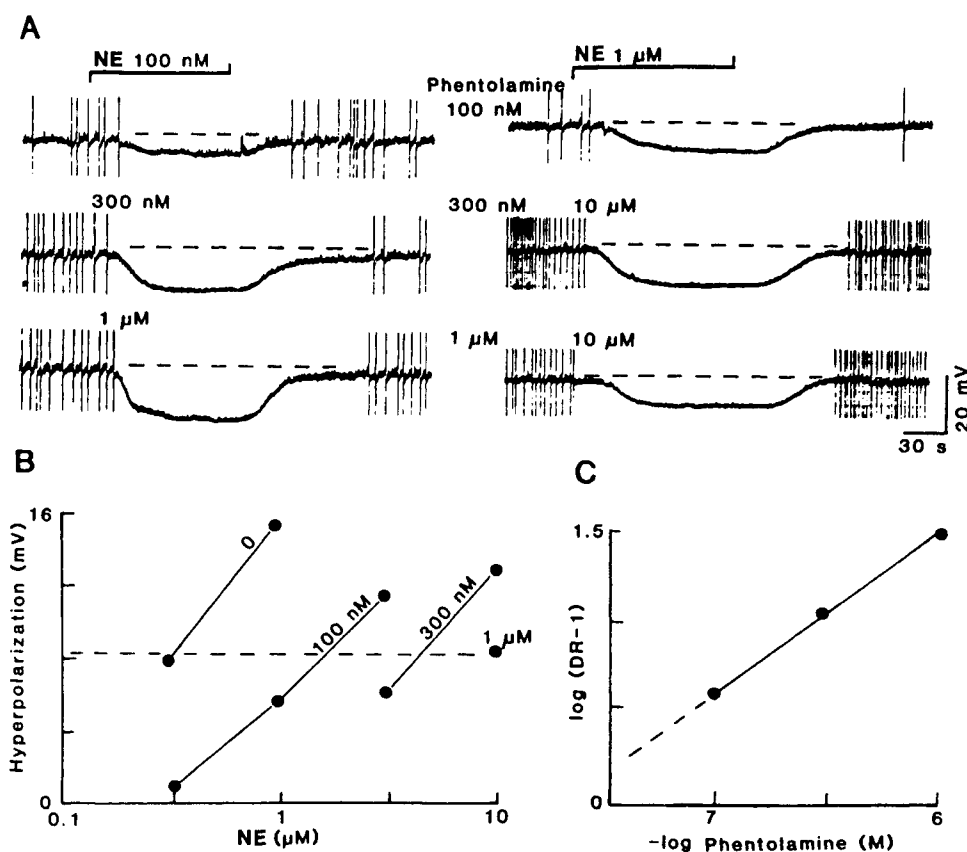


Figure 6.18. Competitive antagonism of norepinephrine (NE) by phentolamine on a single *in vitro* locus coeruleus neuron. A, left panel shows the concentration dependent hyperpolarization produced by superfusion of NE ($1 \mu\text{M}$ desmethylimipramine added to block NE uptake), and the right panel shows the antagonistic effect of addition of the indicated concentrations of phentolamine. B, concentration response curves for NE in the presence of 0, 100, and 300 μM concentrations of phentolamine. The broken line indicates the effect level selected for the Schild Plot, shown in C. The slope is not significantly different from 1.0 and the intercept gives a phentolamine K_i of $19 \mu\text{M}$. Modified from Williams *et al.* (1985).

Voltage clamp recordings have clarified the nature of K^+ conductances in LC neurons [79]. At membrane potentials more negative than about -60 mV, the steady-state slope conductance increased with successive hyperpolarizations, that is, inward rectification was present, confirming some inferences [80]. The I/V relationship of the LC neurons in this voltage range was modeled with excellent fit as the result of a voltage independent K^+ conductance and a voltage sensitive conductance in series. Experimentally, the voltage sensitive conductance had the characteristics of the “classical” inward rectifier [11] in terms of rapid kinetics of activation. This inward rectifier conductance, G_{ir} , was well-described by a sigmoid curve with half maximal conductance centered at about E_k and, as is true for G_{ir} in a number of tissues [81], had a slope dependent on external K^+ concentration. Thus, increasing external K^+ concentrations shifted the curve to less negative potentials and steepened its slope.

Two classes of agonists (α_2 adrenoceptor and μ opioid) increased K^+ conductance in LC neurons and occlusion experiments suggested they acted on the same K^+ conductance [82]. Furthermore, the μ and α_2 agonist-induced shifts in the I/V curve were identical [79]. Both μ and α_2 agonists produced a voltage sensitive, inwardly rectifying K^+ conductance; the steady-state I/V values for an agonist (μ and α_2 agonists gave similar results) are compared with control values in Fig. 6.19A. The agonist K^+ conductance could not be accounted for by a simple increase in the voltage-insensitive K^+ conductance, G_{ir} , or its maximum value. Rather, an additional agonist-induced K^+ conductance, G_{ag} , with different voltage sensitivity was present. While G_{ag} could be mathematically described by a sigmoid function of the same form as G_{ir} , G_{ag} differed in having a half maximal value that was approximately -50 mV vs the more negative value (E_k) for G_{ir} . Furthermore, altering external K^+ concentration did not appreciably shift the half maximal value for G_{ag} although the slope increased with increasing external K^+ concentration. In summary, the μ and α_2 agonist-induced conductance shows inward rectification centered around the resting potential instead of being centered around E_k , as is true for the classical “inward rectifier.”

The G_{ag} was similar to the G_{ir} in terms of activation kinetics and sensitivities to blocking agents, leading to the speculation [79] that the same channels were involved but that when they bind G-protein, thought to be activated by μ and α_2 agonists [82], the half maximal activation point was shifted from close to E_k to close to the resting potential (-55 mV). The functional implication of the agonist conductance curve is that the conductance increase by the

[79] Williams *et al.* (1988a).

[80] Osmanovic and Shefner (1987).

[81] Noble (1985).

[82] North and Williams (1985); North *et al.* (1987).

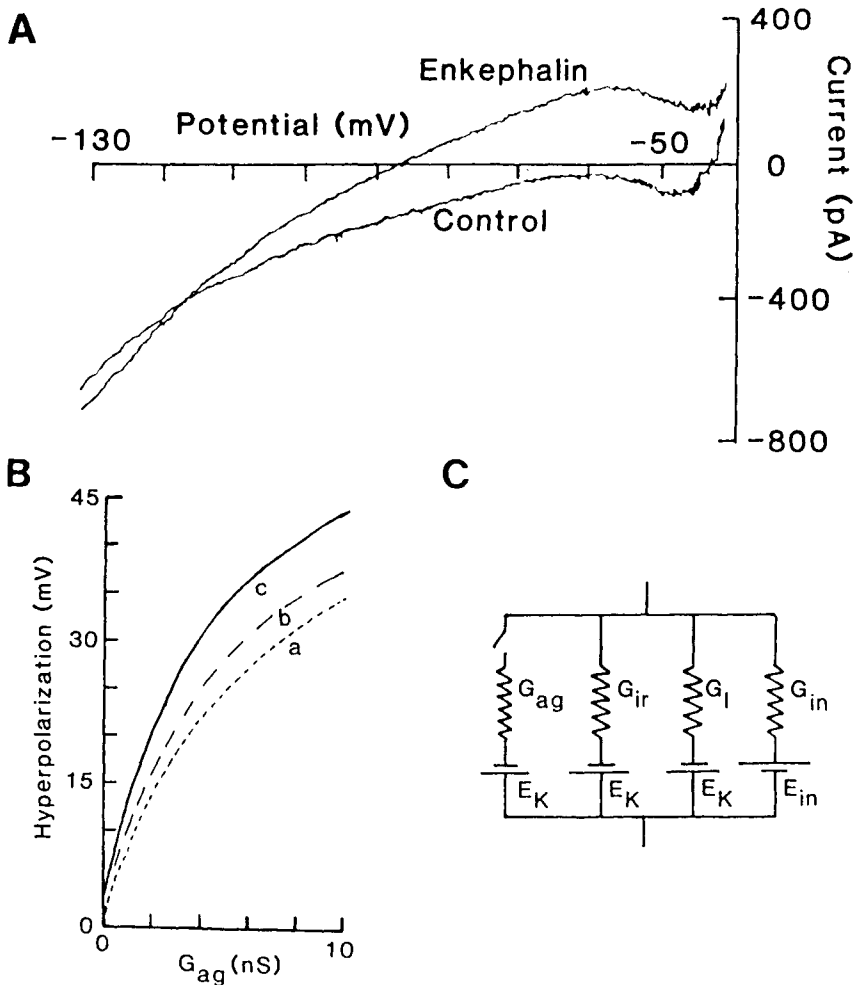


Figure 6.19. A, control and agonist steady-state I/V plots for an locus coeruleus (LC) neuron recorded *in vitro*. The agonist generating this plot was [Met]enkephalin ($10 \mu\text{M}$) in superfusate, but the shape is also characteristic of the I/V plots generated by α -2 agonists (Williams *et al.*, 1988). Note the voltage sensitivity (inward rectification) of both the control and agonist plots at values more negative than -60 mV. B, amplification of hyperpolarizing agonist responses by voltage-sensitive LC membrane conductances. The ordinate shows the hyperpolarization caused by a given increase in K^+ conductance caused by an agonist (abscissa) under three models. Curve a assumes a linear membrane response: $G_{\text{total}} = \text{voltage independent conductance (leak, } G_l) + G_{\text{ag,constant}}$. Curve b assumes an inward rectifier membrane, whose voltage sensitivity is indicated by $G_{ir}(V)$: $G_{\text{total}} = G_l + G_{ir}(V) + G_{\text{ag,constant}}$. Curve c assumes both an inward rectifier membrane and a rectifying agonist conductance, $G_{ag}(V)$: $G_{\text{total}} = G_l + G_{ir}(V) + G_{ag}(V)$. Note that for a 1 nS agonist conductance increase the linear, voltage-insensitive model (curve a) predicts only a 5 mV hyperpolarization while the correct voltage-sensitive model (curve c) indicates a 12 mV hyperpolarization will occur. For these computations: resting conductance at -60 mV = 4.2 nS; $G_{ir}(V) = \text{maximum } G_{ir} / \{1 + \exp[(V_{\text{membrane}} - E_k)/k]\}$, where $E_k = -116$ mV, $k = 15$; $G_{ag}(V) = \text{maximum } G_{ag} / \{1 + \exp[(V_{\text{membrane}} - V^*)/k]\}$, where $V^* = \text{half max } G_{ag} = -50$ mV. C, equivalent circuit for modeling K^+ conductances in part B for LC neuron. G_{ag} , G_{ir} , G_l , as in B. G_{in} = non-specific conductance for all other ions; it and E_{in} were calculated so that there was zero membrane current at -60 mV. Modified from Williams *et al.* (1988)

agonists is high at the resting potential, and its voltage sensitivity means it continues to increase with further hyperpolarization, and this effect is further amplified by the presence of the G_{ir} . Figure 6.19B graphs the difference in conductance changes brought about by the agonist and inward rectifier voltage-sensitivity compared with a purely linear membrane response, and Fig. 6.19C shows the membrane equivalent circuit for these K^+ currents. Other α -mediated hyperpolarizations have been reported in the spinal cord [83] and the cerebellum [84].

The second class of LC response to NE was an inhibition of the Ca^{2+} action potential [85] mediated by an α receptor of unknown subtype. Neither the α_1 antagonist prazosin nor the α_2 antagonist yohimbine were effective in antagonizing this response. Although an increase in K^+ conductance could not be ruled out as the mechanism for inhibition of the Ca^{2+} action potential, a direct effect on Ca^{2+} currents was thought to be more probable.

In the vertebrate peripheral nervous system, high-threshold Ca^{2+} currents responsible for high-threshold Ca^{2+} action potentials have been shown to be antagonized by NE [86]. A low-threshold Ca^{2+} current was reported to be antagonized by α receptor activation in Purkinje neurons of the cerebellum [87]. This antagonism was blocked by the α_1 -receptor antagonist prazosin but not by the α_2 -receptor antagonist yohimbine. A similar NE effect has also been observed in cultured chick dorsal root ganglia neurons and sympathetic neurons recorded with patch clamp techniques [88].

The α -receptor activation in Purkinje neurons also resulted in a hyperpolarization, an effect similar to that observed in LC neurons. In marked contrast to the LC, however, the NE-elicited hyperpolarization in Purkinje neuron was accompanied by an increase in resistance, which was antagonized by the α_1 -receptor antagonist, prazosin. The mechanism of action for this hyperpolarization and conductance decrease remains to be examined, especially with respect to its sensitivity to Ca^{2+} channel blockers and alterations in external K^+ ion concentrations. Furthermore, receptor type mediating both this response and the reduction of low-threshold Ca^{2+} current is not clear since the α_2 agonist clonidine elicited them and the α_1 -antagonist blocked them.

In the young rat (8–26 days) slice preparation, a depolarizing response was observed to phenylephrine that was antagonized by prazosin, consistent with an α_1 -mediation [89]. This response was not present in slices from older animals, where phenylephrine either had no effect or hyperpolarized neurons. This developmentally transient response was consistent with that observed earlier in LC

[83] North and Yoshimura (1984); Wohlberg *et al.* (1986).

[84] Bloom (1978).

[85] Williams and North (1985).

[86] Dunlap and Fischbach (1981); Galvan and Adams (1982); Forscher and Oxford (1985); Marchetti *et al.* (1986).

[87] Crepel *et al.* (1987).

[88] Marchetti *et al.* (1986).

[89] Williams and Marshall (1987).

[90] Finlayson and Marshall (1986).

[91] Jones *et al.* (1985b). This paper did not provide data on changes in brain-stem α_1 receptors.

[92] Jones *et al.* (1985a).

[93] Young and Kuhar (1980).

neurons in culture [90]. This electrophysiological demonstration of a transient α_1 response is paralleled by an *in vitro* autoradiography developmental study in rats utilizing [125I] HEAT (2-beta-[4-hydroxyphenylethylamino-methyl]tetralone) as the α_1 ligand. In globus pallidus, HEAT-binding sites increased in the first 2 weeks of neonatal life before decreasing to near adult levels at day 35 [91]. Using the same ligand in adult rats showed a moderate labeling of mesencephalic reticular formation, with increased density in central gray, dorsal, and median raphe nuclei and lateral reticular nucleus [92], but medial pontine and bulbar reticular formation did not label strongly. The HEAT ligand showed a dense labeling of the LC, but it should be cautioned that other authors [93] found little LC binding of another α_1 antagonist, [3H]-WB 4101, but did find binding of the α_2 receptor ligand p-[3H]aminoclonidine, and the physiological studies cited above suggest α_2 receptors. The latter authors [93] did not indicate a high density of either α_1 or α_2 receptors in medial reticular formation, but they, as is true of most binding studies, did not take into account the lower "packing density" of mPRF neurons because of the presence of extensive fiber tracks in the reticular formation.

6.2.1.2. Dorsal Raphe

[94] Aghajanian (1985).

[95] Burlhis and Aghajanian (1987).

α_1 -receptor activation in dorsal raphe (DR) neurons was observed to antagonize A-current [94]. Phenylephrine had no direct effect on the low-threshold calcium current [95].

6.2.1.3. Pontine Reticular Formation

[96] Greene and Carpenter (1985).

[97] Greene *et al.* (1989b; see also Chapter 5).

With respect to the mPRF, *in vivo* microiontophoretic experiments [96] indicated that both reticulospinal and unidentified mPRF neurons were inhibited by NE, although the *in vivo* nature of the experiment precluded analysis of effects on membrane potential, resistance, or specific ionic conductances. Initial data utilizing the pontine reticular formation slice preparation [97] have shown that some mPRF neurons respond to bath applied NE in the presence of TTX with a hyperpolarization that reversed with wash-out of NE, consonant with the *in vivo* work. This response was mimicked by clonidine and accompanied by a decrease in input resistance (Fig. 6.20B); data on the reversal potential suggest it may be due to an increase in a K^+ current. These effects of NE are consistent with an α_2 inhibitory response, and with the model of sleep cycle control presented in Chapter 12. Still other mPRF neurons in the slice preparation responded to

bath-applied NE with a depolarization and an increase in input resistance. This response was mimicked by phenylephrine (Fig. 6.20A), and was thus consistent with an α_1 response. The α_1 agonists increased the frequency of inhibitory PSPs (Fig. 6.20A). Both the depolarizing and hyperpolarizing effects were seen in the presence of TTX, indicating the effect was direct, and not synaptically mediated.

The α_1 depolarizing effects were seen in a majority of mPRF neurons—a result that was somewhat unexpected in view of the *in vivo* results [96] showing that NE uniformly produced suppression of firing. It is possible that the *in vivo* firing suppression might have resulted from shunting of excitatory input by the NE-induced inhibitory PSPs. It is also possible that the α_1 depolarizing response found in slices from young rats might be developmentally transient, as was reported for α_1 depolarizing response in LC neurons (see Section 6.2.1.1). Another possible reason for differences between the cat *in vivo* and rat *in vitro* work is species differences.

6.2.2. Basal Forebrain

Work in guinea pig slices from cholinergic and non-cholinergic nucleus basalis neurons showed that more

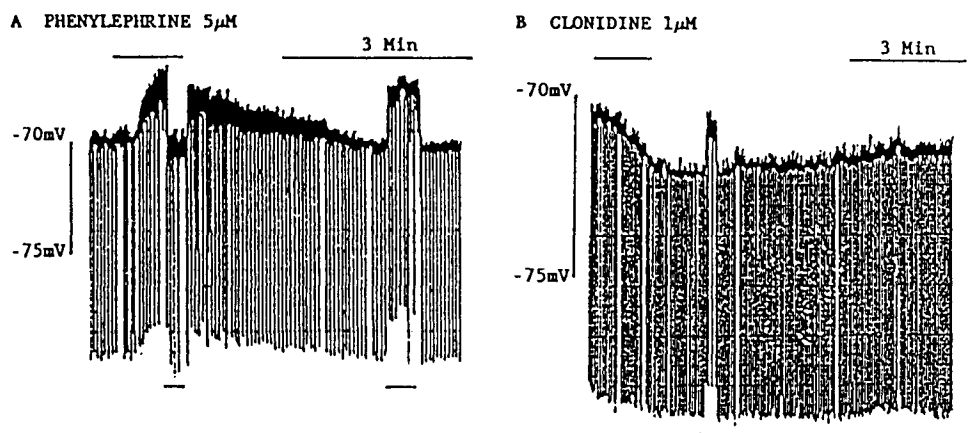


Figure 6.20. Depolarizing and hyperpolarizing responses of mPRF neurons *in vitro* to noradrenergic α agonists. A, depolarization from bath application of an α_1 agonist, phenylephrine, 5 μ M, at the time indicated by the bar. Downward deflections result from constant current pulses injected intracellularly to monitor input resistance, and at the times indicated by the bars membrane potential was returned to resting or to maximal depolarized levels to control for the nonspecific effects of intrinsic voltage sensitive currents on input resistance. Note that phenylephrine produces an increase in input resistance. Note also the increase in postsynaptic potentials (thickened baseline); KMeSO₄ recording electrodes indicated these were hyperpolarizing. B, hyperpolarizing response to bath application of the α_2 agonist, clonidine, 1 μ M. Chart record and downward deflections as in part A; note that clonidine produces a decrease in input resistance. Modified from Greene *et al.* (1989b).

[98] Fort *et al.* (1995, 1998).

than half of those cells were depolarized by NE, whereas approximately 15% were hyperpolarized by both NE and muscarine [98]. In cholinergic cells, the excitatory effect of NE was blocked by the α_1 receptor antagonist prazosin, but not by the α_2 antagonist yohimbine, and it was mimicked by the α_1 agonist 1-phenylephrine, thus indicating mediation by an α_1 adrenergic receptor.

6.2.3. Thalamus

[99] Rogawski and Aghajanian (1980a, b); Kayama *et al.* (1982).
[100] Phillis and Tebecis (1967); Pape and Eysel (1987).
[101] McCormick and Prince (1988).

NE actions studied *in vivo* were generally described as excitatory in the rat LG and PG nuclei [99], but mainly depressive on spontaneous and evoked activities of cat LG neurons [100]. *In vitro* studies of LG neurons of guinea pig and cat showed that NE slowly depolarizes the cell and induces an increase in membrane resistance [101]. The slow depolarization is caused by blockage of a resting K^+ conductance. Thus, NE acts similarly to ACh in blocking the burst firing mode and transforming it into single spike discharges. Of course, this NE action (namely, that NE activates thalamic neurons synergically with ACh) is only possible during waking, when LC neurons are tonically active. The only source for thalamic and cortical activation during the other EEG-activated state, REM sleep, are brainstem and basal forebrain cholinergic neurons, which are active during both wakefulness and REM sleep (see Chapter 9).

[102] Foote *et al.* (1975); Phillis and Kostopoulos (1977); Stone and Taylor (1977b); Waterhouse and Woodward (1980); Waterhouse *et al.* (1981, 1982).
[103] Foehring *et al.* (1989). The depolarizing effects elicited by NE on sensorimotor cortical neurons have been confirmed in a study on corticotectal and corticopontine layer V neurons (Wang and McCormick, 1993). The latter authors showed a mediation by α_1 adrenoreceptor, as the effects were mimicked by phenylephrine and blocked by prazosin. That the NE-induced increased excitability of neocortical neurons can also be mediated by β adrenergic agonists (such as isoprenaline) was shown by Dodt *et al.* (1991).
[104] Madison and Nicoll (1986a, b).

6.2.4. Neocortex and Hippocampus

The different results obtained in extracellular recordings of neocortical neurons *in vivo*, showing depressive as well as excitatory effects [102], varied with different anesthetics and cellular types that were not fully identified in those earlier studies. Studies *in vitro* on large-size neurons from layer V of cat sensorimotor cortex revealed that NE usually caused a small depolarization and reversibly reduced the slow afterhyperpolarizing potential (sAHP) [103]. These effects on membrane potential and sAHP were mimicked by the β -adrenergic agonist, isoproterenol.

NE effects have been extensively studied in hippocampus, but, since these data have been reviewed extensively elsewhere, we here will sketch only a broad outline of effects, so as to serve for comparison with the more detailed exposition of brainstem effects (see Section 6.2.1). Hippocampal CA1 neurons respond to NE with a reduction in the Ca^{2+} -dependent long duration AHP and associated accommodation [104], an effect mediated by

β_1 -receptor activation. This results in an increase in cyclic AMP that, in turn, reduces the Ca^{2+} -dependent K^+ current responsible for accommodation and the long duration AHP. No effect was observed on Ca^{2+} current in these neurons. Activation of the β receptor also elicits a membrane depolarization in 80% of the neurons, probably as a result of reduction of Ca^{2+} -dependent K^+ current [105]. In 70% of CA1 neurons, an α -mediated membrane hyperpolarization (possibly α_2) accompanied by a decrease in input resistance was also reported. The activation of an α receptor presynaptic to the CA1 neurons has been reported to reduce IPSP amplitude while increasing the frequency of spontaneous IPSPs [106]. In granule cells of the hippocampus, β -receptor activation elicits an increase in Ca^{2+} current [107]. As with β effects in CA1 neurons, this may have been mediated by cyclic AMP. Also similar to effects on CA1 neurons, NE was observed to antagonize the long duration AHP and associated accommodation in granule cells [108].

[105] Haas and Greene (1986).

[106] Madison and Nicoll (1988).

[107] Gray and Johnston (1987).

[108] Malenka *et al.* (1986); Haas and Rose (1987).

6.3. Serotonin

It is now clear from intracellular recordings of *in vitro* preparations of both invertebrate and vertebrate CNS that serotonin (5-HT) elicits a wide variety of changes in ionic conductances.

At least seven different responses to 5-HT have been described in neurons from the molluscan CNS. The first six involve increases in conductance to Na^+ (fast and slow), K^+ , and Cl^- , and decreases in conductance to K^+ and to a cation nonselective conductance of Na^+/K^+ [109]. The 5-HT-elicited reduction of K^+ conductance has been further characterized as a reduction in an outwardly rectifying, steady-state current with no threshold for activation (thus, distinguishing it from M-current). It has been named "S-current" and is suggested to mediate the facilitation responsible for sensitization of the tail and siphon-gill withdrawal reflexes [110]. The increase in K^+ conductance by 5-HT results from an increase in the anomalous rectifier K^+ current probably due to an increased number of functional channels [111]. A seventh response was described as an increase in voltage-sensitive Ca^{2+} conductance [112].

[109] Gerschenfeld and Paupardin-Tritsch (1974).

[110] Siegelbaum *et al.* (1982); Pollock *et al.* (1985).

[111] Gunning (1987).

[112] Pellmar and Carpenter (1980); Paupardin-Tritsch *et al.* (1986).

In the peripheral nervous system of vertebrates, at least four types of 5-HT receptors have been classified [113]: 5-HT_{1A}, 5-HT_{1B} (both evoke inhibition), 5-HT₂ (excitatory), and 5-HT₃ (excitatory). There are selective antagonists: spiperone (for 5-HT_{1A}), ketanserin (for 5-HT₂),

[113] Reviewed in Richardson and Engel (1986).

and ICS205-930 (for 5-HT₃). Agonists are 5-carboxyamidotryptamine (5-CT) for 5-HT_{1A-B}, 5-alpha-methyl-5-HT for 5-HT₂ and 2-methyl-5-HT for 5-HT₃ receptors. Radioligand binding studies, models of 5-HT agonist mediated motor disturbances, microiontophoretic electrophysiological studies, and cellular studies of cultured neurons suggest the presence of at least four 5-HT receptors in mammalian CNS [114]. However, classification based on the interaction of the above mentioned agents with electrophysiologically identified serotonergic receptors in *in vitro* preparations is yet not extensive, although current work in these areas is both promising and growing.

[114] Aghajanian (1981);
Pedigo *et al.* (1981);
Peroutka *et al.* (1981);
Lucki *et al.* (1984);
Goodwin and Green
(1985); Yakel *et al.* (1988).

6.3.1. Brainstem

6.3.1.1. Dorsal Raphe

Intrinsic and ligand-induced K⁺ conductances in presumptively serotonergic DR neurons *in vitro* have been investigated [115]. Two intrinsic and one 5-HT-induced inwardly rectifying conductances have been described. One intrinsic conductance exhibited the characteristics of the classic inward rectifier, and thus was similar to the G_{ir} described for LC neurons (see Section 6.2) in that there was a rapid activation (5 ms), Ba²⁺-sensitive, with a voltage sensitivity centered about E_k. The second intrinsic, inwardly rectifying K⁺ conductance was seen at potentials negative to -70 mV where there was a slowly activating (0.3–1 s), noninactivating, and Ba²⁺-insensitive but Cs⁺-sensitive inward current. This current thus resembled the Q-current described previously [69]. The Q-like current had only a minor role in total membrane conductance under conditions of normal K⁺ concentrations, but the G_{ir} had a relatively prominent role in many neurons. For the DR population as a whole, the slope conductance increase for G_{ir} was about one-half that seen in LC neurons.

[115] Williams *et al.*
(1988b).

The 5-HT₁ agonist 5CT produced a hyperpolarization by means of an increased K⁺ conductance that was inwardly rectifying (Fig. 6.21). The 5CT-induced hyperpolarization was dose dependent and was blocked by prior treatment with pertussis toxin, suggesting a G-protein linked between the 5-HT₁ receptor and the K⁺ channel. It is of interest that the GABA_B agonist baclofen had parallel effects, both producing the inwardly rectifying K⁺ conductance, and being blocked by pertussis toxin. Further, occlusion experiments suggested the same channel was affected by both 5CT and baclofen.

Focal electrical stimulation of the DR produced hyperpolarizing potentials in DR neurons; these were

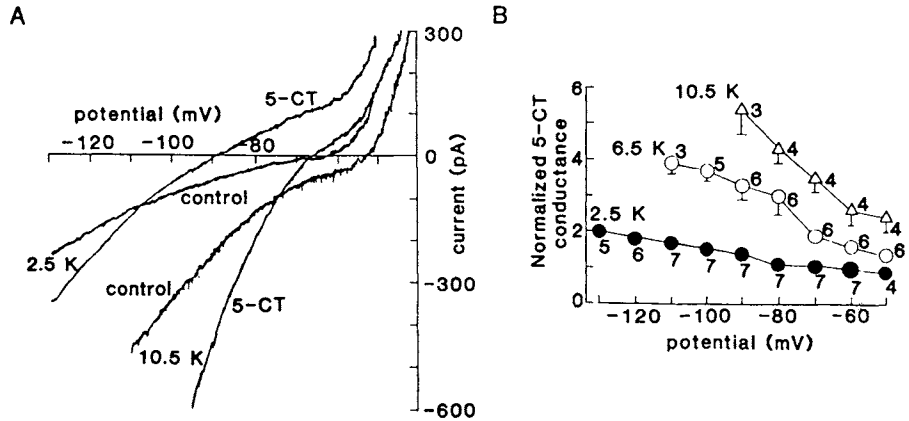


Figure 6.21. The 5-HT₁ receptor-induced increase in K⁺ conductance in dorsal raphe neurons *in vitro* rectifies inwardly. A, steady-state current-voltage plots in the presence and absence of the 5-HT₁ agonist 5-carboxyamidotryptamine (5-CT) in two concentrations of K⁺. Note the reversal potential shifts to a less negative potential in high K⁺. B, the 5-CT conductance increases as the membrane potential is made more negative and the slope increases in high K⁺ concentrations. Normalized conductance is expressed in terms of the conductance obtained at -60 mV in 2.5 mM potassium for each of the DR neurons sampled; each point is an averaged value for the given N. Modified from Williams *et al.* (1988b).

5–20 mV in amplitude, 1–2 s in duration, reversed at the K⁺ equilibrium potential, and were reversibly antagonized by LSD and methylsergide and enhanced by the 5-HT uptake inhibitor imipramine, thus suggesting they were caused by synaptic release of 5-HT, presumably from recurrent collaterals of DR neurons [116]. The electrically induced hyperpolarizations were similar to those caused by the 5-HT₁ agonist 5CT, since they were mediated by an inwardly rectifying K⁺ conductance with comparable characteristics [115] (see Fig. 6.22). It may be noted that these data provide strong support for the hypothesis of 5-HT-mediated DR-to-DR feedback inhibition, much as was noted for the LC-LC α₂-mediated feedback inhibition in Section 6.2.1.1. This postulate is important for the model of sleep cycle control to be presented in Chapter 12.

[116] Yoshimura and Higashi (1985).

6.3.1.2. Pontine Reticular Formation and Facial Motoneurons

In vitro studies using 5-HT application to neurons in the pontine reticular formation slice preparation [117] suggest two major 5-HT effects. One population of neurons responded with a membrane hyperpolarization and decreased input resistance (Fig. 6.23A). Data on reversal potential indicate that a change in K⁺ conductance may be responsible. This would be compatible with a 5-HT₁ response, although appropriate agonists and antagonists have yet to be tested. Still another group of neurons shows

[117] Stevens *et al.* (1989).

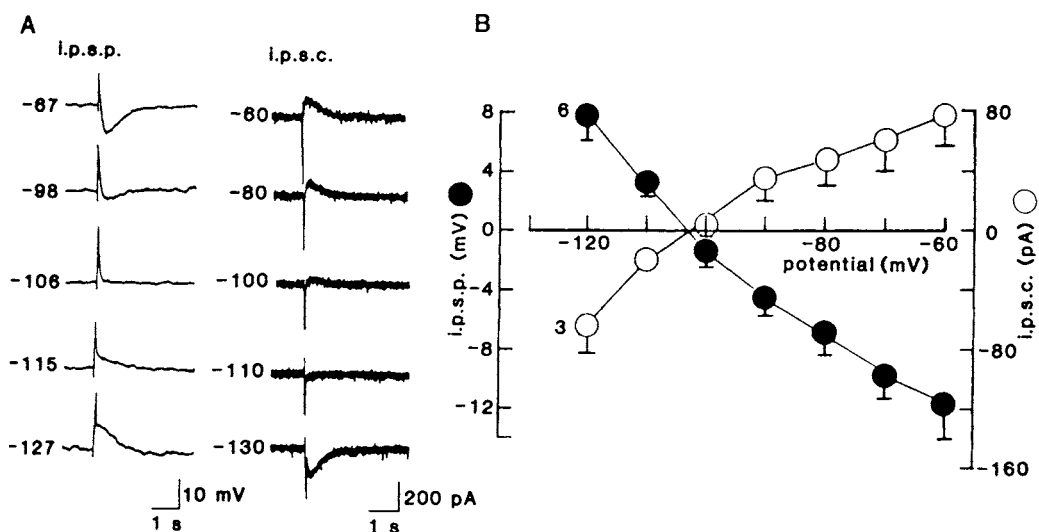


Figure 6.22. Focal electrical stimulation of the dorsal raphe *in vitro* elicits inhibitory synaptic potentials in DR neurons, which is caused by an inwardly rectifying K^+ conductance. A, voltage (left) and current (right) recordings from a single DR neuron held at various membrane potentials. At potentials near resting the focal stimulation induces a hyperpolarizing

response (i.p.s.p.) with outward current (i.p.s.c.). B, the amplitude of the postsynaptic potential and of the current is a nonlinear function of membrane potential, with a marked increase in inward current at negative potentials (inward rectification) comparable to that induced by the 5-HT_1 agonist 5HC. Modified from Williams *et al.* (1988b).

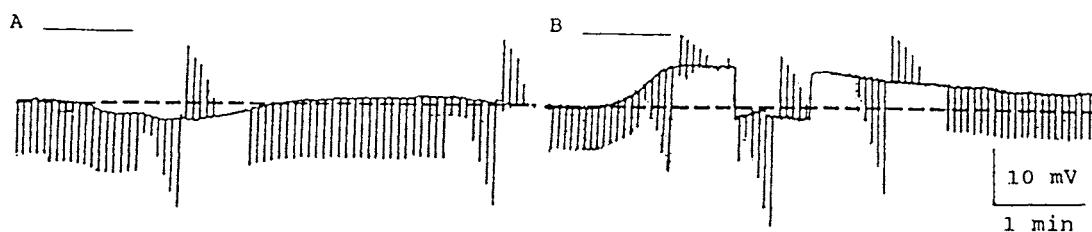


Figure 6.23. Hyperpolarizing response (A) and depolarizing response (B) of two mPRF neurons recorded *in vitro* to the bath application of 5-HT (10 μM , in the presence of 0.5 μM tetrodotoxin) superfused during the period indicated by the horizontal bar above the trace. Deflections are from constant current

pulses used to measure input resistance. Note the hyperpolarizing response is associated with a decrease in input resistance and the depolarizing response with an increase in input resistance. Modified from Stevens *et al.* (1989).

[118] VanderMaelen and Aghajanian (1980).

[119] Luebke *et al.* (1992); Leonard and Llinás (1994); Leonard *et al.* (1995b). In chronic experiments using extracellular unit recordings and microdialysis, discharge activity of REM-on neurons recorded from mesopontine cholinergic nuclei was completely suppressed by local microdialysis perfusion of 5-HT_{1A} agonists (Thakkar *et al.*, 1998).

a depolarization and increased input resistance, compatible with a non- 5-HT_1 response (Fig. 6.21B). Excitatory responses to 5-HT associated with a small decrease in membrane potential and increase in input resistance (probably mediated by a decrease in K^+ conductance) have been observed in facial motoneurons recorded *in vivo* [118].

6.3.1.3. Mesopontine Cholinergic Nuclei

Data on 5-HT effects on neurons recorded from mesopontine cholinergic (PPT/LDT) neurons, including low-threshold bursting ones, consistently showed inhibitory actions, through activation of an inwardly rectifying K^+ conductance, mediated by 5-HT_{1A} receptors [119].

CHAPTER 6

Compared to the consistent results from *in vivo* and *in vitro* intracellular studies with ACh application (see Sections 6.1.3 and 6.1.4), extracellular and intracellular data using 5-HT application report depressive effects on thalamic neurons [120] and both depressant and excitatory actions upon neocortical cells [121].

Recordings from hippocampal neurons *in vitro* have revealed that 5-HT evokes a hyperpolarization mediated by an increase in K^+ conductance that was not dependant on Ca^{2+} but the voltage sensitivity has not been examined [122]. The inhibitory actions of 5-HT in the hippocampus appear to be mediated by a 5-HT_{1A} receptor, as identified by the use of the agonists 5-CT and 8-hydroxy-2-(di-*n*-propylamine)tetralin (8-OH-DPAT) and the antagonistic actions of spiperone [123]. Application of 5-HT to DR neurons *in vitro* produced a hyperpolarization by altering a K^+ conductance [116]; this response was reversibly antagonized by LSD and methylsergide and was enhanced by the 5-HT uptake inhibitor imipramine.

6.4. Excitatory Amino Acids

6.4.1. Summary of Excitatory Amino Acid Receptor Types

As an orientation to excitatory amino acids (EAA) receptor types and physiological characteristics, we summarize previous work on EAA at nonbrainstem sites in Table 6.2. As defined by their specific agonists, three main classes of EAA receptors have been described in the mammalian CNS: the NMDA receptor and two non-NMDA receptors, a quisqualate, and a kainate [124]. Characterization of the receptors in terms of their voltage and ionic sensitivities has now been accomplished by voltage and patch clamp recordings in cultured mammalian CNS neurons. Channels preferentially activated by the non-NMDA receptors had little voltage sensitivity, were selective for monovalent cations (Na^+ and K^+), and had reversal potentials of near 0 mV in physiological media. Channels preferentially activated by the NMDA receptor were voltage sensitive and were selectively permeable to divalent (Ca^{2+} in particular) as well as monovalent cations. Single channel conductance evaluation showed each receptor activated a family of conductances ranging from 2–50 pS; kainate and quisqualate receptors primarily opened channels with smaller conductances (kainate

[120] Kemp *et al.* (1982); Pape and Eysel (1987).

More recently, these depressive effects exerted by 5-HT on thalamic neurons have been confirmed in thalamic slices from ferrets (Monckton and McCormick, 2002). Data showed hyperpolarization of thalamic neurons in a variety of nuclei (mainly associational and intralaminar), due to a direct action on thalamic relay cells through an increase in K^+ conductance and an indirect action through activation of local interneurons. [121] Reader (1978); Olpe (1981). The receptors and underlying cellular mechanisms of these effects remain to be elucidated.

[122] Segal (1980);

Andrade *et al.* (1986).

[123] Beck *et al.* (1985);

Andrade *et al.* (1986).

[124] Watkins and Evans (1981).

Table 6.2. Excitatory Amino Acid Receptor Type (Agonist)^a

Characteristics	NMDA	Quisqualate ^b	Kainate
Voltage sensitivity	+	—	—
Magnesium block	+	—	—
Calcium permeability	+	—	—
Na ⁺ /K ⁺ permeability	+	+	+
Modulation	Glycine ↑, zinc and opiates ↓	—	—
Antagonist	Kynurenate, CPP, APV	Kynurenate, CNQX	Kynurenate, CNQX

^aNMDA = *N*-methyl-D-aspartate; CPP = 3-((+)-2-carboxypiperazin-4-gamma-1)-propyl-1-phosphonic acid; APV = 5-amino-phosphonovaleric acid; CNQX = 2,3-dihydroxy-6-cyano-7-nitroquinoxalone.

^bBeta-L-ODAP (beta-*N*-oxaly-L-alpha, beta-diaminopropionic acid) binds strongly to the quisqualate class of receptors, less strongly to the kainate class, and only very weakly to the NMDA class.

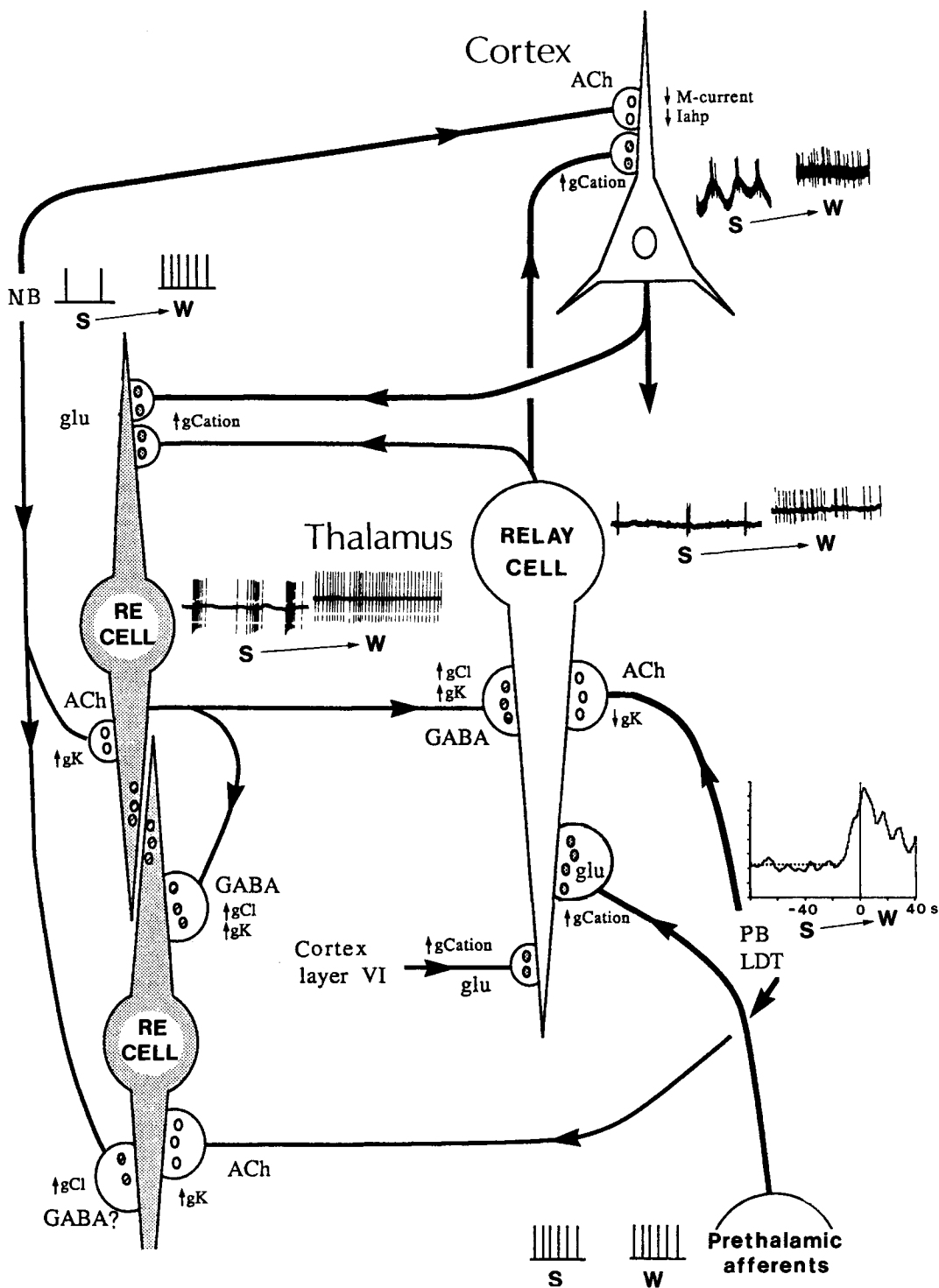
[125] Cull-Candy and Usowicz (1987); Jahr and Stevens (1987).
[126] Nowak *et al.* (1984); Mayer *et al.* (1984).
[127] Herrling (1985).
[128] MacDermott *et al.* (1986).
[129] Collingridge and Bliss (1987).
[130] Ascher and Nowak (1987).
[131] Johnson and Ascher (1987).
[132] Peters *et al.* (1987); Westbrook and Mayer (1987).
[133] Cotman *et al.* (1987).
[134] Perkins and Stone (1982); Cotman *et al.* (1986).
[135] Harris *et al.* (1986).

activation tended toward openings of <5 ps while quisqualate towards 10–15 ps) and NMDA receptors preferentially activated channels with larger conductances of 45–50 ps [125]. The NMDA receptor is of special interest due to its voltage sensitivity, which has been attributed to a voltage sensitive blockade by Mg²⁺ at physiological concentrations [126]. This blockade is removed by depolarization and endows the NMDA response with some regenerative properties. For example, NMDA may only slightly alter the resting properties of a neuron with membrane potential at rest, but once membrane potential is depolarized past the threshold for removal of the magnesium blockade, NMDA may elicit a large burst of action potentials [127].

The Ca²⁺ conductance activated by the NMDA receptor is of importance and interest because it is of sufficient magnitude to raise significantly the intracellular Ca²⁺ concentration of the neuron [128]. This likely affects intracellular signal processing and, in fact, has already been implicated as an integral part of the development of long-term potentiation in hippocampal CA1 neurons [129].

Finally, the NMDA response has been found to be modulated by glycine, zinc, and likely also by opiates [130]. Glycine potentiated the NMDA response with maximal effects occurring at such low concentrations (<2 μM) [131] that it raises the possibility that NMDA responses are modulated by synaptically released glycine in areas with glycinergic transmission, such as may occur in mPRF [23]. Glycine potentiation of NMDA responses was not antagonized by strychnine. Zinc antagonized the NMDA response [132]. Sigma opiate compounds acted as noncompetitive antagonists to the NMDA receptors, but the electrophysiological effects are still unknown [133].

Antagonists, as summarized in Table 6.2, include the nonspecific EAA antagonist kynurenate [134] and the specific NMDA receptor antagonist 3-((+)-2-carboxypiperazin-4-gamma-1)-propyl-1-phosphonic acid (CPP) [135].



6.4.2. Brainstem

6.4.2.1. Mesopontine and Bulbar Reticular Formation

In vivo studies have shown that EPSPs characterized by a distinctive fast time to peak (<3 ms) were readily evoked in the mPRF by stimulation of all areas of the brainstem reticular formation, including mPRF [136]. Such types of EPSPs are also present in mPRF stimulation-recording paradigms in the slice. This fast rise time characteristic was mimicked by iontophoretic application of glutamate or aspartate [23]. In contrast, no other putative transmitter candidate tested (including ACh, NE, 5-HT, and thyrotropin-releasing hormone) elicited such an mPRF response. Behavioral data also indicate the responsiveness of the reticular formation muscle suppression zone in dorsolateral pons to applications of EAA agonists [137]. The phasic depolarizations of alpha lumbar motoneurons during REM sleep are mediated by non-NMDA receptors; some of these PSPs may be mediated by reticulospinal fibers (see Chapter 3). Data supporting an EAA pathway from the nucleus paragigantocellularis in the medulla to the LC are discussed in the next section. At this point we conclude that it is highly likely, although not yet demonstrated in rigorously controlled *in vitro* studies, that EAA are an important class of excitatory brainstem reticular formation neurotransmitters.

Studies on slices from mesopontine cholinergic nuclei showed that the synaptic activation of neurons is mediated by both non-NMDA and NMDA receptors, and indicated that NMDA receptors contribute to the fast excitatory transmission in those neurons [138].

[136] Ito and McCarley (1987); McCarley *et al.* (1987).

[137] Siegel and Lai (1988).

[138] Sanchez and Leonard (1996).

Figure 6.24. Schematic diagram of excitatory amino acids (EAA) and ACh effects on pyramidal-shaped neocortical, thalamocortical (relay), and thalamic reticular (RE) neurons. Direction of axons is indicated by arrows. ACh is released in the thalamus by mesopontine cholinergic peribrachial (PB, or pedunculopontine tegmental) and laterodorsal tegmental (LDT) neurons. In the neocortex, ACh is released by nucleus basalis (NB) neurons. In thalamic relay and reticular neurons, as well as in pyramidal neocortical neurons, EEG-synchronized sleep (S) is characterized by rhythmic inhibitory periods and bursts of action potentials. The information transfer of thalamic relay cells is dramatically reduced during S (see details in Chapter 9). In neocortical cells, the activity evoked by incoming signals is further reduced by due to a relatively uninhibited M-current and slow afterhyperpolarization current (I_{ahp}) that underlie spike frequency adaptation. Upon transition from S to waking (W), the cholinergic PB/LDT neurons increase their rates of spontaneous firing about 20 s before the time 0 of W; an increased activity is also seen in NB cells (see details in Chapter 10). Note that no significant change is seen in neurons recorded from prethalamic relay stations. Increased firing and tonic activity of thalamic relay cells is due to increased release of ACh, as well as glutamate (glu) released by corticothalamic neurons as many brainstem reticular neurons projecting to thalamus, because both these neurotransmitters produce a decrease in a "leak" K^+ current. The hyperpolarization (associated with increased K^+ conductance) of thalamic reticular cells by ACh further excites (by disinhibition) thalamic relay cells. However, reticular neurons increase firing rates upon arousal because of excitatory influences mediated by EAA released by thalamic relay and corticothalamic cells. Scheme of changes in ionic conductances modified from McCormick's review (1990). Data related to S-W behavior of various types of brainstem, thalamic, and neocortical neurons are from chronic experiments by Steriade *et al.* (1974a, 1986, 1990a).

6.4.2.2. Locus Coeruleus

The short latency excitatory response of LC neurons to focal stimulation of the slice has been illustrated in Fig. 6.17. In the *in vitro* LC slice preparation evidence was presented that this fast EPSP results from activation of an EAA receptor [139], complementing *in vivo* data indicating an EAA projection from the nucleus paragigantocellularis in medulla (see Chapter 3).

[139] Williams (1988).

6.4.3. Thalamus and Neocortex

Thalamic and cortical neurons possess both NMDA and non-NMDA receptors [140].

The excitatory responses of thalamic LG cells to optic afferent stimulation are blocked by both NMDA and non-NMDA antagonists [141]. The corticothalamic pathways also use EAA as transmitters since unilateral decortication results in a decline of terminal uptake of aspartate and glutamate in the ipsilateral appropriate thalamic nuclei [142] and D-(³H)-aspartate injected in various thalamic nuclei is taken up by corticothalamic neurons [143]. The TC projections also use EAA as transmitters [144]. This was also inferred from the blockade of visually-evoked responses of simple neurons in the striate cortex by kynurenic acid, a general EAA antagonist [145].

[140] Cotman *et al.* (1987).

[141] Crunelli *et al.* (1985).

[142] Baughman and Gilbert (1980, 1981).

[143] Rustioni *et al.* (1983).

[144] Streit (1980); Ottersen *et al.* (1983).

[145] Tsumoto *et al.* (1986).

The actions of EAA appear mediated by at least three types of receptors. Aspartate seems to act on NMDA receptor [140, 146]. The other types are non-NMDA receptors, quisqualate and kainite [130]. Glutamate appears to act at both NMDA and non-NMDA receptors. Whereas non-NMDA receptor activation induces a fast-rising EPSP with a short decay time, the NMDA receptor activation produces a depolarization with a longer duration [147]. The long-term characteristic of the NMDA response probably accounts for NMDA involvement in plasticity processes of the visual cortex [148], similarly to the long-term potentiation described in the hippocampus [149].

[146] Watkins and Evans (1981).

[147] McLennan (1983); Mayer and Westbrook (1987); Watkins and Olverman (1987).

[148] Artola and Singer (1987).

[149] Collingridge and Bliss (1987).

The striking depolarization produced in cortical cells by EAA is associated with a marked fall in membrane resistance [150], like EEA effects on spinal cord [151] and hippocampal [152] neurons. The excitatory effect of EAA on cortical pyramidal-shaped neurons was also studied *in vitro* [153]. It was found that the depolarizing response to NMDA is voltage-dependent, decreasing in amplitude and duration with membrane hyperpolarization, and that it is associated with an apparent increase in input resistance.

[150] Krnjević (1974).

[151] MacDonald and Wojtowicz (1980).

[152] Dingledine (1983).

[153] Flaunan *et al.* (1983); Thompson (1986a, b).

The combined effects of EAA and ACh exerted on thalamic and neocortical neurons are summarized in Fig. 6.24.

Synchronized Brain Oscillations Leading to Neuronal Plasticity during Waking and Sleep States

The physiological bases of the principal synchronized rhythms of brain electrical activity (EEG) are discussed here because these rhythms are used to objectively identify waking and sleep states. Most of their alterations are induced by increased or decreased activity in brainstem, posterior hypothalamic, and basal forebrain neurons with thalamic, neocortical, and hippocampal projections. The knowledge of cellular mechanisms underlying the synchronization of low- and high-frequency brain oscillations is therefore necessary to understand the role played by generalized modulatory systems in central physiological correlates of behavioral states.

Various types of EEG synchronized waves display slow as well as fast frequencies, from less than 1 Hz to more than 60 Hz or even ultra-fast (80–200 Hz) oscillations. The notion of synchronization supposes the coactivation of large neuronal aggregates whose summated synaptic events and/or intrinsic currents reach such a magnitude that they can be recorded with rather gross recording techniques. There is now ample evidence that EEG activity mainly results from extracellular current flow associated with summated excitatory and inhibitory postsynaptic potentials (EPSPs and IPSPs). However, the long-lasting $I_{K(Ca)}$ and a series of other intrinsic neuronal properties should also be considered as playing a role in the genesis of various EEG waves.

Conventionally, the term EEG synchronization is used as a label for the state of quiet (NREM) sleep. This is justified by the diffuse occurrence over the neocortical mantle of the three major synchronized rhythms (spindles, delta, and slow oscillations) during the state of sleep preceding REM sleep. However, the synonymy between EEG synchronization and

quiet sleep is an oversimplification, since synchronized (sometimes high-amplitude) high-frequency rhythms appear in thalamus and cortical foci during states of increased alertness and synchronized theta waves occur in some species during REM sleep and active wakefulness.

In what follows, we discuss the frequency characteristics and behavioral connotation of the main types of synchronized EEG activity. To a large extent, the identification of pacemakers and the disclosure of cellular bases have been achieved for spindle waves and theta waves. The mechanisms of other synchronized rhythms, such as alpha waves, are as yet poorly understood at the cellular level. We first describe in Section 7.1 four types of synchronized oscillations that appear during the brain-activated states of waking and REM sleep. In Section 7.2, we discuss the mechanisms of generation and synchronization of three types of low-frequency oscillations that characterize the state of NREM sleep. Finally (Section 7.3), we discuss some pathological oscillations that develop during waking and NREM sleep.

Throughout this chapter, we will emphasize that the thalamus and cerebral cortex have to be considered as a unified oscillatory machine under the control of brain-stem and forebrain modulatory systems. This complexity requires investigations in intact-brain preparations.

7.1. Rhythms during Brain-Active States of Waking and REM Sleep

7.1.1. Alpha

Although the description of alpha rhythm (8–13 Hz) dates back to the late 1920s [1], there is no knowledge about its cellular mechanisms because alpha waves have been mainly analyzed from scalp recordings in humans and laminar profiles of cortical field potentials in animals. The mechanisms of this rhythm have been searched by recording spindle oscillations under barbiturate anesthesia [2]; however, although the frequencies of these two rhythms may overlap, their origins, mechanisms, and especially their behavioral context are very dissimilar.

Alpha waves usually occur during relaxed wakefulness and may be a central timing mechanism regulating afferent and efferent signals [3]. The conventional wisdom that the occipital alpha rhythm is associated with reduced visual attention is challenged by the fact that the incidence of alpha waves increases during responses to visual stimuli or concentration on visual imagery [4] and the reports about augmentation of alpha activity during attention

[1] Berger (1929). For a description of different EEG patterns of alpha rhythms in the waking adult, see Niedermeyer (1999).

[2] Andersen and Andersson (1968).

[3] Sanford (1971).

[4] Mulholland (1969).

[5] Creutzfeldt *et al.* (1969); Ray and Cole (1985).

[6] Steriade *et al.* (1969a); Steriade (1991).

[7] Lopes da Silva *et al.* (1973, 1980); Lopes da Silva and Storm van Leeuwen (1977).

[8] Roth *et al.* (1967).
[9] Serman and Wyrwicka (1967).

[10] Gastaut (1952); Pfurtscheller and Neuper (1994).

[11] Howe and Serman (1972).

[12] Rougeul-Buser *et al.* (1983).

tasks [5]. In contrast, spindle oscillations are associated with blockage of synaptic transmission through the thalamus from the very onset of sleep [6], which explains the disconnection from the external world and unconsciousness. Thus, the idea of alpha viewed as an embryo of spindle oscillations is untenable.

The origins of spindle and alpha waves are also different. At variance with the thalamic origin of spindle oscillations (see Section 7.2.1), a series of experimental and modeling data toward the understanding of the origin of alpha rhythm in the dog suggested that alpha waves are mainly generated and spread within the cerebral cortex [7]. Thus, in the visual cortex, alpha waves are generated by an equivalent dipole layer centered at the level of the somata and basal dendrites of pyramidal neurons in layers IV and V. The coherence between alpha rhythms recorded in adjacent (~ 2 mm) foci of the visual cortex is larger than any thalamocortical (TC) coherences measured in the same animal. These findings led to the conclusion that a system of surface-parallel intracortical connections is mainly involved in the spread of alpha activity, while the influence of visual thalamic nuclei over the cerebral cortex is only moderate.

7.1.2. Oscillations during Waking Immobility: The Sensorimotor Rhythm

Synchronized EEG waves within the frequency range of 12–16 Hz have been described during wakefulness associated with complete absence of phasic motor activity. Such oscillations were initially termed the “sensorimotor rhythm” [8], have been postulated to reflect active suppressive or inhibitory processes [9], and are homologous to the μ -rhythm that appears over the central sulcus in humans, which is also related with the blockage of motor activity [10]. Subsequently, this rhythm was more precisely localized within the somatosensory system, as it was recorded in the ventroposterolateral (VPL) thalamic nucleus and its cortical projection area [11].

The patterns of EEG activity during waking immobility (with the exception of occasional eye and tail movements) were analyzed in detail in cats [12]. Different frequencies of oscillations were described while placing the cat in experimental conditions that may be qualified as “hunting” situations. Two distinct behavioral conditions were associated with two different frequencies and cortical locations of oscillations. When the animal was in a position of expectancy, waiting for the unseen mouse to come out through a hole, the rhythms were around 14 Hz and were localized over the

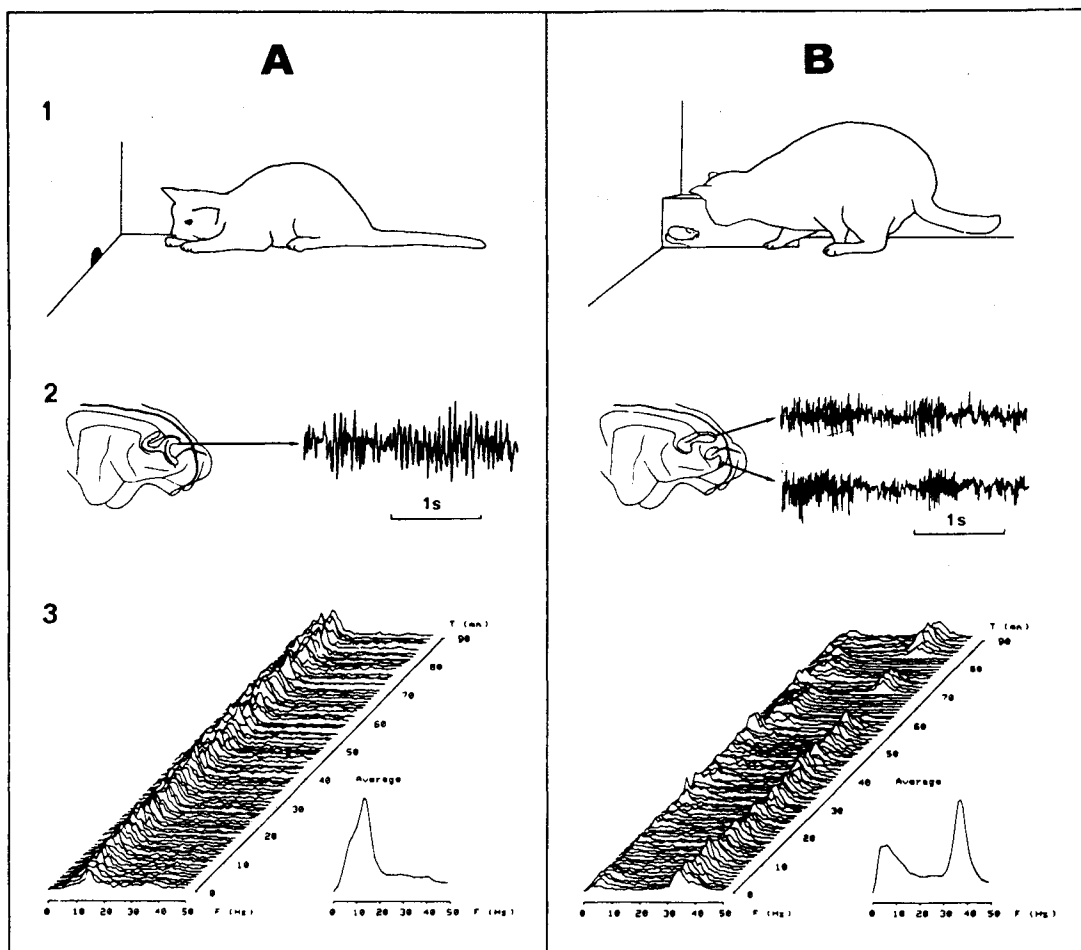


Figure 7.1. Cortical rhythms during waking immobility in cat. A, expectancy, rhythm frequency 14 Hz. B, focused attention, rhythm frequency 36 Hz. See text for behavioral paradigms. In both A and B, 1 illustrates the animal's most common attitudes in the used experimental design and 2 depicts types of rhythmic patterns and their localization: one focus in the primary somatosensory cortex (in A) and

one motor and one parietal focus (in B). In 3, evulsive spectra taken during 90-min recording time. Each spectrum was computed from 1 min recording. Heights of peaks indicate spectral power (in μV^2) in the frequency band 0–50 Hz. Added to each set of evulsive spectra is the average spectrum computed over the 90 min recording time. From Rougeul-Buser *et al.* (1983).

anterior limb zone of primary somatosensory area (Fig. 7.1A). However, when the cat was watching the visible but unsizable mouse, high-frequency (35–45 Hz) rhythms appeared in two foci, one in the pericruciate (motor) cortex, the other in the periansate (parietal association) area (Fig. 7.1B). Similar fast rhythms have been described in the monkey [13].

On the basis of macroelectrode recordings and lesions in the cat thalamus, it was hypothesized that the thalamic source of the 14 Hz rhythm is the VPL nucleus, while the medial part of the posterior thalamic complex (POm) was thought to generate the fast (35–45 Hz) rhythms that

[13] Rougeul *et al.* (1979).

[14] Bouyer *et al.* (1980, 1981, 1987).

[15] Delagrèze *et al.* (1987).

[16] Montaron *et al.* (1982).

[17] Semba and Komisaruk (1984).

[18] Fanselow *et al.* (2001) and Nicolelis and Fanselow (2002) described the neural activity in the VPM thalamus during three behavioral states in rats: quiet waking, whisking (with back-and-forth movements of whiskers at a rate of 4–6 Hz), and whisker twitching (with small movements at a rate of 7–12 Hz). The authors referred to the whisker-twitching-related activity as “bursting” and challenged the idea that bursts of fast action potentials crowning LTSs only occur during the hyperpolarization states of TC neurons (such as slow-wave sleep) on the basis that some studies in the visual thalamus reported “spike-bursts” during wakefulness. With respect to this idea, see note 58 in Chapter 5 showing the absence or extreme paucity (<1%) of bona fide spike-bursts during wakefulness, and a recent commentary (Steriade, 2001c) explaining that, to demonstrate the presence of spike-bursts during wakefulness, intracellular recordings are needed. Otherwise, spike-bursts crowning LTSs may be confounded with brisk firing consisting of trains of single spikes that occur at a depolarized level. That, indeed, wakefulness is associated with depolarization (membrane potential more positive than –60 or –55 mV) of TC cells (Hirsch *et al.*, 1983), when no LTSs can be elicited, was

appear over the pericruciate and periansate cortices [14]. A microelectrode exploration revealed that a very limited number (13%) of VPL thalamic cells changed their discharges when the 14 Hz rhythm occurred in the cortex, and those few neurons displayed various firing patterns during cortical oscillations: tonic firing or phasic discharges related to the cortical rhythm [12]. The spontaneous activity of VPL thalamic neurons fluctuates with the degree of vigilance and with the presence or absence of the cortical 14-Hz rhythm being higher between the trains of 14-Hz waves than during those trains [15].

Despite apparent similarities with spindle waves, the rhythms during waking immobility are basically different from sleep spindles. The dissimilarities do not only concern the 35–45 Hz rhythm that is far beyond the frequency range (7–14 Hz) of spindles, but also the slower (14 Hz) “sensorimotor” rhythm. Indeed: (a) sleep spindles are recorded over extensive cortical areas, whereas the 14-Hz oscillations related to expectancy are restricted within a cortical territory that does not exceed 5 mm²; and (b) cortical spindles are generated by rhythmic high-frequency bursts in TC neurons (see Section 7.2.1), which also contrasts with the few thalamic cells found to discharge in phase with the expectancy rhythm. The location of driving forces and the cellular mechanisms of the 14-Hz expectancy rhythm remain to be elucidated. As to the fast (35–45 Hz) oscillations of pericruciate and periansate cortices, they are suppressed after bilateral electrolytic lesions of the ventral tegmental area of the mesencephalon, thus suggesting that a dopaminergic mechanism is involved in their genesis [16].

When rats are standing or sitting still, whisker twitching is very rhythmic, at a rate of 7–12 Hz [17]. This state is associated with synchronous oscillatory neuronal activity in primary somatosensory (SI) cortex and ventroposteromedial (VPM) thalamus [18].

The intrinsic and network neuronal mechanisms as well as synchronization features of fast (beta and gamma) oscillations occurring spontaneously or triggered by sensory volleys are discussed below (Section 7.1.4).

7.1.3. Theta

The theta rhythm consists of high-amplitude regular waves that appear in the septohippocampal system and related subsystems of nonprimate mammals. Theta waves have a frequency of 4–7 Hz in rabbit and cat, and 6–10 Hz in rat. The relation between theta rhythm and brain-activated states (arousal and REM sleep) is clearly established in rodents. In rat, the animal of choice for the study of theta

rhythm in relation to different types of waking behavior, hippocampal theta waves appear during walking, running, jumping, head movements, and manipulation of objects with the forelimbs, but not during automatic or simple reflexive behavior, such as licking, chewing, or face-washing [19]. In cat, hippocampal theta is more evident during REM sleep than during alertness.

Initially, the septum was regarded as the pacemaker of theta rhythm, a nodal relay between the brainstem and hippocampus, which transforms the steady flow of impulses from the brainstem reticular (RE) core into rhythmic discharges transferred to the hippocampus [20]. The brainstem sites whose electrical stimulation induces hippocampal theta are found along the entire longitudinal extent of the reticular formation, as far caudal as the magnocellular nucleus in the medulla. The frequency and amplitude of theta waves increase by stimulating progressively rostral in the brainstem reticular core [21]. Brainstem reticular impulses reach the septum through the medial forebrain bundle. Septohippocampal neurons have been anatomically traced [22], antidromically-identified [23], and their cholinergic nature is well-established [24].

The mechanism of theta waves was first investigated intracellularly [25]. It was proposed that impulses of septal origin excite hippocampal pyramidal cells that display depolarization-hyperpolarization sequences related to the negative-positive phases of the extracellularly recorded theta. These authors considered the theta rhythm as mainly due to rhythmic EPSPs. The somatic hyperpolarizations were believed to result from the recurrent collateral activation of local-circuit inhibitory cells following the rhythmic discharges of pyramidal neurons driven by septal afferents. A study of the relations between discharges of different types of CA1 and dentate gyrus neurons (pyramidal cells, granule cells, and interneurons) and focal waves in the behaving rat reached the conclusion that, in addition to the recurrent collateral pathway, hippocampal interneurons are driven directly from septal pacemaker neurons as well as from the entorhinal cortex [26]. The noncholinergic entorhinal input was required to explain the failure to eliminate hippocampal theta after atropine administration. In fact, after lesions of the entorhinal cortex, atropine completely eliminates theta rhythm [27]. On the other hand, the direct access of septal cholinergic neurons to hippocampal interneurons is supported by anatomical evidence [28] and by the strong AChE activity coinciding with the distribution of the local-circuit cells in the stratum oriens, radiatum, and the hilus of the dentate gyrus [29]. As to the role played by the entorhinal cortex as a local generator of theta waves, it was found that rhythmic discharges

also demonstrated by increased probability of antidromic responses in these neurons (Glenn and Steriade, 1982).

[19] Vanderwolf and Robinson (1981).

[20] Petsche *et al.* (1965); Gogolak *et al.* (1968).

[21] Vertes (1982).

[22] Segal and Landis (1974).

[23] Lamour *et al.* (1984).

[24] Fibiger (1982).

[25] Fujita and Sato (1964).

[26] Buzsáki *et al.* (1983).

[27] Vanderwolf and Robinson (1981).

[28] Mosko *et al.* (1973).

[29] Mathisen and Blackstad (1964); Vijayan (1979).

[30] Alonso and García-Ausús (1987a–b).

[31] Alonso and Llinás (1988).

[32] Nuñez *et al.* (1987).

[33] Leung and Yim (1986); Soltesz and Deschênes (1993); Buzsáki (1996). A recent review by Buzsáki (2002) discussed in detail the theta dipoles in the CA1 region and the origin of IPSPs in pyramidal neurons produced by the firing of basket and chandelier (GABAergic) neurons.

[34] Krnjević and Ropert (1982); Krnjević *et al.* (1988).

[35] Kamondi *et al.* (1998).

[36] Leung and Borst (1987).

[37] Borst *et al.* (1987).

[38] Traub *et al.* (1987, 1989); Miles *et al.* (1988); Pedley and Traub (1990).

(time-locked with theta waves) are fired by neurons located in layers II and III of this structure [30]. In fact, theta waves can probably be generated within multiple sites of the limbic system. Neurons recorded from the medial subdivision of mammillary bodies display spontaneous oscillations of the membrane potential sustaining rhythmic bursts of discharges; the basic mechanism of these oscillations is a Ca^{2+} -dependent plateau potential [31], different from the Ca^{2+} -dependent low-threshold spike (see Chapter 5). Thus, theta rhythm can no longer be viewed as exclusively generated by a unique pacemaker, the septum, but by an interaction between coupled oscillators within the limbic system.

Although some claimed that theta waves reflect EPSPs and presumably Ca^{2+} -mediated slow spikes in CA1 and CA3 pyramids and concluded that IPSPs do not play an essential role in the genesis of the focal theta waves [32], the prevalent view is that IPSPs are major events in CA1 pyramidal cells during theta activity [33]. It was also proposed that the sustained depolarization of pyramidal neurons during theta is due to a disinhibitory process which is in turn due to a septum-induced suppression of tonic inhibition arising in hippocampal local-circuit inhibitory interneurons [34]. *In vivo* intracellular recordings from distal dendrites of CA1 pyramidal neurons showed theta phase-locked Ca^{2+} potentials (Fig. 7.2) [35].

There are reports indicating that theta waves recorded from the neocortex may result from hippocampal volume conduction. However, at least for the cingulate cortex, the intracortical generation of theta was suggested by neuronal firing at the theta frequency [36] and by persistence of theta rhythm (even with increased amplitude) after lesions of medial septum that produced abolition of hippocampal theta [37]. The origin of the cingulate theta in the absence of the septohippocampal and direct septomammillary systems, which are generally thought to transmit theta waves to the cingulate cortex through a prior relay in the anterior thalamic nuclei, is not known.

Because the main origin of EEG waves should be searched in the synchronized PSPs and simultaneous intracellular recordings from a great number of neurons are impossible at this time, computer simulations have been used to produce oscillations similar to those observed in living animals. Models of the CA3 area with 200–20,000 pyramidal neurons (as well as bursting and nonbursting inhibitory cells were used) and pyramidal neurons were endowed with slow inward currents to produce spontaneous spike bursts [38]. Such a system displays a highly organized rhythmic activity at the population level, while individual elements show chaotic firing. These synchronized activities are similar to those seen experimentally.

Intradendritic theta oscillation

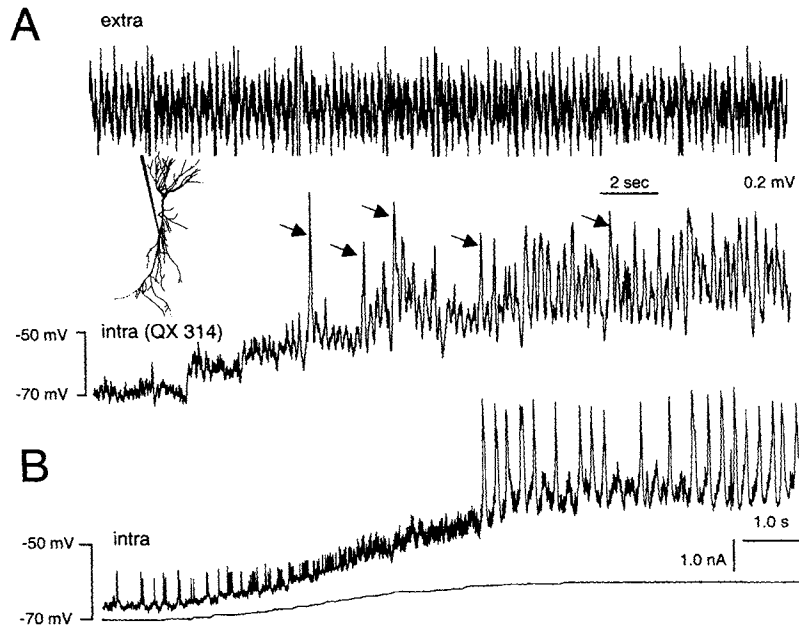


Figure 7.2. Voltage-dependent theta oscillation in pyramidal cell dendrites *in vivo*. A, continuous recording of extracellular (extra; CA1 pyramidal layer) and intradendritic (intra) activity in the rat. Holding potential was manually shifted to progressively more depolarized levels by intradendritic current injection. Inset: location of the dendritic penetration. The recording electrode contained QX 314 to block fast (Na^+) spikes. Some of the high-threshold Ca^{2+} spikes are marked by arrows. B, another dendritic recording without QX 314 (0.37 mm from pyramidal layer). Note large amplitude Ca^{2+} spikes and small amplitude fast spikes. Modified from Kamondi *et al.* (1998).

Theta waves may be implicated in hippocampal plasticity, as suggested by optimal induction of long-term potentiation when the time interval between stimuli is approximately the period of theta rhythm [39].

7.1.4. Fast (Beta/Gamma) and Ultrafast (Ripple) Rhythms

The first demonstration that the EEG activated response to brainstem reticular stimulation [40] is not only a negative event (namely, the blockage of low-frequency waves that characterize NREM sleep or most types of anesthesia) but also includes the appearance of synchronized fast rhythms, belongs to Bremer and his colleagues [41]. They reported that a clear-cut enhancement in the amplitude of spontaneous rhythms and their regular acceleration to 40–45 Hz (*accélération synchronisatrice*) appeared on the cortical EEG of the cat with bulbospinal transection, simultaneously with the ocular syndrome of arousal [42]. Since Bremer's 1960 study, a series of studies in various cortical

[39] Larson and Lynch (1986); Greenstein *et al.* (1988).

[40] Moruzzi and Magoun (1949). In that pioneering study, "activation" of the EEG only consisted of obliteration of slow waves.

When present, fast activity had a low voltage and, during chloralose anesthesia, "fast activity was not elicited" (p. 456).

[41] Bremer *et al.* (1960). See legend of Fig. 5 in that article, showing an example of "*activation synchronisatrice et amplifiante de l'écorce cérébrale par la stimulation réticulaire de l'éveil*." Recordings were done from the primary auditory cortex and fast waves elicited by brainstem reticular stimulation were within the frequency of approximately 45 Hz.

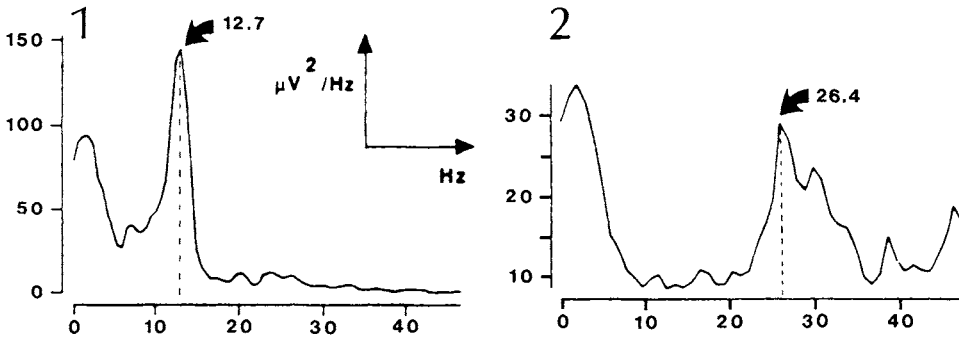


Figure 7.3. Fast (beta) rhythms during focused attention. Power spectra of EEG signals from dog visual cortex. Spectrum 1 was obtained while the awake animal kept its eyes closed and that in 2 when the animal paid attention to a visual object. Alpha activity dominates in 1 and beta activity (peak around 26 Hz) dominates in 2. Modified from Lopes da Silva *et al.* (1970).

[42] The fact that brain arousal is associated with *synchronization* of fast waves in the beta (~ 15 – 30 Hz) and gamma (~ 30 – 60 Hz) band led us (Steriade *et al.*, 1996a) to postulate that the term “EEG desynchronization,” used by most epigones of Moruzzi and Magoun [40], is inadequate, and that the term *cortical activation* is more appropriate. It is known that, during brainstem RE-elicited arousal, activation of neocortex (Bremer and Stoupe, 1959; Dumont and Dell, 1960) and visual thalamus (Steriade and Demetrescu, 1960) was demonstrated by enhancement of potentials evoked by afferent stimuli. [43] Lopes da Silva *et al.* (1970). [44] Murthy and Fetz (1992, 1997a–b); Chen and Fetz (1993). [45] Freeman (1975). [46] Eckhorn *et al.* (1988); Singer *et al.* (1988); Gray *et al.* (1989); Gray *et al.* (1990); Engel *et al.* (1990, 1991). [47] Galambos *et al.* (1981); Llinás and Ribary (1992). [48] Steriade *et al.* (1968). [49] Singer (1990a). [50] Singer (1990b, 1993, 1994). [51] Llinás and Ribary (1993).

areas have reported the presence of 20–40 Hz waves, during different conditions of increased alertness. The fast rhythms were observed in the occipital cortex while the dog paid intense attention to a visual stimulus [43] (Fig. 7.3); in monkey, neocortical cells during motor tasks, such as retrieving raisins or requiring focused attention [44] (Fig. 7.4), and during behavioral immobility associated with an enhanced level of vigilance while the cat was watching a visible but unseizable mouse [12–14] (see above, Fig. 7.1B). Stimulus-dependent oscillations at 25–45 Hz of the focal EEG and/or neuronal firing have been described in the olfactory [45], visual [46], and auditory [47] cortices of animals and humans. It was also reported that brainstem reticular stimulation selectively enhances the oscillatory waves at 60–80 Hz that compose the afterdischarge of the flash-evoked response in the visual cortex [48] and facilitates the coherency of 40-Hz responses in visual cortical neurons [49]. The possible significance of this rhythm resides in the fact that, in addition to the spatial mapping that allows a limited number of representations, a temporal component is brought about by synchronized oscillatory responses across spatially separate cortical columns. The cell assemblies link spatially distributed elements and may be the bases for global and coherent properties of patterns, a prerequisite for scene segmentation and figure-ground distinction [50].

The fast rhythms elicited by sensory stimuli are only the tip of the iceberg, as these oscillations are also present in the background (spontaneous) activity of the thalamus and cerebral cortex. Magnetoencephalographic (MEG) recordings in awake humans have revealed the presence of a 40-Hz oscillation over the entire cortical mantle and a synchronization of the 40-Hz activity by presentation of auditory stimuli with random frequencies [51] (Fig. 7.5). Beta (~ 15 – 30 Hz) and gamma (~ 30 – 60 Hz) activity does

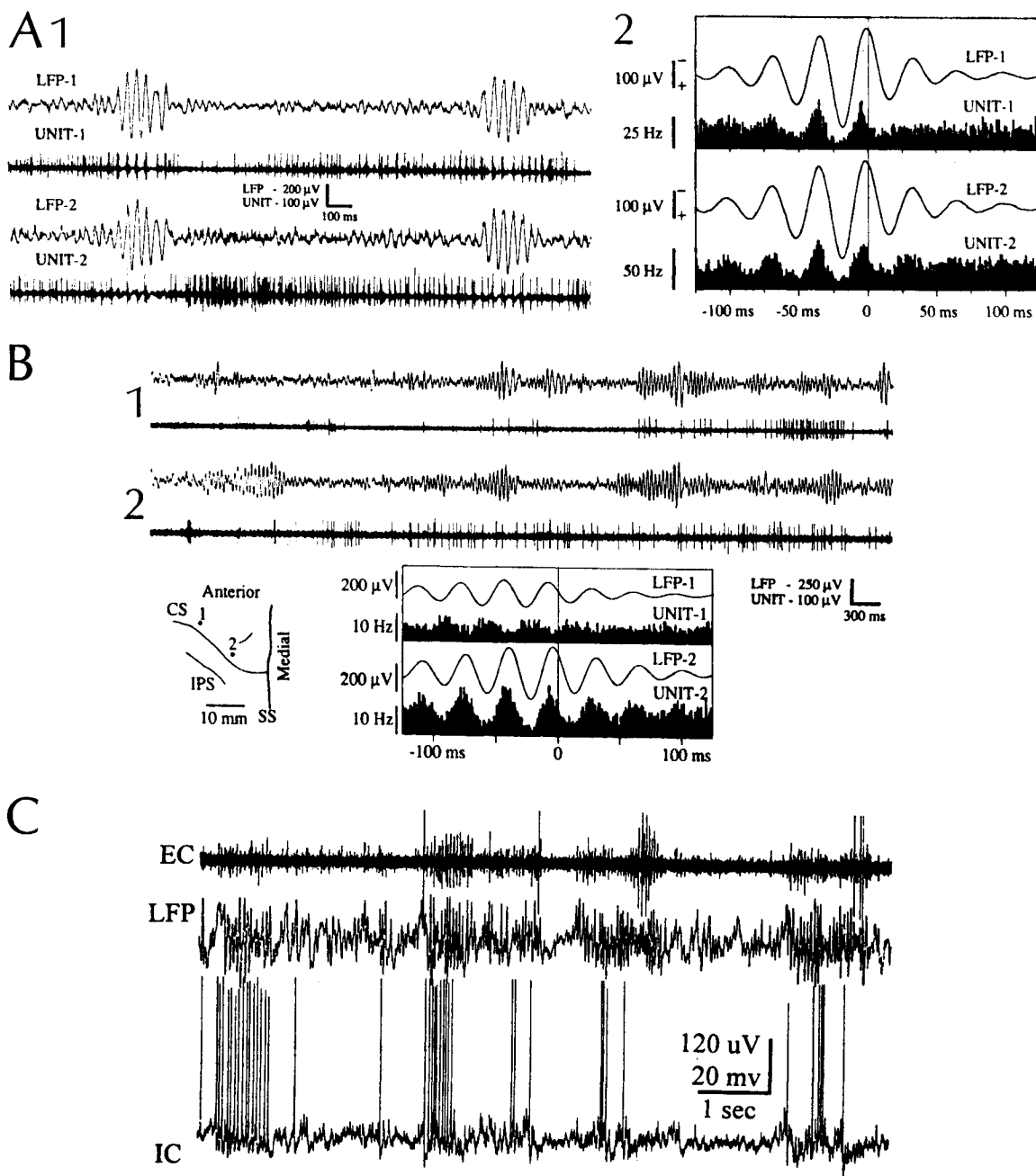
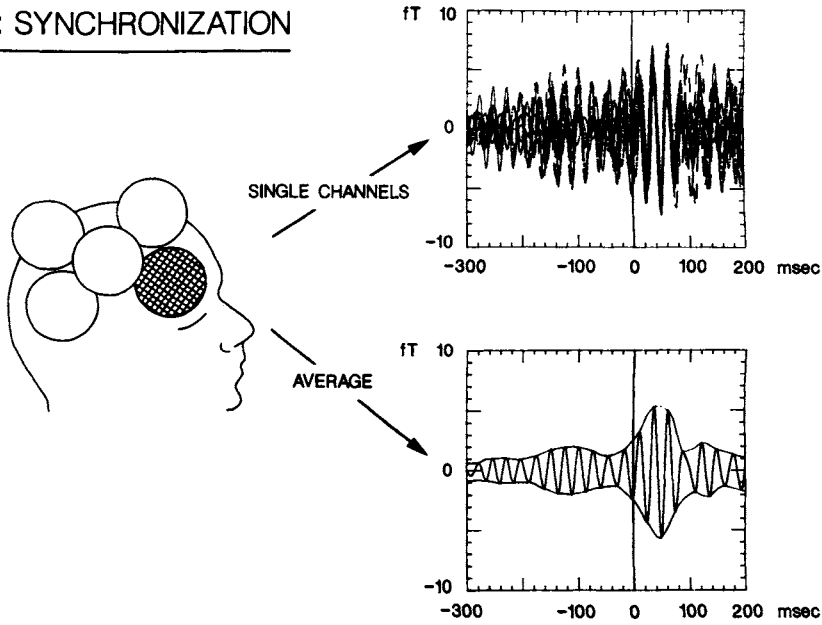


Figure 7.4. Coherent 25–35 Hz oscillations in the sensorimotor cortex of an awake behaving monkey. **A1**, local field potentials (LFPs) and unit activity recorded at two nearby sites in the motor cortex of a monkey retrieving a raisin from a Klüver board. Upper and lower pairs of traces show LFPs and unit activity from electrodes 1 and 2, respectively. **A2**, cycle-triggered averages of LFPs and unit activity (sites in **A1**). **B**, LFPs from sites in

the motor cortex separated by approximately 14 mm. Below, cycle-triggered averages of LFPs and units aligned on cycles in LFP-2. Abbreviations: SS, saggittal sinus; CS, central sulcus; IPS, intraparietal sulcus. **C**, oscillations in LFPs, extracellular multi-unit activity (EC), and intracellular membrane potential (IC), all recorded simultaneously in the monkey motor cortex. Modified from Murthy and Fetz (1992) and Chen and Fetz (1993).

40Hz : SYNCHRONIZATION



40Hz : PHASE-SHIFT

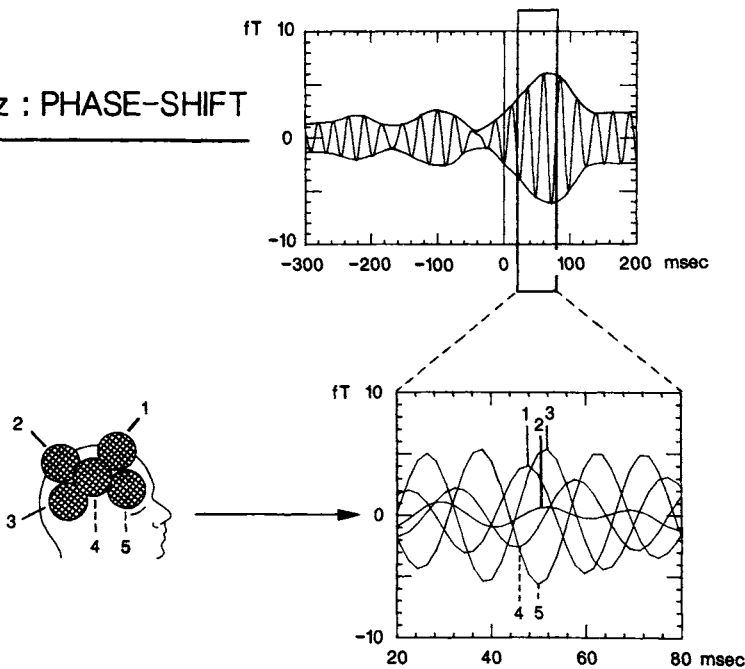


Figure 7.5. Fast (40-Hz) rhythm in magnetoencephalographic recordings from awake humans. Top: synchronization of 40-Hz oscillatory activity during auditory processing with seven single channels of one probe placed over lower frontal areas. The graph on the top right shows a superimposition of 40-Hz activities, time-locked to the stimulus onset, recorded from the seven channels. The graph on the lower right shows an average of the seven individual channels, demonstrating synchronization over a large area (around 25 cm²). Bottom: phase-shift of 40-Hz oscillatory activity during auditory processing. The time period between 20 and 80 ms after the onset of the auditory stimuli is enlarged in the lower panel. The lowest panel shows the superimposition of averaged responses from all sensors in each of the five probe positions (hatched and numbered at left). Note the large, consistent phase-shifts from region to region, indicating a continuous rostrocaudal shift over the hemisphere. Modified from Llinás and Ribary (1992).

not occur spontaneously only during wakefulness when information processing is expected to occur, but also during deep anesthesia and natural slow-wave sleep [52]. During the slow oscillation ($\sim 0.5\text{--}1$ Hz), a hallmark of natural slow-wave sleep and also a characteristic feature of ketamine–xylazine or some other anesthetics (see Section 7.3.3), fast (beta or gamma) activity appears over the depolarizing phase of this sleep oscillation, whereas this fast activity is absent during the hyperpolarizing phase of the slow oscillation. This is depicted in Fig. 7.6 for intracellular activity recorded under ketamine–xylazine anesthesia, and is strikingly similar to the same correspondence during natural sleep [52]. Thus, fast rhythms are sustained during wakefulness and REM sleep, and are selectively occurring during the depolarizing phase of the slow oscillation in slow-wave sleep. The difference between the increased power of fast waves (15–50 Hz) throughout activated periods, compared to epochs in which the slow oscillation is present only during its depolarizing component, is illustrated with intracellular and field potential recordings in Fig. 7.7.

The voltage(depolarization)-dependent occurrence of fast oscillations was demonstrated for both neocortical and thalamic neurons, recorded *in vitro* and *in vivo*. Fast oscillations have been recorded in cortical slices upon depolarizing current pulses in sparsely spinous, presumably inhibitory local-circuit cells located in layer IV [53] (Fig. 7.8) and other types of neocortical neurons [54]. Similar types of fast oscillatory activity were recorded *in vivo*, from antidromically identified corticothalamic and callosal neurons in the association cortex [55]. A peculiar type of cortical neurons, discharging fast-rhythmic (20–60 Hz) spike-bursts, therefore called fast-rhythmic-bursting (FRB) neurons, was recorded from the superficial layers of visual cortex [56] as well as from all layers II–VI in a variety of other (sensory, motor and association) areas [57]. Some of these neurons, located in layers V–VI, are corticothalamic and can, therefore, bind the fast cortical oscillatory activity with the thalamically generated one (see below). Figure 7.9 illustrates such FRB neurons, bursting at frequencies from 30 to 80 Hz, recorded from somatosensory and association cortical areas. Intracellularly recorded TC neurons also oscillate at fast frequencies ($\sim 30\text{--}40$ Hz), firing single-spikes (Fig. 7.10) or spike-bursts during states of depolarization [58].

The demonstration that both cortical and thalamic neurons oscillate at fast frequencies leads to the discussion of the origin and synchronization of this rhythm. Initially, only intracortical connections have been considered in the synchronization process of fast oscillations in the visual

[52] Steriade *et al.* (1996a). See Fig. 14 in that paper for relations between fast oscillations and the depth-negative phase of the slow oscillation (reflecting depolarizing events in a pool of neurons) during natural slow-wave sleep. [53] Llinás *et al.* (1991). [54] Amitai (1994); Gutfreund *et al.* (1995). [55] Nuñez *et al.* (1992b). [56] Gray and McCormick (1996). [57] Steriade *et al.* (1996a); Steriade (1997a); Steriade *et al.* (1998a). FRB neurons, as called in our studies, were also termed “chattering” cells and their firing pattern recorded from superficial layers of the visual cortex was exclusively described as consisting of fast spike-bursts [56]. However, in our hands, the firing pattern of a regular-spiking (RS) neuron could change, with increased depolarization, into that of an FRB neuron that with further depolarization was transformed into the firing pattern of an FS cell (see Section 5.6.1 and Fig. 5.36 in Chapter 5). Such a transformation, from RS to FRB and FS patterns, was observed in antidromically identified corticothalamic neurons as well as in formally identified, intracellularly stained local-circuit, sparsely spiny neurons (Steriade *et al.*, 1998a). [58] Steriade *et al.* (1991b, 1993c). In the 1993 paper, we reported the presence of special type of neurons, recorded from the large-cell part of the thalamic intralaminar CL nucleus, which upon depolarizing pulses from the resting membrane potential triggered fast oscillations (30–40 Hz) crowned by short spike-bursts with unusually high (800–1,000 Hz) frequencies

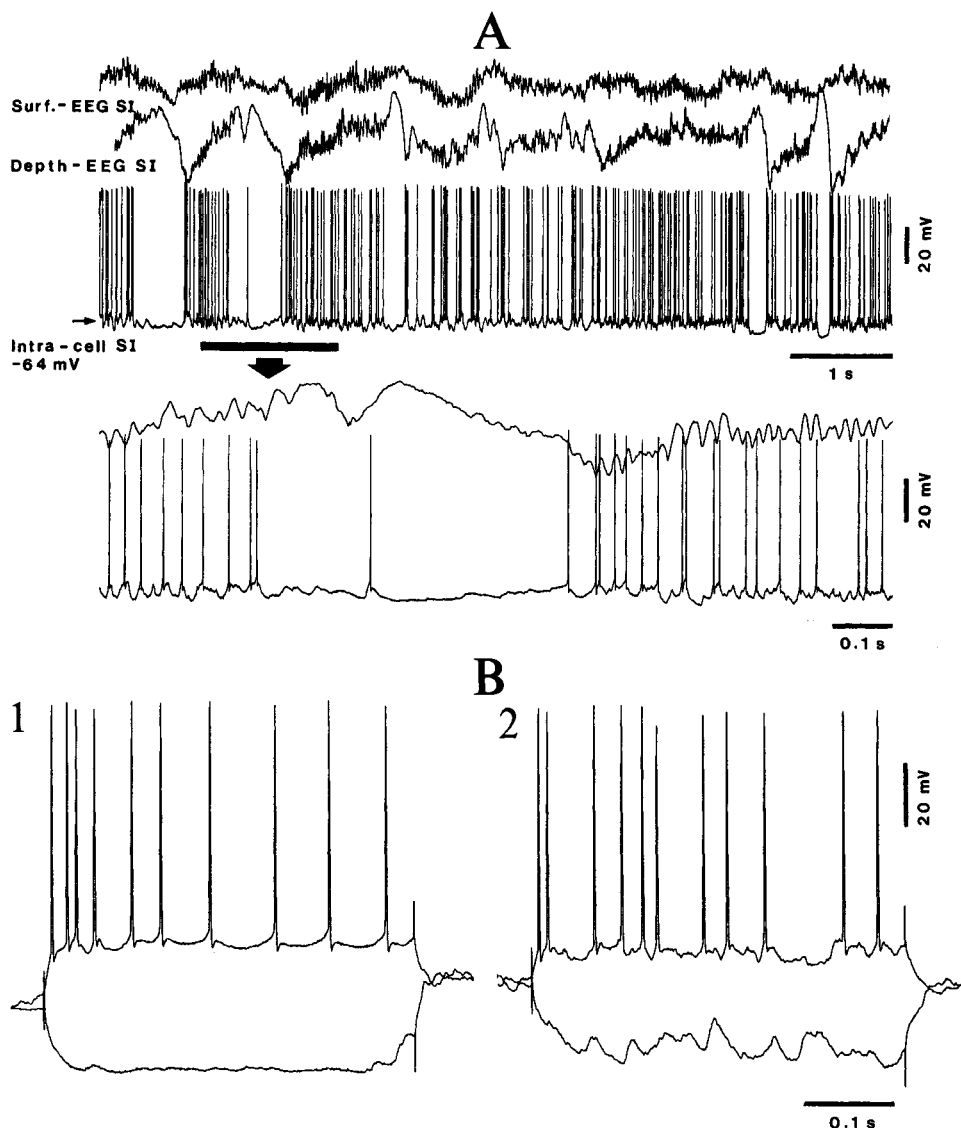


Figure 7.6. Fast (40–50 Hz) oscillations during the depolarizing phase of the slow oscillation. Cat under ketamine–xylazine anesthesia. A, strikingly reduced synaptic activity during the prolonged hyperpolarizations phases of the slow oscillation associated with depth-positive EEG waves (upward deflections) and increased synaptic activity during the fast activity (40–50 Hz) that follows the sharp depth-negative EEG deflection (part marked by horizontal bar is expanded below; arrow). B, differential responses to depolarizing and hyperpolarizing current pulses (1 nA) applied during the prolonged hyperpolarization of the spontaneously occurring slow oscillation (1) and during periods with increased synaptic activities (2). From Steriade *et al.* (1996a).

(see Fig. 5 in Steriade *et al.*, 1993c).

[59] Gray *et al.* (1989). The role of thalamic neurons was denied by these authors because they thought that collaterals of TC axons did not span sufficiently long

cortex [59]. However, the proportion of oscillatory responses in neurons recorded from the visual thalamic relay (lateral geniculate, LG) nucleus is higher than in the visual cortex, and the frequency of oscillation is also higher [60] (Fig. 7.11). It seems that the general rule is an increased frequencies of fast oscillations from cortex

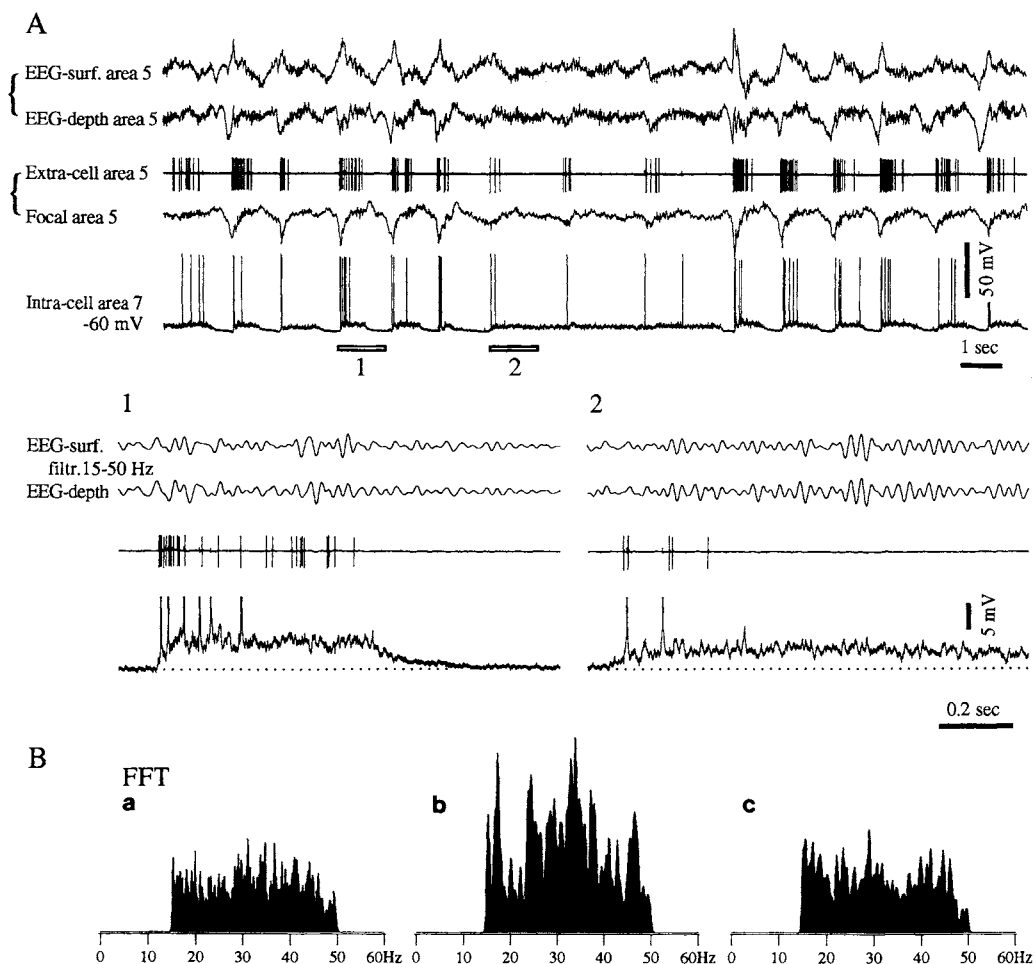


Figure 7.7. Increased power of fast waves (15–50 Hz, peak around 35 Hz) during spontaneous epoch of EEG activation associated with sustained depolarization of cortical neuron. Cat under ketamine–xylazine anesthesia. A, multisite recording of surface- and depth-EEG from area 5, extracellular unit activity and local field potentials (through the same microelectrode) from area 5, and intracellular activity of area 7 neuron. Parts 1 (during slow sleep oscillation) and 2 (onset of shortly activated epoch) are expanded below, depicting EEG waves filtered between 15 Hz and 50 Hz, extracellular discharges of area 5 neuron, and intracellular activity of area 7 neuron. In 2, note sustained depolarization of area 7 neuron (dotted line

tentatively indicates the baseline) and in-phase fast EEG waves recorded from the surface and depth of area 5 (see also Fig. 5 in that paper for the in-phase relations between surface and depth fast waves; also, see such data in Steriade and Amzica, 1996). B, surfaces of fast-Fourier transforms (FFTs) from area 5 EEG waves (filtered between 15 and 50 Hz) in a control period before activation (a), during activation (b), and during a postactivation period (c). The power spectrum in the 15–50 Hz band (peak around 35 Hz) was enhanced by 93%, compared with the preactivation period, because of the absence of prolonged hyperpolarization phases of the slow oscillation. From Steriade *et al.* (1996a).

(30–40; but see below) to thalamic relays (50–60 Hz) and, down to prethalamic stations, such as retina [61] and cerebellum [62] where frequencies may reach 100 Hz or above. The decreased frequencies of fast oscillations by passing from prethalamic to thalamic and cortical neurons may be ascribed to increased inhibitory processes, but this is not yet elucidated. In fact, some studies demonstrated

distances in cortex to account for coherent rhythmicity in distant columns of visual cortex. [60] Ghose and Freeman (1992). A modeling study of the same authors (Ghose and Freeman, 1997), in the

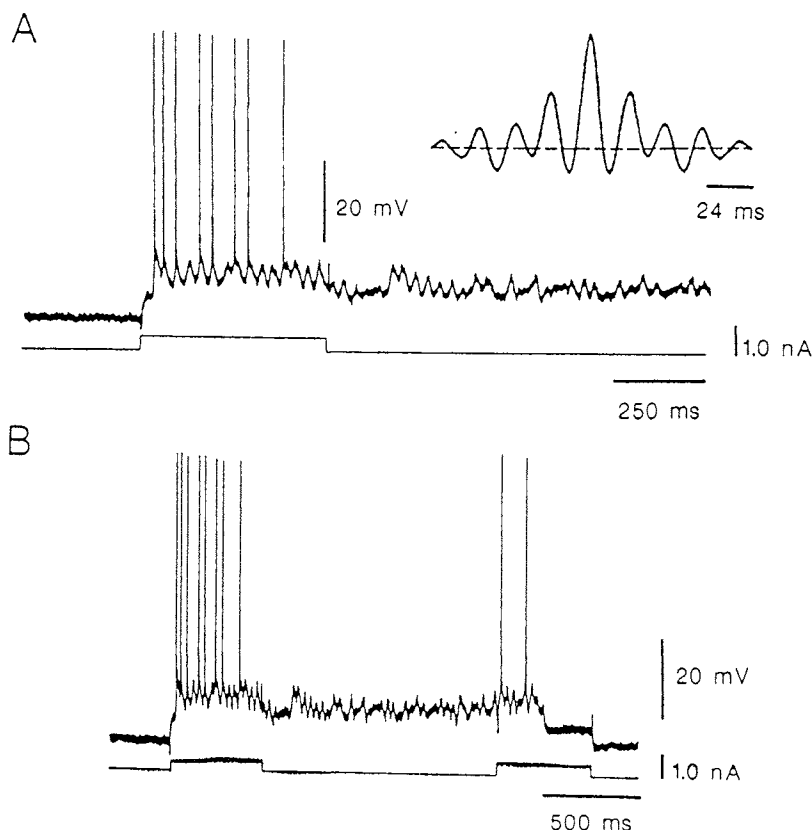


Figure 7.8. *In vitro* intracellular recording from a sparsely spinous neuron in layer IV of the frontal cortex of a guinea-pig. A, the characteristic response obtained in the cell following direct depolarization, consisting of a sustained subthreshold activity on which single spikes can be observed. The intrinsic oscillatory frequency was 42 Hz, as demonstrated by the autocorrelogram shown in the upper right corner. B, the same record as above, but at a slower speed, demonstrating how the response outlasts the first stimulus but comes to an abrupt cessation in the middle of a second stimulus. Modified from Llinás *et al.* (1991).

absence of intracortical connections, led to the conclusion that oscillatory discharges around 50 Hz can arise from the integration of signals within the LG nucleus. Fast oscillations in the visual thalamus, elicited by photic stimuli, have been repeatedly reported in the past (Fuster *et al.*, 1965; Steriade, 1968, 1969). Intracellular recordings of LG neurons demonstrate fast prepotentials and full action potentials with a frequency of 40–50 Hz during light stimulation—an effect that was virtually obliterated after inactivation of retinal cells with

that the magic “40-Hz” frequency of oscillating neocortical neurons might be as low as that of beta or even alpha band (10–20 Hz). Indeed, oscillations at 7–20 Hz were observed in an overwhelming majority (93%) of neurons, using intracellular recordings from primary visual area 17, thus precluding the possibility that some subthreshold intracellular events were not accounted for in the frequency [63]. Also, the frequency of synchronized fast oscillations in nonhuman primate and human motor cortex and hand electromyogram during performance of tasks is about 10–15 to 20 Hz [64].

The fact that thalamic and neocortical neurons oscillate in-phase during fast, so-called beta and/or gamma [65], activities was documented by simultaneous intracellular and field potential recordings from thalamus and projection neocortical areas showing that action potentials

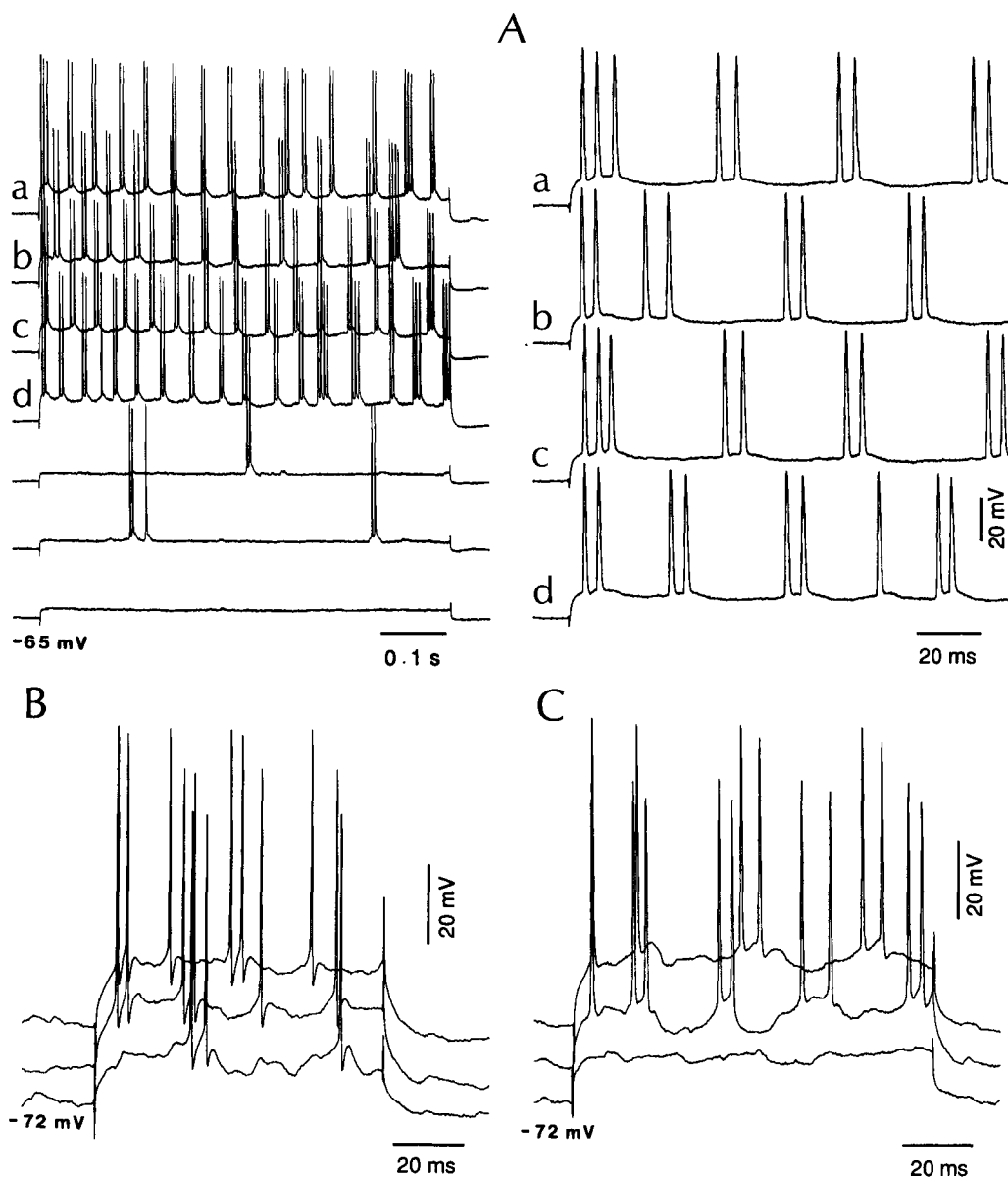


Figure 7.9. Fast rhythmic spike-bursts elicited in neocortical neurons by depolarizing current pulses. Cats under ketamine-xylazine anesthesia. A, neuron at a depth of 0.4 mm in anterior suprasylvian area 5. Depolarizing current pulses of 600 ms, 0.5 nA in a–d, and 0.2 nA in the bottom three traces. At right, expanded traces of a–d. Note, in a–d, spike-doublets and triplets (interspike intervals: 4 ms) recurring at approximately 30 Hz. B, neuron at a depth of 0.8 mm in the primary somatosensory cortex. Depolarizing current pulses (duration

60 ms) with increasing amplitudes (0.7, 0.8, and 1 nA) applied at the same membrane potential. Pulses of 0.8 and 1 nA elicited spike-doublets at 50–80 Hz. C, neuron at a depth of 0.5 mm in the primary somatosensory cortex. Depolarizing current pulses (duration 100 ms) with increasing intensities (0.6, 0.7, and 1.1 nA) at the same membrane potential. Pulses of 0.7 and 1.1 nA elicited three to four spike-doublets at approximately 40 Hz. From Steriade *et al.* (1996a).

of the TC neuron are fired in good time-relations with the depth-negative cortical field potentials reflecting excitatory events in cortical neuronal pools (Fig. 7.12A). This figure also shows the fast coherent activity, over short

lidocaine (Nuñez *et al.*, 1992c).

[61] See Figs. 11–12 in Steriade (1968).

Synchronization of retinal

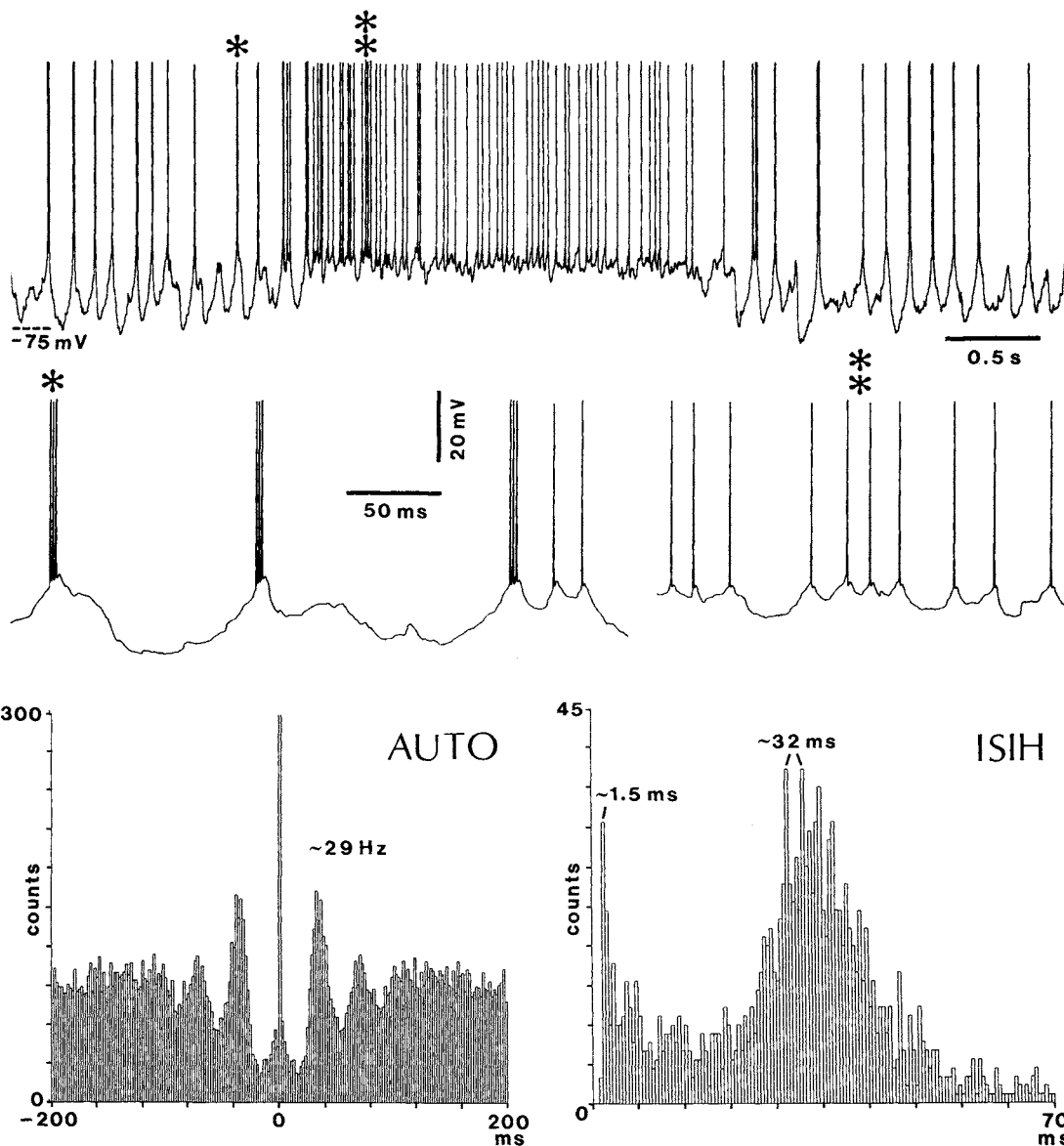


Figure 7.10. Fast (~ 30 Hz) oscillation of intracellularly recorded thalamic centrolateral (CL) neuron, from for the dorsolateral, large-cell part of the nucleus. Cat under barbiturate anesthesia. Uppermost trace depicts transition from spindle oscillation to the tonic (depolarized) firing mode, thereafter followed by another spindle sequence. Parts indicated by one

or two asterisks are expanded below. Below, autocorrelogram (AUTO) computed from tonic (interspindle) epochs (2-ms bins); and interspike interval histogram (ISIH) computed from both spindling and tonic epochs (0.5-ms bins). AUTO and ISIH were generated from a period of 145 s. From Steriade *et al.* (1993c).

and visual thalamic neurons within the frequency of fast rhythms was also reported by Neuenschwander and Singer (1996). Retinal ganglion and amacrine cells

distances, within the association cortex (Fig. 7.12B) and the act that fast oscillatory activities in intracellularly recorded cortical neurons exclusively occur over the depolarizing phase of the slow sleep oscillation, thus demonstrating their voltage-dependency (Fig. 7.12C).

Beyond the usual fast frequencies (20–80 Hz) that are superimposed on the depolarizing phase of slow sleep

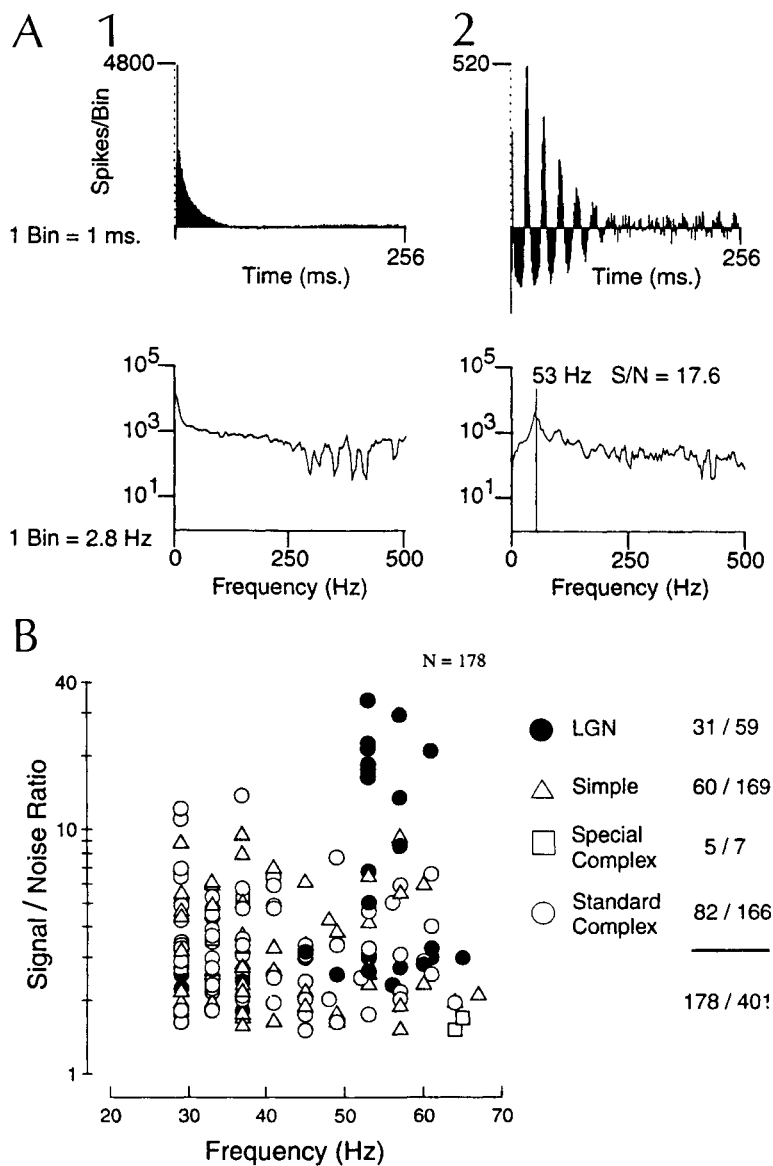


Figure 7.11. Fast oscillatory responses in the thalamic lateral geniculate (LG) and visual cortical responses. Cats under anesthesia. A, autocorrelograms and power spectra corresponding to a nonoscillatory visual cortex complex cell (1) and a strongly oscillatory LG neuron (2). Autocorrelograms are reflected to span intervals from -256 to +256 ms before the Fourier transform. For the cell in 1, a smooth correlogram based on 25,787 spikes accumulated during reverse correlation stimulation yields a power spectrum whose sole peak is 0 Hz. This indicates that the 0-Hz frequency is dominant in the spike train. By contrast, the cell shown in 2 exhibits very rhythmic discharge. The power spectrum of this discharge (which contains 3,800 spikes) shows a distinguishable peak at 53 Hz. B, signal-to-noise ratios and frequencies of oscillatory discharge are summarized according to cell type. Of the LG cells studied, 10 of 59 showed stable oscillatory discharge that was stimulus independent. This group of cells, seen in the top right corner, has signal-to-noise ratios that are an order of magnitude larger than those typically seen over brief periods of time with cortical cells. See further details in that paper. Modified from Ghose and Freeman (1992).

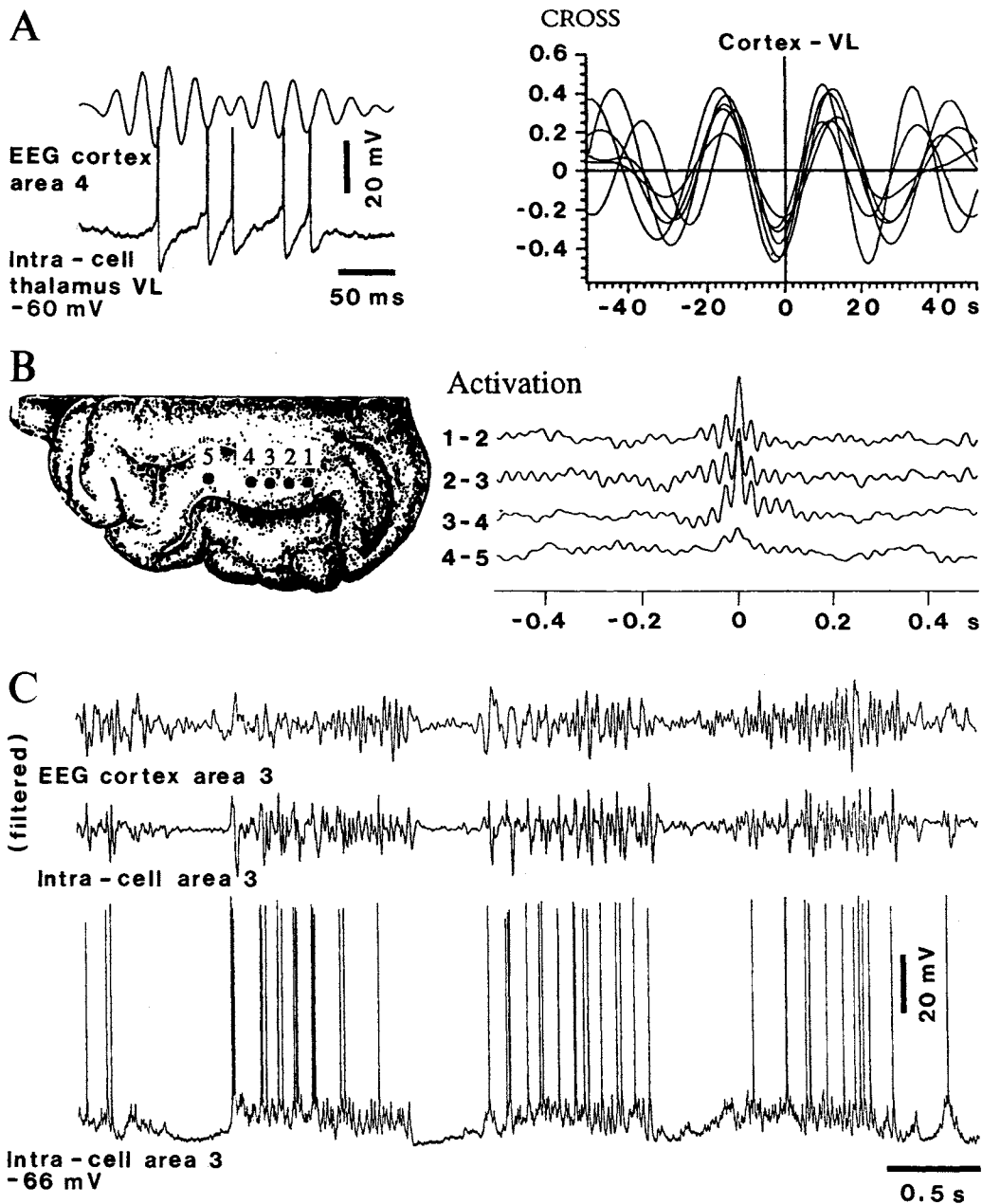


Figure 7.12. Activation and fast rhythms of neocortical and thalamic electrical activity. Cats under ketamine–xylazine anesthesia. **A**, during a brief period of EEG activation, fast rhythms (~ 40 Hz) are synchronous in an intracellularly recorded thalamocortical (TC) neuron from the ventrolateral (VL) nucleus (spikes truncated) and negative peaks of depth-EEG are recorded from the depth of area 4. Cross-correlogram between cortex and VL thalamus shows a clear-cut relation, with opposition of phase between depth-negative EEG and intracellular potentials in the TC cell. **B**, EEG activation induced by a pulse-train (300 Hz) applied to the PPT nucleus. Disruption of the slow sleep-like oscillation was associated with the appearance

of fast activity whose amplitude exceeded that of fast waves during sleep-like patterns (not shown). Numbers of recorded cortical foci (1 to 5) correspond to those indicated on the suprasylvian gyrus (areas 5 and 7) of the brain figurine. Cross-correlations between different leads demonstrate synchronization of fast rhythms. **C**, slow sleep-like oscillation (0.7 Hz) in an intracellularly recorded neuron from cortical area 3, and EEG from the same area. Both intracellular and EEG activities were filtered between 10 and 100 Hz (two top traces). Note fast activity (~ 30 – 40 Hz) during the depolarizing phase of the slow oscillation and coherent activity between cell and field EEG potentials. Modified from Steriade *et al.* (1996a–b).

oscillation, ultra-fast oscillations (80–200 Hz), termed ripples, are selectively related to the cortical depth-negative field potentials (reflecting depolarization in neuronal pools) of the slow oscillation, and also during the sustained depolarization of neurons in natural waking and REM sleep [66]. Similar oscillations are found during anesthesia, behavioral immobility, and natural sleep in CA1 hippocampal area and perirhinal cortex [67]. Multisite recordings of field potentials in neocortex showed grouped ripples in spindle-shaped sequences (see filtered traces in Fig. 7.13). Since the slow oscillation shows coherence across different areas of the cortex [68] (see below, Section 7.2.3), ripples had also a tendency to appear at about the same time in different cortical sites. Correlations between ripples from distant sites were restricted to the same gyrus (Fig. 7.13).

Intracellular recordings of the four electrophysiological neuronal types of neocortex (see Chapter 5, Section 5.6.1) revealed that FRB and fast-spiking (FS) neurons displayed the highest firing rates during ripples (Fig. 7.14). In FRB neurons, compound EPSPs have a structure consistent with their being produced by the signature bursts from another FRB neuron [56, 57] so that a network of interconnected FRB neurons could mutually reinforce each other's excitation, and thus help sustain the excitation level concurrent with field ripples.

As to the functional role of ripples, it has been postulated that hippocampal ripples constitute a replay at a faster time-scale of firing sequences coding for important events so that they can be encoded in a more permanent manner [69]. The possible involvement of ripples in plasticity processes is consistent with a role of slow-wave sleep in the consolidation of memory traces [70], as ripples reach their strongest amplitudes during slow-wave sleep. These periods of higher activities and ripples in a state during which the neocortex is disconnected from the outside world might be relevant for synaptic reorganizations involved in memory processes.

In sum, fast and ultra-fast activities are not exclusively related to brain-active behavioral states, waking, and REM sleep, because they are dependent on neuronal depolarization and, thus, also occur over the depolarizing phase of the slow oscillation in non-REM sleep.

may oscillate up to 100 Hz (Adrian, 1937).

[62] Timofeev and Steriade (1997).

[63] Bringuier *et al.* (1997).

[64] Sanes and Donoghue (1993); Baker *et al.* (1997); Farmer (1998).

[65] We do not see any convincing reason to dissociate beta from gamma activities since the neurons may double the frequency of fast oscillation in periods as short as 0.5–1 s, as a function of increased depolarization (Steriade *et al.*, 1996a).

EEG recordings during the sleep–wake cycle and cognitive activity in humans also showed that beta and gamma activities may fluctuate simultaneously (Gross and Gotman, 1999).

[66] Grenier *et al.* (2001).

[67] Ylinen *et al.* (1995); Chrobak and Buzsáki (1997); Csicsvari *et al.* (1998, 1999); Collins *et al.* (1999).

[68] Amzica and Steriade (1995a–b).

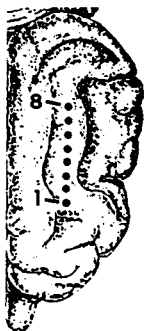
[69] Nádasdy *et al.* (1999).

[70] Steriade (2001a).

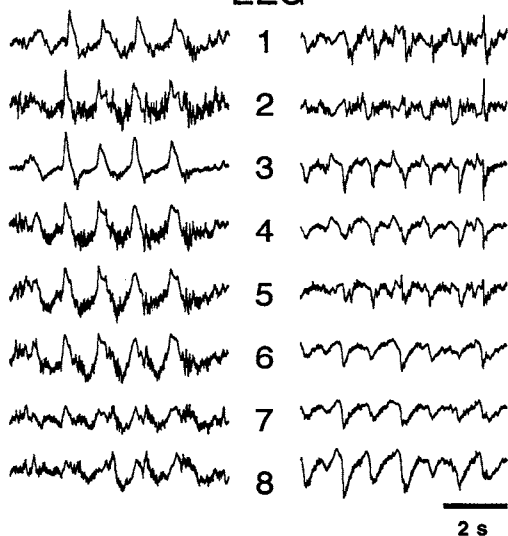
Figure 7.13. Ripples are more strongly correlated among sites along the same gyrus than among different gyri. Cat under ketamine–xylazine anesthesia. Depth field potential recordings with an array of eight electrodes, separated by 1.5 mm, and aligned along the anteroposterior axis over the suprasylvian gyrus or the mediolateral axis, covering the medial, suprasylvian, and ectosylvian gyrus (see brain figurine). An epoch of the slow oscillation is shown in *left middle* panels. The traces of the same epoch were filtered between 80 and 200 Hz (*bottom left* panels). Wave-triggered averages (WTAs) from sites 2, 4, and 6 were calculated for all leads and for both electrode placement and are shown at *right*. Note that correlation is stronger for recordings from the same gyrus. From Grenier *et al.* (2001).

Same gyrus

Three different gyri



EEG



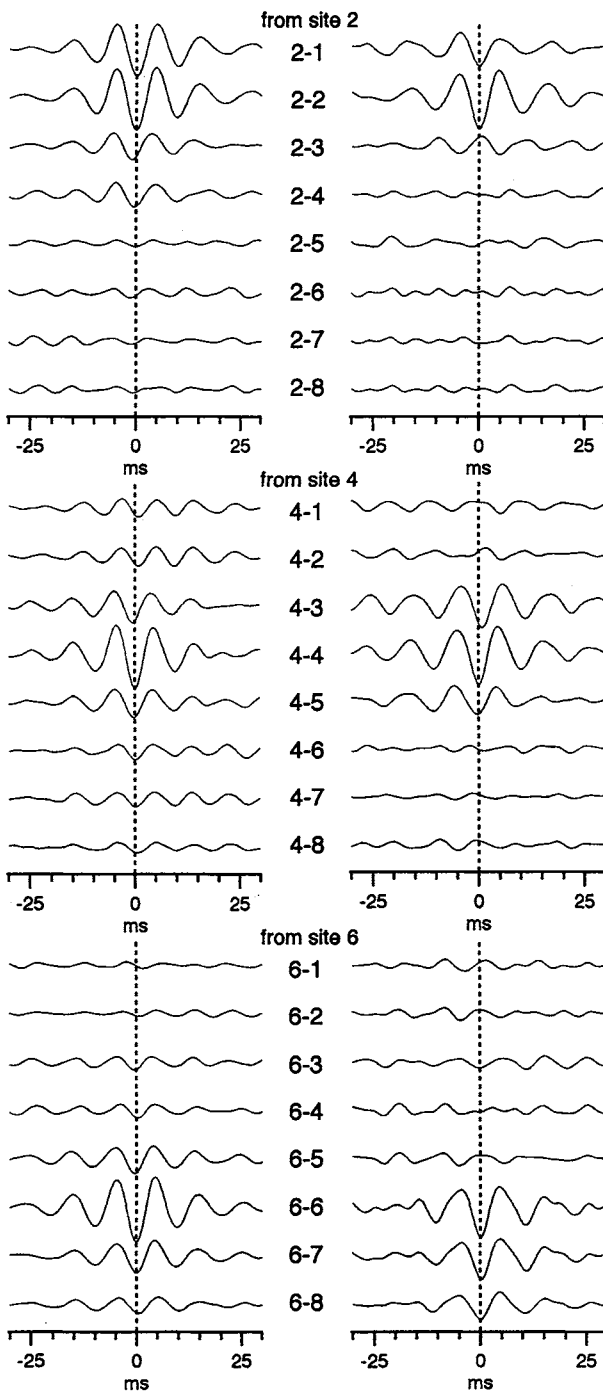
Filtered 80-200 Hz



Same gyrus

Three different gyri

WTAs



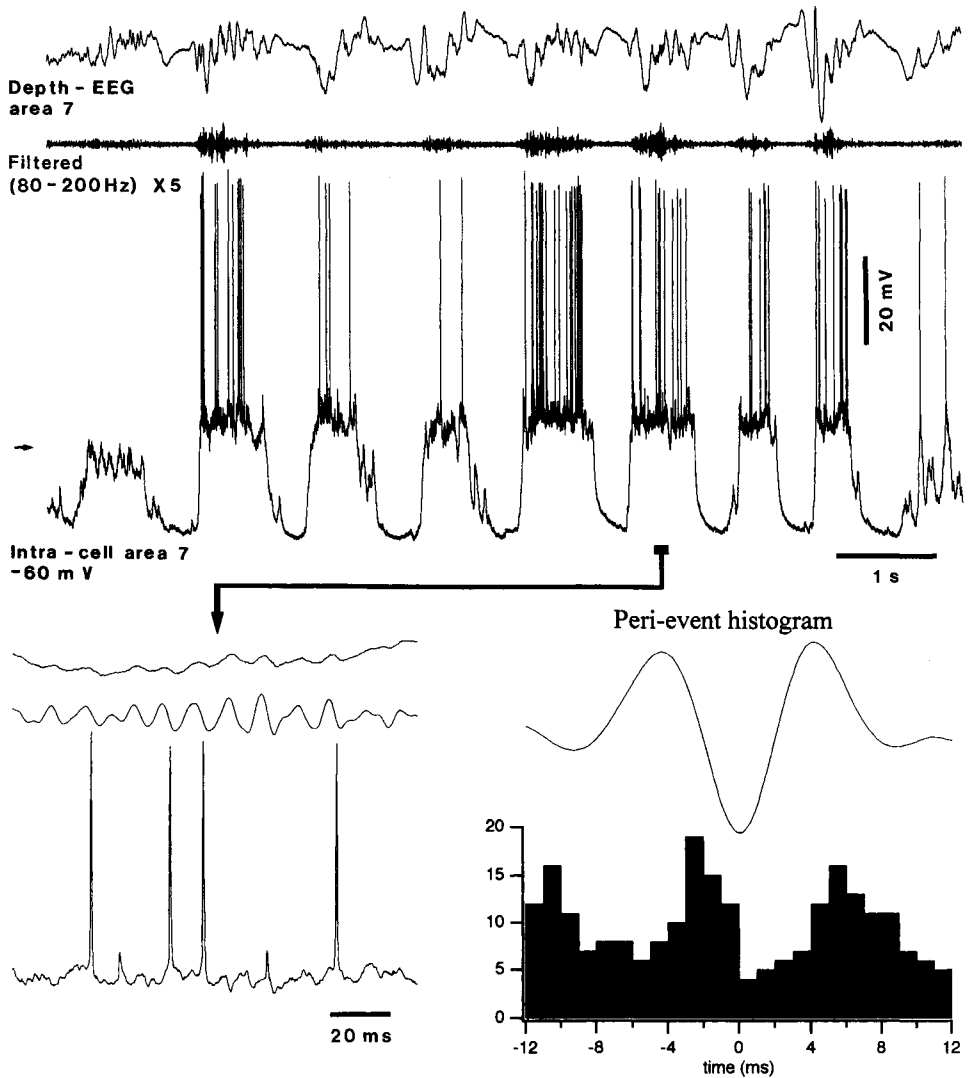


Figure 7.14. Fast-spiking (FS) cortical neurons fire in phase with ripples. Cat under ketamine–xylazine anesthesia. Intracellular and depth-field potential recordings from area 7. Top panel illustrates an epoch with the slow oscillation. The neuron was an FS neuron, identified by responses to depolarizing current pulses. Below the field trace, a filtered trace (80–200 Hz) is also shown. Part indicated by horizontal bar and arrow is expanded below. A peri-event histogram of the neuron firing in relation to ripple depth-negative peak is shown at right, revealing that the neuron fired preferentially around 2.5 ms before the depth-negative peak of ripples. From Grenier *et al.* (2001).

7.2. Low-Frequency Rhythms during Non-REM Sleep

As conventionally described, three major rhythms characterize slow-wave (non-REM) sleep: spindles (7–15 Hz), delta waves (1–4 Hz), and slow oscillations (mainly 0.5–1 Hz). Each of these activities stems from distinct

neuronal networks and is generated by interplay among different synaptic mechanisms and/or voltage-gated currents. Although any of these sleep rhythms may be recorded in the thalamus or neocortex after complete disconnection of these structures, in the intact brain they are all coalesced because of reciprocal (thalamocorticothalamic) loops. This is mainly due to the virtue of the cortically generated slow oscillation that impinges upon the thalamus and triggers complex wave-sequences including all three types of rhythmic patterns within one oscillatory cycle (see Section 7.2.3). It is then obvious why cellular studies of sleep rhythms, similar to those occurring in natural life, require investigations in brains with not only intact connectivity of corticothalamic systems but also with the presence of generalized activating systems whose absence or presence may decisively impact on the occurrence and normal configuration of sleep oscillations.

7.2.1. Spindles

7.2.1.1. Chronology of Spindles and Other NREM Sleep Rhythms

The wake-to-sleep transition is marked by repeated transitions between an activated, low-frequency and fast, electrical pattern and short sequences of low-frequency synchronized waves. This transitional period between waking and sleep is termed WS in Fig. 7.15A1, and is mainly characterized by the appearance of spindle sequences. Thereafter, EEG grapho-elements during NREM sleep become more complex. We can distinguish a light and a deep slow-wave sleep in cats, which correspond to sleep stage 2 and stages 3–4 in man. During light sleep as well as during stage 2 sleep in humans, spindles (7–15 Hz) are coalesced with the slow oscillation (0.5–1 Hz). During light sleep, every cycle of the slow oscillation generally leads to a sequence of spindle waves, on one, another, or all cortical leads [71]. As will be shown in Section 7.2.3, this is due to the synaptic engagement of thalamic neurons implicated in spindle genesis. Notably, though deep sleep displays less spindles, toward the end of deep sleep, just before EEG activation occurs in REM sleep, spindles recover their power as during the initial stages of NREM sleep [71]. This can be explained by the voltage-dependency of sleep rhythms in TC cells. Indeed, at the single-cell level, spindles occur at the resting membrane potential of TC neurons, whereas at more hyperpolarized levels, spindles are progressively replaced by intrinsically generated, clock-like delta potentials (see Section 7.2.2). These intracellular

[71] Steriade and Amzica (1998). See Fig. 3 in that paper, showing more pronounced spindles at the end of deep NREM sleep.

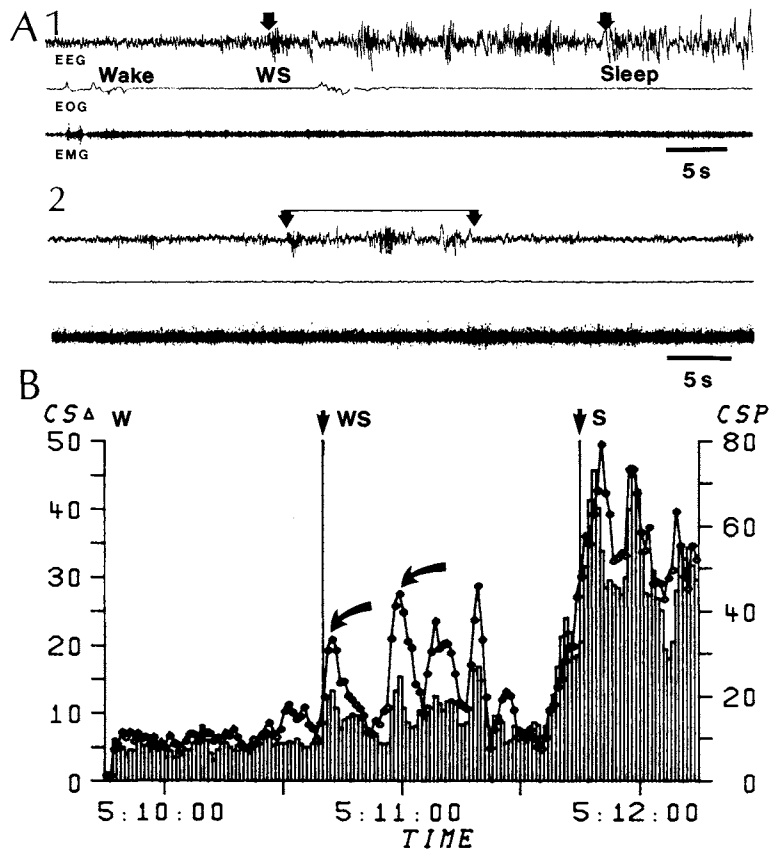


Figure 7.15. Electrographic signs of transition from behavioral states of wakefulness (W) to slow-wave sleep (S) in a chronically implanted cat. A1, EEG waves from the surface of anterior precruciate area, eye movements (electro-oculogram, EOG) and electromyogram (EMG) of neck muscles. Transition from W to S through an intermediate stage (WS) period during which spindles appear. A2, short period of EEG synchronization including spindles (between arrows) within the steady-state of waking. B, normalized amplitudes (ordinate) of cortical spindle waves (line-circle trace, CSP, filtered to 7–14 Hz) and cortical slow as well as delta waves (filtered together to 0.5–4 Hz). Abscissa indicates real time. Note slowly recurring, rhythmic sequences of spindles (arrows), with periods of 8–10 s, beginning with the transitional WS period, and increased amplitudes of both spindles and slow/delta waves, beginning with S. Modified from Steriade *et al.* (1982a, 1986).

data from anesthetized preparation found support in results obtained in naturally sleeping animals and humans, showing that thalamic spindles are maximal at sleep onset and decrease thereafter, whereas thalamic delta waves increase gradually during NREM sleep. Thus, with increasing hyperpolarization of TC cells during NREM sleep, due to the progressive diminished firing rates of brainstem–thalamic reticular activating cells, the incidence and amplitude of spindles are largely diminished during deep sleep stages. On the other hand, the reappearance of spindles toward the end of resting sleep is attributable to a relative depolarization of TC cells, due to the increased firing rates

of brainstem–thalamic reticular neurons that display precursor increased rates of spontaneous firing, 30–60 s before the onset of REM sleep [72].

[72] Steriade *et al.* (1982a, 1990a).

7.2.1.2. Cellular Basis of Spindles

Spindles are generated within the thalamus even in the absence of the cerebral cortex [73] although the neo-cortex has a decisive role in the induction and widespread synchronization of this sleep oscillation (see below). Briefly (Fig. 7.16), thalamic reticular GABAergic neurons impose spike-bursts in the frequency range of spindles onto TC neurons, which display rhythmic IPSPs that, when large and long enough, succeed in de-inactivating the Ca^{2+} -dependent current (I_T), which produces a low-threshold spike (LTS) crowned by high-frequency bursts consisting of fast, Na^+ -mediated action potentials. These spike-bursts are transferred to cortical neurons, where they elicit EPSPs, occasionally leading to action potentials. This mechanism, discovered *in vivo* [74], was repeatedly confirmed in subsequent experimental and modeling studies [75].

[73] Morison and Bassett (1945).

[74] Steriade and Deschênes (1984, 1988).

[75] Reviewed in Destexhe and Sejnowski (2001).

Several differences distinguish the spindle-related spike-bursts in reticular and target TC neurons, as follows. These differences also relate to some dissimilarity between the results from *in vivo* and *in vitro* experiments.

(a) During natural NREM sleep as well as during anesthetic states, reticular neurons fire long bursts, approximately 50 ms and even longer when considering the prolonged tail of tonic discharges that follow the high-frequency bursts, whereas TC neurons fire much shorter spike-bursts, approximately 5–15 ms [76, 77].

[76] Domich *et al.* (1986).

[77] Steriade *et al.* (1986).

(b) The spike-bursts in reticular neurons, often followed by a prolonged tail of discharges, are superimposed on a depolarizing plateau that was recorded *in vivo* (Figs. 7.16 and 7.17) [74, 78] but was absent in initial experiments performed *in vitro*, a condition under which reticular cells underwent a progressive hyperpolarization during spindle sequences [79]. This difference between the results *in vivo* and the initial experiments *in vitro* may be explained by several factors, among them the fact that thalamic slices are deprived of brainstem modulatory systems and corticothalamic depolarizing inputs. Subsequent work in thalamic slices [80] has succeeded in revealing the depolarizing plateau during spindle sequences, at membrane potentials closer to those recorded *in vivo*, thus confirming the results on reticular neurons from intact-brain preparations. It must be emphasized that the prolonged depolarizing plateau described *in vivo* cannot be ascribed to deterioration of

[78] Contreras and Steriade (1996).

[79] Von Krosigk *et al.* (1993).

[80] Kim and McCormick (1998). The depolarizing plateau of spindle sequences in thalamic reticular (PG) neurons was blocked by tetrodotoxin, suggesting that it is mediated by a persistent Na^+ current.

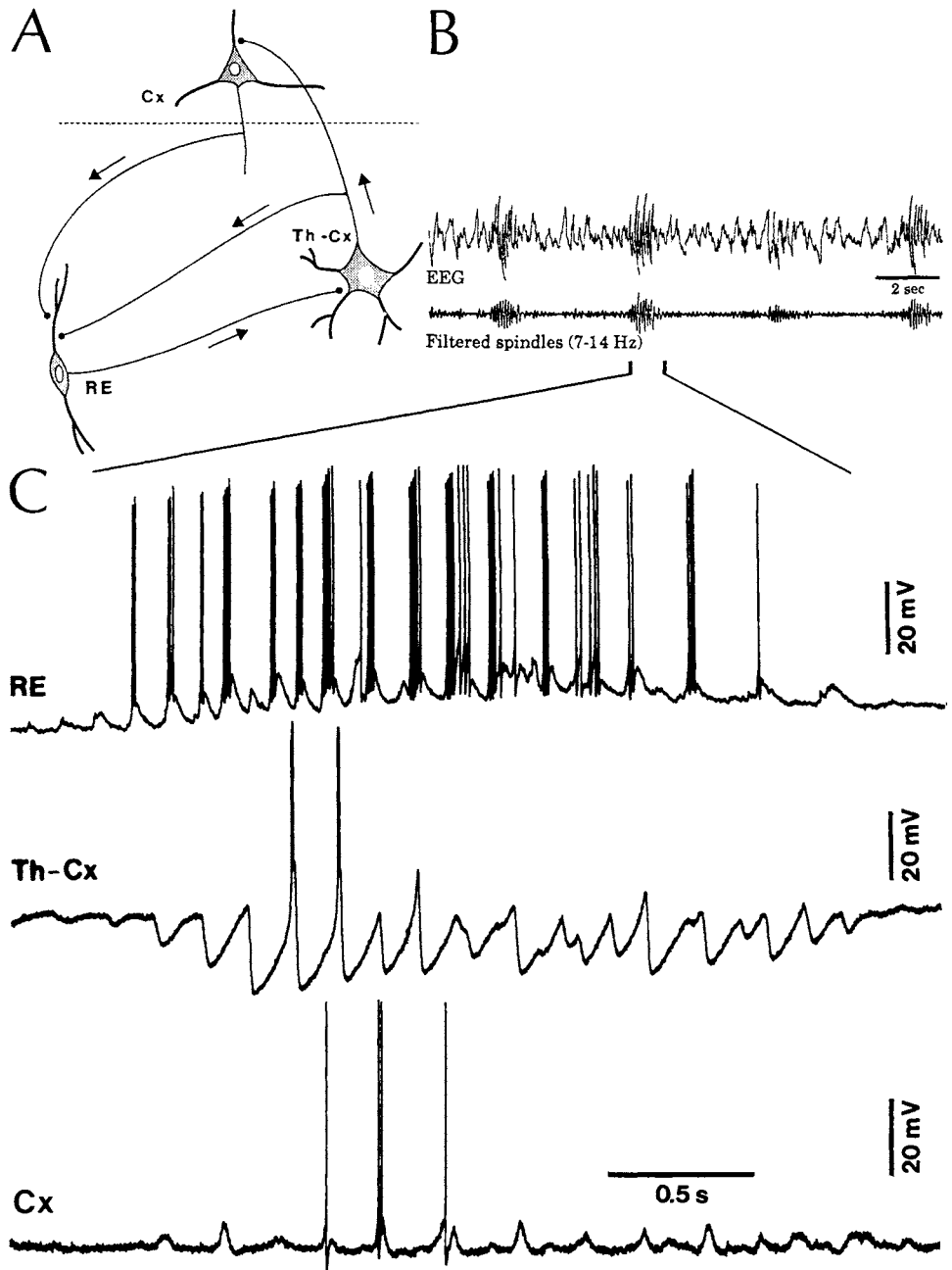


Figure 7.16. Spindle oscillations in thalamic reticular (RE), thalamocortical (Th-Cx, ventrolateral nucleus), and cortical (Cx, motor area) neurons. A, circuit of three neuronal types. B, two rhythms (7–14 Hz and 0.1–0.2 Hz) of spindle oscillations in cortical EEG. C, one EEG spindle sequence is depicted below with intracellular recordings in cats under barbiturate anesthesia. See text. Modified from Steriade and Deschênes (1988).

membrane potential because the same prolonged train of action potentials was recorded extracellularly, during natural NREM sleep [77], in a position that precludes modifications due to impalement. The voltage-dependency of the

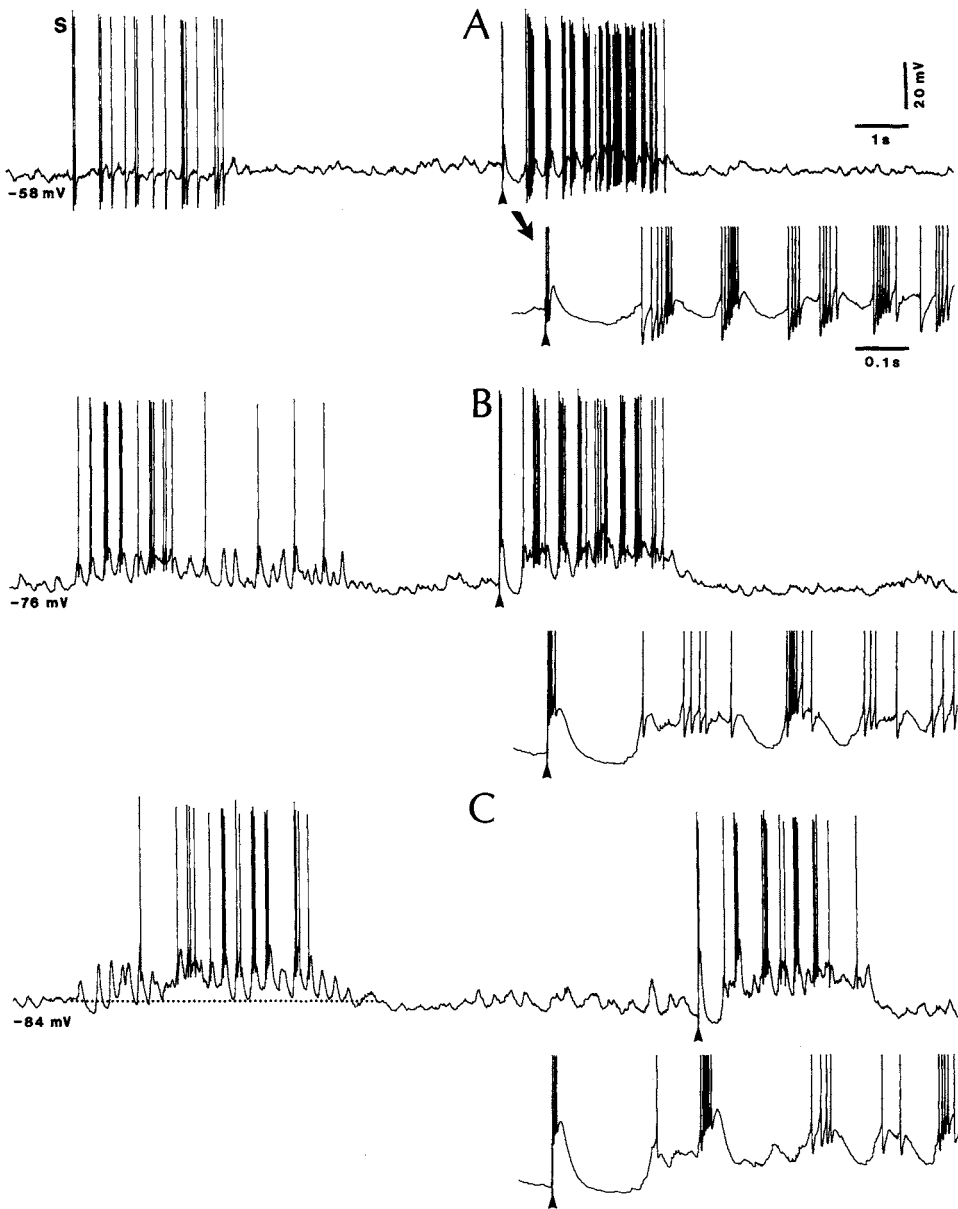


Figure 7.17. Voltage dependency of spindle oscillations in rostral thalamic reticular (RE) neurons. Cat under barbiturate anesthesia. Three panels are depicted (A–C), at different membrane potentials. The cell was depolarized (-58 mV; A) or hyperpolarized (-84 mV; C) from the resting level (-76 mV; B) by means of current injection through the micropipette (in B, no current). The cell displayed spontaneous spindle oscillations (at left in each trace, S in the upper trace) and spindles evoked by cortical stimulation (at right in each trace, arrowhead). Expanded details of the beginning of evoked spindles are depicted below at right (indicated by the arrow in A). From Contreras and Steriade (1996).

Reticular-cells' depolarizing plateau during spindles is illustrated in Fig. 7.17 showing increased amplitude of this plateau at more hyperpolarized levels of the membrane potential [78]. This behavior applies to both spontaneously occurring and cortically evoked spindles.

(c) In contrast to reticular neurons, TC neurons display a hyperpolarizing envelope during spindles and, at depolarized levels from rest, TC neurons exhibit rhythmic IPSPs that do not succeed in de-inactivating spike-bursts (Fig. 7.18). When they do, at more hyperpolarized levels at which I_T is de-inactivated, only some spike-bursts are fired throughout a spindle sequence (see Figs. 7.16 and 7.18), which contrasts with reticular neurons that discharge spike-bursts almost continuously during spindles (see Figs. 7.16 and 7.17). Only one class of TC neurons, recorded from the dorsolateral, large-cell part of the rostral intralaminar CL nucleus, display the propensity to fire spike-bursts after virtually all spindle-related IPSPs (Fig. 7.19) [81]. The ability of these peculiarly bursting neurons to fire a spike-burst after each IPSP is due to the short refractory period (less than 65 ms) of their LTS, whereas other TC neurons show LTS' refractoriness for

[81] Steriade *et al.* (1993c).

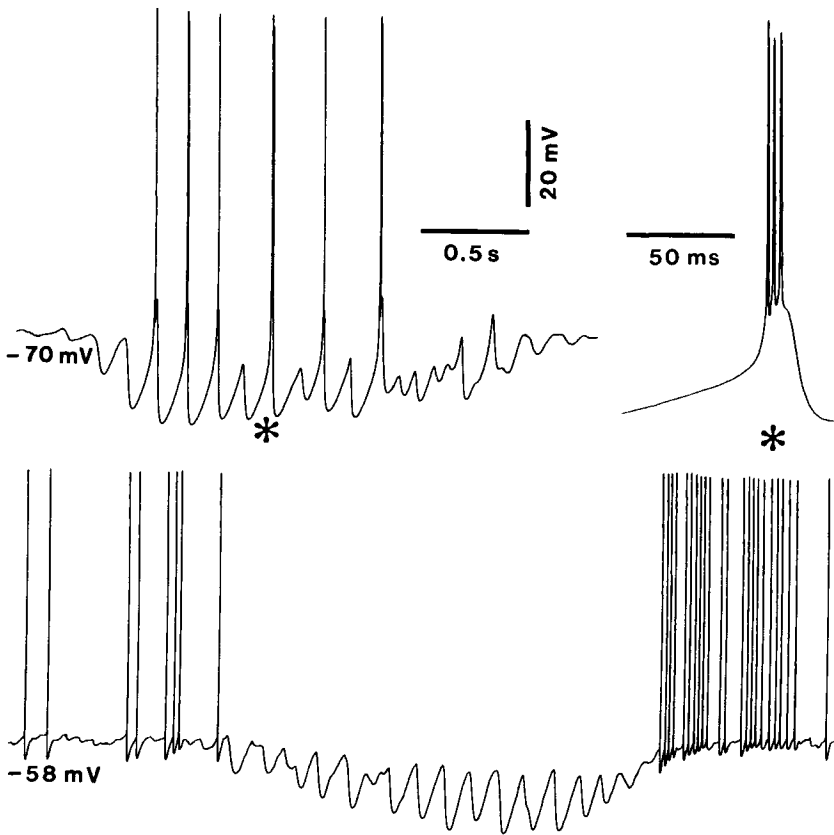


Figure 7.18. Changes in spindle-related rhythmic burst firing of thalamocortical neurons with alterations in the membrane potential. Cat under barbiturate anesthesia. At the resting membrane potential (–70 mV), six spike-bursts were fired during the spindle sequence (burst with asterisk is expanded at right). Upon DC depolarization (0.5 nA), at –58 mV, no spike-burst was fired during the spindle sequence. Modified from Steriade (1993) and unpublished data.

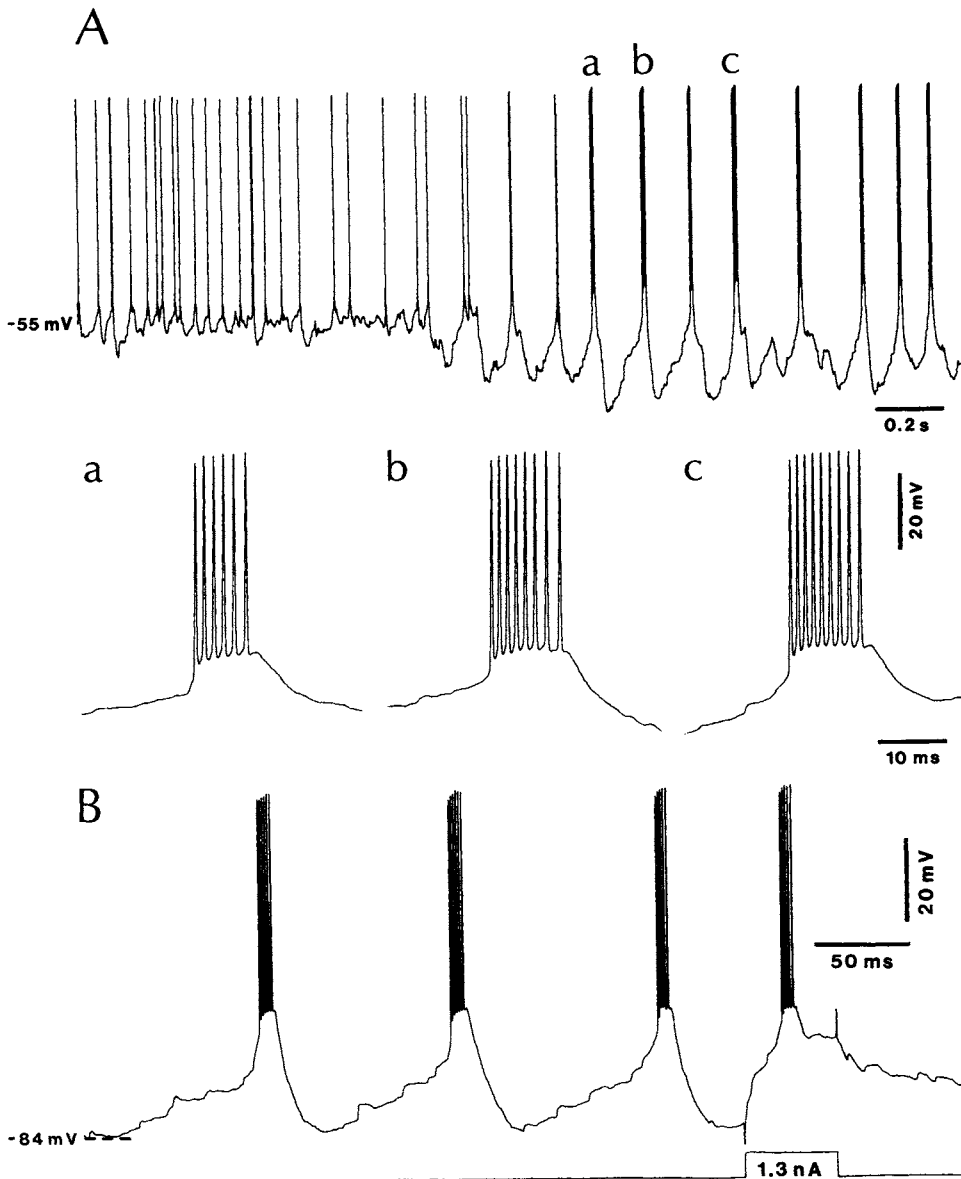


Figure 7.19. Tonic and burst firing of an intracellularly recorded thalamic centrolateral (CL) TC neuron in barbiturate-anesthetized cat. A, tonic firing followed by spontaneously occurring spindle oscillation. Parts a–c are expanded below. Note exceedingly high intraburst frequency of action potentials (800 Hz). Membrane potential was -55 mV during tonic firing and -75 mV at the trough of spindle-related hyperpolarizations. Spike-bursts ride on low-threshold spikes (LTSs) following virtually all IPSPs. B, a sequence of 3 rebound bursts followed by a depolarizing current pulse to show the unusually short (65 ms) refractory phase of the LTS. From Steriade *et al.* (1993c).

170–200 ms (see Chapter 5, Section 5.5.1.1). The widespread projections of CL neurons over the neocortex make them well-suited for the distribution of thalamically generated spindles over the cortical mantle.

7.2.1.3. The Pacemaking Role of Thalamic Reticular Neurons in Spindle Genesis

Since the 1980s, evidence has been accumulated demonstrating that reticular neurons are pacemakers of spindle oscillations. It was first shown that some thalamic nuclei are devoid of afferents from reticular nucleus of cat, the species of choice to study spindles. The nuclei deprived from reticular inputs are the anterior complex (interposed in the limbic circuit between the hippocampus and the cingular cortex) and the lateral habenular nucleus [82]. This connectional feature has a physiological counterpart: spindling is absent in anterior thalamic nuclei (Fig. 7.20) [83], in

[82] Steriade *et al.* (1984a); Velayos *et al.* (1989).
[83] Paré *et al.* (1987).

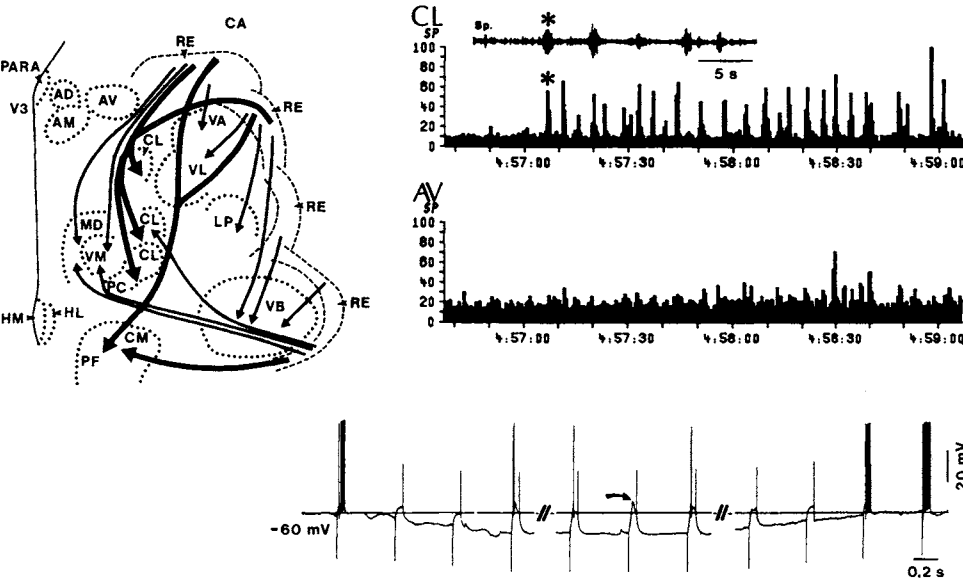


Figure 7.20. Anterior thalamic (AT) nuclei of cat are devoid of afferences from the reticular (RE) nucleus and, despite the fact that the intrinsic property of low-threshold spike (LTS) is present in AT neurons, they do not display spindles because of absence of synaptic connections from the pacemaking reticular nucleus. Left diagram summarizes the reticular projections to various dorsal thalamic nuclei, as resulting from retrograde tracing experiments in cats. Heavy lines indicate prominent projections to intralaminar nuclei. Note absence of projections to AT nuclei. Abbreviations are as follows: AD, AM, and AV, anterodorsal, anteromedial, and anteroventral nuclei; CA, caudate nucleus; CL-PC, centrolateral and paracentral (rostral intralaminar) nuclei; CM-PF, centro median-parafascicular (caudal intralaminar) nuclei; LP, lateroposterior nucleus; MD, mediodorsal nucleus; PARA, paraventricular nucleus; VA, ventroanterior nucleus; VL, ventrolateral nucleus; VM, ventromedial nucleus; VB, ventrobasal complex; reticular, reticular nucleus; V3, third ventricle. Right part depicts simultaneous recordings of field potentials (filtered for spindles, *Sp.*, between 7 and 14 Hz) from CL and AV nuclei in cat. Unanesthetized *cerveau isolé* (collicular-transected) preparation. Abscissa indicate real time (hr, min, s). Data were obtained by applying each filtered EEG signal (see above CL trace, filtered EEG spindles, the first sequence corresponding to the one depicted below) to a full-wave rectifier, a voltage controlled oscillator, and to a laboratory computer (see technical details in that paper). Note regularly recurring spindle sequences in CL nucleus and absence of spindles in the AV nucleus. Below, intracellular recording of an AT neuron, showing tonic firing at a relatively depolarized V_m (−60 mV), LTSs crowned by spike-bursts under steady hyperpolarization when the V_m reaches −72 mV, and recovery of tonic firing at −60 mV. Modified from Steriade *et al.* (1984a) and Paré *et al.* (1987).

[84] Leung and Borst (1987).

[85] Wilcox *et al.* (1988).

the projection areas of the cingular cortex [84], as well as in habenular neurons [85]. All these structures, devoid of reticular afferences, but part of circuits comprising the septum, hippocampus, and entorhinal cortex, display theta rhythmicity that globally characterizes the limbic system. These data emphasize that dorsal (cortically projecting) thalamic nuclei require connections from the reticular nuclear complex to generate spindles and also show that activities in synaptic networks, rather than intrinsic properties, generate spindles. As will be shown below (Section 7.2.2.1), another NREM sleep oscillations, clock-like delta waves, exclusively rely on an interplay between intrinsic currents of TC cells, although their synchronization also require long-range synaptic activities.

The pacemaking role of the reticular nucleus was demonstrated by two major pieces of evidence: (a) spindles disappear in TC systems after disconnection from reticular neurons, and spindle-related long-lasting hyperpolarizations are replaced after disconnection from reticular nucleus by short-lasting IPSPs generated by local interneurons (Fig. 7.21) [86]; and (b) spindles are preserved within the reticular nucleus disconnected from the remaining thalamus and cerebral cortex (Fig. 7.22) [87]. These experimental data were corroborated in different types of computational models of isolated reticular neurons, which displayed oscillations within the frequency range of spindles [88].

The concept of causal relations between rhythmic bursts of GABAergic reticular thalamic neurons and cyclic hyperpolarizations of TC neurons underlying spindle oscillations was also supported by *in vitro* studies in which stimulation was applied to the reticular nucleus at the periphery of the slice and relay cells in adjacent thalamic nuclei were recorded intracellularly [89]. The chloride-mediated IPSPs in TC cells generated by train of pulses to the reticular nucleus gave rise to postinhibitory rebounds (Fig. 7.23A). In contrast to the absence of self-maintained oscillations after current pulses in TC cells, membrane potential oscillations within spindle frequencies were observed after long trains of IPSPs induced by stimulation of the reticular nucleus (Fig. 7.23B). It is worth mentioning that the most effective frequency of reticular stimulation for inducing self-maintained oscillations in TC neurons was around 160 Hz, that is, within the range of usual intraburst frequencies of reticular neurons during spindling in naturally sleeping animals [76, 77]. Detailed analyses of spindle oscillations were performed in slices from ferret visual thalamus [79, 90].

The major differences between the results from *in vivo* [87] and *in vitro* [79] experiments are: the presence of spindles in the disconnected reticular nucleus *in vivo* and the failure to obtain these oscillations after disconnecting

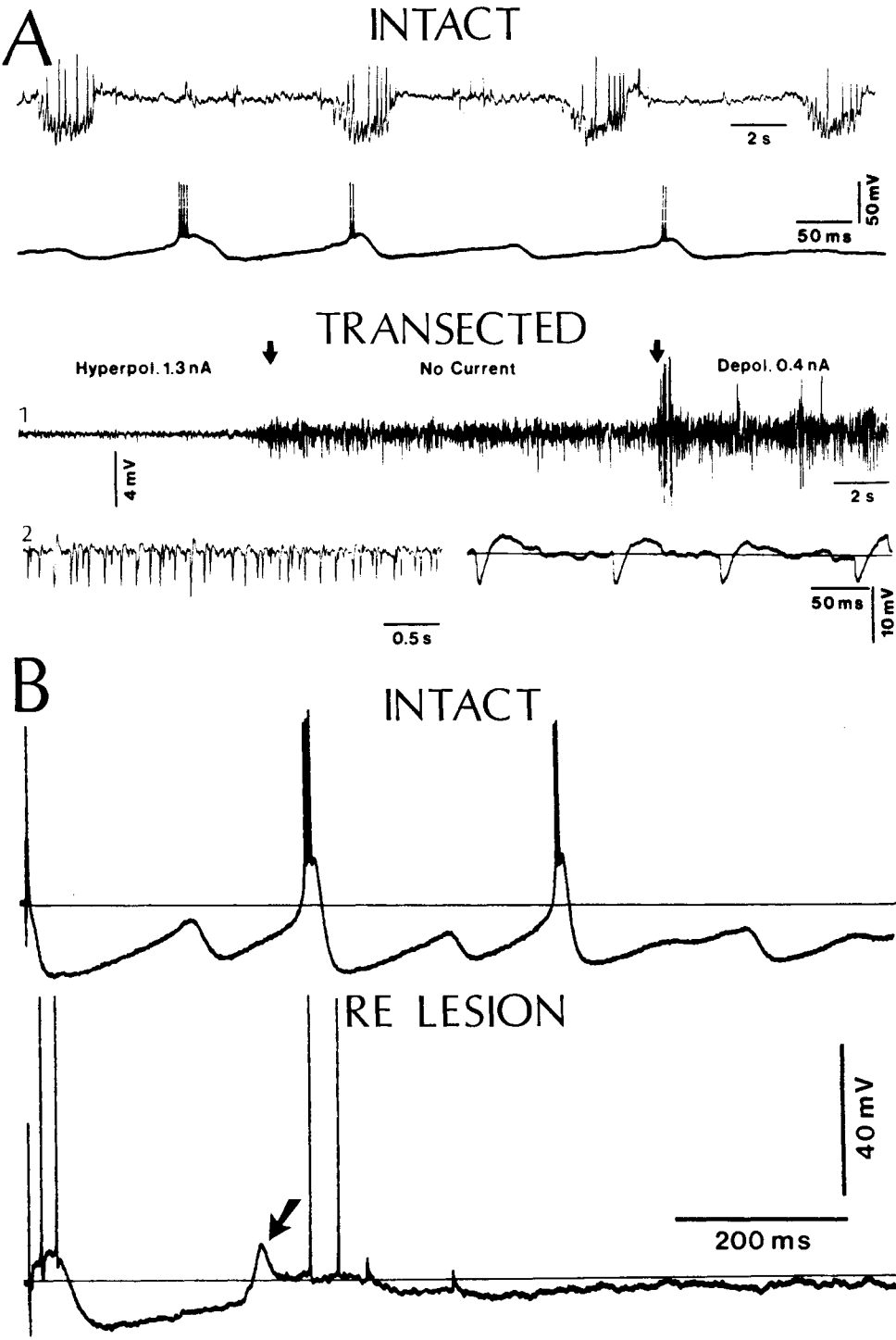
[86] Steriade *et al.* (1985).

[87] Steriade *et al.* (1987a).

[88] Wang and Rinzel (1993); Destexhe *et al.* (1994a); Golomb *et al.* (1994). See also the recent monograph [75] with emphasis on computational studies of spindle oscillations and related phenomena.

[89] Thomson (1988a–b).

[90] Bal *et al.* (1995a–b).



the reticular nucleus *in vitro*; and the nearly simultaneous occurrence of spindles over widespread thalamic and cortical territories *in vivo*, contrasting with the systematic propagation of spindles in a specially cut (sagittal) thalamic slice maintained *in vitro*. These differences are discussed below.

In a collaborative article of *in vivo*, *in vitro*, and *in computo* investigators, it was concluded that the absence of spindles in slices of the isolated reticular nucleus may be ascribed to the incomplete network after slicing the reticular nucleus, as “a larger and more intact collection of reticular thalamic cells may be able to generate spindle waves autonomously” [91]. It is indeed known that the very long dendrites of reticular neurons, which are likely to be cut during the slicing procedure, play a major role in generating and synchronizing spindles within the reticular nucleus [92]. The implication of RE-cells’ in the bursting properties that lead to synchronized spindle oscillations was demonstrated in a combined experimental (*in vivo* and *in vitro*) and modeling study [93]. In contrast to reticular cells with intact dendritic arborizations in which there is a high density of low-threshold transient Ca^{2+} current (I_T), reticular cells in which most of the dendritic arborizations were removed have a much lower density of I_T . With a high density of I_T in distal dendrites, the simulated spike-bursts showed accelerando–decelerando patterns, as is the case with reticular neurons during natural slow-wave sleep [76, 77]. Thus, a reduction in dendritic I_T due to the slicing procedure may diminish the propensity of reticular cells to display spike-bursts similar to those seen in the intact brain and may explain the absence of spindles in the disconnected reticular nucleus *in vitro*. In addition to the slicing of long dendrites of reticular neurons, studies of thalamic spindling mechanisms *in vitro* lack the modulatory influences from brainstem cellular aggregates. A computational study [94] predicted that the depolarization of reticular neurons by inputs arising in monoamine-containing systems [95] would

[91] Steriade *et al.* (1993d). See note 13 in that *Science* article.

[92] The LTSs of reticular neurons are located in the dendrites (Mulle *et al.*, 1986; Huguenard and Prince, 1992). Dendritic LTSs have a graded nature; and the prolonged spike-bursts in these neurons can be modulated both by the level of membrane hyperpolarization and by the intensity of depolarizing inputs (Contreras *et al.*, 1993). The highly excitable dendritic tree and graded bursting behavior of thalamic reticular neurons support their role as generator and synchronizer of spindle rhythmicity *in vivo* [87].

[93] Destexhe *et al.* (1996).

[94] Destexhe *et al.* (1994b).

[95] McCormick and Wang (1991).

Figure 7.21. Abolition of spontaneous and evoked spindle oscillations in thalamocortical (TC) neurons disconnected from the thalamic reticular (RE) nucleus. Intracellular recordings in cats under barbiturate anesthesia. A, spindle oscillations in intact preparation (the two traces represent ink-written recording at the top, and oscilloscopic recording at the bottom) and, below, after thalamic transections that disconnected dorsal thalamic nuclei from the reticular nucleus. In transected preparation, spindle-related rhythmic long-lasting hyperpolarizations are abolished. In 1 of the transected preparation (ink-written recording), polarizing currents (arrows) were passed through the cell membrane to reveal the presence of numerous low-amplitude IPSPs (for comparison, the speed of recording was identical to that in top trace of the intact preparation). In 2, left part shows ink-written recording of IPSPs at higher speed, while right part depicts the same events in oscilloscopic recordings; note the depolarizing hump of the short-lasting IPSP. B, absence of evoked spindle-like oscillatory response in TC neuron after kainic lesion of reticular perikarya. 1, typical oscillatory response of a ventrolateral (VL) TC cell to cortical stimulation (arrowhead) in an intact preparation. 2, response of a VL cell to cortical stimulation after reticular kainic lesion; note absence of oscillations and the presence of a single period of hyperpolarization followed by a low-threshold rebound spike. See the histology of thalamic transections and kainate-induced lesions of the reticular nucleus in Steriade *et al.* (1985). Modified from Steriade *et al.* (1985) and Steriade and Deschênes (1988).

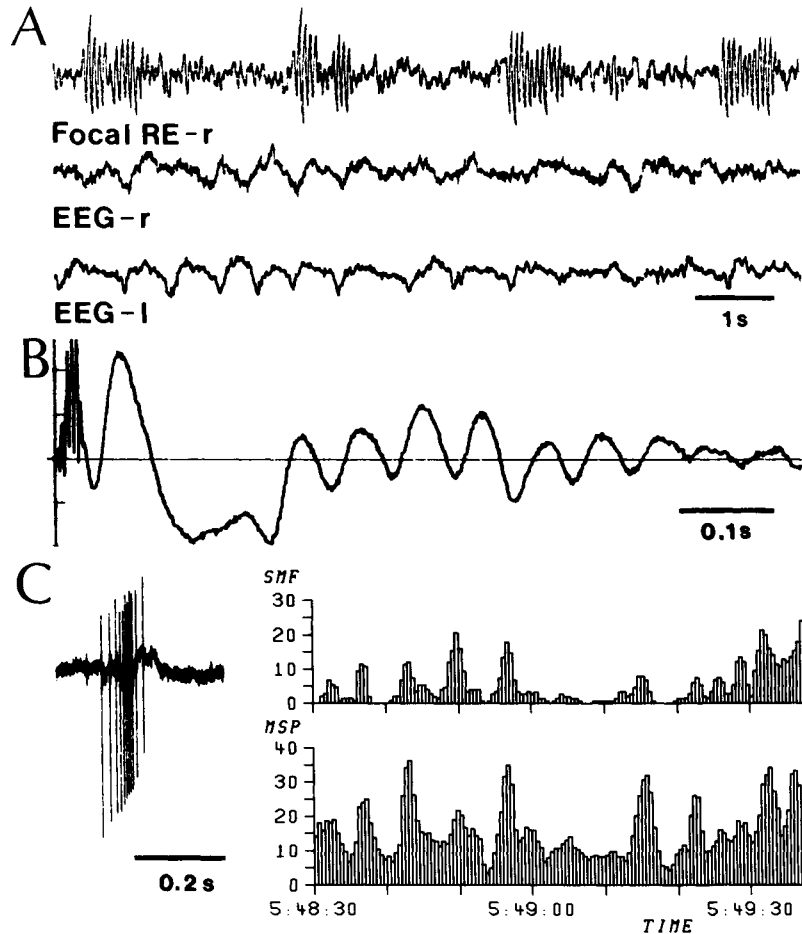


Figure 7.22. The deafferented thalamic reticular (RE) nucleus of cat generates spindle rhythmicity. For histology of transections that created an isolated island containing the rostral pole of the reticular nucleus, see Figs. 1–2 in Steriade *et al.* (1987a). A, normal cyclic recurrence of spindle sequences in the rostral pole of the deafferented reticular nucleus recorded by means of a microelectrode; absence of spindle rhythms (but persistence of slow waves) on cortical EEG recordings due to bilateral thalamic transections. B, oscillations within spindle frequency evoked in the rostral pole of the deafferented reticular nucleus by stimulating (5-shock train) the white matter overlying the caudate nucleus (50 averaged traces). C, slow rhythm of spindle sequences and related cell's burst oscillations in the rostral pole of the reticular nucleus deafferented by thalamic and corona radiata transections. Discharges of a single reticular neuron were simultaneously recorded with focal spindle oscillations by the same microelectrode. Sequential mean frequency (SMF) of the neuron is depicted with the normalized amplitudes of focal waves filtered for spindle waves (MSP). Abscissa indicates real time. At top, two (short and long) spike-bursts from the same period. Modified from Steriade *et al.* (1987a).

promote the sensitivity of reticular neurons to the IPSPs generated by intra-RE GABAergic connections, with the consequence of generating spontaneous oscillations within the frequency range of spindles (Fig. 7.24). This computational study [94] predicted that a medium level of monoaminergic-induced depolarization might change the state of isolated reticular neuronal networks from silence to oscillations within the frequency range of spindles.

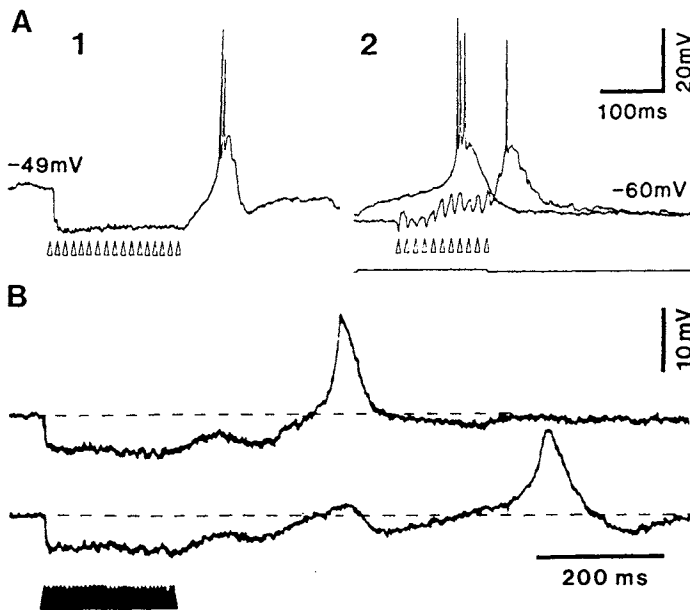


Figure 7.23. Oscillations following trains of inhibitory postsynaptic potentials (IPSPs) induced in rat thalamic neurons studied *in vitro* by stimulating the thalamic reticular (RE) nucleus. A, left, low-threshold spike (LTS) evoked in dorsal thalamic cell by trains of hyperpolarizing IPSPs induced by stimulation of reticular nucleus in the slice; stimulation artifacts indicated by arrowheads. A, right, same cell; comparison between LTS induced from a depolarizing current pulse and LTS following RE-evoked depolarizing IPSPs from a more negative membrane potential. Resting membrane potentials are indicated. B, a high-frequency (160 Hz) train of RE-evoked IPSPs evokes oscillations in dorsal thalamic neuron. Modified from Thomson (1988a).

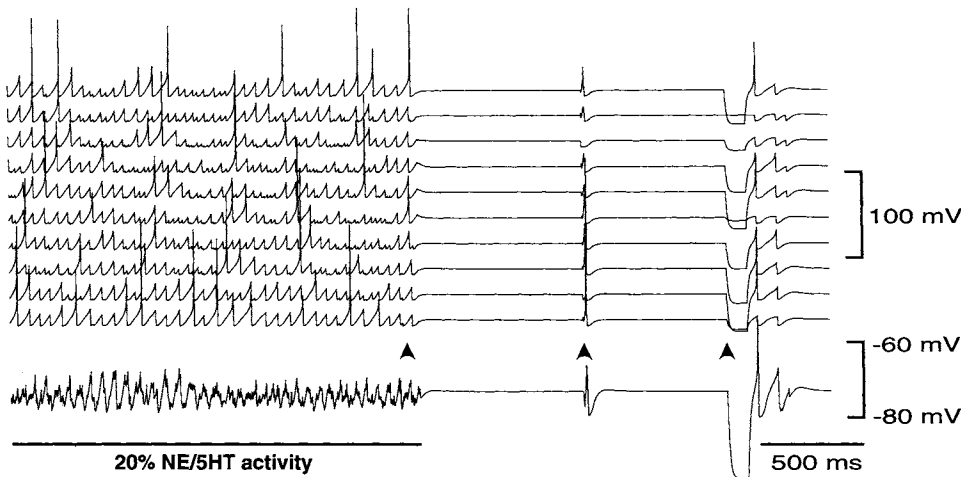


Figure 7.24. Dependence of spindle oscillatory behavior on the membrane potential of model thalamic reticular (RE) neurons. Simulation of a network of 100 RE cells interconnected with their neighbors through GABAergic synapses. The top 10 traces represent the activity of 10 neurons in the network and the bottom trace is the average membrane potential. Twenty percent of norepinephrine (NE)/serotonin (5-HT) synapses were initially activated. In this condition, the network displayed self-sustained oscillation at a frequency of 10–16 Hz and the average membrane potential displayed waxing-and-waning fluctuations in amplitude. After 2 s (first arrow), all NE/5-HT synaptic activity was suppressed; the resulting hyperpolarization prevented the network from sustaining oscillations. Depolarizing (second arrow) or hyperpolarizing (third arrow) current pulses injected simultaneously in all neurons (with random amplitudes) could not restore spontaneous oscillations. From Destexhe *et al.* (1994b).

We proposed that the deafferented reticular cells support oscillations through an avalanche process within the dendrodendritic synaptic junctions of the reticular nucleus [87]. Hyperpolarization through dendrodendritic synapses of GABAergic reticular cells would produce an LTS in the postsynaptic element (say *a*); Ca^{2+} entry in neuron *a* will be followed by GABA exocytosis and hyperpolarization of other dendrites, postsynaptic to those of cell's *a* dendrites; hyperpolarization in the latter elements would succeed in triggering an LTS. In this way, oscillations could spread to adjacent neurons and, ultimately, to large sectors of the reticular nuclear complex. However, we have assumed that any excitatory drive (such as that arising in TC or cortical neurons) impinging upon RE-cells' dendrites could start the process. Although TC-RE loops may assist in developing spindles [91], the synchronization of the whole thalamus during spindling is possible only by invoking the widespread projections of reticular neurons to the dorsal thalamus [82], because there is little cross-talk between dorsal thalamic nuclei.

The other difference between the results from *in vivo* and *in vitro* experiments concerns the increased coherence of spindles in intact-brain animals and is discussed in the next section.

7.2.1.4. The Role of Neocortex in Synchronizing and Terminating Spindle Sequences

One of the most efficient experimental methods to elicit spindles are cortical volleys, applied either ipsilaterally, which directly activates pacemaking reticular neurons (Fig. 7.25), or contralaterally, to avoid antidromic invasion of TC-cells' axons and axon-reflex activation of reticular neurons [96].

This powerful effect of neocortex on spindling explains the cortical influence on spindle synchronization. During natural NREM sleep, spindle oscillations occur simultaneously over vast territories, in the thalamus and cerebral cortex of intact brains, in both humans and animals (Fig. 7.26) [97]. In contrast, spindles propagate systematically in slices from visual thalamus [98]. We hypothesized that this major discrepancy between the results in intact-brain and sliced preparations is due to the absence of neocortex in thalamic slices. Following decortication, we recorded spindle sequences from the same thalamic foci as in intact-brain animals and observed that spindles are no longer simultaneous in the thalamus (Fig. 7.26) [97] without, however, displaying propagation as in slices. The role of the cortex in the simultaneous occurrence of spindles was also shown by diminished coherence of spindles during states, such as barbiturate

- [96] Steriade *et al.* (1972). In those experiments, elicitation of spindles by contralateral stimulation of motor cortex was produced by callosal synaptic excitation of antidromically identified corticothalamic neurons. This bisynaptic pathway, first described in behaving monkeys (Steriade *et al.*, 1974b), was also found using intracellular recordings of cat cortical association neurons (Cissé *et al.*, 2003).
 [97] Contreras *et al.* (1996a, 1997a).
 [98] Kim *et al.* (1995).

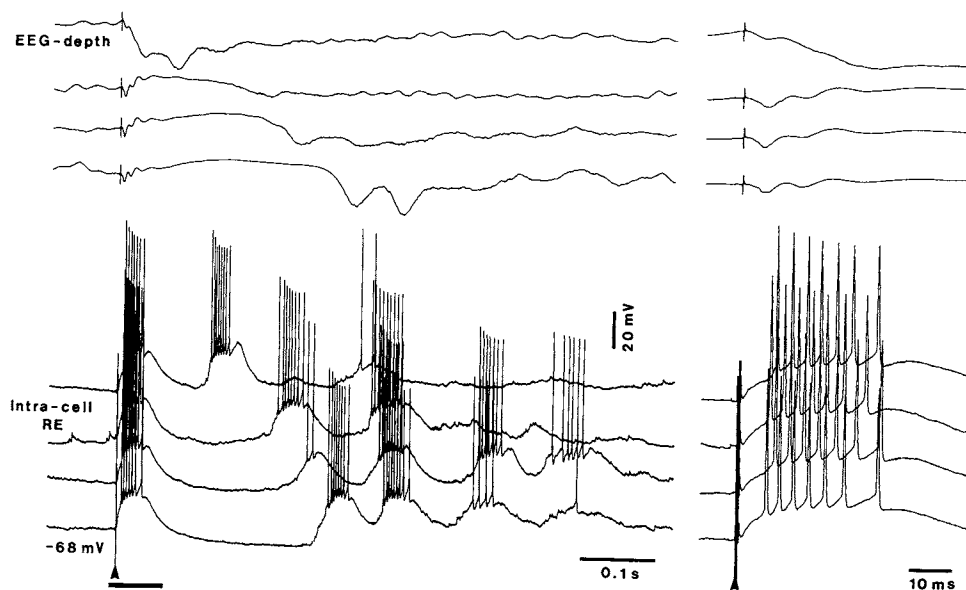


Figure 7.25. Cortically evoked spindle oscillations in thalamic rostralateral reticular (RE) neuron. Cat under ketamine-xylazine anesthesia. The duration of the evoked hyperpolarization varied in parallel with the duration of the depth-positive cortical EEG field potentials. Responses to internal capsule stimuli (arrowheads) consisted of an early spike-burst followed by a long-lasting hyperpolarization that gave rise to a depolarizing spindle sequence. The depth-EEG from the motor cortex was recorded simultaneously. Four different responses (stimuli with constant amplitudes) were selected for their differences in the duration of the evoked hyperpolarization and, consequently, the number of cycles in the spindle sequence. The EEG and intracellular traces correspond 1 : 1, from top to bottom. From Contreras and Steriade (1995).

[99] Contreras *et al.*
(1997b).

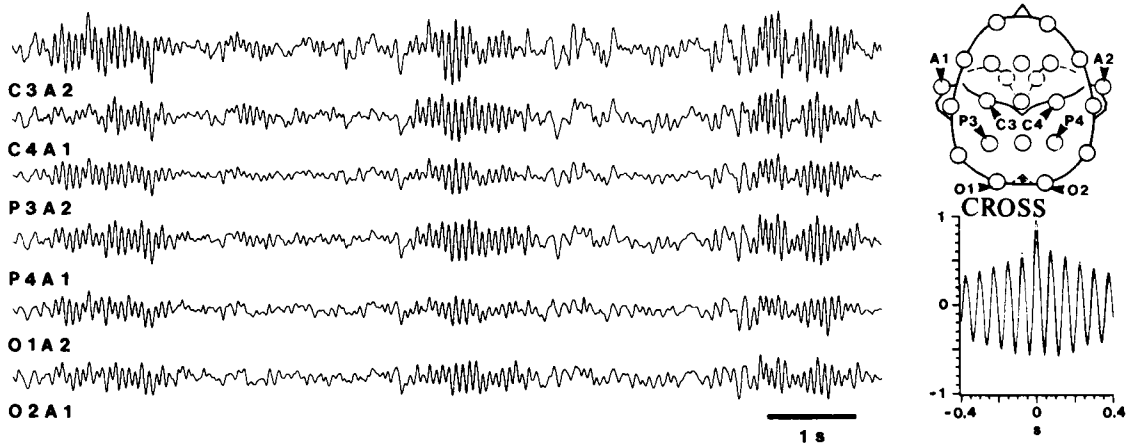
[100] Destexhe *et al.*
(1999a).

[101] Gottselig *et al.*
(2002).

anesthesia or spreading depression induced by topical application of K^+ on cortex, during which corticothalamic neurons display no or negligible spontaneous activity [99]. Computational studies also showed that the simultaneity of spindle oscillations is increased and the phase shift is reduced by increasing the activity of corticothalamic neurons [100]. The powerful role of corticothalamic projections in the high coherence of spindle oscillations was also demonstrated in humans by showing that cortical-damaged patients display significantly reduced coherence spectra from derivations ipsilateral to the lesion [101].

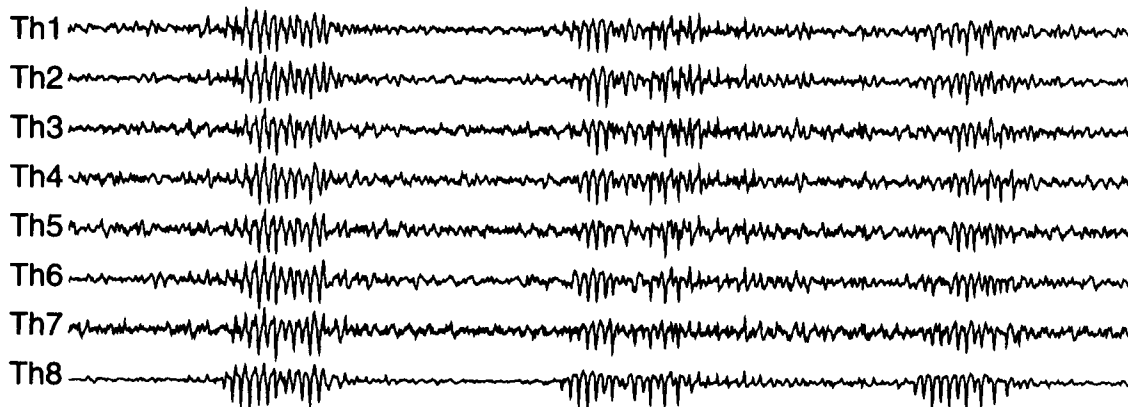
Corticothalamic activity is not only implicated in the long-range synchronization of spindles but also in the termination of individual spindle sequences. One of the factors that may account for the termination of spindle sequences is asynchrony in the thalamic circuit, stemming from the different durations of spindle-related IPSPs in TC cells, resulting in different times at which postinhibitory rebound spike-bursts are fired, so that the synchrony in the TC-RE circuit is disrupted and spindles are terminated. The variability of LTSs generated in the same neuron at the break of a hyperpolarizing current pulse and during

HUMAN



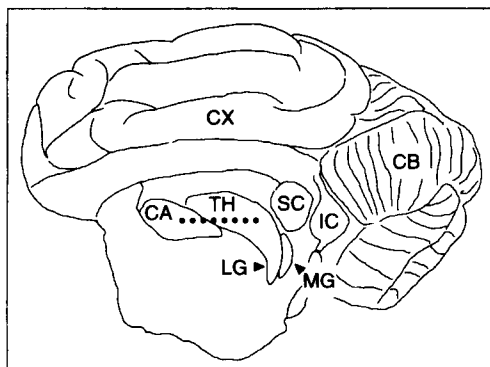
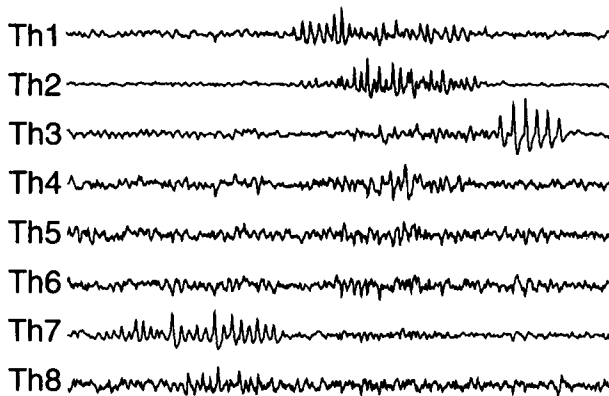
CAT

Intact



Decorticated

200 μ V |



1 sec

[102] Steriade *et al.*
(1998b).

[103] Timofeev *et al.*
(2001a).

[104] *In vitro* studies proposed that up-regulation of the hyperpolarization-activated depolarizing current (I_H) have a role in terminating spindle sequences in TC neurons (Bal and McCormick, 1996; Lüthi and McCormick, 1998).

spontaneously occurring spindles is illustrated in Fig. 7.27. The asynchronous spike-bursts of TC neurons would keep at relatively depolarized level the membrane potential of reticular neurons and thus prevent their LTSS. However, the most important source of spindle desynchronization is cortical input. Some corticothalamic neurons, such as FRB neurons (see Chapter 5, Section 5.6.1), discharge nonaccommodating spike-trains throughout a spindle sequence [102] and may also recruit other cortical neurons into a state that may be out-of-phase with thalamic neurons. During the late phase of spindles, neocortical neurons become tonically depolarized, eventually leading to firing (Fig. 7.28), and spike-triggered-averages by cortical neurons do not reveal a phase relationship between cortical and TC neurons [103]. This depolarization of cortical neurons during the late part of a spindle sequence may be effective in desynchronizing thalamic networks and terminate spindles. This hypothesis was tested in a model of thalamic and neocortical neurons. The RE–TC isolated network oscillated infinitely and up-regulation of I_H alone was not sufficiently strong to terminate spindling [104]. With the addition of the corticothalamic feedback, the spindles in the RE–TC network were shorter. We can then summarize the evolution of individual spindle sequences in the following way: (a) the first part of a spindle sequence is generated in the pacemaker reticular nucleus [87]; (b) during the first 2–4 IPSPs composing the spindles, TC neurons do not display rebound spike-bursts (see Figs. 7.16 and 7.28), thus they do not return signals to reticular neurons and do not contribute to this phase of a spindle sequence; (c) the middle part of a spindle sequence is due to the activity in the RE–TC–RE loop [79, 91]; and (d) the termination of spindles is due to the depolarizing action of I_H and/or the depolarizing action of corticothalamic neurons [103, 104].

One of the functional roles of spindles is to disconnect the cerebral cortex from the external world. The thalamus is the first relay structure where blockage of afferent signals occurs during drowsiness and early stages of NREM sleep, despite the fact that the magnitude of the presynaptic

Figure 7.26. Spindle sequences occur nearly simultaneously in humans and cats, but decortication disorganizes the widespread coherence of thalamic spindles. In the top panel illustrating natural sleep in *HUMAN*, spindles were recorded from six standard EEG derivations (indicated in the schematic at right, arrowheads) in a normal subject, during sleep stage 2. Cross-correlations of individual spindle sequences ($n = 15$) were calculated between C3A2 and each one of the other channels. Averaged correlations (*CROSS*) showed rhythmicity at 14 Hz and central peak values between 0.7 and 0.9. Below, spindles were simultaneously recorded from 7 leads in the thalamus of intact-cortex cat under barbiturate anesthesia. Note the virtual simultaneity of spindle sequences. After decortication (see scheme), recordings from virtually same thalamic sites showed disorganization of spindle simultaneity. Modified from Contreras *et al.* (1996a, 1997a).

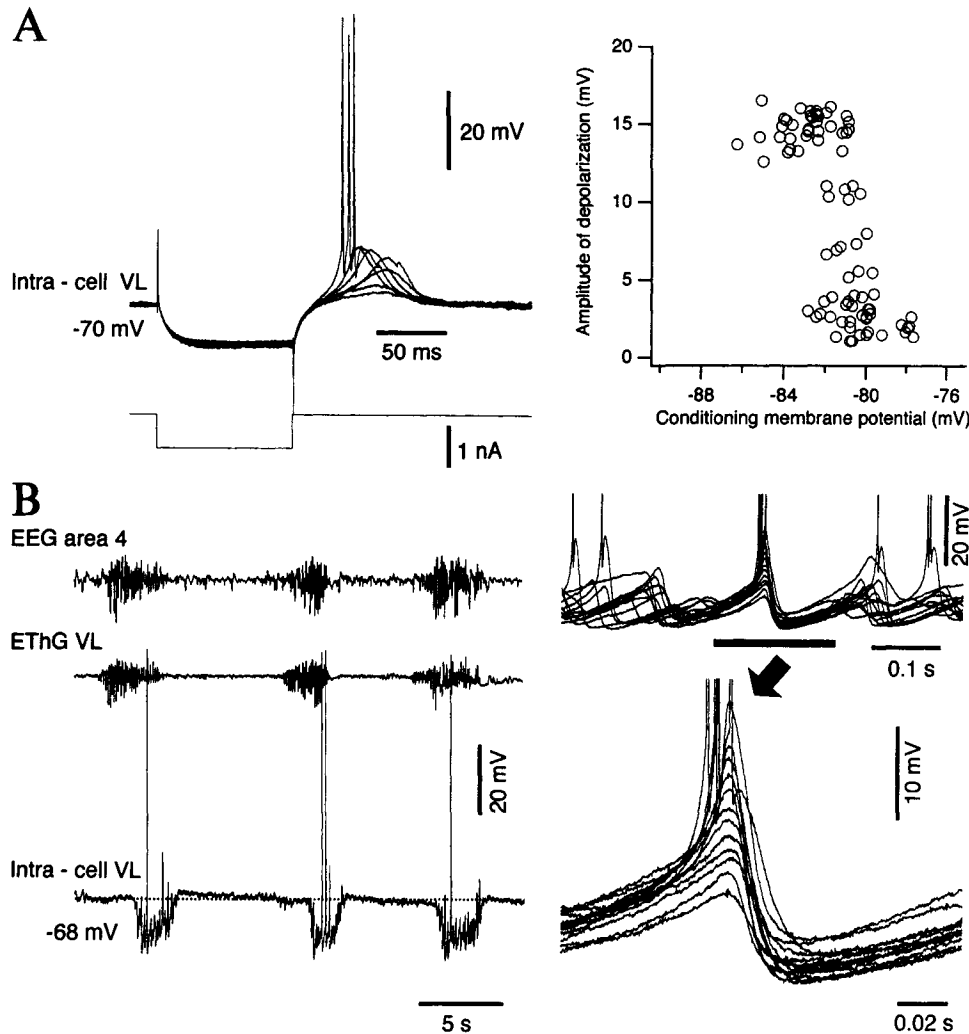


Figure 7.27. Low-threshold spikes (LTSs) in cat thalamocortical neurons are graded in amplitude during spindle oscillation. A, ketamine–xylazine anesthesia. Intracellular recording from the thalamic ventrolateral (VL) nucleus. Fluctuations in time-to-peak and amplitude of LTS at the break of the threshold hyperpolarizing current pulse (-0.8 nA, 0.1 s). Plot at right: conditioning V_m is the V_m just before the end of the current pulse; amplitude of maximal depolarization was calculated from baseline V_m . B, barbiturate anesthesia. Simultaneous field potential from cortical area 4 and VL nucleus, together with intracellular from VL nucleus. Right, an expanded spindle sequence, further expanded below (arrow). Modified from Timofeev *et al.* (2001a).

volley is unchanged, thus showing that no significant changes are seen prior to the thalamus (Fig. 7.29) [105]. The sustained hyperpolarization of TC cells during NREM sleep [106] partially accounts for the blockade of signal transmission to cortex, but the epochs during which afferent messages are most powerfully inhibited are the declining phases of the hyperpolarizations in each spindle wave [107].

[105] Steriade (1991).

[106] Hirsch *et al.* (1983).

[107] Timofeev *et al.* (1996).

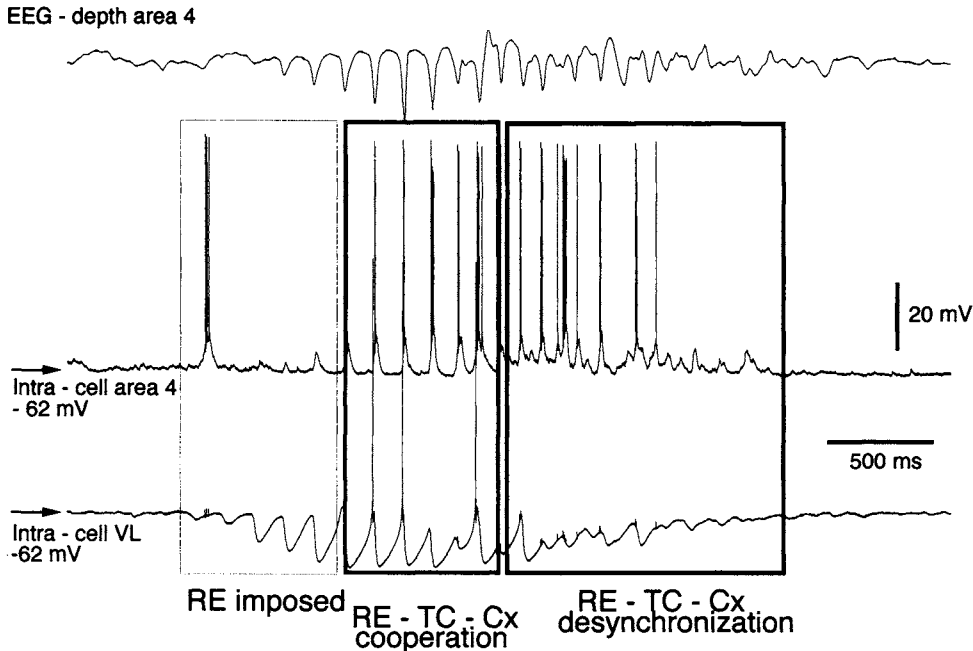


Figure 7.28. Role of corticothalamic input in terminating thalamic spindle sequences. Cat under barbiturate anesthesia. Dual intracellular recording of cortical and thalamocortical (TC) neurons, together with EEG. Three phases of a spindle sequence. Initial phase is imposed by pacemaking reticular (RE) network. During the middle phase of spindle, the activity of cortical, reticular and TC neurons is phase-locked. At the end of spindles, cortical firing induces depolarization of both reticular and TC neurons, which creates conditions for spindle termination. Modified from Timofeev *et al.* (2001a).

7.2.1.5. Blockage of Spindles by Brainstem Activating Influxes

It is known that natural arousal or brainstem reticular stimulation readily blocks spontaneous or evoked spindle waves and transforms the oscillatory mode in TC systems into a relay functional mode, with tonically increased firing rates and enhanced cellular excitability [108]. In addition to the two factors represented by the pacemaking reticular neurons that generate spindles and some intrinsic properties of TC neurons that contribute to the patterning of oscillations, spindles appear as a consequence of dampening activities in brainstem reticular neurons with thalamic projections. Midbrain reticular neurons significantly decrease their firing rates during the transitional period from waking to sleep and reliably slow or completely stop their discharges about 1 s in advance of the first spindle sequence and in repeated transitions from EEG-desynchronized to spindling periods during the drowsiness state (Fig. 7.30) [109].

The generalized spindle rhythmicity is under the control of reticular neurons and the mechanism of diffuse

[108] See previous reviews and monographs (Steriade and Llinás, 1988; Steriade *et al.*, 1990b, 1997a).

[109] Steriade (1980, 1984).

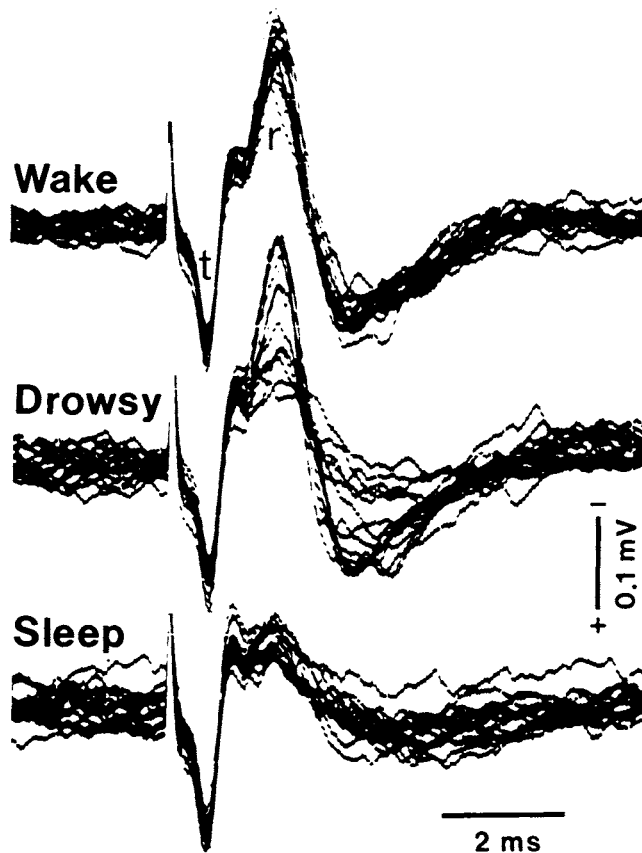


Figure 7.29. Blockade of synaptic transmission in the thalamus at sleep onset in the behaving cat. Field potentials evoked in the thalamic ventrolateral (VL) nucleus by stimulation of cerebellothalamic axons. Note progressively diminished amplitude of monosynaptically relayed (*r*) wave during drowsiness, up to its complete disappearance during full-blown sleep, in spite of lack of changes in the afferent volley monitored by the presynaptic (tract, *t*) component. Modified from Steriade (1991).

spindle disruption by brainstem ascending influxes, as is the case upon natural arousal, should be searched at the very site of spindle genesis, the reticular nucleus. As shown below, the basic mechanism of generalized spindle desynchronization is probably a decoupling in the reticular network due to a cholinergic hyperpolarization of brainstem reticular origin.

The blockage, during natural EEG activation or brainstem reticular stimulation, of spindle-related rhythmic IPSPs and postinhibitory rebound spike-bursts was reported for TC neurons recorded extra- and intracellularly from the dorsal lateral geniculate (LG), lateroposterior (LP), ventrolateral (VL), and intralaminar CL nuclei [110]. In lightly anesthetized or unanesthetized (brainstem-transected or chronic) preparations, the brainstem-induced blockage of spindle sequences is associated with tonic firing of TC neurons, which may outlast the stimulation period. Under barbiturate anesthesia, however, spindling is

[110] Singer (1973); Steriade *et al.* (1971, 1977b); Glenn and Steriade (1982); Steriade (1984); Hu *et al.* (1989b).

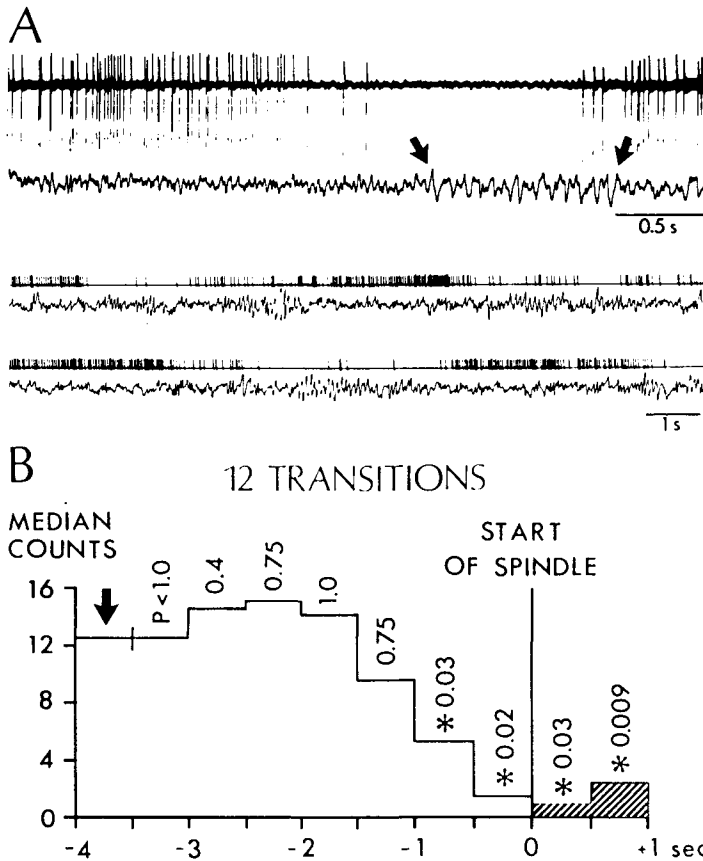


Figure 7.30. Midbrain reticular formation neuron with antidromically identified projection to the intralaminar thalamus decreases discharge rate in advance of the first spindle sequence during transition from waking (W) to EEG-synchronized sleep (S) in cat. A, top two traces depict original spikes and EEG waves simultaneously recorded on oscilloscope. First spindle sequence in W-S transition indicated between arrows. Bottom traces: same activities during repeated EEG desynchronization-synchronization transitions (ink-written recordings). B, 12 transitions of unit firing with respect to start of EEG spindle (time 0). Arrow at left: level of discharge (median rate) during W. Asterisks: bins with significant (<0.05) decrease in firing rate compared with median rate during W. Significantly decreased firing rate occurred 1 s before spindle onset. Modified from Steriade (1980, 1984).

blocked without the occurrence of any tonic discharges in TC cells, and a single rebound spike terminates the aborted spindle sequence (Fig. 7.31).

The origin of spindle disruption in TC cells by brain-stem reticular stimulation is the blockage of spindles at the site of their generation, the reticular nucleus. Short pulse-trains to the cholinergic pedunculopontine tegmental nucleus (PPT) prevent the occurrence of spindles in the perigeniculate (PG) sector of the reticular nuclear complex or block ongoing spindle sequences (Fig. 7.32) [111]. As shown above, spindle oscillations of reticular cells develop on a depolarizing envelope. The brainstem cholinergic stimulation induces a large hyperpolarization that

[111] Hu *et al.* (1989a).

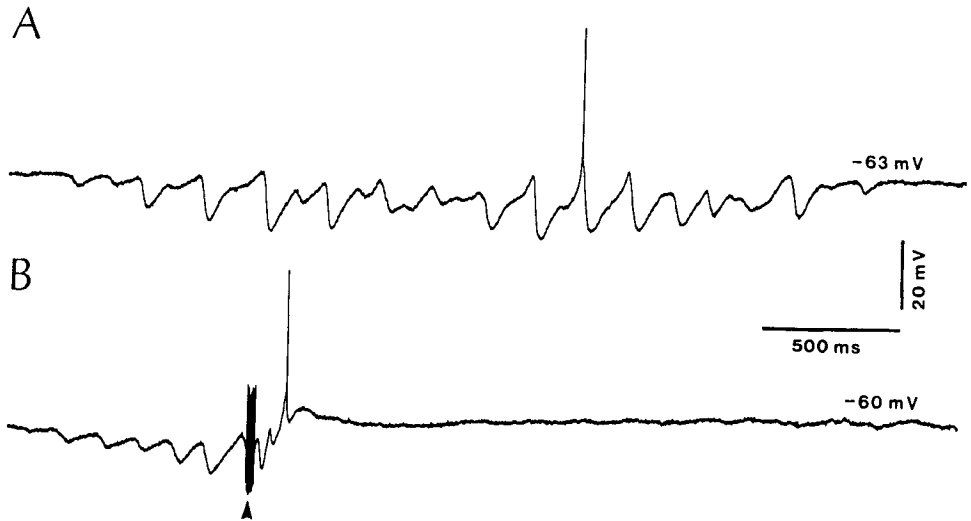


Figure 7.31. Blockage of spindle oscillations in thalamic relay neurons by stimulating the brainstem peribrachial (PB) area (pedunculo pontine tegmental nucleus) in cat. Intracellular recordings from relay cell recorded from the LG nucleus. Resting potential is indicated. A–B, spontaneous spindle sequence (A) and disruption of a spindle sequence by PB stimulation (arrow head in B). Modified from Hu *et al.* (1989b).

blocks the spindles in PG neurons (Fig. 7.32A). Measurements of conductance changes associated with the hyperpolarizing response of PG neurons showed an increased conductance of about 40–50% (Fig. 7.32B). Since the PB-induced hyperpolarization of reticular neurons is abolished after administration of the muscarinic blocker, scopolamine [111], the main mechanism of the spindling blockage by PB stimulation seems to be a cholinergic hyperpolarization. This assumption is further supported by the fact that data similar to those depicted in Fig. 7.32 were also obtained after amine depletion in reserpine-treated animals.

We dealt with the projections from brainstem reticular core to basal forebrain neurons and with the projection from cholinergic and GABAergic basal forebrain neurons to the rostral pole and rostromedial districts of the reticular nucleus in Chapter 3 (Sections 3.3.2–3.6.2). The existence of these circuits indicates that whenever brainstem reticular stimulation is applied, the spindle blockage may arise from an inhibition of spindle genesis in the reticular nucleus from the brainstem–RE neurons as well as from the parallel activation of the basal forebrain structures. The latter circuit is not responsible for data reported in the PG zone of the reticular nucleus (see Fig. 7.32) since there are no basal forebrain projections to that caudal part of the reticular nucleus. However, for most dorsal thalamic nuclei that receive powerful projections from the rostral pole and rostromedial zones of the reticular nucleus, one should

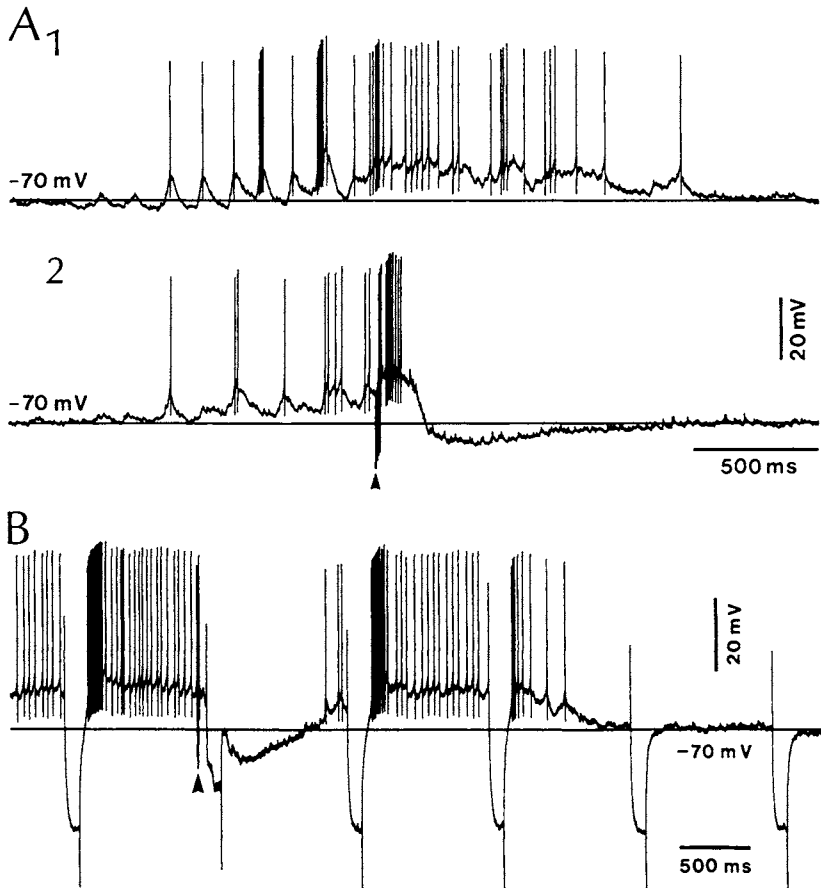


Figure 7.32. Blockage of spindles at the very site of their genesis, the reticular (RE) thalamic nuclear complex, by brainstem peribrachial (PB) stimulation in cat. Intracellular recordings of two (A and B) neurons from the perigeniculate (PG) sector of the reticular nuclear complex. Resting potential is indicated. A, an expanded spindle sequence is shown in 1, and another spindle sequence was aborted by PB stimulation (arrowhead in 2). B, change in membrane resistance induced by PB stimulation in a PG thalamic cell. Current pulse intensity: 2 nA. In the right part of the trace, a sustained hyperpolarizing current was injected to estimate the amount of anomalous rectification in the conductance change observed during the response. Note that, in spite of anomalous rectification, the drop in membrane resistance was of the order of 50%. Modified from Hu *et al.* (1989a).

consider that basal forebrain neurons play a role in spindle blockage. In keeping with this idea, chemical lesions of rat basal forebrain perikarya are followed by a statistically significant increase in the incidence of spindle activity [112]. Thus, a decrease in discharge rates of basal forebrain neurons would be associated with spindle oscillations in TC systems. These data suggest that a dampening activity in basal forebrain cholinergic and/or GABAergic neurons is a permissive factor for spindle genesis in the reticular nucleus, and corroborate similar results concerning the actions of thalamically projecting brainstem reticular neurons (see above, Fig. 7.30).

[112] Buzsáki *et al.* (1988b).

In conclusion then, the blockage of spindle rhythms during EEG desynchronization is due to a decoupling in the synaptic networks of reticular nucleus by brainstem and basal forebrain axons.

7.2.2. Two (Thalamic and Neocortical) Components of Delta Waves

With deepening of NREM sleep, slower EEG rhythms progressively develop. These waves are conventionally termed “delta,” whence the term “delta sleep” applied to stages 3–4 of sleep in humans or to the later part of EEG-synchronized sleep in cats. However, the origin and cellular mechanisms of the slow oscillation (less than 1 Hz) are distinct from those that built up the delta waves (1–4 Hz). Hereafter, the term *delta* will be conventionally used for oscillations within the frequency range of 1–4 Hz, and the term *slow* for waves below 1 Hz (see next Section, 7.2.3). Delta waves are generated at two levels, in TC neurons and in neocortex, through quite different mechanisms.

7.2.2.1. Clock-like Thalamic Delta Rhythm: Generation, Synchronization, and Suppression

The thalamic component of delta waves has a clock-like pattern and depends on two inward currents of TC neurons: a hyperpolarization-activated current, I_H , carried by Na^+ and K^+ , which is expressed as a depolarizing sag of membrane potential toward rest; and a transient Ca^{2+} current, I_T , underlying the LTS (see Chapter 5, Section 5.5.1). The mechanisms of generation and synchronization of this thalamic oscillation were revealed using intracellular studies *in vitro* [113] and *in vivo* [114].

The prerequisite for the appearance of this rhythm is the hyperpolarization of TC neurons, generally to levels more negative than -65 or -70 mV, while depolarization of TC neurons leads to abolition of this rhythm (Fig. 7.33A). Thus, in contrast to the spindle oscillation that is generated by synaptic interactions that necessarily include reticular nucleus, the delta oscillation is an intrinsic oscillation of TC neurons.

The incompatibility between spindles and delta waves, which only occurs at the level of single neurons (and not at the EEG level), is due to the fact that these two rhythms appear at different membrane potentials of TC neurons. Around -60 mV, TC neurons display spindles, whereas at membrane potentials more negative than -65 or -70 mV spindles progressively decrease in amplitude and oscillations

[113] Leresche *et al.* (1990, 1991); McCormick and Pape (1990a); Soltesz *et al.* (1991).

[114] Steriade *et al.* (1991a); Curró Dossi *et al.* (1992a); Nuñez *et al.* (1992a,c).

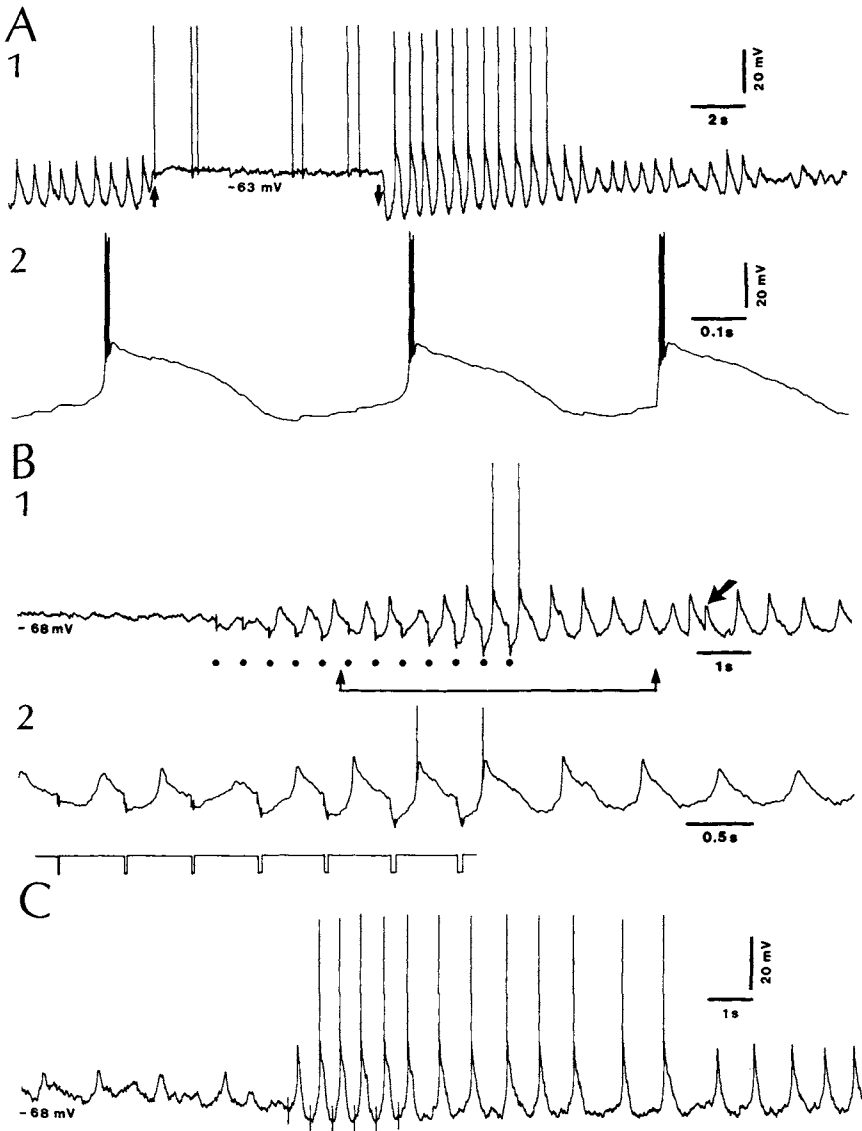


Figure 7.33. Clock-like delta oscillation in thalamocortical (TC) neurons *in vivo*, and its facilitation by corticothalamic volleys. Cats under urethane or ketamine and xylazine anesthesia. A, lateroposterior (LP) TC neuron. At “rest,” the cell oscillated spontaneously at 1.7 Hz. A 0.5 A depolarizing current (between arrows) prevented the oscillation and its removal set the cell back in the oscillatory mode. Three cycles after removal of depolarizing current in 1 are expanded in 2 to show high-frequency spike-bursts crowning low-threshold spikes (LTSs). B, induction of self-sustaining delta oscillation by injecting short rhythmic hyperpolarizing current pulses (1). TC neuron from LP nucleus recorded at “rest” during an oscillation-free period. The frequency of the pulse was chosen according to previously recorded oscillatory epochs. Pulse duration was progressively increased until rebound LTSs with Na^+ spikes could be triggered. Pulse amplitude was 0.4 nA. The portion between arrows is depicted at higher speed in 2 with the current monitor trace. Note progressive development from subthreshold to suprathreshold self-sustaining delta oscillations. Oblique arrow in 1 marks the spontaneous occurrence of a fast prepotential. C, cortical potentiation of thalamic delta oscillation. At a membrane potential of -68 mV, a subthreshold oscillation at 0.8 Hz appeared. Six cortical volleys induced LTSs and, after cessation of stimuli, a self-sustained delta oscillation at approximately 1.5 Hz ensued for 15 s. Modified from Steriade *et al.* (1991a, panels A and C) and Curró Dossi *et al.* (1992a).

are within the delta frequency range [114]. We have, thus, postulated a progressive hyperpolarization of TC cells with the deepening of NREM sleep, which is attributable to the progressive decrease in firing rates, during NREM sleep, of corticothalamic, midbrain core, and mesopontine cholinergic neurons with thalamic projections, and some monoaminergic nuclei (see Chapter 9).

Cortical volleys potentiate delta oscillation in TC cells by transforming subthreshold depolarizing waves into rhythmic LTSs crowned by fast Na^+ action potentials, which may persist for 10–20 s as a self-sustained activity (Fig. 7.33C). Although delta is an intrinsic rhythm of single TC cells, cortical volleys succeed in synchronizing different TC neurons and induce field potentials oscillating in the delta frequency range (Fig. 7.34) and are also capable of synchronizing delta-oscillating TC cells that were uncoupled prior to cortical stimuli (Fig. 7.35). This synaptic action is mediated by thalamic reticular GABAergic neurons that set the membrane potential of TC neurons at the hyperpolarized level required for delta oscillations. Thus, an intrinsic property of TC cells is powerfully modulated by synaptic network operations.

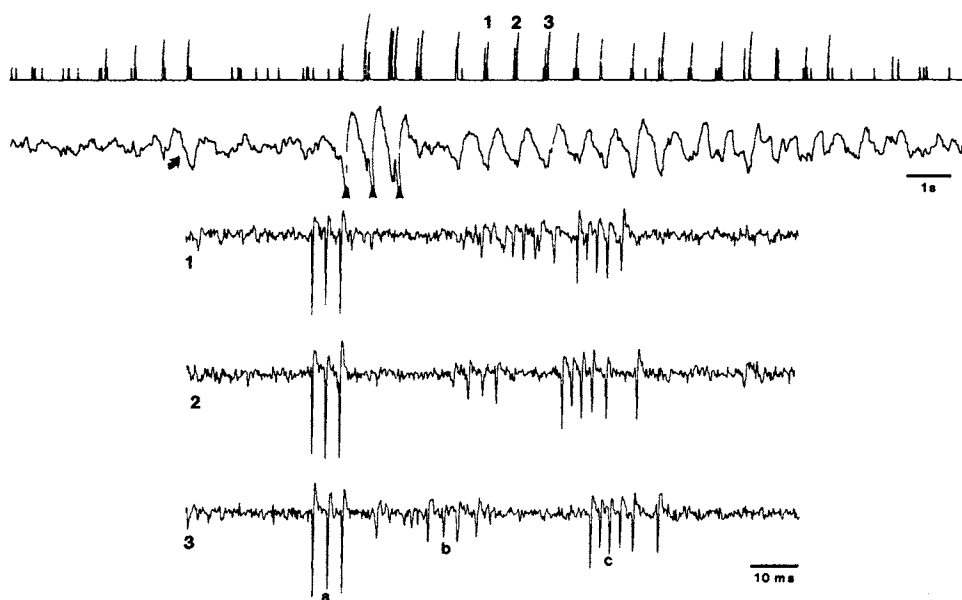


Figure 7.34. Cortically induced synchronization of three cells (a–c), simultaneously recorded in the thalamic lateroposterior (LP) nucleus, and occurrence of focal delta waves. Cat under urethane anesthesia. Top two traces, firing of three cells (deflections exceeding the lowest level indicate spike-bursts of one, two, or all three cells) and focal waves recorded by the same microelectrode. Note appearance of episodic delta waves (oblique arrow) preceded by burst firing. After three cortical stimuli (arrowheads), buildup of delta waves (1.5 Hz) lasted for 8 s, associated with synchronous spike-bursts in all three cells (epochs 1, 2, and 3 are expanded in the bottom three traces and depicted with original spikes). Note regular sequence of high-frequency (300–400 Hz) spike-bursts in cells a–c. From Steriade *et al.* (1991a).

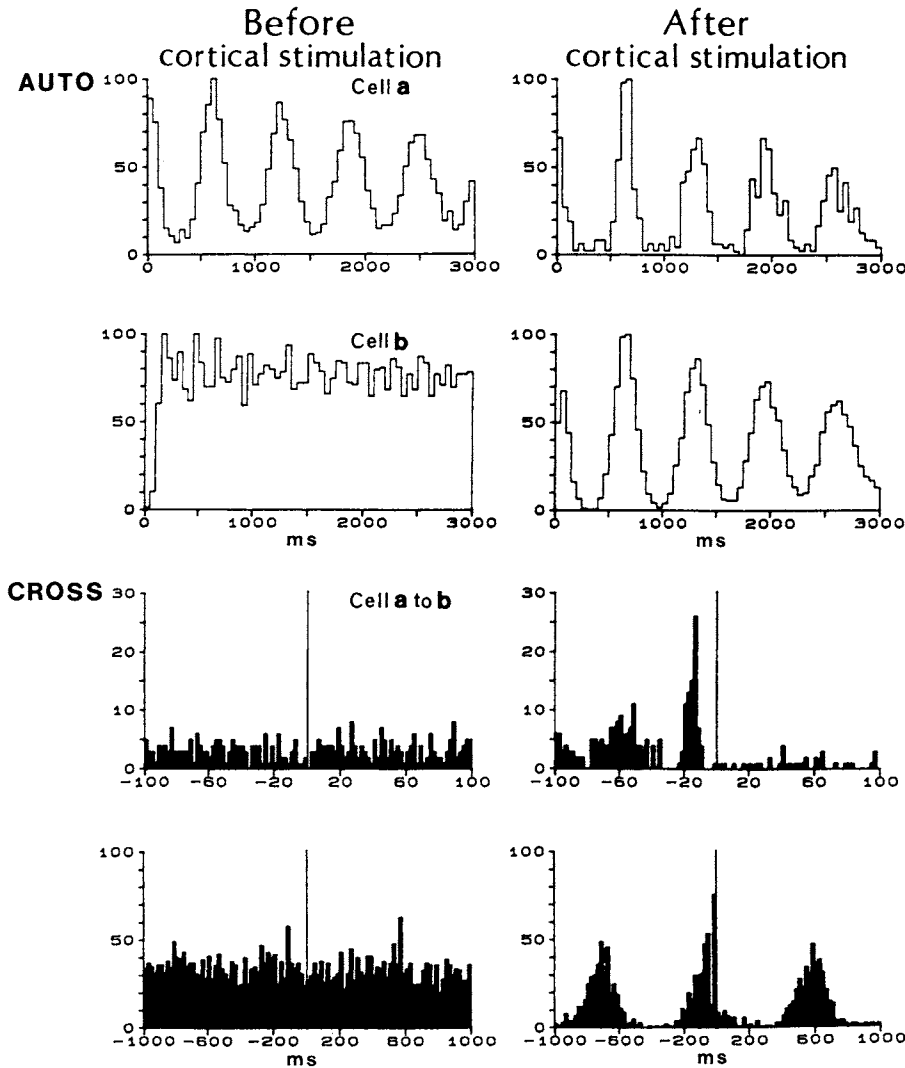


Figure 7.35. Clock-like delta oscillation in TC neurons, and synchronization of this intrinsic oscillation in different TC neurons by corticothalamic synaptic volleys. Cat under urethane anesthesia. Auto- and cross-correlograms of two cells (a and b), recorded simultaneously in the thalamic ventrolateral nucleus. Four correlograms (before and after cortical stimulation) depict, from top to bottom, autocorrelogram of cells a and b, and cross-correlograms of both cells (cell b is the reference cell) with different bins (2 and 20 ms). Note, before cortical stimulation, delta rhythm (1.6 Hz) of cell a, flat contour (absence of rhythmicity in cell b), and absence of coupling between these neurons. After corticothalamic synaptic volleys, the background noise in cell a was reduced, cell b became rhythmic at the same frequency as cell a (1.6 Hz), and cross-correlograms show that cell a firing preceded cell b firing by about 10–20 ms. Modified from Steriade *et al.* (1991a).

The obliteration of thalamic clock-delta oscillation is due to the depolarization of TC cells exerted by ascending influxes from mesopontine cholinergic nuclei, thus bringing TC neurons out of the voltage range at which clock-like delta rhythm is generated [114]. Besides, impulses arising in afferent specific pathways are capable of preventing thalamic delta-oscillating neurons. Figure 7.36 depicts

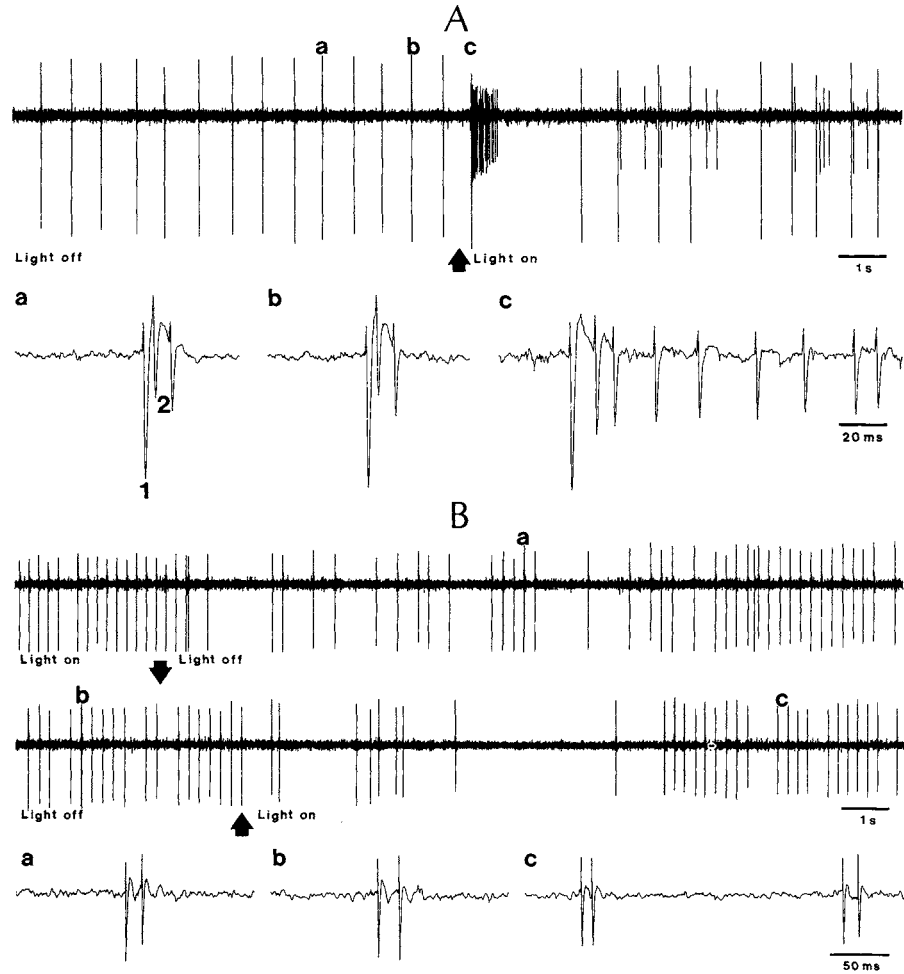


Figure 7.36. Disruption of intrinsic delta oscillation in thalamocortical (TC) neurons from thalamic lateral geniculate (LG) nucleus by changes in ambient luminosity. Extracellular recordings in cats under urethane anesthesia. A. two simultaneously recorded neurons (1, 2) were synchronized during darkness, with an oscillation at 1.8 Hz. Light-on induced tonic firing of neuron 2, blocked cells' synchronization, and disrupted the clock-like oscillation. Parts a–c are expanded below. B, an oscillation at 4 Hz was initially present during light-on, was blocked by light-off but resumed after 10 s, and was also blocked by light-on with recovery after 9 s. Three episodes (a–c) are expanded below to show the stereotyped spike-doublets. From Nuñez *et al.* (1992c).

visual thalamic neurons oscillating with rhythmic spike-bursts in the frequency range of delta oscillation, and the replacement of this oscillation by ambient light.

7.2.2.2. Cortical Delta Waves

The cortical origin of at least one component of delta waves was shown by their persistence in animals with bilateral [115] or unilateral [116] thalamic destruction and their disappearance at subcortical levels after large neo-cortical ablations [117].

[115] Villablanca (1974).
[116] Steriade *et al.* (1993f).
[117] Jouvet (1962).

[118] Calvet *et al.* (1964).

[119] Petsche *et al.* (1984).

[120] Ball *et al.* (1977).

[121] Steriade and Buzsáki (1990).

[122] Schwindt *et al.* (1988a–b).

[123] Steriade *et al.* (1974a).

[124] Oakson and Steriade (1982, 1983).

[125] Steriade *et al.* (1993e). In that initial paper, data from human sleep EEG were also reported showing the grouping of delta waves (1–4 Hz) within the frequency of the slow oscillation (<1 Hz).

[126] Steriade *et al.* (1996a).

[127] Steriade *et al.* (2001a).

[128] Achermann and Borbély (1997).

[129] Amzica and Steriade (1997).

[130] Simon *et al.* (1999, 2000).

[131] Steriade *et al.* (1993f).

There is no systematic intracellular study of slow waves. Laminar profiles in cat suprasylvian cortex indicate that the generator of slow waves is at a depth between 0.6 and 0.9 mm [118], between layers III and V. Current source density analyses showed that 4-Hz waves in rabbit visual cortex display dipoles between layers II–III and V, while waves within higher frequency bands are more pronounced in deeper cortical layers [119]. The surface-negative component of slow waves reverses abruptly at the upper border of layer V, and the depth-positive wave is typically associated with silence in neuronal firing [112]. Similar relations have been reported for pathological slow waves induced by thalamic or midbrain reticular lesions [120]. It was suggested [121] that cortical delta waves reflect summated long-lasting after-hyperpolarizations (AHPs) produced by K^+ currents (mainly $I_{K(Ca)}$) in pyramidal neurons [122]. The decreased excitability that accompanies the slow AHPs is consistent with the decreased synaptic and antidromic responsiveness of pyramidal tract and other corticofugal neurons during EEG epochs with delta waves [123].

The amplitudes of cortical slow waves display oscillations (periods 6–12 s) and increase progressively from the transitional period of drowsiness to fully developed sleep, in close temporal relationship to a progressive decrease in discharge rates of upper midbrain reticular neurons [124]. Since neurons in the rostral reticular core do not have direct cortical projections (see Chapter 3, Section 3.4.1), this relationship is presumably transmitted by intercalated neurons. In particular, basal forebrain cholinergic neurons seem to influence the genesis of cortical slow waves since their unilateral destruction produces an asymmetric map of delta distribution, with an increase in the delta band ipsilateral to the lesion [112].

7.2.3. The Neocortical Slow Oscillation: Its Role in Grouping NREM Sleep and Fast Rhythms

The slow oscillation (~ 0.5 –1 Hz) was first described in 1993, using intracellular recordings from different neuronal types in anesthetized cats [125]. It was confirmed, with the same features, using extracellular [126] and intracellular [127] recordings in chronically implanted, naturally sleeping animals, and was also detected in EEG [128, 129] and MEG [130] recordings during natural NREM sleep in humans. The grouping of two oscillatory types, within frequency bands of 1–4 Hz and 0.3–1 Hz [125, 131], is one of the arguments supporting the distinctness between delta and slow sleep oscillations (see below, Section 7.3.3.2).

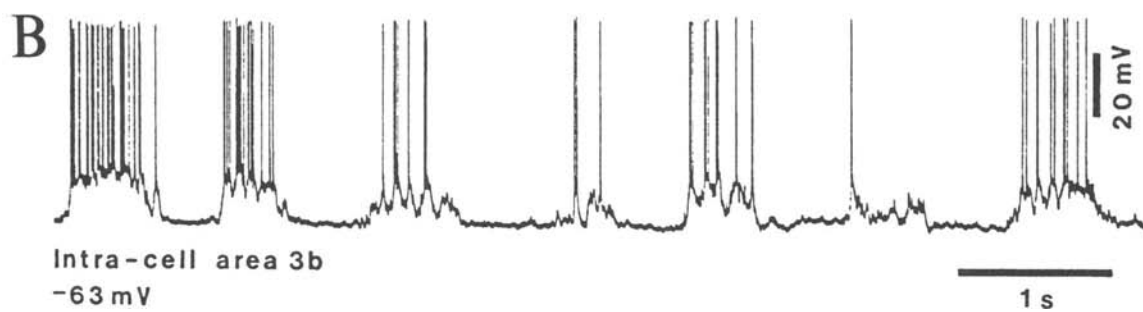
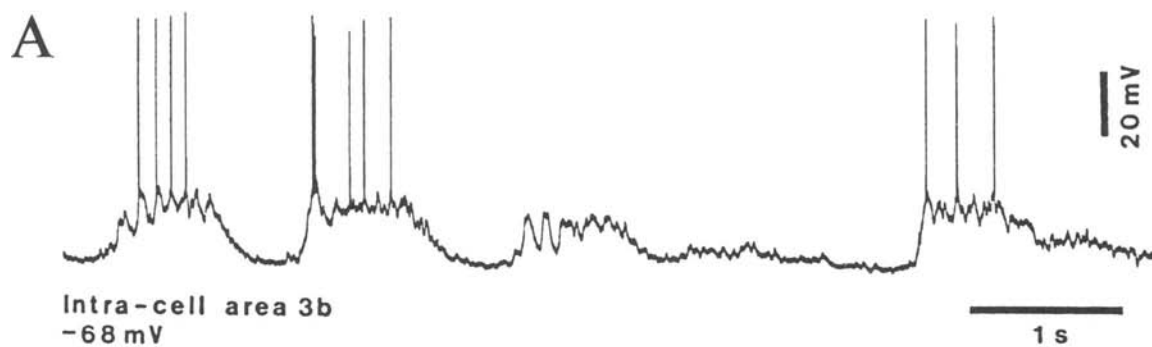
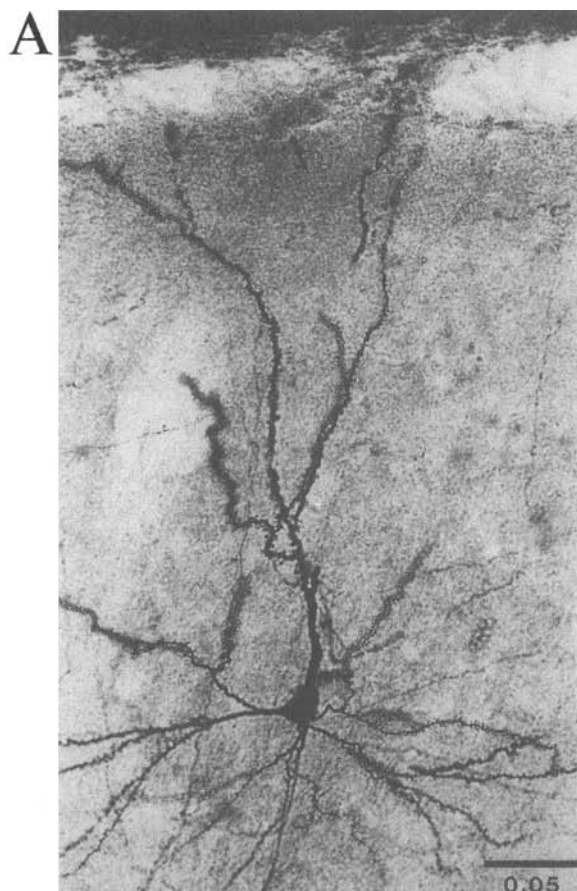
The cortical nature of the slow oscillation was demonstrated by its absence in the thalamus of decorticated animals [132]; its survival in the cerebral cortex after thalamectomy [131]; and its presence in large, isolated cortical slabs in *in vivo* cortical slices [133] and cortical slices maintained *in vitro* [134].

7.2.3.1. Cellular Basis of the Slow Oscillation

The slow oscillation consists of prolonged depolarizations, associated with brisk firing ($\sim 8\text{--}40$ Hz), and prolonged hyperpolarizations during which neurons are silent (Fig. 7.37). Generally, the depolarization lasts for approximately 0.3–0.6 s [135]. In addition to NMDA-mediated events [135], the depolarizing phase consists of non-NMDA-mediated EPSPs, fast prepotentials (FPPs), a voltage-dependent persistent Na^+ current ($I_{\text{Na(p)}}$), and fast IPSPs reflecting the action of synaptically coupled GABAergic local-circuit cortical cells [125]. As to the hyperpolarizing phase of the slow oscillation, it is *not* due to the action of local inhibitory neurons, but to disfacilitation (removal of synaptic, mainly excitatory, inputs) in intracortical and TC networks, and to some K^+ currents. Several pieces of evidence support this conclusion. (a) Neurons identified electrophysiologically as fast-spiking cells and morphologically as basket (aspiny) cells, during either natural sleep (Fig. 7.38) or ketamine–xylazine anesthesia, behave in phase with regular-spiking (pyramidal) neurons, firing during the depolarizing phase and being silent during the hyperpolarizing phase. (b) Intracellular recordings with Cl^- -filled pipettes during naturally sleeping animals did not affect the prolonged hyperpolarizations of the slow oscillation in NREM sleep (see fast-spiking cell in Fig. 7.38) [127]. (c) Recordings with Cs^+ -filled pipettes strikingly reduced or abolished the hyperpolarizations [136]. Cs^+ blocks nonspecifically K^+ currents; then, hyperpolarizations during the slow oscillation are produced, at least partially, by a series of K^+ currents, most probably $I_{\text{K(Ca)}}$. Finally, (d) disfacilitation in cortical networks is the other factor accounting for the prolonged hyperpolarizations, as under anesthesia [137] as well as during natural NREM sleep [127], the apparent input resistance was almost double

[132] Timofeev and Steriade (1996).
 [133] Timofeev *et al.* (2000a).
 [134] Sanchez-Vives and McCormick (2000). In that *in vitro* study, neurons in layer V were found to initiate the slow oscillation because of their high excitability, which may be ascribed to the concentration of extracellular K^+ (3.5 mM K^+), slightly higher than is the case *in vivo* (2.7–3.2 mM K^+ ; Lux and Neher, 1973; Gutnick *et al.*, 1979). The abnormally high excitability of deeply lying neurons in the study by Sanchez-Vives and McCormick (2000) can be seen in Fig. 2 in that paper showing that layers V/VI neurons discharged heavily during the silent phases of neurons from other layers. It is known that, *in vivo*, during the hyperpolarizing (“down-state”) phase of the slow oscillation, there is virtually no action potential in any type of neurons (see main text and Figs. 7.37–7.45, with intracellular recordings in anesthetized and unanesthetized, naturally sleeping animals).
 [135] The duration of the depolarizing phase of the slow oscillation is approximately 0.8–1.5 s under urethane, but it is much shorter ($\sim 0.3\text{--}0.5$ s) under ketamine–xylazine [125] or natural NREM sleep [127]. This suggests the involvement of NMDA-mediated events in this phase.
 [136] Timofeev *et al.* (2001b).

Figure 7.37. Intracellularly recorded and stained pyramidal neurons from cat primary somatosensory cortical display a slow oscillation. Ketamine–xylazine anesthesia. A, neuron at 0.3 mm from the surface (seen in the upper part of the photo) oscillated with periodic depolarizing–hyperpolarizing sequences at a frequency of about 0.6 Hz. This cell was extremely spiny and showed a prominent local arborization of its axon. Note oscillations within the frequency of spindle waves (10–12 Hz) during the depolarizing phase of the slow oscillation. B, pyramidal neuron at a depth of 1 mm, with two apical dendrites. Note the track left by the recording pipette on the left side of the cell. Both these neurons were regular-spiking cells. Modified from Contreras and Steriade (1995).



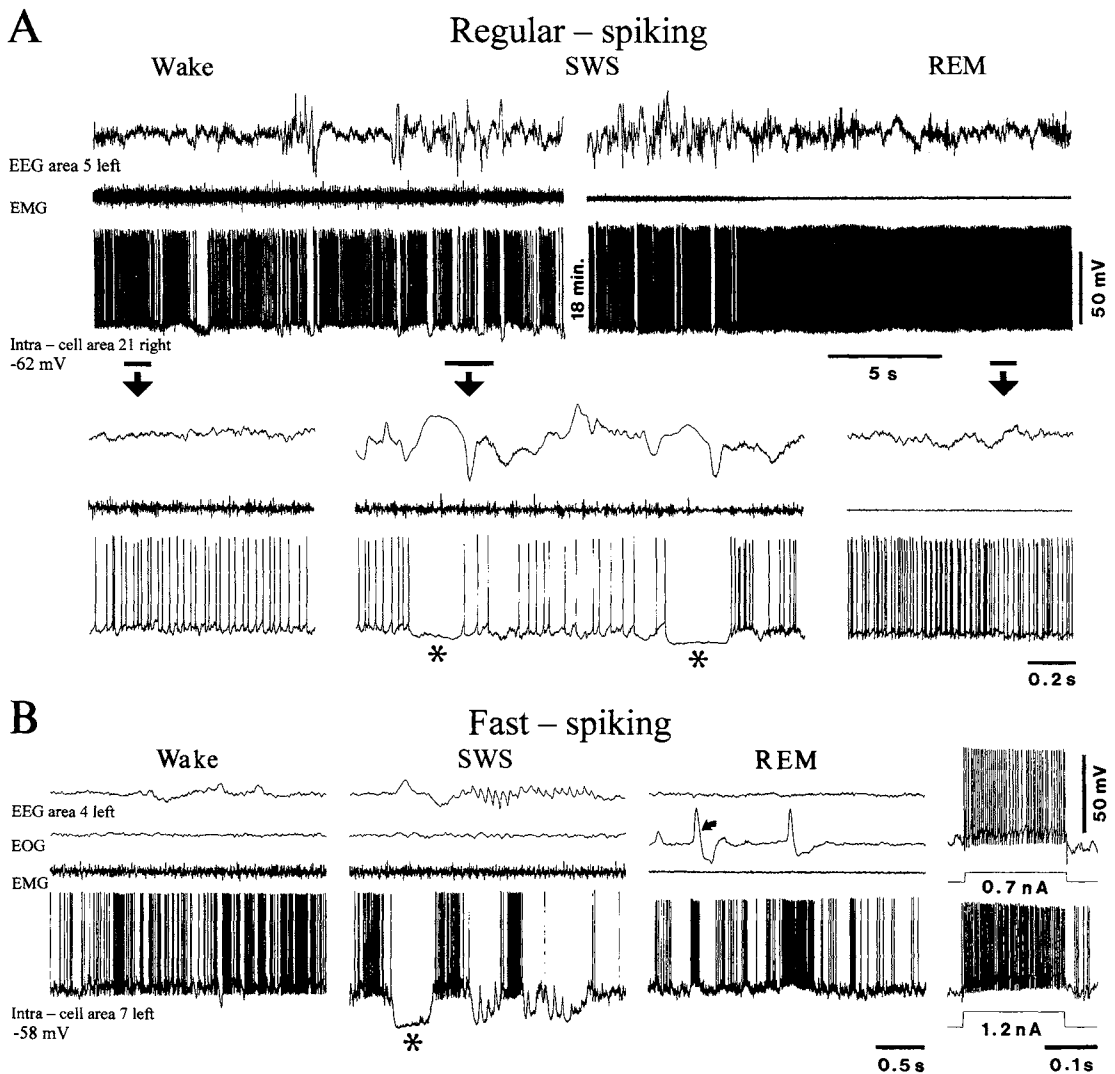


Figure 7.38. Changes in membrane potential and firing patterns during natural wake and sleep states. Intracellular recordings in chronically implanted cats. A, regular-spiking (RS) neuron from posterior association suprasylvian area 21 was intracellularly recorded (together with EMG and EEG from area 5) during transition from wake to NREM sleep (SWS) and, further, to REM sleep (there is a nondepicted period of 18 min during SWS). Periods marked by horizontal bars are expanded below (arrows). Note tonic firing during both waking and REM sleep, and cyclic hyperpolarizations associated with depth-positive EEG field potentials during SWS. B, activity of fast-spiking (FS) neuron (characterized by fast and tonic firing without frequency adaptation; see at right responses to depolarizing current pulses) during waking, SWS, and REM sleep. Recording with KCl-filled pipette. Tonic firing during waking and REM sleep was interrupted during SWS by long periods of hyperpolarizations and spindles, corresponding to EEG depth-positive waves and spindles. Some prolonged hyperpolarizations during SWS are indicated by asterisks. From Steriade *et al.* (2001a).

during the hyperpolarizing phase of the slow oscillation in NREM sleep, compared to the depolarizing phase of this oscillation [31]. The disfacilitation might be explained by a progressive depletion of $[Ca^{2+}]_0$ during the depolarizing phase of the slow oscillation [138], which would produce a decrease in synaptic efficacy and an avalanche reaction that

[137] Contreras *et al.* (1996b).

[138] Massimini and Amzica (2001).

would eventually lead to the functional disconnection of cortical networks.

The slow oscillation was recorded in all four major types of neocortical neurons (regular-spiking, RS; fast-spiking, FS; fast-rhythmic-bursting, FRB; and intrinsically-bursting, IB; see Chapter 5, Section 5.6.1), as identified electrophysiologically (Fig. 7.39) and by intracellular staining (Fig. 7.37). Identical oscillations were detected in all (primary sensory, association, and motor) explored cortical areas. Although the pattern of the slow oscillation recorded from the primary visual cortex is similar to that in other cortical fields (Fig. 7.40), the incidence of the slow oscillation in this area is lower.

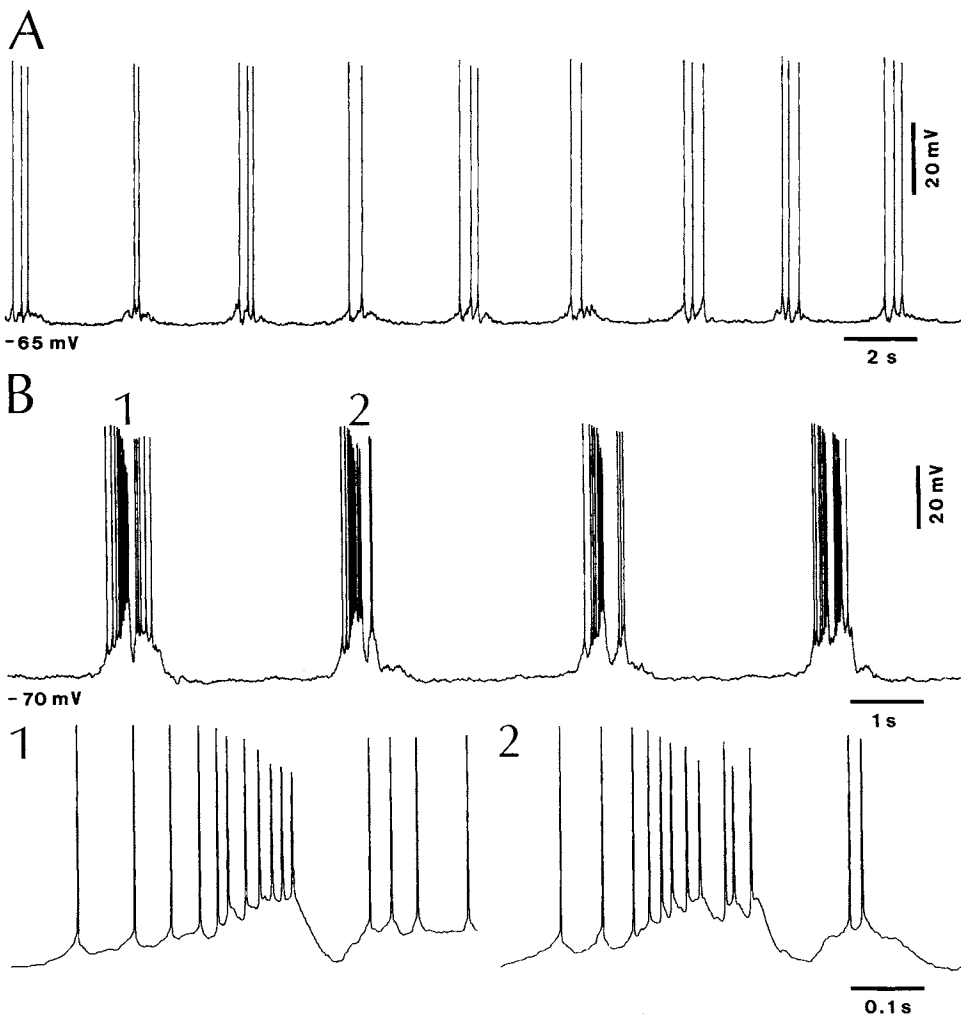


Figure 7.39. Slow oscillation in regular-spiking (RS, panel A) and intrinsically-bursting (IB, panel B) neocortical neurons. Intracellular recordings from suprasylvian area 5 in cats under urethane anesthesia. Depolarizing components B1–2 are expanded below. From Steriade *et al.* (1993a).

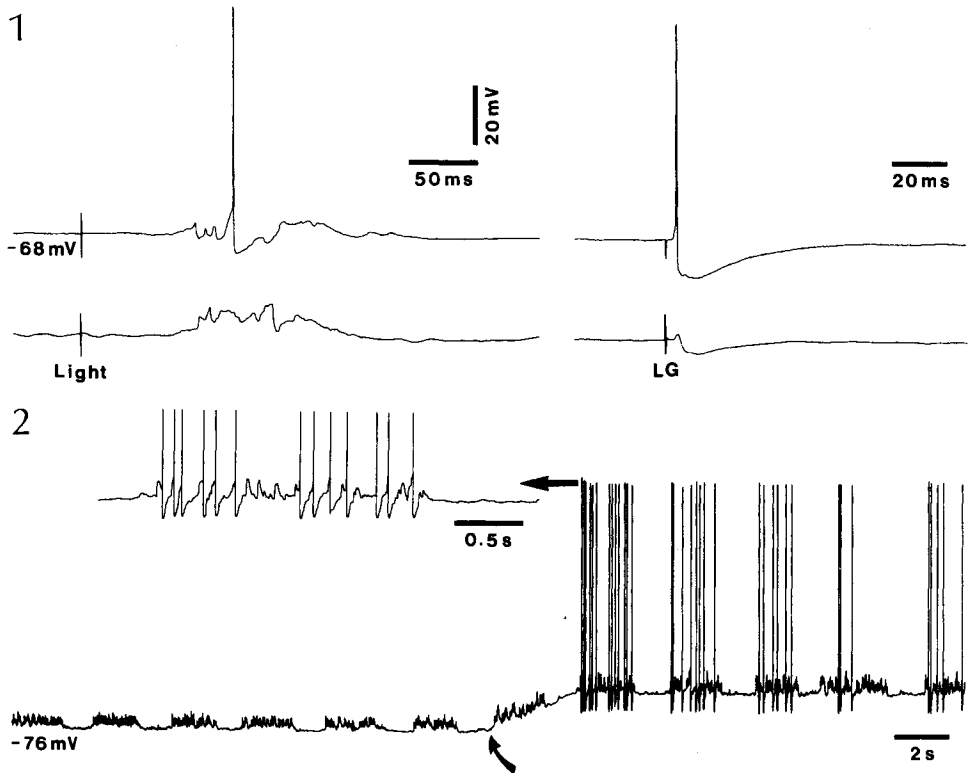


Figure 7.40. Slow oscillation in regular-spiking (RS), slowly adapting neuron, recorded from primary visual area 17 (depth 0.8 mm) in cat under urethane anesthesia. 1, cell identification by two depolarizing responses to flashes (1 ms in duration) and responses to thalamic lateral geniculate stimuli (through two different stimulating electrodes). 2, spontaneous activity under -0.2 nA DC and, at oblique arrow, back to the resting membrane potential (-68 mV). The first spike-train is expanded at left (see arrow; spikes truncated). From Steriade *et al.* (1993e).

7.2.3.2. Intracellular Recording of the Slow Oscillation during Natural NREM Sleep

During the transition from wakefulness to natural NREM sleep, the occurrence of the slow oscillation is, together with spindles, the first major electrical sign in cortical neurons. Long-lasting hyperpolarizations, associated with neuronal silence, are defining features from the very onset of sleep. In histograms of membrane potential distribution, the change from waking-related tonic firing (accompanied by Gaussian-like histograms with peaks around -60 to -65 mV) to NREM sleep patterns is reflected by a hyperpolarizing tail reaching almost -80 to -90 mV (Fig. 7.41) [127, 139]. Conversely, the transition from NREM sleep to wakefulness (Fig. 7.42) or to REM sleep (Fig. 7.43) is associated with complete obliteration of prolonged hyperpolarizations that characterize the slow oscillation.

[139] Steriade (2000).

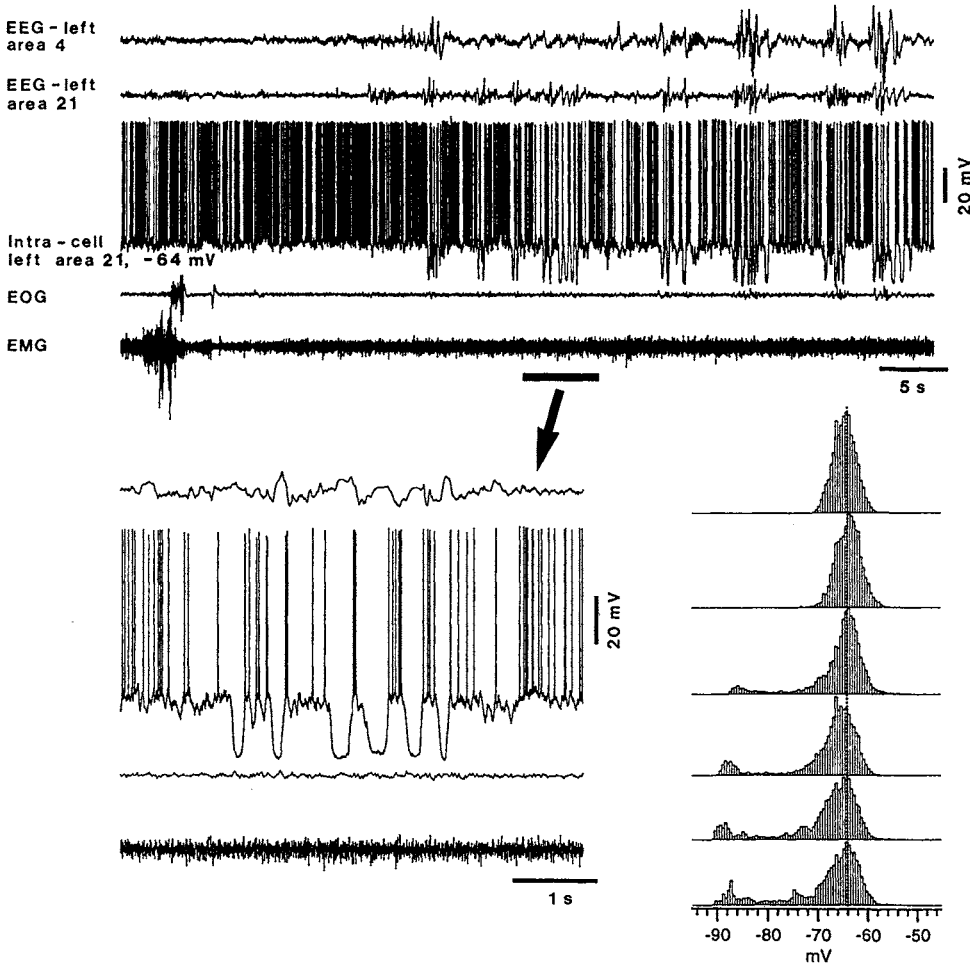


Figure 7.41. Natural NREM sleep is characterized by prolonged hyperpolarizations in neocortical neurons, but rich spontaneous firing during the depolarizing epochs. Chronically implanted cat. Five traces in top panel depict EEG from the depth of left cortical areas 4 (motor) and 21 (visual association), intracellular recording from area 21 neuron (resting membrane potential is indicated), electro-oculogram (EOG) and electromyogram (EMG). Part marked by horizontal bar is expanded below left (arrow). Note relation between the hyperpolarizations and depth-positive EEG field potentials. Below right, histograms of membrane potential (10-s epochs) during the period of transition from waking to slow-wave sleep depicted above. Note membrane potential around -64 mV during the 20 s of waking and progressively increased tail of hyperpolarizations, up to -90 mV, during sleep. Data from experiments by M. Steriade, I. Timofeev, and F. Grenier (see Steriade, 2000).

7.2.3.3. Intracortical Synchronization of Slow Oscillation

Dual intracellular recordings *in vivo* demonstrated that the synchronization of EEG patterns during NREM sleep is associated with simultaneous hyperpolarizations in cortical neurons (Fig. 7.44) [140, 141]. The intracortical

[140] Steriade *et al.* (1994b).

[141] Contreras and Steriade (1995).

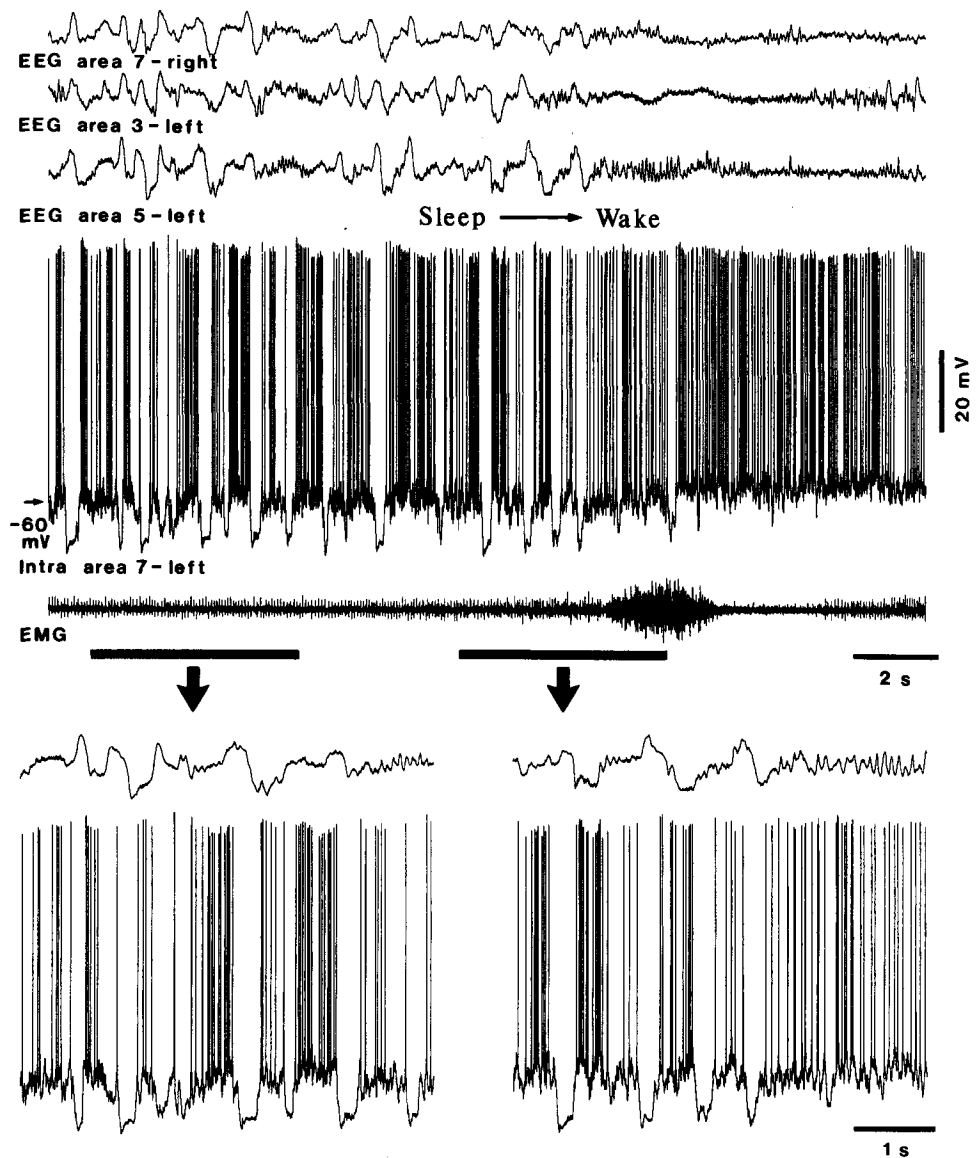


Figure 7.42. The slow oscillation during natural NREM sleep and its obliteration during transition to wakefulness. Chronically implanted cat. Five traces depict (from top to bottom): depth-EEG from right area 7 and left areas 3 and 5; intracellular activity of regular-spiking neuron from left area 7; and electromyogram (EMG). Two epochs marked by horizontal bars are expanded below (arrows). Cyclic hyperpolarizations characterize neocortical neurons during NREM sleep, but their firing rate during the depolarizing phases of the slow sleep oscillation is as high as during the activated behavioral state of waking. Note phasic hyperpolarizations in area 7 neuron, related to depth-positive EEG field potentials, during sleep, tonic firing upon awakening marked by EEG activation and increased muscular tone, and slight depolarization occurring only after a few seconds after awakening and blockage of hyperpolarizations. Modified from Steriade *et al.* (2001a).

synchronization of the slow oscillation was demonstrated by dual intracellular, extracellular multiunit, and field potential recordings from distant cortical foci, and by the disruption of synchronization after lidocaine injection

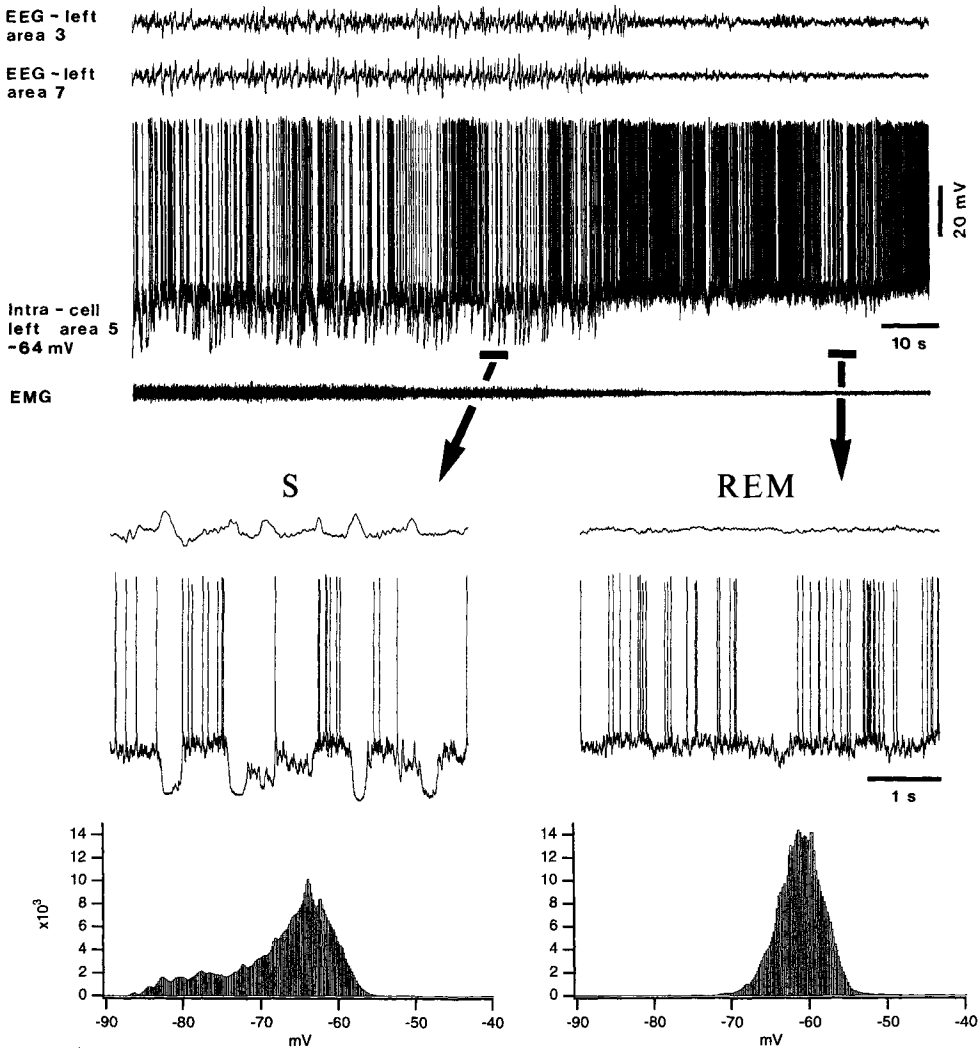


Figure 7.43. Cyclic hyperpolarizations characterize neocortical neurons during NREM sleep (S) and they are blocked during REM sleep. Intracellular recording of area 5 regular-spiking (RS) neuron, together with EEG from areas 3 and 7, and EMG. Periods marked by horizontal bars and arrows are expanded below. The bottom plots show the membrane potential during S (with a tail extending up to -85 mV) and a Gaussian-type histogram during REM sleep, around -60 mV. Note also slight depolarization upon entering REM sleep, preceding by a few seconds EEG activation and muscular atonia. From Steriade *et al.* (2001a).

[142] Destexhe *et al.* (1999b). This study demonstrated high values of spatial correlation for large distances among cortical leads during NREM sleep, in contrast with the steeper decline, with distance, of spatial correlations among neuronal activities during brain-activated states of waking and REM sleep.

between the two foci [68]. These studies, under anesthesia, demonstrated that closely located neurons are also “closer” in time. The shortest mean time lag was found between neurons within adjacent foci, while the longest time lags were found in distant recordings from motor and visual areas [68]. The long-range coherence of the slow oscillation was also demonstrated in naturally sleeping animals [142].

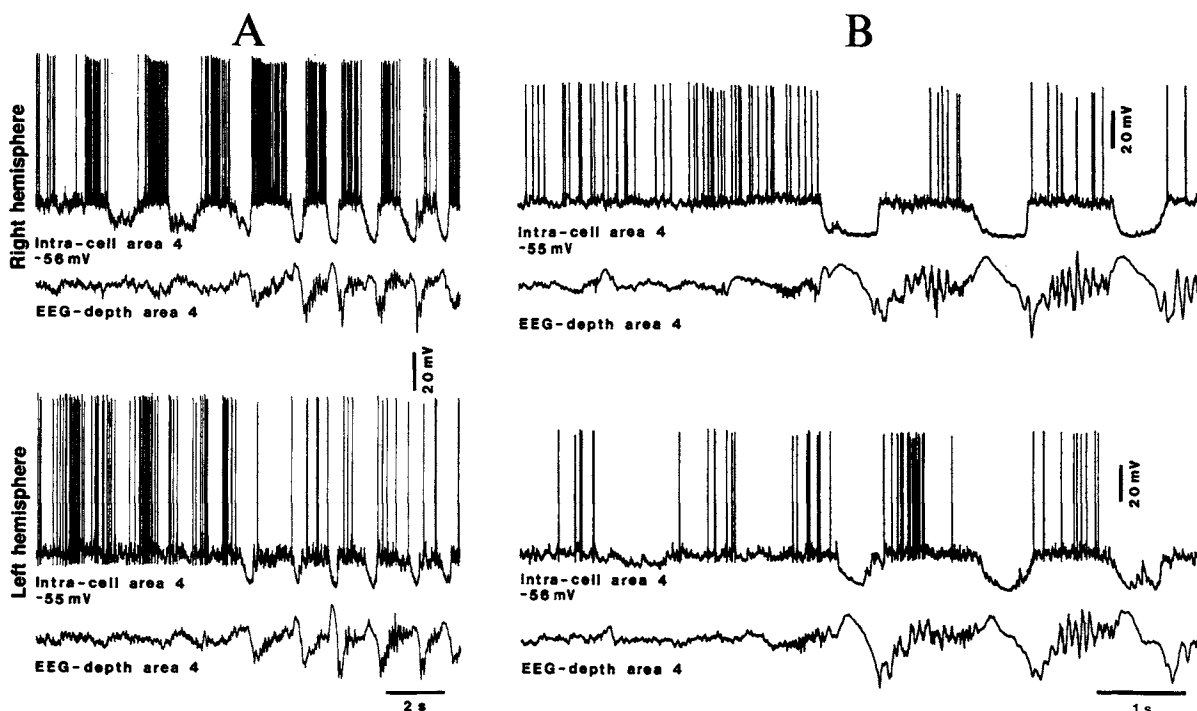


Figure 7.44. Dual intracellular recordings of neocortical neurons during the slow oscillation. Cats under ketamine-xylazine anesthesia. A, dual simultaneous intracellular recordings from right and left cortical area 4. Note spindle during the depolarizing envelope of the slow oscillation and synchronization of EEG when both neurons synchronously display prolonged hyperpolarizations. B, dual intracellular recordings from cortical neurons (right and left areas 4) show that

EEG synchronization is concomitant with simultaneous hyperpolarizations in neocortical neurons. EEG activated pattern at left, and occurrence of EEG synchronization. Only when both cells simultaneously displayed large hyperpolarizations, was the EEG fully synchronized with the patterns of slow oscillation and brief spindle sequences. Modified from Steriade *et al.* (1994b, panel A) and Contreras and Steriade (1995, panel B).

The intracortical synchronization of the slow oscillation is not only observed among neurons, but also between neurons and glial cells. Dual intracellular recordings from neurons and adjacent glial cells [143] showed that the onset of the depolarizing phase in neurons is followed, after approximately 90 ms, by the depolarization of simultaneously recorded glial cells and, toward the end of the depolarizing phase, the glial membrane begins to repolarize before neurons. These data suggested that glial cells might control the pace of the oscillation through changes in $[K^+]_{out}$, which is known to modulate neuronal excitability.

[143] Amzica and Steriade (1998b, 2000); Amzica and Neckelmann (1999); Amzica *et al.* (2002).

7.2.3.4. Synaptic Reflection of the Slow Oscillation in Thalamus and Other Structures

The neuronal synchronization also implicates thalamic neurons. reticular neurons, electrophysiologically identified by their very long spike-bursts with accelerando-decelerando pattern, whose intrinsic properties are quite different from

[144] Steriade *et al.*
(1993b).

those of neocortical neurons, exhibit patterns of the slow oscillation, with prolonged depolarizations interrupted by prolonged hyperpolarizations, which are very similar to those of cortical neurons (Fig. 7.45; see also below, Fig. 7.47) [141, 144]. The depolarizing component of the cortically generated slow oscillation is transmitted to reticular thalamic neurons at which level it triggers rhythmic spike-bursts and, consequently, is reflected in TC cells as rhythmic IPSPs

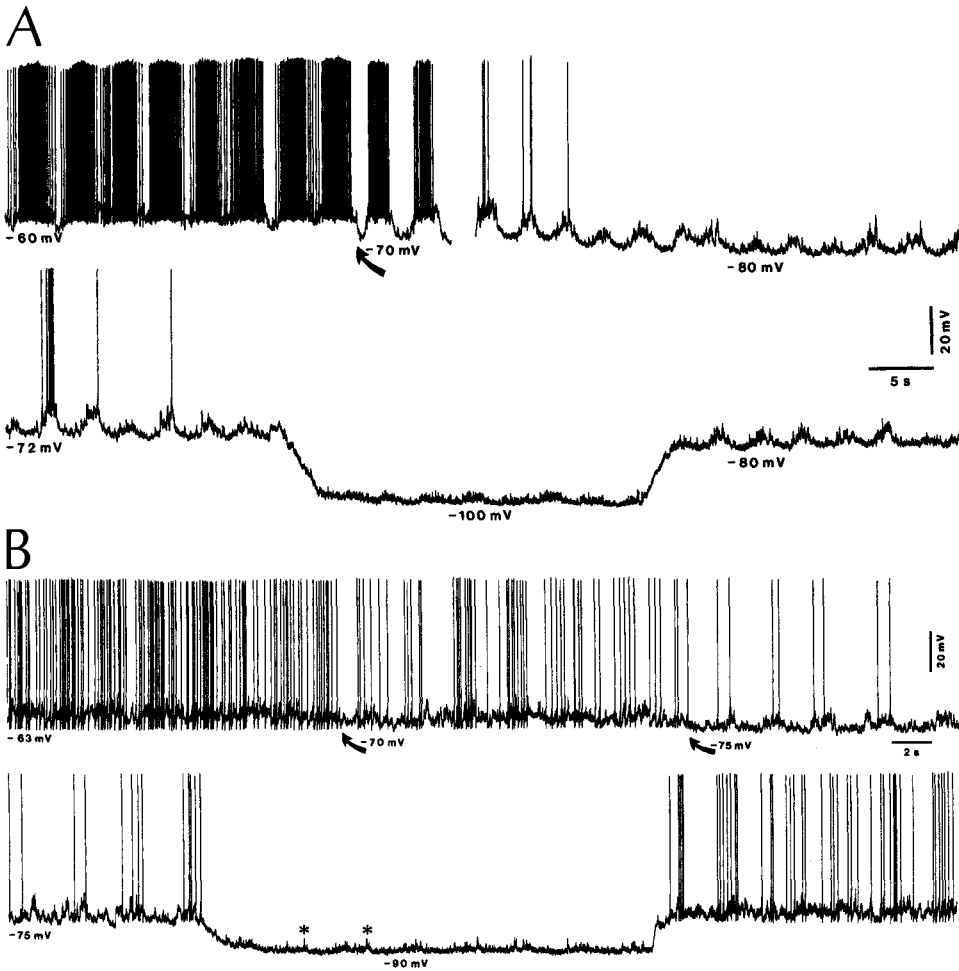


Figure 7.45. Thalamic reticular (RE) neurons during the cortically generated slow oscillation. Effect of hyperpolarization on the depolarizing components of the slow oscillation. Cats under urethane anesthesia. A–B, two different neurons. A, oscillation at 0.3 Hz. Top trace: at the resting V_m (–60 mV); under slight hyperpolarization (–0.2 nA at oblique arrow) bringing the V_m to –70 mV; and further DC hyperpolarization (–0.5 nA) to –80 mV (after interruption of trace). Bottom trace: slow depolarizing rhythm at –72 mV; its drastic reduction in amplitude (while the synaptic noise was left intact) by further hyperpolarization (–1 nA) to –100 mV; and recovery of depolarizing envelopes at –80 mV. B, another neuron, with a slow rhythm at 0.4 Hz. Top trace: slightly removing the DC depolarizing current, from +0.05 nA and +0.03 nA (V_m at –63 mV and –70 mV, respectively) to the resting V_m (–75 mV). Bottom trace: suppression of rhythmic depolarizing envelopes by DC hyperpolarization (–0.3 nA) bringing the V_m to –90 mV; however, the initial phasic events of the slowly rhythmic depolarizations remained intact (asterisks). From Steriade *et al.* (1993b).

leading to rebound spike-bursts (Fig. 7.46). This is the mechanism underlying the brief sequence of spindles that follows every cycle of the slow oscillation (see below, Section 7.3.3.5).

Thus, the thalamic slow oscillation is a consequence of the neocortical slow oscillation. This is *not* a passive

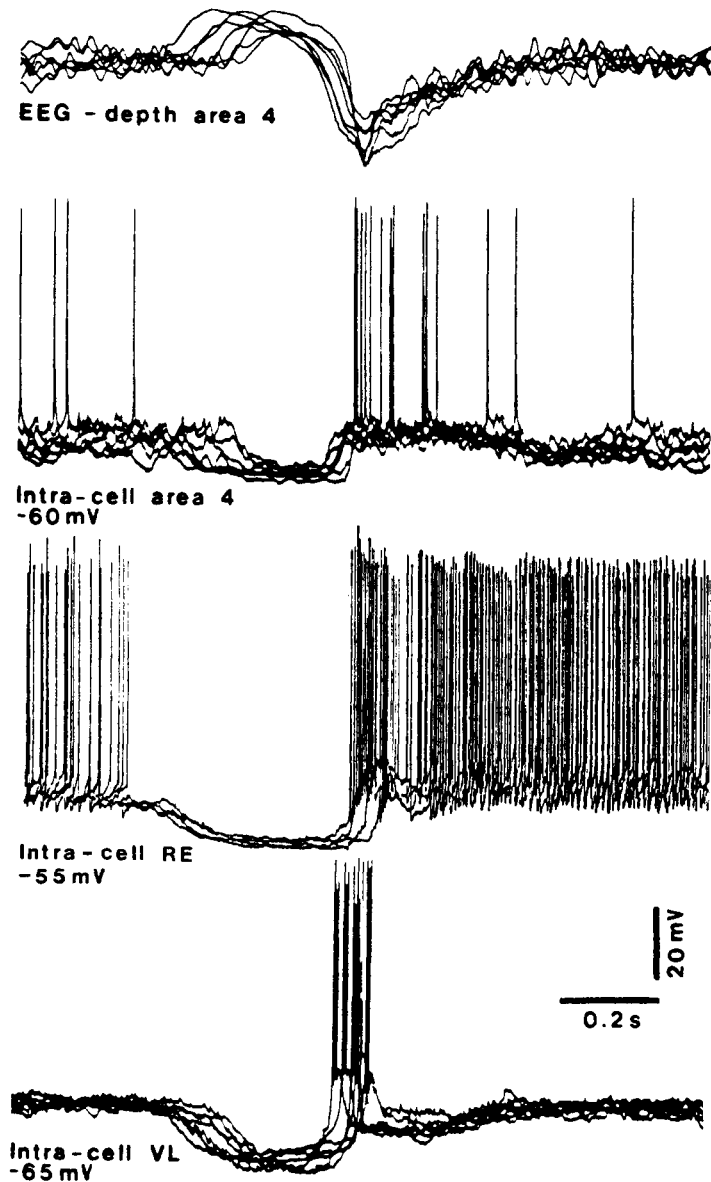


Figure 7.46. Synchronization of the slow oscillation in cortical and thalamic neurons. Intracellular recordings in a cat under ketamine–xylazine anesthesia. Simultaneous recordings of depth-cortical EEG and intracellular activity of an area 4 cortical neuron and thalamocortical neurons from ventrolateral (VL) nucleus. The intracellular activity of the thalamic reticular (RE) neuron was similar with respect to the EEG. All activities aligned on the peak of depth-negativity EEG (downward). Note simultaneity of long-lasting hyperpolarizations (related to the depth-positive EEG component) in all cortical and thalamic cell-types. The depth-negative EEG component of the slow oscillation was associated with spike-trains in the cortical neuron and spike-bursts in thalamic reticular and VL neurons. Modified from Contreras and Steriade (1995).

[145] Hughes *et al.* (2002). A slow oscillation in TC neurons was also observed *in vitro* by Williams *et al.* (1997) in a subset (<15%) of these neurons. This oscillation, possessing a similar feature with that described in our experiments *in vivo* [141, 144], was generated by a bistable interaction between the “window” component of the Ca^{+2} -dependent I_T and the leak K^+ current (I_{leak}). In the more recent study by

reflection, but a synaptically induced effect of cortical discharges, which occur during the depth-negative field potentials, onto thalamic neurons, as demonstrated since our 1993–1995 intracellular studies [141, 144]. This view was recently confirmed in work on thalamic slices [145], showing that by activating metabotropic glutamate receptors (mGluR1a), corticothalamic inputs can recruit neuronal mechanisms in TC neurons, which are identical to those observed in our *in vivo* studies. In the intact brain, synchronous corticothalamic volleys, as they occur naturally during the depolarizing phase of the slow oscillation, excite reticular neurons (Figs. 7.45 and 7.47) that, in turn, impose IPSPs on TC neurons, followed by low-threshold

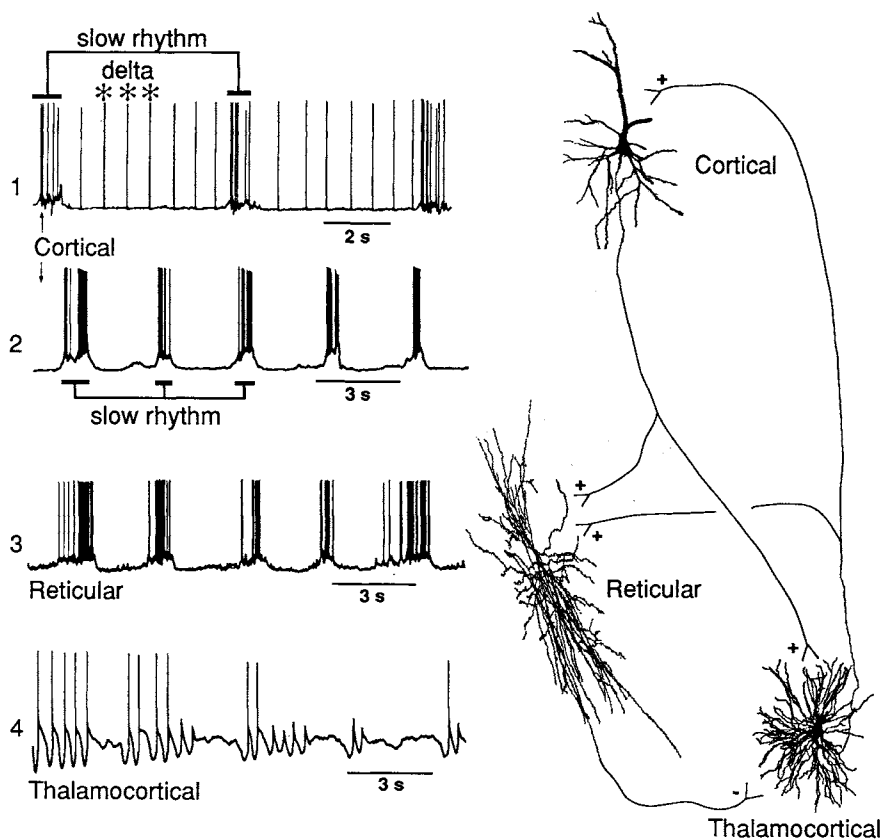


Figure 7.47. The slow cortical oscillation and its synaptic reflection in thalamic neurons. Coalescence of cortically generated slow oscillation with thalamic clock-like delta oscillation. Intracellular recordings of four neurons in anesthetized cats. From top to bottom: two pyramidal cortical neurons (1 and 2), one thalamic reticular (RE) neuron (3) and one thalamocortical (TC) neuron (4). Intracellularly stained neurons are shown at right. Neuron 1 from cortical association area 5 displayed the slow rhythm (less than 1 Hz) and, between the slow depolarizing phases, clock-like action potentials (asterisks) recurring at the delta frequency range (1.6 Hz), arising in TC neurons. Cortical cell 2 exhibited the slow rhythm at 0.3 Hz. Thalamic reticular neuron 3 oscillated at 0.3 Hz, at the same frequency as slowly oscillating cortical neurons. TC neuron 4, from the ventrolateral nucleus, oscillated within the clock-like delta frequency (2.5 Hz); the oscillation tended to dampen and was periodically revived, within the frequency range of the slow oscillation (0.2–0.4 Hz). Modified from Steriade *et al.* (1993b,d,f).

spike-bursts. These opposite effects (excitation in reticular neurons, inhibition-rebound sequences in TC neurons) are due to the fact that the numbers of some subunits of glutamate receptors are approximately four times higher at corticothalamic synapses in reticular neurons, compared to TC neurons, and the amplitude of corticothalamic EPSCs is about 2.5 times higher in reticular than in TC neurons [146].

7.2.3.5. Grouping of Delta, Spindles, and Fast Oscillations by the Slow Oscillation

Two pieces of evidence mark the difference between the slow (generally, 0.5–1 Hz) and delta (1–4 Hz) oscillations, the latter consisting of two (thalamic and cortical) components. (a) The first one is the distinct occurrence of cortically generated slow oscillation and the clock-like delta oscillation generated in TC neurons within the same cortical neuron (see neuron 1 in Fig. 7.47). It should be emphasized, however, that, because of the intrinsic nature of the clock-like delta rhythm (see Section 7.2.2.1), this activity appears in single TC neurons and, although can be synchronized by corticothalamic inputs (see Fig. 7.35), it is quite rare to have pools of TC neurons enough synchronized so that their rhythmic activity be reflected at the macroscopic EEG level. (b) The second fact pointing to the difference between the slow and delta activities is that cortically generated delta waves are grouped in sequences recurring within the frequency range of the slow oscillation. This grouping of two distinct sleep rhythms can be seen using both intracellular and extracellular unit recordings (Fig. 7.48).

The synaptic reflection of the cortical slow oscillation in thalamic reticular neurons (see Figs. 7.45–7.47), which are pacemakers of spindles, is behind the fact that the synchronous firing of cortical neurons during the depolarizing phase of the slow oscillation creates conditions for generation of spindles in both experimental animals and humans (Fig. 7.49). Thus, a cycle of the slow oscillation is followed by a brief spindle sequence in TC neurons, which is transferred to the cortical EEG. The sequence consisting of a surface-positive EEG transient, corresponding to the excitation in deeply lying neocortical neurons, followed by surface-negative component and a short sequence of spindle waves, represents the combination between the slow and spindle oscillation, and is termed in clinical EEG as the K-complex (KC), a reliable sign for stage 2 of human sleep, but apparent in all stages of NREM sleep (Fig. 7.49, *HUMAN*) [147]. Spectral analysis in humans demonstrated the periodic recurrence of KCs, with main peaks at 0.5–0.7 Hz, reflecting the slow oscillation (S); the other frequency band (1–4 Hz) represents delta activity (Δ); and 12–15 Hz reflects the presence of spindles (σ) (Fig. 7.49).

Hughes *et al.* (2002), the exogenous or synaptic activation of mGluR1 produced a slow oscillation in TC neurons, similar to that observed in our *in vivo* studies. Activation of mGluR1 in thalamic slices mimics the corticothalamic synaptic activation that was demonstrated in the intact brain [141, 144].

[146] See note [35] and related main text in Chapter 4.

[147] Loomis *et al.* (1938); Roth *et al.* (1956). The cellular substrates of the KC, a landmark of EEG sleep in humans, have been investigated in cats (Amzica and Steriade, 1997, 1998a). Our studies indicate that the KCs are the expression of the spontaneously occurring, cortically generated slow oscillation. KCs may also be triggered by auditory or other stimuli, though such evoked events are the exception since sleep usually occurs in environments free of sensory stimuli.

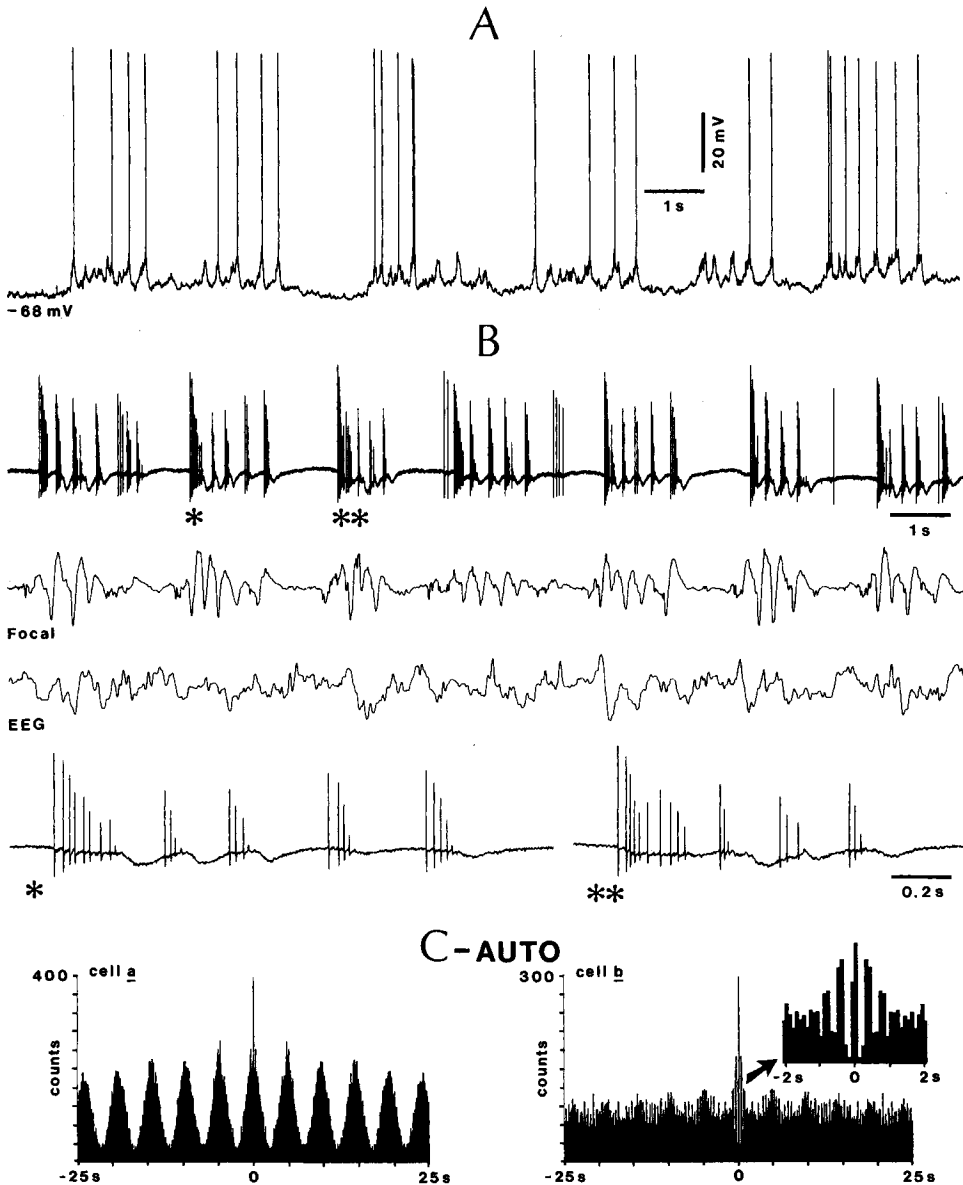
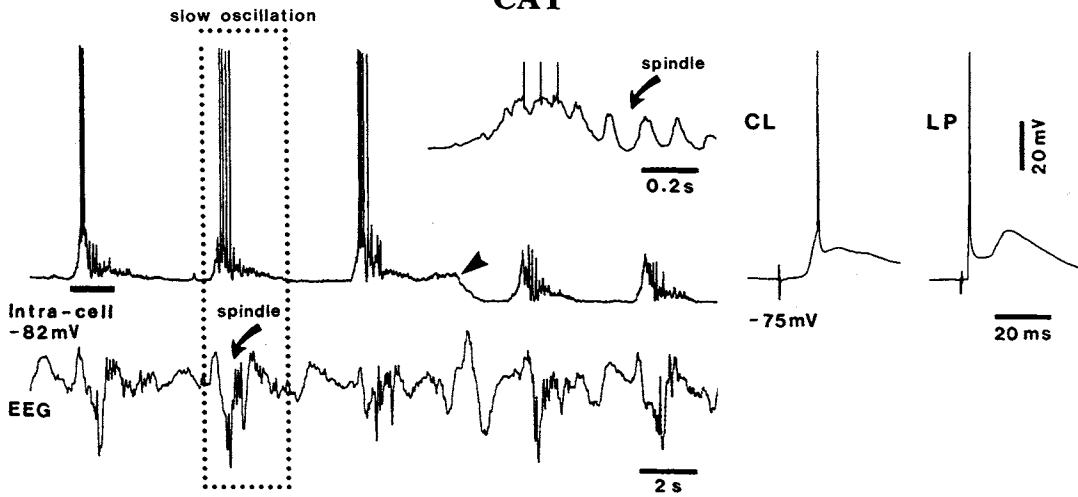
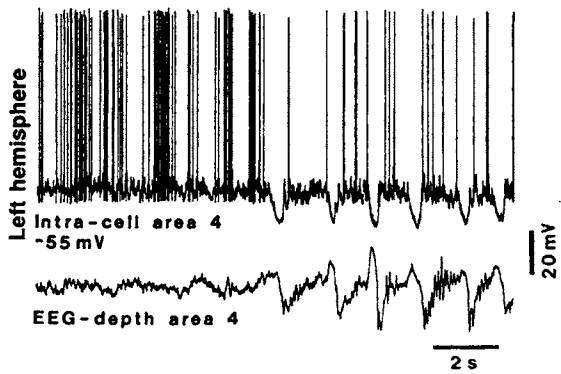
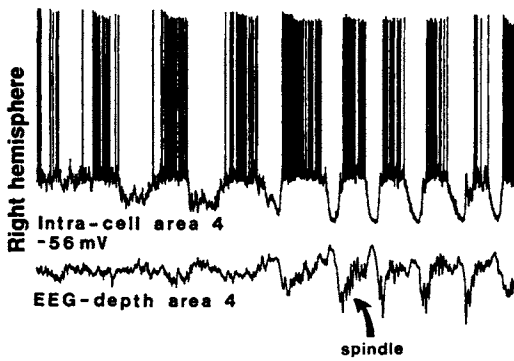


Figure 7.48. Delta oscillation (3–4 Hz) grouped within sequences recurring with a slow rhythm (0.3–0.4 Hz) in cortical neurons. Cats under urethane anesthesia. A, intracellular recording of a regular-spiking, slow adapting corticothalamic neuron in anterior suprasylvian area 5, excited synaptically from the thalamic lateroposterior (LP) nucleus and backfired (3.5 ms latency) from the thalamic rostral intralaminar centrolateral (CL) nucleus. B, extracellular recording of an intrinsically-bursting neuron at 0.6 mm in suprasylvian area 7, convergently excited by stimulation of the LP and CL nuclei. Below the cellular traces, focal waves (field potentials) recorded through the same micropipette used to record action potentials and EEG waves recorded from the cortical surface are depicted. The sequences of spike-bursts marked by one or two asterisks are expanded below. Note delta waves grouped by the slow rhythm. C, AUTO (autocorrelograms) of two (a and b) neurons recorded simultaneously by the same extracellular microelectrode at a depth of 1.3 mm in motor cortical area 4. AUTO (0.1 bin width) shows the slow rhythm (0.2 Hz) in both neurons. The delta rhythm (2.5 Hz) within the slowly (0.2 Hz) recurring discharge sequences in neuron b is depicted in the expanded inset (arrow). Modified from Steriade *et al.* (1993f).

CAT



CAT



HUMAN

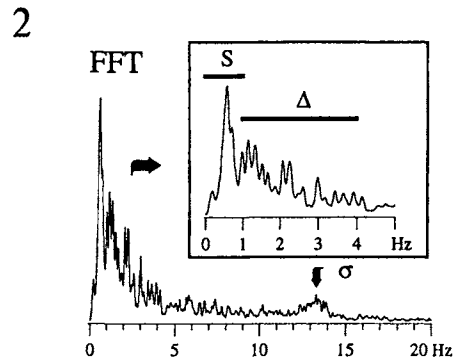
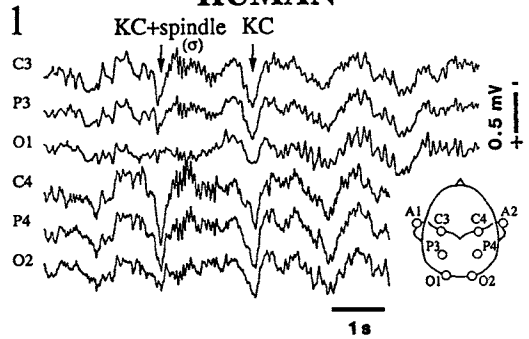


Figure 7.50 illustrates the neuronal circuits that give rise to grouped slow oscillation and spindles or thalamic/cortical components of delta waves. The sharp, depth-negative deflection of the slow oscillation is termed KC. Thus, panel A depicts a KC in the cortex that travels through the corticothalamic pathway and triggers in the thalamic reticular nucleus a spindle sequence that is transferred to TC neurons and thereafter back to the cortex where it shapes the tail of the KC. Panel B shows how KC is modulated by a sequence of clock-like delta waves originating in the thalamus. The KC travels along the corticothalamic pathway eliciting EPSP–IPSPs sequences in TC cells. The IPSPs generate low-threshold potentials crowned by high-frequency spike-bursts at delta frequency that may reach the cortex through the TC link. Finally, panel C shows the modulation of a KC by a sequence of delta waves originating in the cortex.

The slow oscillation also generates fast oscillations in the beta/gamma frequency bands (Fig. 7.51). As these fast activities are voltage (depolarization)-dependent in both thalamic and cortical neurons (see Section 7.1.4), they selectively appear on the depolarization phase of the slow sleep oscillation. Thus, gamma rhythms occur not only during brain-active states of wakefulness and REM sleep, as conventionally assumed, but also during the slow oscillation in NREM sleep.

During the depolarizing phase of the slow oscillation, very fast rhythms (ripples, 80–200 Hz) are also observed. Intracellular recordings revealed a strong relation between ripples in filtered field potentials (80–200 Hz) and neuronal depolarization and firing, with ampler ripples in the field potentials when neurons are more depolarized and fired more frequently. This is documented in Fig. 7.52 depicting a fast-rhythmic-bursting neuron, but was observed in a great majority of recordings from all neuronal classes.

Figure 7.49. The cortical slow oscillation groups thalamically generated spindles. *CAT top*, intracellular recording in cat under urethane anesthesia from area 7 (1.5 mm depth). Electrophysiological identification (at right) shows orthodromic response to stimulation of thalamic centrolateral (CL) intralaminar nucleus and antidromic response to stimulation of lateroposterior (LP) nucleus. Note slow oscillation of neuron and related EEG waves. One cycle of the slow oscillation is framed in dots. Part marked by horizontal bar below the intracellular trace (at left) is expanded above (right) to show spindles following the depolarizing envelope of the slow oscillation. *CAT bottom left*, dual simultaneous intracellular recordings from right and left cortical area 4. Note spindle during the depolarizing envelope of the slow oscillation and synchronization of EEG when both neurons synchronously display prolonged hyperpolarizations. *HUMAN*, the K-complex (KC) in natural sleep. Scalp monopolar recordings with respect to the contralateral ear are shown (see figure). Traces show a short episode from a stage 3 non-REM sleep. The two arrows point to two KCs, consisting of a surface-positive wave, followed (or not) by a sequence of spindle (sigma) waves. Note the synchrony of KCs in all recorded sites. Below, frequency decomposition of the electrical activity from C3 lead (see head figure with leads) into three frequency bands: slow oscillation (S, 0–1 Hz), delta waves (Δ , 1–4 Hz), and spindles (σ , 12–15 Hz). Modified from Steriade *et al.* (1993f and 1994b, *CAT*) and from Amzica and Steriade (1997, *HUMAN*).

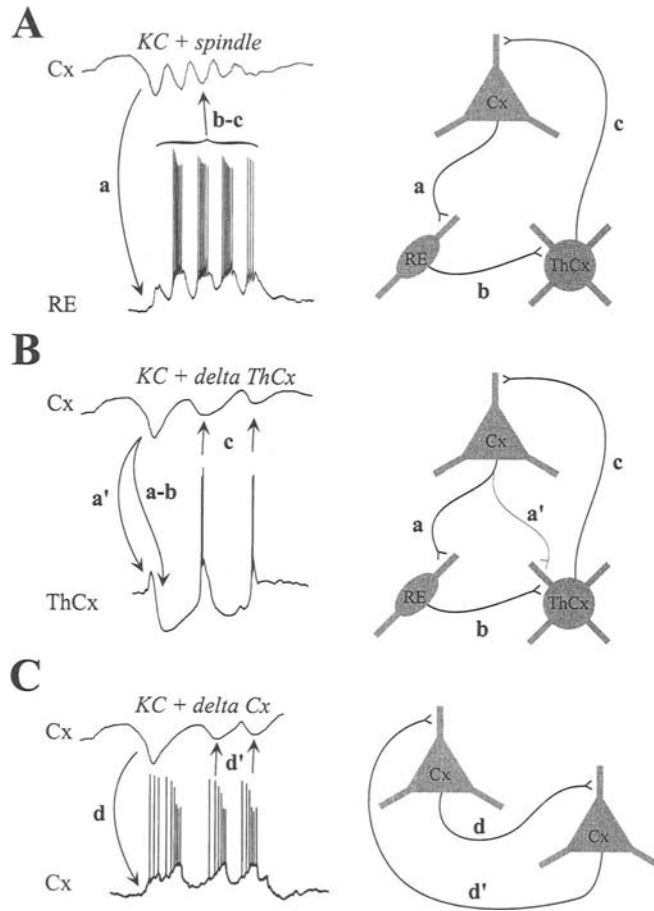


Figure 7.50. Coalescence of the depolarizing phase of the slow oscillation (K-complex, KC) with other sleep rhythms. In the left column, field potential and intracellular recording. In the right column, scheme of the circuit involved in the generation of the respective EEG pattern. The synaptic projections are indicated with small letters, corresponding to the arrows at left, which indicate the time sequence of the events. A, combination of a KC with a spindle sequence. A KC in the cortex (Cx) travels through the corticothalamic pathway (a) and triggers in the thalamic reticular nucleus (RE) a spindle sequence that is transferred to thalamocortical cells (ThCx) of the dorsal thalamus (b) and thereafter back to the cortex (c) where it shapes the tail of the KC. B, modulation of a KC by a sequence of clock-like delta waves originating in the thalamus. The KC travels along the corticothalamic pathway (a') eliciting an excitatory postsynaptic potential (EPSP) curtailed by an inhibitory postsynaptic potential (IPSP) produced along the cortico-RE (a) and RE-ThCx (b) projections. The hyperpolarization of the thalamocortical cell generates a sequence of low-threshold potentials crowned by high-frequency spike-bursts at delta frequency that may reach the cortex through the thalamocortical link (c). C, modulation of a KC by a sequence of delta waves originating in the cortex. When the KC impinges upon bursting cells (d), it triggers a series of rhythmic bursts of spikes at delta frequency that may have a greater impact on target cells (d') than single action potentials, thus synchronizing several neurons whose membrane potentials will be reflected in local field potentials as delta waves. From Amzica and Steriade (2002).

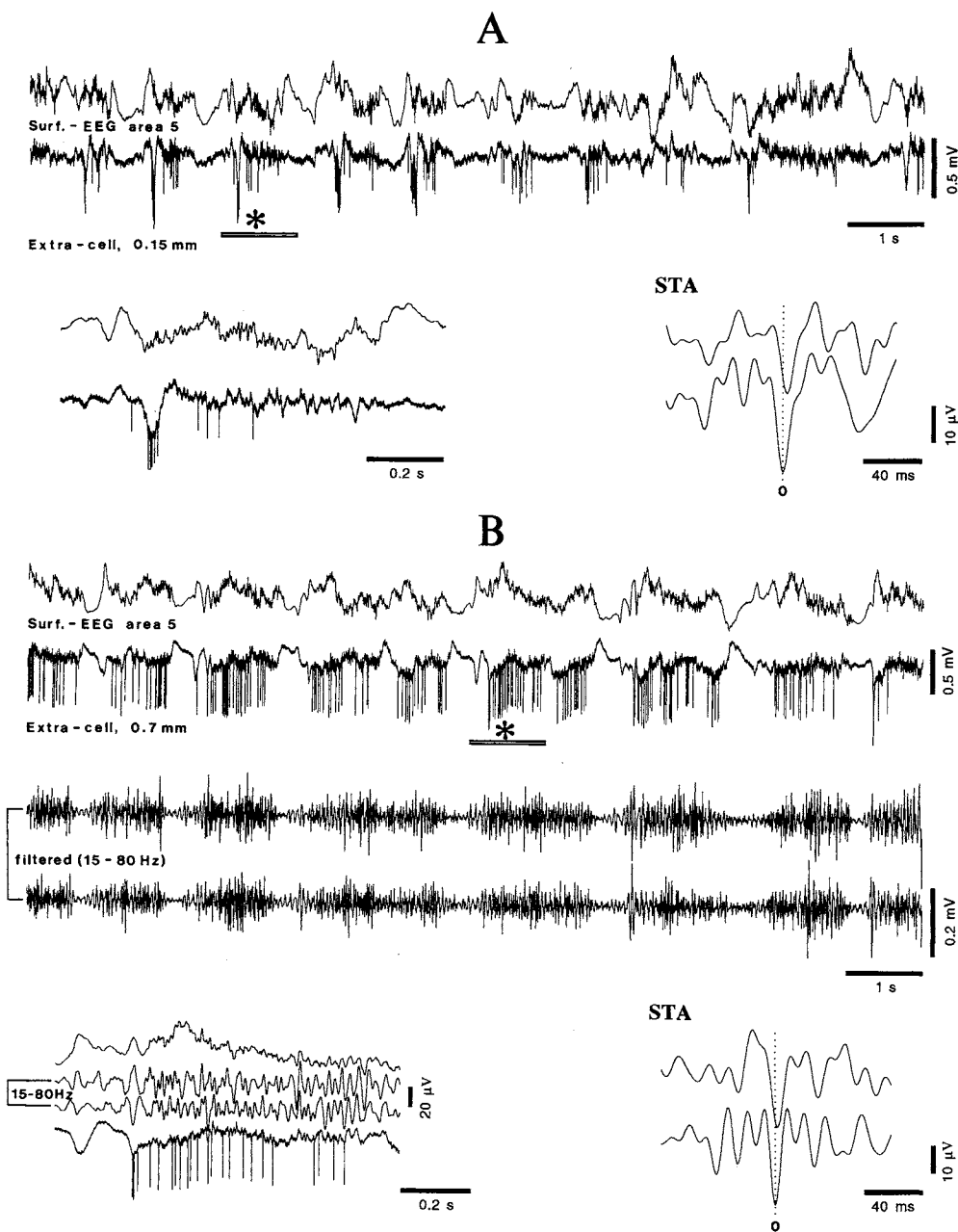
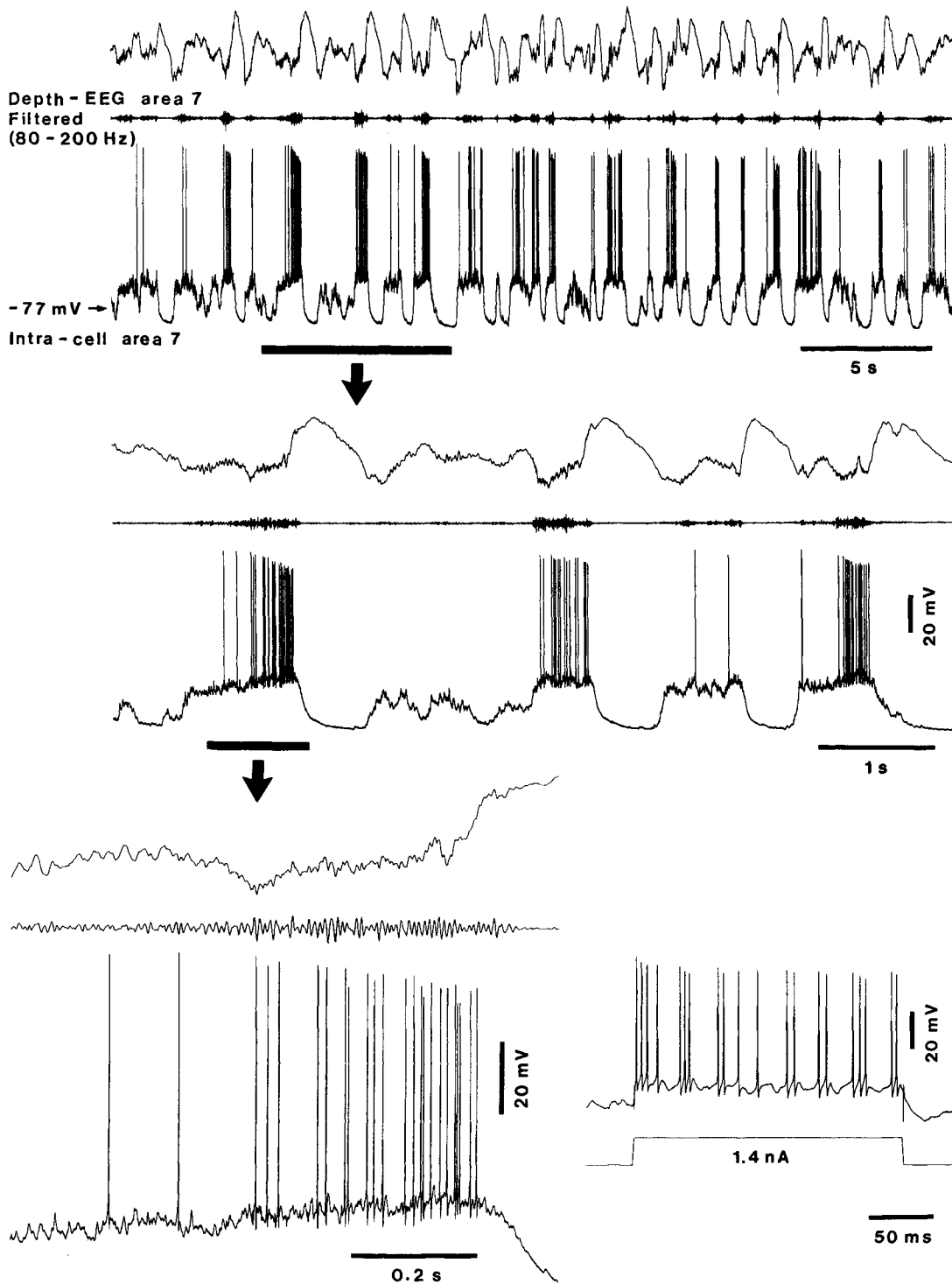


Figure 7.51. Fast waves (gamma band, ~ 40 Hz), superimposed on the excitatory phase of the slow oscillation, occurring in-phase at various cortical depths and crowned by action potentials in both superficial and deep cortical layers. Cat under ketamine-xylazine anesthesia. A, simultaneous recording through a ring placed on the surface of anterior suprasylvian area 5 and through a microelectrode picking up local field potentials and unit discharges at 0.15 mm from the surface. Period marked by horizontal bar (asterisk) is expanded below. At right, spike-triggered average (STA); 50 sweeps with waves at the surface and 0.15 mm, 80 ms before and after the action potentials. B, same track with microelectrode at a depth of 0.7 mm. Below the original traces, activity was filtered between 15 and 80 Hz to show reduction or disappearance of fast waves

during the depth-positive component of the slow oscillation (reflecting cells' hyperpolarization). The part marked by the horizontal bar (asterisk) is expanded below (left). The top and bottom traces represent the nonfiltered traces from the surface and depth, while the middle traces represent the same waves after filtering (15–80 Hz) and increasing their amplitudes to show 40-Hz activity. At right, STA (50 sweeps, as in A), showing in-phase relation, with the surface lagging the depth by 2–3 ms, as in A. Note that the prolonged surface negativity of the slow oscillation reversed in polarity at 0.7 mm, whereas fast oscillations were in-phase. Also, at both 0.15 mm (where the slow oscillation was not yet reversed) and 0.7 mm, neuronal discharges were consistently associated with focal negative waves of the fast oscillation. From Steriade



7.3. Abnormal Oscillations during Non-REM Sleep

325

SYNCHRONIZED
BRAIN
OSCILLATION

7.3.1. Electrical Seizures Developing from NREM Sleep Oscillations

The most common abnormal developments of NREM sleep oscillations are electrographic paroxysms that accompany different types of clinical seizures. As this was the topic of a recent monograph on sleep and epilepsy [148], we will only briefly mention some major aspects.

Epileptic seizures of different types preferentially occur during NREM sleep, whereas REM sleep is a relatively nonepileptic state [149]. Both low-frequency rhythms (0.5–1 Hz and 7–15 Hz), that is, slow oscillation and spindles, respectively, and very fast (ripples, 80–200 Hz) oscillations may develop into paroxysmal discharges.

The spontaneous development of the slow oscillation into paroxysmal discharges similar to the electrographic correlates of Lennox–Gastaut syndrome [150] is illustrated with intracellular recording from a neocortical neuron in Fig. 7.53. Clinically, the close relation between NREM sleep and Lennox–Gastaut syndrome is firmly established [151]. At the EEG level, this paroxysmal pattern is characterized by spike–wave (SW) complexes at 1.5–3 Hz and fast runs at 10–20 Hz. The amplitude of the membrane potential from hyperpolarized to depolarized levels increased from the slow oscillation (~0.9 Hz) during the preseizure epoch to that during the electrographic paroxysm. The shift from the depolarized to hyperpolarized membrane potential was also steeper. During the initial part of the seizure, characterized by SW and polyspike-wave (PSW) complexes, the action potentials were partially inactivated and the AHP disappeared. The following period, with fast runs, was characterized by EEG “spikes” at 10–20 Hz and, at the neuronal level, a tonically depolarized membrane potential. The end of the seizure was associated with a short period of hyperpolarization. What Fig. 7.53 emphasizes is the basically similar field-cellular relation in sleep and seizure patterns. During the slow oscillation, there was a close time-relation between the depolarizing component of the neuron and

[148] Steriade (2003a).

[149] Mahowald and Schenck (1997).

[150] The Lennox–Gastaut syndrome is a clinical entity related to infantile spasms and to the EEG notion of hypsarrhythmia.

[151] Halasz (1991); Niedermeyer (1999b–c).

Figure 7.52. Progressively increased amplitude of very fast oscillations (ripples, 80–200 Hz) with increased depolarization of cortical neurons during the slow oscillation. Cat under ketamine–xylazine anesthesia. Intracellular and depth-EEG recordings from area 7. Top panel illustrates an epoch with the slow oscillation (0.6–0.7 Hz). The neuron was a fast-rhythmic-bursting (FRB) neuron; see electrophysiological identification of this neuronal type at bottom right. Below the EEG trace, a filtered trace (80–200 Hz) is also shown. Part indicated by horizontal bar and arrow is expanded below and the cycle at left is further expanded at the bottom. Note, in the bottom left panel, the progressively increased amplitude of ripples in EEG field potentials, in parallel with neuronal depolarization and increased frequency of action potentials. From Grenier *et al.* (2001).

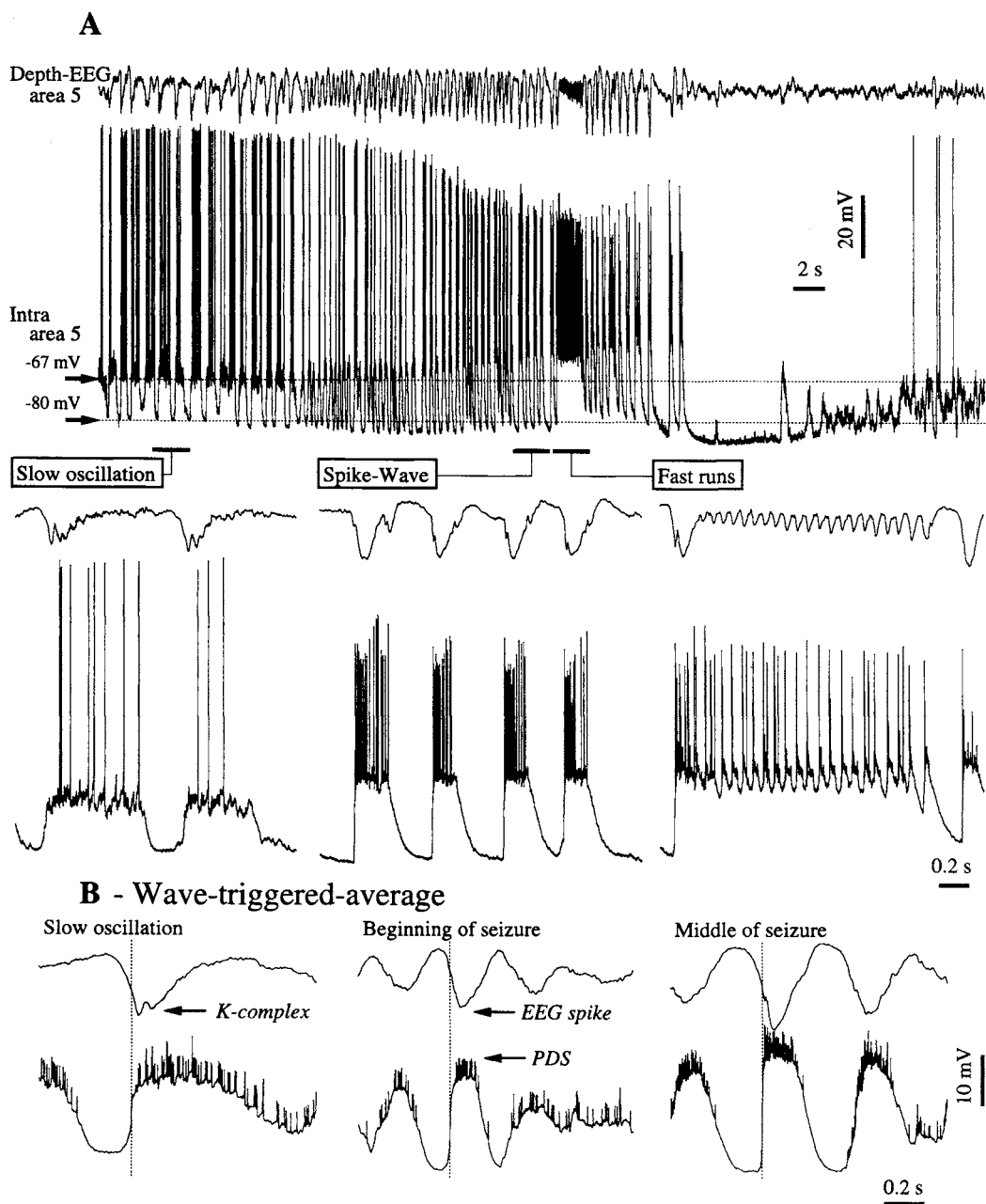


Figure 7.53. Spontaneously occurring seizure, developing without discontinuity from slow sleep oscillation. Intracellular recording from area 5 regular-spiking neuron together with depth-EEG from the vicinity in area 5, in cat under ketamine-xylazine anesthesia. A, smooth transition from slow oscillation to complex seizure consisting of spike-wave (SW) complexes at approximately 2 Hz and fast runs at approximately 15 Hz. The seizure lasted for approximately 25 s. Epochs of slow oscillation preceding the seizure, SW complexes, and fast runs are indicated and expanded below. Note postictal depression (hyperpolarization) in the intracellularly recorded neuron (~6 s), associated with suppression of EEG

slow oscillation (compare to left part of trace). B, wave-triggered-average during the slow oscillation, at the beginning of seizure and during the middle part of seizure. Averaged activity was triggered by the steepest part of the depolarizing component in cortical neuron (dotted lines), during the three epochs. The depth-negative field component of the slow oscillation (associated with cell's depolarization) is termed K-complex. During the seizure, the depolarizing component reaches the level of a paroxysmal depolarizing shift (PDS), associated with an EEG spike. Note fast runs developing upon a plateau of depolarization during the SW seizure. From Steriade *et al.* (1998a).

[152] Steriade *et al.* (1998a).

[153] Kellaway (1985); Kellaway *et al.* (1990). These studies were performed during NREM sleep in humans. The relation between spindles and SW seizures elicited by systemically administered penicillin was also observed in an experimental model, the feline generalized penicillin epilepsy (reviewed in Gloor *et al.*, 1990; Kostopoulos, 2000), in which spindles were totally replaced by sequences of SW discharges. At variance, both spindles and SW complexes are present during the natural SWS in humans (Kellaway *et al.*, 1990).

[154] Steriade and Contreras (1995). These data demonstrated that the majority of TC neurons are steadily hyperpolarized and display phasic IPSPs during SW seizures, but no spike-bursts, due to the faithful following of all paroxysmal depolarizing shifts in cortical neurons by GABAergic reticular neurons (*see also* Slaght *et al.*, 2002). These data have been confirmed by Pinault *et al.* (1998) in a genetic rat model of absence epilepsy. See a comprehensive review on this topic by Crunelli and Leresche (2002).

[155] Marcus *et al.* (1968a–b); Steriade and Contreras (1998).

[156] Steriade (1974).

[157] Steriade and Amzica (1994); Neckelmann *et al.* (1998). The cortical origin of SW seizures was recently corroborated in a genetic rat model of absence epilepsy (Meeren *et al.*, 2002). In the latter study, the important observation was made that cortical SW seizures could sometimes occur without concomitant thalamic SW discharges,

the depth-negative cortical field potential (called KC). During seizure, the depolarizing component increased in amplitude, reaching the level of paroxysmal depolarizing shifts (PDSs). As well, there was an increased frequencies of PDSs (EEG “spikes”), compared to the frequency of the slow sleep oscillation (~ 0.9 Hz), to become SW complexes at approximately 2–3 Hz [152].

The other major NREM sleep oscillation, spindles, can also lead to SW discharges, as seen in absence (petit-mal) of epilepsy [153]. These relations between spindles and SW seizures are valid in intact-brain animals, in which only a minority of TC neurons may fire low-threshold spike-bursts during SW seizures [154], but the minimal substrate for generation of these seizures is the neocortex as they occur in thalamectomized preparations in which spindles are absent [155]. Indeed, SW seizures originate in cortex, and even in circumscribed pools of cortical neurons, sometime without reflection at the cortical surface [156], and they are transferred to adjacent and more distant cortical areas before they reach the thalamus [157]. The conclusion of these studies is that the cortex alone can generate SW seizures, while this is not the case with the thalamus [157–158].

The occurrence of very fast oscillations (ripples, 80–200 Hz) over the depolarizing phase of the slow sleep oscillation was discussed in Sections 7.1.4 and 7.3.3.5. That ripples recorded during the slow sleep oscillation could play a role in initiating seizures is suggested by strong correlation between neuronal excitation and the intensity of ripples and their presence at the transition between normal and paroxysmal activity [159]. Also, halothane antagonizes both ripples and seizures [159]. Ripples of strong amplitude are present from the very onset of the transition between normal and paroxysmal activities (Fig. 7.54).

7.3.2. Burst-Suppression

In humans, the pattern of EEG burst-suppression appears in the cortex infiltrated with tumors, after trauma associated with cerebral anoxia, during coma with dissolution of cerebral function [160], but also in deeply anesthetized animals [161], and consists of sequences of high-amplitude waves alternating with periods of electrical silence. The neuronal substrate of this EEG pattern was recently described, using intracellular recordings in cats by administration of the same anesthetic on a background of already synchronized activity or by administering other anesthetic agents after the initial anesthesia [162]. Briefly, the membrane potential of neocortical neurons hyperpolarizes

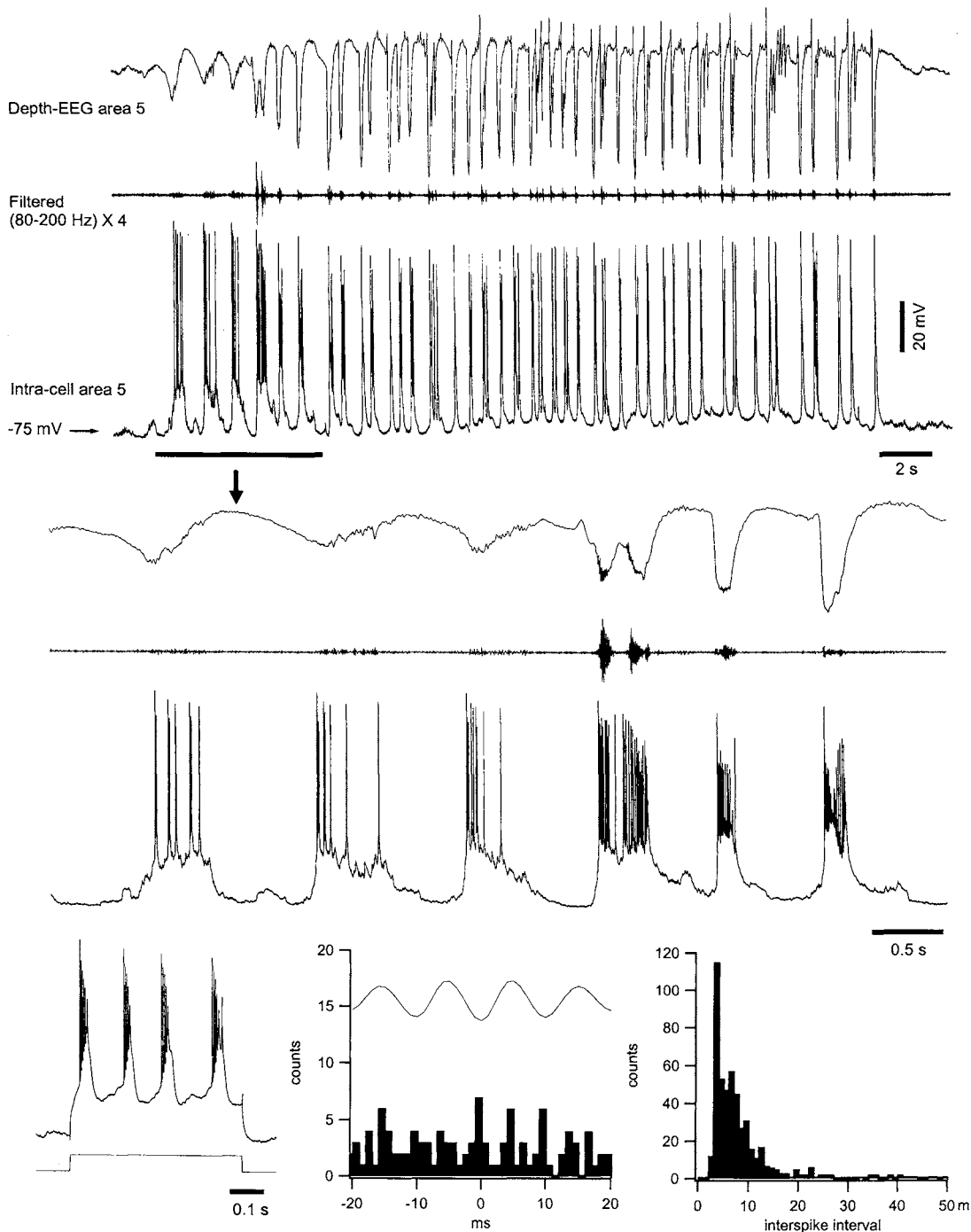


Figure 7.54. Intrinsically-bursting neuron firing in relation with ripples during seizures. Intracellular and field potential recordings from area 5 in cat under ketamine–xylazine anesthesia. The top panel depicts an epoch comprising an entire seizure along with the EEG trace filtered between 80–200 Hz. The neuron was an intrinsically-bursting cell as revealed by its response to depolarizing current pulse (bottom left panel). The beginning of the seizure (underlined epoch)

is expanded in the middle panel. The neuron fired in phase with ripples, but its bursting tendency probably accounts for spikes occurring also out of phase (bottom middle panel), and for the interspike interval histogram showing a peak at 3.5 ms (bottom right plot). Note, in the middle panel, increased amplitudes of ripples at the very onset of seizure, developing from the slow oscillation. Modified from Grenier *et al.* (2003).

whereas the reverse was never observed (see [154]). [158] The concept of a deeply located “centrencephalic” system was postulated by Jasper and Kershman (1941) and Penfield and Jasper (1954). It was also claimed that “absence” seizures were induced in cortex by electrical stimulation of midline thalamic nuclei at 3 Hz, at a critical level of barbiturate anesthesia (Jasper and Drooglever-Fortuyn, 1949). In that study, only SW-like *responses* were evoked in cortex, but no self-sustained activity. As to the existence of a “centrencephalic” system, which would produce bilaterally synchronous SW complexes, it should be stressed that there are no bilaterally projecting thalamic neurons. [159] Grenier *et al.* (2003). [160] Fischer-Williams (1963); Stockard *et al.* (1975); Bauer and Niedermeyer (1979). [161] Swank (1949). [162] Steriade *et al.* (1994a).

[163] Greenstein *et al.* (1988); Pavlides and Winson (1989); Wilson and McNaughton (1994); Qin *et al.* (1997); Buzsáki (1998, 2002). [164] Pavlov (1923). [165] Eccles (1961).

[166] Steriade *et al.* (2001a); Timofeev *et al.* (2001b).

[167] Reviewed in Steriade (2001a,b).

[168] Steriade *et al.* (1993b,d).

[169] Maquet *et al.* (1997).

by approximately 10 mV before any EEG change announcing the transition from the normal slow sleep oscillation to burst-suppression. During flat EEG periods (suppression epochs), the apparent input resistance decreases and neuronal responsiveness to synaptic volleys is dramatically reduced. In contrast with the consistent behavior of all tested cortical neurons, only 60–70% of thalamic relay cells cease firing during periods of flat EEG activity [162]. We hypothesized that the full-blown burst-suppression pattern is achieved through complete disconnection of brain circuits and this assumption was corroborated by revival of normal EEG and neuronal activities after stimuli setting into action cortical and thalamic networks.

7.4. Plastic Changes in Thalamocortical Systems during Sleep and Waking Oscillations

Plasticity can be defined as an alteration in neuronal responsiveness and in the strength of connections among neurons, which depends on the history of a given neuronal circuit, a mechanism through which information is stored.

We will focus on experimental data in the thalamus and neocortex, placing emphasis on neuronal plasticity that occurs during and outlasting sleep and waking oscillations. While the effects of activities (some of them in the theta frequency range) occurring in rodent hippocampus on plasticity and consolidation of memory processes have been hypothesized and intensively investigated during the past decade [163], the effects of NREM sleep oscillations on neuronal plasticity in the thalamus and neocortex have been hindered by traditional views that considered sleep as associated with global cortical inhibition [164] that produces an “abject annihilation of consciousness” [165]. However, recent intracellular recordings during natural states of vigilance of behaving cats demonstrate that neocortical neurons display a rich spontaneous activity during NREM sleep [166], despite the fact that, simultaneously, the thalamus undergoes a global inhibition that prevents the transfer of signals from the external world to the neocortex [167]. These data suggest that, during NREM sleep, cortico-cortical operations are preserved and may lead to reorganization and specification of neuronal circuits in cortex and target structures. This hypothesis [168] was corroborated by studies using indicators of neuronal activities during NREM sleep in humans, revealing more marked changes in those neocortical areas that are implicated in memory tasks and decision-making during wakefulness [169].

It has also been demonstrated in humans that the overnight improvement of visual discrimination tasks requires steps depending on the early night NREM sleep, associated with spindles and slow oscillation, which led to the conclusion that procedural memory formation is prompted by NREM sleep [170]. It was suggested that a massive Ca^{2+} entry in cortical pyramidal neurons during low-frequency sleep oscillations, such as spindling, may activate a molecular “gate” mediated by protein kinase A, opening the door to gene expression—this process allowing permanent changes to subsequent inputs following sleep spindles [171].

In this section, we will present the neuronal substrates of plasticity developing from a major oscillation of NREM sleep, spindles, and their experimental model, augmenting responses. We will also discuss the plastic changes occurring following 10-Hz stimuli to TC systems (mimicking sleep spindles) compared to those induced by 40-Hz stimulation of callosal pathways (mimicking fast oscillations in the gamma frequency band that occur during brain-active states of wakefulness and REM sleep). Although we will mainly present data on cortical plasticity, the thalamus is also implicated in this process [172].

The data presented below demonstrate that spindle oscillations and augmenting responses, known for a long time as a model of spindles [173], produce long-lasting alterations in tested synaptic responses of thalamic and neocortical neurons. First, we will describe the neuronal basis of augmenting responses.

7.4.1. Augmenting or Incremental Responses

Augmenting responses are thalamically or cortically evoked potentials that grow in size during the first stimuli at a frequency of 5–15 Hz (optimal frequency being ~ 10 Hz), like the waxing of waves at the onset of spontaneously occurring spindle sequences. These responses have been investigated at the intracellular level in the thalamus of decorticated animals [174], the intact neocortex of thalamectomized animals [175], or cortical slabs *in vivo* [176], and cortical slices maintained *in vitro* [177]. Such incremental responses have also been investigated in realistic models of thalamic and cortical neurons [178].

Some remarks are necessary concerning the conventional view that two different types of incremental TC responses, augmenting and recruiting, should be distinguished. The distinction between two types of incremental responses, *augmenting* and *recruiting*, was suggested on the basis that augmenting responses are elicited in localized cortical areas by stimulation of “specific” thalamic nuclei and their polarity is positive at the cortical surface,

[170] Gais *et al.* (2000); Stickgold *et al.* (2000). After extensive training on a declarative learning task, the density of sleep spindles in humans is significantly higher as compared to nonlearning control task (Gais *et al.*, 2002). See a comprehensive review on sleep and neuronal processes of consciousness and learning by Hobson and Pace-Schott (2002). [171] Sejnowski and Destexhe (2000). [172] Thalamic neurons display reorganization after deafferentation (Jones, 2000) and brainstem cholinergic stimulation produces a prolonged enhancement of thalamic synaptic responsiveness (Paré and Steriade, 1990; Paré *et al.*, 1990b). Plasticity of TC and thalamic reticular neurons following low-frequency thalamic stimulation, in the frequency range of sleep spindles, is discussed in the main text. [173] Dempsey and Morison (1942); Morison and Dempsey (1942). In their paper, Morison and Dempsey referred to a personal communication by Lorente de Nó who helped to explain the “specific” augmenting responses with restricted cortical distribution and the “nonspecific” recruiting responses with broad distribution. In particular, the recruiting responses to intralaminar thalamic stimulation were attributed to “cell groups, not ordinarily thought of as projection nuclei (that) send fibers to the cortex which make more diffuse connections than do the specific projection fibers, and may be especially rich in association areas” (Morison and Dempsey, 1942, p. 291).

[174] Steriade and Timofeev (1997).
 [175] Steriade *et al.* (1993f).
 [176] Timofeev *et al.* (2002).
 [177] Castro-Alamancos and Connors (1996a–b)
 [178] Bazhenov *et al.* (1998a–b); Houweling *et al.* (2002).
 [179] Spencer and Brookhart (1961a–b).

[180] Purpura *et al.* (1964); Creutzfeldt *et al.* (1966).

[181] Morin and Steriade (1981).

[182] Steriade (1978).

[183] Ferster and Lindström (1986).

whereas recruiting responses are elicited by stimulation of “nonspecific” thalamic nuclei, are negative at the cortical surface, and occur with a longer latency than that of augmenting responses [173].

Depth-profile analyses indicate that the surface-positivity of the augmenting response results from excitatory TC inputs that create sinks mostly in mid-layers (IV–III), with current flow along the vertical core conductors represented by the apical dendrites of pyramidal neurons [179]. During the 1960s, it was postulated that the basic mechanism of augmenting responses is an increased secondary depolarization and an attenuation of hyperpolarizing potentials beginning with the second stimulus in the pulse-train [180] (concerning the attenuation of hyperpolarization, see below more recent data). The increased amplitude of the depth-negative secondary excitatory component is associated, during the augmenting process, with decreased amplitude of the primary excitatory component (Fig. 7.55) [181]. Such a differential evolution of focal waves in the cortical depth is paralleled by an increased number of spike discharges superimposed on the secondary (augmented) field potential. Simultaneously, there is a decreased probability of unit discharges associated with the primary TC excitation. This phenomenon was observed in both somatosensory and parietal association cortices (Fig. 7.56) [182]. That the augmenting potential develops simultaneously with a reduced amplitude primary response was confirmed in an analysis of augmentation in the visual cortex [183]. Since maximal augmentation develops when the second stimulus is delivered at time-intervals of 60–120 ms following the first stimulus (see Fig. 7.55C), that is, at a time when cortical neurons are in a hyperpolarized state after the initial excitation induced by the first stimulus, the augmented wave may well reflect a summation of low-threshold rebound spikes (LTSs) de-inactivated by hyperpolarization (see Chapter 5). In support of this assumption, the second stimulus in the train fails to elicit an augmenting potential when delivered after the postinhibitory rebound potential induced by the first stimulus (see Fig. 7.55C), because of the refractory phase of the LTS. While inhibitory-rebound phenomena at the thalamic stimulated site may play a role in cortical augmentation (see below recent intracellular data in [174]), the cerebral cortex has the required circuitry to generate augmenting responses in the absence of the thalamus. This was shown by eliciting augmenting responses in the somatosensory cortex to direct stimulation of radiation axons in preparations with destruction of ventrobasal thalamus [181]. Similarly, the visual cortex may display augmenting responses by antidromic activation of corticogeniculate axons after destruction of the LG nucleus [183].

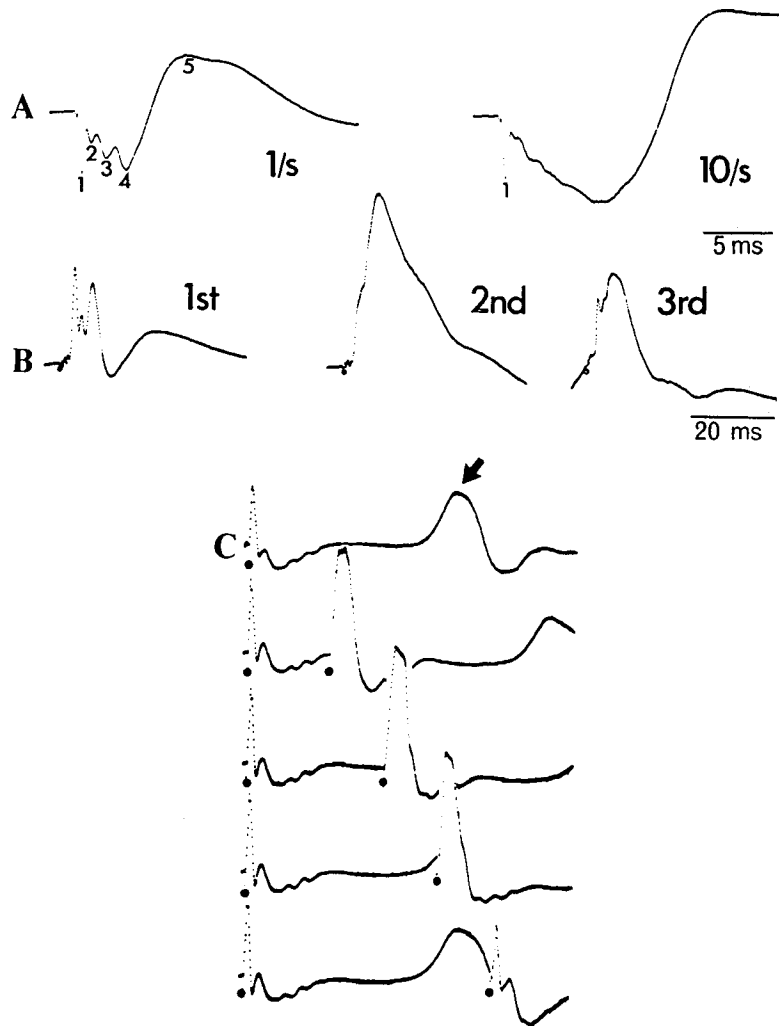


Figure 7.55. Primary and augmenting responses of primary somatosensory (S1) cortex by stimulating the ventroposterior (VP) thalamic complex in the *encéphale isolé* cat. 50-averaged traces. A, surface recording of responses evoked by 1/s and 10/s VP stimulation; responses consist of 5 components (numbered 1 to 5); note unchanged presynaptic (1) component. B, another *encéphale isolé* cat; depth (0.7 mm) recording of the first, second, and third response to a pulse-train at 10/s; presynaptic deflection was not evident in this case; note, during augmentation, reduced amplitude of early postsynaptic rapid components and protracted duration of the slow negative wave. C, depth (0.5 mm) recording of responses to single VP stimulus (first trace) and to paired VP stimuli separated by 60, 100, 140, and 180 ms. Rebound component (peak latency: 150 ms) indicated by arrow on the first trace. Modified from Morin and Steriade (1981).

Concerning recruiting responses, the initial negativity at the cortical surface that distinguishes the recruiting from the augmenting responses is due to the superficial projection over cortical layer I of those thalamic nuclei whose stimulation characteristically induces recruiting. This applies to the three main recruiting systems: the centrolateral–paracentral (CL–PC) rostral intralaminar nuclei, the ventromedial (VM) nucleus, and the

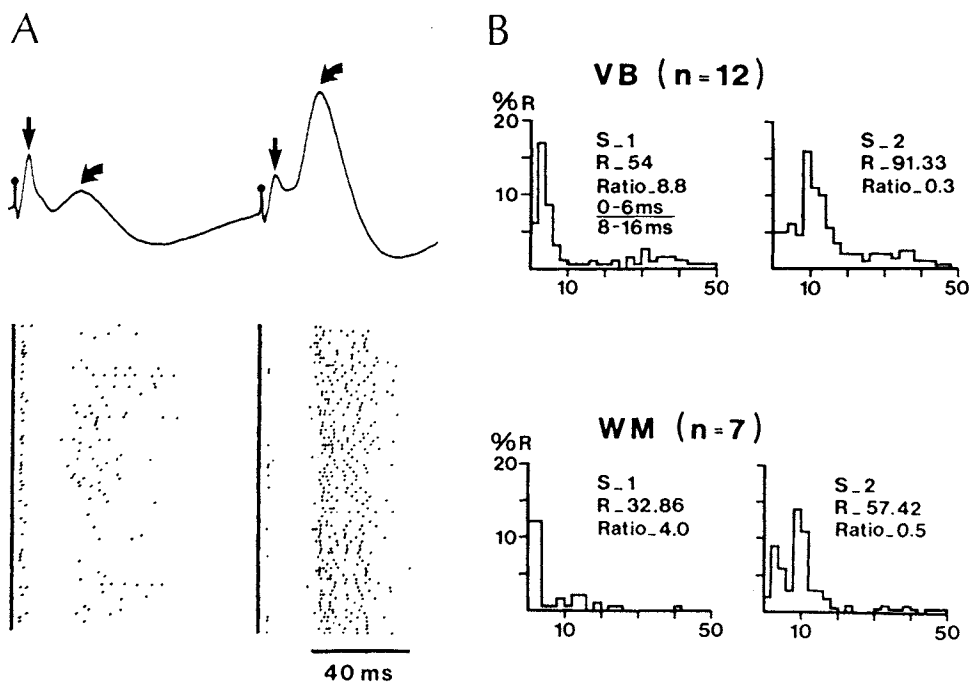


Figure 7.56. Increased secondary excitation during thalamocortical augmenting responses in the *encéphale isolé* cats. A, neuron recorded from parietal association cortex, simultaneously with focal waves. Two 100-ms-delayed shocks: applied to the lateral posterior (LP) thalamic nucleus. Top: 50-averaged traces of focal waves; bottom: 50-sweep dotgram (each dot represents one action potential). Note that the response to the second stimulus had decreased amplitude of the early slow depolarizing field potential (right arrows) and decreased probability of firing in the first part of the unitary response, whereas the second depolarizing field potential (oblique arrows) increased in amplitude and there was an increased number of repetitive discharges. B, augmentation phenomenon in primary somatosensory (S1) cortex by stimulating at 10/s the ventrobasal (VB) thalamic complex and the white matter (WM) underlying S1 cortex after destruction of the VB complex. Poststimulus histograms (2-ms bins) of unit discharges pooled on a bin-by-bin basis in a group of 12 VB-driven and 7 WM-driven units. Testing VB and WM stimuli applied at time 0 on the abscissa. S, stimulus number (first stimulus in the train and second stimulus delayed by 100 ms). R, responsiveness (total number of discharges to 100 stimuli). Ratios indicate the probability of evoked discharges in the 0–6 ms bins (primary excitation) over the probability of discharges in 8–16 ms bins (secondary excitation). Modified from Steriade *et al.* (1978) and Steriade and Morin (1981).

[184] Herkenham (1979); Oka *et al.* (1982); Cunningham and LeVay (1986).
[185] Jones (1985).

[186] Glenn *et al.* (1982).
[187] Foster (1980); Jibiki *et al.* (1986).
[188] Sasaki *et al.* (1970, 1975); Steriade *et al.* (1978).

ventroanterior (VA) nucleus [184]. While CL–PC intralaminar and VM nuclei project diffusely over the cerebral cortex, the projection of VA nucleus is more restricted and primarily directed to the anterior parietal region [185]. The surface-negativity of the VM-evoked recruiting response and its superficial (0.25–0.3 mm) reversal, together with the reduction in amplitude of the surface-negative wave by cortical superfusion with manganese, indicated that direct depolarizing actions of VM-cortical axons are exerted on apical dendrites reaching layer I [186]. Similar superficial depolarizing actions are postulated for CL-cortical [187] and VA-cortical [188] recruiting systems.

Laminar analyses show that augmenting TC potentials are homologous with type I (surface-positive) cortical spindles, whereas recruiting responses are homologous with type II (surface-negative) spindles [179]. The mixed pattern of waves within spindle sequences, with both type I and type II components, is due to afferent connections to cortical areas from multiple thalamic nuclei that project to mid-layers IV–III and to the superficial layer I. For example, the parietal association area 5 of cat receives TC axons from three main nuclei: the lateroposterior (LP) nucleus projecting mainly to mid-layers IV–III; the VA nucleus projecting to layer I; and the intralaminar CL nucleus projecting to both layers I and VI. In the same corticopontine neuron recorded from cat area 5, LP-evoked discharges are superimposed upon augmenting (depth-negative) potentials, whereas VA-evoked discharges are superimposed upon recruiting (depth-positive) potentials (Fig. 7.57).

In reality, augmenting and recruiting responses are not so distinct. Many evidence point in this direction. The longer latency of recruiting responses suggested a “diffuse

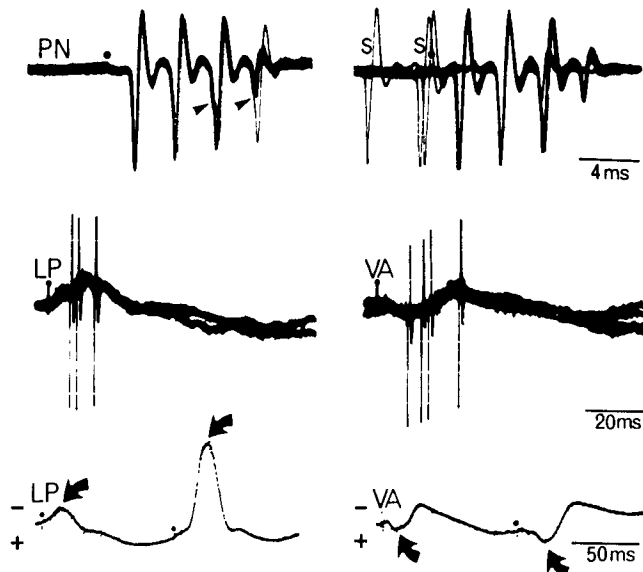


Figure 7.57. Synaptic excitation of a corticopontine neuron from two thalamic nuclei inducing augmenting and recruiting responses in the parietal association cortex of chronically implanted cat. Top: antidromic responses of cortical neuron by stimulation of pontine nuclei (PN) with 4-shock train (only the first shock is marked by dot). Arrowheads in left superimposition indicate break between initial segment (IS) and somatodendritic (SD) spikes. Right superimposition depicts collisions of responses to the first shock with 3 spontaneously (S) occurring discharges. Middle: synaptically evoked discharges of the same neuron by stimulating the lateral posterior (LP) and ventroanterior (VA) thalamic nuclei. Bottom: 50-averaged sweeps of field potentials evoked by LP and VA thalamic stimulation with 2 stimuli separated by 100 ms. Unit discharges were cut off. Note depth-negative augmenting responses induced by LP stimuli (reflecting the prevalent mid-layers termination of LP-cortical axons) and depth-positive recruiting responses induced by VA stimuli (reflecting the prevalent termination of VA axons in the superficial cortical layers). Modified from Steriade *et al.* (1978).

[189] Jasper (1949).
[190] Ramón y Cajal
(1911).

[191] One of these nuclei is the ventromedial nucleus whose neurons are antidromically invaded at long latencies from the cerebral cortex (Steriade, 1995a).
[192] Steriade *et al.* (1998c). See Fig. 4 in that paper showing that TC incremental responses evoked by rhythmic stimulation of rostral intralaminar nuclei (conventionally known as typically inducing recruiting responses) are of the recruiting type in one cortical area and of the augmenting type in another area of the same gyrus (because intralaminar nuclei project preferentially to layer I but also to deep layers); as well, the latencies of both augmenting and recruiting responses evoked by thalamic intralaminar stimulation are equally short (<4 ms).

[193] Timofeev and Steriade (1998).

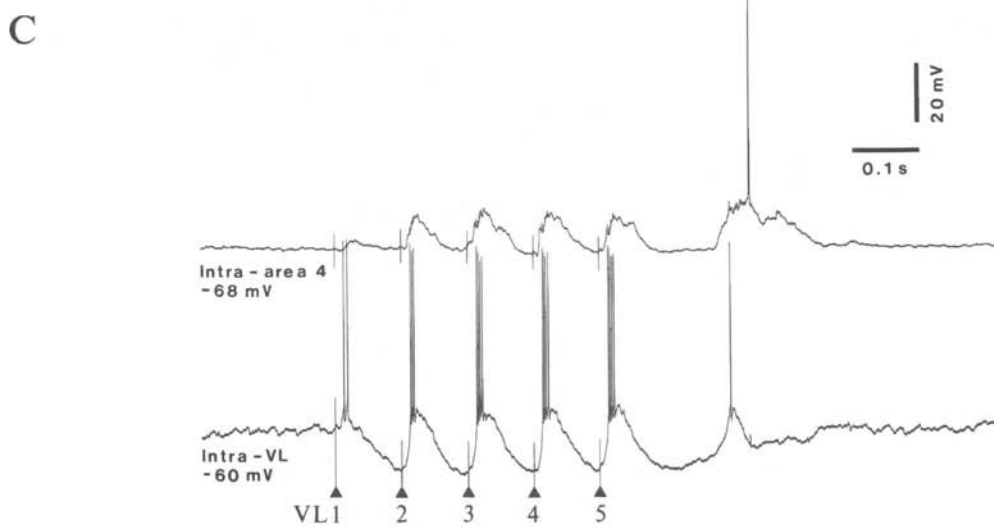
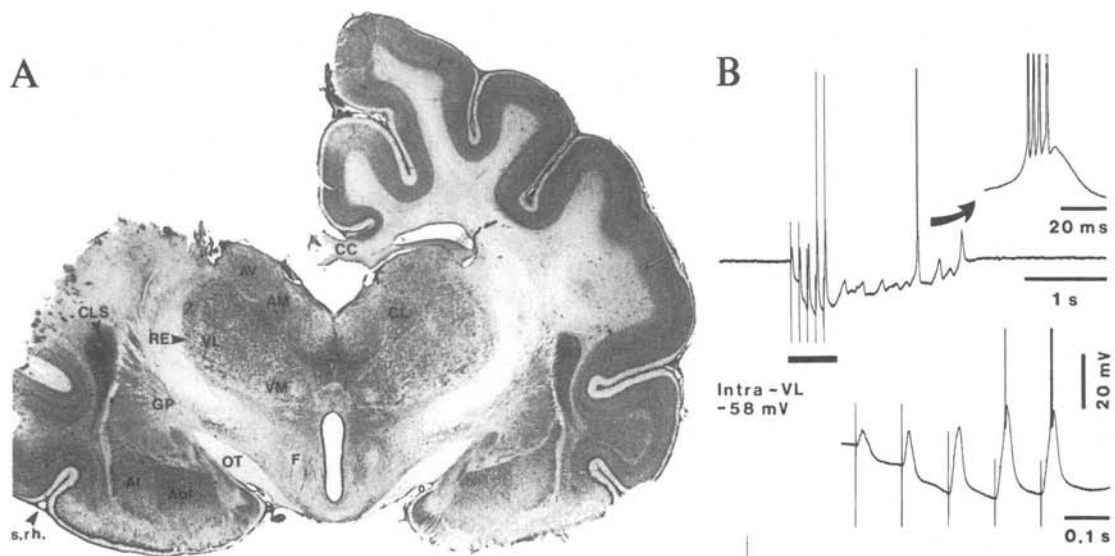
[194] Grenier *et al.* (1998).

multineuronal system,” with intralaminar nuclei serving as an intrathalamic association system and the thalamic reticular nucleus as a final step in the course of influxes to the cerebral cortex [189]. However, it is known since Ramón y Cajal [190] that reticular nucleus does not project to cortex, that there are virtually no direct pathways linking different dorsal thalamic nuclei [185], that the longer latency of cortical recruiting responses is not due to the intrathalamic spread of multisynaptic activity but to slower conduction velocities of axons from some thalamic nuclei projecting directly to the neocortex [191], and that some recruiting (depth-positive) responses may display latencies as short as those of augmenting (depth-negative) responses [192]. There are no pure augmenting or recruiting responses as most are mixed responses, with augmenting preceding the recruiting or vice-versa [179], because of the multilaminar distribution of thalamic projections to cortex (see above). Therefore, the distinction between augmenting and recruiting responses is no longer necessary and we will use throughout this section the term augmenting or incremental.

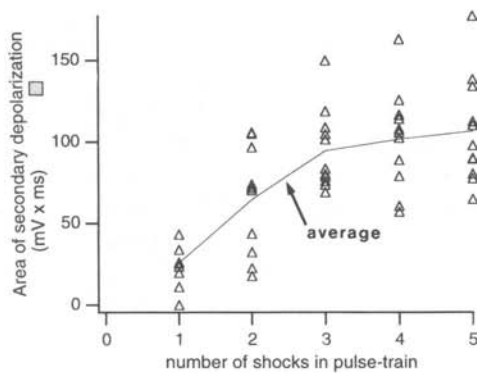
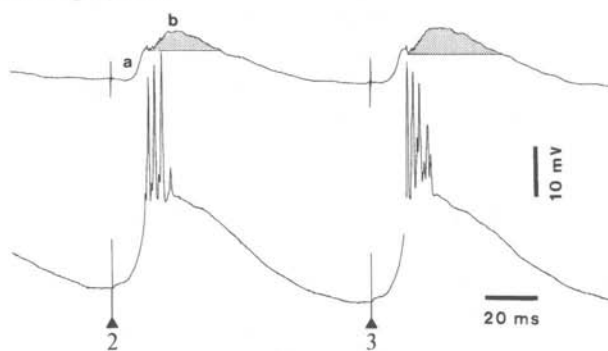
7.4.2. Plasticity Following Spindles and Their Experimental Model, Augmenting Responses

In the thalamus of decorticated cats (Fig. 7.58A), TC neurons display two types of augmenting responses to local thalamic stimulation at 10 Hz [174]. (a) Low-threshold augmenting responses are based on progressively increased LTSs, which are de-inactivated by the increasing hyperpolarization produced by repetitive stimuli in the train (Fig. 7.58B). (b) High-threshold augmenting responses are associated with progressively decreased IPSPs elicited by successive stimuli in the train and with progressive depolarization of neurons, thus leading to high-threshold spike-bursts, with increasing number of action potentials [174]. Whereas low-threshold augmentation is due to the parallel excitation in a pool of thalamic reticular GABAergic neurons, high-threshold augmenting responses are due to decremental responses in a pool of reticular neurons [193].

Dual intracellular recordings from TC and cortical neurons demonstrated that the augmentation in neocortical neurons is expressed by a selective increase in the secondary depolarizing component of thalamically evoked responses as this secondary depolarization follows by about 3 ms the postinhibitory spike-burst in simultaneously recorded TC neurons (Fig. 7.58C) [192, 194]. Thus, cortical augmenting responses primarily depend upon the



Average (n=10)



LTS-type of augmentation and related spike-bursts in TC neurons. Deeply lying pyramidal neurons, and especially FRB cells with thalamic projections (see Chapter 5, Section 5.6.1), consistently showed a higher propensity, shorter latencies, and greater number of action potentials during augmenting responses compared to more superficially located neurons.

Augmenting responses and spindles are associated with short-term plasticity processes. During repetitive thalamic stimuli at 10 Hz in decorticated animals, the IPSPs of TC neurons are progressively diminished (Fig. 7.59) [195]. Conversely, the depolarization area of augmenting responses increases continuously with the repetition of pulse-trains at 10 Hz (Fig. 7.60) [192]. Similar data can be elicited by using testing stimuli to the neocortex. After spontaneously occurring spindle sequences, single-spike responses of cortical association neurons evoked by stimulating the same cortical area, are transformed into greatly increased responses—a potentiation that lasts for several minutes (Fig. 7.61) [176]. The same phenomenon occurs when mimicking spontaneously occurring spindles with pulse-trains within the frequency range (10 Hz) of spindles. In the cerebral cortex of animals with ipsilateral thalamectomy, augmenting responses progressively develop with the depolarization of membrane potential, and the spike-bursts acquire more and more action potentials, eventually developing into self-sustained paroxysmal

[195] Grenier *et al.* (2002).

Figure 7.58. Augmenting responses in thalamic neurons and in thalamocortical (TC) systems. A, hemidecortication (ipsilateral to thalamic recordings) and cut of corpus callosum. Nissl-stained section. Abbreviations: AV, AM, CL, RE, VL, and VM, anteroventral, anteromedial, centrolateral, reticular, ventrolateral, and ventromedial thalamic nuclei; CA, caudate nucleus; CC, corpus callosum; F, fornix; Al and Abl, lateral and basolateral nuclei of amygdala; CLS, claustrum; GP, globus pallidus; OT, optic tract; s.rh., rhinal sulcus (arrowhead). B, intrathalamic augmenting responses in decorticated cat (see A). Intracellular recordings from the thalamic ventrolateral (VL) nucleus under ketamine–xylazine anesthesia show low-threshold augmenting responses of VL cell developing from progressive increase in IPSP-rebound sequences and followed by a self-sustained spindle. Arrow indicates expanded spike-burst (action potentials truncated). The part marked by horizontal bar and indicating augmenting responses is expanded at right. During thalamically-evoked augmenting responses, the cortical augmented component (secondary depolarization, b) follows the rebound spike-burst in TC neuron, and the depolarization area in cortical neuron increases as a function of number of action potentials in the rebound spike-burst of TC cell. C, dual intracellular recording from cortical area 4 and thalamic VL nucleus in cat under ketamine–xylazine anesthesia. *Below*, average of second and third responses in cortical and VL cells. The area of secondary depolarization in cortical neuron (b), which develops during augmentation, is marked by dots. *Right plot*, area of secondary depolarization of cortical cell as a function of the number of stimuli in the pulse-trains (the line represents the mean). In a sample of 92 cells, the maximum number of fast spikes of TC cells triggered by the LTS occurred at the third to fifth stimuli. After having reached the maximum, the number of spikes in TC cells could decrease. The area of secondary depolarization of cortical cells also reached levels close to saturation at the third to fifth stimuli; however, the decrease of the depolarizing area in cortical cells was only exceptionally observed. This suggests that high levels of cortical excitability may be maintained by intracortical mechanisms. Modified from Steriade and Timofeev (1997, A–B) and Steriade *et al.* (1998c, C).

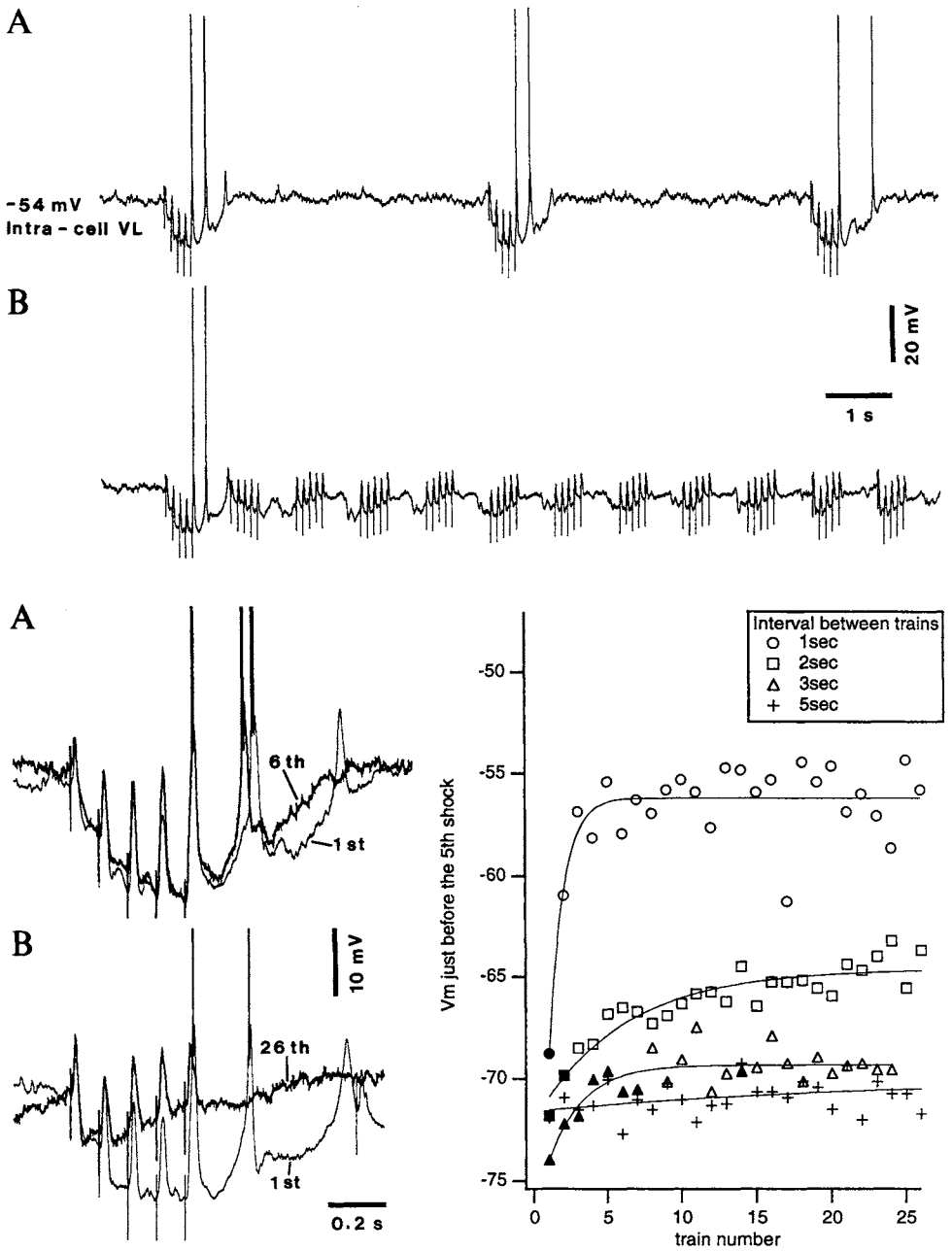


Figure 7.59. Decremental effect of repetitive thalamic stimulation on inhibitory postsynaptic potentials (IPSPs) in thalamocortical (TC) neurons during augmenting stimulation. Cat under ketamine-xylazine anesthesia. Intracellular recording of a TC cell from ventrolateral (VL) nucleus. VL stimulation with trains of 5 stimuli at 10 Hz with different time intervals between the trains. In panel A, pulse-trains are given every 5 s, while in panel B the period is 1 s. In the bottom left panel, the responses to the first and sixth pulse-trains, and the responses to the first and 26th pulse-trains are superimposed. The decremental effect on evoked IPSPs by repetitive stimulation is plotted at bottom right. The V_m at 5 ms before the fifth shock in each train is plotted for series of stimulation of different periods (trains every 1, 2, 3, and 5 s). The impact of repetitive stimulation on the IPSPs is very strong at a period of 1 s, while at 5 s there is almost no effect. Note that the decrease in evoked IPSP eventually led to the disappearance of the rebound low-threshold spike (26th train, bottom left panel). Modified from Grenier *et al.* (2002).

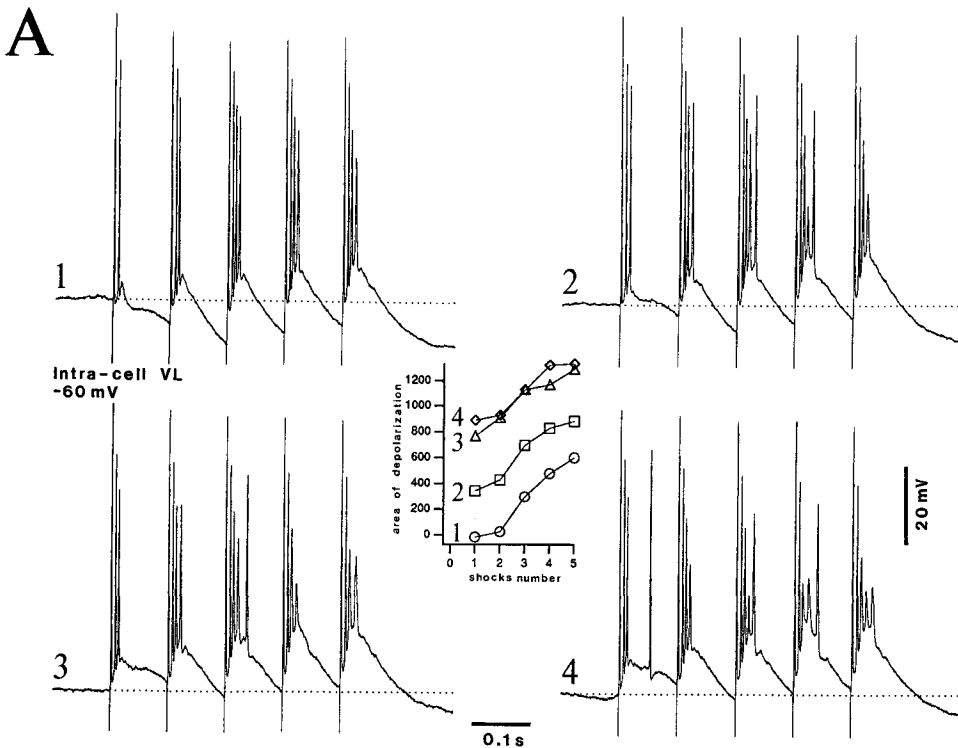


Figure 7.60. Short-term plasticity from repetitive intrathalamic augmenting responses of the high-threshold type. Intracellular recording of ventrolateral (VL) neuron in cat with ipsilateral hemidecortication and callosal cut (as in Fig. 7.55A). Ketamine–xylazine anesthesia. Progressive and persistent increase in the area of depolarization by repeating the pulse-trains. Pulse-trains consisting of five stimuli at 10 Hz were applied to the VL every 2 s. The VL cell was recorded under $+0.5$ nA (-60 mV); at rest, the membrane potential was -72 mV. Responses to four pulse-trains (1–4) are illustrated (1 and 2 were separated by 2 s; 3 and 4 were also separated by 2 s and followed 14 s after 2). The responses to five-shock train consisted of an early antidromic spike, followed by orthodromic spikes displaying progressive augmentation and spike inactivation. Note that, with repetition of pulse-trains, inhibitory postsynaptic potentials elicited by preceding stimuli in the train were progressively reduced until their complete obliteration and spike-bursts contained more action potentials with spike inactivation. The graph depicts the increased area of depolarization from the first to the fifth responses in each pulse-train as well as from pulse-train 1 to pulse-trains 3 and 4. From Steriade *et al.* (1998c).

discharges, as in a seizure (Fig. 7.62) [175]. Thus, in cortex-intact animals, the cortical networks possess the necessary equipment to develop some forms of augmentation even after thalamectomy. As augmenting responses may lead to self-sustained paroxysmal activity in thalamectomized animals (Fig. 7.62A), this finding further strengthens the idea that the cerebral cortex is the minimal substrate of major types of seizures.

The rich spontaneous firing of neocortical neurons [127] and the potentiation of synaptic responses following repetitive stimulation mimicking oscillations occurring during NREM sleep (Figs. 7.61–7.62), together suggest that this behavioral state disconnected from the outside world may sustain mental events. Repeated spike-bursts

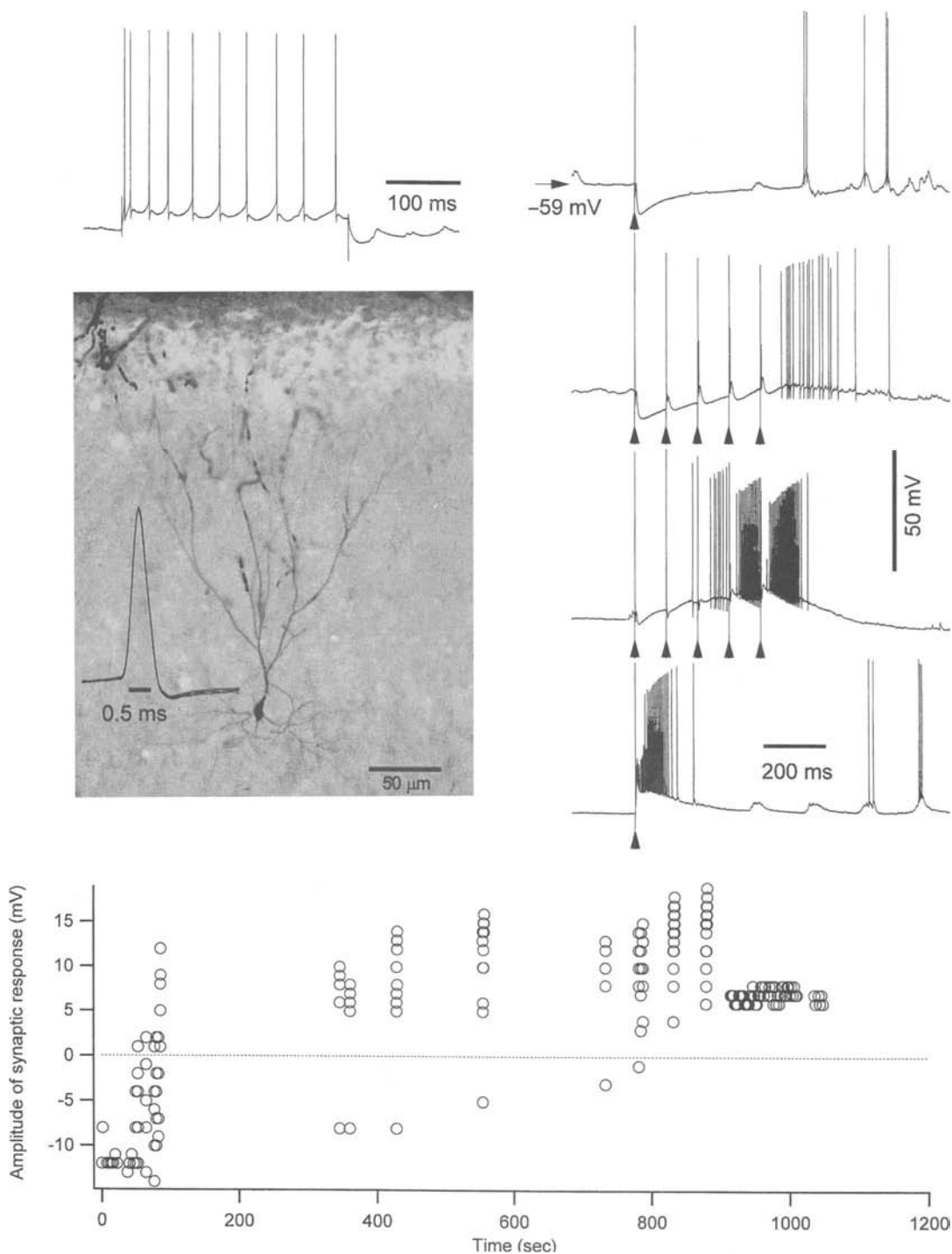


Figure 7.61. Cortical augmenting responses lead to long-lasting enhancement of depolarizing responses in intact cortex. Cat under barbiturate anesthesia. Intracellular recording from electrophysiologically (left upper panel) and morphologically (left middle panel) identified area 7 pyramidal regular-spiking neuron with thin spike (see expanded action potential close to the stained neuron). Right panel shows (from top to bottom): control response to a single stimulus to cortex, early responses to pulse-trains at 10 Hz, responses to pulse-train with the same parameters applied 12 min later, and response to a single stimulus applied 16 min after the onset of rhythmic stimulation. Below, plot showing the amplitude of stimulus-evoked response at 20 ms after stimulus onset. Note that initially hyperpolarizing responses became depolarizing after pulse-trains at 10 Hz. From Timofeev *et al.* (2002). See also color plate 4.

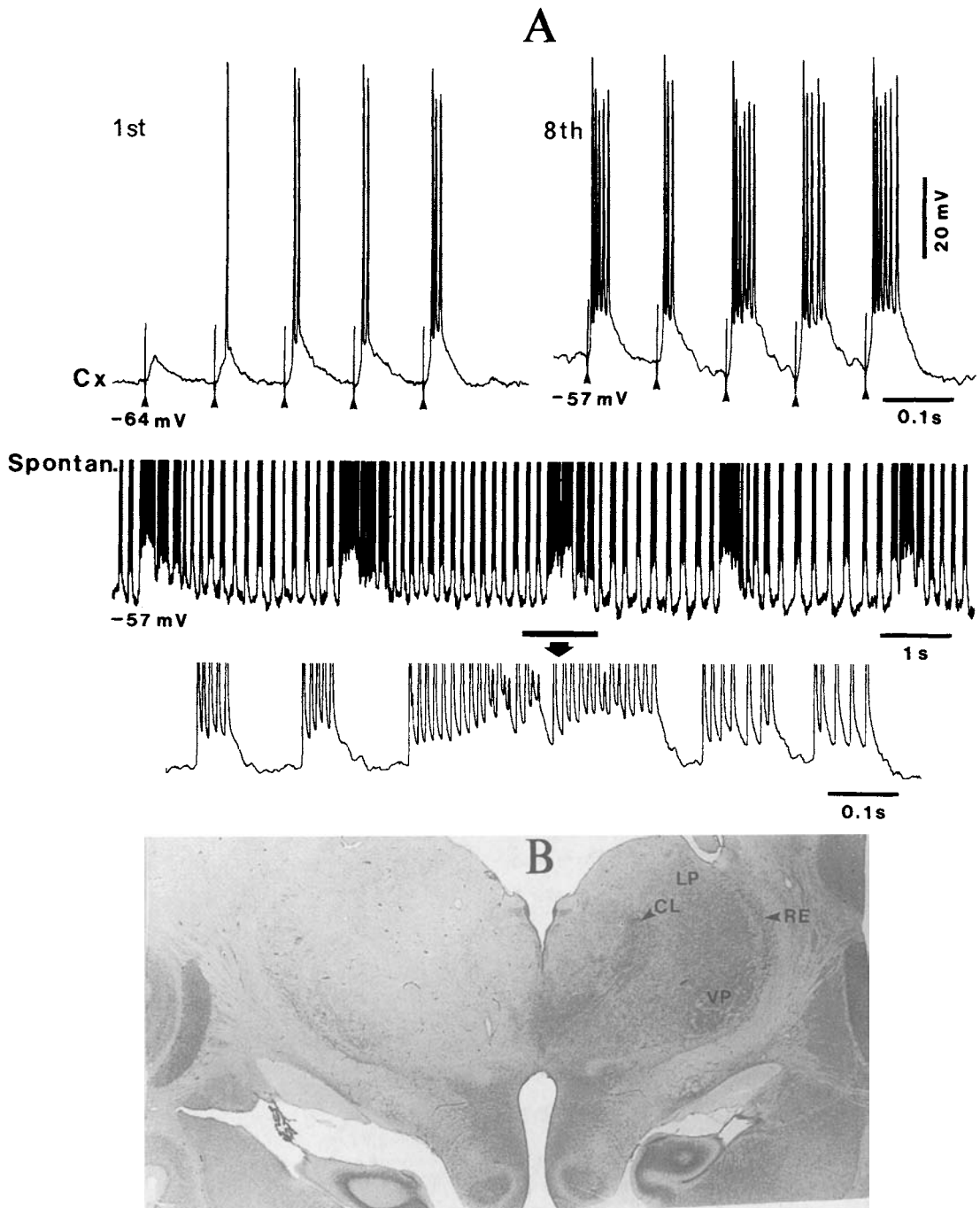


Figure 7.62. Changes in properties of neocortical neuron after repetitive callosal stimulation in a thalamically lesioned cat (see bottom panel with kainic thalamic lesion, ipsilateral to the recorded cortical neuron). Intracellular recording from intrinsically bursting neuron recorded at 1.5 mm depth in area 7. Urethane anesthesia. A, neuronal responses to repetitive stimulation (five-shock trains at 10 Hz, repeated every 3 s) of the contralateral area 7. The intracortical augmenting responses to

the first and eighth trains are illustrated. Note depolarization by about 7 mV and increased number of action potentials within bursts after repetitive stimulation. Following repeated responses to 10 Hz stimuli, spontaneous seizure. Abbreviations in bottom panel: CL, LP, RE, and VP, centrolateral, lateroposterior, reticular and ventroposterior thalamic nuclei. Modified from Steriade *et al.* (1993f).

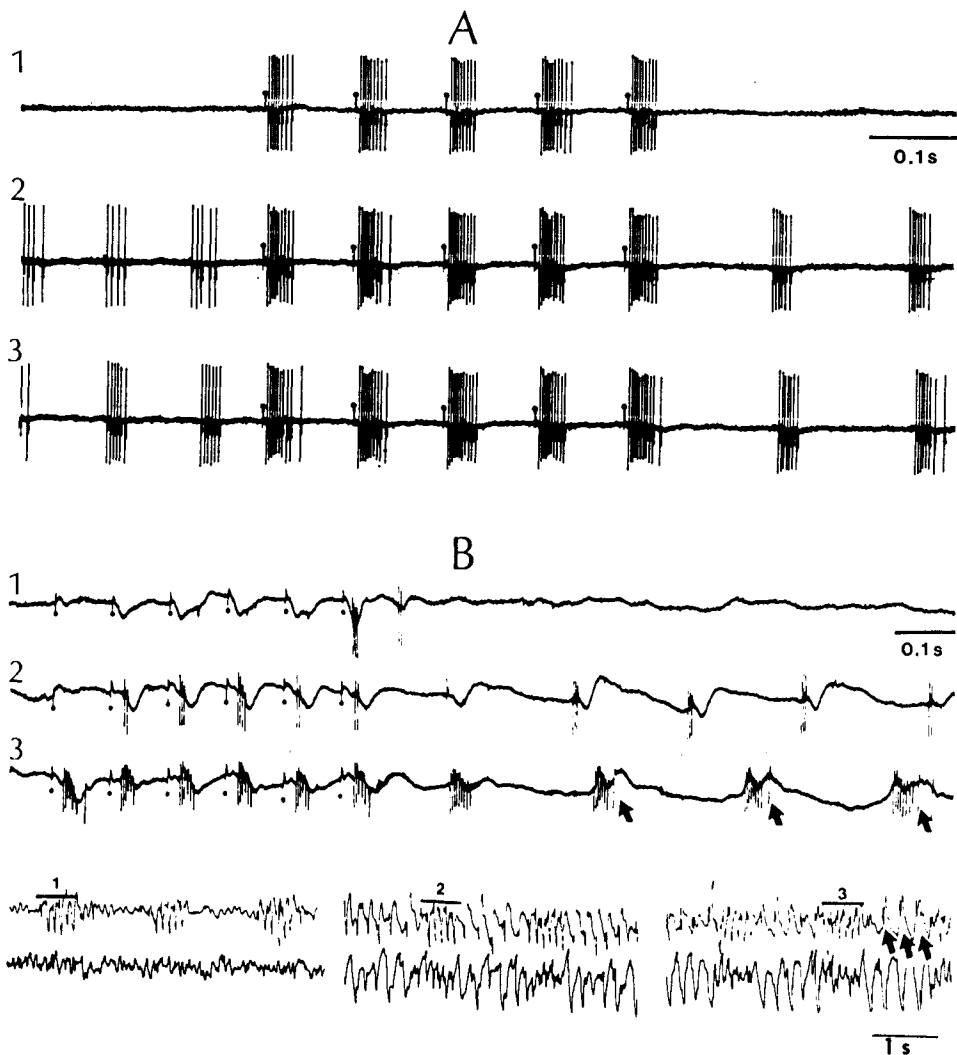


Figure 7.63. Cortically-evoked responses in bursting thalamic neurons of *encéphale isolé* cats, leading to self-sustained spike-and-wave (SW) complexes. A, a ventrolateral (VL) thalamic cell driven by motor cortex stimulation with five stimuli at 10/s (in 1), delivered every 2 s. Note appearance of “spontaneous” bursts resembling the evoked ones at a late stage of stimulation (in 2 and 3). B, effects of stimulation of the suprasylvian area 7 with trains of six stimuli at 10/s (as in 1) upon a bursting cell recorded from the lateral posterior (LP) thalamic cell. Beginning with the 12th pulse-train, the cell was regularly driven and displayed self-sustained rhythmic bursts at 5/s, between cortical pulse-trains. In 3 (28th pulse-train), self-sustained SW complexes appeared (arrows). Below, the two ink-written traces represent focal waves in the LP nucleus, recorded by the same microelectrode used for unit recording (upper trace, negativity upward) and EEG rhythms from the surface of the suprasylvian gyrus (bottom trace). Figures (1–3) on the EEG recordings correspond to the periods of stimulation depicted with the same figures in oscilloscopic recordings. The three SW complexes are indicated by arrows on oscilloscopic trace 3 and EEG recordings. Modified from Steriade *et al.* (1976) and Steriade (1991).

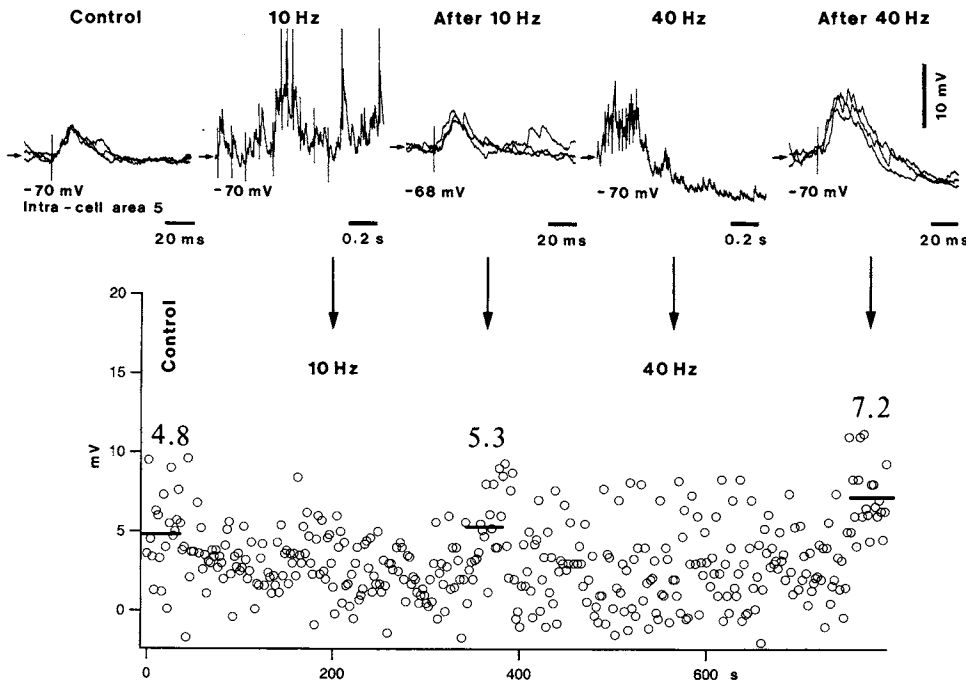


Figure 7.64. Greater facilitation of synaptic responses to callosal stimulation following pulse-trains at 40 Hz, compared to response potentiation following callosal stimulation with pulse-trains at 10 Hz. Cat under barbiturate anesthesia. Intracellular recording from area 5. Upper panel shows superimposed responses to homotopic site in contralateral area 5: before rhythmic stimulation (Control), to 10 Hz stimuli, after repeated pulse-trains at 10 Hz, to 40 Hz stimuli, and after repeated pulse-trains at 40 Hz. Bottom panel shows amplitudes (ordinate) of responses to different periods in the upper panel (see arrows). Note greater facilitation after conditioning stimulation at 40 Hz. Unpublished experiments by Y. Cissé, I. Timofeev, and M. Steriade (see Steriade *et al.*, 2003).

evoked by volleys applied to corticothalamic pathways or occurring during spontaneous sleep oscillations may lead to self-sustained activity patterns resembling those evoked in the late stages of stimulation, as in “memory” processes, eventually leading to paroxysmal events (Fig. 7.63) [196].

[196] Steriade (1991).

7.4.3. Potentiation of Cortical Responses Following Fast Oscillations

Experiments in progress have demonstrated a greater potentiation of cortical responses to stimulation of callosal pathway following 40-Hz stimuli (see Section 7.1.4), compared to the facilitation produced by stimulation with pulse-trains at 10 Hz (Fig. 7.64) [197].

[197] Steriade *et al.* (2003).

7.4.4. Concluding Remarks

The above data show that naturally occurring, low-frequency oscillations during NREM sleep (but also fast

oscillations that characterize both NREM and brain-active states) and their experimental models, such as augmenting responses that mimic sleep spindles, produce progressive depolarization in the membrane potential of neocortical neurons, increased responsiveness that may be short- or medium-range (up to 15 min), self-sustained oscillations with the same waveform and frequencies as those of evoked responses in prior stages of stimulation, and may develop into paroxysmal activity. The full development of these alterations is best seen with intact corticothalamic loops, but plastic changes in cortical neuronal responsiveness are also seen in the absence of thalamus. These results suggest that neocortical neurons are the sites of processes leading to consolidation of memory traces during NREM sleep. It was suggested that early NREM sleep stages favor retention of declarative memories, whereas sleep during late night, when episodes of REM sleep prevail, favors the retention of nondeclarative memories [198]. The role of NREM sleep in memory consolidation is substantiated by results using ocular dominance plasticity during the critical period in cats [199] and by potentiation of discrimination tasks in humans if the training period is followed by sleep, the enhancement correlating more closely to NREM sleep [170, 200].

[198] Plihal and Born (1997).

[199] Frank *et al.* (2001).

[200] Maquet (2001).

Brainstem and State dependency of Thalamocortical Systems

We now examine the state dependency of thalamic and cortical neuronal responses to afferent signals, and the underlying mechanisms of the enhanced excitability in those neurons during the EEG-activated states of wakefulness and REM sleep, compared to EEG-synchronized (NREM) sleep. Data showing the striking electrophysiological similarities between two behavioral states that were initially considered as two poles of the waking-sleep cycle led to the conclusion that both waking and REM sleep are brain-activated states, notwithstanding great differences in their mental content and despite that central motor commands are blocked at the spinal motoneuronal level during REM sleep. During waking, the increased neuronal responsiveness is associated with an increased efficacy of sculpturing inhibition involved in discriminatory tasks. We shall examine the control exerted by brainstem and forebrain ascending systems upon both excitatory and inhibitory processes in the thalamus and neocortex. Inhibitory processes have recently begun to be investigated at the intracellular level during REM sleep; this promising avenue of research may eventually lead to substantiate, at a neuronal level, some of the basic psychological differences between the two brain-activated states, otherwise similar from various electrophysiological points of view.

We first discuss the mechanisms of enhanced synaptic excitability in thalamic and cortical neurons to peripheral or central stimuli during the state of generalized arousal. In this context, we will examine the direct excitation of thalamocortical (TC) neurons by brainstem cholinergic and norepinephrinergic systems, and the disinhibition of TC neurons resulting from the inhibition of GABAergic thalamic reticular (RE) neurons by brainstem and basal forebrain cholinergic systems (Sections 8.1 and 8.2). Thereafter, we deal with investigations of neocortical neurons and with selective attention from studies using field potentials in humans and

unit activities in primates (Section 8.3). Data on electrophysiological processes mediated by two GABA receptors may explain the blockage of long-lasting cyclic inhibitions upon awakening, with preservation of short-range inhibitory processes involved in center-surround antagonism and other feature detection properties of central neurons. The thalamic and cortical transfer of the brainstem-generated signals during dreaming sleep is discussed in Section 8.4.

8.1. Thalamocortical Neurons

The thalamus is the first station where synaptic transmission is facilitated during arousal and where blockade of incoming messages occurs from the very onset of drowsiness. This was first shown by recording photically evoked responses with enhanced amplitudes in the thalamic lateral geniculate (LG) nucleus during EEG activation produced by midbrain reticular core stimulation, in spite of no change in responses simultaneously recorded from optic tract fibers [1]. Subsequent studies, using extra- and intracellularly recorded neuronal responses to peripheral or central stimuli, have confirmed and expanded the notion that an enhanced responsiveness in the thalamus upon arousal does *not* depend on modifications of excitability in prethalamic relays of specific sensory and motor pathways. To a large extent, what goes on in the cerebral cortex depends on fluctuations in thalamic excitability, and minimal increases in thalamic output may generate marked enhancement in cortical responses.

[1] Steriade and Demetrescu (1960).

Data presented below derive from experiments employing both peripheral sensory stimulation and electrical stimuli applied to central pathways. While the latter are abnormally synchronous, they allow analytical investigations of changes in excitability in thalamic neurons (using testing stimuli applied to prethalamic axons) or in cortical neurons (by stimulating radiation axons), thus avoiding unknown modifications at multiple intercalated synapses, as is the case when using natural sensory stimulation.

First, we discuss changes in background firing of TC neurons during different states of vigilance: NREM sleep as opposed to both waking and REM sleep. Next, we analyze the state-dependent responsiveness of TC neurons.

8.1.1. Two Modes of Spontaneous Firing During NREM Sleep and Brain-Active States

The potentiation of synaptic transmission during the two EEG-activated states of waking and REM sleep is

associated with a relative depolarization of thalamic and neocortical neurons in both these states that is reflected in their modes of spontaneous firing.

We have discussed in Chapter 5 that the tonic repetitive firing at a relatively depolarized level of membrane potential develops into burst firing by displacing the membrane potential of TC cells in a hyperpolarizing direction (see Section 5.5.1). Then, the burst of TC neurons is an intrinsic property uncovered by the state of hyperpolarization and the number of spikes within a burst is not related to any feature of an incoming message. In other words, the bursting mode is associated with a low or null transfer function. Conversely, the tonic firing mode during waking and REM sleep allow TC neurons to faithfully follow quite rapid rates of stimuli and to insure an accurate transfer of incoming messages in their route toward the cerebral cortex. Since the early 1960s it was shown that thalamic LG neurons discharge high-frequency spike bursts during EEG-synchronized sleep, a pattern that is not accompanied by similar alterations in the activity of afferent optic tract axons [2]. The independence of bursting firing mode of TC neurons upon the activity in prethalamocortical afferents was also shown by unchanged interspike interval distribution of burst discharges in ventrolateral (VL) thalamic neurons after destruction of their input sources, the deep cerebellar nuclei [3]. The rhythmic spike bursts of TC neurons during EEG-synchronized sleep, compared to the tonic firing patterns during waking and REM sleep, is illustrated in Fig. 8.1 (see also these two modes of firing, bursting and tonic, in intracellular recordings illustrated in Fig. 7.10, Chapter 7). The spindle-related rhythmicity of spike bursts was documented by autocorrelogram analysis [4]. The structure of thalamic bursts was quantitatively analyzed in studies of thalamic LG [5], intralaminar centrolateral-paracentral (CL-PC) [6], and other cortically projecting thalamic neurons [7]. That TC neurons are hyperpolarized by about 7–10 mV in EEG-synchronized sleep, that is the necessary level to de-inactivate the low-threshold spike crowned by high-frequency discharges (see Chapter 5, Section 5.5.1), was demonstrated using intracellular recordings in the naturally sleeping cat [8].

[2] Hubel (1960).

[3] Steriade *et al.* (1971).

[4] Steriade *et al.* (1985).

[5] McCarley *et al.* (1983).

[6] Glenn and Steriade (1982).

[7] Domich *et al.* (1986).

[8] Hirsch *et al.* (1983).

8.1.2. Evoked Potential Studies

The advantage of using the method of field potentials evoked by central stimuli (Fig. 8.2) is that one can monitor the magnitude of the incoming volley by measuring the amplitude of the presynaptic (or tract, *t*) deflection and, thus, one can ascertain whether changes in the postsynaptic

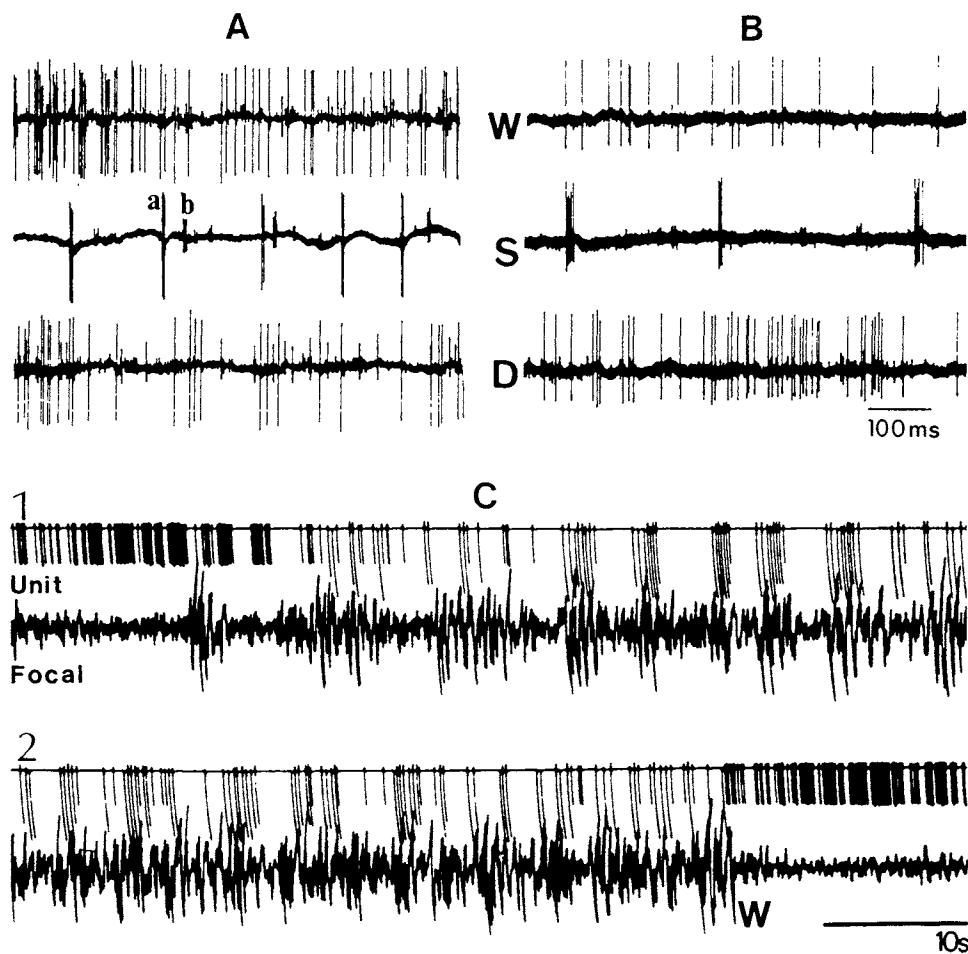


Figure 8.1. Tonic and bursting firing of thalamocortical (TC) neurons during EEG-activated and EEG-synchronized behavioral states in the cat. A–B, two thalamic rostral intralaminar centrolateral–paracentral (CL–PC) neurons. Note high-frequency spike bursts in EEG-synchronized sleep (S) and their replacement by sustained discharges in both behavioral states of waking (W) and EEG-activated (desynchronized) sleep (D). C, neuron in the thalamic ventrolateral (VL) nucleus. Ink-written recording: VL unit spikes were used to deflect a pen of the EEG machine (each deflection exceeding the common level represents a group of high-frequency, >250 Hz, spikes); focal waves simultaneously recorded by the same microelectrode are also depicted. Note close time-relation between groups of spike bursts and high-amplitude spindles; EEG activation is associated with tonic firing and increased discharge rates. Modified from Steriade and Glenn (1982, A–B) and Steriade *et al.* (1971, C).

(or relayed, r) components of the response are intrinsic to the explored structure or depend upon changes in afferent pathways. In this way, it has been demonstrated that EEG activation elicited by stimulation of the midbrain reticular formation (MRF) or natural awakening from EEG-synchronized sleep is accompanied by an increased amplitude of the monosynaptic thalamic response evoked by prethalamic stimulation, without any measurable change in the presynaptic component [9] (Fig. 8.2) (see [9] Steriade (1970).

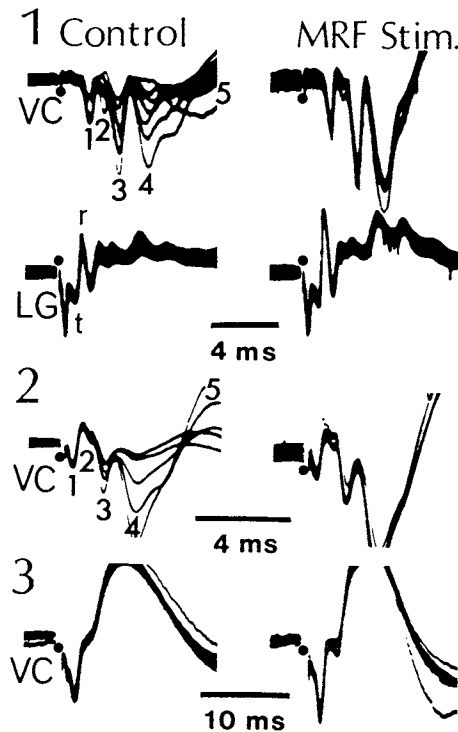


Figure 8.2. Effects of midbrain reticular formation (MRF) stimulation upon thalamic and cortical field responses in cat. Evoked potentials in control periods with EEG synchronization (left column) and effects of MRF stimulation (right column). In 1, simultaneous recording of field potentials evoked in the thalamic lateral geniculate (LG) nucleus and at the surface of the visual cortex (VC) by optic tract stimulation. The LG response consists of a presynaptic (tract, t) component and a monosynaptically relayed (r) component. Different components of the VC response are numbered from 1 to 5. Note, during MRF stimulation, enhancement of the monosynaptically relayed LG response without alteration in the presynaptic deflection; also note the increased amplitude of the VC response. In 2 and 3, same MRF-induced potentiation of the VC response with testing stimulation applied to the underlying white matter or to deep layers in the VC, respectively. Modified from Steriade (1970).

also Fig. 7.29 in Chapter 7, illustrating the obliteration of synaptic responses in the thalamus at the very onset of natural NREM sleep [10]). The idea that the arousal-related enhancement in thalamic excitability does not depend upon activity in prethalamic relays is supported by absence of excitability changes in bulbothalamic somatosensory neurons from sleep to wakefulness [11].

The increased thalamic output upon arousal results in an increased amplitude of simultaneously recorded cortical responses (Fig. 8.2). However, cortical facilitation is not merely due to facilitation of synaptic transmission through specific thalamic relays since a significant potentiation of cortical responses occurs upon MRF stimulation even when testing stimuli are applied to the white matter just beneath the recorded cortical area or to deep cortical layers [9, 12] (Fig. 8.2, panels 2–3). Since there are

[10] Steriade (1991).

[11] Carli *et al.* (1967).

[12] Steriade (1969).

virtually no direct MRF–cortical projections in cat (see Chapter 3, Section 3.4.1.1), two intermediate relays of brainstem ascending influxes (other than specific thalamic nuclei) account for the facilitation at the cortical level. (1) One circuit involves the cholinergic and noncholinergic neurons of the basal forebrain and their widespread cortical projections. The neurotransmitters and physiological actions in the circuit between the brainstem core and the basal forebrain [13] have been investigated at the intracellular level after a series of extracellular studies [14]. Morphologically, it was reported that the majority of brainstem reticular core inputs to cholinergic cells in nucleus basalis (NB) of the basal forebrain appear to arise from neurons other than the mesopontine cholinergic ones as only <1% of cholinergic pedunculopontine and laterodorsal tegmental (PPT/LDT) neurons project to NB [15]. Even if direct PPT/LDT to NB cholinergic-to-cholinergic projections were to be thought, acetylcholine (ACh) elicits a muscarinic-mediated hyperpolarization of NB cells [16]. Among monoamine-containing cells, those of locus coeruleus that release norepinephrine exert depolarizing actions on NB cells [17]. (2) The other circuit consists of the excitatory projections from the upper brainstem reticular core to rostral intralaminar thalamic nuclei [18] that, in turn, have excitatory cortical projections [19] to large territories, including primary sensory areas. Indeed, stimulation of intralaminar thalamic nuclei potentiates visual cortex responses [1] and lesions of those nuclei reduce the MRF-induced facilitation to more than 50% of the control values [20].

The increased responsiveness in thalamic nuclei and cortical areas is at least as high during REM sleep as during wakefulness, both compared to EEG-synchronized sleep [21].

The field potentials have also been used to investigate, during waking and sleep states, the fluctuations in amplitudes of different components recorded across various cortical layers in monkeys and over the scalp in humans.

In monkey, the amplitude of the early surface positivity evoked in the primary somatosensory cortex by a cutaneous stimulation (P1, latency around 12 ms) varies solely as a function of stimulus intensity, whereas the amplitude of the surface negativity (N1) that peaks at a latency of 50 ms predicts the behavioral discrimination response [22]. Current–source–density analyses and multiunit activities showed that the excitatory events which characterize the monkey's N1 component during waking are replaced during EEG-synchronized sleep by a period of inhibition, with large current sources through layer III [23].

- [13] Jones *et al.* (1976); Hallanger *et al.* (1988); Semba *et al.* (1988).
- [14] Earlier extracellular data reported excitatory responses of cortical neurons to stimulation of peripallidal and basal forebrain areas (Edstrom and Phillis, 1980). Contradictory results have been obtained by investigating the action of muscarinic and nicotinic blockers, administered systemically, upon the brainstem-induced potentiation of electrically evoked field responses in the visual cortex (Bremer and Stoupe, 1959; Singer, 1979) since the action could have been exerted either at the thalamic LG level or at the cortical level (see note [20]).
- [15] Jones and Cuello (1989).
- [16] Khateb *et al.* (1997).
- [17] Fort *et al.* (1995). Contrary to the depolarizing effect on cholinergic neurons, norepinephrine hyperpolarizes and inhibits noncholinergic neurons in the basal forebrain (Fort *et al.*, 1998).
- [18] Steriade and Glenn (1982).
- [19] Endo *et al.* (1977).
- [20] Adams *et al.* (1988). Those experiments also attempted to dissociate the thalamic from the cortical level of action after administration of cholinergic blockers (see note [14]).
- [21] Steriade *et al.* (1969).
- [22] Kulics *et al.* (1977); Kulics (1982).
- [23] Cauller and Kulics (1988).

In humans, the early cortically generated components of the somatosensory field potentials are indented by multiple fast-frequency (40–50 Hz) potentials that are markedly attenuated or totally disappear when the subject is in stages II-to-IV of EEG-synchronized sleep; these fast potentials return to waking values in REM sleep [24]. These data, along with the similar morphology of the somatosensory evoked potentials (SEPs) in neonates during waking and REM sleep [25], are in line with the demonstrated similarity between waking and REM sleep as far as the electrophysiological processes of the thalamus and cerebral cortex are concerned.

[24] Emerson *et al.* (1988); Yamada *et al.* (1988).

[25] Desmedt *et al.* (1980).

8.1.3. Extracellular Recordings

In general, the results of studies using extracellular recordings of thalamic and cortical cells are congruent with those obtained by means of field potentials, discussed above.

The synaptic excitability of cortically projecting neurons recorded from relay and intralaminar thalamic nuclei, tested with central stimuli, is enhanced during both EEG-activated behavioral states of waking and REM sleep as well as during MRF stimulation [26]. The state-dependent transfer properties of TC neurons have been mainly studied in the LG nucleus by using different forms of visual stimulation. The transfer ratio of an LG cell was determined in “quasi-intracellular” recordings (that allowed estimations of ratios between actions potentials, as output, and “EPSPs,” as input) and was found to be twice as high during wakefulness compared to EEG-synchronized sleep [27]. During behavioral and EEG signs of wakefulness in the midpontine pre-trigeminal preparations, the oscillation of firing rate of thalamic LG neurons is the perfect replica of the sine-wave photic stimulation, whereas this relation disappears during EEG-synchronized sleep even with a 3-fold increase in the amplitude of the intensity of testing stimulation [28].

The potentiation of thalamic-cells’ excitability can be elicited by setting into motion two neuromodulatory systems: cholinergic [29] and norepinephrinergic-NE [30]. While the cholinergic excitation was reported in virtually all thalamic nuclei so far investigated, the facilitatory effects of locus coeruleus stimulation and NE application are more controversial. In cat’s LG cells, NE iontophoresis resulted in inhibitory effects in 91% of tested LG cells [31] and locus coeruleus stimulation inhibits the spontaneous firing and the evoked responses of thalamic VL neurons [32].

The increased probability of monosynaptic thalamic responses upon arousal or MRF stimulation is simultaneous

[26] Sakakura (1968); Steriade *et al.* (1977b); Glenn and Steriade (1982).

[27] Coenen and Vendrik (1972).

[28] Maffei *et al.* (1965a, b, c).

[29] The cholinergic nature of the effects induced by stimulating the upper brainstem reticular core was shown by Francesconi *et al.* (1988; see also intracellular data in Section 8.1.4).

[30] Stimulation of locus coeruleus increases the spontaneous firing as well as the responses of thalamic LG neurons to optic tract stimulation (Kayama *et al.*, 1982), a response mediated by alpha-1 adrenergic receptors (Rogawski and Aghajanian, 1982).

[31] Pape and Eysel (1988). Opposite, facilitatory effects were obtained *in vitro* by McCormick and Prince (1988).

[32] Rivner and Sutin (1981).

with a decreased probability of spike bursts appearing at a longer (5–12 ms) latency [33]. This change in response pattern is explained by the depolarization of TC neurons during arousal [34], a state during which the low-threshold burst response of TC cells is inactivated [35] (see also Chapter 5, Section 5.5.1).

As also observed with field potential recordings, the facilitation of synaptically evoked cortical discharges upon arousal or MRF stimulation is not merely a result of an enhanced output from TC neurons since the potentiation at cortical level may be observed even when no change is detected in recordings from TC axons just beneath the cortex [36] and when testing stimuli are applied to the radiation axons after destruction of the appropriate thalamic nuclei [37]. The circuits subserving this potentiation that bypasses thalamic relay neurons are discussed in Section 8.1.2.

8.1.4. Intracellular Studies

8.1.4.1. Excitatory Responses

Under barbiturate anesthesia, MRF stimulation facilitates the synaptic transmission of the specific afferent inflow through the LG thalamic nucleus, without, however, exerting direct depolarizing effects on LG cells [38]. At that time, the conclusion was that the brainstem-induced facilitation of synaptic transmission through the thalamus, hypothesized to be cholinergic in nature, is exclusively due to a global disinhibition of TC neurons, through the inhibition of both thalamic reticular and local-circuit inhibitory neurons [39]. It is now known that the excitatory effects of ACh on TC neurons are extremely sensitive to low doses of barbiturates (see Chapter 6, Section 6.1). On the other hand, brainstem reticular stimulation induces a direct and powerful excitation of reticular thalamic neurons in unanesthetized intact animals (see Section 8.2), probably mediated by glutamate release, and dendrites of local-circuit inhibitory neurons also seem to be excited by ACh application, as inferred from the analysis of short-term inhibitory processes in TC cells [40] (see intracellular data in Section 8.1.4.1). These data are hardly reconcilable with the hypothesis of global disinhibition of TC neurons upon brainstem reticular stimulation and arousal.

The effect of stimulating the brainstem cholinergic peribrachial (PB) area, which is part of the PPT nucleus or Ch5 group, on intracellularly recorded thalamic LG neurons in unanesthetized cats (brainstem-transected preparations with trigeminal deafferentation) provided evidence

- [33] Fillion *et al.* (1971); Steriade *et al.* (1971); MacLeod *et al.* (1984).
- [34] Curró Dossi *et al.* (1991); Steriade *et al.* (1991a, 1993a); Timofeev *et al.* (1996).
- [35] Steriade (2001c).

- [36] Gucer (1979).

- [37] Steriade and Morin (1981).

- [38] Singer (1973).

- [39] Singer (1977, 1979).

- [40] Sillito *et al.* (1983); Sillito (1987).

[41] Hu *et al.* (1989b).

for direct excitation of TC neurons from the brainstem reticular core [41]. The brainstem-induced excitation is direct, as it was also obtained in animals deprived of their retinal and visual cortex inputs. The coactivation of passing fibers issuing from the locus coeruleus or other monoaminergic cell-aggregates was avoided by pretreating the animals with reserpine (in fact, the brainstem–LG depolarization was enhanced after monoamine depletion; see Fig. 8.3).

Two types of responses are seen in TC neurons recorded from LG neurons after brainstem PB stimulation. (1) An early transient depolarization appears with a latency of 20–30 ms, has a duration of 150–300 ms, and is interrupted by a short-duration unitary inhibitory postsynaptic potential (IPSP) (Fig. 8.3). This response is the intracellular counterpart of the field pontogeniculoccipital (PGO) wave in the thalamus. (2) The occurrence of a longer-latency (1–2 s), long-lasting (2–5 s) depolarization usually requires more than a single PB stimulus [42] (Fig. 8.4). While the early depolarization is abolished by very low doses of barbiturate (as is the case with the effect of ACh application), the late depolarization can be elicited under barbiturate anesthesia.

[42] Steriade and Deschênes (1988).

The late depolarization depicted in Fig. 8.4. is quite labile. The constancy of the early depolarization interrupted by a unitary IPSP allowed a detailed investigation.

1. At rest (–60 mV), PB stimulation triggers a 5–8 mV depolarizing response, transiently interrupted by an IPSP, and giving rise to a few spike discharges (Fig. 8.5A). The same stimulation leads to long periods of tonic discharges when the membrane potential is kept slightly depolarized (Fig. 8.5B). This prolonged activation reflects a voltage-dependent inward current, probably the persistent Na^+ current ($I_{\text{Na(p)}}$) described in thalamic neurons (see Chapter 5, Section 5.5.1.4), since current pulse injections produce similar protracted firing when delivered on a background of slight depolarization (Fig. 8.5C).

2. The amplitude of the early depolarization and its rate of rise increase with membrane hyperpolarization, eventually triggering a low-threshold rebound spike when the membrane potential is sufficiently negative (Fig. 8.6A). The early depolarization is associated with a marked drop in input resistance in LG relay neurons (Fig. 8.6B). This conductance change is similar to that associated with the fast nicotinic excitation observed in TC neurons from other thalamic nuclei by stimulating another cholinergic neuronal aggregate at the mesopontine junction, the LDT nucleus, and the conductance change was abolished by the nicotinic antagonist

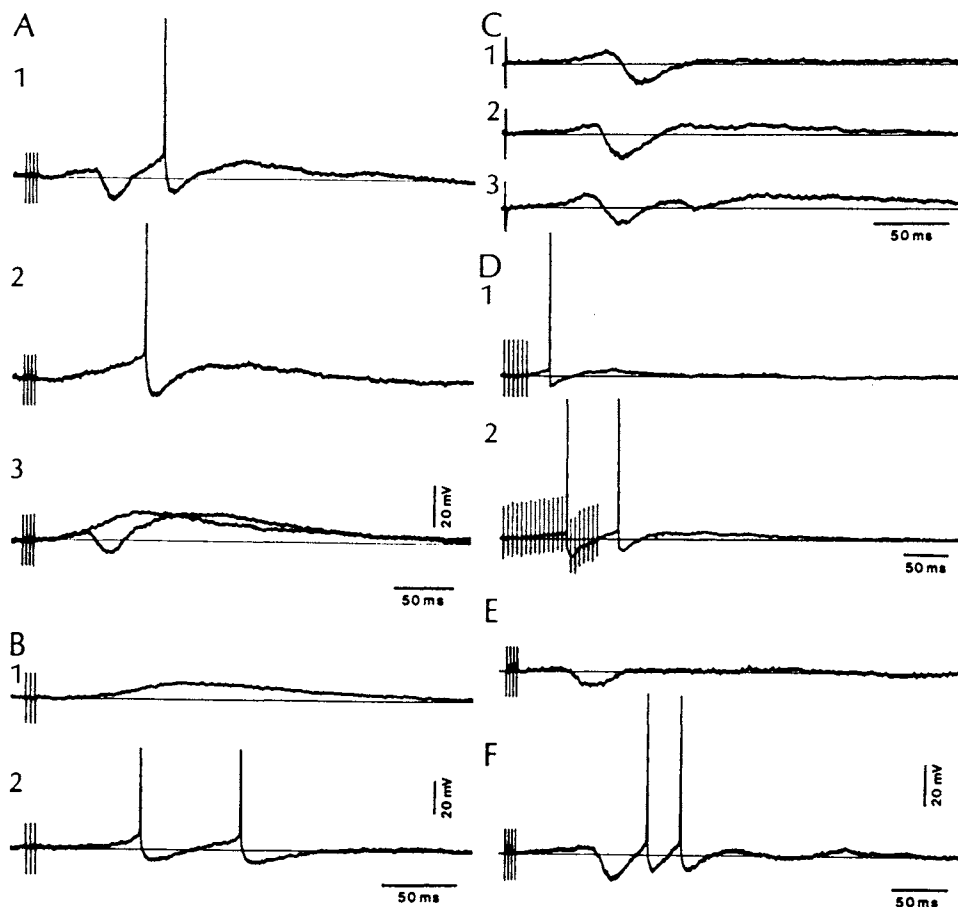


Figure 8.3. Responses to brainstem peribrachial (PB) stimulation in LG thalamic relay cells of cat. Intracellular recordings. A, typical response obtained under urethane anesthesia after reserpine treatment. In A3, the cell was slightly hyperpolarized to prevent spike discharges. Note the all-or-none character of the IPSP. Responses in B–C were recorded from two LG neurons in a reserpine-treated animal with bulbospinal transection and deafferentation of trigeminothalamic pain pathways. Note in C the occasional occurrence of a second IPSP and the shift in latency of the first IPSP. Responses in D were recorded in a deafferented cat without reserpine treatment. Note the smaller amplitude of the response even when a long stimulus train was used (D2). Traces E–F show the responses of two different cells recorded in the same animal under urethane anesthesia. Traces E–F were recorded respectively 30 min and 5 hr after reserpine administration. Voltage calibration in F applies also in C–D–E. From Hu *et al.* (1989b).

mecamylamine [43] (Fig. 8.7). The rapid nicotinic excitation of TC neurons is related to the transmission of brainstem-generated PGO potentials through TC systems. PGO waves appear during natural REM sleep or in reserpine-treated animals and are produced by several classes of bursting and tonic PPT/LDT neurons (see Chapter 10). Reserpine-induced PGO negative field potentials in the thalamic LG nucleus are associated with 5a short depolarizing response (0.2–0.3 s) of TC neurons [44].

[43] The increased membrane conductance during the early nicotinic depolarization ranges from 10% up to 50% in animals treated with reserpine to avoid costimulation of axons arising from locus coeruleus. The increased conductance is sometimes observed even in the absence of overt membrane depolarization

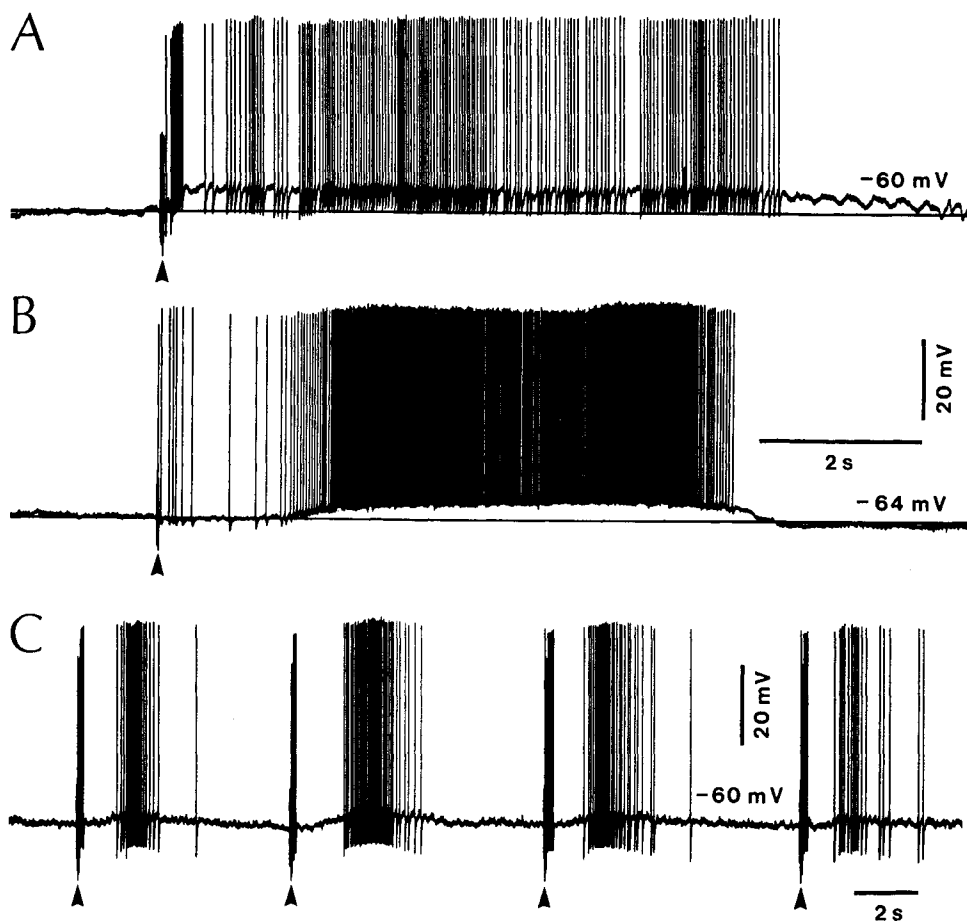


Figure 8.4. Direct excitation of thalamic LG relay neurons of cat by stimulating the brainstem PB area. Intracellular recordings in unanesthetized preparations, brainstem-transected (bulbospinal cut) with deafferentation of trigeminothalamic pathways. A and B, a few stimuli to the PB area (arrowheads) elicited a short-latency excitation, followed by a long-latency (1–1.5 s) and prolonged (1.5–2.5 s) excitation. C, a series of successive PB-evoked responses (early and late excitations) at a lower speed. Modified from Steriade and Deschênes (1988).

and is reflected by the decreased amplitude of the voltage deflection to a hyperpolarizing current pulse and by reduction of the rebound LTS (Carró Dossi *et al.*, 1991). These results obtained by stimulating synaptic brainstem–thalamic pathways *in vivo* are similar to the effects elicited by applying ACh *in vitro* (McCormick and Prince, 1987a, b). [44] Hu *et al.* (1989c).

3. The early excitatory response is interrupted by an IPSP with a shorter duration (50–60 ms), as illustrated in Fig. 8.3. The IPSP that interrupts the early depolarization is a Cl^- -mediated event, and the reversed response by Cl^- injection is made by a series of depolarizing wavelets, suggesting that a bursting element is at the origin of the IPSP [41]. Since in these acute experimental conditions, the brainstem-evoked early depolarization (which is not cholinergic) in GABAergic perigeniculate (PG) (RE) neurons does not usually lead to spike discharges (see below, Section 8.2), it was postulated that the short-duration IPSP evoked in LG relay cells by PB stimulation originates in GABAergic intra-LG inhibitory elements, activated in

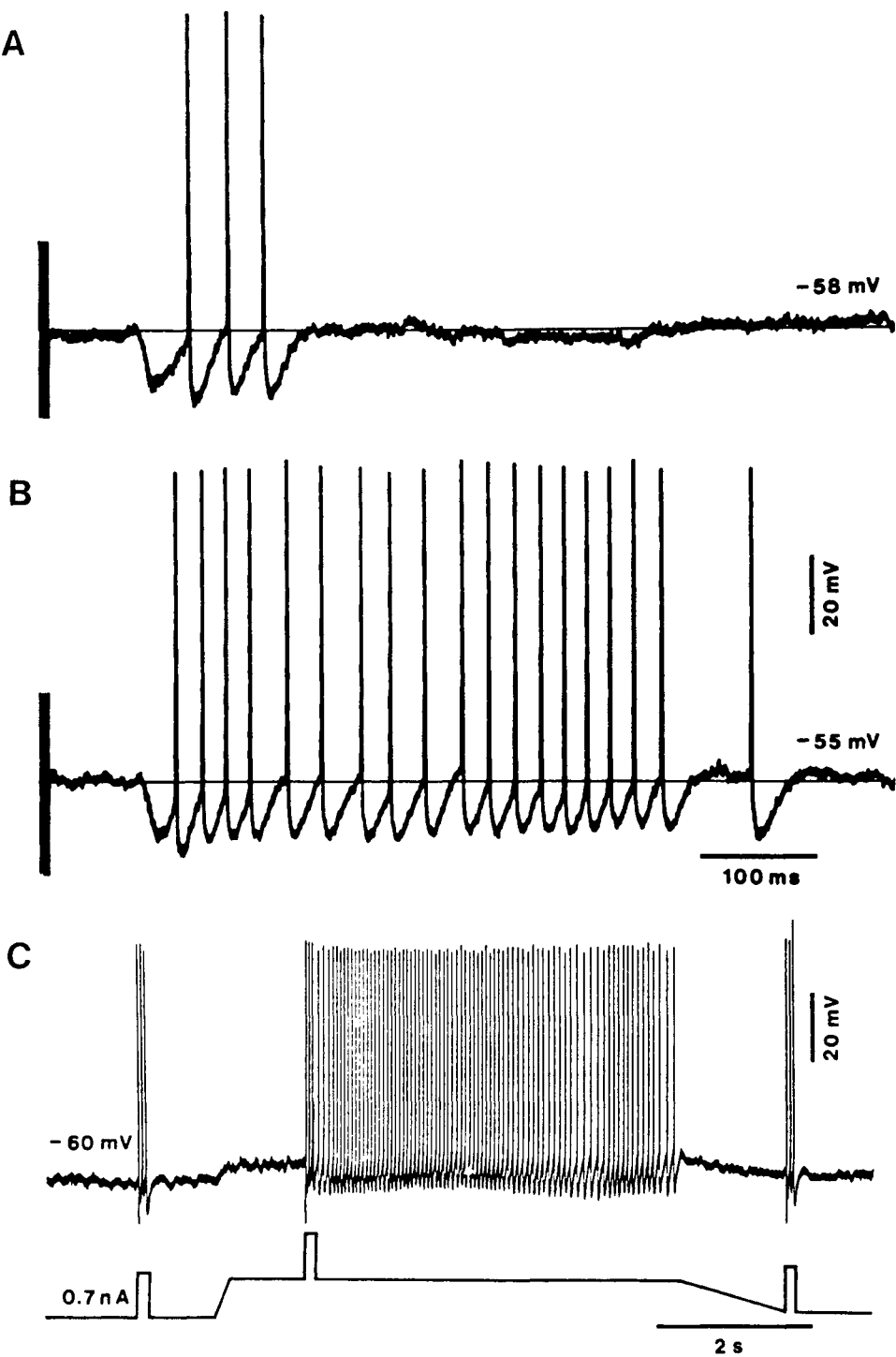


Figure 8.5. Effect of subthreshold depolarizing currents on brainstem PB-evoked responses of LG thalamic neurons of cat. Same neuron from A to C, recorded in a nonreserpinized animal under urethane anesthesia. The control response in A was transformed into a longer duration tonic barrage (B) by a subthreshold outward current of 0.4 nA. Tonic discharges appear to result from the activation of a persistent inward current since they could also be generated by short-duration current pulses when the membrane potential was set just below the spike trigger level (in C). From Hu *et al.* (1989b).

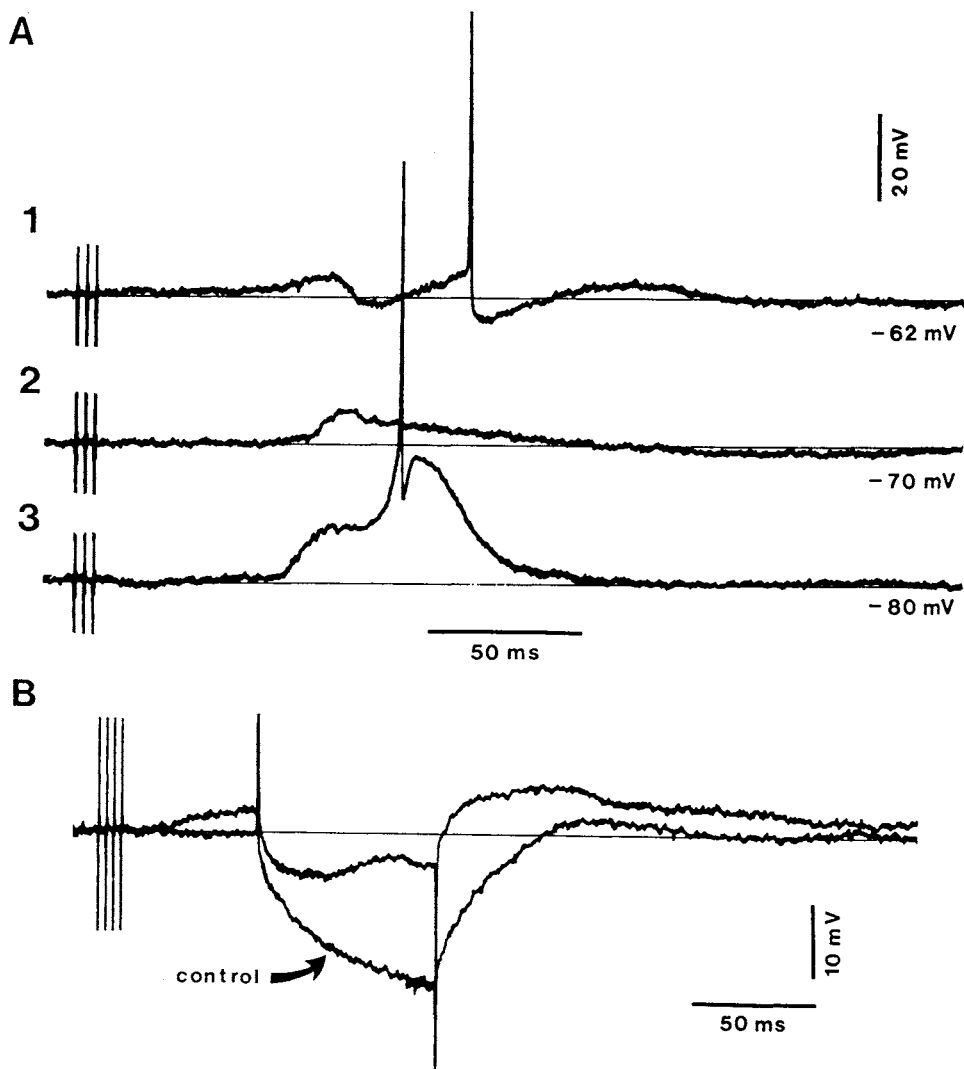


Figure 8.6. Brainstem PB-evoked response in intracellularly recorded LG thalamic neurons of reserpine-treated cat under urethane anesthesia. A, effect of membrane hyperpolarization. At rest, the response consisted of a slow depolarization interrupted by an IPSP that was followed by a single spike discharge. Upon hyperpolarization, the depolarizing component increased, the IPSP amplitude decreased, and a delayed low-threshold response was triggered after the IPSP occurrence. B, increase in membrane conductance during the PB-evoked response in another LG cell. Modified from Hu *et al.* (1989b).

parallel by the cholinergic brainstem–LG projection. The conclusion is that a nicotinic excitation underlies the early response of TC neurons from LG nucleus to brainstem PB stimulation and that a parallel activation affects at least one category of LG local-circuit interneurons (see Section 8.2). It must be emphasized, however, that other transmitters or modulators are colocalized in cholinergic brainstem reticular neurons (see Chapter 3, Section 3.1.1.1) and that the identification of the role played in concert by

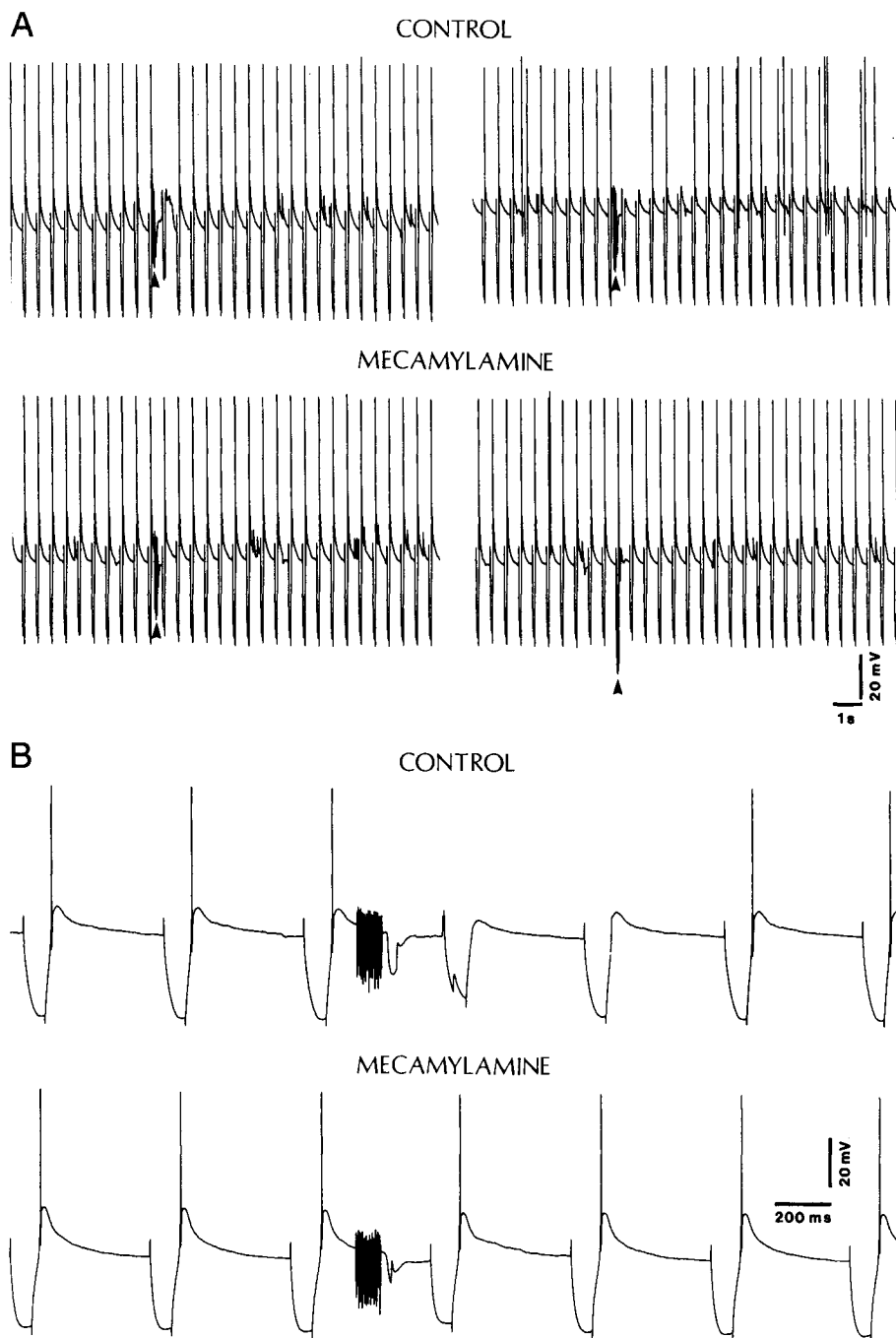


Figure 8.7. Blockage of increased conductance induced by stimulation of laterodorsal tegmental nucleus (LDT) by nicotinic antagonist mecamylamine. Cat under urethane anesthesia, after reserpine treatment. Intracellular recording from anterior thalamic (AT) neuron. LDT stimulation with pulse-train (30 stimuli) at 300 Hz. AT neuron recorded before and after intravenous administration of mecamylamine (30 $\mu\text{g}/\text{kg}$). Membrane input resistance tested by injecting hyperpolarizing current pulses. A, four different trials are depicted, before (top) and after (bottom) mecamylamine administration. B, expanded traces to show in more detail the LDT-induced increased conductance and its blockage by mecamylamine. Membrane potential, -64 mV. From Curró Dossi *et al.* (1991).

all these substances in synaptic transmission through the thalamus is still difficult to assess.

4. Following the early nicotinic excitation, stimulation of brainstem cholinergic (PPT/LDT) nuclei (or PB area) elicits in TC neurons a prolonged depolarization, with a latency of about 1 s, a peak amplitude of 5–14 mV, and the shortest duration of 1.5–2 s but up to 15–20 s [45]. The long duration requires the feedback excitatory projections from the cerebral cortex as the duration of this depolarizing phase is reduced in decorticated animals. The prolonged depolarization is dissociated from the short-lasting nicotinic response by contrasting changes in membrane conductance, differential sensitivity to changes in membrane potential, and blockage by muscarinic antagonists. Thus, the long-lasting depolarization is associated with a 30–40% increase in the apparent input resistance, that is visible about 2 s after the diminished input resistance during the nicotinic response (Fig. 8.8). The depression or disappearance of the muscarinic depolarization during membrane hyperpolarization stands in contrast with the absence of such alterations in the earlier (nicotinic) depolarizing response. The voltage-dependency of the prolonged muscarinic depolarization in TC neurons explains why application of cholinergic agonists induces clear-cut facilitatory influences on TC neurons only during waking and REM sleep [46], two behavioral states that are similarly associated with sustained membrane depolarization in TC cells [47], due to equally increased firing rates of brainstem cholinergic PPT/LDT neurons [48] and equally increased ACh release in the dorsal thalamus [49] (see also Chapter 9). Setting into action brainstem cholinergic projections leads to depolarization and firing of TC neurons, and consequently to activation of cortical electrical rhythms.

The prolonged muscarinic depolarization and increase in input resistance are major factors in switching the functional state of TC neurons, from high-frequency rhythmic spike bursts and depressed responsiveness during NREM sleep to single-spike firing associated with increased antidromic and synaptic excitability during brainstem-induced arousal [50] (Fig. 8.9) as well as during behavioral states of waking and REM sleep [6]. These cholinergic effects also underlie long-lasting potentiation of synaptic responses to mammillary nucleus (MN) stimulation in anterior thalamic (AT) neurons, which may be involved in mnemonic processes [51]. This potentiation is associated with an increase in input resistance that allows synaptic events of small amplitude to depolarize patches of the dendritic membrane so that to trigger fast prepotentials and,

[45] Under reserpine treatment, the duration of the late (muscarinic), long-lasting depolarization is prolonged to 40–60 s (see [42]). The late and very prolonged excitation in LG relay cells depicted in Fig. 8.4. may well be due to the action of peptides that are found in brainstem cholinergic neurons (Vincent *et al.*, 1983, 1986).

[46] Marks and Roffwarg (1987).

[47] Hirsch *et al.* (1983).

[48] Steriade *et al.* (1990a).

[49] Williams *et al.* (1994).

[50] Timofeev *et al.* (1996).

[51] Paré and Steriade (1990); Paré *et al.* (1990b).

The anterior nuclear group of cat thalamus was chosen to investigate the long-term activation process induced by brainstem cholinergic stimulation because it is devoid of inputs from the thalamic reticular complex (Steriade *et al.*, 1984a; Velayos *et al.*, 1989) and, thus, the prolonged potentiation (up to 4 min) is not attributable to disinhibition through the cholinergic inhibition of GABAergic thalamic reticular cells.

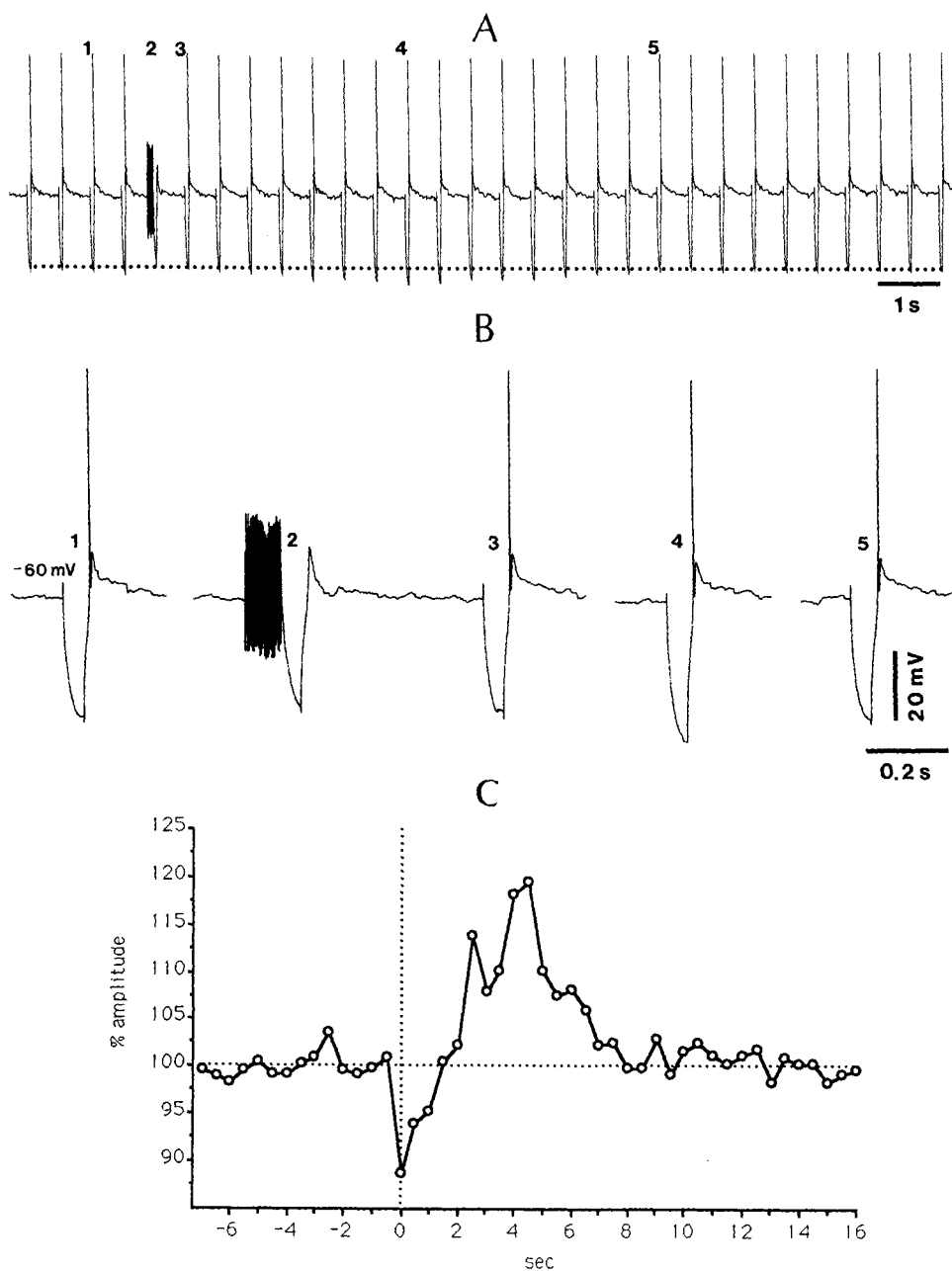


Figure 8.8. Biphasic effect (increase and decrease) on membrane conductance evoked in thalamic intralaminar centrolateral (CL) neuron by brainstem LDT cholinergic nucleus in cat under urethane anesthesia. LDT stimulation consisted of a pulse-train (30 stimuli) at 300 Hz. Different parts of panel A are expanded in B. Part 1 is before the LDT pulse-train; 2-3 depict the increased conductance shortly after LDT stimulation; 4 is taken from the period with increased input resistance; and 5 is back to the control value. C, histogram of the LDT-induced conductance changes in the same neuron. Ordinate: percent voltage pulse amplitudes as compared with the averaged values (horizontal dotted line) in the control condition, before application of LDT stimulation. Abscissa: elapsed time with respect to LDT stimulation. Modified from Curró Dossi *et al.* (1991).

[52] The monkey model of severe amnesia consists of mammillary nuclei and midline/medial thalamic lesions (Aggleton and Mishkin, 1983a,b; Bentivoglio *et al.*, 1997).

[53] See Squire and Alvarez (1995).

[54] This statement is based, among many other data, on the following evidence showing that thalamic (1) LG neurons exhibit far greater reduction in response to stimuli including the field surround than do retinal ganglion cells or optic tract axons (Hubel and Wiesel, 1961) and larger coefficient of variation than retinal cells, with little variability added at the cortical level (Hartveit and Heggelund, 1994); and (2) ventroposterior (VP) thalamic neurons have receptive fields that are different from those of neurons in brainstem relay stations and dynamic responses demonstrating that they are not simple relays for somatosensory signals (Alloway *et al.*, 1994; Nicolelis and Chapin, 1994).

[55] Hicks *et al.* (1986); Salt (1989). Selective lesions of thalamic reticular GABAergic neurons increase the receptive field size of VP neurons by ~3-fold (Lee *et al.*, 1994).

[56] Jones (1985); Steriade *et al.* (1997a).

[57] Liu *et al.* (1995).

[58] Steriade *et al.* (1985). We showed that, after thalamic transections separating the thalamic reticular nucleus from the remaining thalamus or after excitotoxic lesions of reticular neurons, there was an increased number of GABA_A-receptor-mediated IPSPs in TC neurons, as if local-circuit inhibitory neurons were released from the inhibition arising

eventually, somatic action potentials. These data, showing that prolonged facilitation of responsiveness occurs in AT neurons that relay signals from mammillary nuclei (a major output structure of the hippocampus) toward various fields of the cingulate cortex, may be related to data showing that medial thalamic lesions lead to cognitive impairments in primates [52]. The results indicating a prolonged potentiation of neuronal responsiveness in AT nuclei after brief pulse-trains to mesopontine nuclei suggest that the cholinergic system regulates the flow of information along the mammillothalamic axis and modify the strength of the functional relationship between the hippocampal formation and cortical memory storage sites [53].

8.1.4.2. Differential Brainstem Reticular Effects on Three Phases of Inhibitory Responses

In contrast to the old view considering TC neurons as merely synaptic relays for incoming signals in their route to the cerebral cortex, accumulating evidence indicate that these neurons display integrative properties and higher selectivity compared to those recorded from their input sources [54]. These data indicate the importance of inhibitory processes in discriminative responses of TC neurons. The importance of thalamic inhibitory mechanisms was shown by an increase in the receptive field size after inactivation of GABA_A receptors [55].

Two types of thalamic GABAergic neurons may account for the response selectivity of TC neurons: local-circuit neurons, whose actions are confined within the limits of different dorsal thalamic nuclei, and neurons of the reticular nucleus (see Chapter 4, Section 4.1). Local-circuit neurons are involved in stimulus-specific inhibitory responses, while reticular neurons also contribute to more widespread inhibitory effects implicated in long-range thalamic oscillations. It is important to note that most *in vitro* studies are conducted in rodents that, with the exception of LG nucleus, do not possess local GABAergic cells in dorsal thalamic nuclei, whereas in carnivores and primates there are significant numbers (~25%) of local inhibitory interneurons in all dorsal thalamic nuclei [56]. This peculiarity may explain some differences between *in vivo* investigators (working on cats or monkeys) and *in vitro* investigators (who use rodents as experimental animals) concerning their conceptual views on thalamic inhibitory processes. Besides, a given proportion of thalamic reticular neurons project to local inhibitory neurons [57], thus possibly leading to disinhibitory effects on TC neurons [58].

Within thalamic glomeruli, the dendritic appendages of local inhibitory neurons are equipped with presynaptic

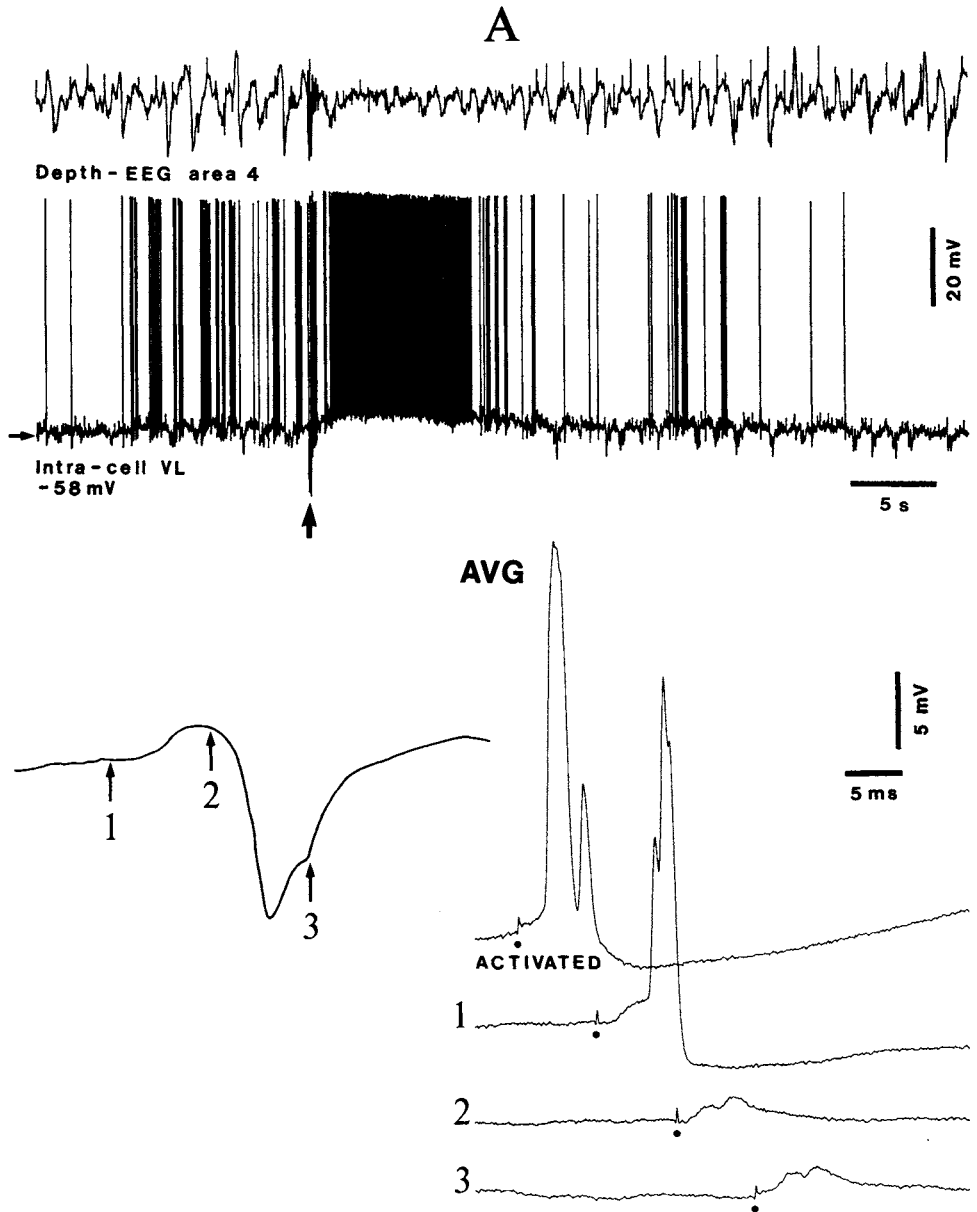


Figure 8.9. Responsiveness of TC neuron from ventrolateral (VL) nucleus during slow oscillation and during activation elicited by stimulation of mesopontine cholinergic PPT nucleus. Intracellular recording in cat at under ketamine–xylazine anesthesia. Activation was elicited by brief PPT pulse-train (0.3 s, 300 Hz; arrow). Stimuli to axons of brachium conjunctivum (BC) were applied every 1 s, before and after PPT stimulation. Note PPT-evoked EEG activation and VL-cell depolarization, lasting for more than 10 s. Below are illustrated averaged ($n = 10$) BC-evoked EPSPs (shortest latency 1.4 ms), as a function of their occurrence prior to the long-lasting depth-positive EEG wave of the slow oscillation (1), during that wave (2), after it (3), and during the PPT-elicited activated epoch. From Timofeev *et al.* (1996).

in reticular neurons. See also Fig. 4.4 in Chapter 4, depicting the circuitry of reticular, local-circuit, and TC neurons.

[59] Jones and Powell (1969); Ralston (1971); Ohara and Lieberman (1993).

[60] Paré *et al.* (1991).

[61] Hirsch and Burnod (1987); Crunelli *et al.* (1988).

[62] Curró Dossi *et al.* (1992b).

vesicles and they contact the dendrites of TC cells with symmetrical synaptic profiles [59]. The intraglomerular circuitry may be implicated in the discrete localization of inhibition. With GABAergic contacts are confined to the region of dendritic protrusions, the depolarization caused in relay cells by specific afferents is shunted, without however reducing electrical activity in the rest of the cell. The role of presynaptic dendrites in inhibitory processes has been determined by analyzing, with somatic impalements, the responses of AT neurons to activation of corticothalamic axons, that do not have access to the presynaptic dendritic terminals, and the responses to activation of mamillothalamic axons that end in the glomeruli [60]. This study revealed the presence of an early, short-lasting, Cl^- -dependent IPSP (termed the α -IPSP), selectively elicited by mamillary stimulation and distinct from the following biphasic ($\text{GABA}_{\text{A-B}}$) sequence of IPSPs (Fig. 8.10). The latter have been described in earlier studies [61]. The initial α -IPSP can be involved in the enhancement of center-surround antagonism and high-fidelity transfer of information during the waking and attentive states since stimulation of brainstem cholinergic cells results in the reduction or suppression of the long-lasting GABA_{A} and GABA_{B} IPSPs (Fig. 8.11), but the preservation or even enhancement of the initial GABA_{A} IPSP [62] (Fig. 8.12).

8.2. Thalamic Reticular Neurons: Dual Types of Responses

High-frequency stimulation of rostral brainstem reticular formation in acutely prepared animals under different anesthetics depresses the spontaneous firing and evoked discharges of reticular neurons [63]. The brainstem-induced blockade of RE-cells' activities was interpreted as a cholinergic effect, as ACh application results in a powerful hyperpolarization of reticular cells (see Chapter 6, Section 6.1.3.2). However, large application of atropine is ineffective against the early phase of the brainstem-induced inhibition of reticular neurons, and weakly antagonizes only a late phase of inhibition [64].

In unanesthetized behaving animals recorded in chronic experiments, brainstem reticular stimulation was applied in the rostral midbrain or in the PB area of the PPT nucleus after chronic bilateral lesions of locus coeruleus to allow anterograde degeneration of axons passing through the stimulated focus [65]. In those conditions, brainstem reticular stimulation induces a short-latency (5–10 ms) excitation, followed by a longer period of

[63] Schlag and Waszak (1971); Yingling and Skinner (1975, 1977).

[64] Dingledine and Kelly (1977).

[65] Steriade *et al.* (1986).

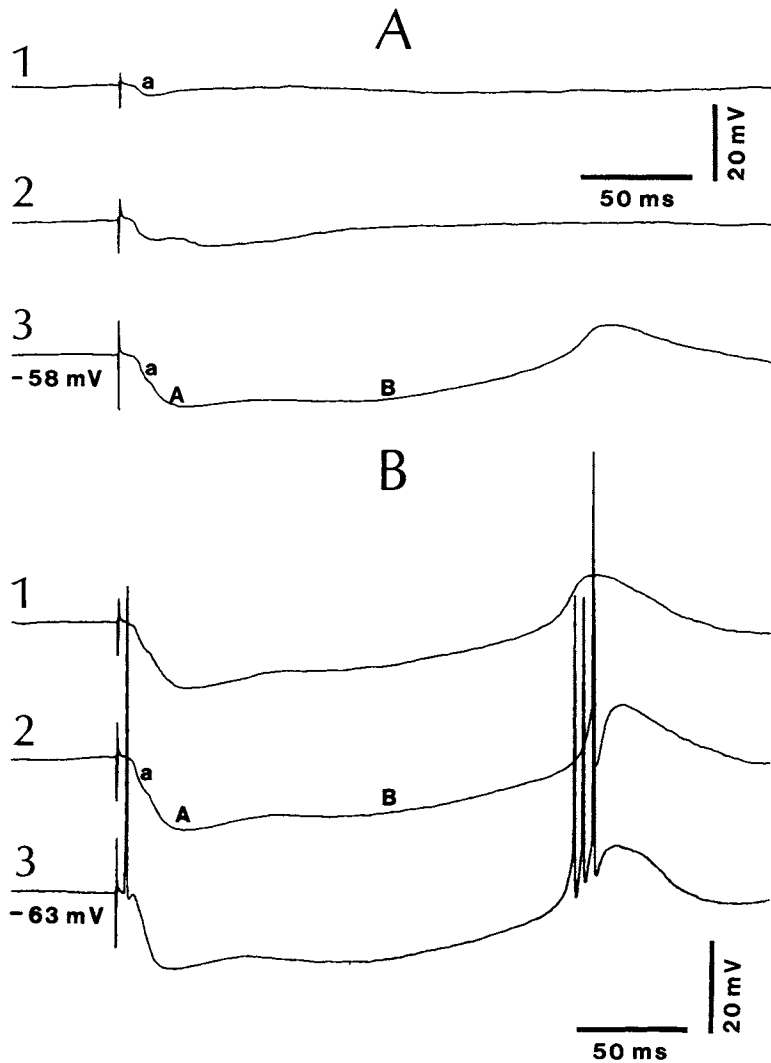


Figure 8.10. Triphasic IPSPs elicited by local interneurons in anterior thalamic (AT) neurons of cat, a species that is devoid of afferents from thalamic reticular (RE) neurons. Intracellular recordings under urethane anesthesia. A–B, two different AT neurons. Triphasic IPSPs evoked by mammillary nucleus (MN) stimuli. Increasing intensities of stimulation (from top to bottom traces). Components *a*, A, and B of IPSPs are described in text. With the higher intensities, the long-lasting IPSPs led to a low-threshold spike crowned by high-frequency fast action potentials. Membrane potential is indicated. Modified from Curró Dossi *et al.* (1992b).

suppressed firing, in neurons recorded from the rostral pole and rostromedial districts of the reticular nuclear complex. Both components of the response are state-dependent (Fig. 8.13). During wakefulness, the latencies of short spike bursts in reticular neurons are grouped between 5 and 10 ms, with modes around 6 ms; a secondary excitation occurs between 50 and 150 ms. During EEG-synchronized sleep, the latency mode of the early excitation lengthens to 15–20 ms and the duration of the evoked burst increases, reaching 50 ms. The histograms in

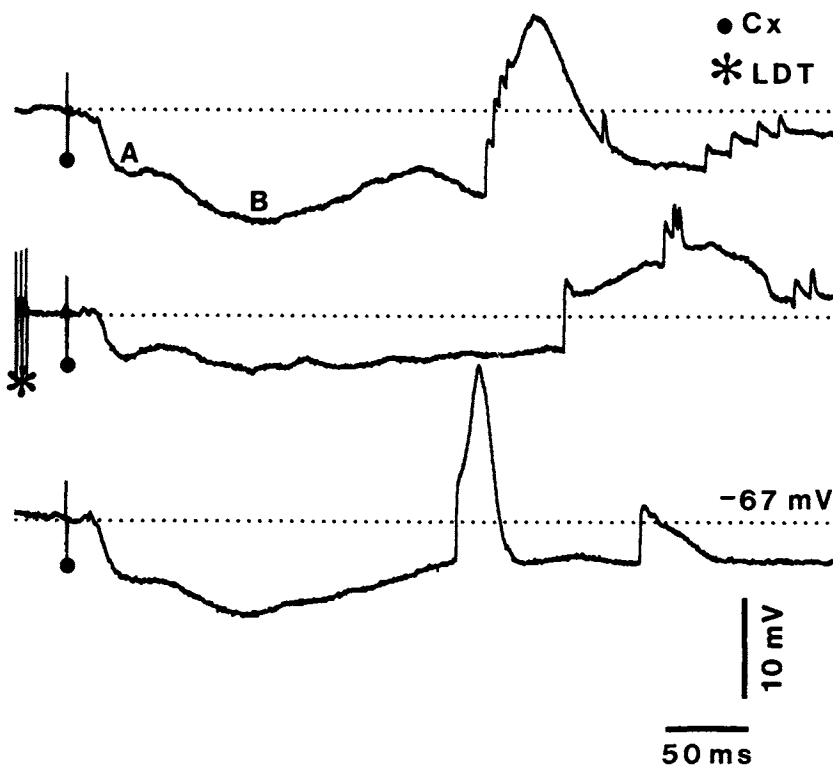


Figure 8.11. Depressant effect of a short pulse-train (350 Hz) to the laterodorsal tegmental (LDT) cholinergic nucleus on cortically (Cx) evoked, biphasic (A–B) IPSP. From Curró Dossi *et al.* (1992b).

Fig. 8.13 suggest that the underlying EPSPs are much faster-rising and shorter-lasting during waking than during EEG-synchronized sleep. As to the period of suppressed neuronal firing, it is much longer during NREM sleep than during wakefulness. The initially excitatory effects of brainstem reticular stimulation upon reticular neurons are consistent with the tonically increased firing rates of the same neurons upon arousal from quiet sleep (Fig. 8.14) [65].

The two, excitatory and inhibitory, components of the reticular-cells' response to brainstem reticular PB stimulation were further substantiated in intracellular recordings from the rostral pole and the PG sectors of the reticular nucleus [66].

[66] Hu *et al.* (1989a).

1. The depolarizing response started at a latency of 8–10 ms, lasted up to 200 ms, and was followed by a long-lasting hyperpolarization (Fig. 8.15). The early brainstem-evoked depolarization can be considered as a direct excitatory effect on rostral reticular (or PG) neurons. The following experimental precautions were taken to preclude that the early depolarization was due to costimulation of noradrenergic fibers coursing through the

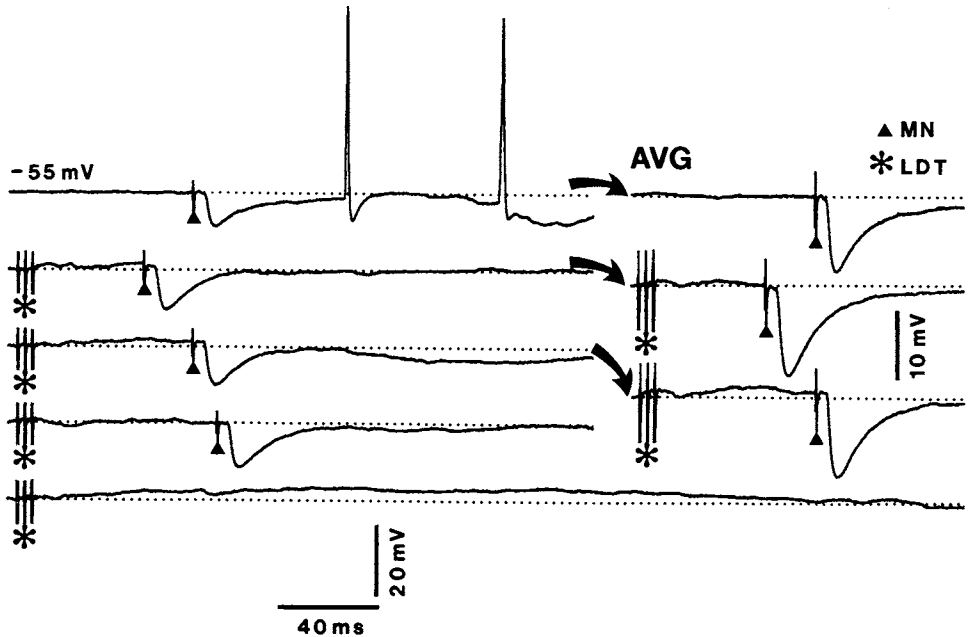


Figure 8.12. Effect of stimulation of laterodorsal tegmental (LDT) stimulation on isolated α -IPSP evoked by mammillary nucleus (MN) stimulation. Cat under urethane anesthesia (with ablation of the cingulate gyrus). Left, the three traces depict (from top to bottom) MN-evoked control responses; LDT + MN stimulation at different delays; and LDT stimulation alone. Right, averages (AVG) of five responses to MN and LDT + MN as indicated by curved arrows. From Curró Dossi *et al.* (1992b).

brainstem stimulated focus, that it was transmitted by prior excitation of LG relay cells or other TC cells, or that it was relayed by corticofugal pathways projecting to various sectors of the reticular nuclear complex. Experiments were conducted on reserpine-treated animals, with cortical ablation, and the direct depolarization of rostral reticular (or PG cells) was also obtained under barbiturate anesthesia (see Fig. 8.15, B–C), a condition that is known to block the brainstem-induced excitation of thalamic relay neurons (see Chapter 6, Section 6.1.3.1). Besides, the latency of brainstem-PG depolarizing response was shorter (8–10 ms) than that (>20 ms) of the brainstem-LG excitation.

2. As to the hyperpolarizing response, its amplitude decreased with inward injections or when the cell hyperpolarized spontaneously (Fig. 8.15C), and it was associated with a conductance increase of the order of 40–50% [66]. The cholinergic nature of this component was demonstrated by its abolition after scopolamine administration, a condition that prolonged the early depolarization and led to repetitive discharges (Fig. 8.16).

The above results [65, 66] indicate that brainstem reticular stimulation induces a dual response in thalamic

[67] Ahlsén (1984).

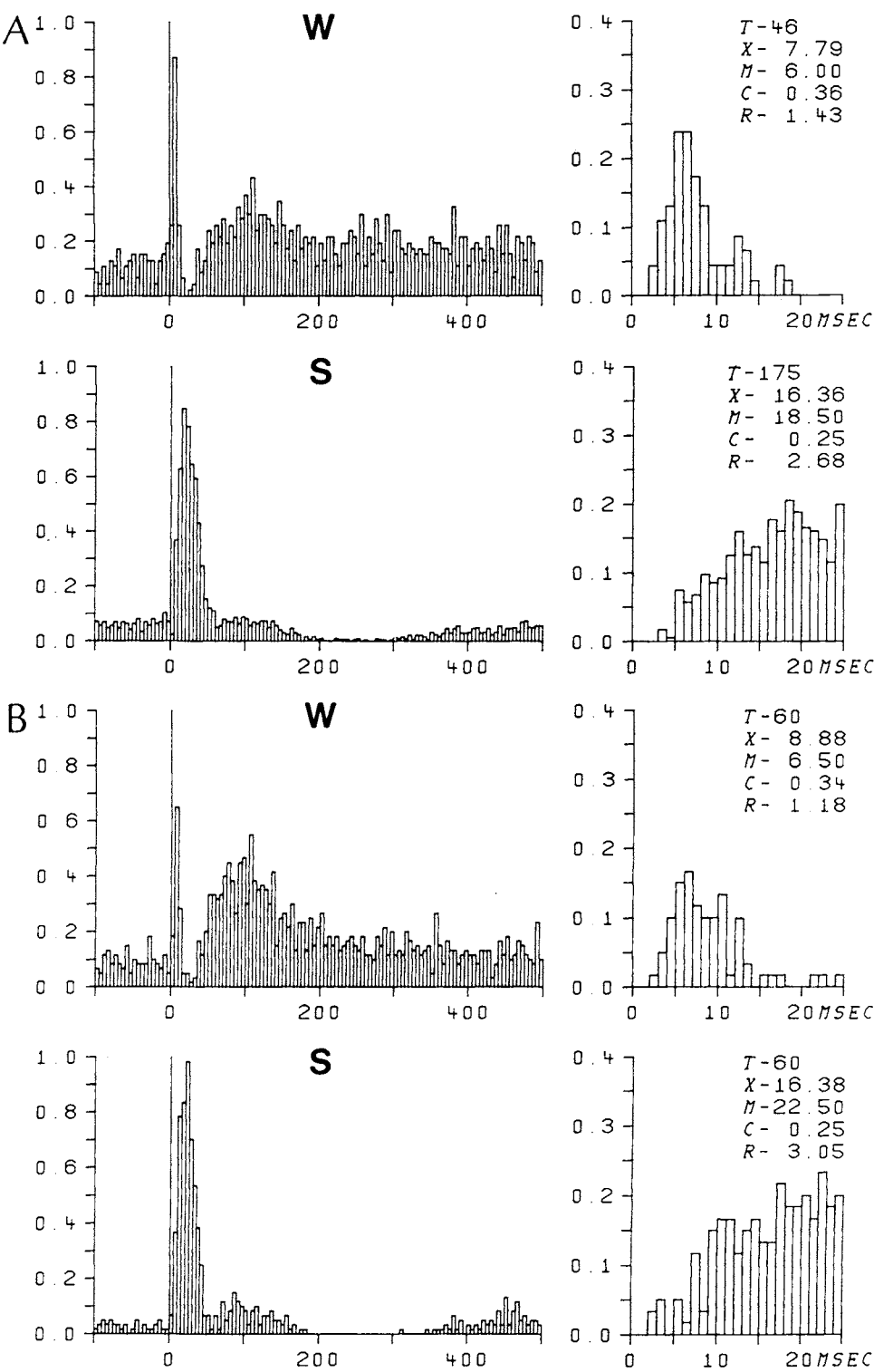
rostral reticular (or PG) neurons. Both excitatory and inhibitory components of the response sequence are dependent upon the behavioral state (see Fig. 8.13) and both are direct. This is shown for the excitatory component by its latency (8–10 ms) that fits with the slow conduction velocities of PB–PG axons [67]. The hyperpolarization is also direct and starts almost simultaneously with the depolarization. This is indicated by PB-induced depression of PG-cells' burst discharges evoked by optic tract stimulation, even when the optic tract stimulus is delivered during the PB-evoked early depolarization (Fig. 8.17). This result strongly suggests that the mechanism of PB-induced cholinergic inhibition in PG or other reticular thalamic neurons involves a large drop in membrane input resistance that renders those neurons transparent to synaptic currents and may also short-circuit intrinsic inward currents.

While the hyperpolarization depends on muscarinic receptors, as it is abolished by scopolamine, the nature of the early excitation remains to be elucidated. It may be induced by an unknown transmitter colocalized in brainstem cholinergic cells, such as glutamate, or it may be mediated by a nicotinic receptor [68].

[68] The failure to observe a nicotinic response in reticular neurons maintained *in vitro* (McCormick and Prince, 1986a) could well be attributed to the mode of ACh application leading to a rapid desensitization of the response. Nicotinic receptors have been mapped within the reticular thalamic nucleus of monkeys (Jones, 1985) and rats (Clarke *et al.*, 1985). The suggestion that the early excitation in reticular neurons is produced by nicotinic receptors (Hu *et al.*, 1989a) was subsequently confirmed in work done in thalamic slices (Lee and McCormick, 1995).

The difference between the two types of experiments, one conducted in behaving animals [65], the other under acute experimental conditions with anesthetics or with brainstem transection and trigeminal deafferentation [66], is that in the latter studies the brainstem-induced early depolarization does not induce tonic firing in reticular thalamic neurons. Most likely, this is ascribable to the difference in the level of membrane polarization between an anesthetized/deafferented preparation and an intact unanesthetized animal. The dramatic increase in tonic discharges of reticular neurons upon arousal from sleep (see Fig. 8.14) are due to the depolarizing pressure exerted by TC neurons projecting to reticular neurons and cortico-reticular neurons that discharge tonically in an intact vigil animal and, thus, create favorable conditions for overwhelming the concomitant inhibition arising in the cholinergic neurons of the brainstem core. These conditions result in an increased spontaneous and evoked firing of reticular cells, as is the case during natural awakening [65].

Until the discovery that brainstem reticular neurons with ascending axons directly excite reticular thalamic neurons, only the second part of the dual brainstem-reticular response (namely, the long-lasting hyperpolarization of reticular neurons) was taken into consideration. The brainstem-induced cholinergic inhibitory effect upon GABAergic reticular neurons was commonly regarded as the basis of generalized disinhibition of TC neurons upon arousal. Such an interpretation obviously reflects only one aspect of



the more complex reality. Indeed, since GABAergic reticular neurons discharge quite rapidly and are highly responsive to brainstem and cortical volleys during waking [65], the parallel increase in spontaneous firing rates and synaptic excitability of both reticular neurons and their inhibited targets, the TC neurons, raises difficult questions that

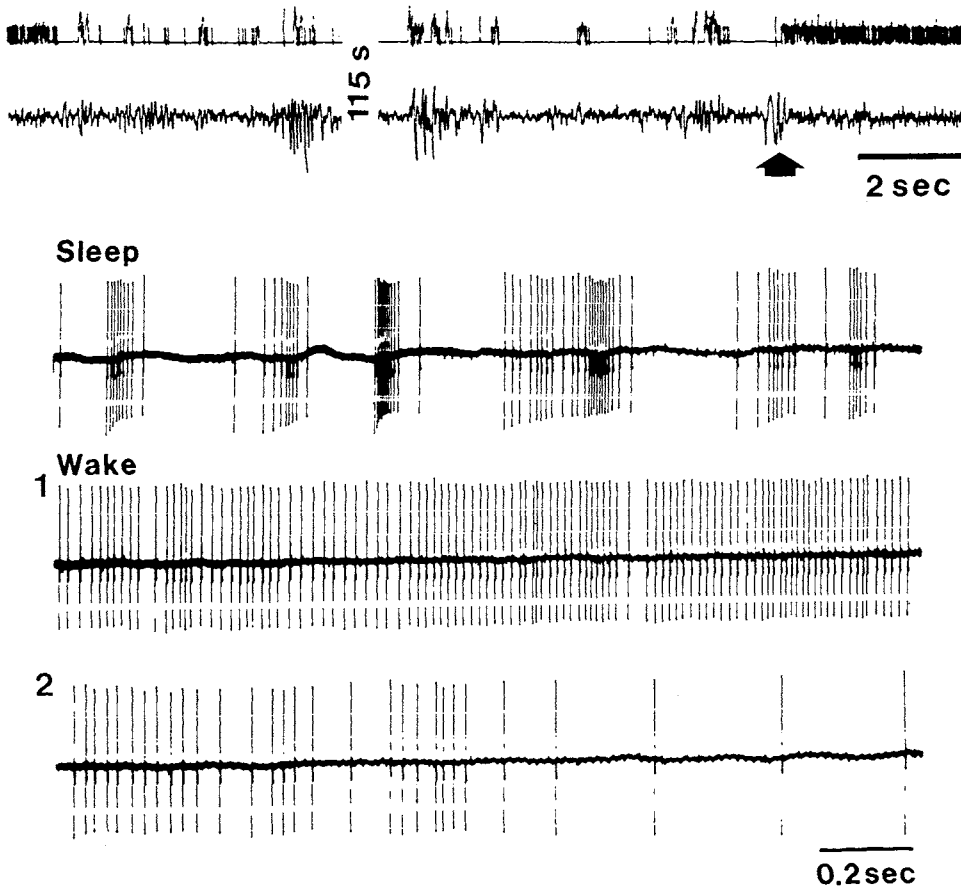


Figure 8.14. Increased firing rates of thalamic reticular neurons upon natural arousal in chronically implanted cat. Top: ink-written recording (unit firing and EEG waves; arrow points to arousal). Below, oscilloscopic recordings display typical RE-cell's barrages during EEG-synchronized sleep and tonic firing at onset of awakening (1) and toward the end of waking state, just before the appearance of EEG-synchronization (2). Modified from Steriade *et al.* (1986).

Figure 8.13. Short-latency excitation followed by firing suppression, elicited by brainstem peribrachial (PB) stimulation in rostral thalamic reticular neurons of cat, after chronic bilateral lesions of locus coeruleus. See histology of locus coeruleus lesions in Steriade *et al.* (1986). Extracellular recordings in chronically implanted, behaving preparation. In both (A and B) neurons, two 3-ms-delayed stimuli were applied at time 0 (stimuli artifacts deleted from peristimulus histograms, PSHs). For both neurons, 2 PSHs are depicted in behavioral states of waking (W) and EEG-synchronized sleep (S): left PSH with 5-ms bins, right PSH with 1-ms bins. Symbols: T , number of trials; X , mean latency (in ms); M , latency mode; C , coefficient of variation; R , sum of all bin responsiveness. Description in main text. From Steriade *et al.* (1986).

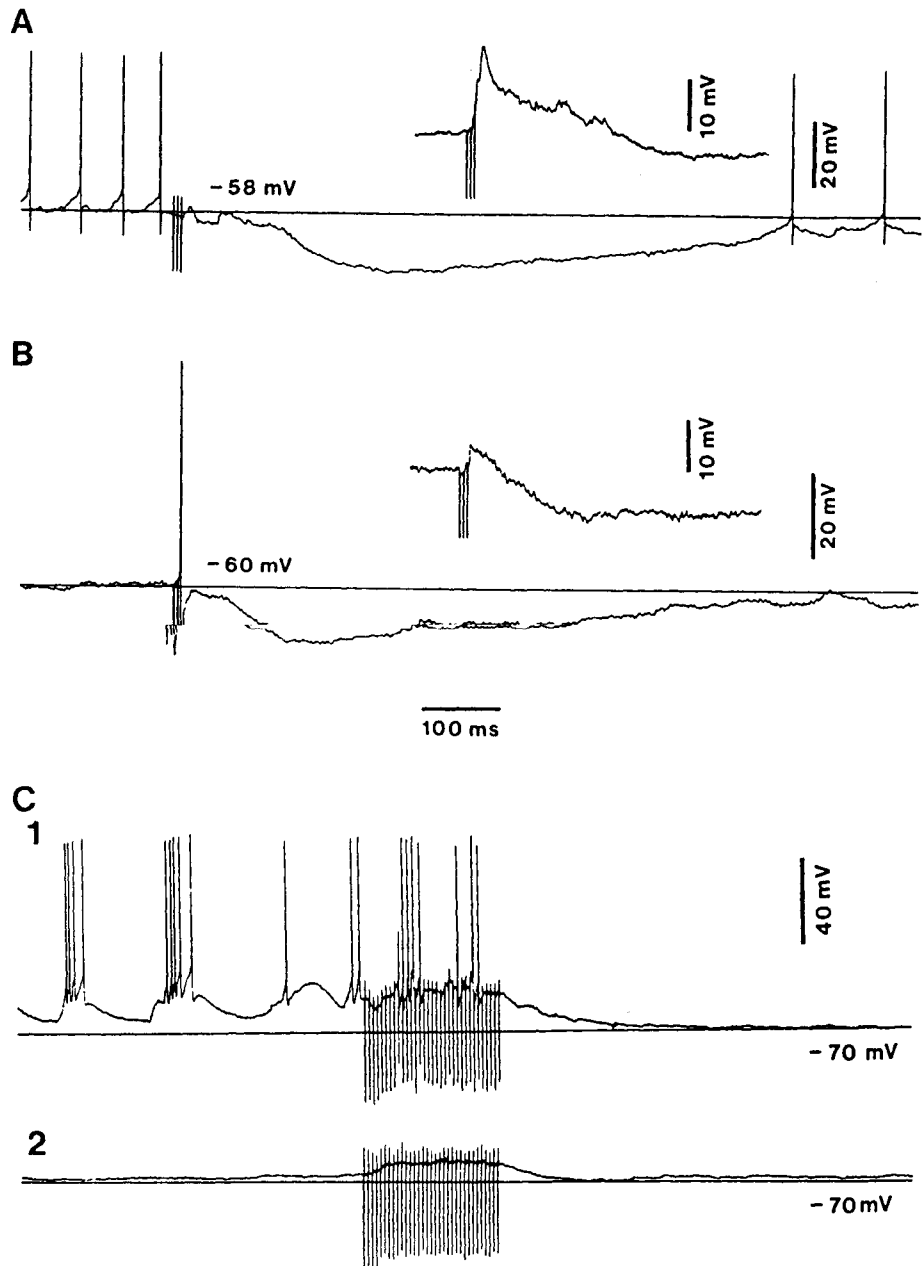


Figure 8.15. Effects of brainstem peribrachial (PB) stimulation on intracellularly recorded thalamic reticular (RE) neurons in the cat. A, unanesthetized deafferented preparation. Three PB stimuli evoked a series of fast depolarizations followed by a long period of hyperpolarization. B, cell recorded under barbiturate anesthesia in the rostral part of the reticular nucleus. The response to PB stimulation was also characterized by a depolarizing-hyperpolarizing sequence. Note, however, the shorter duration of the hyperpolarizing envelope. The right-hand inserts show in greater details the early part of the response evoked in each cell. C, effect of membrane potential on the PB-evoked hyperpolarization in perigeniculate (PG) neurons. Cell recorded under barbiturate anesthesia. In C1, the cell displayed a depolarizing shift of its membrane potential during a spindle sequence. The membrane potential was hyperpolarized to -70 mV by a long PB pulse-train. During the interspindle lull (in C2), when the membrane potential was already at -70 mV , no net hyperpolarization resulted after the PB stimulation; note the PB-evoked depolarization plateau during the pulse-train. Modified from Hu *et al.* (1989a).

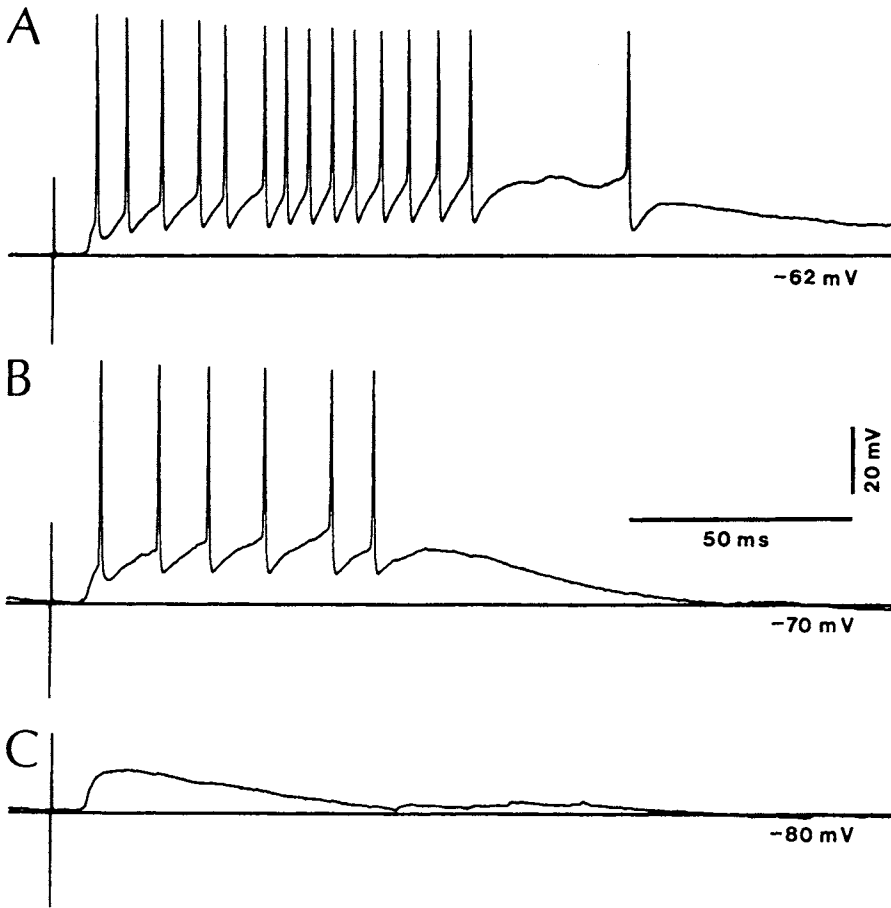


Figure 8.16. Absence of brainstem PB-evoked hyperpolarization in a rostral thalamic reticular (RE) neuron recorded under barbiturate anesthesia after i.v. injection of scopolamine (1 mg/kg). After scopolamine, the PB stimulus triggered a prolonged burst (A) that was eventually reduced to a subthreshold EPSP by hyperpolarizing the cell membrane (B–C). From Hu *et al.* (1989a).

remain to be answered. The suggestion that, upon arousal, reticular-induced inhibition upon TC cells may, in some instances, be overwhelmed by disinhibition (via inhibitory contacts between reticular and local-circuit inhibitory neurons) was substantiated by occurrence of very numerous and short IPSPs in TC neurons following disconnection from the reticular nucleus [58].

8.3. Selective Increase in Cortical Excitability During Attentional Tasks

The above two sections (8.1 and 8.2) dealt with the diffuse excitability enhancement in thalamic neurons during both

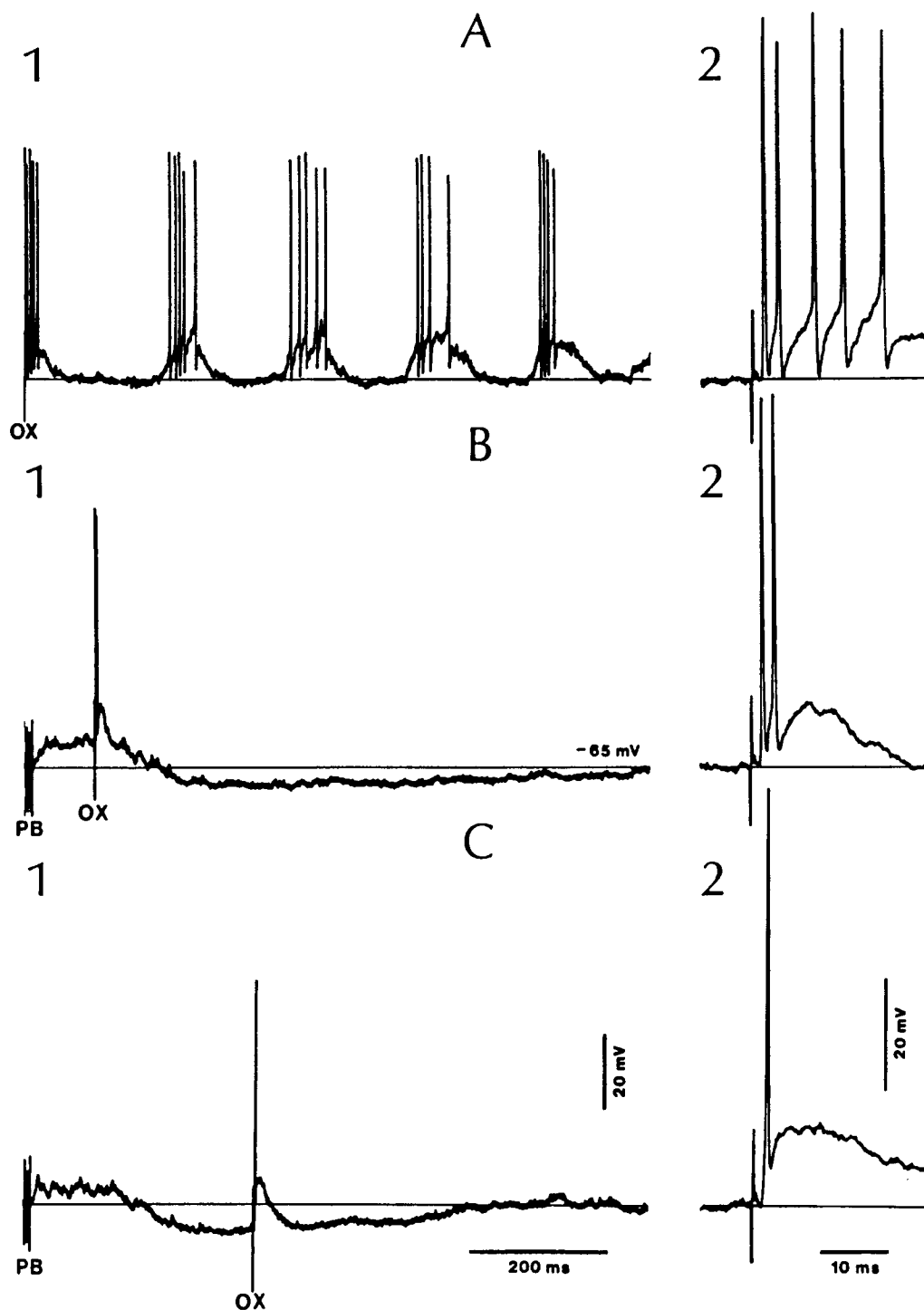


Figure 8.17. Decreased responsiveness of thalamic reticular neuron after a conditioning brainstem PB stimulation in cat. Intracellular recording of a PG cell under urethane anesthesia. The control response to optic chiasm (OX) stimulation is shown in A1. The first part of the response is expanded in A2.

In B–C, the same OX stimulus was delivered at different intervals after a short PB pulse-train. The respective responses are depicted in B2 and C2. Note that the cell responsiveness to OX stimulus was already decreased in B during the early depolarization induced by PB stimulation. From Hu *et al.* (1989a).

brain-activated states of waking and REM sleep. In those studies, the term “waking” state was used rather globally since experimental animals were not submitted to tests of selective attention. We now briefly turn to investigations using scalp-recorded evoked potentials in humans and extracellular unit recordings in monkeys that employed sophisticated experimental paradigms to distinguish focused attention from diffuse arousal.

8.3.1. Event-Related Potentials in Humans

A warning stimulus gives rise to a slow negative shift recorded from the scalp, termed *expectancy wave* or *contingent negative variation* (CNV) [69], which is followed by an imperative stimulus that evokes an event-related potential (ERP). The amplitude of CNV increases when more attention is required or when there is greater incentive for prompt action [70]. The CNV was thought to originate in diffusely projecting brainstem systems and a corticofugal feedback control was hypothesized to suppress irrelevant response tendencies [71]. As to the ERP, it consists of various subcortically and cortically generated components whose latencies signal the arrival of input through different relays and may differ from one sensory modality to another.

The early components of peripherally elicited ERPs, up to a latency of 20 ms, reflect far-field events originating in the spinal cord, brainstem, and thalamic nuclei. For example, in the somatosensory system, all components of the ERP up to and including P14 (a scalp-recorded positive wave with 14-ms peak latency) are believed to be generated below the thalamus (Fig. 8.18A) [72] because wave P14 can be recorded in patients with thalamic lesions [73]. Cortically generated components begin with N20 that occurs over the parietal scalp, contralateral to the stimulus, and P22 that appears in the prerolandic field [72]. It seems that subcortically generated potentials in the somatosensory and auditory modalities do not vary with the attentional state [74]. It is, however, possible that the absence of changes in components that precede the entry of the afferent volley in the cerebral cortex is due to difficulties in recording discrete alterations of distant events over the scalp. Future investigations in humans by means of deep electrodes should explore the possibility that thalamic neurons are capable of discriminatory processes.

The cortically generated components of ERPs are enhanced during selective attention tasks. Subjects were instructed to attend an infrequent somesthetic stimulus (e.g., to the left thumb) designated as target and to press a

[69] Walter *et al.* (1964).

[70] Reviewed in Hillyard and Picton (1987).

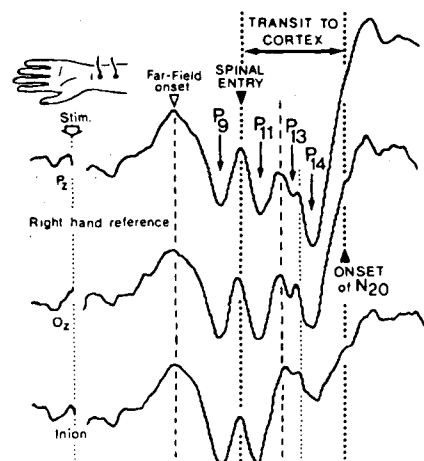
[71] Lang *et al.* (1983).

[72] Desmedt and Bourguet (1985).

[73] Mauguière and Courjon (1983).

[74] Picton *et al.* (1977, 1978); Schulman-Galambos and Galambos (1979); Desmedt (1981).

A



B

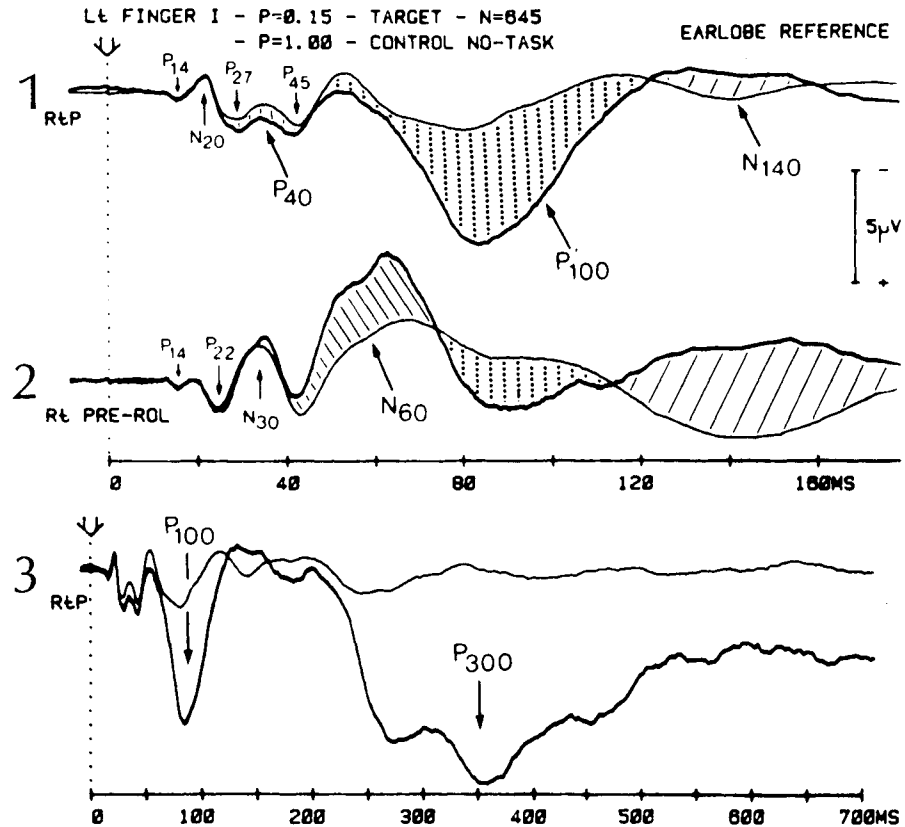


Figure 8.18. Cognitive components of somatosensory evoked potentials (SEPs) in humans. A, far-field SEPs. Stimulation of the left median nerve indicated by the vertical dotted line at left. Negativity upwards. Active electrode at the parietal midline (Pz), occipital midline (Oz) and 2 cm above the inion. Onset of first far-field indicated by white arrow head and vertical interrupted line. B, SEPs to electrical stimuli delivered to the left thumb. The thicker SEP traces were averaged in runs when the thumb stimuli are infrequent ($p = 0.15$) targets to which the subject has to respond by pressing a microswitch with the

[75] Desmedt *et al.* (1983).

button as quickly as possible (with the right index finger) for each of such target [75]. In such conditions, ERP changes consist of increased amplitudes of waves P40, N60, and especially P100 and P300 (Fig. 8.18B). While P40 and N60 are confined to the contralateral parietal and prerolandic areas, respectively, P100 is distributed bilaterally with a contralateral predominance, and P300 is a generalized event, like the CNV. These data suggested that P40 and N60 are the signs of “priming” for infrequent signals, that P100 is the electrical index for identification of input signals, and that P300 reflects a nonspecific postdecision closures, related to the diffuse control of brainstem modulatory systems upon the telencephalon [75].

The understanding of mechanisms underlying the amplitude fluctuations of ERP components while attending or not a stimulus will probably come with animal models of ERPs that would allow combined field potential and unit analyses in cortical and thalamic structures. Attempts at identifying the homologs of P300 wave were made in cat [76], squirrel monkey [77], and macaques [78]. While the significance of P300 is still debated, earlier attention-sensitive components, such as N170, were found to be similarly enhanced in unitary neuronal recordings in monkeys [79] and in human ERPs [80] (Fig. 8.19).

[76] Wilder *et al.* (1981).

[77] Neville and Foote (1984); Pineda *et al.* (1988).

[78] Arthur and Starr (1984).

[79] Wurtz *et al.* (1980).

[80] Galambos and Hillyard (1981).

8.3.2. Neuronal Recordings During Set-Dependent Tasks in Monkeys

[81] Hebb (1972).

Hebb's [81] model of set includes the possibility of different responses to an identical sensory stimulus, depending upon prior instructions. It is generally assumed that the site of this behavioral flexibility is the cerebral cortex, which would explain why cellular studies are overwhelmingly conducted in the cerebral cortex of monkeys. The cerebral cortex is probably not the unique site of flexible decisions, and this should be further assessed. Various methods were used to study the switching mechanisms

right index finger. Thicker traces were obtained by redrawing three times the same trace. These SEPs are superimposed on control SEPs averaged in other runs of the same experiment when identical thumb stimuli were delivered alone ($p = 1.0$) at the same intervals and not mixed with any other stimuli. 1, right parietal scalp derivation. 2, right prerolandic scalp derivation. 3, same trace as 1 displayed on a slower time base. The vertical dotted line on the left side indicates the time of delivery of the thumb stimulus. The small arrows identify standard early SEP components, namely the P14 far-field, the parietal N20-P27-P45, and the prerolandic P22-N30. Cognitive components identified through divergence of the superimposed traces are indicated by the following symbols: P40 (vertical lines), N60 (oblique lines), P100 (vertical rows of dots), N140 (widely spaced oblique lines). Vertical calibration, 5 μ V. Horizontal calibration in ms. Negativity of the active scalp electrodes is upward in all traces. Modified from Desmedt *et al.* (1983) and Desmedt and Bourguet (1985).

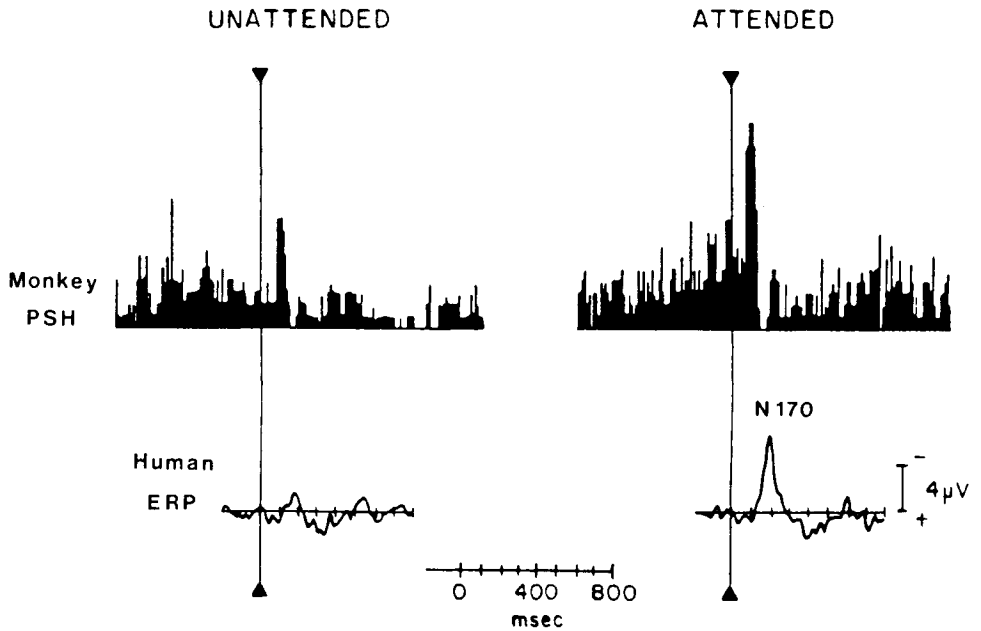


Figure 8.19. Effects of visual attention on unit activity in posterior parietal cortex of a rhesus monkey and on event-related potentials (ERPs) recorded from the parietal scalp in a human subject. Two peristimulus histograms (PSHs) are depicted in the monkey experiment, comparing conditions when the testing flash of light was not attended and when it was attended. Note similar modulation of flash-evoked activity, with similar enhancement when testing stimulus was attended, in the two species. Monkey experiment, from Wurtz *et al.* (1980). Human experiment, from Galambos and Hillyard (1981).

involved in the flexible control of input–output information processing [82].

In general, the macaque receives an instruction consisting of a sensory cue (relevant stimuli are differentiated from irrelevant ones) signaling what type of motor response must be executed after a waiting period in order to receive a reward (delayed alternation task). It must be noted that, usually, cortical neurons are recorded without precise knowledge of their direct inputs and targets, as one could ascertain by standard electrophysiological procedures of monosynaptic and antidromic activation [83]. Instructions to push or pull a handle elicited increases or decreases in activity of the same pyramidal tract neuron; and when the monkey responded incorrectly, the neuronal activity corresponded to the animal's motor preparation rather than the sensory nature of the instructive stimulus (Fig. 8.20A). Similar conclusions, namely that activity changes are specifically related to the state of motor preparation, were drawn from studies on premotor cortical neurons (Fig. 8.20B).

The differentiation between the effects of diffuse activation and those of selective attention leading to initiation

[82] Evarts *et al.* (1984).

[83] Notable exceptions are Evarts and his colleagues (Evarts and Tanji, 1976; Tanji and Evarts, 1976) who have recorded identified pyramidal tract neurons in the primary motor cortex.

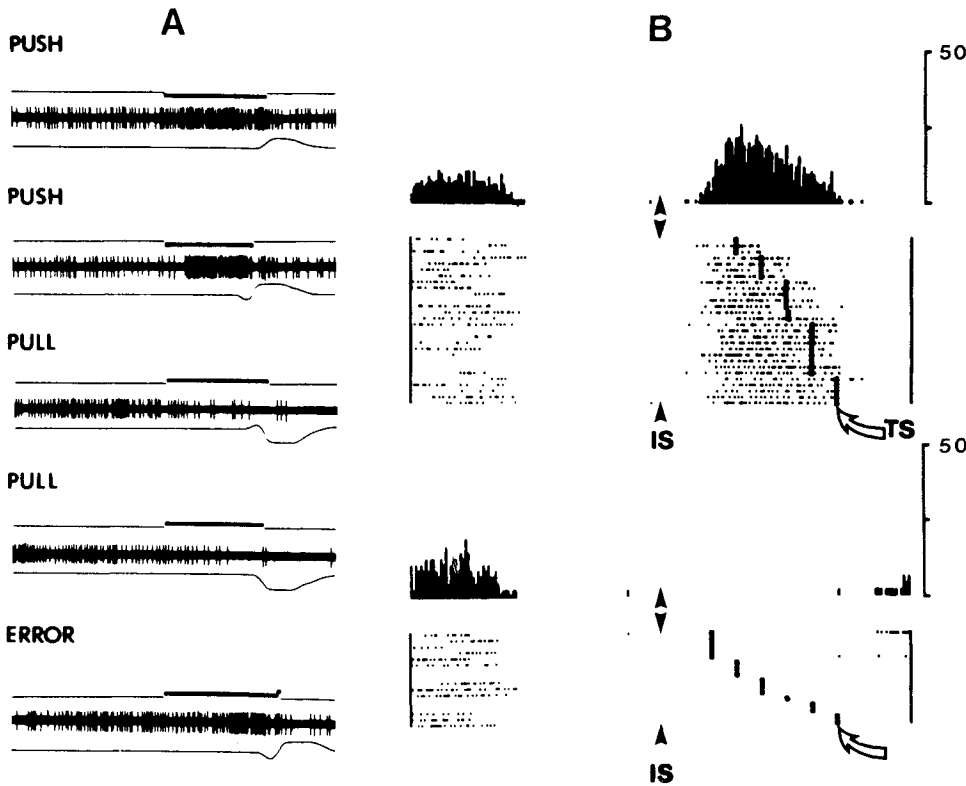


Figure 8.20. Set-related neuronal activity in primary motor (A) and premotor (B) cortices of monkey. A, time of instruction presentation is indicated by the thickening of the horizontal bar above each electrode trace; the instruction delivered is indicated above each trace. Below each electrode trace is an indication of the animal's arm position. Push instructions lead to increases in activity, and pull instructions lead to decreases. Note that in the bottom record the monkey responds incorrectly (he was instructed to pull, but instead pushes, the handle), and in this case the activity resembles other trials in which the monkey ultimately pushes the handle. Thus, the activity appears to reflect the animal's (inferred) motor set, regardless of the instruction. B, top: trials in which the monkey is instructed (IS) to make an arm movement in a certain direction and later is given a triggering stimulus (TS) that allows him to execute the movement. In the bottom raster and histogram, the same cell shows no activity when an identical visual stimulus instructs him to withhold movement. Modified from Tanji and Evarts (1976, A) and from Wise *et al.* (1983, B).

[84] Mountcastle *et al.* (1984). Mountcastle has also studied the command functions for the exploration of extrapersonal space and attentive fixation in monkeys (Mountcastle *et al.*, 1975).

[85] Wurtz and Mohler (1976).

[86] Wurtz *et al.* (1984).

[87] Mountcastle *et al.* (1981).

of movements was emphasized in studies of primary visual and posterior parietal cortices by Mountcastle and his colleagues [84]. In the primary visual cortex, neurons increase their firing rates by diffuse arousal but not by selective attention [85]. This fact suggested that striate cortical cells are not committed in a given circuit but are used for subsequent processing stages [86], such as those involving the posterior parietal cortex and frontal eye fields where saccadic movements are initiated. Mountcastle *et al.* [87] used three types of behavioral conditions in their studies on light-sensitive neurons recorded from the posterior parietal cortex: (1) a no-trial state, that is a state

of quiet waking with no involvement in a behavioral task; (2) a trial state, that is a condition of attentive fixation of a target during which the monkey is engaged in a dimming detection task; and (3) an intertrial mode, that alternates with the trial mode. The light-sensitive neurons of the posterior parietal cortex significantly increase their excitability in the trial mode, compared to both no-trial mode and the intertrial state, with the conclusion that the enhanced synaptic excitability is specifically related to the directed visual attention to the target light, and is not merely due to changes in generalized arousal.

8.3.3. Differential Alterations in Two Phases of Inhibitory Responses During Brain Activation

However efficiently brainstem reticular stimulation and natural arousal obliterate the long-lasting phase of inhibition and its cyclic repetition, these conditions do not eliminate the early *short-lasting* period of inhibition during which spontaneous and evoked discharges are suppressed. This statement [88] was based on extracellular recordings of thalamic relay neurons in the lateral posterior nucleus. Since that time, this notion was expanded at the intracellular level (see above, Section 8.1.4.2).

The emphasis on a differential action exerted by brainstem reticular arousing systems upon the two phases of thalamic inhibitory processes is of importance since, during the 1960s, arousal was regarded as an “inhibition of inhibition” [89] and, until quite recently, activation phenomena elicited by brainstem reticular stimulation or ACh application were thought to be associated with a global blockade of thalamic inhibitory processes through inhibition of both GABAergic thalamic cell-classes, reticular, and local-circuit neurons [90]. The idea of a global blockade of inhibitory mechanisms upon awakening was supported by some data reporting an increase in receptive-field diameter of LG thalamic neurons during “arousal” in acutely prepared unanesthetized animals [91]. These results were regarded as embarrassing [92] and perplexing [93] because loss of center-surround antagonism and other feature detection properties that assist thalamic and cortical neurons in their discrimination tasks would be difficult to conceive during the adaptive state of wakefulness. It is now demonstrated that the long-lasting period of hyperpolarization elicited in thalamic neurons by a synchronous testing stimulus to the prethalamic or corticofugal pathways consists of two distinct components mediated by GABA_A and GABA_B receptors that are blocked by brainstem cholinergic stimulation, whereas the earliest (GABA_A)

[88] Steriade *et al.* (1977b).

[89] Purpura *et al.* (1966).

[90] Singer (1977); Ahlsén *et al.* (1984); McCormick and Prince (1986b); McCormick and Pape (1988).

[91] Godfraind and Meulders (1969); Meulders and Godfraind (1969).

[92] Steriade *et al.* (1974b).

[93] Livingstone and Hubel (1981).

[94] See details for the visual thalamocortical system in Steriade *et al.* (1990e).

[95] Steriade and Deschênes (1974).

IPSP is unaffected and may even be enhanced (see above, Section 8.1.4.2).

The progenitors of inhibitory processes and their circuitries in the thalamus and cerebral cortex are dissimilar [94]. In spite of these notable differences, inhibitory events in TC and corticofugal neurons of cats and monkeys are similarly altered during brainstem reticular stimulation or natural arousal. In TC neurons, the cortically evoked cyclic repetition of the long-lasting inhibitory periods and postinhibitory rebound bursts are blocked by mid-brain reticular stimulation, but the first inhibitory phase is left intact [88]. This was observed with both extracellular and intracellular recordings (see above, Figs. 8.11–8.12). In corticospinal neurons too, the recovery of responsiveness following inhibition evoked by antidromic or synaptic volleys is twice as long during EEG-synchronized sleep compared to waking, but the early phase of inhibition (15–25 ms) is preserved or even enhanced during wakefulness (Fig. 8.21) [95]. These results were interpreted as

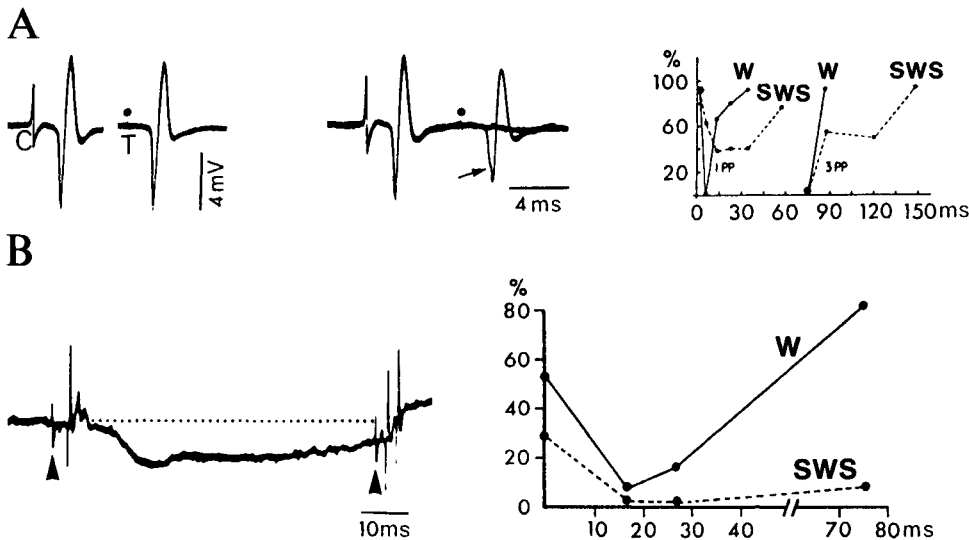


Figure 8.21. Effects of midbrain reticular formation (MRF) stimulation and natural arousal on inhibitory processes of corticospinal neurons in cat and monkey. A, left: method of testing recurrent inhibition acting on antidromic discharges elicited in cat pyramidal tract (PT) neuron. Conditioning (C) volley was delivered at 13 V, that was the minimal voltage required to elicit inhibitory effects on testing (T) response induced by shock at 5 V, which was the minimal voltage required to evoke 100% antidromic invasion. At paired C–T stimulation, complete inhibition of T response or spike fragmentation (arrow). A, right: graph depicts much longer inhibition with three antidromic (pes peduncular, PP) conditioning stimuli than with single shock. With both conditioning procedures (1 PP and 3 PP), recovery of antidromically elicited spike was slower in EEG-synchronized sleep (SWS) than during waking (W). Note deep but short inhibition in W. B, inhibition of synaptic discharges evoked by stimulation of posterior part of the thalamic VL nucleus in precentral PT neuron of chronically implanted macaque monkey. Left, field positive (inhibitory) wave evoked by first VL stimulus and facilitation (during W) of evoked discharges by second stimulus at 75-ms interval toward the end of inhibition. Right, percentage responsiveness of discharge evoked by first stimulus (tome 0) and by second stimulus at 3 time intervals (15 ms, 27 ms, and 75 ms) during W and SWS. Modified from Steriade and Deschênes (1974).

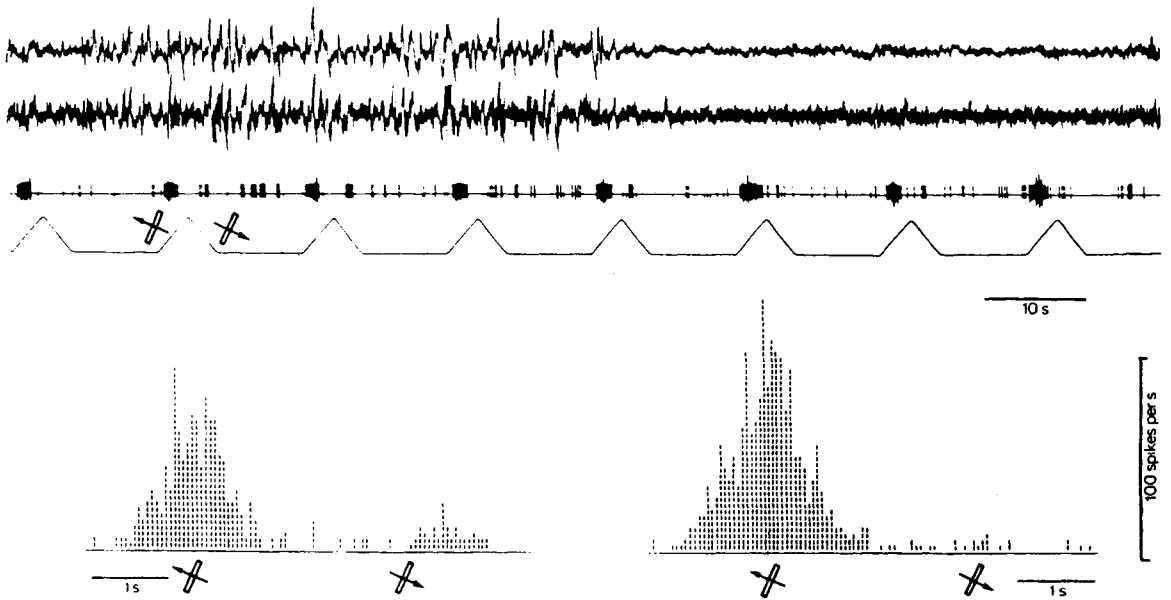


Figure 8.22. Effects of arousal from slow-wave sleep on responses and response selectivity of a cell in layer II of striate cortex in cat. About half-way through the 2-min record, the cat is aroused by a noise. An optimal split, $1/2^\circ/3^\circ$, oriented 25° clockwise to vertical, evokes a response (third trace) that is much greater to movement up and to the left than down and

to the right. Arousal results in a moderate increase in the response to leftward movement, and a virtual elimination of the response to rightward movement (see histograms). Arousal also produces suppression and smoothing of the spontaneous firing. From Livingstone and Hubel (1981).

subserving accurate discrimination of incoming information during waking and are supported by more recent data indicating an improvement of response specificity and directional selectivity upon arousal from EEG-synchronized sleep (Fig. 8.22) [93] and an arousal-induced potentiation of cortical inhibition induced by visual or LG thalamic stimulation [96].

Inhibitory processes have not yet been systematically investigated during REM sleep. The light-evoked inhibition in cortical association neurons is much less conspicuous during REM sleep than during other states of vigilance, and inhibition sculpts again the initial response upon awakening from REM sleep [10]. The study of inhibitory processes may open new avenues for differentiating at the cellular level the two EEG-activated behavioral states of waking and REM sleep that are otherwise quasi-identical from the point of view of electrical activity in thalamic and neocortical neurons.

[96] Swadlow and Weyand (1987).

Neuronal Activities in Brainstem and Basal Forebrain Structures Controlling Waking and Sleep States

The first chapter of this book has described the history of much of the early lesion and stimulation work, as well as the cardinal signs of sleep and the definition of behavioral state. Other chapters describe the neurophysiological and anatomical substrates of various components of waking and sleep states.

In this chapter, we focus on how neuronal activities in brainstem and forebrain structures lead to activation of thalamus and cerebral cortex. Chapter 7 has discussed how the characteristic oscillations of non-REM (NREM) sleep occur in the absence of activating and disrupting influences from the brainstem. The first section of this chapter (Section 9.1) takes up the source of these influences in brainstem and bulbar reticular (RE) neurons, and the brainstem cholinergic neurons in pedunculopontine tegmental and laterodorsal tegmental (PPT/LDT) nuclei, with data from extracellular recordings of antidromically identified, thalamically projecting neurons. Based on these data, we suggest that the synchronizing phenomena in thalamocortical (TC) systems depend, at least in great part, on the removal of brainstem influences. The sudden drop in both cholinergic and noncholinergic brainstem reticular input at sleep onset disfacilitates TC neurons while, at the same time, the reduction in cholinergic input facilitates the genesis of spindle oscillations in the thalamic reticular nucleus. Thus, the return of brainstem cholinergic and brainstem noncholinergic activating influences with REM sleep abolishes these synchronizing events. Next (Section 9.2), we discuss neuronal activities in basal forebrain nuclei and their possible effects on thalamic and cortical activities. Finally, in Section 9.3, we discuss the

neuronal generation of pontogeniculo(thalamo)cortical (PGO) phasic potentials during REM sleep and their neuronal mechanisms in thalamic neurons. Chapter 11 will discuss REM sleep control mechanisms and how the components discussed in this chapter and Chapter 10 (motor control) are orchestrated into the occurrence of a full REM sleep episode. Chapter 12 will take up the property of REM sleep as an ultradian rhythm, with a period of about 90 min in humans and 24 min in the cat, and present a model for its generation. Chapter 13 will discuss the role of active forebrain systems and humoral systems in sleep control.

9.1. Brainstem–Thalamic Neurons Implicated in Tonic Electrical Activation of the Cerebrum

Studies conducted during the early 1980s investigated the waking- and sleep-related activities of rostral midbrain [1] and bulbar reticular neurons [2] with antidromically identified projections to the thalamic intralaminar and ventromedial (VM) nuclei. These thalamic targets were chosen because rostral intralaminar centrolateral–paracentral (CL–PC) and VM nuclei project over widespread cortical territories and may thus account for the diffuse cortical excitatory processes associated with tonic EEG activation. Discharges of brainstem neurons were temporally correlated to the most precocious signs of EEG activation during transition from NREM sleep to either waking or REM sleep. These data were used to evaluate the hypothesis that an increase in firing rates of brainstem neurons precedes overt signs of EEG activation.

At that time, before 1985, the thalamic projections of cholinergic cell-groups located at the junction between the caudal mesencephalon and the rostral pons had not yet been documented. The rationale behind searching at rostral midbrain levels for neuronal candidates involved in EEG desynchronization processes was that classical studies using stimulation and lesions pointed to the upper brainstem reticular stimulation as the critical area for inducing arousal (see Chapter 1, Section 1.1) and that midbrain reticular neurons directly excite thalamic intralaminar CL–PC cells projecting widely over the neocortex [3]. There are virtually no cholinergic cells in the rostral mesencephalon, and the transmitters used by those midbrain neurons have not yet been definitely elucidated. However, the established direct brainstem–thalamic excitatory actions suggest that rostral midbrain neurons probably use excitatory amino acids as neurotransmitters.

[1] Steriade *et al.* (1980, 1982a).

[2] Steriade *et al.* (1984b).

[3] Steriade and Glenn (1982).

[4] Kitsikis and Steriade (1981).

[5] Steriade (1983).

[6] Webster and Jones (1988).

[7] Sastre *et al.* (1981). Data on pontine reticular neurons with thalamic projections and slow conduction velocities (Fuller, 1975), presumably small-size cells, may suggest that these neurons also play a role in EEG activation.

[8] Steriade (2001b).

[9] Reviewed in Steriade and Buzsáki (1990). See also Steriade (2003b).

As to the hypothesis that bulbothalamic neurons may act synergistically with midbrain–thalamic neurons in the process of EEG activation, this was based on the fact that electrolytic or chemical lesions of the upper brainstem reticular core failed to disrupt EEG activation for long periods of time. Indeed, the excitation of midbrain perikarya by glutamate analogs induces a long-lasting (12–36 hr) EEG activation associated with highly aroused behavior [4]. At stages corresponding to the period of kainate-induced neuronal destruction, a 40–60% decrease in duration of the waking state was observed, with only phasic EEG activation reactions, contrasting with the tonic activation observed in the same animals before the kainate injection into the midbrain core [5]. However, this picture lasted for only 3–4 days, and both behavioral and EEG correlates of wakefulness returned to control values after 5–6 days. Subsequent data, using chemical lesions of upper brainstem reticular territories, including cholinergic cell-groups, also indicated that, 10–14 days after the kainate injection, EEG activation during REM sleep is not altered [6]. These results led to call upon an additional source of forebrain activation processes involved in EEG activation. This source may be located in thalamically projecting neurons of the reticular formation, other than mesencephalic fields. Since kainate-induced lesions of the pontine reticular formation do not apparently affect EEG desynchronization during REM sleep, although these lesions may have spared neurons other than the giant cells [7], the bulbar reticular formation was investigated.

In fact, we do not believe that the EEG-activating neurons are restricted within confined regions of the brainstem reticular core, as may be the case with the mesopontine PGO-on cells (see Section 9.3). While the role of bulbothalamic neurons involved in EEG activation during REM sleep (see below, Fig. 9.2) has not yet been tested by lesion experiments, we do not expect that such lesions would succeed in disrupting for long periods of time EEG activation because this process depends upon activities in distributed brainstem as well as supramesencephalic networks, such as posterior hypothalamus, nucleus basalis (NB) and amygdala [8]. The activation of spindle oscillations takes place in the thalamus and depends upon brainstem–thalamic cholinergic neurons (see Chapter 7), whereas the disruption of slow oscillation and delta waves is mainly due to cholinergic actions exerted by NB neurons upon the cerebral cortex [9].

In what follows, we briefly review data on activities of thalamically projecting neurons located in the rostral midbrain, bulbar reticular core, and cholinergic neurons at the PPT/LDT nuclei at the mesopontine junction, which are temporally related to shifts in EEG activation upon awakening and transition from NREM to REM sleep.

9.1.1. Midbrain Reticular Noncholinergic Neurons

The median firing rate of midbrain reticular neurons is twice as high in waking and REM sleep (about 20/s) as in EEG-synchronized sleep. This is valid for neurons receiving multiple converging inputs and antidromically identified as projecting to the intralaminar thalamus, but is not valid for neurons with projections to the paramedian pontine reticular formation that have low firing rates ($<1/s$) and do not increase upon awakening [1]. Both the relatively high discharge rates of thalamically projecting midbrain reticular neurons and their extremely tonic discharge patterns during both waking and REM sleep distinguish them from paramedian pontine reticular neurons that do not seem to be related to ascending activation processes.

The role played by midbrain noncholinergic neurons in EEG activation was determined by using the criterion of a statistically significant change in firing rate preceding the first change in brain electrical activity from NREM sleep to wakefulness. Time 0 in this case is the earliest sign of decreased amplitude and increased frequency of EEG rhythms that eventually lead to generalized EEG activation and overt behavioral manifestations of waking, as reflected by increased muscular tone and eye movements. In these analyses, time 0 is the onset of the transitional period between NREM sleep and waking (see SW epoch in Fig. 9.1, A2) that precedes by more than 15 s the overt EEG activation and motor events associated with behavioral arousal. Precursor signs of increased activity were seen in different midbrain cells 8 to 22 s before any change in the fully synchronized EEG activity (Fig. 9.1B). The pooled analysis of a 25-cell-group revealed that a statistically significant increase in firing rate occurs 15 s before the end of NREM sleep epochs that developed into waking state (Fig. 9.1C) [1]. Similarly, midbrain reticular neurons increase firing rates in the transition from NREM sleep to REM sleep.

There also precursor signs of decreased neuronal activity in thalamically projecting midbrain cells, 1 s before the first sequence of spindle waves during the drowsiness period, were documented in Chapter 7 (see Fig. 7.30).

9.1.2. Bulbar Reticular Noncholinergic Neurons

The bulbar reticular neurons were recorded from the magno- and gigantocellular fields and their ascending projections were antidromically identified from the midbrain reticular core, intralaminar, and VM thalamic

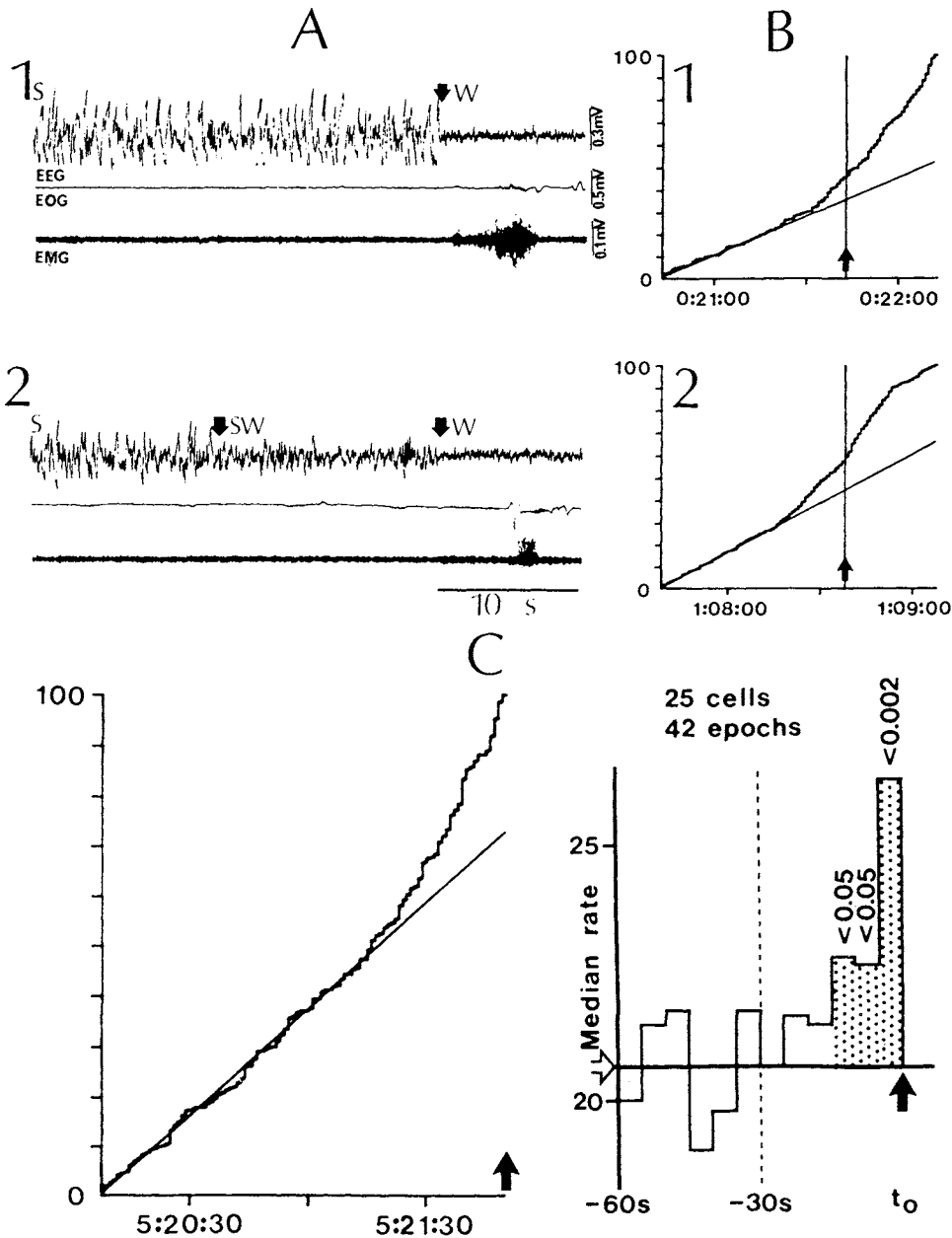
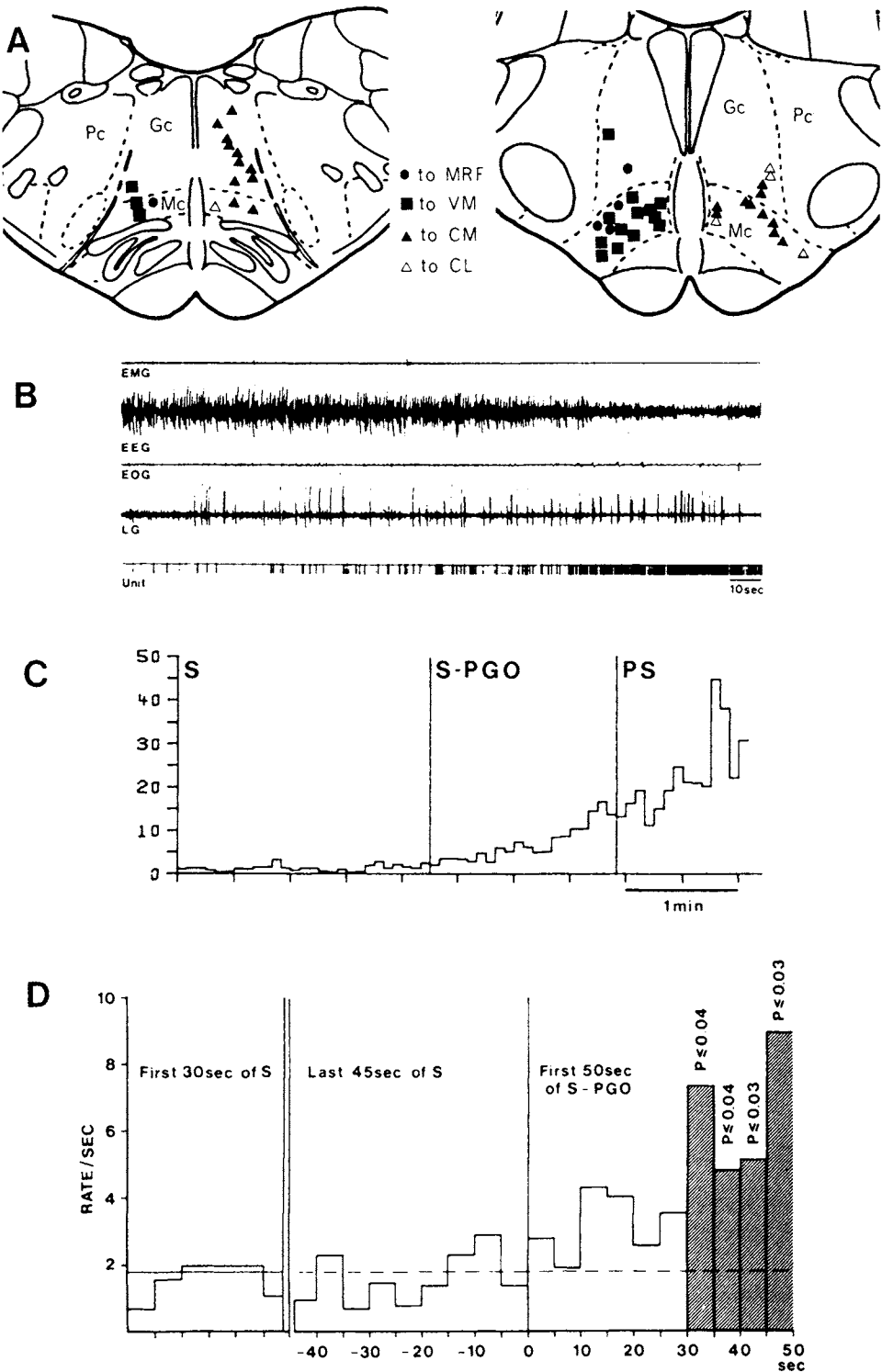


Figure 9.1. Midbrain reticular formation (MRF) neurons with thalamic projections increase discharge rates in advance of EEG and behavioral signs of awakening from EEG-synchronized sleep in the chronically implanted cat. A, electrographic criteria of transitional state (SW) from slow-wave sleep (S) to waking (W). Abrupt (in 1) and progressive transition, with an intermediate SW period (in 2). B, percent cumulative histogram (1-s bins) of 2 MRF neurons. Abscissas, real time of recording; arrows and vertical lines, earliest signs of reduced amplitude and/or increased frequency of EEG waves (as in A, panel 2, arrow indicates time 0 of SW period). Inflection points are seen to occur 10–22 s in advance of any change in EEG; overt signs of wakefulness (eye movements and increased muscular tone) appeared several seconds after arrows (as in A, panel 2). C, increase in firing rate of MRF neurons before the end of S epochs developing into W. Left: percent cumulative histogram of neuron belonging to sample analyzed in graph depicted on right; arrows indicate first change in fully synchronized EEG waves. Right: 25 cells whose global mean rate in S was at least 4/s were analyzed during last minute of S in 42 epochs leading to SW or directly to W. Mann-Whitney test was used to compare reference rate during first 30 s for all cells with their respective rates in the last six 5-s bins. Note significantly increased rates in the three 5-s bins before end of S (arrow) compared with discharge rate in the first 30 s. Modified from Steriade *et al.* (1982a).



nuclei (Fig. 9.2A) [2]. The antidromic identification from the thalamus was necessary to differentiate bulbar reticular neurons involved in EEG activation from other types of medullary neurons that are related to muscular atonia (see Chapter 10). Some of the bulbothalamic neurons were phasically related to REMs and PGO waves. The focus in that study was, however, on tonically discharging neurons in order to relate their activity with the enduring event of EEG desynchronization during REM sleep.

The time 0 of EEG activation associated with REM sleep follows by about 30–60 s the onset of PGO waves during the pre-REM epoch (Fig. 9.2), but in some instances the earliest sign of EEG desynchronization appears more than 2 min after the onset of PGO waves (Fig. 9.2B). To obtain evidence whether the precursor signs of increased discharge rates of bulbothalamic neurons are related to the appearance of PGO waves during the fully synchronized EEG of the pre-REM epoch or if they are really related to EEG activation (Fig. 9.2C), a group of 8 cells was analyzed during at least 75 s of NREM sleep followed by pre-REM transitional epochs of at least 50 s, eventually leading to REM sleep. Data showed that there was no significant difference in firing rate between the EEG-synchronized sleep and the first 30-s period of the transitional pre-REM stage accompanied by PGO waves. Statistically significant increase in discharge frequencies began 30 s after the onset of the pre-REM stage and continued to further increase by approaching the earliest change from NREM sleep to EEG activation (Fig. 9.2D) [2]. These results indicate that bulbothalamic neurons with tonic discharge patterns significantly increase their rates of firing 20 s in advance of EEG activation with transition from EEG-synchronized sleep to REM sleep. The transmitter(s) used by these precursor neurons remain(s) to be elucidated.

Figure 9.2. Bulbar reticular (RE) neurons with midbrain and thalamic projections increase firing rates in advance of EEG activation during REM sleep in chronically implanted cat. A, localization of various gigantocellular (Gc), magnocellular (Mc), and parvocellular (Pv) medullary neurons projecting to mid-brain reticular formation (MRF), ventromedial (VM), centrum medianum (CM), and centrolateral (CL) thalamic nuclei, as identified by antidromic invasion. Rostrally projecting neurons are indicated on both parts of the medullary core to allow the anatomical localization of various neuronal groups (identified cells were usually found ipsilaterally to stimulating electrodes). Left section is at posterior plane 11–10, right section at posterior plane 9–8. B, ink-written recording (EMG, cortical EEG, ocular movements-EOG, PGO waves in the lateral geniculate (LG) thalamic nucleus, and discharges of a bulbothalamic cell) during transition from EEG-synchronized sleep (S) to pre-REM epoch characterized by appearance of PGO waves (S-PGO) and to paradoxical sleep (PS). Time 0 of PS (or REM sleep) is the earliest sign of EEG activation. C, sequential mean frequency (SMF), 5-s bins, of one bulbothalamic neuron during transition from S to S-PGO and further to PS. D, statistical evidence showing that the increased firing rate of thalamically projecting bulbar reticular (RE) neurons prior to onset of EEG activation in REM sleep (during the pre-REM epoch or S-PGO) is not related to PGO waves. See details on method used in Steriade *et al.* (1984b). Modified from Steriade *et al.* (1984b).

This chapter focuses on the relationship of mesopontine cholinergic neurons to cortical EEG activation during waking and REM sleep, while Chapter 11 will examine the activity of these neurons with respect to their role in generation of the entire state of REM sleep. Extracellular recordings have been performed in cat's PPT and LDT cholinergic nuclei at the mesopontine junction to investigate the relation between the activity of their neurons and the tonic process of EEG activation during waking and REM sleep. The location of recorded neurons within PPT or LDT nuclei was assessed by means of lesions along microelectrode tracks combined with micrometer readings, and the sections were stained with NADPH-diaphorase histochemistry that selectively stains cholinergic PPT and LDT neurons in the brainstem core (Fig. 9.3) [10]. Of course, this method can only ascertain that the recorded cell was within a pool of cholinergic neurons. However, at this rostral PPT level (the cat peribrachial (PB) area that mainly extends between stereotaxic planes anterior 1 and posterior 1), where this investigation was conducted [10], cholinergic neurons represent about 85–90% of those neurons labeled by choline acetyltransferase (ChAT) and tyrosine hydroxylase (TH) immunohistochemistry [11]. Significant numbers of catecholaminergic neurons within the PPT nucleus appear only more caudally, at posterior planes 2 to 5 (see Chapter 3). Therefore, the probability that neurons located in the rostral part of the PPT nucleus are cholinergic is very high. In addition, these neurons were antidromically identified as projecting to the different thalamic nuclei, mostly to LG, PUL-LP, and CL-PC intralaminar nuclei (Figs. 9.4 and 9.5) [10, 12].

The majority of thalamically projecting neurons of the cholinergic PPT nucleus displayed tonic discharge patterns and increased their firing rates about 1 min before the earliest change from EEG synchronization during NREM sleep to EEG activation during REM sleep [10]. This was shown by analyses of sequential mean frequency (SMF) in individual (Fig. 9.6) and in pooled PPT cells. Since this long period of precursor changes comprises the transitional SD epoch (NREM to REM sleep) between EEG-synchronized sleep (S) and EEG-desynchronized sleep (REM sleep), whose onset is the first PGO wave, and because many PPT cells are also PGO-on (see below, Section 9.3.1), separate SMFs were computed in which the time 0 was the onset of the transitional SD (or pre-REM) epoch. In these cases, precursor signs of increased activity were seen about 40 s before the first PGO wave (Fig. 9.6C). These data demonstrate that neurons recorded from the cholinergic PPT nucleus, with

[10] Steriade *et al.* (1990a).

[11] See Tables III and IV in [6].

[12] Steriade *et al.* (1990d).

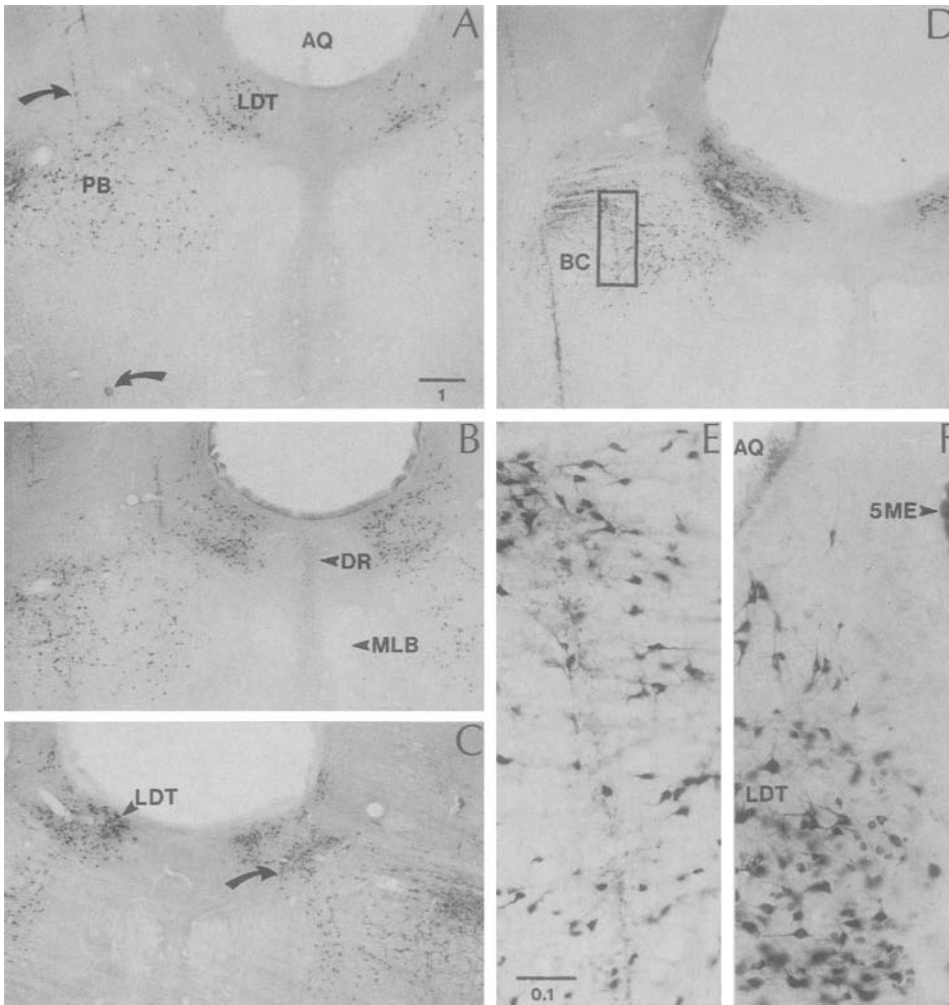


Figure 9.3. Histological localization of microelectrode tracks in mesopontine cholinergic pedunculopontine tegmental (PPT) and laterodorsal tegmental (LDT) nuclei. Chronically implanted, naturally awake and sleeping cat. Frontal sections stained for NADPH-diaphorase activity and counterstained with Neutral red. Sections A–D are rostral to caudal, between frontal planes 0 and –1.5. The rectangle in D is depicted at higher magnification in E. Panel F shows the cholinergic neurons in the LDT nucleus and the adjacent non-cholinergic neurons (stained in red) in the locus coeruleus. Microelectrode tracks through the peribrachial (PB) area of the PPT nucleus and LDT nucleus are marked with arrows in A and C. A small electrolytic lesion (bottom arrow in A) was made a few millimeters ventral to the last recorded neuron on that track. Horizontal bars indicate millimeters (bar in A is valid for other panels, with the exception of E and F). Abbreviations other than PB and LDT: AQ, aqueduct; BC, brachium conjunctivum; DR, dorsal raphe; MLB, medial longitudinal bundle; 5ME, mesencephalic nucleus of the 5th nerve. From Steriade *et al.* (1990a). See also color plate 5.

identified thalamic projections, increase their firing rates well before the EEG activation associated with REM sleep. Thus, PPT neurons may be considered as the best candidates for inducing the cholinergic processes associated with EEG activation, namely, direct excitation of TC cells and blockage of synchronized spindle oscillations by inhibiting

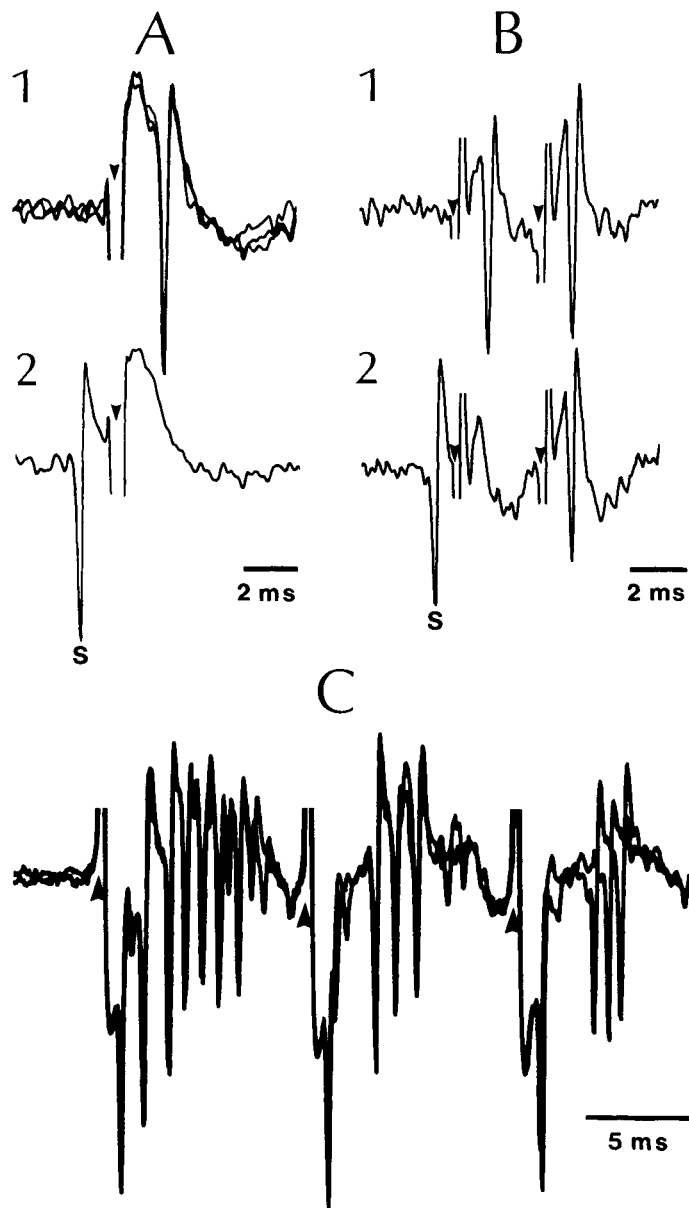


Figure 9.4. Antidromic identification of thalamic projections of mesopontine PPT/LDT neurons. Stimuli marked by arrowheads. A-B, PGO-on sluggish-burst neuron projecting to the medial thalamus. In 2, collision with a spontaneous (S) discharge. C, PGO-on high-frequency burst cell, with antidromic spike evoked from the lateral geniculate nucleus, followed by spike burst. Note progressive decrease in spikes within bursts evoked by 2nd and 3rd stimuli. From Steriade *et al.* (1990b).

reticular thalamic neurons (see Chapter 7). In other studies, presumptive cholinergic neurons from the PPT nucleus were antidromically identified from the posterior hypothalamus and also found to display tonic discharges during both waking and REM sleep or highly specifically during REM sleep [13].

[13] El Mansari *et al.* (1989). Our data [10] also documented a class of thalamically projecting, slowly discharging (less than 2 Hz in waking) PPT/LDT neurons that increased

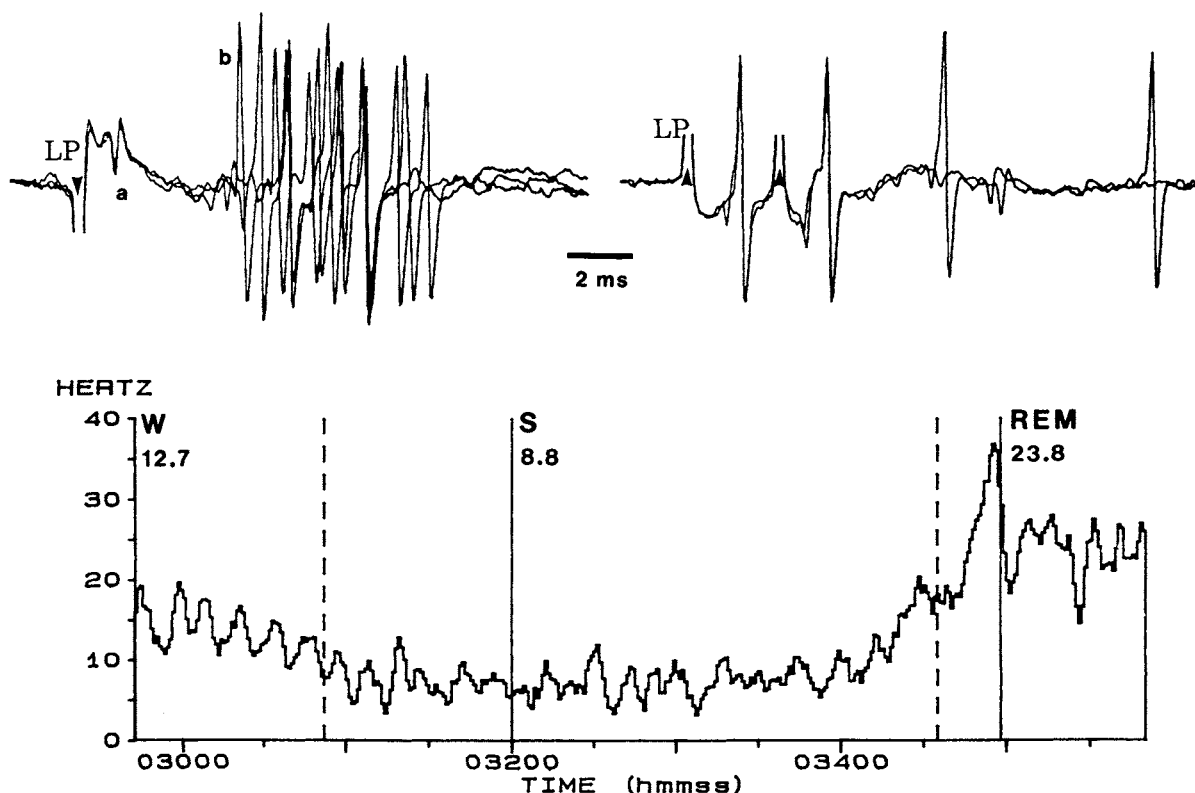


Figure 9.5. Antidromic identification of PPT neuron and sequential firing rate (SFR) of PPT neuron during the waking-sleep cycle. Top panel, two simultaneously recorded PPT neurons (small action potential a and large action potential b). Left: antidromic activation of cell a and synaptic excitation of cell b by stimulating thalamic lateroposterior (LP) nucleus. Right: changing the polarity of stimulation led to antidromic

invasion of cell b. Bottom panel, SFR of thalamically projecting neuron across the wake-sleep cycle. Abscissa indicates real time. Mean firing rates during waking (W), slow-wave sleep (S), and REM sleep are indicated (Hz) for each state. Transitional WS and pre-REM epochs are indicated by vertical interrupted lines (at 0:30:53 and 0:34:34, respectively). Note cyclic activity toward the end of W state. Modified from Steriade *et al.* (1990a).

firing rates from waking to NREM sleep and further to REM sleep, but this class represented only one third of the neuronal population that increased tonically firing frequencies during both waking and REM sleep. In another study, El Mansari *et al.* (1990) reported the suppressive action of microinjections of a cholinergic agonist, carbachol, on PPT neurons with firing frequencies of less than 5 Hz during wakefulness (see also the review by Sakai and Crochet, 2002). [14] The projection from PPT/LDT neurons to

The role of cholinergic neurons with descending projections in the induction and maintenance of REM sleep phenomena originating in pons and bulb is discussed in Chapter 11.

9.2. Basal Forebrain Neurons Implicated in Tonic Cortical Activation

Whereas the first step in the bisynaptic (PPT/LDT to TC to neocortex) activating pathway is cholinergic and the second glutamatergic, the parallel activating bisynaptic pathway from brainstem to NB and to cortex is different, in the sense that the first step is glutamatergic [14] and the second one, from NB to cortex, is, at least in part, cholinergic. The presence of these two parallel activating pathways

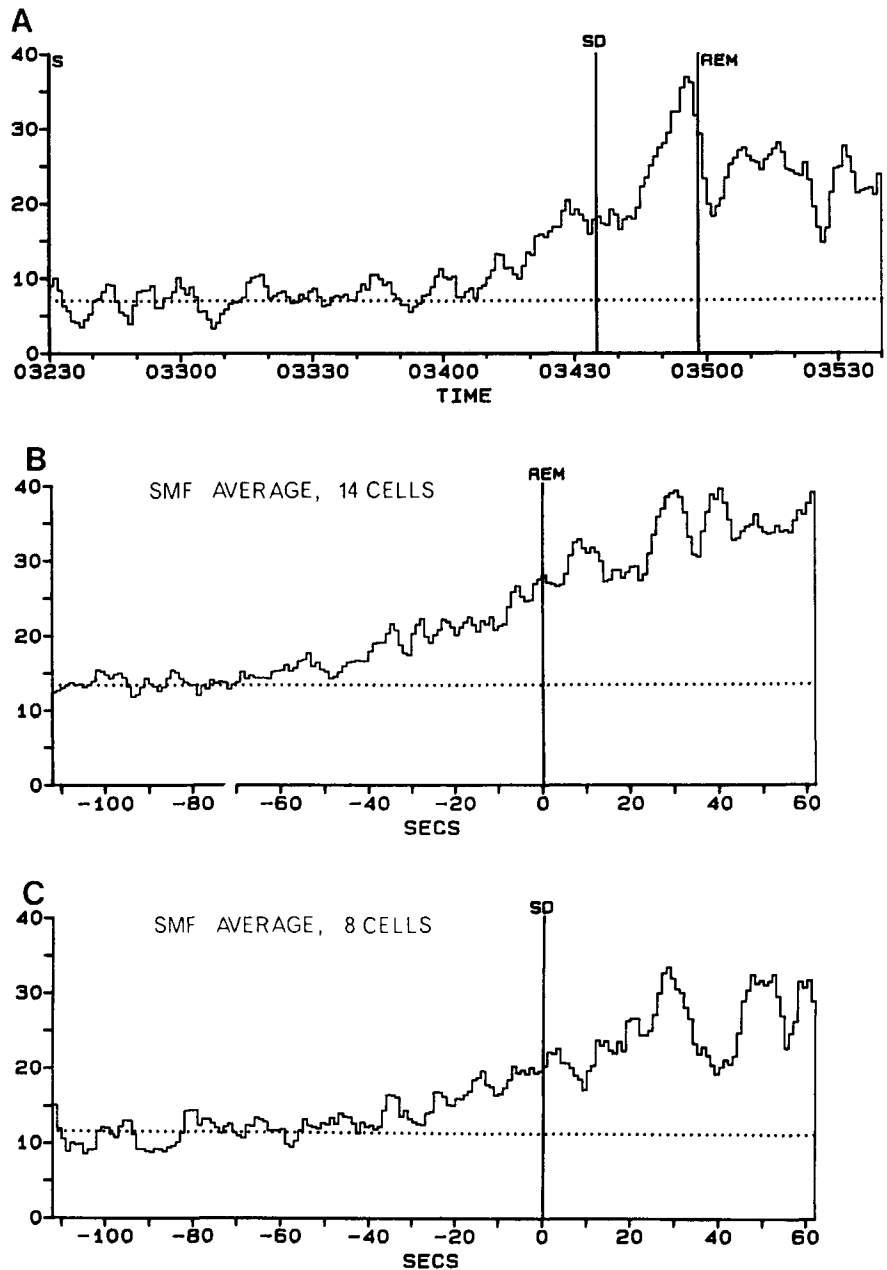


Figure 9.6. Pedunculo-pontine tegmental (PPT) neurons of cat increase firing rates in advance of EEG activation during REM sleep. A, sequential mean frequency (SMF) of a PPT neuron during transition from EEG-synchronized sleep (S) to transitional epoch (SD) from S to EEG-desynchronized (activated) sleep (REM). Time 0 of SD (or pre-REM) epoch is the appearance of the first PGO wave. Time 0 of REM sleep is the earliest change from EEG synchronization to EEG activation. Abscissa indicates real time. In this and two following panels, the spontaneous firing baseline in S is indicated by dotted line. B, an averaged SMF in a pool of 14 PPT neurons during transition from S to REM sleep. Note increased firing rates about 40 s in advance of the first sign of EEG activation. C, since the transitional SD period comprises PGO waves, and in order to preclude that the precursor signs of increased activity in B were due to the appearance of PGO waves, the averaged SMF in C (a pool of 8 PPT neurons) shows that an increase in firing rate occurs well before (about 30 s) the time 0 of the SD epoch. Unpublished data by M. Steriade, G. Oakson, S. Datta, and D. Paré.

nucleus basalis (NB) neurons is excitatory but cannot be ascribed to cholinergic actions because ACh hyperpolarizes NB neurons (Khateb *et al.*, 1991), much the same as the action of ACh on brainstem cholinergic neurons (Leonard and Llinás, 1994). We suggested that the excitatory actions from the brainstem reticular neurons to nucleus basalis (NB)

(from brainstem to cortex, via synaptic relays within the thalamus or NB) is supported by *in vivo* experiments showing that brainstem-induced depolarization of cortical neurons, their enhanced excitability, and replacement of slow oscillations by fast rhythms, can be achieved after extensive lesions of either ipsilateral thalamus (Fig. 9.7) or NB [15].

The input–output organization of cholinergic and noncholinergic neurons of basal forebrain (including NB) nuclei is discussed in Chapter 3 (Sections 3.3.2 and 3.6) [16]. Suffice it to mention that the cholinergic projection from NB to cortex depolarizes cortical neurons and

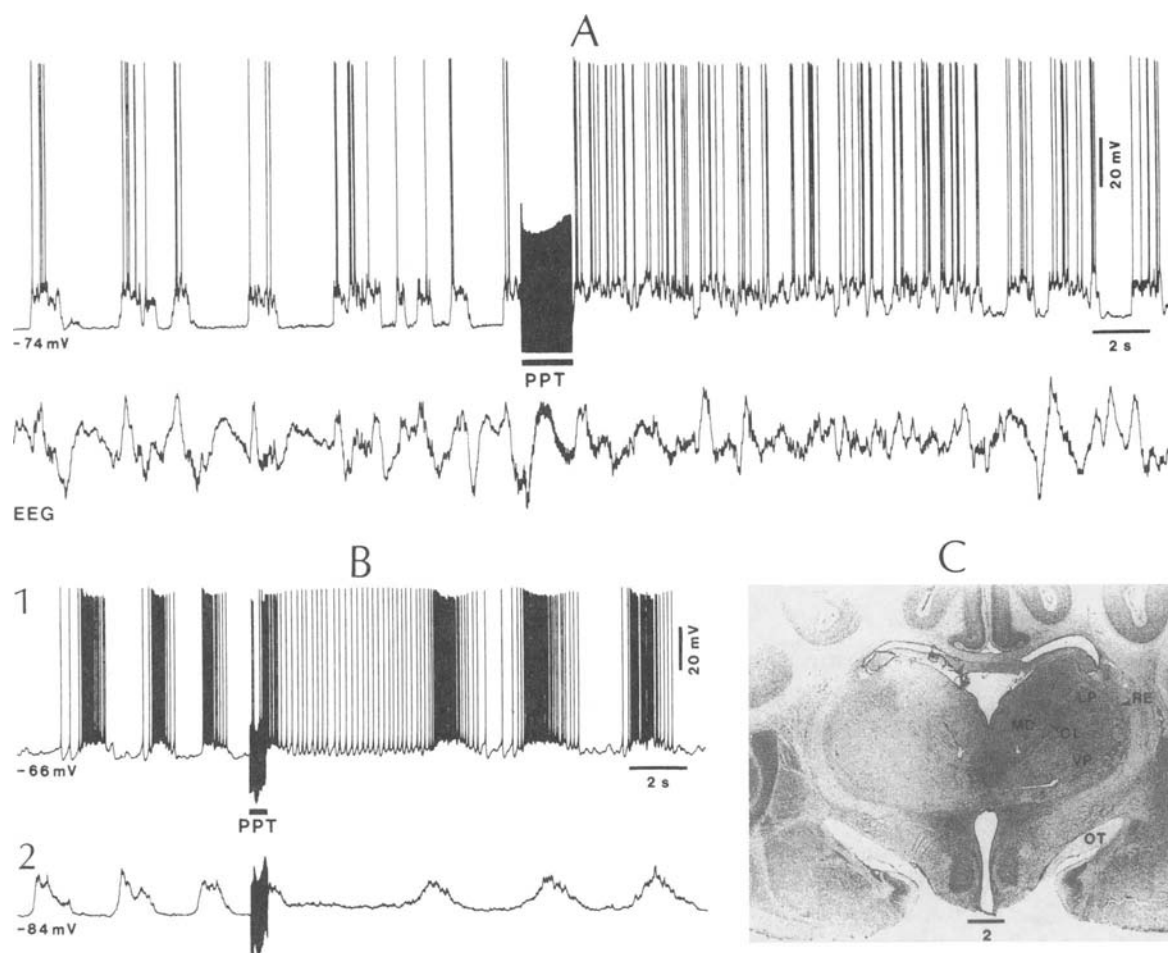


Figure 9.7. Blockage of slow cortical oscillation by mesopontine PPT nucleus stimulation in thalamically lesioned animals, thus implicating activation of the parallel pathway through the basal forebrain. Cats under urethane anesthesia. A, area 7 neuron, oscillating with depolarizing components separated by silent periods of 1–3 s, in close relation with EEG wave complexes initiated by surface-positive waves (upward deflections). PPT pulse-train (1.8 s, 30 Hz; horizontal

line) replaced the slow oscillation by tonic firing. B, effect of PPT pulse-train (0.6 s, 30 Hz; horizontal bar) on slow oscillation in area 5 neuron. B1, under DC depolarizing current (+0.5 nA). B2, at the resting V_m . C, kainate-induced lesion of the thalamus ipsilateral to recorded cortical neurons. Abbreviations: MD, mediodorsal nucleus; OT, optic tract; RE, reticular nucleus. Calibration bar is in millimeters. From Steriade *et al.* (1993a).

changes their slow oscillatory potentials to fast rhythms [17]. Neurons recorded in NB nucleus of chronically implanted rats display the highest frequency activity during waking behavior and decrease their firing with the increase in power of slow waves in the cerebral cortex, with further diminished discharges at the onset of high-voltage cortical spindles [18]. Extracellular studies on juxtacellularly labeled and immunohistochemically identified cholinergic neurons in rat NB nucleus under urethane anesthesia show that such neurons fire in a rhythmic bursting fashion and at high rates during theta-like activity accompanied by fast rhythms [19], as is the electrical pattern of behavioral waking in unanesthetized animals. As yet, there is no study of identified NB cholinergic neurons with cortical projections that would tonically increase their firing rates in advance of the earliest signs of EEG activation during transition from NREM sleep to either waking or REM sleep, as is the case for upper midbrain and bulbar reticular formation neurons with identified thalamic projections (see Figs. 9.1–9.2) and PPT/LDT neurons (see Figs. 9.5–9.6). However, as will be discussed in Chapter 13, inhibition of cholinergic and noncholinergic neurons of the NB by adenosine has marked effects on the cortical EEG, increasing delta activity and increasing the percentage of non-REM sleep.

In addition to their cortical projections, NB cholinergic and noncholinergic (GABAergic) cells project to some dorsal thalamic nuclei and, notably, to the thalamic reticular GABAergic nucleus [20]. As both ACh and GABA inhibit reticular neurons, this projection is implicated in the inhibition of reticular neurons, pacemakers of sleep spindles [21], and thus contributes to activation processes.

9.3. Brainstem Neurons and the Genesis of Pontogeniculo(thalamo)cortical Potentials

PGO waves are stigmatic events of REM sleep when dreaming episodes occur. They are generated in different neuronal groups of the brainstem reticular core and are transferred to many TC systems, in addition to the visual one where they were originally thought to be confined. The interest for the PGO waves stemmed from the discovery that eye movement direction is related to gaze direction in dream imagery, coupled with data from animal experiments showing that saccadic REMs are coincident with PGO events [22]. These observations led to the consensus that PGO waves are physiological correlates of brain activation during dreaming sleep, “the stuff that dreams are made of.”

are glutamatergic (Steriade *et al.*, 1993a) and further experiments corroborated this assumption (Rasmusson *et al.*, 1994, 1996). Indeed, glutamate is colocalized with ACh in PPT/LDT neurons (Lavoie and Parent, 1994).

[15] See Fig. 7 in Steriade *et al.* (1993a).

[16] See also recent reviews of multiple output pathways of the basal forebrain and their functional roles in Semba (2002) and Jones (2003).

[17] Metherate *et al.* (1992).

[18] Buzsáki *et al.* (1988a-b).

[19] Manns *et al.* (2000a). Distinctly from NB cholinergic neurons, GABAergic neurons in the same nucleus are more active during irregular EEG slow wave cortical activity than during activation induced by stimuli (Manns *et al.*, 2000b).

[20] Steriade *et al.* (1987b); Parent *et al.* (1988); Asanuma (1989, 1997); Asanuma and Porter (1990).

[21] Steriade *et al.* (1987a).

[22] Dement and Kleitman (1957b); Jouvet (1972).

In this chapter, we first discuss data on PGO genesis in the brainstem (Section 9.3.1). Thereafter (Section 9.3.2), we deal with the thalamic responses to the brainstem-generated PGO potentials, as revealed by intracellular studies of reserpine-induced PGO waves and by neuronal recordings in the lateral geniculate–perigeniculate (LG–PG) thalamic nuclear complex in naturally sleeping animals.

9.3.1. Brainstem Genesis of PGO Waves

A long series of experimental evidence, including stimulation, lesion, reversible cooling, and recordings of cellular activities have established that neurons which transfer the brainstem-generated PGO waves to the thalamus are located in and around the PPT cholinergic nucleus [23]. That these thalamically projecting brainstem neurons are cholinergic is an assumption resulting from the demonstration that systemic administration [24] and iontophoretic application [25] of nicotinic antagonists into the thalamic LG thalamic abolish the thalamic PGO waves. Recent experiments have indeed shown that, at chronic stages after chemical lesions of PPT cholinergic perikarya, PGO waves are largely suppressed during REM sleep (Fig. 9.8) [6].

The electrophysiology of neurons implicated in the brainstem–thalamic transfer of PGO waves was worked out since the late 1970s. It was reported that some PB neurons from the PPT nucleus discharge groups of 3–5 spikes, reliably preceding by 10–25 ms the LG–PGO wave [26]. Antidromic identification of PGO-on burst cells was achieved by stimulating thalamic intralaminar nuclei [27]. There is a three-way correlation between eye movement direction and the discharge of PB burst neurons related to the LG–PGO wave: rightward eye movements drive right PB neurons that lead to predominantly right LG–PGO waves (Fig. 9.9). In addition to short-lead (10–25 ms) PB burst neurons, longer lead (50–150 ms) PGO-on neurons have been recorded from the medial pontine reticular formation (Fig. 9.10) [28].

It should be mentioned that PGO-on bursting cells recorded from the PPT nucleus merely represent <5% of the sampled brainstem population [26]. The question then arises: how does the vast majority of thalamically projecting PPT neurons behave during PGO waves? Another question concerns the discharge patterns of PGO-on neurons during the waking–sleep continuum, including periods of REM sleep free of PGO waves, and in particular: do PGO-on neurons selectively discharge spike bursts temporally related to PGO waves, or do they also display other

[23] Reviewed in Sakai (1980); Hobson and Steriade (1986).

[24] Ruch-Monachon *et al.* (1976).

[25] Hu *et al.* (1988).

[26] McCarley *et al.* (1978); Sakai and Jouvet (1980); Nelson *et al.* (1983).

[27] Sakai (1985a,b).

[28] McCarley and Ito (1983).

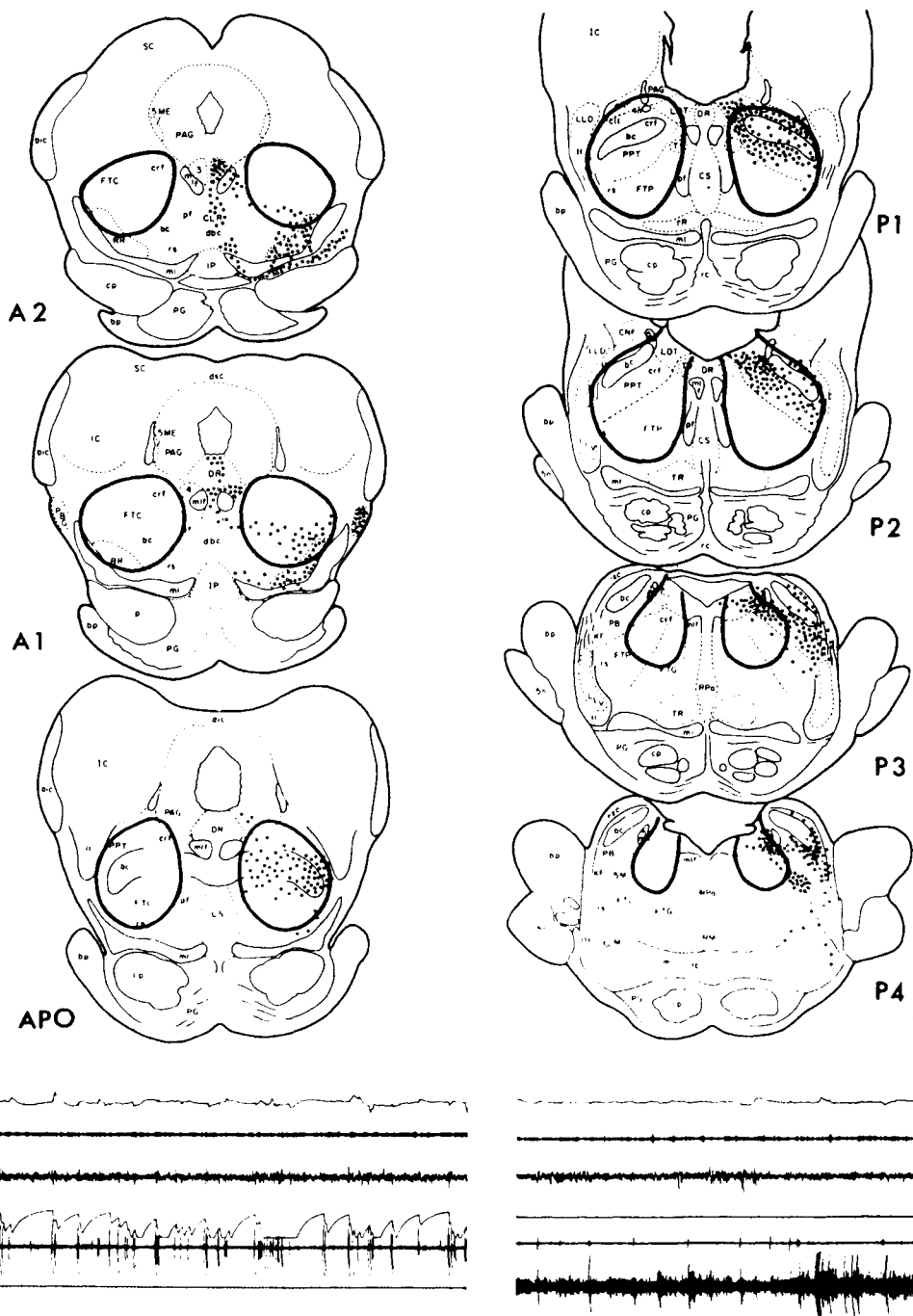


Figure 9.8. Kainate-induced destruction of PPT cholinergic neurons is followed by PGO suppression during REM sleep of chronically implanted cat. The frontal brainstem sections show encircled territories of cell loss after kainic acid injections. Filled circles indicate choline acetyltransferase (ChAT)-positive

cells and empty circles indicate tyrosine hydroxylase (TH)-positive cells as revealed in normal animals. At bottom, control polygraphic record of a cat before kainic injection and 22 days after the injection; note disappearance of PGO waves in the thalamic LG nucleus. Modified from Webster and Jones (1988).

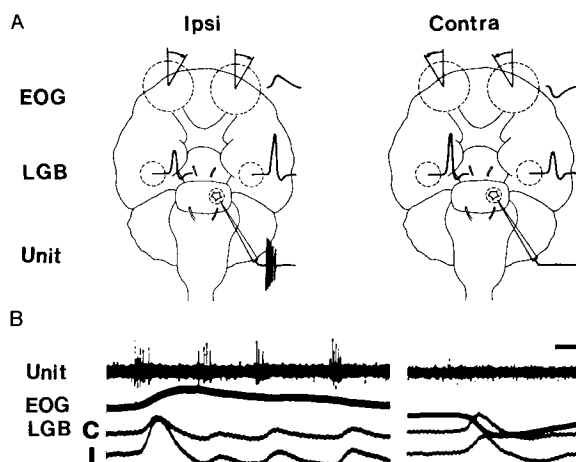


Figure 9.9. Three-way correlation between PGO burst cell discharge, eye movement directionality, and primary PGO waves in the cat. A, two dorsal view drawings of the brain schematize eye movement direction (EOG), laterality of amplitudes of PGO waves in thalamic LG nucleus, and a PGO burst cell being extracellularly recorded by a microelectrode. The left diagram (Ipsi) shows an eye movement toward the side of the recorded burst cell in the pons; the EOG trace is upward, the larger (primary) PGO wave is in the ipsilateral LGB, and there is a burst of spikes in the unit recording. In contrast, the right diagram (Contra) shows that with an eye movement away from the side of the recorded neuron, there is no burst of spikes, and the larger (primary) PGO wave is in the contralateral LGB. B, filmstrips show the raw data from which the diagrammatic conclusions in A were drawn. LGBi is PGO wave recording in the LG nucleus ipsilateral to the unit recording. Upward EOG traces are eye movements toward the side of the recorded neuron. Calibration, 50 ms. From Nelson *et al.* (1983).

types of activity during wake and sleep states? Until quite recently, the only indication was that some of the PGO-on bursting cells also displayed short bursts or single spikes in association with eye movement potentials (EMPs) during the waking state [26].

Since the thalamus is the major site where PGO waves are usually recorded, and the PGO thalamic response is a nicotinic event (see above), the assessment of the role played by PGO-on brainstem neurons should start with the antidromic identification of brainstem–thalamic cells recorded within the limits of cholinergic PPT/LDT nuclei. These identification procedures are shown above (see Figs. 9.3 to 9.5). The extracellular data reported below, related to brainstem PGO-on elements, resulted from analyses of such neurons.

Recordings of different classes of PGO-on cells located within the cholinergic PPT/LDT nuclei and activated antidromically from various dorsal thalamic nuclei were performed during natural REM sleep of chronically implanted cats [12]. This study revealed various neuronal groups, discharging single spikes, trains of single spikes, or spike bursts with different patterns, preceding the negative peak of PGO field potential recorded from the thalamic LG nucleus.

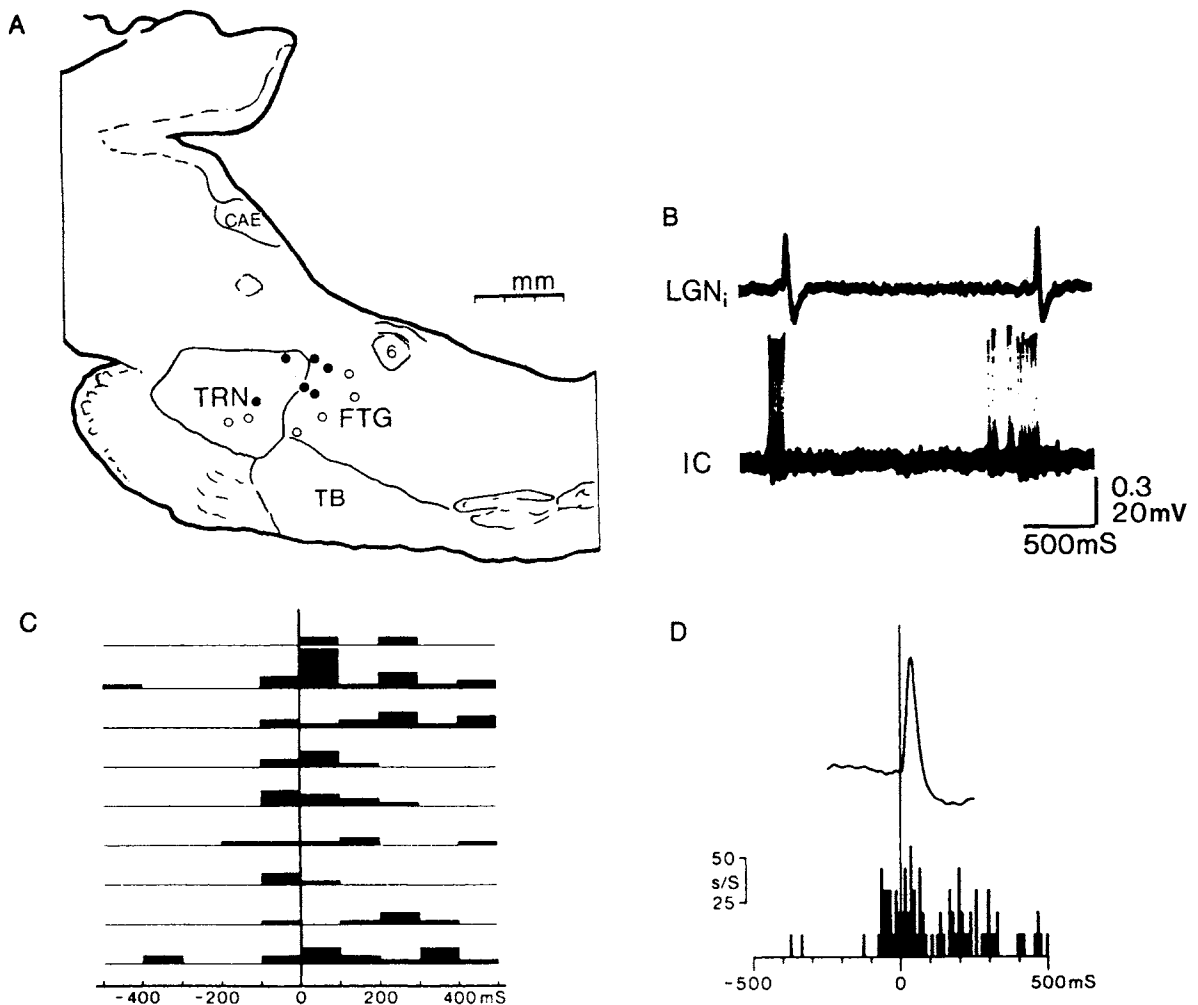


Figure 9.10. Intracellularly recorded long-lead PGO-on neurons in the cat medial pons. A, brainstem schematic at 0.8 mm lateral showing location of intracellularly recorded long-lead PGO-on neurons (closed circles) and neurons with lesser PGO wave correlation and/or no phase-leading relationship (open circles). Abbreviations: CAE, locus Coeruleus; TRN, tegmental reticular nucleus of Bechterew; FTG, gigantocellular tegmental field; 6, abducens nucleus; TB, trapezoid body. B, intracellular record (IC) of a medial pontine reticular formation (mPRF) long lead PGO-on neuron in the transition period, showing phase-leading discharge prior to primary PGO waves (upper trace) in the LGN ipsilateral to recording site. C (different neuron than in B), raster display showing that long lead

PGO-on neuronal discharges began prior to time of onset (0 ms) of eight of nine (89%) ipsilateral LGN primary PGO waves. The height of each black bar is proportional to the number of discharges in each 100 ms bin; scale is provided by the bin in the second row from top with maximal number of discharges, $n = 10$ (rate of 100 spikes/s). Note consistency of discharge-PGO relationship. D, PGO wave-discharge cross-correlogram (same neuron as in part C). Top is average waveform of 9 PGO waves (peak voltage is 400 μ V); below is the associated discharge level of the long lead PGO-on neuron in spikes/s. Note marked acceleration of discharge rate at 80 ms prior to PGO wave onset (binwidth = 10 ms). From McCarley and Ito (1983).

1. Some PPT/LDT neurons fired single spikes preceding by 15–25 ms the negative peak of the LG-PGO field potential [29].
2. Another cell-class discharged trains of single spikes whose onset preceded by 100–200 ms the thalamic PGO

[29] Intracellular recordings of similar neurons (firing single action potentials before

the thalamic PGO potential) in reserpine-treated preparations disclosed that these single spikes rose from large composite EPSPs whose amplitudes grew with hyperpolarization (Paré *et al.*, 1990a).

wave. The tonic firing patterns of these PGO-on neurons was substantiated by interspike interval histograms of cellular activity taken during the period of PGO-related increased neuronal firing, indicating the presence of medium (10–25 ms) intervals and the virtual absence of short (<8 ms) intervals that would reflect spike bursts (Fig. 9.11).

The class of PGO-on bursting neurons comprises a series of different neuronal types, displaying spike bursts with quite different structures.

3. Some neurons discharge a group of 3–5 spikes, as already reported in previous investigations (see above, Fig. 9.9). However, the intraburst frequency in those neurons is well below (130–170 Hz) the frequency generated by a typical low-threshold somatic spike that usually ranges

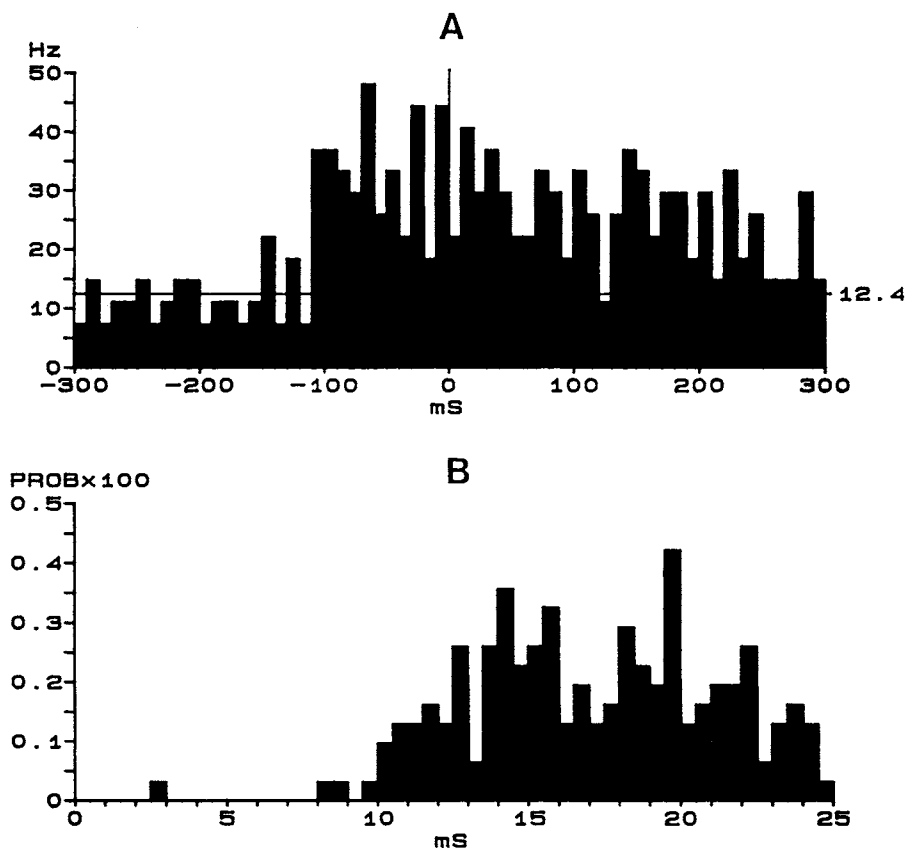


Figure 9.11. PGO-on PPT cell with tonic discharge patterns during REM sleep of chronically implanted cat. A, peri-PGO histogram (10-ms bins) of PPT-cell's discharges. Time 0 is the negative peak of the PGO wave recorded from the ipsilateral thalamic LG nucleus. Note increased firing about 110 ms before the thalamic PGO wave. The level of spontaneous discharge during REM sleep (12.4 Hz) is indicated. B, interspike interval histogram (0.5-ms bins) of cell's activities during the period of increased firing rate around time 0. Note medium intervals (10–25 ms) and virtual absence of short interval (below 8 ms) that would reflect presence of spike bursts. Unpublished data by M. Steriade, S. Datta, G. Oakson, and D. Paré.

above 250 Hz (see Chapter 5). Further intracellular studies should test the possibility that such PGO-on bursts of PPT/LDT neurons originate at the level of their dendrites. It is known that the spike bursts of thalamic reticular neurons have lower frequencies (160–170 Hz) than those (>250 Hz) of TC cells [30]. Correlatively, the rebound bursts of the former neurons originate in dendrites, whereas the rebound bursts of the latter neurons originate mainly the soma [31]. Anyway, the mechanism underlying stereotyped spike bursts, like those displayed during REM sleep by such brainstem PGO-on bursting cells, is probably the de-inactivation of a low threshold spike by membrane hyperpolarization (see Chapter 5). If so, the hypothesis that postulates that the genesis of PGO-on bursts involves a disinhibition of brainstem cholinergic neurons, consequent to the suppressed activity in monoaminergic elements, should be revised. Instead, we should rather investigate possible sources of inhibition acting upon PPT/LDT neurons, during which impulses of different origin may trigger the low-threshold spike and the superimposed bursts of fast action potentials. One of the likely source of inhibition acting upon PPT cells is substantia nigra pars reticulata that consists of GABAergic neurons which project directly to PPT [32].

4. Other PPT neurons discharge high-frequency (500–600 Hz) spike bursts in close temporal relation with thalamic PGO waves. However, distinctly from what is known in literature, these bursts occur on a background of tonically increased discharge rates during REM sleep (Fig. 9.12) [12]. These data raise the intriguing possibility that high-frequency bursts may be generated at a depolarized level, at variance to what is expected for a common low-threshold Ca^{2+} spike.

5. Still another type of PPT/LDT neurons fire tonically, at high rates (>30 Hz), during epochs of REM sleep without PGO events and stop firing prior to and during thalamic PGO waves (Fig. 9.13). The behavior of these PGO-off cells is unexpected for cells located within the limits of brainstem cholinergic nuclei and is the functional counterpart of the heterogeneity of PPT/LDT nuclei. The admixture of cholinergic and monoaminergic neurons in the cat PPT nucleus was already discussed (see Chapter 3, Section 3.1.1), but such PGO-off cells are obviously not aminergic in the light of the virtual silence of aminergic neurons during REM sleep. The disclosure of GABAergic neurons within brainstem cholinergic nuclei [33] raises the possibility that PGO-off neurons, such as that illustrated in Fig. 9.13, are GABAergic, and that their silenced firing prior and during PGO waves could disinhibit adjacent neurons with tonically increased discharges during PGO waves.

[30] Domich *et al.* (1986).

[31] Steriade and Llinás (1988).

[32] Datta *et al.* (1991).

[33] Kosaka *et al.* (1987).

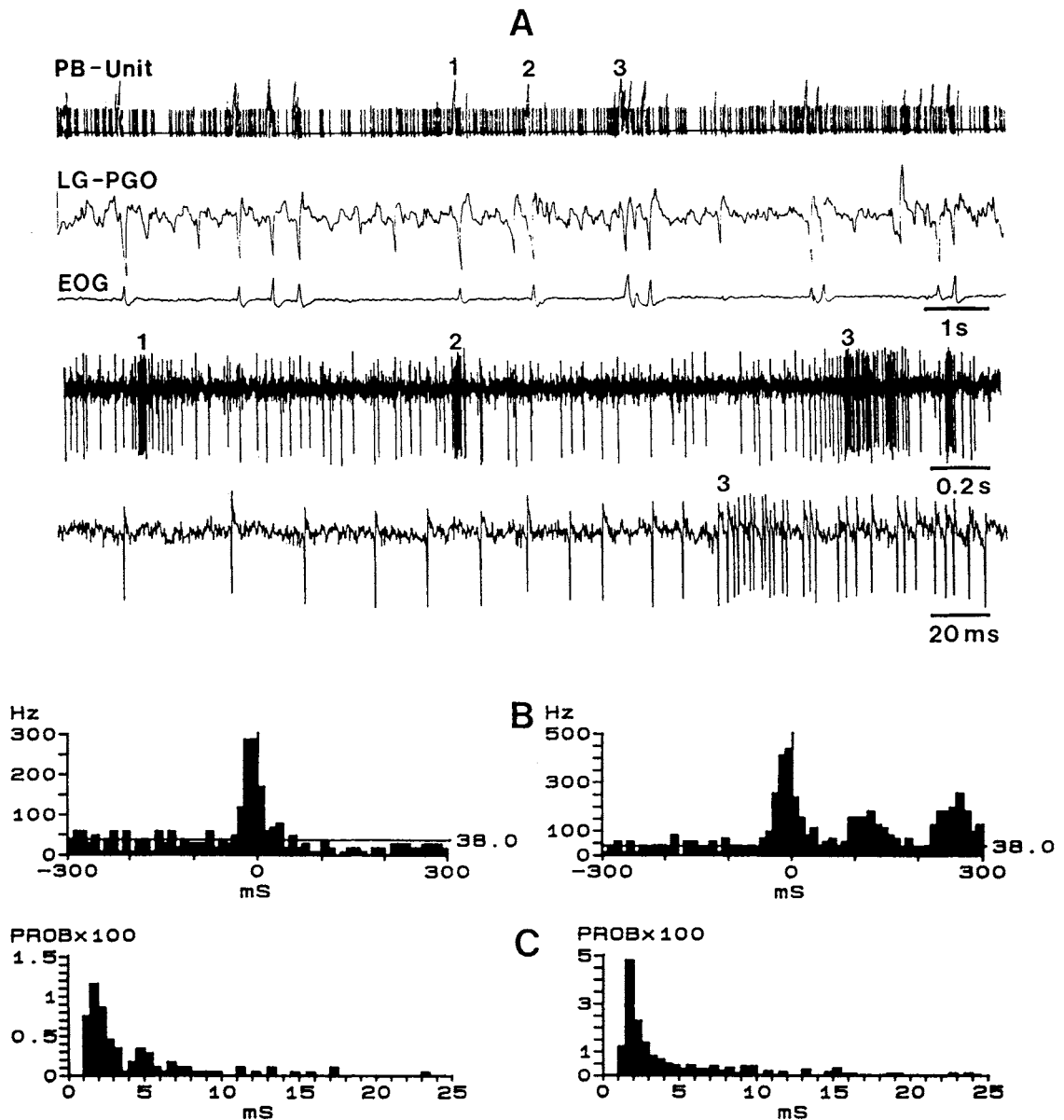


Figure 9.12. Activity of PGO-on burst neuron in the PPT nucleus during REM sleep of chronically implanted cat. A, polygraphic ink-written record (unit discharges, deflections exceeding the common level represent high-frequency spike bursts; LG-PGO waves; and EOG) and original spikes with two different speeds, showing three (1 to 3) PGO-related bursts, as indicated on the first trace of the ink-written records. B, peri-PGO histograms (10-ms bins) of PPT cell's discharges (time 0 is the negative peak of

the LG-PGO wave) for single and clustered PGO waves (left and right panels, respectively). The level of overall spontaneous discharges in REM sleep (38 Hz) is also indicated. C, interspike interval histograms (0.5-ms bins) of PPT cell's activity during the period of increased firing rate around the PGO events for single and clustered PGP wave (left and right panels, respectively). Note very short intervals (<3 ms) reflecting high-frequency bursts. Modified from Steriade *et al.* (1990d).

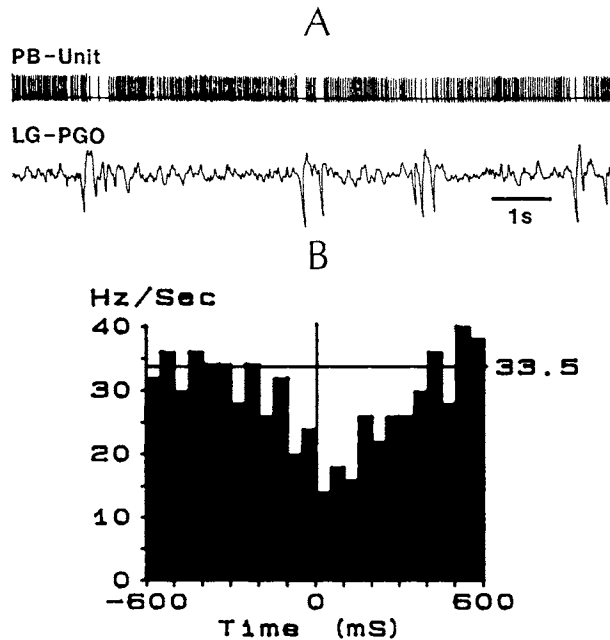


Figure 9.13. Neuron in the PPT nucleus diminishing its firing rate or ceasing its discharges prior and during PGO waves during REM sleep of chronically implanted cat. A, ink-written recording with unitary discharges and LG-PGO waves. B, peri-PGO histogram (50-ms bins) showing decreased firing rate beginning about 300 ms prior to the negative peak of the LG-PGO wave. The level of overall spontaneous discharges during REM sleep (33.5 Hz) is also indicated. Modified from Steriade *et al.* (1990d).

These investigations in behaving animals [12] reveal the variety of PPT/LDT neurons related to the genesis of PGO waves (Fig. 9.14) as well as the organizational complexity of PPT/LDT circuits and related structures (Fig. 9.15), which defy simplistic statements on the properties of neurons transferring PGO waves to the thalamus.

The disclosure of these neuronal properties in the behaving animal are now followed by intracellular studies on reserpine-induced PGO waves in acutely prepared animals.

9.3.2. Cellular Mechanisms of Thalamic PGO Waves

Thalamic PGO waves are spiky, biphasic (initially negative) field potentials that are usually recorded in the thalamic LG nucleus where they display their maximum amplitudes because of the LG laminated structure. Other thalamic nuclei that exhibit PGO waves include especially the associational visual (pulvinar and lateral posterior), rostral intralaminar, and the anterior nuclear group. This diffusion throughout the thalamus of a phenomenon that

was initially regarded as restricted to the geniculostriate system is not surprising since brainstem cholinergic neurons which give rise to PGO waves project to virtually all relay, associational, and intralaminar thalamic nuclei in cats and monkeys [34].

PGO herald REM sleep by about 30 to 90 s, appearing as high-amplitude isolated events that precede the other key signs of REM sleep (EEG activation, muscular atonia, and ocular saccades), and they continue throughout the state of REM sleep as clustered waves with lower amplitudes. Thus, the thalamic transfer of brainstem-generated PGO signals has to be considered in two distinct stages: (1) the transitional period between EEG-synchronized and EEG-activated (REM) sleep, during which PGO waves appear over the background of a fully synchronized EEG (see Fig. 1.5 in Chapter 1, up to EEG activation; and panel B in Fig. 9.2 in this chapter); this period is termed hereafter *pre-REM*; and (2) the REM sleep associated with EEG activation. Besides the change from high-amplitude isolated PGO waves to clustered PGO waves with lower amplitudes, the *pre-REM* and REM sleep should be dissociated because thalamic neurons display opposite firing modes during behavioral states associated with EEG synchronization versus states accompanied by EEG activation: they are hyperpolarized during the former, and tonically depolarized by 7–10 mV during the latter [35]. These two distinct stages have not been analyzed in previous works dealing with the PGO-related neuronal activity in the thalamus [36].

We shall discuss the thalamic transfer of PGO on the basis of recent experiments using intracellular recordings of LG TC neurons in acute experiments on reserpine-treated cats [37] and extracellular recordings of LG neurons in chronically implanted, naturally sleeping cats.

The intracellular studies on reserpine-induced thalamic PGO waves [38] were carried out in cats under urethane anesthesia because the brainstem–thalamic PGO response is a cholinergic event (see below) and the cholinergic activation of TC neurons is blocked by very low doses of barbiturates. The animals were acutely deprived of retinal and visual cortex inputs to prevent massive synaptic bombardment and to avoid activation of LG neurons through circuitous pathways involving cortical neurons. In such simplified experimental conditions, the intracellular response of LG cells to “spontaneous” PGO waves occurring under reserpine treatment are quite stereotyped and they resemble the LG response to stimulation of brainstem PB area in the PPT nucleus, which contains the neurons of the final common path transferring brainstem-generated PGO waves to the thalamus. The thalamic field PGO waves

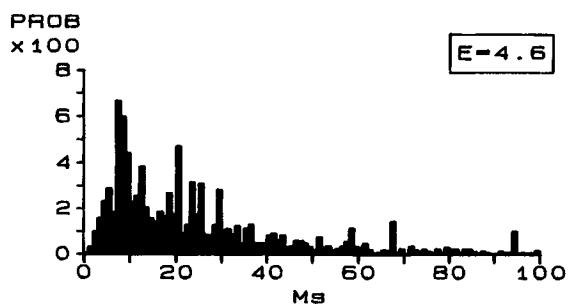
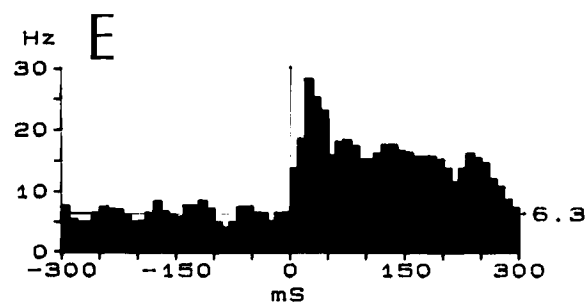
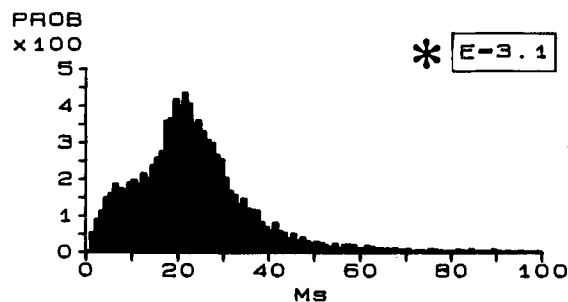
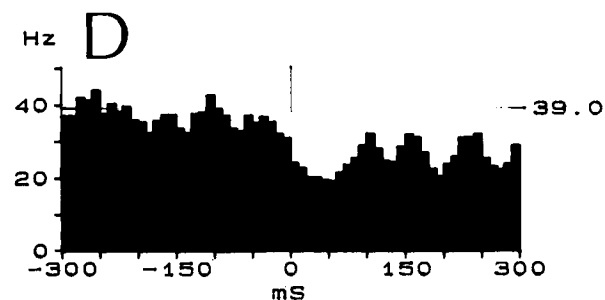
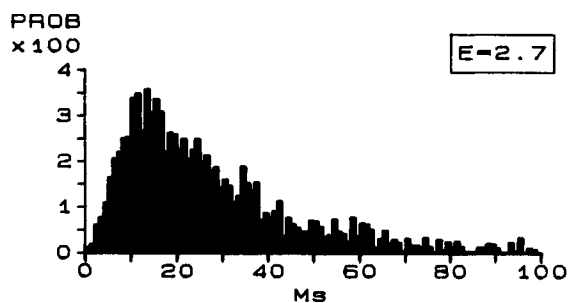
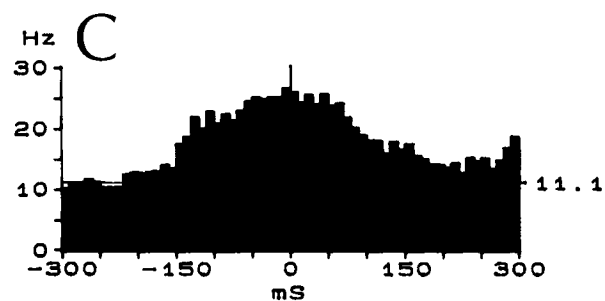
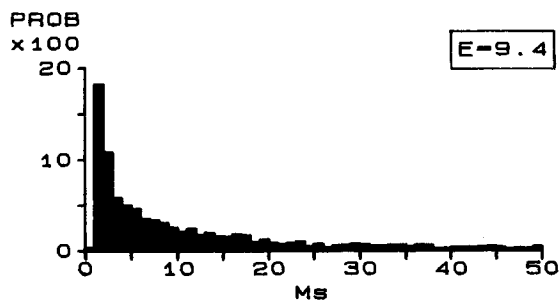
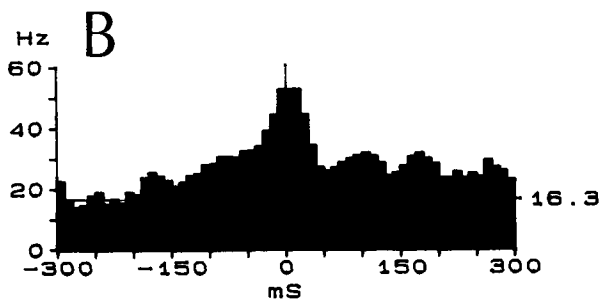
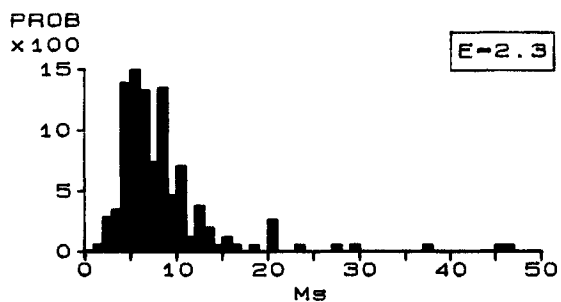
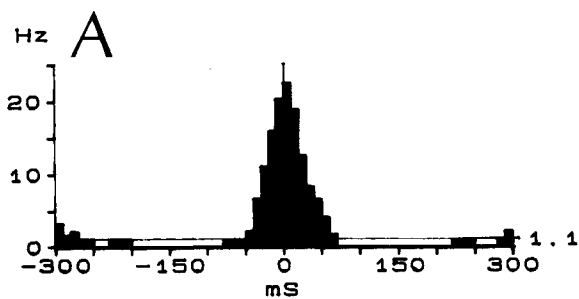
[34] Paré *et al.* (1988); Steriade *et al.* (1988).

[35] See Steriade *et al.* (1993d).

[36] For a review of those early studies, see Steriade and Hobson (1976).

[37] See Jouvet (1972) and Hobson and Steriade (1986) for reviews of monoamine depletors leading to the appearance of REM sleep signs.

[38] Deschênes and Steriade (1988); Hu *et al.* (1989c).



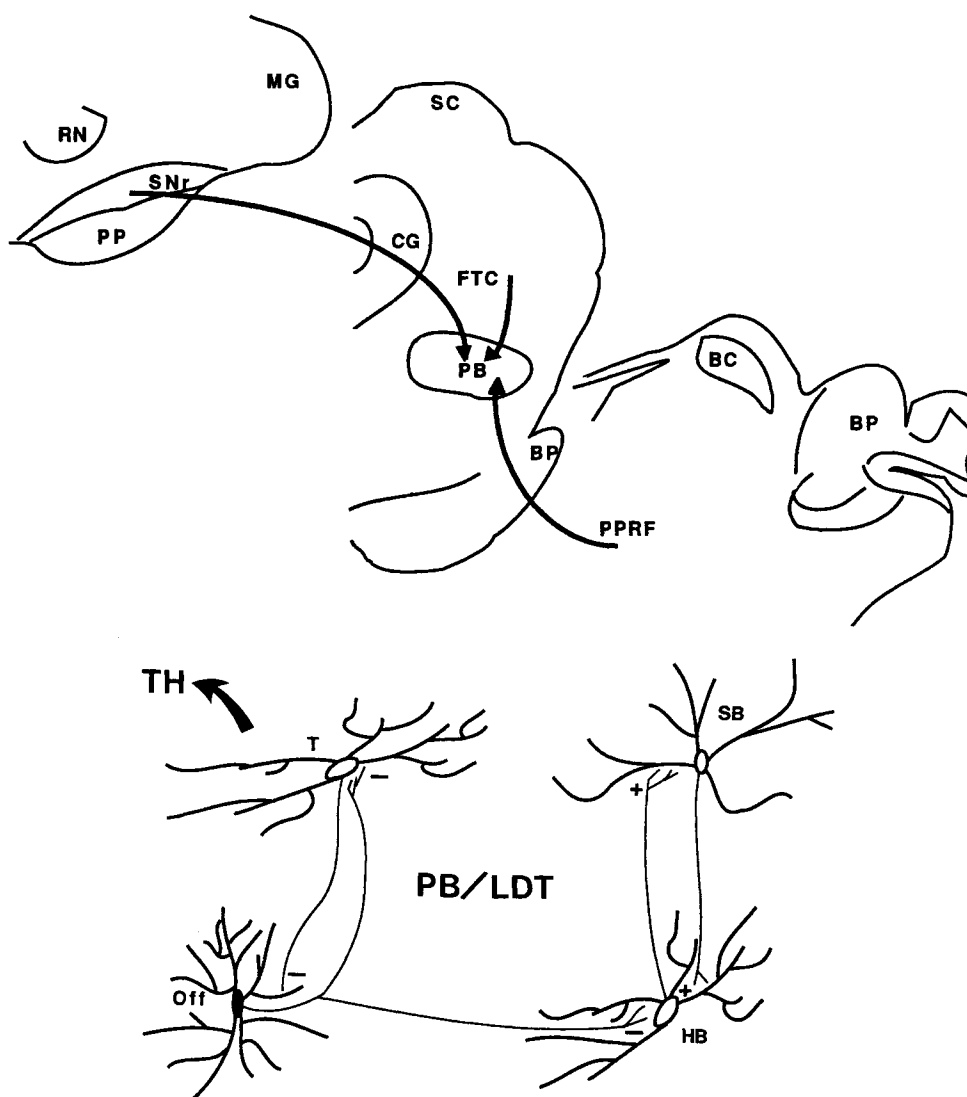


Figure 9.15. Tentative schemes of cellular interactions underlying the genesis of PGO waves and their transfer from PB(PPT)/LDT nuclei to the thalamus (TH). Top, three frontal sections (from rostral to caudal) depicting the inputs to PB area from substantia nigra pars reticulata (SNr), central tegmental field (FTC), and the paramedian pontine reticular formation (PPRF). Other abbreviations: BC, brachium conjunctivum; BP, brachium pontis; CG, central gray; MG, medial geniculate nucleus; PP, pes pedunculi; RN, red nucleus; SC, superior colliculus. Bottom, hypothesized excitatory (+) and inhibitory (-) interactions between four cellular types (PGO-on and PGO-off) in PB(PPT)/LDT nuclei. Symbols: SB, sluggish burst; HB, high-frequency burst; Off, PGO-off cell; T, tonic cell. See also main text. From Steriade *et al.* (1990d).

Figure 9.14. Analyses of PGO-related activities in pools of PGO-on sluggish-burst neurons (A, $n = 5$), PGO-on high-frequency burst neurons with tonically increased firing rates in REM sleep (B, $n = 11$), PGO-on tonic neurons (C, $n = 10$), REM-on but PGO-off neurons (D, $n = 3$), and post-PGO-on neurons (E, $n = 11$). Peri-PGO spike histograms (PPSHs) are depicted in left columns for all cellular types. Peri-PGO interval

histograms (PPIHs) are depicted in right columns for A–C and E cellular types. Symbol E in PPIHs: percentage of PGO-related intervals in excess of the depicted time range. In D (right column), asterisk depicts a pooled interspike interval histogram from REM sleep, instead of a PPIH, since the peri-PGO activity consists of a drop in firing rate. From Steriade *et al.* (1990d).

obtained in these restricted acute experimental conditions are almost identical to those described in chronically implanted, naturally sleeping animals [39, 40], namely: they start with an initial focal negativity, followed by a longer duration positivity that may have a negative notch on its rising phase or may be followed by a second full negative component whose peak follows the peak of the first negativity by about 80 ms (see Figs. 9.16A and 9.17). Thus, the total duration of PGO waves varies between 200 and 500 ms, depending upon the time-course of the positive phase.

[39] Brooks and Gershon (1971).

[40] Steriade *et al.* (1989).

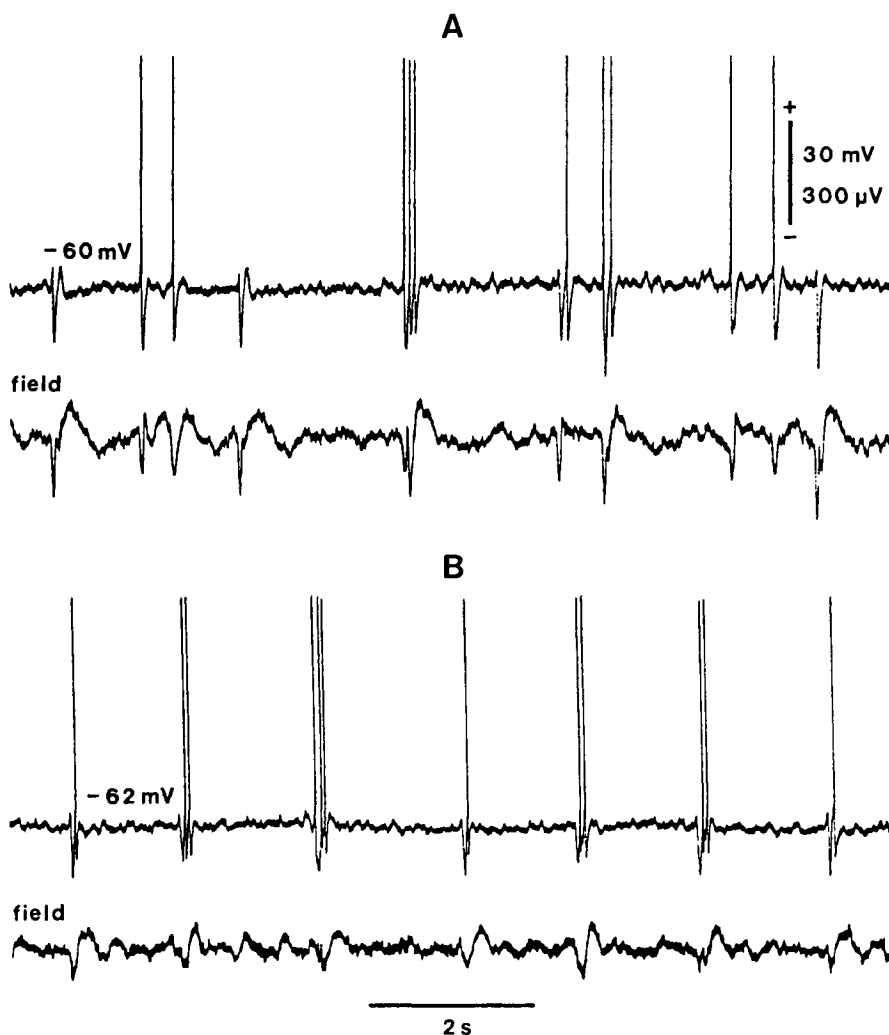


Figure 9.16. Simultaneous recordings of spontaneous PGO waves and intracellular events in two LG thalamic relay neurons of cat. Traces in A were recorded under urethane anesthesia, and those in B in a brainstem-transected cat. Both animals were treated with reserpine (1 mg/kg, i.p.) 24 hr before the recording sessions. From Hu *et al.* (1989c).

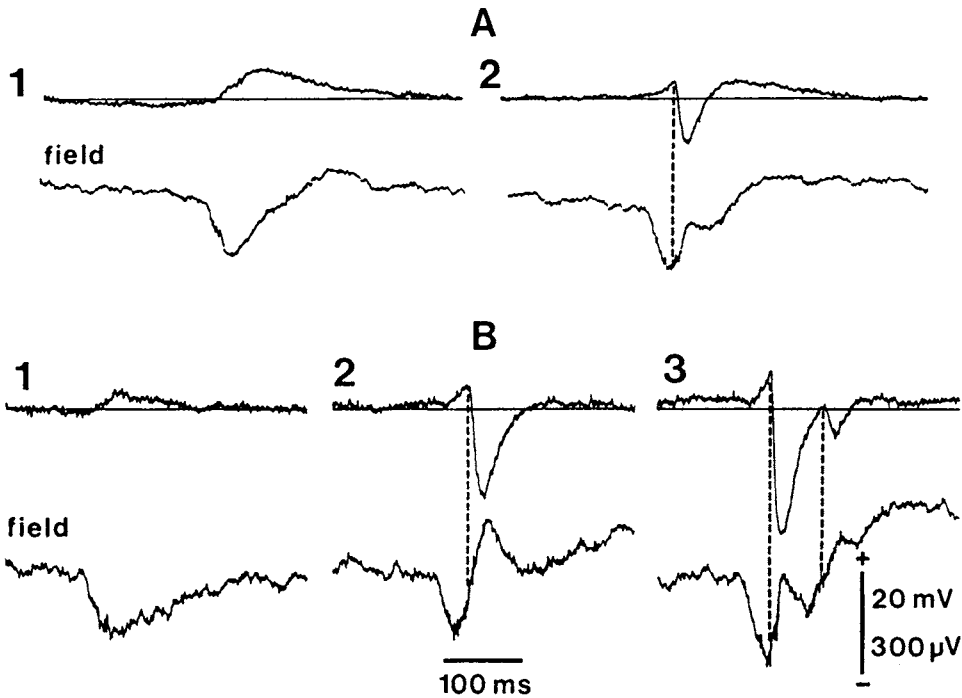


Figure 9.17. Sample of spontaneous PGO waveforms with their intracellular counterparts taken from two LG thalamic neurons (A and B) in cats under urethane anesthesia and reserpine treatment. Negative PGO waves showing a smooth return toward the baseline were usually correlated with pure depolarizing events in LG neurons (A1 and B1). When the negativity was interrupted by a positive going deflection, a prominent IPSP was always present in the intracellular traces (A2, B2–3). Double-notched PGO waveforms were correlated with the appearance of a second IPSP in the traces (B3). Vertical lines indicate the IPSP onset and emphasize the close time relation between IPSPs and the positive upswing in the field potentials. All cells were slightly hyperpolarized to prevent spike discharges. From Hu *et al.* (1989c).

The intracellular events of LG TC neurons associated with the PGO field potential recorded in the vicinity of the micropipette can be summarized as follows. Each PGO field potential is associated in the intracellular recording with a depolarizing potential, interrupted by a short-lasting (50–60 ms) hyperpolarization whose initiation lags the onset of the depolarizing component by 40 to 80 ms (Fig. 9.16). The total duration of the depolarization is about 200–300 ms and firing may occur during the early phase (2nd and 3rd PGO waves in Fig. 9.16A) or after the completion of the hyperpolarizing component (6th PGO wave in Fig. 9.16A, and 1st PGO wave in Fig. 9.18, A1).

The expanded intracellular records in Fig. 9.17 show that: (1) the field negativity is associated with a purely depolarizing potential (A1 and B1); (2) a positive-going upswing deflection correlates with a transient hyperpolarization (A2); and (3) a second positive upswing in the field potential is associated with a second hyperpolarization (B3). Upon passage of hyperpolarizing currents, the

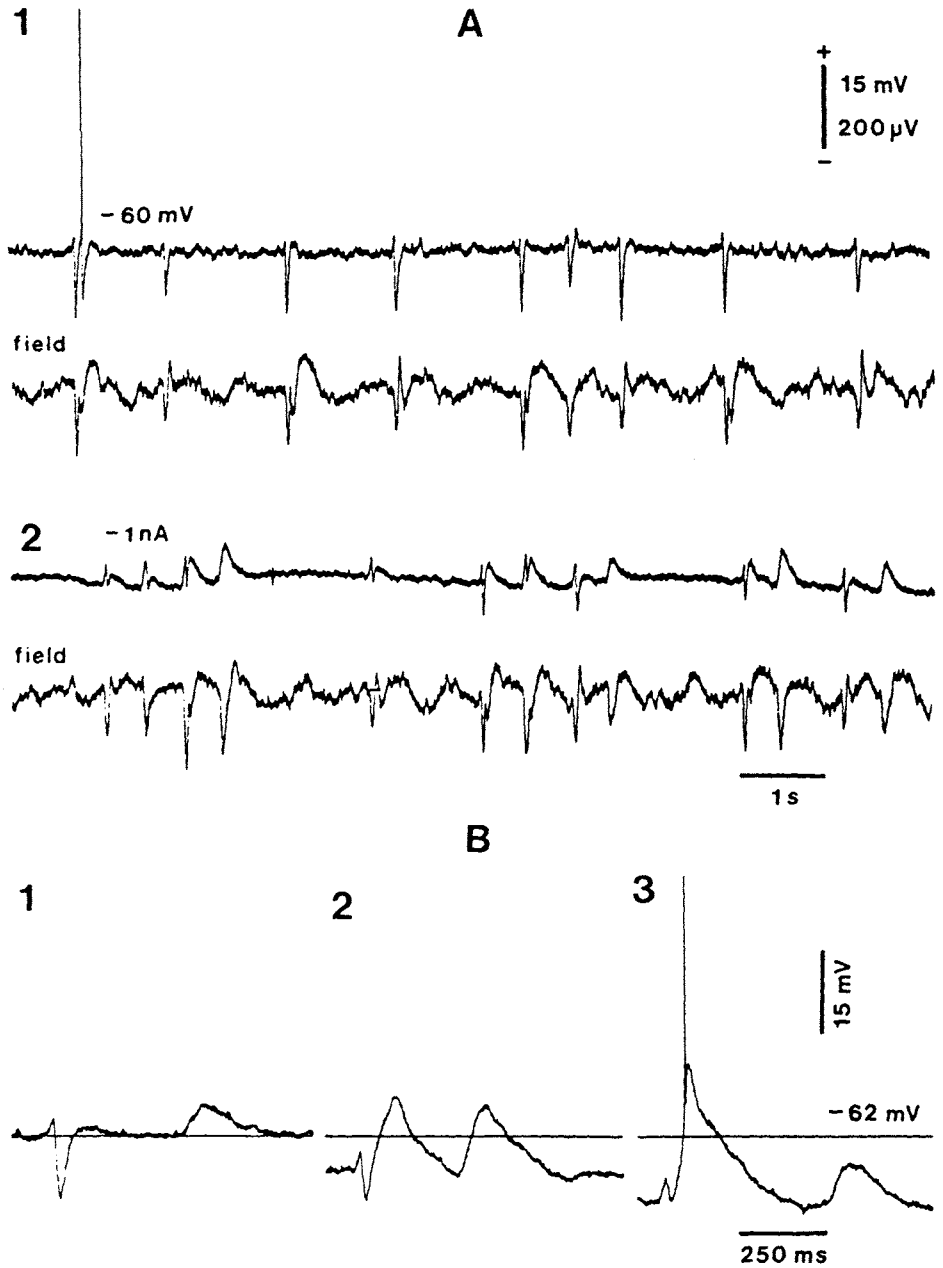


Figure 9.18. Effect of membrane hyperpolarization on PGO waves recorded intracellularly in LG neurons of reserpinized cats under urethane anesthesia. Spontaneous PGO waves were recorded at rest (A1) and during a sustained injection of inward current (A2). Note that the depolarization increased in amplitude while the size of IPSPs decreased. In the other example (B), the cell displayed at rest a stereotyped PGO activity consisting of doublets: a biphasic PGO wave followed by a monophasic one. Membrane hyperpolarization to -68 mV (B2) increased the size of the depolarization and when the membrane potential reached -74 mV (B3), a low-threshold response with a fast action potential was triggered by the first PGO event. From Hu *et al.* (1989c).

amplitude of the depolarizing potential increases, whereas the amplitude of the hyperpolarization decreases (Fig. 9.18, A2). When PGO waves occur in doublets, the first wave is made of a depolarization followed by a hyperpolarization, while the second one consists of a pure depolarization (Fig. 9.18, B1). Upon hyperpolarization by 8 mV, the depolarization becomes larger (B2) and further hyperpolarization reaching 12 mV from the resting membrane potential triggers a low-threshold spike (B3); simultaneously, the hyperpolarizing component becomes smaller and eventually is no longer visible. The membrane conductance increases by 25–40% during the PGO wave, and this is observed even when the hyperpolarizing event is not detectable [38].

Iontophoresis of nicotinic blockers (mecamylamine or hexamethonium) in the thalamic LG nucleus strongly depresses the unit activity related to “spontaneous” PGO waves under reserpine or to PGO waves evoked by brainstem PPT stimulation, while muscarinic blockers (scopolamine) have no significant effect on PGO-related unit activities [25]. These data are in line with earlier results obtained by means of systemically injected mecamylamine [24].

In conclusion, the thalamic PGO wave involves a direct nicotinic excitation of LG relay cells by brainstem cholinergic neurons and an activation of intra-LG inhibitory interneurons that is reflected in the PGO-related inhibitory postsynaptic potential (IPSP) seen in LG relay cells. In fact, presumed LG interneurons display an initial depolarization during PGO field potentials that may reach firing that is closely coupled with the IPSP onset in LG relay cells [41]. While the GABAergic neurons in the PG sector of the thalamic reticular nucleus are also activated during PGO waves in the chronically implanted, naturally sleeping animal [40], the PG neurons do *not* fire in response to the brainstem PB volley in the restricted, acute experimental conditions involving visual cortex ablation [38], probably because their discharges require a certain depolarizing pressure from corticofugal fibers. Thus, in the acute intracellular recordings reported above, the only source for the IPSPs observed in LG relay cells is the pool of intra-LG GABAergic interneurons.

[41] See Fig. 9 in Hu *et al.* (1989c).

9.3.3. PGO-Related Thalamic Neuronal Activities During Natural Sleep

By contrast with reserpine-induced PGO waves in acutely prepared animals, which do not exhibit fluctuations in behavioral states (so-called state-independent PGO waves), the naturally sleeping animal provides the

advantage of studying the cellular correlates of thalamic PGO waves during two different stages of the sleep cycle: the pre-REM transitional epoch accompanied by EEG synchronization (see Fig. 1.5 in Chapter 1) and the full-blown REM sleep associated with EEG activation. As mentioned above and in Chapter 5, thalamic neurons operate in two distinct modes during states associated with EEG synchronization as opposed to EEG-activated behavioral states. During EEG-synchronized sleep, almost 50% of interspike intervals of LG-cells' spontaneous discharges are grouped between 2 and 3 ms, thus reflecting the high intraburst frequencies (>300 Hz) characteristic for this stage of sleep, and the relation between LG thalamic bursts and spindle waves at 7 Hz is reflected by a late mode at 120–160 ms in the interspike interval histogram, representing the silent periods between 7-Hz spike bursts (see top panel in Fig. 9.19). On the other hand, during REM sleep, the proportion of intervals within the 2–3 ms class is negligible, betraying the inactivation of bursts due to the tonic depolarization of LG relay cells (bottom panel in Fig. 9.19). The pre-REM stage is intermediate between the EEG-synchronized sleep and REM sleep.

What is then the thalamic response to the brainstem-generated PGO volley during the pre-REM stage when TC neurons are hyperpolarized by about 7–10 mV and during REM sleep when the same neurons are tonically depolarized? And how do these possibly different responses of LG neurons influence the signal-to-noise ratio in the visual channel, that is, the ratio between the neuronal activity related to the PGO signal and the background firing of the same cell? As PGO waves are commonly regarded as the physiological correlate of dreaming, the last question may give clues as to the vivid imagery during the pre-REM stage, as compared to REM sleep. These topics have been investigated in the chronically implanted, behaving cat [40]. Thus, the activity of LG neurons related to PGO field potentials, simultaneously recorded with the same microelectrode, is quite different during pre-REM and REM sleep. (1) During pre-REM, the activity of LG TC cells starts with a short (7–15 ms), high-frequency (300–500 Hz) spike burst coinciding with the initial negativity of the PGO wave, and continues with a train of single spikes at 50–80 Hz, lasting for 200–400 ms (Fig. 9.20, top panel). (2) During REM sleep, the rate of LG-cells' spontaneous firing is 1.5- to 3-fold higher than in pre-REM, the peak-to-peak amplitudes of PGO waves are 2–3 times lower, and the PGO-related activity of LG neurons lack the initial high-frequency burst that is characteristic for the pre-REM stage (Fig. 9.20, bottom panel). The peri-PGO histograms of neuronal activities in the two LG elements

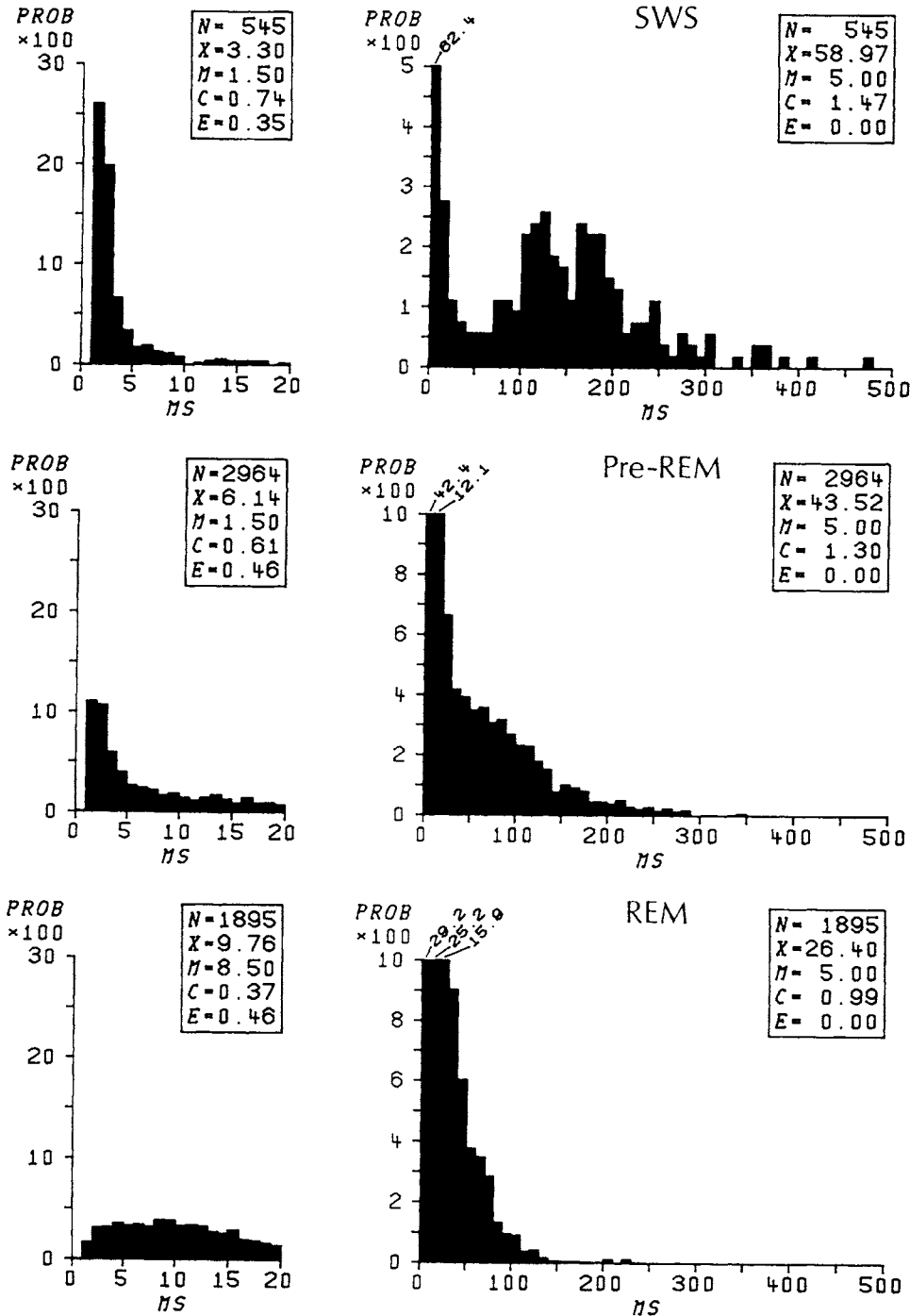


Figure 9.19. Interspike interval histogram (ISIh) of an LG thalamocortical cell during slow-wave sleep (SWS), pre-REM stage, and REM sleep in chronically implanted cat. In each state, two ISIh's are shown, with 1-ms bins (left) and 10-ms bins (right). Symbols: N , number of intervals; \bar{X} , mean interval (in ms); M , interval mode (in ms); C , coefficient of variation; E , proportion of intervals in excess of the depicted time range. Since the percentages of intervals exceed the ordinate maximum in first bins of right panels, the real percentages are indicated. From Steriade *et al.* (1989).

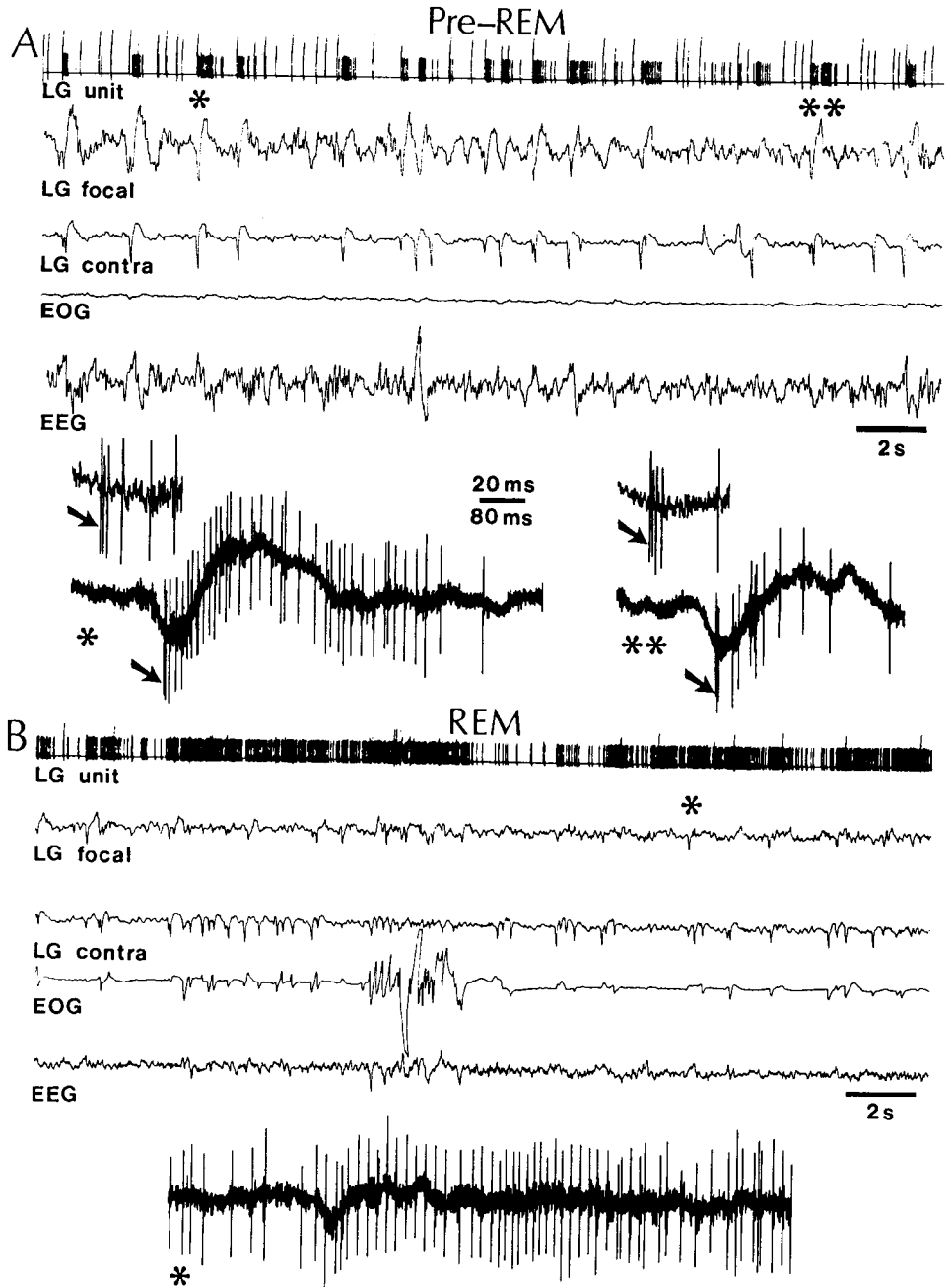


Figure 9.20. PGO-related activity of an LG thalamocortical (TC) cell during pre-REM epoch and REM sleep in chronically implanted cat. Ink-written records depict unit discharges (deflections exceeding the common level of single spikes represent high-frequency spike bursts), focal waves recorded by the same microelectrode, electrical activity in the contralateral LG nucleus recorded by a coaxial electrode, eye movements (EOG), and cortical EEG. In both pre-REM (A) and REM (B) sleep, PGO-related unit activity is depicted with original spikes below each ink-written recording. Note the tonically increased firing rate in REM, the smaller amplitudes of PGO field potentials in REM (compared with pre-REM), and the absence of PGO-related spike bursts in REM (contrasting with their presence, arrows, in pre-REM). From Steriade *et al.* (1989).

depicted in Fig. 9.21 show that the signal-to-noise ratio reaches values of about 6 to 7 during the pre-REM epoch, whereas the ratio values during REM sleep are between 1.5 and 2.5. Less dramatic but consistent effects are seen when examining the pooled signal-to-noise ratio in all analyzed LG neurons, with values of 2.4 during pre-REM and 1.6 during REM sleep (Fig. 9.22).

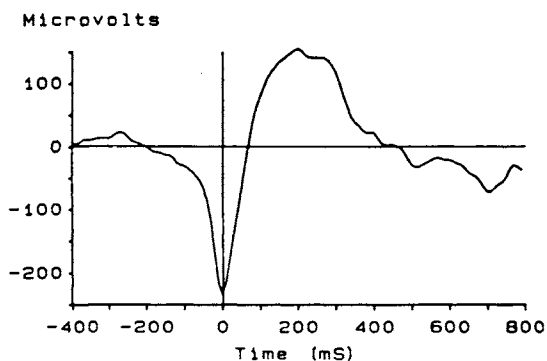
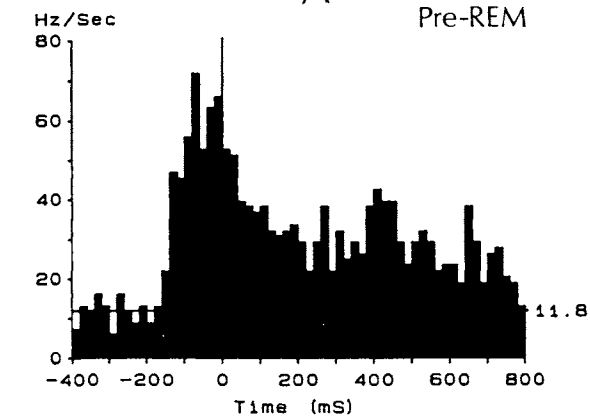
The stereotyped features of the burst which starts the PGO-related activity of LG neurons during the pre-REM stage indicates that it is probably a low-threshold Ca^{2+} spike crowned by high-frequency Na^+ action potentials (see Chapter 5). Further evidence for this assumption comes from the peri-PGO burst occurrence showing a markedly decreased probability of bursts for 300–400 ms after the PGO wave (Fig. 9.23). It is known that the relative refractory period of the low-threshold spike in thalamic neurons may reach 200–300 ms [31]. The hypothesis then emerged that the much larger amplitude of spiky PGO field potentials during the pre-REM stage, as compared to PGO waves during REM sleep (see averaged PGO field potentials in Fig. 9.21), is due to synchronous bursts in pools of LG neurons.

The greater signal-to-noise (PGO-to-spontaneous discharge) ratio in the geniculostriate channel during the pre-REM stage than during REM sleep suggests that the vivid imagery associated with dreaming sleep may appear well before REM sleep, during a period of apparent EEG-synchronized sleep. As to whether or not one may speak about dreaming behavior when discussing results obtained in animal studies, a positive answer is provided by experiments in which a behavioral repertoire typical for dreaming mentation was obtained after having prevented muscular atonia by adequate lesions of certain brainstem structures (see Chapter 1). The idea that PGO waves with greater amplitudes during the pre-REM stage may reflect more vivid imagery during that epoch than even during REM sleep [40] corroborates earlier data [42] in which the rebound (or compensation) phenomenon was studied after REM sleep deprivation in cats. Instead, however, of the standard deprivation of REM sleep, those investigators interrupted sleep immediately after the occurrence of the first PGO wave (during the period we term pre-REM) and eliminated about 30 s of the EEG-synchronized sleep that precedes fully developed REM sleep [42]. The comparison between the standard REM sleep deprivation and the “PGO deprivation” led to the conclusion that “the crucial factor in the so-called REM sleep deprivation–compensation phenomenon is the deprivation of phasic events.” And the increase in total REM time after deprivation was regarded “as a response to an accumulated need for phasic events,

[42] Dement *et al.* (1969; pp. 310–311).

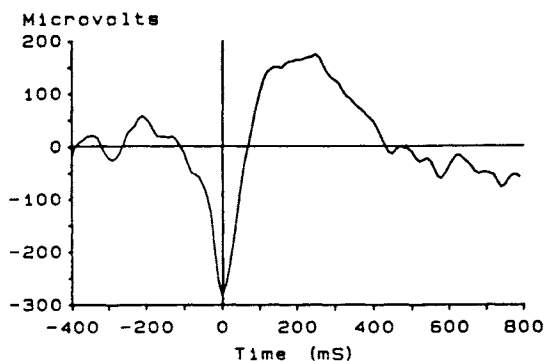
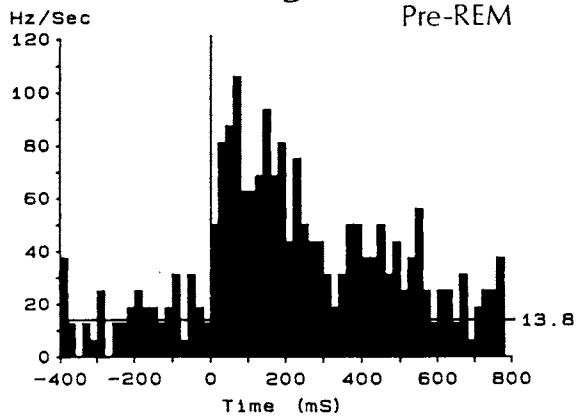
A

Pre-REM

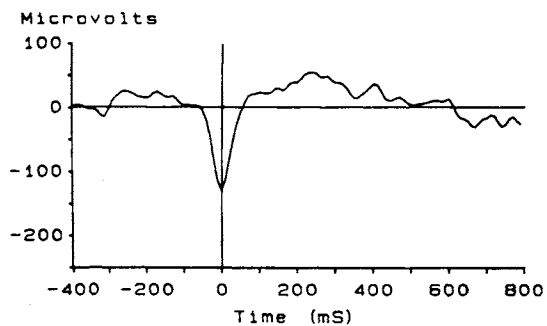
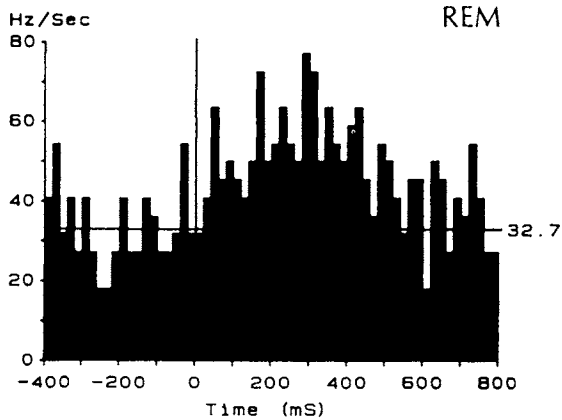


B

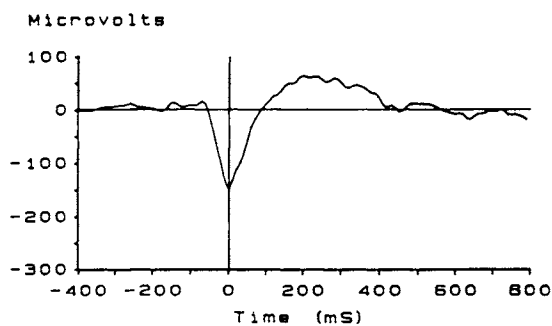
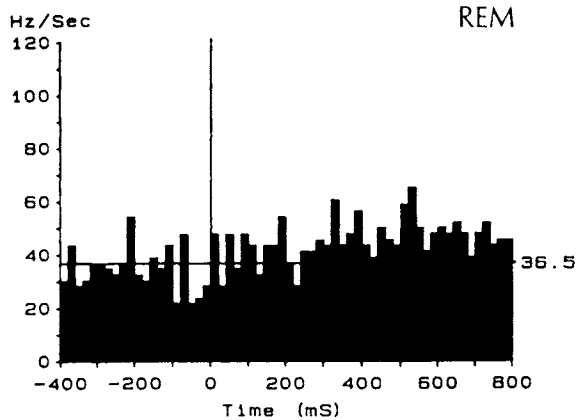
Pre-REM



REM



REM



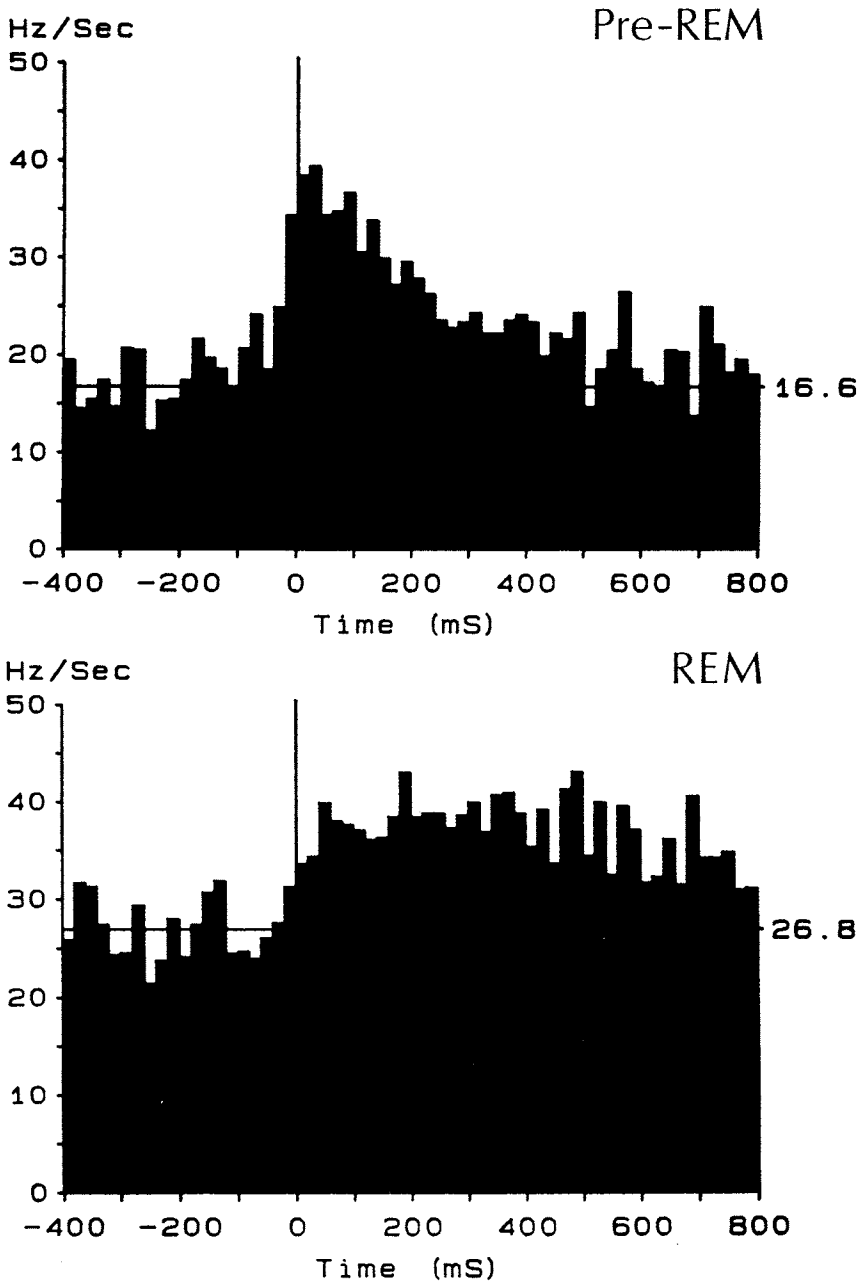


Figure 9.22. Pooled peri-PGO histograms of unit discharges in a sample of 15 LG thalamic relay neurons during pre-REM and REM sleep in naturally sleeping cats. Time 0 taken at the same point as in Figure 9.21. Level of spontaneous firing (16.6 and 26.8 Hz) is also indicated. From Steriade *et al.* (1989).

Figure 9.21. Peri-PGO histogram of LG unit discharges and averaged focal PGO waves from the same epochs during pre-REM and REM sleep in chronically implanted cat. A and B, two LG thalamocortical (TC) neurons. The average level of

spontaneous discharges (11.8 Hz, etc) is also indicated in each histogram. A, 19 PGO events in pre-REM, 11 PGO events in REM sleep. B, 8 PGO events in pre-REM, 23 PGO events in REM sleep. From Steriade *et al.* (1989).

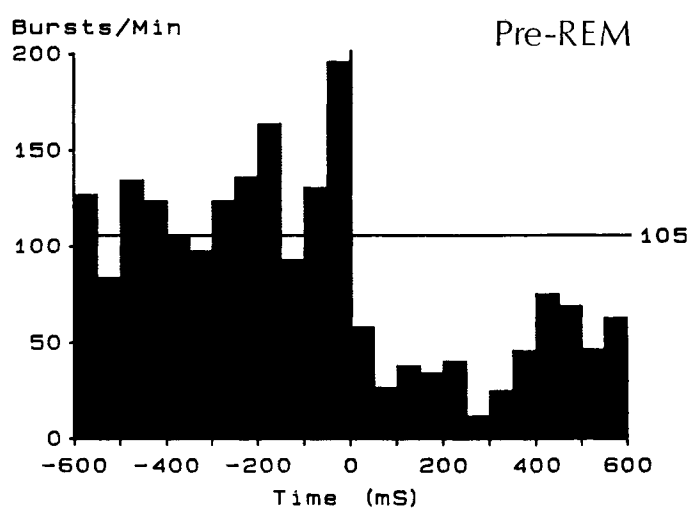


Figure 9.23. Probability of high-frequency spike bursts before and after pre-REM PGO waves in a sample of 11 LG neurons. Time 0 is the peak of the negative PGO wave (as in two preceding figures). For criteria of bursts and their computer-detection, see Methods in Steriade *et al.* (1989).

rather than a response to the loss of REM sleep per se". The observation that some of the dream reports from EEG-synchronized sleep are indistinguishable from those obtained from REM sleep awakenings [43] suggests that such dreams occur during the pre-REM stage and invites researchers to explore the dreaming imagery during the period immediately preceding REM sleep in humans.

[43] Hobson (1988); see also Hobson and Pace-Schott (2002).

Motor Systems

The first seven sections of this chapter review the brainstem oculomotor system, while the last sections will review mechanisms involved in production of the muscle atonia of REM sleep. With respect to the oculomotor system, conjugate eye movements include saccades, pursuit movements, and the eye movements associated with optokinetic and vestibular nystagmus. In this chapter we shall review in some depth the brainstem role in production of one of these conjugate eye movements, saccades, since these play such a prominent role in both waking and REM sleep and much has been learned about their brainstem mechanisms.

10.1. Saccadic Eye Movements

Saccades are rapid eye movements comprised of a rapid acceleration to peak velocity and a deceleration that brings the eye to its final position. In primates, saccades usually last 15–100 ms and may have peak velocities of more than 500 degrees per second. All saccades are thought to share a common generator, and it is this common brainstem generator that has been the subject of intense and productive work over the last 20 years [1]. We will adopt an “outside in” approach and describe the system beginning at the oculomotor neurons and then move centrally. The anatomical locus of the various neuronal types involved in saccade generation will be described in conjunction with the physiology. It is worth emphasizing that the somewhat vague term “paramedian pontine reticular formation” (PPRF) used in early papers to describe the locus of reticular neurons participating in saccade generation can, in most cases, be replaced by more precise anatomical terms.

[1] Fuchs *et al.* (1985).

10.1.1. Physiological Properties of Oculomotor Neurons

During visual fixation, oculomotor neurons discharge tonically at a fixed rate proportional to the degree of muscle tension required to maintain the fixation. Hence, rate is maximal at the extreme “on” direction of the controlled muscle, such as extreme leftward fixation for the left abducens motoneurons. Threshold for the onset of this tonic discharge is usually within $10\text{--}20^\circ$ in the “off” direction, that is, rightward fixation for left abducens motoneurons. Between threshold and maximal rate each neuron has its own constant of proportionality, termed K , relating firing rate and fixation change in degrees. Typical K values range from 1–12 spikes per second per degree.

For saccadic changes in position in the “on” direction, there is a rapid acceleration of firing rate some 8 ms prior to saccade onset, then a slight decrease in frequency during the saccade, with a rapid deceleration and cessation of discharge some 10 ms prior to saccade end (Fig. 10.1). The duration of this heightened firing rate codes saccade duration, which in turn determines the magnitude of eye position change. The convention in the oculomotor literature is to refer to the heightened firing rate as a “burst,” and to designate neurons with a firing pattern consisting of short-term or phasic discharges as “burst” neurons. Because this convention is so well entrenched we will use it, but the reader is warned that the term “burst” pattern would, in our opinion, be better rendered as “phasic” pattern so as to reserve the term “burst” for truly stereotyped

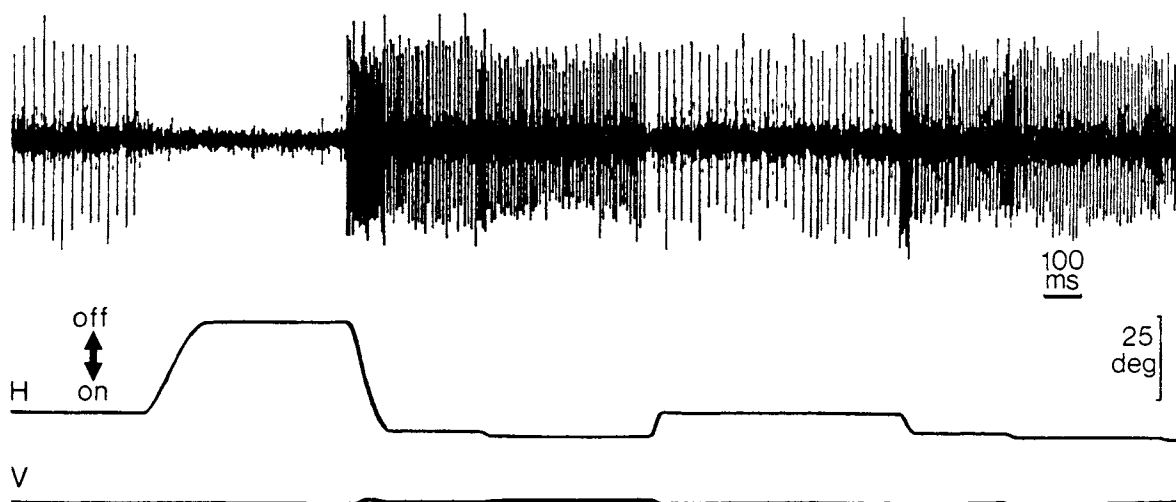


Figure 10.1. Discharge pattern of an identified motoneuron in the abducens nucleus of the monkey. The arrow above the horizontal channel (H) indicates the “on” and “off” directions of this motoneuron. From Fuchs *et al.* (1985).

clusters of spikes, such as those seen with Ca^{2+} spikes in thalamic and brainstem reticular neurons (see Chapter 5). It is of interest from the point of view of intrinsic properties of neurons that abducens neuronal discharge frequencies during a saccade are frequently 400 spikes/s and may peak at 800 spikes/s. However, only the first 3–5 spikes have shorter interspike intervals than the steady-state level, which is always reached within 50 ms, shorter than the usual burst [2]. Thus, while it is indeed possible that the initial spikes might reflect a pattern determined by intrinsic membrane properties (see Chapter 5), the entire run of clustered spikes characteristic of an oculomotor system “burst neuron,” is too long for this explanation. Other characteristics of motoneuron firing during saccades are determined by input from afferent neurons. It is thought that in general the “tonic” and “phasic” components are coded separately. Special cases are medial and lateral rectus motoneurons, which receive inputs from the contralateral abducens and from the prepositus hypoglossi, respectively, which have combined “tonic–phasic” information.

[2] Grantyn and Grantyn (1978).

10.1.2. Afferents to Oculomotor Neurons: Lesion Studies

That the site of afferent input generating the saccade-related discharge of motoneurons was the nearby reticular formation was suggested by early electrolytic [3] and, later, kainic acid lesions [4] placed in the pontine reticular formation (PRF) region rostral to abducens and bounded dorsally by medial longitudinal fascicle (MLF) and ventrally by nucleus reticularis tegmenti pontis. Unilateral lesions in this reticular zone produce an enduring paralysis of horizontal eye movements toward the side of the lesions. Vertical eye movement deficits are produced by unilateral lesions in the rostral interstitial nucleus of the MLF (riMLF, a portion of midbrain reticular formation) in the monkey [5] and of the homologous nucleus of the pre-rubral field in the cat [6]. Bilateral kainic acid lesions, even small, in caudal PRF lead to a severe disruption of rapid eye movements in all directions (Fig. 10.2). These studies suggest that a population of neurons important for horizontal eye movements is present in the rostral PRF and that a population important for vertical eye movements is present in the midbrain reticular formation, whereas the caudal PRF may be important for all saccades. Anatomical studies described below have more specifically implicated these and other portions of brain stem reticular formation as projecting to abducens and other oculomotor nuclei.

[3] Goebel *et al.* (1971).

[4] Lang *et al.* (1982);
Henn *et al.* (1984b).

[5] Büttner-Ennever and Büttner (1978).

[6] Graybiel (1977a).

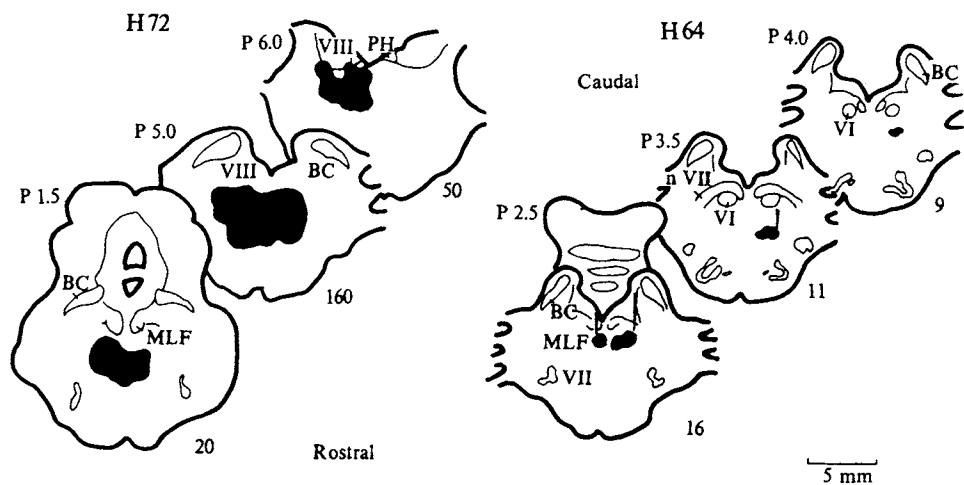


Figure 10.2. Bilateral kainic acid lesions in the caudal PPRF of two monkeys (H72 and H64) that disrupted saccades in all directions, even when the lesions were small (H64). Numbers above drawings of sections indicate stereotaxic planes of coronal sections. BC, brachium conjunctivum; MLF, medial longitudinal fasciculus; PH, nucleus prepositus hypoglossi; VI, abducens nucleus; VII, facial nucleus; n. VII, facial nerve. From Henn *et al.* (1984b).

10.1.3. Efferent Projections of Abducens Neurons

In addition to neurons innervating the lateral rectus, and the projections of internuclear neurons to the group of medial rectus motoneurons in the oculomotor complex, there are projections to other oculomotor structures. About one-third of the internuclear neurons have axon collaterals that extend caudal to the abducens nucleus [7] where they may innervate the nucleus prepositus hypoglossi and parts of the vestibular complex [8]. There is also a population of abducens neurons that project directly to the flocculus of the cerebellum [9]. Thus, the abducens neurons have a much larger function than simple contraction of the lateral rectus muscle.

Physiological studies have described three types of brainstem neuron with discharge patterns linked to saccades. These are “burst” neurons, “omnipause” neurons and “tonic” neurons, and will be discussed in this order.

[7] Highstein *et al.* (1982).

[8] Baker and McCrea (1979).

[9] Alley *et al.* (1975); Langer *et al.* (1985).

10.2. Burst Neurons

10.2.1. Burst Neuron Physiology

Short-lead burst neurons (SLBNs) is the term used to designate the reticular neurons whose discharge commences about 8–10 ms prior to saccades, and continues

until near saccade offset (Fig. 10.3). Originally these neurons were called "medium-lead" to distinguish them from motoneurons, but short-lead is now in general use. The term "short-lead" is used in contradistinction to

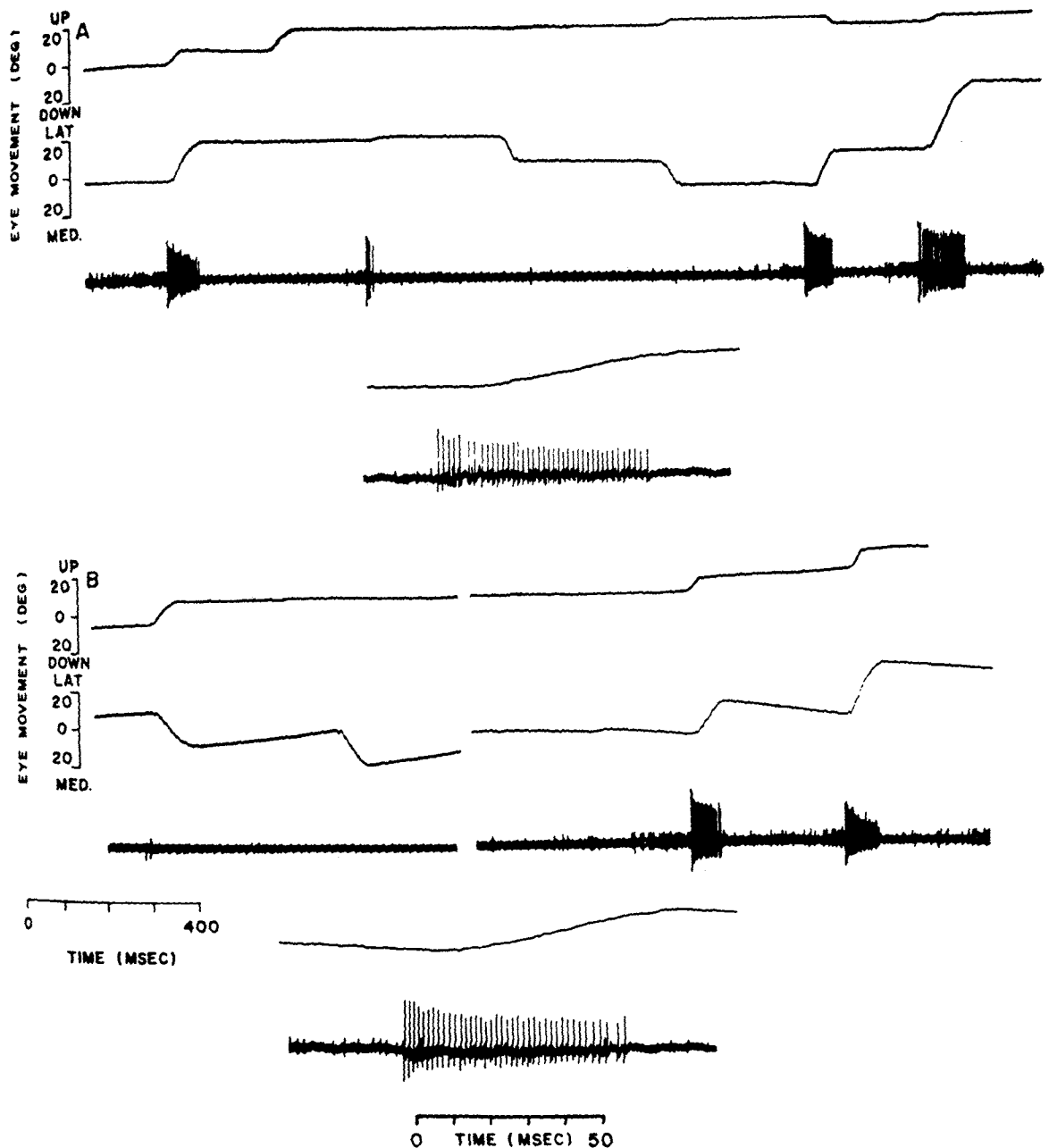


Figure 10.3. Activity of an ipsilateral short-lead burst unit in the cat during saccadic eye movement (A) and the quick-phase movements of rotationally induced vestibular nystagmus (B). In A and B, upper trace is vertical and middle trace is horizontal eye position. The time calibration for both shown below B.

Insets in A and B are high-speed records of one horizontal rapid eye movement and associated unit activity; inset time calibration is shown below B and eye movement calibration is the same as in low-speed records. From Keller (1974).

“long-lead” burst neurons (LLBNs), whose discharge onset may occur 100 ms or more prior to saccade onset. (Fig. 10.4 schematizes the discharge patterns of the various types of burst neurons described in this section.) While the SLBNs and LLBNs were originally described as separate [10], they now appear to be on a continuum, since intermediate lead times have now been described in cat and monkey [11]. Most pontobulbar burst neurons discharge most vigorously and earliest for ipsilateral horizontal saccades, although these neurons also show some discharge for vertical saccades. A smaller population of pontine neurons have near-vertical on-directions and still fewer have oblique on-directions.

There are two sub-classes of burst neurons.

Excitatory burst neurons (EBN) make monosynaptic excitatory connections with the ipsilateral abducens nucleus [12] and are localized to the ipsilateral dorsal PRF in both cat and monkey, as is more fully described below. These neurons are most dense within 2.0 mm of the midline in the cat [13]. Both SLBNs and LLBNs are found in this region, although in monkey LLBNs tend to occur more rostrally in the nongiant cell portion of PRF [10, 14].

Inhibitory burst neurons (IBN) [15] monosynaptically inhibit contralateral abducens neurons, are located in the dorsomedial pontobulbar reticular formation caudal and

[10] Luschei and Fuchs (1972).
[11] Kaneko *et al.* (1981); Scudder *et al.* (1982).
[12] Sasaki and Shimazu (1981).
[13] Keller (1974).
[14] Hepp and Henn (1983).
[15] Hikosaka *et al.* (1978).

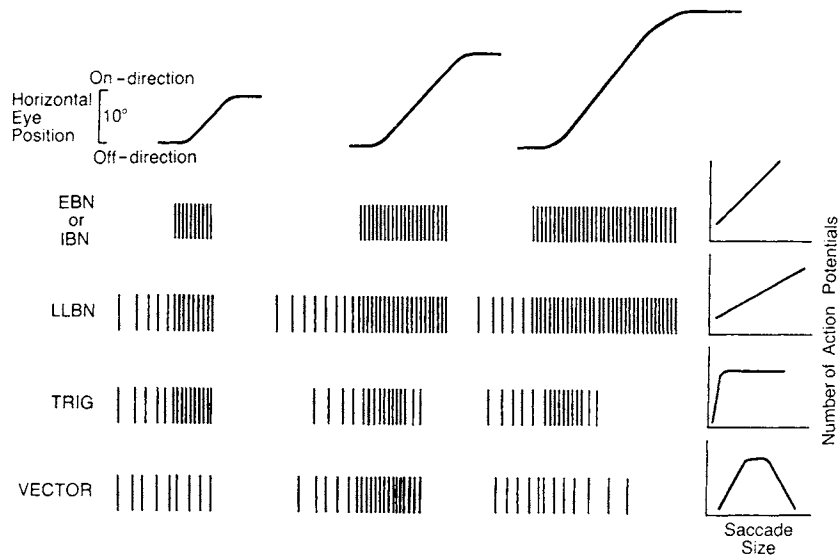


Figure 10.4. Schematic discharge patterns of the different types of burst neurons for three sizes of horizontal on-direction saccades. To the right, the number of action potentials in the burst is plotted as a function of saccade size for each unit type. The units are an excitatory (EBN) or an inhibitory (IBN) burst neuron, a long-lead burst neuron (LLBN), a trigger burst neuron (TRIG), and a vector burst neuron (VECTOR). From Fuchs *et al.* (1985).

- [16] Kaneko and Fuchs (1981); Scudder *et al.* (1988).
- [17] Büttner and Henn (1979); King and Fuchs (1979).
- [18] Nakao and Shiraishi (1983).
- [19] Büttner *et al.* (1977).
- [20] Robinson and Zee (1981).
- [21] van Gisbergen *et al.* (1981).
- [22] Yoshida *et al.* (1981).
- [23] Henn and Cohen (1976).

ventromedial to the abducens nucleus, and consist of both SLBNs and LLBNs in both cat and monkey [16].

Burst neurons with vertical on-directions have been recorded in the riMLF [17]. They resemble pontine SLBNs, but have shorter lead times. Within this area are both excitatory and IBN [18].

Most SLBNs have nearly horizontal or vertical preferred directions, and this may reflect coding either along the pulling planes of the extraocular muscles [19] or along the planes of the semicircular canals [20]. One approach to decoding saccade generation has been to evaluate certain parameters of SLBN discharge as determining saccade duration, peak velocity, and saccade size [10, 13, 16, 21, 22]. Another approach has been to consider saccades as vectors, with both angle and magnitude encoded by properties of pontine reticular neurons [14, 23] and it was concluded that SLBNs are the final common pathway for all rapid eye movements. Targets are initially centrally coded not in retinal but in head (spatial) coordinates. This centrally available target information is processed into a neuronal signal encoding an *eye displacement vector* to the target in the superior colliculus (SC) and the frontal eye fields (see below for discussion of these zones). The transformation of this spatial coding to the temporally coded discharges of SLBNs has been the object of a study that quantitatively analyzed the rapid eye movement parameters of LLBNs in monkey PRF in relationship to the corresponding firing patterns of SLBNs [14]. It was found that burst neurons in rostral PRF have predominantly *spatially coded* movement fields while in the caudal PRF there is *temporal coding* of burst strength in the pulling directions of extraocular eye muscles (near horizontal or near vertical). Both rostral and caudal PRF populations have ipsilateral on-directions and contain LLBNs. The temporally coded long-lead bursters, termed “direction bursters or D-burster” have discharge patterns similar to SLBNs, save for earlier “on” latencies and some preferences for small or large oblique saccades. The new feature postulated [14] is that the spatially coded burst neurons form a motor map of saccadic vectors. These spatially coded LLBNs are called “vector bursters or V-bursters” and discharge only for saccades to a limited region of the visual field, termed the cell’s “motor field.” The following signal transformation sequence was postulated. SC projects to V-bursters in spatial coding (head coordinates). V-bursters project to D-bursters in both PRF and mesencephalic reticular formation (MRF) and it is this projection which effects the transformation from head coordinates to eye position coordinates.

10.2.2. Anatomical Connectivity of Burst Neurons

10.2.2.1. Anatomy of Pontobulbar Reticular Projections to Abducens

Pontine reticular formation projections to abducens were first shown in anterograde tracing experiments in the cat [24]. In the region rostral to the abducens in the monkey, neurons projecting to the abducens are confined almost entirely to the ipsilateral region dorsomedial or medial to the large cell regions of the rostral and caudal medial PRF, while in the cat they are somewhat more dispersed and mingled with the large neurons of this region [25]. These neurons undoubtedly correspond to the physiologically defined EBNs.

In the cat just at and slightly caudal to the level of abducens, is another cluster of neurons in a contralateral region just lateral to the MLF but medial to the lateral border of abducens and extending dorsoventrally from the ventral border of abducens approximately to the same level ventrally as the MLF. This region is devoid of giant cells, being both somewhat dorsal to the giant cell zone and also in the pontomedullary junction portion of PFTG and BFTG that is without giant cells. In the monkey, the abducens projecting cells occupy approximately the same contralateral nongiant cell region as in the cat. These contralaterally situated neurons correspond to the physiologically defined group of IBNs. In the monkey, but not the cat, a few contralateral neurons are seen in reticular core rostral to the rootlets of the abducens nerve, in accord with physiologically defined burst neurons that fire before contralateral saccades [10, 23].

[24] Büttner and Henn (1976); Graybiel (1977b).

[25] Langer *et al.* (1986).

10.2.2.2. Nonreticular Brainstem Projections to Abducens

In both the cat and the monkey, the largest source of abducens afferents was found to be bilateral projections from the ventrolateral vestibular nucleus and the rostral pole of the medial vestibular nucleus [25]. This suggests the heavy vestibular labeling found in previous retrograde tracing studies [26] was due to Horse-radish peroxidase (HRP) deposition in the abducens nucleus and not in the PRF, which, by contrast was shown to have only relatively sparse afferents from vestibular nuclei (Fig. 10.5) [27]. Large numbers of abducens-projecting neurons are also found in the ventral margin of the nucleus prepositus hypoglossi in the cat and the common margin of this nucleus and the medial vestibular nucleus in the monkey.

[26] Stanton and Greene (1981).

[27] Shammah-Lagnado *et al.* (1987).

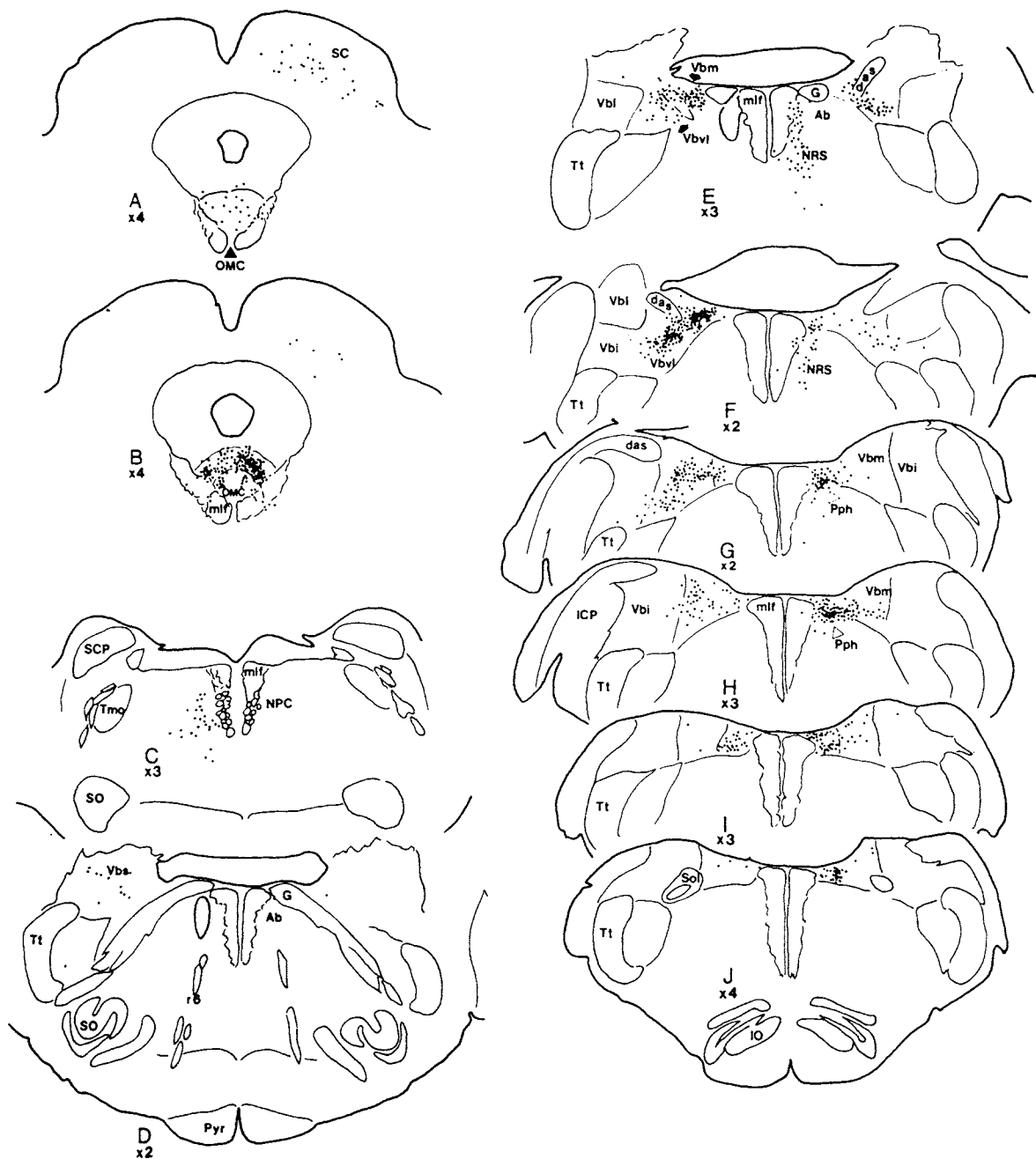


Figure 10.5. Distribution of retrogradely labeled neurons after HRP injection in cat right abducens nucleus. The ellipsoid shape just to the left of MLF in sections E and D indicates the injection site. Each dot represents one retrogradely labeled neuron. The numbers under the section letters indicate the number of histological sections that were compressed into the illustrated section.

Abbreviations: Ab, abducens nucleus; SC, superior colliculus; OMC, oculomotor complex; NPC, nucleus reticularis pontis caudalis; G, Genu of VII; Vb, vestibular nuclei; i, l, m, and s, inferior, lateral, medial, and superior, respectively; NRS, nucleus reticularis supragigantocellularis (a nongiant cell zone dorsal to the FTG); Pph, prepositus hypoglossi. From Langer *et al.* (1986).

The prepositus/medial vestibular complex and projection to oculomotor neurons may be the source of the “neural integrator”; these neurons show burst-tonic discharge patterns (see below). In the monkey, large numbers of neurons are present in contralateral medial rectus subdivision of the oculomotor complex, while in the cat large numbers of retrogradely labeled neurons are seen in a small periaqueductal gray nucleus just dorsal to the caudal pole of the oculomotor complex. Both species have a few contralateral SC neurons projecting to the abducens. The monkey but not the cat has abducens-projecting neurons in the nucleus reticularis tegmenti pontis and in the ipsilateral riMLF and bilateral interstitial nucleus of Cajal.

10.2.2.3. Superior Colliculus and Frontal Eye Field Projections to Reticular Formation

The paramedian pontine reticular region involved in saccade generation receives important input from higher centers. The contralateral SC provides a monosynaptic excitatory input to medial pontobulbar reticular formation in both cat [28]. Recordings in alert monkeys indicate this short-latency input is to LLBNs and to omnipause neurons (OPNs) (see below) but not to SLBNs [29]. The likely cellular source of this SC input has been identified using intraaxonal labeling of squirrel monkey SC neurons whose saccadic parameters had been defined in the alert animal [30]. One type of tectal efferent neuron morphologically identified as the T group was found to send axonal projections to the contralateral predorsal bundle (Fig. 10.6A), whose targets include the pontine nuclei reticularis pontis oralis and caudalis [31]. Axonal collaterals also contact eye movement-related areas of MRF as well as other tectal neurons. These neurons discharge with intense bursts beginning about 20 ms before spontaneous saccades within their movement field (see Fig. 10.6B) and hence were termed “vectorial” bursters. This wiring is compatible with the notion of the SC as transforming retinal error signals into motor commands and transmitting them to preoculomotor structures.

In addition to a frontal eye field to SC projection [32], there is a direct frontal eye field (prearcuate frontal cortex) to PPRF projection [33].

[28] Grantyn and Grantyn (1976).

[29] Raybourn and Keller (1977).

[30] Moschovakis *et al.* (1988a, b).

[31] Harting (1977).

[32] Segraves and Goldberg (1987).

[33] Leichnetz *et al.* (1984).

10.3. Omnipause Neurons

Omnipause neurons (OPNs, Fig. 10.7) are characterized by pauses that begin shortly before saccades in all directions (latency of 13–16 ms) and are thought to exert

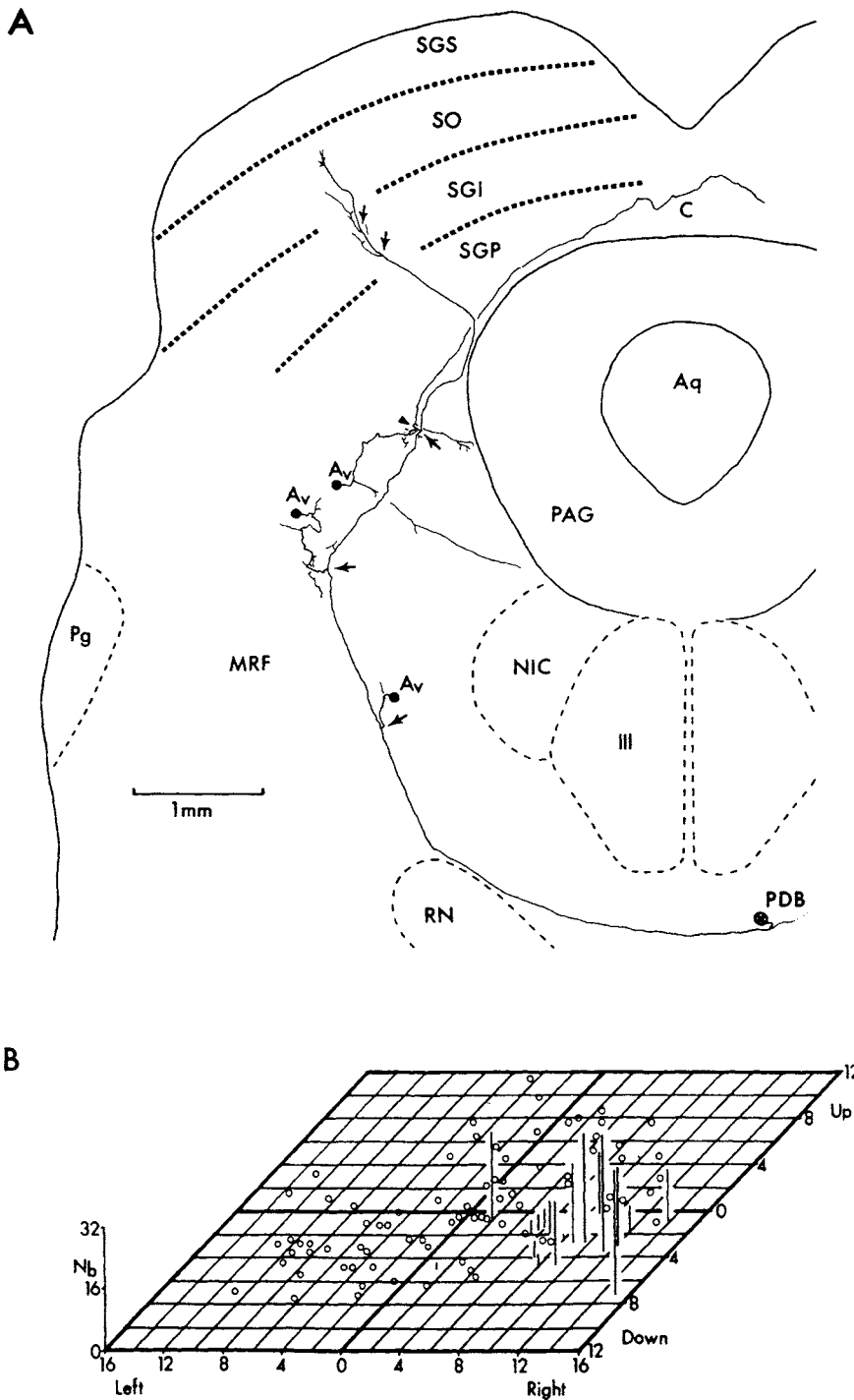


Figure 10.6. A: Camera lucida reconstruction of initial axonal system of a centrally located tectal long-lead burst neuron. Solid triangle in the reticular formation points to origin of the commissural (C) branch from one of the ascending fibers. X in circle indicates the point of descent to pons in the predorsal bundle (PDB). B: Plot of the number of spikes in burst (N_b) for the neuron shown above, as a function of amplitude of horizontal and vertical displacement of the eyes. Axis labels indicate number of degrees displacement. Modified from Moschovakis *et al.* (1988b).

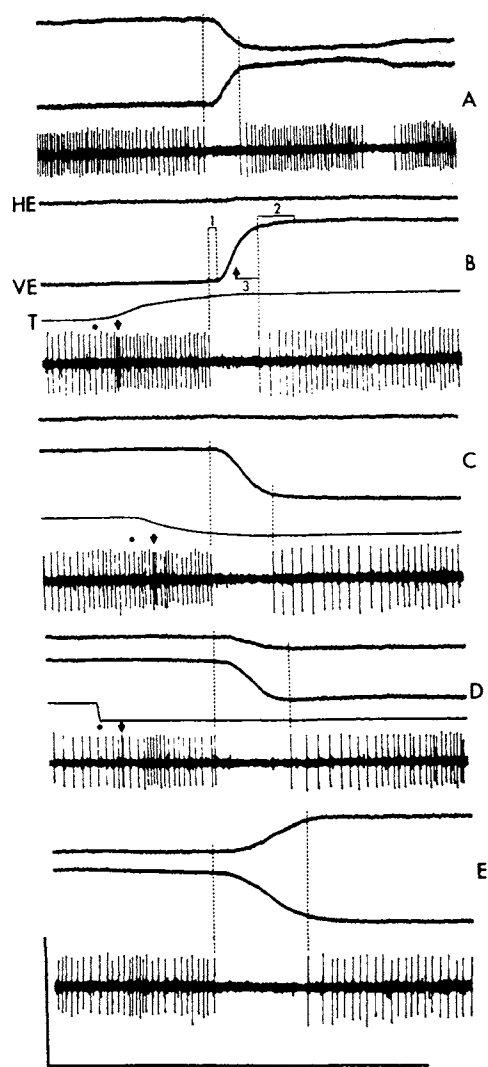


Figure 10.7. Discharge patterns of OPNs during spontaneous (A, E) and visually elicited (B–D) saccades. In B–D, the onset of the target movement (T) is indicated by a dot and the downward arrows point to the visual response. In B, period 1 is the interval from the beginning of the pause to the beginning of the saccade, period 2 is from the end of the saccade to the end of the pause, and period 3 is from maximum velocity (upward arrow) to the end of the pause. Calibration is 25° and 500 ms. From Evinger *et al.* (1982).

a tonic inhibition on the SLBNs of the medial PRF [34]. The arrest of the high frequency firing of OPNs (100–200 Hz) releases the SLBNs, whose activity, in turn, directly and indirectly excites the extraocular muscle motoneurons and leads to saccades. OPNs likely also project to riMLF [35].

In the monkey, the nucleus raphe interpositus (rip) has been identified as the anatomical locus of the OPNs [36]. The rip lies in the midline area at the same rostrocaudal level as the descending 6th nerve rootlets, that is, in caudal pons and including the most rostral

[34] Raybourn and Keller (1977); Evinger *et al.* (1982).

[35] Büttner-Ennever (1977).

[36] Büttner-Ennever *et al.* (1988).

portion of bulb. The rip is dorsal to the raphe pontis. Extracellular recordings were used to define units with omnipauser characteristics. As shown in Fig. 10.8, rip neurons in the monkey are arranged in a distinctive, narrow, orderly band on either side of the midline; these neurons have very large horizontally oriented dendritic trees that cross the midline. A similar morphology is found in the human, while in the cat and rat similar cell types are present but are not arranged in two distinct, bilateral groups. Rip is distinguished from raphe pontis by the presence in the latter nucleus of clustered neurons without large dendritic fields, and, in cytochrome oxidase stain, a darkly staining neuropile. Also, in contrast to raphe pontis, anterograde tritiated leucine studies indicate a direct projection from deep layers of SC, primarily crossed, to rip in contrast to no direct connectivity to raphe pontis and magnus.

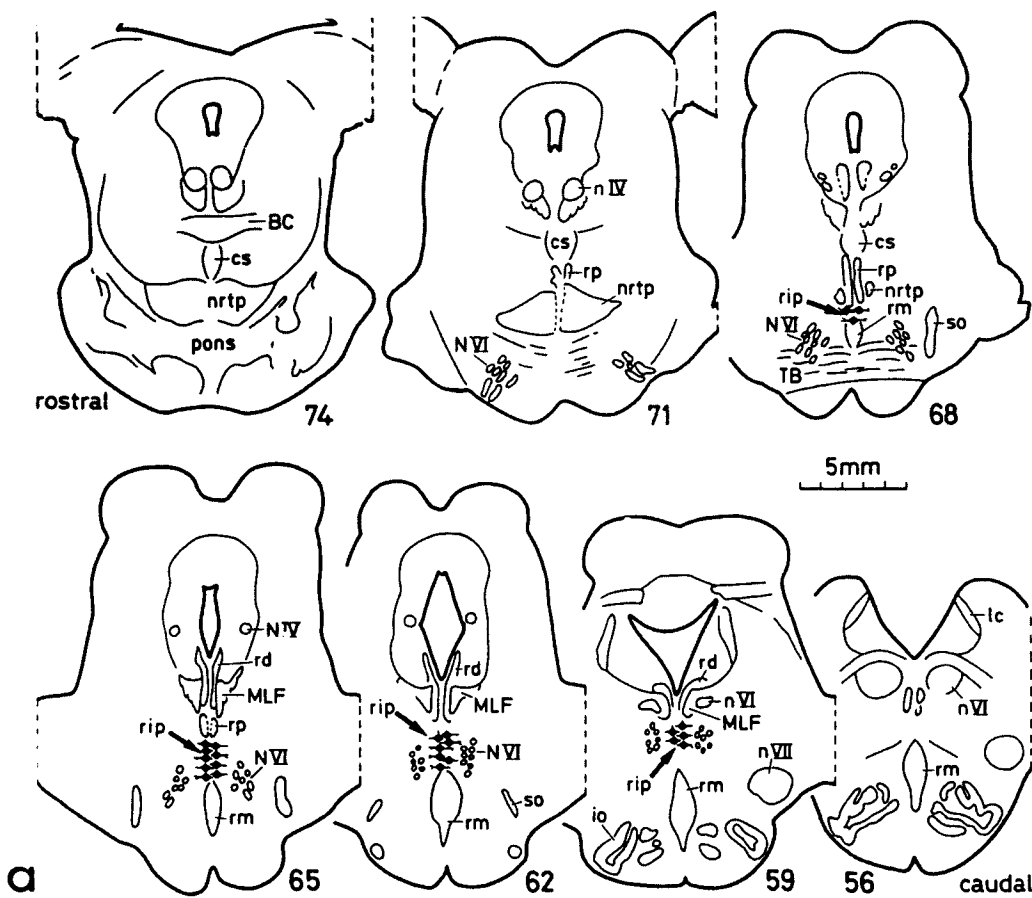
10.4. Tonic Neurons

We have previously discussed the saccade-related burst neuron input to the oculomotor system motoneurons. These motoneurons not only have a “burst” coding a change in eye position but a steady, tonic firing that codes eye position during fixation. How is the input to motoneurons for the steady fixation generated? As illustrated in Fig. 10.9, it was proposed that the “burst” discharge of excitatory and IBNs (which codes eye velocity) is integrated over time (in the mathematical sense) by a set of neurons called “the neural integrator” and that this integrator serves all systems using conjugate eye movements, that is, the saccadic, vestibuloocular, optokinetic, and smooth pursuit systems [37].

[37] Robinson (1975).

A few units have been found in PRF that carried a pure position signal [10, 13], compatible with the output of a neural integrator. However, PRF lesions did not produce neural integration deficits [4], suggesting the integrator might lie elsewhere. Kainic and ibotenic acid lesion experiments showed that the medial vestibular nucleus and nucleus prepositus hypoglossi are the locus of the neural integration of horizontal eye movements [38]. Microinjections of these neurotoxins into the prepositus medial vestibular nucleus complex of the monkey produced the characteristic stigmata of a “leaky integrator”: saccades were made with accuracy to targets but the fixation did not hold, and eye position drifted back to a null position with an exponential time constant whose rate of decay reflected the leakiness or damage to the integrator. The dynamism of this lesion is shown in Fig. 10.10,

[38] Cannon and Robinson (1987).



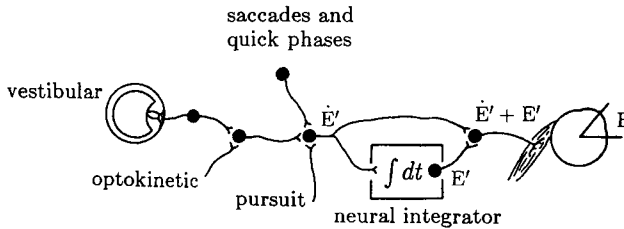


Figure 10.9. The final common integrator hypothesis. All eye movement commands are initiated as eye-velocity encoded signals, E' , which then enter the neural integrator to provide the eye-position encoded signal, E , present on the motoneuron. The arrangement is schematic and is only intended to show that all eye-velocity signals are passed directly to the motoneurons along with the integrated eye-position signals and is not intended to represent neurons actually involved in this process. From Cannon and Robinson (1987).

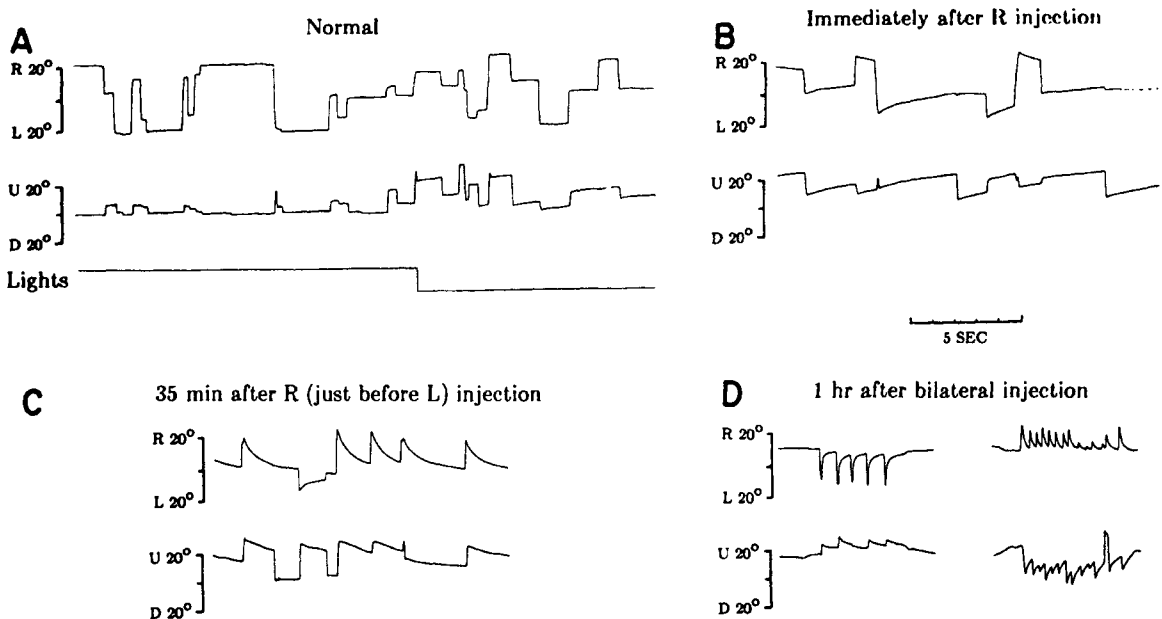


Figure 10.10. Saccadic eye movements before and after ibotenate injection in prepositus hypoglossi. Horizontal eye position is on upper trace, vertical on lower. A: target-directed and spontaneous saccades recorded from a normal monkey. In the first half of the record the fixation target was alternated between right and left 20° . For the second half, spontaneous eye movements were recorded in total darkness. Notice that even in total darkness horizontal gaze holding is steady. The upward drift in darkness is a form of downbeat nystagmus found in many normal rhesus monkeys. B–D: each panel shows

spontaneous saccades recorded in total darkness from the same monkey as in A at various times after the injection of $30 \mu\text{g}$ ibotenate in right (R) and left (L) prepositus hypoglossi. The records in D are two excerpts from a continuous record to demonstrate that eye position drifts centripetally after both leftward and rightward saccades. The time constant of the horizontal drift decreases progressively from 2 to 0.6 to 0.2 s in B–D. A–D were recorded at the same time scale as indicated. R, L, U, D are right, left, up, and down. From Cannon and Robinson (1987).

Figure 10.8. (a): The brainstem of a macaque monkey drawn from cresyl-violet-stained sections, cut in the stereotaxic plane, to show the location of the cell-group nucleus raphe interpositus (rip). The cells of rip are indicated by arrows and drawn diagrammatically. Consecutively numbered sections are $240 \mu\text{m}$ apart. (b): Cytochrome-oxidase-stained section. Note

the darkly stained cell bodies of rip around the midline, and their extensive horizontally oriented dendritic fields. Calibration = 1 mm. Abbreviations cs, nucleus centralis superior; rp, nucleus raphe pontis; nrtp, nucleus reticularis tegmenti pontis; rm, nucleus raphe magnus. Modified from Büttner-Ennever *et al.* (1988).

illustrating progressively more severe effects following injection in the alert monkey. As predicted for a common integrator system, the vestibuloocular reflex, optokinetic responses, and smooth pursuit were also affected. Independent data [39] indicate that electrolytic lesions of the prepositus hypoglossi in the cat also cause a complete loss of the neural integrator.

[39] Chéron *et al.* (1986a, b).

10.5. Saccade Generation: Interaction of Neurons in the Circuit

Figure 10.11 summarizes the known and postulated connectivity of the horizontal saccade generator [1]. During fixation OPNs fire at high rates, inhibit EBNs and IBNs, and prevent saccades. For saccade generation an excitatory signal proportional to the desired saccade size is fed to the appropriate EBNs while at the same time an inhibitory trigger signal is given to the OPNs. Note that the excitatory signal to EBNs derives from input from SC that reflects the horizontal distance of the target from the current foveal position, and is fed through the LLBNs. EBNs are disinhibited when OPNs cease firing, respond to the excitatory input, and drive ipsilateral motoneurons to produce the burst component of their discharge. EBNs also excite IBNs which in turn inhibit the OPNs for the duration of the saccade. This feature means the saccade continues even if initiated by a transient trigger signal.

Some comment on the postulated anatomical underpinnings of portions of this sketch is useful. In one model [37], the EBNs project to tonic neurons, which both lesion data and recent electrophysiological recordings have suggested may be localized to the medial vestibular/prepositus complex. These tonic neurons might be part of a network that integrates the EBN signal to yield an eye position signal. The “trigger” input to OPN may come from SC, either directly and/or through a relay involving the LLBNs, and the frontal eye field is yet another possible input source.

Both SC and the frontal eye fields could provide excitatory inputs into the burst generator since stimulation of either evokes short-latency saccades and both project to PRF. In particular, the saccade-related cells of deep and intermediate layers of SC which discharge only during saccades are particularly appealing sources since physiological data suggest they project to LLBNs, which in turn may project to EBNs. The frontal eye fields, which project directly to PRF, are also postulated to initiate saccades via projections to LLBNs.

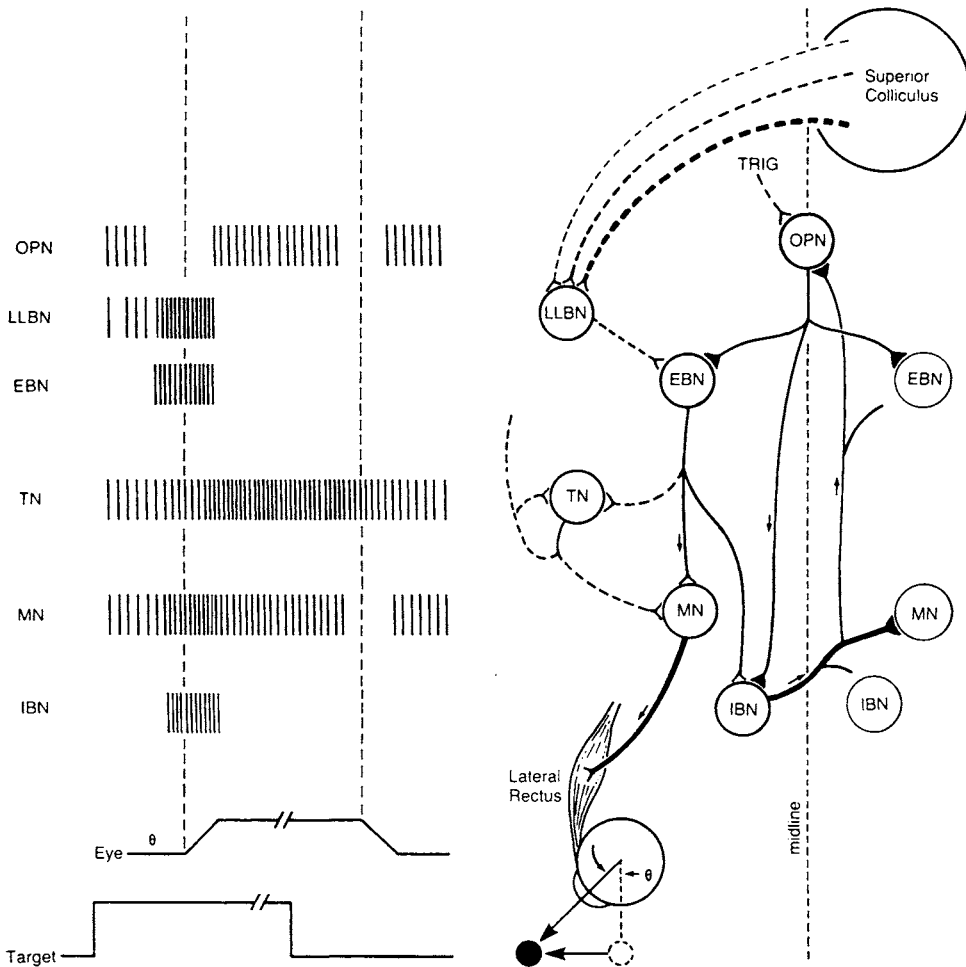


Figure 10.11. The discharge patterns and connections of neurons in the horizontal burst generator. Left: Firing patterns for an on-direction (first vertical dashed line) and off-direction (second dashed line) horizontal saccade of size θ to a target step (schematized in the eye and target traces below). Right: Excitatory connections are shown as open endings, inhibitory connections are shown as filled triangles, and axon collaterals of unknown destination (revealed by intracellular HRP injections or postulated in models) are shown without terminals. Connections known with certainty are represented by thick lines, uncertain connections by thin lines, and hypothesized connections by dashed lines. A description of the behavior of this neural circuit is found in the text. The abbreviations identify excitatory (EBN) and inhibitory (IBN) burst neurons, long-lead burst neurons (LLBN), trigger input neurons (TRIG), omnipause neurons (OPN), tonic neurons (TN), and motoneurons (MN). From Fuchs *et al.* (1985).

10.5.1. Role of Superior Colliculus in Saccades

Cells in the intermediate layer of SC discharge before saccadic eye movements. As illustrated in Fig. 10.6, each cell has its own movement field, and discharges only before saccades with a particular range of directions and amplitude. Most SC neurons increase their discharge rate before saccades made under any condition (to visual targets, spontaneously in the light or in the dark). Cells in the

intermediate layers of the SC are organized so that their movement fields form a topographic map, which is congruent with a visual map in the superficial layers. Electrical stimulation in the SC elicits saccadic eye movements in all mammals thus far studied, including monkey [40], cat [41], and rodent [42]. Microinjections of muscimol, a GABA agonist, into the monkey SC selectively suppress saccades to the movement field of the cells near the injection site [43]. There is a striking decrease in velocity of saccades to visual targets and markedly distorted trajectories of remembered saccades, findings consistent with the initiation of saccadic vectors by SC, and with an inhibitory role of GABA. By contrast, the GABA antagonist bicuculline caused “irrepressible saccades” initially specific to the movement field at the injection site. Subsequent injections of muscimol and bicuculline into the pars reticulata of substantia nigra (SNPR) showed that the GABAergic projection was presumably via action on the GABA-receptive neurons of SNPR [44]. (Because GABA is inhibitory to SNPR and the SNPR-to-SC input is inhibitory, bicuculline in SNPR acts like muscimol in SC, whereas muscimol in SNPR acts like the bicuculline in SC.) It is to be noted that in similar SNPR injections in rats there is a circling behavior to the side contralateral to the injection, suggesting that the SNPR may control all orienting movements, which are more eye-oriented in the fovea-dominant monkey and more body-oriented in the rat.

[40] Schiller and Stryker (1972).

[41] Hyde and Eason (1959).

[42] McHaffie and Stein (1982).

[43] Hikosaka and Wurtz (1985a).

[44] Hikosaka and Wurtz (1985b).

10.5.2. Saccade Trajectories: Mutable or Immutable?

An early assumption was that the burst generator was controlled by a retinal error signal (position of the target relative to the fovea) and that the course of saccades was immutable once initiated. Newer data suggest that, in fact, there is internal feedback control in terms of eye position. Monkeys viewing a quick sequence of two targets whose presentation is terminated before any saccade onset make successive and accurate saccades to the first and then to the second target. This is true despite the fact that the “retinal error signal” at the time of presentation of the second target is not equivalent to the size and angle of the saccade that moved the fovea from target one to target two. (“Retinal error signal” is the difference between foveal position and either of the targets.) This consequently suggests current eye position is used in conjunction with retinal error to generate saccades [45]. Target position in space (see definition below) rather than retinal error may be the driving signal for saccades.

[45] Mays and Sparks (1980).

In 1975, Robinson proposed an enormously influential and useful model that incorporated the above findings and that has been of great impetus to research. He suggested that the EBNs are driven by a signal proportional to (target position in space) – (eye position) (see Fig. 10.12):

TIS = target position in space = (neural representation
of eye position, from integration of EBN output by
tonic neurons) + (retinal error signal)

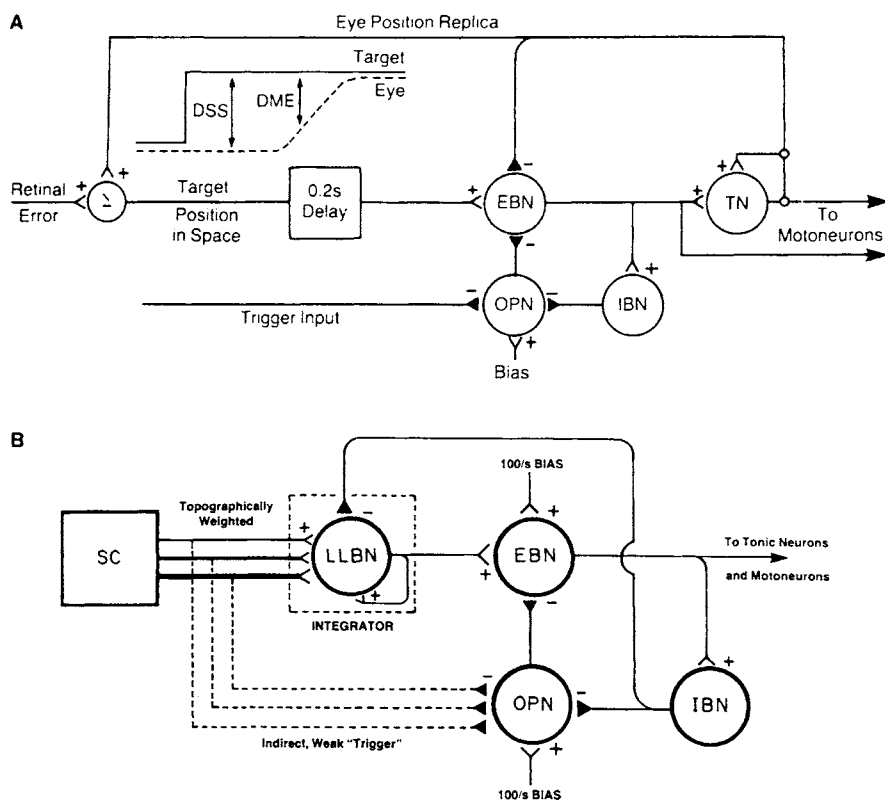


Figure 10.12. Models of the saccade generator. A. The Robinson model, in which a neural replica of eye position is added to retinal error to create target position in space, and later subtracted to generate motor error at the EBN membrane. The physical variables that exist as neural replicas in the model include (inset) target and eye position relative to the head, desired saccade size (DSS, the motor error that exists before the saccade begins), and dynamic motor error (DME, the motor error that exists while the saccade is in progress). The bias signal to the OPN produces its steady firing between saccades. B. The Scudder model. The model uses local (i.e., neural) feedback, but unlike the Robinson model, it matches change in target position (the output of the colliculus) with change in eye position (the output of the IBN). Topographical weighting of the colliculus projection is symbolized by the lines of different thickness. The unweighted and indirect inhibitory projection from the SC to the OPN is symbolized by the dotted lines of constant thickness. The LLBN is wired to integrate its two inputs as symbolized by the recurrent positive feedback with a gain of 1.0. The EBN projects to the IBN, as shown, and is also assumed to project to the tonic neurons and motoneurons (not shown) as in the Robinson model. Modified from Fuchs *et al.* (1985) and Scudder (1988).

Since this signal is delayed by 0.2 s, the neural representation of the target position in space does not change in the course of a normal saccade. Also, the neural representation of eye position is subtracted by the EBN to produce a motor error signal in retinal coordinates. Note that the initial motor error for single saccades is exactly equal to retinal error. However, before the second saccade in the above double step paradigm the initial motor error will be:

$$\text{Dynamic motor error} = (\text{target position in space}) - (\text{current eye movement})$$

Note also that as the eye approaches the target, the dynamic motor error declines, and reaches zero, thus leading to a zero net drive on EBNs and silencing them, thus terminating the saccade. The control is not ballistic, since the feedback loop will correct for an unexpected perturbation and allow the eyes to reach the target. This feedback control is supported by experiments [46] showing that stimulation of the SC in the middle of a targeting saccade, thereby perturbing the system by altering eye position, led a subsequent new saccade that compensated for this perturbation. Other groups [1] have also stimulated the OPNs during an ongoing saccade; the interrupted saccade accurately reached the target.

[46] Sparks and Mays (1983).

Several modifications to the original Robinson model have now been proposed, and we present one of these to give a flavor of the kind of modifications being made [47]. It was suggested that a more realistic representation of SC influence in that the LLBNs receive a topographically weighted output (represented by lines of different strength) of the SC (SLBN do not receive direct superior colliculus input). The eye position (motor) error feedback in this model is on the LLBN and is via an inhibitory recurrent projection from an IBN, whose discharge pattern is essentially identical to that of an EBN. (It has also been proposed that the neural replica of eye position is sent to the SC, where it is compared with target position to generate motor error [48].) When the number of spikes added by the colliculus equals the number of spikes subtracted by the IBN feedback (note that the LLBN is connected to perform as an integrator), there is a cessation of LLBN discharge, the EBN ceases firing and the saccade ends. In addition to the absence of any documented SC-to-SLBN input, the colliculus already encodes initial motor error (= desired saccade size) in the topographic distribution of its neurons. Another feature of the model [47] is that there is a nonspecific SC trigger output to OPNs, assisting in saccade initiation although the degree of OPN inhibition and hence its role in saccade initiation is less critical in this model.

[47] Scudder (1988, see Fig. 10.12B).

[48] Keller (1980).

[49] Sparks *et al.* (1987).

The effect of pontine reticular stimulation in the monkey on eye movements was studied [49] and the authors reasoned that if a copy of the motor command is used as a feedback signal of eye position, then failure to compensate for stimulation-induced movements would indicate that stimulation occurred at a site distal to (e.g., closer to the motoneurons) the point from which the eye position signal was derived. Thus, in the sketch in Fig. 10.11, stimulation would occur at a point nearer to the motoneurons than the takeoff point of the feedback signals. It is known, for example, that animals do not compensate for direct stimulation of the trochlear nerve or of sites close to the abducens nucleus. Briefly, the results were that animals compensated for stimulation at about one-half of all pontine sites where SLBN have been reported. Only the compensation is predicted by Robinson's model. (This of course assumes that the electrical stimulation is indeed a fair test of SLBN activation, since activation of fibers of passage with unknown effects would complicate the interpretation.) An unexpected finding was that pontine stimulation at times prematurely triggered impending visually directed saccades. The time course of this effect suggested that the build-up of input to saccadic generator circuits occurs over an epoch of some 100 ms. A further point of theoretical importance was that the "saccade trigger signal" was dissociated from the signal providing the metrics of the upcoming saccade.

In concluding this portion of the chapter, it is again useful to emphasize the important role of formal modeling in making explicit the assumptions of various hypotheses of neural control and processing. Although the pure empiricist may object to the "postulation" of more circuitry than is known, and to the substitution of simplified schemes for the full complexity of neural circuitry and physiological actions, we suggest that the history of the development of knowledge about the oculomotor system provides one of the best "case examples" of the usefulness of models for the experimental neurophysiologist.

10.6. Gaze Control

The previous sections have discussed control of eye movement, considered independently of movements of the head directed toward visual targets. It is however apparent that control of gaze, defined as cooperative movements of both eye and head in targetting, is also an important topic, although one that has been less intensely investigated. Stimulation of caudal PRF led to ipsilateral head and eye

movements [50] and it was found that electrolytic lesions of this zone eliminated ipsiversive head movements as well as the ipsilateral quick phases of ocular nystagmus [51]. Because these lesions could have involved fibers of passage, more reliable information appears in more recent studies using intraaxonal recordings and HRP labeling.

Intraaxonal recordings in the caudal pons of alert, head-restrained cats, revealed that, among the many axons sampled, a small group met the criteria of antidromic activation from ipsilateral cervical spinal cord, monosynaptic activation from ipsilateral SC, and whose soma location could be determined [52]. The soma were in caudal pons rostral to abducens, and some neurons had a discharge pattern that led to their description as “eye-neck” reticulospinal neurons (EN-RSN). EN-RSN had discharge patterns correlated with ipsiversive eye movements, eccentric eye fixations, and the EMG profile of ipsilateral neck muscles in the course of the behaviors of spontaneous visual scanning or tracking objects presented in the visual field. These neurons were silent when the eyes were deviated contralaterally (beyond the vertical meridian) and the ipsilateral neck muscles were relaxed. However they became phasically active before saccades terminating close to the vertical meridian or further in the ipsilateral hemifield, with the onset and time course of activity correlating with ipsilateral neck EMG activation. Overall discharge rate was approximately proportional to the eccentricity of gaze shift in this “head-fixed” condition, although with prolonged eccentric eye fixation discharge rate declined, thus suggesting a predominant role in phasic components of gaze. The functional inference is that, at eye positions in the ipsilateral hemifield, targets located still further (ipsi-) laterally in the visual field would demand a neck movement to bring the target on the fovea. The firing pattern of EN-RSN neurons was distinct from that of EBN (see previous discussion) although the EN-RSN were located in the same caudal PRF region just rostral to abducens (pontine FTG region) as EBN.

In two neurons intraaxonal HRP labeling was sufficiently complete to label the axon course as far as the medullary pyramidal decussation and also to label its extensive collaterals. Figure 10.13 shows the reconstruction of an intraaxonally stained neuron. Its axonal collateral distribution pattern and a bouton density analysis indicated extensive projections to abducens, VII nucleus, prepositus hypoglossi, vestibular nucleus (especially medial), and bulbar reticular formation, especially the giant cell field. This neuron is of interest also in terms of reticular neuronal morphology. Its axonal pathway in the bulbar reticular formation labels it as an iBRF neuron in the reticular neuronal axonal classification scheme derived from the

[50] Bender *et al.* (1964).

[51] Sirkin *et al.* (1980).

[52] Grantyn and Berthoz (1987); Grantyn *et al.* (1987).

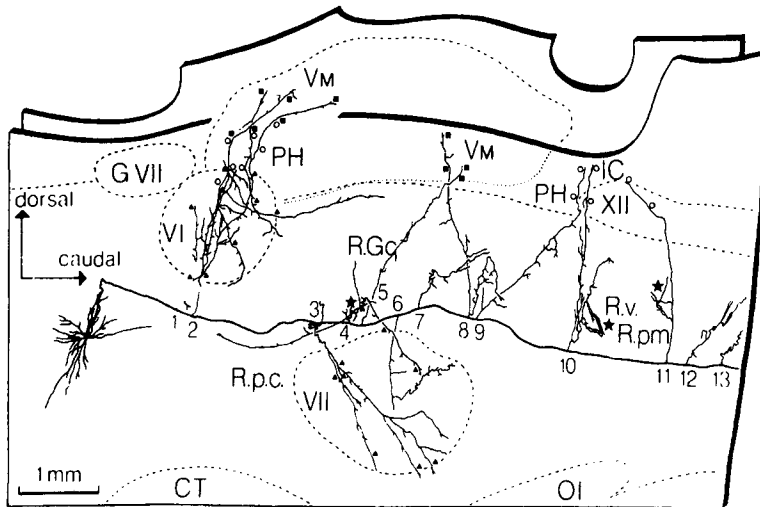


Figure 10.13. Parasagittal plane reconstruction of an intraaxonally HRP-stained eye-neck reticulospinal neuron (EN-RSN) in the cat. Physiologically this neuron was characterized by a monosynaptic response to contralateral superior colliculus (SC) stimulation and antidromic invasion from stimulating electrodes in C2. The axon courses 0.8–0.9 mm lateral to the midline and ventral to the MLF, while the soma is about 1.3 mm lateral to midline. Collateral projections are widespread but are clustered in particular target zones rather than being diffusely distributed throughout the rhombencephalon. Symbols denote portions of collaterals restricted to the abducens (VI) or facial (VII) nuclei (filled triangles); to the prepositus hypoglossi (PH) and nucleus intercalatus Staderini (IC, open circles); and to the medial (Vm) vestibular nucleus (filled squares). Other abbreviations: R.p.c., nucleus reticularis pontis caudalis. GVII, genu of VII. R.Gc., R.v., R.pm. Nucleus reticularis gigantocellularis, ventralis, and paramedianus respectively. IC, nucleus intercalatus. Adapted from Grantyn *et al.* (1987).

[53] See Mitani *et al.* (1988a, b).

[54] This pattern was suggested by Scheibel and Scheibel (1958) as a predominant mode of brainstem reticular organization.

larger sample study of descending PRF neurons described in Chapter 4 [53]. The reticular and nuclear projection zones of the EN-RSN neurons targeted those areas demonstrated to be involved in control of eye, ear, and axial movements, making the point that, while reticular formation neurons may have widespread projections, it is, at least in the case of these two neurons, misleading to call the projections diffuse. It was of interest that some collaterals and their ramifications in reticular formation a “segmental” pattern of distribution, for example, projecting to a “poker-chip shaped” discoid area [54]; however, many collaterals in the adult cats did not have this pattern.

10.7. State-Dependent Alterations in Oculomotor System Function

10.7.1. Waking to Synchronized Sleep Transitions

The characteristic waking eye movement pattern of fixation, alternating with high-velocity saccades, or of slow movements in response to visual or vestibular stimuli, is

transformed during the transition to sleep. As drowsiness occurs, saccadic velocity and number are reduced, and the transition to light slow-wave sleep is marked by an abrupt change to slow, drifting eye movements. In the transition to slow-wave sleep the discharge activity of brainstem oculomotor system neurons is also characteristically altered. OPNs suddenly become silent coincident with the loss of ability to maintain fixation [55, 56]; they just as suddenly resume their firing on a slow-wave sleep to waking transition (Fig. 10.14). It is of interest that multiunit recordings showed this omnipauser silence occurs throughout the population and that this “moment of sleep” change is completed in less than 10 ms [56]. However, although the degree and latency of responsivity to synaptic input is altered during sleep, omnipause units retain sufficient responsivity to discharge in response to SC stimulation [55].

[55] Raybourn and Keller (1977).

[56] Henn *et al.* (1984a).

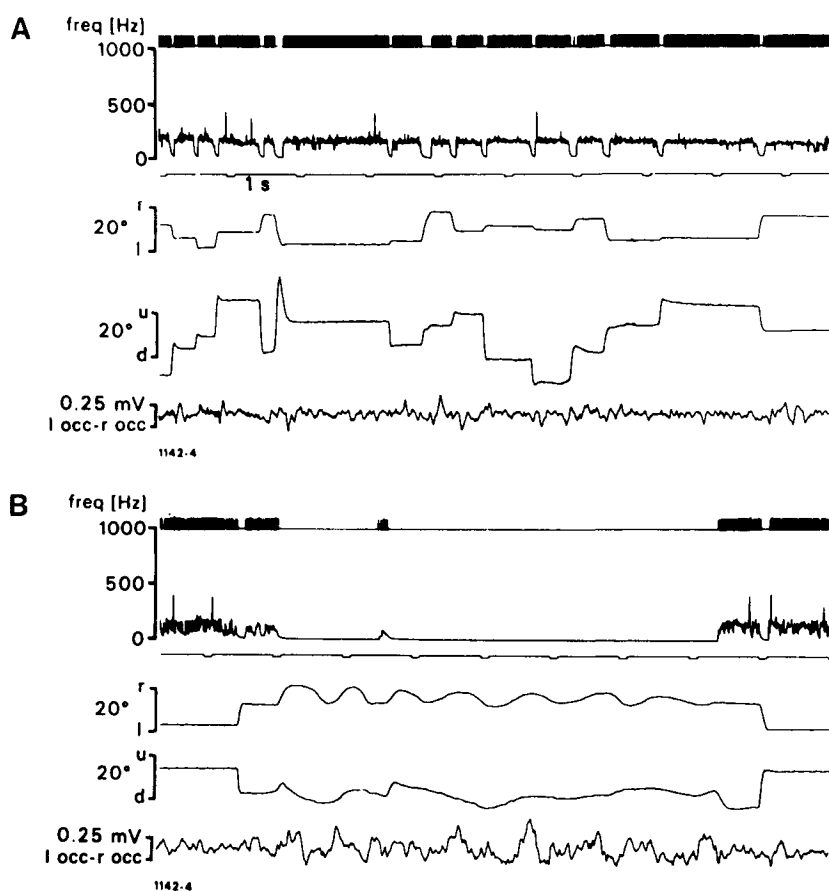


Figure 10.14. Pause neuron from the monkey pontine reticular formation (PRF). A. During alertness there is continuous regular discharge at about 180 Hz which is only interrupted prior to and during rapid eye movements. B. During a period of light sleep there is cessation of neuronal activity and concomitant irregular continuous eye movements. Legend is, from above: blips marking the occurrences of spikes, instantaneous firing rate, horizontal and vertical eye position, and EEG traces (either left right occipital or left parietooccipital). From Henn *et al.* (1984a).

During slow-wave sleep, both medial rectus and vertical eye movement motoneurons show a decreased amount of tonic firing for a given eye position as compared to the waking state, the decrease reaching approximately 50% in the monkey for longer sleep episodes [56], with similar findings being present in the cat abducens and internuclear motoneurons [57]. This suggests the coactivation of the extraocular muscles is strongly relaxed during slow-wave sleep.

[57] Delgado-Garcia *et al.* (1986 a, b).

Short-lead burst neurons in slow-wave sleep show a marked decrease in the sharpness of “bursting,” that is, the occurrence of a high peak of firing frequency as the burst begins, and the duration of bursts tends to be prolonged [56]. This neuronal activity corresponds to the presence of slow, drifting eye movements during slow-wave sleep as contrasted with the rapid, saccadic eye movements of waking. About one half of short-lead bursters show tonic activity after waking–sleep transition, but this activity decreases as sleep becomes deeper. In general, the distinction between short- and long-lead bursters blurs further as sleep is entered and both discharge types show increased burst-on latencies. Burst-tonic neurons and vectorial long-lead bursters, like SLBNs, show decreased peak frequency and increased burst duration. PRF tonic reticular units also became silent during drowsiness and light slow wave sleep, while PRF burst-tonic neurons remained active [55]. In contrast to the disruption in the oculomotor system, activity in vestibular-only neurons in the vestibular nuclei remains unchanged during head rotation in sleep [56]. These workers reasoned that the observed sharp drop of vestibulooculomotor reflex (VOR) gain in sleep might consequently be the result of oculomotor system changes (although, it may be noted parenthetically, vestibular-only neurons may not participate in VOR). The sharp wake to sleep change in the oculomotor system has been modeled as a nonequilibrium phase transition [14]. It should be appreciated that the results described here have, in general, been obtained during “light” or initial slow-wave sleep, and that the system has not been thoroughly explored in deep slow-wave sleep.

10.7.2. Activity During REM Sleep

The eye movements of REM sleep have been characterized in monkeys by use of the search coil technique and have been found to differ considerably from those in waking. The first report [58] found that most (60%) of “rapid” eye movements of REM sleep had velocities less than 50 degrees per second, whereas those with velocities

[58] Fuchs and Ron (1968).

>200 degrees per second, the usual lower velocity cut-off for waking saccades, accounted for only 14% of eye movements in REM. These REM saccades usually had very short duration with very short intersaccade intervals (often 100 ms), much shorter than seen in waking. In waking with and without targets, eye movement velocities clustered at two extremes: most movements were saccades with velocities between 250 and 1,000 degrees per second while smooth pursuit movements with velocities <50 degrees per second were less frequent. In REM sleep, about 30% of eye movements had velocities between 50–200 degrees per second, whereas such velocities were quite rare in waking. Furthermore, records of REM sleep saccades had a “round-shouldered” appearance, indicating the absence of high frequency components present in waking.

Perhaps the most distinctive difference between waking and REM eye movements was a “loop” pattern observable in REM-sleep eye movements displayed in an two-dimensional format on an oscilloscope (Fig. 10.15). These loops were composed of both saccadic and slower movements with a usual range of 3–11 movements/loop. Loops occupied almost 30% of the REM period, with each loop lasting an average of 2.5 s and loops occurring at a “remarkably constant” rate of about 7/min. Often the same starting point would be used for several loops, as seen in Fig. 10.15B. This loop pattern was in marked contrast to eye movements in waking with and without targets present where loops were only very rarely present. Similar findings were reported using the search coil technique in the semichronic *encephale isolé* cat, and described REM-sleep

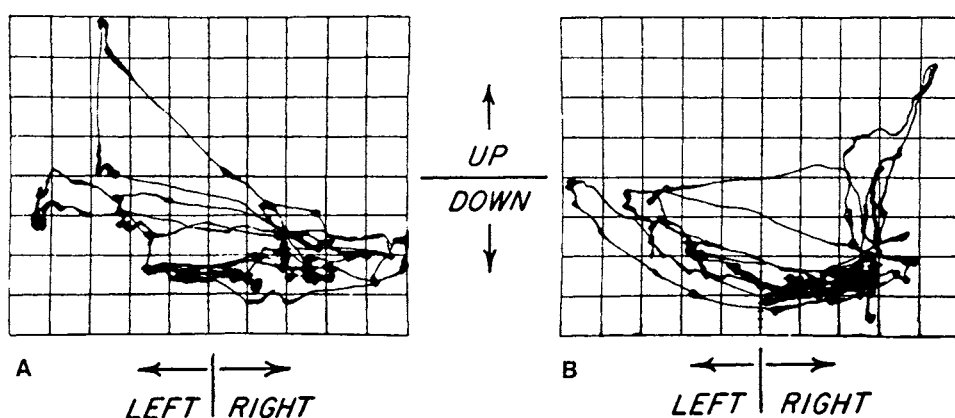


Figure 10.15. Two-dimensional displays of eye position during two short intervals within a REM sleep episode in the monkey. Each small square is 10° on a side. The primary direction of gaze lies at the center of the oscilloscope screen. The trace intensity provides a qualitative measure of eye velocity ranging from dark spots showing fixation points to thin traces indicating a very rapid movement. Note the presence of many loop patterns. From Fuchs and Ron (1968).

eye movements as having “loop shaped trajectories” that frequently returned to the original position, a pattern also not seen in waking in this cat preparation [59]. Saccades in REM, as in waking, consist of conjugate eye movements, as contrasted with the disjunctive movements of slow-wave sleep.

We note that many studies have characterized eye movements in REM using AC coupling of EOG signals; this technique is inferior to the search coil technique, as it is unable to establish the absolute position of the eyeball. The technical limitations of earlier studies may have led to the belief that REM eye movements resembled those of waking in the monkey [60], in the human [61], and in the cat [62]. This belief, in turn, suggested the plausibility of the “scanning” hypothesis, that the REM eye movements represented a “scanning” of the dream image. This hypothesis is obviously rendered implausible on the basis of the marked differences in animals between REM and waking eye movements described above. In addition, data from humans indicate the eye movements of REM are considerably slower than waking saccades of comparable amplitude (a finding compatible with the animal data) and that this slowing is greater than that attributable to either eye closure or eye movements in total darkness [63], thus disputing earlier findings [64].

It may be somewhat surprising to the reader that the neuronal activity underlying the distinctive eye movements of REM sleep has not yet been thoroughly described. Unfortunately, laboratories interested in precise characterization of waking eye movements and neuronal activity have not done unit recordings during REM sleep, while laboratories interested in REM-sleep neuronal activity have not employed the search coil or DC recording electrode techniques necessary for precise characterization of eye movement direction, velocity, and amplitude. Data using AC-coupled EOG electrodes showed eye movement-associated discharge of neurons extracellularly recorded in various regions of the PRF; since direction, velocity, and amplitude of eye movements could not be precisely specified, essentially only discharge latency and intensity relative to eye movement onset were available [65]. These data did suggest that among the units recorded were neurons that might be characterized as SLBNs and LLBNs and burst-tonic neurons in the oculomotor literature. These units discharged in association with waking eye movements but had markedly reduced discharge in slow-wave sleep; during the rapid eye movements of REM sleep, the eye movement-correlated firing again appeared, with both similarities and dissimilarities of discharge latency and intensity being present in waking and REM sleep. Many of

[59] Bon *et al.* (1980).

[60] Weitzman (1961).

[61] Roffwarg *et al.* (1962).

[62] Jeannerod *et al.* (1965).

[63] Aserinsky *et al.* (1985).

[64] Herman *et al.* (1983).

[65] Pivik *et al.* (1976).

these units were recorded in the giant-cell field; more recent data make it unlikely that these were giant cells, but the short-lead burst patterns observed may have been derived from recordings from the nongiant neurons in this region that project to abducens [25, 53].

10.8. Mechanisms of the Muscle Atonia of REM Sleep: Motoneurons

One of the most striking features of REM is the paradoxical presence of muscle atonia coupled with a high level of activity of central neurons, including those in motor systems. In fact, one of the synonyms for REM sleep, paradoxical sleep, was coined by Jouvet as an expression of this feature of REM. The next portion of the chapter will discuss cellular mechanisms for production of atonia. As with the oculomotor system, we will take an “outside in” approach and discuss REM mechanisms for inhibition of spinal and trigeminal motoneurons before taking up the central mechanisms.

10.8.1. Inhibition and Diminished Excitability of Trigeminal Jaw-Closer Motoneurons During REM Sleep

Chase and his colleagues [66], using intracellular recordings in naturally sleeping cats, first identified jaw-closer motoneurons in the trigeminal motor nucleus by their monosynaptic response to stimulation of mesencephalic V and further identified masseter motoneurons by antidromic activation following masseter nerve stimulation. They then tracked membrane potential (MP) and other motoneuron parameters over the sleep–wake cycle. The most dramatic changes in MP occurred on transition from slow-wave sleep to REM sleep where all neurons underwent a tonic hyperpolarization that lasted throughout REM, and was of a 2–10 mV magnitude (Fig. 10.16). Upon transition to waking, the MP invariably depolarized. The MP on transition from waking to slow-wave sleep showed either a slight hyperpolarization or remained the same. Spontaneous discharge activity diminished and usually ceased with the hyperpolarization of REM, with the occasional exception of discharges in association with the rapid eye movements or facial muscle twitches.

It was concluded that active inhibition rather than disfacilitation was responsible for this REM-specific hyperpolarization [67]. In REM sleep, antidromic spikes were

[66] Chase *et al.* (1980).

[67] Chandler *et al.* (1980).

[68] Mariotti *et al.* (1986).

either blocked or showed a decrease in spike-peak potential, with absolute amplitude also frequently reduced; in addition there was a decrease in amplitude and increased rate of decay of monosynaptic excitatory postsynaptic potentials (EPSPs) from stimulation of the trigeminal mesencephalic nucleus, data all consistent with an increased conductance and hence increased inhibitory rather than decreased excitatory input. (The degree of spike peak potential reduction was not correlated with the degree of MP hyperpolarization that occurred in REM.) Since these effects were less pronounced than those obtainable with inferior alveolar nerve inhibitory input, an input thought to be on the soma, it was concluded that the REM inhibition was likely mediated not only by synapses on the soma but also on more distant sites, that is, on dendrites [68]. A final feature of the REM-associated changes was presynaptic inhibition of jaw-closer Ia muscle afferents. This was inferred from a decrease in amplitude of the monosynaptic Ia EPSP without the changes in rise or decay time that would have suggested membrane conductance changes

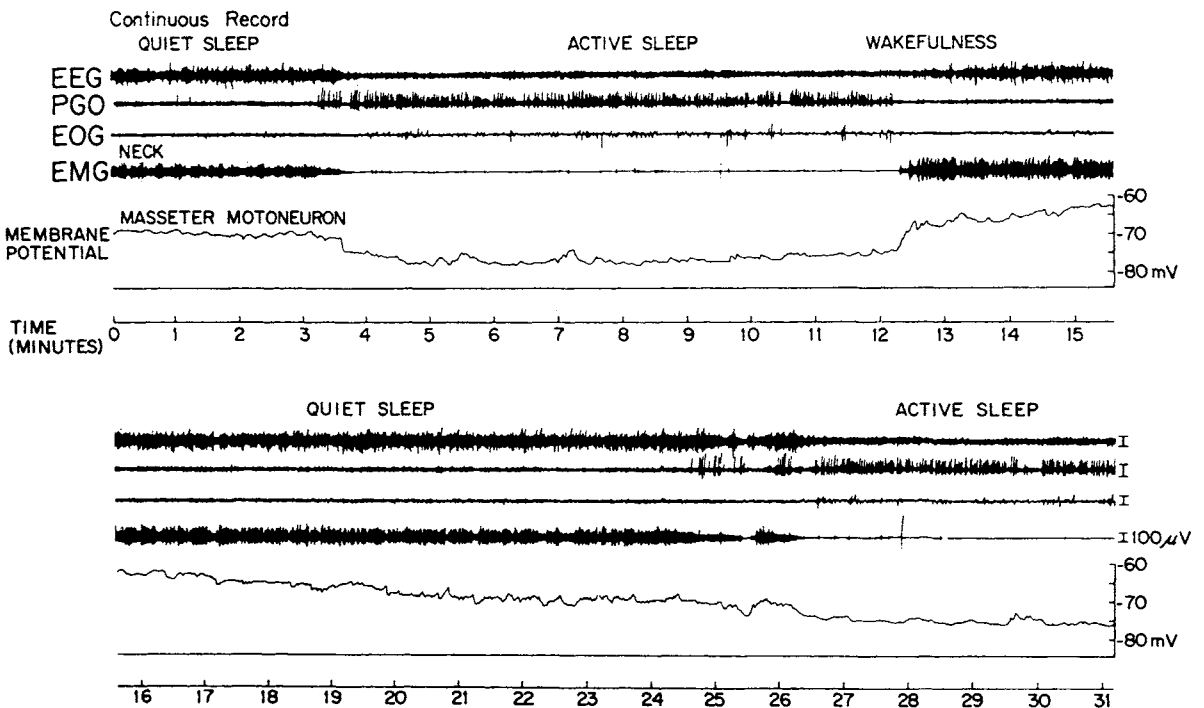


Figure 10.16. Intracellular recording from a trigeminal jaw-closer motoneurons: correlation of membrane potential (MP) and state changes. The MP hyperpolarized rather abruptly at 3.5 min in conjunction with the decrease in neck muscle tone and transition from quiet (slow-wave) sleep to active sleep (REM). At 12.5 min the membrane depolarized and the animal

awakened. After the animal passed into quiet sleep again, a brief, aborted episode of active sleep occurred at 25.5 min that was accompanied by a phasic period of hyperpolarization. A minute later the animal once again entered active sleep and the MP increased. EEG trace, marginal cortex, MP band pass on polygraphic record, DC to 0.1 Hz. From Chase *et al.* (1980).

associated with postsynaptic inhibition. Subsequent pharmacological studies [69] using microinjection techniques have suggested that the REM sleep suppression of the masseteric jaw-closer reflex during active sleep is partly but not completely due to strychnine-sensitive postsynaptic inhibition, suggesting glycinergic mechanisms of inhibition.

[69] Soja *et al.* (1987a).

10.8.2. Spinal Alpha Motoneurons During the Sleep–Wake Cycle

10.8.2.1. Changes in Membrane Potential of Alpha Lumbar Motoneurons During Waking and Sleep

Antidromically identified lumbar motoneurons have been studied in naturally sleeping cats, using intracellular recording techniques [70]. The low-pass filtered record of MP during a sleep–wake cycle is shown in Fig. 10.17. Mean resting potential in waking was -65 mV, and there was a slight hyperpolarization from active waking to slow-wave sleep. During the passage from slow-wave sleep to REM sleep, there was a marked membrane hyperpolarization, averaging 6.7 mV with a range of 4 – 10 mV; this hyperpolarization was temporally coincident with the loss of nuchal EMG activity. On transition to W, the level of polarization decreased. Similar findings have been observed by another team [71]. Overall these data establish the basis of one of the hallmarks of REM, muscle atonia, as a result of motoneuronal hyperpolarization, and confirmed hypotheses made in earlier extracellular and reflex studies by Pompeiano and coworkers [72].

[70] Morales and Chase (1978, 1981).

[71] Glenn and Dement (1981).

[72] Pompeiano *et al.* (1967). See also review in Chase and Morales (1985).

Lines of experimentation similar to those described for jaw-closer motoneurons suggested the presence of a tonic increased membrane conductance in REM sleep and hence of increased inhibition, rather than disfacilitation as the basis of the REM hyperpolarization [70]. During REM sleep, there was an increased duration of the initial segment–somadendritic (IS–SD) delay, an increased rheobase not accounted for by hyperpolarization alone, and there was a directly measured decrease in input resistance from 1.8 to 1.0 M Ω in slow-wave sleep, as compared with REM sleep. (Input resistance was not measured with the MP returned to the same baseline in slow-wave sleep and REM, a manipulation more difficult to accomplish in the chronic preparation.) In addition to the tonic inhibition just described, there were phasic episodes of enhanced postsynaptic inhibition of lumbar motoneurons coincident with the occurrence of phasic runs of rapid eye movements [73]. Thus, both phasic presynaptic inhibition and postsynaptic inhibition occur during REM sleep.

[73] Chase and Morales (1983).

10.8.2.2. Hyperpolarizing PSPs in Alpha Lumbar Motoneurons During Waking and Sleep

447

MOTOR SYSTEMS

[74] Morales *et al.* (1988).

Subsequent work has examined in detail the spontaneous, discrete inhibitory postsynaptic potentials (IPSPs) impinging on lumbar motoneurons that were automatically detected and classified according to amplitude and parameters of rise and decay times [74]. Figure 10.18 is a high gain intracellular record showing the presence of distinctive large amplitude PSPs during REM that are not present during waking and slow-wave sleep, and Fig. 10.19

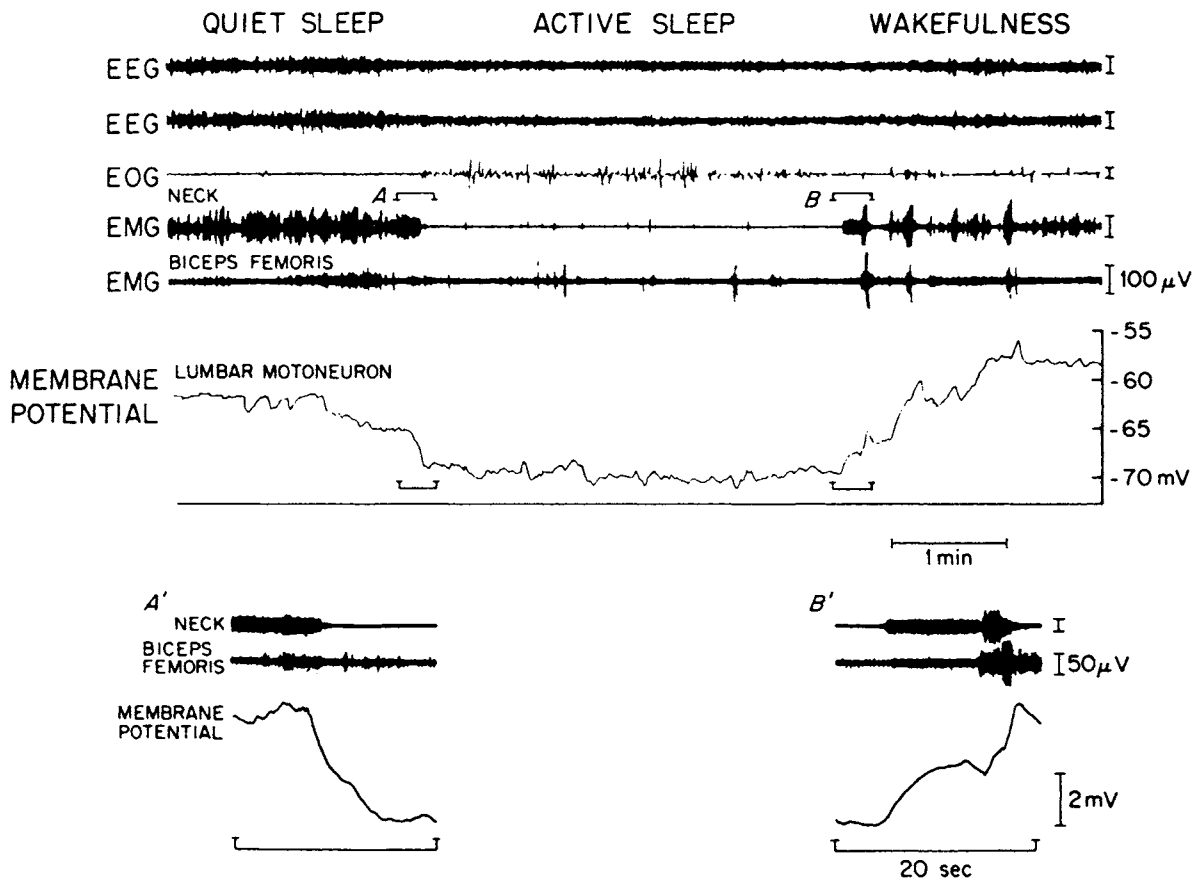


Figure 10.17. Intracellular record from a lumbar motoneuron during sleep and wakefulness: correlation of membrane potential (MP) and behavioral state. This figure highlights the membrane hyperpolarization which accompanies REM (active) sleep. Hyperpolarization commenced prior to the cessation of muscle tone, which was accompanied by a further and rather sharp increase in membrane polarization [(A), and shown oscilloscopically at higher gain and expanded time base in (A')]. At the termination of REM sleep, the membrane depolarized coincident with the resumption of muscle tone and behavioral awakening (B, B'). Note the brief periods of

depolarization during REM sleep and wakefulness, which were accompanied by phasic increases in muscle activity (i.e., muscular twitches during active sleep and leg movements during wakefulness). Spike potentials often occurred during these periods of depolarization but are not evident in this figure because the DC record was passed through a 0.1-cps high-frequency polygraphic filter. This motoneuron was recorded for 28 min; the traces shown were obtained 12 min after the cell was impaled. The first and second polygraph traces are those of EEG activity recorded from left and right frontal-parietal cortex, respectively. From Morales and Chase (1978).

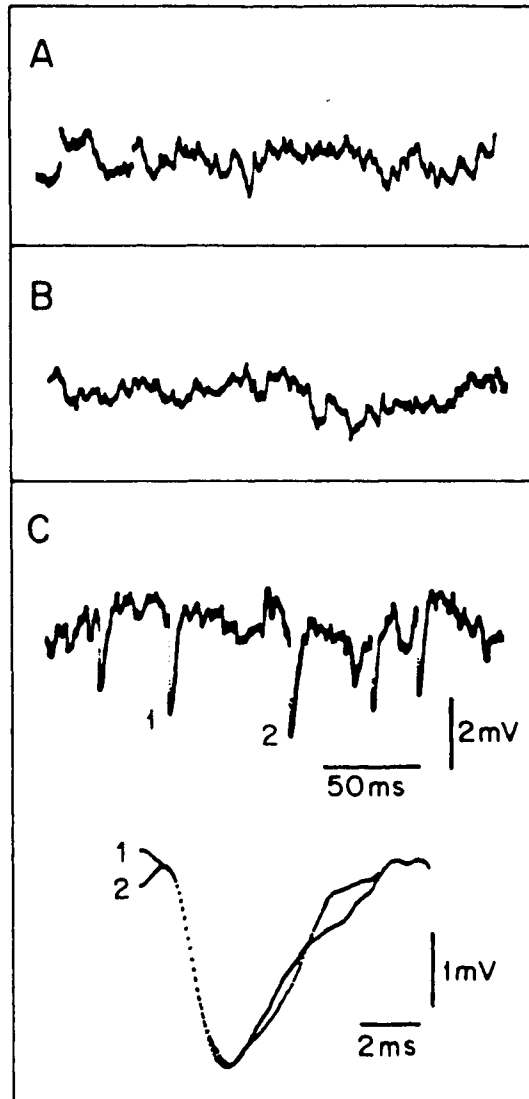


Figure 10.18. High-gain intracellular recording of the membrane potential (MP) activity of a tibial motoneuron during wakefulness (A), slow-wave sleep (B = SWS), and active sleep (C = REM). Note the appearance de novo during REM sleep, of large amplitude and repetitively occurring inhibitory postsynaptic potentials. Two representative potentials, which were aligned by their origins, are shown at higher gain and at an expanded time base (C1, 2). These potentials were photographed from the screen of a digital oscilloscope. The analog-to-digital conversion rate was 40 μ s/bin. The MP level during these recording was during active sleep -67.0 mV; the antidromic action potential was 78.5 mV. From Morales *et al.* (1988).

shows that the REM potentials are distinct in that (1) they have larger amplitudes, and (2) they have a faster rise time/unit of IPSP amplitude. It was thus concluded that they arose from a distinct set of inhibitory neurons that became active during REM. Microiontophoretic application of strychnine (but not picrotoxin or bicuculline) onto

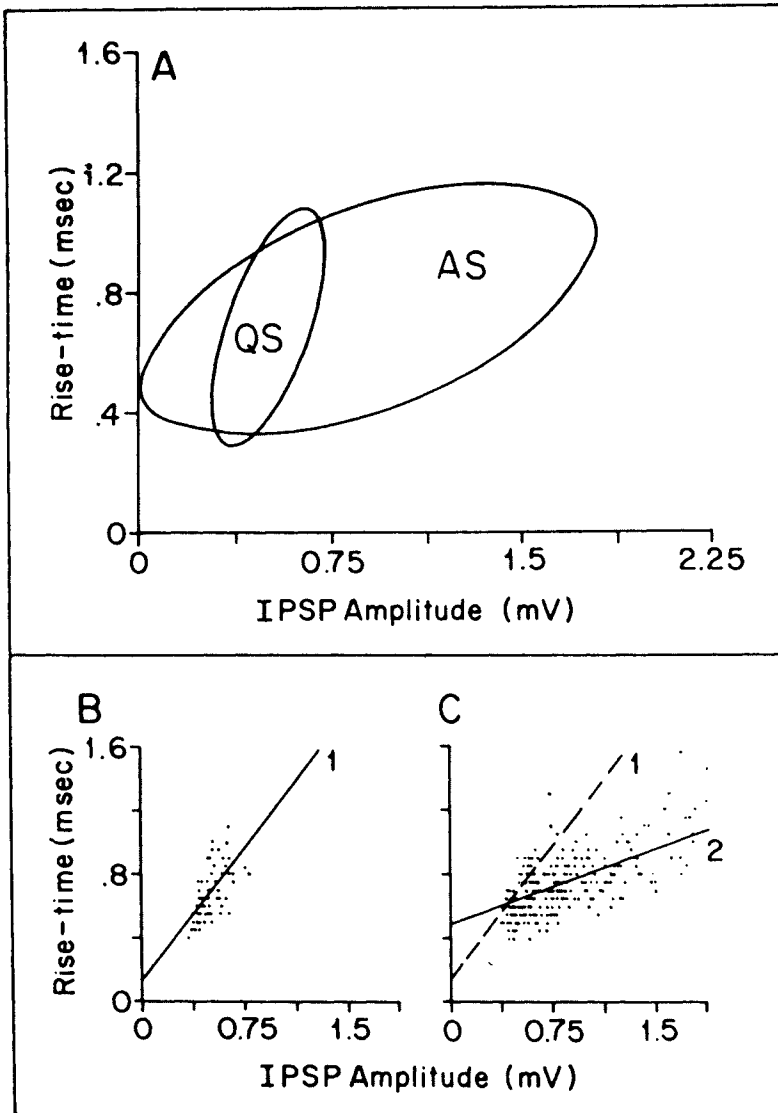


Figure 10.19. Definition of a population of REM-sleep IPSPs utilizing the relationship between the waveform parameters of amplitude and rise time. The two ellipses in A illustrate the 90% confidence region of the data points corresponding to the potentials recorded during quiet sleep (QS) and active sleep (AS). Note that the ellipse corresponding to the AS episode is shifted to the right (i.e., to the region of potentials of larger amplitude) and that the major axis of the larger AS ellipse has a lesser slope than that of the QS ellipse (see text). The original data from which these ellipses were constructed are illustrated in the scattergrams B (QS) and C (AS). Also included in these plots are the regression lines for the correlations B₁ and C₁ (QS and AS, respectively). In both sets of data, there was a direct relationship between rise time and amplitude (data obtained during active sleep: $r = 0.69$, slope = 0.31, $n = 294$, $p < 0.01$; during quiet sleep: $r = 0.63$, slope = 1.09, $n = 65$, $P < 0.01$). The regression line in B₁ is also depicted in C in order to illustrate that the large amplitude active-sleep IPSPs are all situated beneath this line. From Morales *et al.* (1988).

lumbar motoneurons is effective in abolishing the large amplitude spontaneous IPSPs of REM sleep, suggesting that glycine is the principal neurotransmitter mediating these potentials in lumbar motoneurons [75].

[75] Chase *et al.* (1989).

10.8.2.3. Excitatory Activity in Alpha Lumbar Motoneurons During Waking and Sleep

Excitatory processes occurring during REM, primarily occurring at the same time as the runs of rapid eye movements, and different from waking have also been examined [73] (Fig. 10.20). In waking, action potentials usually occurred following a prolonged depolarization

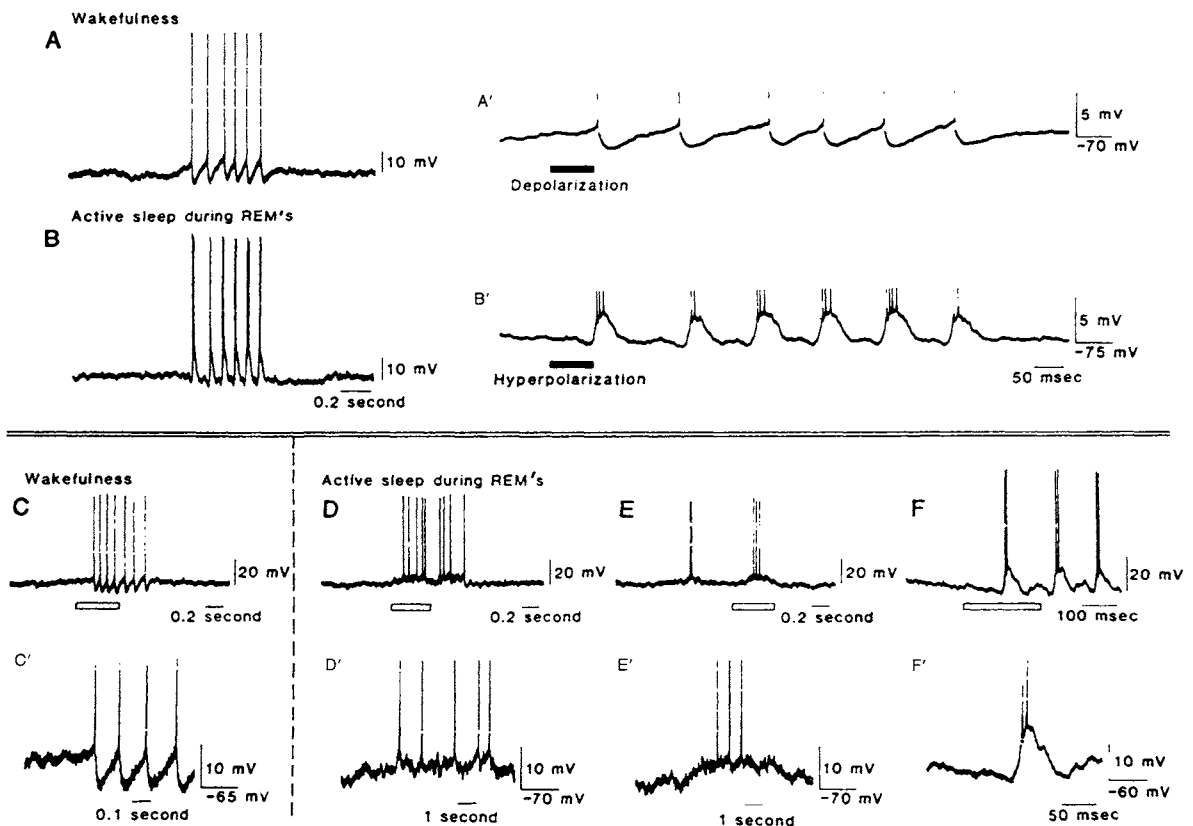


Figure 10.20. Patterns of spike generation during REM periods of active sleep. (A) During wakefulness, depolarization (bar in A') was the initial membrane potential (MP) event. (B) During REM periods, each depolarization shift was preceded by hyperpolarization (bar in B') (see also F and F'). Full-sized spikes developed in both examples; in B doublets, triplets, and quadruplets accompanied each depolarizing shift. The open bars indicate the period of the traces shown in C'-F'. (C) Spike

generation during wakefulness. (D) An irregular pattern of spike activity, (E) intermittent bursts, and (F) spike doublets during REM periods. An increase in hyperpolarizing subthreshold synaptic activity during interspike intervals is present in D' and E'. (A) and (B) are records from a single tibial motoneuron and (C) through (E) from a single peroneal motoneuron; (F) is from another peroneal cell. From Chase and Morales (1983).

(Fig. 10.20A) whereas in REM the majority of action potentials were observed to occur following a hyperpolarization followed by a depolarizing potential on which rode a burst of 2–4 spikes, and with an absence of the spike after hyperpolarization typical of waking (Fig. 10.20B). This was interpreted as indicating simultaneous coactivation of inhibitory and excitatory drives, a pattern not found in waking but distinctive to REM. Another possibility, not considered in that 1983 paper [73], but raised by us, is the presence of a low-threshold Ca^{2+} spike that was de-inactivated at the hyperpolarized MP of REM and was triggered either as a rebound following a hyperpolarization or following a depolarization (see discussion in Chapter 5). A frequent concomitant of a long duration Ca^{2+} spike is a burst of fast (Na^+) action potentials riding on it. It should be noted that not all REM spikes occurred with this particular pattern, and some appeared to arise from depolarizing potentials like those seen in waking (Fig. 10.20D–E); these spikes did not occur in as bursts. The possibility that Ca^{2+} spikes may be present in these records is strengthened by a study [76] reporting Ca^{2+} -dependent low-threshold rebound potentials in the *in vitro* lumbar motoneurons in the spinal cord preparation from neonatal rats, although it was not observed in mature motoneurons in this preparation.

[76] Walton and Llinás (1986).

The non-NMDA excitatory amino acid may mediate some of the EPSPs of REM sleep. The phasic depolarizations of lumbar motoneurons occurring during the rapid eye movement portions of REM sleep are blocked by microiontophoretic application of kynurenic acid, a nonselective EAA receptor blocker [77], but not by 5-aminophosphonovaleric acid (APV), a selective blocker of NMDA receptors [78]. In those experiments APV was applied in doses that were sufficient to antagonize the effects of microiontophoretically applied NMDA.

[77] Soja *et al.* (1988).

[78] Chase *et al.* (1986).

10.8.2.4. Sources of REM Sleep IPSPs and EPSPs

As to the possible source of the hyperpolarization during REM, it was found that electrical stimulation of the bulbar FTG during REM produced prominent long-latency (28 ms to onset, 43 ms to peak) hyperpolarizing potentials in lumbar motoneurons during REM. That these potentials were IPSPs was indicated by their reversal by Cl^- injection or by hyperpolarization, and by their being abolished upon the microiontophoretic application of strychnine [79]. These IPSPs were only intermittently present with the same stimulation parameters in waking and slow-wave sleep. It is of interest that short-latency (~5–10 ms) hyperpolarizing potentials did not vary with

[79] Soja *et al.* (1987b).

state. Our view of these data would agree with the interpretation [78] that bulbar RF may be an important source of descending inhibition, and add that the long-latency, REM-state-specific hyperpolarizing potential may be due to recruitment of more reticular formation neurons by the stimulus in REM, an effect related to the REM-state-specific population depolarization of reticular neurons. There is a REM-sleep selective effect of stimulation of the PRF (nucleus reticularis pontis oralis) in producing hyperpolarizing potentials in lumbar motoneurons [80], an effect not seen in other states, and conceptualized by these workers as resulting from more recruitment of reticular neurons in REM by these stimuli. This interpretation is compatible with the data in Chapter 3 indicating dense excitatory pontobulbar connectivity.

Finally, in view of the possible role of cholinergic neurons in REM phenomena (Chapter 11), it is of interest that microinjections of carbachol into the PRF of decerebrate cats produced postsynaptic inhibitory effects on lumbar motoneurons that were "remarkably similar" to those described above in the chronic cat during natural REM, including changes in input resistance, rheobase, and development of large discrete inhibitory PSPs [81]. That MP was hyperpolarized only 2.2 mV following carbachol vs 6.7 in natural REM may have been due, at least in part, to the 3 mV greater baseline hyperpolarization of neurons in the decerebrate cat vs the intact cat in slow-wave sleep.

[80] Fung *et al.* (1982).

[81] Morales *et al.* (1987).

10.9. Central Mechanisms of REM-Sleep Muscle Atonia

10.9.1. Lesion Data and REM Without Atonia

The Lyon group reported that bilateral lesions of the pontine reticular region just ventral to the locus coeruleus (LC), termed by this group the LC α and peri-LC α , and its descending pathway to the bulbar reticular formation abolished the muscle atonia of REM sleep [82] (Fig. 10.21). (The projections of this region to BRF and whether they are to magno- or gigantocellular field are discussed in Chapter 3.) This group also reported that not only was the nuchal muscle atonia of REM suppressed, but that cats so lesioned exhibited "oneiric behavior," including locomotion, attack behavior, and behavior with head raised and with horizontal and vertical movements "as if watching something."

[82] Jouvet (1979); Sastre and Jouvet (1979).

The basic finding of REM without atonia with bilateral pontine tegmental lesions were confirmed but, in

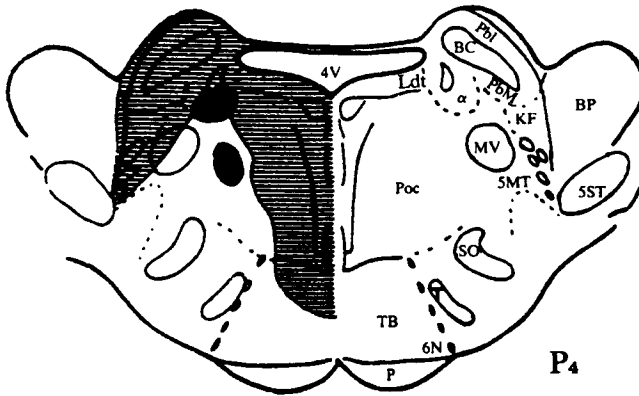


Figure 10.21. Frontal section of the pons of the cat. The solid areas indicate the localization of the lesions which suppress postural atonia during REM. These lesions coincide with the locus coeruleus α or its descending pathway. The horizontal hatching corresponds to lesions that do not suppress postural atonia. Pbl: n. parabrachialis lateralis; Ldt: n. lateralis tegmenti dorsalis; PbM: n. parabrachialis medialis; KF: n. Kölliker-Fuse; Poc: n. pontis caudalis; BP: brachium pontis; 5MT: motor nucleus of trigeminal nerve; 5ST: sensory nucleus of trigeminal nerve; BC: brachium conjunctivum; 4V: fourth ventricle. From Jouvet (1979).

addition, it was found that lesions extending beyond the LC α region and its efferent pathway to bulb were necessary for more than a minimal release of muscle tone and to produce the elaborate “oneiric behaviors” [83]. These authors found particular lesion locations were associated with particular sets of behaviors: For example, attack behavior with lesions that extended into midbrain and interrupted amygdalar pathways, locomotion with lesions near the brainstem locomotor region, and orienting-like behavior with small, symmetrical dorsolateral pontine lesions (Fig. 10.22). Finally, the presence of attack and locomotion behaviors in REM without atonia was reported to be associated with an increased incidence of these behaviors in waking, leading to the interpretation that the lesions may have done more than simply counteract a behaviorally nonspecific muscle inhibition during REM: they may have released the particular behaviors appearing in both REM and waking. Chapter 13 discusses the relationship of these “oneiric behaviors” in animals to similar phenomena seen in cases of human pathology, and their relationship to dreaming.

Quisqualate lesions of bulbar gigantocellular tegmental field (FTG) and FTM led to a marked decrease of the muscle atonia of REM sleep, and to the appearance of paddling behavior during this state [84]. The percentages of time spent in REM and non-REM sleep and in waking were not greatly altered. These data further support a role of bulbar FTG/FTM in REM-sleep muscle atonia.

[83] Hendricks *et al.* (1982).

[84] Holmes *et al.* (1988).

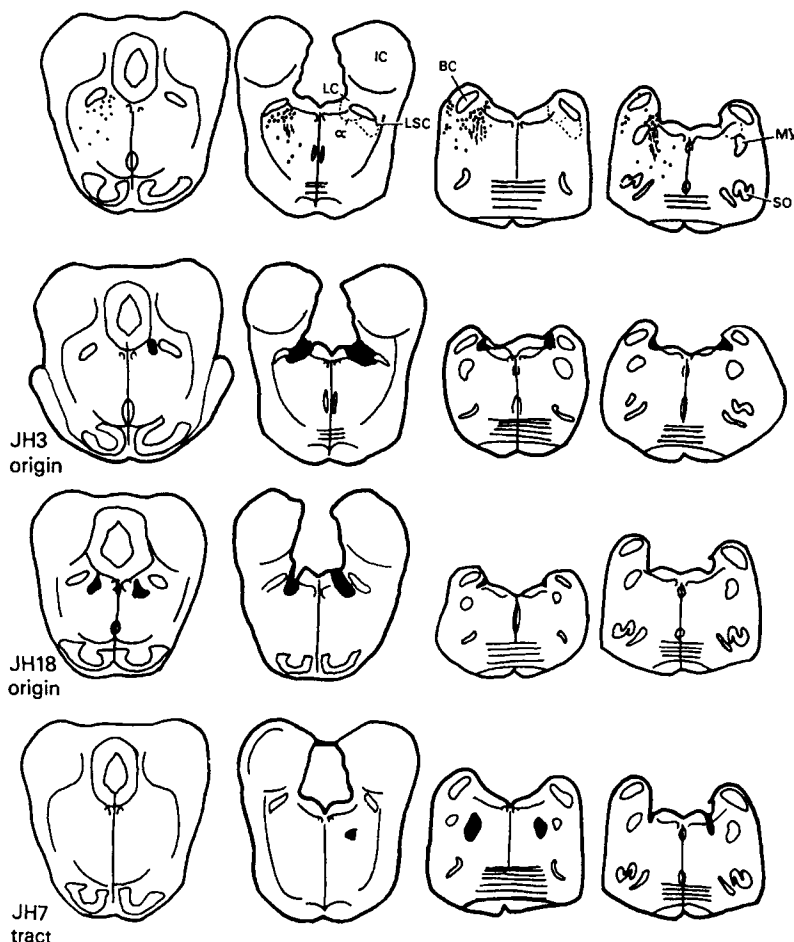


Figure 10.22. Lesions releasing minimal limb and neck movements, compared with the tegmentoreticular tract. Top row: coronal sections at levels P1,2,3,4 from left to right. Left side: cells of origin and projection fibers of tegmentoreticular tract proposed by Sakai *et al.* (1979) to mediate the atonia of REM. Right side: dashed lines outline components of the locus coeruleus complex in the terminology of Sakai *et al.* (1979). Second and third rows: lesions which bilaterally damaged the origin of the tegmentoreticular tract: the medial α locus coeruleus and medially adjacent reticular formation. Fourth row: lesion placed bilaterally in the projection of the tract as it descends medial to the motor nucleus of the trigeminal nerve. Abbreviations for all figures; LC α , locus coeruleus α ; BC, brachium conjunctivum; IC, inferior colliculus; LC, principal locus coeruleus; LSC, locus subcoeruleus; MV, motor nucleus of trigeminal nerve; SO, superior olive; VII, seventh nerve. From Hendricks *et al.* (1982).

10.9.2. Electrophysiological Data and REM-Muscle Atonia

Near half extracellularly recorded units in peri-LC α region show a selective, tonic discharge during REM, and decreased firing rate during deep slow-wave sleep and no discharge activity during waking [85]. Of those REM-on neurons, some were antidromically activated from the bulbar magnocellular field. Some REM-on neurons have also

[85] Sakai (1980, 1985a, b, 1986); Sakai *et al.* (1981).

been found within the magnocellular reticular formation [86] (Fig. 10.23). These neurons had discharge rates that were virtually zero in waking, even in the presence of sensory stimulation and voluntary movements, discharges remained near zero in early slow-wave sleep, and then in slow-wave sleep with PGO waves (5–20 s prior to REM) discharges increased to about 5/s, and further increased to approximately 30/s in REM, with intense acceleration of firing concomitant with runs of PGO waves and eye movements. Electrical stimulation of the peri-LC α resulted in synaptic excitation of some neurons with latencies of 2 and 4.5 ms; in the data from one neuron that is included in a

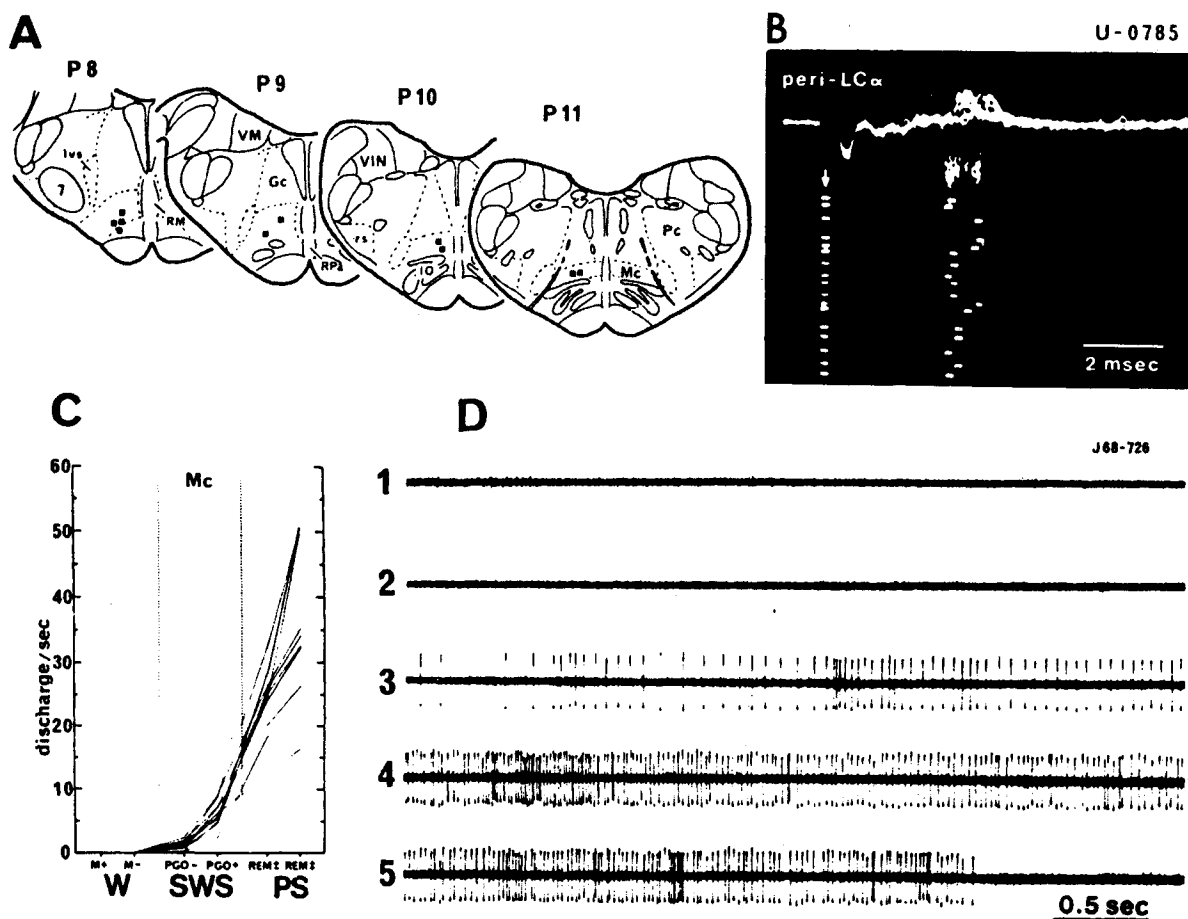


Figure 10.23. A: Location of the magnocellular (Mc) REM-specific neurons. B: Effects of stimulation of the peri-LC α (B) on a Mc REM-specific cell. Superimpositions of several synaptic responses and dotgrams of 17 successive sweeps (the first dot represents the shock artifact) following stimulation of the peri-LC α . C: a summary of neuronal discharge rates of Mc PS-specific cells during the sleep-waking cycle. D: an example of single unit discharges recorded in the Mc during: W (1); SWS without PGO

waves (2); SWS with PGO waves to REM (3); REM (4); and REM to W (5). Abbreviations: 7, facial nucleus; FLM, fasciculus longitudinalis medialis; Gc, n. reticularis gigantocellularis; IO, inferior olivary complex; lvs, direct lateral vestibulospinal tract; Mc, n. reticularis magnocellularis; Pc, n. reticularis parvocellularis; RM, n. raphe magnus; RPA, n. raphe pallidus; rs, rubrospinal tract; VIN, inferior vestibular nucleus; VM, medial vestibular nucleus; S, nucleus of the solitary tract. From Kanamori *et al.* (1980).

Fig. 10.23B, spike latency varies by 1 ms, indicating this response may not be monosynaptic. Some neurons had antidromic responses to stimulation of the ventral reticulospinal tract. It may also be noted that the magnocellular bulbar RF area recorded includes the classic medullary inhibitory zone [87].

These data were interpreted [85] as consistent with an hypothesis that nonmonoaminergic neurons of the peri-LC α (e.g., reticular neurons) become active just before and during REM, and, via tegmentoreticular tract projections to the bulbar magnocellular field, excite neurons in this reticular zone which, in turn, via projections in the ventrolateral reticulospinal tract may cause the postsynaptic inhibition of spinal motoneurons. (The data cite to support a role of the lateral reticulospinal tract involvement in the postural atonia mechanisms of REM sleep derive from studies by Pompeiano [88].)

Our own view of these data is, in general, consistent with the possibility of such an interpretation. However, we think it useful to emphasize the possibility of involvement of other portions of reticular formation. This is because, first of all, Sakai and coworkers [85] tend to call reticular zones "magnocellular" that others label "gigantocellular" (see Chapter 3), and thus much of the localization question may be purely terminological; another reason is that more sensitive HRP chromogens and even smaller injection zones in cord have indicated the presence of bulbar FTG as well as FTM projections to the ventral portion of lateral funiculus (see Chapter 3 and [53]). Finally, other data [89] indicate that projections in the peri-LC α area are primarily to bulbar FTG. With respect to the electrophysiology, the evidence for monosynaptic projections from peri-LC α to FTM is not compelling. Also, other investigators [90] have recorded similar cells in head-restrained cats in a small-cell bulbar reticular zone outside the FTM, perhaps in FTL. With extracellular recordings in head-restrained cats, neurons were recorded in bulbar nucleus gigantocellularis (FTG) [91], a part of the zone that stimulation experiments in acute cats had implicated in inhibitory projections to jaw-closer motoneurons [92]. Chase and coworkers describe these neurons have discharges that increased in a continuum from waking to slow-wave sleep to REM sleep [91] (Fig. 10.24). These discharge rates were in a reciprocal relationship with the magnitude of the state-related amplitude of the trigeminal monosynaptic reflex, which is suppressed in REM sleep. Supporting the hypothesis that these neurons may be responsible for the inhibition of trigeminal jaw-closer motoneurons was the fact that two of the ten cells had spike-triggered averaging data consistent with a monosynaptic inhibitory input to the jaw-closer motoneuron pool.

[87] Magoun and Rhines (1946). Tohyama *et al.* (1979a-b) have provided data from retrograde labeling of HRP placed in the ventral portion of the lateral funiculus that magnocellular neurons indeed project to this spinal zone.

[88] Pompeiano (1976).

[89] Rye *et al.* (1988).

[90] Netick *et al.* (1977).

[91] Chase *et al.* (1984).

[92] Nakamura *et al.* (1975).

[93] Pompeiano (1985). This reference should also be consulted for a general review of brainstem postural control mechanisms, a subject not reviewed in the present book.

Finally, with respect to the peri-LC α neurons, it is somewhat difficult to base a comprehensive theory of REM-muscle atonia on this sample size, and we wonder if the paucity of neurons that have been found to show this discharge signature may not reflect the participation of other neurons in REM-sleep atonia. It seems entirely possible and even plausible that the neurons active in the muscle atonia of REM might also be also active in the normal patterns of muscle inhibition of waking, as indeed suggested by the studies of Pompeiano [93]. In this case there might not be a pure "REM selective" pattern [91], but the population of neurons participating in REM atonia might have subsets of its members active in other states as a function of various postural adjustment mechanisms. The distinctive feature of REM atonia would then lie in the simultaneous involvement of the entire population of neurons providing muscle tone suppression, a concept akin to the notion discussed in Chapter 12 that the distinctive characteristic of REM in reticular formation is a population-specific activation and MP depolarization. In fact, intracellular recordings have demonstrated the presence in REM

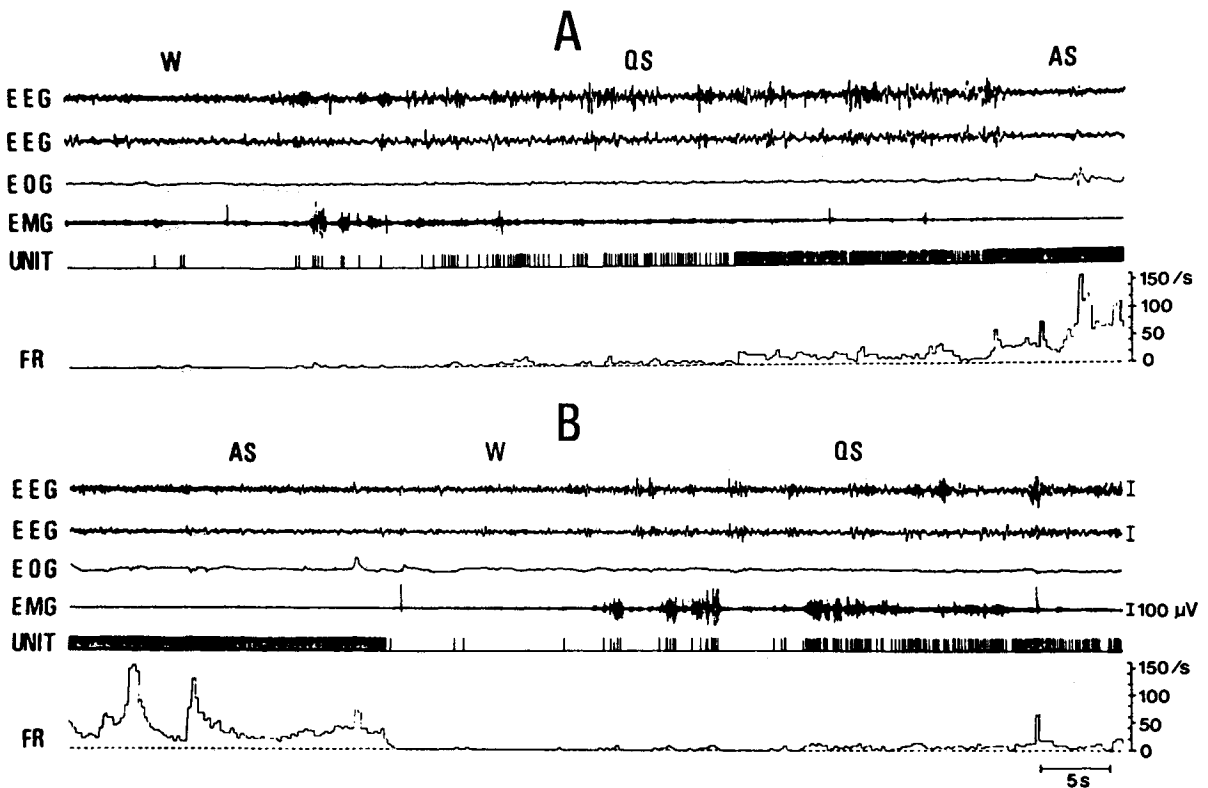


Figure 10.24. Discharge pattern of an extracellularly recorded medullary reticular neurons during the transition from SWS (QS) to REM (AS) (A) and from REM (AS) to W (B). Between

A and B, records were omitted for 2 min. FR—firing rate—the number of spikes/sec. Binwidth 250 ms. From Chase *et al.* (1984).

of an MP depolarization of bulbar reticular formation neurons [94] in the same area as the extracellular recordings were performed [91].

[94] Chase *et al.* (1981).

10.9.3. Role of Other Pontine Structures and the Pharmacology of REM-Sleep Muscle Atonia

With respect to the localization of descending inhibitory pathways, it was found that electrical stimulation of a midline zone in the pons (from P3 to P7, and 1–2 mm below the ventricular surface) produces a long lasting suppression of postural muscle tone in both decerebrate and awake freely moving cats [95]. That region was termed the dorsal tegmental field (DTF). It was believed that were fibers of passage were activated and anatomical studies suggested the most likely fiber pathway was that leading from the nucleus RPO (nongiant cell field) directly to the bulbar FTG, although the possibility of activation of the tegmentoreticular tract was not excluded [96]. In a synaptic connectivity study, spike-triggered averaging was used to study the relationship of extracellularly recorded discharge fluctuations of bulbar giant cell field neurons antidromically identified as projecting in L1 spinal cord (in ventral or lateral funiculus) to the fluctuations in MP of intracellularly recorded extensor and flexor motoneurons at L5–S1 [97]. The bulbar neurons so studied also were orthodromically activated by DTF stimulation at mono- or disynaptic latencies and had antidromic conduction velocities of 90 m/s. The latency from the bulbar neuronal spike to the motoneuronal IPSP was 5 ms (3.7–8 ms range), and the segmental delay, time from the arrival of the presynaptic axonal volley to the onset of the hyperpolarizing potential, was about 1.5 ms. Since monosynaptic connections usually have synaptic delays in the range of about 0.4 ms, and disynaptic connections often have delays in the 1.5 ms time range, these workers postulated a disynaptic pathway with the inhibitory interneuron located in spinal cord. In addition, other parameters of the IPSP, such as time to peak, were not congruent with a monosynaptic projection.

[95] Mori (1987).

[96] Ohta *et al.* (1988).

[97] Takakusaki *et al.* (1988a,b).

This group [97] also used carbachol (100 mM, 0.1–0.25 μ l) microinjected into nucleus reticular pontis oralis (P2–P3, lateral 1–2), and found this zone produced a very short latency (less than 1 min) postural atonia with suppression of both flexors and extensors in acute decerebrate cats. (It may be noted parenthetically that carbachol injections in a similar dorsal pontine area [P1–P3; lateral 2] produce a short-latency [<5 min] induction of all REM

[98] Yamamoto *et al.*
(1988).

components in intact cats [98]). The NRPO carbachol injections also induced tonic firing in bulbar FTG neurons [97]. Electrical stimulation of the bulbar FTG evoked mixed PSPs in intracellularly recorded spinal α motoneurons that became predominantly hyperpolarizing upon carbachol microinjections. Atropine blocked this effect and noradrenaline and serotonin reduced the hyperpolarizing PSPs, indicating the presence of a muscarinic cholinergic–adrenergic reciprocity in this system, a finding previously reported for postural atonia systems [93]. Electrical stimulation of medial pons (FTP and FTG) had the same effect as bulbar FTG stimulation, further suggesting the presence of pontine to bulbar reticular projections carrying muscle suppression information.

[99] Katayama *et al.*
(1984).

With respect to the pharmacology of muscle atonia, in addition to the above-cited elicitation of atonia [95, 96], it has been recognized that direct microinjection of cholinergic agonists into the dorsolateral PRF (approximating the peri-LC α zone) may, at times, produce muscle atonia without the other components of REM sleep [99]. Within the medial bulb, cholinergic microinjection in the caudal portion of the muscle suppression zone [87] produces atonia, while, in contrast, non-NMDA excitatory amino acid but not cholinergic agonists were effective in the more rostral portion [100]; these workers also reported that non-NMDA excitatory amino acids were effective in producing muscle atonia when injected into dorsolateral pons.

[100] Siegel and Lai
(1988).

Thus, evidence is accumulating that the muscle atonia of REM sleep may involve more than one anatomically and pharmacologically specific brainstem system.

Color Plates

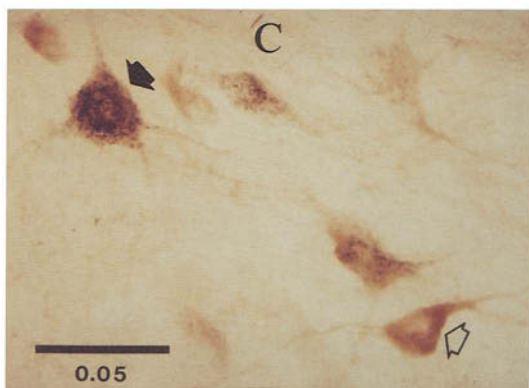


Plate 1

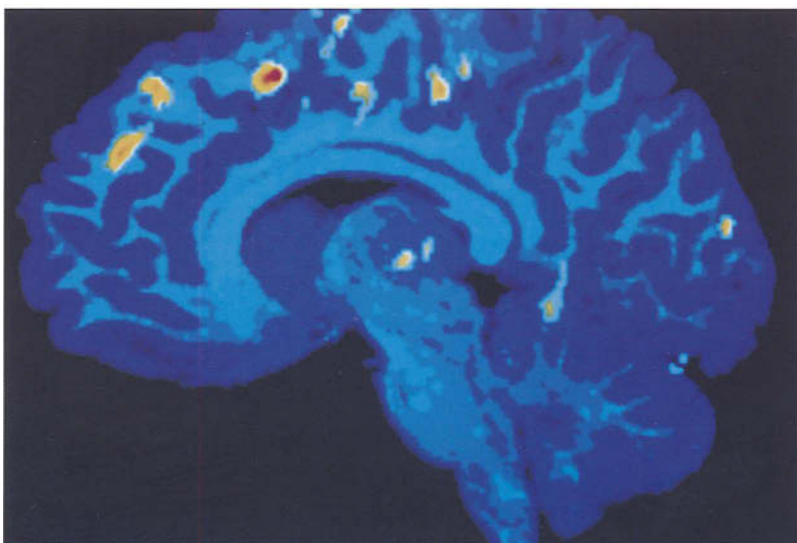
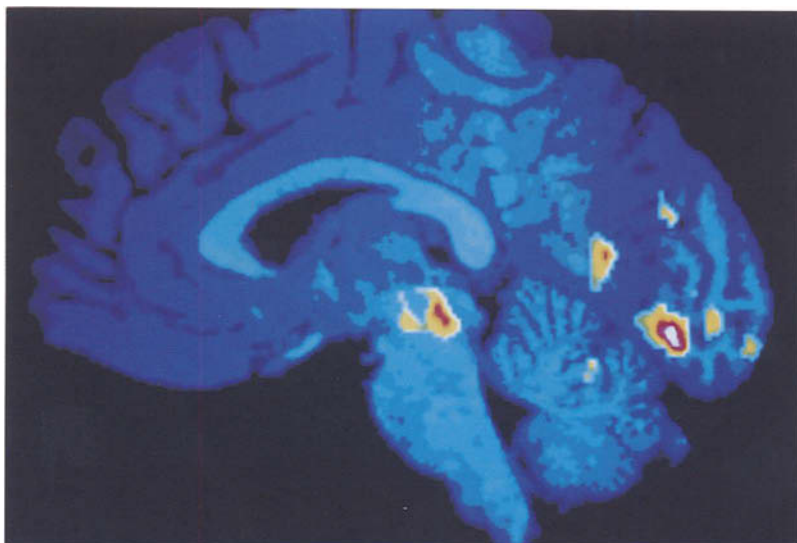


Plate 2

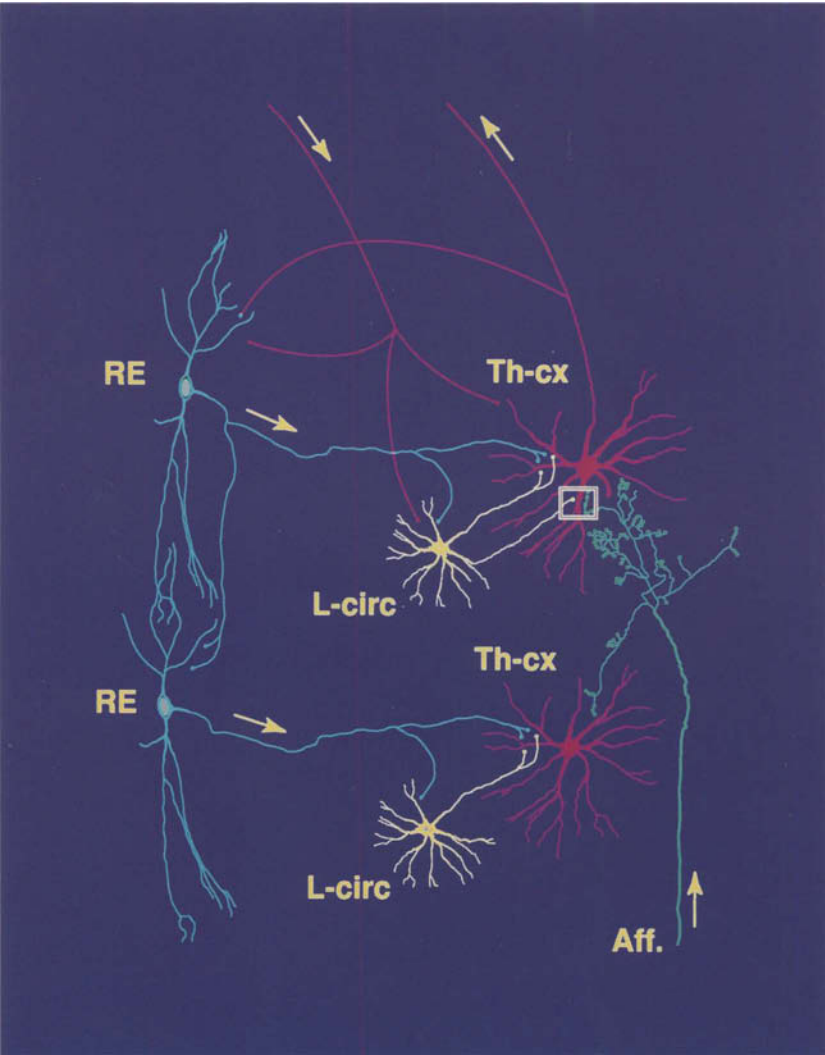


Plate 3

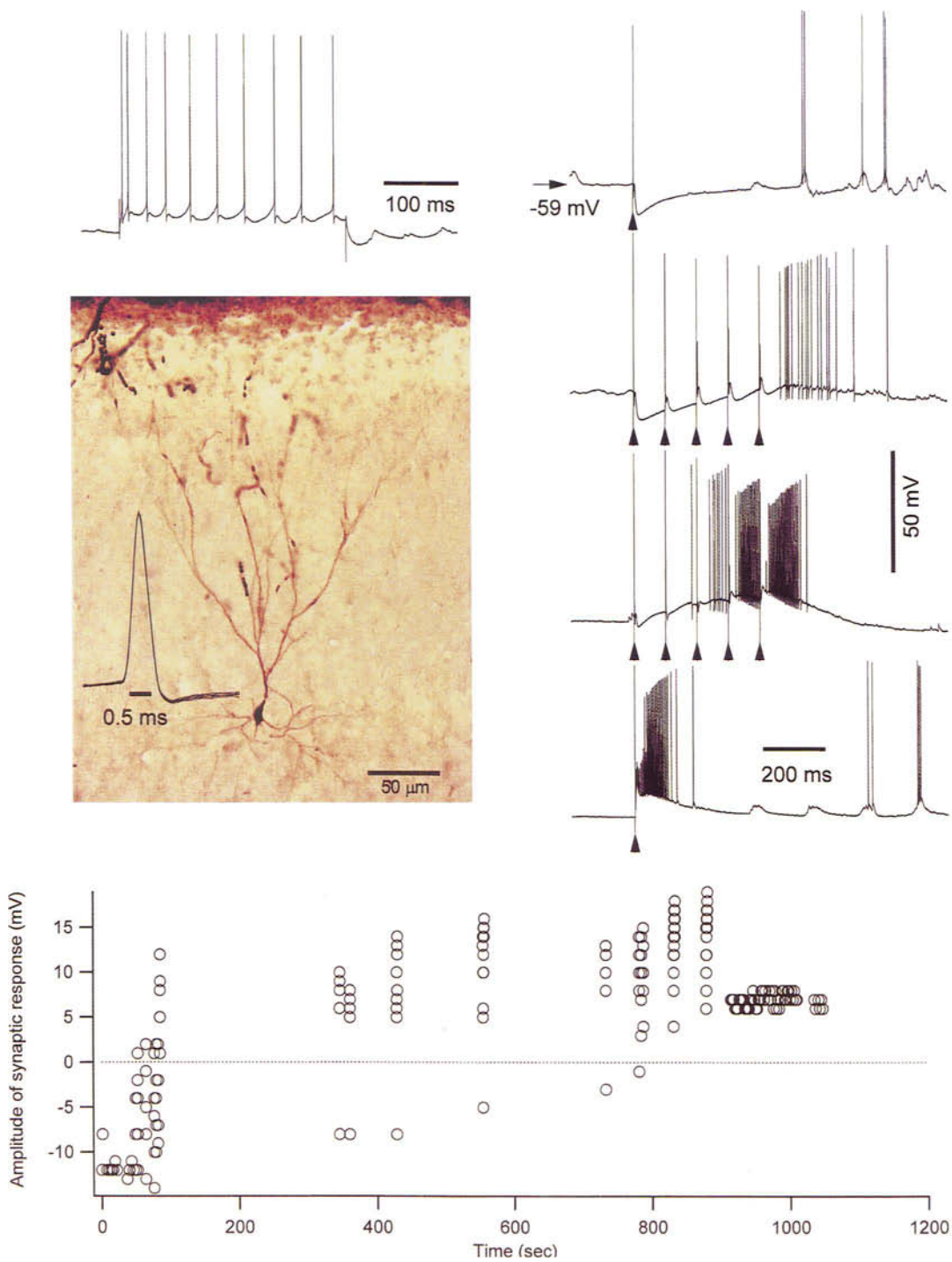


Plate 4

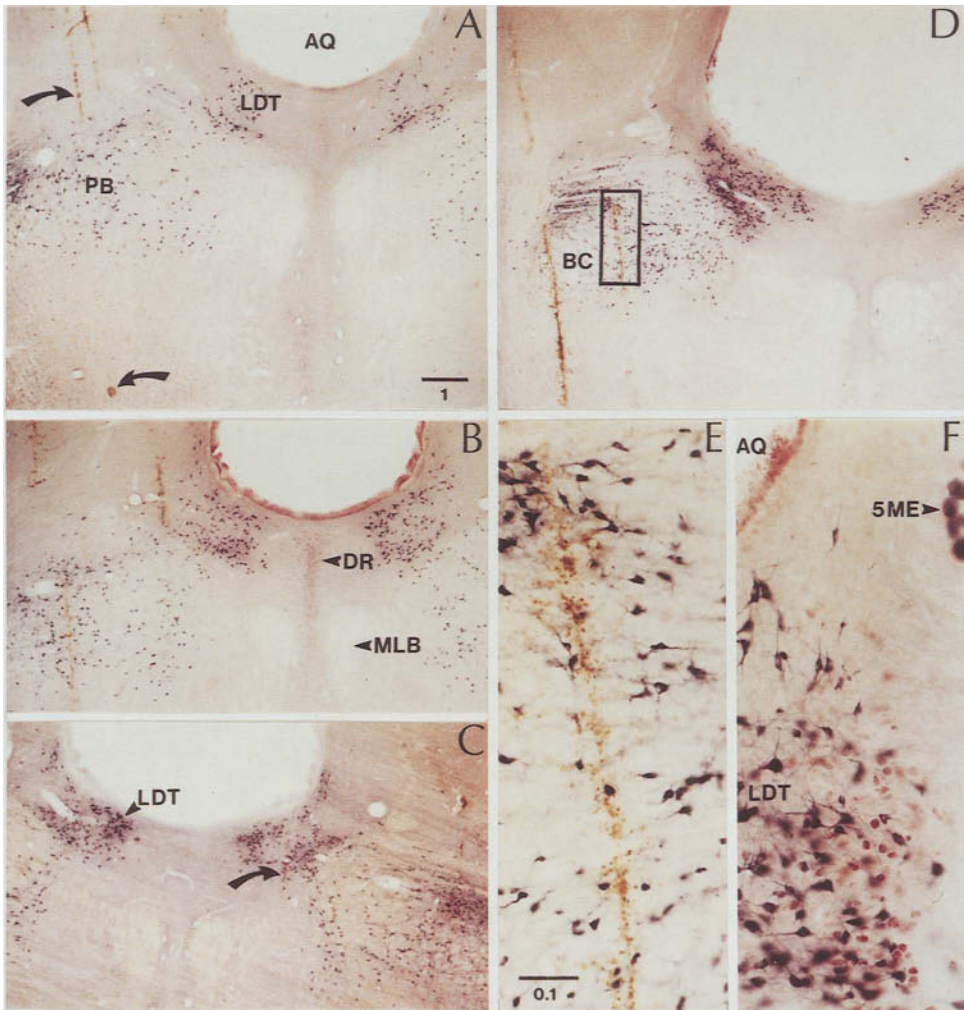
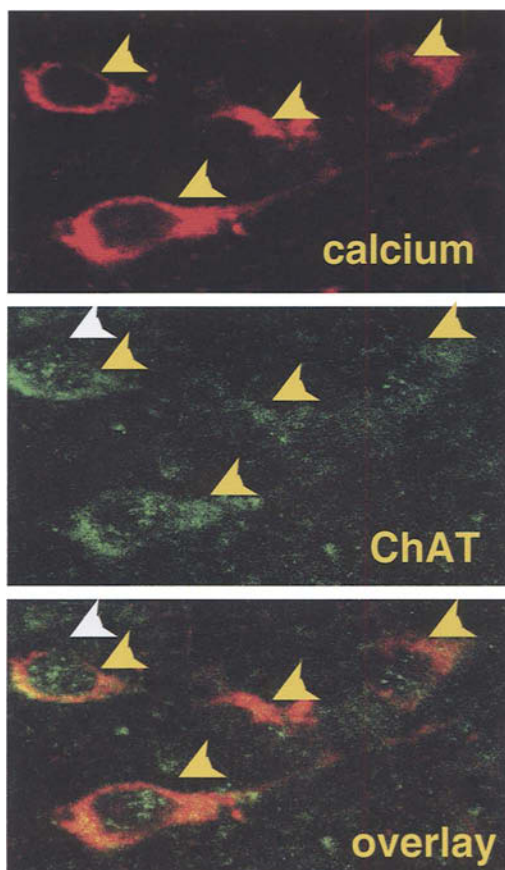
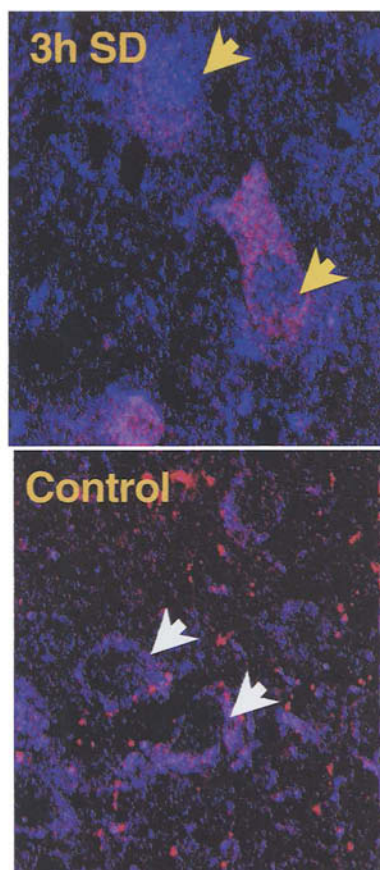


Plate 5

A



B



Neuronal Control of REM Sleep

11.1. Introduction and Overview

The first chapter of this book has described the history of much of the early lesion and stimulation work, as well as the cardinal signs of sleep and the definition of behavioral state. Other chapters have described the neurophysiological and anatomical substrates of various components of EEG-synchronized sleep and REM sleep. These include the synchronized oscillations of non-REM sleep in Chapter 7, the REM sleep components of Ponto-Geniculo-Occipital (PGO) waves and tonic cortical activation in Chapter 9, and the muscle atonia and the rapid eye movements in Chapter 10.

In this chapter, we focus on how these various components are orchestrated into the complex behavior of sleep. Chapter 7 has discussed how the characteristic components of EEG-synchronized sleep occur in the absence of activating and disrupting influences from the brainstem. Chapter 9 takes up the source of these influences in brainstem reticular neurons and the brainstem cholinergic neurons in the pedunculopontine tegmental (PPT) and laterodorsal tegmental (LDT) nuclei, with data from extracellular recordings of antidromically identified, thalamically projecting brainstem neurons. Our present viewpoint of EEG-synchronized sleep mechanisms is essentially a passive one; we suggest that synchronizing phenomena depend on the removal of influence from the brainstem and the wakefulness-active neurons in the basal forebrain (discussed in the next chapter). The sudden drop in both cholinergic and noncholinergic brainstem reticular input at sleep onset disfacilitates thalamocortical neurons while, at the same time, the reduction in cholinergic input facilitates the genesis of spindle oscillations in the reticular thalamic nucleus. Thus, the return of brainstem cholinergic and brainstem noncholinergic activating influences with REM sleep abolishes these synchronizing events.

In the next section (11.2), we address the question of the nature of neuronal population change in the reticular formation during REM sleep that leads to the production of the various REM components. The brainstem reticular formation may be viewed as “the final common pathway,” as effector neurons for the brainstem components of REM sleep. Intracellular recordings suggest that a common feature of REM sleep in the brainstem is a REM sleep-specific tonic membrane depolarization that lasts throughout the state. Data from extracellular recordings show the timing of the gradual onset of this influence. Sleep–wake behavioral state control can be viewed as stemming from modulation of excitability in neuronal pools underlying the components of REM sleep. The final section (11.3), addresses the question of what might cause these modulations of excitability in neuronal pools. Since the first edition of this book, great progress has been made in understanding the influences on reticular formation neurons and their interactions with each other, although much remains to be learned. We will discuss in some detail the role of the neurotransmitters acetylcholine, serotonin, norepinephrine, and GABA in the orchestration of REM sleep.¹

11.2. Brainstem Reticular Neuronal Activity over the REM Sleep Cycle

This section will present the brainstem reticular neuronal activity characteristic of REM sleep. We begin with the reticular formation since, for the most part, these neurons can be viewed as the “effector” or “final common pathway” set of neurons for REM sleep. We will emphasize cellular electrophysiology as offering the most definitive data about REM characteristics, but will include auxiliary methods as appropriate. The reason for the field’s focus on the brainstem dates back to probably the most influential of the many lesion experiments—the early transection studies in the cat by Jouvet [1]. When the neuraxis was cut at the midbrain level (Fig. 11.1), rostral to the pons, signs of the state of REM sleep were not present rostral to the cut (with the cut between brainstem and forebrain, the pathway for all brainstem-mediated REM cortical desynchronization was absent). However, the essential signs of REM sleep were preserved in the brainstem caudal to the cut, as shown by the major REM indicator variables available for analysis in this preparation. The “pontine cat,” as this preparation was called, showed periodically occurring

[1] Jouvet (1962).

¹ This chapter draws upon material from a recent review by McCarley (2004)

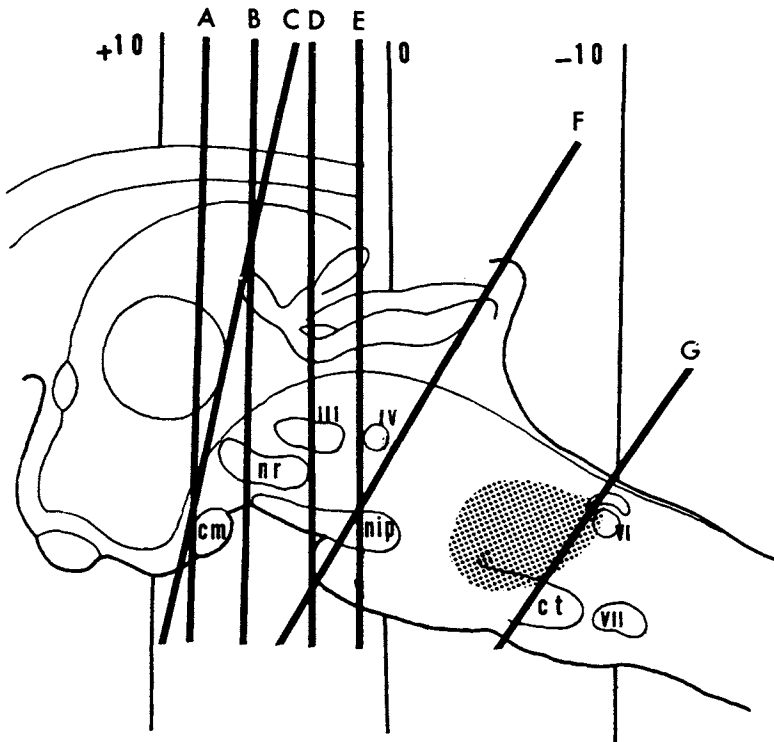


Figure 11.1. Neuraxis transections in the cat by Jouvett (1962). Transections A through F left the essential signs of REM sleep present caudal to the plane of the section, but not rostral to it. Section G abolished the signs of REM sleep. Stippling indicates the zone where electrolytic lesions abolished REM sleep. Midline sagittal section; -10, 0, +10 are HC coordinates; roman numerals indicate cranial nerve nuclei; red nucleus, nr; mammillary body, cm; interpeduncular nucleus, nip; and trapezoid body, ct. Adapted from Jouvett (1962).

states characterized by (1) rapid eye movements, although they were reduced in number and complexity, (2) antigravity muscle atonia, especially remarkable since they abolished the decerebrate rigidity otherwise present, and (3) spiky waves in the pontine tegmentum, the pontine component of PGO waves. The important implication of this study was that the structures caudal to the cut were necessary and sufficient for basic REM phenomena, including rhythmicity. (This is not to say that more rostral structures do not enter into elaboration of REM phenomena; the phenomena in the pontine cat are simpler than those in the intact animal.) However, the presence of the major indicators of REM sleep below this transection has led to a fairly general consensus that the mechanisms for REM production are localized in the lower brainstem, although, as will be discussed, more precise specification of localization and the neurotransmitter influences is still controversial (see, for example, later discussion in this chapter.)

The perspective one obtains from extracellular recordings is useful because this technique enables long-term recordings and is of historical importance for the development of concepts in the field, although the level of mechanistic insight into the nature of state-related alterations and mechanisms is necessarily less than with intracellular recordings. Extracellular unit recordings in the head-restrained cat done in the early 1970s showed that cells in the pontine reticular formation gigantocellular field (FTG), had REM sleep discharge rates considerably higher than those in EEG-synchronized sleep and waking [2]. An early formulation was that this area might be a REM sleep “center.” However, the work of Siegel and coworkers in cats and Vertes in rats showed that FTG neurons discharged in association with movements in waking in freely moving animals, and that if the animals performed the movement associated with a higher discharge rate throughout the recorded waking segment, then the discharge rate in waking approximated that of REM [3]. These studies indicated that a simple notion of the FTG as a “REM center” was not appropriate, at least in one classical definition of a center: an anatomical locus of neurons associated with one behavioral or physiological function and no other (see discussion of the center concept in Chapter 1). In fact, in extracellular recordings, Siegel and Vertes did not observe any state-specific activity in any portion of the pontobulbar reticular formation; obviously, these extracellular recordings could not monitor the REM state-specific population membrane depolarization observable in intracellular recordings and described next in this chapter.

Extracellular recordings are particularly valuable because they enable long-duration recordings of brainstem activity, and hence a clear perspective of changes in activity profile over repeated sleep–waking cycles. Figure 11.2 is such an extracellular multiple cycle recording that clearly shows the magnitude of state-related modulation of discharge activity and the periodicity of this remarkable modulation of activity. Extracellular recordings indicated that, within pontine reticular formation, the pattern of discharge varies from “phasic,” defined by runs of clustered discharges, to “tonic,” with relatively little moment-to-moment discharge variation [4]; as a general rule, neurons with the most pronounced REM sleep discharge rate increase tended to have phasic discharge patterns (clusters of discharges, but without the presence of low-threshold spike “bursts” as defined in Chapter 5) and to be localized in medial pontine reticular formation

[2] McCarley and Hobson (1971); Hobson *et al.* (1974a, b).

[3] Siegel (1979); Siegel and Tomaszewski (1983a); Siegel *et al.* (1983b); Vertes (1977, 1982).

[4] McCarley and Hobson (1975a).

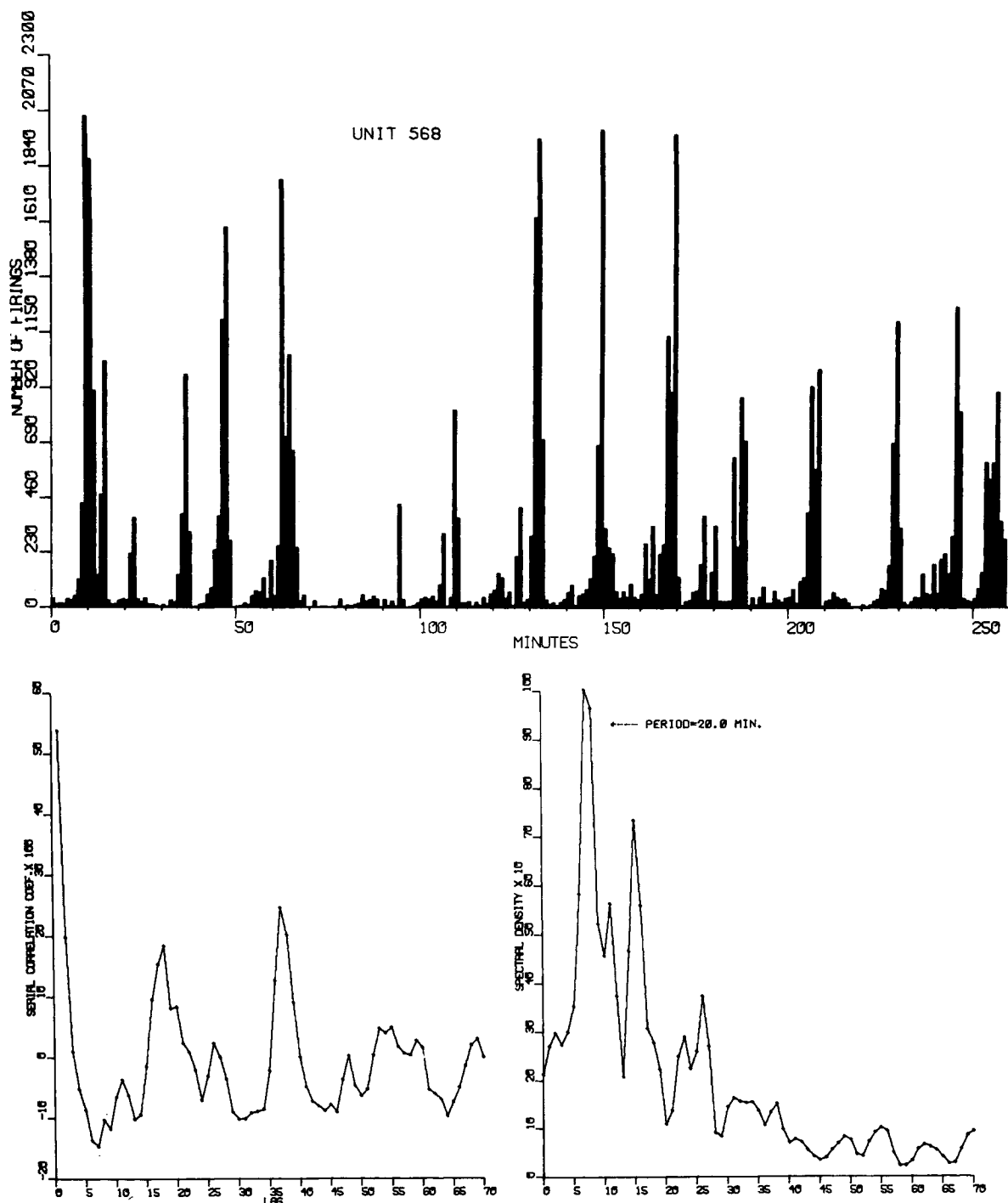


Figure 11.2. Extracellular recording of a pontine FTG neuron over many sleep-wake cycles in a head-restrained cat (Top Panel) and spectral analysis to show the periodicity. Each of the peaks of discharge activity corresponds to the occurrence of a REM sleep episode; the use of head restraint renders waking activity minimal and further emphasizes the obligatory nature of REM sleep discharge enhancement against the behavior-dependent changes of waking. Bottom

Left Panel. Autocorrelogram analysis. Note periodic peaks at approximately 20 min intervals. Bottom Right Panel Spectral analysis: maximal power is concentrated at a frequency corresponding to a period of 20 min, the period of REM sleep in this animal. The presence of substantial power on the flank of the peak is attributable to the non-sinusoidal (nonlinear) components of the activity. Adapted from McCarley (1980a).

(mPRF, in the FTG), while those recorded more laterally were more tonic and had less change. (The neurons with discharge activity associated with muscle atonia and described in the preceding chapter were a conspicuous exception.) The neuron illustrated in Fig. 11.2 had a “phasic” discharge pattern.

Later in this chapter, we will address the important question of what might cause the state-related changes in pontine reticular formation neurons, but we first look at lesion data bearing on the functional role of reticular subdivisions in the production of REM sleep components. The reader will again be reminded of our suggestion that lesions are not the most suitable technique for resolving questions of function of small groups of neurons. We list here the following potential confounds (1) fibers of passage (electrolytic lesions may destroy fibers as well as somata), (2) imprecise boundaries (all types of lesions are not controllable with respect to extent and the precise boundary of functional destruction/disturbance is not known), (3) ambiguity of interpretation even with complete lesions. The latter point is worthy of some elaboration. If a behavioral component vanishes, it is not known whether this implies (i) destruction of output pathways, (ii) nonspecific interference, for example, the animal may be rendered so ill that REM sleep will not occur, (iii) the area destroyed indeed normally mediates the behavioral component in question but other areas may be sufficient for its continued production, or (iv) the behavior, such as REM sleep, being investigated is so radically changed by the lesion that it is not clear whether or not it is present.

We have earlier discussed the Jouvét transection experiments suggesting a pontobulbar location for most of REM sleep components [1]. Transections at the pontomedullary level show preservation of many REM sleep indicator variables rostral to the transection suggesting that medullary components are not essential for REM, and thus pointing to the primacy of pontine and pontomesencephalic components [5]. Early reports by Jouvét and coworkers pointed to abolishment of REM sleep by electrolytic pontine reticular (FTG) lesions [1]. Later, kainic acid lesions of pontine FTG by two sleep research groups were reported to have no effects on REM signs, including no effect on eye movements in waking or REM [6]—a finding in conflict with the lesion studies reported by the oculomotor researchers in the preceding chapter. While it is difficult to reconcile these differences, absence of complete lesions of the medial pontine reticular zones important for eye movements (see Chapter 10, Fig. 10.2) may account for the differences; it is of interest that, while giant cells were reported as destroyed by the two sleep

[5] Siegel *et al.* (1984).

[6] Sastre *et al.* (1981); Drucker-Colin and Pedraza (1983).

research groups, we now know (Chapter 4) that these giant neurons are primarily reticulospinal neurons, and the smaller neurons critical for saccade generation may have been left unlesioned. This sparing appears likely from the histological photographs presented. Lesions of the zones that may be involved in muscle atonia have been discussed in the previous chapter. It is of note that much of the early lesion work was fraught with such controversies over precise localization; as a case example of the difficulty of resolution of lesion data, the reader is referred to the detailed discussion of the precise role of various vestibular nuclei in production of the PGO bursts of REM sleep furnished in an annotated bibliography [7].

[7] Hobson and McCarley (1974).

11.2.2. The View from Intracellular Recordings

Our viewpoint is that intracellular recordings provide a unique window on data relevant to the mechanisms of behavioral state control. In view of the transection evidence for the presence of the basic mechanisms of REM sleep in brainstem, recordings in this zone may be regarded as potentially the most informative with respect to mechanism. We introduce the topic of cellular phenomena of REM sleep in the brainstem by an illustration in Fig. 11.3 of a prototypical continuous intracellular recording in the cat of a mPRF neuron during state passages from W(Waking) to S(Synchronized sleep) to REM sleep, and back to W. The inkwriter traces serve to highlight the indicator variables defining the various behavioral states, and illustrate the temporal progression of phenomena. It can be seen that the lateral geniculate nucleus (LGN) PGO waves herald the occurrence of REM sleep, while the occurrence of atonia, EEG desynchronization, and rapid eye movements mark the REM period proper. The time period prior to REM with PGO waves but no other signs of REM has been termed the “transition period” between slow-wave sleep and REM and is abbreviated by “T” [8]. The data on the time course of membrane potential and occurrence of action potentials over the sequence of states illustrated in Fig. 11.3 described below are from Ito *et al.* [9].

[8] McCarley and Hobson (1970).

[9] Ito *et al.* (2002).

11.2.2.1. Synchronized Sleep

During synchronized sleep, the membrane potential is polarized at about -58 mV, and there is little postsynaptic potential (PSP) activity. Little change in membrane polarization is present in quiet waking-to-synchronized sleep transitions.

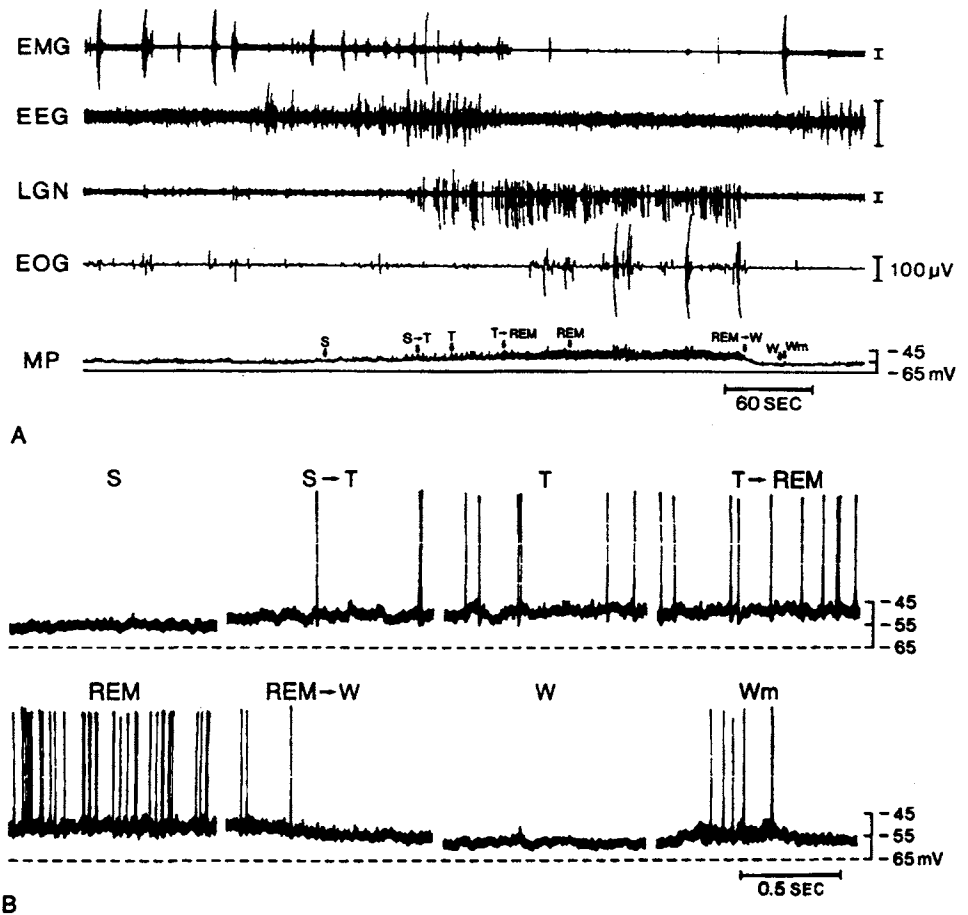


Figure 11.3. Changes in the membrane potential (MP) of a medial pontine gigantocellular tegmental field neuron over a sleep-wake cycle. The five traces (from EMG through MP) in the top panel (A) are a set of inkwriter recordings defining behavioral states in relationship to the MP level. Note that the inkwriter sensitivity is not high enough to trace individual action potentials (MP trace). In the bottom panel (B), oscilloscope photographs detail changes in the frequency of action potentials together with the MP level. The first trace of the top panel is EMG from the deep nuchal muscles. The second trace is EEG from the frontal cortex. The third trace of LGN activity shows PGO waves, which consist of high-amplitude pre-REM waves in T, irregular, high-frequency waves during REM sleep, and rather high-amplitude waves near the end of REM sleep. The fourth trace is EOG from the lateral rectus extra-ocular muscles. The fifth trace is the inkwriter MP record in which the many single spike-like deflections on the trace are prominent excitatory postsynaptic potentials (EPSPs) or compounds of EPSPs and action potentials. The MP records in the bottom panel (B) are eight photographs of the oscilloscope display of the tape-recorded MP. The labels indicate the corresponding segment on the inkwriter MP trace. See also detailed text description. Adapted from Ito *et al.*, 2002.

11.2.2.2. Pre-REM Sleep Changes: The Transition Period to REM Sleep, T

Even while the electrographic indicators are still those of synchronized sleep, the membrane potential of mPRF neurons begins to depolarize—a depolarization that progresses in the rather long, gradual approach to REM sleep. As the membrane potential depolarization

progresses and the electrographic indicators of the transition period appear (onset of PGO waves), there is increased frequency and amplitude of PSPs and the onset of action potential discharge.

11.2.2.3. REM Sleep

During REM sleep, the membrane potential is maintained at a depolarized level, some 7–10 mV more depolarized than during quiet waking or early synchronized sleep. This state-long, “tonic” depolarization is accompanied by increased frequency and amplitude of PSPs and action potential discharge. In addition to tonic depolarization, there are short duration, “phasic” runs of increased PSPs and action potentials.

11.2.2.4. Wakefulness: The REM Sleep–Wake Transition, and Motor Activity in Wakefulness

In the REM sleep to waking state transition, there is a fairly abrupt membrane repolarization of 7–10 mV, with the baseline membrane potential returning to the levels of the previous waking and early synchronized sleep periods. There is a marked reduction of PSP activity in quiet waking compared to REM sleep. While the intracellular data discussed here were obtained in animals whose heads were atraumatically restrained to facilitate the intracellular recordings, the animals remained free to make ocular or somatomotor movements. When a somatic motor movement occurred, there was often a transient membrane depolarization and action potential activity (see Fig. 11.3 at the portion of the record marked Wm). After the end of the movement, the membrane potential returned to a polarized level and action potentials ceased. In waking periods without movement, there was no membrane depolarization. Other mPRF neurons showed transient depolarizations and action potentials in waking in association with ocular movements, but a tonic membrane depolarization that persisted throughout waking was not characteristic of mPRF neurons.

To summarize: intracellular recordings in mPRF show a tonic depolarization in REM sleep that is not present either in EEG-synchronized sleep or waking. In waking, transient depolarizations may occur with ocular or somatic motor movements, but do not persist beyond the movement. Thus, REM sleep in the mPRF may be regarded as a state always characterized by a membrane potential depolarization, whereas in waking any depolarization is dependent on the presence of a particular behavior.

11.2.2.5. State-Dependent Alterations in Reticular Excitability

Corresponding to these changes of membrane polarization level were alterations in excitability, as measured by responses to electrical microstimulation from reticular sites in contralateral mPRF and in bulbar reticular formation, BRF, (Fig. 11.4). Increased excitability was present in REM sleep as contrasted with EEG-synchronized sleep or waking, as measured by the effects of constant current stimulation on monosynaptic PSP amplitude, propensity to evoke action potentials, and percentage of stimuli leading to antidromic activation. Differences with REM sleep were most prominent in EEG-synchronized sleep (Fig. 11.4A) but were also present in waking (Fig 11.4B) and were pervasive in the mPRF neuronal pool.

11.2.2.6. Summary of Behavioral State Alterations in the mPRF

The intracellular analyses show that each behavioral state has distinctive characteristics in the mPRF neuronal pool. REM sleep is a state of heightened excitability and decreased membrane potential (e.g., depolarization) that is both extensive in the mPRF pool present in almost all (>90%) of the neurons sampled, and persistent throughout the REM sleep state. EEG-synchronized sleep is a state where mPRF neurons show lessened excitability, increased membrane polarization, and little spontaneous excitatory postsynaptic potential (EPSP) activity. Waking, in contrast to REM sleep, does not have a temporally persistent heightened excitability and membrane depolarization throughout the pool. Rather, in waking, phasic membrane depolarizations appear to occur in a limited subset of the mPRF pool and in temporal association with the occurrence of specific behavioral events.

11.2.3. Sleep–Wake Control as Resulting from Modulation of Excitability in Neuronal Pools

11.2.3.1. The Concept

The classic Sherringtonian concept of a neuronal pool with varying degrees of facilitation and suppression [10] is useful for dealing with behavioral state alterations observable in brainstem reticular formation. Data to be presented suggest that the most salient alterations in the course of behavioral state changes are the result of different levels of

[10] Sherrington (1906).

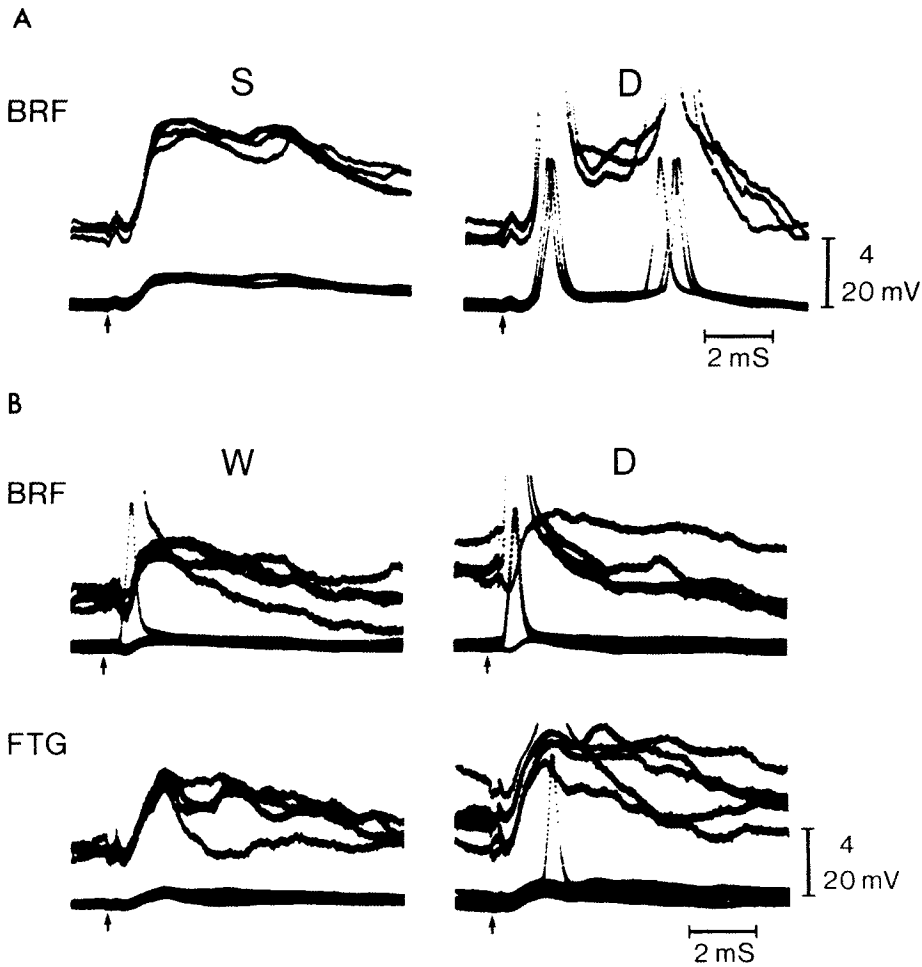


Figure 11.4. State-dependent excitability changes in intracellularly recorded mPRF neurons in the cat. A. Intracellular recording from a medial pontine reticular formation (mPRF) neuron showing effects of 70 μ A stimulation in ipsilateral giant cell field of bulbar reticular formation (BRF) at arrow. Upper traces are high-gain AC-coupled (cal: 4 mV) and lower traces are low-gain DC (cal: 20 mV). In S, BRF stimulation evoked excitatory postsynaptic potentials (EPSPs) with components at both monosynaptic and polysynaptic latencies, but no action potentials. When the state of the animal changed to REM sleep (abbreviated as D for Desynchronized sleep), stimulation at the same intensity elicited action potentials from both EPSP components. In a series of neurons and trials, the probability of a monosynaptically elicited action potential in S was 0.13 and in REM sleep was 0.9. B. Intracellular recording of an mPRF neuron with calibration as in A. BRF stimulation of 60 μ A in waking (W, upper row) produced one antidromic action potential in four trials, but in REM sleep (D), three of four trials showed antidromic invasion. Note the monosynaptic EPSP that was present when no antidromic invasion occurred. Criteria for antidromic invasion were: microstimulation latency < 0.6 mS with < 0.1 ms variability and no preceding PSP. The lower row shows that stimulation of 75 μ A in the gigantocellular tegmental field (FTG) portion of the contralateral mPRF evoked monosynaptic EPSPs with a steeper rising phase in D than in W; mean peak EPSP amplitude was also slightly (0.7 mV) higher in D than in W. One spike potential was elicited in D but none in W. Note also that the membrane potential fluctuations due to spontaneous postsynaptic potentials were more prominent in D. Modified from Ito and McCarley (1984).

membrane polarization in different neuronal pools, which, in turn, lead to different levels of excitability and to different discharge pattern propensities due to the presence of voltage-sensitive membrane currents, as discussed in detail in Chapter 5. We shall frequently use the shorthand term of “bias” as a way of indicating alterations of excitability in neuronal pools. Figure 11.5 schematizes this concept of behavioral state operation by alteration of “bias” on different neuronal pools important in production of REM components. While we here primarily discuss bias alterations from changes in membrane potential, there is the strong possibility that the state-induced bias of neuronal pools may also utilize other mechanisms, such as intracellular second messengers. Unfortunately, these other mechanisms have not been, as yet, thoroughly investigated in the brainstem in relation to sleep–wake states. The basic argument is straightforward: increasing the excitability of neurons in a particular brain region or nucleus will increase the probability of behaviors or physiological functions controlled or mediated by that region. We, thus, see REM sleep as composed of relatively discrete “physiological modules,” REM sleep components, which

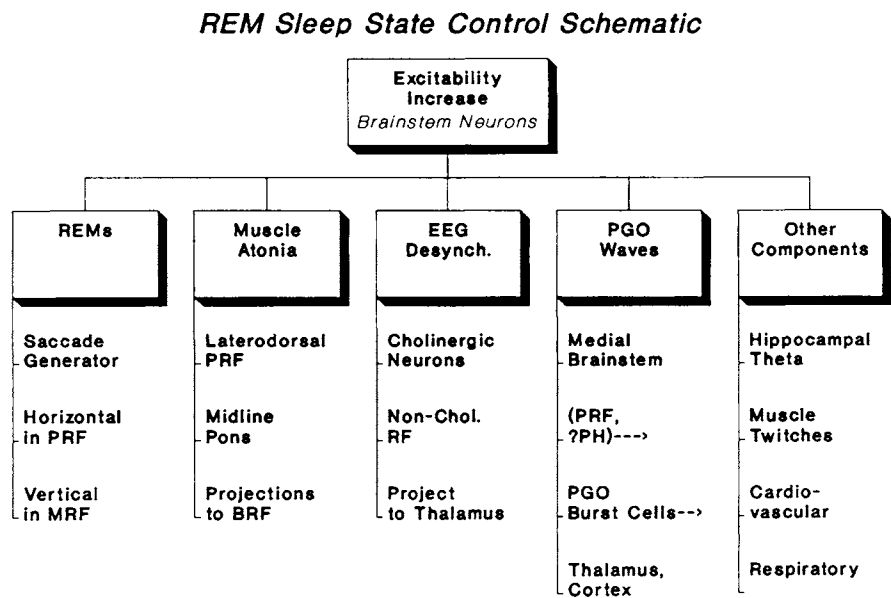


Figure 11.5. Schematic of REM sleep behavioral state control by alteration of bias (= excitability) within brainstem neuronal pools subserving each of the major components of the state. For example, the neuronal pool important for the rapid eye movements is suggested to be the brainstem saccade generating system whose main machinery is in paramedian pontine reticular formation (PRF) (Chapter 6). Although vertical saccades are fewer in REM, their presence suggests similar involvement of the mesencephalic reticular formation (MRF). Information under the other system components sketches the major features of the anatomy and projections of neuronal pools important for muscle atonia, EEG desynchronization, PGO waves, and other components of REM sleep. PH=Prepositus Hypogloss.

become active in concert because they share a common mechanism(s) of excitability modulation and which, in pathological states, are subject to inappropriate expression, such as the muscle atonia seen in narcolepsy.

11.2.3.2. Experimental Evidence for Modulation of Excitability in Neuronal Pools

11.2.3.2.1. Brainstem Reticular Formation. Figure 11.6 schematizes the sleep cycle membrane polarization levels in terms of relative levels for waking, EEG-synchronized sleep, and REM sleep for the three neuronal pools on which intracellular recordings are available.

Pontine reticular formation. We have shown that, in mPRF neurons, membrane depolarization and increased excitability persist throughout the state [9]. Since, as discussed in detail in Chapters 9 and 10, much of the neuronal generating machinery for the rapid eye movements and PGO waves events lies in this zone, the increased excitability will favor the occurrence of these events. In waking, the pattern of mPRF excitability alteration revealed by the intracellular recordings is also functionally reasonable in terms of the set of the behaviors occurring in waking. In this state, discrete activation of subsets of reticular neurons with a circumscribed time duration is associated with a heightened specificity of response to particular inputs and of specificity of output (a higher signal-to-noise ratio). Were waking accompanied by the same state-long tonic increase in excitability and depolarization throughout the entire neuronal pool as found in REM sleep, behavioral responses would lose their specificity in the face of a diffuse excitation of all systems.

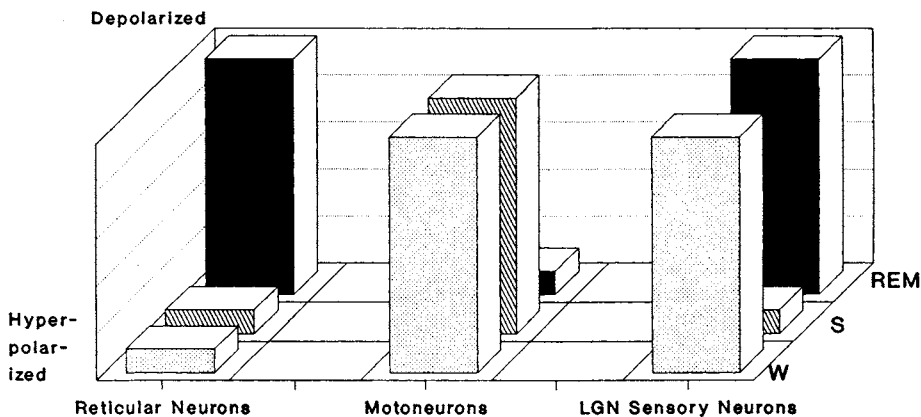


Figure 11.6. Sleep-wake cycle membrane polarization levels. Values are schematized as either depolarized or hyperpolarized and are relative values for waking, synchronized sleep, and REM sleep *within* each pool. Values represent average tonic levels and do not schematize phasic alterations; they are drawn from the neuronal populations for which intracellular data are available.

Bulbar reticular formation neurons. Intracellular recordings of medial BRF neurons by Chase and collaborators indicate the presence of a REM-specific tonic membrane potential depolarization, with approximately the same level of membrane potential shift as mPRF neurons [11]. It is of note that the membrane depolarization in BRF neurons appeared to occur later than seen in many mPRF neurons; in BRF neurons, membrane depolarization occurred near the onset of muscle atonia, which, together with other data on the role of this region in atonia (Chapter 10), suggested that some of the recorded neurons may be effectors of the muscle atonia of REM sleep. State-related membrane potential changes lasted throughout the REM sleep state, thus supporting the thesis that REM sleep behavioral state changes are mediated by excitability alteration, and that membrane potential alteration is one important agent of this change throughout the pontobulbar reticular pool.

[11] Chase *et al.* (1981).

11.2.3.2.2. Peripheral Motoneurons. In both *spinal alpha-motoneurons* and *trigeminal jaw closer motoneurons*, there is a strong modulation of excitability during REM sleep by modulation of membrane potential. The membrane potential in these neurons is hyperpolarized during the state of REM sleep (see Fig. 11.6 and data from the studies of Chase and coworkers and of others cited in Chapter 9). The reduction in excitability in these motoneuronal pools is reflected in the muscle atonia of REM sleep.

11.2.3.2.3. Sensory System Neurons. Only lateral geniculate (LG) thalamocortical neurons have been recorded intracellularly during sleep-wake states, but these data also support the thesis of behavioral state control through excitability modulation, with membrane potential alteration being an important mechanism. As schematized in Fig. 11.6, during EEG-synchronized sleep, LG neurons are relatively hyperpolarized compared with REM sleep, and the REM sleep membrane depolarization is maintained throughout the state [12]. It is of interest that these LG neurons begin to depolarize coincident with the onset of PGO waves in the transition period from synchronized sleep to REM sleep, consistent with the notion that, during REM sleep, these neurons are targets of brainstem excitatory input associated with PGO waves (see Chapter 9). It is also of functional interest that, unlike most brainstem reticular neurons, the LG relay neurons are depolarized throughout waking. This is, of course, functionally reasonable since they function throughout the state of waking to transmit and modulate information from retina. In contrast,

[12] Hirsch *et al.* (1983).

pontine reticular formation neurons do not function as a homogeneous group during waking, and, thus, the absence of a tonic depolarization throughout waking is also functionally reasonable.

In summary, we suggest that experimental evidence supports the concept of modulation of excitability as a key factor in behavioral state control, and that modulation of membrane potential is an important mechanism of excitability modulation.

11.2.3.3. Summary of Orchestration of REM Sleep Components

In this section we indicate the evidence for localizing generation of a particular component of REM to a particular set of neurons; in most cases, the data have been presented in detail elsewhere in the volume and this section and Fig. 11.6 will act as a summary. The order of presentation follows the left-to-right ordering of REM components in Fig. 11.6. Although intracellular recordings and direct monitoring of membrane potential have not been done for all sets of neurons implicated in control of REM components, the state-long persistence of changes in each component is compatible with our hypothesis of membrane potential alteration as an important mechanism of behavioral state change.

11.2.3.3.1. Rapid Eye Movements. Chapter 10 has discussed the saccade generation system, most of which lies in mPRF structures. The REM sleep membrane depolarization and increased excitability biases the system toward increased saccade production during REM sleep, especially lateral saccades. The presence of rapid eye movements in the REM-like states of the “pontine cat” indicates clearly that this component of REM sleep can be generated exclusively within the brainstem, even without the forebrain input so important in waking control.

11.2.3.3.2. Muscle Atonia. Chapter 10 has described the extracellular recordings of dorsolateral tegmental neurons projecting to BRF; their discharge activity is highly correlated with onset and offset of REM sleep muscle atonia. Chapter 10 also has described electrical and chemical stimulation evidence suggesting a possible midline component to the muscle atonia system, but there are neither extra- nor intracellular recordings of neurons in this zone relating their activity to muscle atonia. The previous chapter has also described evidence for reticulotrigeminal input important in muscle atonia.

11.2.3.3.3. EEG Desynchronization. Chapter 9 has described data from Steriade and coworkers supporting a role for cholinergic neurons in PPT and noncholinergic neurons in mesencephalic and BRF in mediating this component of REM sleep [13].

[13] Steriade *et al.* (1982a, 1984b, 1989).

11.2.3.3.4. PGO Waves. Chapter 9 has described intracellular data from McCarley and Ito indicating the presence of neurons in medial PRF and the tegmental reticular nucleus, which discharged with long lead times before PGO waves, and thus may serve to initiate the eye-movement-related PGO waves of REM sleep [14]. Anatomical data by Higo and coworkers suggest the possibility of involvement of the prepositus hypoglossi (PH) in the genesis of the pontine component of PGO waves [15], although REM sleep recordings have not yet been done in this zone. The PGO burst neurons in the PPT zone are described in Chapter 9 and likely form one component of the output pathway from brainstem to thalamus. They have been recorded extracellularly in sleep (see Section 9.1) but not intracellularly.

[14] McCarley and Ito (1983).

[15] Higo *et al.* (1989b).

11.2.3.3.5. Other Components of REM Sleep

Theta rhythm. Studies by Vertes using macropotential recordings, electrical stimulation, and lesion techniques have pointed to the pontine reticular formation at more lateral sites as important for production of the hippocampal theta rhythm of REM [16]. Unit recordings showed neurons whose onset and offset of activity was correlated with onset and offset of theta; it is of interest that this subset of neurons was tonically active in both REM sleep and waking, suggesting a state-dependent activation of this pool that may be different from the set of medial pontine reticular neurons discussed above. These neurons have not been recorded intracellularly. The most effective site within the reticular formation for the elicitation of hippocampal theta was found to be the rostral pontis oralis (RPO). As Vertes and Kocsis conclude, RPO may be the primary brainstem source for septohippocampal theta generation [17].

[16] Vertes (1981, 1982).

[17] See reviews in Vertes and Kocsis (1997); Bland and Oddie (1998).

Phasic muscle twitches. One of the behavioral characteristics of REM sleep is the presence of muscle twitches, especially of distal flexor muscles and, in cats, of the vibrissae and ears. These are present in the “pontine cat” and, thus, brainstem structures are necessary and sufficient for their occurrence. Cellular data bearing on their occurrence has been presented by Wyzinski *et al.*, who recorded extracellularly from mPRF neurons antidromically identified as projecting to ventral spinal cord [18]. These neurons showed high correlations of runs of action potentials with

[18] Wyzinski *et al.* (1978).

the presence of muscle twitches, suggesting brainstem mediation of this component of REM sleep.

Autonomic nervous system changes. The cardiovascular, the respiratory, and the thermoregulatory systems undergo profound alterations during slow-wave sleep and REM sleep. We shall not here review the extensive literature because several books have discussed this aspect of sleep physiology in some detail [19]. We do think it useful, however, to give a brief overview vis-à-vis brainstem control mechanisms. With respect to respiration, extracellular recording studies in cats conditioned to arrest inspiration on signal have led to Orem's thesis that the voluntary/behavioral and the automatic/metabolic aspects of breathing are integrated at the brainstem level [20], and extracellular recordings indicate that some respiratory neurons have relatively "pure" respiration-related discharge activity while that of others is greatly influenced by behavioral state. Orem hypothesizes that non-REM sleep reflects a predominance of automatic/metabolic system control, while breathing during REM sleep represents a predominance of voluntary/behavioral system control [20]. An obvious possibility is that the state-modulated respiratory neurons may have input from areas greatly affected by behavioral state changes, while the others do not.

State-related changes are similarly important in the cardiovascular system. In waking, there is a high degree of heart rate variability, which is transformed to a great regularity in EEG-synchronized sleep, except for a nearly sinusoidal modulation from respiratory influences (sinus arrhythmia is accentuated in this state). REM sleep consistently shows much episodic variability of cardiac rate. These state-related respiratory and cardiovascular changes are sufficiently distinctive to allow machine classification of state [21]. As with the respiratory system, the locus of neurons accounting for the REM sleep variability has not yet been firmly identified although influences from the brainstem parabrachial region and from the forebrain, including central nucleus of the amygdala, have been postulated [22]. Parmeggiani has described the vascular bed-specific changes in blood pressure during REM sleep [23]. Much of the recent interest in the cardiovascular field is driven by an effort to discover associations between clinical pathology and state; in pigs, synchronized sleep, but not REM sleep, is associated with arrhythmias in ischemic heart although such a clear-cut relationship between sleep stage and arrhythmias in humans is still uncertain [24].

Thermoregulation is profoundly affected during sleep, and extracellular recordings in hypothalamus

[19] Lydic and Biebuyck (1988); Saunders and Sullivan (1994); Lugaresi and Parmeggiani (1997).

[20] Orem (1988).

[21] Harper *et al.* (1987).

[22] Harper *et al.* (1988); Verrier (1988).

[23] Parmeggiani (1985).

[24] For pigs see Skinner *et al.* (1975); for humans see Verrier (1988).

suggest a decrease in thermosensitivity in synchronized sleep and an absence of thermoregulation in REM sleep, at least in cats and kangaroo rats [25]. Parmeggiani has summarized the behavioral state-related changes as an absence of hypothalamic and telencephalic regulation in REM sleep, and a “rhombencephalic” dominance of thermoregulation in this state, as well as a rhombencephalic dominance of other physiological systems during this state [26].

[25] For cats see Parmeggiani *et al.* (1987); for kangaroo rats see Glotzbach and Heller (1984).

[26] Parmeggiani (1988).

11.2.3.4. Approach to Factors Producing Modulations of Excitability

In the previous section, we presented the phenomenology of membrane potential changes over the sleep–wake cycle. We suggested that the components of REM were elicited by an alteration of bias of the neuronal pool subserving each component. With the increased excitability associated with REM sleep, the neuronal machinery controlled by a particular neuronal pool would be set into motion, but we have not yet presented data relevant to how the membrane potential alterations of REM sleep are caused. In the current section on reticular formation we discuss reticuloreticular excitatory connections as facilitating recruitment of reticular neurons. Succeeding sections then take up the major brainstem neuromodulators of REM sleep.

11.2.3.5. Recruitment through Reticuloreticular Excitatory Connections

Chapters 3 and 4 have extensively documented evidence for the presence of dense reticuloreticular excitatory connectivity. It is immediately apparent that the onset of discharge activity within this pool as REM sleep is approached would lead to the recruitment of other members through the reticuloreticular excitatory connections, and that this excitatory connectivity would similarly contribute to the maintenance of REM sleep depolarization. Stated in systems terminology, the monosynaptic excitatory connectivity in pontobulbar reticular formation may furnish the substrate for a self-augmenting positive feedback process that will result in the progressive membrane depolarization in T, and will help maintain the depolarization and excitability throughout the state of REM sleep. Indeed, the data show the time course of depolarization in reticular neurons prior to REM sleep onset is compatible with their playing this role in the process leading to initiation of this state. Figure 11.7 summarizes the extracellular

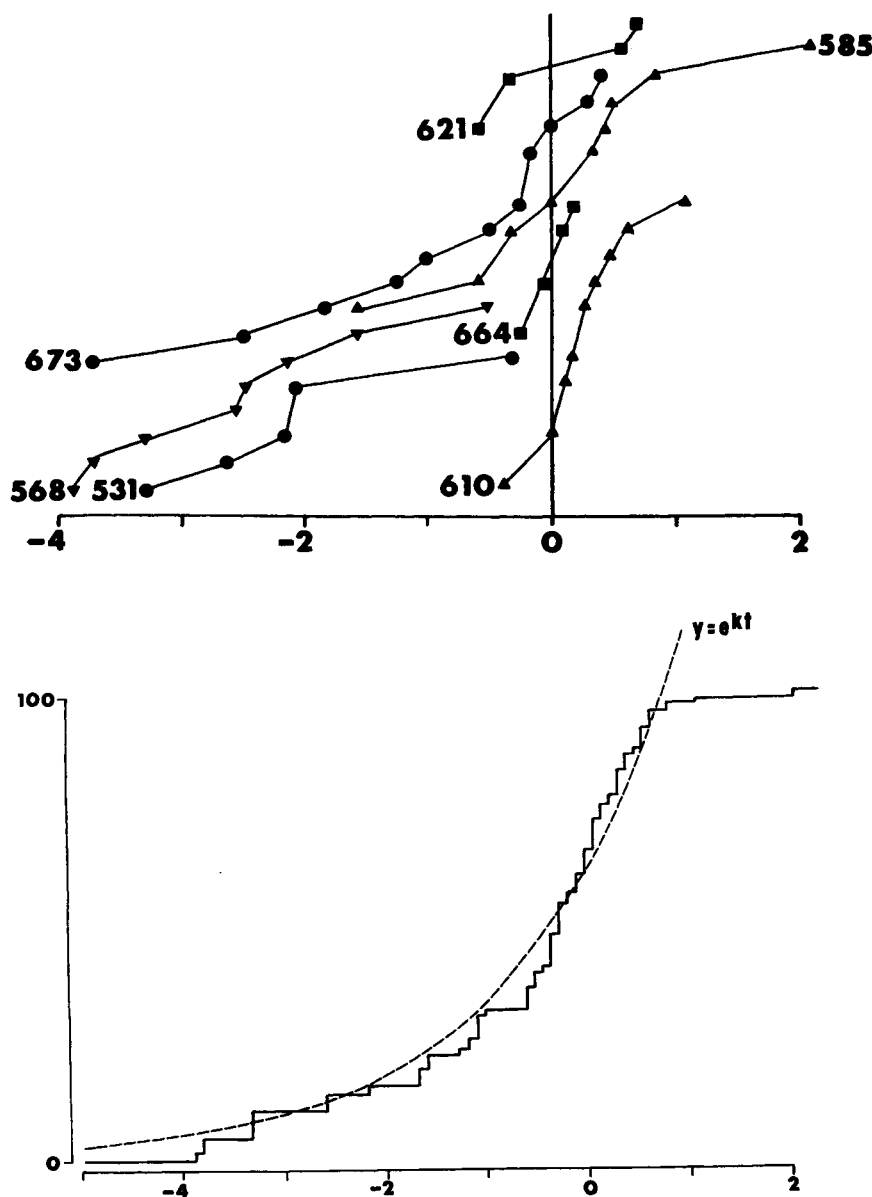


Figure 11.7. Time course of REM sleep-related increase in discharge rate of brainstem reticular neurons extracellularly recorded over many sleep-wake cycles. Top panel shows the “REM recruitment” time onset of 5 FTG neurons and 2 FTC neurons (531 and 673) relative to the electrographically defined time of onset of REM sleep, 0 min on the abscissa. “Recruitment” is defined as a persistent, significant discharge rate increase over the synchronized sleep baseline period ($p \geq .001$). The data are displayed as a cumulative histogram with the increment for each transition period shown. Each point for each numbered neuron represents the occurrence of one or more transition periods with the increment at this time. Thus, for example, the curve of unit 610 presents 12 transition period changes as 9 points because there were three pairs of identical recruitment times. Bottom Panel. Pooled cumulative histogram for the data of the top panel. Time ordinate is as top panel and abscissa is the percentage of the pool of 7 neurons showing recruitment, with the time curve for each of the neurons showing the recruitment distribution of the top panel, and with the contribution of each of the neurons weighted equally. The dotted line is a plot of $y = \exp(kt)$, the exponential growth curve. Note the correspondence is quite close until 1 min after REM sleep onset, at which time the experimental data reach an asymptote, indicating all neurons have changed discharge rate. Modified from Hobson *et al.* (1974a).

recording data on the time course of recruitment, and shows that these data are matched quite nicely by an exponential curve, indicating that mutual augmentation is a good model of recruitment within the population.

11.2.3.5.1. Intracellular Evidence on Recruitment Within the Reticular Pool. In naturally sleeping cats, Ito *et al.* used intracellular recordings and neurobiotin labeling of 39 medial pontine gigantocellular tegmental field (mPFTG) neurons to evaluate the process of recruitment from the standpoint of membrane potential depolarization and soma size [9] (see Fig. 11.8). Most of these neurons (80%) were antidromically activated by stimulation in the BRF and all had excitatory PSPs, often monosynaptic, in response to BRF stimulation.

Most (82%) of the neurons had the onset of membrane depolarization prior to REM sleep onset, and there was a strong correlation between soma size and the time of onset of depolarization prior to REM sleep. Neurons with larger somata began the process of membrane depolarization prior to REM sleep onset earlier than neurons with smaller somata (Pearson correlation coefficient = 0.86), and it was the neurons with smaller somata that depolarized at the beginning of or just after REM sleep onset. In contrast to membrane depolarization, the pre-REM lead times for onset of sustained PSPs and action potentials showed this measure not to be dependent on somata size, but to be rather uniform, occurring just before the onset of REM sleep. Thus, in the reticular pool, larger neurons may take longer to depolarize to an MP level critical for generating sustained action potentials, while smaller neurons may require less time. The final step in recruitment of the mPFTG population to high, sustained levels of discharge may be a process of reticuloreticular feedback, whereas the initial phase of depolarization may largely result from mesopontine cholinergic input (see next section).

11.3. Criteria for Neuromodulation in REM Sleep

The next several sections will address neurotransmitters and neuromodulators of various cell groups thought to be important in REM sleep. What are the criteria for demonstration of this putative causal role? We suggest the following, with the direction of change depending on whether the postulated influence is promoting/suppressive.

In each case, the prediction with promotion is listed first and suppression second.

1. *Discharge profile criterion.* Neurons utilizing the putative modulating neurotransmitter should show a discharge profile consistent with causality, there should be an appropriate increase/decrease in discharge rate prior to the putative controlled REM state or event.

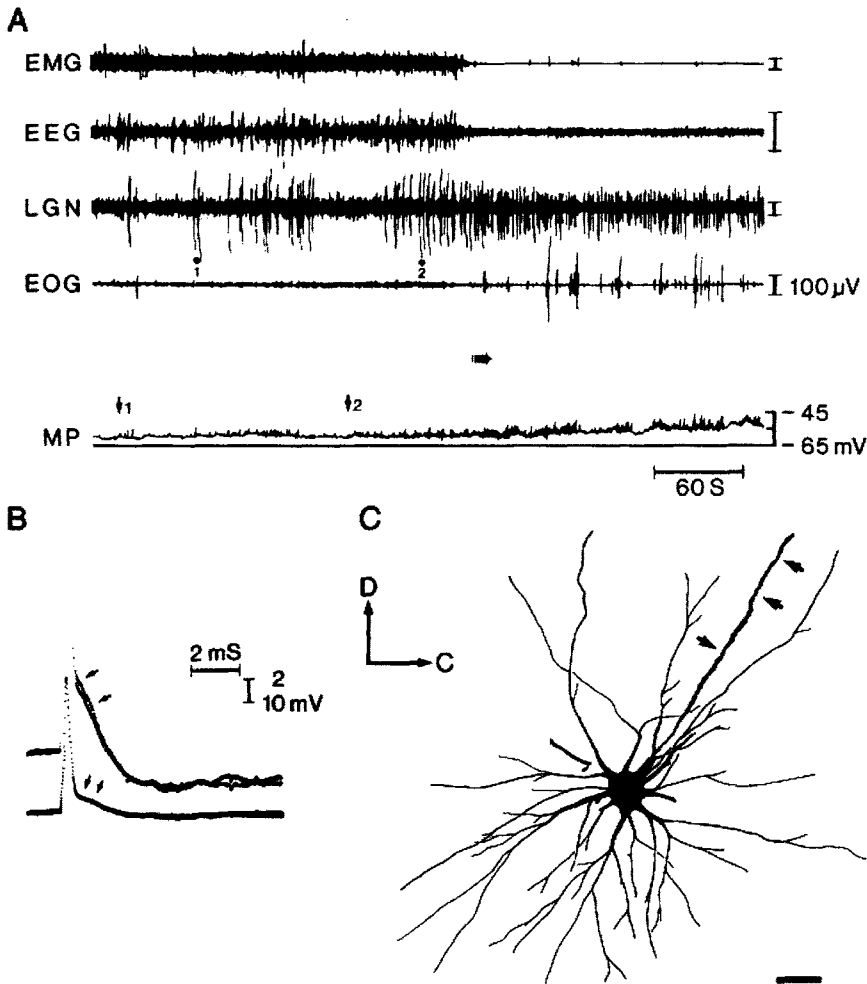


Figure 11.8. A. Correlation between electrographic signs and the membrane potential (MP) from an average size medial pontine gigantocellular tegmental field (mPFTG) neuron during a sleep cycle. There are two pre-REM sleep episodes; while the first episode (vertical arrow 1 on MP trace and dot 1 on the LGN trace) failed to advance to REM sleep, the second episode (vertical arrow 2 and dot 2) did lead to a full REM sleep episode, whose onset is marked by a horizontal arrow. B. Antidromic spike potentials from BRG stimulation in the same mPFTG neuron as 4A. Note monosynaptic excitatory postsynaptic potentials superimposed on the falling phase of the action potentials, indicated by arrows. The top trace is a high-gain, AC-coupled record (2 mV calibration) and the bottom trace is a low-gain DC record (10 mV calibration). C. Reconstruction drawing of this average size neuron. The arrows indicate its dorso-caudally coursing axon. Soma size, $3905 \mu\text{m}^2$; D, dorsal; C, caudal; calibration, $100 \mu\text{m}$. Adapted from Ito *et al.*, 2002.

2. *Anatomical connectivity criterion.* The putative modulating neurons should show connectivity with the controlled group.

3. *Neurotransmitter release criterion.* Microdialysis or other measurements of release in the controlled population should reveal the predicted increase/decrease in the controlled state.

4. *Controller activity criterion*

a. Effect of abolishing activity. Pharmacological or lesion silencing of the putative controlling group will decrease/increase the controlled state.

b. Stimulation Effects. Increasing activity in the putative controlling neural population through pharmacological or electrical stimulation will increase/decrease the controlled state or event.

5. *Pharmacological agonist criterion.* Application of the agonists of the putative neurotransmitter to the controlled neurons will increase/decrease the controlled event or neuronal population. Because of possible spill-over to other receptors or nonphysiological effects of the pharmacological agent, this demonstration should not be regarded as definitive.

6. *Pharmacological antagonist criterion.* Application of the antagonists of the putative neurotransmitter to the controlled neurons will decrease/increase the controlled event or neuronal population. Note that this is a stronger criterion than number 5.

7. *Molecular biological analogs of criteria 5 and 6.* Application of antisense/RNAi directed at the putative receptor or ligand will block the effect of the putative neurotransmitter. Because of biological adaptation, we do not think constitutive knockouts of receptors or a ligand constitute firm proof of a relationship or absence of a relationship, but inducible, reversible genetic knockdowns are a very useful technology.

Perhaps the most salient comment on these criteria is that *purely pharmacological criteria are never sufficient*, since one does not know whether the observed agonist/antagonist effects are, or are not, seen in natural REM sleep, a fact that should be kept in mind as the reader assays the strength of the evidence presented for REM neuromodulators in the next sections.

11.4. Cholinergic Influences on REM Sleep

11.4.1. Cholinergic Induction of REM Sleep-Like Phenomena

Chapter 4 presented anatomical evidence of cholinergic projections to mPRF from the LDT and PPT nuclei

and Chapter 6 presented *in vitro* data indicating the strong excitatory response of over 60% of mPRF neurons to carbachol, administered in micromolar concentrations. Thus, there is strong supporting evidence that acetylcholine is a physiological neurotransmitter acting on mPRF neurons. (A final, but critical, piece of evidence is to show that stimulation of LDT/PPT produces PSPs with the same effects and that the PSPs are blocked by antagonists in the same low concentrations as described in Chapter 6.) Given this information, one might, thus, on an ad hoc basis, choose cholinergic agonists as reasonable agents to alter the excitability of reticular neuronal pools.

In fact, the history of cholinergic injections into the brainstem began in the 1960s on a much more empirical basis. Cordeau *et al.* and George *et al.* reported the induction of a REM-sleep-like state by these injections [27]. In the two decades that followed, numerous published studies have reported the elicitation of some or all components of REM sleep by brainstem injections of cholinergic agonists, with most of these studies using the cat [28].

In certain application sites in the pontine reticular formation, cholinergic agonists produce a "full" REM-sleep-like syndrome, with the simultaneous presence of all major indicator variables (Fig. 11.9); these sites tend to be in the mPRF rostral to VI and in the dorsal one-half (see also discussion of localization of cholinergic agonist effects in the final section of Chapter 10). Carbachol application at other sites, such as near the peribrachial zone and, hence, near PPT may produce isolated PGO waves without other signs of REM sleep [29]. Datta *et al.* found that cholinergic stimulation of the PPT produced immediate and prolonged increases in PGO waves [30]. Chapter 10 has discussed how the muscle atonia of REM sleep may be produced by application of cholinergic agonists to the dorsolateral pontine reticular formation. Applications of cholinergic agonists to mesencephalic or BRF have not, at least in the sites so far tested, produced the full REM-sleep-like syndrome [31].

Early studies in the rat also showed that carbachol was capable of producing a REM sleep syndrome, as did later ones using microinjections [32]; compared with cats, the magnitude of the REM sleep enhancement was less, about two-fold instead of four-fold, and the rat episodes were shorter, close to normal duration, and had a longer latency to onset. Interestingly, Taguchi *et al.* found that carbachol-induced REM-sleep like episodes of atonia and respiratory depression in the decerebrate rat were of short latency and long duration, suggesting that, in part, descending forebrain influences might account for the differential response in the chronic rat [33]. It may be also that, in the smaller volume brainstem of the rat, diffusion

[27] Cordeau *et al.* (1963);
George *et al.* (1964).

[28] Baxter (1969);
Kostowski (1971); Mitler
and Dement (1974);
Amatruda *et al.* (1975);
Velasco *et al.* (1979);
Silberman *et al.* (1980); van
Dongen (1980); Vivaldi
et al. (1980); Hobson *et al.*
(1983b); Katayama *et al.*
(1984); Baghdoyan *et al.*
(1984a, b, 1987);
Shiromani and McGinty
(1986); Shiromani *et al.*
(1986).

[29] Vivaldi *et al.* (1980).

[30] Datta *et al.* (1992).

[31] Baghdoyan *et al.*
(1984b).

[32] For carbachol Gnadt
and Pegram (1986);
Shiromani and Fishbein
(1986); for microinjections
see also Velazquez-
Moctezuma *et al.* (1989);
Bourgin *et al.* (1995);
Okabe *et al.* (1998).

[33] Taguchi *et al.* (1992).

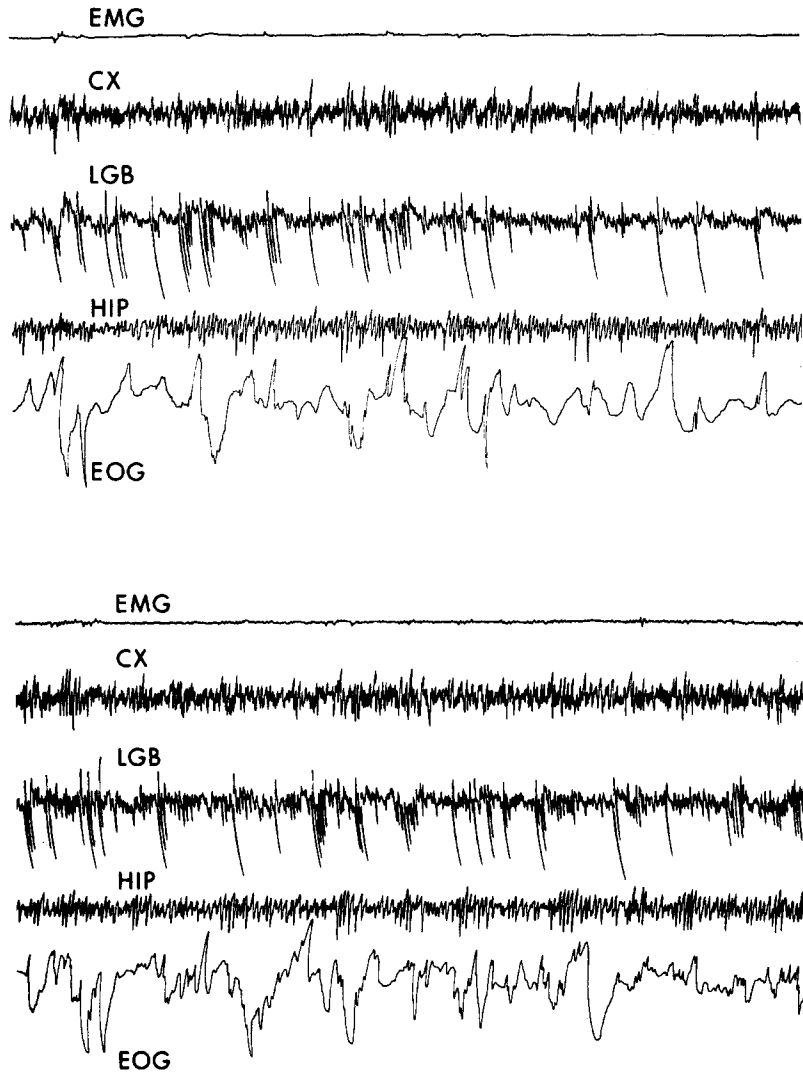


Figure 11.9. Electrographic signs of natural REM sleep (top panel) and a REM sleep-like state (bottom panel) in the same cat induced by diffusion from a cannula filled with 4 μ g carbachol in 1 μ l of saline. Note the similarity of the indicator variables of EMG atonia, cortical EEG (CX) desynchronization, PGO waves in the lateral geniculate body (LGB), hippocampal theta (HIP), and the EOG record of rapid eye movements. This full REM-like syndrome, shown in the bottom panel, is typical of carbachol application to anterodorsal pons. From Vivaldi *et al.* (1980).

of microinjected carbachol is more prone to activate ventral wakefulness-promoting sites than in the cat [34]. In urethane-anesthetized rats and cats, carbachol produces partial REM signs, and Fenik *et al.* have found that by careful titration of the depth of anaesthesia it was possible to produce a 2–3 min state with cortical desynchronization, hippocampal theta rhythm, and motoric suppression with small injections of carbachol [35].

[34] See Kubin (2001).

[35] Fenik *et al.* (1999).

11.4.2. Cholinergic LDT Stimulation Produces Scopolamine-Sensitive EPSPs in mPRF Neurons

Imon *et al.* used single pulse electrical stimulation of the LDT in urethane anaesthetized acute cats to determine the synaptic effects on pontine reticular formation neurons, identified by antidromic activation from BRF and neurobiotin intracellular labeling [36]. This stimulation produced EPSPs in more than 95% of recorded neurons with a latency consistent with the conduction velocity of unmyelinated cholinergic fibers—2 m/s. Also consistent with cholinergic EPSPs was their abolition by intravenous administration of the muscarinic receptor antagonist, scopolamine (N = 40 neurons), by acute transverse cuts separating the LDT and the recorded neurons (N = 40), and by their reduction under barbiturate anaesthesia. These *in vivo* data thus support the anatomical and *in vitro* data indicating an excitatory, cholinergic LDT projection to pontine reticular formation.

[36] Imon *et al.* (1996).

11.4.3. Cholinergic Unit Activity During Sleep and Wakefulness

Chapter 9 has presented extracellular data relevant to LDT/PPT projections to thalamus and forebrain and EEG desynchronization, and we here discuss data relevant to brainstem projections and REM sleep. Perhaps the most important fact is that some LDT/PPT neurons have markedly increased discharge activity during *both* states of EEG activation, wakefulness and REM sleep. We refer to these neurons as Wake/REM-on. Other LDT/PPT neurons show markedly increased discharge *only* in REM sleep. We refer to these neurons as REM-on. Previously presented data indicate a strong cholinergic influence in REM sleep: cholinergic agonists in pontine tegmentum produce a REM sleep-like state; cholinergic projections of LDT/PPT to pontine reticular formation (Chapter 4) that produce EPSPs, and *in vitro* data indicating cholinergic agonists produce depolarization and increased excitability in pontine reticular formation (Chapter 5). It seems obvious that the REM-on neurons must be the ones mediating all the cholinergic REM-promoting effects save for EEG desynchronization.

Data on the discharge activity of LDT/PPT REM-on neurons over the sleep cycle are not as extensive as for extra-cellular recordings of mPRF neurons (see Fig. 11.2).

Electrophysiological studies reveal that a subpopulation of LDT/PPT neurons preferentially discharges just before and during REM sleep (see EEG activation discussion above) [37]. The data from Thakkar *et al.* are particularly useful since they were obtained from both LDT and PPT in freely moving cats and hence were able to use active wakefulness as a state measure and rule out any potential confounds from the absence of head and neck movements [38]. The El Mansari *et al.* study did not restrict recordings to the PPT (although PPT was included) and the recordings were biased toward those units antidromically identified as projecting to thalamus [39]. The Thakkar *et al.* data included both LDT ($n = 11$) and PPT ($n = 23$) neurons [40]. These data, although limited in number, suggest that LDT neurons in general have somewhat lower discharge rates than PPT neurons and tend to show more phasic modulation during REM than PPT neurons. Thakkar and colleagues (in submission) recorded 137 PPT neurons, of which 35% were REM-on, 62% were Wake/REM-on while 3% were REM-off. Figure 11.10 illustrates the discharge profile of this group of REM-on and Wake/REM-on neurons. The REM-on neurons discharged preferentially during REM sleep and showed a statistically significant increase in discharge rate in the 50 sec prior to REM sleep compared with non-REM sleep, and with quiet and active wakefulness (movement). Note also the much higher discharge rate in REM+ (REM with eye movements) compared with REM− (no eye movements). This within REM selectivity suggests an important role in control of phasic events. The discharge profile of REM-on and REM/Wake-on neurons over the sleep cycle is further illustrated below in Section 11.5.3 and Fig. 11.16.

Identification of the recorded neurons in Thakkar *et al.* as cholinergic is consistent with several criteria, although tentative [40]. First, histological reconstruction indicated that all cells were recorded in the anatomically defined cholinergic zones of LDT or PPT. Anatomical studies indicate that in these regions, about 80% of the large neurons ($>20\ \mu\text{m}$ cell body diameter) are ChAT positive, indicative of their being cholinergic [41]. Second, the recording method used fine wires of $32\ \mu\text{m}$ and $64\ \mu\text{m}$ diameter—a method that preferentially records larger cells ($>20\ \mu\text{m}$). Finally, studies have argued that cells in the cholinergic LDT/PPT with long duration action potentials, or slow conduction velocity are likely to be cholinergic [42]. The majority of the neurons recorded had long duration action potentials. These data suggest, but do not prove, that the large majority of REM-on and Wake/REM-on described are cholinergic.

[37] El Mansari *et al.* (1989); Steriade *et al.* (1990a); Kayama *et al.* (1992); Thakkar *et al.* (1998).

[38] Thakkar *et al.* (1998); for potential confounds see Siegel *et al.* (1977); Steriade *et al.* (1990a) and Kayama *et al.* (1992) used head restraints.

[39] El Mansari *et al.* (1989).

[40] Thakkar *et al.* (1998).

[41] Steriade *et al.* (1990a); Jones (1993).

[42] For long duration action potentials see Steriade *et al.* (1990a); for slow conduction velocity see El Mansari *et al.* (1989).

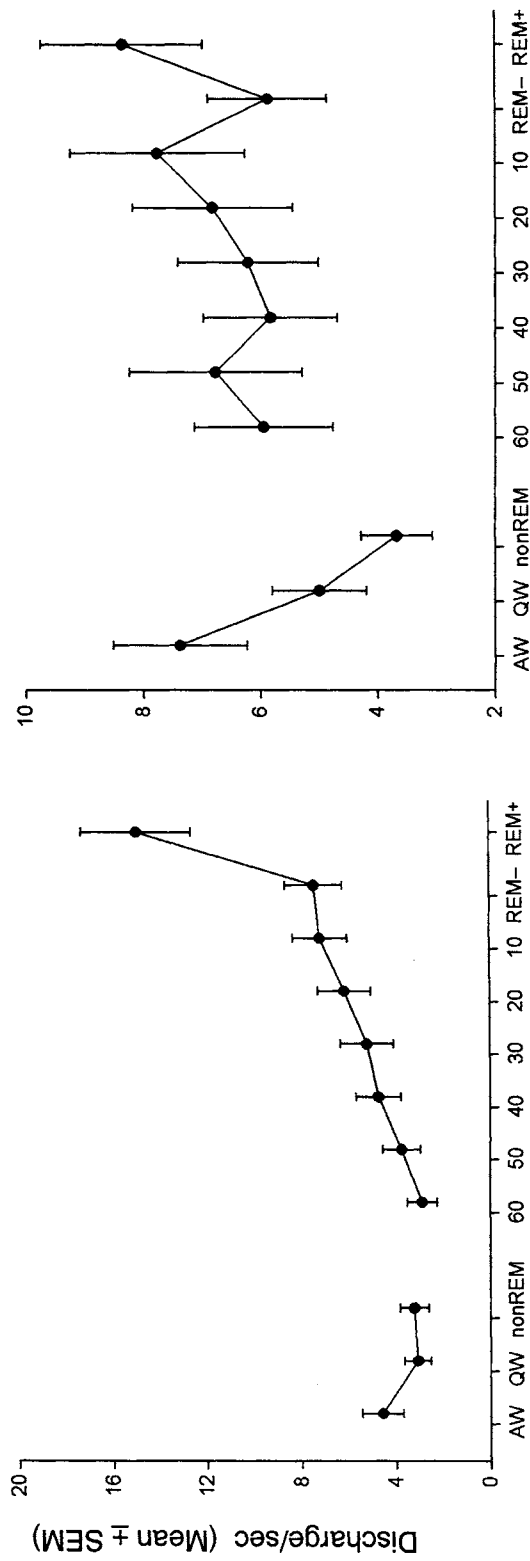


Figure 11.10. State-related discharge profile of 45 REM-on neurons (left panel) and 85 REM/Wake-on neurons in the cholinergic PPT. AW and QW = active and quiet Wake respectively, REM+ and REM- = REM with and without eye movements respectively. Pre-REM activity is graphed for 60 sec prior to REM onset. Adapted from Thakkar *et al.*, in submission.

11.5. Monoaminergic Influences—REM-Off Neurons

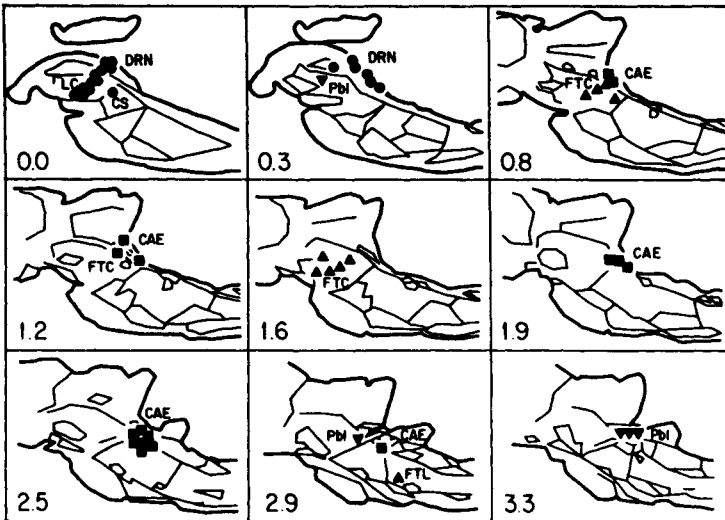
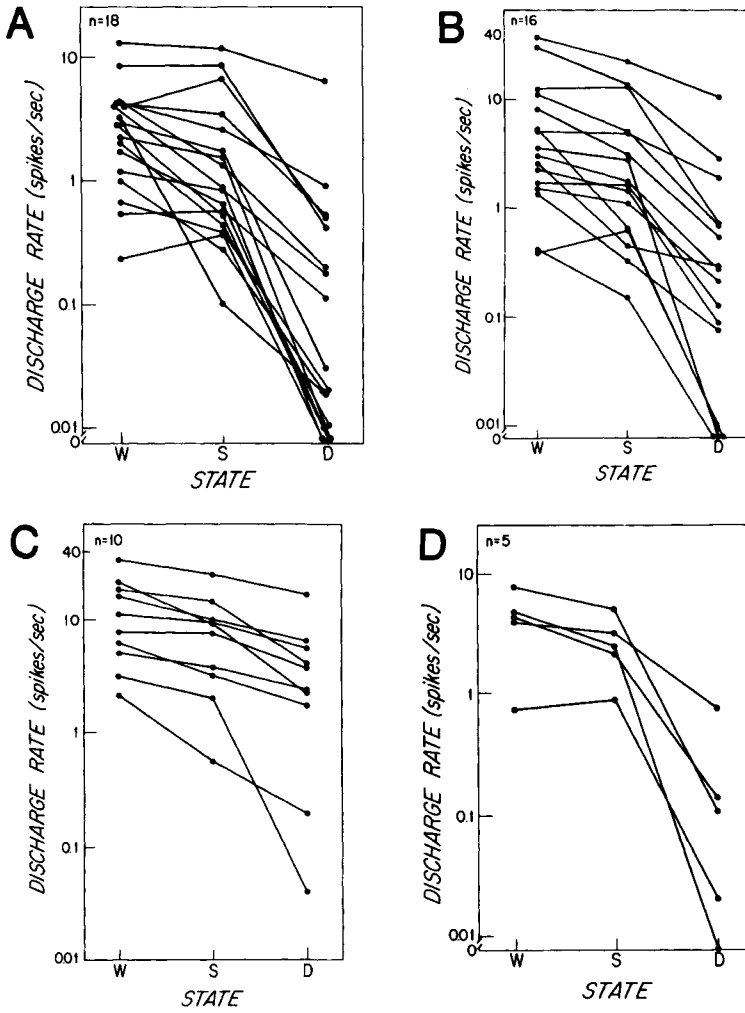
The neurons described in the previous section that increase discharge rate with the advent of REM have been termed “REM-on neurons.” In contrast, groups of other neurons radically decrease and may nearly arrest discharge activity with the approach and onset of REM; these are often termed “REM-off” neurons. The typical discharge activity profile is for discharge rates to be highest in waking, then decrease in synchronized sleep, with near cessation of discharge in REM sleep. REM-off neurons are distinctive both because they are in the minority in the brain and also because they are recorded in zones with neurons that use biogenic amines as neurotransmitters. The loci include a midline zone of the brainstem raphe nuclei, and a more lateral band-like zone in the rostral pons/midbrain junction that includes the nucleus locus coeruleus, a reticular zone, and the peribrachial zone, as illustrated in Fig. 11.11.

11.5.1. Raphe Nuclei

Neurons with a REM-off discharge profile were first described by Harper and McGinty in the dorsal raphe nucleus (DRN)—a finding confirmed by other workers [43]. Neurons with the same REM-off discharge pattern have been found in the other raphe nuclei, including nucleus linearis centralis, centralis superior, raphe magnus, and in raphe pallidus [44]. Identification of these extracellularly recorded neurons with serotonin-containing neurons was made on the basis of recording site location in the vicinity of histochemically identified serotonin neurons and the similarity of the extracellularly recorded slow, regular discharge pattern to that of histochemically identified serotonergic neurons (see Chapters 5 and 6). Nonserotonergic

[43] McGinty and Harper (1976); for confirmation see Trulson and Jacobs (1979); Hobson *et al.* (1983a); Lydic *et al.* (1987a, b).
[44] For nucleus linearis centralis see McCarley (1978) and Hobson *et al.* (1983a); for centralis superior see Rasmussen *et al.* (1984); for raphe magnus see Cesputio *et al.* (1981) and Fornal *et al.* (1985); for raphe pallidus see Sakai *et al.* (1983b).

Figure 11.11. Top panel shows mean discharge rate by state of four groups of REM-off neurons extracellularly recorded in the cat in waking (W), synchronized sleep (S), and REM sleep (D), and the bottom panel shows their anatomical location on computerized reconstructions of sagittal plates from Berman (1968). Note the near uniformity of the discharge rate profile, $W > S > D$. A: The raphe group (bottom panel, circles) includes dorsal raphe, linearis centralis, and centralis superior. B: The locus coeruleus group (bottom panel, squares). C: The reticular group (bottom panel, upright triangles) D: The peribrachial group (bottom panel, inverted triangles). Note that these three latter REM-off groups form a band-like zone across the anterodorsal tegmentum. This particular illustrated sample of REM-off neurons, adapted from Hobson *et al.* (1983a), did not include neurons from the pontine and bulbar raphe nuclei.



neurons in the raphe system have been found to have different discharge pattern characteristics (Chapter 6). While this extracellular identification methodology does not approach the “gold standard” of intracellular recording and labeling, the circumstantial evidence that the raphe REM-off neurons are serotonergic appears strong.

11.5.2. Locus Coeruleus

The second major locus of REM-off neurons is the locus coeruleus, as described in cat, rat, and monkey [45]. The argument that these extracellularly recorded discharges are from norepinephrine-containing neurons parallels that for the putative serotonergic REM-off neurons. Extracellularly recorded neurons that are putatively noradrenergic have the same slow, regular discharge pattern as identified in norepinephrine-containing neurons (see Chapter 5) and have the proper anatomical localization of recording sites, including recording sites in the compact locus coeruleus in the rat, where the norepinephrine-containing neurons are rather discretely localized. Thus, while the evidence that these REM-off neurons are norepinephrine-containing is indirect and circumstantial, it nonetheless appears quite strong.

Finally, the remaining groups of REM-off neurons are principally localized to the anterior pontine tegmentum/midbrain junction either in the peribrachial zone, or in a more medial extension of it (Fig. 11.13), recording sites that correspond to the presence of aminergic neurons scattered through this zone (see Chapters 3 and 4). The “stray” REM-off neurons in other reticular locations also correspond to dispersed adrenergic neuronal groups, although adrenergic identification in this case is much less secure. At this point, we note that putatively dopaminergic neurons in substantia nigra and midbrain *do not* alter their discharge rate or pattern over the sleep–wake cycle [46], and, thus, are unlikely to play important roles in sleep–wake cycle control.

[45] For cat see Hobson *et al.* (1973); Chu and Bloom (1974); Hobson *et al.* (1975); for rat see Aston-Jones and Bloom (1981a, b); for monkey see Foote *et al.* (1980).

[46] Steinfels *et al.* (1983).

11.5.3. Do REM-Off Neurons Play a Permissive, Disinhibitory Role in REM Sleep Genesis?

11.5.3.1. Dorsal Raphe Discharge and REM Events: An Inverse Association

The intriguing reciprocity of the discharge time course of REM-off and REM-on neurons led to the initial

[47] McCarley (1973);
Hobson *et al.* (1973);
Hobson *et al.* (1975);
McCarley and Hobson
(1975b).

hypothesis of interaction of these two groups, as originally proposed for the REM-off adrenergic neurons [47]. The strongest kind of evidence for this interaction would be demonstration of the proper anatomical connectivity and inhibitory actions of aminergic neurotransmitters upon REM effector neurons; while much is known about the connectivity that is, in general, consistent, we are just beginning to learn about cellular effects of aminergic transmitters in reticular formation and other sites of interest, as discussed in Chapter 6. In spite of the absence of these critical data, the phenomenological and behavioral data have been sufficiently strong so that diverse groups of investigators have proposed that the REM-off neurons, as a complete or partial set, act in a permissive, disinhibitory way on some or all of the components of REM sleep, and we will here summarize these postulates, as well as presenting the phenomenology on which they are based. Many of these theories arose in the mid 1970s as increased technical capability led to extracellular recordings of REM-off neurons.

11.5.3.1.1. *Raphe System REM-Off Neurons and PGO Waves.*

The possibility that the dorsal raphe serotonergic neurons act to suppress PGO waves was explicitly proposed by Simon *et al.* on the basis of lesion data and the *in vivo* pharmacological experiments using reserpine, which depleted brainstem serotonin and simultaneously produced nearly continuous PGO-like waves [48]. McGinty and Harper, in their study of extracellularly recorded dorsal raphe REM-off neurons, also noted the inverse relationship between PGO waves and dorsal raphe unit activity [49]. With respect to REM sleep onset, the decrease in discharge activity of presumptively serotonergic raphe neurons is remarkably consistent, as shown in Fig. 11.12. This time course of dorsal raphe unit activity (and other components of the sleep-wake cycle) can be averaged over multiple cycles—a procedure described in Fig. 11.13—so as to form a picture of the average time course. Using this technique, the time course of presumptively serotonergic dorsal raphe neuronal activity over the sleep-wake cycle and its relationship to PGO waves has been described by Lydic *et al.* [50]. Figure 11.14, derived from this work, shows clearly the inverse relationship between PGO waves and dorsal raphe discharge. Note also the premonitory increase in dorsal raphe activity prior to the end of the REM sleep episode—a phenomenon also observed and commented upon by Trulson and Jacobs [51].

[48] Simon *et al.* (1973);
for reserpine experiments
see Brooks *et al.* (1972).

[49] McGinty and Harper
(1976).

[50] Lydic *et al.* (1983).

[51] Trulson and Jacobs
(1979).

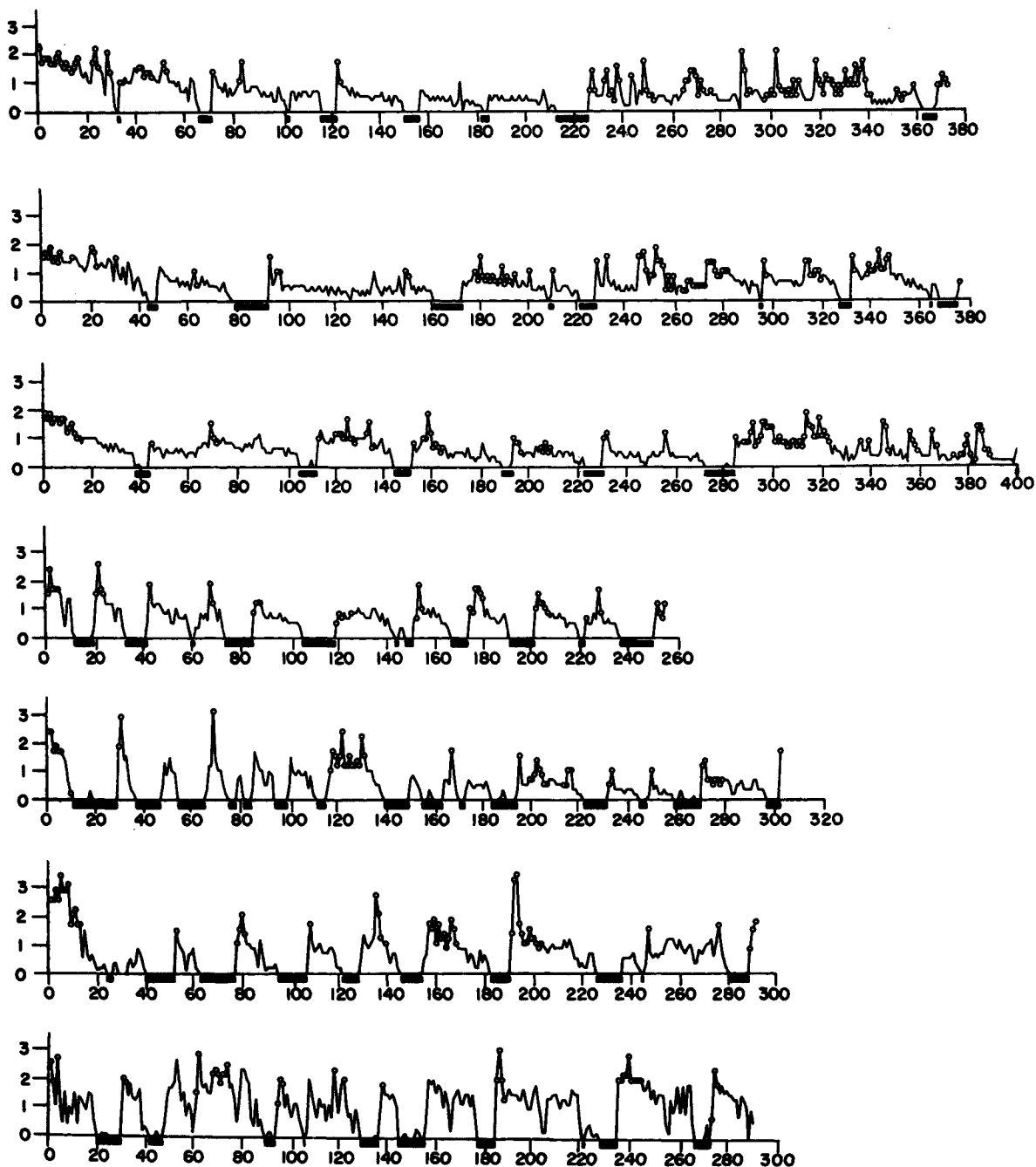


Figure 11.12. Long-term extracellular recording of dorsal raphe discharge over multiple sleep-wake cycles in the cat. The four sets of discharge profiles, each from the same presumably serotonergic dorsal raphe neuron recorded on four separate days show action potentials/per second on the ordinate and time in minutes on the abscissa. Unit activity has been grouped into 1 min bins, with the open circles representing samples during wakefulness while the dark bars below the

abscissa indicate the occurrence of REM sleep episodes. Note the consistence of the discharge profile, with highest rates in waking and lowest in REM sleep. The tendency of REM sleep to occur rhythmically is evident in these recordings, a tendency that was accentuated by recording in sessions following REM deprivation by forced locomotor activity on a slowly moving treadmill. Modified from Lydic *et al.* (1987a).

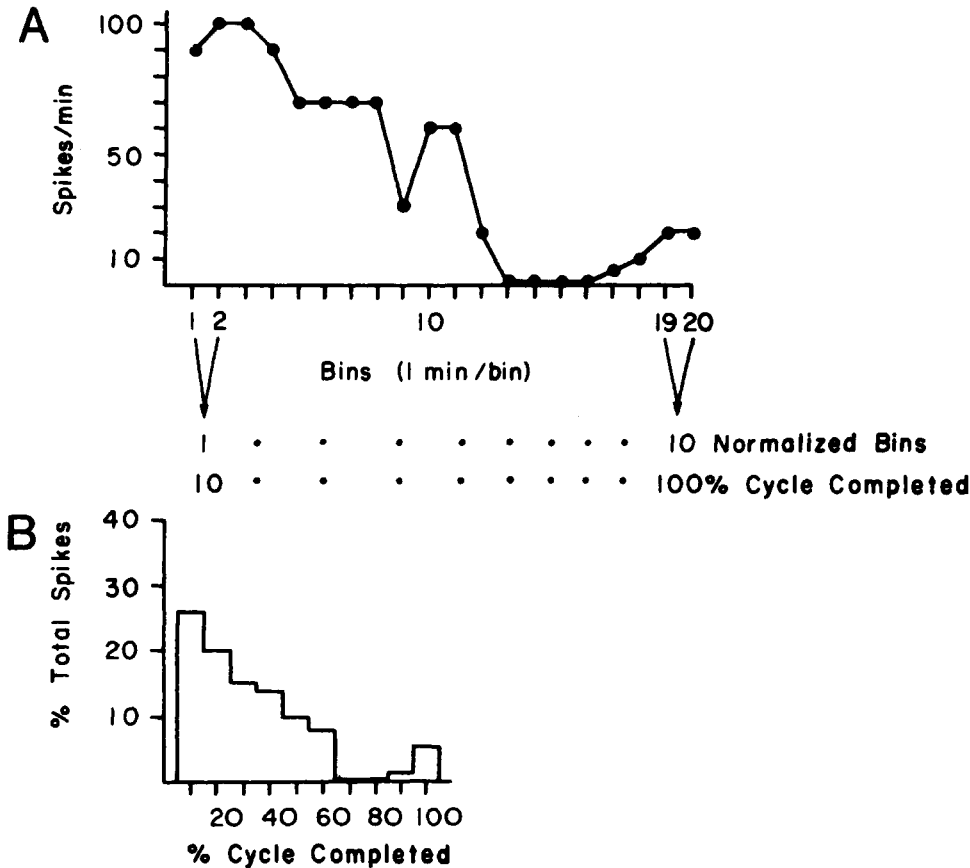


Figure 11.13. Illustration of the method of time normalization used for averaging neuronal activity over multiple sleep-wake cycles, using dorsal raphe neuronal activity as an example. A. The continuous time course of discharge activity of a single dorsal raphe neuron recorded over a sleep-wake cycle of 20 min duration, with the beginning of the cycle (0 min) and the end of the cycle (20 min) defined by the end of REM sleep. The computer program for time normalization converts the real time bins into 10 time-normalized bins of part B. This example shows a 2 to 1 compression for transformation of 20 real time bins into 10 normalized bins, and the same procedure is followed for other real time sleep-wake cycle durations, e.g. a 24 min cycle would use a 2.4 to 1 compression, etc. In B, it will be seen that the 10 normalized bins are read as a percentage of cycle completed and that the actual discharge rate has been converted into the percentage of total dorsal raphe spikes over the entire sleep-wake cycle that are included in each time normalized bin. The final step is simply averaging each cycle of time-normalized and of discharge activity-normalized data so as to produce histograms such as seen in Fig. 11.14. Modified from Lydic *et al.* (1983).

[52] Ruch-Monachon *et al.* (1976).

On the basis of *in vivo* pharmacological experiments, Ruch-Monachon and coworkers hypothesized that serotonergic neurons inhibited PGO waves, and also included adrenergic neurons as playing a suppressive role [52]; they further suggested that cholinergic/cholinoceptive systems were actively responsible for PGO wave generation. Experiments by Cespuglio and coworkers utilized local cooling of the dorsal raphe in the unanesthetized

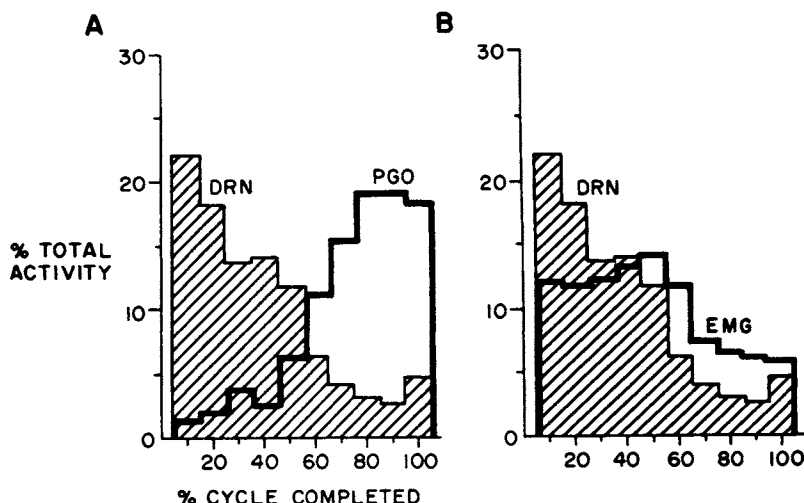


Figure 11.14. Simultaneously recorded time course of a single presumptively serotonergic dorsal raphe neuron (DRN) and PGO waves averaged over 11 sleep–wake cycles. The time bins on the abscissa represent the percentage (10–100%) of the sleep cycle completed, with the cycle beginning and ending at the end of REM sleep, as described in Fig. 11.13. The histograms show the percent of activity in each bin relative to the total number of events; overall 10,021 DRN action potentials and 5,124 PGO waves were recorded. Note the reciprocal time course between discharge activity and PGO waves. Note also that DRN activity is lowest in the portion of the cycle with the maximal probability of REM (80–90% of cycle completed) but that there is an increase in DRN activity prior to the electrographically defined end of REM sleep, suggesting a phase advance of DRN activity that may contribute to termination of the REM sleep episode. Chapter 12 discusses this possibility in detail. Adapted from Lydic *et al.* (1983).

“semi-chronic cat” [53] (spinal cord transected at T2 and deafferented above T2). This preparation showed spontaneous sleep cycles. Local cooling consistently produced PGO waves and full REM sleep in 35% of the trials. Cryocoagulations at the end of the experiment produced a state with cortical desynchronization and continuous PGO waves, much as in previous pure lesion experiments [54].

This postulate of monoaminergic inhibition of cholinergic neurons was originally regarded as extremely controversial. However, interest was quickened in the 1990s by (1) documentation of serotonergic projections from the dorsal raphe to the mesopontine cholinergic neurons in the LDT and PPT nuclei that are implicated in the production of REM sleep [55]; (2) *in vitro* demonstration of serotonergic inhibition of mesopontine cholinergic neurons [56]; and (3) the report that microinjection of a serotonergic 5-HT_{1A} agonist into the PPT inhibits REM sleep [57]. It was also demonstrated that the level of serotonin release in the cat DRN parallels the time course of presumptively serotonergic neuronal activity: waking (W) > slow-wave sleep (SWS) > REM sleep [58], suggesting that this would also be true at axonal release sites in

[53] Cesputio *et al.* (1979).

[54] Jouvet (1969).

[55] Semba and Fibiger (1992); Honda and Semba (1995); Steininger *et al.* (1997).

[56] Leonard and Llinas (1994); Luebke *et al.* (1992).

[57] Sanford *et al.* (1994).

[58] Portas and McCarley (1994).

the LDT/PPT, since serotonin levels at distant DRN projection sites had the same behavioral state ordering of levels as those in the DRN: W > SWS > REM sleep [59].

[59] For cats see Wilkinson *et al.* (1991); for rats see Auerbach *et al.* (1989) and Imeri *et al.* (1994).

11.5.3.2. Suppressing Dorsal Raphe Activity Increases REM Sleep

Since axon collaterals of DRN serotonergic neurons inhibit this same DRN population via somatodendritic 5-HT_{1A} receptors [60], it follows that the introduction of a selective 5-HT_{1A} receptor agonist in the DRN via microdialysis perfusion should produce strong inhibition of serotonergic neural activity, which would be indicated by a reduction of 5-HT release in the DRN. Moreover, if the hypothesis of serotonergic inhibition of REM-promoting neurons were correct, the inhibition of DRN serotonergic activity should disinhibit REM-promoting neurons, producing an increase in REM sleep concomitant with the changes in DRN extracellular serotonin. Portas and collaborators tested the effects of microdialysis perfusion of 8-hydroxy-2-(di-*n*-propylamino)tetralin (8-OH-DPAT), a selective 5-HT_{1A} receptor agonist, in freely moving cats [61]. In perfusions during W, DRN perfusion of 8-OH-DPAT decreased 5-HT levels by 50% compared with ACSF, presumptively through 5-HT_{1A} autoreceptor-mediated inhibition of serotonergic neural activity. Concomitantly, as illustrated in Fig. 11.15, this 8-OH-DPAT perfusion produced a short latency, three-fold increase in REM sleep, from 10 to 30% of the total recorded time ($p < 0.05$), while waking was not significantly affected. In contrast, and suggesting DRN specificity, 8-OH-DPAT delivery through a probe in the aqueduct did not increase REM sleep, but rather tended to increase waking and decrease SWS.

[60] Sprouse and Aghajanian (1987).

[61] Portas *et al.* (1996).

These data in the cat were confirmed in the rat. Bjorvatn *et al.* used microdialysis to perfuse 8-OH-DPAT (10 mM) into the DRN of rats and found a four-fold increase in REM sleep compared to control perfusion with ACSF, while the other vigilance states were not significantly altered [62].

[62] Bjorvatn *et al.* (1997).

[63] Sakai and Crochet (2001); Portas *et al.* (1996).

Sakai and Crochet failed to replicate the findings of Portas *et al.* in the cat and Bjorvatn *et al.* in the rat [63, 62]. Sakai and Crochet used microdialysis to perfuse 8-OH-DPAT (10, 50, 100, and 500 mM) into the DRN of cats and found a dose-dependent increase in wakefulness and decrease in SWS, but there was no significant effect on the generation of REM sleep [64]. They suggested that the Portas *et al.* data were flawed because the control period had "relatively high amounts of wakefulness and low amounts of

[64] Sakai and Crochet (2001).

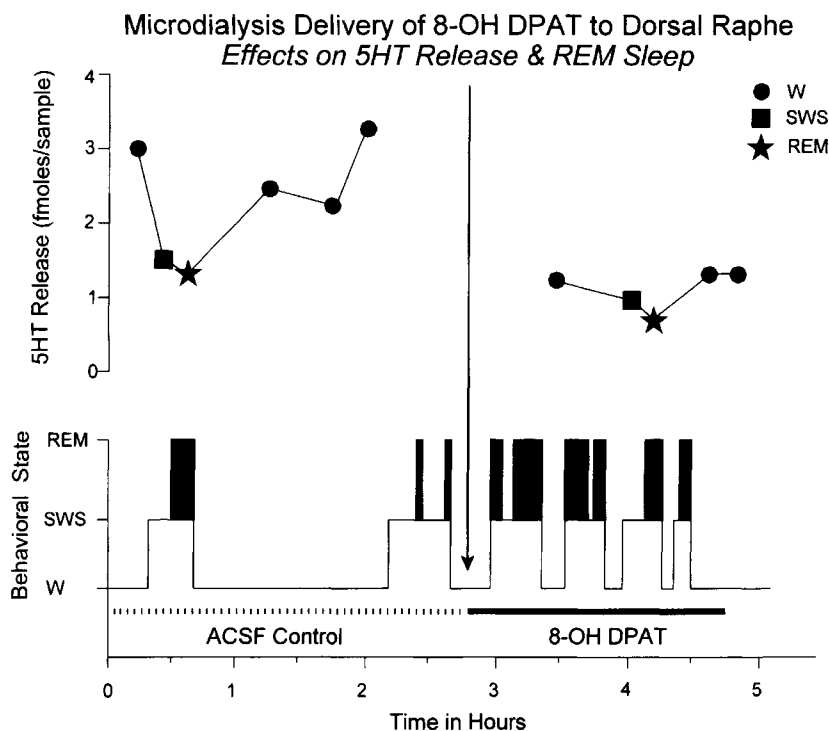


Figure 11.15. Time course of 5-HT levels (top portion of figure) and behavioral state (bottom portion of figure) during control DRN ACSF perfusion (interrupted horizontal line) and during DRN 8-OH-DPAT perfusion (solid horizontal line) in a typical experiment. Note that, prior to perfusion, waking DRN 5-HT levels (circles) are higher than those in slow-wave sleep (SWS) (squares) and REM sleep (stars). Each 5-HT value is expressed as fmol per 7.5 μ l sample, and was obtained during an uninterrupted 5 min sequence of the behavioral state. Upon the onset of 10 μ M 8-OH-DPAT perfusion (arrow) the 5-HT level dropped quickly to levels as low as those normally present in SWS or REM. Behaviorally, 8-OH-DPAT administration markedly increased REM sleep (black bars in the hypnogram). Adapted from *Portas et al.*, 1996.

REM sleep,” and this allowed the comparison with REM sleep after 8-OH-DPAT to become statistically significant. However, as described above, *Portas et al.* reported that the mean percentage time in REM sleep after 8-OH-DPAT was 30% (18 min/hr)—a value considerably higher than Sakai and Crochet’s control values for any of their 7 control hr ($p < 0.007$, binomial test), and, overall, more than two-fold higher than their average control value of about 14%. It is difficult to be certain why Sakai and Crochet did not find this effect. However, Sakai and Crochet did not, unlike *Portas et al.*, monitor 5-HT release before and during 8-OH-DPAT to verify that the expected pharmacological effect of 8-OH-DPAT was occurring (reduction in 5-HT release), and hence indicating adequate delivery to DRN. It is thus difficult to be certain that the expected delivery of 8-OH-DPAT to a sufficiently large number of neurons in DRN occurred (although effects on single neurons were monitored); possible causes of delivery

problems include gliosis on the microdialysis membrane and/or localization problems. Portas *et al.* reported findings similar to Sakai and Crochet of increased wakefulness and decreased SWS with 8-OH-DPAT delivery from probes not in the DRN [61, 64].

11.5.3.3. LDT/PPT REM-On Neurons are Inhibited by a 5-HT1A Agonist

The data of Portas *et al.*, however, did not directly demonstrate serotonergic inhibition of neurons in the cholinergic LDT/PPT [61]. Moreover, the presence of some neurons with REM-on and other neurons with Wake/REM-on activity in LDT/PPT was a puzzle in terms of the global changes in monoaminergic inhibition. McCarley *et al.* postulated that while monoamines might inhibit REM-on cholinergic neurons, Wake/REM-on neurons might not be inhibited, thus explaining their continued activity in waking [65]—since serotonergic activity is highest during wakefulness, the observed high discharge rate of Wake/REM-on neurons during wakefulness would not be consistent with a high level of serotonergic inhibition from a high level of DRN activity. *In vitro* data were also consistent with a subset, not the entire population, of LDT/PPT cholinergic neurons inhibited by serotonin acting at 5-HT1A receptors [66]. Thakkar and collaborators developed a novel methodology allowing both extracellular single cell recording and local perfusion of neuropharmacological agents via an adjacent microdialysis probe in freely behaving cats to test this hypothesis of differential serotonergic inhibition as an explanation of the different state-related discharge activity [40]. Discharge activity of REM-on neurons was almost completely suppressed by local microdialysis perfusion of the selective 5-HT1A agonist 8-OH-DPAT, while this agonist had minimal or no effect on the Wake/REM-on neurons (Fig. 11.16).

The finding that only a subpopulation of the recorded LDT/PPT cells were inhibited by 8-OH-DPAT is consistent with rat pontine slice data, where, in combined intracellular recording and labeling to confirm the recorded cell's cholinergic identity, 64% of the cholinergic neurons in the LDT/PPT were inhibited by serotonin [67]. However, it is obviously not possible to determine if the cells recorded *in vitro* are REM-on, or Wake/REM-on, since there are no purely electrophysiological criteria sufficient to identify the cell's state-related characteristics. The different percentages of LDT/PPT neurons that are inhibited by serotonin or serotonin agonists *in vitro* (64%) compared

[65] McCarley *et al.* (1995).

[66] Luebke *et al.* (1992); Muhlethaler *et al.* (1990); Leonard and Llinas (1994).

[67] Luebke *et al.* (1992).

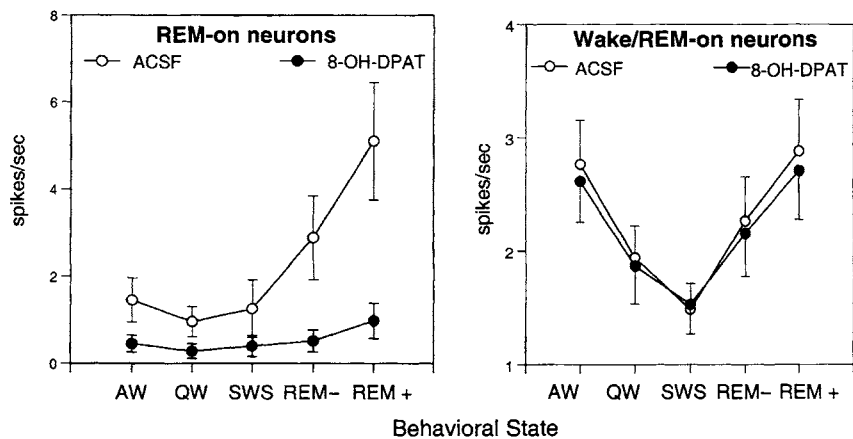


Figure 11.16. Left panel. REM-on units ($N = 9$): Grand mean (\pm SEM) of discharge rate in each behavioral state before (open circle, ACSF) and after (closed circle) $10\ \mu\text{M}$ 8-OH-DPAT was added to the perfusate. Note suppression of activity (highly statistically significant). Abbreviations are defined in text. Right panel, Wake/REM-on units ($N = 25$): Grand mean (\pm SEM) of discharge rate of before (open circle, ACSF) and after (closed circle) $10\ \mu\text{M}$ 8-OH-DPAT was added to the perfusate. Note minimal effect of 8-OH-DPAT on Wake/REM-on neurons, not statistically significant. Adapted from Thakkar *et al.*, 1998.

with our *in vivo* findings (36.4%) may be due to anatomical differences between species (rat vs cat) and/or different concentrations of agents at the receptors. Luebke *et al.* did not do a concentration–response study and their bath-applied serotonin agonists may have had a higher concentration at receptor sites than in the Thakkar *et al.* study [67]. Further research will be needed to determine whether differential serotonergic inhibition in LDT/PPT results from differing serotonergic innervation and/or different receptor distribution or sensitivity on different neurons. Anatomical studies in the cat of the percentage of meso-pontine cholinergic neurons with 5-HT1A receptors are needed, as has been done in rat forebrain [68]. It should be noted that serotonin inhibition of rat mesopontine neurons *in vitro* has been confirmed, and that an additional suppression of dendritic calcium influx has been reported [69].

[68] Kia *et al.* (1996).
[69] For confirmation see Leonard and Llinas (1994); for reporting see Leonard *et al.* (2000).

**11.5.3.4. Locus Coeruleus Lesions and Cooling
Increase REM Sleep**

Lesion studies furnish an unclear picture of the role of the LC in REM sleep. *Bilateral* electrolytic lesions of LC in cat by Jones *et al.* led these workers to conclude the LC was not necessary for REM sleep [70]. In the REM sleep-like state following the lesion, there was a two-fold reduction of PGO spikes while the number in deep

[70] Jones *et al.* (1977).

synchronized sleep increased approximately three-fold, so that the total number of spikes remained approximately the same—a picture much like that following acute raphe lesions. Over time, the total number of PGO spikes declined and the percentage of a REM sleep-like state increased from about 5 to 10%, vs a control value of 15%. We use the term “REM sleep-like” because muscle atonia was abolished and there was, in fact, motor activity like that described in the previous chapter for the “REM sleep without atonia” state following tegmental lesions; this syndrome likely resulted from spread of the lesion to the reticular area subserving atonia. Other lesion effects included loss of spontaneous micturition and defecation, a rise in mean temperature from 37.1 to 38.3°C, and loss of grooming, coordination and balance.

The picture following *unilateral* LC lesions was quite strikingly different. Caballeros and De Andres found a 50% *increase* in the percentage of REM sleep ($p < 0.001$) following unilateral electrolytic lesions of LC in cats; cats with lesions in neighboring tegmentum and sham-operated controls showed no change [71]. The postoperative condition of animal with unilateral lesions was much better than after bilateral lesions; in only one unilaterally LC-lesioned animal was there urinary retention, and this was transient and no “alteration in any other vegetative function” was observed. Accordingly, Caballeros and DeAndres attributed the differences between their study and that of Jones *et al.* to nonspecific effects of the larger lesions that, as with almost any CNS insult, may have led to a REM sleep reduction [70, 71].

[71] Caballeros and
De Andres (1986).

11.5.3.4.1. Locus Coeruleus Cooling Induces REM Sleep. Cespuglio and coworkers performed unilateral and bilateral cooling of the LC, using the same methodology as described above for the dorsal raphe cooling [72]. The effects of cooling were quite clear-cut. Three cats each had 5 trials of bilateral cooling, and in *all* 15 trials, there was progression to synchronized sleep (30–60 s), then to the transition phase with PGO waves (2–3 min), and then, in 40–50% of the trials, to full-blown REM sleep (3–4 min after cooling onset). Unilateral cooling produced exactly the same picture in 92% of the trials. In repeated cooling trials, REM sleep was repetitively induced and the percentage of REM sleep increased by 120% over control periods. Figure 11.17 shows that LC cooling to +10°C induced, in sequence, synchronized sleep, then PGO waves (transition period, 2 min latency), and finally, 2.5 min after the onset of cooling, a full-blow REM sleep episode. Note that both phasic and tonic components

[72] Cespuglio *et al.*
(1982).

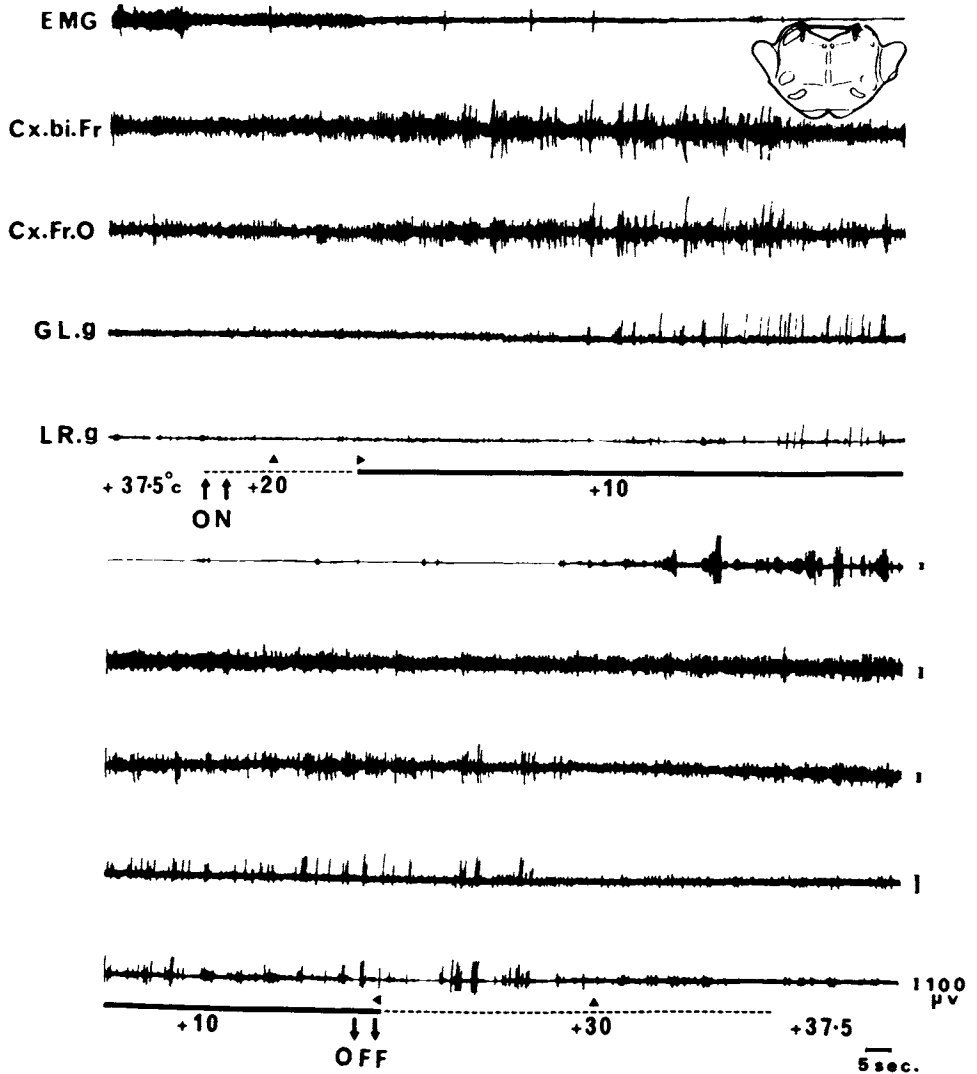


Figure 11.17. In the cat, bilateral localized cooling of the locus coeruleus (LC) induces cortical synchronization, then PGO waves, then both the tonic and phasic components of REM sleep. The frontal section insert is at P3 (Berman, 1968) and shows the position of the tip of the cryode in the LC zone. The dotted and solid lines indicate the time duration of cooling to +20 and then to +10°C; at +10°C, REM sleep is induced and maintained. Abbreviations: EMG, electromyogram of neck muscle; Cx.bi.Fr and Cx.Fr.O are cortical EEG from bifrontal and fronto-occipital electrodes respectively; GL.g is record of PGO wave activity from the left (= gauche in French) lateral geniculate nucleus; and LR.g. is electromyographic record of the left lateral rectus muscle, indicating the presence of leftward eye movements. From Cespuglio *et al.* (1982).

of REM sleep were present: muscle atonia, cortical desynchronization, PGO waves, and rapid eye movements.

Cooling experiments produced repeatable effects implying temporary inactivation and not destruction of neuronal elements, and also because they clearly enhanced REM. This raises the general point that nonspecific effects

[73] Satinoff (1988).

of destructive lesions always decrease REM, as do other CNS insults. Satinoff's comment about nonspecific effects is that, "One might also say that rendering an animal unconscious by a blow to the head eliminates REM sleep. In a sense it does, but that sense is completely trivial" [73]. It is, consequently, hard to draw definitive and interpretable conclusions about destructive lesions, especially those that do not enhance REM sleep. Jones, for example, concluded that her lesions showed the LC was not necessary for REM sleep, in the sense of being a region actively promoting REM, as had been proposed in the early Jouvet theory. While this interpretation appears reasonable, an important alternative interpretation was not ruled out: namely, that the LC plays a permissive, disinhibitory role but that nonspecific effects of the large lesions prevented the appearance of increased REM sleep—as we have seen taking place with both unilateral LC lesions and cooling that inactivated monoamine neurons. Later studies in the Jones laboratory were consistent with this disinhibition hypothesis (see below and [74]). In summary, many nonspecific factors decrease REM and few, if any, increase it; consequently, lesions or manipulations that increase REM are always more directly interpretable.

[74] Maloney *et al.* (1999).

11.5.3.4.2. Site(s) of REM-Off and REM-On interaction. The model for REM sleep control proposed in the next chapter discusses REM-off suppression of REM-on neurons. It must be emphasized that there are several, nonmutually exclusive, possible sites of interaction. These include direct ACh-NE interactions in the LDT and PPT. For example, there is now evidence that ChAT-labeled fibers are present in LC and it has long been known that the NE-containing LC neurons also stain intensely for the presence of acetylcholinesterase [75]. NE varicosities are present throughout the reticular formation and the LDT and the peribrachial area that is the site of ChAT-positive neurons. Thus adrenergic-cholinergic interactions may take place directly between these two species of neurons and/or may take place at reticular neurons.

[75] See review of NE-ACh anatomical interrelationship in Jones (2003a).

11.6. GABAergic Influences and REM Sleep

In addition to the monoamines and acetylcholine as modulators and controllers of the sleep cycle, there is accumulating evidence that GABAergic influences may play an important role. Defining the role of GABA with certainty is difficult, however. Since GABA is an ubiquitous

inhibitory neurotransmitter, purely pharmacological experiments using agents that increase or decrease GABA do not answer a key question, namely whether the results so obtained were representative of the increases or decreases in GABA that occur naturally in the course of the sleep cycle, or were simply and trivially the result of a pharmacological manipulation of GABA systems not naturally playing a role in sleep-cycle control. Microdialysis is potentially a very useful way of sampling naturally occurring changes in GABA levels over the sleep cycle, but is often limited in sensitivity and, hence, in time resolution of when the changes occur in the sleep cycle.

This section surveys GABA data from dorsal raphe, LC, and pontine reticular formation that are relevant to sleep-wakefulness control. From the standpoint of sleep-cycle control, one of the most puzzling aspects has been defining what causes the “REM-off” neurons in the LC and DRN to slow and cease discharge as REM sleep is approached and entered. The reciprocal interaction model (see below) hypothesized a recurrent inhibition of LC/DRN, which might account for this effect. While recurrent inhibition is present, there is no clear evidence that it might be the causal agent in REM-off neurons turning off. Thus, the prospect that a GABAergic mechanism might be involved is of great intrinsic interest. We go into some detail about the GABA levels reported, since GABA sampling is evolving technically.

11.6.1. Dorsal Raphe Nucleus

11.6.1.1. Microdialysis

Nitz and Siegel obtained *in vivo* microdialysis samples from the DRN in naturally sleeping cats, noting that “cessation of firing of serotonergic dorsal raphe neurons is a key controlling event of rapid eye movement (REM) sleep” [76]. This study is the single extant microdialysis study of GABA release in DRN, and reported a significant increase in GABA levels in REM sleep (0.072 pmol/ μ L or 72 fmol/ μ L) compared with wakefulness (0.042 pmol/ μ L), while SWS (0.049 pmol/ μ L) did not significantly differ from wakefulness. Glutamate and glycine release did not change over the sleep cycle. Further supporting a GABA role in REM control via inhibition of serotonergic neurons was the 67% increase in REM sleep observed with microinjections of the GABA agonist muscimol into the DRN and the observation that reverse microdialysis of the GABA antagonist picrotoxin completely abolished REM sleep. For comparative purposes we note that the increase in

[76] Nitz and Siegel (1997a).

REM sleep observed with microdialysis application of the 5-HT_{1A} agonist 8-OH-DPAT to DRN by Portas *et al.* was greater (190%) suggesting that factors other than GABA might influence serotonergic neurons [61].

Although the data did not directly support GABAergic inhibition as a mechanism of the slowing of serotonergic unit discharge in the passage from wakefulness to SWS, Nitz and Siegel noted the possibility that a small increase in the release of GABA, possibly beyond the resolution of the microdialysis technique, might be sufficient to reduce DRN unit discharge in SWS.

11.6.1.2. Microiontophoresis

Levine and Jacobs showed in cats that iontophoretic application of bicuculline reversed the typical suppression of DRN serotonergic neuronal activity seen during SWS but had no effect on maintained activity during W and the more complete suppression of activity occurring during PS [77]. An interpretation of this finding offered by Nitz and Siegel was that bicuculline was able to antagonize the lesser GABAergic inhibition during SWS, but not the greater inhibition during REM sleep, since bicuculline is a competitive GABA-A receptor blocker, unlike the picrotoxin used by Nitz and Siegel [76].

Gervasoni *et al.* reported that, in the unanesthetized but head-restrained rat, the iontophoretic application of bicuculline on DRN serotonergic neurons, identified by their discharge characteristics, induced a tonic discharge during SWS and REM sleep (see Fig. 11.18) and an increase of discharge rate during quiet waking [78]. They postulated that an increase of a GABAergic inhibitory tone present during wakefulness was responsible for the decrease of activity of the DRN serotonergic cells during slow-wave and REM sleep. In addition, by combining retrograde tracing with cholera toxin B subunit and glutamic acid decarboxylase immunohistochemistry, they provided evidence that the GABAergic innervation of the dorsal raphe nucleus arose from multiple distant sources and not only from interneurons as classically accepted. Among these afferents, they suggested GABAergic neurons located in the lateral preoptic area and the pontine ventral periaqueductal gray, including the DRN itself, could be responsible for the reduction of activity of the DRN serotonergic neurons during SWS and REM sleep, respectively.

However, a report from the same laboratory in the same year described results at variance with those of Gervasoni *et al.* [78]. Sakai and Crochet used *in vivo* extracellular unit recordings combined with microdialysis infusion in the cat but were unable to block the cessation of

[77] Levine and Jacobs (1992).

[78] Gervasoni *et al.* (2000).

Bicuculline restores DRN unit discharge during REM sleep

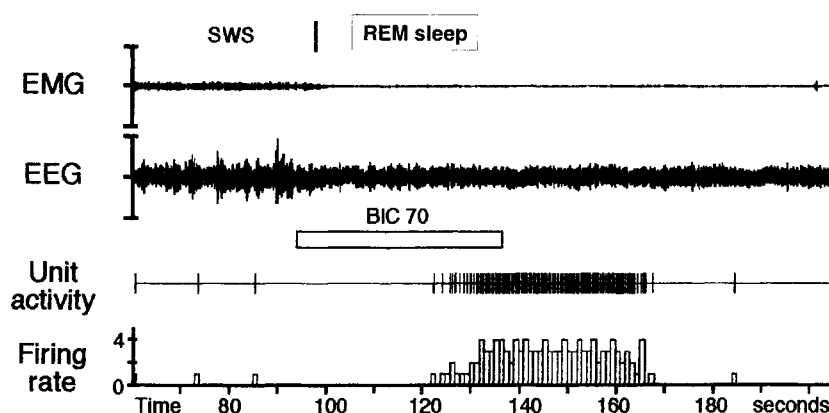


Figure 11.18. Effect of an iontophoretic application of bicuculline on a presumptively serotonergic dorsal raphe nucleus (DRN) cell during REM sleep. In control conditions, the DRN neuron does not discharge during REM sleep (100–120 s). Thirty seconds after the onset of the bicuculline application (70 nA, 42 s), the neuron increased its discharge rate to a mean frequency of 3.6 Hz. The effect lasted 43 s and disappeared 31 s after the end of the bicuculline application. Note that the REM sleep period is not disrupted by the iontophoretic application of bicuculline. Adapted from Gervasoni *et al.* (2000).

discharge of presumed serotonergic DRN neurons during REM sleep by either bicuculline or picrotoxin application [79]. Rather, in subpopulations of DRN neurons, cessation of REM sleep discharge was completely blocked by either histamine (2 or 5 mM, in 19/27 neurons), or phenylephrine, an α_1 adrenoceptor agonist (0.2 mM, in 10/21 neurons). (No neuron responded both to histamine and to phenylephrine.) Suppression of spontaneous discharge of DRN neurons during quiet wake and SWS occurred with microdialysis application of mepyramine, a specific H1 histamine receptor antagonist (N = 9 histamine-responsive neurons) or prazosin, a specific α_1 adrenoceptor antagonist (N = 2 phenylephrine-responsive neurons). Sakai and Crochet concluded that the suppression of REM-off neuronal discharge was the result of SWS and REM sleep disfacilitation of excitatory histaminergic and noradrenergic projections to DRN [79]. We note that no data were presented on whether DRN application of mepyramine and/or prazosin was able to increase REM sleep percentages, as were GABA antagonists and serotonin agonists, as described above by Nitz and Siegel [76] and Portas *et al* [61]. Sakai and Crochet found an increase in DRN neuronal antidromic excitability during REM sleep, mainly due to a decreased spontaneous discharge rate, a cause that could be due to either disfacilitation or inhibition [64]. While it is entirely possible that GABA pharmacological actions could differ radically in

[79] Sakai and Crochet (2000).

[80] Nitz and Siegel
(1997b).

the cat and rat, the most parsimonious interpretation is that the Gervasoni *et al.* studies in the rat and Sakai and Crochet in the cat differed in technical aspects [79, 80]. The argument for a different pharmacology in the cat and rat is weakened also by the results of Nitz and Siegel, which agreed with the Gervasoni *et al.* rat data [76, 78].

11.6.2. Locus Coeruleus

11.6.2.1. Microdialysis

The single published study on sleep–wake analysis of GABA release in the LC region placed microdialysis probes on the border of LC or in the peri-LC region in the cat [80]. GABA release was found to increase during REM sleep (1.9 fmol/ μ L) as compared to both waking values (1.2 fmol/ μ L) and SWS (1.6 fmol/ μ L) (see Fig. 11.19). GABA release during SWS showed a trend-level significance ($p < 0.06$) when compared with waking. The concentration of glutamate and glycine in microdialysis samples was unchanged across sleep and wake states. These data, because of the SWS differences, appear to offer more direct support for LC than for DRN neurons for the hypothesis of GABA-induced inhibition causing the reduction in LC/DRN discharge in SWS and virtual cessation of firing in REM sleep. Incidentally, the authors did not explicitly comment on the reason for their finding a 35-fold greater GABA concentration in the DRN than in the LC during waking; this may have been due to various methodological differences, thus calling to attention the difficulty in measuring GABA.

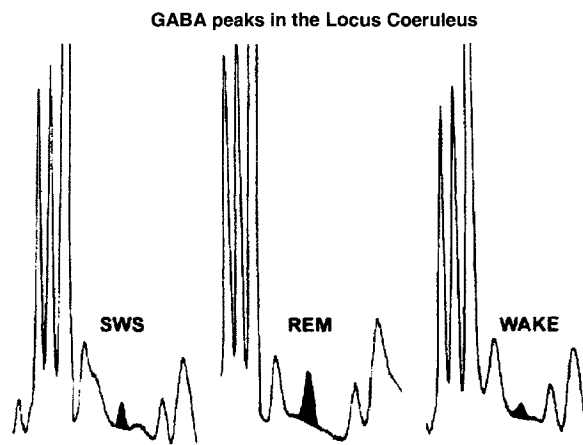


Figure 11.19. Chromatographic peaks corresponding to GABA from a single sleep/wake cycle. The GABA peak is indicated by blackening. Modified from Nitz and Siegel, 1997a.

11.6.2.2. Microiontophoresis

Gervasoni and colleagues applied their methodology of microiontophoresis and single-unit extracellular recordings in the LC of unanesthetized, head-restrained rats [81]. Bicuculline, a GABA-A receptor antagonist, was able to restore tonic firing in the LC noradrenergic neurons during both REM sleep and SWS. Application of bicuculline during wakefulness increased discharge rate. These data, combined with Nitz and Siegel [80], are thus consistent with GABAergic inhibition in the LC during REM and SWS.

[81] Gervasoni *et al.* (1998).

11.6.3. Source of State-Related GABAergic Input to DRN and LC

Overall, the DRN and LC studies just surveyed are consistent with, but do not prove, the hypothesis that increased GABAergic inhibition leads to REM-off cells turning off. The increased GABAergic tone could simply be a *consequence* of other state-related changes without causing these changes. Here, as with other neurotransmitters, it would be helpful to have unit recordings of GABAergic neurons with inputs to LC/DRN. One could see if these neurons had the requisite lead times and state-related discharge time course to cause the changes. Where might these neurons be located?

11.6.3.1. Periaqueductal Gray?

The Gervasoni *et al.* study on DRN pointed to the periaqueductal gray (PAG) as a possible source of the GABAergic input proposed to inhibit DRN neurons [78]. The PAG is involved in the control of a number of behavioral and physiological functions, many related to autonomic and visceral function, as well as to pain [82]. With respect to behavioral state control, there are reports that suggest the ventrolateral division of the PAG (vlPAG) may be involved in the regulation of REM sleep since both vlPAG lesions and muscimol injections produced a large increase in REM sleep [83]. Thakkar and colleagues thus decided to record vlPAG unit activity in freely behaving cats to determine if neurons selectively increased their tonic discharge activity before and during REM sleep, and hence might furnish GABAergic inhibition of monoaminergic neurons [84]. Several types of state-specific neuronal populations were found in the PAG, but none of the 33 neurons showed a tonic discharge increase before and during REM, but rather were phasic in pattern and increased

[82] Reviewed in Behbehani (1995).

[83] For vlPAG lesions see Petitjean *et al.* (1975); for muscimol see Sastre *et al.* (1996).

[84] Thakkar *et al.* (2002).

discharge rate too late in the cycle to be a cause of the DRN SWS suppression. These data thus suggest that although vlPAG neurons may regulate phasic components of REM sleep, they do not have the requisite tonic pre-REM and REM activity to be a source of GABAergic tone to monoaminergic neurons responsible for their REM-off discharge pattern. This (and any) study with negative findings can be critiqued on failure to study more potential exemplars. However, compared with other unit studies, this study did record more neurons than most; its negative findings would suggest that, at a minimum, neurons with the requisite activity are not abundant in the vlPAG.

11.6.3.2. Ventrolateral Preoptic Area? (VLPO)

This forebrain site was retrogradely labeled by Gervasoni *et al.* as projecting to the DRN [78]. Forebrain influences on REM sleep are discussed in the next chapter, but the Jouvet transection experiments suggest, however, these are not essential for the basic REM cyclicity found in the pontine cat.

11.6.4. GABA and the Pontine Reticular Formation: Disinhibition and REM Sleep

11.6.4.1. Pharmacological Studies in Cats on the Behavioral State Effects of GABA Agents

In three chronic, unanesthetized cats, Xi *et al.* micro-injected GABA, muscimol (GABA-A receptor agonist), and bicuculline (GABA-A receptor antagonist), separately, into the nucleus pontis oralis (NPO). This was in a region about 2 mm lateral to the midline and more than 1 mm ventral to LC—a region where carbachol induced a short latency (<4 min) onset of REM sleep [85]. The injection of either GABA or muscimol-induced wakefulness caused SWS and REM sleep to be suppressed. In contrast, the injection of bicuculline induced a prolonged state that was similar to naturally occurring REM sleep with muscle atonia, EEG desynchronization, and rapid eye movements. This REM-like state was three-fold more prominent than natural REM sleep (36% and 12%, respectively, of recording time).

Xi *et al.* elaborated on their 1999 data and micro-injected GABA-B agents baclofen (GABA-B agonist) and phaclofen (GABA-B antagonist) as well as muscimol and bicuculline into the NPO [86, 85]. Microinjection of 10 mM muscimol into RPO in cats significantly and

[85] Xi *et al.* (1999).

[86] Xi *et al.* (2001).

immediately increased wakefulness at the expense of REM and NREM, whereas 10 mM bicuculline enhanced REM, producing increases in the percentage of time in this state its frequency, and reducing the latency to onset. In contrast, injections of bicuculline or phaclofen produced active sleep. The percentage of time spent in active sleep and the frequency of active sleep increased while the percentage of time spent in wakefulness and the latency to active sleep were significantly reduced. The effects of baclofen and phaclofen were similar to the GABA-A agents but less strong. These data suggested that pontine GABAergic processes acting on both GABA-A and GABA-B receptors might play a critical role in generating and maintaining wakefulness and in controlling the occurrence of the state of REM sleep.

11.6.4.2. Pharmacological Studies in Rats on the Behavioral State Effects of GABA Agents

In the head-restrained rat, Boissard *et al.* used microiontophoresis of the GABA-A antagonists bicuculline and gabazine in the pontine reticular formation just ventral to the LC and LDT [87], termed the dorsal and alpha subcoeruleus nuclei by Paxinos and Watson atlas and the sublateralodorsal (SLD) nucleus by Swanson [88]. These agents produced a REM-like state with some, but not all, of the electrographic characteristics of REM sleep. Muscle atonia was a prominent and consistent feature, and an anatomical study showed anterogradely labeled fibers originating from the SLD were apposed on glycine- and C-Fos-positive neurons (labeled after 90 min of pharmacologically induced REM-like state) in the medullary gigantocellular and parvicellular reticular nuclei, likely sources of muscle inhibition during REM sleep. The EEG spectrum of natural REM sleep was not consistently present in this pharmacological state; the EEG spectrum was either intermediate between W and REM (39% of trials) or similar to W (61% of trials), including little theta activity. Rapid eye movements and penile erections were notably absent in this pharmacologically induced state. In contrast to the cat, carbachol applied to the SLD in these head-restrained rats produced wakefulness and not REM sleep. The authors interpreted these data as supporting the production of the REM-like phenomena through GABA disinhibition, especially the muscle atonia.

Sanford *et al.* assessed REM after bilateral microinjections into NPO and nucleus pontis caudalis (NPC) of muscimol and bicuculline in rats during the light (inactive) period [89]. In NPO, muscimol (1,000 μ M) suppressed REM while bicuculline (1,000 μ M) enhanced REM. In NPC,

[87] Boissard *et al.* (2002).

[88] Paxinos and Watson (1997); Swanson (1992).

[89] Sanford *et al.* (2003).

muscimol (200 μM , 1,000 μM) suppressed REM but bicuculline (1,000 μM and less) did not significantly affect REM. Higher concentrations of bicuculline (10,000 μM) injected into NPO and NPC produced wakefulness, circling, and escape behavior. Of note, bicuculline induced an overall increase in REM across the 6-hr recording period that was greatest in the third and fourth hours after the injection, but the pronounced short-latency, long-duration increase in REM seen in cats [85] was not observed.

This observation is similar to the absence of short-latency, long-duration enhancement of REM sleep with carbachol in the rat and its presence with these very different agents suggests a species difference in REM organization, perhaps related to the more circadian rats. Repeating the experiments of Sanford *et al.* and Boissard *et al.* [89, 87] in the dark, active phase would be of interest in determining whether circadian phase is an important variable in response to these agents in the rat. It is puzzling that such dark phase experiments have not been done.

11.6.4.3. Microdialysis Measurements of GABA in the Pontine Reticular Formation

Recently, Thakkar, Tao, and McCarley (unpublished data) have studied GABA release in pontine reticular formation of freely moving cats. They validated GABA measurements by increasing/decreasing GABA release by local microdialysis perfusion of (1) high (100 mM) K^+ ; (2) GABA uptake blockers (SKF 89976A and nipecotic acid); and (3) 10% procaine. The sensitivity in 5 μL samples was 0.04 pmol/sample. In the four animals thus far tested, multiple episodes of REM sleep had consistently lower levels of GABA than wakefulness (see Fig. 11.20). Although wake was not statistically different from SWS, there was a trend toward lower GABA levels in SWS. Moreover, extracellular levels increased during forced wakefulness and decreased markedly during carbachol-induced REM. These data provide very preliminary but direct evidence compatible with GABA disinhibition in the pontine reticular formation during REM sleep.

11.6.5. The Pedunculopontine Tegmental (PPT) Nucleus

Tortorolo *et al.* microinjected muscimol and bicuculline into the PPT of four chronic cats [90]. Muscimol increased the time spent in REM sleep by increasing the frequency and duration of REM episodes; this increase was at the expense of the time spent in wakefulness. A decrease in PGO density during REM sleep was also observed following

[90] Tortorolo *et al.* (2002).

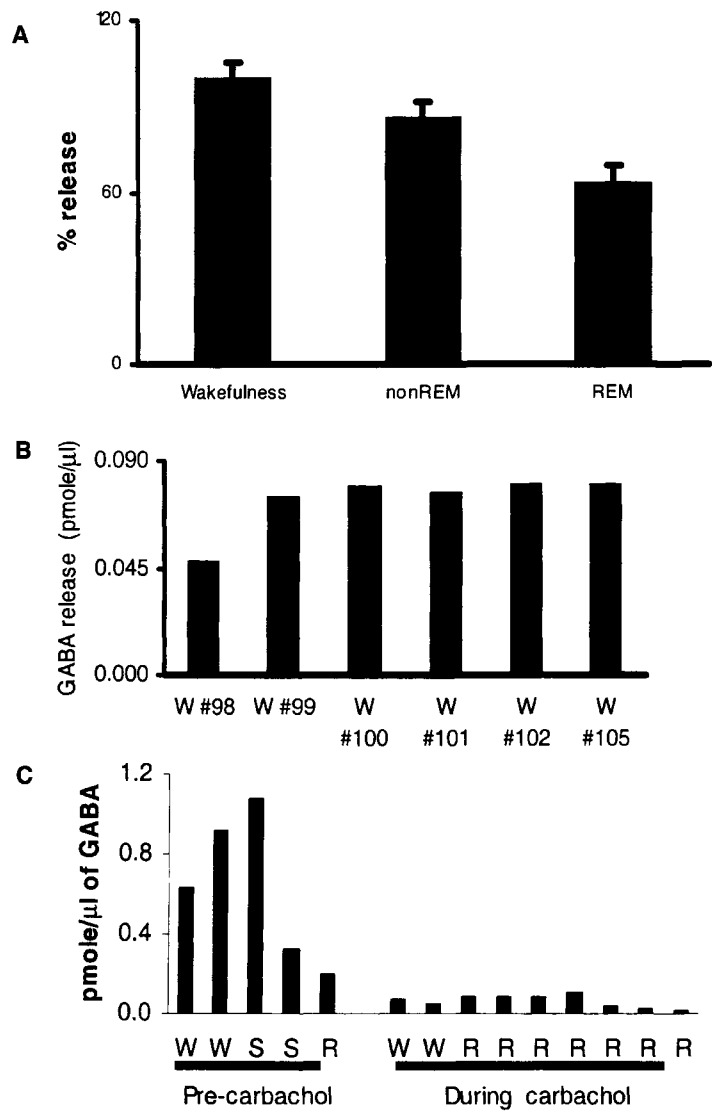


Figure 11.20. Extracellular concentrations of GABA in the pontine reticular formation in freely moving cats as measured by microdialysis. A. Release is lowest during REM sleep. B. Extracellular levels of GABA in the medial pontine reticular formation (mPRF) during 6 hr of sleep deprivation show an increase. C. Microdialysis perfusion of carbachol in the mPRF causes a significant reduction in GABA release in mPRF. Abbreviations: W = Wakefulness, S = SWS = non-REM sleep, R = REM sleep. Thakkar, Tao, and McCarley, unpublished data.

the microinjection of muscimol. On the other hand, bicuculline decreased both REM sleep and SWS and increased the time spent in wakefulness. These data were somewhat paradoxical in that an inhibitory agent increased REM sleep; the authors suggest that the GABA-A agonist acted primarily to suppress the activity of wakefulness-promoting PPT neurons, which are in a majority. We think there is an

alternate explanation: GABA agonists may primarily act to inhibit the GABAergic PPT neurons that inhibit cholinergic REM-on neurons. Since the PPT Wake/REM-on neurons are active in natural REM sleep as well as in wake, it is highly unlikely they would act to suppress REM sleep. Similarly, bicuculline might act to disinhibit PPT GABA neurons; however, their actions on PPT cholinergic neurons would also be blocked, as would other incoming GABAergic influences from outside the ipsilateral PPT, thus, producing a net disinhibition of PPT cholinergic neurons.

REM Sleep as a Biological Rhythm: The Phenomenology and a Structural and Mathematical Model with Application to Depression

12.1. Introduction and Overview

This chapter first presents a structural model of REM sleep cyclicity based on the data discussed in Chapter 11. The next sections discuss the characteristics of the REM sleep rhythm and the need for a mathematical model incorporating a limit cycle. Later sections of this chapter take up the more formal modeling aspects using the simplifying and unifying concept of interactions of REM-on and REM-off neurons. A final section (12.8) addresses the application of the model to understanding the abnormalities of REM sleep in patients suffering from depression.

12.2. A Structural Model of REM Sleep Organization

The history of the development of structural models encompasses the history of discovery of neurons and neurotransmitters important in REM sleep, and is one of growing complexity. The first formal structural and mathematical model was presented in 1975 by McCarley and Hobson [1]. This model, termed the Reciprocal Interaction model, was based on the interaction of populations of REM-on and REM-off neurons and mathematically described by the Lotka–Volterra (LV) equations, derived

[1] McCarley and Hobson (1975b).

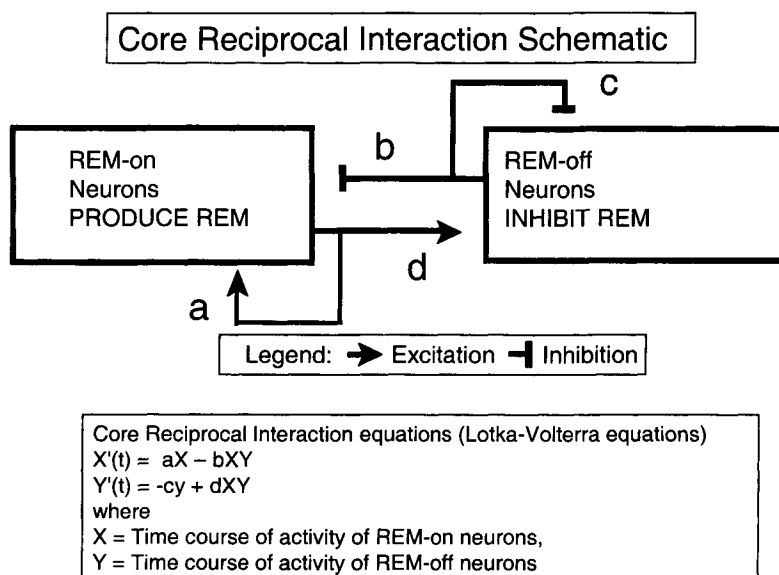


Figure 12.1. Summary of the “core” features of the reciprocal interaction model. The REM-on neuronal population has a positive feedback so that activity grows (see connection labeled “a”). This activity gradually excites the REM-off population (connection “d”). The REM-off population then inhibits the REM-on population (connection “b”), terminating the REM episode. The REM-off population is also self-inhibiting (connection “c”), and as REM-off activity wanes, the REM-on population is released from inhibition and is free to augment its activity. This begins a new cycle of events. This interaction is formally described by the Lotka–Volterra equations, where X = REM-on activity and Y = REM-off activity.

from population models of prey–predator interaction. This chapter will suggest that the basic notion of interaction of REM-on and REM-off neuronal populations is a very useful one for modeling and conceptualization, even though the description of the populations of neurons characterized as REM-on and REM-off has been altered and made much more detailed. Before getting into the details of the anatomy and the interaction, we first point the reader to Fig. 12.1, which describes the “core” features of the structural and mathematical model, and provides nonmathematical descriptions of the dynamics. The subsequent parts of this section elaborate on this core model in terms of current knowledge of the physiology and anatomy.

12.2.1. REM-On Neurons and Interaction with Other Elements in the Model

12.2.1.1. REM-On Neurons and the Postulate of Self-Excitation (Positive Feedback) and Exponential Growth—Term “a” in Fig. 12.1

The 1975 model was constructed before ChAT identification of cholinergic neurons and the REM-on population was simply characterized as pontine reticular formation

population, and should be referred to for details of the current anatomical/structural model. Additional positive feedback occurs via reticuloreticular connections (see Chapter 11; for simplicity, this feature is not shown in Fig. 12.2).

Supporting data for the PRF → LDT/PPT excitation include the presence of reticulo → LDT/PPT projections, evidence that excitatory amino acids (EAA) are the principal excitatory transmitters of PRF, and *in vitro* evidence for excitation of LDT/PPT neurons by EAA [4]. Further supporting the concept of PRF–LDT/PPT interaction during REM sleep are data showing that medial PRF microinjection of carbachol that induced REM sleep also increased the release of ACh in the medial PRF contralateral to the injection site, presumably as a result of PRF excitation of LDT/PPT neurons [5]. Finally, as described in Chapter 11, unit recording data indicate that a subset of LDT/PPT neurons becomes selectively active just before and during REM sleep, as would be expected of neurons promoting this state.

12.2.1.2. Reticular Formation and GABAergic Influences

Not only may LDT/PPT cholinergic input excite PRF neurons but there is the intriguing possibility that inhibitory LDT/PPT projections from REM-on neurons impinge onto GABAergic PRF interneurons with projections onto PRF neurons. This would have the effect of disinhibiting glutamatergic PRF neurons as REM sleep was approached and entered. Gerber *et al.* found that about one-fourth of PRF neurons *in vitro* were inhibited by muscarinic cholinergic agents [6]. Whether these neurons that were inhibited were GABAergic or not, however, is still not known. Preliminary data in the cat support cholinergic inhibition of GABAergic neurons, since microdialysis application of carbachol to the PRF not only induced REM but decreased GABA concentrations in samples from the same microdialysis probe [7]. Moreover, as outlined in Chapter 11, there is considerable evidence that reduction of GABA inhibition in the PRF might play a role in production of REM sleep. First, there are preliminary microdialysis data in both the cat [7] and the rat [8] that GABA levels in the PRF are decreased during REM sleep compared to wakefulness and the Thakkar *et al.* data indicate levels in non-REM sleep are intermediate between wakefulness and REM sleep. Second, pharmacological experiments support this concept since GABA antagonists applied to the rostral PRF produced REM sleep in both the cat and the rat [9]. This postulated pathway of LDT/PPT muscarinic inhibition of GABA

[4] For anatomical data on PRF projections to mesopontine cholinergic LDT/PPT see Higo *et al.* (1989a, 1990); for EAA as an excitatory neurotransmitter in PRF see Stevens *et al.* (1992); for *in vitro* evidence for excitation of cholinergic mesopontine neurons by EAA see Sanchez and Leonard (1994, 1996).

[5] Lydic *et al.* (1991).

[6] Gerber *et al.* (1991).

[7] Thakkar *et al.* (2004).

[8] Marks *et al.* (2003).

[9] For cats see Xi *et al.* (1999); Xi *et al.* (2001); for rats see Sanford *et al.* (2003).

PRF neurons during REM sleep is illustrated in Fig. 12.2. The dotted lines for this and other GABAergic pathways indicate the more tentative nature of identification of both the projections and their source. This figure graphically emphasizes that inhibition of PRF GABAergic neurons that inhibit PRF neurons would “Dis-Inhibit” the PRF neurons and so constitute an additional source of positive feedback. Of note, the GABA levels in wake and in REM in the PRF [7] are almost the exact inverse of Nitz and Siegel’s measurements of GABA in the locus coeruleus (LC) (see Chapter 11) suggesting a possible common source in the REM on neuronal activity of disinhibition in PRF and inhibition in LC REM-on neurons (PRF Wake/REM ratio = 1.7 and LC REM/Wake ratio = 1.7).

12.2.2. Excitation of REM-Off Neurons by REM-On Neurons (Fig. 12.1 term “d”)

There is anatomical evidence for cholinergic projections to both LC and dorsal raphe nucleus (DRN) [10]. *In vitro* data indicate excitatory effects of ACh on LC neurons, but data do not support such direct effects on DR neurons [11]. The REM-on neuronal excitation of DR neurons may be mediated through the reticular formation; there is *in vitro* evidence for EAA excitatory effects on both LC and DR neurons.

[10] Jones (1993).

[11] Li *et al.* (1998).

12.2.3. Inhibition of REM-On Neurons by REM-Off Neurons (Fig. 12.1 term “b”)

As noted in Chapter 11, for many years, this aspect of the model was most controversial, since the indirect evidence from *in vivo* data, although generally supportive, was subject to alternative explanations. Now *in vitro* data indicate that a subpopulation of cholinergic neurons in the LDT are inhibited by serotonin [12]. Inhibition is especially consistent for the population of LDT neurons that fire in bursts; such burst firing has been shown by *in vivo* extracellular recordings to be tightly correlated with lateral geniculate nucleus PGO waves, which other data indicate are cholinergically mediated. The action potential burst itself is caused by a particular calcium current, the *low-threshold spike* (LTS), which causes calcium influx and depolarization to a level that produces a burst of sodium-dependent action potentials. Some nonburst cholinergic neurons are also hyperpolarized by serotonin. Other data indicate effects of norepinephrine (NE) on

[12] Luebke *et al.* (1992).

LDT/PPT cholinergic neurons are also inhibitory [13]. Moreover, noncholinergic, presumptively GABAergic, interneurons are excited by NE [14]; GABAergic interneurons acting to inhibit cholinergic neurons would furnish yet another possible mechanism of inhibition of cholinergic mesopontine neurons by NE, thus further strengthening the model's postulates.

[13] Williams and Reiner (1993).

[14] Kohlmeier and Reiner (1999).

12.2.4. Inhibitory Feedback of REM-Off Neurons (Fig. 12.1 term "c")

There is strong *in vitro* physiological evidence for NE inhibition of LC neurons and of serotonergic inhibition of DR neurons, and anatomical studies indicate the presence of recurrent collaterals (see Chapter 11). These recurrent collaterals, which have been demonstrated to be inhibitory, could be the source of suppression of raphe activity, with the prolonged silence during REM resulting from long-duration neurotransmitter effects, perhaps from coupling with second or third messengers. It has been suggested that there may also be an unconventional mode of serotonin release during REM sleep that leads to increased extracellular serotonin and hence to inhibition. *In vivo* voltammetry data from Cespuglio and coworkers in the Jouvet laboratory suggest that, even though action potential activity in dorsal raphe neurons during REM sleep is low, the levels of serotonin metabolites increase [15]. This suggests a release of serotonin not coupled with soma depolarization. While this at first might be viewed as a highly improbable mechanism, Pan and Williams have obtained *in vitro* data compatible with such an unconventional release of serotonin in DR neurons [16]. However, direct measurements by *in vivo* microdialysis of serotonin release in the cat DRN parallels the time course of presumptively serotonergic neuronal activity: waking (W) > slow-wave sleep (SWS) > REM sleep [17] (see Fig. 11.15 in Chapter 11), and so it seems unlikely that there is a large serotonin release in DRN during REM sleep.

[15] Cespuglio *et al.* (1990).

[16] Pan and Williams (1989).

[17] Portas and McCarley (1994).

12.2.4.1. GABAergic Influences in the LC and DRN during REM Sleep

DRN. From the standpoint of sleep-cycle control, one of the most puzzling aspects has been defining what causes the "REM-off" neurons in the LC and DRN to slow and cease discharge as REM sleep is approached and entered. While LC-LC and DRN-DRN recurrent inhibition is present, there is no clear evidence that it might be the causal agent in REM-off neurons' turning off. Thus, the prospect that a GABAergic mechanism might be involved is of great

[18] Nitz and Siegel
(1997a).

[19] Portas *et al.* (1996);
Nitz and Siegel (1997a).

[20] Nitz and Siegel
(1997b).

[21] Gervasoni *et al.*
(1998).

intrinsic interest. As reviewed in Chapter 11, supporting a GABAergic mechanism in the DRN is the *in vivo* microdialysis finding of Nitz and Siegel in naturally sleeping cats that there is a significant increase in DRN GABA levels in REM sleep (0.072 pmol/ μ L or 72 fmol/ μ L) compared with wakefulness (0.042 pmol/ μ L), while SWS (0.049 pmol/ μ L) did not significantly differ from wakefulness [18]. Moreover, as discussed in the preceding chapter, the balance of pharmacological studies support a GABA-induced suppression of DRN activity. We think it important to emphasize that the issue of GABAergic and serotonergic inhibition is important in suppression of DRN discharge as not an either/or but likely one of joint influences. For example, we note that the 190% increase in REM sleep observed with microdialysis application of the 5-HT1A agonist 8-OH-DPAT to DRN by Portas *et al.* was greater than that observed with the GABA agonist muscimol by Nitz and Siegel, suggesting that factors other than GABA might influence serotonergic neurons [19]. Determination of whether the GABA time course of release parallels the decrease in activity of DRN serotonergic neurons during SWS as REM is approached awaits better technology for measurement of GABA.

LC. Nitz and Siegel placed microdialysis probes on the border of LC or in the peri-LC region in the cat [20]. GABA release was found to increase during REM sleep (1.9 fmol/ μ L) as compared to both waking values (1.2 fmol/ μ L) and SWS (1.6 fmol/ μ L) [20]. GABA release during SWS showed a trend-level significance ($p < 0.06$) when compared with waking. These data, because of the SWS differences, appear to offer more direct support for LC than for DRN neurons relative to the hypothesis of GABA-induced inhibition causing the reduction in LC/DRN discharge in SWS and virtual cessation of firing in REM sleep. In pharmacological experiments, Gervasoni and colleagues found that microiontophoresis application of bicuculline, a GABA-A receptor antagonist, during extracellular recordings in the LC was able to restore tonic firing in the LC noradrenergic neurons during both REM sleep and SWS in unanaesthetized, head-restrained rats [21].

12.2.4.2. Source of GABAergic Inputs to LC and DRN

The major missing piece of evidence on GABAergic inhibition of LC/DRN and REM-off neurons is the recording of GABAergic neurons whose activity has the proper inverse time course to that of LC and DRN neurons (see Chapter 11 review). In our diagram of the brainstem anatomy of REM sleep-cycle control, we have suggested

that GABAergic neurons in the PRF might provide the input to DRN/LC. Certainly, neurons in the PRF have the requisite time course of activity, but there is, to date, no evidence that these are GABAergic neurons. Within the LC and DRN, Maloney *et al.* found the extent of C-Fos labeling of GAD-positive neurons in DRN and LC to be inversely correlated with REM sleep percentage, and to decrease in recovery from REM sleep deprivation [22]. This is of course compatible with a local source of GABA increase during REM. However, unit recordings in DRN and LC have not found evidence for neurons with an inverse time course to that of the presumptively monoaminergic LC and DRN neurons.

[22] Maloney *et al.* (1999).

12.3. Characteristics of the REM Sleep Rhythm

Biological rhythms are processes characterized by recurrence over a particular time period, with the period of recurrence often referred to as tau. The inverse of the *period* of a rhythm is its frequency, a measure less often used. Circadian rhythms, for example, refer to processes with a period of about a day, while ultradian rhythms are those with periods shorter than a day. REM sleep has a period of about 90 min in the adult human, about 22 min in the cat, and about 12 min in the rat. This feature of alteration of ultradian REM period with body and brain size is not seen in circadian rhythms, which maintain an approximately 24 hr period across all species, regardless of size. This constancy of circadian period likely reflects function; circadian rhythms prepare behavior and physiology for events in the external world that are clocked by the circadian period of the earth's rotation, such as sunrise or sunset. While the function(s) of REM remain speculative, adjusting internal events to coincide with timing of external events seems excluded as a function. A point relating circadian rhythms and the ultradian REM rhythm is that, in many species including man, the time of occurrence and other parameters of REM sleep are modulated by circadian rhythms although the occurrence of REM is not dependent on the presence of either a circadian rhythm or an intact circadian oscillator.

12.3.1. Phenomenology of the REM Sleep Rhythm

The long duration of the period of the human REM cycle (90 min) and the consequent paucity of the number

of consecutive cycles available for analysis, usually only 3 or 4, and, in addition, its variability of duration makes statistical and experimental analysis of the rhythmicity difficult. Hence, study of many characteristics of REM cycle is easier in animals with a more rapid rhythm, and consequently more consecutive cycles are available for analysis. We use the term “*REM cycle*” or “*sleep cycle*” to refer to the time duration from the end of one REM period to the end of the next. Figure 12.3 shows the rhythmicity of

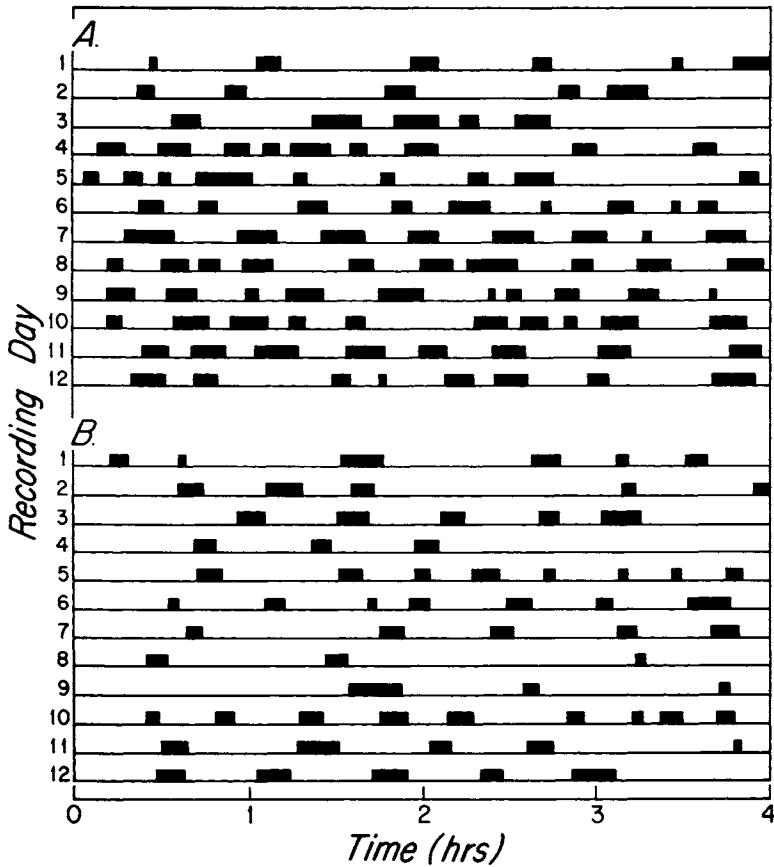


Figure 12.3. Phenomenology of the REM sleep ultradian rhythm. The occurrence of REM sleep epochs (black bars) in the cat during the initial 4 h (abscissa) from a randomly selected sample of 12 daily recordings, each of which followed REM sleep deprivation by means of forced locomotor activity (A) and 12 different days of recordings, which were not preceded by forced activity (B). Note the marked reduction in time to onset of the first REM sleep epoch on each recording day (from zero on the abscissa to the first black bar) and the increased frequency of REM sleep epochs after REM deprivation during forced activity (contrast number of black bars in A and B). This figure also illustrates the variability of REM sleep episodes, with episode to episode variability being less following REM sleep deprivation by forced activity. (Duration of forced activity on a very slowly moving treadmill was 8 h for the data in Figs. 12.3–12.6. Other studies cited in Lydic *et al.* (1987a) suggest that REM sleep deprivation was the major cause of the REM sleep increase; for the present purpose of illustrating how the REM sleep control system increases the percentage of REM sleep, the possible presence of other major effects on recovery REM is not important.) Adapted from Lydic *et al.* (1987a).

REM sleep occurrence in the cat recorded in the laboratory. This figure also shows that REM deprivation, produced by forced activity for 12 hr, has the effect of increasing the regularity of the REM cycle and the percentage of recording time occupied by REM [23].

Examining the effects of this mild REM deprivation is important in allowing us to make statements about the properties of the “REM oscillator,” as we shall refer to the system producing this ultradian rhythm. The following statements summarize the characteristics revealed by REM deprivation:

1. The number of REM episodes is increased by deprivation (Figs. 12.4A, B).
2. The duration of REM sleep episodes is only slightly, if at all, increased by REM deprivation (Fig. 12.4C). (The duration of a REM sleep episode is the time from onset of REM to the end of the same REM episode, and is to be contrasted with the term “REM cycle” duration—the time from the end of one REM episode to the end of the next.)
3. Without REM deprivation, the average time from end of one REM episode to the end of the next is increased; more time is spent in waking and slow-wave sleep, but not in the “transition period”—the pre-REM time characterized by the occurrence of PGO waves. The effect of deprivation is summarized in the histograms of REM cycle duration; deprivation produces a regularization of REM cycle lengths to the median duration of about 22 min, whereas without deprivation there are more long REM cycles characterized by long episodes of waking and slow wave sleep (Fig. 12.5).

A simple summary of these data is that the REM oscillator has relatively fixed characteristics: REM episode duration is relatively constant, as is the “preferred” or modal REM cycle length. We conclude that what varies with REM deprivation is the probability of the REM oscillator being turned on. When the oscillator is not “on,” the animal is in waking or slow-wave sleep. Figure 12.6 emphasizes this point.

12.3.2. Mathematical Characterization of Oscillators

A mathematical characterization of these phenomena would, thus, seem to require a REM oscillator with a variable probability of being “on” and with a limit cycle organization. By a limit cycle organization one means that

[23] Where no citation is given, the data in this section are taken from Lydic *et al.* (1987a–b).

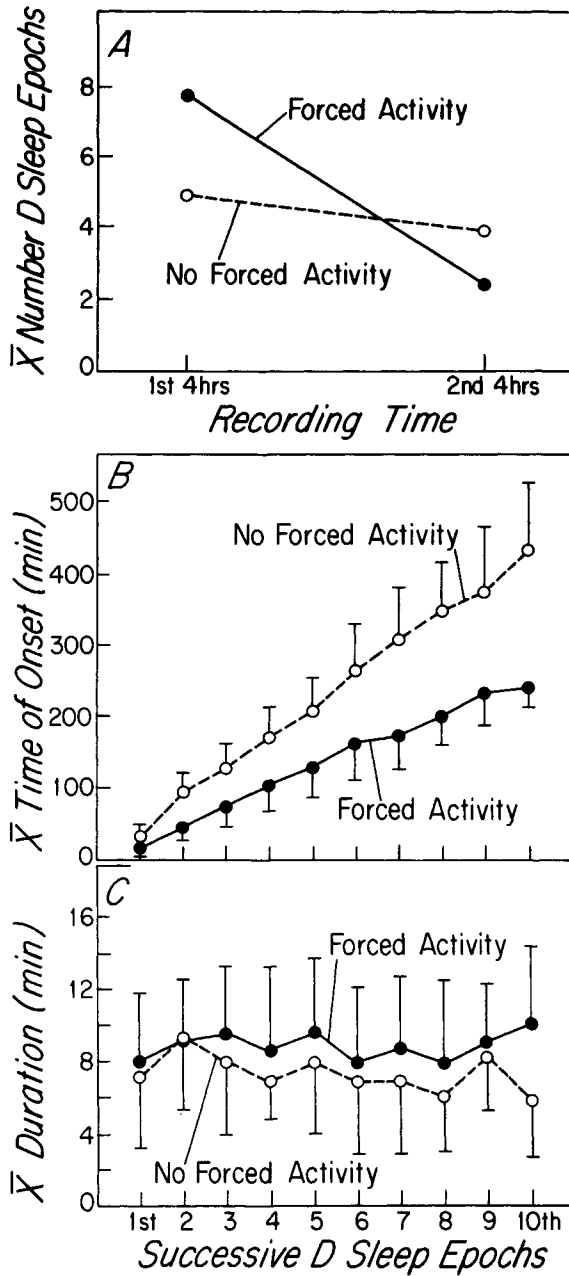


Figure 12.4. Forced activity and REM sleep deprivation effects. The average number (A), time of onset (B), and duration (C) of 265 REM sleep episodes recorded following forced and no forced locomotor activity in the cat. Part A shows that forced activity doubled the number of REM sleep episodes in the first 4 h of the subsequent recording sessions, but this effect was not seen in the second 4 h of recording. Part B summarizes the decreased latency to REM sleep onset, which followed forced activity. Frame C shows that forced activity produced no significant increase in the average duration of REM sleep. Thus, forced activity and REM sleep deprivation act primarily to increase the number of REM sleep episodes. Adapted from Lydic *et al.* (1987a).

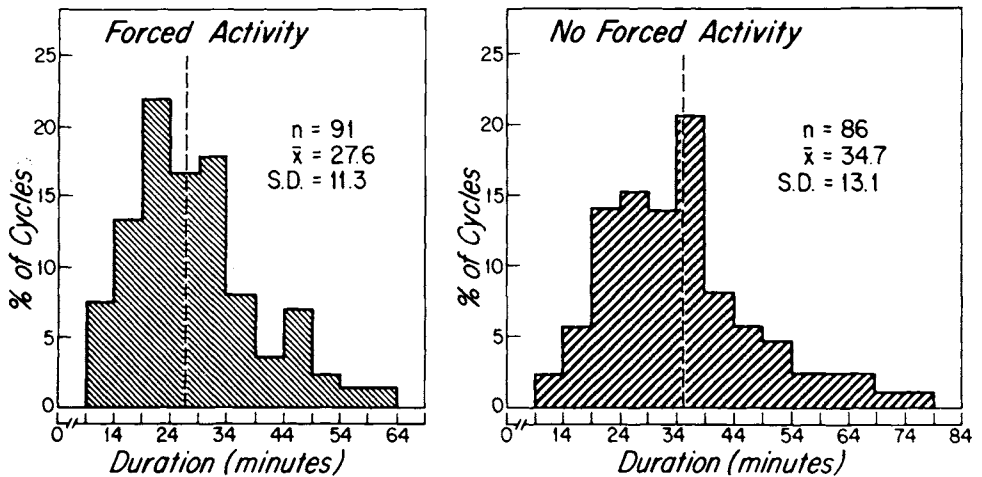


Figure 12.5. Constancy of REM sleep cycle preferred duration. Frequency histograms of sleep cycle duration in the cat following forced activity (left panel) and no forced activity (right panel). Note that forced activity had the effect of reducing the number of long duration sleep cycles and increasing the number of shorter duration cycles, with a stronger tendency to cluster around the modal sleep cycle duration in the cat, 22 min. Legend: n = number of sleep cycles (sleep cycle = time from end of one REM sleep episode to the end of the next), \bar{x} = mean (broken vertical lines), S.D. = standard deviation. Adapted from Lydic *et al.* (1987a).

the oscillator system, once turned on, tends to follow a relatively fixed time course of oscillatory activity after the first cycle or so, no matter what the state of the organism when the oscillator is turned on.

In describing the organization of the oscillator, there are two main classes of systems to consider. The first are those depending on timing mechanisms intrinsic to individual cells, often referred to as “pacemakers.” There is growing evidence that the suprachiasmatic circadian oscillator system has this kind of structure, although the pacemaker neurons themselves are sensitive to Zeitgeber (time-resetting) inputs from outside the suprachiasmatic nucleus and also are linked to, and perhaps modulate, each other. In contrast, there is no positive evidence that any such pacemaker neurons are responsible for the REM cycle. Currently, the most popular class of models, and, indeed, the only class of models for the generation of the REM cycle, are those depending on the interaction of neuronal populations.

We next present a simple model of REM control based on the simple LV model adapted to interaction of neuronal populations, together with a broad sketch of the relevant neurophysiology, and link these to data presented above and in previous chapters. We then discuss a more realistic and complex model—the limit cycle model (Section 12.5). The next two sections of this

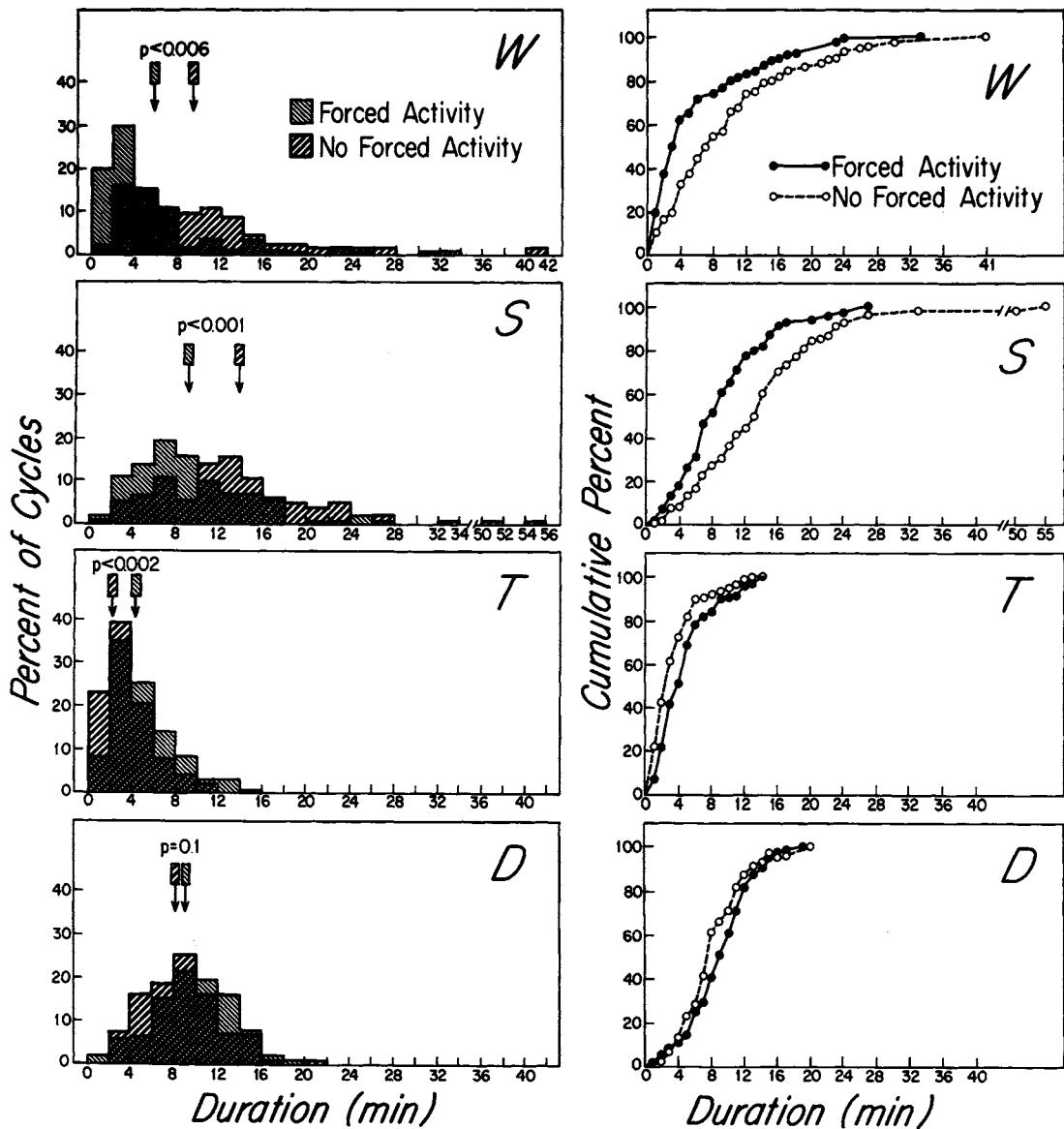


Figure 12.6. Histograms describing the effect of forced activity on the temporal organization of the four behavioral states comprising the sleep cycle in the cat: wakefulness (W), synchronized (S) sleep, transition (T), and REM sleep (abbreviated D for desynchronized sleep). The left panels are histograms of the durations of the individual states within each sleep cycle, while the right panels present the same data in cumulative histogram form. At a glance, the panels show that forced activity decreases W and S ($p < 0.01$) by decreasing the number of long duration episodes; note also the shift in the means. The transition period (T) duration is reduced slightly but significantly by forced activity. In

contrast, REM sleep (abbreviated as D) duration is not significantly affected. These data thus support the concept of a REM oscillator with a propensity to generate a relatively constant amount of REM sleep per sleep cycle. REM sleep percentage is increased by increasing the number of REM sleep episodes, but the duration of the episodes is not greatly altered. A simple summary is that, following REM sleep deprivation, the REM oscillator remains "on" for more time; with less REM sleep pressure, the oscillator is "off" and this is reflected in more waking and non-REM sleep. (Kolmogorov-Smirnov nonparametric statistical tests were used.) Adapted from Lydic *et al.* (1987a).

chapter (12.6 and 12.7) present details of the postulates and of construction of the two models.

12.4. The Reciprocal Interaction Model and the Lotka–Volterra Equations

This mathematical model was first proposed in 1975, and used the simple LV equations to describe interactions of populations of neurons postulated to be involved in REM cycle production [1]. Although this model does not have the limit cycle feature, the basic features of the interaction of neuronal populations and the dynamics are the same as the more later limit cycle REM models [24]. The first section of this chapter has given a nonmathematical description of the dynamics of the simpler LV equations.

[24] McCarley and Massaquoi (1986a, b, 1992); Massaquoi and McCarley (1992).

12.4.1. Postulated Steps in Production of a REM Sleep Episode

To aid in intuitive understanding of the model, we here summarize in words the model's postulate of steps in production of a REM sleep episode and the repetition of this REM cycle, and will later introduce the mathematical equations. We point out the approximate time points of these steps by noting the percentage of cycle completed values on the time-averages of neuronal activity shown in Fig. 12.7. (Zero indicates the beginning of a REM cycle with the end of the previous REM period, and the subsequent figures indicate the percentage of the cycle completed, with REM onset occurring at about 75% of cycle completed.) These data are taken from recordings of REM-on neurons in the PRF and REM-off neurons in the LC. In addition to Fig. 12.7, Fig. 12.2 (the structural model) should also be referred to when reading this account of the dynamics of the REM sleep cycle.

1. The slowing and near-cessation of firing of REM-off neurons disinhibit the population of REM-on neurons (0–25% of cycle duration).

2. As a result of this disinhibition, the population of REM-on neurons becomes increasingly active and this activity augments because of: (a) the excitatory interconnections in this REM-on population (LDT/PPT–reticular interaction) and (b) disinhibition of reticular effector neurons from reticular GABAergic neurons, which are inhibited by increasing LDT/PPT activity. Note also that Fig. 12.2 shows that REM-off neurons may also be inhibited by

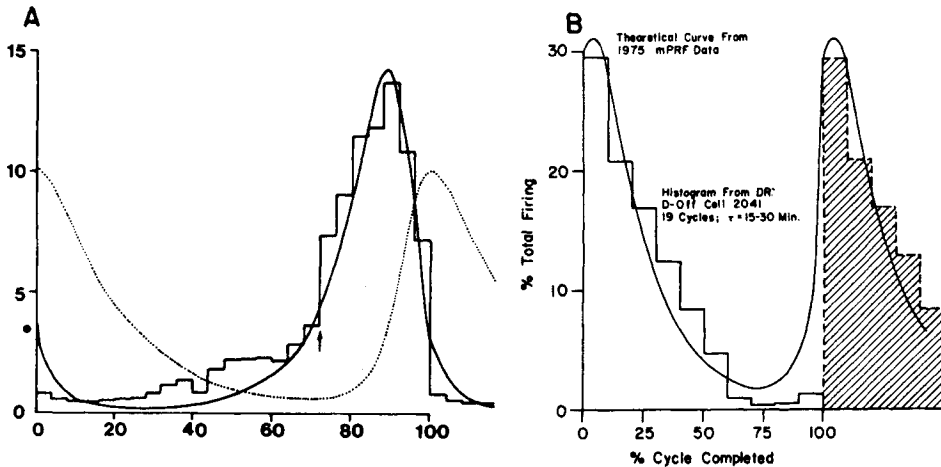


Figure 12.7. A. Match of the time course of averaged medial pontine reticular formation neuronal activity (data in bins) to time course of activity from model simulation using the simple Lotka–Volterra (LV) equations (equations 1 and 2). For Model: solid line = X population; broken line = Y population. Ordinate = discharge activity in spikes/s. Point 0 on the graph represents the end of one REM episode (the start of the cycle) and 100 represents the end of the next REM episode (cycle end, 100% complete). The arrow points to the start of the bin with the most probable time of REM sleep onset. Initial conditions and the values of model constants were set to match the observed modulation during the sleep cycle. Adapted from McCarley and Hobson (1975b). B. Theoretical curve (smooth line) for the Y population derived from data for the X population described in part A compared with averaged neuronal activity data from 10 cycles of a dorsal raphe neuron (Adapted from Lydic *et al.*, 1987a; tau = sleep cycle duration). Abscissa as in A. Averages from REM-off locus coeruleus neurons showed approximately the same goodness of fit (McCarley and Hobson, 1975b). We note that the ratio of a to c reflects the fundamental nature of X–Y interaction (see text); this ratio in the new limit cycle model presented here is approximately the same as that of the 1975 simple LV model.

GABAergic inputs from REM-on neurons. This augmenting of REM-on population activity continues until the REM episode is produced (25–75% of cycle duration).

3. The REM-off population becomes active as a result of excitatory input from the REM-on population (75–100% of cycle duration). When the REM-off population becomes sufficiently active, the REM episode is terminated because of the REM-off neurons' inhibition of the REM-on population.

4. The population of REM-off neurons is postulated to become less active because of inhibitory feedback, and this leads to step 1 and a resumption of the cycle. The exact circuitry responsible for REM-off neurons turning off over the sleep cycle remains undefined, and is one of the principal current questions in REM sleep control. The sketch in Fig. 12.2 indicates that REM-off neuronal autoinhibition might not only occur through monoaminergic autoreceptors (the original postulate of the reciprocal interaction model) but also through GABAergic mechanisms, with REM-off neuronal activity producing GABAergic inhibition in the initial stage of the sleep cycle (0–25% in

Fig. 12.7) either through local interneurons and/or distant sources.

The more mathematically inclined reader will also have noticed that the oscillatory system, as described, continues to oscillate indefinitely. Below, we will give a more detailed account of the model and describe the turning on and off of the oscillator through interaction with circadian and other systems.

12.4.2. Simple Lotka–Volterra Equations

The interaction situation described nonmathematically in Section 12.2 and in the structural model of Fig. 12.1 corresponds to the structural model for the most simple of stable two-population oscillatory systems, namely the LV equations [25]. These were initially used in population biology to describe the interaction of a predator population (corresponding to the REM-suppressive REM-off neurons) with a prey population (corresponding to the REM-promoting REM-on neurons).

[25] Lotka (1956);
Volterra (1931).

For the convenience of the reader, the simple LV equations, with X representing REM-on and Y REM-off activity, are repeated here. These and the constants in the structural model were first presented in Fig. 12.1.

$$X'(t) = aX - bXY \quad (1)$$

$$Y'(t) = -cY + dXY \quad (2)$$

These simple LV equations (equations 1 and 2) yield time courses of activity that mimic the time course of REM-on neuronal discharge and also of REM-off discharge, as illustrated in Fig. 12.7. The data fitting for the cat neuronal data to the simple LV model were done by setting the strengths of the equations' constants to match the observed time course of rise of REM-on (mPRF) neuronal activity at the approach of REM sleep [26]. We will not describe the "time domain" behavior of the system further, but call attention to Fig. 12.8A, which describes the "phase plane" of the system and will be useful in understanding the differences between the simple LV model and the limit cycle model. A *phase plane graph* (refer to Fig. 12.8A) is constructed by plotting the level of activity of one component (X , REM-on discharge activity) vs that of the other (Y , REM-off discharge activity) at successive points in time. In particular, the simple LV solutions appear as families of simple oval orbits (paths) in the phase plane; Fig. 12.8 provides a schematic illustration of three such paths (P1,

[26] See description in McCarley and Hobson (1975b); see also Hobson *et al.* (1975) for a discussion of the structural features of the model.

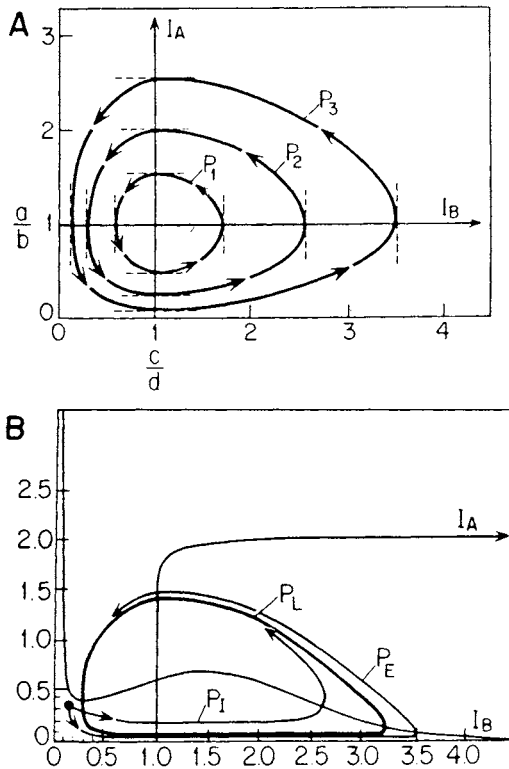


Figure 12.8. Schematic of phase plane paths for simple Lotka-Volterra (LV) system (*part A*) and for limit cycle system with circadian modulation (*part B*). Part A. The simple LV solutions appear as families of simple oval orbits (paths) in the phase plane. A phase plane graph is constructed by plotting the level of activity of one component (X axis, REM-on discharge activity) vs that of the other (Y axis, REM-off discharge activity) at successive points in time. Three such paths (P_1 , P_2 , P_3) correspond to separate solutions generated by choosing different initial conditions but having the same values for a , b , c , and d . P_3 is most similar to the solution used in the 1975 model (McCarley and Hobson, 1975b); note that this, like any stable oscillation of the X and Y population, is represented by a single closed orbit which is traversed repeatedly over time in a counterclockwise direction (note direction of arrows). All orbits have zero slope on the isocline, I_A , while all orbits have infinite slope on the other isocline, I_B . See also text sections 12.4 and 12.6. Part B is the phase plane graph of the limit cycle system with circadian modulation. Here, the system points (X-Y values) cluster in the upper left hand corner during waking [high Y values (REM-off neurons), low X values (REM-on neurons)]. At sleep onset, there is falling Y activity and rising X activity and thus the graph shows a downward and rightward drift and eventually begins to orbit. (For the feline model without circadian variation this time course of decline is postulated to be relatively constant, with the probability of the system being allowed to oscillate being, in part, a function of whether REM deprivation had occurred previously.) In a limit cycle system, all orbits by definition eventually converge to the limit cycle and the graph of later cycles is insensitive to the details of the trajectory of the initial transition into sleep. The limit cycle model solutions are families of spirals, which all converge to a common, unique final oval, termed the limit cycle (P_L in the figure, thick line). This same limit cycle is approached regardless of whether the initial approach is exterior (P_E) or interior (P_I). The critical feature of this human sleep model is that an interior approach (P_I) results from a slow decline in Y (see closed circle and upper arrow in lower left corner of graph), and occurs near a temperature maximum (a measure of the activity of the "deep" circadian oscillator); this results in a quick onset, short duration, low amplitude first REM period. An exterior approach (P_E) results, in contrast, from a rapid decline in Y (same closed circle and lower arrow) and occurs near a temperature minimum; this results in a slow onset, long duration, high amplitude first REM period. Sections 12.5 and 12.7 describe other details of the system including the altered shape of the isoclines, I_A and I_B . Whether the approach is exterior or interior to the limit cycle depends entirely on the starting conditions and not on any alteration of a property of the oscillator. Adapted from McCarley and Massaquoi (1986a).

P2, P3), which correspond to separate solutions generated by choosing different initial conditions but having the same values for a , b , c , and d . P3 is most similar to the solution used in the 1975 model [1]; note that, like any stable oscillation of the X and Y population, it is represented by a single closed orbit that is traversed repeatedly over time in a counterclockwise direction (note direction of arrows). All orbits have zero slope on the isocline, I_A , while all orbits have infinite slope on the other isocline, I_B . Section 12.6 provides more details of system behavior in terms of the phase plane.

12.4.3. Limitations of the Simple Lotka–Volterra System

The fundamental difficulty with the simple LV equation system was that it displayed only neutral stability. That is, the system's long-term behavior was determined entirely by its initial conditions. This would imply that, in order to generate the regular pattern of sleep cycles, the REM oscillator would have to be set into motion each night with a highly reproducible precision alien to physiological systems. Furthermore, a REM oscillator governed by simple LV dynamics would be unreasonably sensitive to any perturbation such as external stimuli so that even a momentary alteration of the components of the oscillator would disturb the period and other properties of REM sleep system forever (or until specifically reset). These properties are clearly not typical of physiological oscillators; these must be able to maintain stability in the face of continuously changing internal and external influences. An additional complication of the neutral stability condition was the difficulty in modeling circadian influences, which would have necessitated postulating the existence of unreasonable phase resetting mechanisms.

Central to the LV system's neutral stability problem was that there was no inherent limit on the frequency of neuronal discharge and even swings to infinite frequency were possible. A reasonable first step in modeling was, thus, to add factors to the equation, which effectively produced realistic physiological constraints on neuronal firing rates. In addition, factors were added that better described neuronal firing characteristics at low discharge rates. These changes led to a model, which displayed limit cycle stability, and the new model will be hereafter described as the limit cycle model.

12.5.1. Summary of Changes from the Simple
Lotka–Volterra Model

The limit cycle feature of the new model resulted from the addition of the following postulates to the simple LV equations: (1) Constraints on maximal neuronal firing rates in both REM-on (X) and REM-off (Y) populations; further, the strength of inhibition of the REM-off population on the REM-on population is limited when the REM-on population activity is at low levels. (2) The term for growth rate of the REM-on population resulting from excitatory feedback is now a function of the current discharge rate (X level), and is less for lower values of X whereas it was constant in the simple LV model.

The other major category of change in the model was the addition of circadian modulation—a point not addressed in the original model. This feature is primarily of use for modeling human REM sleep (and other animals with a strong circadian REM modulation); it is not utilized in the feline version because cat circadian modulation is weak, especially that observed in the usual laboratory recording session. (Circadian REM modulation in cats is relatively minimal, and consists of a tendency to have more REM at dawn and dusk, a “crepuscular” circadian REM organization.) In the limit cycle model for humans, all circadian sleep fluctuation is modeled by: (a) circadian variation in the way the system begins oscillation, modeled by variation in the strength of excitatory influences on the REM-off (Y) population at sleep onset and consequent alteration of the time course of decline of this population at sleep onset. This “start-up” variation accounts for most of the observed circadian changes in REM sleep percentage. (b) A small continuous circadian modulation (accounting for about $\pm 5\%$ variation in REM parameters) that results from changing the constant “ d ” in the simple LV equations to a sinusoidally modulated circadian variable, $d(\text{circadian time phase}) = d(\text{circ})$. The rationale for each of these changes is discussed in detail in Section 12.7 of this chapter. We also note that Chapter 13 discusses orexin as one of the possible circadian controlling factors for REM sleep. The equations for the limit cycle model, which incorporate these changes, are:

$$X'(t) = a(X) * X * S_1(X) - b(X) * X * Y \quad (3)$$

$$Y'(t) = -c * Y + d(\text{circ}) * X * Y * S_2(Y) \quad (4)$$

where $*$ = multiplication.

X = REM-off neuronal activity; Y = REM-on neuronal activity.

S_1 and S_2 are saturation functions constraining X and Y .

$a(X)$ = X growth rate, smaller with smaller X .

$b(X)$ = limitation on inhibitability of X by Y for low X values.

$d(\text{circ}) = d(\text{circadian time}) = \text{circadian variation in amplitude of } d$.

The graphs and discussion of the construction of S_1 , S_2 , $a(X)$, $b(X)$, and $d(\text{circ})$ are presented in Section 12.7 of this chapter.

12.5.2. Modeling Events at Sleep Onset, Human Sleep Patterns, and Circadian Variation

12.5.2.1. Events at the Onset of Sleep

Neuronal recordings in cats indicate that during waking, the activity of the REM-off population is generally elevated ($1 \leq Y \leq 2$, cf. Fig. 12.5) and intracellular recordings indicate population activity and excitability of the REM-on (X) population is low, with X typically < 0.2 , although, as discussed below, subsets of REM-on neurons may be phasically active during waking. Thus, in the phase plane graph (Fig. 12.8B graphs the phase plane), the system points (X - Y values) cluster in the upper left hand corner during waking (high Y values, low X values). At sleep onset, there is falling Y activity and rising X activity and thus the graph shows a downward and rightward drift and eventually begins to orbit. For the feline model without circadian variation, this time course of decline is postulated to be relatively constant, with the probability of the system being allowed to oscillate being, in part, a function of whether REM deprivation had occurred previously. In a limit cycle system, all orbits, by definition, eventually converge to the limit cycle and the graph of later cycles is insensitive to the details of the trajectory of the initial transition into sleep, providing the necessary stability in the feline cycle.

12.5.2.2. Modeling Human Sleep Patterns

However, the shape of the first cycle is critically dependent on the precise trajectory taken at sleep onset and it is this variation that is important for modeling the human sleep pattern. Although no specific physiological mechanism has yet been clearly identified as maintaining the system in the upper left portion of the phase plane in waking, we suggest a simple, plausible explanation: that

tonic excitatory input to REM-off neurons maintains the system at high Y values during waking, and that one important component of the strength of this input may be circadian influences arising from the hypothalamus. Computer simulations show that such an input suppresses oscillations by keeping Y high and thus X activity low. In the limit cycle model applied to adult human sleep, the circadian waxing and waning of this input is an important factor turning the REM sleep oscillator on and off. We add that we do not wish to suggest that other physiological mechanisms having the equivalent mathematical effect are ruled out, but only that this currently appears the most plausible postulate.

In summary, for the human sleep model, the difference in the time course of decline of Y (as controlled by excitation withdrawal) at sleep onset determines whether the limit cycle is entered from the interior (slow time course of decline) or from exterior (rapid time course of decline), and, thus, this parameter is by far the most critical one for determining changes in REM sleep values, since it is the first REM cycle that varies the most from all others in human sleep.

12.5.2.3. Circadian Variation in the REM Cycle

The experimentally observed circadian phase sensitivity of the initial sleep cycle parameters (cycle period duration, REM intensity, REM latency, and REM duration) are simply modeled by varying the time course of withdrawal of excitatory influences on the Y population with circadian phase: withdrawal is more rapid near a temperature minimum and slower at a temperature maximum.

Figure 12.8B graphically illustrates the concept of the limit cycle and external and internal entry points. The limit cycle model solutions are families of spirals that all converge to a common, unique final oval, termed the limit cycle (P_L in the figure). This same limit cycle is approached regardless of whether the initial approach is exterior (P_E) or interior (P_I). The critical feature of this human sleep model is that an interior approach (P_I) results from a slow decline in Y , and occurs near a temperature maximum (a measure of the activity of the "deep" circadian oscillator); this results in a quick-onset, short-duration, low-amplitude first REM period. An exterior approach (P_E) results, in contrast, from a rapid decline in Y and occurs near a temperature minimum; this results in a slow-onset, long-duration, high-amplitude first REM period. Section 12.7 describes other details of the system including the altered shape of the isoclines, I_A and I_B . Whether the approach is exterior or interior to the limit

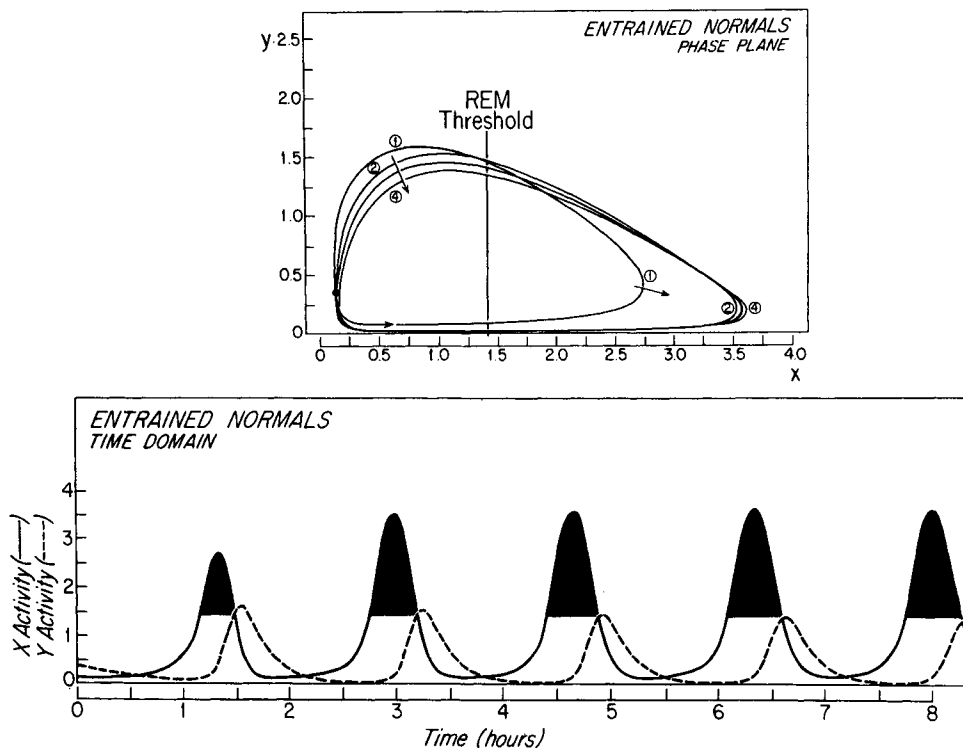


Figure 12.9. Model simulation of night's course of REM sleep in entrained normal humans. The top part is the Phase Plane and the bottom part the Time Domain representation of this data. In the bottom panel, the solid portions of the X graph show those portions of the night with REM sleep and the height of these peaks indicates the intensity of the REM sleep episode. Note the short-duration, lesser intensity first REM episode with subsequent variations being slight. The activity of the Y (REM inhibitory) population is indicated by the dotted line. In the phase plane representation in the top panel, each point on the graph represents the X-Y values at a particular time. The dot represents the starting point and the interior curve with the arrow shows the first REM sleep episode values, with this curve being interior to the limit cycle values obtained in subsequent REM cycles, labeled 2, 3, 4 in the order of their occurrence (for simplicity, sleep cycle 5 has not been graphed in the phase plane). The smaller variations in sleep cycles 2 through 4 are due to circadian modulation. Adapted from McCarley and Massaquoi (1986a).

cycle depends entirely on the starting conditions and not on any alteration of a property of the oscillator.

In this model, when sleep is begun at the usual point on the circadian temperature cycle, soon after the occurrence of a temperature maximum, the activity trajectories illustrated in Fig. 12.9 for the phase plane and time domain are produced. This starting point produces an interior entry into the limit cycle and a long-latency, short-duration first REM period. In contrast, when sleep is begun near a temperature minimum, there is an exterior entry into the limit cycle and a short latency, long-duration first REM period (Fig. 12.10).

The fit between the model and data from actual human sleep is good, both for percentage of REM in thirds

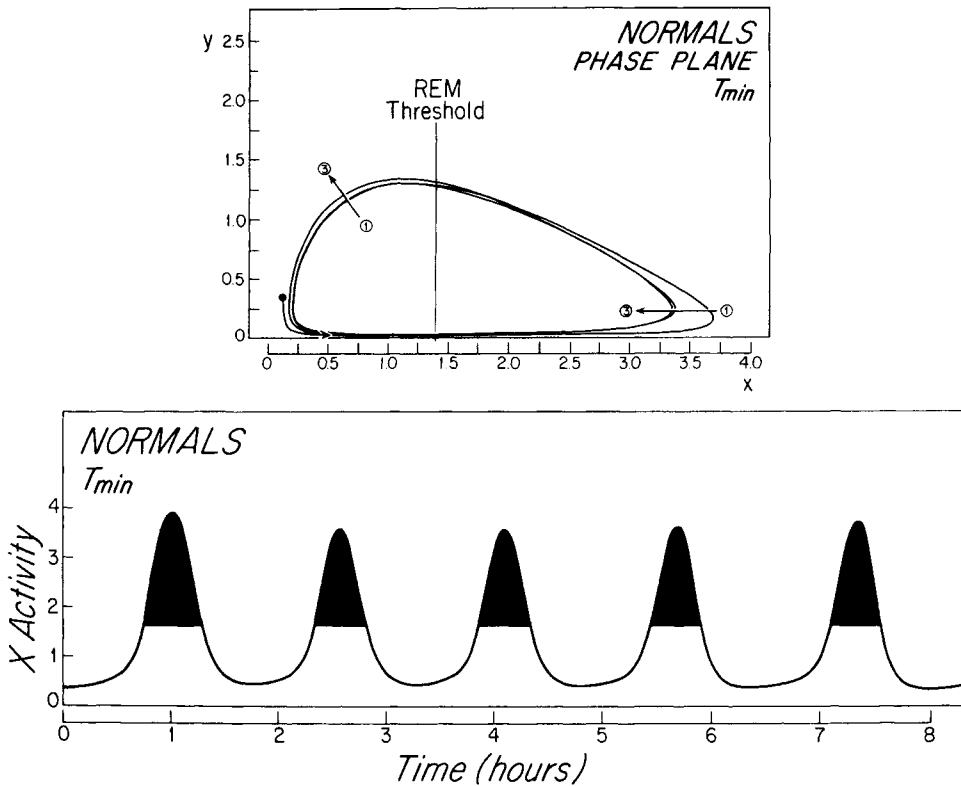


Figure 12.10. Phase Plane (top) and Time Domain (bottom) representation of model results for sleep begun near a temperature minimum (Circadian Phase = 4.72 radians, 270 degrees). Note that, in contrast to Fig. 12.8, the phase plane graph shows an entry into the limit cycle from a point *exterior* to the cycle; arrows indicate the direction of change successive phase plane trajectories for cycles 1, 2, and 3. As can be seen, this is associated with a shorter-latency, longer duration, and higher intensity first REM episode than does the interior entry that occurs near a temperature maximum (cf. Fig. 12.9, Phase Plane). Adapted from McCarley and Massaquoi (1986a).

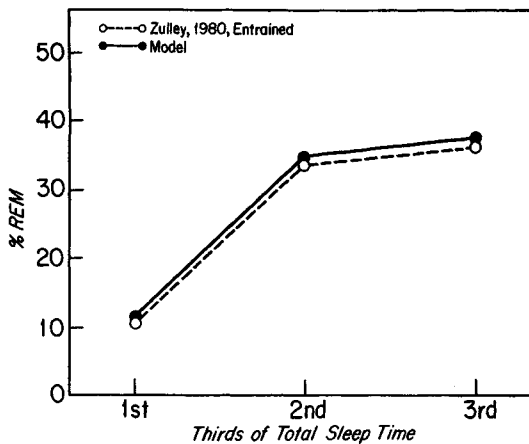


Figure 12.11. Empirical data (Zulley, 1980) and Model indicate a low REM percentage in first third of the night and a tendency for the last third of the night to show more REM than the middle portion. Note the near-exact fit of model and data. Adapted from McCarley and Massaquoi (1986a).

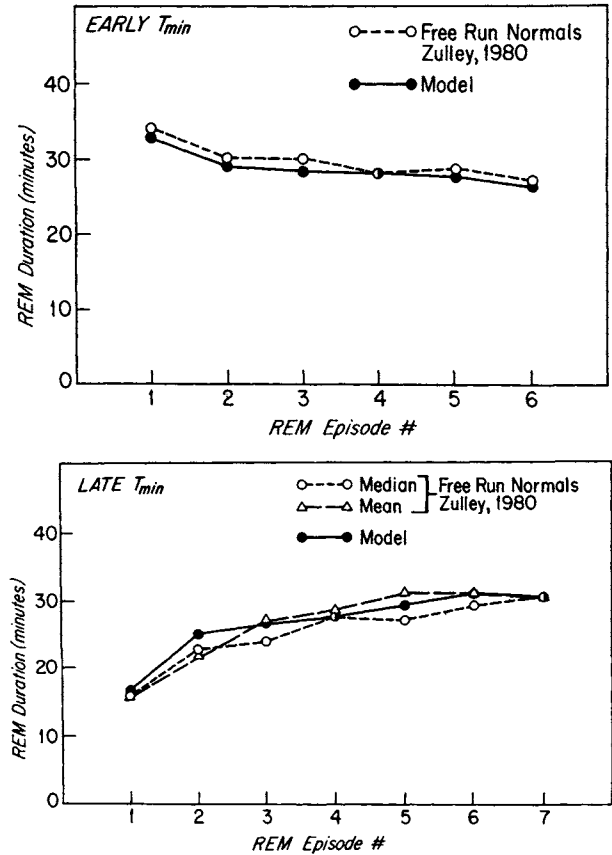


Figure 12.12. (Top) Match of Model and Zulley's data (median = open circle) for REM duration in sleep begun at temperature minimum (Circadian Phase = 4.72 radians) in free-run normals. Note excellent fit in general and, in particular, that the first to second REM episode change is the largest and the subsequent gradual duration decrease in both model and data REM duration. (Bottom) Match of Model and Zulley's data (median = circle, mean = triangle; both included because of variation in this data set) for REM duration in sleep begun near temperature maximum in free-run normals (Zulley labels these data as "late temperature minimum"). Note close approximation of model prediction, in particular: the first to second REM episode increase is the largest and there is a subsequent gradual duration increase in both model and data. Adapted from McCarley and Massaquoi (1986a).

of the night in entrained normals (Fig. 12.11) and for a match between duration of successive REM episodes in free-run normal subjects when sleep is begun at a temperature minimum or at a temperature maximum (Fig. 12.12).

It perhaps does not need to be emphasized that much additional work will be needed before this model can be said to be solidly grounded on empirical data. Our reading is, however, that the currently available behavioral, pharmacological, and cellular neurophysiological data indicate the utility of such a model in terms of aiding conceptualization and for suggesting experiments. For example, the concept of interacting REM-on and REM-off populations has been used by Sakai and also has been useful in

[27] Sakai (1985a).

modeling REM alterations in depression, as described below in Section 12.8 [27].

12.6. Details of Simple Lotka–Volterra Model

This section provides a more detailed account of the concepts and mathematics than presented in the earlier overview.

12.6.1. Significance of the Terms in the Equations

This initial formulation of the sleep cycle control model employed a simple system of first order nonlinear differential equations known as the LV system after the two mathematical biologists who first used it to model the interaction of predator and prey species. As REM-on neurons excite themselves via recurrent collaterals, they behave mathematically as an autonomous, self-replicating prey population. REM-off neurons, conversely, inhibit the growth in activity of REM-on neurons while their own activity dies off in the absence of REM-on input. Thus, REM-off neurons behave as a predatory population. The LV system is:

$$X'(t) = aX - bXY \quad Y'(t) = -cY + dXY$$

where X represents the aggregate firing rate of REM-on neurons and Y represents the aggregate firing rate of REM-off neurons.

The reciprocal interaction between the two populations is characterized by the LV system. The different terms in the system represent the contribution of each type of synapse in the model (Figs. 12.5 and 12.12) to overall system behavior.

First term: REM-on neurons' response to self-excitation: $X'(t) = aX$, which alone would yield unbridled exponential growth:

$$X(t) = e^{+at} \text{ with growth constant } a.$$

Second term: REM-on neurons' response to REM-off neurons' inhibition: $Y'(t) = -(bY)X$, which alone would yield exponential decay of X activity with a rate dependent on Y activity and b :

$$X(t) = e^{-(by)t}$$

Third term: REM-off neuronal response to self inhibition: $Y'(t) = -cY$, which alone would yield an exponential decay in Y activity with decay constant c :

$$Y(t) = e^{-ct}$$

Fourth term: REM-off response to REM-on excitation: $Y'(t) = (dX)Y$, which alone would yield exponential growth of REM-off activity with a growth rate dX :

$$Y(t) = e^{+(dX)t}$$

12.6.2. Phase Plane Representation

In the phase plane representation, any stable oscillation of X and Y populations is represented graphically as a single closed orbit that is traversed repeatedly over time in a counterclockwise direction. In particular, the simple LV solutions appear as families of simple oval orbits (paths) in the phase plane; Fig. 12.8A provides a schematic illustration of three such paths (P1, P2, P3) that correspond to separate solutions generated by choosing different initial conditions but having the same values for a , b , c , and d . P3 is most similar to the solution used in the 1975 model [1].

Line I_A in Fig. 12.8A represents the vertically oriented isocline, the set of loci where all paths must have zero slope (hashed lines). Line I_B is the horizontally oriented isocline where all crossing paths have infinite slope. The isocline equations are: $I_A: X = c/d$ and $I_B: Y = a/b$ where a , b , c , and d are the LV parameters of equations 1 and 2. Since in this figure $a = b = 2c = 2d$, the isoclines are located at $X = 1$ and $Y = 1$. The values c/d and a/b are termed the X and Y equilibrium values because they represent the average X and Y values over time and represent the coordinates for the system center, where no oscillation occurs.

Fig. 12.8B and the limit cycle system are discussed in detail below. For here we note that the limit cycle model solutions are families of spirals, which all converge to a common, unique final oval, termed the limit cycle (P_L in the figure). This same limit cycle is approached regardless of whether the initial approach is exterior (P_E) or interior (P_I); the presence of such a limiting oval graphically demonstrates the stability of the oscillatory system. Whether the approach is exterior or interior to the limit cycle depends entirely on the starting conditions and not on any alteration of a property of the oscillator.

This section discusses the mathematical form and the rationale for the changes in the simple LV system that lead to the limit cycle model. We will discuss the changes in approximate order of occurrence in the equations. For convenience of reference, we here list the limit cycle model equations:

$$X'(t) = a(X) * X * S_1(X) - b(X) * X * Y \quad (3)$$

$$Y'(t) = -c * Y + d(\text{circ}) * X * Y * S_2(Y) \quad (4)$$

12.7.1. Use of $a(X)$

$a(X)$ = the REM-on autoexcitation growth function that has X dependence and replaces the constant “ a ” in the simple LV system. This term makes the effectiveness of the REM-on to REM-on neuron positive feedback a function of REM-on activity level. In the limit cycle model, the term for the X population feedback is changed from the constant “ a ” in the simple LV equations into a function dependent on X , with a lesser growth rate at lower values of X . This is physiologically analogous to an assumption of a “kindling effect” since, as the mean activity level grows so does the growth term, a (autoexcitability) with near

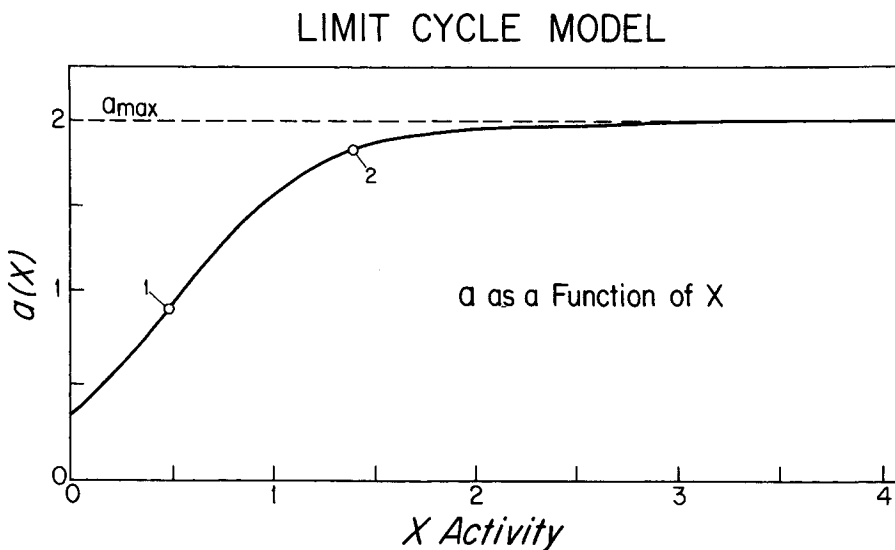


Figure 12.13. Shape of logistic curve describing the alteration in “ a ” with changes in the level of activity of the X population. See text Section 12.7.1 for further description. Adapted from McCarley and Massaquoi (1986a).

maximal levels of $a(X)$ being reached at the threshold for REM onset (see graph in Fig. 12.13). Mathematically, making “ a ” a function of X in this manner destabilizes the system in the center region. In the phase plane representation, it accounts for the system’s spiraling outward toward the limit cycle when initiated in the region interior to the limit cycle (Fig. 12.8B, P_1).

The term $a(X)$ has the form $a_{\max}L(X)$ where $L(X)$ is a logistic (sigmoid) function that slopes upward from zero to 1 with peak slope occurring at $X = 0.5$ (marked by circle 1 on graph in Fig. 12.13) (the equation of the logistic function is given below in 12.7.3). a_{\max} is taken to be equal to 2, such that for large X , $a = a_{\max} = 2$ —the same value used in the earlier nonlimit cycle model. Note that at REM threshold (circle 2), $a(X)$ is nearly at its maximum.

This central destabilization can be heuristically understood as follows: as REM-on activity becomes suppressed by REM-off activity, it declines to low levels where it remains for a duration slightly longer than that of the standard LV equations. This further removes excitation from REM-off neurons and allows REM-off firing intensity to diminish to lower levels. This, in turn, facilitates a much more explosive growth of REM-on firing rate on the next cycle. Without this reduction in REM-on excitability at low levels and the consequent additional decrease in REM-off activity, REM-off activity would remain relatively high and constrain REM-on firing rate to progressively less rapid growth on successive cycles and ultimately oscillations would cease entirely. In the phase plane representation, this would be seen as a progressive spiral to the center of the phase plane to a single stable equilibrium point. Thus, reduction of the X (REM-on) firing rate growth term at low values of X is one simple mathematical postulate that leads to the repeated oscillations found physiologically.

It must be acknowledged that, at present, while there is general evidence for increased REM-on excitability and rate of REM-on membrane potential change for a given stimulus input in REM as compared with waking [28], there are currently no specific empirical data indicating the shape of the excitability curve or suggesting the physiological mechanisms of excitability alteration.

[28] Ito and McCarley (1984).

12.7.2. Limitations on Growth of Firing Rates, $S_1(X)$, $S_2(Y)$

An unrealistic feature of the simple LV model was the absence of limitation on neuronal firing rates; when the system was perturbed, firing rates could become arbitrarily and thus unreasonably high, even infinite. In the new

[29] Eccles (1964).

model, we have included constraining functions on firing rates of neurons; the shape of these constraining curves is sigmoid, in accord with data from a number of neuronal pools suggesting this to be the general form of frequency limitation [29]. As discussed below, physiological data dictated that the REM-off population curve have a sharper cut-off than that for the REM-on population. Below, we also list the sample values for neuronal discharge activity for various components of the REM-on and REM-off populations; the values used for X and Y discharge rate activity in the graph ordinates are scaled, relative values since it would be too cumbersome to label all graphs with absolute firing rates for each of the subpopulations. We further note that, technically, the sigmoidal functions act to constrain X and Y levels by sharply attenuating the rate of neuronal firing rate growth at high firing levels of X or Y , but do not directly impose a boundary on firing levels.

[30] Hobson *et al.* (1974a);
McCarley (1980b).

$S_1(X)$ = sigmoidal saturation function (Fig. 12.14.), which slopes from 1 to 0 as X increases, thereby effectively constraining the growth of REM-on neurons to finite levels. A logistic function is used to generate this sigmoid curve (circle in Fig. 12.14 indicates point of maximum slope). The particular parameters of the X population curve were selected to produce a curve consistent with extensive data indicating the reticular population is heterogeneous with respect to both maximal firing rates and mean rates [30]. The slow rate of descent of the function reflects the heterogeneity of the X population, that is, some reticular units are rate-limited at relatively low rates and others at relatively high discharge rates. It will be noted that we have placed the cut-off value close to maximal REM discharge rate values; we have done this because extracellular recordings during carbachol stimulation of reticular areas suggest very little in the way of additional

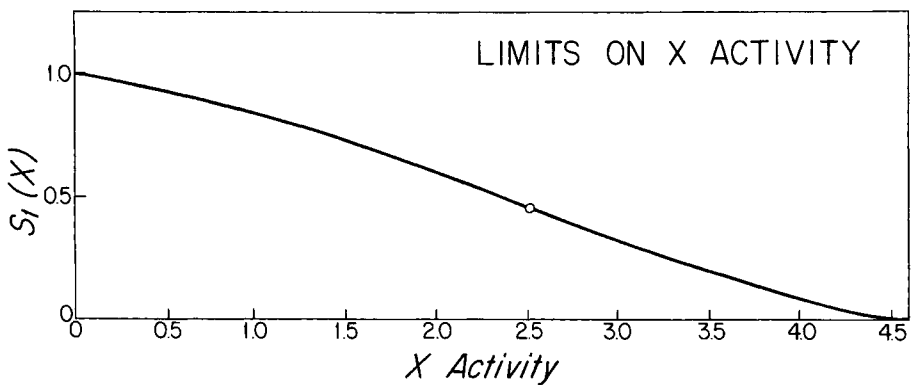


Figure 12.14. Shape of logistic curve indicating limitation on X population maximal firing rates; note a slower cut-off than for the Y population in Fig. 12.15. Adapted from McCarley and Massaquoi (1986a).

increase of reticular activity under these conditions of probable near-maximal stimulation as compared with that in REM sleep. With respect to the ordinate values, X activity units should be thought of in terms of mean population discharge activity values, with each reticular group having a different absolute maximum, but rescaled so that the peak rate is 3.2 spikes/sec and, therefore, a mean rate of 1.0 spikes/sec. For the mPRF cell-group, the example used in this paper, maximal values are 10.8 spikes/second (s/sec) in REM and minimal values as a population are 0.231 s/sec (geometric mean values). We note that the dynamics of our system of equations are not greatly altered by changes in the details of the shape of these sigmoid functions. For example, making this saturation function begin at higher values of X simply shifts the peak of REM intensity more toward the start of the REM period.

$S_2(Y)$ = a sigmoidal saturation function, which slopes steeply from 1 to 0 as Y increases; thereby effectively limiting the growth of REM-off discharges to finite levels. A logistic function is used to generate this sigmoid. Fig. 12.15 indicates the point of maximum slope by a circle. The Y activity values in Fig. 12.15 and other figures in this paper represent scaled mean neuronal discharge rates for the entire REM-off population. For the various subgroups of REM-off neurons, sample values for the mean peak rates and, in parentheses, median peak rates are: LC population, 7.9 spikes/sec (3.4 s/s); DR neurons, 3.25 s/s (2.57 s/s); and peribrachial neurons, 4.4 s/s (4.46 s/s) [31]. Because it would be cumbersome for each graph to indicate absolute maximal firing levels for each of these populations, the ordinates of the graphs are relative (scaled) firing rates, and we refer to these

[31] Data from Hobson *et al.* (1983a).

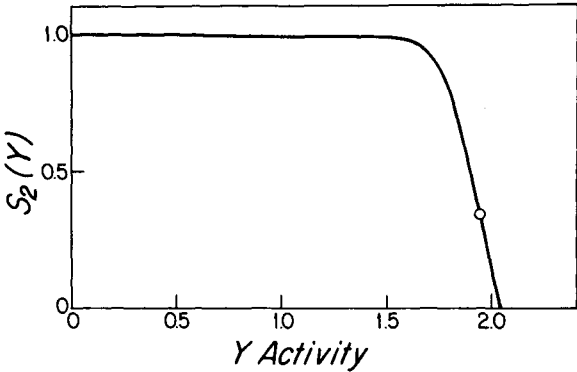


Figure 12.15. Shape of logistic curve indicating limitation on Y population maximal firing rates. Adapted from McCarley and Massaquoi (1986a).

relative firing rates as “ Y units.” (We originally selected the peak Y population activity to be about 2.5 Y units such that the mean activity value would lie at $Y = 1.0$ on order to facilitate computation of parameters.)

Extensive extracellular data have shown that the firing rate of all of these REM-off populations is severely limited at the upper end and that each population is also fairly homogeneous in terms of the firing rate of its members and the upper frequency limitation. We have accordingly used a sigmoid curve with a rapid cut-off at the upper end, and a high maximum slope value of 3.

12.7.3. Use of $b(X)$ and c

$b(X)$ = REM-on dependence on REM-off inhibitory input. Compared with the simple LV system, this is no longer a simple constant but as with the growth function $a(X)$, depends on X , the REM-on firing level.

$$b(X) = b_{\max} * \text{Logistic Function}(X)$$

where $\text{Logistic Function}(X) = 1/\{1 + \exp[-80(X - 0.11)]\}$ and $b_{\max} = 2$. The logistic function has a point of maximum slope at $X = 0.11$ and is very steeply sloped so that at X is greater than 0.2; this function is virtually identical to $b(X) = 2$. This function provides a limitation on inhibitability of X by Y population when X activity level is low, and is significantly different from the constant “ b ” in the simple LV equations only at very low levels of X (approximately < 0.2). Its addition prevents the X population activity level becoming zero at high and sustained levels of REM-off activity, as is postulated to occur during waking; in terms of system dynamics, this alteration was empirically found to be necessary to prevent degeneration of the system to the origin. Physiologically, this corresponds to a nonzero basal level of REM-on activity, which cannot be suppressed by REM-off inhibition; experimental observations confirm the presence of some reticular activity throughout all behavioral states.

$$c = 1.0. \quad (\text{As in simple LV system.})$$

12.7.4. Circadian Variation, $d(\text{circ})$ and Entry into the Limit Cycle

$d(\text{circ})$ = the REM-off dependence on REM-on firing rate is made dependent on the phase of the circadian temperature oscillator (“circadian time,” abbreviated

“circ”). Circadian variation in “ d ” is described by the following equation:

$$d(\text{circadian time}) = d(\text{circ}) = d + A * \sin(f * t) + p_o,$$

where:

d = average level, set at 0.975 in the simulations

A = amplitude of the oscillations, set at 0.125

p_o = circadian phase in radians at start of simulation

t = time since start of simulation

f = frequency of oscillation (period = 24 hr)

The introduction of continuous circadian variation of the parameter “ d ,” which describes the sensitivity of the Y population to activity in the X population allows: (1) modeling of small amounts of sleep cycle parameter variation that occur in concert with the temperature rhythm after the first sleep cycle and are especially visible in humans in extended sleep (e.g. circabidean days); (2) a more accurate modeling of the shorter latency of REM near sleep onset near temperature minima. Specifically, the amplitude of “ d ” sinusoidally covaries with temperature; $d = 1.1$ at temperature maximum and is 0.85 at temperature minimum.

The alterations of $d(\text{circ})$ over many cycles have relatively little effect on REM parameters other than those of the first REM cycle. In humans, it is the first REM cycle that is most strongly affected by circadian variation.

The experimentally observed circadian phase sensitivity of the initial sleep cycle parameters (cycle period duration, REM intensity, REM latency, and REM duration) are simply modeled by varying the time course of withdrawal of excitatory influences on the Y population with circadian phase: withdrawal is more rapid near a temperature minimum and slower at a temperature maximum.

Specifically, this is modeled by having a constant rate of decay of excitatory input to Y but having the starting strength of Y excitation at sleep onset vary sinusoidally and in phase with the circadian temperature oscillator [32]. For sleep onset at all circadian phases the rate of decay of Y excitation is 0.05 units/time unit (i.e. -0.05 firing rate units per 10.7 min, scaled) but the higher starting amplitude of excitation with sleep onset at T_{\max} leads to a longer time course of decline in Y and, therefore, to an internal approach to the limit cycle, resulting in a longer latency, shorter duration, and lesser intensity of the first REM period. In contrast, with sleep onset near T_{\min} , there is a lower starting level of Y excitation that leads to a more rapid decline in Y and, thus, to an external approach to the limit cycle. An earlier version of this limit cycle model was termed the “Karma model” to emphasize that the “fate” of the system during the first cycle depended on the way in which it was set into motion [33].

[32] Czeisler *et al.* (1980); Akerstedt and Gillberg (1981); Endo *et al.* (1981); Zulley *et al.* (1981); Kronauer *et al.* (1982).

[33] Massaquoi and McCarley (1982).

The sleep onset starting level of the residual excitation was sinusoidally covaried with a maximum of 0.69 occurring at temperature maximum and a minimum of 0.09 at temperature minimum. Thereafter, the rate of linear decay was a constant 0.05 X units/10.7 minutes (scaled) with a resultant longer time course of decay near temperature maximum and a consequent interior entry into the limit cycle.

Specifically, the sleep onset level of residual excitation, E_s , is:

$$E_s = E_m + A * \sin[(f * t) + p_o]$$

where E_m = midpoint level of residual excitation = 0.39,

A = amplitude of variation = 0.3,

f = frequency of oscillation; period fixed at 24 hr,

t = time since start of simulation = 0 at start of simulation,

p_o = circadian phase in radians at start of simulation.

It will be noticed that this construction exactly parallels that for $d(\text{circ})$ described above. This starting level of residual excitation is then decreased linearly until it becomes zero, and then remains zero throughout the simulation. Thus, until the decay of residual excitation, equation (4) becomes:

$$Y'(t) = -c * Y + d(\text{circ}) * (X + E) * Y * S_2 \quad (4')$$

where E = level of residual excitation, same units as X .

In summary, we note that it is the difference in the time course of decline of Y (as controlled by excitation withdrawal) at sleep onset, which determines whether the limit cycle is entered from the interior (slow time course of decline) or from exterior (rapid time course of decline), and, thus, this parameter is by far the most critical one for determining changes in REM sleep values, since it is the first REM cycle that varies the most from all others.

12.7.5. Phase Plane Representation of Entry into the Limit Cycle

With this model, the trajectory into sleep cycling is controlled by the time course of the decline in excitatory input to Y , residual excitation. Slow withdrawal allows the system very slowly to begin a gentle oscillation that increases in amplitude as the limit cycle is approached. In the phase plane graph, this corresponds to an initial

trajectory that is interior to the limit cycle with a subsequent outward spiraling to reach the limit cycle (cf. Fig. 12.8B, path P_I , and Fig. 12.9). In contrast, rapid withdrawal of excitation from Y allows the system to accelerate into a rapid, large amplitude oscillation, which then decays slightly to the limit cycle amplitude; this is represented in the phase plane graph as an external approach to the limit cycle (cf. Fig. 12.8B, path P_E , and Fig. 12.10).

It is useful to use Fig. 12.8B to summarize some of the dynamics of the limit cycle system. The equations governing the limit cycle isoclines are:

$$I_A, X = c/[S_2(Y)d(\text{circ})] \text{ and } I_B, Y = a(X)S_1(X)/b(X)$$

with the terms as in equations 3 and 4. These isoclines are clearly “bent” compared with those of the simple LV system in Fig. 12.8A. Since all solution paths must have zero slope at the point of crossing I_A , it can be seen heuristically that if I_A is bent clockwise against the sense of path rotation, then solution paths are “forced” to curve earlier and more tightly than in the standard system. Therefore, solutions spiral inward toward the limit cycle. At larger radii from the center (>0.75 units), I_B produces the same constraining effect by being similarly bent against the direction of solution rotation. At smaller radii, however, I_B is bent counterclockwise and in the same direction as that of solution rotation. In this case, solution paths near the center bend later and less tightly than in the standard system. Thus, solution paths tend to spiral outward on each revolution when initiated interior to the limit cycle. This counterclockwise bending of I_B at small radii is the graphical reflection of depressed REM-on autoexcitation at low firing rates—a property we propose is fundamental to the presence of limit cycle behavior of the system. There are two further technical points. First, the position of I_A is shown for $d(\text{circ}) = 1$; however since d varies with circadian phase between 0.85 and 1.1, the position of I_A will vary also with circadian phase by ± 0.125 abscissa units. The second point has to do with the different vertical scale factors of 12.8A and B; these do not affect system behavior or the final values of subsequently scaled neuronal discharge rates [34].

[34] This point is discussed in detail in McCarley and Massaquoi (1986a).

12.8. Sleep Abnormalities in Depression and Quantitative Modeling

We here discuss those neurobiological control mechanisms likely important for both sleep and depression, and

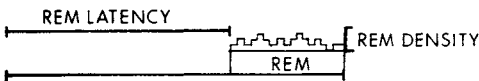
thought to have important brainstem components. No attempt to cover the entire neurobiology of major mood disorders will be made; this is an overly large topic for this book. However, the overlap between the mood disorders and sleep disorders is considerable and quite important, since about 90% of patients with major endogenous depressive disorders show some electrographic sleep abnormality [35]. These abnormalities may be grouped

[35] Kupfer (1982);
Reynolds (1989).

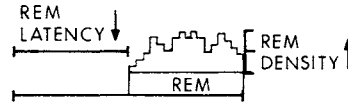
THE FIRST SLEEP CYCLE IN NORMALS AND DEPRESSIVES

EEG MEASURES

Normals:



Depressives:



NEURONAL ACTIVITY

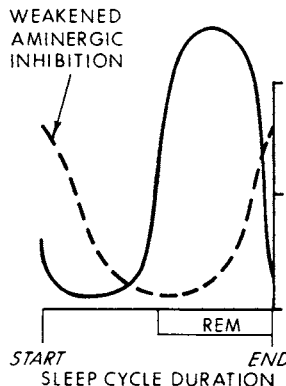
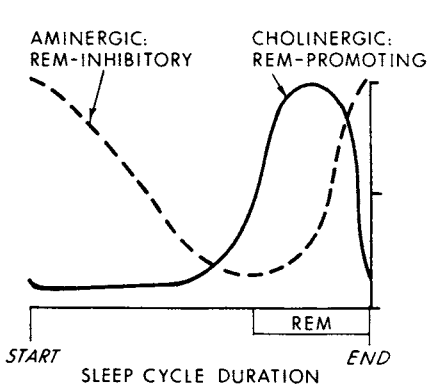


Figure 12.16. Schematic of EEG measures in the first sleep cycle of normal and depressive subjects (top) and of the postulated underlying neuronal activity (bottom) according to the aminergic-cholinergic interaction model. Top panel. EEG measures show patients with endogenous depression have, in the first sleep cycle, a decreased REM sleep latency and increased frequency of rapid eye movements (REM density) within the REM phase of sleep as compared with normals. Depressives also tend to have a slightly longer duration of the first REM period than normals (not illustrated in this schematic). Bottom. The sketch of the hypothesized corresponding neuronal activity over the sleep cycle in normal subjects shows that REM sleep occurs when cholinergic and REM-promoting (REM-on) neuronal activity becomes dominant with the gradual offset of aminergic (noradrenergic, adrenergic, and serotonergic) inhibition. The hypothesized weakened aminergic inhibition in depression produces a quicker release from inhibition of the cholinergic, REM-promoting neurons and a consequently quicker onset of REM (decreased REM latency) and an increased intensity of the REM sleep episode (increased REM density). To be compared with quantitative simulation of Fig. 12.17. From McCarley (1982).

into three categories:

1. *REM sleep abnormalities.* (a) *shortened "REM latency,"* a shortened interval between sleep onset and the beginning of the first REM sleep period; (b) *increased "REM density" in the first REM sleep episode,* an increased number of rapid eye movements per unit time; and (c) a tendency to *increased duration of the first REM sleep episode* (Fig. 12.16 top, schematizes these abnormalities). REM density and REM sleep duration may also be increased in other early night REM sleep episodes in addition to the first. A number of studies suggest that these abnormalities persist beyond the stage of clinical recovery from the depressive episode [36].

2. *Synchronized sleep abnormalities. Delta sleep reduction.* There is a reduction in stage 3 and 4 sleep, often called delta sleep. This reduction is especially marked in the first non-REM sleep episode (e.g., the interval between sleep onset and the first REM episode)—a time when delta sleep ordinarily is at a maximum. Initial analyses also indicate a reduction in power in the delta bandwidth on frequency analysis (0.5–3.0 Hz) [37].

3. *Sleep continuity disturbances.* These include difficulty in falling asleep, early morning awakenings, and increased nocturnal awakenings, and appear to be the least specific for depression [38].

Three major theories have been advanced to account for the observed links between sleep state disturbances and mood state disturbances:

1. *Monoaminergic–cholinergic alterations.* McCarley has proposed commonality of monoamine and cholinergic biological control systems to explain covarying aspects of REM sleep and mood control [39]. This thesis grew out of the cholinergic–monoaminergic reciprocal interaction model of sleep cycle control, and posits at least partial parallelism with the mood regulation system, in terms of disturbances of monoaminergic control, cholinergic control, and of cholinergic–adrenergic balance [40].

2. *Deficient Process S.* Borbély, Daan, Beersma, and coworkers have proposed a two process model of control of the synchronized phase of sleep [41]. Process C (for circadian) regulates the circadian variation in sleep propensity while Process S is the momentary physiological need for sleep that is dependent on the prior history of sleep and wakefulness, and is measured by the power spectral density in the delta bandwidth. "Factor S" builds up in wakefulness and declines during sleep. A deficiency in Factor S is postulated for depressives, who are hypothesized not to produce

[36] For more details see Gresham *et al.* (1965); Hartmann (1968); Kupfer and Foster (1972); Coble *et al.* (1976); Foster *et al.* (1976); McPartland *et al.* (1979).

[37] See Borbély *et al.* (1984); Kupfer *et al.* (1984).

[38] See reviews in Kupfer (1982); Gillin *et al.* (1988).

[39] McCarley (1980a); McCarley (1982).

[40] For monoaminergic control see Schildkraut and Kety (1967); for cholinergic control see Gillin *et al.* (1982, 1988); for cholinergic–adrenergic balance see Janowsky *et al.* (1972).

[41] Borbély (1982); Daan *et al.* (1984); Beersma *et al.* (1987).

[42] Borbely and Wirz-Justice (1982).

sufficient Factor S to cause deep delta sleep at sleep onset [42]. The postulated inhibition of REM sleep by Factor S (indexed by delta sleep) means that reduced Factor S (and consequently reduced delta sleep) has, as a consequence, a quicker onset first REM sleep period (shortened REM latency). Finally, it is postulated that the deficiency in Factor S causes the shortening of sleep duration found in depressives.

3. *Phase-advance theories of sleep disturbance in depression.*

This chapter has earlier described how the latency to the first REM sleep episode and the intensity and duration of REM sleep episodes is under control of a circadian oscillator that also controls the temperature cycle and endocrine rhythms, such as cortisol. The phase advance theory of depression simply states that the abnormalities of sleep and mood in depressives are a function of a phase advance in the circadian oscillator controlling both temperature and REM sleep propensity relative to the phase of the rest-activity circadian rhythm. Thus, it is postulated, the observed pattern of REM sleep in depressives at sleep onset is like that seen near the temperature nadir of normals, which in entrained subjects occurs at about 4 a.m. [43]. This out of phase relationship of the temperature-REM sleep oscillator and the oscillator controlling the rest-activity cycle is postulated to lead to a mood disturbance.

[43] Kripke *et al.* (1978); Wehr *et al.* (1979).

Before reviewing the theories and relevant data, it is first important to emphasize that the separation of these theories has been done for didactic purposes and that, in fact, they are not mutually incompatible. For example, it is entirely possible that there is disturbance in both Process S (synchronized sleep) and in cholinergic-adrenergic balance (controlling REM sleep). The other key point to be made is that the factors controlling circadian rhythms, REM sleep, and non-REM sleep interact, and, in fact, our review of the theories and data will emphasize interactions.

The reader should note that, in spite of limitations in a simple monoamine deficiency theory of depression, more recent data still convincingly point to the involvement of monoamine systems, albeit at a more sophisticated level of understanding. For example, there is now emerging evidence that the individuals with variations in the alleles of the serotonin transporter promotor show differing vulnerability to depression, to antidepressant treatment, and to tryptophan depletion [44]. There is less work on the relationship to sleep in depression. Benedetti *et al.* reported that bipolar depressed patients, who were homozygotic for the long variant, showed a better mood amelioration after

[44] See, for example, discussion and data in Moreno *et al.* (2002).

total sleep deprivation than patients who were heterozygotic and those who were homozygotic for the short variant, although they did not look at sleep stage-specific responses [45]. They did note that the effect was similar to that observed in patients treated with serotonin-specific reuptake inhibitors used as antidepressants. Nonetheless, the relationship between abnormalities at the single gene level and depression remains complex, since, for example, psychiatric conditions such as anxiety disorders also share in the transporter promoter polymorphism [46]. Duman and colleagues suggest that, rather than simple neurotransmitter concentration alterations, intracellular signaling systems may be disturbed [47], which may have important consequences in production of growth factors, such as brain-derived neurotrophic factor, which may, in turn, influence function and survival of neurons. Newport *et al.* have reviewed data more directly related to norepinephrine, reporting that animal studies consistently indicate disrupted parenting produces offspring behaviors reminiscent of the cardinal features of mood disorders; at a biochemical level, disrupted parenting uniformly produces persistent hyperresponsivity in hypothalamic–pituitary–adrenal axis activity secondary to hypersecretion of corticotropin-releasing factor (CRF), which, among other actions excites LC noradrenergic neurons [48]. This chronic overstimulation may, in turn, eventually lead to lower concentrations or less receptor effectiveness of NE. We note that, despite this more sophisticated and deeper level of understanding, it remains true that the monoamine and cholinergic systems, even if downstream from the main causative factors in depression, remain a vital point of intersection between mood disorders and sleep abnormalities. The following review thus focuses on these systems.

12.8.1. Monoaminergic–Cholinergic Factors in Mood Disorders and Associated Sleep Abnormalities

12.8.1.1. Monoamines

The monoamine theory of depression proposes that a deficiency in monoamine activity (NE and/or serotonin systems) is responsible for the occurrence of some or all of the major types of depression [49]. Almost all varieties of clinically effective tricyclic antidepressants, including those atypical ones not associated with acute blocking of monoamine reuptake such as iprindole, have been reported to change NE and serotonin receptor binding [50]. Long

[45] Benedetti *et al.* (1999).

[46] See review and data in Mann (1999); Mann *et al.* (2000).

[47] Duman *et al.* (1997).

[48] Newport *et al.* (2002).

[49] Schildkraut and Kety (1967); Maas (1975).

[50] Peroutka and Snyder (1980); Wolfe *et al.* (1978).

- [51] DeMontigny and Aghajanian (1978); Menkes and Aghajanian (1980).
[52] Blier and DeMontigny (1983).

- [53] Cortes *et al.* (1988).

- [54] Kupfer *et al.* (1981b).

- [55] See review by Vogel (1989).

- [56] Vogel *et al.* (1980).

- [57] Mogilnicka *et al.* (1980).

term administration of these agents decrease beta adrenergic and serotonin-2 (high affinity to [H^3]-spiroperidol) receptors. Neuronal recordings indicate that long term administration of tricyclic antidepressants, including the atypical ones, act on monoamine systems by increasing responsiveness to iontophoretically applied monoamines [51]. A study by Blier and DeMontigny has provided some insight into the mechanism of antidepressant action at the neuronal level [52]; after 2 weeks of antidepressant administration, serotonergic transmission in the rat dorsal raphe-hippocampal pathway was potentiated. The initial effect of antidepressants was to cause reduced dorsal raphe firing because of depolarization blockade, with this effect vanishing over 2 weeks; it is of note that a similar lag period is present before tricyclics become clinically effective in improving human depressive symptoms. Cortes and coworkers have recently examined the binding sites in human brain of both a tricyclic antidepressant, [H^3]-imipramine, and a nontricyclic antidepressant, [H^3]-paroxetine—a more specific and potent serotonin uptake inhibitor [53]. These antidepressant binding sites paralleled the serotonin system, with highest values in the midbrain raphe nuclei and ascending projections. Also of interest in view of the augmentation of REM sleep phenomena in depression and their suppression by antidepressants was the finding of fairly dense labeling in brainstem zones related to PGO waves and eye movements (Chapter 10), namely in the nucleus reticularis tegmenti pontis and gigantocellular portions of reticular formation (cf. Figs 6 and 7 in [53]).

The implication of monoamine systems in both the regulation of mood (the monoamine theory) and in REM sleep (the reciprocal interaction theory) suggest the possibility of a link between these two systems through the monoamines. Kupfer and coworkers have shown that one of the first indications of effectiveness of the tricyclic action on depression is the abolition of the abnormally short latency of the first REM period [54]. In fact, almost all clinically effective antidepressants (tricyclics, monoamine oxidase inhibitors, and others) markedly suppress REM sleep, and induce a characteristic REM sleep rebound on their discontinuance [55]. Further supporting the link between control mechanisms of REM sleep and depression is a study by Vogel and coworkers [56]; REM sleep deprivation, known to increase monoamine neuronal discharge activity in animals, acts to improve depression, and with about the same efficacy as tricyclic antidepressants. REM sleep deprivation has also been shown to decrease rat cortical high affinity binding sites for the antidepressant imipramine [57], with the likely

mediating event being the deprivation-induced increased firings of monoamine neurons. This monoamine commonality of mood and REM control systems forms one basis of the model of REM sleep abnormalities in depression.

12.8.1.2. Cholinergic Abnormalities and the Sleep of Depressives

In addition to the monoamine abnormalities in depression, Gillin, Sitaram, and coworkers have found that increased sensitivity to acetylcholine agonist induction of REM sleep appears to be a hallmark of many patients subject to endogenous depression [58]. These patients may have a primary cholinergic abnormality. The shorter REM latencies in rats with increased number of muscarinic receptors (Flenders Sensitive Line [59]) suggest the possibility of cholinergic causation of this event, although these animals also had an increased percentage of REM sleep—a finding not present in depressives [60]. Another possibility given the monoaminergic–cholinergic duality of control is that the monoamine deficiency is responsible for the enhanced effectiveness of cholinergic agonists in inducing REM sleep. In general, it appears likely that various kinds of depression involve more than one causative factor and that both acetylcholine and/or monoamine abnormalities (in addition to other factors) could be present. The evidence on parallelism of monoaminergic and cholinergic features in depression and REM sleep control has been summarized [39]. Overall, the evidence appears stronger for a monoamine role in depression and for more parallelism between monoamine controls in depression and sleep than for cholinergic systems. Fig. 12.16, bottom panel, is a qualitative sketch of how lessened monoaminergic inhibition might lead to short latency, higher intensity first REM sleep episode in depressives.

The availability of quantitative predictions about the effects of monoaminergic and cholinergic factors may be of use in specifying subtypes of depression and in classifying other pathological syndromes with REM abnormalities, and will be discussed in the next section, as will the “phase advance” theories of REM sleep alterations in depression.

12.8.2. Quantitative Modeling of the REM Sleep Abnormalities in Depression

This section addresses the quantitative modeling of REM sleep abnormalities in depression—a procedure that

[58] Gillin *et al.* (1982, 1988); Sitaram *et al.* (1982).

[59] See Overstreet (1986).

[60] Shiromani *et al.* (1988b).

furnishes more precise predictions and tests than do simple qualitative assertions. This modeling uses aspects of the limit cycle reciprocal interaction model of sleep cycle control presented above. The first and most elementary question is whether a simple phase advance, as modeled by the limit cycle model, could account for the REM sleep abnormalities. Figure 12.10 shows that, for sleep begun at temperature minimum, there is indeed a more intense, longer duration REM sleep episode that has a shorter REM latency than with sleep begun near temperature maximum, as shown in Fig. 12.9.

However, the REM latency shortening to about 45 min is *not sufficient* to mimic that seen in depressives, although it does match quite well the empirical findings of REM sleep changes in normals with sleep begun at different points on the circadian oscillator. The match to empirical circadian phase data is important, since the failure to mimic could represent a problem with the limit cycle model and not the phase advance theory. Additional evidence against the simple phase advance hypothesis comes from the fact that depressives also show short REM latencies compared with normals when they nap in the daytime and when they are awakened later in the night [61]; the phase advance theory would predict a longer duration REM latency during at least some point of the circadian cycle. Thus, both the limit cycle model and empirical data suggest that simple phase change could not explain the REM sleep abnormalities in depression.

Nonetheless, examination of the latency, intensity, and duration of the first REM sleep episode when sleep is begun near a circadian temperature minimum (T_{\min}) in free-running normal subjects (Fig. 12.10) is instructive for suggesting the kind of changes that might occur in depression. In the limit cycle model, at T_{\min} there is a more rapid decline of the REM-suppressive monoamine (Y) population activity; this leads to entry into the limit cycle from the outside and hence produces a shorter latency, larger amplitude, and longer duration REM episode than at points nearer circadian T_{\max} .

These results suggest that the REM sleep abnormalities in depressives might be quite simply and realistically modeled by alterations in the monoamine population activity at sleep onset (although these would need to be more pronounced than those seen with circadian modulation). A lessened monoamine influence is also compatible with evidence (cited above) on monoamine alterations in depressives and the normalization of REM sleep abnormalities by antidepressants. Thus, both an initial qualitative approach [39] (see Fig. 12.16) and subsequent quantitative modeling [31, 62] have worked on the postulate that

[61] For daytime see Kupfer *et al.* (1981a); for nighttime see Schulz and Tetzlaff (1982).

[62] McCarley and Massaquoi (1986a, b).

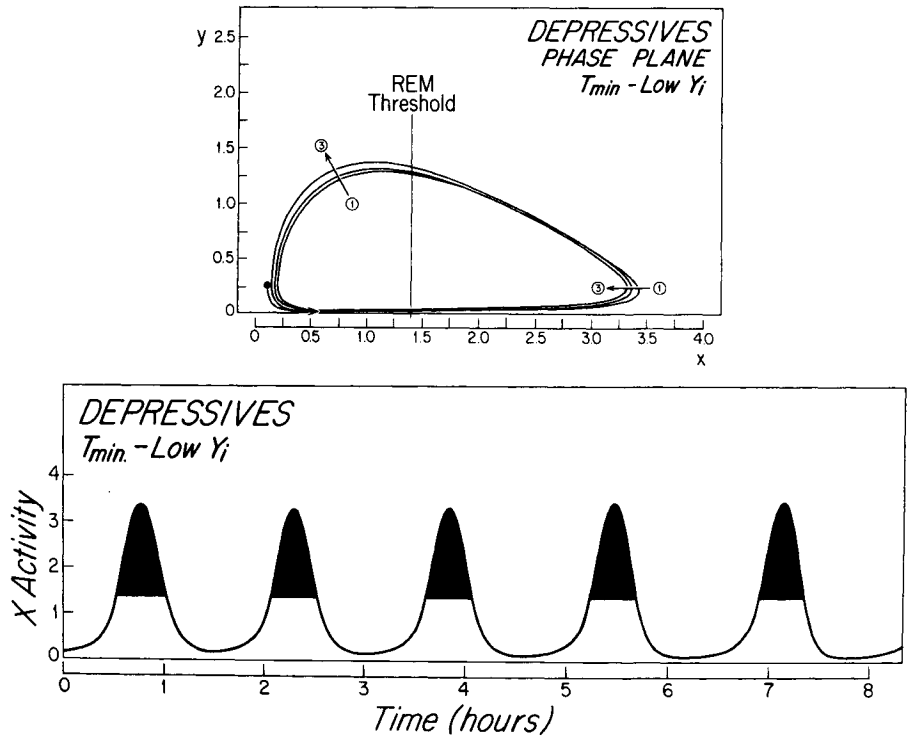


Figure 12.17. Quantitative simulation of REM activity of depressives by the reciprocal interaction–limit cycle model. Time Domain (bottom) representation of REM-on neuronal activity is to be compared with Fig. 13.3; as in the figures of Chapter 12, X represents REM-on neuronal activity, and the darkened portions of the time domain graph represent REM sleep episodes, and Y represents REM-off neuronal activity. The main point of this figure is that use of a lower value of $Y_{initial}$ than for the entrained normal simulation leads to a first REM episode with a shortened latency (here about 35 min), increased intensity, and longer duration compared with that of the normal first REM episode (Fig. 12.9). The phase plane representation (top) shows that entry into the limit cycle is external; legends and interpretation are as in Figs 12.9 and 12.10. In this particular simulation, the circadian phase used was T_{min} , but the same alterations in the first REM period were present when T_{max} was used as a circadian phase. Comparison with a simulation at T_{min} and normal Y_i (Fig. 12.10) shows further that a lower Y_i is required to achieve a shortened REM latency in the range of depressives. Circadian phase is as in Fig. 12.10 (temperature minimum, 4.72 radians) and $Y_{initial}$ is 0.25 vs the 0.35 for all simulations of normal REM in Chapter 12. See also description in text. From McCarley and Massaquoi (1986a).

the level of monoamine population activity at sleep onset is less in depressives than in normals.

For simplicity, the level of monoamine population activity at sleep onset will be described as $Y_{initial} = Y_i$. Setting the value of Y_i at 0.25 units, compared with a normal value of 0.35 produces a first REM sleep latency of 35 min, as shown in Fig. 12.17. This shortened REM sleep latency is almost exactly in accord with the mean values for depressives in the literature and also has the desirable feature of being less than most extreme values for the first REM sleep latency in normals as tabulated by Schulz *et al.* [63]. Figure 12.17 further indicates that alteration of Y_i is

[63] Schulz *et al.* (1984).

not only able to mimic the shortened REM sleep latency characteristic of depressives but also produces a first REM sleep episode with a heightened amplitude (= heightened REM sleep intensity) and duration, also characteristics of the first REM sleep episode of depressives. It is to be emphasized that the critical feature of the limit cycle model that produces a short latency REM sleep episode is the rapid decline of the Y (monoamine) population activity. This change in Y_i is able to produce short REM sleep latencies regardless of whether the simulation is begun at times near circadian T_{\min} (as in the illustration in Fig. 12.17) or near circadian T_{\max} . In both cases, subsequent REM sleep cycles tend to converge to the limit cycle, preserving a realistic replica of sleep patterning after the initial short latency REM sleep episode; this important feature of the limit cycle model was not present with the earlier simple LV model [1].

12.8.2.1. Modeling the Bimodal Distribution of REM Sleep Latencies in Depression

The REM sleep latency histogram from patients in at least some types of depression has been reported to show a “bimodal distribution”; there is one peak at near sleep-onset REM sleep latency and another peak at much longer latencies, with relatively few REM sleep episodes in the intermediate zone [64]. The limit cycle model simulations have suggested a possible mechanism for this phenomenon. In the limit cycle model [62], Y (monoamine population activity) values less than approximately 0.3 were progressively less able to “hold” the X (REM-on) population at low values, that is, 0.2 or less. If the Y values dropped below this critical zone of about 0.3 in the presleep period, there was a progressively increasing tendency for an “escape” and a gradual increase of the X (REM-on) population toward a higher value prior to onset of stage 2 sleep, which is conventionally used to define “sleep onset,” and, as such, begins the graph of depressives in Fig. 12.18 and those of normals. (“Presleep,” as prestage 2, thus includes stage 1; REM sleep latency is measured as the time from stage 2 onset to REM sleep onset. It will be noted that this model assumes that the initial non-REM sleep abnormalities of depression [lessened initial delta sleep] are reflections of the REM sleep abnormalities.) This “passive” model of non-REM sleep seems plausible, as discussed in Chapter 11, but the more “active” non-REM systems described in the next chapter may very well play a role, although there is currently no clear evidence for this.

[64] Schulz *et al.* (1979).

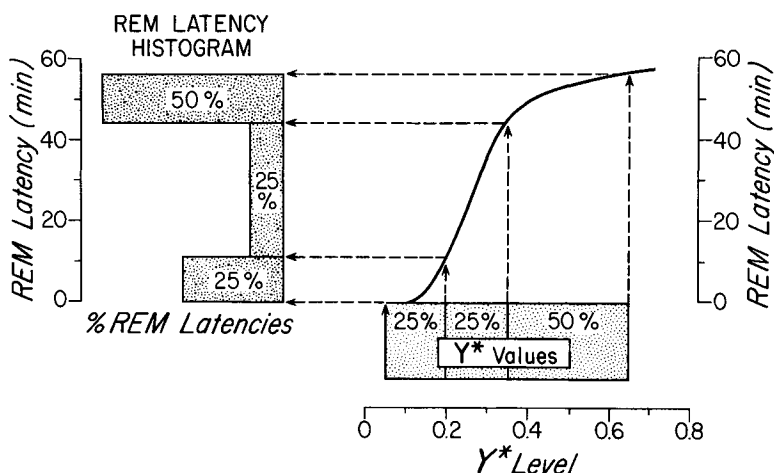


Figure 12.18. Reciprocal interaction limit cycle model simulation of bimodal REM latency distribution for depressives. Pre-sleep variation in the value of the monoamine population activity (Y^* , abscissa) is nonlinearly related to REM latency (ordinate), producing a bimodal distribution of REM latencies, due to the nonlinear, sigmoid nature of the function relating them (illustrated sigmoid function). For simplicity of computation it is assumed that the probability of a given Y^* is uniformly distributed in the range 0.05–0.65. The resulting map of this probability distribution onto the probability distribution of REM latencies is highly nonlinear. Note that 50% of the Y^* range from 0.35 to 0.65 but that this range maps into a much smaller latency range, 43–56 min or 23% of latency range, producing a peak at longer REM latencies. There is a second strongly nonlinear region at the lower end where 25% of Y^* values map into a latency range of 0–11 min (20%), producing a peak at the lower range of REM latencies. In contrast, 25% of the Y^* values map into a large middle value REM latency range, 11–43 min (57% of entire range). Thus, a pre-sleep stage 2 increase in X values secondary to low Y^* values produces a bimodal REM latency distribution. In this series of simulations, Y^* was held constant for 30 min prior to stage 2 onset (stage 2 onset = sleep onset); in all cases, other parameters including circadian phase were held constant at the values used in Fig. 12. 17. From McCarley and Massaquoi (1986a).

This “escape” of the X (REM-on) population activity because of the lowered Y (monoamine) population activity hastened the onset of the first REM sleep episode. Simulations showed the degree of shortening of REM sleep latency as Y values became less dependent on the prestage 2 values of Y , which were termed Y^* . The shape of the function relating REM sleep latency and the level of Y^* (presleep Y) was highly nonlinear, resulting in a bimodal distribution of REM sleep latencies, as illustrated in Fig. 12.18, whose legend should be consulted for a more detailed description of the simulation. The very short REM sleep latencies reflect the “escape” of the X population.

It is evident that the exact form of the REM sleep latency distribution is contingent on the level and rate of change of Y_{presleep} , as well as the probability distribution assumed for Y^* , but McCarley and Massaquoi noted that the production of a bimodal REM sleep latency distribution occurs under a wide variety of assumptions about the form of Y^* density and the rapidity of Y^* decline [65].

[65] McCarley and Massaquoi (1986a).

12.8.2.2. Earlier Quantitative Models of REM Sleep Latency in Depression

All of the previous work has been based on the simple LV model of McCarley and Hobson (equations 1 and 2 of the previous chapter) [1]. Vogel *et al.* used cycle-to-cycle alterations of the connectivity constants “a” and “c” without explicit use of the Y population values at sleep onset [56]. McCarley suggested that alterations in the Y_{initial} value might mimic the findings in depression and Massaquoi and McCarley provided quantitative evidence for this in the context of presenting the initial version of the limit cycle model [66, 33].

[66] McCarley (1980a).

Beersma and colleagues were the first to realize the value of a stochastic model of Y_{initial} values and used this model to generate a bimodal REM sleep latency histogram with the simple LV equations [67]. With respect to the use of Y_{initial} alteration to model the sleep of depressives, both the papers of Beersma *et al.* and Massaquoi and McCarley emphasized that use of a single parameter change (Y) was to be preferred to the more elaborate suppositions about system changes used in the Vogel *et al.* work [56].

[67] Beersma *et al.* (1983, 1984).

However, the neutral stability of the simple LV model used by Beersma *et al.* meant that altering initial conditions created persisting alterations and consequently did not reproduce the actual data of the REM sleep cycles: (1) In the simple LV equations with parameters used by Beersma *et al.*, lowering Y_i does shorten the REM sleep latency but unfortunately also produces a first REM sleep episode with a less than normal intensity, not in agreement with the higher intensity found in empirical studies of depression. (2) Because of the neutral stability feature of the simple LV equations, creating a short latency first REM sleep episode also creates distortions of later REM/nonREM sleep cycles and the REM/nonREM sleep values obtained by the LV simulation do not match those observed in empirical studies. Thus, use of the limit cycle model appears to offer marked improvements over the simple LV model.

12.8.2.3. Modeling the Cholinergically Induced Hastened Onset of REM Sleep

The ability of cholinergic agonists to hasten the onset of a REM sleep episode has been mimicked by the limit cycle model (Fig. 12.19), which has also produced a prediction of the normal phase response curve to cholinergic agonists (Fig. 12.20). Patients with predisposition to affective disorder not only should have a single time point abnormality in their response to acetylcholine agonist but also should show an abnormal phase response curve to

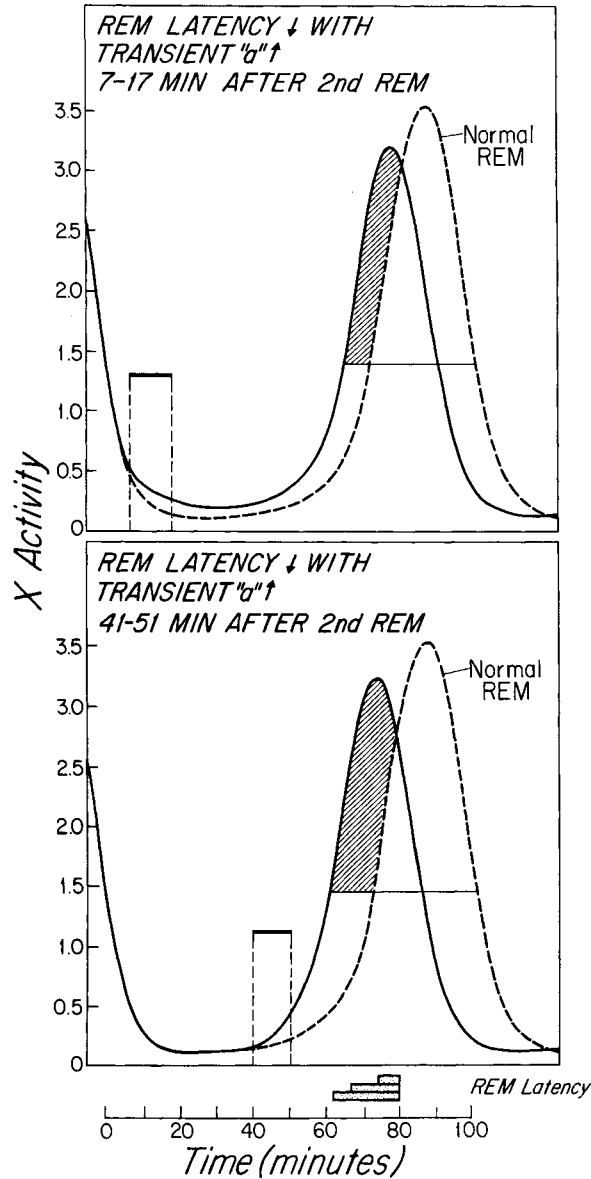


Figure 12.19. Examples of modeling of REM latency shortening by experimental application of an acetylcholinesterase inhibitor. In the reciprocal interaction limit cycle model, the parameter "a" is increased for the same duration in A and B but the phase advance of REM (shaded area) is greater for application at the time in B. The curves model REM-on neuronal activity with REM onset defined as the point of crossing a threshold (horizontal line). In the model, "a" is the term indicating the strength of positive feedback in the excitatory, REM-on population and thus the strength of cholinergic activity. As a first approximation to the experimental conditions, simulations doubled the strength of "a" (cholinergic feedback) for 10.7 min (step function). These values produced clear-cut effects but did not severely distort the time curves, and produced a phase advance of the REM episode of roughly the same order of magnitude as the single time point experiments of Sitaram and Gillin [58]. These differential phase response effects can be understood as REM being much easier to induce when the X population is on the rising rather than in the falling phase of the sleep cycle. This has to do with both an ease of moving the X population into an exponential growth phase and also the absence of Y inhibition later in the cycle. From McCarley and Massaquoi (1986a).

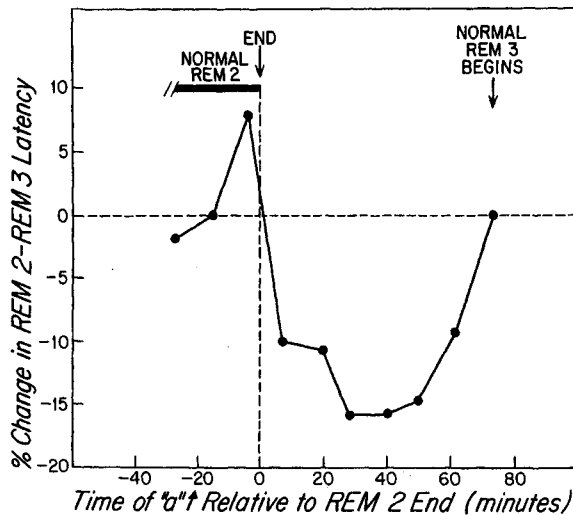


Figure 12.20. Predicted REM latency phase response curve to cholinergic agonists, reciprocal interaction limit cycle model. Each point on the curve was constructed by a simulation like the two described in Fig. 12.19, with “ a ” increased for the same 10.7 min duration but with different times of onset. Onset times of “ a ” increase are relative to the end of the REM period at the start of the graph, the second REM episode of the night. Negative times indicate the time before the normal (unperturbed) end of this REM sleep episode. Note that there is a time zone just at the end of the previous REM sleep episode when increasing “ a ” prolongs the latency of the subsequent REM episode. This is due to an increase in the duration of the second REM episode. The phase of the response then changes rapidly; a shortening of the REM latency of the order of 10% occurs on administrations starting after the end of the second REM episode; an increase to maximal effect (17% latency reduction) occurs with administrations about 25–50 min after the end of the second REM sleep episode. Following this, there is relatively less effect, due to the fact that the third REM sleep episode normally occurs very soon thereafter, and thus there is very little room left for shortening. This phase response curve is both a useful test of the predictions of the model in normals and also draws attention to the prediction that cholinergic system abnormalities in depressives should be marked by phase response abnormalities as well as single time point abnormalities. From McCarley and Massaquoi (1986a).

cholinergic agonists administered at various points in the sleep–wake cycle.

12.8.2.4. Circadian Rhythms in Depression: Decreased Amplitude Instead of a Phase Advance?

Although empirical studies cited above have failed to provide strong empirical support for a theory of phase advance in depression, work has suggested that the amplitude of circadian rhythms may be reduced in endogenous depression [68]; Czeisler and coworkers have suggested this may also hold for seasonal affective disorder [69]. It may be useful to point out that a reduced amplitude of circadian rhythms would be highly compatible with the model just presented, since there would be a low level of monoamine activity at sleep onset, with a consequent production of the abnormalities of the first REM sleep episode.

[68] Schulz and Lund (1983, 1985).

[69] Czeisler *et al.* (1987).

12.8.3. Deficient Process S and Sleep Abnormalities in Depression

12.8.3.1. REM Sleep

Borbély and Wirz-Justice, modifying the reciprocal interaction model of McCarley and Hobson, have suggested that there may be a reciprocal interaction between the processes inducing REM sleep and the processes inducing non-REM sleep [42, 1]. Indeed data discussed in the next chapter suggests the possibility of this interaction. However, the presence of the REM cycle in the pontine cat indicates the sufficiency of brainstem mechanisms for normal cycling. Although the possibility remains that an abnormality in one of the forebrain systems discussed in the next chapter could influence REM sleep, there is currently no strong empirical data for this effect.

12.8.3.2. Non-REM Sleep

The hypothesis of deficient Process S has stimulated considerable research and remains as a possible explanation of the disturbed synchronized sleep in depression. Reynolds *et al.*, using automated scoring of delta waves, have confirmed decreased delta wave activity prior to the first REM sleep episode in depressives as compared with normals [70]. However, whether this delta deficiency is responsible for the short REM latency has been questioned. Schulz and Lund found no inpatient correlation between very short REM latencies and the amount of stage 3 and 4 sleep [71], contrary to the deficient “Process S” hypothesis, which would predict a covariation of REM latency and amount of delta sleep. Also not supporting the deficient Process S-short REM latency hypothesis was a study by Van den Hoofdakker and Beersma [72]; the accumulation curves of delta sleep in depressives with very short and longer REM latencies were similar, in contrast to this theory’s prediction of a covariation of REM latency and accumulation of delta sleep. These workers concluded that best explanatory model for the short REM latencies of depression abnormalities was the mathematical reciprocal interaction model [1]. Beersma and colleagues have also suggested that postulating a deficiency in Process S is not necessary to account for shortening and interruption of sleep in depressives [73]; by superimposing random noise on the circadian rhythm, they were able to simulate both the shortening and decreased continuity of sleep in depressives.

[70] Reynolds *et al.* (1985).

[71] Schulz and Lund (1985).

[72] Van den Hoofdakker and Beersma (1985).

[73] Beersma *et al.* (1985).

The Role of Active Forebrain and Humoral Systems in Sleep Control

In Chapter 9 we developed the theme of thalamocortical influences on sleep, putting forward the thesis that the synchronizing phenomena in thalamocortical systems depend, at least in great part, on the removal of brainstem influences. This present chapter takes up new data on active forebrain and humoral systems which influence sleep. Because some of these systems also act on brainstem mechanisms controlling REM sleep we have placed this chapter following the discussion of REM sleep control.

We first discuss humoral factors, with an emphasis on adenosine (AD) and its role in the induction of sleep, and then take up the ventrolateral preoptic (VLPO) system and its role in control of the duration of non-REM sleep. We conclude with a discussion of the orexin system and its role in REM sleep control and narcolepsy. This chapter draws upon reviews of these topics by McCarley and coworkers [1].

[1] Strecker *et al.* (2000);
McCarley (2002); Basheer
et al. (2004).

To provide background for our discussion of sleepiness, it is useful here to summarize briefly the role of circadian and homeostatic factors.

1. *Circadian factors in sleepiness.* In adult humans, the period of maximal sleepiness occurs at the time of the circadian low point of the temperature rhythm; as discussed in Chapter 12, the circadian rhythm of man can be thought of as a sine wave function with a minimum that occurs between 4:00–7:00 A.M. in subjects with a normal daytime activity schedule. It is no accident that accidents are most frequent at the time near circadian temperature minima, since this is the time of maximal sleepiness. Per vehicle mile, the risk for truck accidents is greatest at this time and the nuclear reactor incidents at both Chernobyl and Three Mile Island also occurred in the early

morning hours. There is a secondary peak of sleepiness that occurs about 3 P.M., corresponding to a favored time for naps. Human newborns do not have a strong circadian modulation of sleep, and, as discussed in Chapter 11, some species, such as the cat, do not have much circadian modulation even as adults.

2. *The second factor determining sleepiness is the extent of prior wakefulness.* Mathematical models of sleep propensity have been developed by Kronauer and coworkers [2], who emphasize circadian control and by Borbély [3], who emphasize the extent of prior wakefulness. Borbély and coworkers' model postulates that the intensity and amplitude of delta wave activity (as measured by power spectral analysis) indexes the level of sleep factor(s) and slow-wave sleep (SWS) drive. In this model the time course of delta activity over the night, a declining exponential, reflects the dissipation of the sleep factor(s). These workers have not specified the nature of the underlying sleep factor(s), but the principal candidates are discussed below.

[2] Kronauer *et al.* (1982).

[3] Borbély (1982).

The main short-term functional consequence of deprivation of sleep seems to be the presence of "microsleeps" that is, very brief episodes of sleep during which sensory input from the outside is diminished and cognitive function is markedly altered [4]. Furthermore, there are also long-duration effects of sleep loss/restriction on performance and physiology, termed "sleep debt," which persist even after a night of recovery sleep. Sleep loss-induced transcriptional changes may underlie the presence of sleep debt. Further discussion of this topic is provided below in the context of AD as a sleep factor.

[4] Dinges *et al.* (1997).

13.1. Adenosine

13.1.1. Adenosine as a Mediator of the Sleepiness Following Prolonged Wakefulness (Homoeostatic Control of Sleep)

A growing body of evidence supports the role of purine nucleoside adenosine as a mediator of the sleepiness following prolonged wakefulness, a role in which its inhibitory actions on the basal forebrain wakefulness-promoting neurons may be especially important. Common-sense evidence for an adenosine role in sleepiness comes from the nearly universal use of coffee and tea to increase alertness, since these beverages contain the adenosine receptor antagonists caffeine and theophylline [5].

[5] Reviewed in Fredholm *et al.* (1999).

McCarley and coworkers have advanced the hypothesis that, during prolonged wakefulness, adenosine accumulates selectively in the basal forebrain and promotes the transition from wakefulness to slow-wave sleep (SWS) by inhibiting, via the adenosine A1 receptor, cholinergic and noncholinergic wakefulness-promoting basal forebrain neurons.

Adenosine, a ubiquitous nucleoside, serves as a building block of nucleic acids and energy storage molecules, as a substrate for multiple enzymes, and, most importantly for this review, as an extracellular modulator of cellular activity [6]. Since its first description in 1929 by Drury and Szent-Gyorgyi, adenosine has been widely investigated in different tissues [7]. The endogenous release of adenosine exerts powerful effects in a wide range of organ systems [8]. For example, adenosine has a predominantly hyperpolarizing effect on the membrane potential of excitable cells, producing inhibition in smooth muscle cells both in the myocardium and coronary arteries, as well as in neurons in brain. From an evolutionary point of view, adenosine's postulated promotion of sleep following activity could be considered as an extension of its systemic role in protecting against overactivity, as seen most clearly in the heart.

Adenosine in the central nervous system functions both as a neuromodulator and as a neuroprotector. The modulatory function, reviewed as early as 1981 by Phillis and Wu, is exerted under physiological conditions both as a homeostatic modulator as well as a modulator at the synaptic level [9]. The most profound effect of adenosine is inhibitory modulation of cellular activity and neurotransmitter release, and it consequently has been described as a "retaliatory modulator" [10].

In terms of a neuroprotective response, extracellular adenosine levels have been shown to increase under abnormal cell-threatening conditions such as cell injury, trauma, ischemia, or hypoxia, and adenosine is widely studied as an endogenous neuroprotective agent in the central nervous system [11]. The increased levels of extracellular adenosine exert neuroprotective effects by reducing excitatory amino acid release and/or Ca^{2+} influx, as well as by reducing cellular activity and hence metabolism [12]. Pharmacological agents which enhance extracellular adenosine levels have been shown to reduce neuronal damage in animal models of cerebral ischemia [13]. An increase in adenosine levels and adenosine A1 receptor activation have been described as essential to development of ischemic tolerance [14]. In addition, adenosine has also been implicated in locomotion, analgesia, chronic drug use, and mediation of the effects of ethanol, topics reviewed in Dunwiddie and Masino [15].

[6] Illes *et al.* (2000).

[7] Drury and Szent-Gyorgyi (1929).

[8] Olah and Stiles (1992).

[9] Phillis and Wu (1981); Newby (1984); Williams (1989); Cunha (2001).

[10] Newby (1984); Dunwiddie (1985); Williams (1989).

[11] Rudolphi *et al.* (1992); Fredholm (1997); Ongini and Schubert (1998); Von Lubitz (1999); for review see Latini and Pedata (2001).

[12] Schubert *et al.* (1997).

[13] Rudolphi *et al.* (1992); Park and Rudolphi (1994); Fredholm (1997).

[14] Heurteaux *et al.* (1995).

[15] Dunwiddie and Masino (2001).

Initial evidence that adenosine (AD), a purine nucleoside, was a sleep factor came from pharmacological studies describing the sleep-inducing effects of systemic or intracerebral injections of adenosine and adenosine agonist drugs [16]. The hypnogenic effects of adenosine were first described in cats by Feldberg and Sherwood [17] and later in dogs by Haulica *et al.* [18]. Since then the sedative, sleep-inducing effects of systemic and central administrations of adenosine have been repeatedly demonstrated [19]. These effects and the fact that adenosine is a byproduct of energy metabolism, led to postulates that adenosine may serve as a homeostatic regulator of energy in brain during sleep, since energy restoration has been proposed as one of the functions of sleep [20]. Fig. 13.1A schematizes adenosine metabolism and its relationship to adenosine triphosphate.

Reasoning that adenosine's control of sleepiness might best be understood as an inhibition of wakefulness-promoting neuronal activity, Portas *et al.* [21] used microdialysis to apply adenosine to the cholinergic neuronal zones of the feline basal forebrain and LDT/PPT, known to be important in production of wakefulness (see Chapter 9). At both sites, adenosine produced a decrease

[16] Ticho and Radulovacki (1991); reviewed in Radulovacki (1985).
[17] Feldberg and Sherwood (1954).
[18] Haulica *et al.* (1973).
[19] Dunwiddie and Worth (1982); Virus *et al.* (1983); Radulovacki *et al.* (1984), Radulovacki (1985); Ticho and Radulovacki (1991).
[20] Chagoya de Sanchez *et al.* (1993); Benington and Heller (1995).
[21] Portas *et al.* (1997).

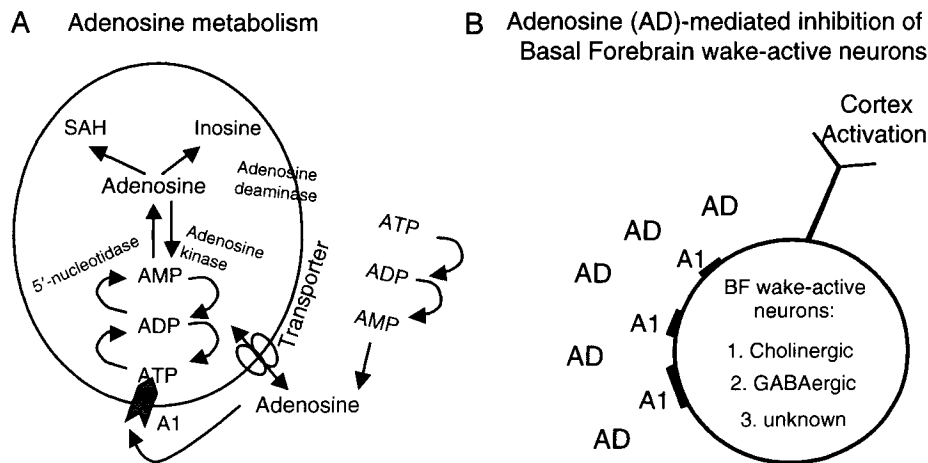


Figure 13.1. A. Schematic of main intra- and extracellular metabolic pathways of adenosine. The intracellular pathway from ATP (adenosine 5'-triphosphate) to ADP (adenosine diphosphate) to AMP (adenosine monophosphate) to Adenosine is respectively regulated by the enzymes ATP-ase, ADP-ase, and 5'-nucleotidase and extracellularly by the respective ectoenzymes. Adenosine kinase converts adenosine to AMP, while adenosine deaminase converts adenosine to inosine. The third enzyme to metabolize adenosine is Sadenosylhomocysteine hydrolase, which converts adenosine to Sadenosylhomocysteine (SAH). Adenosine concentration between the intra- and extracellular spaces is equilibrated by nucleoside transporters. B. Schematic of adenosine effects on cells in the basal forebrain. Extracellular adenosine (AD) acts on the A1 adenosine receptor subtype to inhibit neurons of various neurotransmitter phenotypes that promote EEG activation and wakefulness. Modified from McCarley, 2002.

in wakefulness and in the activated EEG. (Fig. 13.1B provides a schematic of this wakefulness-suppressing action in basal forebrain.)

However, these were pharmacological experiments, and the remaining critical piece of evidence was a study of the changes in extracellular concentration of adenosine as sleep–wake state was varied (cf. our sketch of criteria for establishing a relationship of neurotransmitter/neuro-modulator to a state change in Chapter 11). Using cats to take advantage of the predominance of homeostatic vs circadian control of sleep, Porkka-Heiskanen *et al.* [22] found extracellular adenosine concentrations in the basal forebrain were higher during spontaneously occurring episodes of wake compared with SWS. Moreover, adenosine concentrations progressively increased with each succeeding hour of wakefulness during atraumatic sleep deprivation (Fig. 13.2A).

To determine if the increased adenosine concentrations played a causal role in the sleep–wake alterations, unilateral microdialysis perfusion of the adenosine transport inhibitor *S*-(4-nitrobenzyl)-6-thioinosine (NBTI, 1 mM) was performed. This produced slightly more than a 2-fold increase in extracellular adenosine in basal forebrain, about the same as prolonged wakefulness (see Section 13.1.2, for further explanation of the increase in adenosine). Both prolonged wakefulness and NBTI infusion in the basal forebrain produced the same pattern of sleep–wakefulness changes, with a reduction in wakefulness and an increase in SWS (Fig. 13.2B). Power spectral analysis showed that both prolonged wakefulness and NBTI infusion, compared with control values of spontaneous sleep–wakefulness states with artificial cerebrospinal fluid (ACSF) perfusion, produced an increase in delta band and a decrease in gamma band power. These data were seen as compatible with a causal role of adenosine in producing sleep–wake changes through actions in the basal forebrain. In contrast, in the ventroanterior/ventrolateral (VA/VL) thalamus, a relay nucleus without the widespread cortical projections of the basal forebrain, increasing adenosine concentrations 2-fold with NBTI had no effect in sleep–wakefulness.

13.1.2. Site Specificity and Sources of Adenosine Increases with Prolonged Wakefulness

1. *Site specificity of adenosine increases with prolonged wakefulness.* An important issue is whether adenosine exerts its effects on sleep–wakefulness at localized brain regions, or globally throughout the brain. The initial study

[22] Porkka-Heiskanen
et al. (1997).

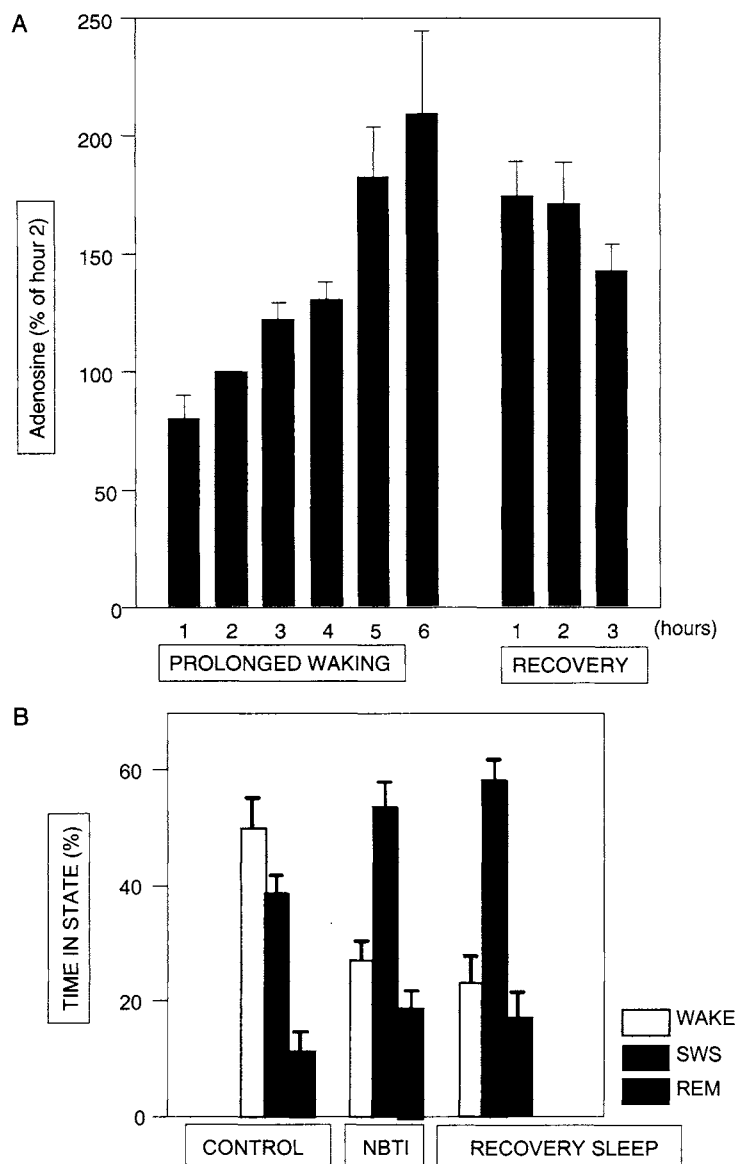


Figure 13.2. A. Mean basal forebrain extracellular adenosine values by hour during 6 hr of prolonged wakefulness and in the subsequent 3 hr of spontaneous recovery sleep. Microdialysis values in the six cats are normalized relative to the second hour of wakefulness. Adapted from Porkka-Heiskanen *et al.*, 1997. B. Comparison of the effects of prolonged wakefulness and NBTI perfusion in the feline basal forebrain on the percent of time spent in each behavioral state. During both the NBTI treatment and the recovery sleep conditions, slow-wave sleep (SWS) was increased as compared with control sleep ($p < 0.05$), and this increase in SWS did not differ between the NBTI and recovery sleep conditions (post hoc Neumann Keul). Wakefulness was decreased in both experimental conditions as compared to control sleep ($p < 0.01$), whereas the two experimental conditions did not differ from each other. REM sleep in the NBTI-treated and recovery sleep groups had similar percentage increases. Effects of NBTI perfusion in the VA/VL thalamus did not differ from control conditions (not shown). Adapted from Porkka-Heiskanen *et al.*, 1997.

[23] Porkka-Heiskanen
et al. (2000).

of Porkka-Heiskanen *et al.* [22] reported no increases in adenosine concentration in VA/VL thalamus with prolonged wakefulness, although short spontaneous episodes of wakefulness showed higher levels in wake relative to spontaneous episodes of SWS. This suggested that all brain sites might not show an increase in adenosine with prolonged wakefulness and hence might not be the source of a homeostatic signal. A systematic study [23] in multiple brain areas showed that sustained and monotonic increases in adenosine concentrations in the course of prolonged wakefulness (6 hr) occurred only in the cat basal forebrain, and to a lesser extent in cerebral cortex. Of note, adenosine concentrations did not increase elsewhere during prolonged wakefulness even in regions known to be important in behavioral state control, such as the preoptic-anterior hypothalamus region (POAH), dorsal raphe nucleus (DRN), and PPT nucleus; nor did it increase in the VL/VA thalamic nuclei (Fig. 13.3), although adenosine concentrations were higher in all brain sites sampled during the naturally occurring (and shorter duration) episodes of wakefulness as compared to sleep episodes in the freely moving and behaving animals. The possibility that other brain sites not surveyed here might show a similar pattern to basal forebrain remains open. Obviously, not all brain sites were surveyed and so it is possible that some other site(s) might show the same pattern as basal forebrain. For example, diurnal variations

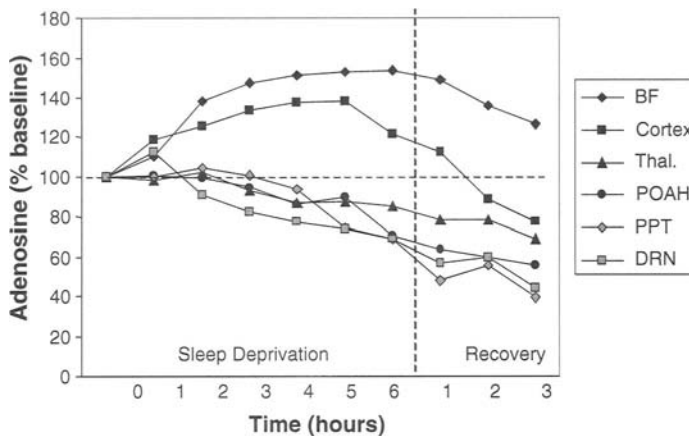


Figure 13.3. Adenosine concentrations in six different brain areas during sleep deprivation and recovery sleep. Note that in basal forebrain (BF, top line) adenosine levels increase progressively during the 6 hr of sleep deprivation, then decline slowly in recovery sleep. Visual Cortex most closely resembles BF, but adenosine levels decrease during the last hour and fall precipitously in during recovery. Other brain areas show no sustained rise in adenosine levels with deprivation. This pattern and other data (see text) suggest basal forebrain is likely a key site of action for adenosine as a mediator of the sleepiness following prolonged wakefulness. Abbreviations: Thal., Thalamus; POAH, preoptic-anterior hypothalamus region; PPT, pedunculopontine tegmental nucleus; DRN, dorsal raphe nucleus. Modified from Porkka-Heiskanen *et al.*, 2000.

in adenosine concentrations have been found in hippocampus, although lack of sleep state recording in this study makes it difficult to know if these are primarily sleep–wake state or circadian related [24].

These data suggest the presence of brain region-specific differences in factors controlling extracellular adenosine concentration, and this section next addresses several potential factors controlling the concentration of extracellular adenosine.

2. *Metabolism.* Data suggest the level of extracellular concentration of adenosine is dependent on metabolism, with increased metabolism leading to reduced high energy phosphate stores and increased adenosine which, via an equilibrative nucleoside transporter, might lead to increases in extracellular adenosine (see Fig. 13.1A). For example, in the *in vitro* hippocampus, extracellular adenosine release, shown by ATP labeling with [³H]adenine to be secondary to ATP breakdown, was induced both by hypoxia/hypoglycemia and by electrical field stimulation [25]. Thus, when the energy expenditure exceeded energy production, adenosine levels increased in the extracellular space. Of note also, pharmacologically induced local energy depletion in the basal forebrain, but not in adjacent brain areas, induces sleep [26]. It is worth emphasizing at this point that the equilibrative transporter for adenosine is a nucleoside transporter, and *in vitro* data [25] suggest that the transporter inhibitor NBTI has the effect of increasing adenosine and decreasing inosine and hypoxanthine release, in agreement with the *in vivo* measurements of the effects of NBTI on adenosine [22]. Support for an adenosine-metabolism link hypothesis comes from the facts that EEG arousal is known to diminish as a function of the duration of prior wakefulness and also with brain hyperthermia, both associated with increased brain metabolism [27].

3. *Extracellular breakdown of adenine nucleotides.* Another potential factor in the increase of extracellular adenosine during wakefulness is the dephosphorylation of adenine nucleotides by ectonucleotidases. This may occur through degradation of ATP, released as a cotransmitter during synaptic activity, as illustrated in Fig. 13.3 [15]; this degradation and cellular uptake is ordinarily rapid, occurring within 1 s, but the possibility exists that increased intracellular adenosine could decrease the rate of uptake through the facilitated nucleoside transporter. Still another potential source of extracellular adenosine is through cyclic adenosine 3',5'-menophosphate (cAMP) released into the extracellular space by a probenidic-sensitive transporter [28], although no data are currently present supporting a role for sleep–wake modulation of this effect.

[24] Huston *et al.* (1996).

[25] Fredholm *et al.* (1994).

[26] Kalinchuk *et al.* (2003a).

[27] Borbély (1982) and Fineberg *et al.*, (1985) report the effect of wakefulness on reducing EEG arousal. Brain metabolism during delta SWS is considerably less than in wakefulness. In humans, a 44% reduction in the cerebral metabolic rate (CMR) of glucose during delta-wave sleep, compared with that during wakefulness, was determined by Maquet *et al.* (1992), and a 25% reduction in the CMR of O₂ was determined by Madsen *et al.* (1991). Horne (1992) has reviewed metabolism and hyperthermia. [28] Rosenberg and Li (1995).

4. *Changes in activity of adenosine-related enzymes.* The biochemistry of enzymes responsible for adenosine production as well as its conversion to inosine or phosphorylation to adenosine monophosphate (AMP) have been well characterized, although the factors regulating their activity are still not well known [15, 29] (see sketch in Fig. 13.1A). In view of the observed selective increase in the levels of extracellular adenosine in cholinergic basal forebrain with prolonged waking, changes in the activity of regulatory enzymes have been examined following 3 and 6 hr of sleep deprivation in rat. None of the enzymes in basal forebrain including adenosine kinase, adenosine deaminase, and both ecto- and endo-5'-nucleotidases showed any change in activity following sleep deprivation [30].

5. *Nucleoside transporters.* It is possible that adenosine concentration increases and the regional selectivity might be related to differences in activity of the nucleoside transporters in the membrane, although the lack of knowledge about these transporters and their regulation has hindered sleep-related research. The human (h) and rat (r) equilibrative (Na(+)-independent) nucleoside transporters (ENTs) hENT1, rENT1, hENT2, and rENT2 belong to a family of integral membrane proteins with 11 transmembrane domains and are distinguished functionally by differences in sensitivity to inhibition by NBTI; ENT1 but not ENT2 has pharmacological antagonists, such as NBTI [31]. Very little is known about the active transporter. After 6 hr of sleep deprivation in the rat, NBTI binding to the ENT1 transporter, a possible indirect measure of ENT1 activity, was found to be decreased in basal forebrain but not in cortex, although ENT1 mRNA did not change [32].

6. *Nitric oxide.* Another candidate for contributing to the increased adenosine concentration following prolonged wakefulness is the release of nitric oxide (NO) as demonstrated in hippocampal slices and forebrain neuronal cultures [33]. Infusion of the nitric oxide donor diethylamine-NONOate into cholinergic basal forebrain has been shown to mimic the effects of sleep deprivation by increasing non-REM sleep [34].

Thus, the mechanism for sleep deprivation-induced increase in extracellular adenosine that is specific to the basal forebrain is not yet clear, and remains an important area for further research. It is the authors' opinion that extracellular adenosine increases with prolonged wakefulness are linked to increased metabolism, and that the most likely source is from inside the neurons, secondary to a decrease in ATP, which, even though small, would produce

[29] Fredholm *et al.* (2000).

[30] Alanko *et al.* (2003a); Mackiewicz *et al.* (2003).

[31] Yao *et al.* (1997, 2002).

[32] Alanko *et al.* (2003b).

[33] For hippocampal slices see Fallahi *et al.* (1996); for forebrain neuronal cultures see Rosenberg *et al.* (2000).

[34] Kalinchuk *et al.* (2003b).

larger increases in ADP, AMP, and adenosine because of the equilibrium constants in the reactions illustrated in Fig. 13.1A. Data are even more scanty on the mechanism for basal forebrain selectivity, but transporter differences are, in the authors' opinion, excellent candidates.

13.1.3. Neurophysiological Mechanisms of Adenosine Effects

Using an *in vitro* rat brainstem slice preparation, Rainnie and coworkers [35] demonstrated that mesopontine cholinergic neurons are under the tonic inhibitory control of endogenous adenosine. Whole-cell and extracellular recordings of identified cholinergic neurons showed an adenosine inhibitory tone that was mediated postsynaptically by an inwardly rectifying potassium conductance and by an inhibition of a hyperpolarization-activated current (*I_h*). Similar inhibition of discharges mediated by the adenosine A1 receptor occurred in basal forebrain cholinergic and noncholinergic neurons. Arrigoni and colleagues [36] performed whole cell patch-clamp *in vitro* recordings on basal forebrain cholinergic neurons, identified by prelabeling *in vivo* with the fluorescent marker, Cy3-192IgG, which is selectively internalized by p75-receptor-expressing basal forebrain cholinergic neurons. Under fluorescent microscopy the prelabeled neurons in the slice appeared bright red and were targeted for electrophysiological recordings, with cholinergic identity confirmed by post-recording injection with lucifer yellow and subsequent cholineacetyl transferase (ChAT) labeling. Adenosine (50–100 μ M) reduced the cholinergic neuronal firing rate by inducing membrane hyperpolarization and decreasing input resistance, effects persisting in the presence of TTX (1 μ M), indicating a postsynaptic action. Voltage-clamp recordings suggested adenosine evoked an inwardly rectifying potassium current. Application of the adenosine A1 receptor antagonist 8-cyclopentyl-theophylline (CPT, 200 nM) blocked adenosine effects and, when applied alone, decreased the current evoked by a voltage ramp protocol, consistent with removal of a tonic inhibition by endogenous adenosine. These effects were similar to those previously described in LDT, with the exception that no *I_h* current was present in basal forebrain cholinergic neurons. The effects of adenosine on most of the noncholinergic neurons recorded in this protocol were similar but more data are needed.

[35] Rainnie *et al.* (1994).

[36] Arrigoni *et al.* (2003).

13.1.4. Receptor Mediation of Adenosine Effects: A1 and A2A Subtypes

To date four different adenosine receptors (A1, A2A, A2B, A3) have been cloned in a variety of species, including man [15, 37]. All of the adenosine receptors are seven transmembrane domain, G-protein-coupled receptors, and they are linked to a variety of transduction mechanisms. The A1 receptor has the highest abundance in the brain and is coupled to activation of K⁺ channels (primarily postsynaptically) and inhibition of Ca²⁺ channels (primarily presynaptically), both of which would inhibit neuronal activity [38]. The A2A receptor is expressed at high levels in only a few regions of the brain, such as the striatum, nucleus accumbens, and olfactory bulb, and is primarily linked to activation of adenylyl cyclase. Evidence is available for both A1 and A2A adenosine receptor subtypes in mediating the sleep inducing effects of adenosine.

[37] Olah and Stiles (1995).

[38] See review in Brundage and Dunwiddie (1997).

13.1.4.1. Receptor Mediation of Adenosine Effects: The A1 Subtype

A1 receptor. ICV administration of the highly selective A1 receptor agonist, N⁶-cyclohexyladenosine (CHA) was found to result in an increased propensity to sleep and increased delta waves during sleep, suggesting a role of the A1 adenosine receptor [39]. Studies in cat and in rat revealed that the somnogenic effects of adenosine in the cholinergic region of the basal forebrain appear to be mediated by the A1 adenosine receptor, since the unilateral infusion of the A1 receptor selective antagonist, cyclopentyl-1,3-dimethylxanthine (CPT) increased waking and decreased sleep [40]. More-over, single unit recording of basal forebrain wake-active neurons in conjunction with *in vivo* microdialysis of the A1 selective agonist CHA decreased, and the A1 selective antagonist CPT increased discharge activity of basal forebrain wake-active neurons [41] in a dose-dependent manner [42] (Fig. 13.4).

[39] Bennington *et al.* (1995); Schwierin *et al.* (1996).

[40] Strecker *et al.* (1999, 2000).

[41] Alam *et al.* (1999).

[42] Thakkar *et al.* (2003a).

Of particular note, blocking the expression of basal forebrain A1 receptors with microdialysis perfusion of antisense oligonucleotides designed to hybridize with A1 receptor mRNA and thereby preventing its translation, resulted in a significant reduction in non-REM sleep and increase in wakefulness in the rat (Fig. 13.5). Moreover, as illustrated in Fig. 13.5, following microdialysis perfusion of A1 receptor antisense and 6 hr of sleep deprivation, the animals spent a significantly reduced (50–60%) amount of time in non-REM sleep during hours 2–5 in the

post-deprivation period with an increase in delta activity in each hour [43]. The absence of a sleep stage difference in post-deprivation hour 1 suggested that other regions in addition to basal forebrain, perhaps cortex, might mediate the immediate sleep response following deprivation. The neocortex is suggested because of the initial deprivation-induced rise in adenosine in the neocortex, but not in other brain regions outside of basal forebrain (see

[43] Thakkar *et al.* (2003b).

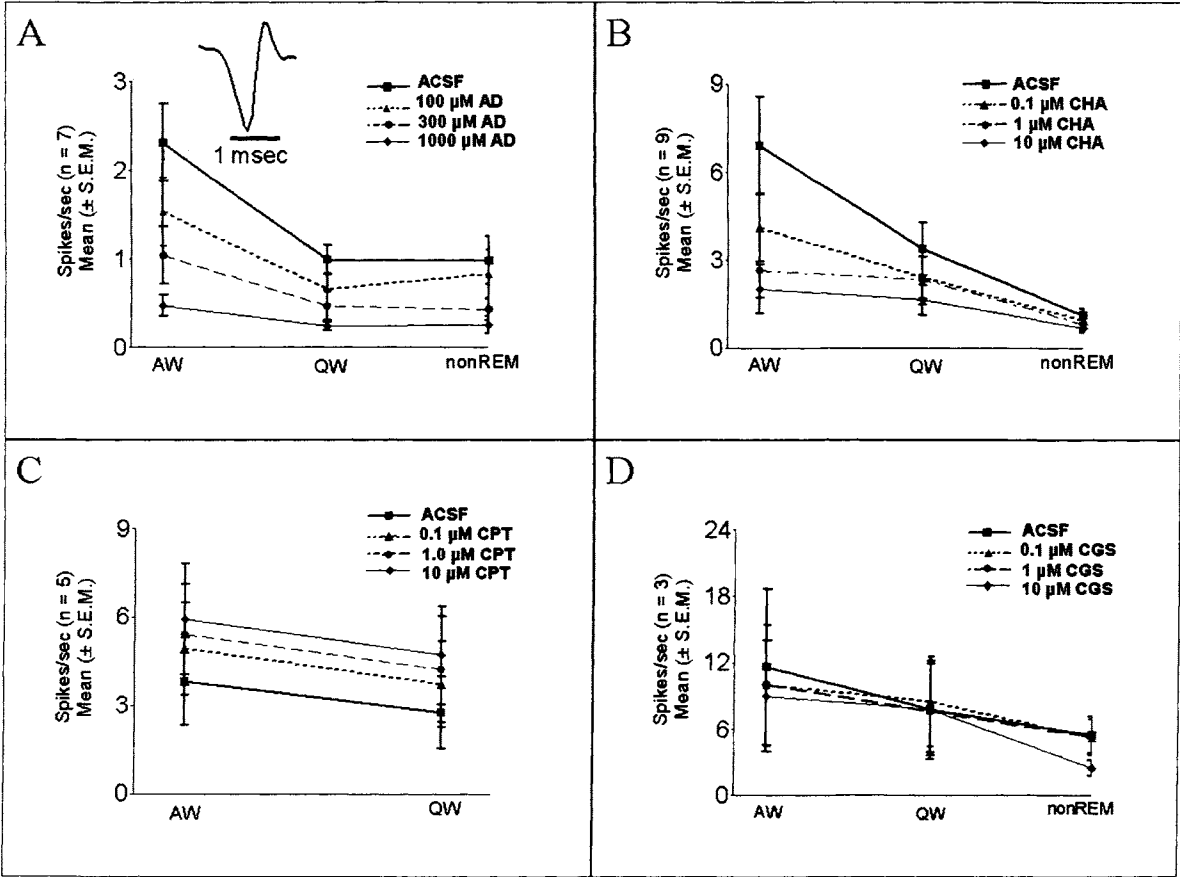


Figure 13.4 Basal forebrain wakefulness-active units: responses to adenosine and to adenosine A1 and A2a pharmacological agents. A. Microdialysis perfusion of adenosine decreases the discharge activity of wakefulness-active neurons in the cholinergic BF in a dose-dependent manner (dose-dependency $p < 0.05$). The graph shows the group mean values (\pm SEM) of discharge activity (spikes/s) during active wakefulness (AW), quiet wakefulness (QW), and non-REM sleep during ACSF (solid line), or adenosine perfusion (three doses; dashed lines). The digital recording trace of a typical extracellular action potential is also shown. B. Microdialysis perfusion of the specific adenosine A1 receptor agonist CHA in the BF reduces the discharge activity of wakefulness-active neurons in a dose-dependent manner (dose-dependency $p < 0.05$). The graph shows mean (\pm SEM)

discharge activity during ACSF (solid line), and CHA perfusion (three doses; dashed lines). Subsequent analysis revealed that CHA significantly reduced the activity of wakefulness-active neurons only during AW. C. Microdialysis perfusion of the specific adenosine A1 receptor antagonist CPT in the BF induces a significant increase in the discharge activity of wakefulness-active neurons both during AW and QW (Wilcoxon Signed-Ranks Test in AW and QW; p 's = 0.042). A permutation test indicated dose-dependence. This graph shows mean (\pm SEM) discharge activity during ACSF (solid line), and CPT perfusion (three doses; dashed lines). D. Microdialysis perfusion of the specific adenosine A2a agonist CGS 21680 in the BF has no effect on the discharge activity of wakefulness-active neurons. Adapted from Thakkar *et al.*, 2003a.

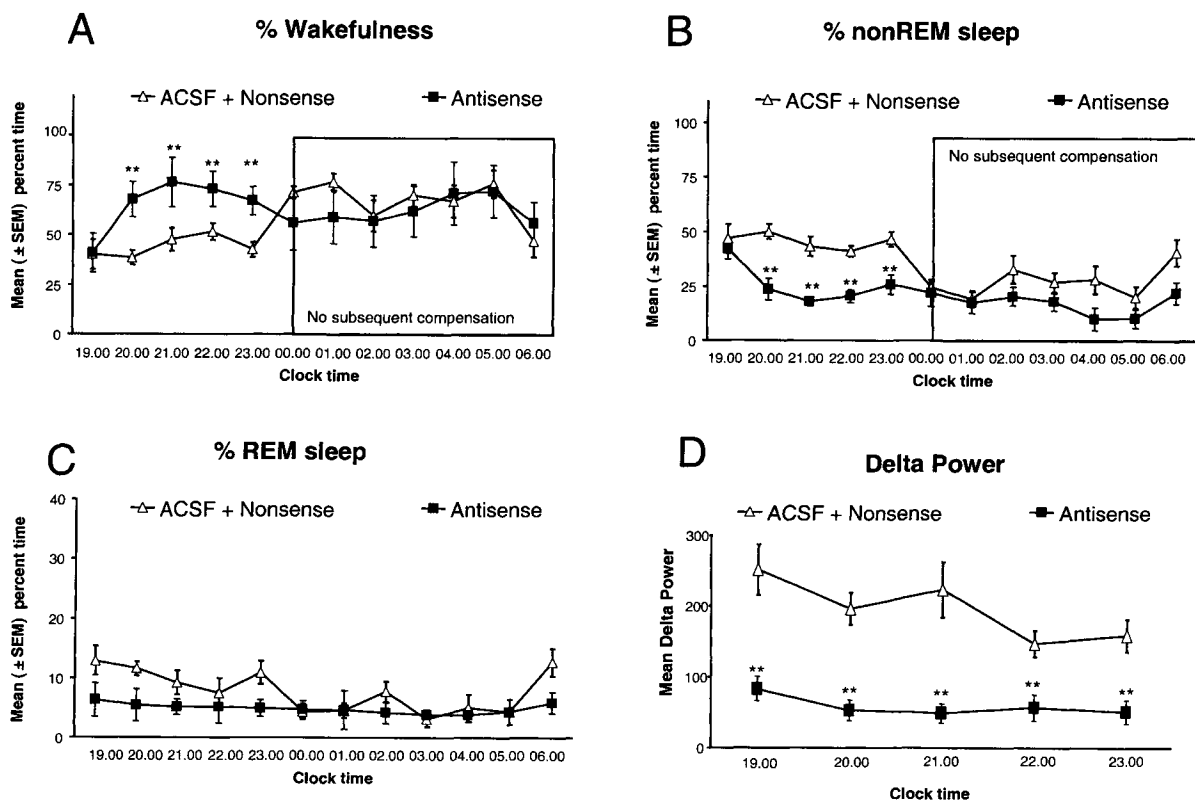


Figure 13.5. Effects of basal forebrain perfusion of antisense oligonucleotides against the mRNA of the adenosine A1 receptor compared with controls (ACSF and nonsense pooled) on recovery sleep following 6 hr of sleep deprivation in rats. Note increased wakefulness (Panel A) and decreased non-REM sleep (Panel B) during the first 5 hr of the recovery sleep period in the antisense group as compared with controls. There was a significant increase in wakefulness and a decrease in non-REM sleep during the 2nd, 3rd, 4th, and the 5th hour. REM sleep (Panel C) did not show significant differences. The right part of the graphs (within box) shows that, for the

subsequent 7 hr, there was no compensation for the antisense-induced changes in wakefulness and non-REM. Ordinate is mean % time spent in each behavioral state (\pm SEM) and abscissa is time of day, with lights off occurring at 1900 hr and lights on occurring at 0700 hr. Panel D describes differences in delta power (1–4 Hz, Mean \pm SEM) for the antisense and the control group for the first 5 hr of recovery sleep. Note the significant decrease in the delta activity in antisense treated animals during each of the 5 hr of recovery sleep as compared to the pooled controls (** = $p < 0.01$). Adapted from Thakkar *et al.*, 2003b.

Fig. 13.3 above). Together, these observations suggested a rather strong site-specific somnogenic effect of adenosine in basal forebrain, with a lesser effect in neocortex. The section on intracellular signaling below describes the A1 selectivity of this pathway.

In contrast to the findings of the A1 receptor knock-down just described, mice with a constitutive A1 receptor knockout did not show a reduced non-REM sleep and delta activity following deprivation [44]. Stenberg *et al.* note that possible determinants of this unexpected finding were the mixed and variable genetic background of the mice and developmental compensation, perhaps with another adenosine receptor compensating. Based on the

presence of some overlap in the effects of the A3 and A1 receptor, the authors of this volume suggest the A3 receptor might possibly compensate (see Section 13.1.5 below). An inducible knockout would help obviate developmental compensatory factors (Scammell *et al* 2003).

13.1.4.2. Receptor Mediation of Adenosine Effects: The A2A Subtype and the Prostaglandin D2 System

The adenosine A2A receptor subtype mediates sleep-related effects in the subarachnoid space below the rostral basal forebrain, but not in the basal forebrain parenchyma. In the subarachnoid space data suggest that there is prostaglandin D2 (PGD2) receptor activation-induced release of adenosine which exerts its somnogenic effects via the A2A adenosine receptor, as documented in a series of studies by the Osaka Bioscience Institute investigators and collaborators [45]. Data supporting the somnogenic effects of PGD2 have been reviewed by Hayaishi [46]. PGD2 has been implicated as a physiological regulator of sleep because PGD2 is the major prostanoid in the mammalian brain and the ICV infusion of femtomolar amounts per minute of PGD2 induced both non-REM and REM sleep in rats, mice, and monkeys. Sleep promoted by PGD2 was indistinguishable from natural sleep as judged by several electrophysiological and behavioral criteria, in contrast to sleep induced by hypnotic drugs.

The PGD2 link to adenosine to exert its somnogenic effects is apparently mediated by PGD2 receptors in the leptomeninges in the subarachnoid space ventral to the basal forebrain [47]. Infusion of the A2A agonist CGS 21680 (0.02 to 20 pmol/min) in the subarachnoid space of rats for 6 hr during their active period (night) induced SWS sleep in a dose-dependent manner [48]. Infusion at the rate of 20 pmol/min was effective during the first night, but became ineffective 18 hr after the beginning of infusion, resulting in a wakefulness rebound and almost complete insomnia during the first and second days of infusion, a finding attributed to A2A receptor desensitization [49]. These data provide pharmacological evidence for the role of the A2A receptor in mediating the somnogenic effects of PGD2 [48]. Moreover infusion of PGD2 into the subarachnoid space increased the local extracellular adenosine concentration, although dose-dependency was not described in this preliminary (abstract) communication [50]. Scammell *et al.* [51] found robust Fos expression in the basal leptomeninges, as well as the VLPO of rats treated with subarachnoid CGS 21680. The mediator and pathway for leptomeningeal activation of VLPO Fos

- [45] For example, Matsumura *et al.* (1994); Urade and Hayaishi (1999); Mizoguchi *et al.* (2001); Scammell *et al.* (2001); Hayaishi (2002).
[46] Hayaishi (2002).

- [47] Mizoguchi *et al.* (2001).

- [48] Satoh *et al.* (1996, 1998, 1999).

- [49] Gerashchenko *et al.* (2000).

- [50] Mochizuki *et al.* (2000).

- [51] Scammell *et al.* (2001).

expression is currently unknown. Scammell *et al.* [51] speculated, "Stimulation of leptomeningeal cells by an A2a receptor agonist could induce production of a paracrine mediator that activates nearby VLPO neurons, and studying the effects of PGD2 and A2A receptor agonists on isolated or cultured leptomeningeal cells may help define this local signal," a possibility illustrated in Fig. 13.6. These authors suggested that presynaptic inhibition of VLPO might be effected by this paracrine mediator; however, the extant data on presynaptic inhibition of VLPO neurons implicate adenosine [52], and this effect is likely A1-mediated. Scammell *et al.* [51] noted that data did not support an alternate hypothesis of A2A effects being mediated by the shell of the nucleus accumbens, since, in reviewing the pattern of Fos-immunoreactive neurons from previous work with PGD2 [53], they could not identify any change in accumbens Fos expression with infusion of PGD2 (Fig. 13.6).

Data indicate that the PGD2–Adenosine A2A system plays a special role in pathological conditions affecting the leptomeninges and producing alterations in sleep. Roberts and coworkers [54] reported that the endogenous production of PGD2 increased up to 150-fold in patients with systemic mastocytosis during deep sleep episodes. Subsequently, the PGD2 concentration was shown to be elevated progressively and selectively up to 1,000-fold in the cerebrospinal fluid (CSF) of patients with African sleeping sickness [55]. It is possible that the A2AR system is specialized for the mediation of sleepiness that occurs with leptomeningeal inflammation in contrast to the more homeostatically regulated A1 system.

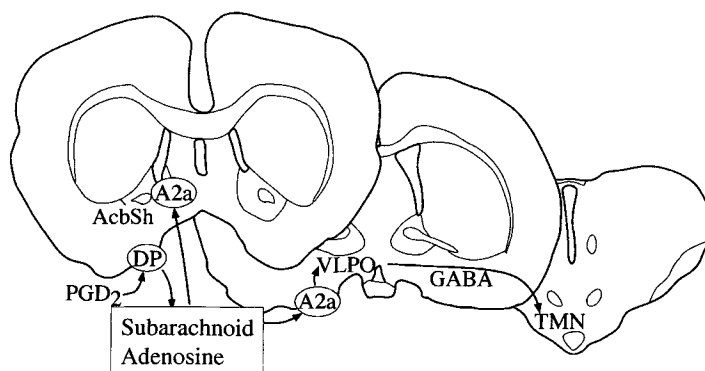


Figure 13.6. Potential mechanisms through which prostaglandin D2 (PGD2) and adenosine A2a receptor agonists may promote sleep. PGD2 may bind to PGD2 (DP) receptors in leptomeningeal cells that increase the concentration of adenosine in the subarachnoid space. This adenosine then binds to A2a receptors in the leptomeninges or in the shell of the accumbens nucleus. Through synaptic or paracrine signals, these regions then activate sleep-active neurons in the ventrolateral preoptic area (VLPO) that inhibit the tuberomammillary nucleus (TMN) and other arousal regions via GABAergic projections. Adapted from Scammell *et al.*, 2001.

[52] Morairty *et al.* (2004).

[53] Scammell *et al.* (1998).

[54] Roberts *et al.* (1980).

[55] Pentreath *et al.* (1990).

It is useful to mention that in the cholinergic basal forebrain, only A1 but not A2A receptor mRNA (*in situ* hybridization and reverse-transcription coupled polymerase chain reaction (RT-PCR) studies) and protein (receptor autoradiography) have been detected [56]. These data provide strong evidence that in HDB/SI/MCPO area of cholinergic basal forebrain the effects of adenosine on sleep–wake behavior are mediated through the A1 adenosine receptor, in contrast to the A2A receptor found in the leptomeninges.

[56] Basheer *et al.* (2001a).

13.1.5. Adenosine A1 Receptor-Coupled Intracellular Signal Transduction Cascade and Transcriptional Modulation

Introduction. Prolonged waking or sleep restriction produces progressive, additive effects such as decreased neurobehavioral alertness, decreased verbal learning, and increased mood disturbances, often referred to as “sleep debt” [4, 57]. These effects are cumulative over many days and thus, unlike the shorter term effects described in previous sections, are likely to have sleep deprivation or restriction-induced alterations in transcription as a basis for these long-term effects. The next sections describe investigations of the adenosine signal transduction pathways that may be responsible for the relevant transcriptional alterations.

[57] Drummond *et al.* (2000); Van Dongen *et al.* (2003).

The sleep-deprivation induced presence, over several hours, of increased extracellular adenosine in the cholinergic basal forebrain suggested the utility of investigating the intracellular effects of A1 receptor activation that involved second messenger actions impacting activation of protein kinases and transcription factors that alter gene expression. A series of reports from the Basheer/McCarley laboratory have demonstrated that A1 adenosine receptors on cholinergic neurons activate a signal transduction pathway mobilizing intracellular stores of calcium that impacts intracellular changes in enzyme activities, transcription factor activation, and gene expression. A schematic of the postulated pathway is presented in Fig. 13.7 so as to help orient the reader. The initial part of the cascade is consistent with reports that the A1 adenosine receptor, coupled to the inhibitory Gi3 subtype of G-protein, is capable of “dual signaling,” that is, inhibition of adenylate cyclase and stimulation of phospholipase C (PLC) [58]. Also, Biber *et al.* [59] have shown that increased expression and/or stimulation of A1 receptor results in PLC activation that, in turn, activates protein kinase C (PKC) via the production of the second messenger inositol trisphosphate (IP3) [60].

[58] Gerwins and Fredholm (1992); Freund *et al.* (1994); Biber *et al.* (1997).

[59] Biber *et al.* (1997).

[60] Berridge (1993); Fisher (1995).

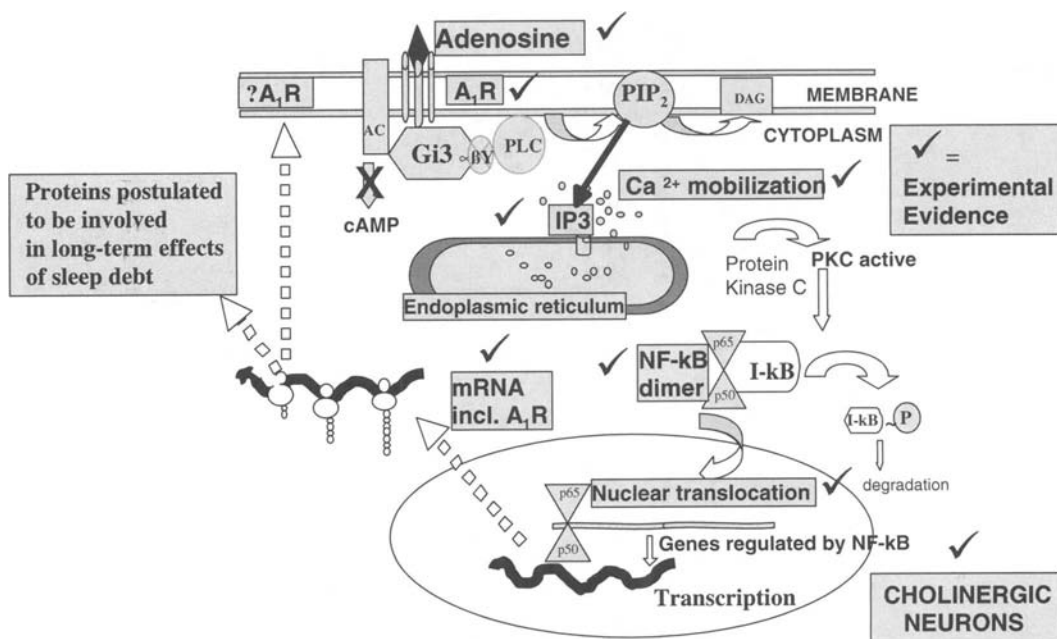


Figure 13.7. Model of intracellular signaling pathway of the adenosine A1 receptor in the cholinergic basal forebrain. In brief, Adenosine binds to the A1 receptor subtype, proceeds through a second messenger pathway producing IP3 receptor-mediated intracellular calcium increase and leading to an activation of the transcription factor NF-κB. The activated NF-κB

translocates to the nucleus and binds to the promotor regions of genes, one of which is the gene for A1 receptor. See text for a description of the steps in the pathway and supporting experimental evidence. The checks in the figure indicate steps for which supporting evidence is present. Basheer and McCarley, unpublished figure.

In basal forebrain adenosine mobilizes intracellular calcium predominantly via A1 adenosine receptor. Real-time changes in intracellular calcium in individual neurons were measured in 300 μm thick acute brain slices of basal forebrain using multiphoton microscopy. Adenosine treatment (100 μM) induced an increase in cytoplasmic calcium reaching a maximum of 4–6 fold increase in 45 s [61] (Fig. 13.8A). This increase was closely matched with an A1 selective agonist, CHA (100 nM) whereas the A2A selective agonist, N6-[2-(3, 5-dimethoxyphenyl)-2-(methylphelyl)-ethyl] adenosine (DPMA, 100 nM) did not produce significant change. The A3 selective agonist, 4-aminobenzyl-methylcarbonyl-beta-D-ribofuranosyl-adenine (AB-MECA, 1 μM), produced a smaller but significant increase (Fig. 13.8B). Thus, the adenosine-induced calcium increase appears to be primarily mediated by the A1 receptor.

Adenosine mediates mobilization of calcium from intracellular stores via the IP3 receptor. An intracellular origin for the cytoplasmic calcium response to adenosine was indicated by (1) its presence in the absence of calcium in the external medium and (2) absence with pretreatment of slices with thapsigargin to deplete the cells of internal stores.

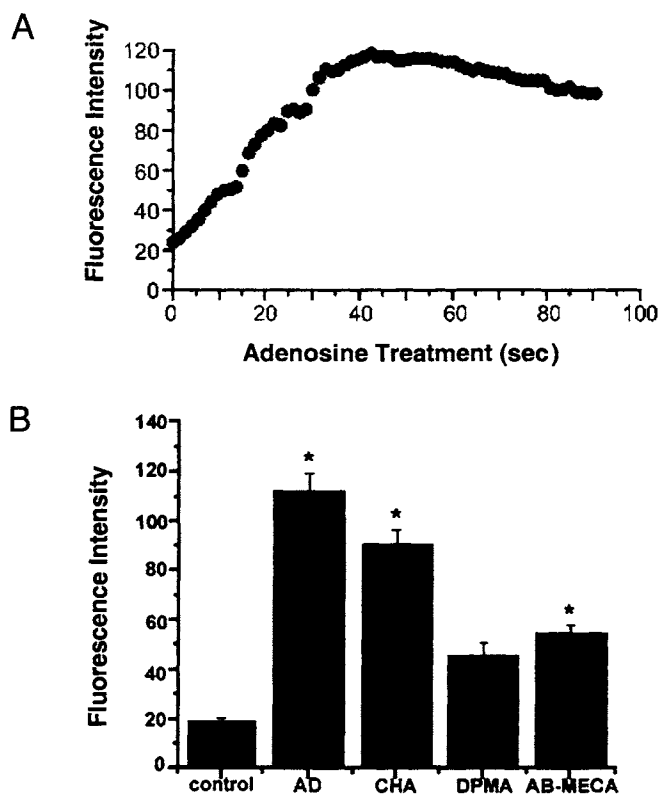


Figure 13.8. Adenosine-mediated mobilization of cytoplasmic calcium via binding to the A1 receptor. Panel A shows a typical time course of calcium increase, measured as increase in calcium orange fluorescence in a live neuron in an acute slice after treatment with 100 μ M adenosine (measurements with a two-photon microscope). Panel B: The significant 5-fold increase in intracellular calcium produced by adenosine was closely approximated by treatment with the A1 agonist CHA treatment (both p 's < 0.01) but treatment with the A2 agonist DPMA had no significant effect. Treatment with the A3 agonist AB-MECA produced a smaller, but still statistically significant (p < 0.05), fluorescence increase than the A1 agonist (* = p < 0.05). The adenosine effect was partially blocked by pretreatment with an A1 antagonist, and completely blocked by pretreatment with an A1 plus an A3 antagonist (not illustrated). Abbreviations: AD, Adenosine; CHA, Cyclohexyladenosine; DPMA, N6-[2-(3,5-dimethoxyphenyl)-2-(methylphenyl)-ethyl] adenosine; AB-MECA, 4-aminobenzyl-methylcarbonyl-beta-D-ribofuranosyladenine. Adapted from Basheer *et al.*, 2002.

A major source of internal calcium in neurons is the stores present in the elaborately distributed network of the endoplasmic reticulum, with both IP3 and ryanodine receptors mediating calcium release from this internal source [62]. Blocking the IP3 receptor with Xestospongine C, a potent cell permeable blocker of IP3 receptor [63], or with 2-aminoethoxydiphenylborane (2APB), a functional and membrane permeable IP3 receptor antagonist [64], prevented calcium increase. However, blocking the ryanodine receptor with 1,1'-diheptyl-4,4'-bipyridinium did not have any effect. These observations suggest that mobilization of intracellular calcium is mediated via IP3 receptors and not ryanodine receptors.

[62] Kostyuk and Verkhratsky (1994); Simpson *et al.* (1995).
[63] Gafni *et al.* (1997).
[64] Hamada *et al.* (1999).

[65] Gritti *et al.* (1993);
Semba (2000); Zábrosky
et al. (1999).

Adenosine-mediated mobilization of intracellular calcium occurs almost exclusively in cholinergic neurons. The basal forebrain contains cells with several neurotransmitter phenotypes, including cholinergic, GABAergic, glutamatergic, and peptidergic [65]. A long-standing conundrum is the relative role of cholinergic and noncholinergic neurons in mediation of basal forebrain control of wakefulness. Interestingly, immunohistochemical labeling of basal forebrain sections for the cholinergic marker ChAT showed that all the cells responding to adenosine by mobilizing intracellular calcium were cholinergic in nature (Fig. 13.9A) and 65% of all the cholinergic cells examined

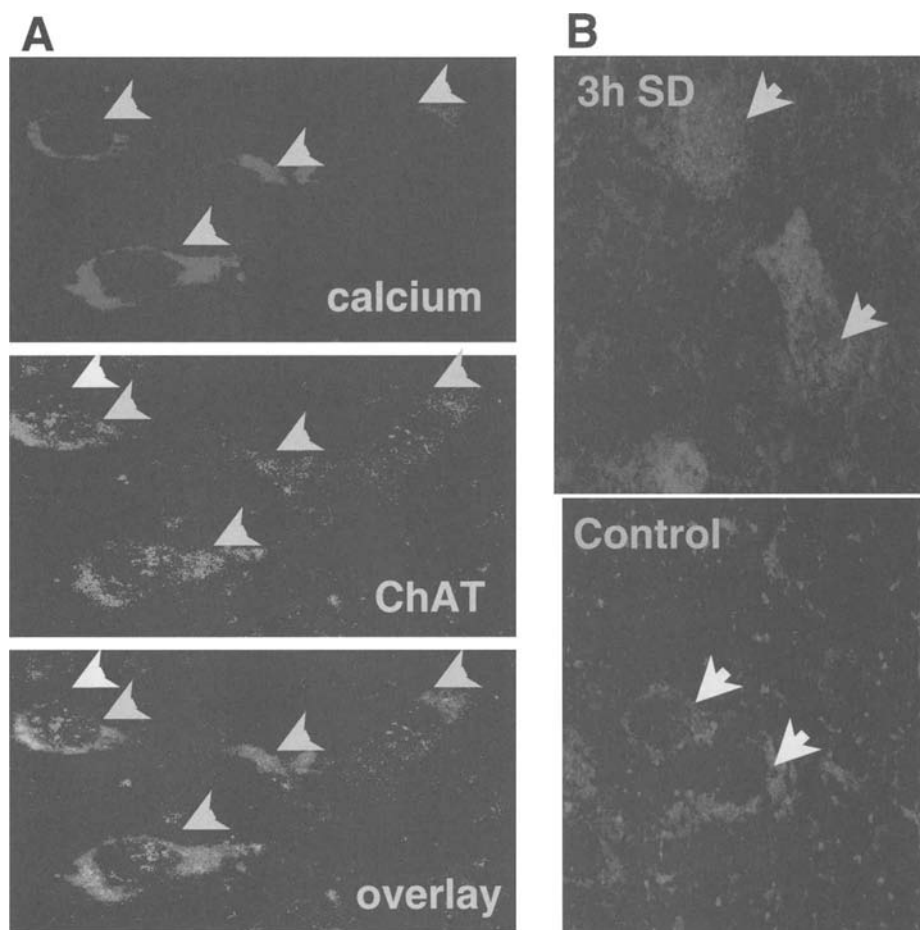


Figure 13.9. Panel A. Adenosine-induced cytosolic calcium increase was seen only in cholinergic neurons of basal forebrain. The neurons that showed an increase in calcium (orange fluorescence) after 60 s treatment with adenosine were also positive for ChAT (green fluorescence) (yellow arrowheads). One cholinergic neuron (white arrowhead) does not show calcium orange fluorescence. (Adapted from Basheer *et al.*, 2002). Panel B: Nuclear translocation of NF- κ B following 3 hr sleep deprivation (SD). Overlay of double-labeled neurons for ChAT (red fluorescence) and NF- κ Bp65 (blue fluorescence) in rat basal forebrain section. After 3 hr of SD (sleep deprivation) there is nuclear translocation of NF- κ B (blue in the nucleus, yellow arrowhead) which is not seen in sleeping controls (bottom panel, hollow nucleus, white arrowhead) (Basheer, Ramesh, McCarley, unpublished data). See also color plate 6.

showed an increase in intracellular calcium in response to adenosine. There is preliminary evidence that sleep deprivation induced nuclear translocation of NF- κ B is also limited to cholinergic neurons [66] (Fig. 13.9B). These observations thus present evidence for a selective activation of an adenosinergic pathway in a subset of BF cholinergic neurons in response to increased levels of extracellular adenosine. This suggests the possibility of a functional role of cholinergic cells in the response to sleep deprivation.

Adenosine intracellular signaling and transcriptional alterations: Introduction. A common functional feature of inhibitory receptors (such as the A1R) is their rapid attenuation in response to agonists, the most common response being receptor downregulation, that is, loss of receptors from the cell surface following prolonged exposure to their agonists [67]. Recent evidence also indicates the presence of upregulation of receptors following exposure to agonists [68]. The receptor-coupled effector pathways regulate the synthesis and stability of receptor mRNA as clearly demonstrated for receptors of substance P, β -adrenergic, serotonin, (5-HT₂), somatostatin, (SST2A) [69], and neurotensin, (NT1) [68]. Thus, prolonged presence of agonists results either in the downregulation of its receptor in order to reduce the response to the over abundant agonist or upregulation for continued maintenance of cell sensitivity to the increasing levels of endogenous agonists.

Sleep deprivation-induced increase in A1 receptor mRNA in basal forebrain. To examine A1 receptor regulation in response to sleep deprivation-induced elevated levels of adenosine, Bashen *et al.* [56] investigated the ligand binding efficiency and mRNA of adenosine A1 and A2A receptors. *In situ* hybridization and RT-PCR of total RNA from basal forebrain and cingulate cortex showed that 6 hr of sleep deprivation resulted in significant increases in A1 receptor mRNA in basal forebrain, but not in cortex (Fig. 13.10). This upregulation of mRNA in basal forebrain was accompanied by unchanged levels of A1 receptor ligand-binding efficiency and overall receptor density after 6 hr of sleep deprivation. A2a mRNA and ligand binding was undetectable in this region [56]. Thus, increased mRNA and absence of any decrease in ligand binding for A1 receptor suggested that sleep deprivation-induced increase in extracellular adenosine might be upregulating the levels of A1 receptor in order to maintain steady levels of receptor density and continued response to the agonist, adenosine. The physiological significance of the sleep deprivation-induced upregulation of A1 receptor mRNA in basal forebrain is not yet clear. The neuroprotective effects of adenosine have been suggested to involve

[66] Ramesh *et al.* (2002).

[67] Bohm *et al.* (1997); Grady *et al.* (1997).

[68] Souzae (2001).

[69] For substance P see Hershey *et al.* (1991); for β -adrenergic see Collins *et al.* (1992); for serotonin (5-HT₂) see Rydelek-Fitzgerald *et al.* (1993); for somatostatin (SST2A) see Boudin *et al.* (2000).

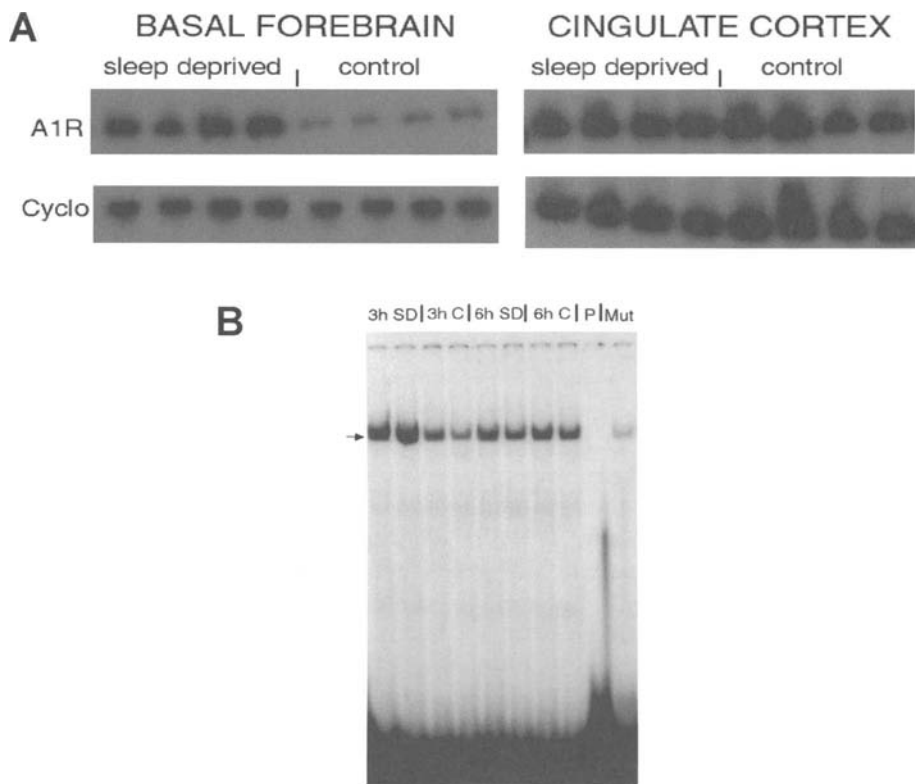


Figure 13.10. Effects of sleep deprivation on A1 receptor mRNA and NF-kB DNA binding activity in basal forebrain of rat: Panel A shows the autoradiograph of RT-PCR product for the A1 receptor and the housekeeping gene cyclophyllin mRNA from basal forebrain and cortex of sleep deprived and control rats. In basal forebrain, A1 receptor mRNA levels are higher than the sleeping control. No significant change was observed in cortex. Panel B: Gel shift assays of the crude nuclear extracts of basal forebrain shows that NF-kB DNA binding is higher after 3 hr of sleep deprivation compared to controls. SD, sleep deprived; C undisturbed circadian control; P probe only loaded, Mut, mutant oligonucleotide. Modified from Basheer *et al.*, 2001a.

[70] Biber *et al.* (2001).

upregulation of A1 receptor in cortical astrocytes [70]. It seems evident that prolonged sleep deprivation might act to enhance the sleep-inducing effects of a given level of extracellular adenosine concentrations beyond that observed before the deprivation, a “resetting of the set point” or positive feedback that would further promote sleepiness.

[71] O’Hara *et al.* (1993); Cirelli *et al.* (1995); Basheer *et al.* (1997); Chen *et al.* (1999).

Sleep deprivation-induced nuclear translocation and DNA binding activity of NF-kB. There are many reports of sleep deprivation-induced increase in transcription factors [71]. One of the documented transcription factors that binds to the A1R promoter region and enhances transcription of the A1 receptor (among many other proteins) is NF-kB [72]. Adenosine, acting via the A1 receptor, has been shown to activate a signal transduction pathway leading to PKC activation. Activation of PKC is known to impact many downstream events including phosphorylation of inhibitory protein I-kB and the release of NF-kB allowing

[72] Nie *et al.* (1998).

its translocation to the nucleus [73]. Indeed there is a sleep deprivation-induced activation of NF- κ B, evinced by an increase in DNA binding of NF- κ B, in the basal forebrain but not in the control region of cingulate cortex (Fig. 13.10B). In *in vitro* slices the adenosine-induced DNA binding of NF- κ B was significantly blocked by pretreatment with the A1 receptor antagonist CPT, suggesting that A1 receptor activation might be responsible for the NF- κ B activation [74]. In summary, sleep deprivation resulted in the upregulation of A1 receptor mRNA and increased NF- κ B DNA binding in basal forebrain. Moreover, pharmacological evidence indicated that the activation of NF- κ B was mediated via A1 receptor activation.

As outlined in Fig. 13.7, the data delineated an adenosinergic pathway, starting from its binding to the A1 subtype adenosine receptor, proceeding through a second messenger pathway producing IP₃ receptor-mediated intracellular calcium increase and leading to an activation of the transcription factor NF- κ B. These studies are of interest since NF- κ B has been reported to have a role in regulating the expression of several sleep regulatory substances, such as interleukin-1 beta (IL-1 beta), tumor necrosis factor alpha (TNF alpha), nitric oxide synthase, and cyclooxygenase-2 (COX-2), as discussed in the next section of this chapter [75]. The role of NF- κ B in the positive feedback regulation of the adenosine A1 receptor is currently being investigated. Basheer *et al.* (unpublished data) have found that blocking translocation of NF- κ B by a cell-permeable inhibitor protein (IP) prevents the increase in ADAIR mRNA in the cholinergic basal forebrain that occurs following 3 hr sleep deprivation. The IP was SN 50 (amino-acid sequence, AAVALLPAVLLALLAPVQRKRQKLMP) and the control peptide (CP) was SN (amino-acid sequence, AAVALLPAVLLALLAPVQRNGQKLMP). The CP and IP were prepared in ACSF and were microinjected unilaterally. Double-labeling immunohistochemistry of cholinergic basal forebrain sections demonstrated that sleep deprivation-induced nuclear translocation of NF- κ B occurred almost exclusively in cholinergic neurons in the side contralateral to IP injection and in rats injected with a CP, confirming earlier findings that sleep deprivation-induced NF- κ B translocation in the cholinergic basal forebrain was confined to the cholinergic neuronal population. Since Adenosine A1 receptor-mediated mobilization of calcium from intracellular stores was also observed exclusively in cholinergic neurons [61] the current data provide further supporting evidence that adenosine A1-mediated calcium release leads to activation of NF- κ B in cholinergic neurons. Only about one-third of the entire cellular population of the cholinergic basal forebrain is cholinergic [76] while almost all cells express

[73] Siebenlist *et al.* (1994); McKinsey *et al.* (1997).

[74] Basheer *et al.* (2001b).

[75] Borbély and Tobler (1989); Opp and Krueger (1991, 1994); Krueger and Majde (1994); Xie *et al.* (1994); Yamamoto *et al.* (1997).

[76] Gritti *et al.* (1993); Jones and Mühlethaler (1999).

the adenosine A1 receptor. The finding that IP treatment produced a reduction of 19% in adenosine A1 receptor mRNA in the entire tissue volume, suggested that there was approximately a 57% reduction in adenosine A1 receptor mRNA in cholinergic neurons, since only the cholinergic neurons show NF- κ B translocation. This percentage is hence highly compatible with the observed sleep deprivation-induced nuclear translocation of NF- κ B in 75–80% of cholinergic neurons. This evidence thus provides more support for the intracellular signaling pathway outline in Fig. 13.7.

13.1.6. Sleep-Mediated Alterations in Behavior: Possible Relationship to Adenosine-Induced Changes in the Basal Forebrain Cholinergic System

In the basal forebrain, both cholinergic and noncholinergic neuronal activity are associated with promoting wakefulness [77]. The somnogenic effects of adenosine may be due to the inhibition of neuronal activity in both cholinergic and noncholinergic neurons of the basal forebrain. In addition, the modulatory effects of sleep deprivation on the A1 adenosine receptor mRNA and transcription factor NF- κ B activation in the cholinergic basal forebrain, suggest the significance of an adenosiner-gic pathway in the long-term effects of sleep deprivation on the quality of ensuing sleep and/or neurobehavioral alertness, cognitive functions, and mood. The cholinergic neurons in HDB/SI/MCPO target the entorhinal cortex, neocortex, and amygdala and regulate aspects of cognition and attention, sensory information processing, and arousal [78]. Cognitive functions such as learning and memory show a correlated decline with degenerating cholinergic neurons, as reported in Alzheimer's patients [79]. Wiley *et al.* [80] developed a technique involving 192IgG-saporin-induced lesioning of p75 nerve growth factor (NGF) receptor containing cholinergic cells in rats. The cholinergic lesions using this technique resulted in severe attentional deficit in a serial reaction-time task [81]. The cholinergic basal forebrain is important in cortical arousal. Animals with lesioned basal forebrain show decreased arousal and increased slow waves in cortex [82]. The effects of adenosine on cholinergic basal forebrain are thus potentially important as the related sleep deprivation-induced "cognitive" effects may be mediated through adenosine. As an initial step, the effects of sleep deprivation on five choice serial reaction time behavior in the rat have

[77] Lo Conte *et al.* (1982); Szymusiak (1995); Jones (1993, 1998, 2003b); Semba, (2000).

[78] Nagai *et al.* (1982); Pearson *et al.* (1983); Gallagher and Holland (1994); Sarter and Bruno (1997, 2000); Everitt and Robbins (1997).

[79] See reviews by Everitt and Robbins (1997); Wenk (1997); Baxter and Chiba (1999); Perry *et al.* (1978).

[80] Wiley *et al.* (1991).

[81] Muir *et al.* (1996); McGaughy and Sarter (1998).

[82] Buzsáki and Gage (1989); Berntson *et al.* (2002).

been examined. Preliminary data [83] on this selective attention task indicate a sleep deprivation duration-dependent decrease in accuracy, an increased response latency, and increased omitted responses but a decreased impulsiveness (premature responses). These resemble effects of deprivation in man and are highly compatible with the effects of basal forebrain cholinergic lesions (saporin) in rats [81], but direct microdialysis acetylcholine measurements in rats will be needed to prove a relationship with decreased cholinergic activity.

[83] Cordova *et al.* (2003).

13.2. Cytokines and Other Humoral Factors

Overview of this section. Early experiments on humoral factors relied on transfer of substances from sleep-deprived animals including the classic experiments of Ishimori [84] and of Legendre and Pieron [85], as did the pioneering work of Pappenheimer [86] which directly led into the current investigations of the cytokines, including IL-1 beta. However, transfer experiments do not currently play a role in this field. We have just discussed AD and PGD2 in terms of adenosine mediation of its effects. Other major factors include IL-1 beta and TNF alpha, discussed in detail below, and, to a somewhat lesser extent, growth hormone releasing hormone (GHRH). They promote non-REM sleep in various species, inhibition of their action or endogenous production results in loss of spontaneous sleep, and their synthesis and/or release display variations correlating with sleep-wake activity. Although the source of these substances vary, they all may be characterized as primarily enhancing sleep by acting in the basal forebrain/anterior hypothalamus-preoptic region. It is also characteristic of these substances that they interact in multiple ways, often resulting in mutual stimulation or potentiation of each other. Finally, there is a third group of substances whose significance in sleep regulation is less clear but for which there is some evidence suggesting that they may have a role in modulating non-REM sleep. In addition to nitric oxide, this group includes oleamide, cortistatin, cholecystokinin (CCK), uridine, and insulin and are not further discussed in this chapter but are reviewed in detail in Obal and Krueger [87]. This section first discusses the cytokines (IL-1 beta and TNF alpha) in some detail and then takes up GHRH and concludes with a brief discussion of somatostatin and its role in inhibiting GHRH.

[84] Dialysates of brain homogenates, reviewed in Inoué (1989).

[85] CSF, serum, and emulsion of cerebral cortex, Legendre and Pieron (1913).

[86] Miller *et al.* (1967).

[87] Obal and Krueger (2003), the present chapter draws on the information in this review.

13.2.1. Introduction and Overview of the Cytokines: Interleukin-1 Beta and Tumor Necrosis Factor Alpha (IL-1 Beta and TNF Alpha)

[88] Krueger has commented, "Every substance thus far identified as being part of the sleep regulatory cascade also has additional biologic activities. This issue of specificity of response elicited by substances within multiple pleiotropic redundant pathways is a central problem in biology. A major challenge to sleep research is to define how and where these molecular steps produce sleep." Krueger *et al.* (1998).

[89] Breder *et al.* (1988, 1993).

[90] See Saper and Sawchenko (2003).

[91] This is a controversial area. The review by Vitkovic *et al.* (2000) summarizes the studies showing and not showing IL-1 in neurons (strongest evidence in hypothalamus, cortex has mixed results), with weaker evidence for TNF alpha. These authors conclude that the evidence is equivocal for genes in neurons coding for these factors. Renauld and Spengler (2002) present evidence in cultures of primary hippocampal neurons and of tumor cells for TNF mRNA in the cells and protein in the supernatant following alpha 2 adrenergic receptor activation and potassium depolarization. Ringheim *et al.* (1995) found evidence for IL-6 mRNA in cultured murine cortical neurons.

[92] Krueger and Obal (2003).

Cytokines act in autocrine, paracrine, and endocrine systems to regulate important facets of the immune response, such as the acute phase response, where they trigger constitutional symptoms of acute illness such as malaise as well as behavioral manifestations such as somnolence, anorexia, fever, and social withdrawal. Most aspects of the acute phase immune response are driven by a complex array of cytokines in association with classical stress hormones. Cytokines have also been hypothesized to be involved in processes such as sleep, food intake, development, and gastrointestinal function.

A difficulty facing sleep researchers is disambiguating the sleep-related control features of the cytokines from those involved in immune and stress responses, both of which increase cytokine production. There seems to be little doubt that the cytokines are responsible for the somnolence accompanying immune responses (see below) and the evidence for the cytokines' role in sleep independent of the immune response has been detailed [87]. However the involvement of cytokines in multiple processes and their complicated interactions make clear-cut conclusions about mechanism of action difficult. Fig. 13.11 summarizes this complexity of interaction [88].

An important issue with cytokines is their cellular origin in the brain. There is ample evidence of their origin in glia (see below), but data on their origin in neurons is less strong due to uncertainties of immunostaining. Although early studies suggested that both IL-1 beta and TNF alpha can be localized to neurons in the brain with immunocytochemistry [89], it has been difficult to confirm these observations with other antisera or by *in situ* hybridization histochemistry (Saper, personal communication, January 2004), and these older results were not subject to the modern criterion that immunostaining should be abolished in genetic knockout animals [90]. Because these and other cytokines can be expressed by microglial cells and by astrocytes, the presence of cytokines in neurons in normal brains and under pathological conditions must be considered with caution [91].

Krueger and Obal [92] have stated a theory of local generation of sleep in brain regions active in wakefulness. Their theory of sleep function and generation postulates that cytokines serve a key role in local generation of sleep.

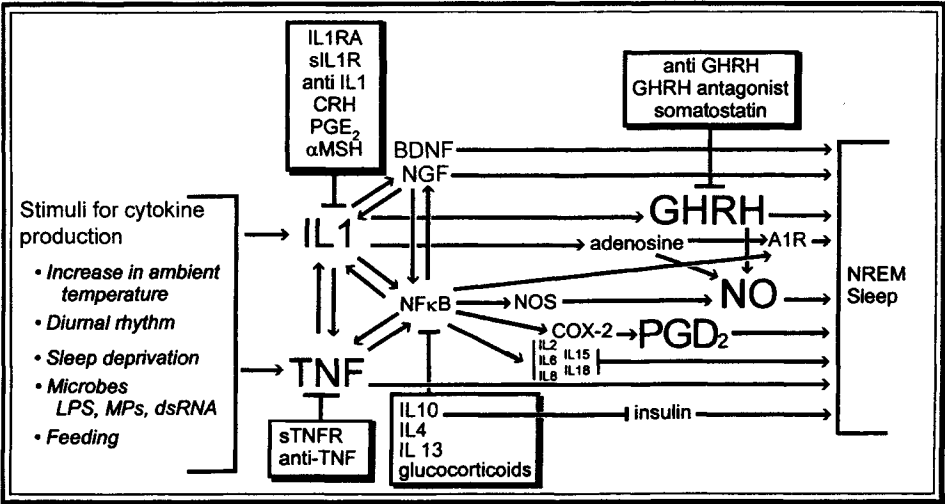


Figure 13.11. Interleukin (IL)-1 beta and TNF alpha are part of the cascade of events involving several other endogenous somnogenic substances and sleep inhibitory substances. Substances in boxes inhibit non-REM sleep and inhibit either the production of or action of substances in the somnogenic pathways. Note that inhibition of any one step does not result in complete sleep loss. Krueger and colleagues postulate that animals compensate for the loss of any one step by relying on parallel somnogenic pathways and that these redundant pathways provide stability to the sleep regulatory system as well as alternative mechanisms by which a variety of sleep-promoting or sleep inhibitory stimuli may affect sleep. Solid arrow indicates stimulation; solid line indicates inhibition. Courtesy of Dr. J. Krueger.

The theory postulates that cellular electrical activity within neuronal groups (use-dependent activity) leads to the production of cytokines which act as sleep-promoting substances within the local neuronal network. The somnogenic cytokine growth factors induce molecules necessary for synaptic connectivity, thereby changing the synaptic activation patterns within neuronal groups, inducing changes in the input–output relationships of neuronal groups and causing a neuronal group state shift. Altered input–output relations result in increased efficacy of some synapses. Sleep is thus targeted to active neuronal groups and functionally serves to incorporate novel stimulus patterns into a synaptic contextual network and also to preserve that network. After the neuronal group state shift, environmental input is divorced from output. Sleep is useful to keep the animal stationary at a time when its brain is most dysfunctional.

We note that the very small amounts of cytokines produced has made it difficult to test the theory of localized, use-dependent production of cytokines by direct measurement of their production, although Section 13.2.3 below discusses the use of cytokine inhibitors [93]. As reviewed below, in addition to this “local” theory of sleep, Obal and Krueger [87] also postulate that cytokines may act to induce sleep through more centralized sleep control systems [94].

[93] A potential problem in the mechanism of the state-shifting paradigm is that lasting synaptic connectivity change would require a longer time duration than the six or fewer hours of sleep deprivation required to cause the sleep synchronization effects. We note that, even without neuronal localization, cytokines could be produced by glia as a result of neuronal activity, and thus the neuronal locus of production does not appear critical to this theory, although it makes the mechanism more complex. [94] Krueger and Majde (2003) have a thoughtful review of the major research questions and issues in cytokines and sleep.

[95] Krueger *et al.* (1984).

[96] Takeuchi and Akiara (2001).

[97] Reviewed in Sporri *et al.* (2001).

[98] For example, Breder *et al.* (1988); as discussed above, evidence for neuronal production of IL-1 beta is not strong.

[99] Reviewed in Krueger *et al.* (2001).

[100] Krueger (1990).

[101] Opp *et al.* (1991); Susic and Totic (1989).

[102] Opp *et al.* (1991).

IL-1 beta has a molecular weight of about 17 kD, and was the first cytokine for which sleep-promoting activity was described [95]. There are two IL-1 receptors, Types I and II, and the three IL-1 ligands (alpha, beta, and the antagonist, IL-1 RA) bind to both receptors, although only the beta ligand appears to have substantial sleep promoting properties. The receptors are part of the Toll-like receptor family [96] with other members of this family also contributing to host defense and perhaps probably to sleep as well. (*Drosophila* Toll protein is a transmembrane receptor whose function is to recognize the invasion of microorganisms as well as to establish dorsoventral polarity.) The Type I receptor is the signal transduction receptor, triggering complex signaling cascades leading to NF-kB activation, activation of mitogen-activated protein kinases and PKC, as well as induction of other second messengers including intracellular calcium (see below), cAMP, and ceramide [97]. IL-1 beta is produced by glia and endothelial cells and the receptors are also found on a variety of cell types, including neurons [98]. The steps in the release of IL-1 beta with respect to sleep-cycle control are poorly defined, although release with inflammation and infection is well documented. As discussed above, while "use-dependent release" of IL-1 beta has been postulated to occur, there is no direct evidence.

Injection of IL-1 beta either directly into brain areas, ICV, intravenously (IV), or intraperitoneally (IP) enhances SWS [99] and also produces hyperthermia. Hyperthermia itself may increase SWS, but blocking the hyperthermic effects of IL-1 beta does not block the non-REM sleep-inducing effects [100]. The argument that IL-1 beta is important in the hypersomnia associated with infections is thus strong.

The sleep-promoting effects have complex dependencies on injection dose and timing. In rats and cats low doses of IL-1 beta promote non-REM sleep while higher doses inhibit non-REM sleep [101]. Moreover, some doses of IL-1 beta promote non-REM sleep after nighttime injections while the same dose given during the day suppresses this sleep phase [102]. In addition to enhancing the duration of non-REM sleep, IL-1 beta also induces enhanced EEG slow-wave activity [95].

As illustrated in Fig. 13.12, Obal and Krueger [87] suggest that the somnogenic effects of IL-1 beta occur both through local action and also through effects on other somnogenic systems in the brain, including stimulation of sleep-active neurons in the POAH, upregulation of the GHRH system, stimulation of PGD2 production,

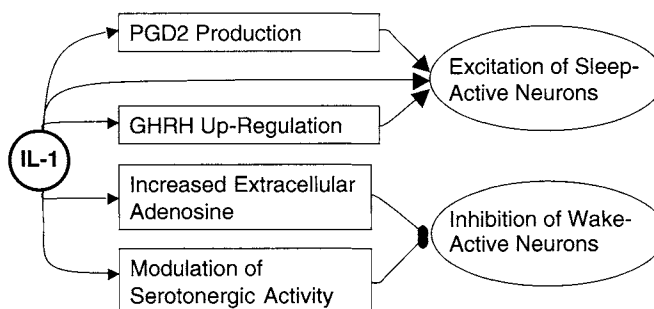


Figure 13.12. Hypothesized mechanisms of action of IL-1 in production of non-REM sleep. Note there are both local actions on sleep-active neurons as well as activation of other systems important in non-REM sleep. Adapted from Obal and Krueger, 2003.

modulation of 5HT activity in the DRN, and enhancement of adenosine release. The strongest evidence for adenosine release is in hippocampus where, *in vitro*, application of IL-1 beta decreased glutamate neurotransmission, an effect obviated by pharmacological blockade of adenosine A1 receptors, and thus suggestive of adenosine release; the authors proposed that the adenosine release may have been mediated by the metabolic effects of IL-1 beta [103]. Injection of IL-1 beta into the locus coeruleus (LC) [104] or dorsal raphe [105] induces enhanced non-REM sleep. In contrast application of IL-1 beta into the hypothalamic PVN induces wakefulness [106] perhaps through activation of the corticotropic system. In a more extensive study, IL-1 beta injection into several ventricular sites and subarachnoid sites resulted in enhanced sleep [107]. The most active sites were those in close proximity to the anterior hypothalamus. Within the anterior hypothalamus/preoptic area, there is preliminary (abstract) data indicating IL-1 beta excites sleep-active neurons and inhibits wake-active neurons [108].

Mutant mice lacking the IL-1 type I receptor do not exhibit sleep responses if given IL-1, thereby implicating the type I receptor in IL-1 beta-induced sleep responses; these mutant mice also have less spontaneous non-REM sleep than their control strain and this effect is greatest during dark hours [109].

Brain levels of IL-1 or IL-1 beta mRNA vary with sleep propensity. CSF levels of IL-1-like activity in cats vary with the sleep-wake cycle [110]. In rats, highest hypothalamic levels of IL-1 beta and IL-1 beta mRNA occur at the beginning of daylight hours, a time when rat non-REM sleep is maximal [111]. Further, sleep deprivation results in enhanced hypothalamic IL-1 mRNA levels [112]. In humans, peak levels of IL-1 occur at sleep onset, and levels also increase during sleep deprivation [113].

[103] Luk *et al.* (1999).

[104] De Sarro *et al.* (1997).

[105] Imeri *et al.* (2002).

[106] Slisli and De Beaurepaire (1999).

[107] Terao *et al.* (1998).

[108] Alam *et al.* (2001).

[109] Fang *et al.* (1998).

[110] Lue *et al.* (1998).

[111] For IL-1 beta see Nguyen *et al.* (1998); for IL1 beta mRNA see Taishi *et al.* (1997).

[112] Mackiewicz *et al.* (1996).

[113] e.g. Uthgenannt *et al.* (1995).

[114] Nguyen *et al.* (1998).

Relevant to the task of disambiguating stress effects from sleep control aspects of IL-1, the Nguyen *et al.* [114] study found that stress increased IL-1 beta protein in hypothalamus and hippocampus but not in cerebellum or posterior cortex. However, without stress there was a clear diurnal rhythm in these regions, compatible with an IL-1 beta role in sleep control. These data do suggest the need to consider the possibility of stress-induced effects in sleep deprivation experiments looking at effects on cytokines.

The site(s) of action of IL-1 beta responsible for sleep remains to be determined in a definitive way. Results from microinjection studies suggest that IL-1 beta may act at multiple action sites (Fig. 13.10), while there is an extensive literature implicating the anterior hypothalamus for the site of IL-1-induced fevers as well as suggestions that diurnal variations are also localizable to the hypothalamus (e.g., see 114).

13.2.3. Tumor Necrosis Factor Alpha (TNF Alpha)

[115] Kriegler *et al.* (1998).

TNF alpha is synthesized as a 26 kD membrane associated protein [115]. Soluble TNF alpha, a 17 kD protein, is cleaved from the 26 kD membrane associated protein by TNF alpha converting enzyme. TNF alpha production is tightly regulated in a tissue-specific manner [116] with transcription, translation, and secretion all controlled at multiple points.

[116] Reviewed by Spriggs *et al.* (1992).

[117] Breder *et al.* (1993);
Cheng *et al.* (1994).

TNF alpha is expressed by microglia and astrocytes, with some limited evidence for its presence in neurons (see above); it has a variety of biological actions in the central nervous system including a role in mediating brain damage and in neuroprotection [117]. TNF alpha, like IL-1 beta, may serve as either a neuroprotective or cell death agent, although the neuroprotective function dominates. Both TNF receptors signal by recruitment of cytosolic proteins via protein-protein interaction domains. The receptor type (55 or 75 kD) and associated intracellular protein adaptor molecules are likely important determinants of cellular specificity of action [118]. TNF alpha participates in mediating whole organism processes including fever and food intake [119]. The effects of systemic bacterial products such as endotoxin may also involve TNF. For instance, in humans, endotoxin doses that induce transient increases in sleep also induce concomitant increases in circulating TNF alpha [120]. TNF alpha also plays a role in brain development and plasticity [121].

[118] See, for example,
Yang *et al.* (2002).

[119] For fever see Saper
and Breder (1992); for
food intake see Plata-
Salaman (2000).

[120] Haack *et al.* (2001).

[121] Merrill (1992).

[122] Shoham *et al.* (1987).

The ability of TNF alpha to promote non-REM sleep was first described in 1987 by Shoham *et al.* [122]. TNF enhances non-REM sleep when given to mice, rats, rabbits,

or sheep [87, 123]. Its inhibition results in reduced spontaneous non-REM sleep and reduced sleep rebound after sleep deprivation [124]. TNF mRNA levels and TNF protein vary in the hypothalamus and cerebral cortex with sleep propensity; for example, highest levels occur in rats at the onset of daylight hours, the rat sleep period [125]. Sleep deprivation increases hypothalamic TNF alpha mRNA, brain expression of the 55 kD TNF receptor mRNA, and circulating levels of TNF and the 55 kD TNF soluble receptor, and in healthy humans blood levels of TNF alpha correlate with EEG slow wave activity [87].

Several disorders which affect sleep are associated with elevated TNF and sleepiness, including sleep apnea, AIDS, and chronic fatigue patients; the sleep response to endotoxin also may be related to the higher levels of TNF elicited by this substance [87].

Mice lacking the TNF 55 kD receptor sleep less than corresponding control strains; the reduced non-REM sleep occurs mostly during daylight hours [126]. In contrast, mice lacking the IL-1 Type I receptor sleep less than controls during dark hours [109].

Krueger and Obal [92] suggest that TNF alpha, like IL-1 beta, may be produced as a consequence of use-dependent neuronal activity and thus may be one of the factors providing local control of sleep. In addition, Obal and Krueger [87] cite studies indicating that TNF likely acts on other sleep-wake systems including PGD2, LC, and the pre-optic area, where microinjection of TNF alpha enhanced and a TNF alpha inhibitor suppressed spontaneous non-REM sleep in rats. Yoshida *et al.* [127] have demonstrated in rats that ipsilateral cortical injections of TNF alpha increase slow-wave activity and delta power on the injected side. Moreover, sleep deprivation-induced increased slow wave activity and delta power are ipsilaterally attenuated on the side of the microinjection of an inhibitor of TNF alpha action, TNF soluble receptor, as illustrated in Fig. 13.13.

[123] Dickstein *et al.* (1999).

[124] Takahashi *et al.* (1996).

[125] Bredow *et al.* (1997);
Floyd and Krueger (1997).

[126] Fang *et al.* (1997).

[127] Yoshida *et al.* (2004).

13.2.4. Other Humoral Systems

13.2.4.1. Growth Hormone Releasing Hormone (GHRH)

GHRH-containing neurons reside in the arcuate nucleus (Arc), around the ventral surface of the ventromedial nucleus (periVMN), and in the parvicellular portion of the PVN. The GHRH released from terminals in the median eminence is taken up by the blood and is carried into the anterior pituitary where it stimulates GH secretion. A much smaller number of GHRHergic neurons are found

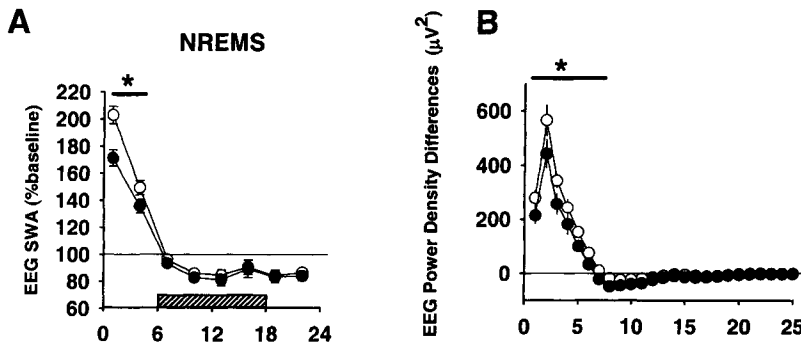


Figure 13.13. The TNF soluble receptor (TNFSR) attenuates sleep-deprivation enhancements of EEG slow-wave power. A: EEG Slow Wave Activity (SWA) during non-REM sleep (NREMS). B: Power spectrum analyses of data obtained in hours 0–6 post sleep deprivation. The power (μV^2) for each rat in each 1-Hz frequency bandwidth was determined on a saline baseline day and on another day after sleep deprivation plus unilateral TNFSR injection. Open circles represent values obtained from the noninjection side after sleep deprivation minus values obtained from that same side during the baseline day. Closed circles are values obtained from the TNFSR-injected side after sleep deprivation minus values obtained from the same side during the baseline day. * indicates $p < 0.05$. The bars indicate the frequencies at which the significant differences occurred. Wake and REM slow-wave activity and delta power were not affected. Adapted from Yoshida *et al.*, 2004.

around the VMN, close to the Arc nucleus, and in the parvicellular portion of the PVN. These extraarcuate GHRHergic neurons seem to innervate the PVN and the anterior hypothalamus/preoptic area (POAH). Promotion of sleep is the function of intrahypothalamic GHRH action: microinjection of GHRH into the POAH enhances non-REM sleep, whereas administration of a GHRH antagonist into this region inhibits spontaneous non-REM sleep and recovery after sleep deprivation [128]. That diurnal and sleep deprivation-induced changes in GHRH mRNA are detected in the periventricular and paraventricular neurons suggests that the extraarcuate GHRHergic neurons are important for sleep regulation, although some intraarcuate neurons may innervate the hypothalamus and thus may also modulate sleep. There is relatively little direct information on cellular and membrane effects of GHRH in the POAH, although GHRH has been reported to increase cytosolic calcium in GABAergic cultured hypothalamic neurons obtained from fetal rats [129].

There is considerable evidence in a number of species that injections of GHRH promote non-REM sleep [87]. Data also indicate that decreases in GHRH lead to decreases in SWS. Suppression of endogenous GHRH actions by means of immunoneutralization of GHRH [130] or by means of a competitive antagonist [131] is followed by decreases in SWS. SWS decreases are found in mutant dwarf rats (dw/dw rats) [132] and, in preliminary (abstract) data, in mice (lit/lit mice) with GHRH receptor deficiencies [133], and in transgenic mice with decreased GHRH production [134].

[128] Zhang *et al.* (1999).

[129] Churchill *et al.* (2002).

[130] Obal *et al.* (1992).

[131] Obal *et al.* (1991).

[132] Obal *et al.* (2001).

[133] Alt *et al.* (2002).

[134] Hajdu *et al.* (2002).

With respect to response to sleep deprivation, immunoneutralization of GHRH blocks the non-REM sleep response to a 3-hr sleep deprivation in rats [130]. Further, deprivation-induced increases in EEG slow-wave activity are greatly attenuated in the dw/dw rats with a defect in GHRH receptor signaling [132]. However, the sleep responses to sleep deprivation are essentially normal in the lit/lit mouse (4-hr sleep deprivation) with nonfunctional GHRH receptors [87]. Recovery sleep after 12 hr of sleep deprivation is also normal in the transgenic Mt-rGH mice, which express rat GH stimulated by the promoter region of the metallothionein gene, although these mice have less GHRH [134]. The cause of these differences is currently not known but suggests that mediation of the sleepiness following sleep deprivation is not likely a primary function of the GHRH system.

With respect to function, the GHRH system is capable of synchronizing the anabolic processes of the body to a state when rest occurs, and, indeed, most GHRH release occurs during the first part of the sleep phase. However the precise nature of regulation of this system, for example, potential feedback through the GHRH system about anabolic needs and the subsequent transmission to POAH, remains unclear.

13.2.4.2. Somatostatin

Somatostatin is a cyclic peptide found both in pancreas and in the gastrointestinal system as well as in brain. While there are other brain actions, its suppressive effects on non-REM sleep appear to be mediated by its inhibition of GHRH-containing neurons. Somatostatinergic neurons that project to hypothalamic GHRH neurons and to their terminals in the median eminence are located in the periventricular nucleus while somatostatinergic interneurons act on GHRH neurons in the Arc nucleus [135]. Somatostatin also inhibits the release of growth hormone by GHRH. As in the case of GHRH, the details of how this particular system might be regulated with respect to sleep function are currently unclear.

[135] See data and review in Lanneau *et al.* (2000).

13.3. The Ventrolateral Preoptic Area (VLPO) and Active Control of Sleep

13.3.1. Identification of Sleep-Active Neurons in the VLPO

Based on his neuropathological observations on patients who were victims of the encephalitis lethargica

[136] von Economo
(1930).

epidemic at the time of World War I, von Economo [136] predicted that the anterior region of the hypothalamus near the optic chiasm would be found to contain sleep-promoting neurons, whereas the posterior hypothalamus would contain neurons that promote wakefulness. Indeed, electrophysiological recordings of basal forebrain/anterior hypothalamic neurons indicated that some of these neurons selectively discharge during non-REM sleep, and this might represent an active sleep-promoting mechanism although the precise anatomical localization remained unclear [137].

[137] For review see
Szymusiak (1995).
[138] Sherin *et al.* (1996).

In 1996 Sherin and colleagues [138] used Fos immunohistochemistry in the hypothalamus to identify sleep-active neuron cells, which were found to be clustered in the VLPO area. As shown in Fig. 13.14, the extent of Fos immunoreactivity was directly proportional to the duration of time the experimental animals slept, regardless of circadian phase. An important feature of the data was that the animals that failed to fall asleep following sleep deprivation showed little or no Fos expression in the VLPO, indicating this area was not involved in the induction of non-REM sleep, in contrast to adenosine, but rather the maintenance of this state.

[139] Sherin *et al.* (1998).

Double labeling with the retrograde tracer cholera toxin B showed that these neurons projected to the tuberomammillary nucleus. This nucleus is the locus of the histamine neurons that are selectively active in arousal and may comprise an important element of arousal systems. Nearly 80% of the retrogradely labeled VLPO neurons contained both the GABA-synthesizing enzyme glutamic acid decarboxylase (GAD) and the peptide galanin [139]. Electron microscopy confirmed that the VLPO terminals onto tuberomammillary nucleus (TMN) neurons were immunoreactive for GABA and made symmetric synapses. VLPO neurons also innervated, although less intensely, the dorsal and median raphe nuclei and the LC [140]. Fig. 13.15 Part A schematizes the most important VLPO efferent connections and Part B summarizes the afferents.

[140] See also Steininger
et al. (2001).

Since Fos expression does not necessarily imply increased discharge activity, it is important that chronic microwire recordings in the lateral POA found that neurons with increased discharge rates during sleep compared with wakefulness were most densely located in the same VL hypothalamic region, the VLPO, as those with Fos expression [141] (Fig. 13.16). Following sleep deprivation, VLPO neuronal discharge rates during non-REM sleep were increased, but discharge rates in wakefulness were not changed, thus agreeing with the Fos data indicating that VLPO neuronal activation is related to sleep

[141] Szymusiak *et al.*
(1998).

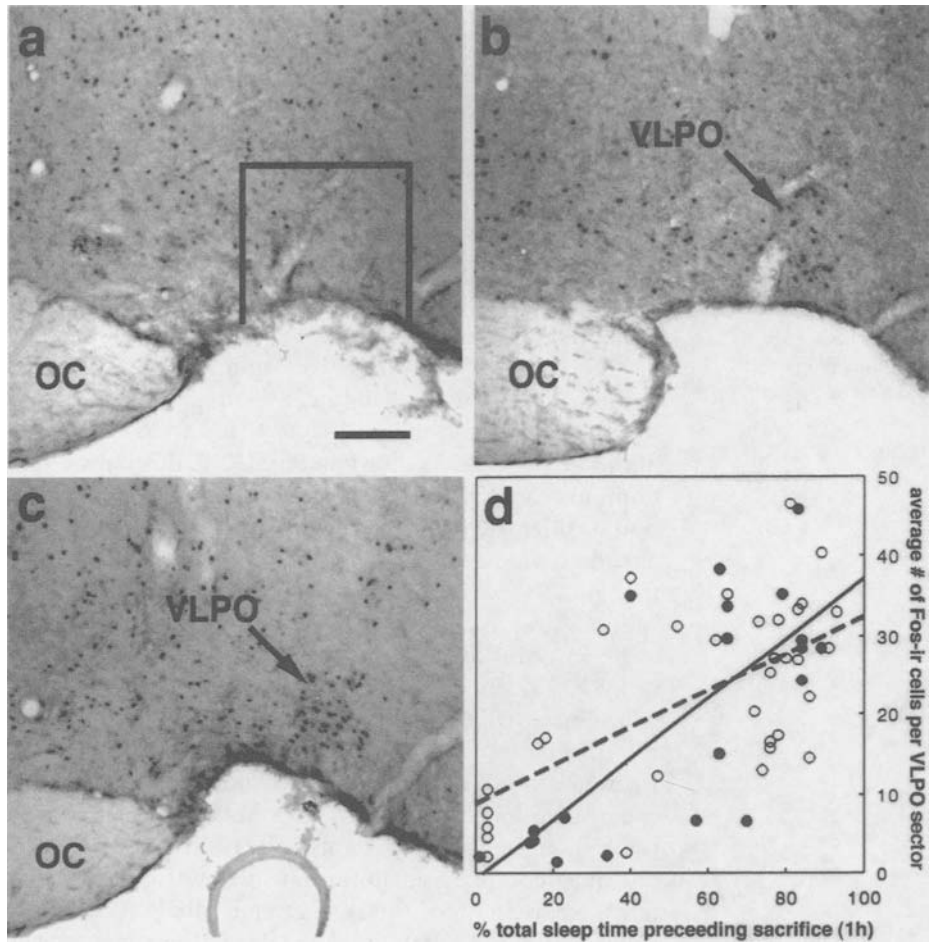


Figure 13.14. Panels a through c are Fos-immunostained coronal sections through the preoptic hypothalamus of freely behaving rats that slept 15% (a) and 63% (b) and a sleep-deprived rat that slept 83% (c) of the hour before they were killed. Panel d is the correlation between the number of Fos-immunoreactive (Fos-ir) cells counted in each preoptic sector containing the ventrolateral preoptic area (VLPO) (shown in a) and % total sleep time for the freely behaving rats (closed circles, solid regression line, $r = 0.74$, $p < 0.0001$) and sleep-deprived rats (open circles, dashed regression line, $r = 0.70$, $p < 0.0001$). OC, optic chiasm. Scale = 150 μ M. Modified from Sherin *et al.*, 1996.

occurrence and not to sleep propensity. For the group of VLPO neurons with increased discharge rate during sleep vs wakefulness, mean non-REM and REM sleep discharge rates did not differ. Szymusiak and colleagues [141] noted that increased discharge from the non-REM sleep-selective neurons tended to increase prior to the onset of sleep, leading to a postulate that these neurons might play a role in sleep induction. This finding is not easily reconciled with the Fos data in which animals with sleep deprivation but no sleep did not show increased Fos expression.

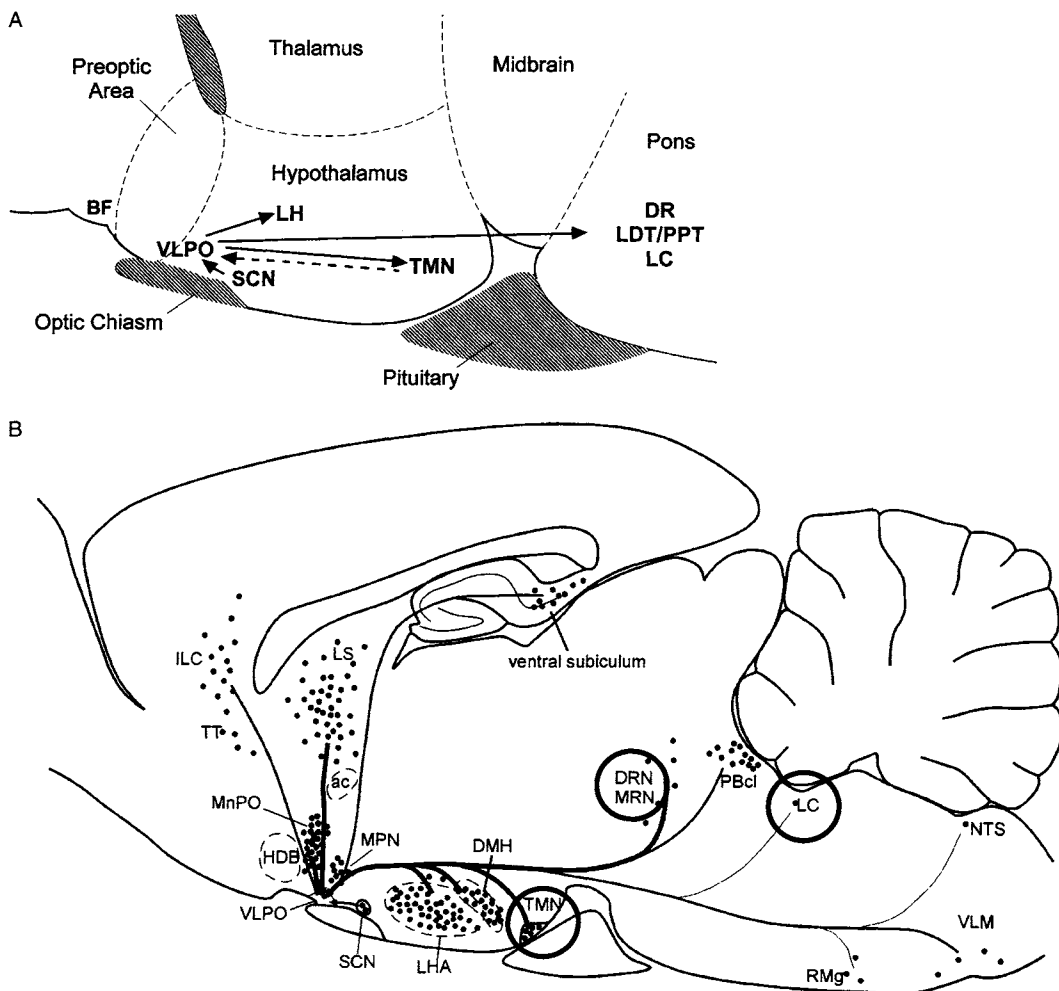


Figure 13.15. Panel A. Schematic of a sagittal section of the basal forebrain and hypothalamic areas in the mammalian brain showing important ventrolateral preoptic area (VLPO) connections. Note projections to brainstem sleep–wake related centers and to lateral hypothalamus. Only two efferents are indicated here: very strong histaminergic input from the tuberomammillary nucleus (TMN) and the polysynaptic input from suprachiasmatic nucleus (SCN). Unpublished figure, C. Sinton and R. McCarley. Panel B furnishes more detail. Sagittal summary diagram of the afferents to the VLPO. Major regions projecting to the VLPO are indicated by dots, with one dot indicating roughly 10 retrogradely labeled neurons (counted in every fifth section, average of 3 cases). *Line thickness* roughly indicates intensity of varicosity density in VLPO core, which does not always correlate with density of retrograde labeling. Circles indicate the sources of greatest densities of varicosities labeled for arousal neurotransmitters or

anterograde tracer in the VLPO core. Because the ventral subiculum does not appear in the sagittal level shown, retrogradely labeled neurons in the ventral subiculum are depicted more dorsally than they appear in the brain. Adapted from Chou *et al.*, 2002. Abbreviations for panels A and B: VLPO, ventrolateral preoptic area; LH or LHA, lateral hypothalamus area; DMH, Dorsomedial hypothalamic nucleus; TMN, tuberomammillary nucleus; BF, basal forebrain; MnPO, Median preoptic nucleus; MPN, Medial preoptic nucleus; LS, lateral septal nucleus; ILC, Infralimbic cortex; TT, Tenia tecta; ac, anterior commissure; HDB, Horizontal limb of the nucleus of the diagonal band; SCN, suprachiasmatic nucleus (SCN); DR or DRN/MRN, dorsal/median raphe nucleus; PBcl, Parabrachial nucleus, central lateral subdivision; LDT/PPT, laterodorsal tegmental and pedunculopontine tegmental (LDT/PPT); LC, locus coeruleus; RMg, Raphe Magnus; VLM, ventrolateral medulla; NTS, nucleus of the solitary tract.

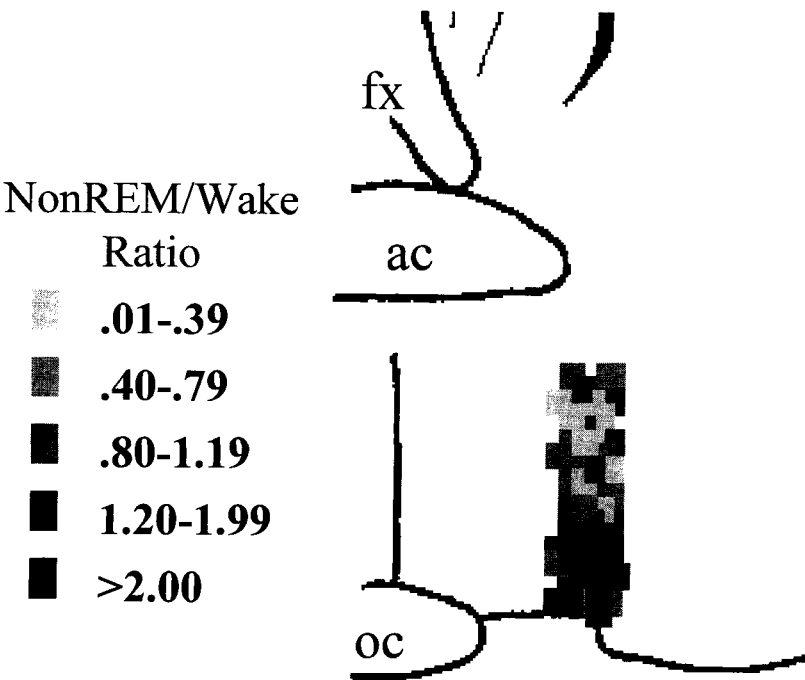


Figure 13.16. Superimposed reconstructions of microwire passes from 7 animals, showing the location and sleep-waking discharge rate ratios of recorded cells, displayed on a drawing of a coronal section through the preoptic-anterior hypothalamic area. The gray scale coding of non-REM/waking discharge rate ratio is shown on the left. Note the concentration of cells with sleep-related discharge in the ventral one-third of the microwire passes. Abbreviations: ac anterior commissure; oc optic chiasm; fx fornix. Modified from Szymusiak *et al.*, 1998.

13.3.2. Lesions of VLPO and the Extended VLPO and Effects on Sleep

To study the effects of cellular loss on sleep, Lu *et al.* [142] made small excitotoxic lesions in the lateral preoptic area by microinjecting ibotenic acid and comparing the numbers of remaining Fos-ir cell bodies in the VLPO cluster and the surrounding area, termed the extended VLPO, with the changes in sleep behavior. In animals with more than 70% bilateral cell loss in the VLPO proper, the amounts of both NREM and REM sleep were reduced by about 55%. The loss of neurons in the VLPO proper correlated closely with the loss of NREM ($r = 0.77$), but did not correlate significantly with loss of REM sleep. However, the loss of Fos-ir neurons in the extended VLPO correlated closely with the loss of REM sleep ($r = 0.74$), but did not show a significant correlation with the loss of NREM sleep. Conversely, when rats were exposed to a period of darkness during the day, a condition that doubles REM sleep time, there was a concomitant increase in Fos expression in the extended VLPO, but not the VLPO cluster

[142] Lu *et al.* (2000).

[143] Lu *et al.* (2002).

[144] Schonrock *et al.* (1991); Yang and Hatton (1997); Seutin *et al.* (1989).

[143] (Fig. 13.17). Retrograde tracing from the LDT, DRN, and LC demonstrated more labeled cells in the extended VLPO than the VLPO cluster, and 50% of these in the extended VLPO were sleep-active. Anterograde tracing showed that projections from the extended VLPO and VLPO cluster targeted the cell bodies and dendrites of DRN serotonergic neurons and LC noradrenergic neurons but that the projections did not target the cholinergic neurons in the LDT. Because galanin and GABA are known to inhibit both TMN and neurons of the LC [144], these projections from the VLPO and extended VLPO are likely to be inhibitory, and, by implication, so are the DRN and cholinergic zone projections.

In summarizing their functional view of these findings, Lu and colleagues in the Saper laboratory [143] propose that, during NREM sleep, the sleep-active neurons in the VLPO cluster inhibit the activity of the cells in the TMN, DRN, and LC by releasing galanin and GABA, thus maintaining SWS. During the transition from NREM to REM sleep, the firing of DRN and LC is further decreased. Lu and colleagues proposed that this transition may be attributable at least in part to the recruitment of inhibitory neurons in the extended VLPO that further decrease LC and DRN firing, thus disinhibiting the LDT and PPT cholinergic cells (see discussion in Chapter 11). In addition, if extended VLPO efferents end on inhibitory interneurons in the LDT/PPT, they could further promote their firing during the transition to REM sleep. The connections of the extended VLPO neurons and their REM active pattern would make them prime candidates to fulfill this role.

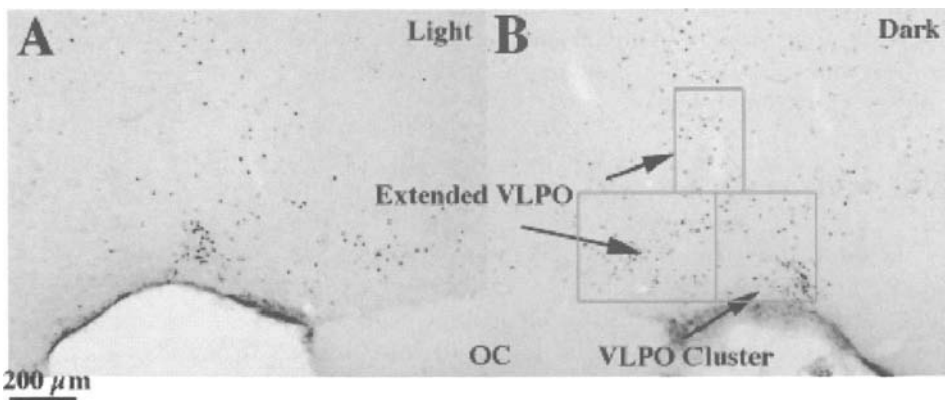


Figure 13.17. A pair of photomicrographs showing the distribution of Fos-immunoreactive cells in the extended VLPO and VLPO cluster in an animal exposed to light (12% REM sleep, A) and in an animal exposed to dark treatment (30% REM sleep, B) during the early part of the sleep cycle. The counting boxes used for VLPO cluster and dorsal and medial extended VLPO are shown in B. These sections are approximately at the level of AP 0.5 in Paxinos and Watson (1986). OC, optic chiasm. Adapted from Lu *et al.*, 2002.

13.3.3. Relationship of VLPO to Other Preoptic Regions and the Suprachiasmatic Nucleus

With respect to other preoptic regions, Gong *et al.* [145] have reported increased Fos expression with spontaneous sleep (09–11 A.M.) compared with forced wakefulness in the rat median preoptic nucleus (MnPO) as well as in VLPO. They postulated that this area, particularly at high ambient temperatures, where Fos expression increased in MnPO, might act in concert with VLPO to promote sleep. Subsequently unit recordings in MnPO by this lab [146] revealed that most neurons showed a heightened discharge in both non-REM and REM sleep and it was hypothesized that this region might, like VLPO, have GABAergic/galaninergic cells that inhibited wakefulness promoting systems. While there is evidence for MnPO projections to monoaminergic nuclei, to VLPO [147], as well as preoptic projections to cholinergic basal forebrain [148], the neurotransmitter identity of MnPO cells is unknown.

The relationship of VLPO to other state control areas is currently under vigorous investigation. The suprachiasmatic nucleus (SCN) projections to the VLPO have been shown to be sparse, but the heavy input to the VLPO from the dorsomedial hypothalamus (DMH), which receives direct and indirect SCN inputs, could provide an alternate pathway regulating the circadian timing of sleep [149]. Other inputs to VLPO include histaminergic, noradrenergic, and serotonergic fibers, lateral hypothalamic area, autonomic regions including the infralimbic cortex and parabrachial nucleus, and limbic regions including the lateral septal nucleus and ventral subiculum. Light to moderate inputs arose from orexin and melanin concentrating hormone neurons, but cholinergic or dopaminergic inputs were extremely sparse.

13.3.4. VLPO and Adenosine

In vitro studies in the rat of VLPO neurons have indicated the presence of inhibitory postsynaptic currents (IPSCs) that were fully blocked by bicuculline suggesting they are GABA-A-mediated events [52, 150]. Adenosine reduced the frequency of spontaneous IPSC's in 11 of 17 VLPO neurons (mean reduction 63%). Chamberlin *et al.* [151] confirmed and extended this effect of adenosine on IPSCs, finding it present with bath application of tetrodotoxin, and occurring in neurons expressing galanin mRNA. Thus, in addition to a possible direct action of anatomically defined inputs to VLPO, it is possible that

[145] Gong *et al.* (2000).

[146] Suntsova *et al.* (2002).

[147] Chou *et al.* (2002).

[148] Cullinan and Zaborszky (1991).

[149] Chou *et al.* (2003).

[150] Strecker *et al.* (2000).

[151] Chamberlin *et al.* (2003).

adenosine might activate VLPO neurons through presynaptic inhibition of GABAergic inhibitory inputs (see Fig. 13.18.) Microdialysis in the cat in the VLPO region provided no evidence of adenosine concentration increases with prolonged wakefulness [23]. However, the VLPO is a small target and it is possible the probe did not

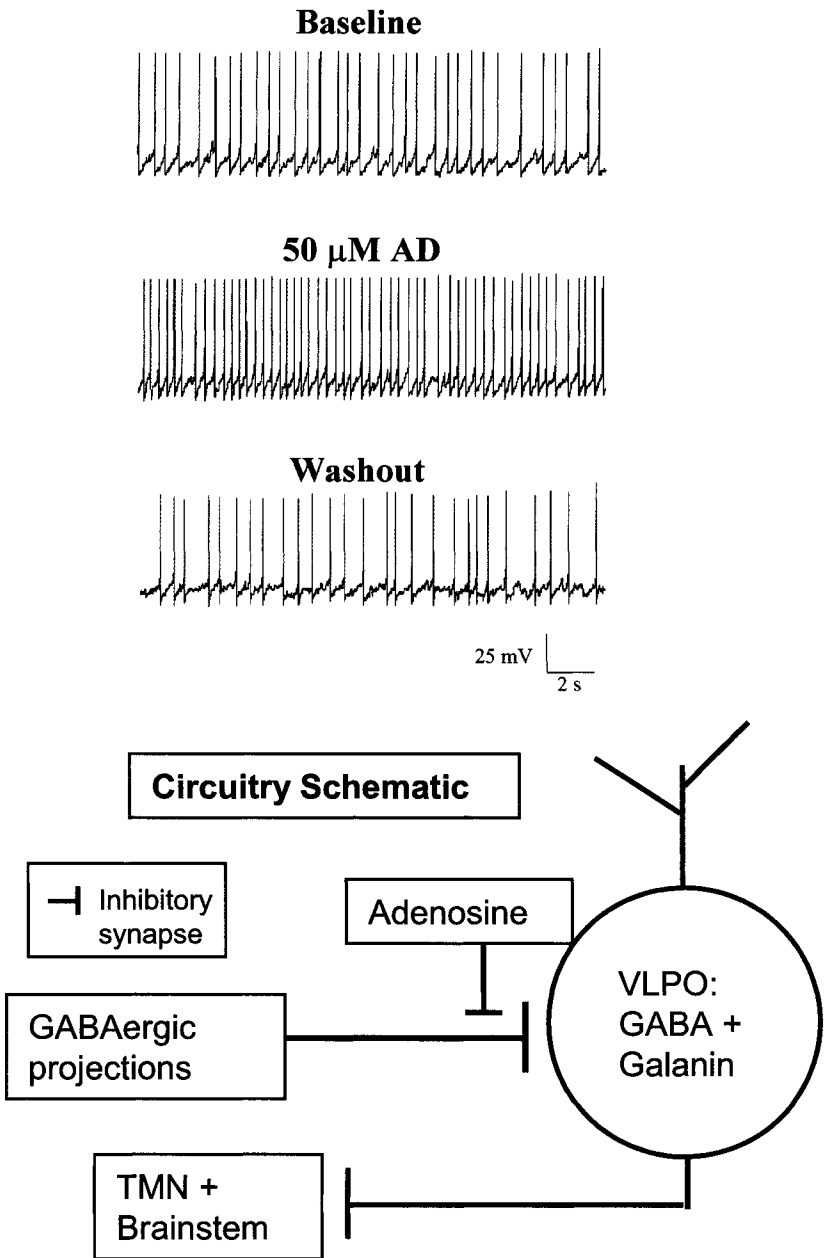


Figure 13.18. Top. Current clamp recording in VLPO. 50 μ M adenosine (AD) increased discharge rate. Since other experiments indicated GABA-mediated IPSCs were prominent, presynaptic inhibition of GABAergic inputs seemed the most likely explanation of this result, as schematised in the bottom portion of the figure. Adapted from Morairty *et al.*, 2004.

precisely or exclusively sample the small VLPO region. As discussed and referenced in Section 13.1.4.2 and illustrated in Fig. 13.6., the Hayaishi laboratory has shown that subarachnoid administration of adenosine or its agonists promotes sleep and induces expression of Fos protein in VLPO neurons.

It is possible that the VLPO GABAergic inputs arise from the lateral hypothalamus or lateral septum [147, 149]. Although the function of the lateral septum neurons is unknown, they receive extensive inputs from the hippocampus, amygdala, midline thalamus, and brainstem monoaminergic arousal system [152] and thus may relay emotional and arousal signals that inhibit VLPO neurons during periods of stress or anxiety. Much work remains to be done to identify the sources of control of VLPO neurons.

[152] Staiger and Nurnberger (1989).

13.3.5. Modeling the VLPO Control of Sleep

The precise mechanism controlling the “turning on” of the VLPO non-REM sleep-active neurons is unknown, although adenosine is a candidate. Disinhibition of VLPO neurons by adenosine should inhibit the monoaminergic ascending arousal system, and thus induce sleep [138–140]. Chou and colleagues recently proposed that mutual inhibition between the VLPO and ascending monoamine systems can act as a bistable “flip-flop” switch [147, 153]. The tendency for each side of the switch to reinforce its own activity by inhibiting the other side may be a mechanism for ensuring rapid state transitions, from wakefulness to sleep and vice versa. By reducing GABAergic inhibition of the VLPO, adenosine may act as a homeostatic sleep signal, tilting the balance toward sleep [154].

[153] Saper *et al.* (2001).
 [154] The presence of the REM cycle in the Jouvett pontine cat transection (Chapter 11) suggests that forebrain is not essential for the REM cycle. One might think of the VLPO as providing a “latch” for non-REM sleep: It does not initiate the state, based on the absence of Fos-ir prior to occurrence of the sleep state. However the strong correlation between the duration of sleep and intensity of Fos-ir suggests that it may maintain the state of non-REM sleep. The “flip-flop” switch analogy of Saper and collaborators seems in accord with this notion since the mechanism, once switched on, remains on. In terms of modeling, it should be noted that bistable mutually inhibitory centers are incapable of generating transitions between states on their own, since they remain in one state until reset by external forces. These forces remain to be identified in the case of the VLPO.

13.4. Orexin/Hypocretin, Narcolepsy, and the Control of Sleep and Wakefulness

13.4.1. Background and Identification of Orexin/Hypocretin

An exciting development in sleep research in the late 1990s was discovery of the important role of neurons principally located in the perifornical and lateral hypothalamus containing the neuropeptide orexin (alternatively known as hypocretin) in behavioral state regulation and narcolepsy/cataplexy. Narcolepsy is a chronic sleep disorder

[155] Aldrich (1998);
Sinton and McCarley
(2001).

[156] Lin *et al.* (1999).

[157] Chemelli *et al.*
(1999).

[158] Mignot (1998).

[159] Nishino *et al.* (2000).

[160] Thannickal *et al.*
(2000).

that is characterized by excessive daytime sleepiness, fragmented sleep, and other symptoms that are indicative of abnormal REM sleep expression; these latter symptoms include cataplexy, hypnogogic hallucinations, sleep-onset REM periods, and sleep paralysis [155]. An abnormality in the gene for the orexin type II receptor has been found to be the basis of canine inherited narcolepsy [156] whereas orexin gene knockout mice ($-/-$) have increased REM sleep, sleep-onset REM periods and also cataplexy-like episodes entered directly from states of active movement [157] (see Fig. 13.19). Cataplexy in canines and rodents consists of attacks of sudden bilateral atonia in anti-gravity muscles, with consequent collapse; these episodes last from a few seconds to a few minutes and are often provoked by emotion or excitement, such as food presentation to dogs [157, 158]. Confirmation in man of orexin's importance has been provided by Nishino *et al.* [159] who reported that narcoleptic humans often have undetectable levels of orexin in CSF, and by Thannickal *et al.* [160] who found an absence or greatly reduced number of orexin-containing neurons in post-mortem studies of individuals suffering

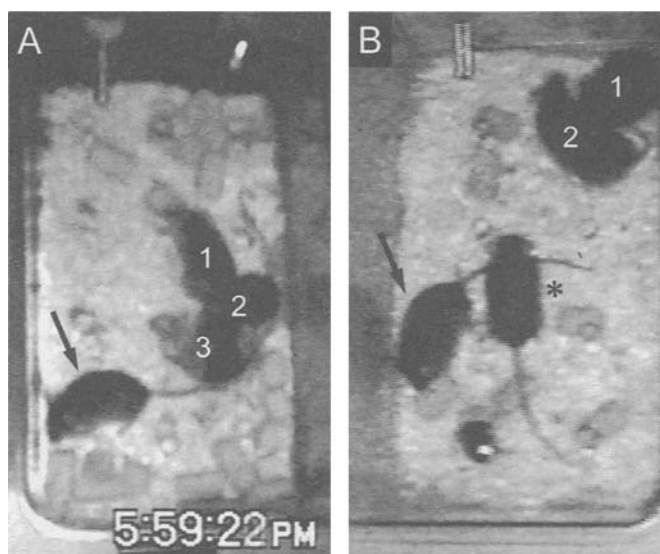


Figure 13.19. Panel A. Digitally captured infrared video image of orexin knockout mice at 4 weeks of age. Note that one mouse (arrow) has completely fallen onto his side in a cataplexy episode (confirmed in other mice by EEG). The film shows the fuzziness (motion artifact) associated with body movement in behaving acting littermates designated 1 to 3. Panel B. Digitally captured infrared video image of orexin knockout mice at 4 weeks of age. Note that one mouse has fallen completely onto his side (arrow), while another is collapsed onto his ventral surface (asterisk). Littermates designated 1 and 2 are quietly sleeping in their usual corner of the cage. In both A and B, the dark (active) phase onset was at 5:30 P.M. and panel B was recorded at 8:26 P.M. (Panels A and B reproduced with permission from Fig. 3 in Chemelli *et al.*, 1999; a video of these episodes is available at <http://www.cell.com/cgi/content/full/98/4/437/DC1>).

from narcolepsy. As well as the control of wakefulness and sleep, orexins may have a neuromodulatory role in several neuroendocrine/homoeostatic functions such as food intake, body temperature regulation, and blood pressure regulation, [157, 161].

In late 1997, orexin/hypocretin was identified by two independent groups. De Lecea *et al.* [162] identified two related peptides, which they termed hypocretin-1 and -2, using a direct tag PCR subtraction technique to isolate mRNA from hypothalamic tissue. Shortly thereafter, and using a different approach, Sakurai *et al.* [163] identified these same two peptides, which they termed orexin-A (= hypocretin-1) and orexin-B (= hypocretin-2). Sakurai *et al.* [163] used a systematic biochemical search to find endogenous peptide ligands that would bind to G protein-coupled cell surface receptors that had no previously known ligand (orphan receptors) [164]. These first two reports indicated that neurons containing the orexins are found exclusively in the dorsal and lateral hypothalamic areas [162, 163], and that the orexins may function as neurotransmitters since they were localized in synaptic vesicles and had neuroexcitatory effects on hypothalamic neurons [162]. Orexin-A and -B are neuropeptides of 33 and 28 amino acids, respectively; they are derived from a single precursor protein.

13.4.2. Orexin Neuronal Projections and Orexin Receptors

As illustrated in Fig. 13.20, immunohistochemical studies revealed a distribution of orexin projections that is remarkable for the targeting of a number of distinct brain regions known to be involved in the regulation of sleep and wakefulness including both brainstem and forebrain systems [165]. Orexin projections to forebrain include the cholinergic basal forebrain (in the rat this includes the horizontal limb of the diagonal band of Broca, the magnocellular preoptic nucleus, and the substantia innominata) and the histaminergic TMN. Brainstem targets include the pontine and medullary brainstem reticular formation, the cholinergic mesopontine tegmental nuclei (including the LDT), the LC, and the DRN.

Two orexin receptors have been identified [163]. Orexin-A is a high-affinity ligand for the orexin receptor type I (orexin-I), whose affinity for orexin-B is 1–2 orders of magnitude lower. The orexin receptor type II (orexin-II) exhibits equally high affinity for both peptides. Currently there are no ligands sufficiently specific for orexin-I and -II receptors to define their distribution. *In situ* hybridization

[161] de Lecea *et al.* (1998); Peyron *et al.* (1998); van den Pol (1999).
[162] de Lecea *et al.* (1998).

[163] Sakurai *et al.* (1998).

[164] de Lecea and colleagues (1998) chose hypocretin as a name to indicate the hypothalamic localization and the similarity to the gut hormone, secretin. Sakurai and colleagues chose orexin because of their initial assumption that the peptides would be tied to feeding behavior. Both names are currently in common use in the literature, although a preferred name will likely emerge. (In general in the English language, shorter names come to predominate over competing longer ones.) We use orexin because we find it simpler and more euphonious, while recognizing others may prefer hypocretin. As used in sleep research, both orexin and hypocretin suffer from an inappropriate derivation relative to the gut and feeding.
[165] Elias *et al.* (1998); Peyron *et al.* (1998); Date *et al.* (1999); Horvath *et al.* (1999b); Nambu *et al.* (1999).

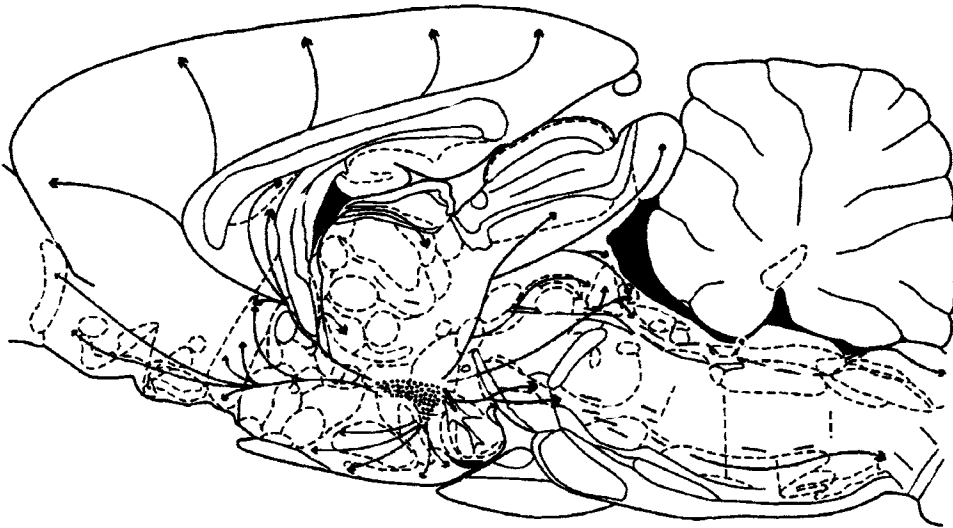


Figure 13.20. Schematic sagittal section drawing of location of orexin-containing neurons (dots in hypothalamus) and their widely distributed projection pathways in the rat brain. Modified from Peyron *et al.*, 1998.

[166] Trivedi *et al.* (1998); Chemelli *et al.* (1999), citing their own unpublished data.

studies of orexin receptor mRNAs [166] have shown a diffuse pattern, consistent with the widespread nature of orexin projections, although there was a marked differential distribution of the orexin type I and II mRNAs. Of the brainstem regions involved in state control, only the DRN and the LC appear to show a predominance of mRNA for type I receptors. While orexin-A and -B-positive fibers with varicosities were detected in almost all brainstem regions, the highest densities were found in the DRN, the LDT, and the LC [167]. *In vitro* [^{35}S]GTPgammaS autoradiography for activated G proteins in the rat revealed dose-dependent increases following localized orexin-A administration in brainstem LC, pontis oralis and caudalis, and DRN, and an increased ACh releases in pontis oralis following administration in this region [168].

[167] Zhang *et al.* (2004).

[168] Bernard *et al.* (2003).

13.4.3. Actions of Orexin at the Cellular Level

Orexin-A has been shown to excite the noradrenergic neurons of the LC, providing a mechanism by which orexin can promote wakefulness [169] and suppress REM sleep in a dose-dependent manner. *In vitro* work in a transgenic mouse with strong GFP expression in the LC that was colocalized with immunoreactive tyrosine hydroxylase showed that orexin-A and -B increased spike frequency, with orexin-A being an order of magnitude more potent; the postsynaptic excitation was thought to be mediated by

[169] Hagan *et al.* (1999); Horvath *et al.* (1999a); Bourgin *et al.* (2000).

an inward cation current since effects of orexin were blocked by substitution of choline-Cl for NaCl [170]. Another report suggests excitation occurs through suppression of G-protein-coupled inward rectifier (GIRK) channel activity [171].

In vitro work in the rat has shown that orexin rather uniformly excited GABAergic neurons of the ventral tegmental area (VTA) while effects on dopaminergic neurons were more complex, with approximately one-third being excited, one-third showing development of oscillatory burst firing, and one-third showing no response [172]. Most neurons depolarized in response to both orexin-A and -B (100 nM), a postsynaptic effect (persisting with tetrodotoxin application). Single-cell PCR experiments showed that both orexin receptors were expressed in both dopaminergic and nondopaminergic neurons. Somewhat surprisingly, dopaminergic neurons in substantia nigra pars compacta were unaffected by orexins, while, in contrast, bath application of orexin-A (100 nM) or orexin-B (5–300 nM) greatly increased the firing rate of GABAergic neurons in pars reticulata [173].

In the dorsal raphe, orexin-A and -B acting postsynaptically increased the firing rate of serotonin neurons; the excitatory effects of orexin were occluded by previous application of phenylephrine, suggesting that orexin and noradrenergic systems act via common effector mechanisms [174]. Orexin-I-receptor-mediated effects appeared to be somewhat stronger than Orexin-II-receptor-mediated effects based on both signal strength in single-cell PCR in tryptophan hydroxylase-positive neurons and a slightly greater number of serotonin neurons responsive to orexin-A than -B. Interestingly, agonists of three arousal-related systems impinging on the dorsal raphe (orexin/hypocretin, histamine and the noradrenaline systems) caused an inward current and increase in current noise in whole-cell patch-clamp recordings from these neurons in brain slices. In most cases orexin appeared to activate a mixed cation channel with relative permeabilities for sodium and potassium of 0.43 and 1, respectively.

In an *in vitro* study of the tuberomammillary nucleus, both orexin-A and orexin-B depolarized the histaminergic neurons and increased their firing rate via an action on postsynaptic receptors [175]. The depolarization was associated with a small decrease in input resistance and was likely caused by activation of both the electrogenic Na(+)/Ca(2+) exchanger and a Ca(2+) current. A single-cell RT-PCR study in this nucleus revealed that most tuberomammillary neurons express both orexin-A and -B, with stronger expression of the orexin-2 receptor. Immunocytochemistry showed that the histamine and

[170] van den Pol (2002).

[171] Hoang *et al.* (2003).

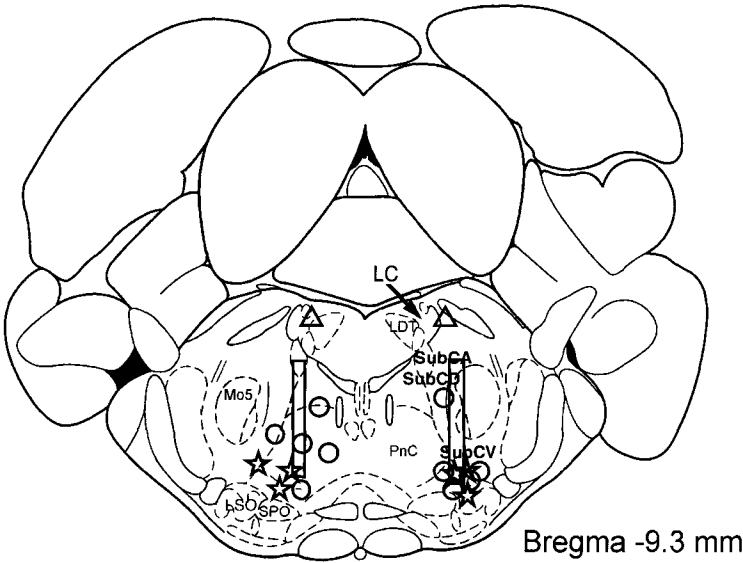
[172] Korotkova *et al.* (2003).

[173] Korotkova *et al.* (2002).

[174] Brown *et al.* (2002).

[175] Eriksson *et al.* (2001).

orexin neurons were often located very close to each other, and appeared to be reciprocal. Other data suggest presynaptic effects of orexin [176].



Schematic of Orexin Influences on REM
Sleep via Brainstem Projections

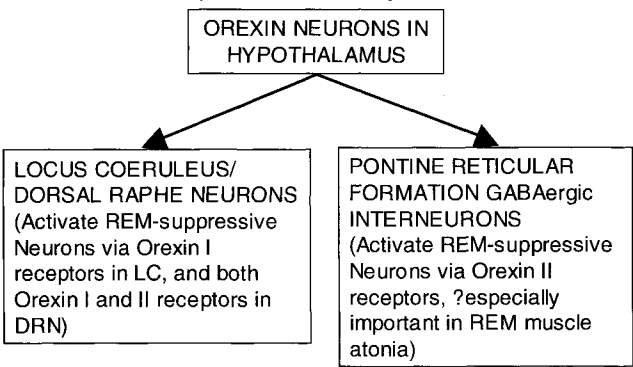


Figure 13.21. Top Panel. Localization of effective sites for cataplexy and REM enhancement by microdialysis perfusion of antisense to the orexin receptor II in the pons. Size of the bilateral probe is represented by rectangles (.25 × 2mm) and probe tip localization for the effective sites is indicated by open circles; note these are in reticular formation ventral to the Locus Coeruleus. Triangles represent the ineffective sites that received antisense perfusion in a site dorsal (as shown) and caudal (AP -10.25) to the target site. All other sites were located between AP -8.8 and -9.5 and are all mapped onto this one coronal brainstem section (-9.3, adapted from Paxinos and Watson, 1997). Probe tips for nonsense perfusion are represented by stars (nonsense = scrambled order of the amino acids in antisense). Probes were placed bilaterally in each animal. Antisense perfusion sites are represented by open circles (N = 5 subjects), whereas the nonsense perfusion sites are represented by stars (N = 1). LC, locus coeruleus; LDT, laterodorsal tegmental nucleus; LSO, lateral superior olive; Mo5, motor trigeminal nucleus; PnC, caudal pontine reticular nucleus; SPO, superior paraolivary nucleus; subCA, subcoeruleus, alpha; subCD, subcoeruleus, dorsal; subCV, subcoeruleus, ventral. For identification of unlabeled structures see Paxinos and Watson (1997). Adapted from Thakkar et al. 1999. Bottom Panel. Schematic of orexin influences on REM control mechanisms. The data from the top panel suggest the orexinergic projections to GABAergic neurons may be especially important in control of REM muscle atonia.

13.4.4. Orexin and the Control of REM-Related Phenomena and Wakefulness

The knockout and canine narcolepsy data suggested that an absence of orexin or a defective orexin-II receptor will produce cataplexy. Where might this cataplexy effect be mediated? In the absence of an effective antagonist to orexin receptors, the author's laboratory decided to use antisense oligodeoxynucleotides (ODN) against the mRNA for orexin type II receptors [177], thereby producing a "reversible knockout" or "knockdown" of the type II orexin receptor. As illustrated in Fig. 13.21 Spatial specificity was obtained by microdialysis perfusion of orexin type II receptor antisense in the rat pontine reticular formation (PRF) just ventral to the LC (but presumably not affecting the LC, which has predominantly type I receptors). This treatment, as predicted, increased REM sleep 2- to 3- fold during both the light period (quiescent phase) and the dark period (active phase). Furthermore, this manipulation produced increases in behavioral cataplexy suggesting that the REM sleep and narcolepsy-related role of orexin is mediated via the action of orexin in the brainstem nuclei that control the expression of REM sleep signs.

[177] Thakkar *et al.* (1999).

Chemelli *et al.* [157] as well as others (David Rye, personal communication) have noted a heavy concentration of orexin-containing fibers around the somata of cholinergic neurons of the basal forebrain. This suggested that orexin might not only act on REM-related phenomena but also on wakefulness control. Indeed, microdialysis perfusion of orexin into the cholinergic basal forebrain of the rat was found to produce a dose-dependent enhancement of wakefulness, with the highest dose producing more than a 5-fold increase in wakefulness [178].

[178] Thakkar *et al.* (2001).

13.4.5. Orexin Release: Linked to Circadian Cycle and/or to Behavioral State?

Remarkably, relatively little is known with certainty about whether orexin release is a function of the circadian cycle and/or a function of behavioral state. This is an important theoretical question, since simulations based on the McCarley–Massaquoi–Hobson model described in Chapter 12 showed that circadian effects on the REM cycle could be faithfully mimicked by postulating an excitatory drive on LC and DRN neurons during times of circadian activity, with withdrawal of the drive during times of circadian inactivity leading to sleep, an excitatory drive that might stem from orexinergic activity. Taheri *et al.* [179] described diurnal variation in orexin-A immunoreactivity

[179] Taheri *et al.* (2000).

and prepro-orexin mRNA expression in the rat, findings suggestive of a circadian fluctuation in orexin release, as did preliminary ELISA orexin assays [180].

[180] Strecker *et al.* (2002).

[181] Espana *et al.* (2003).

In the rat, Espana and colleagues [181] evaluated differences in the number of neurons immunohistochemically double-labeled for Fos and either prepro-orexin in the lateral hypothalamus or orexin-A receptors in the LC and basal forebrain regions during behaviorally scored, spontaneous states of daytime sleeping (DS), daytime wakefulness (DW), and nighttime wakefulness (NW) and during a “high-arousal” wake state induced by an 80 dB white noise (HW). These values were compared with double labeling induced by 0.07 or 0.7 nmol orexin-A administered ICV. Daytime spontaneous waking was not different from DS in the number of Fos-ir nuclei, suggesting a predominating time of day effect rather than a state effect per se. Nighttime spontaneous waking was associated with an increased number of Fos-ir nuclei in orexin-expressing neurons. For all other regions only high arousal waking was associated with increased number of Fos-ir nuclei in either orexin-expressing or orexin-I receptor-expressing neurons; this increase was relative to DW, to DS, and to NW. Orexin-A administration dose-dependently increased Fos-ir within orexin-I-expressing neurons. The authors concluded that, combined, these observations support the hypothesis that hypocretin neuronal activity varies across the circadian cycle and that waking per se does not alter orexin neurotransmission, but that particular behaviors that occur during wakefulness are associated with increased Fos-ir in both orexin-synthesizing neurons and Orexin-I receptor-expressing neurons.

[182] Yoshida *et al.* (2001).

Yoshida and colleagues [182] used microdialysis and ¹²⁵I RadioImmunoAssay to measure changes in extracellular orexin-A levels in the lateral hypothalamus and medial thalamus of freely moving rats with simultaneous sleep recordings. As illustrated in Fig. 13.22, orexin levels exhibited a robust diurnal fluctuation; levels slowly increased during the dark period (active phase), and decreased during the light period (rest phase). Levels were not correlated with the amount of wake or sleep in each period. Although an acute 4-hr light-shift did not alter orexin levels, 6-hr sleep deprivation significantly increased orexin release during the forced-wake period. Orexin activity is, thus, likely to build up during wakefulness and decline with the occurrence of sleep. These findings, together with the fact that a difficulty in maintaining wakefulness during the daytime is one of the primary symptoms of orexin-deficient narcolepsy, suggest that orexin activity may be critical in opposing sleep propensity during periods of prolonged wakefulness.

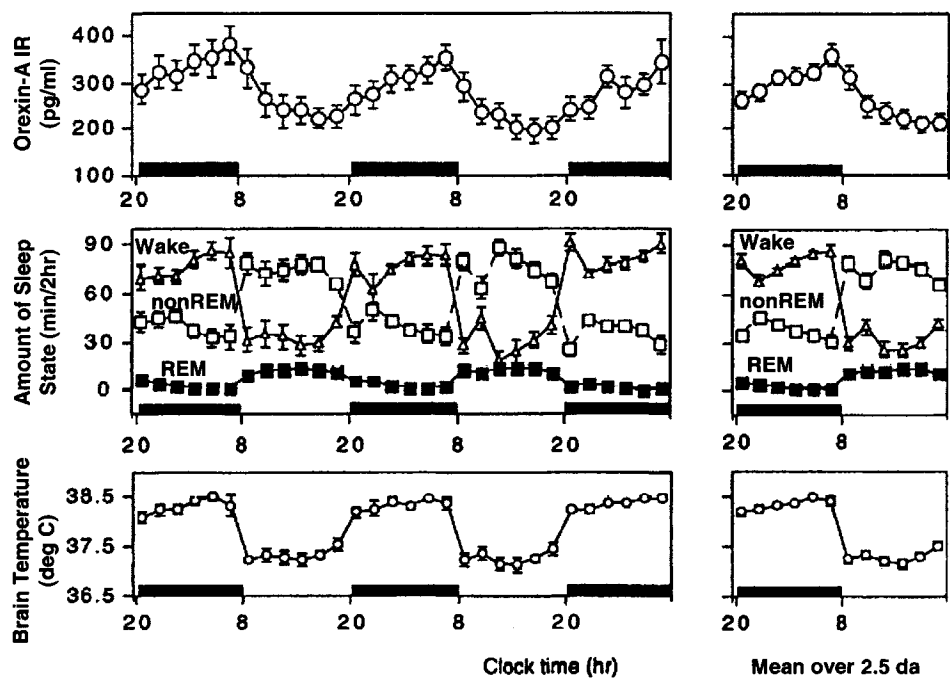


Figure 13.22. Fluctuation of extracellular orexin-A levels in the lateral hypothalamic region in rats under 12-hr light : 12-hr dark conditions in relation to sleep state and brain temperature (2 hr sample bins, data are mean \pm SD.) Dark periods are indicated by black bars. Open circles (large) represent orexin-A level, open triangles represent wakefulness, open squares represent SWS, Filled squares represent REM sleep, and open circles (small) represent brain temperature. On the right side, the mean of each time point over the 2.5 days is re-plotted. Adapted from Yoshida *et al.*, 2001.

The state-related release of orexin-A has been assayed by a solid phase radioimmunoassay of microdialysis collected samples in the freely moving cat [183]. In the perifornical hypothalamus and basal forebrain highest levels in this minimally circadian animal were present during active wakefulness (movement) and in REM sleep, with lower levels in non-REM sleep. However no statistically significant differences were detected across states in the LC. The high values in wake with movement are compatible with the Espana data, but the high REM values seem paradoxical in view of the finding that antisense knockdown of the orexin-II receptor in the subcoerulean region is associated with more REM sleep and muscle atonia [177], as is narcolepsy with the inappropriate expression of REM sleep signs.

The construction of transgenic mice and rats in which orexin-containing neurons are destroyed postnatally by orexinergic-specific expression of a truncated Machado-Joseph disease gene product (ataxin-3) with an expanded polyglutamine stretch under control of the human prepro-orexin promoter has provided a valuable animal model of narcolepsy [184]. The transgenic model is useful because there is a gradual post-natal development of cell loss, as in

[183] Kiyashchenko *et al.* (2002).

[184] Mice: Hara *et al.* (2001); Mieda *et al.* (2003); Rats: Beuckmann *et al.* (2004).

human narcolepsy, and the rat is a useful animal for a transgenic model since sleep recordings are of higher quality and the sleep behavior of the rat is more fully documented than the mouse. In the rat at 4 weeks the number of orexin-expressing cells was diminished and continued to decline; at 17 weeks, the time of recording, orexin-expressing cells were virtually absent, as were their projections.

This transgenic rat, compared with wild types, showed a markedly different REM sleep profile. Sleep onset REM (SOREM) episodes were present during the normal wakefulness period (dark), averaging 3.8/12 hr recording period, but occurred rarely during the light period (0.3/12 hr), but SOREM were less frequent than normal REM periods (43/light period, 28/dark period). A SOREM episode in these rats was essentially identical to a normal REM sleep episode with respect to both the EEG frequency distribution (marked by the presence of theta), muscle atonia, and episode duration. (A SOREM sleep episode was defined as REM sleep preceded by not more than 30 s of non-REM sleep—in the wild type there is usually about 2 min of non-REM preceding REM—following at least 60 s of wakefulness.) Another behavior resembled human cataplexy, with behavioral collapse, absence of muscle tone, but with wakefulness-like EEG without the theta peak characterizing REM. These arrests occurred both during the dark (mean 4.7 times/12 hr) and light (mean 2.8 times) phases and were generally short in duration (10–20 s). They could not be triggered by emotional stimuli.

Perhaps the most striking change in REM percentage was the difference in diurnal distribution, as illustrated in Fig. 13.23. REM sleep (including SOREM) was approximately 2-fold increased over the wild type in the normally REM-poor dark period, whereas there was a reduction in REM%. These data in animals without orexinergic neurons argue strongly that diurnal control of the distribution of REM sleep is under the control of orexin, and combined with the Yoshida *et al.* [182] data indicate that orexinergic activity suppresses the occurrence of REM sleep. These data also seem compatible with the McCarley–Massaquoi–Hobson model described in Chapter 12 in that REM episode duration and overall interREM interval were not affected. It is as if the removal of orexin greatly altered the probability of the REM oscillator being permitted to turn on, allowing it to run during the normally suppression period of darkness. This failure to consolidate REM sleep into the sleep (inactive) circadian phase is highly characteristic of human narcolepsy [185]. To our mind this transgenic construct and its REM data provide the strongest evidence for orexin functioning as a circadian control mechanism for the consolidation of REM sleep into the

[185] This was first clearly documented by Passouant and colleagues (1969).

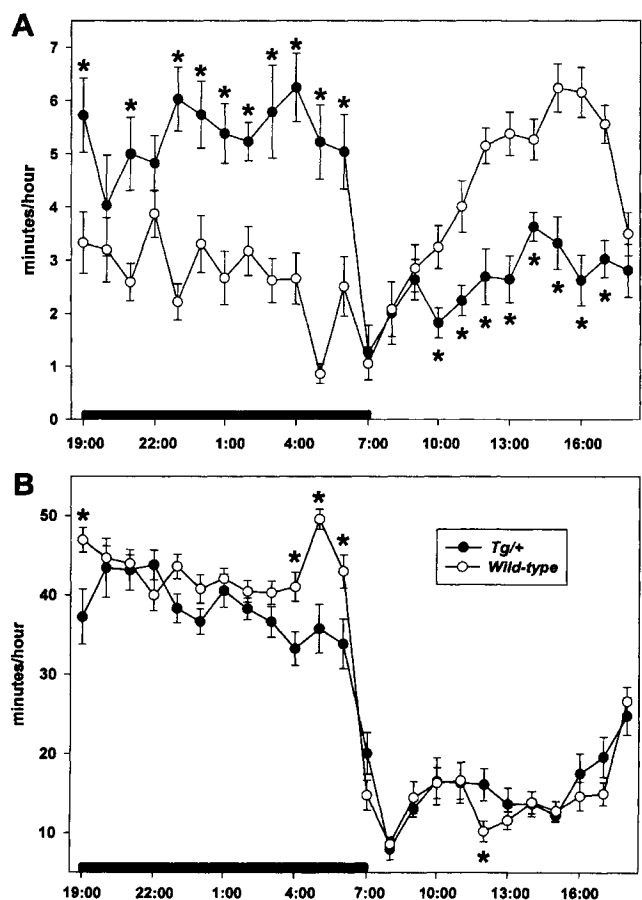


Figure 13.23. Time spent each hour (minutes, mean \pm SEM) in (A) REM sleep and (B) wakefulness for wild-type rats and their *orexin/ataxin-3* hemizygous transgenic littermates. Significant differences between the genotypes (*t*-test, $p < 0.05$) are marked by an asterisk. The dark period is denoted by the horizontal bar. Adapted from Beuckmann *et al.*, 2004.

inactive phase. It also argues strongly against the theory that the role of orexin is a necessary factor in the expression of sleep–wake behavioral state changes per se, but argues for orexin as a modulatory factor shaping the circadian phase of occurrence of REM sleep.

As also shown in Fig. 13.23, in the transgenic rat there was an absence of the surge of wakefulness near the end of the dark period, corresponding to the peak of orexinergic secretion (see Fig. 13.23). This provides further evidence of the control of wakefulness by orexin. However, what is evident is that the 15% reduction in wakefulness percentage during the dark period in the transgenic rat is of a much lesser degree than the 100% increase in REM percentage. This suggests that the diurnal control over REM sleep exerted by orexin is a much stronger effect than that over wakefulness, perhaps because of the multiple system control of wakefulness.

References

- Achermann, P. and Borbély, A. (1997) Low-frequency (< 1 Hz) oscillations in the human sleep EEG. *Neuroscience* 81: 213–222.
- Adams, D.J., Constanti, A., Brown, D.A., and Clark, R.B. (1982) Intracellular Ca^{2+} activates a fast voltage-sensitive K^+ current in vertebrate sympathetic neurones. *Nature* 296: 746–749.
- Adams, D.J., Smith, S.J., and Thompson, S.H. (1980) Ionic currents in molluscan soma. *Annual Review of Neuroscience* 3: 141–167.
- Adams, R.W., Lambert, G.A., and Lance, J.W. (1988) Brainstem facilitation of electrically evoked visual response in the cat. Source, pathway and role of nicotinic receptors. *Electroencephalography and Clinical Neurophysiology* 69: 45–54.
- Adrian, E.D. (1936) The spread of activity in the cerebral cortex. *Journal of Physiology (London)* 88: 127–161.
- Adrian, E.D. (1937) Synchronized reactions in the optic ganglion of *Dysticus*. *Journal of Physiology (London)* 91: 66–89.
- Aggleton, J.P. and Mishkin, M. (1983a) Visual recognition impairment following medial thalamic lesions. *Neuropsychologia* 21: 189–197.
- Aggleton, J.P. and Mishkin, M. (1983b) Memory impairments following restricted medial thalamic lesions in monkeys. *Experimental Brain Research* 52: 199–209.
- Aghajanian, G.K. (1981) The modulatory role of serotonin of multiple receptors in brain. In B.L. Jacobs and A. Gelperin, eds., *Serotonin Neurotransmission and Behavior*, pp. 156–185, Cambridge (MA): The MIT Press.
- Aghajanian, G.K. (1985) Modulation of a transient outward current in serotonergic neurones by alpha 1-adrenoceptors. *Nature* 315: 501–503.
- Aghajanian, G.K. and Lakoski, J.M. (1984) Hyperpolarization of serotonergic neurons by serotonin and LSD: studies in brain slices showing increased K^+ conductance. *Brain Research* 305: 181–185.
- Aghajanian, G.K. and VanderMaelen, C.P. (1982a) Intracellular recordings from serotonergic dorsal raphe neurons: pacemaker potentials and the effect of LSD. *Brain Research* 238: 463–469.
- Aghajanian, G.K. and VanderMaelen, C.P. (1982b) Intracellular identification of central noradrenergic and serotonergic neurons by a new double labeling procedure. *Journal of Neuroscience* 2: 1786–1792.
- Aghajanian, G.K. and Wang, E.Y. (1977) Habenular and other midbrain raphe afferents demonstrated by a modified retrograde tracing technique. *Brain Research* 122: 229–242.
- Aghajanian, G.K., Cedarbaum, J.M., and Wang, R.Y. (1977) Evidence for norepinephrine mediated collateral inhibition of locus coeruleus neurons. *Brain Research* 136: 570–577.
- Aghajanian, G.K., Wang, R.Y., and Baraban, J. (1978) Serotonergic and nonserotonergic neurons of the dorsal raphe: reciprocal changes in firing induced by peripheral nerve stimulation. *Brain Research* 153: 169–175.
- Ahlsén, G. (1984) Brain stem neurones with differential projection to functional subregions of the dorsal lateral geniculate complex in the cat. *Neuroscience* 12: 817–838.
- Ahlsén, G., Lindstrom, S., and Lo, F.S. (1984) Inhibition from the brain stem of inhibitory interneurons in the cat's dorsal lateral geniculate nucleus. *Journal of Physiology (London)* 347: 593–609.
- Airaksinen, M.S. and Panula, P. (1988) The histaminergic system in the guinea pig central nervous system: an immunocytochemical mapping study using an antiserum against histamine. *Journal of Comparative Neurology* 273: 163–186.

- Akerstedt, T. and M. Gillberg (1981) The circadian variation of experimentally displaced sleep. *Sleep* 4: 159–169.
- Akiskal, H.S., Rosenthal, T.L., Haykal, R.F., Lemmi, H., Rosenthal, R.H., and Scott-Strauss, A. (1980) Characterological depressions. Clinical and sleep EEG findings separating “subaffective dysthymias” from “character spectrum disorders”. *Archives of General Psychiatry* 37: 777–783.
- Alam, M.N., Szymusiak, R., Gong, H., King, J., and McGinty, D. (1999) Adenosinergic modulation of rat basal forebrain neurons during sleep and waking: neuronal recording with microdialysis. *Journal of Physiology* 521: 679–690.
- Alam, N., McGinty, D., Imeri, L., Opp, M., and Szymusiak, R. (2001) Effects of interleukin-1 beta on sleep- and wake-related preoptic anterior hypothalamic neurons in unrestrained rats. *Sleep* 24: A59.
- Alanko, L., Heiskanen, S., Stenberg, D. and Porkka-Heiskanen, T. (2003a) Adenosine kinase and 5'-nucleotidase activity after prolonged wakefulness in the cortex and the basal forebrain of rat. *Neurochemistry International* 42: 449–454.
- Alanko, L., Stenberg, D., and Porkka-Heiskanen, T. (2003b) Nitrobenzylthioinosine (NBMPR) binding and nucleoside transporter ENT1 mRNA expression after prolonged wakefulness and recovery sleep in the cortex and basal forebrain of rat. *Journal of Sleep Research* 12: 299–304.
- Albanese, A. and Butcher, L.L. (1980) Acetylcholinesterase and catecholamine distribution in the locus coeruleus of the rat. *Brain Research Bulletin* 5: 127–124.
- Albe-Fessard, D., Levante, A., and Lamour, Y. (1974) Origin of spinothalamic and spinoreticular pathways in cats and monkeys. In J.J. Bonica, ed., *Advances in Neurology*, vol. 4, pp. 157–166, New York: Raven Press.
- Aldrich, M.S. (1998) Diagnostic aspects of narcolepsy. *Neurology* 50: S2–S7.
- Aldrich, R.W., Jr., Getting, P.A., and Thompson, S.H. (1979) Mechanism of frequency-dependent broadening of molluscan neurone soma spikes. *Journal of Physiology (London)* 291: 531–544.
- Alley, K., Baker, R., and Simpson, J.I. (1975) Afferents to the vestibulocerebellum and the origin of the visual climbing fibers in the rabbit. *Brain Research* 98: 582–589.
- Alloway, K.D., Wallace, M.B., and Johnson, M.J. (1994) Cross-correlation analysis of cuneothalamic interactions in the rat somatosensory system: influence of receptive field topography and comparisons with thalamocortical interactions. *Journal of Neurophysiology* 72: 1949–1972.
- Alonso, A. and Garcia-Ausst, E. (1987a) Neuronal sources of theta rhythm in the entorhinal cortex of the rat. I. Laminar distribution of theta field potentials. *Experimental Brain Research* 67: 493–501.
- Alonso, A. and Garcia-Ausst, E. (1987b) Neuronal sources of theta rhythm in the entorhinal cortex of the rat. II. Phase relations between unit discharges and theta field potentials. *Experimental Brain Research* 67: 502–509.
- Alonso, A. and Klink, R. (1993) Differential electroresponsiveness of stellate and pyramidal-like cells of medial entorhinal cortex layer II. *Journal of Neurophysiology* 70: 128–143.
- Alonso, A. and Köhler, C. (1984) A study of the reciprocal connection between the septum and the entorhinal area using anterograde and retrograde axonal transport methods in the rat brain. *Journal of Comparative Neurology* 225: 327–343.
- Alonso, A. and Llinás, R. (1988) Voltage-dependent calcium conductances and mammillary body neurons autorhythmicity: an *in vitro* study. *Society for Neuroscience Abstracts* 14: 900.
- Alonso, A. and Llinás, R. (1989) Subthreshold Na⁺-dependent theta-like rhythmicity in stellate cells of entorhinal cortex layer II. *Nature* 342: 175–177.
- Alonso, A., Khateb, A., Fort, P., Jones, B.E., and Mühlethaler, M. (1996) Differential oscillatory properties of cholinergic and noncholinergic nucleus basalis neurons in guinea pig brain slices. *European Journal of Neuroscience* 8: 169–182.
- Alt, J., Obal, F. Jr., Gardi, J., and Krueger, J.M. (2002) Sleep in mutant mice with non-functional GHRH receptor: responses to GHRH, ghrelin, and somatostatin. *Journal of Sleep Research* 11: 3–4.
- Amacher, P. (1965) Freud's Neurological Education and Its Influence on Psychoanalytic Theory. *Psychological Issues, Monograph* 16, New York: International Universities Press.
- Amaral, D.G. and Witter, M.P. (1989) The three-dimensional organization of the hippocampal formation: a review of anatomical data. *Neuroscience* 31: 571–591.
- Amatruda, T.T., Black, D.A., McKenna, R.M., McCarley, R.W., and Hobson, J.A. (1975) Sleep cycle control and cholinergic mechanisms: differential effects of carbachol injections at pontine brain stem sites. *Brain Research* 98: 501–515.
- Amitai, Y. (1994) Membrane potential oscillations underlying firing patterns in neocortical neurons. *Neuroscience* 63: 151–161.
- Amzica, F. and Neckelmann, D. (1999) Membrane capacitance of cortical neurons and glia during sleep oscillations and spike-wave seizures. *Journal of Neurophysiology* 82: 2731–2746.

- Amzica, F. and Steriade, M. (1995a) Disconnection of intracortical synaptic linkages disrupts synchronization of a slow oscillation. *Journal of Neuroscience* 15: 4658–4677.
- Amzica, F. and Steriade, M. (1995b) Short- and long-range neuronal synchronization of the slow (<1 Hz) cortical oscillation. *Journal of Neurophysiology* 75: 20–38.
- Amzica, F. and Steriade, M. (1996) Progressive cortical synchronization of ponto-geniculo-occipital potentials during rapid eye movement sleep. *Neuroscience* 72: 309–314.
- Amzica, F. and Steriade, M. (1997) The K-complex: its slow (<1 Hz) rhythmicity and relation to delta waves. *Neurology* 49: 952–959.
- Amzica, F. and Steriade, M. (1998a) Cellular substrates and laminar profile of sleep K-complex. *Neuroscience* 82: 671–686.
- Amzica, F. and Steriade, M. (1998b) Electrophysiological correlates of sleep delta waves. *Electroencephalography and Clinical Neurophysiology* 107: 69–83.
- Amzica, F. and Steriade, M. (2000) Neuronal and glial membrane potentials during sleep and paroxysmal oscillations in the cortex. *Journal of Neuroscience* 20: 6648–6665.
- Amzica, F. and Steriade, M. (2002) The functional significance of K-complexes. *Sleep Medicine Reviews* 6: 139–149.
- Amzica, F., Massimini, M., and Manfridi, A. (2002) Spatial buffering during slow and paroxysmal oscillations in cortical networks of glial cells *in vivo*. *Journal of Neuroscience* 22: 1042–1053.
- Andersen, P. and Andersson, S.A. (1968) *Physiological Basis of Alpha Rhythm*. New York: Appleton-Century-Crofts.
- Andersen, P. and Curtis, D.R. (1964a) The excitation of thalamic neurones by acetylcholine. *Acta Physiologica Scandinavica* 61: 85–99.
- Andersen, P. and Curtis, D.R. (1964b) The pharmacology of the synaptic and acetylcholine-induced excitation of ventrobasal thalamic neurones. *Acta Physiologica Scandinavica* 61: 100–120.
- Andersen, P. and Eccles, J.C. (1962) Inhibitory phasing of neuronal discharges. *Nature* 196: 645–647.
- Andersen, P. and Sears, T.A. (1964) The role of inhibition in the phasing of spontaneous thalamo-cortical discharges. *Journal of Physiology (London)* 173: 459–480.
- Andersen, P., Eccles, J.C., and Løysing, Y. (1964) Location of postsynaptic inhibitory synapses on hippocampal pyramids. *Journal of Neurophysiology* 27: 592–607.
- Andersen, P., Gross, G.N., Lømo, T., and Sveen, O. (1969) Participation of inhibitory and excitatory interneurons in the control of hippocampal cortical output. In M. Brazier, ed., *The Interneuron*, pp. 415–465. Los Angeles: University of California Press.
- Andersen, P., Silfvenius, H., Sundberg, S.H., and Sveen, O. (1980) A comparison of distal and proximal dendritic synapses on CA1 pyramids in hippocampal slices *in vitro*. *Journal of Physiology (London)* 307: 273–299.
- Andrade, R., Malenka, R.C., and Nicoll, R.A. (1986) A G-binding protein couples serotonin and GABA_B receptors to the same channels in hippocampus. *Science* 243: 1261–1265.
- Andrezik, J.A., Chan-Palay, V., and Palay, S. (1981a) The nucleus paragigantocellularis lateralis in the rat. Conformation and cytology. *Anatomy & Embryology* 161: 355–371.
- Andrezik, J.A., Chan-Palay, V., and Palay, S. (1981b) The nucleus paragigantocellularis lateralis in the rat. Demonstration of afferents by the retrograde transport of horseradish peroxidase. *Anatomy & Embryology* 161: 373–390.
- Araki, M., McGeer, P.L., and McGeer, E.G. (1984) Presumptive gamma-aminobutyric acid pathways from the midbrain to the superior colliculus studied by a combined horseradish peroxidase-gamma-aminobutyric acid transaminase pharmacohistochemical method. *Neuroscience* 13: 433–439.
- Arkin, A.M., Sanders, K.I., Ellman, S.J., Antrobus, J.S., Farber, J., and Nelson, W.T. (1975) The rarity of pain sensation in sleep mentation reports. *Sleep Research* 4: 179.
- Armstrong, D.M., Saper, C.B., Levey, A.I., Wainer, B.H., and Terry, R.D. (1983) Distribution of cholinergic neurons in rat brain demonstrated by the immunocytochemical localization of choline acetyltransferase. *Journal of Comparative Neurology* 216: 53–68.
- Arrigoni, E., Chamberlin, N.L., Saper, C.B., and McCarley, R.W. (2003) The effects of adenosine on the membrane properties of basal forebrain cholinergic neurons. *Sleep* 26: A45.
- Arsenault, M.Y., Parent, A., Séguéla, P., and Descarries, L. (1988) Distribution and morphological characteristics of dopamine-immunoreactive neurons in the midbrain of the squirrel monkey (*Saimiri sciureus*). *Journal of Comparative Neurology* 267: 489–506.
- Arthur, D.L. and Starr, A. (1984) Task-relevant late positivity component of the auditory event-related potential in monkeys resembles P300 in humans. *Science* 223: 186–188.
- Artola, A. and Singer, W. (1987) Long-term potentiation and NMDA receptors in rat visual cortex. *Science* 230: 649–662.

- Asanuma, C. (1989) Basal forebrain projections to the reticular thalamic nucleus in rat. *Proceedings of the National Academy of Sciences of the USA* 86: 4746–4750.
- Asanuma, C. (1997) Distribution of neuromodulatory inputs in the reticular and dorsal thalamic nuclei. In: M. Steriade, E.G. Jones, and D.A. McCormick, eds., *Thalamus*, vol. 2 (*Experimental and Clinical Aspects*) pp. 93–153, Oxford: Elsevier.
- Asanuma, C. and Porter, L.L. (1990) Light and electron microscopic evidence for a GABAergic projection from the caudal basal forebrain to the thalamic reticular nucleus in rats. *Journal of Comparative Neurology* 302: 159–172.
- Asanuma, H. and Rosen, I. (1973) Spread of mono- and polysynaptic connections within the cat's motor cortex. *Experimental Brain Research* 16: 507–520.
- Ascher, P. and Nowak, L. (1987) Electrophysiological studies of NMDA receptors. *Trends of Neuroscience* 10: 284–287.
- Aserinsky, E. and Kleitman, N. (1953) Regularly occurring periods of eye motility, and concomitant phenomena during sleep. *Science* 118: 273–274.
- Aserinsky, E. and Kleitman, N. (1955) Two types of ocular motility occurring in sleep. *Journal of Applied Physiology* 8: 11–18.
- Aserinsky, E., Lynch, J.A., Mack, M.E., Tzankoff, S.P., and Hurn, E. (1985) Comparison of eye motion in wakefulness and REM sleep. *Psychophysiology* 22: 1–10.
- Aston-Jones, G. and Bloom, F.E. (1981a) Activity of norepinephrine-containing locus coeruleus neurons in behaving rats anticipates fluctuations in the sleep-waking cycle. *Journal of Neuroscience* 1: 876–886.
- Aston-Jones, G. and Bloom, F.E. (1981b) Norepinephrine-containing locus coeruleus neurons in behaving rat exhibit pronounced responses to non-noxious environmental stimuli. *Journal of Neuroscience* 1: 887–900.
- Aston-Jones, G., Ennis, M., Pieribone, V.A., Nickell, W.T., and Shipley, M.T. (1986) The brain nucleus locus coeruleus: restricted afferent control of a broad efferent network. *Science* 234: 734–737.
- Aston-Jones, G., Foote, S.L., and Segal, M. (1985) Impulse conduction properties of noradrenergic locus coeruleus axons projecting to monkey cerebrocortex. *Neuroscience* 15: 765–777.
- Aston-Jones, G., Segal, M., and Bloom, F.E. (1980) Brain aminergic axons exhibit marked variability in conduction velocity. *Brain Research* 195: 215–222.
- Aston-Jones, G., Shaver, R., and Dinan, T. (1984) Cortically projecting nucleus basalis neurons in rat are physiologically heterogeneous. *Neuroscience Letters* 46: 19–24.
- Auerbach, S.B., Minzenberg, M.J., and Wilkinson, L.O. (1989) Extracellular serotonin and 5-hydroxyindoleacetic acid in hypothalamus of the unanesthetized rat measured by in vivo dialysis coupled to high-performance liquid chromatography with electrochemical detection: dialysate serotonin reflects neuronal release. *Brain Research* 499: 281–90.
- Avendaño, C., Raussel, E., Perez-Aguilar, D., and Isorna, S. (1988) Organization of the association cortical afferents of area 5: a retrograde tracer study in the cat. *Journal of Comparative Neurology* 278: 1–33.
- Avoli, M. (1986) Inhibitory potentials in neurons of the deep layers of the *in vitro* neocortical slice. *Brain Research* 370: 165–170.
- Bachelor, P.E., Armstrong, D.M., Blaker, S.N., and Gage, F.H. (1989) Nerve growth factor receptor and choline acetyltransferase colocalization in neurons within the rat forebrain: response to fimbria-fornix transection. *Journal of Comparative Neurology* 284: 187–204.
- Baghdoyan, H.A., McCarley, R.W., and Hobson, J.A. (1985) Cholinergic manipulation of brainstem reticular systems: effects on desynchronized sleep generation. In A. Waquier, J. Monti, J.P. Gaillard, and M. Radulovacki, eds., *Sleep: Neurotransmitters and Neuromodulators*, pp. 15–27, New York: Raven Press.
- Baghdoyan, H.A., Monaco, A.P., Rodrigo-Angulo, M.L., Assens, F., McCarley, R.W., and Hobson, J.A. (1984a) Microinjection of neostigmine into the pontine reticular formation enhances desynchronized sleep signs. *Journal of Pharmacology and Experimental Therapy* 231: 173–180.
- Baghdoyan, H.A., Rodrigo-Angulo, M.L., McCarley, R.W., and Hobson, J.A. (1984b) Site-specific enhancement and suppression of desynchronized sleep signs following cholinergic stimulation of three brainstem regions. *Brain Research* 306: 39–52.
- Baghdoyan, H.A., Rodrigo-Angulo, M.L., McCarley, R.W., and Hobson, J.A. (1987) A neuroanatomical gradient in the pontine tegmentum for the cholinceptive induction of desynchronized sleep signs. *Brain Research* 414: 245–261.
- Bagnoli, P., Beaudet, A., Stella, M., and Cuénod, M. (1981) Selective retrograde labeling of cholinergic neurons with (^3H)choline. *Journal of Neuroscience* 1: 691–695.
- Baker, R. and McCrea, R. (1979) The parabrachial nucleus. In H. Asanuma and V.J. Wilson, eds., *Integration in the Nervous System*, pp. 97–121, New York: Igaku-Shoin.
- Baker, S.N., Olivier, E., and Lemon, R.N. (1997) Coherent oscillations in the monkey motor cortex and hand muscle EMG show task-dependent modulation. *Journal of Physiology (London)* 501: 225–241.

- Baker, T.L. and Dement, W.C. (1985) Canine narcolepsy-cataplexy syndrome: evidence for an inherited monoaminergic-cholinergic imbalance. In D. McGinty, R. Drucker-Colin, A. Morrison, and P.L. Parmeggiani, eds., *Brain Mechanisms of Sleep*, pp. 63–80, New York: Raven Press.
- Bal, T. and McCormick, D.A. (1993) Mechanisms of oscillatory activity in guinea-pig nucleus reticularis thalami *in vitro*: a mammalian pacemaker. *Journal of Physiology (London)* 466: 669–691.
- Bal, T. and McCormick, D.A. (1996) What stops synchronized thalamocortical oscillations? *Neuron* 17: 297–308.
- Bal, T., von Krosigk, M., and McCormick, D.A. (1995a) Synaptic and membrane mechanisms underlying synchronized oscillations in the ferret lateral geniculate nucleus *in vitro*. *Journal of Physiology (London)* 483: 641–663.
- Bal, T., von Krosigk, M., and McCormick, D.A. (1995b) Role of the ferret perigeniculate nucleus in the generation of synchronized oscillations *in vitro*. *Journal of Physiology (London)* 483: 665–685.
- Ball, G.J., Gloor, P., and Schaul, N. (1977) The cortical electromicrophysiology of pathological delta waves in the electroencephalogram of cats. *Electroencephalography and Clinical Neurophysiology* 43: 346–361.
- Baraban, J.H. and Aghajanian, G.K. (1981) Noradrenergic innervation of serotonergic neurons in the dorsal raphe: demonstration by electron microscopic autoradiography. *Brain Research* 204: 1–11.
- Barbaresi, P., Minelli, A., and Manzoni, T. (1994) Topographical relations between ipsilateral cortical afferents and callosal neurons in the second somatic sensory area of cats. *Journal of Comparative Neurology* 343: 582–596.
- Barrett, E.F. and Barrett, J.N. (1976) Separation of two voltage-sensitive potassium currents, and demonstration of a tetrodotoxin-resistant calcium current in frog motoneurons. *Journal of Physiology (London)* 255: 737–774.
- Bartee, T.C., Lebow, I.L., and Reed, I.S. (1962) *Theory and Design of Digital Machines*. New York: McGraw-Hill.
- Basbaum, A.I., Clanton, C.H., and Fields, H.L. (1978) Three bulbospinal pathways from the rostral medulla of the cat: an autoradiographic study of pain modulating systems. *Journal of Comparative Neurology* 178: 209–224.
- Basheer, R., Arrigoni, E., Thatte, H.S., Greene, R.W., Ambudkar, I.S., and McCarley, R.W. (2002) Adenosine induces inositol 1, 4, 5-trisphosphate receptor-mediated mobilization of intracellular calcium stores in basal forebrain cholinergic neurons. *Journal of Neuroscience* 22: 7680–7686.
- Basheer, R., Halldner, L., Alanko, L., McCarley, R.W., Fredholm, B.B., and Porkka-Heiskanen, T. (2001a) Opposite changes in adenosine A₁ and A_{2A} receptor mRNA in the rat following sleep deprivation. *Neuroreport* 12: 1577–1580.
- Basheer, R., Rainnie, D.G., Porkka-Heiskanen, T., Ramesh, V., and McCarley, R.W. (2001b) Adenosine, prolonged wakefulness, and A₁ activated NF- κ B DNA binding in the basal forebrain of the rat. *Neuroscience* 104: 731–739.
- Basheer, R., Sherin, J.E., Saper, C.B., Morgan, J.I., McCarley, R.W., and Shiromani, P.J. (1997) Effects of sleep on wake-induced c-fos expression. *Journal of Neuroscience* 17: 9746–9750.
- Basheer, R., Strecker, R.E., Thakkar, M. and McCarley, R.W. (2004) Adenosine and sleep–wake regulation. *Progress in Neurobiology* 73: 379–396.
- Batini, C., Moruzzi, G., Palestini, M., Rossi, G.F. and Zanchetti, A. (1958) Persistent patterns of wakefulness in the pretrigeminal midpontine preparation. *Science* 128: 30–32.
- Batsel, H.L. (1960) Electroencephalographic synchronization and desynchronization in the chronic “cervau isolé” of the dog. *Electroencephalography and Clinical Neurophysiology* 12: 421–430.
- Bauer, G. and Niedermeyer, E. (1979) Acute convulsions. *Clinical Neurophysiology* 10: 127–144.
- Baughman, R.W. and Gilbert, C.D. (1980) Aspartate and glutamate as possible neurotransmitters of cells in layer 6 of the visual cortex. *Nature* 287: 848–849.
- Baughman, R.W. and Gilbert, C.D. (1981) Aspartate and glutamate as possible neurotransmitters in the visual cortex. *Journal of Neuroscience* 1: 427–439.
- Baxter, B.L. (1969) Induction of both emotional behavior and a novel form of REM sleep by chemical stimulation applied to cat mesencephalon. *Experimental Neurology* 23: 220–229.
- Baxter, M.G. and Chiba, A.A. (1999). Cognitive functions of the basal forebrain. *Current Opinion in Neurobiology* 9: 178–183.
- Bazhenov, M., Timofeev, I., Steriade, M., and Sejnowski, T.J. (1998a) Cellular and network models for intrathalamic augmenting responses during 10-Hz stimulation. *Journal of Neurophysiology* 79: 2730–2748.
- Bazhenov, M., Timofeev, I., Steriade, M., and Sejnowski, T.J. (1998b) Computational models of thalamocortical augmenting responses. *Journal of Neuroscience* 18: 6444–6465.
- Bazhenov, M., Timofeev, I., Steriade, M., and Sejnowski, T.J. (1999) Self-sustained rhythmic activity in the thalamic reticular nucleus mediated by depolarizing GABA_A receptor potentials. *Nature Neuroscience* 2: 168–174.

- Beaudet, A. and Descarries, L. (1978) The monoamine innervation of rat cerebral cortex: synaptic and non-synaptic axon terminals. *Neuroscience* 3: 851–860.
- Beaudet, A. and Descarries, L. (1984) Fine structure of monoamine axon terminals in cerebral cortex. In Descarries, L., Reader, T., and Jasper, H.H., eds., *Monoamine Innervation of Cerebral Cortex*, pp. 77–93, New York: Liss.
- Beck, S.G., Clarke, W.P., and Goldfarb, J. (1985) Spiperone differentiates multiple 5-hydroxytryptamine responses in rat hippocampal slices *in vitro*. *European Journal of Pharmacology* 116: 195–197.
- Beckstead, R.M. (1983) Long collateral branches of substantia nigra pars reticulata axons to thalamus, superior colliculus and reticular formation in monkey and cat. Multiple retrograde neuronal labeling with fluorescent dyes. *Neuroscience* 10: 767–779.
- Beckstead, R.M. and Frankfurter, A. (1982) The distribution and some morphological features of substantia nigra neurons that project to the thalamus, superior colliculus and pedunculopontine nucleus in the monkey. *Neuroscience* 10: 2377–2388.
- Beckstead, R.M., Edwards, S.B., and Frankfurter, A. (1981) A comparison of the intranigral distribution of nigroreticular neurons labeled with horseradish peroxidase in the monkey, cat, and rat. *Journal of Neuroscience* 1: 121–125.
- Beersma, D.G.M., Daan, S., and Dijk, D.J. (1987) Sleep intensity and timing – a model for their circadian control. In G.A. Carpenter, ed., *Lectures on Mathematics in the Life Sciences* (vol. 19, *Some Mathematical Questions in Biology: Circadian Rhythms*), Providence (RI): The American Mathematical Society.
- Beersma, D.G.M., Daan, S., and van den Hoofdakker, R.H. (1984) Distribution of REM latencies and other sleep phenomena in depression as explained by a single ultradian rhythm disturbance. *Sleep* 7: 126–136.
- Beersma, D.G.M., Daan, S., and van den Hoofdakker, R.H. (1985) The timing of sleep in depression: theoretical considerations. *Psychiatric Research* 16: 253–262.
- Beersma, D.G.M., van den Hoofdakker, R.H., Daan, S., and van Berkestijn, J.W.B.M. (1983) REM sleep and depression. *Abstracts of the 6th European Congress of Sleep Research*, pp. 349–351, Basel: Karger.
- Behbehani, M.M. (1995) Functional characteristics of the midbrain periaqueductal gray. *Progress in Neurobiology* 46: 575–605.
- Belin, M.F., Aguera, M., Tappaz, M., McRae-Dequeueur, A., Bobillier, P., and Pujol, J.F. (1979) GABA-accumulating neurons in the nucleus raphe dorsalis and periaqueductal gray in the rat: a biochemical and radioautographic study. *Brain Research* 170: 279–297.
- Benardo, L.S. and Prince, D.A. (1981) Acetylcholine induced modulation of hippocampal pyramidal neurons. *Brain Research* 211: 227–234.
- Benardo, L.S. and Prince, D.A. (1982a) Cholinergic pharmacology of mammalian hippocampal pyramidal cells. *Neuroscience* 7: 1703–1712.
- Benardo, L.S. and Prince, D.A. (1982b) Cholinergic excitation of mammalian hippocampal pyramidal cells. *Brain Research* 249: 315–331.
- Ben-Ari, Y., Dingledine, R., Kanazawa, I., and Kelly, J.S. (1976) Inhibitory effects of acetylcholine on neurones in the feline nucleus reticularis thalami. *Journal of Physiology (London)* 261: 647–671.
- Ben-Ari, Y., Krnjević, K., Reiffenstein, R.J., and Reinhardt, W. (1981a) Inhibitory conductance changes and action of γ -aminobutyrate in rat hippocampus. *Neuroscience* 6: 2445–2463.
- Ben-Ari, Y., Krnjević, K., Reinhardt, W., and Ropert, N. (1981b) Intracellular observations on the disinhibitory action of acetylcholine in the hippocampus. *Neuroscience* 6: 2475–2484.
- Bender, M.B., Shanzer, S., and Wagman, I.H. (1964) On the physiologic decussation concerned with head turning. *Confinia Neurologica* 24: 169–181.
- Benedetti, F., Serreti, A., Colombo, C., Campori, E., Barbini, B., di Bella D., and Smeraldi, E. (1999) Influence of a functional polymorphism within the promoter of the serotonin transporter gene on the effects of total sleep deprivation in bipolar depression. *American Journal of Psychiatry* 156: 1450–1452.
- Bennington, J.H. and Heller, H.C. (1995) Restoration of brain energy metabolism as the function of sleep. *Progress in Neurobiology* 45: 347–360.
- Bennington, J.H., Kodali, S.K., and Heller, H.C. (1995) Stimulation of A₁ adenosine receptors mimics the electroencephalographic effects of sleep deprivation. *Brain Research* 692: 79–85.
- Bentivoglio, M., Aggleton, J.P., and Mishkin, M. (1997) The thalamus and memory formation. In M. Steriade, E.G. Jones, and D.A. McCormick (eds.), *Thalamus*, vol. 2 (*Experimental and Clinical Aspects*), pp. 689–720, Oxford: Elsevier.
- Bentivoglio, M., Macchi, G., and Albanese, A. (1981) The cortical projections of the thalamic intralaminar nuclei, as studied in cat and rat with the multiple fluorescent retrograde tracing technique. *Neuroscience Letters* 26: 5–10.
- Berger, H. (1929). Über das Elektroencephalogramm des Menschen. *Archives für Psychiatrie und Nervenkrankheiten* 87: 527–570.

- Berger, H. (1930) Über das Elektroenkephalogram des Menschen. Zweite Mitteilung. *Journal für Psychologie und Neurologie* 40: 160–179.
- Berger, H. (1933) Über das Elektroenkephalogram des Menschen. Sechste Mitteilung. *Archives für Psychiatrie und Nervenkrankheiten* 99: 555–574.
- Berlucchi, G., Aglioti, S., Marzi, C.A., and Tassinari, G. (1995) Corpus callosum and simple visuomotor integration. *Neuropsychologia* 33: 923–936.
- Berlucchi, G., Maffei, L., Moruzzi, G., and Strata, P. (1964) EEG and behavioral effects elicited by cooling of medulla and pons. *Archives Italiennes de Biologie* 102: 372–392.
- Berman, A.L. (1968) *The Brain Stem of the Cat*. Madison: University of Wisconsin Press.
- Bernard, R., Lydic, R., and Baghdoyan, H.A. (2003) Hypocretin-1 causes G protein activation and increases ACh release in rat pons. *European Journal of Neuroscience* 18: 1775–1785.
- Berntson, G.G., Shafi, R., and Sarter, M. (2002) Specific contributions of the basal forebrain corticopetal cholinergic system to electroencephalographic activity and sleep/waking behavior. *European Journal of Neuroscience* 16: 2453–2461.
- Berridge, M.J. (1993) Inositol trisphosphate and calcium signaling. *Nature* 362: 315–325.
- Berry, D.J., Ohara, P.T., Jeffery, G., and Lieberman, A.R. (1986) Are there connections between the thalamic reticular nucleus and the brainstem reticular formation? *Journal of Comparative Neurology* 243: 347–362.
- Besset, A., Billiard, M., Brissaud, L., and Touchon, J. (1988) Effects of toloxatone on sleep architecture. *Abstracts of European Sleep Research Society*: 205.
- Beuckmann, C.T., Sinton, C.M., Williams, S.C., Richardson, J.A., Hammer, R.E., Sakurai, T., and Yanagisawa, M. (2004) Expression of a poly- glutamine-ataxin-3 transgene in orexin neurons induces narcolepsy-cataplexy in the rat. *Journal of Neuroscience* 24: 4469–4477.
- Biber, K., Klotz, K.-N., Berger, M., Gebicke-Härter, P.J., and van Calker, D. (1997) Adenosine A₁ receptor-mediated activation of phospholipase C in cultured astrocytes depends on the level of receptor expression. *Journal of Neuroscience* 17: 4956–4964.
- Biber, K., Lubrich, B., Fiebich, B.L., Hoddede, H.W.G.M., and van Calker, D. (2001). Interleukin-6 enhances expression of adenosine A₁ receptor mRNA and signaling in cultured rat cortical astrocytes and brain slices. *Neuropsychopharmacology* 24: 86–96.
- Biggall, K.E., Imbert, M., and Buser, P. (1966) Optic projections to non visual cortex in the cat. *Journal of Neurophysiology* 29: 396–409.
- Billard, J. and Seignalet, J. (1985) Extraordinary association between HLA-DR2 and narcolepsy. *Lancet* 2: 226–227.
- Bizzi, E. (1966) Discharge patterns of single geniculate neurons during the rapid eye movements of sleep. *Journal of Neurophysiology* 29: 1087–1095.
- Bizzi, E., Pompeiano, O. and Somogyi, I. (1964) Spontaneous activity of single vestibular neurons of unrestrained cats during sleep and wakefulness. *Archives Italiennes de Biologie* 104: 425–458.
- Björklund, A. and Hökfelt, T. (eds.) (1986) *Handbook of Chemical Neuroanatomy (vol. 4, GABA and Neuropeptides in the CNS)*. Amsterdam: Elsevier.
- Björklund, A. and Lindvall, O. (1984) Dopamine-containing systems in the CNS. In A. Björklund, and T. Hökfelt eds., *Handbook of Chemical Neuroanatomy, vol. II: Classical Transmitters in the CNS*, Part I, pp. 55–122, Amsterdam: Elsevier.
- Björklund, A. and Lindvall, O. (1986) Catecholaminergic brain stem regulatory systems. In V.B. Mountcastle, and F.E. Bloom, eds., *Handbook of Physiology, Section 1, Vol. IV: Intrinsic Regulatory Systems of the Brain*, pp. 155–235, Bethesda (MD): American Physiological Society.
- Björvatn, B., Fagerland, S., Eid, T., and Ursin, R. (1997) Sleep/waking effects of a selective 5-HT_{1A} receptor agonist given systemically as well as perfused in the dorsal raphe nucleus in rats. *Brain Research* 770: 81–88.
- Blake, J.F., Brown, M.W., and Collingridge, G.L. (1988) CNQX blocks amino acid depolarizations and synaptic components mediated by non-NMDA receptors in rat hippocampal slices. *Neuroscience Letters* 55: 89–94.
- Bland, B.H. and Oddie, S.D. (1998) Anatomical, electrophysiological and pharmacological studies of ascending brainstem hippocampal synchronizing pathways. *Neuroscience & Biobehavioral Reviews* 22: 259–273.
- Blier, P. and De Montigny, C. (1983) Electrophysiological investigations on the effect of repeated zimelidine administration on serotonergic neurotransmission in the rat. *Journal of Neuroscience* 3: 1270–1278.
- Bloom, F. (1978) Central noradrenergic systems: physiology and pharmacology. In M.A. Lipton, A. Di Mascio, and K.S. Killam, eds., *Psychopharmacology: Generation of Progress*, pp. 131–141, New York: Raven Press.
- Bloom, F.E., Battenberg, E., Rossier, J., Ling, N., and Guillemin, R. (1978) Neurons containing beta-endorphin in rat brain exist separately from those containing enkephalin: immunocytochemical studies. *Proceedings of the National Academy of Sciences of the USA* 75: 1591–1595.

- Bobillier, P., Sequin, S., Petitjean, F., Salvart, D., Touret, M., and Jouvet, M. (1976) The raphe nuclei of cat brain stem: a topographical atlas of their efferent projections as revealed by autoradiography. *Brain Research* 113: 449–486.
- Boehme, R.H., Baker, T.L., Mefford, I.N., Barchas, J.D., Dement, W.C., and Ciaranello, R.D. (1984) Narcolepsy: cholinergic receptor changes in an animal model. *Life Sciences* 34: 1824–1828.
- Bohm, S.K., Grady, E.F., and Bunnett, N.W. (1997). Mechanisms attenuating signaling by G-protein coupled receptors. *Biochemical Journal* 322: 1–18.
- Boissard, R., Gervasoni, D., Schmidt, M.H., Barbagli, B., Fort, P., and Luppi, P.H. (2002) The rat pontomedullary network responsible for paradoxical sleep onset and maintenance: a combined microinjection and functional neuroanatomical study. *European Journal of Neuroscience* 16: 1959–1973.
- Bon, L., Corazza, R. and Inchingolo, P. (1980) Eye movements during the waking sleep cycle of the encephale isolé semichronic cat preparation. *Electroencephalography and Clinical Neurophysiology* 48: 327–340.
- Borbély, A.A. (1982) A two process model of sleep regulation. *Human Neurobiology* 1: 195–204.
- Borbély, A.A. and Tobler, I. (1989) Endogenous sleep-promoting substances and sleep regulation. *Physiological Review* 69: 605–670.
- Borbély, A.A. and Wirz-Justice, A. (1982) Sleep, sleep deprivation and depression—a hypothesis derived from a model of sleep regulation. *Human Neurobiology* 1: 205–210.
- Borbély, A.A., Tobler, I., Loepfe, M., Kupfer, D.J., Ulrich, R.F., Grochocinski, V., Doman, J., and Matthews, G. (1984) All-night spectral analysis of the sleep EEG in untreated depressives and normal controls. *Psychiatry Research* 12: 27–33.
- Borst, J.G.G., Leung, L.W.S., and MacFabe, D.F. (1987) Electrical activity of the cingulate cortex. II. Cholinergic modulation. *Brain Research* 407: 81–93.
- Boudin, H., Sarret, P., Mazella, J., Schonbrunn, A., and Beaudet, A. (2000). Somatostatin-induced regulation of SST2A receptor expression and cell surface availability in central neurons: role of receptor internalization. *Journal of Neuroscience* 20: 5932–5939.
- Bourgin, P., Escourrou, P., Gaultier, C., and Adrien, J. (1995) Induction of rapid eye movement sleep by carbachol infusion into the pontine reticular formation in the rat. *Neuroreport* 6: 532–536.
- Bourgin, P., Huitron-Resendiz, S., Spier, A.D., Fabre, V., Morte, B., Criado, J.R., Sutcliffe, J.G., Henriksen, S.J., and de Lecea, L. (2000) Hypocretin-1 modulates rapid eye movement sleep through activation of locus coeruleus neurons. *Journal of Neuroscience* 20: 7760–7765.
- Bouyer, J.J., Montaron, M.F., and Rougeul, A. (1981) Fast fronto-parietal rhythms during combined focused attentive behaviour and immobility in cat: cortical and thalamic localizations. *Electroencephalography and Clinical Neurophysiology* 51: 244–252.
- Bouyer, J.J., Montaron, M.F., Rougeul-Buser, A., and Buser, P. (1980) A thalamo-cortical rhythmic system accompanying high vigilance levels in the cat. In G. Pfurtscheller, P. Buser, F.H. Lopes da Silva, and H. Petsche, eds., *Rhythmic EEG Activities and Cortical Functioning*, pp. 63–77, Amsterdam: Elsevier/North Holland.
- Bouyer, J.J., Montaron, M.F., Vahnée, J.M., Albert, J.M., and Rougeul, A. (1987) Anatomical localization of cortical beta rhythms in cat. *Neuroscience* 22: 863–869.
- Bowsher, D. and Westman, J. (1970) The gigantocellular reticular region and its spinal afferents: a light and electron microscopic study in the cat. *Journal of Anatomy (London)* 106: 23–36.
- Boylan, M.K., Fisher, R.S., Hull, C.D., Buchwald, N.A., and Levine, M.S. (1986) Axonal branching of basal forebrain projections to the neocortex: a double-labeling study in the cat. *Brain Research* 375: 176–181.
- Bradshaw, C.M., Sheridan, R.D., and Szabadi, E. (1987) Involvement of M1-muscarinic receptors in the excitation of neocortical neurones by acetylcholine. *Neuroscience* 26: 1195–1200.
- Brashear, H.R., Zaborski, L., and Heimer, L. (1986) Distribution of GABAergic and cholinergic neurons in the rat diagonal band. *Neuroscience* 17: 439–451.
- Braun, A.R., Balkin, T.J., Wesensten, N.J., Carson, R.E., Varga, M., Baldwin, P., Selbie, S., Belenky, G., and Herscovitch, P. (1997) Regional cerebral blood flow throughout the sleep–wake cycle. *Brain* 120: 1173–1197.
- Brazier, M.A.B. (1961) *A History of the Electrical Activity of the Brain*. London: Pitman.
- Breder, C.D., Dinarello, C.A., and Saper, C.B. (1988) Interleukin-1 immunoreactive innervation of the human hypothalamus. *Science* 240: 321–324.
- Breder, C.D., Tsujimoto, M., Terano, Y., Scott, D.W., and Saper, C.B. (1993) Distribution and characterization of tumor necrosis factor-alpha-like immuno-reactivity in the murine central nervous system. *Journal of Comparative Neurology* 337: 543–567.
- Bredow, S., Taishi, P., Guha-Thakurta, N., Obal, F. Jr., and Krueger, J.M. (1997) Diurnal variations of tumor necrosis factor alpha mRNA and alpha-tubulin mRNA in rat brain. *Journal of Neuroimmunomodulation* 4: 84–90.

- Breitwieser, G.E. and Szabo, G. (1985) Uncoupling of cardiac muscarinic and beta-adrenergic receptors from ion channels by a guanine nucleotide analogue. *Nature* 317: 538–540.
- Bremer, F. (1935) Cerveau "isolé" et physiologie du sommeil. *Comptes Rendus de la Société de Biologie (Paris)* 118: 1235–1241.
- Bremer, F. (1937) L'activité cérébrale au cours du sommeil et de la narcose. Contribution à l'étude du mécanisme du sommeil. *Bulletin de l'Académie Royale de Médecine de Belgique* 4: 68–86.
- Bremer, F. (1938) L'activité électrique de l'écorce cérébrale et le problème physiologique du sommeil. *Bolletino de la Societa Italiana della Biologia Sperimentale* 13: 271–290.
- Bremer, F. (1954) The neurophysiological problem of sleep. In E.D. Adrian, F. Bremer, and H.H. Jasper, eds., *Brain Mechanisms and Consciousness*, pp. 137–162, Oxford: Blackwell.
- Bremer, F. (1975) The isolated brain and its aftermath. In F.G. Worden, J.P. Swazey, and G. Adelman, eds., *The Neurosciences: Paths of Discovery*, pp. 267–274, Cambridge (MA): The MIT Press.
- Bremer, F. and Stoupe, N. (1959) Facilitation et inhibition des potentiels évoqués corticaux dans l'éveil cérébral. *Archives Internationales de Physiologie* 67: 240–275.
- Bremer, F. and Terzuolo, C. (1954) Contribution à l'étude des mécanismes physiologiques du maintien de l'activité vigile du cerveau. Interaction de la formation réticulée et de l'écorce cérébrale dans le processus de l'éveil. *Archives Internationales de Physiologie* 62: 157–178.
- Bremer, F., Stoupe, N., and Van Reeth, P.C. (1960) Nouvelles recherches sur la facilitation et l'inhibition des potentiels évoqués corticaux dans l'éveil réticulaire. *Archives Italiennes de Biologie* 98: 229–247.
- Brezina, V., Eckert, R., and Erxleben, C. (1987) Modulation of potassium conductances by an endogenous neuropeptide in neurones of *Aplysia californica*. *Journal of Physiology (London)* 382: 267–290.
- Bridges, R.J., Stevens, D.R., Kahle, J.S., Nunn, P.B., Kadri, M., and Cotman, C.W. (1989) Structure-function studies on N-oxalyl-diamino-dicarboxylic acids and excitatory amino acid receptors: evidence that beta-L-ODAP is a selective non-NMDA agonist. *Journal of Neuroscience* 9: 2073–2079.
- Bringuier, V., Frégnac, Y., Baranyi, A., Debanne, D., and Shulz, D.E. (1997) Synaptic origin and stimulus dependency of neuronal oscillatory activity in the primary visual cortex of the cat. *Journal of Physiology (London)* 500: 751–774.
- Brodal, A. (1957) *The Reticular Formation of the Brain Stem: Anatomical Aspects and Functional Correlations*. Edinburgh: Oliver & Boyd.
- Brooks, D.C. and Gershon, M.D. (1971) Eye movement potentials in the oculomotor and visual systems of the cat: a comparison of reserpine induced waves with those present during wakefulness and rapid eye movement sleep. *Brain Research* 27: 223–239.
- Brooks, D.C., Gershon, M.D., and Simon, R.P. (1972) Brain stem serotonin depletion and pontogeniculo-occipital wave activity in the cat treated with reserpine. *Neuropharmacology* 11: 511–520.
- Brown, A.M., Schwindt, P.C., and Crill, W.E. (1993) Voltage dependence and activation kinetics of pharmacologically defined components of high-threshold calcium current in rat neocortical neurons. *Journal of Neurophysiology* 70: 1530–1543.
- Brown, D.A. and Adams, P.R. (1980) Muscarinic suppression of a novel voltage-sensitive K current in a vertebrate neurone. *Nature* 283: 673–676.
- Brown, R.E., Sergeeva, O.A., Eriksson, K.S., and Haas, H.L. (2002) Convergent excitation of dorsal raphe serotonin neurons by multiple arousal systems (orexin/hypocretin, histamine and noradrenaline). *Journal of Neuroscience* 22: 8850–8859.
- Brownstein, M. (1975) Biogenic amine content of the hypothalamic nuclei. In W.E. Stumpf and L.D. Grant, eds., *Anatomical Neuroendocrinology*, pp. 393–396, Basel: Karger.
- Brundage, J.M. and Dunwiddie, T.V. (1997) Role of adenosine as a modulator of synaptic activity in the central nervous system. *Advances in Pharmacology* 39: 353–391.
- Budde, T., Mager, R., and Pape, H.C. (1992) Different types of potassium outward current in relay neurons acutely isolated from the rat lateral geniculate nucleus. *European Journal of Neuroscience* 4: 708–722.
- Burlhis, T.M. and Aghajanian, G.K. (1987) Pacemaker potentials of serotonergic dorsal raphe neurons: contribution of a low-threshold Ca^{2+} conductance. *Synapse* 1: 582–588.
- Buser, P., Richard, D., and Lescop, J. (1969) Contrôle, par le cortex sensori-moteur, de la réactivité des cellules réticulaires mésencéphaliques chez le chat. *Experimental Brain Research* 9: 83–95.
- Butcher, L.L., Talbot, K., and Bilezikian, L. (1975) Acetylcholinesterase neurons in dopamine-containing regions of the brain. *Journal of Neural Transmission* 37: 127–153.
- Buttner, J.A. and Henn, V. (1976) An autoradiographic study of the pathways from the pontine reticular formation involved in horizontal eye movements. *Brain Research* 108: 155–164.
- Buttner, U. and Henn, V. (1977) Vertical eye movement related unit activity in the rostral mesencephalic reticular formation of the alert monkey. *Brain Research* 130: 239–252.
- Buttner, U., Hepp, K., and Henn, V. (1977) Neurons in the rostral mesencephalic and paramedian pontine reticular formation generating fast eye movements. In R. Baker and A. Berthoz, eds., *Control of Gaze by Brain Stem Neurons*, vol. 1, pp. 309–318, New York: Elsevier/North Holland.

- Buttner-Ennever, J.A. (1977) Pathways from the pontine reticular formation to structures controlling horizontal and vertical eye movements in the monkey. In R. Baker and A. Berthoz, eds., *Control of Gaze by Brain Stem Neurons*, vol. 1, pp. 89–98, New York: Elsevier/North Holland.
- Buttner-Ennever, J.A. and Buttner, U. (1978) A cell group associated with vertical eye movements in the rostral mesencephalic reticular formation of the monkey. *Brain Research* 151: 31–47.
- Buttner-Ennever, J.A., Cohen, B., Pause, M., and Fries, W. (1988) Raphe nucleus of the pons containing omnipause neurons of the oculomotor system in the monkey, and its homologue in man. *Journal of Comparative Neurology* 267: 307–321.
- Buzsáki, G. (1996) The hippocampal-neocortical dialogue. *Cerebral Cortex* 6: 81–92.
- Buzsáki, G. (1998) Memory consolidation during sleep: a neurophysiological perspective. *Journal of Sleep Research* 7 (Suppl. 1), 17–23.
- Buzsáki, G. (2002) Theta oscillations in the hippocampus. *Neuron* 33: 325–340.
- Buzsáki, G. and Gage, F.H. (1989) The nucleus basalis: a key structure in neocortical arousal. In M. Frotscher and U. Misgeld, eds., *Central Cholinergic Synaptic Transmission*, pp. 159–171, Basel: Birkhauser Verlag.
- Buzsáki, G., Bickford, R.G., Armstrong, D.M., Ponomareff, G., Chen, K.S., Ruiz, R., Thal, L.G., and Gage, F.H. (1988a) Electrical activity in the neocortex of freely moving young and aged rats. *Neuroscience* 26: 735–744.
- Buzsáki, G., Bickford, R.G., Ponomareff, G., Thal, L.J., Mandel, R., and Gage, F.H. (1988b) Nucleus basalis and thalamic control of neocortical activity in the freely moving rat. *Journal of Neuroscience* 8: 4007–4026.
- Buzsáki, G., Leung, L.W.S., and Vanderwolf, C.H. (1983) Cellular bases of hippocampal EEG in the behaving rat. *Brain Research Reviews* 6: 139–171.
- Caballero, A. and De Andres, I. (1986) Unilateral lesions in locus coeruleus area enhance paradoxical sleep. *Electroencephalography and Clinical Neurophysiology* 64: 339–346.
- Cairns, H., Oldfield, R.C., Pennybacker, J.B., and Whitteridge, D. (1941) Akinetic mutism with an epidermoid cyst of the 3rd ventricle. *Brain* 64: 273–290.
- Calvet, J., Calvet, M.C., and Scherrer, J. (1964) Etude stratigraphique corticale de l'activité EEG spontanée. *Electroencephalography and Clinical Neurophysiology* 17: 109–125.
- Calvo, J.M., Badillo, S., Morales-Ramirez, M., and Palacios-Salas, P. (1987) The role of the temporal lobe amygdala in ponto-geniculo-occipital activity and sleep organization in cats. *Brain Research* 403: 22–30.
- Cannon, S.C. and Robinson, D.A. (1987) Loss of the neural integrator of the oculomotor system from brain stem lesions in monkey. *Journal of Neurophysiology* 57: 1383–1409.
- Cannon, W.B. and Rosenblueth, A. (1949) *The Supersensitivity of Denervated Structures: A Law of Denervation*. New York: Macmillan.
- Carbone, E. and Lux, H.D. (1984) A low voltage-activated, fully inactivating Ca^{2+} channel in vertebrate sensory neurones. *Nature* 310: 501–502.
- Carey, R.G. and Rieck, R.W. (1987) Topographic projections to the visual cortex from the basal forebrain in the rat. *Brain Research* 424: 205–215.
- Carli, G., Diete-Spiff, K., and Pompeiano, O. (1967) Presynaptic and postsynaptic inhibition of somatic afferent volleys through the cuneate nucleus during sleep. *Archives Italiennes de Biologie* 105: 52–82.
- Carskadon, M.A. and Dement, W.C. (2000) Normal human sleep: an overview. In M.H. Kryger, T. Roth, and W.C. Dement, eds., *Principles and Practice of Sleep Medicine*, pp. 15–25, Philadelphia: W.B. Saunders.
- Carstens, E. and Trevino, D.L. (1978) Laminar origins of spinothalamic projections in the cat as determined by the retrograde transport of horseradish peroxidase. *Journal of Comparative Neurology* 182: 151–166.
- Carter, D.A. and Fibiger, H.C. (1977) Ascending projections of presumed dopamine-containing neurons in the ventral tegmentum of the rat as demonstrated by horseradish peroxidase. *Neuroscience* 2: 569–576.
- Castaigne P., Buge, A., Escourolle, R., and Masson, M. (1962) Ramollissement pédonculaire médian, tegmento-thalamique avec ophtalmoplégie et hypersomnie. *Revue de Neurologie (Paris)* 106: 357–367.
- Castro-Alamancos, M.A. and Connors, B.W. (1996a) Spatiotemporal properties of short-term plasticity in sensorimotor thalamocortical pathways of the rat. *Journal of Neuroscience* 16: 2767–2779.
- Castro-Alamancos, M.A. and Connors, B.W. (1996b) Cellular mechanisms of the augmenting response: short-term plasticity in a thalamocortical pathway. *Journal of Neuroscience* 16: 7742–7756.
- Catsman-Berrevoets, C.E. and Kuypers, H.G.J.M. (1975) Pericruciate cortical neurons projecting to brain stem reticular formation, dorsal column nuclei and spinal cord in the cat. *Neuroscience Letters* 1: 257–262.
- Catsman-Berrevoets, C.E. and Kuypers, H.G.J.M. (1981) A search for corticospinal collaterals to the thalamus and mesencephalon by means of multiple retrograde fluorescent tracers in cat and rat. *Brain Research* 218: 15–33.

- Caulier, L.J. and Kulics, A.T. (1988) A comparison of awake and sleeping cortical states by analysis of the somatosensory-evoked response of postcentral area 1 in rhesus monkey. *Experimental Brain Research* 72: 584–592.
- Cechetto, D.F., Standaert, D.G., and Saper, C.B. (1985) Spinal and trigeminal dorsal horn projections to the parabrachial nucleus in the rat. *Journal of Comparative Neurology* 240: 153–160.
- Cederbaum, J.M. and Aghajanian, G.K. (1976) Noradrenergic neurons of the locus coeruleus: inhibition by epinephrine and activation by the alpha-antagonist piperhexane. *Brain Research* 112: 413–419.
- Cederbaum, J.M. and Aghajanian, G.K. (1978) Afferent projections to the rat locus coeruleus as determined by a retrograde tracing technique. *Journal of Comparative Neurology* 178: 1–16.
- Celesia, G.G. and Jasper, H.H. (1966) Acetylcholine released from cerebral cortex in relation to state of activation. *Neurology* 16: 1053–1064.
- Cespuglio, R., Faradji, H., Gomez, M.E., and Jouvet, M. (1981) Single unit recordings in the nuclei raphe dorsalis and magnus during the sleep-waking cycle of semi-chronic prepared cats. *Neuroscience Letters* 24: 133–138.
- Cespuglio, R., Faradji, H., Hahn, Z., and Jouvet, M. (1984) Voltammetric detection of brain 5-hydroxyindolamines by means of electrochemically treated carbon fibre electrodes: chronic recordings for up to one month with movable cerebral electrodes in the sleeping or waking rat. In C.A. Marsden, ed., *Measurement of Neurotransmitter Release In Vivo*, IBRO Handbook Series, vol. 6, pp. 173–191, New York: Wiley.
- Cespuglio, R., Gomez, M.E., Walker, E., and Jouvet, M. (1979) Effets du refroidissement et de la stimulation des noyaux du système du raphé sur les états de vigilance chez le chat. *Electroencephalography and Clinical Neurophysiology* 47: 289–308.
- Cespuglio, R., Gomez, M.E., Faradji, H., and Jouvet, M. (1982) Alterations in the sleep-waking cycle induced by cooling of the locus coeruleus area. *Electroencephalography and Clinical Neurophysiology* 54: 570–578.
- Cespuglio, R., Sarda, N., Gharib, A., Chastrette, N., Houdouin, F., Rampin, C., and Jouvet, M. (1990) Voltammetric detection of the release of 5-hydroxyindole compounds throughout the sleep-waking cycle of the rat. *Experimental Brain Research* 80: 121–128.
- Chagnac-Amitai, Y., Luhmann, H.J., and Prince, D.A. (1990) Burst generating and regular spiking layer 5 pyramidal neurons of rat neocortex have different morphological features. *Journal of Comparative Neurology* 296: 598–613.
- Chagoya de Sanchez, V., Hernandez, M.R., Suarez, J., Vidrio, S., Yanez, L., and Diaz Munoz, M. (1993) Day-night variations of adenosine and its metabolizing enzymes in the brain cortex of the rat—possible physiological significance for the energetic homeostasis and the sleep-wake cycle. *Brain Research* 612: 115–121.
- Chamberlin, N.A., Arrigoni, E., Chou, T.C., Scammell, T.E., Greene, R.W., and Saper, C.B. (2003) Effects of adenosine on GABAergic synaptic inputs to identified ventrolateral preoptic neurons. *Neuroscience* 119: 913–918.
- Champagnat, J., Jacquin, T., and Richter, D.W. (1986) Voltage-dependent currents in neurones of the nuclei of the solitary tract of rat brainstem slices. *Pflügers Archives* 406: 372–379.
- Chandler, S.H., Chase, M.H., and Nakamura, Y. (1980) Intracellular analysis of synaptic mechanisms controlling trigeminal motoneuron activity during sleep and wakefulness. *Journal of Neurophysiology* 44: 359–371.
- Charara, A. and Parent, A. (1998) Chemoarchitecture of the primate dorsal raphe nucleus. *Journal of Chemical Neuroanatomy* 15: 111–127.
- Chase, M.H. and Morales, F.R. (1983) Subthreshold excitatory activity and motoneuron discharge during REM periods of active sleep. *Science* 221: 1195–1198.
- Chase, M.H. and Morales, F.R. (1985) Postsynaptic modulation of spinal cord motoneuron membrane potential during sleep. In D.J. McGinty, A. Morrison, R. Drucker-Colin, and P.L. Parmeggiani, eds., *Brain Mechanisms of Sleep*, pp. 45–61, New York: Raven Press.
- Chase, M.H., Chandler, S.H., and Nakamura, Y. (1980) Intracellular determination of membrane potential of trigeminal motoneurons during sleep and wakefulness. *Journal of Neurophysiology* 44: 349–358.
- Chase, M.H., Enomoto, Murakami, R., Nakamura, Y., and Taira, M. (1981) Intracellular potential of medullary reticular neurons during sleep and wakefulness. *Experimental Neurology* 71: 226–233.
- Chase, M.H., Enomoto, S., Hiraba, K., Katoh, M., Nakamura, Y., Sahara, Y., and Tiara, M. (1984) Role of medullary reticular neurons in the inhibition of trigeminal motoneurons during active sleep. *Experimental Neurology* 84: 364–373.
- Chase, M.H., Morales, F.R., Boxer, P.A., Fung, S.J., and Soja, P.J. (1986) Effect of stimulation of the nucleus reticularis gigantocellularis on the membrane potential of cat lumbar motoneurons during sleep and wakefulness. *Brain Research* 386: 237–244.

- Chase, M.H., Soja, P.J., and Morales, F.R. (1989) Evidence that glycine mediates the postsynaptic potentials that inhibit lumbar motoneurons during the atonia of active sleep. *Journal of Neuroscience* 9: 743–751.
- Chemelli, R.M., Willie, J.T., Sinton, C.M., Elmquist, J.K., Scammell, T., Lee, C., Richardson, J.A., Williams, S.C., Xiong, Y., Kisanuki, Y., Fitch, T.E., Nakazato, M., Hammer, R.E., Saper, C.B., and Yanagisawa, M. (1999) Narcolepsy in orexin knockout mice: molecular genetics of sleep regulation. *Cell* 98: 437–451.
- Chen, D.F. and Fetz, E.E. (1993) Effect of synchronous neural activity on synaptic transmission in primate cortex. *Society for Neuroscience Abstracts* 19: 781.
- Chen, S. and Bentivoglio, M. (1993) Nerve growth factor receptor-containing cholinergic neurons of the basal forebrain project to the thalamic reticular nucleus in the rat. *Neuroscience Letters* 606: 207–212.
- Chen, W., Zhang, J.J., Hu, G.Y., and Wu, C.P. (1996) Electrophysiological and morphological properties of pyramidal and non-pyramidal neurons in the cat motor cortex *in vitro*. *Neuroscience* 73: 39–55.
- Chen, Z., Gardi, J., Kushikata, T., Fang, J., and Krueger, J.M. (1999) Nuclear factor- κ B like activity increases in murine cerebral cortex after sleep deprivation. *American Journal of Physiology* 276: R1812–R1818.
- Cheng, B., Christakos, S., and Mattson, M.A. (1994) Tumor necrosis factors protect neurons against metabolic excitotoxic insults and promote maintenance of calcium homeostasis. *Neuron* 12: 139–153.
- Chéron, G., Gillis, P., and Godaux, E. (1986b) Lesions in the cat prepositus complex: effects on the optokinetic system. *Journal of Physiology (London)* 372: 95–111.
- Chéron, G., Godaux, E., Laune, J.M., and VanDerkelen, B. (1986a) Lesions in the cat prepositus: effects on the vestibulo-ocular reflex and saccades. *Journal of Physiology (London)* 372: 75–94.
- Chevalier, G., Deniau, J.M., Thierry, A.M., and Féger, J. (1981a) The nigro-tectal pathway. An electrophysiological reinvestigation in the rat. *Brain Research* 213: 253–263.
- Chevalier, G., Thierry, A.M., Shibazaki, T., and Féger, J. (1981b) Evidence for a GABAergic inhibitory nigrotectal pathway in the rat. *Neuroscience Letters* 21: 67–70.
- Chi, C.C. and Flynn, J.P. (1971) Neuroanatomic projections related to biting attack elicited from hypothalamus in cats. *Brain Research* 35: 49–66.
- Childs, J.A. and Gale, K. (1983) Neurochemical evidence for a nigrosegmental GABAergic projection. *Brain Research* 258: 109–114.
- Chou, T.C., Bjorkum, A.A., Gaus, S.E., Lu, J., Scammell, T.E., and Saper, C.B. (2002) Afferents to the ventrolateral preoptic nucleus. *Journal of Neuroscience* 22: 977–990.
- Chou, T.C., Scammell, T.E., Gooley, J.J., Gaus, S.E., Saper, C.B., and Lu, J. (2003) Critical role of dorso-medial hypothalamic nucleus in a wide range of behavioral circadian rhythms. *Journal of Neuroscience* 23: 10691–10702.
- Chrobak, J.J. and Buzsáki, G. (1996) High-frequency oscillations in the output networks of the hippocampal-entorhinal axis of the freely behaving rats. *Journal of Neuroscience* 16: 3056–3066.
- Chu, N.S. and Bloom, F.E. (1974) Activity patterns of catecholamine-containing neurons in the dorsolateral tegmentum of unrestrained cats. *Journal of Neurobiology* 5: 527–544.
- Churchill, A.L., Obal, F. Jr., Simasko, S.M., and Krueger, J.M. (2002) GHRH and IL1 β increase cytoplasmic Ca^{2+} levels in cultured hypothalamic GABAergic neurons. *Brain Research* 949: 209–212.
- Cirelli, C., Pompeiano, M., and Tononi, G. (1995) Sleep deprivation and c-fos expression in the rat brain. *Journal of Sleep Research* 4: 92–106.
- Cissé, Y., Grenier, F., Timofeev, I., and Steriade, M. (2003) Electrophysiological properties and input-output organization of callosal neurons in cat association cortex. *Journal of Neurophysiology*, submitted.
- Claes, E. (1939) Contribution à l'étude physiologique de la fonction visuelle. I. Analyse oscillographique de l'activité spontanée et sensorielle de l'aire visuelle corticale chez le chat non anesthésié. *Archives Internationales de Physiologie* 48: 181–237.
- Clarke, P.B.S., Schwartz, R.D., Paul, S.M., Pert, C.B., and Pert, A. (1985) Nicotinic binding in rat brain: autoradiographic comparison of (^3H) acetylcholine, (^3H) nicotine, and (^{125}I)-a-bungarotoxin. *Journal of Neuroscience* 5: 1307–1315.
- Clarke, P.B.S., Schwartz, R.D., Paul, S.M., Pert, C.B., Coben, L.A., Danzinger, W.L., and Berg, L. (1983) Frequency analysis of the resting awake EEG in mild senile dementia of Alzheimer type. *Electroencephalography and Clinical Neurophysiology* 55: 372–380.
- Coben, L.A., Danziger, W.L., and Berg, L. (1983) Frequency analysis of the resting awake EEG in mild senile dementia of Alzheimer type. *Electroencephalography and Clinical Neurophysiology* 55: 372–380.
- Coble, P., Foster, F.G., and Kupfer, D.J. (1976) Electroencephalographic sleep diagnosis of primary depression. *Archives of General Psychiatry* 33: 1124–1127.
- Coenen, A.M.L. and Vendrik, A.J.H. (1972) Determination of the transfer ratio of cat's geniculate neurons through quasi-intracellular recordings and the relation with the level of alertness. *Experimental Brain Research* 14: 227–242.

- Cohen, A.H., Rossignol, S., and Grillner, S. (eds.) (1988) *Neural control of Rhythmic Movements in Vertebrates*. New York: Wiley.
- Cole, A.E. and Nicoll, R.A. (1983) Acetylcholine mediates a slow synaptic potential in hippocampal pyramidal cells. *Science* 221: 1299–1301.
- Collier, B. and Mitchell, J.F. (1967) The central release of acetylcholine during consciousness and after brain lesions. *Journal of Physiology (London)* 188: 83–98.
- Collingridge, G.L. and Bliss, T.V.P. (1987) NMDA receptors-their role in long-term potentiation. *Trends in Neurosciences* 10: 288–293.
- Collins, D.R., Lang, E.J., and Paré, D. (1999) Spontaneous activity of the perirhinal cortex in behaving rats. *Neuroscience* 89: 1025–1039.
- Collins, S., Caron, M.G., and Lefkowitz, R.J. (1992) From ligand binding to gene expression: new insights into the regulation of G-protein-coupled receptors. *Trends in Biochemical Science* 17: 37–39.
- Conner, J.A. and Stevens, C.F. (1971) Voltage clamp studies of a transient outward membrane current in gastropod neural somata. *Journal of Physiology (London)* 213: 21–30.
- Connors, B.W. and Gutnick, M.J. (1990) Intrinsic firing patterns of diverse neocortical neurons. *Trends in Neurosciences* 13: 99–104.
- Connors, B.W., Gutnick, M.J., and Prince, D.A. (1982) Electrophysiological properties of neocortical neurons *in vitro*. *Journal of Neurophysiology* 48: 1302–1320.
- Connors, B.W., Malenka, R.C., and Silva, L.R. (1988) Two inhibitory postsynaptic potentials, and GABA_A and GABA_B receptor-mediated responses in neocortex of rat and cat. *Journal of Physiology (London)* 406: 443–468.
- Consolazione, A., Priestley, J.V., and Cuello, A.C. (1984) Serotonin-containing projections to the thalamus in the rat revealed by a horseradish peroxidase and peroxidase antiperoxidase double-staining technique. *Brain Research* 322: 233–243.
- Contreras, D. and Steriade, M. (1995) Cellular basis of EEG slow rhythms: a study of dynamic corticothalamic relationships. *Journal of Neuroscience* 15: 604–622.
- Contreras, D. and Steriade, M. (1996) Spindle oscillation: the role of corticothalamic feedback in a thalamically generated rhythm. *Journal of Physiology (London)* 490: 159–179.
- Contreras, D., Curró Dossi, R., and Steriade, M. (1993) Electrophysiological properties of cat reticular neurones *in vivo*. *Journal of Physiology (London)* 470: 273–294.
- Contreras, D., Destexhe, A., and Steriade, M. (1997b) Spindle oscillations during cortical spreading depression in naturally sleeping cats. *Neuroscience* 77: 933–996.
- Contreras, D., Destexhe, A., Sejnowski, T.J., and Steriade, M. (1996a) Control of spatiotemporal coherence of a thalamic oscillation by corticothalamic feedback. *Science* 274: 771–774.
- Contreras, D., Destexhe, A., Sejnowski, T.J., and Steriade, M. (1997a) Spatiotemporal patterns of spindle oscillations in cortex and thalamus. *Journal of Neuroscience* 17: 1179–1196.
- Contreras, D., Dürmüller, N., and Steriade, M. (1997c) Absence of a prevalent laminar distribution of IPSPs in association cortical neurons of cat. *Journal of Neurophysiology* 78: 2742–2753.
- Contreras, D., Timofeev, I., and Steriade, M. (1996b) Mechanisms of long-lasting hyperpolarizations underlying slow sleep oscillations in cat corticothalamic networks. *Journal of Physiology (London)* 494: 251–264.
- Coombs, S.J., Eccles, J.C., and Fatt, P. (1955) The electrical properties of the motoneurone membrane. *Journal of Physiology (London)* 130: 291–325.
- Cordeau, J.P., Moreau, A., Beaulnes, A., and Laurin, C. (1963) EEG and behavioral changes following microinjections of acetylcholine and adrenaline in the brain stem of cats. *Archives Italiennes de Biologie* 101: 30–47.
- Cordeau, J.P., Moreau, A., Beaulnes, A., and Laurin, C. (1983) EEG and behavioral changes following microinjections of acetylcholine and adrenaline in the brain stem of cats. *Archives Italiennes de Biologie* 101: 30–47.
- Cordova, C.A., Mulkern, K.J., McCarley, R.W., Baxter, M.G., Chiba, A.A., and Strecker, R.E. (2003) Behavioral assessment of sleepiness in rats: 10h of sleep deprivation disrupts serial reaction time performance. *Society for Neuroscience 33rd Annual Meeting Oral Presentation*, Monday Nov. 10, 2003, New Orleans, LA.
- Cortes, R., Soriano, E., Pazos, A., Probst, A., and Palacios, J.M. (1988) Autoradiography of antidepressant binding sites in the human brain: localization using [³H]imipramine and [³H]paroxetine. *Neuroscience* 27: 473–496.
- Cotman, C.W., Flatman, J.A., Ganong, A.H., and Perkins, M.N. (1986) Effects of excitatory amino acid antagonists on evoked and spontaneous excitatory potentials in guinea-pig hippocampus. *Journal of Physiology (London)* 378: 403–415.
- Cotman, C.W., Monaghan, D.T., Ottersen, O.P., and Storm-Mathisen, J. (1987) Anatomical organization of excitatory amino acid receptors and their pathways. *Trends in Neurosciences* 10: 273–280.

- Cowan, W.M., Gottlieb, D.I., Hendrickson, A.E., Price, J.L., and Woolsey, T.A. (1972) The autoradiographic demonstration of axonal connections in the central nervous system. *Brain Research* 37: 21–51.
- Cowan, W.M., Woolsey, T.A., Wann, D.F., and Dierker, M.L. (1975) The computer analysis of Golgi-impregnated neurons. In M. Santini, ed., *Golgi Centennial Symposium*, pp. 81–85, New York: Raven Press.
- Crawford, J.M. and Curtis, D.R. (1966) Pharmacological studies on feline Betz cells. *Journal of Physiology (London)* 186: 121–138.
- Crepel, F., Debono, M. and Flores, R. (1987) Alpha-adrenergic inhibition of rat cerebellar purkinje cells *in vitro*: a voltage-clamp study. *Journal of Physiology (London)* 383: 487–498.
- Creutzfeldt, O., Grunewald, G., Simonova, O., and Schmiz, H. (1969) Changes of the basic rhythms of the EEG during the performance of mental and visuomotor tasks. In C.R. Evans and T.B. Mulholland, eds., *Attention in Neurophysiology*, pp. 148–168, London: Butterworths.
- Creutzfeldt, O.D., Watanabe, S., and Lux, H.D. (1966) Relations between EEG phenomena and potentials of single cells. I. Evoked responses after thalamic and epicortical stimulation. *Electroencephalography and Clinical Neurophysiology* 20: 1–18.
- Cropper, E.C., Eisenman, J.S., and Azmitia, E.C. (1985) An immunocytochemical study of the serotonergic innervation of the thalamus of the rat. *Journal of Comparative Neurology* 234: 38–50.
- Crosby, E., Humphrey, T., and Lauer, E. (1962) *Correlative anatomy of the nervous system*. New York: Macmillan.
- Crunelli, V. and Leresche, N. (2002) Childhood absence epilepsy: genes, channels, neurons and networks. *Nature Reviews Neuroscience* 3: 371–382.
- Crunelli, V. and Segal, M. (1985) An electrophysiological study of neurones in the rat median raphe and their projections to septum and hippocampus. *Neuroscience* 15: 47–60.
- Crunelli, V., Haby, M., Jassik-Gerschenfeld, D., Leresche, N., and Pirchio, M. (1988) Cl^- and K^+ dependent inhibitory postsynaptic potentials evoked by interneurons in the rat lateral geniculate nucleus. *Journal of Physiology (London)* 399: 153–176.
- Crunelli, V., Kelly, J.S., Leresche, N., and Pirchio, M. (1987a) The ventral and dorsal lateral geniculate nucleus of the rat: intracellular recordings *in vitro*. *Journal of Physiology (London)* 384: 587–601.
- Crunelli, V., Kelly, J.S., Leresche, N., and Pirchio, M. (1987b) On the excitatory postsynaptic potential evoked by stimulation of the optic tract in the rat lateral geniculate nucleus. *Journal of Physiology (London)* 384: 603–618.
- Crunelli, V., Leresche, N., and Parnavelas, J.G. (1987c) Membrane properties of morphologically identified X and Y cells in the lateral geniculate nucleus of the rat *in vitro*. *Journal of Physiology (London)* 390: 243–256.
- Crunelli, V., Leresche, N., and Pirchio, M. (1985) Non-NMDA receptors mediate the optic nerve input to the rat LGN *in vitro*. *Journal of Physiology (London)* 360: 40P.
- Crutcher, M.D., Branch, M.H., DeLong, M.R., and Georgopoulos, A.P. (1980) Activity of zona incerta neurons in the behaving primate. *Society for Neuroscience Abstracts* 6: 676.
- Csicsvari, J., Hirase, H., Czurkó, A., and Buzsáki, G. (1998) Reliability and state dependence of pyramidal cell—interneuron synapses in the hippocampus: an ensemble approach in the behaving rat. *Neuron* 21: 179–189.
- Csicsvari, J., Hirase, H., Czurkó, A., Mamiya, A., and Buzsáki, G. (1999) Fast network oscillations in the hippocampal CA1 region of the behaving rat. *Journal of Neuroscience* 19: RC20.
- Cuenod, M., Bagnoli, P., Beaudet, A., Rustioni, A., Wiklund, L., and Streit, P. (1982) Transmitter-specific retrograde labeling of neurons. In V. Chan-Palay and S. Palay, eds., *Cytochemical Methods in Neuroanatomy*, pp. 17–43, New York: A.R. Liss.
- Cull-Candy, S.G. and Usowicz, M.M. (1987) Multiple-conductance channels activated by excitatory amino acids in cerebellar neurons. *Nature* 325: 525–528.
- Cullinan, W.E. and Zaborszky, L. (1991) Organization of ascending hypothalamic projections to the rostral forebrain with special reference to the innervation of cholinergic projection neurons. *Journal of Comparative Neurology* 306: 631–667.
- Cunha, R.A. (2001) Adenosine as a neuromodulator and as a homeostatic regulator in the nervous system: different roles, different sources and different receptors. *Neurochemistry International* 38: 107–125.
- Cunningham, E.T. and LeVay, S. (1986) Laminar and synaptic organization of the projection from the thalamic nucleus centralis to primary visual cortex in the cat. *Journal of Comparative Neurology* 254: 65–77.
- Curro Dossi, R., Nuñez, A., and Steriade, M. (1992a) Electrophysiology of a slow (0.5–4Hz) intrinsic oscillation of cat thalamocortical neurones *in vivo*. *Journal of Physiology (London)* 447: 215–234.

- Curró Dossi, R., Paré, D., and Steriade, M. (1991) Short-lasting nicotinic and long-lasting muscarinic depolarizing responses of thalamocortical neurons to stimulation of mesopontine cholinergic nuclei. *Journal of Neurophysiology* 65: 393–406.
- Curró Dossi, R., Paré, D., and Steriade, M. (1992b) Various types of inhibitory postsynaptic potentials in anterior thalamic cells are differentially altered by stimulation of laterodorsal tegmental cholinergic nucleus. *Neuroscience* 47: 279–289.
- Curtis, D.R. and Eccles, R.M. (1958) The excitation of Renshaw cells by pharmacological agents applied electrophoretically. *Journal of Physiology (London)* 141: 435–445.
- Curtis, D.R. and Ryall, R.W. (1966a) The excitation of Renshaw cells by cholinomimetics. *Experimental Brain Research* 2: 49–65.
- Curtis, D.R. and Ryall, R.W. (1966b) The acetylcholine receptors of Renshaw cells. *Experimental Brain Research* 2: 66–80.
- Czeisler, C.A., Kronauer, R.E., Mooney, J.J., Anderson, J.L., and Allan, J.S. (1987) Biologic rhythm disorders, depression, and phototherapy. *Psychiatric Clinic of North America* 10: 687–709.
- Czeisler, C.A., Zimmerman, J.C., Ronda, J.M., Moore-Ede, M.C., and Weitzman, E.D. (1980) Timing of REM sleep is coupled to the circadian rhythm of body temperature in man. *Sleep* 2: 329–346.
- Daan, S., Beersma, D.G.M., and Borbely, A.A. (1984) Timing of human sleep: recovery process gated by a circadian pacemaker. *American Journal of Physiology* 246 (*Regulatory Integrative Comparative Physiology* 15): R161–R178.
- Dahlstrom, A. and Fuxe, K. (1964) Evidence for the existence of monoamine-containing neurones in the central nervous system. I. Demonstration of monoamines in the cell bodies of brain stem neurones. *Acta Physiologica Scandinavica* (Suppl. 232) 62: 1–55.
- Daniels, L. (1934) Narcolepsy. *Medicine* 13: 1–122.
- Date, Y., Ueta, Y., Yamashita, H., Yamaguchi, H., Matsukura, S., Kangawa, K., Sakurai, T., Yanagisawa, M., and Nakazato, M. (1999) Orexins, orexigenic hypothalamic peptides, interact with autonomic, neuroendocrine and neuroregulatory systems. *Proceedings of the National Academy of Sciences of the USA* 96: 748–753.
- Datta, S., Calvo, J.M., Quattrochi, J.J., and Hobson, J.A. (1992) Cholinergic microstimulation of the peribrachial nucleus in the cat. I. Immediate and prolonged increases in ponto-geniculo-occipital waves. *Archives Italiennes de Biologie* 130: 263–284.
- Datta, S., Curró Dossi, R., Paré, D., Oakson, G., and Steriade, M. (1991) Substantia nigra reticulata neurons during sleep–waking states: relation with ponto-geniculo-occipital waves. *Brain Research* 566: 344–347.
- de la Peña, E. and Geijo-Barrientos, E. (1996) Laminar localization, morphology, and physiological properties of pyramidal neurons that have low-threshold calcium current in the guinea-pig medial frontal cortex. *Journal of Neuroscience* 16: 5301–5311.
- de Lecea, L., Kilduff, T.S., Peyron, C., Gao, X., Foye, P.E., Danielson, P.E., Fukuhara, C., Battenberg, E.L., Gautvik, V.T., Bartlett, F.S., Frankel, W.N., van den Pol, A.N., Bloom, F.E., Gautvik, K.M., and Sutcliffe, J.G. (1998) The hypocretins: hypothalamus-specific peptides with neuroexcitatory activity. *Proceedings of the National Academy of Sciences of the USA* 95: 322–327.
- De Sarro, G., Gareri, P., Sinopoli, V.A., David, E., and Rotiroli, D. (1997) Comparative, behavioural and electrocortical effects of tumor necrosis factor- α and interleukin-1 microinjected into the locus coeruleus of rat. *Life Sciences* 60: 555–564.
- DeFelipe, J. (1993) Neocortical neuronal diversity: chemical heterogeneity revealed by co-localization studies of classic transmitters, neuropeptides, calcium-binding proteins and cell surface molecules. *Cerebral Cortex* 3: 273–289.
- DeFelipe, J. (1999) Chandelier cells and epilepsy. *Brain* 122: 1807–1822.
- DeFelipe, J. and Jones, E.G. (1992) High-resolution light and electron microscopy immunocytochemistry of colocalized GABA and calbindin D-28k in somata and double bouquet cell axons in the monkey sensory-motor cortex. *European Journal of Neuroscience* 4: 46–60.
- Delagrangé, P., Tadjer, D., Rougeul, A., and Buser, P. (1987) Activité unitaire de neurones du noyau ventral postérieur du thalamus pour divers degrés de vigilance chez le chat normal. *Comptes Rendus de l'Académie des Sciences (Paris)* 305: 149–155.
- Delgado-García, J.M., del Pozo, F., and Baker, R. (1988a) Behavior of neurons in the abducens nucleus of the alert cat. I. Motoneurons. *Neuroscience* 17: 929–952.
- Delgado-García, J.M., del Pozo, F., and Baker, R. (1988b) Behavior of neurons in the abducens nucleus of the alert cat. II. Internuclear neurons. *Neuroscience* 17: 953–973.
- DeLima, A.D. and Singer, W. (1987) The brainstem projection to the lateral geniculate nucleus in the cat: identification of cholinergic and monoaminergic elements. *Journal of Comparative Neurology* 259: 92–121.

- DeLima, A.D., Montero, V.M., and Singer, W. (1985) The cholinergic innervation of the visual thalamus: an EM immunocytochemical study. *Experimental Brain Research* 59: 206–212.
- Dell, P.C. (1958) Some basic mechanisms of the translation of bodily needs into behaviour. In G.E.W. Wolstenholme and C.M. O'Connor, eds., *Neurological Basis of Behaviour*, pp. 187–203. London: Churchill.
- Dement, W.C. (1958) The occurrence of low voltage, fast, electroencephalogram patterns during behavioral sleep in the cat. *Electroencephalography and Clinical Neurophysiology* 10: 291–296.
- Dement, W.C. and Kleitman, N. (1957a) Cyclic variations in EEG during sleep and their relation to eye movements, body motility, and dreaming. *Electroencephalography and Clinical Neurophysiology* 9: 673–690.
- Dement, W.C. and Kleitman, N. (1957b) The relation of eye movements during sleep to dream activity: an objective method for the study of dreaming. *Journal of Experimental Psychology* 53: 339–346.
- Dement, W.C., Ferguson, J., Cohen, H., and Barchas, J. (1969) Non-chemical methods and data using a biochemical model: the REM quanta. In A. Mandell and M.P. Mandell, eds., *Psychochemical Research in Man—Methods, Strategy and Theory*, pp. 275–325. New York: Academic Press.
- DeMontigny, C. and Aghajanian, G.K. (1978) Tricyclic antidepressants: long-term treatment increases responsivity of rat forebrain neurons to serotonin. *Science* 202: 1303–1306.
- Dempsey, E.W. and Morison, R.S. (1942) The production of rhythmically recurrent cortical potentials after localized thalamic stimulation. *American Journal of Physiology* 135: 293–300.
- Descarries, L. and Umbriaco, D. (1995) Ultrastructural basis of monoamine and acetylcholine function in CNS. *Seminars in Neuroscience* 7: 309–318.
- Descarries, L., Berthelot, F., Garcia, S., and Beaudet, A. (1986) Dopaminergic projection from nucleus raphe dorsalis to neostriatum in the rat. *Journal of Comparative Neurology* 249: 511–520.
- Descarries, L., Gisiger, V., and Steriade, M. (1997) Diffuse transmission by acetylcholine in the CNS. *Progress in Neurobiology* 53: 603–625.
- Descarries, L., Watkins, K.C., and Lapierre, Y. (1977) Noradrenergic axon terminals in the cerebral cortex of rat. III. Topometric ultrastructural analysis. *Brain Research* 133: 197–222.
- Deschênes, M. and Steriade, M. (1988) The neuronal mechanism of thalamic PGO waves. In M. Bentivoglio, G. Macchi, and R. Spreafico, eds., *Cellular Thalamic Mechanisms*, pp. 197–206. Amsterdam: Elsevier.
- Deschênes, M., Labelle, A., and Landry, P. (1979) Morphological characterization of slow and fast pyramidal tract cells in the cat. *Brain Research* 178: 251–274.
- Deschênes, M., Madariaga-Domich, A., and Steriade, M. (1985) Dendrodendritic synapses in cat reticularis thalami nucleus, a structural basis for thalamic spindle synchronization. *Brain Research* 334: 169–171.
- Deschênes, M., Paradis, M., Roy, J.P., and Steriade, M. (1984) Electrophysiology of neurons of lateral thalamic nuclei in cat: resting properties and burst discharges. *Journal of Neurophysiology* 51: 1196–1219.
- Deschênes, M., Roy, J.P., and Steriade, M. (1982) Thalamic bursting mechanism: a slow inward current revealed by membrane hyperpolarization. *Brain Research* 239: 289–293.
- Desimone, R. and Duncan, J. (1995) Neural mechanisms of selective attention. *Annual Reviews of Neuroscience* 18: 193–222.
- Desmedt, J.E. (1981) Scalp-recorded cerebral event-related potentials in man as point of entry into the analysis of cognitive processing. In F.O. Schmitt, F.G. Worden, G. Adelman, and S.G. Dennis, eds., *The Organization of the Cerebral Cortex*, pp. 441–473. Cambridge (MA): The MIT Press.
- Desmedt, J.E. and Bourguet, M. (1985) Color imaging of parietal and frontal somatosensory potential fields evoked by stimulation of median or posterior tibial nerve in man. *Electroencephalography and Clinical Neurophysiology* 62: 1–17.
- Desmedt, J.E., Brunko, E., and Debecker, J. (1980) Maturation and sleep correlates of the somatosensory evoked potential. In J.E. Desmedt, ed., *Clinical Uses of Cerebral, Brainstem and Spinal Somatosensory Evoked Potentials*, pp. 146–161. Basel: Karger.
- Desmedt, J.E., Huy, N.T., and Bourguet, M. (1983) The cognitive P40, N60, and P100 components of somatosensory evoked potentials and the earliest electrical signs of sensory processing in man. *Electroencephalography and Clinical Neurophysiology* 56: 272–282.
- Destexhe, A. and Sejnowski, T.J. (2001) *Thalamocortical Assembly*. Oxford: Oxford University Press.
- Destexhe, A., Contreras, D., and Steriade, M. (1999a) Neocortical excitability controls the coherence of thalamic-generated oscillations through corticothalamic feedback. *Neuroscience* 92: 427–443.
- Destexhe, A., Contreras, D., and Steriade, M. (1999b) Spatiotemporal analysis of local field potentials and unit discharges in cat cerebral cortex during natural wake and sleep states. *Journal of Neuroscience* 19: 4595–4608.
- Destexhe, A., Contreras, D., and Steriade, M. (2001) LTS cells in cerebral cortex and their role in generating spike-and-wave oscillations. *Neurocomputing* 38–40: 555–563.

- Destexhe, A., Contreras, D., Sejnowski, T.J., and Steriade, M. (1994a) A model of spindle rhythmicity in the isolated thalamic reticular nucleus. *Journal of Neurophysiology* 72: 803–818.
- Destexhe, A., Contreras, D., Sejnowski, T.J., and Steriade, M. (1994b) Modeling the control of reticular thalamic oscillations by neuromodulators. *NeuroReport* 5: 2217–2220.
- Destexhe A., Contreras D., Steriade M., Sejnowski T.J., and Huguenard J.R. (1996) *In vivo*, *in vitro* and computational analysis of dendritic calcium currents in thalamic reticular neurons. *Journal of Neuroscience* 16: 169–185.
- Detari, L., Juhasz, G., and Kukorelli, T. (1987) Neuronal firing in the pallidal region: firing patterns during sleep-wakefulness cycle in cats. *Electroencephalography and Clinical Neurophysiology* 67: 159–166.
- Deuchars, J. and Thomson, A.M. (1995) Innervation of burst firing spiny interneurons by pyramidal cells in deep layers of rat somatomotor cortex: paired intracellular recordings with biocytin filling. *Neuroscience* 69: 739–755.
- Deurveilher, S., Hars, B., and Hennevin, E. (1997) Pontine microinjection of carbachol does not reliably enhance paradoxical sleep in rats. *Sleep* 20: 593–607.
- Deutch, A.V., Kalivas, P.W., Goldstein, M., and Roth, R.M. (1986) Interconnections of the mesencephalic dopamine cell groups. *Society for Neuroscience Abstracts* 12: 875.
- Dickson, C.T., Kirk, I.J., Oddie, S.D., and Bland, B.H. (1995) Classification of theta-related cells in the entorhinal cortex: cell discharges are controlled by the ascending brainstem synchronizing pathway in parallel with hippocampal theta-related cells. *Hippocampus* 5: 306–319.
- Dickson, C.T., Mena, A.R., and Alonso, A. (1997) Electroresponsiveness of medial entorhinal cortex layer III neurons *in vitro*. *Neuroscience* 81: 937–950.
- Dickstein, J.B., Moldofsky, H., Lue, F.A., and Hay, J.B. (1999) Intracerebroventricular injection of TNF- α promotes sleep and is recovered in cervical lymph. *American Journal of Physiology* 276: R1018–R1022.
- Dijk, D.J. and Beersma, D.G.M. (1988) Effects of seganserine, a 5-HT₂ receptor antagonist, on human SWS and EEG power spectra. *Abstracts of the European Sleep Research Society*, pp. 250.
- Dinges, D.F., Pack, F., Williams, K., Gillen, K.A., Powell, J.W., Ott, G.E., Aptowicz, C., and Pack, A.I. (1997) Cumulative sleepiness, mood disturbances and psychomotor vigilance performance decrements during a week of sleep restricted to 4–5 hour per night. *Sleep* 20: 267–267.
- Dingledine, R. (1983) *N*-methyl aspartate activates voltage-dependent calcium conductance in rat hippocampal pyramidal cells. *Journal of Physiology (London)* 343: 385–405.
- Dingledine, R. and Kelly, J.S. (1977) Brain stem stimulation and the acetylcholine-evoked inhibition of neurones in the feline nucleus reticularis thalami. *Journal of Physiology (London)* 271: 135–154.
- Divac, I. (1975) Magnocellular nuclei of the basal forebrain project to neocortex, brain stem, and olfactory bulb. Review of some functional correlates. *Brain Research* 93: 385–398.
- Dodd, J., Dingledine, R., and Kelly, J.S. (1981) The excitatory action of acetylcholine on hippocampal neurones of the guinea pig and rat maintained *in vitro*. *Brain Research* 207: 109–127.
- Doty, H.U., Pawelzik, H., and Zieglgänsberger, W. (1991) Actions of noradrenaline on neocortical neurons *in vitro*. *Brain Research* 545: 307–311.
- Domich, L., Oakson, G., and Steriade, M. (1986) Thalamic burst patterns in the naturally sleeping cat: a comparison between cortically-projecting and reticularis neurones. *Journal of Physiology (London)* 379: 429–450.
- Donoghue, J.P. and Carroll, K.L. (1987) Cholinergic modulation of sensory responses in rat primary somatic sensory cortex. *Brain Research* 408: 367–371.
- Donoghue, J.P. and Ebner, F.F. (1981) The laminar distribution and ultrastructure of fibers projecting from three thalamic nuclei to the somatic sensory-motor cortex of the opossum. *Journal of Comparative Neurology* 198: 389–420.
- Drew, T., Dubuc, R., and Rossignol, S. (1986) Discharge patterns of reticulospinal and other reticular neurons in chronic unrestrained cats walking on a treadmill. *Journal of Neurophysiology* 55: 375–401.
- Drucker-Colin, R., and Pedraza, J.G.B. (1983) Kainic acid lesions of gigantocellular tegmental field (FTG) neurons does not abolish REM sleep. *Brain Research* 272: 387–391.
- Drummond, A.H., Benson, J.A., and Levitan, I.B. (1980) Serotonin-induced hyperpolarization of an identified Aplysia neuron is mediated by cyclic AMP. *Proceedings of the National Academy of Sciences of the USA* 77: 5013–5017.
- Drummond, S.P.A., Brown, G.G., Gillin, J.C., Stricker, J.L., Wong, E.C., and Buxton, R.B. (2000) Altered brain response to verbal learning following sleep deprivation. *Nature* 403: 655–657.
- Drury, A.N. and Szent-Gyorgyi, A. (1929) The physiological activity of adenine compounds with special reference to their action upon mammalian heart. *Journal of Physiology* 68: 213–237.
- Duggan, A.W. and Hall, J.G. (1975) Inhibition of thalamic neurones by acetylcholine. *Brain Research* 100: 445–449.

- Dugovic, C. and Waquier, A. (1987) 5-HT₂ receptors could be primarily involved in the regulation of slow-wave sleep in the rat. *European Journal of Pharmacology* 137: 145–146.
- Duman, R.S., Heninger, G.R., and Nestler, E.J. (1997) A molecular and cellular theory of depression. *Archives of General Psychiatry* 54: 597–606.
- Dumont, S. and Dell, P. (1960) Facilitation réticulaire des mécanismes visuels corticaux. *Electroencephalography and Clinical Neurophysiology* 12: 769–796.
- Dunlap, K. and Fischbach, G.D. (1981) Neurotransmitters decrease the calcium conductance activated by depolarization of embryonic chick sensory neurones. *Journal of Physiology (London)* 317: 519–535.
- Dunwiddie, T.V. (1985) The physiological role of adenosine in the central nervous system. *International Review of Neurobiology* 27: 63–139.
- Dunwiddie, T.V. and Masino, S.A. (2001) The role and regulation of adenosine in the central nervous system. *Annual Review of Neuroscience* 24: 31–55.
- Dunwiddie, T.V. and Worth, T. (1982) Sedative and anticonvulsant effects of adenosine analogs in mouse and rat. *Journal of Pharmacology and Experimental Therapeutics* 220: 70–76.
- Eccles, J.C. (1961) Chairman's opening remarks. In G.E.W. Wolstenholme and M. O'Connor, eds., *The Nature of Sleep*, 1–3, London: Churchill.
- Eccles, J.C. (1964) *The Physiology of Synapses*. New York: Academic Press.
- Eccles, J.C., Nicoll, R.A., Taborikova, H., and Willey, T.J. (1975) Medial reticular neurons projecting rostrally. *Journal of Neurophysiology* 38: 531–538.
- Eccles, J.C., Nicoll, R.A., Schwarz, D.W.F., Tabórikova, H., and Willey, T.J. (1976) Topographic studies on medial reticular nucleus. *Journal of Neurophysiology* 38: 109–118.
- Eckenstein, F., Barde, Y.A., and Thoenen, H. (1981) Production of specific antibodies to choline acetyltransferase purified from pig brain. *Neuroscience* 6: 993–1000.
- Eckenstein, F.P., Baughman, R.W., and Quinn, J. (1988) An anatomical study of cholinergic innervation in rat cerebral cortex. *Neuroscience* 25: 457–474.
- Eckhorn, R., Bauer, R., Jordan, W., Brosch, M., Kruse, W., Munk, M., and Reitboeck, H.J. (1988) Coherent oscillations: a mechanism of feature linking in the visual cortex? *Biological Cybernetics* 60: 121–130.
- Edstrom, J.P. and Phillis, J.W. (1980) A cholinergic projection from the globus pallidus to cerebral cortex. *Brain Research* 189: 524–529.
- Edwards, D.L., Johnston, K.M., Poletti, C.E., and Foote W.E. (1987) Morphology of pontomedullary raphe and reticular formation neurons in the brainstem of the cat: an intracellular HRP study. *Journal of Comparative Neurology* 256: 257–273.
- Edwards, S.B. (1975) Autoradiographic studies of the projections of the midbrain reticular formation: descending projections of nucleus cuneiformis. *Journal of Comparative Neurology* 161: 341–358.
- Edwards, S.B. (1980) The deep cell layers of the superior colliculus: their reticular characteristics and structural organization. In J.A. Hobson and M.A.B. Brazier, eds., *The Reticular Formation Revisited*, pp. 193–209, New York: Raven Press.
- Edwards, S.B. and DeOlmos, J.S. (1976) Autoradiographic studies of the projections of the midbrain reticular formation: ascending projections of nucleus cuneiformis. *Journal of Comparative Neurology* 165: 417–432.
- Egan, T.M. and North, R.A. (1985) Acetylcholine acts on m₂-muscarinic receptors to excite rat locus coeruleus neurons. *British Journal of Pharmacology* 85: 733–735.
- Egan, T.M. and North, R.A. (1986a) Acetylcholine hyperpolarizes central neurones by acting on a muscarinic receptor subtype. *Nature* 319: 405–407.
- Egan, T.M. and North, R.A. (1986b) Actions of acetylcholine and nicotine on rat locus coeruleus neurons *in vitro*. *Neuroscience* 19: 565–571.
- Egan, T.M., Henderson, G., North, R.A., and Williams, J.T. (1983) Noradrenaline-mediated synaptic inhibition in rat locus coeruleus neurones. *Journal of Physiology (London)* 345: 477–488.
- Ehlers, C., Hendricksen, S.J., Wang, M., Rivier, J., Vale, W., and Bloom, F.E. (1983) Corticotropin releasing factor produces increases in brain excitability and convulsive seizures in rats. *Brain Research* 278: 332–336.
- El Mansari, M., Sakai, K., and Jouvet, M. (1989) Unitary characteristics of presumptive cholinergic tegmental neurons during the sleep-waking cycle in freely moving cats. *Experimental Brain Research* 76: 519–529.
- El Mansari, M., Sakai, K., and Jouvet, M. (1990) Responses of presumed cholinergic mesopontine tegmental neurons to carbachol microinjections in freely moving cats. *Experimental Brain Research* 83: 115–123.
- Elias, C.F., Saper, C.B., Maratos-Flier, E., Tritos, N.A., Lee, C., Kelly, J., Tatro, J.B., Hoffman, G.E., Ollmann, M.M., Barsh, G.S., Sakurai, T., Yanagisawa, M., and Elmquist, J.K. (1998) Chemically

- defined projections linking the mediobasal hypothalamus and the lateral hypothalamic area. *Journal of Comparative Neurology* 402: 442–459.
- Elliott, H.C. (1969) *Textbook of Neuroanatomy*. Philadelphia: Lippincott.
- Emerson, R.G., Sgro, J.A., Pedley, T.A., and Hauser, A. (1988) State-dependent changes in the N20 component of the median nerve somatosensory evoked potential. *Neurology* 38: 64–67.
- Endo, K., Araki, T., and Ito, K. (1977) Short latency EPSPs and incrementing PSPs of pyramidal tract cells evoked by stimulation of the nucleus centralis lateralis of the thalamus. *Brain Research* 132: 541–546.
- Endo, S., Kobayashi, T., Yamamoto, T., Fukuda, H., Sasaki, M., and Ohta, T. (1981) Persistence of the circadian rhythm of REM sleep: a variety of experimental manipulations of the sleep-wake cycle. *Sleep* 4: 319–328.
- Engel, A.K., König, P., Gray, C.M., and Singer, W. (1990) Stimulus-dependent neuronal oscillations in cat visual cortex: inter-columnar interaction as determined by cross-correlation analysis. *European Journal of Neuroscience* 2: 588–606.
- Engel, A.K., König, P., Kreiter, A.K., and Singer, W. (1991) Interhemispheric synchronization of oscillatory neuronal responses in cat visual cortex. *Science* 252: 1177–1179.
- Ennis, M. and Aston-Jones, G. (1988) Activation of locus coeruleus from nucleus paragigantocellularis: a new excitatory amino acid pathway in brain. *Journal of Neuroscience* 8: 3644–3657.
- Eriksson, K.S., Sergeeva, O., Brown, R.E. Haas, H.L. (2001) Orexin/ Hypocretin excites the neurons of the tuberomammillary nucleus. *Journal of Neuroscience* 21: 9273–9279.
- Espana, R.A., Valentino, R.J., and Berridge, C.W. (2003) Fos immunoreactivity in hypocretin-synthesizing and hypocretin-1 receptor-expressing neurons: effects of diurnal and nocturnal spontaneous waking, stress and hypocretin-1 administration. *Neuroscience* 121: 201–217.
- Evarts, E.V. (1964) Temporal patterns of discharge of pyramidal tract neurons during sleep and waking. *Journal of Neurophysiology* 27: 152–171.
- Evarts, E.V. (1965) Relation of discharge frequency to conduction velocity in pyramidal tract neurons. *Journal of Neurophysiology* 28: 216–228.
- Evarts, E.V. and Tanji, J. (1976) Reflex and intended responses in motor cortex pyramidal tract neurons of monkey. *Journal of Neurophysiology* 39: 1069–1080.
- Evarts, E.V., Shinoda, Y., and Wise, S.P. (1984) *Neurophysiological Approaches to Higher Brain Functions*. New York: Wiley.
- Everitt, B.J. and Robbins, T.W. (1997) Central cholinergic systems and cognition. *Annual Review of Psychology* 48: 649–684.
- Evinger, G., Kaneko, C.R.S., and Fuchs, A. (1982) Activity of omnipause neurons in alert cats during saccadic eye movements and visual stimuli. *Journal of Neurophysiology* 47:827–844.
- Exner, S. (1894) *Entwurf zu einer Physiologischen Erklärung der Psychischen Erscheinungen*, Vienna: Deuticke.
- Eysel, U.T., Pape, H.C., and van Schayck, R. (1986) Excitatory and differential disinhibitory actions of acetylcholine in the lateral geniculate nucleus of the cat. *Journal of Physiology (London)* 370: 233–254.
- Façon, E., Steriade, M., and Wertheim, N. (1958) Hypersomnie prolongée engendrée par des lésions bilatérales du système activateur médial. Le syndrome thrombotique de la bifurcation du tronc basilaire. *Revue Neurologique (Paris)* 98: 117–133.
- Fadiga, E. and Pupilli, G.C. (1964) Teleceptive components of the cerebellar function. *Physiological Reviews* 44: 432–486.
- Fallahi, N., Broad, R.M., Jin, S., and Fredholm, B.B. (1996) Release of adenosine from rat hippocampal slices by nitric oxide donors. *Journal of Neurochemistry* 67: 186–193.
- Fallon, J.H. (1981) Collateralization of monoamine neurons: mesotelencephalic dopamine projections to caudate, septum, and frontal cortex. *Journal of Neuroscience* 1: 1361–1368.
- Fang, J., Wang, Y., and Krueger, J.M. (1997) Mice lacking the TNF 55 kD receptor fail to sleep more after TNF alpha treatment. *Journal of Neuroscience* 17: 5949–5955.
- Fang, J., Wang, Y., and Krueger, J.M. (1998) The effects of interleukin-1 beta on sleep are mediated by the type I receptor. *American Journal of Physiology* 274: R655–R660.
- Fanselow, E.F., Sameshina, K., Baccala, L.A., and Nicolelis, M.A.I. (2001) Thalamic bursting in rats during different awake behavioral states. *Proceedings of the National Academy of Sciences of the USA* 98: 15330–15335.
- Farmer, S.F. (1998) Rhythmicity, synchronization and binding in human and primate motor cortex. *Journal of Physiology (London)* 509: 3–14.
- Fatt, P. and Ginsborg, B.L. (1958) The ionic requirements for the production of action potentials in crustacean muscle fibres. *Journal of Physiology (London)* 142: 516–543.
- Faull, K.F., Zeller-DeAmicis, L.C., Radde, L., Bowersox, S.S., Baker, T.L., Kilduff, T.S., and Dement, W.C. (1986) Biogenic amine concentrations in the brains of normal and narcoleptic canines: current status. *Sleep* 9: 107–110.

- Feinberg, I. and March, J.D. (1988) Cyclic delta peaks during sleep: result of a pulsatile endocrine process? *Archives of General Psychiatry* 45: 1141–1142.
- Feinberg, I., March, J.D., Floyd, T.C., Jimison, R., Bossom-Demitrack, L., and Katz, P.H. (1985) Homeostatic changes during post-nap sleep maintain baseline levels of delta EEG. *Electroencephalography and Clinical Neurophysiology* 61: 134–137.
- Feldberg, L.A. and Sherwood, P.D. (1954) Injections of drugs into the lateral ventricle of the cat. *Journal of Physiology* 123: 148–167.
- Fenik, V., Ogawa, H., Davies, R.O., and Kubin, L. (1999) Pontine carbachol produces a spectrum of REM sleep-like and arousal-like electrocortical, motor and noradrenergic cellular responses in urethane-anesthetized rats. *Sleep Research Online* 2 (Suppl. 1): 30.
- Ferster, D. and Lindstrom, S. (1986) Augmenting responses evoked in area 17 of the cat by intracortical axon collaterals of cortico-geniculate cells. *Journal of Physiology (London)* 367: 217–232.
- Fibiger, H.C. (1982) The organization and some projections of cholinergic neurons of the mammalian forebrain. *Brain Research Reviews* 4: 327–388.
- Filion, M., Lamarre, Y., and Cordeau, J.P. (1971) Neuronal discharges of the ventrolateral nucleus of the thalamus during sleep and wakefulness. *Experimental Brain Research* 12: 499–508.
- Finlayson, P.G. and Marshall, K.C. (1986) Locus coeruleus neurons in culture have a developmentally transient alpha-1-adrenergic response. *Developmental Brain Research* 25: 292–295.
- Fischer-Williams, M. (1963) Burst-suppression activity as indication of undercut cortex. *Electroencephalography and Clinical Neurophysiology* 15: 723–724.
- Fisher, S.K. (1995) Homologous and heterologous regulation of receptor-stimulated phosphoinositide hydrolysis. *European Journal of Pharmacology* 288: 231–250.
- Flatman, J.A., Schwindt, P.C., Crill, W.E., and Stafstrom, C.E. (1983) Multiple actions of N-methyl-D-aspartate on cat neocortical neurons *in vitro*. *Brain Research* 266: 169–173.
- Floyd, R.A. and Krueger, J.M. (1997) Diurnal variations of TNF alpha in the rat brain. *Neuroreport* 8: 915–918.
- Foehring, R.C., Schwindt, P.C., and Crill, W.E. (1989) Norepinephrine selectively reduces slow Ca^{2+} and Na^{+} -mediated K^{+} currents in cat neocortical neurons. *Journal of Neurophysiology* 61: 245–256.
- Foote, S.L., Aston-Jones, G., and Bloom, F.E. (1980) Impulse activity of locus coeruleus neurons in awake rats and monkeys is a function of sensory stimulation and arousal. *Proceedings of the National Academy of Sciences of the USA* 77: 3033–3037.
- Foote, S.L., Bloom, F.E., and Aston-Jones, G. (1983) Nucleus locus coeruleus: new evidence of anatomical and physiological specificity. *Physiological Reviews* 63: 844–914.
- Foote, S.L., Freedman, R., and Oliver, A.P. (1975) Effects of putative neurotransmitters on neuronal activity in monkey auditory cortex. *Brain Research* 86: 229–242.
- Ford, B., Holmes, C.J., Mainville, L., and Jones, B.E. (1995) GABAergic neurons in the rat pontomesencephalic tegmentum: codistribution with cholinergic and other tegmental neurons projecting to the posterior lateral hypothalamus. *Journal of Comparative Neurology* 363: 177–196.
- Fornal, C., Auerbach, S., and Jacobs, B.L. (1985) Activity of serotonin containing neurons in nucleus raphe magnus in freely moving cats. *Experimental Neurology* 88: 590–608.
- Forscher, P. and Oxford, G.S. (1985) Modulation of calcium channels by norepinephrine in internally dialyzed avian sensory neurons. *Journal of General Physiology* 85: 743–764.
- Fort, P., Khateb, A., Pegna, A., Mühlethaler, M., and Jones, B.E. (1995) Noradrenergic modulation of cholinergic nucleus basalis neurons demonstrated by *in vitro* pharmacological and immunohistochemical evidence in the guinea-pig brain. *European Journal of Neuroscience* 7: 1502–1511.
- Fort, P., Khateb, A., Serafin, M., Mühlethaler, M., and Jones, B.E. (1998) Pharmacological characterization and differentiation of non-cholinergic nucleus basalis neurons *in vitro*. *Neuroreport* 9: 61–65.
- Fortin, M., Asselin, M.C., Gould, P.V., and Parent, A. (1998) Calretinin-immunoreactive neurons in the human thalamus. *Neuroscience* 84: 537–548.
- Foster, F.G., Kupfer, D.J., Coble, P., and McPartland, R.J. (1976) Rapid eye movement sleep density. *Archives of General Psychiatry* 33: 1119–1123.
- Foster, J.A. (1980) Intracortical origin of recruiting responses in the cat cortex. *Electroencephalography and Clinical Neurophysiology* 48: 639–653.
- Foutz, A.S., Mitler, M.M., Cavalli-Sforza, L.L., and Dement, W.C. (1979) Genetic factors in canine narcolepsy. *Sleep* 1: 413–422.
- Francesconi, W., Muller, C.M., and Singer, W. (1988) Cholinergic mechanisms in the reticular control of transmission in the cat lateral geniculate nucleus. *Journal of Neurophysiology* 59: 1690–1718.
- Frank, M.G., Issa, N.P., and Stryker, M.P. (2001) Sleep enhances plasticity in the developing visual cortex. *Neuron* 30: 275–287.
- Fredholm, B.B. (1997) Adenosine and neuroprotection. *International Review in Neurobiology* 40: 259–280.

- Fredholm, B.B., Arslan, G., Kull, B., Wassermann, W., and Schulte, G. (2000) Structure and function of adenosine receptors and their genes. *Naunyn-Schmiedberg's Archives of Pharmacology* 362: 364–374.
- Fredholm, B.B., Bättig, K., Holmen, J., Nehlig, A., and Zvartau, E.E. (1999) Actions of caffeine in the brain with special reference to factors that contribute to its widespread use. *Pharmacological Review* 51: 83–133.
- Fredholm, B.B., Lindstrom, K., and Wallman-Johansson, A. (1994) Propentofylline and other adenosine transport inhibitors increase the efflux of adenosine following electrical or metabolic stimulation of rat hippocampal slices. *Journal of Neurochemistry* 62: 563–73.
- Freedman, J.E. and Aghajanian, G.K. (1987) Role of phosphoinositide metabolites in the prolongation of afterhyperpolarizations by alpha 1-adrenoceptors in rat dorsal raphe neurons. *Journal of Neuroscience* 7: 3897–3906.
- Freeman, W.J. (1975) *Mass Action in the Nervous System*. New York: Academic Press.
- Freud, S. (1887–1902) *The Origins of Psychoanalysis: Letters to Wilhelm Fliess, Drafts and Notes: 1887–1902*. New York: Basic Books (reprinted 1954).
- Freud, S. (1891) *Zur Auffassung der Aphasien*. Vienna: Deuticke.
- Freud, S. (1895) Project for a scientific psychology. In *Complete Psychological Works*, Standard edition, vol. 1 (Translated and edited by J. Strachey), pp. 294–397, London: Hogarth Press.
- Freud, S. (1900a) Die Traumdeutung. In *Gesammelte Schriften* (1952), vol. II, Vienna: Internationaler Psychoanalytischer Verlag.
- Freud, S. (1900b) The interpretation of dreams. In *Complete Psychological Works*. Standard edition, vols. 4 and 5 (Translated and edited by J. Strachey), London: Hogarth Press (reprinted 1966).
- Freud, S. (1988) Gehirn. In *Handwoerterbuch der gesamten Medizin*, Stuttgart: F. Enke.
- Freund, S., Ungerer, M., and Lohse, M. (1994) A₁ adenosine receptors expressed in CHO-cells couple to adenylate cyclase and to phospholipase C. *Naunyn-Schmiedberg's Archives of Pharmacology* 350: 49–56.
- Freund, T.F. and Buzsáki, G. (1988) Alterations in excitatory and GABAergic inhibitory connections in hippocampal transplants. *Neuroscience* 27: 373–385.
- Freund, T.F. and Buzsáki, G. (1996) Interneurons of the hippocampus. *Hippocampus* 6: 347–470.
- Freund, T.F. and Meskenaite, V. (1992) Gamma-aminobutyric acid-containing basal forebrain neurons innervate inhibitory interneurons in the neocortex. *Proceedings of the National Academy of Sciences of the USA* 89: 738–742.
- Freund, T.J., Powell, J.F., and Smith, A.D. (1984) Tyrosine hydroxylase-immunoreactive boutons in synaptic contact with identified striatonigral neurons, with particular reference to dendritic spines. *Neuroscience* 13: 1189–1215.
- Friedman, L. and Jones B.E. (1984) Study of sleep-wakefulness by computer graphics and cluster analysis before and after lesions of the pontine tegmentum in the cat. *Electroencephalography and Clinical Neurophysiology* 57: 43–56.
- Fuchs, A.F. and Ron, S. (1968) An analysis of rapid eye movements of sleep in the monkey. *Electroencephalography and Clinical Neurophysiology* 25: 244–251.
- Fuchs, A.F., Kaneko, C.R.S., and Scudder C.A. (1985) Brainstem control of saccadic eye movements. *Annual Reviews of Neuroscience* 8: 307–337.
- Fujita, Y. and Sato, T. (1964) Intracellular records from hippocampal pyramidal cells in rabbits during theta rhythm activity. *Journal of Neurophysiology* 27: 1011–1025.
- Fukuda, A., Minami, T., Nabekura, J., and Oomura, Y. (1987) The effects of noradrenaline on neurones in the rat dorsal motor nucleus of the vagus, *in vitro*. *Journal of Physiology (London)* 393: 213–231.
- Fuller, J.H. (1975) Brain stem reticular units: some properties of the course and origin of the ascending trajectory. *Brain Research* 83: 349–367.
- Fulwiler, C.E. and Saper, C.B. (1984) Subnuclear organization of the efferent connections of the parabrachial nucleus in the cat. *Brain Research Reviews* 7: 229–259.
- Fung, S.J., Boxer, P.A., Morales, F.R., and Chase, M.H. (1982) Hyperpolarizing membrane responses induced in lumbar motoneurons during active sleep. *Brain Research* 248: 267–273.
- Fuster, J.M., Therz, A., and Creutzfeldt, O.D. (1965) Interval analysis of cell discharge in spontaneously and optically modulated activity in the visual system. *Archives Italiennes de Biologie* 103: 159–177.
- Gacek, R.R. (1979) Location of abducens afferent neurons in the cat. *Experimental Neurology* 64: 342–353.
- Gafni, J., Munsch, J.A., Lam, T.H., Catlin, C.M., Costa, L.G., Molinski, T.F., and Pessah, I.N. (1997) Xestospngins: potent membrane permeable blockers of the inositol 1,4,5-trisphosphate receptor. *Neuron* 19: 723–733.
- Gais, S., Mölle, M., Helms, K., and Born, J. (2002) Learning-dependent increases in sleep spindle density. *Journal of Neuroscience* 22: 6830–6834.
- Gais, S., Plihal, W., Wagner, U., and Born, J. (2000) Early sleep triggers memory for early visual discrimination skills. *Nature Neuroscience* 3: 1335–1339.

- Galambos, R. and Hillyard, S.A. (eds.) (1981) Electrophysiological approaches to human cognitive processing. *Neuroscience Research Program Bulletin* 20: 141–265.
- Galambos, R., Makeig, S., and Talmachoff, P. (1981) A 40-Hz auditory potential recorded from the human scalp. *Proceedings of the National Academy of Sciences of the USA* 78: 2643–2647.
- Gallagher, M. and Holland, P.C. (1994) The amygdala complex: multiple roles in associative learning and attention. *Proceedings of the National Academy of Sciences of the USA* 91: 11771–11776.
- Galvan, M. and Adams, P.R. (1982) Control of calcium current in rat sympathetic neurons by norepinephrine. *Brain Research* 244: 135–144.
- Ganguli, R., Reynolds, C.F., and Kupfer, D.J. (1987) EEG sleep in young, never medicated, schizophrenic patients: a comparison with delusional and nondelusional depressives and with healthy controls. *Archives of General Psychiatry* 44: 36–45.
- Gastaut, H. (1952) Étude électrographique de la réactivité des rythmes rolandiques. *Revue Neurologique (Paris)* 87: 176–182.
- Gaudin-Chazal, G., Daszuta, A., Faudon, M., and Ternaux, J.P. (1979) 5-HT concentration in cat's brain. *Brain Research* 160: 281–293.
- Geffard, M., Buijs, R.M., Séguéla, P., Pool, C.W., and Le Moal, M. (1984) First demonstration of highly specific and sensitive antibodies against dopamine. *Brain Research* 294: 161–165.
- Geffard, M., Patel, S., Dulluc, J., and Rock, A.M. (1986) Specific detection of noradrenaline in the rat brain using antibodies. *Brain Research* 363: 395–400.
- George, R., Haslett, W.L., and Jenden, D.J. (1964) A cholinergic mechanism in the brainstem reticular formation: induction of paradoxical sleep. *International Journal of Neuropharmacology* 3: 541–552.
- Gerashchenko, D., Okano, Y., Urade, Y., Inoue, S., and Hayaishi, O. (2000) Strong rebound of wakefulness follows prostaglandin D₂- or adenosine A_{2a} receptor agonist-induced sleep. *Journal of Sleep Research* 9: 81–87.
- Gerber, U., Greene, R.W., and McCarley, R.W. (1989a) Repetitive firing properties of medial pontine reticular formation neurones of the rat recorded *in vitro*. *Journal of Physiology (London)* 410: 533–560.
- Gerber, U., Greene, R.W., and McCarley, R.W. (1989b) Muscarinic receptors modulate neuronal membrane properties in medial pontine reticular formation. *Sleep Research* 12: 54.
- Gerber, U., Stevens, D.S., McCarley, R.W., and Greene, R.W. (1991) A muscarinic-gated conductance increase in medial pontine reticular neurons of the rat *in vitro*. *Journal of Neuroscience* 11: 3861–3867.
- Gerfen, C.R. and Sawchenko, P.E. (1984) An anterograde neuroanatomical tracing method that shows the detailed morphology of neurons, their axons and terminals: immunohistochemical localization of an axonally transported plant lectin, *Phaseolus vulgaris* leucoagglutinin (PHA-L). *Brain Research* 290: 219–238.
- Gerschenfeld, H.M. and Paupardin-Tritsch, D. (1974) Ionic mechanisms and receptor properties underlying the responses of molluscan neurones to 5- hydroxytryptamine. *Journal of Physiology (London)* 243: 427–456.
- Gervasoni, D., Darracq, L., Fort, P., Souliere, F., Chouvet, G., and Luppi, P.H. (1998) Electrophysiological evidence that noradrenergic neurons of the rat locus coeruleus are tonically inhibited by GABA during sleep. *European Journal of Neuroscience* 10: 964–70.
- Gervasoni, D., Peyron, C., Rampon, C., Barbagli, B., Chouvet, G., Urbain, N., Fort, P., and Luppi, P.H. (2000) Role and origin of the GABAergic innervation of dorsal raphe serotonergic neurons. *Journal of Neuroscience* 20: 4217–4225.
- Gerwins, P. and Fredholm, B.B. (1992) ATP and its metabolite adenosine act synergistically to mobilize intracellular calcium via the formation of inositol 1, 4, 5-triphosphate in a smooth muscle cell line. *Journal of Biological Chemistry* 267, 16081–16087.
- Ghose, G.M. and Freeman, R.D. (1992) Oscillatory discharge in the visual system: does it have a functional role? *Journal of Neurophysiology* 68: 1558–1574.
- Ghose, G.M. and Freeman, R.D. (1997) Intracortical connections are not required for oscillatory activity in the visual cortex. *Visual Neuroscience* 14: 963–979.
- Giesler, G.J. Jr., Menetrey, D., and Basbaum, A.I. (1979) Differential origin of spinothalamic tract projections to medial and lateral thalamus in the rat. *Journal of Comparative Neurology* 184: 107–126.
- Giesler, G.J. Jr., Yeziarski, R.P., Gerhart, K.D., and Willis, W.D. (1981) Spinothalamic tract neurons that project to medial and/or lateral thalamic nuclei: evidence for a physiologically novel population of spinal cord neurons. *Journal of Neurophysiology* 46: 1285–1308.
- Gilbert, C.D. (1992) Horizontal integration and cortical dynamics. *Neuron* 9: 1–13.
- Gilbert, C.D. and Wiesel, T.N. (1983) Clustered intrinsic connections in cat visual cortex. *Journal of Neuroscience* 3: 1116–1133.
- Gillin, J.C. (1989) Sleep and affective disorders: theoretical perspectives. In M.H. Kryger, T. Roth, and W.C. Dement, eds., *Principles and Practice of Sleep Medicine*, pp. 420–422, Philadelphia: Saunders.

- Gillin, J.C., Mendelson, W.B., and Kupfer, D.J. (1988) The sleep disturbances of depression: clues to pathophysiology with special reference to the circadian rapid eye movement rhythm. In D.J. Kupfer, T.H. Monk, and J.D. Barchas, eds., *Biological Rhythms and Mental Disorders*, pp. 27–54, New York: Guilford.
- Gillin, J.C., Sitaram, N., and Mendelson, W.B. (1982) Acetylcholine, sleep and depression. *Human Neurobiology* 1: 211–219.
- Glaser, E.M. and van der Loos, H. (1965) A semi-automatic computer-microscope for the analysis of neuronal morphology. *IEEE Transactions of Biomedical Engineering* BME-12: 22–31.
- Glenn, L.L. and Dement, W.C. (1981) Membrane potential, synaptic activity and excitability of hindlimb motoneurons during wakefulness and sleep. *Journal of Neurophysiology* 46: 839–854.
- Glenn, L.L. and Steriade, M. (1982) Discharge rate and excitability of cortically projecting intralaminar thalamic neurons during waking and sleep states. *Journal of Neuroscience* 2: 1387–1404.
- Glenn, L.L., Hada, J., Roy, J.P., Deschênes, M., and Steriade, M. (1982) Anterograde tracer and field potential analysis of the neocortical layer I projection from nucleus ventralis medialis of the thalamus in cat. *Neuroscience* 7: 1861–1877.
- Gloor, P. (1969) *Hans Berger on the Electroencephalogram of Man* (Suppl. no. 28 of *Electroencephalography and Clinical Neurophysiology*). Amsterdam: Elsevier.
- Gloor, P. and Fariello, R.G. (1988) Generalized epilepsy: some of its cellular mechanisms differ from those of focal epilepsy. *Trends in Neurosciences* 11: 63–68.
- Gloor, P., Avoli, M., and Kostopoulos, G. (1990) Thalamocortical relationships in generalized epilepsy with bilaterally synchronous spike-and-wave discharges. In M. Avoli, P. Gloor, G. Kostopoulos, and R. Naquet, eds., *Generalized Epilepsies*, pp. 190–212, Boston: Birkhäuser.
- Glotzbach, S.F. and Heller, H.C. (1984) Changes in the thermal characteristics of hypothalamic neurons during sleep and wakefulness. *Brain Research* 309: 17–26.
- Gnadt, J.W. and Pegrum, G.V. (1986) Cholinergic brainstem mechanisms of REM sleep in the rat. *Brain Research* 384: 29–41.
- Godfraind, J.M. (1978) Acetylcholine and somatically evoked inhibition on perigeniculate neurons in the cat. *Journal of Pharmacology* 63: 295–302.
- Godfraind, J.M. and Meulders, M. (1969) Effets de la stimulation sensorielle somatique sur les champs visuels des neurones de la région genouillée chez le chat anesthésié au chloralose. *Experimental Brain Research* 9: 183–200.
- Goebel, H.H., Komatsuzaki, A., Bender, M.B., and Cohen, B. (1971) Lesions of the pontine tegmentum and conjugate gaze paralysis. *Archives of Neurology* 24: 431–440.
- Gogolak, G., Stumpf, C.H., Petsche, H., and Sterc, F. (1968) The firing patterns of septal neurons and the form of hippocampal theta wave. *Brain Research* 7: 201–207.
- Goldman-Rakic, P.S. (1987) Circuitry of the prefrontal cortex and the regulation of behavior by representational memory. In F. Plum and V.B. Mountcastle, eds., *Handbook of Physiology* (vol. V, *The Nervous System*), pp. 373–417, Bethesda (MD): American Physiological Society.
- Goldman-Rakic, P.S. (1988) Changing concepts of cortical connectivity: parallel distributed cortical networks. In P. Kacic and W. Singer, eds., *Neurobiology of Neocortex*, pp. 177–202, New York: Wiley.
- Golomb, D., Wang, X.J., and Rinzel, J. (1994) Synchronization properties of spindle oscillations in a thalamic reticular nucleus model. *Journal of Neurophysiology* 72: 1109–1126.
- Golshani, P., Liu, X.B., and Jones, E.G. (2001) Differences in quantal amplitude reflect GluR4-subunit number at corticothalamic synapses on two populations of thalamic neurons. *Proceedings of the National Academy of Sciences of USA* 98: 4172–4177.
- Gong, H., Szymusiak, R., King, J., Steininger, T., and McGinty, D. (2000) Sleep-related c-Fos protein expression in the preoptic hypothalamus: effects of ambient warming. *American Journal of Physiology—Regulatory, Integrative and Comparative Physiology* 279: R2079–R2088.
- Gonzalez-Lima, F. and Scheich, H. (1985) Ascending reticular activating system in the rat: a 2-deoxyglucose study. *Brain Research* 344: 70–88.
- Goodwin, G.M. and Green, A.R. (1985) A behavioural and biochemical study in mice and rats of putative selective agonists and antagonists for 5-HT₁ and 5-HT₂ receptors. *British Journal of Pharmacology* 84: 743–753.
- Gorman, A.L.F., Hermann, A., and Thomas, M.V. (1982) Ionic requirements for membrane oscillations and their dependence on the calcium concentration in a molluscan pacemaker neurone. *Journal of Physiology (London)* 327: 185–217.
- Gottselig, J.M., Bassetti, C.L., and Achermann, P. (2002) Power and coherence of sleep spindle frequency activity following hemispheric strokes. *Brain* 125: 373–383.
- Grady, E.F., Böhm, S.K., and Bunnnett, N.W. (1997). Turning off the signal: mechanisms that attenuate signaling by G protein-coupled receptors. *American Journal of Physiology* 273: G586–G601.

- Granit, R. (1967) *Charles Scott Sherrington*. Garden City (NY): Doubleday & Co.
- Grantyn, A. and Berthoz, A. (1987) Reticulo-spinal neurons participating in the control of synergic eye and head movements during orienting in the cat. I. Behavioral properties. *Experimental Brain Research* 66: 339–354.
- Grantyn, A. and Grantyn, R. (1976) Synaptic actions of tectofugal pathways on abducens motoneurons in the cat. *Brain Research* 105: 269–285.
- Grantyn, A. and Grantyn, R. (1982) Axonal patterns and sites of termination of cat superior colliculus neurons projecting in the tecto-bulbo-spinal tract. *Experimental Brain Research* 46: 243–256.
- Grantyn, A., Hardy, O., and Berthoz, A. (1988) Activity and ponto-bulbar connectivity of reticulo-spinal neurons subserving visually triggered eye and head movements. *Society for Neuroscience Abstracts* 14: 956.
- Grantyn, R. and Grantyn, A. (1978) Morphological and electrophysiological properties of cat abducens motoneurons. *Experimental Brain Research* 31: 249–279.
- Grantyn, R., Baker, R., and Grantyn, A. (1980) Morphological and physiological identification of excitatory pontine reticular neurons projecting to the cat abducens nucleus and spinal cord. *Brain Research* 198: 221–228.
- Grantyn, R., Jacques, V.O., and Berthoz, A. (1987) Reticulo-spinal neurons participating in the control of synergic eye and head movements during orienting in the cat. II. Morphological properties as revealed by intra-axonal injections of horseradish peroxidase. *Experimental Brain Research* 66: 355–377.
- Gray, B.G. and Dostrovsky, J.O. (1985) Inhibition of feline spinal cord dorsal horn neurons following electrical stimulation of nucleus paragigantocellularis lateralis. A comparison with nucleus raphe magnus. *Brain Research* 348: 261–273.
- Gray, R. and Johnston, D. (1987) Noradrenaline and beta-adrenoceptor agonists increase activity of voltage-dependent calcium channels in hippocampal neurons. *Nature* 327: 620–622.
- Gray, C.M. and McCormick, D.A. (1996) Chattering cells: superficial pyramidal neurons contributing to the generation of synchronous oscillations in the visual cortex. *Science* 274: 109–113.
- Gray, C.M., Engel, A.K., König, P., and Singer, W. (1990) Stimulus-dependent neuronal oscillations in cat visual cortex: receptive field properties and feature dependence. *European Journal of Neuroscience* 2: 607–619.
- Gray, C.M., König, P., Engel, A.K., and Singer, W. (1989) Stimulus-specific neuronal oscillations in cat visual cortex exhibit inter-columnar synchronization which reflects global stimulus properties. *Nature* 338: 334–337.
- Graybiel, A.M. (1977a) Direct and indirect preoculomotor pathways of the brainstem: an autoradiographic study of the pontine reticular formation in the cat. *Journal of Comparative Neurology* 175: 37–78.
- Graybiel, A.M. (1977b) Organization of oculomotor pathways in the cat and rhesus monkey. In R. Baker and A. Berthoz, eds., *Control of Gaze by Brain Stem Neurons*, vol. 1., pp. 79–88, New York: Elsevier/North Holland.
- Graybiel, A.M. (1978a) Organization of the nigrotectal connection: an experimental tracer study in the cat. *Brain Research* 143: 339–348.
- Graybiel, A.M. (1978b) A satellite system of the superior colliculus: the parabigeminal nucleus and its projections to the superficial collicular layers. *Brain Research* 145: 365–374.
- Graybiel, A.M. and Elde, R.P. (1983) Somatostatin-like immunoreactivity characterizes neurons of the nucleus reticularis thalami in the cat and monkey. *Journal of Neuroscience* 3: 1308–1321.
- Greene, R.W. and Carpenter, D.O. (1985) Actions of neurotransmitters on pontine medial reticular formation neurons of the cat. *Journal of Neurophysiology* 54: 520–531.
- Greene, R.W. and McCarley, R.W. (1990) Cholinergic neurotransmission in the brainstem: implications for behavioral state control. In M. Steriade and D. Biesold, eds., *Brain Cholinergic Systems*, pp. 224–235, Oxford: Oxford University Press.
- Greene, R.W., Haas, H.L., and McCarley, R.W. (1986) A low threshold calcium spike mediates firing pattern alterations in pontine reticular neurons. *Science* 234: 738–740.
- Greene, R.W., Gerber, U., and McCarley, R.W. (1989a) Cholinergic activation of medial pontine reticular formation neurons *in vitro*. *Brain Research* 476: 154–159.
- Greene, R.W., Gerber, U., Haas, H.L., and McCarley, R.W. (1989b) Noradrenergic actions on neurons of the medial pontine reticular formation *in vitro*. *Sleep Research* 12: 58.
- Greenstein, Y.J., Pavlides, C., and Wilson, J. (1988) Long-term potentiation in the dentate gyrus is preferentially induced at theta periodicity. *Brain Research* 438: 331–334.
- Grenier, F., Timofeev, I., and Steriade, M. (1998) Leading role of thalamic over cortical neurons during postinhibitory rebound excitation. *Proceedings of National Academy of Sciences of USA* 95: 13929–13934.

- Grenier, F., Timofeev, I., and Steriade, M. (2001) Focal synchronization of ripples (80–200 Hz) in neocortex and their neuronal correlates. *Journal of Neurophysiology* 86: 1884–1898.
- Grenier, F., Timofeev, I., and Steriade, M. (2002) Thalamic short-term plasticity and its impact on the neocortex. *Thalamus & Related Systems* 1: 331–340.
- Grenier, F., Timofeev, I., and Steriade, M. (2003) Neocortical very fast oscillations (ripples, 80–200 Hz) during electrographic seizures: intracellular correlates and possible role in seizure initiation. *Journal of Neurophysiology* 89: 841–852.
- Gresham, S.C., Agnew, H.W., and Williams, R.L. (1965) The sleep of depressed patients. *Archives of General Psychiatry* 13: 503.
- Griffith, W.H. (1988) Membrane properties of cell types within guinea pig basal forebrain nuclei *in vitro*. *Journal of Neurophysiology* 59: 1590–1612.
- Gritti, I., Mainville, L., and Jones, B.E. (1993) Co-distribution of GABA-with acetylcholine-synthesizing neurons in the basal forebrain of the rat. *Journal of Comparative Neurology* 329: 438–457.
- Gritti, I., Mainville, L., and Jones, B.E. (1994) Projections of GABAergic and cholinergic basal forebrain and GABAergic preoptic-anterior hypothalamic neurons to the posterior lateral hypothalamus of the rat. *Journal of Comparative Neurology* 339: 251–268.
- Gritti, I., Mariotti, M. and Mancina, M. (1998) GABAergic and cholinergic basal forebrain and preoptic-anterior hypothalamic projections to the mediodorsal nucleus of the thalamus in the cat. *Neuroscience* 85: 149–178.
- Grofova, I., Ottersen, O.P., and Rinvik, E. (1978) Mesencephalic and diencephalic afferents to the superior colliculus and periaqueductal gray substance demonstrated by retrograde axonal transport of horseradish peroxidase in the cat. *Brain Research* 146: 205–220.
- Gross, D.W. and Gotman, J. (1999) Correlation of high-frequency oscillations with the sleep–wake cycle and cognitive activity in humans. *Neuroscience* 94: 1005–1018.
- Grzanna, R. and Molliver, M.E. (1980) The locus coeruleus in the rat: an immunocytochemical delineation. *Neuroscience* 5: 21–40.
- Gucer, G. (1979) The effect of sleep upon the transmission of afferent activity in the somatic afferent system. *Experimental Brain Research* 34: 287–298.
- Guido, W. and Weyand, T. (1995) Burst responses in thalamic relay cells of the awake, behaving cat. *Journal of Neurophysiology* 74: 1782–1786.
- Guido, W., Lu, S.M., and Sherman, S.M. (1992) Relative contributions of burst and tonic responses to the receptive field properties of lateral geniculate neurons in the cat. *Journal of Neurophysiology* 68: 2199–2211.
- Guilleminault, C. (1989) Narcolepsy syndrome. In M.H. Kryger, T. Roth, and W.C. Dement, eds., *Principles and Practices of Sleep Medicine*, pp. 338–347, New York: Saunders.
- Guilleminault, C., Dement, W.C., and Passouant, P. (eds.) (1975) *Narcolepsy*, New York: Spectrum.
- Guillery, R.W. (1966) A study of Golgi preparations from the dorsal lateral geniculate neurons of the cat. *Journal of Comparative Neurology* 128: 21–50.
- Gunning, R. (1987) Increased numbers of ion channels promoted by an intracellular second messenger. *Science* 235: 80–82.
- Gupta, A., Wang, Y., and Markram, H. (2000) Organizing principles for a diversity of GABAergic interneurons and synapses in the neocortex. *Science* 287: 273–278.
- Gustafsson, B., Galvan, M., Grafe, P., and Wigstrom, H. (1982) A transient outward current in a mammalian central neurone blocked by 4-aminopyridine. *Nature* 299: 252–254.
- Gutfreund, Y., Yarom, Y., and Segev, I. (1995) Subthreshold oscillations and resonant frequency in guinea-pig cortical neurons: physiology and modelling. *Journal of Physiology (London)* 483: 621–640.
- Gutnick, M.J., Heinemann, U., and Prince, D.A. (1979) Stimulus induced and seizure related changes in extracellular potassium concentration in cat thalamus (VPL). *Electroencephalography and Clinical Neurophysiology* 47: 329–344.
- Guyenet, P.G. and Brown, D.L. (1986) Nucleus paragigantocellularis lateralis and lumbar sympathetic discharge in the rat. *American Journal of Physiology* 250: R1081–R1094.
- Guyenet, P.G. and Young, B.S. (1987) Projections of nucleus paragigantocellularis lateralis to locus coeruleus and other structures in rat. *Brain Research* 406: 171–184.
- Haack, M., Schuld, A., Kraus, T., and Pollmacher, T. (2001) Effects of sleep on endotoxin-induced host responses in healthy men. *Psychosomatic Medicine* 63: 568–578.
- Haas, H.L. (1982) Cholinergic disinhibition in hippocampal slices of the rat. *Brain Research* 233: 200–204.
- Haas, H.L. and Greene, R.W. (1986) Effects of histamine on hippocampal pyramidal cells of the rat *in vitro*. *Experimental Brain Research* 62: 123–130.
- Haas, H.L. and Rose, G.M. (1987) Noradrenaline blocks potassium conductance in rat dentate granule cells *in vitro*. *Neuroscience Letters* 78: 171–174.

- Haas, H.L., Schaerer, B., and Vosmanský, M. (1979) A simple perfusion chamber for the study of nervous tissue slices *in vitro*. *Journal of Neuroscience Methods* 1: 323–325.
- Hagan, J.J., Leslie, R.A., Patel, S., Evans, M.L., Wattam, T.A., Holmes, S., Benham, C.D., Taylor, S.G., Routledge, C., Hemmati, P., Munton, R.P., Ashmeade, T.E., Shah, A.S., Hatcher, J.P., Hatcher, P.D., Jones, D.N., Smith, M.I., Piper, D.C., Hunter, A.J., Porter, R., and Upton, N. (1999) Orexin A activates locus coeruleus cell firing and increases arousal in the rat. *Proceedings of the National Academy of Sciences of the USA* 96: 10911–10916.
- Hagiwara, S. and Takahashi, K. (1974) The anomalous rectification and cation selectivity of the membrane of a starfish egg cell. *Journal of Membrane Biology* 18: 61–80.
- Hajdu, I., Obal, F. Jr., Fang, J., Krueger, J.M., and Rollo, C.D. (2002) Sleep of transgenic mice producing excess rat growth hormone. *American Journal of Physiology* 282: R70–R76.
- Halasz, P. (1991) Runs of rapid spikes in sleep: a characteristic EEG expression of generalized malignant epileptic encephalopathies. A conceptual review with new pharmacological data. *Epilepsy Research Supplement* 2: 49–71.
- Halgren, E., Walter, R.D., Cherlow, D.G., and Crandal, P.H. (1978) Mental phenomena evoked by electrical stimulation of the human hippocampal formation and amygdala. *Brain* 101: 83–117.
- Hallanger, A.E. and Wainer, B.H. (1988) Ultrastructure of ChAT-immunoreactive synaptic terminals in the thalamic reticular nucleus of the rat. *Journal of Comparative Neurology* 278: 486–497.
- Hallanger, A.E., Levey, A.I., Lee, H.J., Rye, D.B., and Wainer, B.H. (1987) The origins of cholinergic and other subcortical afferents to the thalamus in the rat. *Journal of Comparative Neurology* 262: 105–124.
- Hallanger, A.E., Price, S.D., Steininger, T., and Wainer, B.H. (1988) Mesopontine tegmental projections to the nucleus basalis of Meynert: an ultrastructural study. *Society for Neuroscience Abstracts* 14: 1184.
- Halliwel, J.V. and Adams, P.R. (1982) Voltage-clamp analysis of muscarinic excitation in hippocampal neurons. *Brain Research* 250: 71–92.
- Hamada, T., Liou, S-Y., Fukushima, T., Maruyama, T., Watanabe, S., Mikoshiba, K., and Ishida, N. (1999) The role of inositol trisphosphate induced Ca^{2+} release from IP_3 -receptor in the rat suprachiasmatic nucleus on circadian entrainment mechanism. *Neuroscience Letters* 263: 125–128.
- Hammer, R.P. Jr., Lindsay, R.D., and Scheibel, A.B. (1981) Development of the brain stem reticular core: an assessment of dendritic state and configuration in the perinatal rat. *Developmental Brain Research* 7: 179–190.
- Hara, J., Beuckmann, C.T., Nambu, T., Willie, J.T., Chemelli, R.M., Sinton, C.M., Sugiyama, F., Yagami, K., Goto, K., Yanagisawa, M., and Sakurai, T. (2001) Genetic ablation of orexin neurons in mice results in narcolepsy, hypophagia, and obesity. *Neuron* 30: 345–354.
- Hari, R. (1993) Magnetoencephalography as a tool of clinical neurophysiology. In E. Niedermeyer and F. Lopes da Silva, eds., *Electroencephalography: Basic Principles, Clinical Applications and Related Fields*, 3rd edn., pp. 1035–1061, Baltimore: Williams & Wilkins.
- Harper, R.M., Frysinger, R.C., Zhang, J., Trelease, R.B., and Terreberry, R.R. (1988) Cardiac and respiratory interactions maintaining homeostasis during sleep. In R. Lydic and J.F. Biebuyck, eds., *Clinical Physiology of Sleep*, pp. 67–78, Bethesda (MD): American Physiological Society.
- Harper, R.M., Schechtman, V.L., and Kluge, K.A. (1987) Machine classification of infant sleep state using cardiorespiratory measures. *Electroencephalography and Clinical Neurophysiology* 67: 379–387.
- Harris, E.W., Ganong, A.H., Monaghan, D.T., Watkins, J.C., and Cotman, C.W. (1986) Action of 3-((+/-)-2-carboxypiperazin-4-yl)-propyl-1-phosphonic acid (CPP): a new and highly potent antagonist of N-methyl-D-aspartate receptors in the hippocampus. *Brain Research* 382: 174–177.
- Harris, R.M. (1987) Axon collaterals in the thalamic reticular nucleus from thalamocortical neurons of the rat ventrobasal thalamus. *Journal of Comparative Neurology* 258: 397–407.
- Harting, J.K. (1977) Descending pathways from the superior colliculus: an autoradiographic analysis in the rhesus monkey (*Macaca mulatta*). *Journal of Comparative Neurology* 173: 583–612.
- Hartmann, E. (1968) Longitudinal studies of sleep and dreams in manic-depressed patients. *Archives of General Psychiatry* 19: 312–329.
- Hartveit, E. and Heggelund, P. (1994) Response variability of single cells in the dorsal lateral geniculate nucleus of the cat. Comparison with retinal input and effect of brain stem stimulation. *Journal of Neurophysiology* 72: 1278–1289.
- Hartzell, H.C., Kuffler, S.W., Stickgold, R., and Yoshikami, D. (1977) Synaptic excitation and inhibition resulting from direct action of acetylcholine on two types of chemoreceptors on individual amphibian parasympathetic neurones. *Journal of Physiology (London)* 271: 817–846.
- Haulica, I., Ababei, L., Branisteanu, D., and Topoliceanu, F. (1973) Preliminary data on the possible hypnogenic role of adenosine. *Journal of Neurochemistry* 21: 1019–1020.
- Hayaishi, O. (2002) Molecular genetic studies on sleep-wake regulation, with special emphasis on the prostaglandin D (2) system. *Journal of Applied Physiology* 92: 863–868.

- Hayashi, H., Takagi, H., Takeda, N., Kubota, Y., Tohyama, M., Watanabe, T., and Wada, H. (1984) Fine structure of histaminergic neurons in the caudal magnocellular nucleus of the rat as demonstrated by immunocytochemistry using histidine decarboxylase as a marker. *Journal of Comparative Neurology* 229: 233–241.
- Head, H. (1923) The conception of nervous and mental energy. II. "Vigilance": a physiological state of the nervous system. *British Journal of Psychology* 14: 126–147.
- Hebb, D.O. (1972) *Textbook of Physiology*. Philadelphia: Saunders.
- Hendricks, J.C., Morrison, A.R., and Mann, G.L. (1982) Different behaviors during paradoxical sleep without atonia depend on pontine lesion site. *Brain Research* 239: 81–105.
- Henn, V. and Cohen, B. (1976) Coding of information about rapid eye movements in the pontine reticular formation of alert monkeys. *Brain Research* 108: 307–325.
- Henn, V., Baloh, R.W., and Hepp, K. (1984a) The sleep–wake transition in the oculomotor system. *Experimental Brain Research* 54: 166–176.
- Henn, V., Lang, W., Hepp, K., and Reisine, H. (1984b) Experimental gaze palsies in monkeys and their relation to human pathology. *Brain* 107: 619–636.
- Hepp, K., and Henn, V. (1983) Neurodynamics of the oculomotor system: space-time recording and a non-equilibrium phase transition. In E. Basar, H. Flohr, and H. Haken, eds., *Springer Series in Synergetics*, pp. 139–154, Berlin-Heidelberg-New York: Springer.
- Herkenham, M. (1979) The afferent and efferent connections of the ventromedial thalamic nucleus in the rat. *Journal of Comparative Neurology* 183: 487–518.
- Herkenham, M. (1987) Mismatches between neurotransmitter and receptor localizations in brain: observations and implications. *Neuroscience* 23: 1–38.
- Herman, J.H., Ellman, S.J., and Roffwarg, H.P. (1978) The problem of NREM dream recall reexamined. In A.M. Arkin, J.S. Antrobus, and S.J. Ellman, eds., *The Mind in Sleep: Psychology and Psychophysiology*, pp. 59–92, Hillsdale (NJ): Lawrence Erlbaum.
- Herman, J.H., Barker, D.R., and Roffwarg, H.P. (1983) Similarity of eye movement characteristics in REM sleep and the awake state. *Psychophysiology* 20: 537–543.
- Hermann, A. and Gorman, A.L.F. (1981) Effects of tetraethylammonium on potassium currents in a molluscan neuron. *Journal of General Physiology* 78: 87–110.
- Hernández-Cruz, A. and Pape, H.C. (1989) Identification of two calcium currents in acutely dissociated neurons from the rat lateral geniculate nucleus. *Journal of Neurophysiology* 61: 1270–1283.
- Herrling, P.L. (1985) Pharmacology of the corticocaudate excitatory postsynaptic potential in the cat: evidence for its mediation by quisqualate- or kainate-receptors. *Neuroscience* 14: 417–426.
- Hershey, A.D., Plazani, L., Woodward, R.M., Miledi, R., and Karausa, J.E. (1991) Molecular and genetic characterization, functional expression and mRNA expression pattern of a rat substance P receptor. *Annals of the New York Academy of Sciences* 632: 63–78.
- Hess, W.R. (1944) Das Schlafsyndrom als Folge dienzephaler Reizung. *Helvetica Physiologica et Pharmacologica Acta* 2: 305–344.
- Heurteaux, C., Lauritzen, I., Widmann, C., and Lazdunski, M. (1995) Essential role of adenosine, adenosine A1 receptors, and ATP-sensitive K⁺ channels in cerebral ischemic preconditioning. *Proceedings of the National Academy of Science* 92: 4666–4670.
- Hicks, T.P., Metherate, R., Landry, P., and Dykes, R.W. (1986) Bicuculline-induced alterations of response properties in functionally identified ventroposterior thalamic neurones. *Experimental Brain Research* 63: 248–264.
- Highstein, S.M., Karabelas, A., Baker, R., and McCrea, R.A. (1982) Comparison of the morphology of physiologically identified abducens motor and internuclear neurons in the cat: A light microscopic study employing the intracellular injection of horseradish peroxidase. *Journal of Comparative Neurology* 208: 369–381.
- Higo, S., Ito, K., Fuchs, D., and McCarley, R.W. (1989a) Pontine and bulbar afferents to the peribrachial PGO burst cell zone in the cat. *Sleep Research* 18: 28.
- Higo, S., Ito, K., Fuchs, D., Rye, D., Wainer, B., and McCarley, R.W. (1989b) Topography of pedunculo-pontine tegmental nucleus (PPT) interconnections with the lateral geniculate nucleus (LGN) and n. Prepositus Hypoglossi (PH) in the cat. *Society for Neuroscience Abstracts* 15: 351.
- Higo, S., Ito, K., Fuchs, D., and McCarley, R.W. (1990) Anatomical interconnections of the pedunculo-pontine tegmental nucleus and the nucleus prepositus hypoglossi in the cat. *Brain Research* 536: 79–85.
- Hikosaka, O. and Wurtz, R.H. (1983a) Visual and oculomotor functions of monkey substantia nigra pars reticulata. I. Relation of visual and auditory responses to saccades. *Journal of Neurophysiology* 49: 1230–1253.
- Hikosaka, O. and Wurtz, R.H. (1983b) Visual and oculomotor functions of monkey substantia nigra pars reticulata. IV. Relation of substantia nigra to superior colliculus. *Journal of Neurophysiology* 49: 1285–1301.

- Hikosaka, O. and Wurtz, R.H. (1985a) Modification of saccadic eye movements by GABA-related substances. I. Effect of muscimol and bicuculline in monkey superior colliculus. *Journal of Neurophysiology* 53: 266–291.
- Hikosaka, O. and Wurtz, R.H. (1985b) Modification of saccadic eye movements by GABA-related substances. I. Effects of muscimol in monkey substantia nigra pars reticulata. *Journal of Neurophysiology* 53: 292–308.
- Hikosaka, O., Igusa, Y., Nakao, S., and Shimazu, H. (1978) Direct inhibitory synaptic linkage of pontomedullary reticular burst neurons with abducens motoneurons in the cat. *Experimental Brain Research* 33: 337–352.
- Hille, B. (1975) Ionic selectivity of Na and K channels of nerve membranes. In G. Eisenman, ed., *Membranes—A Series of Advances*, vol. 3, *Lipid Bilayers and Biological Membranes: Dynamic Properties*, pp. 255–323, New York: Marcel Dekker.
- Hille, B. (1984) *Ionic Channels of Excitable Membranes*. Sunderland (MA): Sinauer Associates.
- Hillyard, S.A. and Picton, T.W. (1987) Electrophysiology of cognition. In V.B. Mountcastle and F. Plum, eds., *Handbook of Physiology*, sect. 1, vol. V, part 2, pp. 519–584, Bethesda (MD): American Physiological Society.
- Hirsch, J.C. and Burnod, Y. (1987) A synaptically evoked hyperpolarization in the rat dorsolateral geniculate neurons *in vitro*. *Neuroscience* 23: 457–468.
- Hirsch, J.C., Fourment, A., and Marc, M.E. (1983) Sleep-related variations of membrane potential in the lateral geniculate body relay neurons of the cat. *Brain Research* 259: 308–312.
- Hoang, Q.V., Bajic, D., Yanagisawa, M., Nakajima, S., and Nakajima, Y. (2003) Effects of orexin (hypocretin) on GIRK channels. *Journal of Neurophysiology* 90: 693–702.
- Hobson, J.A. (1988) *The Dreaming Brain*. New York: Basic Books.
- Hobson, J.A. and McCarley, R.W. (1974) *Neuronal Activity in Sleep: An Annotated Bibliography*. Los Angeles: Brain Information Service.
- Hobson, J.A. and McCarley, R.W. (1977) The brain as a dream state generator: an activation-synthesis hypothesis of the dream process. *American Journal of Psychiatry* 134: 1335–1348.
- Hobson, J.A. and Pace-Schott, E.F. (2002) The cognitive neuroscience of sleep: neuronal systems, consciousness and learning. *Nature Reviews Neuroscience* 3: 679–693.
- Hobson, J.A. and Steriade, M. (1986) Neuronal basis of behavioral state control. In V.B. Mountcastle and F.E. Bloom, eds., *Handbook of Physiology*, sect. 1, vol. IV, pp. 701–823, Bethesda (MD): American Physiological Society.
- Hobson, J.A., Goldberg, M., Vivaldi, E., and Riew, D. (1983b) Enhancement of desynchronized sleep signs after pontine microinjection of the muscarinic agonist bethanechol. *Brain Research* 275: 127–136.
- Hobson, J.A., Lydic, R., and Baghdoyan, H.A. (1986) Evolving concepts of sleep cycle generation: from brain centers to neuronal populations. *Behavioral and Brain Sciences* 9: 371–448.
- Hobson, J.A., McCarley, R.W., and Nelson, J.P. (1983a) Location and spike-train characteristics of cells in anterodorsal pons having selective decreases in firing rate during desynchronized sleep. *Journal of Neurophysiology* 50: 770–783.
- Hobson, J.A., McCarley, R.W., and Wyzinski, P.W. (1975) Sleep cycle oscillation: reciprocal discharge by two brain stem neuronal groups. *Science* 189: 55–58.
- Hobson, J.A., McCarley, R.W., Freedman, R., and Pivik, R.T. (1974b) Time course of discharge rate changes by cat pontine brainstem neurons during the sleep cycle. *Journal of Neurophysiology* 37: 1297–1309.
- Hobson, J.A., McCarley, R.W., Pivik, R.T., and Freedman, R. (1974a) Selective firing by cat pontine brain stem neurons in desynchronized sleep. *Journal of Neurophysiology* 37: 497–511.
- Hobson, J.A., McCarley, R.W., Wyzinski, P.A., and Pivik, R.T. (1973) Reciprocal firing by two neuronal groups during the sleep cycle. *Society for Neuroscience Abstracts* 3: 373.
- Hofle, N., Paus, T., Reutens, D., Fiset, P., Gotman, J., Evans, A.C., and Jones, B.E. (1997) Regional cerebral blood flow changes as a function of delta and spindle activity during slow wave sleep in humans. *Journal of Neuroscience* 17: 4800–4808.
- Hököfelt, T. (1987) Neuronal communication through multiple coexisting messengers. In G.M. Edelman, W.E. Gall, and W.M. Cowan, eds., *Synaptic Function*, pp. 179–211, New York: Wiley.
- Hököfelt, T., Johansson, O., and Goldstein, M. (1984) Central catecholamine neurons as revealed by immunohistochemistry with special reference to adrenaline neurons. In *Handbook of Chemical Neuroanatomy* (vol. 2, *Classical Transmitters in the CNS*), pp. 156–276, Amsterdam: Elsevier.
- Holets, V.R., Hököfelt, T., Rokaeus, A., Terenius, L., and Goldstein, M. (1988) Locus coeruleus neurons in the rat containing neuropeptide Y, tyrosine hydroxylase or galanin and their efferent projections to the spinal cord, cerebral cortex and hypothalamus. *Neuroscience* 24: 893–906.

- Holmes, C.J., Webster, H.H., Zikman, S., and Jones, B.E. (1988) Quisqualic acid lesions of the ventromedial medullary reticular formation: effects upon sleep-wakefulness states. *Society for Neuroscience Abstracts* 14: 1308.
- Holsheimer, J. (1982) Generation of theta activity (RSA) in the cingulate cortex of the rat. *Experimental Brain Research* 47: 309–312.
- Holstege, G. (1987) Some anatomical observations on the projections from the hypothalamus to brainstem and spinal cord: an HRP and autoradiographic tracing study in the cat. *Journal of Comparative Neurology* 260: 98–126.
- Holstege, G. and Kuypers, H.G.J.M. (1982) The anatomy of brain stem pathway to the spinal cord in cat. A labeled amino acid tracing study. *Progress in Brain Research* 57: 145–175.
- Holstege, G. and Kuypers, H.G.J.M. (1988) Brainstem projections to lumbar motoneurons in rat. I. An ultrastructural study using autoradiography and the combination of autoradiography and horseradish peroxidase histochemistry. *Neuroscience* 21: 345–365.
- Holt, R. (1965) A review of some of Freud's biological assumptions and their influence on his theories. In N. Greenfield and W. Lewis, eds., *Psychoanalysis and Current Biological Thought*, pp. 93–124, Madison: University of Wisconsin Press.
- Honda, T. and Semba, K. (1995) An ultrastructural study of cholinergic and non-cholinergic neurons in the laterodorsal and pedunculopontine tegmental nuclei in the rat. *Neuroscience* 68: 837–853.
- Honore, T., Davies, S.D., Drejer, J., Fletcher, E.J., Jacobsen, P., Lodge, D., and Nielsen, E. (1987) Potent and competitive antagonism at non-NMDA receptors by FG9041 and FG9065. *Society for Neuroscience Abstracts* 13: 383.
- Hopkins, D.A. and Holstege, G. (1978) Amygdaloid projections to the mesencephalon, pons and medulla oblongata in the cat. *Experimental Brain Research* 32: 529–547.
- Horne, J. (1992) Human slow wave sleep: a review and appraisal of recent findings, with implications for sleep functions, and psychiatric illness. *Experimentia* 48: 941–54.
- Horsley, V. (1892) *The Structure and Functions of the Brain and Spinal Cord*. Philadelphia: Blakiston.
- Horvath, T.L., Diano, S., and van Den Pol, A.N. (1999b) Synaptic interaction between hypocretin (orexin) and neuropeptide Y cells in the rodent and primate hypothalamus: a novel circuit implicated in metabolic and endocrine regulations. *Journal of Neuroscience* 19: 1072–1087.
- Horvath, T.L., Peyron, C., Diano, S., Ivanov, A., Aston-Jones, G., Kilduff, T.S., and van den Pol, A.N. (1999a) Hypocretin (orexin) activation and synaptic innervation of the locus coeruleus noradrenergic system. *Journal of Comparative Neurology* 415: 145–159.
- Houson, J.R. and Prince, D.A. (1980) A calcium-activated hyperpolarization follows repetitive firing in hippocampal neurons. *Journal of Neurophysiology* 43: 409–419.
- Houser, C.R., Crawford, G.D., Salvaterra, P.M., and Vaughn, J.E. (1985) Immunocytochemical localization of choline acetyltransferase in rat cerebral cortex: a study of cholinergic neurons and synapses. *Journal of Comparative Neurology* 234: 17–34.
- Houser, C.R., Vaughn, J.E., Barber, R.P., and Roberts, E. (1980) GABA neurons are the major cell type of the nucleus reticularis thalami. *Brain Research* 200: 341–354.
- Houweling, A., Bazhenov, M., Timofeev, I., Grenier, F., Steriade, M., and Sejnowski, T.J. (2002) Frequency-selective augmenting responses by short-term synaptic depression in cat neocortex. *Journal of Physiology (London)* 542: 599–617.
- Howe, R.C. and Serman, M.B. (1972) Cortical-subcortical EEG correlates of suppressed motor behavior during sleep and waking in the cat. *Electroencephalography and Clinical Neurophysiology* 32: 681–695.
- Hu, B., Bouhassira, D., Steriade, M., and Deschênes, M. (1988) The blockage of ponto-geniculo-occipital waves in the cat lateral geniculate nucleus by nicotinic antagonists. *Brain Research* 473: 394–397.
- Hu, B., Steriade, M., and Deschênes, M. (1989a) The effects of peribrachial stimulation on reticular thalamic neurons: the blockage of spindle waves. *Neuroscience* 31: 1–12.
- Hu, B., Steriade, M., and Deschênes, M. (1989b) The effects of brainstem peribrachial stimulation on neurons of the lateral geniculate nucleus. *Neuroscience* 31: 13–24.
- Hu, B., Steriade, M., and Deschênes, M. (1989c) The cellular mechanism of thalamic ponto-geniculo-occipital waves. *Neuroscience* 31: 25–35.
- Hubel, D.H. (1960) Single unit activity in lateral geniculate body and optic tract of unrestrained cats. *Journal of Physiology (London)* 150: 91–104.
- Hubel, D.H. and Livingstone, M.S. (1980) A comparison between sleeping and waking spontaneous and visually evoked activity in cat striate cortex examined by single cell recording and 2-deoxyglucose autoradiography. *Society for Neuroscience Abstracts* 6: 314.
- Hubel, D.H. and Wiesel, T.N. (1961) Integrative action in the cat's lateral geniculate body. *Journal of Physiology (London)* 155: 385–398.

- Hughes, H.C. and Mullikin, W.H. (1984) Brainstem afferents to the lateral geniculate nucleus of the cat. *Experimental Brain Research* 54: 253–258.
- Hughes, S.W., Cope, D.W., Blethly, K.L., and Crunelli, V. (2002) Cellular mechanisms of the slow (<1 Hz) oscillation in thalamocortical neurons *in vitro*. *Neuron* 33: 947–958.
- Huguenard, J.R. (1996) Low-threshold calcium currents in central nervous system neurons. *Annual Review of Physiology* 58: 329–348.
- Huguenard, J.R. and Prince, D.A. (1992) A novel T-type current underlies prolonged Ca^{2+} -dependent burst firing in GABAergic neurons of rat thalamic reticular nucleus. *Journal of Neuroscience* 12: 3804–3817.
- Huguenard, J.R., Coulter, D.A., and Prince, D.A. (1991) A fast transient potassium current in thalamic relay neurons, kinetics of activation and inactivation. *Journal of Neurophysiology* 66: 1304–1315.
- Hunt, S.P., Henke, H., Kunzle, H., Reubi, J.C., Schenker, T., Streit, P., Felix, D., and Cuénod, M. (1976) Biochemical neuroanatomy of the pigeon optic tectum. In O. Creutzfeldt, ed., *Afferent and Intrinsic Organization of Laminated Structures in the Brain*, pp. 521–525, *Experimental Brain Research Suppl.* 1, New York: Springer.
- Huston, J.P., Haas, H.L., Pfister, M., Decking, U., Schrader, J., and Schwarting, R.K.W. (1996) Extracellular adenosine levels in neostriatum and hippocampus during rest and activity periods of rats. *Neuroscience* 73: 99–107.
- Hyde, J.E. and Eason, R.G. (1959) Characteristics of ocular movements evoked by stimulation of brain stem of cat. *Journal of Neurophysiology* 22: 666–678.
- Ibuka, N., Inouye, S.T., and Kawamura, H. (1977) Analysis of sleep–wakefulness rhythms in male rats after suprachiasmatic nucleus lesions and ocular enucleations. *Brain Research* 122: 33–47.
- Idzikowski, C., Burton, S.W., and James, R. (1988) The effects on sleep of 1 mg ritanserin given for four weeks. *Abstracts of the European Sleep Research Society*: 199.
- Idzikowski, C., Mills, F.J., and Glennard, R. (1986) 5-Hydroxytryptamine-2 antagonist increases human slow wave sleep. *Brain Research* 378: 164–168.
- Igusa, Y., Sasaki, S., and Shimazu, H. (1980) Excitatory premotor burst neurons in the cat pontine reticular formation related to the quick phase of vestibular nystagmus. *Brain Research* 182: 451–456.
- Illes, P., Klotz, K.-N., and Lohse, M.J. (2000) Signaling by extracellular nucleotides and nucleosides. *Naunyn-Schmiedeberg's Archives of Pharmacology* 362: 295–298.
- Imeri, L., Bianchi, S., Mariotti, M., and Opp, M.R. (2002) Interleukin-1 microinjected into the dorsal raphe nucleus enhances NREMS in rats. *Journal of Sleep Research* 11: 107.
- Imeri, L., De Simoni, M.G., Giglio, R., Clavenna, A., and Mancina, M. (1994) Changes in the serotonergic system during the sleep–wake cycle: simultaneous polygraphic and voltammetric recordings in hypothalamus using a telemetry system. *Neuroscience* 58: 353–358.
- Imon, H., Ito, K., Dauphin, L., and McCarley, R.W. (1996) Electrical stimulation of the cholinergic laterodorsal tegmental nucleus elicits scopolamine-sensitive excitatory postsynaptic potentials in medial pontine reticular formation neurons. *Neuroscience* 74: 393–401.
- Inoué, S. (1989) *Biology of Sleep Substances*. Boca Raton (FL): CRC Press, Inc.
- Inouye, S.T. and Kawamura, H. (1979) Persistence of circadian rhythmicity in a mammalian hypothalamic “island” containing the suprachiasmatic nucleus. *Proceedings of the National Academy of Sciences of the USA* 76: 5962–5966.
- Insel, T.R., Gillin, J.C., Moore, A., Mendelson, W.B., Loewenstein, R.J., and Murphy, D.L. (1982) The sleep of patients with obsessive-compulsive disorder. *Archives of General Psychiatry* 39: 1372–1377.
- Issacson, L.G. and Tanaka, D. Jr. (1986) Cholinergic and non-cholinergic projections from the canine pontomesencephalic tegmentum (Ch5 area) to the caudal intralaminar thalamic nuclei. *Experimental Brain Research* 62: 179–188.
- Ito, K. and McCarley, R.W. (1984) Alterations in membrane potential and excitability of cat medial pontine reticular formation neurons during naturally occurring sleep–wake states. *Brain Research* 292: 169–175.
- Ito, K. and McCarley, R.W. (1987) Physiological studies of brainstem reticular connectivity. I. Responses of mPRF neurons to stimulation of bulbar reticular formation. *Brain Research* 409: 97–110.
- Ito, K., Yanagihara, M., Imon, L., Dauphin, L., and McCarley, R.W. (2002) Intracellular recordings of pontine medial gigantocellular tegmental field neurons in the naturally sleeping cat: behavioral state-related activity and soma size difference in order of recruitment. *Neuroscience* 114: 23–37.
- Ito, M., Udo, M., and Mano, N. (1970) Long inhibitory and excitatory pathways converging onto cat reticular and Deiters' neurons and their relevance to reticulofugal axons. *Journal of Neurophysiology* 33: 210–226.
- Iwamura, Y., Tanaka, M., Sakamoto, M., and Hikosaka, O. (1985) Vertical neuronal arrays in the postcentral gyrus signaling active touch: a receptive field study in the conscious monkey. *Experimental Brain Research* 58: 412–420.

- Jackson, A. and Crossman, A.R. (1981) Basal ganglia and other afferent projections to the peribrachial region in the rat: a study using retrograde and anterograde transport of horseradish peroxidase. *Neuroscience* 6: 1537–1549.
- Jahnsen, H. and Llinás, R. (1984a) Electrophysiological properties of guinea-pig thalamic neurones: an *in vitro* study. *Journal of Physiology (London)* 349: 205–226.
- Jahnsen, H. and Llinás, R. (1984b) Ionic basis for the electroresponsiveness and oscillatory properties of guinea-pig thalamic neurones *in vitro*. *Journal of Physiology (London)* 349: 227–247.
- Jahr, C.E. and Stevens, C.F. (1987) Glutamate activates multiple single channel conductances in hippocampal neurons. *Nature* 325: 522–525.
- Janowsky, D.S., El-Yousef, M.K., and Davis, J.M. (1972) A cholinergic-adrenergic hypothesis of mania and depression. *Lancet* 2: 632–635.
- Janowsky, D.S., Risch, C., Parker, D., Huey, L., and Judd, L. (1980) Increased vulnerability to cholinergic stimulation in affective disorder patients. *Psychopharmacological Bulletin* 16: 29–31.
- Jasper, H.H. (1949) Diffuse projection systems: the integrative action of the thalamic reticular system. *Electroencephalography and Clinical Neurophysiology* 1: 405–420.
- Jasper, H.H. (1958) Recent advances in our understanding of ascending activities of the reticular system. In H.H. Jasper, L.D. Proctor, R.S. Knighton, W.C. Noshay, and R.T. Costello, eds., *Reticular Formation of the Brain*, pp. 319–331, Boston-Toronto: Little-Brown.
- Jasper, H.H. and Droogleever-Fortuyn, J. (1949) Experimental studies on the functional anatomy of petit-mal epilepsy. *Research Publications of the Association of Nervous and Mental Diseases* 26: 272–298.
- Jasper, H.H. and Kershman, J. (1941) Electroencephalographic classification of the epilepsies. *Archives of Neurology and Psychiatry* 45: 903–943.
- Jasper, H.H. and Tessier, J. (1971) Acetylcholine liberation from cerebral cortex during paradoxical (REM) sleep. *Science* 172: 601–602.
- Jasper, H.H., Ricci, G.F., and Doane, B. (1957) Patterns of cortical neuron discharge during conditioned response in monkeys. In G.E.W. Wolstenholme and C.M. Connor, eds., *Neurological Basis of Behavior*, pp. 277–294, Boston: Ciba Foundation Symposium.
- Jasper, H.H., Ricci, G.F., and Doane, B. (1960) Microelectrode analysis of cortical cell discharge during avoidance conditioning in the monkey. *Electroencephalography and Clinical Neurophysiology* (Suppl.) 13: 137–155.
- Jeannerod, M., Mouret, J., and Jouviet, M. (1965) Etude de la motricité oculaire au cours de la phase paradoxale du sommeil chez le chat. *Electroencephalography and Clinical Neurophysiology* 18: 554–566.
- Jibiki, I., Avoli, M., Gloor, P., Giaretta, D., and McLachlan, R.S. (1986) Thalamocortical and intrathalamic interactions during slow repetitive stimulation of n. cnetralis lateralis. *Experimental Brain Research* 61: 245–257.
- Johnson, J.W. and Ascher, P. (1987) Glycine potentiates the NMDA response in cultured mouse brain neurons. *Nature* 325: 529–531.
- Jones, B.E. (1989) The relationship among acetylcholine, norepinephrine and GABA neurons within the pons of the rat. *Anatomical Record* 223: 57.
- Jones, B.E. (1993) The organization of central cholinergic systems and their functional importance in sleep–waking states. *Progress in Brain Research* 98: 61–71.
- Jones, B.E. (1998) The neuronal basis of consciousness across the sleep–waking cycle. *Advances in Neurology* 77: 75–94.
- Jones, B.E. (2000) Basic mechanisms of sleep–wake states. In M.H. Kryger, T. Toth, and W.C. Dement, eds., *Principles and Practice of Sleep Medicine*, pp. 134–154, Philadelphia: Saunders.
- Jones, B.E. (2003a) Activity, modulation and role of basal forebrain cholinergic neurons innervating the cerebral cortex. In L. Descarries, K. Krnjević, and M. Steriade, eds., *Acetylcholine in the Cerebral Cortex*, San Diego: Academic Press.
- Jones, B.E. (2003b) Arousal systems. *Frontiers in Bioscience* 8: S438–S451.
- Jones, B.E. and Beaudet, A. (1987a) Distribution of acetylcholine and catecholamine neurons in the cat brain stem studied by choline acetyltransferase and tyrosine hydroxylase immunohistochemistry. *Journal of Comparative Neurology* 261: 15–32.
- Jones, B.E. and Beaudet, A. (1987b) Retrograde labeling of neurons in the brain stem following injections of (³H) choline into the forebrain of the rat. *Experimental Brain Research* 65: 437–448.
- Jones, B.E. and Cuello, A.C. (1989) Afferents to the basal forebrain cholinergic cell area from the pontomesencephalic—catecholamine, serotonin, and acetylcholine—neurons. *Neuroscience* 31: 37–61.
- Jones, B.E. and Moore, R.Y. (1977) Ascending projections of the locus coeruleus in the rat. II. Autoradiographic study. *Brain Research* 127: 23–53.

- Jones, B.E. and Mühlethaler, M. (1999) Cholinergic and GABAergic neurons of the basal forebrain: role in cortical activation. In *Handbook of Behavioral State Control*, CRC Press, 213–233.
- Jones, B.E. and Yang, T.Z. (1985) The efferent projections from the reticular formation and the locus coeruleus studied by anterograde and retrograde axonal transport in the rat. *Journal of Comparative Neurology* 242: 56–92.
- Jones, B.E., Harper, S.T., and Halaris, A.E. (1977) Effects of locus coeruleus lesions upon cerebral monoamine content, sleep–wakefulness states and the response to amphetamine in the cat. *Brain Research* 124: 473–496.
- Jones, E. (1959) *The Life and Work of Sigmund Freud*. New York: Basic Books.
- Jones, E.G. (1975a) Some aspects of the organization of the thalamic reticular complex. *Journal of Comparative Neurology* 162: 285–308.
- Jones, E.G. (1975b) Varieties and distribution of non-pyramidal cells in the somatic sensory cortex of the squirrel monkey. *Journal of Comparative Neurology* 160: 205–268.
- Jones, E.G. (1985) *The Thalamus*. New York: Plenum.
- Jones, E.G. (1988) What are local circuits? In P. Rakic and W. Singer, eds., *Neurobiology of Neocortex*, pp. 137–152, New York: Wiley.
- Jones, E.G. (1991) Cellular organization in the primate postcentral gyrus. In O. Franzen and J. Westman, eds., *Information Processing in the Somatosensory System*, pp. 95–107, New York: Macmillan.
- Jones, E.G. (2000) Cortical and subcortical contributions to activity-dependent plasticity in primate somatosensory cortex. *Annual Reviews of Neuroscience* 23: 1–37.
- Jones, E.G. and Powell, T.P.S. (1969) An electron microscopic study of the mode of termination of cortico-thalamic fibers within the thalamic relay nuclei of the cat. *Proceedings of the Royal Society, London, Series B, Biological Sciences* 172: 173–185.
- Jones, E.G., Burton, H., Saper, C.B., and Swanson, L.W. (1976) Midbrain, diencephalic and cortical relationships of the basal nucleus of Meynert and associated structures in primates. *Journal of Comparative Neurology* 167: 385–420.
- Jones, E.G., Coulter, J.D., and Hendry, S.H.C. (1978) Intracortical connectivity of architectonic fields in somatic sensory, motor and parietal cortex. *Journal of Comparative Neurology* 181: 291–348.
- Jones, L.S., Gauger, L.L., and Davis, J.N. (1985a) Anatomy of brain alpha 1-adrenergic receptors: *in vitro* autoradiography with [125I]-HEAT. *Journal of Comparative Neurology* 231: 190–208.
- Jones, L.S., Gauger, L.L., Davis, J.N., Slotkin, T.A., and Bartolome, J.V. (1985b) Postnatal development of brain alpha 1 adrenergic receptors: *in vitro* autoradiography with [125I]HEAT in normal rats and rats treated with alpha-difluoromethylornithine, a specific, irreversible inhibitor of ornithine decarboxylase. *Neuroscience* 15: 1195–1202.
- Jouvet, M. (1962) Recherches sur les structures nerveuses et les mécanismes responsables des différentes phases du sommeil physiologique. *Archives Italiennes de Biologie* 100: 125–206.
- Jouvet, M. (1965a) Behavioral and EEG effects of paradoxical sleep deprivation in the cat. *Proceedings of the XXIII International Congress of Physiological Sciences*, Lectures and Symposia Volume, Amsterdam: Excerpta Medica Foundation 344–353.
- Jouvet, M. (1965b) Discussion générale. In *Neurophysiologie des Etats de Sommeil*, pp. 613–650, Paris: Editions du Centre National de la Recherche Scientifique.
- Jouvet, M. (1967) Neurophysiology of the states of sleep. *Physiological Reviews* 47: 117–177.
- Jouvet, M. (1969) Biogenic amines and the states of sleep. *Science* 163: 32–41.
- Jouvet, M. (1972) The role of monoamine and acetylcholine-containing neurons in the regulation of the sleep–waking cycle. *Ergebnisse der Physiologie* 64: 166–307.
- Jouvet, M. (1979) What does a cat dream about? *Trends in Neurosciences* 2: 15–16.
- Jouvet, M. and Delorme, J.F. (1965) Locus coeruleus et sommeil paradoxal. *Comptes Rendus de la Société de Biologie (Paris)* 159: 895–899.
- Jouvet, M. and Michel, F. (1959) Corrélations électromyographiques du sommeil chez le chat décortiqué et mésencéphalique chronique. *Comptes Rendus de la Société de Biologie (Paris)* 153: 422–425.
- Jouvet, M., Michel, F., and Courjon, J. (1959) Sur un stade d'activité électrique cérébrale rapide au cours du sommeil physiologique. *Comptes Rendus de la Société de Biologie (Paris)* 153: 1024–1028.
- Jouvet, M., Mounier, D., and Astic, L. (1968) Etude de l'évolution du sommeil du raton au cours du premier mois post-natal. *Comptes Rendus de la Société de Biologie (Paris)* 162: 119–123.
- Juji, T., Satake, M., Honda, Y., and Doi, Y. (1984) HLA antigens in Japanese patients with narcolepsy—all the patients were DR2 positive. *Tissue Antigens* 24: 316–319.
- Kalia, M. and Fuxe, K. (1985) Rat medulla oblongata. I. Cytoarchitectonic considerations. *Journal of Comparative Neurology* 233: 285–307.

- Kalinchuk, A.V., Urrila, A.-S., Alanko, L., Heiskanen, S., Wigren, H.-K., Soumela, M., Stenberg, D., and Porkka-Heiskanen, T. (2003a) Local energy depletion in the basal forebrain increases sleep. *European Journal of Neuroscience* 17: 863–869.
- Kalinchuk, A.V., Hokkanen, M., Stenberg, D., Rosenberg, P.A., and Porkka-Heiskanen, T. (2003b) The role of nitric oxide in regulation of sleep need. *Sleep* 26: A32.
- Kammermeier, P.J. and Jones, S.W. (1997) High-voltage-activated calcium currents in neurons acutely isolated from the ventrobasal nucleus of the rat thalamus. *Journal of Neurophysiology* 77: 465–475.
- Kamondi, A., Williams, J.A., Hutcheon, B., and Reiner, P.B. (1992) Membrane properties of mesopontine cholinergic neurons studied with the whole-cell patch-clamp technique: implications for behavioral state control. *Journal of Neurophysiology* 68: 1359–1372.
- Kamondi, A., Acsády, L., Wang, X.J., and Buzsáki, G. (1998) Theta oscillations in somata and dendrites of hippocampal pyramidal cells in vivo: activity dependent phase-precession of action potentials. *Hippocampus* 8: 244–261.
- Kanamori, N., Sakai, K., and Jouvet, M. (1980) Neuronal activity specific to paradoxical sleep in the ventromedial medullary reticular formation of unrestrained cats. *Brain Research* 189: 251–255.
- Kaneko, C.R.S. and Fuchs, A.F. (1981) Inhibitory burst neurons in alert trained cats: comparison with excitatory burst neurons and functional implications. In A.F. Fuchs and W. Becker, eds., *Progress in Oculomotor Research*, vol. 12, pp. 63–70, New York: Elsevier North Holland.
- Kaneko, C.R.S., Evinger, C., and Fuchs, A.F. (1981) Role of cat pontine burst neurons in generation of saccadic eye movements. *Journal of Neurophysiology* 46: 387–408.
- Kang, Y. and Kitai, S.T. (1990) Electrophysiological properties of pedunculopontine neurons and their postsynaptic responses following stimulation of substantia nigra reticulata. *Brain Research* 535: 79–95.
- Karabelas, A.B. and Purpura, D.P. (1980) Evidence for autapses in the substantia nigra. *Brain Research* 200: 467–473.
- Katayama, Y., DeWitt, D.S., Becker, D.P., and Hayes, R.L. (1984) Behavioral evidence for a cholinceptive pontine inhibitory area: descending control of spinal motor output and sensory input. *Brain Research* 296: 241–262.
- Katz, B. (1949) Les constantes électriques de la membrane du muscle. *Archives des Sciences Physiologiques* 3: 285.
- Kawaguchi, Y. (1993) Groupings of nonpyramidal and pyramidal cells with specific physiological and morphological characteristics in rat frontal cortex. *Journal of Neurophysiology* 69: 416–431.
- Kawaguchi, Y. and Kubota, Y. (1997) GABAergic cell subtypes and their synaptic connections in rat frontal cortex. *Cerebral Cortex* 7: 476–486.
- Kayama, Y., Negi, T., Sugitani, M., and Iwama, K. (1982) Effects of locus coeruleus stimulation on neuronal activities of dorsal lateral geniculate nucleus and perigeniculate reticular nucleus of the rat. *Neuroscience* 7: 655–666.
- Kayama, Y., Ohta, M., and Jodo, E. (1992) Firing of ‘possibly’ cholinergic neurons in the rat laterodorsal tegmental nucleus during sleep and wakefulness. *Brain Research* 569: 210–220.
- Kayama, Y., Sumitomo, I., and Ogawa, T. (1986a) Does the ascending cholinergic projection inhibit or excite neurons in the rat thalamic reticular nucleus? *Journal of Neurophysiology* 56: 1310–1320.
- Kayama, Y., Takagi, M., and Ogawa, T. (1986b) Cholinergic influence of the laterodorsal tegmental nucleus on neuronal activity in the rat lateral geniculate nucleus. *Journal of Neurophysiology* 56: 1297–1309.
- Kellaway, P. (1985) Sleep and epilepsy. *Epilepsia* 26: 15–30.
- Kellaway, P., Frost, J.D. Jr., and Crawley, J.W. (1990) The relations between sleep spindles and spike-and-wave bursts in human epilepsy. In M. Avoli, P. Gloor, G. Kostopoulos, and R. Naquet, *Generalized Epilepsy*, eds, 36–48, Boston: Birkhäuser.
- Keller, A. (1993) Intrinsic synaptic organization of the motor cortex. *Cerebral Cortex* 3: 43–51.
- Keller, E.L. (1974) Participation of medial pontine reticular formation in eye movement generation in monkey. *Journal of Neurophysiology* 37: 316–332.
- Keller, E.L. (1980) Oculomotor specificity within subdivisions of the brain stem reticular formation. In J.A. Hobson and M.A.B. Brazier, eds., *The Reticular Formation Revisited*, pp. 227–280, New York: Raven Press.
- Kelly, J.P. and Van Essen, D.C. (1974) Cell structure and function in the visual cortex of the cat. *Journal of Physiology (London)* 328: 515–547.
- Kelly, J.S., Godfraind, J.M., and Maruyama, S. (1979) The presence and nature of inhibition in small slices of the dorsal lateral geniculate nucleus of rat and cat incubated *in vitro*. *Brain Research* 168: 388–392.
- Kemp, J.A., Roberts, H.C., and Sillito, A.M. (1982) Further studies on the action of 5-hydroxytryptamine in the dorsal lateral geniculate nucleus of the rat. *Brain Research* 246: 334–337.

- Kennedy, C. (1983) Changes in glucose utilization in relation to activity in the central nervous system. In H.H. Jasper and N.M. van Gelder, eds., *Basic Mechanisms of Neural Hyperexcitability*, pp. 399–421, New York: A.R. Liss.
- Khachaturian, H., Lewis, M.E., and Watson S.J. (1983) Enkephalin systems in diencephalon and brainstem of the rat. *Journal of Comparative Neurology* 220: 273–310.
- Khateb, A., Fort, P., Serafin, M., Jones, B.E., and Mühlethaler, M. (1995a) Rhythmical bursts induced by NMDA in guinea-pig cholinergic nucleus basalis neurones *in vitro*. *Journal of Physiology (London)* 487: 623–638.
- Khateb, A., Fort, P., Pegna, A., Jones, B.E., and Mühlethaler, M. (1995b) Cholinergic nucleus basalis neurons are excited by histamine *in vitro*. *Neuroscience* 69: 495–506.
- Khateb, A., Fort, P., Williams, S., Serafin, M., Jones, B.E., and Mühlethaler, M. (1997) Modulation of cholinergic nucleus basalis neurons by acetylcholine and *N*-methyl-D-aspartate. *Neuroscience* 81: 47–55.
- Khateb, A., Fort, P., Williams, S., Serafin, M., Mühlethaler, M., and Jones, B.E. (1998) GABAergic input to cholinergic nucleus basalis neurons. *Neuroscience* 86: 937–947.
- Khateb, A., Mühlethaler, M., Alonso, A., Serafin, M., Mainville, L., and Jones, B.E. (1992) Cholinergic nucleus basalis neurons display the capacity for rhythmic bursting activity mediated by low-threshold calcium spikes. *Neuroscience* 51: 489–494.
- Khateb, A., Serafin, M., Jones, B.E., Alonso, A., and Mühlethaler, M. (1991) Pharmacological study of basal forebrain neurons in guinea pig brain slices. *Society for Neuroscience Abstracts* 17: 881.
- Kia, H.K., Brisorgueil, M.J., Daval, G., Langlois, X., Hamon, M., and Verge, D. (1996) Serotonin1A receptors are expressed by a subpopulation of cholinergic neurons in the rat medial septum and diagonal band of Broca—a double immunocytochemical study. *Neuroscience* 74: 143–154.
- Kievit, J. and Kuypers, H.G.J.M. (1972) Fastigial cerebellar projections to the ventrolateral nucleus of the thalamus and the organization of the descending pathways. In T. Frigyesi, E. Rinvik, and M.D. Yahr, eds., *Corticothalamic Projections and Sensorimotor Activities*, pp. 91–111, New York: Raven Press.
- Kilduff, T.S., Bowersox, S.S., Kaitin, K.I., Baker, T.L., Ciaranello, R.D., and Dement, W.C. (1986) Muscarinic cholinergic receptors and the canine model of narcolepsy. *Sleep* 9: 102–106.
- Kim, H.G., Beierlein, M., and Connors, B.W. (1995) Inhibitory control of excitable dendrites in neocortex. *Journal of Neurophysiology* 74: 1810–1814.
- Kim, U. and McCormick, D.A. (1998) Functional and ionic properties of a slow afterhyperpolarization in ferret perigeniculate neurons *in vitro*. *Journal of Neurophysiology* 80: 1222–1235.
- Kim, U., Bal, T., and McCormick, D.A. (1995) Spindle waves are propagating synchronized oscillations in the ferret LGNd *in vitro*. *Journal of Neurophysiology* 74: 1301–1323.
- Kimura, H., McGeer, P.L., Peng, J.H., and McGeer, E.G. (1981) The central cholinergic system studied by choline acetyltransferase immunohistochemistry in the cat. *Journal of Comparative Neurology* 200: 151–201.
- King, W.M. and Fuchs, A.F. (1979) Reticular control of vertical saccadic eye movements by mesencephalic burst neurons. *Journal of Neurophysiology* 42: 861–876.
- Kinomura, S., Larsson, J., Gulyás, B., and Roland, P. (1996) Activation by attention of the human reticular formation and thalamic intralaminar nuclei. *Science* 271: 512–515.
- Kiper, D.C., Knyazeva, M.G., Tettoni, L., and Innocenti, G.M. (1999) Visual stimulus-dependent changes in interhemispheric EEG coherence in ferrets. *Journal of Neurophysiology* 82: 3082–3094.
- Kisvárdy, Z.F., Beaulieu, C., and Eysel, U.T. (1993) Network of GABAergic large basket cells in visual cortex (area 18): implication for lateral disinhibition. *Journal of Comparative Neurology* 327: 398–415.
- Kita, H. and Kitai, S.T. (1986) Electrophysiology of rat thalamocortical relay neurons: an *in vivo* intracellular recording and labeling study. *Brain Research* 371: 80–89.
- Kitsikis, A. and Steriade, M. (1981) Immediate behavioral effects of kainic acid injections into the mid-brain reticular core. *Behavioral and Brain Research* 3: 361–380.
- Kitt, C.A., Mitchell, S.J., DeLong, M.R., Wainer, B.H., and Price, D.L. (1987) Fiber pathways of basal forebrain cholinergic neurons in monkeys. *Brain Research* 406: 192–206.
- Kiyashchenko, L.I., Milevskiy, B.Y., Maidment, N., Lam, H.A., Wu, M.F., John, J., Peever, J., and Siegel, J.M. (2002) Release of hypocretin (orexin) during waking and sleep states. *Journal of Neuroscience* 22: 5282–5286.
- Klee, A. (1961) Akinetic mutism: review of the literature and report of a case. *Journal of Nervous and Mental Diseases* 133: 536–553.
- Kleitman, N. (1929) Sleep. *Physiological Reviews* 9: 624–665.
- Kleitman, N. (1963) *Sleep and Wakefulness*. Chicago: Chicago University Press.
- Klink, R. and Alonso, A. (1997a) Muscarinic modulation of the oscillatory and repetitive firing properties of entorhinal cortex layer II neurons. *Journal of Neurophysiology* 77: 1813–1828.
- Klink, R. and Alonso, A. (1997b) Ionic mechanisms of muscarinic depolarization in entorhinal cortex layer II neurons. *Journal of Neurophysiology* 77: 1829–1843.

- Knyazeva, M.G., Kiper, D.C., Vilvadski, V.Y., Despland, P.A., Maeder-Ingvar, M., and Innocenti, G.M. (1999) Visual stimulus-dependent changes in interhemispheric EEG coherence in humans. *Journal of Neurophysiology* 82: 3095–3107.
- Kohlmeier, K.A. and Reiner, P.B. (1999) Noradrenaline excites non-cholinergic laterodorsal tegmental neurons via two distinct mechanisms. *Neuroscience* 93: 619–630.
- Konopacki, J., MacIver, M.B., Bland, B.H., and Roth, S.H. (1987) Carbachol-induced EEG “theta” activity in hippocampal brain slices. *Brain Research* 405: 196–198.
- Korotkova, T.M., Eriksson, K.S., Haas, H.L., and Brown, R.E. (2002) Selective excitation of GABAergic neurons in the substantia nigra of the rat by orexin/hypocretin *in vitro*. *Regulatory Peptides* 104: 83–89.
- Korotkova, T.M., Sergeeva, O.A., Eriksson, K.S., Haas, H.L., and Brown, R.E. (2003) Excitation of ventral tegmental area dopaminergic and non-dopaminergic neurons by orexins/hypocretins. *Journal of Neuroscience* 23: 7–11.
- Kosaka, T., Kosaka, K., Hataguchi, Y., Nagatsu, I., Wu, J.Y., Ottersen, O.P., Storm-Mathisen, J., and Hama, K. (1987) Catecholaminergic neurons containing GABA-like and/or glutamic acid decarboxylase-like immunoreactivities in various brain regions of the rat. *Experimental Brain Research* 66: 191–210.
- Kostopoulos, G. (2000) Spike-and-wave discharges of absence seizures as a transformation of sleep spindles: the continuing development of a hypothesis. *Clinical Neurophysiology* 111 (Suppl. 2): S27–S38.
- Kostowski, W. (1971) Effects of some cholinergic and anticholinergic drugs injected intracerebrally to the midline pontine area. *Neuropharmacology* 10: 595–605.
- Kostyuk, P. and Verkhratsky, A. (1994) Calcium stores in neurons and glia. *Neuroscience* 63: 381–404.
- Kreindler, A. and Steriade, M. (1964) EEG patterns of arousal and sleep induced by stimulating various amygdaloid levels in the cat. *Archives Italiennes de Biologie* 102: 576–586.
- Kriegler, M., Perez, C., DeFay, K., Albert, I., and Lu, S.D. (1998) A novel form of TNF/cachectin is a cell surface cytotoxic transmembrane protein; ramifications for the complex physiology of TNF. *Cell* 53: 45–56.
- Kripke, D.F., Mullaney, D.J., Atkinson, M., and Wolf, S. (1978) Circadian rhythm disorders in manic-depressives. *Biological Psychiatry* 13: 335–351.
- Kristensson, K. and Olsson, Y. (1971) Retrograde axonal transport of protein. *Brain Research* 29: 363–365.
- Krnjević, K. (1974) Chemical nature of synaptic transmission in vertebrates. *Physiological Reviews* 54: 418–540.
- Krnjević, K. and Phillis, J.W. (1963a) Acetylcholine-sensitive cells in the cerebral cortex. *Journal of Physiology (London)* 166: 296–327.
- Krnjević, K. and Phillis, J.W. (1963b) Pharmacological properties of acetylcholine-sensitive cells in the cerebral cortex. *Journal of Physiology (London)* 166: 328–350.
- Krnjević, K. and Ropert, N. (1981) Septo-hippocampal pathway modulates hippocampal activity by a cholinergic mechanism. *Canadian Journal of Physiology and Pharmacology* 59: 911–914.
- Krnjević, K. and Ropert, N. (1982) Electrophysiological and pharmacological characteristics of facilitation of hippocampal population spikes by stimulation of the medial septum. *Neuroscience* 7: 2165–2183.
- Krnjević, K., Pumain, R., and Renaud, L. (1971) The mechanism of excitation by acetylcholine in the cerebral cortex. *Journal of Physiology (London)* 215: 247–268.
- Krnjević, K., Puil, E., and Werman, R. (1976) Is cyclic guanosine monophosphate the internal “second messenger” for cholinergic actions on central neurons? *Canadian Journal of Physiology and Pharmacology* 54: 172–176.
- Krnjević, K., Ropert, N., and Caullo, J. (1988) Septohippocampal disinhibition. *Brain Research* 438: 182–192.
- Kronauer, R.E., Czeisler, C.A., Pilato, S.F., Moore-Ede, M.C., and Weitzman, E.D. (1982) Mathematical model of the human circadian system with two interacting oscillators. *American Journal of Physiology* 242 (Regulatory Integrative Comparative Physiology 11): R3–R17.
- Krueger, J., Walter, J., and Levin, C. (1985) Factor S and related somnogens: an immune theory for slow-wave sleep. In D. McGinty, R. Drucker-Colin, A. Morrison, P.L. Parmeggiani, eds., *Brain Mechanisms of Sleep*, pp. 253–275, New York: Raven Press.
- Krueger, J.M. (1990) Somnogenic activity of immune response modifiers. *Trends in Pharmacological Science* 11: 122–126.
- Krueger, J.M. and Majde, J.A. (1994). Microbial products and cytokines in sleep and fever regulation. *Critical Reviews in Immunology* 14: 355–379.
- Krueger, J.M. and Majde, J.A. (2003) Humoral links between sleep and the immune system: research issues. *Annals of the New York Academy of Sciences* 992: 9–20.
- Krueger, J.M. and Obal, F. Jr. (2003) Sleep function. *Frontiers in Bioscience* 8: d511–519.
- Krueger, J.M., Fang, J., Taishi, P., Chen, Z., Kushikata, T., and Gardi, J. (1998) Sleep: a physiologic role for IL-1 β and TNF- α . *Annals of the New York Academy of Sciences* 856: 148–159.

- Krueger, J.M., Obal, F. Jr., Fang, J., Kubota, T., and Taishi, P. (2001) The role of cytokines in physiological sleep regulation. *Annals of the New York Academy of Sciences* 933: 211–221.
- Krueger, J.M., Obal, F., Jr., Opp, M., Johansen, L., Cady, A.B., and Toth, L. (1989) Immune response modifiers and sleep. In K. Masek and G. Nistico, eds., *Interactions Between Neuroendocrine and Immune Systems*, Rome: Pythagora Press.
- Krueger, J.M., Walter, J., Dinarello, C.A., Wolff, S.M., and Chedid, L. (1984) sleep-promoting effects of endogenous pyrogen (interleukin-1). *American Journal of Physiology* 246: R994–R999.
- Kubin L. (2001) Carbachol models of REM sleep: recent developments and new directions. *Archives Italiennes de Biologie* 139: 147–168.
- Kucera, P. and Favrod, P. (1979) Suprachiasmatic nucleus projection to mesencephalic central gray in the woodmouse (*Apodemus sylvaticus* L.). *Neuroscience* 4: 1705–1715.
- Kulics, A.T. (1982) Cortical neural evoked correlates of somatosensory stimulus detection in the rhesus monkey. *Electroencephalography and Clinical Neurophysiology* 53: 78–93.
- Kulics, A.T., Lineberry, C.G., and Roppolo, J.R. (1977) Neurophysiological correlates of cutaneous discrimination performance in rhesus monkey. *Brain Research* 136: 360–365.
- Kupfer, D.J. (1982) EEG sleep as biological markers in depression. In E. Usdin and I. Hanin, eds., *Biological Markers in Psychiatry and Neurology*, pp. 387–396, New York: Pergamon Press.
- Kupfer, D.J. and Foster, F.G. (1972) Interval between onset of sleep and rapid eye movement as an indicator of depression. *Lancet* 2: 684–686.
- Kupfer, D.J., Gillin, J.C., Coble, P.A., Spiker, D.G., Shaw, D.H., and Holtzer, B. (1981a) REM sleep, naps, and depression. *Psychiatry Research* 5: 195–203.
- Kupfer, D.J., Spiker, D.G., Coble, P.A., Neil, J.F., Ulrich, R., and Shaw, D.H. (1981b) Sleep and treatment prediction in endogenous depression. *American Journal of Psychiatry* 138: 429–434.
- Kupfer, D.J., Ulrich, R.F., Coble, P.A., Jarrett, D.B., Grochocinski, V., Doman, J., Matthews, G., and Borbély, A.A. (1984) Application of automated REM and slow wave sleep analysis. II. Testing the assumptions of the two-process model of sleep regulation in normal and depressed subjects. *Psychiatry Research* 13: 335–343.
- Kuroda, M. and Price, J.L. (1991) Synaptic organization of projections from basal forebrain structures to the mediodorsal thalamic nucleus of the rat. *Journal of Comparative Neurology* 303: 513–533.
- Kuypers, H.G.J.M. (1958) Cortico-bulbar connexions to the pons and lower brain stem in man. An anatomical study. *Brain* 81: 364–388.
- Kuypers, H.G.J.M., Bentivoglio, M., Catsman-Berrevoets, C.E., and Bharos, A.T. (1980) Double retrograde neuronal labeling through divergent axon collaterals, using two fluorescent tracers with the same excitation wave length which label different features of the cell. *Experimental Brain Research* 40: 383–392.
- Lamour, Y., Dutar, P., and Jobert, A. (1982) Excitatory effect of acetylcholine on different types of neurons in the first somatosensory neocortex of the rat: laminar distribution and pharmacological characteristics. *Neuroscience* 7: 1483–1494.
- Lamour, Y., Dutar, P., and Jobert, A. (1983) A comparative study of two populations of acetylcholine sensitive neurons in rat somatosensory cortex. *Brain Research* 289: 157–167.
- Lamour, Y., Dutar, P., and Jobert, A. (1984) Septo-hippocampal and other medial septum—diagonal band neurons: electrophysiological and pharmacological properties. *Brain Research* 309: 227–239.
- Lancaster, B. and Nicoll, R.A. (1987) Properties of two calcium-activated hyperpolarizations in rat hippocampal neurones. *Journal of Physiology (London)* 389: 187–203.
- Lang, W., Henn, V., and Hepp, K. (1982) Gaze palsies after selective pontine lesions in monkeys. In A. Roucoux and M. Crommelinck, eds., *Physiological and Pathological Aspects of Eye Movements*, pp. 209–218, The Hague: Junk.
- Lang, W., Lang, M., Kornhuber, A., Deeke, L., and Kornhuber, H.H. (1983) Human cerebral potentials and visuomotor learning. *Pfluegers Archiv* 399: 342–344.
- Langer, T., Fuchs, A.F., Scudder, C.A., and Chubb, M.C. (1985) Afferents to the flocculus of the cerebellum in the rhesus macaque as revealed by retrograde transport of horseradish peroxidase. *Journal of Comparative Neurology* 235: 1–25.
- Langer, T., Kaneko, C.R.S., Scudder, C.A., and Fuchs, A.F. (1986) Afferents to the abducens nucleus in the monkey and the cat. *Journal of Comparative Neurology* 245: 379–400.
- Lanneau, C., Peineau, S., Petit, F., and Epelbaum, J. (2000) Somatostatin modulation of excitatory synaptic transmission between periventricular and arcuate hypothalamic nuclei *in vitro*. *Journal of Neurophysiology* 84: 1464–1474.
- Larson, J. and Lynch, G. (1986) Induction of synaptic potentiation in hippocampus by patterned stimulation involves two events. *Science* 232: 985–988.
- Lasek, R., Joseph, B.S., and Whitlock, D.G. (1968) Evaluation of a radioautographic neuroanatomical tracing method. *Brain Research* 8: 319–336.

- Latini, S. and Pedata, F. (2001) Adenosine in the central nervous system: release mechanisms and extracellular concentrations. *Journal of Neurochemistry* 79: 463–484.
- LaVail, J.H. and LaVail, M.M. (1972) Retrograde axonal transport in the central nervous system. *Science* 176: 1416–1417.
- Lavoie, B. and Parent, A. (1994) Pedunculopontine nucleus in the squirrel monkey: distribution of cholinergic and monoaminergic neurons in the mesopontine tegmentum with evidence for the presence of glutamate in cholinergic neurons. *Journal of Comparative Neurology* 344: 190–209.
- Le Gros Clark, W.E. and Boggon, R.H. (1933) On the connections of the medial cell groups of the thalamus. *Brain* 56: 83–98.
- Ledberg, A., Akerman, S., and Roland, P.E. (1998) Estimation of the probabilities of 3D clusters in functional brain images. *Neuroimage* 8: 113–128.
- Lee, K.H. and McCormick, D.A. (1995) Acetylcholine excites GABAergic neurons of the ferret perigeniculate nucleus through nicotinic receptors. *Journal of Neurophysiology* 73: 2123–2128.
- Lee, S.M., Friedberg, M.H., and Ebner, F.F. (1994) The role of GABA-mediated inhibition in the rat ventral posterior medial thalamus. I. Assessment of receptive field changes following thalamic reticular nucleus lesions. *Journal of Neurophysiology* 71: 1702–1715.
- Legendre, R. and Piéron, H. (1913) Recherches sur le besoin de sommeil consécutif à une veille prolongée. *Zeitschrift der Allgemeine Physiologie* 14: 235–262.
- Leichnetz, G., Smith, D.J., and Spencer, R.F. (1984) Cortical projections to the paramedian tegmental and basilar pons in the monkey. *Journal of Comparative Neurology* 228: 388–408.
- Leichnetz, G.R., Gonzalo-Ruiz, A., DeSalles, A.A.F., and Hayes, R.L. (1987) The origin of brainstem afferents of the paramedian pontine reticular formation in the cat. *Brain Research* 422: 389–397.
- Leonard, C.S. and Llinás, R.R. (1990) Electrophysiology of mammalian pedunculopontine and laterodorsal tegmental neurons *in vitro*: implications for the control of REM sleep. In M. Steriade and D. Biesold, eds., *Brain Cholinergic Systems*, pp. 205–223, Oxford: Oxford University Press.
- Leonard, C.S. and Llinas, R.R. (1994) Serotonergic and cholinergic inhibition of mesopontine cholinergic neurons controlling REM sleep: an *in vitro* electrophysiological study. *Neuroscience* 59: 309–330.
- Leonard, C.S., Kerman, I., Blaha, G., Taveras, E., and Taylor, B. (1995a) Interdigitation of nitric oxide synthase-, tyrosine hydroxylase- and serotonin-containing neurons in and around the laterodorsal and pedunculopontine tegmental nuclei of the guinea pig. *Neuroscience* 362: 411–432.
- Leonard, C.S., Rao, S., and Sanchez, R.M. (1995b) Patterns of neuromodulation and the nitric oxide signaling pathway in mesopontine cholinergic neurons. *Seminars in the Neurosciences* 7: 319–328.
- Leonard, C.S., Sanjai, R.R., and Takafumi, I. (2000) Serotonergic inhibition of action potential evoked calcium transients in NOS-containing mesopontine cholinergic neurons. *Journal of Neurophysiology* 84: 1558–1572.
- Leontovitch, T.A. and Zhukova, G.P. (1963) The specificity of the neuronal structure and topography of the reticular formation in the brain and spinal cord of carnivora. *Journal of Comparative Neurology* 121: 347–389.
- Leresche, N., Jassik-Gerschenfeld, D., Haby, M., Soltesz, I., and Crunelli, V. (1990) Pacemaker-like and other types of spontaneous membrane potential oscillations of thalamocortical cells. *Neuroscience Letters* 113: 72–77.
- Leresche, N., Lightowler, S., Soltesz, I., Jassik-Gerschenfeld, D., and Crunelli, V. (1991) Low-frequency oscillatory activities intrinsic to rat and cat thalamocortical cells. *Journal of Physiology (London)* 441: 155–174.
- Leung, L.W.S. and Borst, J.G.G. (1987) Electrical activity of the cingulate cortex. I. Generating mechanisms and relations to behavior. *Brain Research* 407: 68–80.
- Leung, L.W.S. and Yim, C.Y. (1986) Intracellular records of theta rhythm in hippocampal CA1 cells of the rat. *Brain Research* 367: 323–327.
- Levey, A.I., Armstrong, D.M., Atweh, S.F., Terry, R.D., and Wainer, B.H. (1983a) Monoclonal antibodies to choline acetyltransferase: production, specificity, and immunohistochemistry. *Journal of Neuroscience* 3: 1–9.
- Levey, A.I., Hallanger, A.E., and Wainer, B.H. (1987a) Choline acetyltransferase-immunoreactivity in the rat thalamus. *Journal of Comparative Neurology* 257: 317–332.
- Levey, A.I., Hallanger, A.E., and Wainer, B.H. (1987b) Cholinergic nucleus basalis neurons may influence the cortex via the thalamus. *Neuroscience Letters* 74: 7–13.
- Levey, A.I., Wainer, B.H., Mufson, E.J., and Mesulam, M.M. (1983b) Co-localization of acetylcholinesterase and choline acetyltransferase in the rat cerebrum. *Neuroscience* 9: 9–22.
- Levine, E.S. and Jacobs, B.L. (1992) Neurochemical afferents controlling the activity of serotonergic neurons in the dorsal raphe nucleus: microiontophoretic studies in the awake cat. *Journal of Neuroscience* 12: 4037–4044.

- Levitt, P. and Moore, R.Y. (1978) Noradrenaline neuron innervation of the neocortex in the rat. *Brain Research* 139: 219–231.
- Levitt, P. and Moore, R.Y. (1979) Origin and organization of brainstem catecholamine innervation in the rat. *Journal of Comparative Neurology* 186: 505–528.
- Lhermitte, F., Gautier, J.C., Marteau, R., and Chain, F. (1963) Troubles de la conscience et mutisme akinétique. *Revue de Neurologie (Paris)* 109: 115–131.
- Li, X., Rainnie, D.G., McCarley, R.W., and Greene, R.W. (1998) Presynaptic nicotinic receptors facilitate monoaminergic transmission. *Journal of Neuroscience* 18: 1904–1912.
- Lidov, H.G.W., Grzanna, R., and Molliver, M.E. (1980) The serotonin innervation of the cerebral cortex in the rat—an immunohistochemical analysis. *Neuroscience* 5: 207–227.
- Lin, J.S., Hou, Y., Sakai, K., and Jouvet, M. (1996) Histaminergic descending inputs to the mesopontine tegmentum and their role in the control of cortical activation and wakefulness in the cat. *Journal of Neuroscience* 16: 1523–1537.
- Lin, J.S., Luppi, P.H., Salvetti, D., Sakai, K., and Jouvet, M. (1986) Neurones immunoréactifs à l'histamine dans l'hypothalamus chez le chat. *Comptes Rendus de l'Académie de Sciences (Paris)* 303: 371–376.
- Lin, J.S., Sakai, K., and Jouvet, M. (1988) Evidence for histaminergic arousal mechanisms in the hypothalamus of cats. *Neuropharmacology* 27: 111–122.
- Lin, J.S., Sakai, K., Vanni-Mercier, G., and Jouvet, M. (1989) A critical role of the posterior hypothalamus in the mechanisms of wakefulness determined by microinjections of muscimol in freely moving cats. *Brain Research* 479: 225–240.
- Lin, L., Faraco, J., Li, R., Kadotani, H., Rogers, W., Lin, X., Qiu, X., de Jong, P.J., Nishino, S., and Mignot, E. (1999) The sleep disorder canine narcolepsy is caused by a mutation in the hypocretin (orexin) receptor 2 gene. *Cell* 98: 365–376.
- Lindsley, D.B., Bowden, J.W., and Magoun, H.W. (1949) Effect upon the EEG of acute injury to the brain stem activating system. *Electroencephalography and Clinical Neurophysiology* 1: 475–486.
- Lindsley, D.B., Schreiner, L.H., Knowles, W.B., and Magoun, H.W. (1950) Behavioral and EEG changes following chronic brain stem lesions in the cat. *Electroencephalography and Clinical Neurophysiology* 2: 483–498.
- Lindvall, O. and Bjorklund, A. (1974) The organization of the ascending catecholamine neuron systems in the rat brain as revealed by the glyoxylic acid fluorescence method. *Acta Physiologica Scandinavica (Suppl.)* 412: 1–48.
- Lindvall, O., Bjorklund, A., and Divac, I. (1978) Organization of catecholamine neurons projecting to the frontal cortex in the rat. *Brain Research* 142: 1–24.
- Lindvall, O., Bjorklund, A., Nobin, A., and Stenevi, U. (1974) The adrenergic innervation of the rat thalamus as revealed by the glyoxylic acid fluorescence method. *Journal of Comparative Neurology* 154: 317–348.
- Liu, X.B., Warren, R.A., and Jones, E.G. (1995) Synaptic distribution of afferents from reticular nucleus in ventroposterior nucleus of cat thalamus. *Journal of Comparative Neurology* 352: 187–202.
- Livingstone, M.S. and Hubel, D.H. (1981) Effects of sleep and arousal on the processing of visual information in the cat. *Nature* 291: 554–561.
- Ljungdahl, A., Hokfelt, T., and Nilsson, G. (1978) Distribution of substance P-like immunoreactivity in the central nervous system of the rat. I. Cell bodies and terminals. *Neuroscience* 3: 861–943.
- Llinás, L.L. and Terzuolo, C.A. (1964) Mechanisms of supraspinal actions upon spinal cord activities. Reticular inhibitory mechanisms on alpha-extensor motoneurons. *Journal of Neurophysiology* 27: 579–591.
- Llinás, R. and Hillman, D.E. (1975) A multipurpose tridimensional reconstruction computer system for neuroanatomy. In M. Santini, ed., *Golgi Centennial Symposium*, pp. 71–79, New York: Raven Press.
- Llinás, R. and Jahnsen, H. (1982) Electrophysiology of mammalian thalamic neurones *in vitro*. *Nature* 297: 406–408.
- Llinás, R. and Mühlethaler, M. (1988) An electrophysiological study of the *in vitro*, perfused brain stem – cerebellum of adult guinea-pig. *Journal of Physiology (London)* 404: 215–240.
- Llinás, R. and Ribary, U. (1992) Rostrocaudal scan in human brain: a global characteristic for the 40-Hz response during sensory input. In E. Basar and T. Bullock, eds., *Induced Rhythms in the Brain*, pp. 147–154, Boston: Birkhäuser.
- Llinás, R. and Sugimori, M. (1980) Electrophysiological properties of *in vitro* Purkinje cell dendrites in mammalian cerebellar slices. *Journal of Physiology (London)* 305: 171–195.
- Llinás, R. and Yarom, Y. (1981) Electrophysiology of mammalian inferior olivary neurones *in vitro*. *Journal of Physiology (London)* 315: 549–567.
- Llinás, R. and Yarom, Y. (1986) Specific blockage of the low threshold calcium channel by high molecular weight alcohols. *Society for Neuroscience Abstracts* 12: 174.

- Llinás, R., Grace, A.A. and Yarom, Y. (1991) *in vitro* neurons in mammalian cortical layer 4 exhibit intrinsic oscillatory activity in the 10- to 50-Hz frequency range. *Proceedings of the National Academy of Sciences USA* 88: 897–901.
- Llinás, R., Paré, D., Deschênes, M., and Steriade, M. (1987) Differences between thalamo-cortical spindling and PGO generation demonstrated by low-threshold Ca blockage by octanol. *Society for Neuroscience Abstracts* 13: 1012.
- Llinás, R.R. (1988) The intrinsic electrophysiological properties of mammalian neurons: insights into central nervous system function. *Science* 242: 1654–1664.
- Llinás, R.R. and Ribary, U. (1993) Coherent 40-Hz oscillation characterizes dream state in humans. *Proceedings of the National Academy of Sciences of the USA* 90: 2078–2081.
- Lo Conte, G., Casamenti, F., Bigl, V., Milaneschi, E., and Pepeu, G. (1982) Effects of magnocellular forebrain nuclei lesions on acetylcholine output from the cerebral cortex electrocorticogram and behavior. *Archives Italiennes de Biologie* 120: 176–188.
- London, E.D., Ernst, M., Grant, S., Bonson, K., and Weinstein, A. (2000) Orbitofrontal cortex and human drug abuse: functional imaging. *Cerebral Cortex* 10: 334–342.
- Loomis, A.L., Harvey, N., and Hobart, G.A. (1938) Distribution of disturbance patterns in the human electroencephalogram, with special reference to sleep. *Journal of Neurophysiology* 1: 413–430.
- Lopes da Silva, F. (1987) Dynamics of EEGs as signals of neuronal populations: models and theoretical considerations. In E. Niedermeyer and F.H. Lopes da Silva, eds., *Electroencephalography*, pp. 15–28, Baltimore: Schwartzberg.
- Lopes da Silva, F.H. and Storm van Leeuwen, W. (1977) The cortical source of alpha rhythm. *Neuroscience Letters* 6: 237–241.
- Lopes da Silva, F.H., Van Lierop, T.H.M.T., Schrijer, C.F.M., and Storm Van Leeuwen, W. (1973) Organization of thalamic and cortical alpha rhythm: spectra and coherences. *Electroencephalography and Clinical Neurophysiology* 35: 627–639.
- Lopes da Silva, F.H., Vos, J.E., Mooibroek, J., and van Rotterdam, A. (1980) Partial coherence analysis of thalamic and cortical alpha rhythms in dog. A contribution towards a general model of the cortical organization of rhythmic activity. In G. Pfurtscheller, P. Buser, and F.H. Lopes da Silva, eds., *Rhythmic EEG Activities and Cortical Functioning*, pp. 33–59, Amsterdam: Elsevier/North Holland.
- Lopes da Silva, F.H., Van Rotterdam, A., Storm van Leeuwen, W., and Thielen, A.M. (1970) Dynamic characteristics of visual evoked potentials in the dog. II. Beta frequency selectivity in evoked potentials and background activity. *Electroencephalography and Clinical Neurophysiology* 29: 260–268.
- Lopes da Silva, F.H., Witter, M.P., Boeijinga, P.H., and Lohman, A.H.M. (1990) Anatomic organization and physiology of the limbic system. *Physiological Reviews* 70: 453–511.
- Losier, B.J. and Semba, K. (1993) Dual projections of single cholinergic and aminergic brainstem neurons to the thalamus and basal forebrain in the rat. *Brain Research* 604: 41–52.
- Lotka, A. (1956) *Elements of Physical Biology*. New York: Dover Press.
- Lu, J., Bjorkum, A.A., Xu, M., Gaus, S.E., Shiromani, P.J., and Saper, C.B. (2002) Selective activation of the extended ventrolateral preoptic nucleus during rapid eye movement sleep. *Journal of Neuroscience* 22: 4568–4576.
- Lu, J., Greco, M., Shiromani, P., and Saper, C.B. (2000) Effects of the lesions of the ventrolateral preoptic nucleus on NREM and REM sleep. *Journal of Neuroscience* 20: 3830–3842.
- Lu, S.T., Kajola, M., Joutsiniemi, S.L., Knuutila, J., and Hari, R. (1992) Generator sites of spontaneous MEG activity during sleep. *Electroencephalography and Clinical Neurophysiology* 82: 182–196.
- Lucki, I., Nobler M.S., and Frazer, A. (1984) Differential actions of serotonin antagonists on two behavioral models of serotonin receptor activation in the rat. *Journal of Pharmacology and Experimental Therapeutics* 228: 133–139.
- Lue, F.A., Bail, F.A., Jephthah-Ocholo, J., Carayanniotis, K., Gorczynski, R., and Moldofsky, H. (1998) Sleep and cerebrospinal fluid interleukin-1 like activity in the cat. *International Journal of Neuroscience* 42: 179–183.
- Luebke, J.L., Greene, R.W., Semba, K., Kamondi, A., McCarley, R.W., and Reiner, P.B. (1992) Serotonin hyperpolarizes cholinergic low-threshold burst neurons in the rat laterodorsal tegmental nucleus *in vitro*. *Proceedings of the National Academy of Sciences of the USA* 89: 743–747.
- Lugaresi, E. and Parmeggiani, P.L. eds. (1997) Somatic and autonomic regulation in sleep: physiological and clinical aspects. New York: Springer-Verlag.
- Luk, W.P., Zhang, Y., White, T.D., Lue, F.A., Wu, C., Jiang, C.G., Zhang, L., and Moldofsky, H. (1999) Adenosine: a mediator of interleukin-1 beta-induced hippocampal synaptic inhibition. *Journal of Neuroscience* 19: 4238–4244.
- Luschei, E.S. and Fuchs, A.F. (1972) Activity of brain stem neurons during eye movements of alert monkeys. *Journal of Neurophysiology* 35: 445–461.

- Lüthi, A. and McCormick, D.A. (1998) Periodicity of thalamic synchronized oscillations: the role of Ca^{2+} -mediated upregulation of I_h . *Neuron* 20: 553–563.
- Lux, H.D. and Neher, E. (1973) The equilibrium time course of $[\text{K}^+]_o$ in cat cortex. *Experimental Brain Research* 17: 190–205.
- Lydic, R. and Biebuyck, J.F. eds. (1988) Clinical physiology of sleep. Bethesda (MD): American Physiological Society.
- Lydic, R., Baghdoyan, H.A., and Lorinc, Z. (1991) Microdialysis of cat pons reveals enhanced acetylcholine release during state-dependent respiratory depression. *American Journal of Physiology* 261: R766–R770.
- Lydic, R., McCarley, R.W., and Hobson, J.A. (1983) The time-course of dorsal raphe discharge, PGO waves, and muscle tone averaged across multiple sleep cycles. *Brain Research* 274: 365–370.
- Lydic R., McCarley, R.W., and Hobson, J.A. (1987a) Serotonin neurons and sleep. I. Long term recordings of dorsal raphe discharge frequency and PGO waves. *Archives Italiennes de Biologie* 125: 317–343.
- Lydic R., McCarley, R.W., and Hobson, J.A. (1987b) Serotonin neurons and sleep. II. Time course of dorsal raphe discharge, PGO waves, and behavioral states. *Archives Italiennes de Biologie* 126: 1–28.
- Lykasowski, A., Wainer, B.H., Bruce, G., and Hersh, L.B. (1989) An atlas of the regional and laminar distribution of choline acetyltransferase immunoreactivity in rat cerebral cortex. *Neuroscience* 28: 291–336.
- Maas, J.W. (1975) Biogenic amines and depression: biochemical and pharmacological separation of two types of depression. *Archives of General Psychiatry* 32: 1357–1361.
- Macchi, G., Bentivoglio, M., Molinari, M., and Minciaccchi, D. (1984) The thalamo-caudate versus thalamo-cortical projections as studied in the cat with fluorescent retrograde double labeling. *Experimental Brain Research* 54: 225–239.
- Macchi, G., Rossi, G., Abbamondi, A.L., Giaccone, G., Mancina, D., Tagliavini, F., and Bugiani, O. (1997) Diffuse thalamic degeneration in fatal familial insomnia. A morphometric study. *Brain Research* 771: 154–158.
- MacDermott, A.B. and Weight, F.F. (1982) Action potential repolarisation may involve a transient, Ca^{2+} -sensitive outward current in a vertebrate neurone. *Nature* 300: 185–188.
- MacDermott, A.B., Mayer, M.L., Westbrook, G.L., Smith, S.J., and Barker, J.L. (1986) NMDA-receptor activation increases cytoplasmic calcium concentration in cultured spinal cord neurones. *Nature* 321: 519–522.
- MacDonald, J.F. and Wojtowicz, J.M. (1980) Two conductance mechanisms activated by applications of L-glutamate, L-aspartate, DL-homocysteate, N-methyl-D-aspartate, and DL-kainate acids to cultured mammalian central neurones. *Canadian Journal of Physiology and Pharmacology* 58: 1393–1397.
- Maciewicz, R.J., Eagen, K., Kaneko, C.R.S., and Highstein, S.M. (1977) Vestibular and medullary brain stem afferents to the abducens nucleus in the cat. *Brain Research* 123: 229–240.
- Mackiewicz, M., Nikonova, E.V., Zimmerman, J.E., Galante, R.J., Zhang, L., Cater, J.R., Geiger, J.D., and Pack, A.I. (2003) Enzymes of adenosine metabolism in the brain: diurnal rhythm and the effect of sleep deprivation. *Journal of Neurochemistry* 85: 348–357.
- Mackiewicz, M., Sollars, P.J., Ogilvie, M.D., and Pack, A.I. (1996) Modulation of IL-1 β gene expression in the rat CNS during sleep deprivation. *Neuroreport* 7: 529–533.
- MacLeod, N.K., James, T.A., and Starr, M.S. (1984) Muscarinic action of acetylcholine in the rat ventromedial thalamic nucleus. *Experimental Brain Research* 55: 553–561.
- MacVicar, B.A. and Dudek, F.E. (1981) Electrotonic coupling between pyramidal cells: a direct demonstration in rat hippocampal slices. *Science* 213: 782–785.
- MacVicar, B.A. and Dudek, F.E. (1982) Electrotonic coupling between granule cells of rat dentate gyrus. Physiological and anatomical evidence. *Journal of Neurophysiology* 47: 579–592.
- Madison, D.V. and Nicoll, R.A. (1984) Control of the repetitive discharge of rat CA1 pyramidal neurones *in vitro*. *Journal of Physiology (London)* 354: 319–331.
- Madison, D.V. and Nicoll, R.A. (1986a) Actions of noradrenaline recorded intracellularly in rat hippocampal CA1 pyramidal neurones, *in vitro*. *Journal of Physiology (London)* 372: 221–244.
- Madison, D.V. and Nicoll, R.A. (1986b) Cyclic adenosine 3',5'-monophosphate mediates beta-receptor actions of noradrenaline in rat hippocampal pyramidal cells. *Journal of Physiology (London)* 372: 245–259.
- Madison, D.V. and Nicoll, R.A. (1988) Norepinephrine decreases synaptic inhibition in the rat hippocampus. *Brain Research* 442: 131–138.
- Madison, D.V., Lancaster, B., and Nicoll, R.A. (1987) Voltage clamp analysis of cholinergic action in the hippocampus. *Journal of Neurosciences* 7: 733–741.
- Madsen, P.L., Schmidt, J.F., Wildschiodtz, G., Friberg, L., Holm, S., Vorstrup, S., and Lassen, N.A. (1991) Cerebral O_2 metabolism and cerebral blood flow in humans during deep and rapid-eye-movement sleep. *Journal of Applied Physiology* 70: 2597–2601.

- Maekawa, K. and Purpura, D.P. (1967a) Properties of spontaneous and evoked synaptic activities of thalamic ventrobasal neurons. *Journal of Neurophysiology* 30: 360–381.
- Maekawa, K. and Purpura, D.P. (1967b) Intracellular study of lemniscal and non-specific synaptic interactions in thalamic ventrobasal neurons. *Brain Research* 4: 308–323.
- Maffei, L., Moruzzi, G., and Rizzolatti, G. (1965a) Geniculate unit responses to sine-wave photic stimulation during wakefulness and sleep. *Science* 149: 563–564.
- Maffei, L., Moruzzi, G., and Rizzolatti, G. (1965b) Influence of sleep and wakefulness on the response of lateral geniculate units to sinewave photic stimulation. *Archives Italiennes de Biologie* 103: 596–608.
- Maffei, L., Moruzzi, G., and Rizzolatti, G. (1965c) Effects of synchronized sleep on the response of lateral geniculate units to flashes of light. *Archives Italiennes de Biologie* 103: 609–622.
- Magni, F. and Willis, W.D. (1963) Identification of reticular formation neurons by intracellular recording. *Archives Italiennes de Biologie* 102: 418–433.
- Magni, F., Moruzzi, G., Rossi, G.F., and Zanchetti, A. (1959) EEG arousal following inactivation of the lower brain stem by selective injection of barbiturate into the vertebral circulation. *Archives Italiennes de Biologie* 97: 33–46.
- Magoun, H.W. (1975) The role of research institutes in the advancement of neuroscience: Ranson's institute of neurology, 1928–1942. In F.G. Worden, J.P. Swazey and G. Adelman, eds., *The Neurosciences: Paths of Discovery*, pp. 515–527, Cambridge (MA) and London (England): The MIT Press.
- Magoun, H.W. and Rhines, R. (1946) An inhibitory mechanism in the bulbar reticular formation. *Journal of Neurophysiology* 9: 119–152.
- Mahowald, M.K. and Schenck, C.H. (1997) Sleep disorders. In J. Engel Jr. and T.A. Pedley, eds., *Epilepsy: A Comprehensive Textbook*, pp. 2705–2715, Philadelphia: Lippincott-Raven Press.
- Mahowald, M.W. and Schenck, C.H. (1989) REM sleep behavior disorder. In M.H. Kryger, T. Roth, and W.C. Dement, eds., *Principles and Practices of Sleep Medicine*, pp. 389–401, New York: Saunders.
- Malenka, R.C. and Nicoll, R.A. (1999) Long-term potentiation – a decade of progress? *Science* 285: 1870–1874.
- Malenka, R.C., Madison, D.V., Perkel, D.J., and Nicoll, R.A. (1986) Actions of norepinephrine and carbachol on granule cells of the dentate gyrus *in vitro*. *Society for Neuroscience Abstracts* 12: 729.
- Maloney, K.J., Mainville, L., and Jones, B.E. (1999) Differential c-Fos expression in cholinergic, monoaminergic, and GABAergic cell groups of the pontomesencephalic tegmentum after paradoxical sleep deprivation and recovery. *Journal of Neuroscience* 19: 3057–3072.
- Manaye, K.F., Zweig, R., Wu, D., Hersh, L.B., De Lacalle, S., Saper, C.B., and German, D.C. (1999) Quantification of cholinergic and select non-cholinergic mesopontine neuronal populations in the human brain. *Neuroscience* 89: 759–770.
- Mancia, M., Mariotti, M., and Spreafico, R. (1974) Caudo-rostral brainstem reciprocal influences in the cat. *Brain Research* 80: 41–51.
- Manetto, V., Medori, R., Cortelli, P., Montagna, P., Tinuper, P., Baruzzi, A., Rancurel, G., Hauw, J.J., Vanderhaeghen, J.J., Mailloux, P., Bugiani, O., Tagliavini, F., Bouras, C., Rizzuto, N., Lugaresi, E., and Gambetti, P. (1992) Fatal familial insomnia: clinical and pathological study of five new cases. *Neurology* 42: 312–319.
- Mann, J.J. (1999) Role of the serotonergic system in the pathogenesis of major depression and suicidal behavior of mood disorders. *Neuropsychopharmacology* 21: 99S–105S.
- Mann, J.J., Huang, Y., Underwood, M.D., Kassir, M.S., Oppenheim, S., Kelly, T.M., Dwork, A.J., and Arango, V. (2000) A serotonin transporter gene promoter polymorphism (5-HTTLPR) and prefrontal cortical binding in major depression and suicide. *Archives of General Psychiatry* 57: 729–738.
- Mannen, H. (1975) Morphological analysis of an individual neuron with Golgi's method. In M. Santini, ed., *Golgi Centennial Symposium*, pp. 61–70, New York: Raven Press.
- Manns, I.D., Alonso, A., and Jones, B.E. (2000a) Discharge profiles of juxtacellularly labeled and immunohistochemically identified cholinergic basal forebrain neurons recorded in association with the electroencephalogram in anesthetized rats. *Journal of Neuroscience* 20: 1505–1518.
- Manns, I.D., Alonso, A., and Jones, B.E. (2000b) Discharge profiles of juxtacellularly labeled and immunohistochemically identified GABAergic basal forebrain neurons recorded in association with the electroencephalogram in anesthetized rats. *Journal of Neuroscience* 20: 9252–9263.
- Maquet, P. (2000) Functional neuroanatomy of normal human sleep. In A.A. Borbély, O. Hayashi, T.J. Sejnowski, and J.S. Altman, eds., *The Regulation of Sleep*, pp. 86–94, Strasbourg: Human Frontier Science Program.
- Maquet, P. (2001) The role of sleep in learning and memory. *Science* 294: 1048–1052.
- Maquet, P., Degueldre, C., Delfiore, G., Aerts, J., Péters, J.P., Luxen, A., and Franck, G. (1997) Functional neuroanatomy of human slow wave sleep. *Journal of Neuroscience* 17: 2807–2812.
- Maquet, P., Dive, D., Salmon, E., Sadzot, B., Franco, G., Poirrier, R., and Franck, G. (1992) Cerebral glucose utilization during stage 2 sleep in man. *Brain Research* 571: 149–53.

- Marchetti, C., Carbone, E., and Lux, H.D. (1986) Effects of dopamine and noradrenaline on Ca channels of cultured sensory and sympathetic neurons of chick. *Pfluegers Archiv*, 406: 104–111.
- Marcus, E.M., Watson, C.W., and Simon, S.A. (1968a) An experimental model of some varieties of petit mal epilepsy. Electrical-behavioral correlations of acute bilateral epileptogenic foci in cerebral cortex. *Epilepsia* 9: 233–248.
- Marcus, E.M., Watson, C.W., and Simon, S.A. (1968b) Behavioral correlates of acute bilateral symmetrical epileptogenic foci in monkey cerebral cortex. *Brain Research* 9: 370–373.
- Mariotti, M., Soja, P.J., Morales, F.R., and Chase, M.H. (1986) The spontaneous IPSPs which bombard trigeminal motoneurons during active sleep appear to be generated at somatic and proximal dendritic loci. *Society for Neuroscience Abstracts* 12: 250.
- Markram, H., Wang, Y., and Tsodyks, M. (1998) Differential signaling via the same axon of neocortical pyramidal neurons. *Proceedings of the National Academy of Sciences of the USA* 95: 5323–5328.
- Marks, G.A. and Roffwarg, H.P. (1987) The role of acetylcholine in the control of state-related activity of thalamic relay cells. *Sleep Research* 16: 20.
- Marks, G.A., Kramer, G.L., and Birabil, C.G. (2003) GABAergic mechanisms in the REM sleep induction zone of the rat. *Sleep* 26 (Abstract Supplement): A8.
- Marshall, K.C. and McLennan, H. (1972) The synaptic activation of neurones of the feline ventrolateral thalamic nucleus: possible cholinergic mechanisms. *Experimental Brain Research* 15: 472–483.
- Marshall, K.C. and Murray, J.S. (1980) Cholinergic facilitation of thalamic relay transmission in the cat. *Experimental Neurology* 69: 318–333.
- Marshall, K.C., Flumerfelt, B.A., and Gwyn, D.G. (1980) Acetylcholinesterase activity and acetylcholine effects in the cerebello-rubro-thalamic pathway of the cat. *Brain Research* 190: 493–504.
- Marshall, L.H. and Magoun, H.W. (1998) *Discoveries in the Human Brain – Neuroscience Prehistory, Brain Structure, and Function*. Totowa (NJ): Humana Press.
- Martin, G.F. and Waltzer R.P. (1984a) A double-labelling study of reticular collaterals to the spinal cord and cerebellum of the North American opossum. *Neuroscience Letters* 47: 185–191.
- Martin, G.F. and Waltzer, R.P. (1984b) A study of overlap and collateralization of bulbar reticular and raphe neurons which project to the spinal cord and diencephalon of the North American opossum. *Brain and Behavior Evolution* 24: 109–123.
- Martin, G.F., Humbertson, A.O., Laxson, C.L., Panneton, W.M., and Tschismadia, I. (1979) Spinal projections from the mesencephalic and pontine reticular formations in the North American opossum: a study using axonal transport techniques. *Journal of Comparative Neurology* 187: 373–400.
- Martin, L.J., Koliatsos, V.E., Nauta, H.J.W., DeLong, M.R., and Price, D.L. (1987) Substantia innominata and pedunculo-pontine tegmental nucleus in the rat: evidence for predominantly noncholinergic reciprocal innervation. *Society for Neuroscience Abstracts* 13: 1567.
- Mash, D.C. and Potter, L.T. (1986) Autogradiographic localization of M1 and M2 muscarine receptors in the rat brain. *Neuroscience* 19: 551–564.
- Mason, A. and Larkman, A. (1990) Correlations between morphology and electrophysiology of pyramidal neurons in slices of rat visual cortex. II. Electrophysiology. *Journal of Neuroscience* 10: 1415–1428.
- Massaquoi, S.G. and McCarley, R.W. (1982) Extension of the reciprocal interaction sleep stage control model: a “Karma” control model. *Sleep Research* 11: 216.
- Massaquoi, S.G. and McCarley, R.W. (1992) Extension of the limit cycle reciprocal interaction model of REM cycle control. An integrated sleep control model. *Journal of Sleep Research* 1: 138–143.
- Massimini M. and Amzica F. (2001) Extracellular calcium fluctuations and intracellular potentials in the cortex during the slow sleep oscillation. *Journal of Neurophysiology* 85: 1346–1350.
- Mathiesen, J.S. and Blackstad, T.W. (1964) Cholinesterase in the hippocampal region. Distribution and relation to architectonics and afferent systems. *Acta Anatomica* 56: 216–253.
- Matsubara, J.A., Chase, R., and Thejomayen, M. (1996) Comparative morphology of three types of projection-identified pyramidal neurons in the superficial layers of cat visual cortex. *Journal of Comparative Neurology* 366: 93–108.
- Matsumura, H., Nakajima, T., Osaka, T., Satoh, S., Kawase, K., Kubo, E., Kantha, S.S.S., Kasahara, K., and Hayaishi, O. (1994) Prostaglandin D₂-sensitive, sleep promoting zone defined in the ventral surface of the rostral basal forebrain. *Proceedings of the National Academy of Sciences of the USA* 91: 11998–12002.
- Matsumura, M., Chen, D.F., Sawaguchi, T., Kubota, K., and Fetz, E.E. (1996) Synaptic interactions between primate precentral cortex neurons revealed by spike-triggered averaging of intracellular membrane potentials *in vivo*. *Journal of Neuroscience* 16: 7757–7767.
- Mauguière, F. and Courjon, J. (1983) The origins of short-latency somatosensory evoked potentials in humans. *Annals of Neurology* 9: 607–611.
- Maunz, R.A., Pitts, N.G., and Peterson, B.W. (1978) Cat spinoreticular neurons: locations, responses and changes in responses during repetitive stimulation. *Brain Research* 148: 365–379.

- May, P.J. and Hall, W.C. (1986) The sources of the nigroreticular pathway. *Neuroscience* 19: 159–180.
- Mayer, M.L. and Westbrook, G.L. (1983) A voltage-clamp analysis of inward (anomalous) rectification in mouse spinal sensory ganglion neurons. *Journal of Physiology (London)* 340: 19–45.
- Mayer, M.L. and Westbrook, G.L. (1987) The physiology of excitatory amino acids in the vertebrate central nervous system. *Progress in Neurobiology* 28: 197–276.
- Mayer, M.L., Westbrook, G.L., and Guthrie, P.B. (1984) Voltage-dependent block by Mg^{2+} of NMDA responses in spinal cord neurones. *Nature* 309: 261–263.
- Mays, L.E. and Sparks, D.L. (1980) Dissociation of visual and saccade-related responses in superior colliculus neurons. *Journal of Neurophysiology* 43: 207–233.
- McCance, I., Phillis, J.W., and Westerman, R.A. (1968a) Acetylcholine-sensitivity of thalamic neurones: its relationship to synaptic transmission. *British Journal of Pharmacology and Chemotherapy* 32: 635–651.
- McCance, I., Phillis, J.W., Tebecis, A.K., and Westerman, R.A. (1968b) The pharmacology of acetylcholine-excitation of thalamic neurones. *British Journal of Pharmacology and Chemotherapy* 32: 652–662.
- McCarley, R.W. (1973) A model for the periodicity of brain stem neuronal discharges during the sleep cycle. *Sleep Research* 2: 30.
- McCarley R.W. (1978) Control of sleep–waking state alteration in *Felix Domesticus*. In J.A. Ferrendelli, ed., *Neuroscience Symposia, Vol III. Society for Neuroscience*, Bethesda, Maryland 90.
- McCarley, R.W. (1980a) Reciprocal discharge of reticular and non-reticular brainstem neurons and a model for state-dependent changes in neuronal activity. In J.A. Hobson and A.B. Schiebel, eds., *The Brainstem Core: Sensorimotor Integration and Behavioral State Control, Neurosciences Research Program Bulletin* 18: 101–112.
- McCarley, R.W. (1980b) Mechanisms and models of behavioral state control. In J.A. Hobson and M.A.B. Brazier, eds., *The Reticular Formation Revisited*, pp. 375–403, New York: Raven Press.
- McCarley, R.W. (1981) Mind–body isomorphisms and the study of dreams. In W. Fishbein, ed., *Advances in Sleep Research*, vol. IV, New York: Spectrum.
- McCarley, R.W. (1982) REM sleep and depression: common neurobiological control mechanisms. *American Journal of Psychiatry* 139: 565–570.
- McCarley, R.W. (1983) REM dreams, REM sleep, and their isomorphisms. In M. Chase and E.D. Weitzman, eds., *Sleep Disorders: Basic and Clinical Research*, pp. 363–392, New York: Spectrum.
- McCarley, R.W. (1988) Foreword. In R. Lydic and J.F. Biebuyck, eds., *Clinical Physiology of Sleep*, pp. 5–9, Bethesda (MD): American Physiological Society.
- McCarley, R.W. (1989) The biology of dreaming sleep. In M.H. Kryger, T. Roth, and W.C. Dement, eds. *Principles and Practices of Sleep Medicine*, pp. 173–183, New York: Saunders.
- McCarley, R.W. (2002) Human electrophysiology: cellular mechanisms and control of wakefulness and sleep. In S. Yudofsky and R.E. Hales, eds., *Handbook of Neuropsychiatry*, Fourth Edition, pp. 43–70, New York (NY): American Psychiatric Press.
- McCarley, R.W. (2004) Mechanisms and models of REM sleep control. *Archives italienne de Biologie* 142: 429–468.
- McCarley, R.W. and Hobson, J.A. (1970) Cortical unit activity in desynchronized sleep. *Science* 167: 901–903.
- McCarley, R.W. and Hobson, J.A. (1971) Single neuron activity in cat gigantocellular tegmental field: selectivity of discharge in desynchronized sleep. *Science* 174: 1250–1252.
- McCarley, R.W. and Hobson, J.A. (1975a) Discharge patterns of cat pontine brain stem neurons during desynchronized sleep. *Journal of Neurophysiology* 38: 751–766.
- McCarley, R.W. and Hobson, J.A. (1975b) Neuronal excitability modulation over the sleep cycle: a structural and mathematical model. *Science* 189: 58–60.
- McCarley, R.W. and Hobson, J.A. (1977) The neurobiological origins of psychoanalytic dream theory. *American Journal of Psychiatry* 134: 1211–1221.
- McCarley, R.W. and Hobson, J.A. (1979) The form of dreams and the biology of sleep. In B. Wolman, ed., *Handbook of Dreams: Research, Theory, and Applications*, pp. 76–130, New York: Van Nostrand Reinhold Co.
- McCarley, R.W. and Hoffman, E.A. (1981) REM sleep dreams and the activation-synthesis hypothesis. *American Journal of Psychiatry* 138: 904–912.
- McCarley, R.W. and Ito, K. (1983) Intracellular evidence linking medial pontine reticular formation neurons to PGO generation. *Brain Research* 280: 343–348.
- McCarley, R.W. and Ito, K. (1985) Desynchronized sleep-specific changes in membrane potential and excitability in medial pontine reticular formation neurons: implications for concepts and mechanisms of behavioral state control. In D. McGinty, R. Drucker-Colin, A. Morrison, and P.L. Parmeggiani, eds., *Brain Mechanisms of Sleep*, pp. 63–80, New York: Raven Press.
- McCarley, R.W. and Massaquoi, S.G. (1986a) A limit cycle mathematical model of the REM sleep oscillator system. *American Journal of Physiology* 251: R1011–R1029.

- McCarley, R.W. and Massaquoi, S.G. (1986b) Further discussion of a model of the REM sleep oscillator. *American Journal of Physiology* 251: R1033–R1036.
- McCarley, R.W. and Massaquoi, S.G. (1992) The limit cycle reciprocal interaction model of REM cycle control: new neurobiological structure. *Journal of Sleep Research* 1: 132–137.
- McCarley, R.W., Benoit, O., and Barrionuevo, G. (1983) Lateral geniculate nucleus unitary discharge in sleep and waking: state and rate specific aspects. *Journal of Neurophysiology* 50: 798–818.
- McCarley, R.W., Ito, K., and Rodrigo-Angulo, M.L. (1987) Physiological studies of brainstem reticular connectivity. II. Responses of mPRF neurons to stimulation of mesencephalic and contralateral pontine reticular formation. *Brain Research* 409: 111–127.
- McCarley, R.W., Greene, R.W., Rainnie, D., and Portas, C.M. (1995) Brain Stem Neuromodulation and REM Sleep. *Seminars in Neurosciences* 7: 341–354.
- McCarley, R.W., Nelson, J.P., and Hobson, J.A. (1978) Ponto-geniculo-occipital (PGO) burst neurons: correlative evidence for neuronal generators of PGO waves. *Science* 201: 269–272.
- McCormick, D.A. (1990) Cellular mechanisms of cholinergic control of neocortical and thalamic neuronal excitability. In M. Steriade and D. Biesold, eds., *Brain Cholinergic Systems*, pp. 236–264, Oxford: Oxford University Press.
- McCormick, D.A. (1991a) Functional properties of a slowly inactivating potassium current I_{As} in guinea pig dorsal lateral geniculate relay neurons. *Journal of Neurophysiology* 66: 1176–1189.
- McCormick, D.A. (1991b) Cellular mechanisms underlying cholinergic and noradrenergic modulation of neuronal firing mode in the cat and guinea pig dorsal lateral geniculate nucleus. *Journal of Neuroscience* 12: 278–289.
- McCormick, D.A. (1992) Neurotransmitter actions in the thalamus and cerebral cortex and their role in neuromodulation of thalamocortical activity. *Progress in Neurobiology* 39: 337–388.
- McCormick, D.A. and Feuser, H.R. (1990) Functional implications of burst firing and single spike activity in lateral geniculate relay neurons. *Neuroscience* 39: 103–113.
- McCormick, D.A. and Pape, H.C. (1988) Acetylcholine inhibits identified interneurons in the cat lateral geniculate nucleus. *Nature* 334: 246–248.
- McCormick, D.A. and Pape, H.C. (1990a) Properties of a hyperpolarization-activated cation current and its role in rhythmic oscillation in thalamic relay neurones. *Journal of Physiology (London)* 431: 291–318.
- McCormick, D.A. and Pape, H.C. (1990b) Noradrenergic and serotonergic modulation of a hyperpolarization-activated cation current in thalamic relay cells. *Journal of Physiology (London)* 431: 319–342.
- McCormick, D.A. and Prince, D.A. (1985) Two types of muscarinic response to acetylcholine in mammalian cortical neurons. *Proceedings of the National Academy of Sciences of the USA* 82: 6344–6348.
- McCormick, D.A. and Prince, D.A. (1986a) Mechanisms of action of acetylcholine in the guinea pig cerebral cortex, *in vitro*. *Journal of Physiology (London)* 375: 169–194.
- McCormick, D.A. and Prince, D.A. (1986b) ACh induces burst firing in thalamic reticular neurones by activating a K^+ conductance. *Nature* 319: 402–405.
- McCormick, D.A. and Prince, D.A. (1987a) Actions of acetylcholine in the guinea-pig and cat medial and lateral geniculate nuclei, *in vitro*. *Journal of Physiology (London)* 392: 147–165.
- McCormick, D.A. and Prince, D.A. (1987b) Acetylcholine causes rapid nicotinic excitation in the medial habenular nucleus of guinea pig, *in vitro*. *Journal of Neuroscience* 7: 742–752.
- McCormick, D.A. and Prince, D.A. (1987c) Neurotransmitter modulation of thalamic neuronal firing pattern. *Journal of Mind and Behavior* 8: 573–590.
- McCormick, D.A. and Prince, D.A. (1987d) Actions of acetylcholine in the guinea-pig and cat medial and lateral geniculate nuclei, *in vitro*. *Journal of Physiology (London)* 392: 147–165.
- McCormick, D.A. and Prince, D.A. (1988) Noradrenergic modulation of firing pattern in guinea-pig and cat thalamic neurons *in vitro*. *Journal of Neurophysiology* 59: 978–996.
- McCormick, D.A. and Wang, Z. (1991) Serotonin and noradrenaline excite GABAergic neurones of the guinea-pig and cat nucleus reticularis thalami. *Journal of Physiology (London)* 442: 235–255.
- McCormick, D.A., Connors, B.W., Lighthall, J.W., and Prince, D.A. (1985) Comparative electrophysiology of pyramidal and sparsely spiny stellate neurons of the neocortex. *Journal of Neurophysiology* 54: 782–806.
- McCormick, D.A., Huguenard, J.R., and Pape, H.C. (1997) Electrophysiological and pharmacological properties of thalamic GABAergic neurons. In M. Steriade, E.G. Jones, and D.A. McCormick, eds., *Thalamus* (vol. 2, *Experimental and Clinical Aspects*), pp. 155–212, Oxford: Elsevier.
- McDonald, A.J. and Augustine, J.R. (1993) Localization of GABA-like immunoreactivity in the monkey amygdala. *Neuroscience* 52: 281–294.
- McGaughy, J. and Sarter, M. (1998) Sustained attention performance in rats with intracortical infusions of 192 IgG-saporin-induced cortical cholinergic deafferentation: effects of physostigmine and FG 7142. *Behavioral Neuroscience* 112: 1519–1525.

- McGinty, D., Drucker-Colin, R., Morrison, A., and Parmeggiani, P.L. (eds.) (1985) *Brain Mechanisms of Sleep*. New York: Raven Press.
- McKinsey, D.J. and Harper, R.M. (1976) Dorsal raphe neurons: depression of firing during sleep in cats. *Brain Research* 101: 569–575.
- McGinty, D.J. and Serman, M.B. (1968) Sleep suppression after basal forebrain lesions in the cat. *Science* 160: 1253–1255.
- McHaffie, J.G. and Stein, B.E. (1982) Eye movements evoked by electrical stimulation in the superior colliculus of rats and hamsters. *Brain Research* 247: 243–253.
- McKinsey, T.A., Chu, Z.I., and Ballard, D.W. (1997) Phosphorylation of the PEST domain of I- κ B β regulates the function of NF- κ B/I- κ B β complexes. *Journal of Biological Chemistry* 272: 22377–22380.
- McLennan, H. (1983) Receptors for the excitatory amino acids in the mammalian central nervous system. *Progress in Neurobiology* 20: 251–271.
- McLennan, H. and Hicks, T.P. (1978) Pharmacological characterization of the excitatory cholinergic receptors of rat central neurons. *Neuropharmacology* 17: 329–334.
- McPartland, R.J., Kupfer, D.J., Coble, P., Shaw, D.H., and Spiker, D.G. (1979) An automated analysis of REM sleep in primary depression. *Biological Psychiatry* 14: 767–776.
- Meeren, H.K.M., Pijn, J.P.M., Van Luijcklaar, J.M., Coenen, A.M.L., and Lopes da Silva, F.H. (2002) Cortical focus drives widespread corticothalamic networks during spontaneous absence seizures in rats. *Journal of Neuroscience* 22: 1480–1495.
- Melker, R.J. and Purpura, D.P. (1972) Maturational features of neurons and synaptic relations in raphe and reticular nuclei of neonatal kittens. *Anatomical Record* 172: 366–367.
- Mendelson, W.B., Martin, J.V., Wagner, R., Milton, J.G., James, S.P., Sack, D.A., Rosenthal, N.E., and Wehr, T.A. (1986) Do depressed patients have decreased delta power in the sleep EEG? *Sleep Research* 15: 146.
- Menetrey, D., Chaouch, A., and Besson, J.M. (1980) Location and properties of dorsal horn neurons at origin of spinoreticular tract in lumbar enlargement of the rat. *Journal of Neurophysiology* 44: 862–877.
- Menkes, D.B. and Aghajanian, G.K. (1980) Chronic antidepressant treatment enhances alpha-adrenergic responses in brain: a microiontophoretic study. *Society for Neuroscience Abstracts* 6: 860.
- Merrill, J.E. (1992) Tumor necrosis factor alpha, interleukin 1 and related cytokines in brain development: normal and pathological. *Developmental Neuroscience* 14: 1–10.
- Mesulam, M.M. (1978) Tetramethyl benzidine for horseradish peroxidase neurohistochemistry: a non-carcinogenic blue reaction-product with superior sensitivity for visualizing neural afferents and efferents. *Journal of Histochemistry and Cytochemistry* 26: 106–117.
- Mesulam, M.M. (1982) Principles of horseradish peroxidase neurohistochemistry and their applications for tracing neural pathways – Axonal transport, enzyme histochemistry and light microscopic analysis. In M.M. Mesulam, ed., *Tracing Neural Connections with Horseradish Peroxidase*, pp. 1–151, New York: Wiley.
- Mesulam, M.M. and Geula, C. (1988) Nucleus basalis (Ch4) and cortical cholinergic innervation in the human brain: observations based on the distribution of acetylcholinesterase and choline acetyltransferase. *Journal of Comparative Neurology* 275: 216–240.
- Mesulam, M.M. and Mufson, E.J. (1980) The rapid anterograde transport of horseradish peroxidase. *Neuroscience* 5: 1277–1286.
- Mesulam, M.M. and Rosene, D.L. (1979) Sensitivity in horseradish peroxidase neurohistochemistry: a comparative and quantitative analysis of nine methods. *Journal of Histochemistry and Cytochemistry* 27: 763–773.
- Mesulam, M.M., Hershey, L.B., Mash, D.C., and Geula, C. (1992) Differential cholinergic innervation within functional subdivisions of the human cerebral cortex: a choline acetyltransferase study. *Journal of Comparative Neurology* 318: 316–328.
- Mesulam, M.M., Mufson, E.J., Levey, A.I., and Wainer, B.H. (1983b) Cholinergic innervation of cortex by the basal forebrain: cytochemistry and cortical connections of the septal area, diagonal band nuclei, nucleus basalis (substantia innominata), and hypothalamus in the rhesus monkey. *Journal of Comparative Neurology* 214: 170–197.
- Mesulam, M.M., Mufson, E.J., Levey, A.I., and Wainer, B.H. (1984) Atlas of cholinergic neurons in the forebrain and upper brainstem of the macaque based on monoclonal choline acetyltransferase immunohistochemistry and acetylcholinesterase histochemistry. *Neuroscience* 12: 669–686.
- Mesulam, M.M., Mufson, E.J., Wainer, B.H., and Levey, A.I. (1983a) Central cholinergic pathways in the rat: an overview based on an alternative nomenclature (Ch1–Ch6). *Neuroscience* 10: 1185–1201.
- Metherate, R., Tremblay, N., and Dykes, R.W. (1987) Acetylcholine permits long-term enhancement of neuronal responsiveness in cat primary somatosensory cortex. *Neuroscience* 22: 75–81.
- Metherate, R., Tremblay, N., and Dykes, R.W. (1988a) Transient and prolonged effects of acetylcholine on responsiveness of cat somatosensory cortical neurons. *Journal of Neurophysiology* 59: 1231–1252.

- Metherate, R., Tremblay, N., and Dykes, R.W. (1988b) The effects of acetylcholine on response properties of cat somatosensory cortical neurons. *Journal of Neurophysiology* 59: 1253–1276.
- Metherate, R., Cox, C.L., and Ashe, J.H. (1992) Cellular bases of neocortical activation: modulation of neural oscillations by the nucleus basalis and endogenous acetylcholine. *Journal of Neuroscience* 12: 4701–4711.
- Meulders, M. and Godfraind, J.M. (1969) Influence de l'éveil d'origine réticulaire sur l'étendue des champs visuels des neurones de la région genouillée chez le chat avec cerveau intact ou avec cerveau isolé. *Experimental Brain Research* 9: 201–220.
- Meynert, T. (1872) Vom Gehirn der Säugetiere. In S. Stricker, ed., *Handbuch der Lehre von den Geweben des Menschen und Tiere*, vol. 2, pp. 694–808, Leipzig: Engelmann.
- Mieda, M., Willie, J.T., Sinton, C.M., Sakurai, T., and Yanagisawa, M. (2003) Pharmacological rescue of narcoleptic orexin-neuron ablated mice. *Sleep* 26: A288.
- Mignot, E. (1998) Genetic and familial aspects of narcolepsy. *Neurology* 50: S16–S22.
- Mignot, E., Guilleminault, C., Bowersox, S., Rapport, A., and Dement, W.C. (1988) Role of central alpha-1 adrenoceptors in canine narcolepsy. *Journal of Clinical Investigations* 82: 885–894.
- Miles, R., Traub, R.D., and Wong, R.K.S. (1988) Spread of synchronous firing in longitudinal slices from the CA3 region of the hippocampus. *Journal of Neurophysiology* 60: 1281–1296.
- Miller, T.B., Goodrich, C.A., and Pappenheimer, J.R. (1967) Sleep-promoting effects of cerebrospinal fluid from sleep-deprived goats. *Proceedings of the National Academy of Sciences of the USA* 58: 513–517.
- Milleret, C., Houzel, J.C., and Buser, P. (1994) Pattern of development of the callosal transfer of visual information to cortical areas 17 and 18 in the cat. *European Journal of Neuroscience* 6: 193–202.
- Milner, T.A. and Pickel, V.M. (1986) Ultrastructural localization and afferent sources of substance P in the rat parabrachial region. *Neuroscience* 17: 687–707.
- Minciacchi, D., Bentivoglio, M., Molinari, M., Kultas-Ilinski, K., Ilinski, I.A., and Macchi, G. (1986) Multiple cortical targets of one thalamic nucleus: the projections of the ventral medial nucleus in the cat studied with retrograde tracers. *Journal of Comparative Neurology* 252: 106–129.
- Mitani, A., Ito, K., Mitani, Y., and McCarley, R.W. (1988a) Descending projections from the gigantocellular tegmental field in the cat: origins of the descending pathways and their funicular trajectories. *Journal of Comparative Neurology* 268: 546–566.
- Mitani, A., Ito, K., Mitani, Y., and McCarley, R.W. (1988b) Morphological and electrophysiological identification of gigantocellular tegmental field neurons. I. Pons. *Journal of Comparative Neurology* 268: 527–545.
- Mitani, A., Ito, K., Mitani, Y., and McCarley, R.W. (1988c) Morphological and electrophysiological identification of gigantocellular tegmental field neurons with descending projections in the cat. II. Bulb. *Journal of Comparative Neurology*.
- Mitani, A., Ito, K., Hallanger, A.H., Wainer, B.H., Kataoka, K., and McCarley, R.W. (1988d) Cholinergic projections from the laterodorsal and pedunculopontine tegmental nuclei to the pontine gigantocellular tegmental field in the cat. *Brain Research* 451: 397–402.
- Mitchell, S.J. and Ranck, J.B.J. (1980) Generation of theta rhythm in medial entorhinal cortex of freely moving rats. *Brain Research* 189: 49–66.
- Mitler, M.M. and Dement, W.C. (1974) Cataplectic-like behavior in cats after micro-injections of carbachol in pontine reticular formation. *Brain Research* 68: 335–343.
- Mize, R.R. and Payne, M.P. (1987) The innervation density of serotonergic (5-HT) fibers varies in different subdivisions of the rat lateral geniculate nucleus complex. *Neuroscience Letters* 82: 133–139.
- Mizoguchi, A., Eguchi, N., Kimura, K., Kiyohara, Y., Qu, W.M., Huang, Z.L., Mochizuki, T., Lazarus, M., Kobayashi, T., Kaneko, T., Narumiya, S., Urade, Y., and Hayaishi, O. (2001) Dominant localization of prostaglandin D receptors on arachnoid trabecular cells in mouse basal forebrain and their involvement in the regulation of non-rapid eye movement sleep. *Proceedings of the National Academy of Sciences of the USA* 98: 11674–11679.
- Mizuno, N., Clemente, C.D., and Sauerland, E.K. (1969) Fiber projections from rostral basal forebrain structures in the cat. *Experimental Neurology* 25: 22–237.
- Mochizuki, T., Satoh, T., Gerashchenko, D., Urade, Y., and Hayaishi, O. (2000) Characterization of prostaglandin D2-induced adenosine increase in the subarachnoid space of rats. *Society for Neuroscience Abstracts* 26: 511–566.
- Mogilnicka, E., Arbilla, S., and Depoortere, H. (1980) Rapid-eye-movement sleep deprivation decreases the density of 3H-dihydroalprenolol and 3H-imipramine binding sites in the rat cerebral cortex. *European Journal of Pharmacology* 65: 289–299.
- Molinari, M., Hendry, S.H.C., and Jones, E.G. (1987) Distributions of certain neuropeptides in the primate thalamus. *Brain Research* 426: 270–289.
- Monckton, J.E. and McCormick, D.A. (2002) Neuromodulatory role of serotonin in the ferret thalamus. *Journal of Neurophysiology* 87: 2124–2136.

- Mongeau, R., Blier, P., and de Montigny, C. (1997) The serotonergic and noradrenergic systems of the hippocampus: their interactions and the effects of antidepressant treatments. *Brain Research Reviews* 23: 145–195.
- Montaron, M.F., Bouyer, J.J., Rougeul, A., and Buser, P. (1982) Ventral mesencephalic tegmentum (VMT) controls electrocortical beta rhythms and associated attentive behavior in the cat. *Behavioral and Brain Research* 6: 129–145.
- Moon-Edley, S. and Graybiel, A.M. (1983) The afferent and efferent connections of the feline nucleus tegmenti pedunculopontinus, pars compacta. *Journal of Comparative Neurology* 217: 187–215.
- Moore, R.Y. and Bloom, F.E. (1978) Central catecholamine systems: anatomy and physiology of the dopamine system. *Annual Review of Neuroscience* 1: 29–69.
- Moore, S.D., Madamba, S.G., Joels, M., and Siggins, G.R. (1988) Somatostatin augments the M-current in hippocampal neurons. *Science* 239: 278–280.
- Morairty, S., Rainnie, D., McCarley, R.W., and Greene, R.W. (2004) Disinhibition of ventrolateral preoptic area sleep-active neurons by adenosine: a new mechanism for sleep promotion. *Neuroscience* 123: 451–457.
- Morales, F.R. and Chase, M.H. (1978) Intracellular recording of lumbar motoneuron membrane potential during sleep and wakefulness. *Experimental Neurology* 62: 821–827.
- Morales, F.R. and Chase, M.H. (1981) Postsynaptic control of lumbar motoneuron excitability during active sleep in the chronic cat. *Brain Research* 225: 279–295.
- Morales, F.R., Boxer, P., and Chase, M.H. (1988) Behavioral state-specific inhibitory postsynaptic potentials impinge on cat lumbar motoneurons during active sleep. *Experimental Neurology* 98: 418–435.
- Morales, F.R., Engelhardt, J.K., Soja, P.J., Pereda, A.E., and Chase, M.H. (1987) Motoneuron properties during motor inhibition produced by microinjection of carbachol into the pontine reticular formation of the decerebrate cat. *Journal of Neurophysiology* 57: 1118–1129.
- Moreno, F.A., Rowe, D.C., Kaiser, B., Chase, D., Michaels, T., Gelernter, J., and Delgado, P.L. (2002) Association between a serotonin transporter promoter region polymorphism and mood response during tryptophan depletion. *Molecular Psychiatry* 7: 213–216.
- Mori, S. (1987) Integration of posture and locomotion in acute decerebrate cats and in awake, freely moving cats. *Progress in Neurobiology* 28: 161–196.
- Morin, D. and Steriade, M. (1981) Development from primary to augmenting responses in primary somatosensory cortex. *Brain Research* 205: 49–66.
- Morison, R.S. and Bassett, D.L. (1945) Electrical activity of the thalamus and basal ganglia in decorticated cats. *Journal of Neurophysiology* 8: 309–314.
- Morison, R.S. and Dempsey, E.W. (1942) A study of thalamo-cortical relations. *American Journal of Physiology* 135: 281–292.
- Morrell, J.L., Greensberger, L.M., and Pfaff, D.W. (1981) Hypothalamic, other diencephalic and telencephalic neurons that project to the dorsal midbrain. *Journal of Comparative Neurology* 201: 589–620.
- Morrison, A.R. (1979) Brain-stem regulation of behavior during sleep and wakefulness. In J.M. Sprague and A.N. Epstein, eds., *Progress in Psychobiology and Physiological Psychology*, vol. 8, pp. 91–131, New York: Academic Press.
- Morrison, J.H., and Foote, S.L. (1986) Noradrenergic and serotonergic innervation of cortical, thalamic, and tectal visual structures in Old and New World monkeys. *Journal of Comparative Neurology*, 243: 117–138.
- Morrisson, J.H., Foote, S.L., O'Connor, D., and Bloom, F.E. (1982) Laminar, tangential and regional organization of the noradrenergic innervation of monkey cortex: dopamine-b-hydroxylase immunohistochemistry. *Brain Research Bulletin* 9: 309–319.
- Morrison, J.H., Molliver, M.E., Grzanna, M.E., and Coyle, J.T. (1981) The intracortical trajectory of the coeruleo-cortical projection in the rat: a tangentially organized cortical afferent. *Neuroscience* 6: 139–158.
- Moruzzi, G. (1963) Active processes in the brain stem during sleep. *Harvey Lectures Series* 58: 233–297.
- Moruzzi, G. (1964) The historical development of the deafferentation hypothesis of sleep. *Proceedings of the American Philosophy Society* 108: 19–28.
- Moruzzi, G. (1969) Sleep and instinctive behavior. *Archives Italiennes de Biologie* 107: 175–216.
- Moruzzi, G. (1972) The sleep–waking cycle. *Ergebnisse der Physiologie* 64: 1–165.
- Moruzzi, G. and Magoun, H.W. (1949) Brain stem reticular formation and activation of the EEG. *Electroencephalography and Clinical Neurophysiology* 1: 455–473.
- Moschovakis, A.K., Karabelas, A.B., and Highstein, S.M. (1988a) Structure-function relationships in the primate superior colliculus. I. Morphological classification of efferent neurons. *Journal of Neurophysiology* 60: 232–262.
- Moschovakis, A.K., Karabelas, A.B., and Highstein, S.M. (1988b) Structure-function relationships in the primate superior colliculus. II. Morphological identity of presaccadic neurons. *Journal of Neurophysiology* 60: 232–262.

- Mosko, S.B. and Jacobs, B.L. (1976) Recording of dorsal raphe unit activity *in vitro*. *Neuroscience Letters* 2: 195–200.
- Mosko, S., Haubrich, D., and Jacobs, B.L. (1977) Serotonergic afferents to the dorsal raphe nucleus: evidence from HRP and synaptosomal uptake studies. *Brain Research* 119: 269–290.
- Mosko, S., Lynch, G., and Cotman, C.W. (1973) The distribution of septal projections to the hippocampus of the rat. *Journal of Comparative Neurology* 152: 163–174.
- Mountcastle, V.B. (1998) *Perceptual Neuroscience—The Cerebral Cortex*. Cambridge, MA: Harvard University Press.
- Mountcastle, V.B., Andersen, R.A., and Motter, B.C. (1981) The influence of attentive fixation upon the excitability of the light-sensitive neurons of the posterior parietal cortex. *Journal of Neuroscience* 1: 1218–1235.
- Mountcastle, V.B., Lynch, J.C., Georgopoulos, A., Sakata, H., and Acuna, C. (1975) Posterior parietal association cortex of the monkey: command functions for operations within extrapersonal space. *Journal of Neurophysiology* 38: 871–908.
- Mountcastle, V.B., Motter, B.C., Steinmetz, M.A., and Duffy, C.J. (1984) Looking and seeing: the visual functions of the parietal lobe. In G.M. Edelman, W.E. Gall, and W.M. Cowan, eds., *Dynamic Aspects of Neocortical Function*, pp. 159–193, New York: Wiley-Interscience.
- Mrzljak, L. and Goldman-Rakic, P.S. (1993) Low-affinity nerve growth factor receptor (p^{75NGFR})- and choline acetyltransferase (ChAT)-immunoreactive axons in the cerebral cortex and hippocampus of adult macaque monkeys and humans. *Cerebral Cortex* 3: 133–147.
- Mrzljak, L., Pappy, M., Leranth, C., and Goldman-Rakic, P. (1995) Cholinergic synaptic circuitry in the macaque prefrontal cortex. *Journal of Comparative Neurology* 357: 603–617.
- Mufson E.J., Martin, T.L., Mash, D.C., Wainer, B.H., and Mesulam, M.M. (1986) Cholinergic projections from the parabrachial nucleus (Ch8) to the superior colliculus in the mouse: a combined analysis of horseradish peroxidase transport and choline acetyltransferase immunohistochemistry. *Brain Research* 370: 144–148.
- Mühlethaler, M., Khateb, A., and Serafin, M. (1990) Effects of monoamines and opiates on pedunculo-pontine neurones. In Mancina, M., Marini, G., eds., *The Diencephalon and Sleep* pp. 367–378, New York: Raven Press.
- Muir, J.L., Everitt, B.J., and Robbins, T.W. (1996) The cerebral cortex of the rat and visual attentional function: dissociable effects of mediofrontal, cingulate, anterior dorsolateral, and parietal cortex lesions on a five-choice serial reaction time task. *Cerebral Cortex* 6: 470–481.
- Mulholland, T. (1969) The concept of attention and the electroencephalographic alpha rhythm. In C.R. Evans and T.B. Mulholland, eds., *Attention in Neurophysiology*, pp. 100–127, London: Butterworth.
- Mulle, C., Madariaga, A., and Deschênes, M. (1986) Morphology and electrophysiological properties of reticularis thalamic neurons in cat: in vivo study of a thalamic pacemaker. *Journal of Neuroscience* 6: 2134–2145.
- Mulle, C., Steriade, M., and Deschênes, M. (1985) The effects of QX314 on thalamic neurons. *Brain Research* 333: 350–354.
- Murthy, V.N. and Fetz, E.E. (1992) Coherent 25- to 35-Hz oscillations in the sensorimotor cortex of awake behaving monkeys. *Proceedings of National Academy of Sciences USA* 89: 5670–5674.
- Murthy, V.N. and Fetz, E.E. (1997a) Oscillatory activity in sensorimotor cortex of awake monkeys: synchronization of local field potentials and relation to behavior. *Journal of Neurophysiology* 76: 3949–3967.
- Murthy, V.N. and Fetz, E.E. (1997b) Synchronization of neurons during local field potential oscillations in sensorimotor cortex of awake monkeys. *Journal of Neurophysiology* 76: 3968–3982.
- Nádasy, Z., Hirase, H., Czurkó, A., Csicsvari, J., and Buzsáki, G. (1999) Replay and time compression of recurring spike sequences in the hippocampus. *Journal of Neurophysiology* 19: 9497–9507.
- Nagai, T., Kimura, H., Maeda, T., McGeer, P.L., Peng, F., and McGeer, E.G. (1982) Cholinergic projections from the basal forebrain of rat to the amygdala. *Journal of Neuroscience* 2: 513–520.
- Nagai, T., McGeer, P.L., and McGeer, E.G. (1983) Distribution of GABA-T-intensive neurons in the rat forebrain and midbrain. *Journal of Comparative Neurology* 218: 220–238.
- Nagai, T., Satoh, K., Imamoto, K., and Maeda, T. (1981) Divergent projections of catecholamine neurons of the locus coeruleus as revealed by fluorescent retrograde double labeling technique. *Neuroscience Letters* 23: 117–123.
- Nakamura, H. and Kawamura, S. (1988) The ventral lateral geniculate nucleus in the cat: thalamic and commissural connections revealed by the use of WGA-HRP transport. *Journal of Comparative Neurology* 277: 509–528.
- Nakamura, Y., Takatori, S., Nozaki, S., and Kikuchi, M. (1975) Monosynaptic reciprocal control of trigeminal motoneurons from the medial bulbar reticular formation. *Brain Research* 89: 144–148.

- Nakao, S. and Shiraishi, Y. (1983) Excitatory and inhibitory synaptic inputs from the medial mesodiencephalic junction to vertical eye movement-related motoneurons in the cat oculomotor nucleus. *Neuroscience Letters* 42: 125–130.
- Nakazato, T. (1987) Locus coeruleus neurons projecting to the forebrain and the spinal cord in the cat. *Neuroscience* 23: 529–538.
- Nambu, T., Sakurai, T., Mizukami, K., Hosoya, Y., Yanagisawa, M., and Goto, K. (1999) Distribution of orexin neurons in the adult rat brain. *Brain Research* 827: 243–260.
- Nauta, W.J.H. (1946) Hypothalamic regulation of sleep in rats. *Journal of Neurophysiology* 9: 285–316.
- Nauta, W.J.H. (1958) Hippocampal projections and related neural pathways to the midbrain in the cat. *Brain Research* 81: 319–340.
- Nauta, W.J.H. and Kuypers, H.G.J.M. (1958) Some ascending pathways in the brain stem reticular formation. In H.H. Jasper, L.D. Proctor, R.S. Knighton, W.C. Noshay, and R.T. Costello, eds., *Reticular Formation of the Brain*, pp. 3–30, Boston: Little Brown.
- Neckelmann, D., Amzica, F., and Steriade, M. (1998) Spike-wave complexes and fast components of cortically generated seizures. III. Synchronizing mechanisms. *Journal of Neurophysiology* 80: 1480–1494.
- Neher, E. (1971) Two fast transient current components during voltage clamp on snail neurons. *Journal of General Physiology* 58: 36–53.
- Neil, J.F., Merikanges, J.R., Foster, F.G., Merikanges, K.R., Spiker, D.G., and Kupfer, D.J. (1980) Waking and all-night sleep EEGs in anorexia nervosa. *Clinical Electroencephalography* 11: 9–15.
- Nelson, J.P., McCarley, R.W., and Hobson, J.A. (1983) REM sleep burst neurons, PGO waves, and eye movement information. *Journal of Neurophysiology* 50: 784–797.
- Netick, A., Orem, J., and Dement, W.C. (1977) Neuronal activity specific to REM sleep and its relationship to breathing. *Brain Research* 120: 197–207.
- Neuenschwander, S. and Singer, W. (1996) Long-range synchronization of oscillatory light responses in the cat retina and lateral geniculate nucleus. *Nature* 379: 728–733.
- Neville, H.J. and Foote, S.L. (1984) Auditory event-related potentials in the squirrel monkey: parallels to human late wave responses. *Brain Research* 298: 107–116.
- Newberry, N.R. and Nicoll, R.A. (1984) A bicuculline-resistant inhibitory postsynaptic potential in rat hippocampal pyramidal cells *in vitro*. *Journal of Physiology (London)* 348: 239–254.
- Newby, A.C. (1984) Adenosine and the concept of “retaliatory metabolites”. *Trends in Biochemical Science* 2: 42–44.
- Newman, D.B. (1985a) Distinguishing rat brainstem reticulospinal nuclei by their morphology. I. Medullary nuclei. *Journal für Hirnforschung* 26: 187–226.
- Newman, D.B. (1985b) Distinguishing rat brainstem reticulospinal nuclei by their neuronal morphology. II. Pontine and mesencephalic nuclei. *Journal für Hirnforschung* 26: 385–418.
- Newman, D.B. and Liu, R.P.C. (1987) Nuclear origins of brainstem reticulocortical systems in the rat. *American Journal of Anatomy* 178: 279–299.
- Newport, D.J., Stowe, Z.N., and Nemeroff, C.B. (2002) Parental depression: animal models of an adverse life event. *American Journal of Psychiatry* 159: 1265–1283.
- Nguyen, K.T., Deak, T., Owens, S.M., Kohno, T., Fleshner, M., Watkins, L.R., and Maier, S.F. (1998) Exposure to acute stress induces brain interleukin-1 beta protein in the rat. *Journal of Neuroscience* 18: 2239–2246.
- Nicolelis, M.A.L. and Chapin, J.K. (1994) Spatiotemporal structure of somatosensory responses of many-neuron ensembles in the rat ventral posterior medial nucleus of the thalamus. *Journal of Neuroscience* 14: 3511–3532.
- Nicolelis, M.A.L. and Fanselow, E.E. (2002) Thalamocortical optimization of tactile processing according to behavioral state. *Nature Neuroscience* 5: 517–523.
- Nie, Z., Mei, Y., Ford, M., Rybak, L., Marcuzzi, A., Ren, H., Stiles, G.L., and Ramkumar, V. (1998). Oxidative stress increases A₁ adenosine receptor expression by activating nuclear factor κ B. *Molecular Pharmacology* 53: 663–669.
- Niedermeyer, E. (1993) Historical aspects. In E. Niedermeyer and F.H. Lopes da Silva, eds., *Electroencephalography: Basic Principles, Clinical Applications and Related Fields* (3rd edn), pp. 1–14, Baltimore: Williams & Wilkins.
- Niedermeyer, E. (1999a) The normal EEG of the waking adult. In E. Niedermeyer and F.H. Lopes da Silva, eds., *Electroencephalography: Basic Principles, Clinical Applications and Related Fields* (3rd edn), pp. 149–173, Baltimore: Williams & Wilkins.
- Niedermeyer, E. (1999b) Abnormal EEG patterns (epileptic and paroxysmal). In *Electroencephalography: Basic Principles, Clinical Applications and Related Fields* (4th edition), E. Niedermeyer and F. Lopes da Silva, eds., 235–260, Baltimore: Williams & Wilkins.

- Niedermeyer, E. (1999c) Epileptic seizure disorders. In E. Niedermeyer and F. Lopes da Silva, eds., *Electroencephalography: Basic Principles, Clinical Applications and Related Fields* (4th edition), pp. 476–585, Baltimore: Williams & Wilkins.
- Nieoullon, A. and Dusticier, N. (1981) Decrease in choline acetyltransferase and in high affinity glutamate uptake in the red nucleus of the cat after cerebellar lesions. *Neuroscience Letters* 24: 267–272.
- Nishimura, Y., Kitagawa, H., Saitoh, K., Asahi, M., Itoh, K., Yoshioka, K., Asahara, T., Tanaka, T. and Yamamoto, T. (1996) The burst firing in the layer III and V pyramidal neurons of the cat sensorimotor cortex *in vitro*. *Brain Research* 727: 212–216.
- Nishimura, Y., Asahi, M., Saitoh, K., Kitagawa, H., Kumazawa, Y., Itoh, K., Lin, M., Akamine, T., Shibuyama, H., Asahara, T., and Yamamoto, T. (2001) Ionic mechanisms underlying burst firing of layer III sensorimotor cortical neurons of the cat: and *in vitro* slice study. *Journal of Neurophysiology* 86: 771–781.
- Nishino, S., Ripley, B., Overeem, S., Lammers, G.J., and Mignot, E. (2000) Hypocretin (orexin) deficiency in human narcolepsy. *Lancet* 355: 39–40.
- Nitz, D.A. and Siegel, J.M. (1997a) Inhibitory amino acid neurotransmission in the dorsal raphe nucleus during sleep/wake states. *American Journal of Physiology* 273: R451–R454.
- Nitz, D.A. and Siegel, J.M. (1997b) GABA release in the locus coeruleus as a function of sleep/wake state. *Neuroscience* 78: 795–801.
- Noble, D. (1985) Ionic mechanisms in rhythmic firing of heart and nerve. *Trends in Neurosciences* 89: 499–504.
- Noda, T. and Oka, H. (1984) Nigral inputs to the pedunculo-pontine region: intracellular analysis. *Brain Research* 322: 223–227.
- Noma, A. and Trautwein, W. (1978) Relaxation of the acetylcholine-induced potassium current in the rabbit sinoatrial node cell. *Pflügers Archiv für Gesamte Physiologie* 377: 193–200.
- North, R.A. (1986a) Mechanisms of autonomic integration. In V.B. Mountcastle and F.E. Bloom, eds., *Handbook of Physiology*, section 1, vol. 4, pp. 115–153, Bethesda (MD): American Physiological Society.
- North, R.A. (1986b) Receptors on individual neurones. *Neuroscience* 17: 899–907.
- North, R.A. and Williams, J.T. (1985) On the potassium conductance increased by opioids in rat locus coeruleus neurones. *Journal of Physiology (London)* 364: 265–280.
- North, R.A. and Yoshimura, M. (1984) The actions of noradrenaline on neurones of the rat substantia gelatinosa *in vitro*. *Journal of Physiology (London)* 349: 43–55.
- North, R.A., Williams, J.T., Surprenant, A., and Christie, M.J. (1987) Mu and delta receptors both belong to a family of receptors which couple to a potassium conductance. *Proceedings of the National Academy of Sciences of the USA* 84: 5487–5491.
- Nowak, L., Bregestovski, P., Ascher, P., Herbet, A., and Prochiantz, A. (1984) Magnesium gates glutamate-activated channels in mouse central neurones. *Nature* 307: 462–465.
- Nowycky, M.C., Fox, A.P., and Tsien, R.W. (1985) Three types of neuronal calcium channel with different calcium agonist sensitivity. *Nature* 316: 440–446.
- Núñez, A., Amzica, F., and Steriade, M. (1992a) Intracellular evidence for incompatibility between spindle and delta oscillations in thalamo-cortical neurons of cat. *Neuroscience* 48: 75–85.
- Núñez, A., Amzica, F., and Steriade, M. (1992b) Voltage-dependent fast (20–40 Hz) oscillations in long-axonated neocortical neurons. *Neuroscience* 51: 7–10.
- Núñez, A., Amzica, F., and Steriade, M. (1992c) Intrinsic and synaptically generated delta (1–4 Hz) rhythms in dorsal lateral geniculate neurons and their modulation by light-induced fast (30–70 Hz) events. *Neuroscience* 51: 269–284.
- Núñez, A., Amzica, F., and Steriade, M. (1993) Electrophysiology of cat association cortical neurons *in vivo*: intrinsic properties and synaptic responses. *Journal of Neurophysiology* 70: 418–430.
- Núñez, A., García-Ausó, E., and Buño, W. (1987) Intracellular theta rhythm generation in identified hippocampal pyramids. *Brain Research* 416: 289–300.
- O'Hara, B.F., Young, K.A., Watson, F.L., Heller, H.C., and Kilduff, T.S. (1993). Immediate early gene expression in brain during sleep deprivation: preliminary observations. *Sleep* 16: 1–7.
- Oades, R.D. and Halliday, G.M. (1987) Ventral tegmental (A10) system: neurobiology. I. anatomy and connectivity. *Brain Research Reviews* 12: 117–165.
- Oakson, G. and Steriade, M. (1982) Slow rhythmic rate fluctuations of cat midbrain reticular neurons in synchronized sleep. *Brain Research* 247: 277–288.
- Oakson, G. and Steriade, M. (1983) Slow rhythmic oscillations of EEG slow-wave amplitudes and their relations to midbrain reticular discharge. *Brain Research* 269: 386–390.
- Obal, F. Jr. and Krueger, J.M. (2003) Biochemical regulation of non-rapid-eye-movement sleep. *Frontiers in Bioscience* 8: d520–d550.

- Obal, F. Jr., Payne, L., Kapas, L., Opp, M., and Krueger, J.M. (1991) Inhibition of growth hormone-releasing factor suppresses both sleep and growth hormone secretion in the rat. *Brain Research* 557: 149–153.
- Obal, F. Jr., Payne, L., Opp, M., Alfoldi, P., Kapas, L., and Krueger, J.M. (1992) Growth hormone-releasing hormone antibodies suppress sleep and prevent enhancement of sleep after sleep deprivation. *American Journal of Physiology* 263: R1078–R1085.
- Obal, F. Jr., Fang, J., Taishi, P., Kacsoh, B., Gardi, J., and Krueger, J.M. (2001) Deficiency of growth hormone-releasing hormone signaling is associated with sleep alterations in the dwarf rat. *Journal of Neuroscience* 21: 2912–2918.
- Oertel, W.H., Graybiel, A.M., Mugnaini, E., Elde, R.P., Schmechel, D.E., and Kopin, I.J. (1983) Coexistence of glutamic acid decarboxylase- and somatostatin-like immunoreactivity in neurons of the feline nucleus reticularis thalami. *Journal of Neuroscience* 3: 1322–1332.
- Ohara, P. and Lieberman, A.R. (1993) Some aspects of the synaptic circuitry underlying inhibition in the ventrobasal thalamus. *Journal of Neurocytology* 22: 815–825.
- Ohta, Y., Mori, S., and Kimura, H. (1988) Neuronal structures of the brainstem participating in postural suppression in cats. *Neuroscience Research* 5: 181–202.
- Oka, H., Ito, J., and Kawamura, M. (1982) Identification of thalamo-cortical neurons responsible for cortical recruiting and spindling activities in cats. *Neuroscience Letters* 33: 13–18.
- Okabe, S., Sanford, L.D., Veasey, S.C., and Kubin, L. (1998) Pontine injections of nitric oxide synthase inhibitor, L-NAME consolidate episodes of REM sleep in the rat. *Sleep Research Online* 1: 41–48.
- Olah, M.E. and Stiles, G.L. (1992) Adenosine receptors. *Annual Review of Physiology* 54: 211–225.
- Olah, M.E. and Stiles, G.L. (1995) Adenosine receptor subtypes: characterization and therapeutic regulation. *Annual Review of Pharmacology and Toxicology* 35: 581–606.
- Olivier, A., Parent, A., and Poirier, L. (1970) Identification of the thalamic nuclei on the basis of their cholinesterase content in the monkey. *Journal of Anatomy (London)* 106: 37–50.
- Olpe, H.R. (1981) The cortical projection of the dorsal raphe nucleus: some electrophysiological and pharmacological properties. *Brain Research* 216: 61–71.
- Olchowaska, J.A., Molliver, M.E., Grzanna, R., Rice, F.L., and Coyle, J.T. (1981) Ultrastructural demonstration of noradrenergic synapses in the rat central nervous system by dopamine- β -hydroxylase immunocytochemistry. *Journal of Histochemistry and Cytochemistry* 29: 271–280.
- Olzewski, J. and Baxter, D. (1954) *Cytoarchitecture of the Human Brain Stem*. Basel: Karger.
- Ongini, E. and Schubert, P. (1998) Neuroprotection induced by stimulating A₁ or blocking A_{2a} adenosine receptors: an apparent paradox. *Drug Development Research* 45: 387–393.
- Onteniente, B., Geffard, M., and Calas, A. (1984) Ultrastructural immunocytochemical study of the dopaminergic innervation of the rat lateral septum with anti-dopamine antibodies. *Neuroscience* 13: 385–393.
- Onteniente, B., Geffard, M., Campistron, G., and Calas, A. (1987) An ultrastructural study of GABA-immunoreactive neurons and terminals in the septum of the rat. *Journal of Neuroscience* 7: 48–54.
- Opp, M.R. and Krueger, J.M. (1991) Interleukin 1 receptor antagonist blocks interleukin 1 induced sleep and fever. *American Journal of Physiology* 260: R453–R457.
- Opp, M.R. and Krueger, J.M. (1994) Anti-interleukin-1 β reduces sleep and sleep rebound after sleep deprivation in rats. *American Journal of Physiology* 266: R688–R695.
- Opp, M.R., Obal, F. Jr. and Krueger, J.M. (1991) Interleukin 1 alters rat sleep: temporal and dose-related effects. *American Journal of Physiology* 260: R52–R58.
- Orem, J. (1988) Neural basis of behavioral and state-dependent control of breathing. In R. Lydic and J.F. Biebuyck, eds., *Clinical Physiology of Sleep*, pp. 79–96, Bethesda (MD): American Physiological Society.
- Osmanovic, S.S. and Shefner, S.A. (1987) Anomalous rectification in rat locus coeruleus neurons. *Brain Research* 417: 161–166.
- Ottersen, O.P., Fisher, B.O., and Storm-Mathisen, J. (1983) Retrograde transport of D-³H-aspartate in thalamo-cortical neurones. *Neuroscience Letters* 42: 19–24.
- Overstreet, D.H. (1986) Selective breeding for increased cholinergic function: development of a new animal model of depression. *Biological Psychiatry* 221: 49–58.
- Pan, Z.Z. and Williams, J.T. (1989) GABA- and glutamate-mediated synaptic potentials in rat dorsal raphe neurons *in vitro*. *Journal of Neurophysiology* 61: 719–726.
- Panneton, W.M. and Burton, H. (1985) Projections from the paratrigeminal nucleus and the medullary and spinal horns to the peribrachial area in the cat. *Neuroscience* 3: 779–797.
- Panula, P., Airaksinen, M.S., Pirvola, U., and Kotilainen, E. (1990) A histamine-containing neuronal system in human brain. *Neuroscience* 34: 127–132.
- Pape, H.C. and Eysel, U.T. (1987) Modulatory action of the reticular transmitters norepinephrine and 5-hydroxytryptamine (serotonin) in the cat's visual thalamus. *Society for Neuroscience Abstracts* 13: 86.

- Pape, H.C. and Eysel, U.T. (1988) Cholinergic excitation and inhibition in the visual thalamus of the cat – influences of cortical inactivation and barbiturate anesthesia. *Brain Research*, 440: 79–86.
- Pape, H.C. and McCormick, D.A. (1995) Electrophysiological and pharmacological properties of interneurons in the cat dorsal lateral geniculate nucleus. *Neuroscience* 68: 1105–1125.
- Pape, H.C., Budde, T., Mager, R., and Kisvárdy, Z.F. (1994) Prevention of Ca^{2+} -mediated action potentials in GABAergic local-circuit neurones of rat thalamus by a transient K^{+} current. *Journal of Physiology (London)* 478: 403–422.
- Paré, D. and Smith, Y. (1993) Distribution of GABA immunoreactivity in the amygdaloid complex of the cat. *Neuroscience* 57: 1061–1076.
- Paré, D. and Smith, Y. (1994) GABAergic projection from the intercalated cell masses of the amygdala to the basal forebrain in cats. *Journal of Comparative Neurology* 344: 33–49.
- Paré, D. and Steriade, M. (1990) Control of mamillothalamic axis by brainstem cholinergic laterodorsal tegmental afferents: possible involvement in mnemonic processes. In M. Steriade and D. Biesold, eds. *Brain Cholinergic Systems*, pp. 337–354, Oxford: Oxford University Press.
- Paré, D., Steriade, M., Deschênes, M., and Oakson, G. (1987) Physiological characteristics of anterior thalamic nuclei, a group devoid of inputs from reticular thalamic nucleus. *Journal of Neurophysiology* 57: 1669–1685.
- Paré, D., Collins, D.R., Pelletier, J.G., and Filali, M. (2002) Neuronal oscillations and coding in the amygdala. *Trends in Cognitive Sciences* 6: 306–314.
- Paré, D., Curró Dossi, R., Datta, S., and Steriade, M. (1990a) Brainstem genesis of reserpine-induced ponto-geniculo-occipital waves: an electrophysiological and morphological investigation. *Experimental Brain Research* 81: 533–544.
- Paré, D., Curró Dossi, R., and Steriade, M. (1990b) Neuronal basis of the Parkinsonian resting tremor: a hypothesis and its implications for treatment. *Neuroscience* 35: 217–226.
- Paré, D., Curró Dossi, R., and Steriade, M. (1991) Three types of inhibitory postsynaptic potentials generated by interneurons in the anterior thalamic complex of cat. *Journal of Neurophysiology* 66: 1190–1204.
- Paré, D., Smith, Y., Parent, A., and Steriade, M., (1988) Projections of upper brainstem cholinergic and non-cholinergic neurons of cat to intralaminar and reticular thalamic nuclei. *Neuroscience* 25: 69–88.
- Paré, D., Smith, Y., Parent, A., and Steriade, M. (1989) Neuronal activity of identified posterior hypothalamic neurons projecting to the brainstem peribrachial area of the cat. *Neuroscience Letters* 107: 145–150.
- Paré, D., Steriade, M., Deschênes, M., and Bouhassira, D. (1990c) Prolonged enhancement of anterior thalamic synaptic responsiveness by stimulation of a brainstem cholinergic group. *Journal of Neuroscience* 10: 20–33.
- Parent, A. (1984) Comparative anatomy of monoaminergic systems. In A. Bjorklund, T. Hokfelt, and M. Kuhar, eds., *Handbook of Chemical Neuroanatomy*, vol. 2, pp. 409–439, Amsterdam: Elsevier.
- Parent, A. and Steriade, M. (1981) Afferents from the periaqueductal gray, medial hypothalamus and medial thalamus to the midbrain reticular core. *Brain Research Bulletin* 7: 411–418.
- Parent, A. and Steriade, M. (1984) Midbrain tegmental projections of nucleus reticularis thalami of cat and monkey: a retrograde transport and antidromic identification study. *Journal of Comparative Neurology* 229: 548–558.
- Parent, A., Descarries, L., and Beaudet, A. (1981) Organization of ascending serotonin systems in the adult rat brain. A radioautographic study after intraventricular administration of (^3H)5-hydroxytryptamine. *Neuroscience* 6: 115–138.
- Parent, A., Mackey, A., and DeBellefeuille, L. (1983) The subcortical afferents to caudate nucleus and putamen in primate: a fluorescent retrograde double labeling study. *Neuroscience* 10: 1137–1150.
- Parent, A., Paré, D., Smith, Y., and Steriade, M. (1988) Basal forebrain cholinergic and non-cholinergic projections to the thalamus and brainstem in cats and monkeys. *Journal of Comparative Neurology* 277: 281–301.
- Park, C.K., and Rudolph, K.A. (1994) Antischismic effect of propentofylline (HWA 283) against focal cerebral infarction in rats. *Neuroscience Letters* 178: 235–238.
- Park, M.R. (1987) Intracellular horseradish peroxidase labeling of rapidly firing dorsal raphe projection neurons. *Brain Research* 402: 117–130.
- Parmeggiani, P.L. (1985) Homeostatic regulation during sleep: facts and hypotheses. In D. McGinty, R. Drucker-Colin, A. Morrison, and P.L. Parmeggiani eds., *Brain Mechanisms of Sleep*, pp. 385–397, New York: Raven Press.
- Parmeggiani, P.L. (1988) Thermoregulation during sleep from the viewpoint of homeostasis. In R. Lydic and J.F. Biebuyck eds., *Clinical Physiology of Sleep*, pp. 159–169, Bethesda (MD): American Physiological Society.

- Parmeggiani, P.L., Cevolani, D., Azzaroni, A., and Ferrari, G. (1987) Thermosensitivity of anterior hypothalamic-preoptic neurons during the waking-sleeping cycle: a study in brain functional states. *Brain Research* 415: 79–89.
- Passouant, P., Halberg, F., Genicot, R., Popoviciu, L., and Baldy-Moulinier, M. (1969) Periodicity of narcoleptic attacks and the circadian rhythm of rapid eye movement sleep. *Revue Neurologique* 121: 155–164.
- Passouant, P., Schwab, R.S., Cadilhac, J., and Baldy-Moulinier, M. (1964) Narcolepsie-cataplexie. Étude du sommeil de nuit et du sommeil de jour. *Revue de Neurologie (Paris)* 3: 415–426.
- Pastel, R.H. (1988) The effects of DOI, a selective 5 HT-2 agonist, on sleep in the rat. *Abstracts of the European Sleep Research Society* 6: 202.
- Paupardin-Tritsch, D., Hammond, C., and Gerschenfeld, H.M. (1986) Serotonin and cyclic GMP both induce an increase of the calcium current in the same identified molluscan neurons. *Journal of Neuroscience* 6: 2715–2723.
- Pavides, C. and Winson, J. (1989) Influences of hippocampal place cell firing in awake state on the activity of these cells during subsequent sleep episodes. *Journal of Neuroscience* 9: 2907–2918.
- Pavlov, I.P. (1923) 'Innere Hemmung' der bedingten Reflexe und der Schlaf—ein und derselbe Prozess. *Skandinavische Archive für Physiologie* 44: 42–58.
- Pavlov, I.P. (1928) *Lectures on Conditioned Reflexes* (translated by H.W. Gantt). New York: International Publications.
- Paxinos, G.T. and Watson, C. (1997) *The Rat Brain: In Stereotaxic Coordinates*. San Diego (CA): Academic Press.
- Pazos, A. and Palacios, J.M. (1985) Quantitative autoradiographic mapping of serotonin receptors in the rat brain. I. Serotonin-1-receptors. *Brain Research* 346: 205–230.
- Pazos, A., Cortes, R., and Palacios, J.M. (1985) Quantitative autoradiographic mapping of serotonin receptors in the rat brain. II. Serotonin-2 receptors. *Brain Research* 346: 231–249.
- Pearson, R.C.A., Gatter, K.C., and Powell, T.P.S. (1983) The cortical relationships of certain basal ganglia and the cholinergic basal forebrain nuclei. *Brain Research* 261: 327–330.
- Pedigo, N. W., Yamamura, H.I., and Nelson, D.L. (1981) Discrimination of multiple [3H]5-hydroxytryptamine binding sites by the neuroleptic spiperone in rat brain. *Journal of Neurochemistry* 36: 220.
- Pedley, T.A. and Traub, R.D. (1990) Physiological basis of EEG. In D.D. Daly and T.A. Pedley, eds., *Current Practice of Clinical Electroencephalography*, pp. 107–137, New York: Raven Press.
- Pellmar, T.C. and Carpenter, D.O. (1980) Serotonin induces a voltage-sensitive calcium current in neurons of *Aplysia californica*. *Journal of Neurophysiology* 44: 423–439.
- Penfield, W. and Jasper, H.H. (1954) *Epilepsy and the Functional Anatomy of the Human Brain*. Boston: Little & Brown.
- Pentreath, V.W., Rees, K., Owolabi, O.A., Philip, K.A., and Duoa, F. (1990) The somnogenic T lymphocyte suppressor prostaglandin D2 is selectively elevated in cerebrospinal fluid of advanced sleeping sickness patients. *Transactions of the Royal Society of Tropical Medicine & Hygiene* 84: 795–799.
- Perkins, M.N. and Stone, T.W. (1982) An iontophoretic investigation of the actions of convulsant kynurenes and their interaction with the endogenous excitant quinolinic acid. *Brain Research* 247: 184–187.
- Peroutka, S.J. and Snyder, S.H. (1980) Long-term antidepressant treatment decreases spiroperidol-labeled serotonin receptor binding. *Science* 210: 88–90.
- Peroutka, S.J., Lebovitz, R.M., and Snyder, S.H. (1981) Two distinct central serotonin receptors with different physiological functions. *Science* 212: 827–829.
- Perry, E.K., Tomlinson, B.E., Blessed, G., Bergmann, K., Gibson, P.H., and Perry, R.H. (1978) Correlation of cholinergic abnormalities with senile plaques and mental test scores in senile dementia. *British Medical Journal* 2: 1457–1459.
- Pessah, M.A. and Roffwarg, H.P. (1972) Spontaneous middle ear muscle activity in man: a rapid eye movement sleep phenomenon. *Science* 178: 773–776.
- Peters, S., Koh, J., and Choi, D.W. (1987) Zinc selectively blocks the action of N-methyl-D-aspartate on cortical neurons. *Science* 236: 589–593.
- Peterson, B.W. (1977) Identification of reticulospinal projections that may participate in gaze control. In R. Baker and A. Berthoz, eds., *Control of gaze by brainstem neurons*, pp. 152–243, New York: Elsevier.
- Peterson, B.W., Franck, J.I., Pitts, N.G., and Dauntton, N.G. (1976) Changes in responses of medial pontomedullary reticular neurons during repetitive cutaneous, vestibular, cortical, and tectal stimulation. *Journal of Neurophysiology* 39: 564–581.
- Petitjean, F., Sakai, K., Blondaux, C., and Jouvet, M. (1975) Hypersomnia by isthmus lesion in cat. II. Neurophysiological and pharmacological study. *Brain Research* 88: 439–453.
- Petrovicky, P. (1980) *Reticular Formation and its Raphe System*. Prague: Acta Universitatis Carolinae Medica.

- Petsche, H., Gogolak, G., and van Zwieten, P.A. (1965) Rhythmicity of septal cell discharges at various levels of reticular excitation. *Electroencephalography and Clinical Neurophysiology* 19: 25–33.
- Petsche, H., Pockberger, H., and Rappelsberger, P. (1984) On the search for the sources of the electroencephalogram. *Neuroscience* 11: 1–27.
- Peyron, C., Tighe, D., van den Pol, A., de Lecea, L., Heller, H., Sutcliffe, J., and Kilduff, T. (1998) Neurons containing hypocretin (orexin) project to multiple neuronal systems. *Journal of Neuroscience* 18: 9996–10015.
- Pfaffinger, P.J., Martin, J.M., Hunter, D.D., Nathanson, N.M., and Hille, B. (1985) GTP-binding proteins couple cardiac muscarinic receptors to a K channel. *Nature* 317: 536–540.
- Pfurtscheller, G. and Neuper, C. (1994) Event-related synchronization of mu rhythm in the EEG over the cortical hand area in man. *Neuroscience Letters* 174: 93–96.
- Phillipson, O.T. (1979) Afferent projections to the ventral tegmental area of Tsai and interfascicular nucleus: a horseradish peroxidase study in the rat. *Journal of Comparative Neurology* 187: 117–144.
- Phillis, J.W. (1970) *The Pharmacology of Synapses*. Oxford: Pergamon.
- Phillis, J.W. (1971) The pharmacology of thalamic and geniculate neurons. *International Review of Neurobiology* 14: 1–48.
- Phillis, J.W. and Kostopoulos, G.K. (1977) Activation of a noradrenergic pathway from the brainstem to rat cerebral cortex. *General Pharmacology* 8: 207–211.
- Phillis, J.W. and Tebecis, A.K. (1967) The responses of thalamic neurones to iontophoretically applied monoamines. *Journal of Physiology (London)* 192: 715–745.
- Phillis, J.W. and Wu, P.H. (1981) The role of adenosine and its nucleotide in central synaptic transmission. *Progress in Neurobiology* 16: 187–193.
- Phillis, J.W. and York, D.H. (1968) Pharmacological studies on a cholinergic inhibition in the cerebral cortex. *Brain Research* 10: 297–306.
- Phillis, J.W., Tebecis, A.K., and York, D.H. (1976) A study of cholinceptive cells in the lateral geniculate nucleus. *Journal of Physiology (London)* 192: 695–713.
- Pickel, V.M., Joh, T.H., and Reis, D.J. (1977) A serotonergic innervation of noradrenergic neurons in nucleus locus coeruleus: demonstration by immunocytochemical localization of the transmitter specific enzymes tyrosine and tryptophan hydroxylase. *Brain Research* 131: 197–214.
- Pickel, V.M., Segal, M., and Bloom, F.E. (1974) A radioautographic study of the efferent pathways of the nucleus locus coeruleus. *Journal of Comparative Neurology* 155: 15–42.
- Pickel, V.M., Joh, T.H., Reis, D.J., Leeman, S.E., and Miller, R.J. (1979) Electron microscopic localization of substance P and enkephalin in axon terminals related to dendrites of catecholaminergic neurons. *Brain Research* 160: 387–400.
- Picton, T.W., Campbell, K.B., Baribeau-Braun, J., and Proulx, G.B. (1978) The neurophysiology of human attention: a tutorial view. In J. Requin, ed., *Attention and Performance*, pp. 429–467, New Jersey: Hillsdale.
- Picton, T.W., Woods, D.L., Baribeau-Braun, J., and Healy, T.M.G. (1977) Evoked potential audiometry. *Journal of Otolaryngology* 6: 90–119.
- Pinault, D., Leresche, N., Charpier, S., Deniau, J.M., Marescaux, C., Vergnes, M., and Crunelli, V. (1998) Intracellular recordings in thalamic neurones during spontaneous spike and wave discharges in rats with absence epilepsy. *Journal of Physiology (London)* 509: 449–456.
- Pineda, J.A., Foote, S.L., Neville, H.J., and Holmes, T.C. (1988) Endogenous event-related potentials in monkey: the role of task relevance, stimulus probability, and behavioral response. *Electroencephalography and Clinical Neurophysiology* 70: 155–171.
- Pivik, R.T., McCarley, R.W., and Hobson, J.A. (1976) Eye movement-associated discharge in brain stem neurons during desynchronized sleep. *Brain Research* 121: 59–76.
- Plata-Salaman, C.R. (2000) Central nervous system mechanisms contributing to the cachexia-anorexia syndrome. *Nutrition* 16: 1009–1012.
- Plihal, W. and Born, J. (1997) Effects of early and late nocturnal sleep on declarative and procedural memory. *Journal of Cognitive Neuroscience* 9: 534–547.
- Plum, F. (1991) Coma and related global disturbances of the human conscious state. In A. Peters and E.G. Jones, eds., *Cerebral Cortex* (vol. 9, *Normal and Altered States of Function*), pp. 359–425, New York: Plenum.
- Pollen, D.A. and Lux, H. (1966) Conductance changes during inhibitory postsynaptic potentials in normal and strychninized cortical neurons. *Journal of Neurophysiology* 29: 367–381.
- Pollock, J.D., Bernier, L., and Camardo, J.S. (1985) Serotonin and cyclic adenosine 3':5'-monophosphate modulate the potassium current in tail sensory neurons in the pleural ganglion of Aplysia. *Journal of Neuroscience* 5: 1862–1871.

- Pompeiano, O. (1967a) The neurophysiological mechanisms of the postural and motor events during desynchronized sleep. *Proceedings of the Association for Research of Nervous and Mental Diseases* 45: 351–423.
- Pompeiano, O. (1967b) Sensory inhibition during motor activity in sleep. In M.D. Yahr and D.P. Purpura, eds., *Neurophysiological basis of Normal and Abnormal Motor Activities*, pp. 323–375, New York: Raven Press.
- Pompeiano, O. (1973) Reticular formation. In A. Iggo, ed., *Handbook of Sensory Physiology*, vol. 2, *Somatosensory System*, pp. 381–488, Berlin: Springer.
- Pompeiano, O. (1976) Mechanisms responsible for spinal inhibition during desynchronized sleep: experimental study. In C. Guilleminault, W.C. Dement, and P. Passouant, eds., *Advances in Sleep Research*, vol. 3, *Narcolepsy*, pp. 411–449, New York: Spectrum.
- Pompeiano, O. (1985) Cholinergic mechanisms involved in the gain regulation of postural reflexes. In A. Wauquier, J.M. Gaillard, J.M. Monti, and M. Radulovacki, eds., *Sleep: Neurotransmitters and Neuromodulators*, pp. 165–184, New York: Raven Press.
- Pompeiano, O. and Valentinuzzi, M. (1976) A mathematical model for the mechanism of rapid eye movements induced by an anticholinesterase in the decerebrate cat. *Archives Italiennes de Biologie* 114: 103–154.
- Porkka-Heiskanen, T., Strecker, R.E., and McCarley, R.W. (2000) Brain site-specificity of extracellular adenosine concentration changes during sleep deprivation and spontaneous sleep: an in vivo microdialysis study. *Neuroscience* 99: 507–517.
- Porkka-Heiskanen, T., Strecker, R.E., Thakkar, M., Bjørkum, A.A., Greene, R.W., and McCarley, R.W. (1997) Adenosine: a mediator of the sleep-inducing effects of prolonged wakefulness. *Science* 276: 1265–1268.
- Portas, C.M. and McCarley, R.W. (1994) Behavioral state-related changes of extracellular serotonin concentration in the dorsal raphe nucleus: a microdialysis study in the freely moving cat. *Brain Research* 648: 306–312.
- Portas, C.M., Thakkar, M., Rainnie, D.G., Greene, R.W., and McCarley, R.W. (1997) Role of adenosine in behavioral state modulation: a microdialysis study in the freely moving cat. *Neuroscience* 79: 225–235.
- Portas, C.M., Thakkar, M., Rainnie, D., and McCarley, R.W. (1996) Microdialysis perfusion of 8-hydroxy-2-(di-*n*-propylamino)tetralin (8-OH-DPAT) in the dorsal raphe nucleus decreases serotonin release and increases rapid eye movement sleep in the freely moving cat. *Journal of Neuroscience* 16: 2820–2828.
- Posner, M.I. and Raichle, M. (1994) *Images of Mind*. New York: Scientific American Library.
- Preuss, T.M. and Goldman-Rakic, P.S. (1987) Crossed corticothalamic and thalamocortical connections of macaque prefrontal cortex. *Journal of Comparative Neurology* 257: 269–281.
- Price, J.L. and Amaral, D.G. (1981) An autoradiographic study of the projections of the central nucleus of the monkey amygdala. *Journal of Neuroscience* 1: 1242–1259.
- Price, J.L. and Stern, R. (1983) Individual cells in the nucleus basalis—diagonal band complex have restricted axonal projections to the cerebral cortex in the rat. *Brain Research* 269: 352–356.
- Puizillout, J.J. and Ternaux, J.P. (1974) Origine pyramidale des variations phasiques bulbaires observées lors de l'endormement. *Brain Research* 66: 85–102.
- Purpura, D.P. and Cohen, B. (1962) Intracellular recording from thalamic neurons during recruiting responses. *Journal of Neurophysiology* 25: 621–635.
- Purpura, D.P., McMurtry, J.G., and Maekawa, K. (1966) Synaptic events in ventrolateral thalamic neurons during suppression of recruiting responses by brain stem reticular stimulation. *Brain Research* 1: 63–76.
- Purpura, D.P., Shofer, R.J., and Musgrave, F.S. (1964) Cortical intracellular potentials during augmenting and recruiting responses. II. Patterns of synaptic activities in pyramidal and nonpyramidal tract neurons. *Journal of Neurophysiology* 27: 133–151.
- Qin, Y.L., McNaughton, B.L., Skaggs, W.E., and Barnes, C.A. (1997) Memory reprocessing in corticocortical and hippocampocortical neurons ensembles. *Philosophical Transactions of the Royal Society (London, Series B)* 352: 1525–1533.
- Radulovacki, M. (1985) Role of adenosine in sleep in rats. *Reviews of Clinical Basic Pharmacology* 5: 327–339.
- Radulovacki, M., Virus, R.M., Djuricic-Nedelson, M., and Green, R.D. (1984) Adenosine analogs and sleep in rats. *Journal of Pharmacology and Experimental Therapeutics* 228: 268–274.
- Rainnie, D.G., Grünze, H.C.R., McCarley, R.W., and Greene, R.W. (1994) Adenosine inhibition of mesopontine cholinergic neurons: implications for EEG arousal. *Science* 263: 689–692.
- Ralston, H.J. (1971) Evidence for presynaptic dendrites and a proposal for their mechanism of action. *Nature* 230: 585–587.

- Ramesh, V., Basheer, R., Thatte, H.S., and McCarley, R.W. (2002) Nuclear translocation of transcription factor NF- κ B in cholinergic neurons: a sleep deprivation and microinjection study. *Sleep* 25: A130.
- Ramón y Cajal, S. (1901–1917) *Recuerdos De Mi Vida* (translated as *Recollections of My Life* by E.H. Cragie with the assistance of J. Cano). Cambridge (MA): The MIT Press, 1966.
- Ramón y Cajal, S. (1911) *Histologie du Système Nerveux de l'Homme et des Vertébrés* (2 vol.), translated by L. Azoulay. Paris: Maloine. Also the 1952 edition, Madrid: Consejo Superior de Investigaciones Científicas, Instituto Ramón y Cajal.
- Ramón-Moliner, E. (1975) Specialized and generalized dendritic patterns. In M. Santini, ed., *Golgi Centennial Symposium*, pp. 87–100, New York: Raven Press.
- Ramón-Moliner, E. and Nauta, W.J.H. (1966) The isodendritic core of the brain stem. *Journal of Comparative Neurology* 126: 311–336.
- Ranson, S.W. (1939) Somnolence caused by hypothalamic lesions in the monkey. *Archives of Neurology and Psychiatry (Chicago)* 41: 1–23.
- Ranson, S.W. and Clark, S.L. (1953) *The Anatomy of the Nervous System* (ninth edition). Philadelphia and London: W.B. Saunders.
- Rapoport, J., Elkins, R., Langer, D.H., Sceery, W., Buchsbaum, M.S., Gillin, J.C., Murphy, D.L., Zahn, T.P., Lake, R., Ludlow, C., and Medelson, W.B. (1981) Childhood obsessive-compulsive disorder. *American Journal of Psychiatry* 138: 1545–1554.
- Rasler, F.E. (1984) Behavioral and electrophysiological manifestations of bombesin: excessive grooming and elimination of sleep. *Brain Research* 321: 187–198.
- Rasmussen, K., Heym, J., and Jacobs, B.L. (1984) Activity of serotonin containing neurons in nucleus centralis superior of freely moving cats. *Experimental Neurology* 83: 302–317.
- Rasmusson, D.D., Clow, K., and Szerb, J.C. (1994) Modification of neocortical acetylcholine release and electroencephalogram desynchronization due to brainstem stimulation by drugs applied to the basal forebrain. *Neuroscience* 60: 665–677.
- Rasmusson, D.D., Szerb, J.C., and Jordan, J.L. (1996) Differential effects of α -amino-3-hydroxy-5-methyl-4-isoxazole propionic acid and *N*-methyl-D-aspartate receptor antagonists applied to the basal forebrain on cortical acetylcholine release and EEG desynchronization. *Neuroscience* 72: 419–427.
- Rausell, E., Bae, C.S., Viñuela, A., Huntley, G.W. and Jones, E.G. (1992) Calbindin and parvalbumin cells in monkey VPL thalamic nucleus: distribution, laminar cortical projections, and relations to spinothalamic terminations. *Journal of Neuroscience* 12: 4088–4111.
- Ray, J.P. and Price, J.L. (1987) Possible interdigitation of basal forebrain afferents in the mediodorsal thalamic nucleus of the rat. *Society for Neuroscience Abstracts* 13: 445.
- Ray, W.J. and Cole, H.W. (1985) EEG alpha activity reflects attentional demands and beta activity reflects emotional and cognitive processes. *Science* 228: 750–752.
- Raybourn, M.S. and Keller, E.L. (1977) Colliculoreticular organization in primate oculomotor system. *Journal of Neurophysiology* 40: 861–878.
- Reader, T.A. (1978) Effects of dopamine, noradrenaline and serotonin in visual cortex of cat. *Experientia* 34: 1568–1588.
- Reader, T.A., Masse, P., and Champlain, J. (1979) The intracortical distribution of norepinephrine, dopamine and serotonin in the cerebral cortex of the cat. *Brain Research* 177: 499–513.
- Reiner, P.B. and McGeer, E.G. (1987) Electrophysiological properties of cortically projecting histamine neurons of the rat hypothalamus. *Neuroscience Letters* 73: 43–47.
- Renaud, L., Kelly, J., and Provini, L. (1974) Synaptic inhibition in pyramidal tract neurons: membrane potential and conductance changes evoked by pyramidal tract and cortical surface stimulation. *Journal of Neurophysiology* 37: 1144–1155.
- Renaud, A.E. and Spengler, R.N. (2002) Tumor necrosis factor expressed by primary hippocampal neurons and SH-SY5Y cells is regulated by α (2)-adrenergic receptor activation. *Journal of Neuroscience Research* 67: 264–274.
- Reynolds, C.F. (1989) Sleep in affective disorders. In M.H. Kryger, T. Roth, and W.C. Dement, eds., *Principles and Practices of Sleep Medicine*, pp. 413–415, New York: Saunders.
- Reynolds, C.F., III, Kupfer, D.J., Taska, L.S., Hoch, C.C., Sewich, D.E., and Grochocinski, V.J. (1985) Slow wave sleep in elderly depressed, demented, and healthy subjects. *Sleep* 8: 155–159.
- Ribary, U., Ioannides, A.A., Singh, K.D., Hasson, R., Bolton, J.P.R., Lado, F., Mogilner, A., and Llinás, R. (1991) Magnetic field tomography of coherent thalamocortical 40-Hz oscillations in humans. *Proceedings of the National Academy of Sciences USA* 88: 11037–11041.
- Richardson, B.P. and Engel, G. (1986) The pharmacology and function of 5-HT₃ receptors. *Trends in Neurosciences* 9: 424–428.
- Ringheim, G.E., Burgher, K.L., and Heroux, J.A. (1995) Interleukin-6 mRNA expression by cortical neurons in culture: evidence for neuronal sources of interleukin-6 production in the brain. *Journal of Neuroimmunology* 63:113–123.

- Rinvik, E., Grofova, I., and Ottersen, O.P. (1976) Demonstration of nigrotectal and nigroreticular projections in the cat by axonal transport of proteins. *Brain Research* 112: 388–394.
- Rivner, M. and Sutin, J. (1981) Locus coeruleus modulation of the motor thalamus: inhibition in nuclei ventralis lateralis and ventralis anterior. *Experimental Neurology* 73: 651–673.
- Roberts, J.L. II, Sweetman, B.J., Lewis, R.A., Austen, K.F., and Oates, J.A. (1980) Increased production of prostaglandin D2 in patients with systemic mastocytosis. *New England Journal of Medicine* 303: 1400–1404.
- Robertson, R.T. and Feiner, A.R. (1982) Diencephalic projections from the pontine reticular formation: autoradiographic studies in the cat. *Brain Research* 239: 3–16.
- Robinson, D.A. (1975) Oculomotor control signals. In G. Lennerstrand and P. Bach-y-Rita, eds., *Basic Mechanisms of Ocular Motility and Their Clinical Implications*, pp. 337–374, Oxford: Pergamon.
- Robinson, D.A. and Zee, D.S. (1981) Theoretical considerations of the function and circuitry of various rapid eye movements. In A.F. Fuchs and W. Becker, eds., *Progress in Oculomotor Research*, vol. 12, pp. 3–9, New York: Elsevier North-Holland.
- Roffwarg, H.P., Dement, W.C., Muzio, J.N., and Fisher, C. (1962) Dream imagery: relationship to rapid eye movements of sleep. *Archives of General Psychiatry* 7: 235–258.
- Rogawski, M.A. and Aghajanian, G.K. (1980a) Activation of lateral geniculate neurons by norepinephrine: mediation by an α -adrenergic receptor. *Brain Research* 182: 345–359.
- Rogawski, M.A. and Aghajanian, G.K. (1980b) Norepinephrine and serotonin: opposite effects on the activity of lateral geniculate neurons evoked by optic pathway stimulation. *Experimental Neurology* 69: 678–694.
- Rogawski, M.A. and Aghajanian, G.K. (1982) Activation of lateral geniculate neurons by locus coeruleus or dorsal noradrenergic bundle stimulation: selective blockade by the α_1 -adrenoreceptor antagonist prozosin. *Brain Research* 250: 31–39.
- Roger, A., Rossi, G.F., and Zirondoli, A. (1956) Le rôle des afférences des nerfs crâniens dans le maintien de l'état vigile de la préparation "encéphale isolé". *Electroencephalography and Clinical Neurophysiology* 8: 1–13.
- Rogers, A.W. (1979) *Techniques of Autoradiography*. Amsterdam: Elsevier/North-Holland Biomedical Press.
- Roldan, M. and Reinoso-Suarez, F. (1981) Cerebellar projections to the superior colliculus in the cat. *Journal of Neuroscience* 1: 827–834.
- Rolls, E.T., Murzi, E., Yaxley, S., Thorpe, S.J., and Simpson, S.J. (1986) Sensory-specific satiety: food-specific reduction in responsiveness of ventral forebrain neurons after feeding in the monkey. *Brain Research* 368: 79–86.
- Room, P., Postema, F., and Korf, J. (1981) Divergent axon collaterals of rat locus coeruleus neurons: demonstration by a fluorescent double labeling technique. *Brain Research* 221: 219–230.
- Report, N. and Steriade, M. (1981) Input-output organization of the midbrain reticular core. *Journal of Neurophysiology* 46: 17–31.
- Rosen, R. (1970) *Dynamical System Theory in Biology, vol. 1: Stability Theory and Its Applications*. New York: Wiley.
- Rosenberg, P.A. and Li, Y. (1995) Adenylyl cyclase activation underlies intracellular cyclic AMP accumulation, cyclic AMP transport, and extracellular adenosine accumulation evoked by beta-adrenergic receptor stimulation in mixed cultures of neurons and astrocytes derived from rat cerebral cortex. *Brain Research* 692: 227–232.
- Rosenberg, P.A., Li, Y., Le, N., and Zhang, Y. (2000) Nitric Oxide-stimulated increase in extracellular adenosine accumulation in rat forebrain neurons in culture is associated with ATP hydrolysis and inhibition of adenosine kinase activity. *Journal of Neuroscience* 20: 6294–6301.
- Ross, C.A., Ruggiero, D.A., and Reis, D.J. (1985) Projections from the nucleus tractus solitarius to the rostral ventrolateral medulla. *Journal of Comparative Neurology* 242: 511–534.
- Rossi, G.F. and Brodal, A. (1956) Corticofugal fibres to the brain stem reticular formation: an experimental study in the cat. *Journal of Anatomy (London)* 90: 42–62.
- Rossi, G., Macchi, G., Porro, M., Giaccone, G., Bugiani, M., Scarpini, E., Scarlato, G., Molini, G.E., Sasanelli, F., Bugiani, O., and Tagliavini, F. (1998) Fatal familial insomnia. Genetic, neuropathologic, and biochemical study of a patient from a new Italian kindred. *Neurology* 50: 688–692.
- Roth, M., Shaw, J., and Green, J. (1956) The form, voltage distribution and physiological significance of the K-complex. *Electroencephalography and Clinical Neurophysiology* 8: 385–402.
- Roth, S.R., Serman, M.B., and Clemente, C.D. (1967) Comparison of EEG correlates of reinforcement, internal inhibition and sleep. *Electroencephalography and Clinical Neurophysiology* 23: 509–520.
- Rotter, S., Martina, M., and Paré, D. (2000a) Polarized synaptic interactions between intercalated neurons of the amygdala. *Journal of Neurophysiology* 83: 3509–3518.
- Rougeul, A., Bouyer, J.J., Dedet, L., and Debray, O. (1979) Fast somatoparietal rhythms during combined focal attention and immobility in baboon and squirrel monkey. *Electroencephalography and Clinical Neurophysiology* 46: 310–319.

- Rougeul-Buser, A., Bouyer, J.J., Montaron, M.F., and Buser, P. (1983) Patterns of activities in the ventrobasal thalamus and somatic cortex SI during behavioral immobility in the awake cat: focal waking rhythms. *Experimental Brain Research Supplement* 7: 69–87.
- Rowntree, C.J. and Bland, B.H. (1986) An analysis of cholinceptive neurons in the hippocampal formation by direct microinfusion. *Brain Research* 362: 98–113.
- Roy, J.P., Clercq, M., Steriade, M., and Deschênes, M. (1984) Electrophysiology of neurons of the lateral thalamic nuclei in cat: mechanisms of long-lasting hyperpolarizations. *Journal of Neurophysiology* 51: 1220–1235.
- Royer, S., Martina, M., and Paré, D. (2000b) Bistable behavior of inhibitory neurons controlling impulse traffic through amygdala: role of a slowly deinactivating K^+ current. *Journal of Neuroscience* 20: 9034–9039.
- Ruch-Monachon, M.A., Jalfre, M., and Haefele, W. (1976) Drugs and PGO waves in the lateral geniculate body of the curarized rat. *Archives Internationales de Pharmacodynamie et Thérapie* 219: 251–346.
- Rudolph, K., Schubert, P., Parkinson, F.E., and Fredholm, B.B. (1992) Neuroprotective role of adenosine in cerebral ischemia. *Trends in Pharmacological Sciences* 13: 1343–1345.
- Rudy, B. and McBain, C.J. (2001) Kv3 channels: voltage-gated K^+ channels designed for high-frequency repetitive firing. *Trends in Neurosciences* 24: 517–526.
- Ruggiero, D.A., C.A. Ross, M. Anwar, D.H. Park, T.H. Joh, and D.J. Reis (1985) Distribution of neurons containing phenylethanolamine N-methyltransferase in medulla and hypothalamus of rat. *Journal of Comparative Neurology* 239: 127–154.
- Russchen, F.T., Amaral, D.G., and Price, J.L. (1985) The afferent connections of the substantia innominata in the monkey. *Macaca fascicularis. Journal of Comparative Neurology* 242: 1–27.
- Russell, G.V. (1955) The nucleus locus coeruleus (dorsolateralis tegmenti). *Texas Rep. of Biological Medicine* 13: 939–988.
- Rustioni, A., Schmelch, D.E., Spreafico, R., Cheema, S., and Cuénod, M. (1983) Excitatory and inhibitory amino acid putative neurotransmitters in the ventralis posterior complex: an autoradiographic and immunocytochemical study in rats and cats. In G. Macchi, A. Rustioni and R. Spreafico, eds., *Somatosensory Integration in the Thalamus*, pp. 365–383, Amsterdam: Elsevier.
- Rydelek-Fitzgerald, L., Wilcox, B.D., Teitler, M., and Jeffrey, J.J. (1993). Serotonin-mediated 5HT₂ receptor gene regulation in rat myometrial smooth muscle cells. *Molecular and Cellular Endocrinology* 92: 253–259.
- Rye, D.B., Lee, H.J., Saper, C.B., and Wainer, B.H. (1988) Medullary and spinal efferents of the pedunculopontine tegmental nucleus and adjacent mesopontine tegmentum in the rat. *Journal of Comparative Neurology*, 269: 315–341.
- Rye, D.B., Saper, C.B., Lee, H.J., and Wainer, B.H. (1987) Pedunculopontine tegmental nucleus of the rat: cytoarchitecture, cytochemistry, and some extrapyramidal connections of the mesopontine tegmentum. *Journal of Comparative Neurology* 259: 483–528.
- Rye, D.B., Wainer, B.H., Mesulam, M.M., Mufson, E.J., and Saper, C.B. (1984) Cortical projections arising from the basal forebrain: a study of cholinergic and non-cholinergic components employing combined retrograde tracing and immunohistochemical localization of choline acetyltransferase. *Neuroscience* 13: 627–643.
- Sakaguchi, T. and Nakamura, S. (1987) The mode of projections of single locus coeruleus neurons to the cerebral cortex in rats. *Neuroscience* 20: 221–230.
- Sakai, K. (1980) Some anatomical and physiological properties of ponto-mesencephalic tegmental neurons with special reference to the PGO waves and postural atonia during paradoxical sleep in the cat. In J.A. Hobson and M.A.B. Brazier, eds., *The Reticular Formation Revisited*, pp. 427–447, New York: Raven Press.
- Sakai, K. (1985a) Anatomical and physiological basis of paradoxical sleep. In D.J. McGinty, A. Morrison, R. Drucker-Colin, and P.L. Parmeggiani, eds., *Brain Mechanisms of Sleep*, pp. 111–137, New York: Raven Press.
- Sakai, K. (1985b) Neurons responsible for paradoxical sleep. In A. Wauquier, J.M. Gaillard, J.M. Monti, and M. Radulovacki, eds., *Sleep: Neurotransmitters and Neuromodulators*, pp. 29–42, New York: Raven Press.
- Sakai, K. (1986) Central mechanisms of paradoxical sleep. *Brain and Development* 8: 402–407.
- Sakai, K. and Crochet, S. (2000) Serotonergic dorsal raphe neurons cease firing by disfacilitation during paradoxical sleep. *Neuroreport* 11: 3237–3241.
- Sakai, K. and Crochet, S. (2001) Role of dorsal raphe neurons in paradoxical sleep generation in the cat: no evidence for a serotonergic mechanism. *European Journal of Neuroscience* 13: 103–112.

- Sakai, K. and Jouvett, M. (1980) Brainstem PGO-on cells projecting directly to the cat lateral geniculate nucleus. *Brain Research* 194: 500–505.
- Sakai, K., Crochet, S., and Onoe, H. (2001) Pontine structures and mechanisms involved in the generation of paradoxical (REM) sleep. *Archives Italiennes de Biologie* 139: 93–107.
- Sakai, K., El Mansari, M., Lin, J.S., Zhang, G., and Vanni-Mercier, F. (1990) The posterior hypothalamus in the regulation of wakefulness and paradoxical sleep. In M. Mancia and G. Marini, eds., *The Diencephalon and Sleep*, pp. 171–198, New York: Raven Press.
- Sakai, K., Salvetti, D., Kitahama, K., Kimura, H., Maeda, T., and Jouvett, M. (1983a) Projections ascendantes et descendantes des neurones de l'hypothalamus postérieur immunoréactifs à la sérotonine après administration de 5-hydroxytryptophane chez le chat. *Comptes Rendus de l'Académie de Sciences (Paris)* 296: 1013–1018.
- Sakai, K., Salvetti, D., Touret, M., and Jouvett, M. (1977a) Afferent connections of the nucleus raphe dorsalis in the cat as visualized by the horseradish peroxidase technique. *Brain Research* 137: 11–35.
- Sakai, K., Sastre, J., Kanamori, N., and Jouvett, M. (1981) State specific neurons in the ponto-medullary reticular formation with special reference to the postural atonia during paradoxical sleep in the cat. In C. Ajmone-Marsan and O. Pompeiano, eds., *Brain Mechanisms of Perceptual Awareness and Purposeful Behavior*, pp. 405–429, New York: Raven Press.
- Sakai, K., Sastre, J.P., Salvetti, D., Touret, M., and Jouvett, M. (1979) Tegmentoreticular projections with special reference to the muscular atonia during paradoxical sleep in the cat: an HRP study. *Brain Research* 176: 233–254.
- Sakai, K., Touret, M., Salvetti, D., Leger, L., and Jouvett, M. (1977b) Afferent projections to the cat locus coeruleus as visualized by the horseradish peroxidase technique. *Brain Research* 119: 21–41.
- Sakai, K., Vanni-Mercier, G., and Jouvett, M. (1983b) Evidence for the presence of PS-Off neurons in the ventromedial oblongata of freely moving cats. *Experimental Brain Research* 49: 311–314.
- Sakakura, H. (1968) Spontaneous and evoked unitary activities of cat lateral geniculate neurons in sleep and wakefulness. *Japanese Journal of Physiology* 18: 23–42.
- Sakmann, B., Noma, A., and Trautwein, W. (1983) Acetylcholine activation of single muscarinic K⁺ channels in isolated pacemaker cells of the mammalian heart. *Nature* 303: 250–253.
- Sakurai, T., Amemiya, A., Ishii, M., Matsuzaki, I., Chemelli, R.M., Tanaka, H., Williams, S.C., Richardson, J.A., Kozlowski, G.P., Wilson, S., Arch, J.R., Buckingham, R.E., Haynes, A.C., Carr, S.A., Annan, R.S., McNulty, D.E., Liu, W.S., Terrett, J.A., Elshourbagy, N.A., Bergsma, D.J., and Yanagisawa, M. (1998) Orexins and orexin receptors: a family of hypothalamic neuropeptides and G protein-coupled receptors that regulate feeding behavior. *Cell* 92: 573–585.
- Sallanon, M., Denoyer, M., Kitahama, K., Aubert, C., Gay, N., and Jouvett, M. (1989) Long-lasting insomnia induced by preoptic lesions and its transient reversal by muscimol injection into the posterior hypothalamus in the cat. *Neuroscience* 32: 669–683.
- Salt, T.E. (1989) Gamma-aminobutyric acid and afferent inhibition in the cat and rat ventrobasal thalamus. *Neuroscience* 28: 17–26.
- Salva, M.A.Q. and Guilleminault, C. (1986) Olivopontocerebellar degeneration, abnormal sleep, and REM sleep without atonia. *Neurology* 36: 576–577.
- Sanchez, R. and Leonard, C.S. (1994) NMDA receptor-mediated synaptic input to nitric oxide synthase-containing neurons of the guinea pig mesopontine tegmentum *in vitro*. *Neuroscience Letters* 179: 141–144.
- Sanchez, R. and Leonard, C.S. (1996) NMDA-receptor-mediated synaptic currents in guinea pig laterodorsal tegmental neurons *in vitro*. *Journal of Neurophysiology* 76: 1101–1111.
- Sanchez-Vives, M.V. and McCormick, D.A. (2000) Cellular and network mechanisms of rhythmic recurrent activity in neocortex. *Nature Neuroscience* 3: 1027–1034.
- Sanes, J.N. and Donoghue, J.P. (1993) Oscillations in local field potentials of the primate motor cortex. *Proceedings of the National Academy of Sciences of the USA* 90: 4470–4474.
- Sanford, A.J. (1971) A periodic basis for perception and action. In W.P. Colquhoun, ed., *Biological Rhythms and Human Perception*, pp. 179–209, New York: Academic Press.
- Sanford, L.D., Ross, R.J., Seggos, A.E., Morrison, A.R., Ball, W.A., and Mann, G.L. (1994) Central administration of two 5-HT receptor agonists: effect on REM sleep initiation and PGO waves. *Pharmacology, Biochemistry and Behavior* 49: 93–100.
- Sanford, L.D., Tang X., Xiao J., Ross R.J., and Morrison, A.R. (2003) GABAergic regulation of REM sleep in reticularis pontis oralis and caudalis in rats. *Journal of Neurophysiology* 90: 938–945.
- Saper, C.B. (1984) Organization of cerebral cortical afferent systems in the rat. I. Magnocellular basal nucleus. *Journal of Comparative Neurology* 222: 313–342.
- Saper, C.B. (1987) Diffuse cortical projection systems: anatomical organization and role in cortical function. In V.B. Mountcastle and F. Plum, eds., *Handbook of Physiology, The Nervous System*, sect. 1, vol. V, pp. 169–210, Bethesda (MD): American Physiological Society.

- Saper, C.B. and Breder, C.D. (1992) Endogenous pyrogens in the CNS: role in febrile response. *Progress in Brain Research* 93: 419–428.
- Saper, C.B. and Loewy, A.D. (1982) Projections of the pedunculopontine tegmental nucleus in the rat: evidence for additional extrapyramidal circuitry. *Brain Research* 252: 367–372.
- Saper, C.B. and Sawchenko, P.E. (2003) Magic peptides, magic antibodies: Guidelines for appropriate controls for immunohistochemistry (Editorial). *Journal of Comparative Neurology* 465: 161–163.
- Saper, C.B., Chou, T.C., and Scammell, T.E. (2001) The sleep switch: hypothalamic control of sleep and wakefulness. *Trends in Neurosciences* 24: 726–731.
- Saper, C.B., Standaert, D.G., Currie, M.G., Schwartz, D., Geller, D.M., and Needleman, P. (1985) Atriopeptin-immunoreactive neurons in the brain: presence in cardiovascular regulatory areas. *Science* 227: 1047–1049.
- Saper, C.B., Swanson, L.W., and Cowan, W.M. (1976) The efferent connections of the ventromedial nucleus of the hypothalamus of the rat. *Journal of Comparative Neurology* 169: 409–442.
- Sarter, M. and Bruno, J.P. (1997) Cognitive functions of cortical acetylcholine: toward a unifying hypothesis. *Brain Research Reviews* 23: 28–46.
- Sarter, M. and Bruno, J.P. (2000) Cortical cholinergic inputs mediating arousal, attentional processing and dreaming: differential afferent regulation of the basal forebrain by telencephalic and brainstem afferents. *Neuroscience* 95: 933–952.
- Sasaki, K., Matsuda, Y., Oka, H., and Mizuno, N. (1975) Thalamo-cortical projections for recruiting responses and spindling-like responses in the parietal cortex. *Experimental Brain Research* 22: 87–96.
- Sasaki, S. and Shimazu, H. (1981) Reticulovestibular organization participating in generation of horizontal fast eye movement. *Annals of New York Academy of Science* 374: 130–143.
- Sasaki, K., Staunton, H.P., and Dieckman, G. (1970) Characteristic features of augmenting and recruiting responses in the cerebral cortex. *Experimental Neurology* 26: 369–392.
- Sastre, J.P. and Jouvet, M. (1979) Le comportement onirique du chat. *Physiology and Behavior* 22: 979–989.
- Sastre, J.P., Buda, C., Kitahama, K., and Jouvet, M. (1996) Importance of the ventrolateral region of the periaqueductal gray and adjacent tegmentum in the control of paradoxical sleep as studied by muscimol microinjections in the cat. *Neuroscience* 74: 415–426.
- Sastre, J.P., Sakai, K., and Jouvet, M. (1981) Are the gigantocellular tegmental field neurons responsible for paradoxical sleep? *Brain Research* 229: 147–161.
- Satinoff, E. (1988) Thermal influences on REM sleep. In R. Lydic and J.F. Biebuyck, eds., *Clinical Physiology of Sleep*, pp. 135–144, Bethesda (MD): American Physiological Society.
- Satinski, D. (1967) Pharmacological responsiveness of lateral geniculate nucleus neurons. *International Journal of Neuropharmacology* 15: 387–397.
- Satoh, K. and Fibiger, H.C. (1986) Cholinergic neurons of the laterodorsal tegmental nucleus: efferent and afferent connections. *Journal of Comparative Neurology* 253: 277–302.
- Satoh, M., Akaike, A., Nakazawa, T., and Takagi, H. (1980) Evidence for involvement of separate mechanisms in the projection of analgesia by electrical stimulation of the nucleus reticularis paragigantocellularis and nucleus raphe magnus in the rat. *Brain Research* 194: 525–529.
- Satoh, S., Matsumura, H., and Hayaishi, O. (1998) Involvement of A_{2A} receptor in sleep promotion. *European Journal of Pharmacology* 351: 155–162.
- Satoh, S., Matsumura, H., Koike, N., Tokunaga, Y., Maeda, T., and Hayaishi, O. (1999) Region-dependent difference in the sleep-promoting potency of an adenosine A_{2A} receptor agonist. *European Journal of Neuroscience* 11: 1587–1597.
- Satoh, S., Matsumura, H., Suzuki, F. and Hayaishi, O. (1996) Promotion of sleep mediated by the A_{2A}-adenosine receptor and possible involvement of this receptor in the sleep induced by prostaglandin D₂ in rats. *Proceedings of the National Academy of Sciences of the USA* 93: 5980–5984.
- Saunders, N.A. and Sullivan, C.E. (eds.) (1994) *Sleep and Breathing*. New York (NY): Marcel Dekker, Inc.
- Scammell, T., Gerashchenko, D., Urade, Y., Onoe, H., Saper, C., and Hayaishi, O. (1998) Activation of ventrolateral preoptic neurons by the somnogen prostaglandin D₂. *Proceedings of the National Academy of Sciences of the USA* 95: 7754–7759.
- Scammell, T.E., Gerashchenko, D.Y., Mochizuki, T., McCarthy, M.T., Estabrook, I.V., Sears, C.A., Saper, C.B., Urade, Y., and Hayaishi, O. (2001) An adenosine A_{2A} agonist increases sleep and induces Fos in ventrolateral preoptic neurons. *Neuroscience* 107: 653–663.
- Scarnati, E., Proia, A., Di Loreto, S., and Pacitti, C. (1987) The reciprocal electrophysiological influence between the nucleus tegmenti pedunculopontinus and the substantia nigra in normal and decorticated rats. *Brain Research* 423: 116–124.
- Scheibel, M.A., Scheibel, A.B., Moruzzi, G., and Mollica, A. (1955) Convergence and interaction of afferent impulses on single units of reticular formation. *Journal of Neurophysiology* 18: 309–331.

- Scheibel, M.E. and Scheibel, A.B. (1958) Structural substrates for integrative patterns in the brain stem reticular core. In H.H. Jasper, L.D. Proctor, R.S. Knighton, W.C. Noshay, and R.T. Costello, eds., *Reticular Formation of the Brain*, pp. 31–55, Boston: Little-Brown.
- Scheibel, M.E. and Scheibel, A.B. (1965) Periodic sensory nonresponsiveness in reticular neurons. *Archives Italiennes de Biologie* 103: 300–316.
- Scheibel, M.E. and Scheibel, A.B. (1975) Dendrites as neuronal couplers: the dendrite bundle. In M. Santini, ed., *Golgi Centennial Symposium*, pp. 347–354, New York: Raven Press.
- Schenck, C.H., Bundlie, S.R., Ettinger, M.G., and Mahowald, M.W. (1986) Chronic behavioral disorders of human REM sleep: a new category of parasomnia. *Sleep* 9: 293–308.
- Schildkraut, J.J. and Kety, S.S. (1967) Biogenic amines and emotion. *Science* 156: 21–30.
- Schiller, P. and Stryker, M. (1972) Single-unit recording and stimulation in superior colliculus of the alert rhesus monkey. *Journal of Neurophysiology* 35: 915–924.
- Schlag, J. and Waszak, M. (1971) Electrophysiological properties of units in the thalamic reticular complex. *Experimental Neurology* 32: 79–97.
- Schonrock, B., Busselberg, D., and Haas, H.L. (1991) Properties of tuberomammillary histamine neurones and their response to galanin. *Agents & Actions* 33: 135–137.
- Schubert, P., Ogata, T., Marchini, C., Ferroni, S., and Rudolphi, K. (1997) Protective mechanisms of adenosine in neurons and glial cells. *Annals of the New York Academy of Sciences* 825: 1–10.
- Schulman-Galambos, C. and Galambos, R. (1979) Brainstem evoked response audiometry in newborn hearing screening. *Archives of Otolaryngology* 105: 86–90.
- Schulz, H. and Lund, R. (1983) Sleep onset REM periods are associated with circadian parameters of body temperature. A study in depressed patients and normal controls. *Biological Psychiatry* 18: 1411–1426.
- Schulz, H. and Lund, R. (1985) On the origin of early REM episodes in the sleep of depressed patients: a comparison of three hypotheses. *Psychiatry Research* 16: 65–77.
- Schulz, H. and Tetzlaff, W. (1982) Distribution of REM latencies after sleep interruption in depressive patients and control subjects. *Biological Psychiatry* 18: 1411–1426.
- Schulz, H., Lund, R., Cording, C., and Dirlich, G. (1979) Bimodal distribution of REM sleep latencies in depression. *Biological Psychiatry* 14: 595–600.
- Schulz, H., Zulley, J., and Dirlich, G. (1984) Statistical properties of the REM-NREM sleep cycle. Unpublished manuscript.
- Schwartz, J.C., Garberg, M., and Pollard, H. (1986) Histaminergic transmission in the brain. In V.B. Mountcastle and F.E. Bloom eds., *Handbook of Physiology, The Nervous System*, sect. 1, vol. IV, pp. 257–316, Bethesda (MD): American Physiological Society.
- Schwartz, J.C., Pollard, H., and Quach, T.T. (1980) Histamine as a neurotransmitter in mammalian brain: neurochemical evidence. *Journal of Neurochemistry* 35: 26–33.
- Schwartzkroin, P.A. and Stafstrom, C.E. (1980) Effects of EGTA on the calcium-activated afterhyperpolarization in hippocampal CA3 pyramidal cells. *Science* 210: 1125–1126.
- Schwierin, B., Borbely, A.A., and Tobler, I. (1996) Effects of N⁶-cyclopentyladenosine and caffeine on sleep regulation in the rat. *European Journal of Pharmacology* 300: 163–171.
- Schwindt, P.C., Spain, W.J., and Crill, W.E. (1989) Long-lasting reduction of excitability by a sodium-dependent potassium current in cat neocortical neurons. *Journal of Neurophysiology* 61: 233–244.
- Schwindt, P.C., Spain, W.J., Foehring, R.C., Chubb, M.C., and Crill, W.E. (1988b) Slow conductances in neurons from cat sensorimotor cortex *in vitro* and their role in slow excitability changes. *Journal of Neurophysiology* 59: 450–467.
- Schwindt, P.C., Spain, W.J., Foehring, R.C., Stafstrom, C.E., Chubb, M.C., and Crill, W.E. (1988a) Multiple potassium conductances and their functions in neurons from cat sensorimotor cortex *in vitro*. *Journal of Neurophysiology* 59: 424–449.
- Scudder, C.A. (1988) A new local feedback model of the saccadic burst generator. *Journal of Neurophysiology* 59: 1455–1475.
- Scudder, C.A., Fuchs, A.F., and Langer, T.P. (1988) Characteristics and functional identification of saccadic inhibitory burst neurons in the alert monkey. *Journal of Neurophysiology* 59: 1430–1454.
- Scudder, C.A., Langer, T.P., and Fuchs, A.F. (1982) Probable inhibitory burst neurons in the monkey. *Society for Neuroscience Abstracts* 8: 157.
- Segal, M. (1980) The action of serotonin in the rat hippocampal slice preparation. *Journal of Physiology (London)* 303: 423–439.
- Segal, M. and Landis, S. (1974) Afferents to the hippocampus of the rat studied with the method of retrograde transport of horseradish peroxidase. *Brain Research* 78: 1–15.
- Segarra, J.M. (1970) Cerebral vascular disease and behavior. I. The syndrome of the mesencephalic artery (basilar artery bifurcation). *Archives of Neurology* 22: 408–418.

- Segraves, M.A. and Goldberg, M.E. (1987) Functional properties of corticotectal neurons in the monkey's frontal eye field. *Journal of Neurophysiology* 58: 1387–1419.
- Séguéla, P., Watkins, K.C., and Descarries, L. (1988) Ultrastructural features of dopamine axon terminals in the anteromedial and the suprarhinal cortex of adult rat. *Brain Research* 442: 11–22.
- Sejnowski, T.J. and Destexhe, A. (2000) Why do we sleep? *Brain Research* 886: 208–223.
- Semba, K. (2000) Multiple output pathways of the basal forebrain: organization, chemical heterogeneity and roles in vigilance. *Behavioural Brain Research* 115: 117–141.
- Semba, K. (2002) Multiple output pathways of the basal forebrain: organization, chemical heterogeneity, and roles in vigilance. *Behavioural Brain Research* 115: 117–141.
- Semba, K. and Fibiger, H.C. (1992) Afferent connections of the laterodorsal and the pedunculopontine tegmental nuclei in the rat: a retro- and antero-grade transport and immunohistochemical study. *Journal of Comparative Neurology* 323: 387–410.
- Semba, K. and Komisaruk, B.R. (1984) Neural substrates of two different rhythmical vibrissal movements in the rat. *Neuroscience* 12: 761–774.
- Semba, K., Reiner, P.B., McGeer, E.G., and Fibiger, H.C. (1988) Brainstem afferents to the magnocellular basal forebrain studied by axonal transport, immunohistochemistry and electrophysiology in the rat. *Journal of Comparative Neurology* 267: 433–453.
- Serafin, M. and Mühlethaler, M. (1988) Spindle activity in the thalamus *in vitro*. *Society for Neuroscience Abstracts* 14: 1024.
- Serafin, M., Williams, S., Khateb, A., Fort, P., and Mühlethaler, M. (1996) Rhythmic firing of medial septum non-cholinergic neurons. *Neuroscience* 75: 671–675.
- Seutin, V., Verbanck, P., Massotte, L., and Dresse, A. (1989) Galanin decreases the activity of locus coeruleus neurons *in vitro*. *European Journal of Pharmacology* 164: 373–376.
- Seymour, S.E., Reuter-Lorenz, P.A., and Gazzaniga, M.S. (1994) The disconnection syndrome. Basic findings reaffirmed. *Brain* 117: 105–115.
- Shammah-Lagnado, S.J., Negrao, N., and Ricardo, J.A. (1985) Afferent connections of the zona incerta: a horseradish peroxidase study in the rat. *Neuroscience* 15: 109–134.
- Shammah-Lagnado, S.J., Negrao, N., Silva, B.A., and Ricardo, J.A. (1987) Afferent connections of the nuclei reticularis pontis oralis and caudalis: a horseradish peroxidase study in the rat. *Neuroscience* 20: 961–989.
- Sherin, J.E., Elmquist, J.K., Torrealba, F., and Saper, C.B. (1998) Innervation of histaminergic tuberomammillary neurons by GABAergic and galaninergic neurons in the ventrolateral preoptic nucleus of the rat. *Journal of Neuroscience* 18: 4705–4721.
- Sherin, J.E., Shiromani, P.J., McCarley, R.W., and Saper, C.B. (1996) Activation of ventrolateral preoptic neurons during sleep. *Science* 271: 216–219.
- Sherrington, C.S. (1906) *Integrative Action of the Nervous System*. New Haven: Yale University Press.
- Shiromani, P.J. and Fishbein, W. (1986) Continuous pontine cholinergic microinfusion via minipump induces sustained alterations in rapid eye movement (REM) sleep. *Pharmacology, Biochemistry and Behavior* 25: 1253–1261.
- Shiromani, P.J. and McGinty, D.J. (1986) Pontine neuronal response to local cholinergic infusion: relation to REM sleep. *Brain Research* 386: 20–31.
- Shiromani, P.J., Armstrong, D.M., and Gillin, J.C. (1988a) Cholinergic neurons from the dorsolateral pons project to the medial pons: a WGA-HRP and choline acetyltransferase immunohistochemical study. *Neuroscience Letters* 95: 19–23.
- Shiromani, P.J., Overstreet, D., Levy, D., Goodrich, C.A., Campbell, S.S., and Gillin, J.C. (1988b) Increased REM sleep in rats selectively bred for cholinergic hyperactivity. *Neuropsychopharmacology* 1: 129–133.
- Shiromani, P.J., Siegel, J.M., Tomaszewski, K.S., and McGinty, D.J. (1986) Alterations in blood pressure and REM sleep after pontine carbachol microinfusion. *Experimental Neurology* 91: 285–292.
- Shoham, S., Davenne, D., Cady, A.B., Dinarello, C.A., and Krueger, J.M. (1987) Recombinant tumor necrosis factor and interleukin 1 enhance slow-wave sleep. *American Journal of Physiology* 253: R142–R149.
- Shute, C.C.D. and Lewis, P.R. (1967a) The ascending cholinergic reticular system: neocortical, olfactory and subcortical projections. *Brain* 90: 497–520.
- Shute, C.C.D. and Lewis, P.R. (1967b) The cholinergic limbic system: projections to hippocampal formation, medial cortex, nuclei of the ascending cholinergic reticular system, and the subfornical organ and supra-optic crest. *Brain* 90: 521–540.
- Siebenlist, U., Franzoso, G., and Brown, K. (1994) Structure, regulation of and function of NF- κ B. *Annual Review of Cellular Biology* 10: 405–455.

- Siegel, J.M. (1979) Behavioral Functions of the reticular formation. *Brain Research Reviews* 1: 69–105.
- Siegel, J.M. and Lai, Y.Y. (1988) Receptors mediating suppression of muscle tone produced by glutamate in dorsolateral pons and medial medulla. *Society for Neuroscience Abstracts* 14: 1309.
- Siegel, J.M. and Tomaszewski, K.S. (1983a) Behavioral organization of reticular formation studies in the unrestrained cat. I. Cells related to axial, limb, eye and other movements. *Journal of Neurophysiology* 50: 696–716.
- Siegel, J.M., McGinty, D.J., and Breedlove, S.M. (1977) Sleep and waking activity of pontine gigantocellular field neurons. *Experimental Neurology* 56: 553–573.
- Siegel, J.M., Nienhuis, R., and Tomaszewski, K.S. (1984) REM sleep signs rostral to chronic transections at the pontomedullary junction. *Neuroscience Letters* 45: 241–246.
- Siegel, J.J., Tomaszewski, K.S., and Wheeler, R.L. (1983b) Behavioral organization of reticular formation: studies in the unrestrained cat. II. Cells related to facial movements. *Journal of Neurophysiology* 50: 717–723.
- Siegelbaum, S.A., Camardo, J.S., and Kandel, E.R. (1982) Serotonin and cyclic AMP close single potassium channels in Aplysia sensory neurones. *Nature* 299: 413–417.
- Siggins, G.R. and Gruol, D.L. (1986) Mechanisms of transmitter action in the vertebrate central nervous system. In V.B. Mountcastle and F.E. Bloom, eds., *Handbook of Physiology*, sect. 1, vol. IV, pp. 1–114, Bethesda (MD), American Physiological Society.
- Siggins, G.R., Champagnat, J., Jacquin, T., and Denavit-Saubie, M. (1987) Somatostatin depresses neuronal excitability in the solitary tract complex (STC) via hyperpolarization and augmentation of the M-current. *Society for Neuroscience Abstracts* 13: 1443.
- Silberman E.K., Vivaldi E., Garfield J., McCarley R.W., and Hobson J.A. (1980) Carbachol triggering of desynchronized sleep phenomena: enhancement via small volume infusions. *Brain Research* 191: 215–224.
- Sillito, A.M. (1987) Synaptic processes and neurotransmitters operating in the central visual system: a system approach. In G.M. Edelman, W.E. Gall, and W.M. Cowan, eds., *Synaptic Function*, pp. 329–371, New York: Wiley.
- Sillito, A.M. and Kemp, J.A. (1983) Cholinergic modulation of the functional organization of the cat visual cortex. *Brain Research* 289: 143–155.
- Sillito, A.M., Kemp, J.A., and Berardi, N. (1983) The cholinergic influence on the function of the cat dorsal lateral geniculate nucleus (dLGN). *Brain Research* 280: 299–307.
- Simon, N.R., Lopes da Silva, F.H., and Manshanden, I. (1999) Preliminary results from a whole-head MEG study of sleep. In T. Yoshimoto, ed. *Recent Advances in Biomagnetism*, pp. 373–376, Sendai: Tohoku University Press.
- Simon, N.R., Mandshanden, I., and Lopes da Silva, F.H. (2000) A MEG study of sleep. *Brain Research* 860: 64–76.
- Simon, R.P., Gershon, M.P., and Brooks, D.C. (1973) The role of the raphe nuclei in the regulation of ponto-geniculo-occipital wave activity. *Brain Research* 58: 313–330.
- Simpson, P.B., Challis, R.A.J., and Nahorski, S.R. (1995) Neuronal Ca^{2+} stores: activation and function. *Trends in Neuroscience* 18: 299–306.
- Singer, W. (1973) The effects of mesencephalic reticular stimulation on intracellular potentials of cat lateral geniculate neurons. *Brain Research* 61: 35–54.
- Singer, W. (1977) Control of thalamic transmission by corticofugal and ascending reticular pathways in the visual system. *Physiological Reviews* 57: 386–420.
- Singer, W. (1979) Central-core control of visual cortex functions. In F.O. Schmitt and F.G. Worden, eds., *The Neurosciences: Fourth Study Program*, pp. 1093–1110, Cambridge (MA): The MIT Press.
- Singer, W. (1990a) Role of acetylcholine in use-dependent plasticity of the visual cortex. In M. Steriade and D. Biesold, eds., *Brain Cholinergic Systems*, pp. 314–336, Oxford: Oxford University Press.
- Singer, W. (1990b) Search for coherence: A basic principle of cortical self-organization. *Concepts in Neuroscience* 1: 1–26.
- Singer, W. (1993) Synchronization of cortical activity and its putative role in information processing and learning. *Annual Reviews of Physiology* 55: 349–374.
- Singer, W. (1994) Time as coding space in neocortical processing: a hypothesis. In G. Buzsáki, R. Llinás, W. Singer, A. Beethoz, and Y. Christen, eds., *Temporal Coding in the Brain*, pp. 51–79, Berlin: Springer.
- Singer, W., Gray, C.M., Engel, A., and König, P. (1988) Spatio-temporal distribution of stimulus-specific oscillations in the cat visual cortex. II. Global interactions. *Society for Neuroscience Abstracts* 14: 899.
- Sinton, C.M. and McCarley, R.W. (2001) Sleep Disorders. In *Encyclopedia of Life Sciences*, www.els.net (Article #1483), London: Macmillan Reference Ltd.
- Sirkin, D.W., Schallert, T., and Teitelbaum, P. (1980) Involvement of the pontine reticular formation in head movements and labyrinthine righting in the rat. *Experimental Neurology* 69: 435–457.

- Sitaram, N., Nurnberger, J.I., Jr., Gershon, E.S., and Gillin, J.C. (1982) Cholinergic regulation of mood and REM sleep: potential model and marker of vulnerability to affective disorder. *American Journal of Psychiatry* 139: 571–576.
- Skinner, J.E., Mohn, D.N., and Kellaway, P. (1975) Sleep-stage regulation of ventricular arrhythmias in the unanesthetized pig. *Circulatory Research* 37: 342–349.
- Slaght, S.J., Leresche, N., Deniau, J.M., Crunelli, V., and Charpier, S. (2002) Activity of thalamic reticular neurons during spontaneous genetically determined spike and wave discharges. *Journal of Neuroscience* 22: 2323–2334.
- Slisli, Y. and De Beaurepaire, R. (1999) Interleukin-1 beta and calcitonin, but not corticotropin-releasing factor, alter sleep cycles when microinjected into the rat hypothalamic lateral paraventricular area. *Neuroscience Letters* 265: 29–32.
- Smiley, J.F. and Mesulam, M.M. (1999) Cholinergic neurons of the nucleus basalis of Meynert receive cholinergic, catecholaminergic and GABAergic synapses: an electron microscopic investigation in the monkey. *Neuroscience* 88: 241–255.
- Smith, S.J. and Thompson, S.H. (1987) Slow membrane currents in bursting pacemaker neurones of *Tritonia*. *Journal of Physiology (London)* 382: 425–448.
- Smith, T.G., Barker, J.L., and Gainer, H. (1975) Requirements for bursting pacemaker potential in molluscan neurones. *Nature* 253: 450–452.
- Smith, Y., Paré, D., Deschênes, M., Parent, A., and Steriade, M. (1988) Cholinergic and non-cholinergic projections from the upper brainstem core to the visual thalamus in the cat. *Experimental Brain Research* 70: 166–180.
- Smith, Y., Parent, A., Séguéla, P., and Descarries, L. (1987) Distribution of GABA-immunoreactive neurons in the basal ganglia of the squirrel monkey. *Journal of Comparative Neurology* 259: 50–64.
- Sofroniew, M.V., Priestley, J.V., Consolazione, A., Eckenstein, F., and Cuellar, A.C. (1985) Cholinergic projections from the midbrain and pons to the thalamus in rat, identified by combined retrograde tracing and choline acetyltransferase immunohistochemistry. *Brain Research* 329: 213–223.
- Soja, P.J., Finch, D.M., and Chase, M.H. (1987a) Effect of inhibitory amino acid antagonists on masseteric reflex suppression during active sleep. *Experimental Neurology* 96: 178–193.
- Soja, P.J., Lopez, F., Morales, F.R., and Chase, M.H. (1988) Depolarizing synaptic events influencing cat lumbar motoneurons during rapid eye movement episodes of active sleep are blocked by kynurenic acid. *Society for Neuroscience Abstracts* 14: 941.
- Soja, P.J., Morales, F.R., Baranyi, A., and Chase, M.H. (1987b) The effect of inhibitory amino acid antagonists on IPSPs induced in lumbar motoneurons upon stimulation of the nucleus reticularis gigantocellularis during active sleep. *Brain Research* 423: 353–358.
- Solomon, J.S., Doyle, J.F., Burkhalter, H., and Nerbonne, J.M. (1993) Differential expression of hyperpolarization-activated currents reveals distinct classes of visual cortical projection neurons. *Journal of Neuroscience* 13: 5082–5091.
- Soloway, A.S., Pucak, M.L., Melchitzky, D.S., and Lewis, D.A. (2002) Dendritic morphology of callosal and ipsilateral projection neurons in monkey prefrontal cortex. *Neuroscience* 109: 461–471.
- Soltesz, I. and Deschênes, M. (1993) Low- and high-frequency membrane potential oscillations during theta activity in CA1 and CA3 pyramidal neurons of the rat hippocampus under ketamine-xylazine anesthesia. *Journal of Neurophysiology* 70: 97–116.
- Soltesz, I., Haby, M., Leresche, N., and Crunelli, V. (1988) The GABA_B antagonist phaclofen inhibits the late potassium-dependent IPSP in cat and rat thalamic and hippocampal neurones. *Brain Research* 448: 351–354.
- Soltesz, I., Lightowler, S., Leresche, N., Jassik-Gerschenfeld, D., and Crunelli, V. (1991) Two inward currents and the transformation of low-frequency oscillations of rat and cat thalamocortical cells. *Journal of Physiology (London)* 441: 175–197.
- Somogyi, P. (1978) The study of Golgi stained cells and of experimental degeneration under the electron microscope: a direct method for the identification in the visual cortex of three successive links in a neuron chain. *Neuroscience* 3: 167–180.
- Somogyi, P. (1989) Synaptic organisation of GABAergic neurons and GABA_A receptors in the lateral geniculate nucleus and visual cortex. In D.K.T. Lam and C.D. Gilbert, eds., *Retina Research Foundation Symposium*, vol. 2, *Neural mechanisms of visual perception*, pp. 35–62, Woodlands (TX): Portfolio.
- Somogyi, P., Hodgson, A.J., and Smith, A.D. (1979) An approach to tracing neuron networks in the cerebral cortex and basal ganglia. Combination of Golgi staining, retrograde transport of horseradish peroxidase and anterograde degeneration of synaptic boutons in the same material. *Neuroscience* 4: 1805–1852.
- Somogyi, P., Freund, T.F., Hodgson, A.J., Somogyi, J., Beroukas, D., and Chubb, I.W. (1985) Identified axo-axonic cells are immunoreactive for GABA in the hippocampus and visual cortex of cats. *Brain Research* 332: 143–149.

- Somogyi, P., Freund, T.F., Wu, J.Y., and Smith, A.D. (1983) The section-Golgi impregnation procedure. 2. Immunocytochemical demonstration of glutamate decarboxylase in Golgi-impregnated neurons and in their afferent synaptic boutons in the visual cortex of the cat. *Neuroscience* 9: 475–490.
- Souaze, F. (2001) Maintaining cell sensitivity to G-protein coupled receptor agonists: neurotensin and the role of receptor gene activation. *Journal of Neuroendocrinology* 13: 473–479.
- Soury, J. (1899) *Le Système Nerveux Central. Histoire Critique des Théories et des Doctrines*. Paris: Carré et Naud.
- Sparks, D.L. and Mays, L.E. (1983) Spatial localization of saccade targets. I. Compensation for stimulation-induced perturbations in eye position. *Journal of Neurophysiology* 49: 45–63.
- Sparks, D.L., Mays, L.E., and Porter, J.D. (1987) Eye movements induced by pontine stimulation: interaction with visually triggered saccades. *Journal of Neurophysiology* 58: 300–318.
- Spencer, W.A. and Brookhart, J.M. (1961a) Electrical patterns of augmenting and recruiting waves in the depths of the sensorimotor cortex of cat. *Journal of Neurophysiology* 24: 26–49.
- Spencer, W.A. and Brookhart, J.M. (1961b) A study of spontaneous spindle waves in sensorimotor cortex of cat. *Journal of Neurophysiology* 24: 50–65.
- Sporri, B., Bickel, M., Dobbelaere, D., Machado, J., and Lottaz, D. (2001) Soluble interleukin-1 receptor—reverse signaling in innate immunoregulation. *Cytokine Growth Factor Review* 12: 27–32.
- Spreafico, R., Amadeo, A., Angoscini, P., Panzica, F., and Battaglia, G. (1993) Branching projections from mesopontine nuclei to the nucleus reticularis and related thalamic nuclei: a double labelling study in the rat. *Journal of Comparative Neurology* 336: 481–492.
- Spriggs, D.R., Deutsch, S., and Kufe, D.W. (1992) Genomic structure, induction and production of TNF alpha. In B.B. Aggarwal and J. Vilcek, eds, *Tumor Necrosis Factor*, pp. 3–34, New York (NY): Marcel Dekker, Inc.
- Sprouse, J.S. and Aghajanian, G.K. (1987) Electrophysiological responses of serotonergic dorsal raphe neurons to 5-HT1A and 5-HT1B agonists. *Synapse* 1: 3–9.
- Squire, L.R. and Alvarez, P. (1995) Retrograde amnesia and memory consolidation: a neurobiological perspective. *Current Opinions in Neurobiology* 5: 169–177.
- Staiger, J.F. and Nurnberger, F. (1989) Pattern of afferents to the lateral septum in the guinea pig. *Cell & Tissue Research* 257: 471–490.
- Standaert, D.G., Saper, C.B., Rye, D.B., and Wainer, B.H. (1986) Colocalization of atriopeptin-like immunoreactivity with choline acetyltransferase and substance P-like immunoreactivity in the pedunculopontine and laterodorsal tegmental nuclei in the rat. *Brain Research* 382: 163–168.
- Stanfield, P.R. (1983) Tetraethylammonium ions and the potassium permeability of excitable cells. *Reviews of Physiology, Biochemistry and Pharmacology* 97: 167.
- Stanton, G.B. and Greene, R.W. (1981) Brain stem afferents to the periauducens reticular formation (PARF) in the cat. *Experimental Brain Research* 44: 419–426.
- Stanton, G.B. and Orr, A. (1985) [³H]choline labeling of cerebellothalamic neurons with observations on the cerebello-thalamo-parietal pathways in cats. *Brain Research* 335: 237–243.
- Stanton, G.B., Goldberg, M.E., and Bruce, C.J. (1988) Frontal eye field efferents in the macaque monkey. *Journal of Comparative Neurology* 271: 493–506.
- Steinbusch, H.W.M. (1981) Distribution of serotonin-immunoreactivity in the central nervous system of the rat. *Neuroscience* 6: 557–618.
- Steinbusch, H.W.M. and Nieuwehuys, R. (1983) The raphe nuclei of the rat brainstem: a cytoarchitectonic and immunohistochemical study. In P.C. Emson, ed., *Chemical Neuroanatomy*, pp. 131–207, New York: Raven Press.
- Steinbusch, H.W.M., van der Kooy, D., Verhofstad, A.A.J., and Pellegrino, A. (1980) Serotonergic and non-serotonergic projections from the nucleus raphe dorsalis to the caudate-putamen complex in the rat, studied by a combined immunofluorescence and fluorescent retrograde axonal labeling technique. *Neuroscience Letters* 19: 137–142.
- Steinfels, G.f., Heym, J., Strecker, R.E., and Jacobs, B.L. (1983) Behavioral correlates of dopaminergic unit activity in freely moving cats. *Brain Research* 258: 217–228.
- Steininger, T.L., Gong, H., McGinty, D., and Szymusiak, R. (2001) Subregional organization of preoptic area/anterior hypothalamic projections to arousal-related monoaminergic cell groups. *Journal of Comparative Neurology* 429: 638–653.
- Steininger, T.L., Wainer, B.H., Blakely, R.D., and Rye D.B. (1997) Serotonergic dorsal raphe nucleus projections to the cholinergic and noncholinergic neurons of the pedunculopontine tegmental region: a light and electron microscopic anterograde tracing and immunohistochemical study. *Journal of Comparative Neuroscience* 382: 302–322.
- Stenberg, D., Litonius, E., Halldner, L., Johansson, B., Fredholm, B.B., and Porkka-Heiskanen, T. (2003) Sleep and its homeostatic regulation in mice lacking the adenosine A1 receptor. *Journal of Sleep Research* 12: 283–290.

- Stephan, F.K., Berkley, K.J., and Moss, R.L. (1981) Efferent connections of the rat suprachiasmatic nucleus. *Neuroscience* 6: 2625–2641.
- Steriade, M. (1968) The flash-evoked afterdischarge. *Brain Research* 9: 169–212.
- Steriade, M. (1969) *Physiologie des Voies et des Centres Visuels*. Paris: Masson.
- Steriade, M. (1970) Ascending control of thalamic and cortical responsiveness. *International Review of Neurobiology* 12: 87–144.
- Steriade, M. (1974) Interneuronal epileptic discharges related to spike-and-wave cortical seizures in behaving monkeys. *Electroencephalography and Clinical Neurophysiology* 37: 247–263.
- Steriade, M. (1978) Cortical long-axonated cells and putative interneurons during the sleep-waking cycle. *Behavioral and Brain Sciences* 3: 465–514.
- Steriade, M. (1980) State-dependent changes in the activity of rostral reticular and thalamocortical elements. *Neuroscience Research Program Bulletin* 18: 83–91.
- Steriade, M. (1981) Mechanisms underlying cortical activation: neuronal organization and properties of the midbrain reticular core and intralaminar thalamic nuclei. In O. Pompeiano and C. Ajmone-Marsan, eds., *Brain Mechanisms and Perceptual Awareness*, pp. 327–377, New York: Raven Press.
- Steriade, M. (1983) Cellular mechanisms of wakefulness and slow-wave sleep. In A. Mayes, ed., *Sleep Mechanisms and Functions in Humans and Animals. An Evolutionary Perspective*, pp. 161–216, Wokingham (UK): Van Nostrand Reinhold.
- Steriade, M. (1984) The excitatory-inhibitory response sequence of thalamic and neocortical cells: state-related changes and regulatory systems. In G.M. Edelman, W.E. Gall, and W.M. Cowan, eds., *Dynamic Aspects of Neocortical Function*, pp. 107–157, New York: Wiley.
- Steriade, M. (1989) Spindling, incremental thalamocortical responses and spike-wave epilepsy. In M. Avoli, P. Gloor, G. Kostopoulos, and R. Naquet, eds., *Generalized Epilepsy*, pp. 161–180, Boston: Birkhäuser.
- Steriade, M. (1991) Alertness, quiet sleep, dreaming. In A. Peters and E.G. Jones, eds., *Cerebral Cortex* (vol. 9, *Normal and Altered States of Function*), pp. 279–357, New York: Plenum.
- Steriade, M. (1993) Cholinergic blockage of network and intrinsically generated slow oscillations promote waking and REM sleep patterns in thalamic and cortical neurons. In A.C. Cuello, ed., *Cholinergic Function and Dysfunction*, pp. 345–355 (vol. 98, *Progress in Brain Research*). Amsterdam: Elsevier.
- Steriade, M. (1994) The thalamus and sleep disturbances. In C. Guilleminault, E. Lugaresi, P. Montagna, and P. Gambetti, eds., *Fatal Familial Insomnia: Inherited Prion Diseases, Sleep, and the Thalamus*, pp. 177–189, New York: Raven Press.
- Steriade, M. (1995a) Two channels in the cerebellothalamocortical system. *Journal of Comparative Neurology* 354: 57–70.
- Steriade, M. (1995b) Brain activation, then (1949) and now: coherent fast rhythms in corticothalamic networks. *Archives Italiennes de Biologie* 134: 5–20.
- Steriade, M. (1997a) Synchronized activities of coupled oscillators in the cerebral cortex and thalamus at different levels of vigilance. *Cerebral Cortex* 7: 583–604.
- Steriade, M. (1997b) Thalamic substrates of disturbances in states of vigilance and consciousness in humans. In M. Steriade, E.G. Jones, and D.A. McCormick, eds., *Thalamus* (vol. 2, *Experimental and Clinical aspects*), pp. 721–742, Oxford: Elsevier.
- Steriade, M. (1999a) Cellular substrates of brain rhythms. In E. Niedermeyer and F. Lopes Da Silva, eds., *Electroencephalography: Basic Principles, Clinical Applications, and Related Fields* (4th edn.), pp. 28–75, Baltimore: Williams & Wilkins.
- Steriade, M. (1999b) Coherent oscillations and short-term plasticity in corticothalamic networks. *Trends in Neurosciences* 22: 337–345.
- Steriade, M. (1999c) Thalamus. In G. Adelman and B. Smith, eds., *Encyclopedia of Neuroscience*, pp. 2031–2034, Amsterdam: Elsevier.
- Steriade, M. (2000) Corticothalamic resonance, states of vigilance, and mentation. *Neuroscience* 101: 243–276.
- Steriade, M. (2001a) Impact of network activities on neuronal properties in corticothalamic systems. *Journal of Neurophysiology* 86: 1–39.
- Steriade, M. (2001b) *The Intact and Sliced Brain*. Cambridge (MA): The MIT Press.
- Steriade, M. (2001c) To burst, or rather, not to burst. *Nature Neuroscience* 4: 671.
- Steriade, M. (2003a) *Neuronal Substrates of Sleep and Epilepsy*. Cambridge (UK): Cambridge University Press.
- Steriade, M. (2003b) Acetylcholine systems and rhythmic activities during the waking-sleep cycle. In L. Descarries, K. Krnjević, and M. Steriade, eds., *Acetylcholine in the Cerebral Cortex*, San Diego: Academic Press.

- Steriade, M. and Amzica, F. (1994) Dynamic coupling among neocortical neurons during evoked and spontaneous spike-wave seizure activity. *Journal of Neurophysiology* 72: 2051–2069.
- Steriade, M. and Amzica, F. (1996) Intracortical and corticothalamic coherency of fast spontaneous oscillations. *Proceedings of National Academy of Sciences of the USA* 93: 2533–2538.
- Steriade, M. and Amzica, F. (1998) Coalescence of sleep rhythms and their chronology in corticothalamic networks. *Sleep Research Online* 1: 1–10.
- Steriade, M. and Buzsáki, G. (1990). Parallel activation of thalamic and cortical neurons by brainstem and basal forebrain cholinergic systems. In M. Steriade and D. Biesold, eds., *Brain Cholinergic Systems*, pp. 3–63, Oxford: Oxford University Press.
- Steriade, M. and Contreras, D. (1995) Relations between cortical and thalamic cellular events during transition from sleep pattern to paroxysmal activity. *Journal of Neuroscience* 15: 623–642.
- Steriade, M. and Contreras, D. (1998) Spike-wave complexes and fast runs of cortically generated seizures. I. Role of neocortex and thalamus. *Journal of Neurophysiology* 80: 1439–1455.
- Steriade, M. and Demetrescu, M. (1960) Unspecific systems of inhibition and facilitation of potentials evoked by intermittent light. *Journal of Neurophysiology* 23: 602–617.
- Steriade, M. and Deschênes, M. (1974) Inhibitory processes and interneuronal apparatus in motor cortex during sleep and waking. II. Recurrent and afferent inhibition of pyramidal tract neurons. *Journal of Neurophysiology* 37: 1093–1113.
- Steriade, M. and Deschênes, M. (1984) The thalamus as a neuronal oscillator. *Brain Research Reviews* 8: 1–63.
- Steriade, M. and Deschênes, M. (1988) Intrathalamic and brainstem-thalamic networks involved in resting and alert states. In M. Bentivoglio, G. Macchi, and R. Spreafico, eds., *Cellular Thalamic Mechanisms*, pp. 37–62, Amsterdam: Elsevier.
- Steriade, M. and Glenn, L.L. (1982) Neocortical and caudate projections of intralaminar thalamic neurons and their synaptic excitation from the midbrain reticular core. *Journal of Neurophysiology* 48: 352–371.
- Steriade, M. and Hobson, J.A. (1976) Neuronal activity during the sleep–waking cycle. *Progress of Neurobiology* 6: 155–376.
- Steriade, M. and Llinás, R. (1988) The functional states of the thalamus and the associated neuronal interplay. *Physiological Reviews* 68: 649–742.
- Steriade, M. and McCarley, R.W. (1990) *Brainstem Control of Wakefulness and Sleep*. New York: Plenum.
- Steriade, M. and Morin, D. (1981) Reticular influences on primary and augmenting responses in the somatosensory cortex. *Brain Research* 205: 67–80.
- Steriade, M. and Stoupe, N. (1960) Contribution à l'étude des relations entre l'aire auditive du cervelet et l'écorce cérébrale chez le chat. *Electroencephalography and Clinical Neurophysiology* 12: 119–136.
- Steriade, M. and Timofeev, I. (1997) Short-term plasticity during intrathalamic augmenting responses in decorticated cats. *Journal of Neuroscience* 17: 3778–3795.
- Steriade, M. and Timofeev, I. (2001) Corticothalamic operations through prevalent inhibition of thalamo-cortical neurons. *Thalamus & Related Systems* 1: 225–236.
- Steriade, M. and Yossif, G. (1974) Spike-and-wave afterdischarges in cortical somatosensory neurons of cat. *Electroencephalography and Clinical Neurophysiology* 37: 633–648.
- Steriade, M., Amzica, F., and Contreras, D. (1994a) Cortical and thalamic cellular correlates of electroencephalographic burst-suppression. *Electroencephalography and Clinical Neurophysiology* 90: 1–16.
- Steriade, M., Amzica, F., and Contreras, D. (1996a) Synchronization of fast (30–40 Hz) spontaneous cortical rhythms during brain activation. *Journal of Neuroscience* 16: 392–417.
- Steriade, M., Amzica, F., and Nuñez, A. (1993a) Cholinergic and noradrenergic modulation of the slow (~0.3 Hz) oscillation in neocortical cells. *Journal of Neurophysiology* 70: 1384–1400.
- Steriade, M., Amzica, F., Neckelmann, D., and Timofeev, I. (1998a) Spike-wave complexes and fast runs of cortically generated seizures. II. Extra- and intracellular patterns. *Journal of Neurophysiology* 80: 1456–1479.
- Steriade, M., Apostol, V., and Oakson, G. (1971) Control of unitary activities in cerebellothalamic pathways during wakefulness and synchronized sleep. *Journal of Neurophysiology* 34: 384–413.
- Steriade, M., Belekova, M., and Apostol, V. (1968) Reticular potentiation of cortical flash-evoked afterdischarge. *Brain Research* 11: 276–280.
- Steriade, M., Botez, M.I., and Petrovici, I. (1961) On certain dissociations of consciousness levels within the syndrome of akinetic mutism. *Psychiatry and Neurology (Basel)* 141: 38–58.
- Steriade, M., Constantinescu, E., and Apostol, V. (1969b) Correlations between alterations of the cortical transaminase activity and EEG patterns of sleep and wakefulness induced by brainstem transections. *Brain Research* 13: 177–180.
- Steriade, M., Contreras, D., and Amzica, F. (1994b) Synchronized sleep oscillations and their paroxysmal developments. *Trends in Neuroscience* 17: 199–208.

- Steriade, M., Contreras, D., and Amzica, F. (1997b) The thalamocortical dialogue during wake, sleep and paroxysmal oscillations. In M. Steriade, E.G. Jones, and D.A. McCormick, eds., *Thalamus* (vol. 2, *Experimental and Clinical Aspects*), pp. 213–294, Oxford: Elsevier.
- Steriade, M., Contreras, D., Amzica, F., and Timofeev, I. (1996b) Synchronization of fast (30–40 Hz) spontaneous oscillations in intrathalamic and thalamocortical networks. *Journal of Neuroscience* 16: 2788–2808.
- Steriade, M., Contreras, D., Curró Dossi, R., and Nuñez, A. (1993b) The slow (<1 Hz) oscillation in reticular thalamic and thalamocortical neurons: scenario of sleep rhythm generation in interacting thalamic and neocortical networks. *Journal of Neuroscience* 13: 3284–3299.
- Steriade, M., Crochet, S., Fuentealba, P., Cissé, Y., and Timofeev, I. (2003) Cortical plasticity and self-sustained activity. *Society for Neuroscience Abstracts* 29: In press.
- Steriade, M., Curró Dossi, R., and Contreras, D. (1993c) Electrophysiological properties of intralaminar thalamocortical cells discharging rhythmic (~40 Hz) spike-bursts at ~1000 Hz during waking and rapid eye movement sleep. *Neuroscience* 56: 1–9.
- Steriade, M., Curró Dossi, R., and Nuñez, A. (1991a) Network modulation of a slow intrinsic oscillation of cat thalamocortical neurons implicated in sleep delta waves: cortical potentiation and brainstem cholinergic suppression. *Journal of Neuroscience* 11: 3200–3217.
- Steriade, M., Curró Dossi, R., Paré, D., and Oakson, G. (1991b) Fast oscillations (20–40 Hz) in thalamocortical systems and their potentiation by mesopontine cholinergic nuclei in the cat. *Proceedings of the National Academy of Sciences of the USA* 88: 4396–4400.
- Steriade, M., Datta, S., Paré, D., Oakson, G., and Curró Dossi, R. (1990a) Neuronal activities in brainstem cholinergic nuclei related to tonic activation processes in thalamocortical systems. *Journal of Neuroscience* 10: 2541–2559.
- Steriade, M., Deschênes, M., and Oakson, G. (1974a) Inhibitory processes and interneuronal apparatus in motor cortex during sleep and waking. I. Background firing and responsiveness of pyramidal tract neurons and interneurons. *Journal of Neurophysiology* 37: 1065–1092.
- Steriade, M., Deschênes, M., Domich, L., and Mülle, C. (1985) Abolition of spindle oscillations in thalamic neurons disconnected from nucleus reticularis thalami. *Journal of Neurophysiology* 54: 1473–1497.
- Steriade, M., Deschênes, M., Wyzinski, P., and Hallé, J.Y. (1974b) Input-output organization of the motor cortex during sleep and waking. In O. Petre-Quadens and J. Schlag, eds., *Basic Sleep Mechanisms*, pp. 144–200. New York: Academic Press.
- Steriade, M., Diallo, A., Oakson, G., and White-Guay, B. (1977a) Some synaptic inputs and ascending projections of lateralis posterior thalamic neurons. *Brain Research* 131: 39–53.
- Steriade, M., Domich, L., and Oakson, G. (1986) Reticularis thalami neurons revisited: activity changes during shifts in states of vigilance. *Journal of Neuroscience* 6: 68–81.
- Steriade, M., Domich, L., Oakson, G., and Deschênes, M. (1987a) The deafferented reticular thalamic nucleus generates spindle rhythmicity. *Journal of Neurophysiology* 57: 260–273.
- Steriade, M., Gloor, P., Llinás, R.R., Lopes da Silva, F.H., and Mesulam, M.M. (1990c) Basic mechanisms of cerebral rhythmic activities. *Electroencephalography and Clinical Neurophysiology* 76: 481–508.
- Steriade, M., Iosif, G., and Apostol, V. (1969) Responsiveness of thalamic and cortical motor relays during arousal and various stages of sleep. *Journal of Neurophysiology* 32: 251–265.
- Steriade, M., Jones, E.G., and Llinás, R.R. (1990b) *Thalamic Oscillations and Signaling*. New York: Wiley-Interscience.
- Steriade, M., Jones, E.G., and McCormick, D.A. (1997a) *Thalamus* (vol. 1, *Organisation and Function*). Oxford: Elsevier.
- Steriade, M., Kitsikis, A., and Oakson, G. (1978) Thalamic inputs and subcortical targets of cortical neurons in areas 5 and 7 of cat. *Experimental Neurology* 60: 420–442.
- Steriade, M., Kitsikis, A., and Oakson, G. (1979a) Excitatory-inhibitory processes in parietal association neurons during reticular activation and sleep–waking cycle. *Sleep* 1: 339–355.
- Steriade, M., Kitsikis, A., and Oakson, G. (1979b) Selectively REM-related increased firing rates in association interneurons during sleep: possible implications for learning. In M.A. Brazier, ed., *Brain Mechanisms in Memory and Learning*, pp. 47–52, New York: Raven Press.
- Steriade, M., McCormick, D.A., and Sejnowski, T.J. (1993d) Thalamocortical oscillation in the sleeping and aroused brain. *Science* 262: 679–685.
- Steriade, M., Nuñez, A., and Amzica, F. (1993e) A novel slow (<1 Hz) oscillation of neocortical neurons *in vivo*: depolarizing and hyperpolarizing components. *Journal of Neuroscience* 13: 3252–3265.
- Steriade, M., Nuñez, A., and Amzica, F. (1993f) Intracellular analysis of relations between the slow (<1 Hz) neocortical oscillation and other sleep rhythms. *Journal of Neuroscience* 13: 3266–3283.
- Steriade, M., Oakson, G., and Diallo, A. (1976) Cortically elicited spike-wave afterdischarges in thalamic neurons. *Electroencephalography and Clinical Neurophysiology* 41: 641–644.

- Steriade, M., Oakson, G., and Diallo, A. (1977b) Reticular influences on lateralis posterior thalamic neurons. *Brain Research* 131: 55–71.
- Steriade, M., Oakson, G., and Ropert, N. (1982a) Firing rates and patterns of midbrain reticular neurons during steady and transitional states of the sleep–waking cycle. *Experimental Brain Research* 46: 37–51.
- Steriade, M., Paré, D., Bouhassira, D., Deschênes, M., and Oakson, G. (1989) Phasic activation of lateral geniculate and perigeniculate neurons during sleep with ponto-geniculo-occipital spikes. *Journal of Neuroscience* 9: 2215–2229.
- Steriade, M., Paré, D., Datta, S., Oakson, G., and Curró Dossi, R. (1990d) Different cellular types in meso-pontine cholinergic nuclei related to ponto-geniculo-occipital waves. *Journal of Neuroscience* 10: 2560–2579.
- Steriade, M., Paré, D., Hu, B., and Deschênes, M. (1990e) *The visual thalamocortical system and modulation thereof by the brainstem core*. Berlin-Heidelberg-New York: Springer.
- Steriade, M., Paré, D., Parent, A., and Smith, Y. (1988) Projections of cholinergic and non-cholinergic neurons of the brainstem core to relay and associational thalamic nuclei in the cat and macaque monkey. *Neuroscience* 25: 47–67.
- Steriade, M., Parent, A., and Hada, J. (1984a) Thalamic projections of nucleus reticularis thalami of cat: a study using retrograde transport of horseradish peroxidase and double fluorescent tracers. *Journal of Comparative Neurology* 229: 531–547.
- Steriade, M., Parent, A., Paré, D., and Smith, Y. (1987b) Cholinergic and non-cholinergic neurons of cat basal forebrain project to reticular and mediodorsal thalamic nuclei. *Brain Research* 408: 372–376.
- Steriade, M., Parent, A., Ropert, N., and Kitsikis, A. (1982b) Zona incerta and lateral hypothalamic afferents to the midbrain reticular core of the cat—an HRP and electrophysiological study. *Brain Research* 238: 13–28.
- Steriade, M., Ropert, N., Kitsikis, A., and Oakson, G. (1980) Ascending activating neuronal networks in midbrain reticular core and related rostral systems. In J.A. Hobson and M.A.B. Brazier, eds., *The Reticular Formation Revisited*, pp. 125–167. New York: Raven Press.
- Steriade, M., Sakai, K., and Jouviet, M. (1984b) Bulbothalamic neurons related to thalamocortical activation processes during paradoxical sleep. *Experimental Brain Research* 54: 463–475.
- Steriade, M., Timofeev, I., and Grenier, F. (2001a) Natural waking and sleep states: a view from inside neocortical neurons. *Journal of Neurophysiology* 85: 1969–1985.
- Steriade, M., Timofeev, I., and Grenier, F. (2001b) Intrinsic, antidromic and synaptic excitability of cortical neurons during natural waking-sleep cycle. *Society for Neuroscience Abstracts* 27: 240.
- Steriade, M., Timofeev, I., Dürmüller, N., and Grenier, F. (1998b) Dynamic properties of corticothalamic neurons and local cortical interneurons generating fast rhythmic (30–40 Hz) spike bursts. *Journal of Neurophysiology* 79: 483–490.
- Steriade, M., Timofeev, I., Grenier, F., and Dürmüller, N. (1998c) Role of thalamic and cortical neurons in augmenting responses: dual intracellular recordings *in vivo*. *Journal of Neuroscience* 18: 6425–6443.
- Steriade, M., Wyzinski, P., and Apostol, V. (1972) Corticofugal projections governing rhythmic thalamic activity. In T.L. Frigyesi, E. Rinvik and M.D. Yahr, ed., *Corticothalamic Projections and Sensorimotor Activities*, pp. 221–272. New York: Raven Press.
- Sterman, M.B. and Clemente, C.D. (1962) Forebrain inhibitory mechanisms: sleep patterns induced by basal forebrain stimulation in the behaving cat. *Experimental Neurology* 6: 103–117.
- Sterman, M.B. and Wyrwicka, W. (1967) EEG correlates of sleep: evidence for separate forebrain substrates. *Brain Research* 6: 143–163.
- Stevens, D.R., Greene, R.W., and McCarley, R.W. (1989) Excitatory and inhibitory actions of serotonin on medial pontine reticular formation neurons mediated by opposing actions on potassium conductance(s). *Sleep Research* 18: 23.
- Stevens, D.R., McCarley, R.W., and Greene, R.W. (1992) Excitatory amino acid-mediated responses and synaptic potentials in medial pontine reticular formation neurons of the rat *in vitro*. *Journal of Neuroscience* 12: 4188–4194.
- Stichel, C.C. and Singer, W. (1985) Organization and morphological characteristics of choline acetyltransferase-containing fibers in the visual thalamus and striate cortex of the cat. *Neuroscience Letters* 53: 155–160.
- Stickgold, R., Whitbee, D., Schirmer, B., Patel, V., and Hobson, J.A. (2000) Visual discrimination improvement. A multi-step process occurring during sleep. *Journal of Cognitive Neuroscience* 12: 246–254.
- Stockhard, J.J., Bickford, R.G., and Aung, M.H. (1975) The electroencephalogram in traumatic brain injury. In P.J. Vinken and G.W. Bruyn, eds., *Handbook of Clinical Neurology*, vol. 23 (1), pp. 217–367, Amsterdam: North Holland.
- Stone, T.W. and Taylor, D.A. (1977a) Microiontophoretic studies of the effects of cyclic nucleotides on excitability of neurones in the rat cerebral cortex. *Journal of Physiology (London)* 266: 523–543.

- Stone, T.W. and Taylor, D.A. (1977b) The nature of adrenoreceptors in the guinea pig cortex. A microiontophoretic study. *Canadian Journal of Physiology and Pharmacology* 55: 1400–1404.
- Stone, T.W., Taylor, D.A., and Bloom, F.E. (1975) Cyclic AMP and cyclic GMP may mediate opposite neuronal responses in the rat cerebral cortex. *Science* 187: 845–847.
- Storm, J.F. (1987) Action potential repolarization and a fast afterhyperpolarization in rat hippocampal pyramidal cells. *Journal of Physiology (London)* 385: 733–759.
- Strachey, J. (1966) Editor's introduction to project for a scientific psychology. In *Complete Psychological Works*, vol. 1 (translated and edited by J. Strachey), pp. 283–293. London: Hogarth Press.
- Strassman, A., Highstein, S.M., and McCrea R.A. (1986) Anatomy and physiology of saccadic burst neurons in the alert squirrel monkey. II. Inhibitory burst neurons. *Journal of Comparative Neurology* 249: 358–380.
- Strecker, R.E., McCarley, R.W., Dauphin, L.J., McKenna, J.T., Sinton, C.M., Wilkemeyer, M., Ramesh, V., and Thakkar, M.M. (2002) Diurnal variation in extracellular orexin-A levels in the rat basal forebrain. *Sleep* 25: A8.
- Strecker, R.E., Morairty, S., Thakkar, M.M., Porkka-Heiskanen, T., Basheer, R., Dauphin, L.J., Rainnie, D.G., Portas, C.M., Greene, R.W., and McCarley, R.W., (2000) Adenosinergic modulation of basal forebrain and preoptic/anterior hypothalamic neuronal activity in the control of behavioral state. *Behavioral Brain Research* 115: 183–204.
- Strecker, R.E., Porkka-Heiskanen, T., Thakkar, M.M., Dauphin, L.J., Stenberg, D., and McCarley, R.W. (1999). Recent evidence that the sleep-promoting effects of adenosine are site specific. *Sleep* 22: 32.
- Streit, P. (1980) Selective retrograde labeling indicating the transmitter of neuronal pathways. *Journal of Comparative Neurology* 191: 429–463.
- Sugimoto, T. and Hattori, T. (1984) Organization and efferent projections of nucleus tegmenti pedunculopontinus pars compacta with special reference to its cholinergic aspects. *Neuroscience* 11: 931–946.
- Sulloway, F.J. (1979) *Freud, Biologist of the Mind*. New York: Basic Books.
- Suntsova, N., Szymusiak, R., Alam, M.N., Guzman-Marin, R., and McGinty, D. (2002) sleep–waking discharge patterns of median preoptic nucleus neurons in rats. *Journal of Physiology* 543: 665–677.
- Surkis, A., Raylor, B., Peskin, C.S., and Leonard, C.S. (1996) Quantitative morphology of physiologically identified and intracellularly labeled neurons from the guinea-pig laterodorsal tegmental nucleus *in vitro*. *Neuroscience* 74: 375–392.
- Susic, V. and Totic, S. (1989) 'Recovery' function of sleep: effects of purified human interleukin-1 on the sleep and febrile response of cats. *Metabolic Brain Disease* 4: 73–80.
- Sutton, R.E., Koob, G.F., Le Moal, M., Rivier, J., and Vale, W. (1982) Corticotropin releasing factor produces behavioral activation in rats. *Nature* 297: 31–33.
- Svensson, T.H. and Engberg (1980) Effect of nicotine on single cell activity in the noradrenergic nucleus locus coeruleus. *Acta Physiologica Scandinavica* (Suppl. 479): 31–34.
- Swadlow, H.A. and Weyand, T.G. (1987) Corticogeniculate neurons, corticotectal neurons, and suspected interneurons in visual cortex of awake rabbits: receptive-field properties, axonal properties, and effects of EEG arousal. *Journal of Neurophysiology* 57: 977–1001.
- Swank, R.L. (1949) Synchronization of spontaneous electrical activity of cerebrum by barbiturate narcosis. *Journal of Neurophysiology* 12: 161–172.
- Swanson, L.W. (1976) The locus coeruleus: a cytoarchitectonic Golgi and immunohistochemical study in the albino rat. *Brain Research* 110: 39–56.
- Swanson, L.W. (1977) Immunohistochemical evidence for a neurophysin-containing autonomic pathway in the paraventricular nucleus of the hypothalamus. *Brain Research* 128: 346–353.
- Swanson, L.W. (1992) *Brain Maps: Structure of the Rat Brain*. Amsterdam: Elsevier Press.
- Swanson, L.W. and Hartman, B.K. (1975) The central adrenergic system. An immunofluorescence study of the location of cell bodies and their efferent connections in the rat utilizing dopamine- β -hydroxylase as a marker. *Journal of Comparative Neurology* 163: 467–506.
- Swanson, L.W., Mogenson, G.J., Gerfen, C.R., and Robinson, P. (1984) Evidence for a projection from the lateral preoptic area and substantia innominata to the "mesencephalic locomotor region" in the rat. *Brain Research* 295: 161–178.
- Swanson, L.W., Mogenson, G.J., Simerly, R.B., and Wu, M. (1987) Anatomical and electrophysiological evidence for a projection from the medial preoptic area to the "mesencephalic and subthalamic locomotor regions" in the rat. *Brain Research* 405: 108–122.
- Szerb, J.C. (1967) Cortical acetylcholine release and electroencephalographic arousal. *Journal of Physiology (London)* 192: 329–345.
- Szymusiak, R. (1995) Magnocellular nuclei of the basal forebrain: substrates of sleep and arousal regulation. *Sleep* 18: 478–500.
- Szymusiak, R. and McGinty, D. (1986) Sleep-related neuronal discharge in the basal forebrain of cats. *Brain Research* 370: 82–92.

- Szymusiak, R., Alam, N., Steininger, T.L., and McGinty, D. (1998) sleep-waking discharge patterns of ventrolateral preoptic/anterior hypothalamic neurons in rats. *Brain Research* 803: 178–188.
- Szymusiak, R., Steininger, T., Alam, N., and McGinty, D. (2001) Preoptic area sleep-regulating mechanisms. *Archives Italiennes de Biologie* 139: 77–92.
- Taber, E. (1961) The cytoarchitecture of the brain stem of the cat. I. Brain stem nuclei of the cat. *Journal of Comparative Neurology* 116: 27–70.
- Taguchi, O., Kubin, L., and Pack, A.I. (1992) Evocation of postural atonia and respiratory depression by pontine carbachol in the decerebrate rat. *Brain Research* 595: 107–115.
- Taheri, S., Sunter, D., Dakin, C., Moyes, S., Seal, L., Gardiner, J., Rossi, M., Ghatei, M., and Bloom, S. (2000) Diurnal variation in orexin A immunoreactivity and prepro-orexin mRNA in the rat central nervous system. *Neuroscience Letters* 279: 109–112.
- Taishi, P., Bredow, S., Guha-Thakurta, N., Obal, F. Jr., and Krueger, J.M. (1997) Diurnal variations of interleukin-1 beta mRNA and beta-actin mRNA in rat brain. *Journal of Neuroimmunology* 75: 69–74.
- Takagi, H., Morishima, Y., Matsuyama, T., Hayashi, H., Watanabe, T., and Wada, H. (1986) Histaminergic axons in the neostriatum and cerebral cortex of the rat: a correlated light and electron microscopic immunocytochemical study using histidine decarboxylase as a marker. *Brain Research* 364: 114–123.
- Takahashi, S., Kapas, L., Seyer, J.M., Wang, Y., and Krueger, J.M. (1996) Inhibition of tumor necrosis factor attenuates physiological sleep in rabbits. *Neuroreport* 7: 642–646.
- Takakusaki, K. and Kitai, S.T. (1997) Ionic mechanisms involved in the spontaneous firing of tegmental pedunculopontine nucleus neurons of the rat. *Neuroscience* 78: 771–794.
- Takakusaki, K., Ohta, Y., and Mori, S. (1988a) Single medullary reticulospinal neurons exert postsynaptic inhibitory effects via inhibitory interneurons upon alpha-motoneurons innervating cat hindlimb muscles. *Experimental Brain Research* 201: 1–13.
- Takakusaki, K., Sakamoto, T., and Mori, S. (1988b) Chemical modulation of medullary output neurons which control excitability of hindlimb alpha-motoneurons in cats. *Society for Neuroscience Abstracts* 14: 180.
- Takakusaki, K., Shiroyama, T., and Kitai, S.T. (1997) Two types of cholinergic neurons in the rat tegmental pedunculopontine nucleus: electrophysiological and morphological characterization. *Neuroscience* 79: 1089–1109.
- Takeuchi, O. and Akira, S. (2001) Toll-like receptors; their physiological role and signal transduction system. *International Immunopharmacology* 1: 625–635.
- Takeuchi, Y., McLean, J.H., and Hopkins, D.A. (1982) Reciprocal connections between the amygdala and parabrachial nuclei: ultrastructural demonstration by degeneration and axonal transport of horseradish peroxidase in the cat. *Brain Research* 239: 583–588.
- Tanji, J. and Evarts, E.V. (1976) Anticipatory activity of motor cortex neurons in relation to direction of an intended movement. *Journal of Neurophysiology* 39: 1062–1068.
- Tebecis, A.K. (1972) Cholinergic and non-cholinergic transmission in the medial geniculate nucleus of the cat. *Journal of Physiology (London)* 226: 153–172.
- Terao, A., Matsumura, H., Yoneda, H., and Saito, M. (1998) Enhancement of slow-wave sleep by tumor necrosis factor alpha is mediated by cyclooxygenase-2 in rats. *Neuroreport* 9: 3791–3796.
- Thakkar, M., Strecker, R., and McCarley, R.W. (2002) Phasic but not tonic REM selective discharge of periaqueductal gray neurons in freely behaving animals: relevance to postulates of GABAergic inhibition of monoaminergic neurons. *Brain Research* 945: 276–280.
- Thakkar, M.M., Delgiacco, R.A., Strecker, R.E., and McCarley, R.W. (2003a) Adenosinergic inhibition of basal forebrain wakefulness – active neurons: a simultaneous unit recording and microdialysis study in freely behaving cats. *Neuroscience* 122: 1107–1113.
- Thakkar, M.M., Ramesh, V., Cape, E.G., Winston, S., Strecker, R.E., and McCarley, R.W. (1999) REM sleep enhancement and behavioral cataplexy following orexin (hypocretin) II receptor antisense perfusion in the pontine reticular formation. *Sleep Research Online* 2: 113–120.
- Thakkar, M.M., Ramesh, V., Strecker, R.E., and McCarley, R.W. (2001) Microdialysis perfusion of orexin-A in the basal forebrain increases wakefulness in freely behaving rats. *Archives Italiennes de Biologie* 139: 313–328.
- Thakkar, M.M., Strecker, R.E., and McCarley, R.W. (1998) Behavioral state control through differential serotonergic inhibition in the mesopontine cholinergic nuclei: a simultaneous unit recording and microdialysis study. *Journal of Neuroscience* 18: 5490–5497.
- Thakkar, M.M., Tao, R., Ma, Z., Winston, S., Yunren, B., and McCarley, R.W. (2004) GABA release in the mPRF: role in the regulation of sleep-wakefulness. *Sleep* 27.
- Thakkar, M.M., Winston, S., and McCarley, R.W. (2003b) A1 receptor and adenosinergic homeostatic regulation of sleep-wakefulness: effects of antisense to the A1 receptor in the cholinergic basal forebrain. *Journal of Neuroscience* 23: 4278–4287.

- Thannickal, T.C., Moore, R.Y., Nienhuis, R., Ramanathan, L., Gulyani, S., Aldrich, M., Cornford, M., and Siegel, J.M. (2000) Reduced number of hypocretin neurons in human narcolepsy. *Neuron* 27: 469–474.
- Thierry, A.M., Chevalier, G., Ferron, A., and Glowinski, J. (1983) Diencephalic efferents of the medial prefrontal cortex in the rat: electrophysiological evidence for the existence of branched neurons. *Experimental Brain Research* 50: 275–282.
- Thompson, S.H. (1977) Three pharmacologically distinct potassium channels in molluscan neurones. *Journal of Physiology (London)* 265: 465–488.
- Thomson, A.M. (1986) Comparison of responses to transmitter candidates at an *N*-methylaspartate receptor mediated synapse, in slices of rat cerebral cortex. *Neuroscience* 17: 37–47.
- Thomson, A.M. (1988a) Inhibitory postsynaptic potentials evoked in thalamic neurones by stimulation of the reticular nucleus evoke slow spikes. *Neuroscience* 25: 491–502.
- Thomson, A.M. (1988b) Biphasic responses of thalamic neurones to gamma-aminobutyric acid in isolated rat brain slices. *Neuroscience* 25: 503–512.
- Thomson, A.M. (1997) Activity-dependent properties of synaptic transmission at two classes of connections made by rat neocortical pyramidal axons *in vitro*. *Journal of Physiology (London)* 502: 131–147.
- Thomson, A.M., West, D.C., and Deuchars, J. (1995) Properties of single axon excitatory postsynaptic potentials elicited in spiny interneurons by action potentials in pyramidal neurons in slices of rat neocortex. *Neuroscience* 69: 727–738.
- Thomson, A.M., West, D.C., Hahn, J., and Deuchars, J. (1996) Single axon IPSPs elicited in pyramidal cells by three classes of interneurons in slices of rat neocortex. *Journal of Physiology (London)* 496: 81–102.
- Ticho, S.R. and Radulovacki, M. (1991) Role of adenosine in sleep and temperature regulation in the preoptic area of rats. *Pharmacology, Biochemistry and Behavior* 40: 33–40.
- Tigges, J. and Tigges, M. (1985) Subcortical sources of direct projections to visual cortex. In A. Peters and E.G. Jones, eds, *Cerebral Cortex*, vol. 3, pp. 351–378, New York: Plenum.
- Tigges, J., Tigges, M., Cross, N.A., McBride, R.L., Lethbetter, W.D., and Anschel, S. (1982) Subcortical structures projecting to visual cortical areas in squirrel monkey. *Journal of Comparative Neurology* 209: 29–40.
- Tigges, J., Walker, L.C., and Tigges, M. (1983) Subcortical projections to the occipital lobe and parietal lobes of the chimpanzee brain. *Journal of Comparative Neurology* 220: 106–115.
- Timofeev, I. and Steriade, M. (1996) Low-frequency rhythms in the thalamus of intact-cortex and decorticated cats. *Journal of Neurophysiology* 76: 4152–4168.
- Timofeev, I. and Steriade, M. (1997) Fast (mainly 30–100 Hz) oscillations in the cat cerebellothalamic pathway and their synchronization with cortical potentials. *Journal of Physiology (London)* 504: 153–168.
- Timofeev, I. and Steriade, M. (1998) Cellular mechanisms underlying intrathalamic augmenting responses of reticular and relay neurons. *Journal of Neurophysiology* 79: 2716–2729.
- Timofeev, I., Grenier, F., and Steriade, M. (2001b) Disfacilitation and active inhibition in the neocortex during the natural sleep–wake cycle: an intracellular study. *Proceedings of the National Academy of Sciences of the USA* 98: 1924–1929.
- Timofeev, I., Bazhenov, M., Sejnowski, T.J., and Steriade, M. (2001a) Contribution of intrinsic and synaptic factors in the desynchronization of thalamic oscillatory activity. *Thalamus & Related Systems* 1: 53–69.
- Timofeev, I., Contreras, D., and Steriade, M. (1996) Synaptic responsiveness of cortical and thalamic neurons during various phases of slow oscillation in cat. *Journal of Physiology (London)* 494: 265–278.
- Timofeev, I., Grenier, F., and Steriade, M. (1998) Spike-wave complexes and fast runs of cortically generated seizures. IV. Paroxysmal fast runs in cortical and thalamic neurons. *Journal of Neurophysiology* 80: 1495–1513.
- Timofeev, I., Grenier, F., Bazhenov, M., Sejnowski, T.J., and Steriade, M. (2000a) Origin of slow oscillations in deafferented cortical slabs. *Cerebral Cortex* 10: 1185–1199.
- Timofeev, I., Grenier, F., Bazhenov, M., Sejnowski, T.J., and Steriade, M. (2000b) Impact of intrinsic properties and synaptic factors on the activity of neocortical networks *in vivo*. *Journal of Physiology (Paris)* 94: 343–355.
- Timofeev, I., Grenier, F., Bazhenov, M., Houweling, A., Sejnowski, T.J., and Steriade, M. (2002) Short- and medium-term plasticity associated with augmenting responses in cortical slabs and spindles in intact cortex of cats *in vivo*. *Journal of Physiology (London)* 542: 583–598.
- Tohyama, M., Sakai, K., Salvetti, D., Touret, M., and Jouvett, M. (1979a) Spinal projections from the lower brain stem in the cat as demonstrated by the horseradish peroxidase technique. I. Origins of the reticulospinal tracts and their funicular trajectories. *Brain Research* 173: 383–403.
- Tohyama, M., Sakai, K., Salvetti, D., Touret, M., and Jouvett, M. (1979b) Spinal projections from the lower brain stem in the cat as demonstrated by the horseradish peroxidase technique. II. Projections from the dorsolateral pontine tegmentum and raphe nuclei. *Brain Research* 176: 215–231.

- Tork, I., Halliday, G., Scheibner, T., and Turner, S. (1984) The organization of the mesencephalic ventromedial tegmentum (VMT) in the cat. In R. Bandler, ed., *Modulation of Sensorimotor Activity during Alterations in Behavioural States*, pp. 39–73, New York: A. Liss.
- Tortella, F.C., Eschevaria, E., Pastel, R.H., Cox, B., and Blackburn, T.P. (1988) Differential effects of ICI 169,369 and ritanserin on 24 h EEG sleep patterns in rats. *British Journal of Pharmacology* 93: 196P.
- Torterolo, P., Morales, F.R., and Chase, M.H. (2002) GABAergic mechanisms in the pedunculopontine tegmental nucleus of the cat promote active (REM) sleep. *Brain Research* 944: 1–9.
- Trachsel, L., Tobler, I., and Borbély, A. (1988) Effect of ritanserin on sleep and sleep EEG in the rat. *European Sleep Research Society Abstracts* 6: 253.
- Traub, R.D. and Llinás, R. (1979) Hippocampal pyramidal cells: significance of dendritic ionic conductances for neuronal function and epileptogenesis. *Journal of Neurophysiology* 42: 476–496.
- Traub, R.D. and Wong, R.K.S. (1981) Penicillin-induced epileptiform activity in the hippocampal slice: a model of synchronization of CA3 pyramidal cell bursting. *Neuroscience* 6: 223–230.
- Traub, R.D., Miles, R., and Wong, R.K.S. (1989) Model of the origin of rhythmic population oscillations in the hippocampal slice. *Science* 243: 1319–1325.
- Traub, R.D., Miles, R., Wong, R.K.S., Schulam, L.S., and Schneiderman, J.H. (1987) Models of synchronized hippocampal bursts in the presence of inhibition. II. Ongoing spontaneous population events. *Journal of Neurophysiology* 58: 752–764.
- Trétiakoff, C. and Bremer, F. (1920) Encéphalite létargique avec syndrome Parkinsonien et catatonie. Rechute tardive. *Revue Neurologique (Paris)* 7: 772–775.
- Trivedi, P., Yu, H., MacNeil, D.J., Van der Ploeg, L.H.T., and Guan, X.M. (1998) Distribution of orexin receptor mRNA in the rat brain. *FEBS Letters* 438: 71–75.
- Trulson, M.E., Howell, G.A., Brandstetter, J.W., Fredrickson, M.H., and Fredrickson, C.J. (1982) *in vitro* recording of raphe unit activity: evidence for endogenous rhythms in presumed serotonergic neurons. *Life Sciences* 31: 785–790.
- Trulson, M.F. and Jacobs, B.L. (1979) Raphe unit activity in freely moving cats: correlation with level of behavioral arousal. *Brain Research* 163: 135–150.
- Trussell, L.O. and Jackson, M.B. (1985) Adenosine-activated potassium conductance in cultured striatal neurons. *Proceedings of the National Academy of Sciences of the USA* 82: 4857–4861.
- Trussell, L.O. and Jackson, M.B. (1987) Dependence of an adenosine-activated potassium current on a GTP-binding protein in mammalian central neurons. *Journal of Neuroscience* 7: 3306–3316.
- Tsumoto, T., Masui, H., and Sato, H. (1986) Excitatory amino acid transmitters in neuronal circuits of the cat visual cortex. *Journal of Neurophysiology* 55: 469–483.
- Uhlich, D.J., Manning, K.A., and Pienkowski, T.P. (1993) The histaminergic innervation of the lateral geniculate complex in the cat. *Visual Neuroscience* 10: 225–235.
- Umbriaco, D., Watkins, K.C., Descarries, L., Cozzari, C., and Hartman, B.K. (1994) Ultrastructural and morphometric features of the acetylcholine innervation in adult rat parietal cortex. An electron microscopic study in serial sections. *Journal of Comparative Neurology* 348: 351–373.
- Urade, Y. and Hayaishi, O. (1999) Prostaglandin D2 and sleep regulation. *Biochimica et Biophysica Acta* 1436: 606–605.
- Ursin, R. and Serman, M.B. (1981) *A Manual for Standardized Scoring of Sleep and Waking States in the Adult Cat*. Los Angeles: Brain Information Service/BRI UCLA.
- Uthgenannt, D., Schoolmann, D., Pietrowsky, R., Fehm, H.-L., and Born, J. (1995) Effects of sleep on the production of cytokines in humans. *Psychosomatic Medicine* 57: 97–104.
- Valverde, F. (1961) Reticular formation of the pons and medulla oblongata. A Golgi study. *Journal of Comparative Neurology* 116: 71–99.
- Valverde, F. (1962) Reticular formation of the albino rat's brain stem: cytoarchitecture and corticofugal connections. *Journal of Comparative Neurology* 119: 25–53.
- Van den Hoofdakker, R.H. and Beersma, D.G.M. (1985) On the explanation of short REM latencies in depression. *Psychiatric Research* 16: 155–163.
- van den Pol, A.N. (1999) Hypothalamic hypocretin (orexin): robust innervation of the spinal cord. *Journal of Neuroscience* 19: 3171–3182.
- van den Pol, A.N., Gao, X.B., Obrietan, K., Kilduff, T.S., and Belousov, A.B. (1998) Presynaptic and postsynaptic actions and modulation of neuroendocrine neurons by a new hypothalamic peptide, hypocretin/orexin. *Journal of Neuroscience* 18: 7962–7971.
- van den Pol, A.N., Ghosh, P.K., Liu, R.J., Li, Y., Aghajanian, G.K., and Gao, X.B. (2002) Hypocretin (orexin) enhances neuron activity and cell synchrony in developing mouse GFP-expressing locus coeruleus. *Journal of Physiology* 541: 169–185.
- Van der Kooy, D., Kuypers, H.G.J.M., and Catsman-Berrevoots, C.E. (1978) Single mammillary cell bodies with divergent axon collaterals. Demonstration by a simple, fluorescent retrograde double labeling technique in the rat. *Brain Research* 158: 189–196.

- Van der Loos, H. and Glaser, E.M. (1972) Autapses in neocortex cerebri: synapses between pyramidal cell's axon and its own dendrites. *Brain Research* 48: 355–360.
- Van Dongen, H.P.A., Maislin, G., Mullington, J.M., and Dinges, D.F. (2003) The cumulative cost of additional wakefulness: dose-response effects on neurobehavioral functions and sleep physiology from chronic sleep restriction and total sleep deprivation. *Sleep* 26: 117–126.
- Van Dongen, P.A.M. (1980) Locus coeruleus region: effects on behavior of cholinergic, noradrenergic and opiate drugs injected intracerebrally into freely moving cats. *Experimental Neurology* 67: 52–78.
- Van Gisbergen, J.A.M., Robinson, D.A., and Gielen, S. (1981) A quantitative analysis of generation of saccadic eye movements by burst neurons. *Journal of Neurophysiology* 45: 417–442.
- VanderMaelen, C.P. and Aghajanian, G.K. (1980) Intracellular studies showing modulation of facial motoneurone excitability by serotonin. *Nature* 287: 346–347.
- VanderMaelen, C.P. and Aghajanian, G.K. (1983) Electrophysiological and pharmacological characterization of serotonergic dorsal raphe neurons recorded extracellularly and intracellularly in rat brain slices. *Brain Research* 289: 109–119.
- Vanderwolf, C.H. and Robinson, T.E. (1981) Reticulo-cortical activity and behavior: a critique of the arousal theory and a new synthesis (with commentaries). *Behavioral and Brain Science* 4: 459–514.
- Vanni-Mercier, G., Sakai, K., and Jouvet, M. (1984) Neurones spécifiques de l'éveil dans l'hypothalamus postérieur du chat. *Comptes Rendus de l'Académie de Sciences (Paris)* 298: 195–200.
- Velasco, M., Velasco, F., Cepeda, C., and Romo, R. (1979) Effect of a push-pull perfusion of carbachol on the pontine reticular formation multiple unit activity. In P. Passouant and I. Oswald, eds., *Pharmacology of the States of Alertness*, pp. 231–233. New York: Pergamon Press.
- Velayos, J.L., Jimenez-Castellanos, J. Jr., and Reinoso-Suárez, F. (1989) Topographical organization of the projections from the reticular thalamic nucleus to the intralaminar and medial thalamic nuclei in the cat. *Journal of Comparative Neurology* 279: 457–469.
- Velazquez-Moctezuma, J., Gillin, J.C., and Shiromani, P.J. (1989) Effect of specific M1, M2 muscarinic receptor agonists on REM sleep generation. *Brain Research* 503: 128–131.
- Verrier, R. (1988) Behavioral state and myocardial excitability. In R. Lydic and J.F. Biebuyck, eds., *Clinical Physiology of Sleep*, pp. 31–51. Bethesda (MD): American Physiological Society.
- Vertes, R.P. (1977) Selective firing of rat pontine gigantocellular neurons during movement and REM sleep. *Brain Research* 128: 146–152.
- Vertes, R.P. (1981) An analysis of ascending brainstem systems involved in hippocampal synchronization and desynchronization. *Journal of Neurophysiology* 46: 1140–1159.
- Vertes, R.P. (1982) Brainstem generation of the hippocampal EEG. *Progress in Neurobiology* 19: 159–186.
- Vertes, R.P. (1984) Brainstem control of the events of REM sleep. *Progress in Neurobiology* 22: 241–288.
- Vertes, R.P. and Kocsis, B. (1997) Brainstem-diencephalo-septohippocampal systems controlling the theta rhythm of the hippocampus. *Neuroscience* 81: 893–926.
- Vertes, R.P. and Martin, G.F. (1988) Autoradiographic analysis of ascending projections from the pontine and mesencephalic reticular formation and the median raphe nucleus in the rat. *Journal of Comparative Neurology* 275: 511–541.
- Vertes, R.P., Martin, G.F., and Waltzer, R. (1986) An autoradiographic analysis of ascending projections from the medullary reticular formation in the rat. *Neuroscience* 19: 873–898.
- Vijayan, V.K. (1979) Distribution of cholinergic neurotransmitter enzymes in the hippocampus and the dentate gyrus of the adult and developing mouse. *Neuroscience* 4: 121–137.
- Villablanca, J. (1965) The electrocorticogram in the chronic *cerveau isolé* cat. *Electroencephalography and Clinical Neurophysiology* 19: 576–586.
- Villablanca, J. (1974) Role of the thalamus in sleep control: sleep–wakefulness studies in chronic diencephalic and athalamic cats. In O. Petre-Quadens and J.D. Schlag, eds., *Basic Sleep Mechanisms*, pp. 51–78. New York: Academic Press.
- Villis, T., Hepp, K., Schwarz, U., Henn, V., and Haas, H. (1987) Unilateral riMLF lesions impair saccade generation along specific vertical planes. *Society for Neuroscience Abstracts* 12: 1187.
- Vincent, S.R. and Reiner, P.B. (1987) The immunohistochemical localization of choline acetyltransferase in the cat brain. *Brain Research Bulletin* 18: 371–415.
- Vincent, S.R., Hökfelt, T., Skirboll, L.R., and Wu, J.-Y. (1983b) Hypothalamic gamma-aminobutyric acid neurons project to the neocortex. *Science* 220: 1309–1311.
- Vincent, S.R., Satoh, K., Armstrong, D.M., and Fibiger, H.C. (1983a) Substance P in the ascending cholinergic reticular system. *Nature* 306: 688–691.
- Vincent, S.R., Satoh, K., Armstrong, D.M., Panula, P., Vale, W., and Fibiger, H.C. (1986) Neuropeptides and NADPH-diaphorase activity in the ascending cholinergic reticular system of the rat. *Neuroscience* 17: 167–182.
- Virus, R.M., Djuricic-Nedelson, M., Radulovacki, M., and Green, R.D. (1983) The effects of adenosine and 2'-doxycyformycin on sleep and wakefulness in rats. *Neuropharmacology* 22: 1401–1404.

- Vitkovic, L., Bockaert, J., and Jacque, C. (2000) "Inflammatory" cytokines: neuromodulators in normal brain? *Journal of Neurochemistry* 74: 457–471.
- Vivaldi, E., McCarley, R.W., and Hobson, J.A. (1980) Evocation of desynchronized sleep signs by chemical microstimulation of the pontine brain stem. In J.A. Hobson and M.A.B. Brazier, eds., *The Reticular Formation Revisited*, pp. 513–529, New York: Raven Press.
- Vizi, E.S. and Kiss, J.P. (1998) Neurochemistry and pharmacology of the major hippocampal transmitter systems: synaptic and nonsynaptic interactions. *Hippocampus* 8: 566–607.
- Vogel, G. (1960) Studies in the psychophysiology of dreams III. The dream of narcolepsy. *Archives of General Psychiatry* 3: 421–425.
- Vogel, G. (1989) Sleep variables and the treatment of depression. In M.H. Kryger, T. Roth, and W.C. Dement, eds., *Principles and Practices of Sleep Medicine*, pp. 419–420, New York: Saunders.
- Vogel, G.W., Vogel, F., McAbee, R.S., and Thurmond, A.J. (1980) Improvement of depression by REM sleep deprivation. New findings and a theory. *Archives of General Psychiatry* 37: 247–253.
- Volterra, V. (1931) *Leçons sur la théorie mathématique de la lutte pour la vie*. Paris: Gauthier-Villars et Cie.
- von Economo, C. (1929) Schlaftheorie. *Ergebnisse der Physiologie* 28: 312–339.
- von Economo, C. (1930) Sleep as a problem of localization. *Journal of Nervous Mental Disorders* 71: 249–259.
- von Krosigk, M., Bal, T., and McCormick, D.A. (1993) Cellular mechanisms of a synchronized oscillation in the thalamus. *Science* 261: 361–364.
- von Lubitz, D.K. (1999) Adenosine and cerebral ischemia: therapeutic future or death of a brave concept? *European Journal of Pharmacology* 365: 9–25.
- Voorn, P., Jorritsma-Byham, B., Van Dijk, C., and Buijs, R.M. (1986) The dopaminergic innervations of the ventral striatum in the rat: a light- and electron microscopical study with antibodies against dopamine. *Journal of Comparative Neurology* 251: 84–99.
- Wada, J.A. and Terao, A. (1970) Effect of parachlorophenylalanine on basal forebrain stimulation. *Experimental Neurology* 28: 501–506.
- Wainer, B.H. and Mesulam, M.-M. (1990) Ascending cholinergic pathways in the rat brain. In M. Steriade and D. Biesold, eds., *Brain Cholinergic Systems*, pp. 65–119. Oxford: Oxford Univ. Press.
- Walker, L.C., Kitt, C.A., DeLong, M.R., and Price, D.L. (1985) Noncollateral projections of basal forebrain neurons to frontal and parietal neocortex in primates. *Brain Research Bulletin* 15: 307–314.
- Walter, W.G., Cooper, R., Aldridge, V.J., McCallum, W.C., and Winter, A.L. (1964) Contingent negative variation: an electric sign of sensorimotor association and expectancy in the human brain. *Nature* 203: 380–384.
- Walton, K. and Fulton, B.P. (1986) Ionic mechanisms underlying the firing properties of rat neonatal motoneurons studied *in vitro*. *Neuroscience* 19: 669–683.
- Walton, K. and Llinás, R. (1986) Calcium-dependent low threshold rebound potentials and oscillatory potentials in neonatal rat spinal motoneurons *in vitro*. *Society for Neuroscience Abstracts* 12: 382.
- Waltzer, R. and Martin, G.F. (1984) Collateralization of reticulospinal axons from the nucleus reticularis gigantocellularis to the cerebellum and diencephalon. A double-labeling study in the rat. *Brain Research* 293: 153–158.
- Wang, R.Y. and Aghajanian, G.K. (1977) Physiological evidence for habenula as major link between forebrain and midbrain raphe. *Science* 197: 89–91.
- Wang, X.J. and Rinzel, J. (1993) Spindle rhythmicity in the reticularis thalami nucleus: synchronization among mutually inhibitory neurons. *Neuroscience* 53: 899–904.
- Wang, Z. and McCormick, D.A. (1993) Control of firing mode of corticotectal and corticopontine layer V burst-generating neurons by norepinephrine, acetylcholine and 1S, 3R-ACPD. *Journal of Neuroscience* 13: 2199–2216.
- Waterhouse, B.D. and Woodward, D.J. (1980) Noradrenergic modulation of somatosensory cortical neuronal responses to iontophoretically applied putative neurotransmitters. *Experimental Neurology* 69: 30–49.
- Waterhouse, B.D., Moises, H.C., and Woodward, D.J. (1981) Alpha-receptor mediated facilitation of somatosensory cortical neuronal responses to excitatory synaptic inputs and iontophoretically applied acetylcholine. *Neuropharmacology* 20: 907–920.
- Waterhouse, B.D., Moises, H.C., Yeh, H.H., and Woodward, D.J. (1982) Norepinephrine enhancement of inhibitory synaptic mechanisms in cerebellum and cerebral cortex: mediation by beta adrenergic receptors. *Journal of Pharmacology and Experimental Therapy* 221: 495–506.
- Watkins, J.C. and Evans, R.H. (1981) Excitatory amino acid transmitters. *Annual Reviews of Pharmacology and Toxicology* 21: 165–204.
- Watkins, J.C. and Olverman, H.J. (1987) Agonist and antagonists for excitatory amino acid receptors. *Trends in Neurosciences* 10: 265–272.
- Watson, R.T., Heilman, B.D., Miller, B.D., and King, F.A. (1974) Neglect after mesencephalic reticular formation lesions. *Neurology* 24: 294–298.

- Webster, H.H. and Jones, B.E. (1988) Neurotoxic lesions of the dorsolateral pontomesencephalic tegmentum cholinergic area in the cat. II. Effects upon sleep-waking states. *Brain Research* 458: 285–302.
- Wehr, T.A., Wirz-Justice, A., Goodwin, F.K., Duncan, W., and Gillin, J.C. (1979) Phase advance of the circadian sleep-wake cycle as an antidepressant. *Science* 206: 710–713.
- Weitzmann, E. (1961) A note on the EEG and eye movements during behavioral sleep in monkeys. *Electroencephalography and Clinical Neurophysiology* 13: 790–794.
- Wenk, G.L. (1997) The nucleus basalis magnocellularis cholinergic system: one hundred years of progress. *Neurobiology of Learning and Memory* 67: 85–95.
- Westbrook, G.L. and Mayer, M.L. (1987) Micromolar concentrations of zinc antagonize NMDA and GABA responses of hippocampal neurons. *Nature* 328: 640–643.
- Westman, J. and Bowsher, D. (1971) Ultrastructural observations on the degeneration of spinal afferents to the nucleus medullae oblongatae centralis (pars caudalis) of the cat. *Brain Research* 26: 395–398.
- Weyand, T.G., Boudreaux, M., and Guido, W. (2001) Burst and tonic response modes in thalamic neurons during sleep and wakefulness. *Journal of Neurophysiology* 85: 1107–1118.
- Wikler, A. (1952) Pharmacologic dissociation on behavior and EEG sleep patterns in dogs: morphine, N-allylnormorphine and atropine. *Proceedings of the Society for Experimental Biology of New York* 79: 261–265.
- Wiklund, L. and Cuénod, M. (1984) Differential labeling of afferents to thalamic centromedian-parafascicular nuclei with ^3H -choline and D- ^3H -aspartate: further evidence for transmitter specific retrograde labeling. *Neuroscience Letters* 46: 275–281.
- Wiklund, L., Léger, L., and Persson, M. (1981) Monoamine cell distribution in the cat brain stem. A fluorescence histochemical study with quantification of indolaminergic and locus coeruleus cell groups. *Journal of Comparative Neurology* 203: 613–647.
- Wilcox, K.S., Grant, S.J., Burkhart, B.A., and Cristoph, G.R. (1989) *In vivo* electrophysiology of neurons in the lateral dorsal tegmental nucleus. *Brain Research Bulletin* 22: 557–560.
- Wilcox, K.S., Gutnick, M.J., and Cristoph, G.R. (1988) Electrophysiological properties of neurons in the lateral habenular nucleus: an *in vitro* study. *Journal of Neurophysiology* 59: 212–225.
- Wilder, M.B., Farley, G.R., and Starr, A. (1981) Endogenous late positive component of the evoked potential in cats corresponding to P300 in humans. *Science* 211: 605–607.
- Wiley, R.G., Oelmann, T.N., and Lappi, D.A. (1991) Immunolesioning: selective destruction of neurons using immunotoxin to rat NGF receptor. *Brain Research* 562: 149–153.
- Wilkinson, L.O., Auerbach, S.B., and Jacobs, B.L. (1991) Extracellular serotonin levels change with behavioral state but not with pyrogen-induced hyperthermia. *Journal of Neuroscience* 11: 2732–2741.
- Williams, J.A. and Reiner, P.B. (1993) Noradrenaline hyperpolarizes identified rat mesopontine cholinergic neurons *in vitro*. *Journal of Neuroscience* 13: 3878–3883.
- Williams, J.A., Comisarow, J., Day, J., Fibiger, H.C., and Reiner, P.B. (1994) State-dependent release of acetylcholine in rat thalamus measured by *in vivo* microdialysis. *Journal of Neuroscience* 14: 5236–5242.
- Williams, J.T. (1988) Amino acid synaptic neurotransmission in locus coeruleus: effects of field stimulation *in vitro*. *Society for Neuroscience Abstracts* 14: 151.
- Williams, J.T. and Marshall, K.C. (1987) Membrane properties and adrenergic responses in Locus Coeruleus neurons of young rats. *Journal of Neuroscience* 7: 3687–3694.
- Williams, J.T. and North, R.A. (1985) Catecholamine inhibition of calcium action potentials in rat locus coeruleus neurones. *Neuroscience* 14: 103–109.
- Williams, J.T., Colmers, W.F., and Pan, Z.Z. (1988b) Voltage- and ligand-activated inwardly rectifying currents in dorsal raphe neurons *in vitro*. *Journal of Neuroscience* 8: 3499–3506.
- Williams, J.T., Henderson, G., and North, R.A. (1985) Characterization of α_2 -adrenoceptors which increase potassium conductance in rat locus coeruleus neurones. *Neuroscience* 14: 95–101.
- Williams, J.T., North, R.A., and Tokimasa, T. (1988a) Inward rectification of resting and opiate-activated potassium currents in rat locus coeruleus neurones. *Journal of Neuroscience* 8: 4299–4306.
- Williams, J.T., North, R.A., Shefner, S.A., Nishi, S., and Egan, T.M. (1984) Membrane properties of rat locus coeruleus neurones. *Neuroscience* 13: 137–156.
- Williams, M. (1989) Adenosine: the prototypical modulator. *Neurochemistry International* 14: 249–264.
- Williams, S.R., Turner, J.P., Tóth, T.I., Hughes, S.W., and Crunelli, V. (1997) The “window” component of the low threshold Ca^{2+} current produces input signal amplification and bistability in cat and rat thalamocortical neurones. *Journal of Physiology (London)* 505: 689–705.
- Willis, W.D., Kenshalo, D.R., and Leonard, R.B. (1979) The cells of origin of the primate spinothalamic tract. *Journal of Comparative Neurology* 188: 543–574.
- Wilson, F.A. and Rolls, E.T. (1990) Learning and memory is reflected in the response of reinforcement-related neurons in the primate basal forebrain. *Journal of Neuroscience* 10: 1254–1267.

- Wilson, M.A. and McNaughton, B.L. (1994) Reactivation of hippocampal ensemble memories during sleep. *Science* 265: 676–679.
- Wilson, P.M. (1985) A photographic perspective on the origin, form, course and relations of the acetylcholinesterase-containing fibers of the dorsal tegmental pathways in the rat brain. *Brain Research Reviews* 10: 85–118.
- Wise, S.P., Weinrich, M., and Mauritz, K.H. (1983) Motor aspects of cue-related neuronal activity in pre-motor cortex of the rhesus monkey. *Brain Research* 260: 301–305.
- Wohlberg, C. J., Davidoff, R.A., and Hackman, J.C. (1986) Analysis of the responses of frog motoneurons to epinephrine and norepinephrine. *Neuroscience Letters* 69: 150–155.
- Wolfe, B.B., Harden, T.K., Sporn, J.R., and Molinoff, P.B. (1978) Presynaptic modulation of beta adrenergic receptors in rat cerebral cortex after treatment with antidepressants. *Journal of Pharmacology and Experimental Therapy* 207: 446–457.
- Woody, C.D., Bartfai, T., Gruen, E., and Nairn, A.C. (1986) Intracellular injection of cGMP-dependent protein kinase results in increased input resistance in neurons of the mammalian motor cortex. *Brain Research* 386: 379–385.
- Woody, C.D., Swartz, B.E., and Gruen, E. (1978) Effects of acetylcholine and cyclic GMP on input resistance of cortical neurons in awake cats. *Brain Research* 158: 373–395.
- Woolf, N.J. and Butcher, L.L. (1986) Cholinergic systems in the rat brain. III. Projections from the pontomesencephalic tegmentum to the thalamus, tectum, basal ganglia and basal forebrain. *Brain Research Bulletin* 16: 603–637.
- Woolf, N.J., Hernit, M.C., and Butcher, L.L. (1986) Cholinergic and non-cholinergic projections from the rat basal forebrain revealed by combined choline acetyltransferase and *Phaseolus vulgaris* leucoagglutinin immunohistochemistry. *Neuroscience Letters* 66: 281–286.
- Woolf, N.J., Gould, E., and Butcher, L.L. (1989) Nerve growth factor receptor is associated with cholinergic neurons of the basal forebrain but not the pontomesencephalon. *Neuroscience* 30: 143–152.
- Wouterlood, F.G. and Groenewegen, H.J. (1984) Neuroanatomical tracing by use of *Phaseolus vulgaris* leucoagglutinin (PHA-L): electron microscopy of PHA-L-filled neuronal somata, dendrites, axons and axon terminals. *Brain Research* 326: 188–191.
- Wright, J.J. and Craggs, M.D. (1978) Changed cortical activation and lateral hypothalamic syndrome: a study in the split-brain cat. *Brain Research* 151: 632–636.
- Wurtz, R.H. and Mohler, C.W. (1976) Enhancement of visual response in monkey striate cortex and frontal eye fields. *Journal of Neurophysiology* 39: 766–772.
- Wurtz, R.H., Goldberg, M.E., and Robinson, D.L. (1980) Behavioral modulation of visual responses in the monkey: stimulus selection for attention and movement. In J.M. Sprague and A.N. Epstein, eds., *Progress in Psychobiology and Physiological Psychology*, vol. 9, pp. 43–83, New York: Academic Press.
- Wurtz, R.H., Richmond, B.J., and Newsome, W.T. (1984) Modulation of cortical visual processing by attention, perception and movements. In G.M. Edelman, W.E. Gall and W.M. Cowan, eds., *Dynamic Aspects of Neocortical Function*, eds. pp. 195–217, New York: Wiley-Interscience.
- Wyziński, P.W., McCarley, R.W., and Hobson, J.A. (1978) Discharge properties of pontine reticulo-spinal neurons during the sleep–waking cycle. *Journal of Neurophysiology* 41: 821–834.
- Xi, M.C., Morales, F.R., and Chase, M.H. (1999) A GABAergic pontine reticular system is involved in the control of wakefulness and sleep. *Sleep Research Online* 2: 43–48.
- Xi, M.C., Morales, F.R., and Chase, M.H. (2001) Induction of wakefulness and inhibition of active (REM) sleep by GABAergic processes in the nucleus pontis oralis. *Archives Italiennes de Biologie* 139: 125–145.
- Xie, Q., Kashiwabara, Y., and Nathan, C. (1994). Role of transcription factor NF- κ B/Rel in induction of nitric oxide synthase. *Journal of Biological Chemistry* 269: 4705–4708.
- Yaari, Y., Hamon, B., and Lux, H.D. (1987) Development of two types of calcium channels in cultured mammalian hippocampal neurons. *Science* 235: 680–682.
- Yakel, J.L., Trussell, L.O., and Jackson, M.B. (1988) Three serotonin responses in cultured mouse hippocampal and striatal neurons. *Journal of Neuroscience* 8: 1273–1285.
- Yamada, T., Kameyama, S., Fuchigami, Y., Nakazumi, Y., Dickins, Q.S., and Kimura, J. (1988) Changes of short latency somatosensory evoked potentials in sleep. *Electroencephalography and Clinical Neurophysiology* 70: 126–136.
- Yamamoto, C. (1974) Electrical activity recorded from thin sections of the lateral geniculate body, and the effects of 5-hydroxytryptamine. *Experimental Brain Research* 19: 271–281.
- Yamamoto, K., Arakawa, T., Taketani, Y., Takahashi, Y., Hayashi, Y., Ueda, N., Yamamoto, S., and Kumegawa, M. (1997). TNF-dependent induction of cyclooxygenase-2 mediated by NF- κ B and NF-IL6. *Advances in Experimental Medicine & Biology* 407: 185–189.

- Yamamoto, K., Mamelak, A., Quattrochi, J., and Hobson, J.A. (1988) Localization of a D sleep induction site with short latency by microinjection of carbachol in a head-restrained cat. *Society for Neuroscience Abstracts* 14: 1307.
- Yamamoto, T., Samejima, A., and Oka, H. (1986) An intracellular analysis of the entopeduncular inputs on the centre median—parafascicular complex in cats. *Brain Research* 348: 343–347.
- Yamashita, H., Inenaga, K., and Kannan, H. (1987) Depolarizing effect of noradrenaline on neurons of the rat supraoptic nucleus *in vitro*. *Brain Research* 405: 348–352.
- Yamoaka, S. (1978) Participation of limbic-hypothalamic structures in circadian rhythm of slow wave sleep and paradoxical sleep in the rat. *Brain Research* 151: 255–268.
- Yang, L., Lindholm, K., Konishi, Y., Li, R., and Shen, Y. (2002) Target depletion of distinct tumor necrosis factor receptor subtypes reveals hippocampal neuron death and survival through different signal transduction pathways. *Journal of Neuroscience* 22: 3025–3032.
- Yang, Q.Z. and Hatton, G.I. (1997) Electrophysiology of excitatory and inhibitory afferents to rat histaminergic tuberomammillary nucleus neurons from hypothalamic and forebrain sites. *Brain Research* 773: 162–172.
- Yao, S.Y., Ng, A.M., Muzyka, W.R., Griths, M., Cass, C.E., Baldwin, S.A., and Young, J.D. (1997) Molecular cloning and functional characterization of nitrobenzylthioinosine (NBMPR)-sensitive (es) and NBMPR-insensitive (ei) equilibrative nucleoside transporter proteins (rENT1 and rENT2) from rat tissues. *Journal of Biological Chemistry* 272: 423–428.
- Yao, S.Y., Ng, A.M., Vickers, M.F., Sundaram, M., Cass, C.E., Baldwin, S.A., and Young, J.D. (2002) Functional and molecular characterization of nucleobase transport by recombinant human and rat equilibrative nucleoside transporters 1 and 2. Chimeric constructs reveal a role for the ENT2 helix 5–6 region in nucleobase translocation. *Journal of Biological Chemistry* 277: 24938–24948.
- Yarom, Y., Sugimori, M., and Llinás, R. (1985) Ionic currents and firing patterns of mammalian vagal motoneurons *in vitro*. *Neuroscience* 16: 719–737.
- Yen, C.T. and Jones, E.G. (1983) Intracellular staining of physiologically identified neurons and axons in the somatosensory thalamus of the cat. *Brain Research* 280: 148–154.
- Yen, C.T., Conley, M., Hendry, S.H.C., and Jones, E.G. (1985) The morphology of physiologically identified GABAergic neurons in the somatic sensory part of the thalamic reticular nucleus in the cat. *Journal of Neuroscience* 5: 2254–2268.
- Yingling, C.D. and Skinner, J.E. (1975) Regulation of unit activity in nucleus reticularis thalami by the mesencephalic reticular formation and the frontal cortex. *Electroencephalography and Clinical Neurophysiology* 39: 635–642.
- Yingling, C.D. and Skinner, J.E. (1977) Gating of thalamic input to cerebral cortex by nucleus reticularis thalami. In J.E. Desmedt, ed., *Attention, Voluntary Contraction and Event-Related Potentials, Progress in Clinical Neurophysiology*, vol. 1, pp. 70–96, Basel: Karger.
- Ylinen, A., Bragin, A., Nádasdy, Z., Jando, G., Szabo, I., Sik, A., and Buzsáki, G. (1995) Sharp wave-associated high-frequency oscillation (200 Hz) in the intact hippocampus: network and intracellular mechanisms. *Journal of Neuroscience* 15: 30–46.
- Yoshida, H., Peterfi, Z., García-García, F., Kirkpatrick, R., Yasuda, T., and Krueger, J.M. (2004) State-specific asymmetries in EEG slow wave activity induced by local application of TNF. *Brain Research* 1009: 129–136.
- Yoshida, K., McCrea, R., Berthoz, A., and Vidal, P.P. (1981) Properties of immediate premotor inhibitory burst neurons controlling horizontal rapid eye movements in the cat. In A.F. Fuchs and W. Becker, eds., *Progress in Oculomotor Research*, eds. pp. 71–80. New York: Elsevier/North-Holland.
- Yoshida, Y., Fujiki, N., Nakajima, T., Ripley, B., Matsumura, H., Yoneda, H., Mignot, E., and Nishino, S. (2001) Fluctuation of extracellular hypocretin-1 (orexin A) levels in the rat in relation to the light-dark cycle and sleep-wake activities. *European Journal of Neuroscience* 14: 1075–1081.
- Yoshimura, M. and Higashi, H. (1985) 5-hydroxytryptamine mediates inhibitory postsynaptic potentials in rat dorsal raphe neurons. *Neuroscience Letters* 53: 69–74.
- Yoshimura, M., Polosa, C., and Nishi, S. (1987) Slow IPSP and the noradrenaline-induced inhibition of the cat sympathetic preganglionic neuron *in vitro*. *Brain Research* 419: 383–386.
- Yoss, R.E. and Daly, D.D. (1957) Criteria for the diagnosis of the narcoleptic syndrome. *Proceedings of Staff Meetings in Mayo Clinic* 32: 320–328.
- Young, W.S. and Kuhar, M.J. (1980) Noradrenergic alpha 1 and alpha 2 receptors: light microscopic autoradiographic localization. *Proceedings of the National Academy of Sciences of the USA* 77: 1696–1700.
- Záborsky, L., Cullinan, W.E., and Braun, A. (1991) Afferents to basal forebrain cholinergic projection neurons: an update. In T.C. Napier, P.W. Kalivas, and I. Hanin, eds., *The Basal Forebrain*, pp. 43–100, New York: Plenum.

- Záborsky, L., Heimer, L., Eckenstein, F., and Leranth, C. (1986) GABAergic input to cholinergic forebrain neurons: an ultrastructural study using retrograde tracing of HRP and double immunolabeling. *Journal of Comparative Neurology* 250: 282–295.
- Zaborsky, L., Pang, K., Somogyi, J., Nadasdy, Z., and Kallo, I. (1999) The basal forebrain corticopetal system revisited. *Annals of the New York Academy of Sciences* 877: 339–367.
- Zarcone, V.P., Benson, K.L., and Berger, P.A. (1987) Abnormal rapid eye movement latencies in schizophrenia. *Archives of General Psychiatry* 44: 45–48.
- Zarcone, V.P. (1989) Sleep abnormalities in schizophrenia. In M.H. Kryger, T. Roth, and W.C. Dement, eds., *Principles and Practices of Sleep Medicine*, pp. 422–423, New York: Saunders.
- Zemlan, F.B., Behbehani, M.M., and Beckstead, R.M. (1984) Ascending and descending projections from nucleus reticularis magnocellularis and nucleus reticularis gigantocellularis: an autoradiographic and horseradish peroxidase study in the rat. *Brain Research* 292: 207–220.
- Zhang, J., Obal, F. Jr., Zheng, T., Fang, J., Taishi, P., and Krueger, J.M. (1999) Intrapreoptic microinjection of GHRH or its antagonist alters sleep in rats. *Journal of Neuroscience* 19: 2187–2194.
- Zhang, J.H., Sampogna, S., Morales, F.R., and Chase, M.H. (2004) Distribution of hypocretin (orexin) immunoreactivity in the feline pons and medulla. *Brain Research* 995: 205–217.
- Zhu, J.J., Lytton, W.W., Xue, J.T., and Uhlich, D.J. (1999a) An intrinsic oscillation in interneurons of the rat lateral geniculate nucleus. *Journal of Neurophysiology* 81: 702–711.
- Zhu, J.J., Uhlich, D.J., and Lytton, W.W. (1999b) Burst firing in identified rat geniculate interneurons. *Neuroscience* 91: 1445–1460.
- Ziegelsgänsberger, W. and Puil, E.A. (1973) Actions of glutamic acid on spinal neurones. *Experimental Brain Research* 17: 35–49.
- Ziegelsgänsberger, W. and Reiter, C.H. (1974) A cholinergic mechanism in the spinal cord of cats. *Neuropharmacology* 13: 519–527.
- Zulley, J. (1979) *Der Einfluss von Zeitgebern auf den Schlaf des Menschen*. Frankfurt: Rita G. Fischer Verlag.
- Zulley, J. (1980) Distribution of REM sleep in entrained 24 hour and free-running sleep–wake cycles. *Sleep* 2: 377–389.
- Zulley, J., Wever, R., and Aschoff, J. (1981) The dependence of onset and duration of sleep on the circadian rhythm of rectal temperature. *Pflügers Archives* 391: 314–318.

Index

- Abducens nerve, 116
 - discharge frequencies during saccade, 419
 - gaze control, 438, 439
 - LDT and PPT neuron distribution, 108
 - nonreticular brainstem projections to, 424–426, 427
 - omnipause neurons, 428
 - pontobulbar reticular projections to, 424
- Absence seizures (petit mal epilepsy), 327
- accelerando-decelerando* pattern, thalamic reticular neurons, 194–195, 196
- acceleration synchronatrice*, 4
- Accumbens nucleus, 88, 132
- Acetylcholine, 55, 61, 355, 359, 363;
 - see also* Cholinergic neurons; Cholinergic nuclei
 - basal forebrain-brainstem connections, 74
 - brainstem neurons, actions of, 212–235
 - basal forebrain, 223
 - hippocampus, 234–235
 - locus coeruleus, 219, 221–223
 - medial pontine reticular formation, 212–219
 - neocortex, 231–234
 - pedunculopontine tegmental cholinergic neurons, 219, 220
 - thalamus, 223–231
 - cholinergic abnormalities in depression, 552
 - cholinergic inputs to PFTG, 110
 - cholinergic neurons in NB nucleus, 394
 - excitatory amino acids and, 253
 - immunohistochemistry, 45
 - intracellular studies
 - excitatory responses, 352
- Acetylcholine-norepinephrine interactions,
 - REM-on and REM-off neuron interaction sites, 501
- Acetylcholinesterase, 23, 260
 - immunohistochemistry, 46
- Acetyl-methylcholine, 226
- Acoustic nerve, spinoreticular pathways, 66
- Action potentials, *see also* Electrophysiology,
 - intrinsic properties
 - extracellular recordings, 351
 - recruitment within reticular pool, 480, 481
 - thalamocortical system, repetitive callosal stimulation and, 341
- Activation
 - historical developments and changing concepts, 4, 5, 11–20
 - inhibitory response during, 378–380
 - long-term, intracellular studies of excitatory responses, 359
 - thalamus and cerebral cortex, *see* Neuronal activities, brainstem and basal forebrain structures
- Activation threshold, medial pontine reticular formation neurons, 160
- Active sleep, historical developments and changing concepts, 24–30
- Active states, thalamocortical system,
 - spontaneous firing modes during, 346–347, 348
- A-current, medial pontine reticular formation neurons, 162–163, 164
- Adenosine, 562–584
 - behavioral alterations, 583–584
 - homeostatic control of sleep, 562–565, 566
 - IL-1 β and, 588
 - neurophysiological mechanisms, 570
 - potassium conductance in cultured cells, 217
 - receptor coupled signal transduction and transcriptional modulation, 576–583
 - receptor mediation of effects
 - A1 subtype, 571–574
 - A2A subtype, 574–576
 - signal transduction and transcriptional modulation, 576–583
 - receptor subtypes, 571–576
 - site specificity and sources after prolonged wakefulness, 565, 567–570
 - VLPO and, 598–600

- Adrenergic-cholinergic interactions
 - modeling REM sleep in depression, 549
 - and muscle tone, 459
- Adrenergic receptors, 236–237, 238, 239
 - basal forebrain, 244–245
 - dorsal raphe nucleus, 243
 - electrophysiology, *see*
 - Norepinephrine/norepinephrinergic systems
 - extracellular recordings, alpha-1 receptors, 351
 - locus coeruleus, 87, 238–245
 - neocortex, 245–246
 - pontine reticular formation, 243–344
 - thalamus, 245–246
- Afterhyperpolarization (AHP), 164, 305
- Alertness, 73, 256
- Alpha motoneurons, spinal, muscle atonia of
 - REM sleep, 446–452
- Alpha rhythms, origins of, 256–257
- Alzheimer's patients, 23
- Amines
 - modeling REM sleep in depression, 547, 548
 - ventral tegmental area, 88
- Amino acid transmitters, *see* Excitatory amino acids
- Aminoclonidine, 243
- Aminophosphonovaleric acid, 251
- Amygdala, 153
 - augmenting response, 336
 - brainstem-thalamic neurons implicated in tonic
 - electrical activation of cerebrum, 383
 - connections
 - basal forebrain, 74
 - dopaminergic, 132
 - locus coeruleus, 85
 - locus coeruleus efferents, 129
 - NB inputs, 89
 - substantia innominata neurons, 89
 - tuberomammillary area afferents, 88
 - ventral tegmental area afferents, 88
 - electrophysiological properties, intrinsic, 208–209
- Anatomical connections, 56–85
 - basal forebrain cholinergic nuclei, afferents to, 88–90
 - modulatory systems, 89–90
 - systematization of cholinergic nuclei, 88–89
 - basal forebrain efferents, 133–138
 - to brainstem cholinergic nuclei, 73–76
 - cortical projections, 133–134
 - posterior hypothalamic projections, 137–138
 - thalamic projections, 134–137
 - brainstem cholinergic nuclei, afferents to, 56–85
 - convergent inputs onto single brainstem reticular neurons, 76–78
 - from basal forebrain and related systems, 73–76
 - from hypothalamic areas, 72–73
 - from intrabrainstem sources, 78
 - from neocortical areas, 76
- Anatomical connections *contd.*
 - from spinal cord and sensory cranial nerves, 63–68
 - from thalamic nuclei, 68–72
 - nuclei with unidentified transmitters, 61–63
 - systematization of cholinergic nuclei, 56–61
 - to midbrain and bulbar reticular formation, 82–85
 - to pontine reticular formation, 78–82, 83
 - brainstem cholinergic nuclei, efferents, 90–128
 - brainstem and spinal cord projections of
 - mesopontine cholinergic and pontobulbar nuclei, 106–117
 - intrinsic cell morphology and projections of
 - pontine and bulbar gigantocellular fields, 117–128
 - rostral projection of cholinergic and noncholinergic nuclei and classical reticular fields, 91–106
 - brainstem monoaminergic nuclei, afferents to, 85–88
 - locus coeruleus, 85–87
 - raphe nuclei, 87
 - tuberomammillary area, 88
 - ventral tegmental area, 87–88
 - diffuse modulatory system targets, *see also*
 - Diffuse modulatory systems, targets of
 - neocortex, 145–153
 - thalamus, 141–142
 - monoamine-containing neurons, efferent connections, 128–133
 - dopaminergic systems, 132
 - histaminergic systems, 133
 - norepinephrinergic systems, 128–130
 - serotonergic systems, 130–132
 - neurotransmitter-modulated brainstem currents, *see* Neurotransmitter-modulated currents
- Anatomic connectivity criterion,
 - neuromodulation of REM sleep, 482
- Anterior hypothalamus/preoptic area,
 - GHRH-containing neurons, 591–592
- Anterograde tracing methods, 39–44
- Antidepressants, 550–552
- 4-AP-sensitive conductance, 162–163, 164, 166, 176
- Arcade cells, 148
- Archicortex, 139
- Arcuate nucleus, 590, 591
- Arousal, 4
 - extracellular recordings, 352
 - fast (beta/gamma) oscillations, 262–263
 - historical developments and changing concepts, 13
 - midbrain reticular noncholinergic neurons and, 384
 - neuropeptides and, 58
 - and thalamic output, 349
 - transition to state of, 13

- Aspartate, 99, 146–147, 254
- Association, thalamic function, 141
- Associational nuclei, 93, 95–96
- Association cortex
- circuitry, 148
 - hippocampal trisynaptic loop, 153
 - interhemispheric integration, 151
 - thalamic projections, 141
- Ataxin-3, 608
- Atonia, muscle, *see* Muscle atonia
- Atriopeptin-like immunoreactivity, 58
- Atropine, 214, 215, 216, 221, 234, 235, 363
- acetylcholine effects, 229
 - and hippocampal theta, 260
 - muscarinic receptors, 217
 - muscle atonia, 459
- Attention/attentional tasks
- cortical excitability during, 371, 373–380
 - differential alterations in two phases of inhibitory response during brain activation, 378–380
 - event-related potentials in humans, 373–375, 376
 - neuronal recordings during set-dependent tasks in monkeys, 375–378
 - fast (beta/gamma) oscillations, 263
 - selective attention versus diffuse activation, 376–377
 - thalamic circuits and, 145
- Auditory cortex, fast (beta/gamma) oscillations, 263
- Auditory signals
- cerebellar relays, 68
 - spinoreticular pathways, 66
- Augmenting response
- plastic changes in thalamocortical system, 330, 331, 333, 334, 335
 - plasticity following spindles, 335, 336–343
 - self-augmenting feedback process, 478
- Autapses, neocortex, 147
- Autoexcitation growth function, Limit Cycle model, 539–540
- Autonomic nervous system, neuronal control of REM sleep, 477
- Autoradiography, anterograde and retrograde tracing, 39–44
- Avalanche process
- slow oscillation, cellular basis of, 308
 - spindles, 290
- Axoaxonic (chandelier) cells, 153
- Axonal collateral bifurcation, BFTG, 128
- Axonal collateralization, 145
- Barbiturates, 25, 231
- Basal forebrain, 139
- activation of thalamus and cerebral cortex by, *see* Neuronal activities, brainstem and basal forebrain structures
 - adenosine and, 564, 565
 - adrenergic receptors, 244–245
- Basal forebrain *contd.*
- brainstem neuron currents
 - acetylcholine-modulated, 223
 - norepinephrine-modulated, 244–245
 - delta waves, 305
 - electrophysiological properties, intrinsic, 179
 - evoked potential studies, 350
 - parallel pathways, 393, 394
 - spindles, 295–300
 - and tonic cortical activation, 391, 393–394
- Basal forebrain connections
- afferents to cholinergic nuclei, 88–90
 - brainstem projections, 90, 91
 - modulatory systems, 89–90
 - systematization of cholinergic nuclei, 88–89
 - diffuse modulatory systems, *see* Diffuse modulatory systems, targets of
 - dual connections of brainstem cholinergic neurons, 106
 - efferent, 133–138
 - to brainstem cholinergic nuclei, 73–76
 - cortical projections, 133–134
 - posterior hypothalamic projections, 137–138
 - thalamic projections, 134–137
 - thalamic, 134
- Basal ganglia, 146
- Basal nucleus, *see* Nucleus basalis
- Basket cells, 150, 153
- Basket circuits, 148
- Behavioral habituation, 66
- Behavioral responses, *see also* Arousal; *specific sleep states*
- evoked potential studies, 350
 - hypothalamus and, 73
- Behavioral states, 359, *see also specific sleep states*
- afferents from diencephalon and telencephalon, 68–85
 - brainstem reticular neuronal activity over REM sleep cycle, 470
 - changing concepts, *see* Historical developments and changing concepts
 - extracellular recordings, 351
 - fast oscillations, 263, 274
 - humoral factors
 - adenosine, 567, 583–584
 - orexin/hypocretin, 606–610
 - medial pontine reticular formation neuron
 - electrophysiology and, 167, 470
 - oscillator characterization, 524, 525
 - plastic changes in thalamocortical system, 339
- Beta-endorphin, 86
- Beta/gamma oscillations
- nucleus basalis, 179
 - origins of, 262–275, 276
- Beta waves, 4, 259
- BFTG (bulbar gigantocellular tegmental field), *see* Bulbar gigantocellular tegmental field
- Bias signal, saccade generation, 435
- Bifurcating axonal collaterals, BFTG, 128

- Bimodal distribution, REM latency in depression, 555–556
- Biocytin, 39
- Biological rhythm, modeling REM sleep as, 513–560
 - characteristics of rhythms, 520–526
 - mathematical characterization of oscillators, 522–526
 - phenomenology of REM sleep rhythms, 520–522
 - depression, 546–560
 - biomodal distribution of REM sleep latencies, 555–556
 - cholinergically hastened onset of REM sleep, 557–559
 - circadian rhythms, 559
 - deficient process S, 560
 - earlier quantitative models, 556
 - monoaminergic-cholinergic factors, 550–552
 - quantitative modeling of sleep abnormalities, 552–559
 - Limit Cycle model, 531–546
 - circadian variation in REM pattern, 533–537
 - details, 539–546
 - limitations on growth of firing rates, 540–543
 - modeling events at sleep onset, 532
 - modeling sleep patterns, 532–533
 - phase plane representation of entry into limit cycle, 545–546
 - REM-on autoexcitation growth function, 539–540
 - REM-on dependence on REM-off inhibitory input, 543–545
 - summary of changes from simple LV model, 531–532
 - Lotka-Volterra model, simple, 537–538
 - phase plane representation, 538
 - significance of terms, 537–538
 - reciprocal interaction model and Lotka-Volterra equations, 526–530
 - postulated steps in production of REM sleep episode, 526–528
 - simple LV equations, 528–530
 - simple LV equations, limits of, 530
 - structural (Reciprocal Interaction) model of organization, 513–520
 - excitation of REM-off neurons by REM-on neurons, 517
 - inhibition of REM-on neurons by REM-off neurons, 517–518
 - inhibitory feedback of REM-off neurons, 518–520
 - REM-on neurons and interaction with other elements in model, 514–517
- Biphasic effect, 360
- Bisynaptic inhibition, thalamic relay cells, 142
- Bombesin, 58
- Bouquet neurons, 147
- Brachial nucleus, 73
- Brachium conjunctivum, 453; *see also* Peribrachial area
 - connections, 60, 64, 57, 95, 114
 - basal forebrain-brainstem, 74
 - brainstem afferents to, 84
 - neocortical projections of intralaminar thalamic neurons and brainstem excitation, 105
- Brachium pontis (BP), 105, 114, 405, 453
- Brainstem, 430
 - activation of thalamus and cerebral cortex by, *see* Neuronal activities, brainstem and basal forebrain structures
 - cholinergic neurons
 - corticothalamic networks, 140
 - spindle generation, 137
 - cholinergic influences on REM sleep, 485–487
 - cholinergic stimulation
 - differential alterations in two phases of inhibitory response during brain activation, 378–379
 - excitatory responses, 359
 - and spindles, 297
 - electrophysiology, *see* Electrophysiology, intrinsic properties
 - excitatory amino acids and, 253, 253–255
 - locus coeruleus, 255
 - mesopontine and bulbar reticular formation, 253–254
 - humoral factors, *see* Forebrain and humoral systems
 - intracellular studies, excitatory responses, 352, 353
 - laterodorsal tegmental nucleus, excitatory responses, 360
 - nonreticular projections to abducens, 424–426, 427
 - oculomotor system, *see* Motor systems
 - orexin neuronal projections, 602
 - neurotransmitter-modulated currents, *see* Neurotransmitter-modulated currents
 - parallel activating pathways, 391
 - peribrachial stimulation, excitatory responses, 354
 - PGO-on bursting cells, 400
 - PGO wave genesis, 394–416
 - brainstem genesis of PGO waves, 395–402
 - cellular mechanisms, 402–409
 - during natural sleep, 409–416
 - reticular neuronal activity over REM sleep cycle, 462–480
 - behavior state alterations in mPRF, 470
 - extracellular recordings, 464–467
 - intracellular recordings, 467–470
 - pre-REM changes, transition period T, 468–469
 - REM sleep, 469
 - sleep-wake control resulting from modulation of excitability in neuronal pools, 470, 472–480

- Brainstem *contd.***
- state-dependent alterations in reticular excitability, 470, 471
 - synchronized sleep, 467
 - wakefulness, sleep-wake transition, 469
 - serotonin effects
 - dorsal raphe nucleus, 247–248
 - facial motoneurons, 248–249
 - mesopontine cholinergic nucleus, 249
 - pontine reticular formation, 248–249
 - spindle blockages, 295–300
 - thalamocortical system dependency, *see* Thalamocortical system, brainstem and state dependency of
- Brainstem-basal forebrain circuit, evoked potential studies, 350**
- Brainstem connections, 56–85**
- basal forebrain, 73–76
 - histaminergic, 133
 - locus coeruleus efferents, 130
 - projections to thalamus, 134
 - cholinergic nuclei, afferents to, 56–85
 - convergent inputs onto single brainstem reticular neurons, 76–78
 - from basal forebrain and related systems, 73–76
 - from hypothalamic areas, 72–73
 - from intrabrainstem sources, 78
 - from neocortical areas, 76
 - from spinal cord and sensory cranial nerves, 63–68
 - from thalamic nuclei, 68–72
 - nuclei with unidentified transmitters, 61–63
 - spinoreticular pathways, 66
 - systematization of cholinergic nuclei, 56–61
 - to midbrain and bulbar reticular formation, 82–85
 - to pontine reticular formation, 78–82, 83
- cholinergic nuclei, efferents, 90–128**
- brainstem and spinal cord projections of mesopontine cholinergic and pontobulbar nuclei, 106–117
 - direct cortical projections, 91–92
 - intrinsic cell morphology and projections of pontine and bulbar gigantocellular fields, 117–128
 - pontobulbar reticular formation, noncholinergic projections from, 112–117
 - rostral projection of cholinergic and noncholinergic nuclei and classical reticular fields, 91–106
 - thalamic projections, 92–106
- cholinergic projection, lateral geniculate nucleus, 357**
- diffuse modulatory systems, *see* Diffuse modulatory systems, targets of**
- monoaminergic nuclei, afferents to, 85–88**
- locus coeruleus, 85–87
 - raphe nuclei, 87
- Brainstem connections *contd.***
- tuberomammillary area, 88
 - ventral tegmental area, 87–88
 - thalamic projections, 141
- Brainstem-evoked depolarization**
- intracellular studies, excitatory responses, 355, 356, 357
 - thalamic reticular neurons, 365
- Brainstem reticular formation, 84**
- cerebral activation, 383
 - connections, 61
 - afferents to pontine reticular formation, 79
 - basal forebrain, 74
 - corticopetal link, brainstem-thalamic projections, 105
 - hypothalamic projections, 73
 - locus coeruleus, 85
 - spinoreticular pathways, 66
 - thalamic projections to midbrain reticular formation, 68–72
- efferent connections, 90**
- fast (beta/gamma) oscillations, 262–263, 263
 - gaze control, 437–439
 - and hippocampal theta, 260
 - inhibitory effects, three phases of, 361, 363
 - monoaminergic nuclei, rostral projections, 91–106
 - neuronal control of REM sleep, 475
 - neuronal morphology, 117–129
 - neuron morphology, 117–128
 - noncholinergic neurons, 55
 - orexin neuronal projections, 602
 - recruitment within reticular pool, 480, 481
 - sleep state control schematic, 472
 - spindles, 295
 - thalamic reticular neuron dual response, 363–371
- Brainstem reticular neurons**
- activity over REM sleep cycle, 462–480
 - connections
 - convergent inputs onto single neurons, 76–78
 - spinoreticular pathways, 66
- Brainstem-thalamic networks, 139**
- electrophysiology, 225–226
 - thalamic reticular neurons, dual types of responses, 363
 - and tonic electrical activation of cerebrum, 382–391, 392
 - bulbar reticular noncholinergic neurons, 384, 386, 387
 - mesopontine cholinergic neurons, 388–391
 - midbrain reticular cholinergic neurons, 384, 385
- Brainstem-ZI axons, 102**
- Bremer, F., 2, 3, 5, 20–21**
- Bulbar gigantocellular tegmental fields (BFTG), 83, 91, 453**
- afferents to pontine reticular formation, 79, 80
 - connections, 117–128

- Bulbar gigantocellular tegmental fields (BFTG)
 - contd.*
 - cholinergic projections, 112
 - noncholinergic brainstem and spinal cord projections, 112–117
 - neuron morphology, 124, 125, 127
 - bifurcating axonal collaterals, organization of, 128
 - cell sending axons to ipsilateral bulbar reticular core, 125–127
 - cell size distribution, 118
 - dendrites, 123–124
 - muscle atonia
 - central mechanisms, 453, 454, 456
 - other pontine structures and pharmacology of, 459
 - pontine FTG stimulation and, 82
 - pontobulbar reticular projections to abducens, 424
 - projections of, intrinsic cell morphology and, 117–128
- Bulbar magnocellular field, 454, 456
- Bulbar nucleus reticularis gigantocellularis, 156
- Bulbar reticular formation, 64, 114
 - adrenergic receptors, 243
 - behavioral state alterations in mPRF, 470
 - brainstem cholinergic nuclei afferents to, 82–85
 - burst neurons, 422–423
 - cholinergic neurons in NB nucleus, 394
 - connections, 90–91
 - brainstem afferents to, 82–85
 - cholinergic projections, 112
 - cholinergic projections to PPT nucleus, 110–112
 - convergent inputs onto single brainstem reticular neurons, 76
 - convergent synaptic excitation of midbrain reticular neurons, 77
 - locus coeruleus, 85–86
 - excitability, modulation of, 474, 478
 - excitatory amino acids and, 253–254
 - gaze control, 438
 - muscle atonia, central mechanisms, 452
 - nuclei of, 63
 - state-dependent alterations in reticular excitability, 470, 471
 - structural (Reciprocal Interaction) model of organization, 515, 516
 - terminology, 61
- Bulbar reticular neurons
 - projections to thalamic nuclei, 382
 - tonic electrical activation of cerebral cortex by brainstem thalamic neurons, 384, 386, 387
- Bulbospinal neurons
 - locus coeruleus afferents, 86
 - paragigantocellularis nucleus, 86
- Bulbothalamic neurons
 - and midbrain thalamic neurons, 383
 - somatosensory, 350
- Burst cells
 - delta waves, 302
 - fast rhythmic, 265
 - motor system, 420–426, 427
 - anatomic connectivity, 424–426, 427
 - physiology, 420–423
 - neural integrator, 429
 - oculomotor system, 418–419
 - PGO, 404, 405
 - PGO-on, 85, 395, 397, 401
 - plastic changes in thalamocortical system
 - repetitive callosal stimulation and, 341
 - repetitive motor cortex stimulation, 342
 - sleep state control schematic, 472
 - slow oscillations, 309
 - spindle generation, 259
 - spindles, 282
 - state-dependent alterations in oculomotor system function, 441
- Burst mode, 139
- Bursts
 - cholinergic neurons in NB nucleus, 394
 - intracellular studies, 355
 - neocortical interneurons, 149
 - PGO-on cells, 395, 397, 399, 400
 - PGO waves, 410, 412, 413
 - thalamic reticular neurons, 152, 367
 - thalamocortical neurons, 347
 - electrophysiological properties, intrinsic, 182–184, 185
 - plastic changes, 327, 329
- Caffeine, 562–563
- Cajal, interstitial nucleus of, 426
- Calbindin, 48
- Calcium action potentials
 - medial pontine reticular formation, 156, 157, 158
 - locus coeruleus, 242–243
- Calcium-binding proteins, 48
- Calcium conductance
 - norepinephrine and, 236, 237
 - serotonin and, 246–250
- Calcium currents
 - spindles, 287
 - thalamocortical neurons
 - high-voltage, 185–187, 188
 - low-threshold, 181–185
- Calcium-dependent currents
 - locus coeruleus pacemaker activity, 172–175, 242–243
 - NMDA receptors and, 250
- Calcium-dependent potassium conductance
 - acetylcholine and, 234
 - norepinephrine and, 246
 - thalamocortical neurons, 189–192
- Calcium depletion, cellular basis of slow oscillation, 308
- Calcium entry, plastic changes in thalamocortical system, 330

- Calcium mediated slow spikes, and theta waves, 261
- Calcium mobilization, adenosine-mediated, 578, 579–580, 582
- Calcium potentials, phase-locked, 261
- Calcium spike, *see also* Electrophysiology, intrinsic properties
 - medial pontine reticular formation neurons, 159–166
 - PGO-related, 413
- cAMP, 217, 246
- Carbachol, 458–459
- Carboxyamidotryptamine, 247
- Cardiovascular system
 - neuronal control of REM sleep, 477
 - sleep state control schematic, 472
- Cataplexy, 604, 605
- Catecholaminergic neurons, 85
 - connections
 - locus coeruleus, 85
 - NB inputs from, 89
 - immunohistochemistry, 44
 - PPT nucleus, 388
- Cation currents
 - excitatory amino acids and, 250
 - locus coeruleus pacemaker activity, 172–175
 - serotonin and, 246
 - thalamic neurons, 181
 - thalamocortical neuron hyperpolarization-activated, 187, 189
- Caudal intralaminar (CM-PF) nuclei, 98
- Caudal mesencephalon, cholinergic cell groups, 382
- Caudal nucleus (RPC) 63, 65, 156, 425, 439, 453
 - afferents to pontine reticular formation, 78, 79
- Caudate nucleus
 - augmenting response, 336
 - basal forebrain projections, 135
 - dopaminergic connections, 132
- Central medial (CeM) nucleus
 - connections, 105
 - convergent synaptic excitation of midbrain reticular neurons, 77
- Central superior raphe nucleus (CS), 92, 430
 - neocortical projections of intralaminar thalamic neurons and brainstem excitation, 105
 - serotonergic connections, 131, 132
- Central tegmental field (FTC), 74, 405
 - afferents to pontine reticular formation, 79
 - cholinergic nuclei, 56–57
 - connections, 91
 - brainstem efferents to thalamic nuclei, 94
 - brainstem reticular projections, 100
 - locus coeruleus efferents, 129
 - terminology, 61–62
- Centrolateral (CL) neurons, thalamic
 - intracellular studies, 360
 - projections of, 141
 - recruiting systems, 332
 - spindles, 283, 296
- Centrolateral-paracentral (CL-Pc) nuclei, 104, 105, 106, 388
 - projections to midbrain reticular formation, 68, 69
 - spontaneous firing in NREM sleep and brain-active states, 347
- Centromedian-parafascicular (CM-Pf) nuclei, 98, 99
 - brainstem reticular projections, 100, 101
 - projections to midbrain reticular formation, 68, 69
- Cerebellum
 - abducens projections, 420
 - adrenergic receptors, 242
 - connections
 - BFTG bifurcating axonal collaterals, 128
 - locus coeruleus, 85
 - sensory signal relays, 68
 - thalamic projections to midbrain reticular formation, 70
 - fast oscillations, 267
 - thalamic nuclei, projections to, 141
 - thalamocortical neuron electrophysiology, 191
- Cerebral cortex, *see also* Neocortex
 - activation by brainstem-thalamic neurons, 382–391, 392; *see also* Neuronal activities, brainstem and basal forebrain structures
 - bulbar reticular noncholinergic neurons, 384, 386, 387
 - mesopontine cholinergic neurons, 388–391
 - midbrain reticular cholinergic neurons, 384, 385
 - alpha rhythms, origins of, 256–257
 - cholinergic projection from NB to, 393
 - connections
 - basal forebrain, 74
 - basal forebrain projections to thalamus, 137
 - brainstem reticular neuron projections, 91–92
 - convergent inputs onto single brainstem reticular neurons, 76
 - corticopetal link, brainstem-thalamic projections, 104, 105
 - dopaminergic systems, 87–88
 - histaminergic, 133
 - NB inputs, 89
 - serotonergic efferents, 131–132
 - thalamocortical neurons, 98
 - ventral tegmental area afferents, 88
 - fast (beta/gamma) oscillations, 263
 - thalamic projections, 382
 - TNF-alpha and, 590
- cerveau isolé* preparation, 3, 5, 6, 8, 21, 24
- cGMP, 233
- Chandelier (axoaxonic) cells, 147, 148, 153
- Chloride conductance, 246
- Chloride-mediated IPSP, 355, 363
- Cholecystokinin, 48, 147, 584
- Choline acetyltransferase (ChAT), 56, 58, 396
 - adenosine and, 577, 578, 579–580, 582

- Choline acetyltransferase (ChAT) *contd.*
 basal forebrain-brainstem connections, 74
 immunohistochemistry, 45, 46–47
 locus coeruleus, 219
 mesopontine cholinergic neurons, 388
 thalamic nuclei connections, 93, 95, 99
- Cholinergic-adrenergic interactions
 modeling REM sleep in depression, 549
 muscle atonia, 459, 549
- Cholinergic mechanisms
 adenosine and, 564
 depression, quantitative modeling of sleep
 abnormalities in, 552, 557–559
 excitatory responses, 352
 GABAergic influences and, 511
 intracellular studies, 359, 361
 modeling
 Limit Cycle model, 557–559
 REM sleep in depression, 547, 548
 monoaminergic inhibition of, 494–495
 REM-on and REM-off neuron interaction
 sites, 501
 REM sleep, 482–487
 in depression, 547, 548
 induction of REM sleep-like phenomena,
 482–484
 LDT stimulation, production of
 scopolamine-sensitive EPSPs in mPRF
 neurons, 485
 unit activity during sleep and wakefulness,
 485–487
 structural (Reciprocal Interaction) model of
 organization, 514–516
 thalamic cell excitation, 351
 thalamic reticular neuron dual response, 367
- Cholinergic neurons, 139
 adenosine signal transduction, 577, 578,
 579–580, 582
 brainstem, actions of, 212–235
 basal forebrain, 223
 hippocampus, 234–235
 locus coeruleus, 219, 221–223
 medial pontine reticular formation, 212–219
 neocortex, 231–234
 pedunculopontine tegmental cholinergic
 neurons, 219, 220
 thalamus, 223–231
 brainstem-LG projection, 357
 brainstem-thalamic neurons implicated
 in tonic electrical activation of
 cerebrum, 383
 centers versus distributed systems for waking
 and sleep, 30–31
 connections
 basal forebrain-brainstem, 75
 basal forebrain projections, 134
 cerebral cortex, efferent connections,
 133–134
 NB inputs from, 89
 PPT/LDT nuclei, 57–58
- Cholinergic neurons *contd.*
 delta waves, 305
 diffuse modulatory systems, 140; *see also* Diffuse
 modulatory systems, targets of
 evoked potential studies, 350
 hippocampal septal neurons, 260
 LDT, *see also* Pedunculopontine/laterodorsal
 tegmental neurons
 neuronal interactions, 517
 lumbar alpha neuron activity during waking
 and sleep, 452
 parallel pathways, 391
 spindles, 297, 298, 299
 thalamic projections, 382
 tonic electrical activation of cerebral cortex by
 brainstem-thalamic neurons
 mesopontine, 388–391, 392
 midbrain, 384, 385
- Cholinergic nuclei
 basal forebrain afferents, 88–90
 modulatory systems, 89–90
 systematization of cholinergic nuclei,
 88–89
 brainstem afferents, 56–85
 convergent inputs onto single brainstem
 reticular neurons, 76–78
 from basal forebrain and related systems,
 73–76
 from hypothalamic areas, 72–73
 from intrabrainstem sources, 78
 from neocortical areas, 76
 from spinal cord and sensory cranial nerves,
 63–68
 from thalamic nuclei, 68–72
 nuclei with unidentified transmitters,
 61–63
 systematization of cholinergic nuclei,
 56–61
 to midbrain and bulbar reticular formation,
 82–85
 to pontine reticular formation,
 78–82, 83
 brainstem efferents, 90–128
 brainstem and spinal cord projections of
 mesopontine cholinergic and
 pontobulbar nuclei, 106–117
 rostral projections, 91–106
 spinal cord projections, 106–117
 monoaminergic cells in, 55
- Cholinergic-to-cholinergic projections, 350
 evoked potential studies, 350
 NB cells, 90
- Cholinoceptive cells, somatosensory
 cortex, 234
- Cingulate cortex, 98
 acetylcholine effects, 231
 cholinergic projections from NB and diagonal
 band nuclei, 133
 spindles, 284, 285
 Cingulate gyrus, 98

- Circadian rhythms, *see also* Biological rhythm,
 modeling REM sleep as characteristics of
 REM sleep, 520
 modeling
 depression, 548, 559
 Limit Cycle model, 533–537
 orexin/hypocretin, 606–610
 sleepiness, 561–562
 suprachiasmatic nucleus and, 73
- Circuits
 diffuse modulatory systems, *see* Diffuse
 modulatory systems, targets of
 neurotransmitter-modulated brainstem
 currents, *see* Neurotransmitter-modulated
 currents
- Clastrum, 146
- Clock-like delta rhythm, 300–304, 317
- Clonidine, 237, 242, 243, 244
- CL-PC neurons, *see* Centrolateral-paracentral
 nuclei
- CM-Pf neurons, *see* Centromedian-parafascicular
 nuclei
- CNQX, 251
- Cochlear nucleus, 130
- Cognitive functions
 adenosine and, 583
 somatosensory evoked potentials and,
 373, 374
- Collaterals, recurrent, 518
- Colliculus, *see* Inferior colliculus; Superior
 colliculus
- Connections, *see* Anatomical connections; Basal
 forebrain connections, Brainstem
 connections; *specific classes of transmitters*
- Contingent negative variation (CNV), 373, 375
- Continuity disturbances, modeling REM sleep in
 depression, 547, 548
- Controller activity criterion, neuromodulation of
 REM sleep, 482
- Cooling, LC influences in REM sleep, 499–501
- Corpus callosum, 135
 cortical connections, 148, 150–151
 plastic changes in thalamocortical system,
 341, 343
- Cortex, *see also* Cerebral cortex; Neocortex
 brainstem reticular neuron projection studies,
 91–92
 connections
 basal forebrain nuclei, 133–134
 corticopetal link, brainstem-thalamic
 projections, 104, 105
 serotonergic efferents, 131–132
 thalamic projections to midbrain reticular
 formation, 70
 thalamic projections, 141
- Cortical activation, 350
 basal forebrain neurons and, 391, 393–394
 brainstem-thalamic neurons implicated
 in tonic electrical activation of
 cerebrum, 382
- Cortical activation *contd.*
 extracellular recordings, 352
 by neuronal activities in brainstem and
 forebrain, *see* Neuronal activities,
 brainstem and basal forebrain structures
- Cortical inhibition, global, 329
- Cortical layers, evoked potential studies, 350
- Cortically evoked responses, 350
 repetitive motor cortex stimulation and, 342
 spindles, 281
- Cortical neurons
 depolarization, cholinergic projection from NB
 and, 393
 plastic changes in thalamocortical system, 329
 seizures, 327
 slow oscillation, cellular basis of, 306
 spindles, 279, 280
- Cortical oscillations, *see also* Slow oscillations,
 neocortical; Thalamocortical system
 oscillations
 alpha rhythms, 256–257
 delta waves, 304–305
 sensorimotor rhythms, 259
- Cortical projections, thalamic nuclei, 141, 382
- Cortical pyramidal neurons, plastic changes in
 thalamocortical system, 330
- Cortical synchronization, locus coeruleus cooling
 and, 499, 500
- Corticocortical pathways, 148
 callosal, *see* Corpus callosum
 plastic changes in thalamocortical system, 329
- Corticofugal projections, 148
- Corticopetal pathways
 brainstem-thalamic projections, 104
 locus coeruleus efferents, 129–130
- Corticopontine neurons, plastic changes in
 thalamocortical system, 334
- Corticoreticular connections
 afferents to pontine reticular formation, 79
 neocortical projections to brainstem, 76
- Corticothalamic neurons/networks, 152
 diffuse modulatory systems, 139, 140, 141; *see*
also Diffuse modulatory systems, targets of
 excitatory amino acids and, 253, 254
- Corticotropin-releasing factor (CRF), 58, 550
- Cranial nerve nuclei, *see also specific nerves*
 connections, 63
 locus coeruleus efferents, 130
 spinoreticular pathways, 66
 muscarinic receptors, 217
- Cranial nerves, gaze control, 438, 439
- CS, *see* Central superior raphe nucleus
- 5-CT, 247, 248, 250
- Cultured cells, cholinergic agonists and, 217
- Cuneate nucleus, 114
- Cuneiform nucleus, 77, 79, 109
- Current-source-density analysis, 350
- Cyclic AMP, 217, 246
- Cyclic GMP, 233
- Cytochrome oxidase, 48, 429, 430

- Cytokines, 584–589
 - IL-1 β , 587–589
 - TNF-alpha, 589–590, 591
- Dampening activity, brainstem, 295
- Deafferented thalamic reticular cells,
 - spindles, 290
- Deep cerebellar nuclei
 - connections
 - thalamic projections to midbrain reticular formation, 70
 - ventral tegmental area afferents, 88
 - thalamocortical neuron electrophysiology, 191
 - ventrolateral thalamic neuron
 - inputs, 347
- De-inactivation, medial pontine reticular
 - formation neurons, 160
- Delta rhythms/waves, 300–305, 383
 - adenosine and, 565
 - cortical component, 304–305
 - modeling REM sleep in depression, 547, 548
 - sleep factor indicators, 562
 - slow oscillations
 - grouping by, 318–324, 326
 - synaptic reflection in thalamic and other structures, 317
 - thalamic component, 300–304
- Delta sleep, 300, 547, 548
- Dendritic patterns, morphological methods,
 - 36–39
- Dendrodendritic synapses, 145
- Dentate gyrus, 153
- Depolarization, *see also* Electrophysiology
 - slow oscillation
 - cellular basis of, 306
 - synaptic reflection in thalamic and other structures, 315
 - soma size and, 480, 481
 - time course, 478
- Depolarizing plateau, spindles, 279, 281
- Depression, 546–560
 - deficient process S, 560
 - monoaminergic-cholinergic factors,
 - 550–552
 - quantitative modeling of sleep abnormalities,
 - 552–559
 - bimodal distribution of REM sleep latencies,
 - 555–556
 - cholinergically hastened onset of REM sleep,
 - 557–559
 - circadian rhythms, 559
 - earlier models, 556
- Desmethylinipramine, 237, 239
- Desynchronized sleep
 - cholinergic influences on REM sleep, 484
 - sleep state control schematic, 472
 - state-dependent alterations in reticular excitability, 470, 471
 - structural (Reciprocal Interaction) model of organization, 515
- Diagonal band nuclei (DB)
 - connections, 73, 74, 75, 88, 90
 - basal forebrain projections, 135, 136
 - cortical, 133
 - hypothalamus, posterior, 138
 - electrophysiological properties,
 - intrinsic, 179
- Diaminobenzidine (DAB), 42
- Diencephalon
 - BFTG bifurcating axonal collaterals, 128
 - giant cell field projections to, 91
 - muscarinic receptors, 217
 - spinoreticular pathways, 66
- Diffuse activation, selective attention versus,
 - 376–377
- Diffuse modulatory systems, targets of,
 - 139–153
 - hippocampus and related systems, 153
 - neocortex, 145–153
 - thalamus, 141–145, 146
- Diffuse spindle disruption, 295–296
- Direction burst neurons, 423
- Disfacilitation, slow oscillation, cellular basis of,
 - 306, 308
- DMPP, 226
- Dopamine
 - immunohistochemistry, 44
 - orexin and, 604
- Dopaminergic systems
 - efferent connections, 132
 - sensorimotor rhythms, 259
 - thalamic nuclei, 96
 - ventral tegmental area, 87–88
- Dorsal lateral geniculate, spindles, 296
- Dorsal mesostriatal pathway, dopaminergic
 - connections, 132
- Dorsal raphe nucleus, 139, 237
 - adrenergic receptors, 243
 - afferents, 86, 87
 - brainstem neuron currents
 - norepinephrine-modulated, 243–244
 - serotonin-modulated, 247–248
 - cholinergic projections, 517
 - connections
 - brainstem efferents to, 93
 - locus coeruleus, 85, 86
 - serotonergic, 130, 131, 132
 - ventral tegmental area afferents, 88
 - electrophysiological properties, intrinsic,
 - 175–179
- GABAergic influences, 518–520
- GABAergic influences in REM sleep,
 - 502–505
 - microdialysis, 502–503
 - microiontophoresis, 503–506
 - source of input to, 506–507
- humoral factors
 - adenosine, 567
 - IL-1 β and, 588
 - orexin, 602, 604, 605, 606

- Dorsal raphe nucleus *contd.*
 monoaminergic influences in REM sleep, 488
 inverse association with REM events, 490–495
 suppression and increases in REM sleep, 495–497
 serotonergic inhibition of cholinergic neurons, 518
 structural (Reciprocal Interaction) model of organization, 515
- Dorsal tegmental bundle, locus coeruleus efferents, 128
- Dorsal tegmental field (DTF), muscle atonia, 458
- Dorsal tegmental nucleus, *see* Laterodorsal tegmental nucleus
- Dorsal thalamic nucleus
 acetylcholine effects, 223–224
 diffuse modulatory systems, cell types and connections, 141
 inhibitory interneurons, 361
 NB cholinergic and GABAergic projections, 394
 plastic changes in thalamocortical system, 335
 spindles, 298
- Dorsolateral funiculus nucleus (DLF), 64, 65, 79
- Dorsolateral pontine reticular formation, 483
- Dorsolateral reticular formation, 111, 112
- Dorsolateral tegmental neurons, 111, 475
- Double bouquet neurons, 147, 148
- Doublets, PGO waves, 409
- Dreaming, PGO waves, 410
- DR (nucleus raphe dorsalis), *see* Dorsal raphe nucleus
- Drowsiness, 15, 295
- Dual nature of sleep, 9–10
- Dynamic motor error, 435, 436
- Eccentric eye fixation, 438
- EEG-activated states, *see* under Electroencephalography
- EGTA, 186
- Electrical stimulation
 muscle atonia, 459
 sleep induction, 25–27
- Electroencephalography
 adenosine and, 565
 EEG-activated states, 403
 brainstem-thalamic neurons implicated in tonic electrical activation of cerebrum, 383
 bulbothalamic neurons and, 386, 387
 historical developments and changing concepts, 5, 12, 16, 33
 intracellular studies, 362
 mesopontine cholinergic neurons, 388
 midbrain reticular noncholinergic neurons, 384
 PGO waves, 410
 PPT neuron firing rates, 392
 thalamic neuron electrophysiology, 179
- Electroencephalography *contd.*
 EEG desynchronization
 brainstem-thalamic neurons implicated in tonic electrical activation of cerebrum, 383
 bulbothalamic neurons and, 386, 387
 mesopontine cholinergic neurons, 388
 neuronal control of REM sleep, 476
 PPT neuron firing rates, 392
 sleep state control schematic, 472
 structural (Reciprocal Interaction) model of organization, 515
 EEG-synchronized activity, *see also* Neuronal control of REM sleep; Synchronized oscillations
 historical developments and changing concepts, 9, 10, 12, 13
 mesopontine cholinergic neurons, 388
 EEG-synchronized sleep, 403
 corticothalamic arousal and inhibitory processes, 379, 380
 evoked potential studies, 350
 extracellular recordings, 351
 PPT neuron firing rates, 392
 thalamic reticular neurons, 364
 thalamic reticular neurons, dual response, 369
 thalamocortical neuron electrophysiology, 182–184, 185
 historical developments and changing concepts, 6, 7, 9, 10, 12–15, 24–30
 IL-1 β and, 587, 588
 methods, 48
 modeling REM sleep in depression, 547, 548
 neocortical projections of intralaminar thalamic neurons and brainstem excitation, 105
 PGO waves, 412
 synchronized rhythms, *see* Synchronized oscillations
 TNF-alpha and, 590
- Electromyography
 atonia, *see* Muscle atonia
 mesopontine cholinergic neurons, 386
 slow oscillations, 311
- Electrooculograms, 397, 401
 slow oscillations, 311
 state-dependent alterations in oculomotor system function, 443
- Electrophysiology
 augmenting response, 336, 337, 350
 diffuse modulatory systems, *see* Diffuse modulatory systems, targets of
 historical developments and changing concepts, 1, 12–13
 methods, 48–54
 muscle atonia of REM sleep, 454–458
 neurotransmitter-modulated currents, *see* Neurotransmitter-modulated currents

- Electrophysiology *contd.*
 plastic changes in thalamocortical system, 333
 cortical augmenting responses and, 340
 repetitive callosal stimulation and, 341
 thalamic reticular cells, GABA inhibitory effect, 137
- Electrophysiology, intrinsic properties, 155–209
 amygdala neurons, 208–209
 basal forebrain and medial septum neurons, 179
 dorsal raphe nucleus neurons, 175–179
 entorhinal complex neurons, 208
 hippocampal neurons, 209
 locus coeruleus neurons, 171–175
 medial pontine reticular formation neurons, 156–167
 classes of neurons, 156–159
 low- and high-threshold spikes, 159–166
 membrane potential, control of repetitive firing, behavioral implications, 167
 neocortical neurons, 197, 199–208
 changes in firing patterns during synaptic activities and shifts in behavioral state, 199, 201–208
 firing patterns in four neuronal types and underlying ionic currents,
 pedunculopontine and laterodorsal tegmental nuclei, 167–171
 thalamic neurons, 179–197, 198
 local-circuit inhibitory cells, 191–194
 thalamic reticular GABAergic neurons, 194–196, 197, 198
 thalamocortical, 181–191
- Encéphale isolé preparation, 2
- Encephalography, historical development, 3
- Endopeduncular nucleus, 112
- Endorphin, 86
- Enkephalin, 241
- locus coeruleus afferents, 86
 paragigantocellularis nucleus, 86
- Entopeduncular nucleus, 89
- Entorhinal complex
 cholinergic projections from NB and diagonal band nuclei, 133
 electrophysiological properties, intrinsic, 208
 theta rhythm origins, 260–261
- Entorhinal cortex, 153
- EPSPs, *see* Excitatory postsynaptic potentials;
 Postsynaptic potentials
- Error signal, retinal, 434, 435
- Event-related potentials (ERPs)
 electrophysiological methods, 49–50, 54
 in humans, 373–375
- Evoked spindles, 281
- Excitatory amino acids (EAAs)
 brainstem neurons, actions of, 250–254
 brainstem, 253–254
 neocortex, 254
 receptor types, 250–252
 thalamus, 254
 locus coeruleus, 87
- Excitatory amino acids (EAAs) *contd.*
 lumbar alpha neuron activity during waking and sleep, 451
 muscle atonia, 459
 rostral midbrain neurons, 382
- Excitatory burst neurons (EBNs), 422
 gaze control, 438
 interactions of neurons in saccade generation, 432–437
 pontobulbar reticular projections to abducens, 424
- Excitatory postsynaptic potentials (EPSPs), *see also* Postsynaptic potentials
 behavioral state alterations in mPRF, 470
 extracellular recordings, 351
 PPT/LDT neurons, 399
 recruitment within reticular pool, 480, 481
 synchronized rhythms, *see* Synchronized oscillations
 thalamic reticular neurons, 365
 thalamic reticular versus TC neurons, 318
 and theta waves, 261
 trigeminal mesencephalic nucleus stimulation, 445
- Excitatory responses
 cerebral activation, 382
 diffuse modulatory systems, *see* Diffuse modulatory systems, targets of
 evoked potential studies, 350
 glutamatergic neurons, 55; *see also* Glutamatergic neurons
 intracellular studies, 342–361
 neocortical projections to brainstem, 76
 slow oscillation, cellular basis of, 306
- Expectancy, sensorimotor rhythms, 257–259
- Expectancy wave, 373
- Extracellular current flow, synchronized rhythms, *see* Synchronized oscillations
- Extracellular recordings, 50–53
 adenosine effects, 0
 brainstem reticular neuronal activity over REM sleep cycle, 464–467
 raphe system REM-off neurons and PGO waves, 491–495
 cholinergic neurons in NB nucleus, 394
 evoked potential studies, 350
 thalamocortical neurons, 351–352
- Extrapyramidal area, 79, 111, 112
- Eye displacement vectors, burst neurons, 423
- Eye movements, 12, 16, 33, 403; *see also* Motor systems
 gaze control, 437–439
 neocortical projections of intralaminar thalamic neurons and brainstem excitation, 105
 neuronal control of REM sleep, 475
 PB burst neurons and, 395, 397
 PGO burst cell discharge and, 397
 PGO waves, 397, 412
 SNr inhibitory projections and, 85
- Eye-neck reticulospinal neurons, 438, 439

- Facial motoneurons, serotonergic modulation, 248–249
- Facial nerve, 109, 114
- Facial nuclei, 63
 - gaze control, 439
 - muscle atonia, central mechanisms, 454, 455
- Factor S, 548–549
- Fasciculus longitudinalis medialis (FLM), 455
- Fast Blue, 43
- Fastigial nucleus, 68, 85
- Fast oscillations
 - grouping of delta spindles and fast oscillation by slow oscillation, 318–324, 325
 - sensorimotor rhythms, 259
- Fast rhythms, cholinergic neurons in NB nucleus, 394
- Fast spiking neurons, slow oscillations, 309
- Fast waves, 4
- Fatal insomnia, 26
- Feedback, 478
 - excitatory projections, 358
 - reticuloreticular, 480, 481
 - self-augmenting feedback process, 478
- Feedback inhibition
 - LC-MC, 237
 - structural (Reciprocal Interaction) model of organization, 515
- Field of Forel, 66, 79
- Field potentials, electrophysiological methods, 49–50, 53, 54,
- Final common integrator hypothesis, 431
- Flocculus, cerebellum, 420
- Fluorescent dyes, 43
- Forebrain, *see also* Basal forebrain; Cerebral cortex; Neocortex
 - dopaminergic connections, 132
 - electrophysiology, *see* Electrophysiology, intrinsic properties
- Forebrain and humoral systems, 561–610
 - adenosine, 562–584
 - behavioral alterations, 583–584
 - homeostatic control of sleep, 562–565, 566
 - neurophysiological mechanisms, 570
 - receptor coupled signal transduction and transcriptional modulation, 576–583
 - receptor subtypes, 571–576
 - site specificity and sources after prolonged wakefulness, 565, 567–570
 - cholinergic influences on REM sleep, 483
 - cytokines, 584–589
 - IL-1 β , 587–589
 - TNF-alpha, 589–590, 591
 - miscellaneous humoral factors, 590–592
 - growth hormone-releasing hormone, 590–592
 - somatostatin, 592
 - orexin/hypocretin, 600–610
 - actions at cellular level, 603–605
 - identification of, 600–602
 - neuronal projection and receptors, 602–603
- Forebrain and humoral systems *contd.*
 - orexin/hypocretin *contd.*
 - release of, circadian cycles versus behavioral states, 606–610
 - REM-related phenomena and wakefulness, 606
 - ventrolateral preoptic area (VLPO), 592–600
 - lesions and extnded VLPO, 595–600
 - modeling, 600
 - sleep-active neurons, identification of, 592–595, 596
- Forel, field of, 66, 79, 91
- 40 Hz frequency, 267, 343
- Fourth ventricle, 60
- Frontal eye fields
 - burst neurons, 423
 - interactions of neurons in saccade generation, 432–437
 - projections to reticular formation, 426
- Frontal lobe connections
 - cholinergic projections from NB and diagonal band nuclei, 133
 - locus coeruleus efferents, 129
- FTG (gigantocellular tegmental field), *see* Gigantocellular tegmental field
- FTM (magnocellular tegmental field), *see* Magnocellular tegmental field
- FTP (paralemniscal tegmental field), *see* Paralemniscal tegmental field
- Funiculus
 - dorsolateral, 64, 65, 79
 - lateral, 115, 116
 - ventral, 80, 113, 114, 115, 116
 - ventrolateral, 130
- GABA
 - adenosine and, 564
 - excitatory amino acids and, 253
 - immunohistochemistry, 48
- GABAergic influences in REM sleep, 501–511
 - dorsal raphe nucleus
 - sources of input to, 506–507
 - suppression and increases in REM sleep, 502–505
 - inhibitory feedback of REM-off neurons, 518–520
 - locus coeruleus, 505–507
 - models, postulated steps in production of REM sleep episode, 524–528
 - pontine reticular formation, distribution and REM sleep, 507–509
 - PPT nucleus, 509–511
 - structural (Reciprocal Interaction) model of organization, 515, 516–517
- GABAergic interneurons, NE excitation, 518
- GABAergic mechanisms
 - differential brainstem reticular effects on inhibitory responses, 363
- NB cholinergic and GABAergic projections, 394

- GABAergic mechanisms *contd.*
 perigeniculate RE neurons, 355
 PGO waves, 400, 409
 thalamic cells
 differential alterations in two phases of
 inhibitory response during brain
 activation, 378–379
 types of, 361, 363
 thalamic reticular neuron dual response,
 367, 369
- GABAergic neurons, 30–31, 139
 connections
 basal forebrain, 74, 89, 90
 basal forebrain projections to thalamus, 137
 histaminergic, 133
 NB-cortical, 134
 NB inputs from, 89
 substantia nigra pars reticulata, 84
 tuberomammillary area afferents, 88
 delta waves, 302
 Golgi staining, 39
 hippocampal trisynaptic loop, 153
 hippocampus, 235
 medial septum, 179
 neocortex, 150
 acetylcholine effects, 231–232
 diffuse modulatory systems, 147–148
 orexin and, 604
 plastic changes in thalamocortical system, 335
 slow oscillation, cellular basis of, 306
 spindles, 279, 285, 298, 299
 thalamocortical electrophysiology, 191
 local circuit inhibitory cells, 191–194
 thalamic reticular neurons, 194–196, 197
 thalamus
 brainstem cholinergic pathways,
 acetylcholine effects, 229–231
 diffuse modulatory systems, 141, 142–145, 146
 electrophysiological properties, intrinsic,
 194–196, 197, 198
- Galanin, 88
 Gamma bands, 4, 565
 Gamma oscillations
 nucleus basalis, 179
 sensorimotor rhythms, 259
 theta rhythm origins, 262–275, 276
 Gastrin-releasing peptide, 58
 Gaze, control of, 437–444; *see also* Motor systems
 Giant cell nucleus, *see* Gigantocellular tegmental
 field
 Gigantocellular fields, 63, 111
 brainstem-thalamic projections, 104
 mesopontine cholinergic projections to, 107
 medulla, 111
 Gigantocellular neurons, 61
 brainstem afferents to, 83
 bulboreticular (RE) neurons with midbrain
 and thalamic projections, 386, 387
 connections of brainstem cholinergic nuclei,
 intrinsic cell morphology and, 117–128
- Gigantocellular neurons *contd.*
 paramedian pons, 63
 PGO-on cells, 398
 spinoreticular pathways, 66
 Gigantocellular tegmental field (FTG), 112
 bulbar, *see* Bulbar gigantocellular tegmental
 fields
 connections, 62–63
 afferents to pontine reticular formation, 79,
 81, 82
 locus coeruleus efferents, 130
 thalamus, 98–99
 electrophysiological recordings, 156
 gaze control, 439
 muscle atonia, central mechanisms, 453,
 454, 456
 neuron morphology, 117–128;
 PGO-on cells, 398
 pontine, 74; *see also* Pontine gigantocellular
 tegmental fields
 state-dependent alterations in reticular
 excitability, 470, 471
- Glial cells, 314
 Glial sheets, thalamic synapses, 142
 Global cortical inhibition, plastic changes in
 thalamocortical system, 329
 Global disinhibition of TC neurons, 352
 Globus pallidus, 71, 89, 112, 136, 243
 Glomeruli, thalamic, 142, 143
 Glutamate, 254
 intracellular studies, 352
 somatosensory cortical responses, 234
 Glutamate decarboxylase, 38
 Glutamatergic neurons, 139
 corticothalamic synapses, 318
 IL-1 β and, 588
 midbrain reticular noncholinergic neurons, 61
 NB activation, 90
 neocortex, 146–147
 parallel pathways, 391
 roles of, 55–56
 thalamus, 141, 152
 Glycine, NMDA receptors, 251
 Golgi staining methods, 35–39
 Gomori's stain AChE, 46
 Growth hormone-releasing hormone, 587, 588,
 590–592
- Habenular nucleus, lateral, 87, 145, 284
 Habituation, behavioral, 66
 HEAT-binding sites, locus coeruleus, 243
 Hebb's model, 375
 Hexamethonium, 221
 Hippocampus
 adenosine in, 568
 adrenergic receptors, 237, 245–246
 brainstem neuron currents
 acetylcholine-modulated, 234–235
 norepinephrine-modulated, 245–246
 cholinergic agonists and, 217

- Hippocampus** *contd.*
- cholinergic influences on REM sleep, 484
 - connections
 - locus coeruleus efferents, 129
 - neocortical projections of intralaminar thalamic neurons and brainstem excitation, 105
 - raphe nuclei afferents, 87
 - thalamic connections, 98
 - diffuse modulatory systems, 153
 - electrophysiological properties, intrinsic, 209
 - excitatory amino acids and, 254
 - IL-1 β and, 589
 - intracellular studies, excitatory responses, 361
 - muscarinic activation, 215
 - neuronal control of REM sleep, 476
 - plastic changes in thalamocortical system, 329
 - serotonin effects, 250
 - sleep state control schematic, 472
 - spindles, 284
 - theta rhythm origins, 259–262
 - theta rhythms, 145
- Histaminergic systems**, 61
- efferent connections, 133
 - tuberomammillary area, 88
- Histogram**, interspike interval, 411
- Historical developments and changing concepts**, 1–33
- centers and distributed systems, 30–33
 - definition of vigilance and activation states, 11–20
 - pioneering discoveries, 2–11
 - sleep-promoting mechanisms, 20–30
 - active sleep, 24–30
 - passive sleep, 20–24
- Homeostatic control of sleep**, adenosine and, 562–565, 566
- Horseradish peroxidase (HRP)**
- anterograde and retrograde tracing, 41–43
 - Golgi staining, 15–19
 - immunohistochemistry, 44–47
- Horsley-Clarke stereotaxic instrument**, 22
- 5-HT1A agonists**
- LDT/PPT REM-on neuron inhibition by, 497–498
 - serotonergic inhibition of cholinergic neurons, 494–495
- Humans**
- event-related potentials in, 373–375
 - motor cortex, fast oscillations, 267
 - sleep patterns, modeling, 532–533, 534, 536
 - thalamocortical neurons, event-related potentials, 373–375
- Humoral systems**, *see* Forebrain and humoral systems
- Hyperpolarization**, *see also* Electrophysiology, intrinsic properties
- brainstem PB-evoked responses, 357
 - burst suppression, 327, 328, 329
 - delta waves, 305
- Hyperpolarization** *contd.*
- evoked potential studies, 350
 - intracellular studies, excitatory responses, 355
 - locus coeruleus cells, 87
 - lumbar alpha neuron activity during waking and sleep, 452
 - muscle atonia, 459
 - NB cells, 90
 - nucleus basalis cells, 350
 - PGO waves, 407, 408
 - doublets, 409
 - PGO-on bursting cells, 400
 - plastic changes in thalamocortical system, cortical augmenting responses and, 340
 - slow oscillations, 308
 - cellular basis of, 306
 - intracellular recording during natural NREM sleep, 310, 311
 - intracortical synchronization of, 311–313
 - synaptic reflection in thalamic and other structures, 315
 - spindles, 279, 281, 282, 285, 294, 298
 - thalamic reticular neurons, 365, 366, 367
 - thalamocortical neurons, 187, 189, 347
- Hypnogenesis**, 24–30
- Hypocretin**, *see* Orexin/hypocretin
- Hypoglossal nerve**, 115
- Hypoglossal nucleus**, 115
- Hypophysis**, 592
- Hypothalamus**
- connections
 - basal forebrain nuclei efferents, 137–138
 - to brainstem cholinergic nuclei, 72–73
 - brainstem reticular neuron projections, 91
 - histaminergic, 133
 - locus coeruleus, 85, 129
 - NB inputs, 89, 90
 - raphe nuclei afferents, 87
 - thalamic projections to midbrain reticular formation, 70
 - tuberomammillary area, 88
 - ventral tegmental area afferents, 88
 - humoral factors
 - adenosine, 567
 - IL-1 β , 588, 589
 - TNF-alpha and, 590
 - neuronal control of REM sleep, 477–478
- ICS205–930**, 247
- IL-1 β** , 582, 587–589
- Imipramine**, 248, 250
- Immobility**, fast (beta/gamma) oscillations, 263
- immunohistochemistry methods**, 5, 44–48
- Incremental response**, plastic changes in thalamocortical system, 330
- Indicator variables**, 11–12, 17–18
- Inferior colliculus**, 63, 156
- LDT and PPT neuron distribution, 108
 - locus coeruleus efferents, 129

- Inferior colliculus *contd.*
 - neocortical projections of intralaminar thalamic neurons and brainstem excitation, 105
- Inferior olivary nucleus, 112, 455
- Inferior vestibular nucleus, 355
- Inhibition-rebound sequences
 - corticothalamic synapses, 318
 - plastic changes in thalamocortical system, 331
- Inhibitory burst neurons (IBNs), 422–423
 - interactions of neurons in saccade generation, 432–437
 - neural integrator, 429
 - pontobulbar reticular projections to abducens, 424
- Inhibitory cells/interneurons, 361; *see also*
 - Local-circuit interneurons
 - GABAergic inhibition in cortex, 134
 - hippocampal trisynaptic loop, 153
 - hippocampus, 235
 - intracellular studies, 352
 - neocortex, 147–148, 150
 - thalamic, 152, 194–196, 197, 198, 361
 - EEG synchronized sleep, 379, 380
 - electrophysiological properties, intrinsic, 191–194
- Inhibitory post synaptic potentials (IPSPs)
 - intracellular studies
 - differential brainstem reticular effects on inhibitory responses, 363
 - excitatory responses, 353, 355
 - local interneurons, 363
 - midbrain reticular cells, bulbar stimulation and, 84
 - PGO waves, 407, 409
 - slow oscillations
 - cellular basis of, 306
 - synaptic reflection in thalamic and other structures, 315
 - spindles, 282, 285, 289
 - synchronized rhythms, *see* Synchronized oscillations
 - thalamocortical system, plastic changes in, 335, 338
 - thalamic circuits, types of, 142–144
 - thalamic reticular neurons, 366
 - and theta waves, 261
- Inhibitory responses
 - during brain activation, 378–380
 - brainstem reticular effects on, 361, 363
 - three phases of, 361, 363
- Initiation/onset of movement, set-dependent tasks, 376–377
- Insomnia, 27–28
- Insomnia, fatal, 26
- Integrator, neural, 429, 432
- Interhemispheric integration, 150–151
- Interlaminar nuclei, mesopontine cholinergic neurons, 388
- Internal capsule, 105
- Interneurons
 - cortical, 134, 147–148, 149
 - acetylcholine effects, 231–232
 - hippocampal trisynaptic loop, 153
 - hippocampus, 235
 - IPSPs elicited by, 364
 - LG local-circuit, 357
 - PGO waves, 409
 - structural (Reciprocal Interaction) model of organization, 515
 - thalamic, 142, 145, 152
 - brainstem cholinergic pathways, acetylcholine effects, 229–231
 - GABAergic neurons, 361, 363
- Internuclear neurons, abducens projections, 420
- Interspike interval histogram, PGO waves, 411
- Interstitial nucleus of Cajal, 426
- Intrabrainstem pontine reticular formation
 - afferents, 78–85
- Intracellular recordings
 - brainstem reticular neuronal activity over REM sleep cycle, 467–470
 - excitatory responses, 352
 - methods, 50–54
 - neuronal control of REM sleep, 475
 - recruitment within reticular pool, 480, 481
 - thalamocortical neurons
 - excitatory responses, 352–361, 362
 - inhibitory responses, differential brainstem reticular effects on, 361, 363
- Intracortical connections, 149–150, 150–151
- Intralaminar centrolateral (CL) nuclei/neurons, 98
 - intracellular studies, excitatory responses, 360
 - plastic changes in thalamocortical system, 335
 - spindles, 283, 296
- Intralaminar nuclei, 62
 - connections
 - brainstem efferents to, 93, 98, 99, 100, 104
 - to midbrain reticular formation, 68, 69
 - neocortical projections, 104, 105, 106
 - electrophysiology, intrinsic, 184
 - evoked potential studies, 350
 - neocortical pyramidal neuron connections, 146
 - projections to, 382
 - spontaneous firing in NREM sleep and brain-active states, 347
 - thalamic nuclei and, 141
- Intrinsically bursting neurons
 - repetitive callosal stimulation and, 341
 - seizures, 328
 - slow oscillations, 309
- Ionic conductances, 1
- IPSPs *see* Inhibitory postsynaptic potentials
- Isodendritic, defined, 36
- Isoproterenol, 237
- Jaw closer motoneurons, 444–446, 456
- Joseph disease gene product, 608

- Jouvet, M., 1, 2, 12, 22, 26
 Jouvet theory, 501
- Kainate, 250, 251, 254
 K-complex, 318
 Ketanserin, 246
 Kleitman, N., 2, 9
 Kölliker-Fuse nucleus, 112, 128, 453
 Kynurenate, 251, 254
- Latency, REM
 deficient process S, 560
 in depression, 547, 548
 bimodal distribution of, 555–556
 quantitative modeling, 553, 554, 555
- Lateral funiculus, 115, 116
 Lateral geniculate interneurons, PGO waves, 409
 Lateral geniculate neurons
 extracellular recordings, 351
 peribrachial area, 352
- Lateral geniculate nucleus (LGN), 95, 361
 acetylcholine effects, 223–224, 225
 brainstem-LG cholinergic projection, 357
 brainstem reticular neuronal activity over REM
 sleep cycle, 467, 468
 cholinergic influences on REM sleep, 484
 connections, 61
 brainstem efferents to, 93, 96
 brainstem reticular projections, 102
 locus coeruleus efferents, 129
 parabigeminal nucleus projections, 58
 serotonergic efferents, 131
 diffuse modulatory systems, 141
 electrophysiology, intrinsic, 191–194
 extracellular recordings, 351
 fast (beta/gamma) and ultrafast (ripple)
 rhythm, 272
 fast oscillations, 267, 268, 269
 intracellular studies, excitatory responses,
 354, 357
 local-circuit interneurons, 357
 mesopontine cholinergic neurons, 388
 modulation of excitability in neuronal pools,
 experimental evidence for, 473, 474–475
 muscarinic activation, 215
 PGO field potential, 397
 PGO waves, 395, 397, 401, 403, 409, 410, 414,
 415, 416; *see also* Ponto-geniculo-occipital
 waves
 spindles, 284, 296
 spontaneous firing in NREM sleep and brain-
 active states, 347, 349
- Lateral geniculate relay neurons
 intracellular studies, excitatory responses, 354,
 355, 359
 PGO waves, 409
- Lateral geniculate thalamic bursts, 410
 Lateral geniculate thalamocortical cells, PGO
 waves, 403, 407, 410, 411, 412
 Lateral habenular nucleus, 87, 145, 284
- Lateral lemniscus, 111
 Lateral reticular nucleus, 115, 243
 Lateral tegmental field (FTL), 62, 63, 74
 afferents to pontine reticular formation, 79
 muscle atonia, central mechanisms, 455, 456
 parvocellular neurons, 61, 386, 387
 pontine, 109
- Lateral tegmentoreticular tract, 111, 112
 Lateral ventricle, connections, 135
 Laterodorsal tegmental (LDT) nucleus, 430;
 see also Pediculopontine/laterodorsal
 tegmental neurons
 acetylcholine, 212–213, 227
 afferents to pontine reticular formation, 79
 connections, 57, 60
 basal forebrain-brainstem, 74, 75
 brainstem efferents to thalamic nuclei, 93,
 95, 94, 97
 brainstem reticular projections, 100, 101
 cholinergic projections to bulbar reticular
 formation, 112
 cholinergic projections to PFTG, 106–110
 LDT and PPT neuron distribution, 108, 109
 thalamus, 99
 excitatory amino acids and, 253
 intracellular studies, 353, 358, 360
 muscle atonia, central mechanisms, 453
 thalamic reticular neurons, 366
- Lateroposterior (LP) nucleus
 antidromic activation of PPT neurons, 391
 connections, 94, 97
 brainstem efferents to, 93
 convergent synaptic excitation of midbrain
 reticular neurons, 77
 locus coeruleus efferents, 129
 cortical projections, 141
 plastic changes in thalamocortical system, 334
- LDT, *see* Laterodorsal tegmental field
 Leak potassium current, 55, 148
 Leaky integrator, 429
- Learning
 acetylcholine and, 233–234
 basal forebrain projections to MD nucleus and,
 134
 hippocampal circuits, 153
- Lectins, anterograde and retrograde tracers, 40,
 41–43
- Lennox-Gastaut syndrome, 325
 Limbic cortex/system, 145
 spindles, 284
 thalamic connections, 98
 and theta waves, 261
- Limit Cycle model, 531–546
 cholinergically induced onset of REM sleep,
 557–559
 circadian variation in REM pattern, 533–537
 depression, 554, 555
 details, 539–546
 limitations on growth of firing rates, 540–543
 modeling events at sleep onset, 532

- Limit Cycle model *contd.*
 - modeling sleep patterns, 532–533
 - phase plane graph, 529
 - phase plane representation of entry into limit cycle, 545–546
 - REM-on autoexcitation growth function, 539–540
 - REM-on dependence on REM-off inhibitory input, 543–545
 - summary of changes from simple LV model, 531–532
- Local-circuit inhibitory cells, *see* Inhibitory cells/interneurons
- Local-circuit neurons, *see also* Interneurons
 - diffuse modulatory systems, cell types and connections, 141
 - neocortex, 145, 147, 148, 150
 - thalamic, 142, 143, 145, 146, 152
- Local field potentials
 - electrophysiological methods, 49–50, 54
 - fast (beta/gamma) oscillations, 264
- Locus coeruleus, 139, 156, 237
 - brainstem neuron currents
 - acetylcholine-modulated, 219, 221–223
 - norepinephrine-modulated, 236–243
 - cholinergically evoked hyperpolarizations, 217
 - cholinergic projections, 517
 - connections, 57, 61
 - histaminergic, 133
 - neocortical projections of intralaminar thalamic neurons and brainstem excitation, 105
 - norepinephrinergic efferents, 128–130
 - connections to brainstem monoaminergic nuclei, 85–87
 - afferents to pontine reticular formation, 79
 - raphe nuclei afferents, 87
 - ventral tegmental area afferents, 88
 - corticotropin-releasing factor and NE neurons, 550
 - electrophysiological properties, intrinsic, 171–175
 - excitatory amino acids and, 255
 - extracellular recordings, 351
 - GABAergic influences, 505–506
 - in REM sleep, 518–520
 - sources of input to, 506–507
 - humoral factors
 - IL-1 β , 588
 - TNF-alpha, 590
 - LC-MC feedback inhibition, 237
 - mesopontine cholinergic PPT-LDT neurons, 389
 - monoaminergic influences in REM sleep, 498–501
 - cooling, 499–501
 - REM-off neurons, 490
 - sites of REM-on and REM-off action, 501
 - muscarinic receptors, 217
 - muscle atonia, central mechanisms, 452, 453, 455, 456, 457
 - NE inhibition of, 518
- Locus coeruleus *contd.*
 - nicotinic excitation, 354
 - orexin actions, 603, 605, 606
 - orexin neuronal projections, 602
 - PGO-on cells, 398
 - structural (Reciprocal Interaction) model of organization, 515
- Long-lead burst neurons (LLBNs), 422, 423, 426
- interactions of neurons in saccade generation, 432–437
- oculomotor system function, wake-sleep transitions, 441
- Long-term activation, intracellular studies, 359
- Lotka-Volterra equations, 513–514
- Lotka-Volterra model, simple, 526–530
 - neutral stability of, 557
 - phase plane representation, 538
 - postulated steps in production of REM sleep episode, 526–528
 - significance of terms, 537–538
 - simple LV equations, 528–530
 - simple LV equations, limits of, 530
 - summary of changes with Limit Cycle model, 531–532
- Low-threshold augmentation, plastic changes in thalamocortical system, 335
- Low-threshold burst neurons (LTBNs), *see also* Electrophysiology, intrinsic properties
 - medial pontine reticular formation neurons, 156, 157, 159–161, 167
- Low-threshold spikes (LTS), 517; *see also* Electrophysiology, intrinsic properties
 - augmenting response, 336
 - brainstem control of corticothalamic networks, 140
 - medial pontine reticular formation neurons, 156, 157, 159–161
 - plastic changes in thalamocortical system, 331
 - PPT-LDT, 170
 - rebound, 355
 - spindles, 282, 294
- Lumbar motoneurons, 446, 447–450, 450–451
- Machine state, 11
- Magnesium blockade, NMDA, 251
- Magnetic resonance imaging, 54
- Magnetoencephalography, 49, 263, 265
- Magnocellular neurons, 61, 386, 387
 - bulbar, 83, 454, 456
 - medullary, brainstem-thalamic projections, 104
- Magnocellular pontine reticular formation, afferents to, 78, 79
- Magnocellular preoptic nucleus, orexin neuronal projections, 602
- Magnocellular tegmental fields (FTM)
 - connections, 63, 74, 111, 112
 - afferents to pontine reticular formation, 79
 - brainstem-thalamic projections, 104
 - thalamus, 98–99
 - muscle atonia, central mechanisms, 453, 454, 456

- Magnocellular zones, reticular formation
 afferents to pontine reticular formation, 79
 muscle atonia, central mechanisms, 456
- Mammillary nuclei
 connections, 88, 98
 intracellular studies, excitatory, 359, 361
- Mammillothalamic axis, 129, 361
- Mathematical models of sleep, 562
- McCarley-Massaquoi-Hobson model,
see Reciprocal Interaction model
- Mecamylamine
 intracellular studies, 358
 neocortex, 231
 thalamic reticular neurons, 227
- Medial forebrain bundle, 129, 260
- Medial geniculate nucleus (MGN), 68, 95, 405
 acetylcholine effects, 224, 225
 diffuse modulatory system connections, 141
 muscarinic activation, 215
- Medial longitudinal fascicle (MLF), 113, 156, 419
 connections, 111
 afferents to pontine reticular formation, 80,
 81, 82
 brainstem afferents to, 83
 bulbar gigantocellular tegmental field, 82
 reticulospinal fibers, 115–116
 gaze control, 439
 LDT and PPT neuron distribution, 108
 pontobulbar reticular projections to abducens,
 424, 425
- Medial pons
 muscle atonia, 459
 PGO-on cells, 399
- Medial pontine gigantocellular tegmental field
 (mPFTG), 480, 481
- Medial pontine reticular formation (mPRF)
 adrenergic receptors, 237, 243–244, 243
 afferents to pontine reticular formation, 81
 behavioral state alterations in, 470
 brainstem cholinergic neuron currents, 212–219
 brainstem reticular neuronal activity over REM
 sleep cycle, 470, 471
 cholinergic influences on REM sleep, 485–488
 electrophysiological properties, intrinsic,
 156–167
 classes of neurons, 156–159
 low- and high-threshold calcium spikes,
 159–166
 membrane potential, control of repetitive
 firing, behavioral implications, 167
 modulation of excitability in neuronal pools,
 experimental evidence for, 473
 PGO-on cells, 398
 pre-REM sleep changes, 468, 469
 state-dependent alterations in excitability, 470,
 471
- Medial raphe nucleus, 243
- Medial rectus motoneurons, abducens
 projections, 420
- Medial reticulospinal tract, 113
- Medial septum, 89, 179
- Medial vestibular nuclei
 gaze control, 439
 leaky integrator, 429
- Mediodorsal (MD) thalamic nuclei
 blockage of slow cortical oscillations by
 mesopontine PPT nucleus, 393
 connections, 60, 62, 94, 97, 98
 basal forebrain projections, 134, 135, 136
 brainstem efferents to, 93
- Medullary glutamatergic neurons, 55–56
- Medullary laminae, 129
- Medullary magnocellular fields, brainstem-
 thalamic projections, 104
- Medullary reticular formation, thalamic
 connections, 91, 93, 98–99, 98
- Membrane conductance, intracellular studies, 354
- Membrane potentials, *see also* Electrophysiology,
 intrinsic properties
 electrographic signs and, 481
 medial pontine reticular formation neurons, 167
 neuronal control of REM sleep, 475
 soma size and, 480, 481
- Memory
 acetylcholine and, 233–234
 basal forebrain projections to MD nucleus
 and, 134
 hippocampal circuits, 153
 plastic changes in thalamocortical system,
 329, 330
- Mesencephalic central gray, 85
- Mesencephalic reticular formation (MRF)
 adrenergic receptors, 243
 afferents to pontine reticular formation, 80
 brainstem efferents to, 93
 brainstem reticular neuronal activity over REM
 sleep cycle, 472
 burst neurons, 423
 nonreticular brainstem projections to
 abducens, 427
 spinoreticular pathways, 67
 superior colliculus and frontal eye field
 projections to, 426
- Mesencephalon
 cholinergic cell groups, 382
 ventral tegmental area, sensorimotor
 rhythms, 259
- Mesopontine cholinergic nuclei
 brainstem neuron currents, serotonin-
 modulated, 249
 connections
 brainstem and spinal cord projections,
 106–117
 dual thalamic connections, 106
 histaminergic, 133
 glutamatergic neurons and, 55–57
 intracellular studies, 361
 stimulation, 362
 tonic electrical activation of cerebral cortex by
 brainstem thalamic neurons, 388–391, 392

- Mesopontine junction
 - intracellular studies, excitatory, 353
 - tuberomammillary area afferents, 88
- Mesopontine neurons, 90
- Mesopontine PGO-on cells, 383, 398, 399
- Mesopontine reticular formation
 - connections, 60–61, 90–91
 - excitatory amino acids and, 253, 253–254
- Mesopontine tegmental nuclei, orexin neuronal projections, 602
- Mesostriatal pathway, dorsal, dopaminergic connections, 132
- Metabolism, adenosine, 568–569
- Methodology, 35–54
 - electrophysiological studies, 48–54
 - morphological studies, 25–48
 - anterograde and retrograde tracing, 39–44
 - immunohistochemistry, 44–48
 - Nissl and Golgi staining, 35–39
 - noninvasive methods, 54
- Methylcholine, 226
- 2-Methyl-5-hydroxytryptamine, 247
- Methylsergide, 250
- Meynert, nucleus basalis of, *see* Nucleus basalis
- Microsleeps, 562
- Midbrain
 - cerebral activation, 382
 - brainstem afferents to, 82–85
 - connections to brainstem cholinergic nuclei, 82–85
 - reticular noncholinergic neurons, 384, 385
- Midbrain extrapyramidal area, 111, 112
- Midbrain-pontine junction, 11, 64, 72, 91
 - brainstem afferents, 83, 84
 - brainstem projections to thalamic nuclei, 93
- Midbrain reticular formation (MRF), 55
 - connections, 55, 105
 - brainstem afferents to, 82–85
 - brainstem cholinergic stimulation, 93
 - brainstem efferents to thalamic nuclei, 97–98
 - central tegmental field, 61–62
 - histaminergic, 133
 - neocortical projections to brainstem, 76
 - preoptic area connections, 73
 - spinoreticular pathways, 68
 - synaptic convergence, 76–78
 - thalamic projections, 68–72
 - thalamic relay, 91
- delta waves, 305
- evoked potential studies, 348, 349, 350
- extracellular recordings, 351, 352
- neuronal activities controlling wake-sleep states
 - cerebral cortex activation by brainstem thalamic neurons, 384, 385, 386
 - bulboreticular (RE) neurons with midbrain and thalamic projections, 386, 387
 - bulbothalamic neurons and, 383
- spindles, 295, 297
- Midpontine pre-trigeminal preparations, extracellular recordings, 351
- MLF (medial longitudinal fascicle), *see* Medial longitudinal fascicle
- Mobility, sensorimotor rhythms, 257–259
- Molecular gate, 330
- Monoaminergic influences on REM sleep, 488–501
 - in depression
 - bimodal distribution of REM sleep latencies, 556
 - modeling REM sleep in, 547, 548, 549–550, 553–554
 - LDT-PPT REM-on neuron inhibition by HTIA agonist, 497–498
 - locus coeruleus, 490, 498–501
 - raphe nuclei, 490
 - inverse association with REM events, 490–495
 - suppression and increases in REM sleep, 495–497
 - REM-off neurons, 490–501
- Monoaminergic neurons/nuclei, 139
 - basal forebrain connections, 74
 - brainstem afferents, 85–88
 - locus coeruleus, 85–87
 - raphe nuclei, 87
 - tuberomammillary area, 88
 - ventral tegmental area, 87–88
 - in cholinergic nuclei, 55
 - depression, quantitative modeling of sleep abnormalities in, 550–552
 - efferent connections, 128–133
 - dopaminergic systems, 132
 - histaminergic systems, 133
 - norepinephrinergic systems, 128–130
 - serotonergic systems, 130–132
 - evoked potential studies, 350
 - immunohistochemistry, 44
 - LG thalamic nucleus projections, 93
 - muscle atonia, central mechanisms, 456
 - spindles, 287
 - thalamic nuclei, projections to, 96
- Mood
 - adenosine and, 583–584
 - depression, *see* Depression
- Morphological methods, 25–48
 - anterograde and retrograde tracing, 39–44
 - immunohistochemistry, 44–48
 - Nissl and Golgi staining, 35–39
- Moruzzi, G., 1, 2–3, 4, 5, 6, 9, 15
- Motor activity, 23
 - midbrain reticular noncholinergic neurons, 384
 - states of vigilance, 12
- Motor area
 - slow oscillations, 311
 - spindles, 280

- Motor cortex
 - circuitry, 148–149
 - connections, 105
 - cholinergic projections from NB and diagonal band nuclei, 134
 - thalamic projections, 141
 - fast (beta/gamma) oscillations, 264, 267
 - plastic changes in thalamocortical system, 342
- Motor field, neuron, 423
- Motor functions, *see also* Sensorimotor cortex
 - spinoreticular pathways, 70, 72
 - thalamic nuclei and, 141
- Motor neurons
 - interactions of neurons in saccade generation, 432–437
 - modulation of excitability in neuronal pools, experimental evidence for, 473, 474
 - reticulospinal projections, 116–117
- Motor relay nuclei, thalamus, 141
- Motor sensory function, *see also* Sensorimotor cortex
 - neocortical projections to brainstem, 76
 - origins of sensorimotor rhythm, 257–259
- Motor systems, 417–459
 - burst neurons, 420–426, 427
 - anatomic connectivity, 424–426, 427
 - physiology, 420–423
 - central mechanisms of REM sleep atonia, 452–459
 - electrophysiological data, 454–458
 - lesion data and REM without atonia, 452–453, 454
 - other pontine structures and pharmacology of, 458–459
 - gaze control, 437–444
 - mechanisms of muscle atonia of REM sleep, 444–452
 - inhibition and diminished excitability of trigeminal jaw closer motoneurons during REM sleep, 444–446
 - spinal alpha motoneurons during sleep-wake cycle, 446–452
 - omnipause neurons, 426, 428–429, 430
 - saccade generation, interactions of neurons in circuit, 432–437
 - model of, 435–437
 - superior colliculus, 433–434
 - trajectories, mutability of, 434
 - saccadic eye movements, 417–420
 - afferents to oculomotor neurons, lesion studies, 419, 420
 - efferent projections of abducens neurons, 420
 - physiological properties of oculomotor neurons, 418–419
 - state-dependent alterations in oculomotor system function, 439–444
 - activity during REM sleep, 441–444
 - waking to synchronized sleep transitions, 439–440
 - tonic neurons, 429, 431–432
- Motor thalamic relay, 93, 98, 99
- Movement, initiation of, 376–377
- Multi-unit activity, evoked potential studies, 350
- Muscarinic cholinergic-adrenergic reciprocity, muscle atonia, 459
- Muscarinic mechanisms
 - cholinergic agonists and, 213, 215
 - evoked potential studies, 350
 - GABA PRF neuron inhibition, 516–517
 - narcolepsy, 110
 - NB cells, 90
 - potassium conductance, 217
 - TC neuron depolarization, 359
- Muscarinic-mediated hyperpolarization of NB cells, 350
- Muscarinic receptors, 217–218
 - hippocampus, 234, 235
 - locus coeruleus, 221, 222
 - neocortex, 231, 232–233
 - thalamic reticular neuron dual response, 367
 - thalamic reticular neurons, 226, 229
- Muscle atonia, 33, 403, 413
 - central mechanisms in REM sleep, 452–459
 - electrophysiological data, 454–458
 - lesion data and REM without atonia, 452–453, 454
 - other pontine structures and pharmacology of, 458–459
 - cholinergic influences on REM sleep, 483, 484
 - gigantocellular fields and, 112
 - mechanisms of in REM sleep, 444–452
 - inhibition and diminished excitability of trigeminal jaw closer motoneurons during REM sleep, 444–446
 - spinal alpha motoneurons during sleep-wake cycle, 446–452
 - modulation of excitability in neuronal pools, experimental evidence for, 474
 - neuronal control of REM sleep, 475
 - orexin actions, 608
 - sleep state control schematic, 472
 - structural (Reciprocal Interaction) model of organization, 515
- Muscle twitches, neuronal control of REM sleep, 476–477
- Narcolepsy, 110, 600–601, 608
- Natural sleep, PGO wave genesis, 409–416
- NB (nucleus basalis), *see* Nucleus basalis
- Neocortex, 139
 - adrenergic receptors, 245–246
 - brainstem neuron currents
 - acetylcholine-modulated, 231–234
 - excitatory amino acid-modulated, 254
 - norepinephrine-modulated, 245–245
 - serotonin-modulated, 250
 - brainstem reticular neuron projection studies, 91–92

- Neocortex *contd.*
- connections
 - to brainstem cholinergic nuclei, 76
 - corticopetal link, brainstem-thalamic projections, 104, 105
 - histaminergic, 133
 - locus coeruleus efferents, 129–130
 - serotonergic efferents, 131–132
 - delta waves, 300–305
 - diffuse modulatory systems, 145–153
 - brainstem control of corticothalamic networks, 139, 140, 142
 - GABAergic transmission, 147–148
 - glutamate, aspartate transmitters, 146–147
 - long-range connections, 148–153
 - neuron classes, 145–146
 - neuron firing patterns, 146–147
 - electrophysiological properties, intrinsic, 197, 199–208
 - changes in firing patterns during synaptic activities and shifts in behavioral state, 199, 201–208
 - firing patterns in four neuronal types and underlying ionic currents, excitatory amino acids and, 253
 - fast oscillations, 267, 274
 - NB-elicited activation, 134
 - parallel activating pathways, 391
 - plastic changes in thalamocortical system, 329, 335, 341
 - PPT-induced activation, 90
 - slow oscillations, 305–327, 328
 - cellular basis of, 306–307, 310
 - grouping of delta spindles and fast oscillation by slow oscillation, 318–324, 325
 - intracellular recording during natural NREM sleep, 310, 311, 312, 313
 - intracortical synchronization of, 311–314
 - synaptic reflection in thalamic and other structures, 314–318
 - spindles, synchronizing and terminating, 290–294, 295, 296
- Neonates, 243
- Neostigmine, 110, 221
- Nerve growth factor, 583
- Nerve growth factor receptor, 137
- Neural integrator, 429, 430, 431, 432
- Neurobiotin, 39
- Neurogliaform cells, 147, 148
- Neuromodulation criteria, neuronal control of REM sleep, 480–482
- Neuromodulators, extracellular recordings, 351
- Neuronal activities, brainstem and basal forebrain structures *contd.*
- cellular mechanisms, 402–409
 - during natural sleep, 409–416
 - brainstem-thalamic neurons implicated in tonic electrical activation of cerebrum, 382–391, 392
 - bulbar reticular noncholinergic neurons, 384, 386, 387
 - mesopontine cholinergic neurons, 388–391
 - midbrain reticular cholinergic neurons, 384, 385
- Neuronal aggregates, synchronized rhythms, *see* Synchronized oscillations
- Neuronal control of REM sleep, 461–511
- brainstem reticular neuronal activity over REM sleep cycle, 462–480
 - behavior state alterations in mPRF, 470
 - extracellular recordings, 464–467
 - intracellular recordings, 467–470
 - pre-REM changes, transition period T, 468–469
 - REM sleep, 469
 - sleep-wake control resulting from modulation of excitability in neuronal pools, 470, 472–480
 - state-dependent alterations in reticular excitability, 470, 471
 - synchronized sleep, 467
 - wakefulness, sleep-wake transition, 469
- cholinergic influences, 482–487
- induction of REM sleep-like phenomena, 482–484
 - LDT stimulation, production of scopolamine-sensitive EPSPs in mPRF neurons, 485
 - unit activity during sleep and wakefulness, 485–487
- GABAergic influences, 501–511
- dorsal raphe nucleus suppression and increases in REM sleep, 502–505
 - locus coeruleus, 505–506
 - pontine reticular formation, distribution and REM sleep, 507–509
 - PPT nucleus, 509–511
 - source of input to dorsal raphe nucleus and locus coeruleus, 506–507
- modeling
- postulated steps in production of REM sleep episode, 524–528
 - REM sleep in depression, 547, 548
- monoaminergic influences, 488–501
- dorsal raphe discharge, inverse association with REM events, 490–495
 - dorsal raphe nucleus suppression and increases in REM sleep, 495–497
 - LDT-PPT REM-on neuron inhibition by HTIA agonist, 497–498
 - locus coeruleus, 490, 498–501
 - raphe nuclei, 490
 - REM-off neurons, 490
- neuromodulation criteria, 480–482

- Neuronal networks, 33
- Neuronal plasticity, *see* Plasticity
- Neuronal pools, sleep-wake control resulting
 - from modulation of, 470, 472–480
- Neurons
 - convergent inputs onto single brainstem
 - reticular cell, 76–78
 - extracellular recordings, 50–53; *see also* Extracellular recordings
 - intracellular recordings, *see* Intracellular recordings
 - intrinsic cell morphology and projections of
 - pontine and bulbar gigantocellular fields, 117–128
 - orexin/hypocretin actions, 603–605
 - PFTG and BFTG morphology, 117–128
 - slow oscillation synchronization, 314
 - soma size, *see* Soma size
- Neuropeptides, *see* Peptide neurotransmitters
- Neuropeptide Y, 128
- Neurophysin, 86
- Neurotransmitter-modulated currents, 211–254
 - acetylcholine, 212–235
 - basal forebrain, 223
 - hippocampus, 234–235
 - locus coeruleus, 219, 221–223
 - medial pontine reticular formation, 212–219
 - neocortex, 231–234
 - pediculopontine tegmental cholinergic neurons, 219, 220
 - thalamus, 223–231
 - excitatory amino acids, 250–254
 - brainstem, 253–254
 - cerebral cortex, 250
 - neocortex, 254
 - receptor types, 250–252
 - thalamus, 254
 - norepinephrine, 236–246
 - basal forebrain, 244–245
 - dorsal raphe nucleus, 243–244
 - hippocampus, 245–246
 - locus coeruleus, 236–243
 - neocortex, 245
 - pontine reticular formation, 243
 - thalamus, 245
 - serotonin, 246–250
 - dorsal raphe nucleus, 247–248
 - facial motoneurons, 248–249
 - mesopontine cholinergic nucleus, 249
 - pontine reticular formation, 248–249
 - thalamus, 250
- Neurotransmitters
 - evoked potential studies, 350
 - immunohistochemistry, 44–48
 - neuromodulation of REM sleep, 481, 482
 - peptide, *see* Peptide neurotransmitters
 - retrograde tracing with, 44
- NF-kB, 581–583
- Nicotinic mechanisms, 221, 357
 - evoked potential studies, 350
 - intracellular studies, 353, 358, 359
 - lateral geniculate nucleus, 224
 - neocortex, 231
 - PGO waves, 409
 - thalamic reticular neurons, 226, 227, 226, 367
 - thalamic reticular neuron dual
 - response, 367
- Nissl staining, 35–39
- Nitric oxide, 569, 584
- NMDA (*N*-methyl-D-aspartate), 179, 223
 - receptors, 250, 251
 - slow oscillation, cellular basis of, 306
- Nonburst (NB) firing pattern, *see also* Electrophysiology, intrinsic properties
 - medial pontine reticular formation neurons, 156, 157, 158, 165, 166
- Noncholinergic neurons, 55, 139
 - cerebral cortex activation by brainstem-thalamic neurons, 384, 386, 387
- basal forebrain
 - hypothalamic projections, 90
 - projections to thalamus, 134, 136, 137
- brainstem
 - centromedian-parafascicular (CM-Pf) nuclei
 - projections, 101
 - rostral projections, 91–106
- evoked potential studies, 350
- medial septum, 89
- midbrain, pontine, and medullary fields, 91
- Noninvasive methods, 54
- Nonmonoaminergic neurons, cortical
 - projections, 91–92
- Non-NMDA receptors, 250, 251
 - thalamocortical, 254
- Non-REM (NREM) sleep, 305–327, 328
 - abnormal oscillations during, 325, 327, 329
 - burst suppression, 327, 329
 - electrical seizures developing from, 325, 327, 328
 - bulbothalamic neurons and, 386, 387
 - EEG activation during transition, 382
 - intracellular studies, excitatory responses, 359
 - mesopontine cholinergic neurons, 388
 - neocortical slow oscillation in, 305–327, 328
 - cellular basis of, 306–307, 310
 - delta spindles and fast oscillation grouping
 - by slow oscillation, 318–324, 325
 - intracellular recording during natural NREM sleep, 310, 311, 312, 313
 - intracortical synchronization of, 311–314
 - synaptic reflection in thalamic and other structures, 314–318
 - synchronized rhythms, *see* Synchronized oscillations
 - thalamocortical system, spontaneous firing
 - modes during, 346–347, 348
 - transition to REM sleep, 383, 384, 384
- Nonspecificity of activation, 4, 5

- Noradrenaline
 - immunohistochemistry, 44
 - muscle atonia, 459
- Noradrenergic neurons, 92
 - cat brainstem, 59
 - centers for states of, 30
 - locus coeruleus, 86, 87
 - neuropeptide colocalization, 128
 - paragigantocellularis nucleus, 86
 - PPT/LDT nuclei, 57–58
 - thalamic nuclei, 93, 95, 96
 - thalamic reticular neurons, 365
 - tyrosine hydroxylase immunohistochemistry, 45, 48
- Norepinephrine/norepinephrinergic systems, 61
 - brainstem neurons, actions of, 236–246
 - basal forebrain, 244–245
 - dorsal raphe nucleus, 243–244
 - hippocampus, 245–246
 - locus coeruleus, 236–243
 - neocortex, 245–245
 - pontine reticular formation, 243
 - thalamus, 245
 - efferent connections, 128–130
 - evoked potential studies, 350
 - LDT/PPT neuronal interactions, 518
 - locus coeruleus, 85, 87
 - modeling REM sleep in depression, 550
 - REM-on and REM-off neuron interaction sites, 501
 - thalamic cell excitation, 351
- Nuclear Yellow, 43
- Nucleus accumbens, 88, 132
- Nucleus basalis (NB), 23, 73, 89–90
 - acetylcholine and, 223
 - brainstem-thalamic neurons implicated in tonic electrical activation of cerebrum, 383
 - connections
 - cortical, 133, 134, 137
 - hypothalamus, posterior, 137–138
 - electrophysiological properties, intrinsic, 179
 - excitatory amino acids and, 253
 - parallel activating pathways, 391, 393
 - PPT/LDT projections, 350
 - projection to dorsal thalamic nucleus, 394
- Nucleus intercalatus, 114, 439
- Nucleus Kölliker-Fuse, 112, 128, 453
- Nucleus lateralis tegmenti dorsalis, *see*
 - Laterodorsal tegmental nucleus
- Nucleus paragigantocellularis (RPG, PGCL), *see*
 - Paragigantocellularis nucleus; Parabrachial nucleus; Peribrachial area
- Nucleus proprius, 64
- Nucleus raphe, *see* Raphe nuclei
- Nucleus raphe dorsalis, *see* Dorsal raphe nucleus
- Nucleus reticularis gigantocellularis, *see*
 - Gigantocellular tegmental field
- Nucleus reticularis paramedianis, gaze control, 439
- Nucleus reticularis pontis caudalis (RPC), *see*
 - Caudal nucleus
- Nucleus reticularis supragigantocellularis (NRS), 425
- Nucleus reticularis tegmenti pontis (NRTP), 426
- Nucleus reticularis ventralis, gaze control, 439
- Nucleus subcoeruleus, locus coeruleus efferents, 130
- Nucleus supragenualis, 114
- Occipital cortex, 133
- Octanol, 170, 171
- Ocular system, *see* Visual signals
- Oculomotor system, 66, 113; *see also* Motor systems
 - lesion studies, 419, 420
 - physiological properties, 418–419
 - state-dependent alterations in, 439–444
- 8-OH-DPAT, 250
- Olfactory cortex, fast (beta/gamma) oscillations, 263
- Omnipause neurons (OPNs)
 - interactions of neurons in saccade generation, 432–437
 - motor system, 426, 428–429, 430
 - oculomotor system, state-dependent alterations in, 439–440
- Onset of sleep
 - modeling, Limit Cycle model, 532
 - transitions, *see* Transitions/state changes
- Opioid agonists, 217
- Opioid peptides, 240, 241, 251
- Optic chiasm, 94
- Optic nerve, 66
- Optic tract stimulation
 - blockage of slow cortical oscillations by mesopontine PPT nucleus, 393
 - evoked potential studies, 349
 - extracellular recordings, 351
 - lateral geniculate oscillations, 193
 - thalamic reticular neuron dual response, 367
- Optokinetic system, neural integrator, 429
- Orexin/hypocretin, 600–610
 - actions at cellular level, 603–605
 - identification of, 600–602
 - neuronal projection and receptors, 602–603
 - release of, circadian cycles versus behavioral states, 606–610
 - REM-related phenomena and wakefulness, 606
- Oscillations, *see also* Rhythms; Synchronized oscillations
 - amygdala, 153
 - cortical, 149
 - corticothalamic networks, 152
 - electrophysiological methods, 48
 - historical developments and changing concepts, 12, 13, 14, 15
 - nucleus basalis, 179
 - thalamic, 143–145
 - thalamic neurons, 181

- Oscillations *contd.*
 thalamic pacemaker, 98
 thalamic reticular neurons and, 142
 thalamocortical neuron electrophysiology, 182–184, 185
- Oscillators, historical developments and changing concepts, 10–11
- Pacemakers, 256, 524
 cholinergic neurons in NB nucleus, 394
 locus coeruleus neurons, 171–175
 spindles, 284–290, 295
 thalamic reticular nucleus, 98, 144, 284–290
- Pain pathways, thalamic nuclei and, 141
- Parabigeminal (PBG) nucleus, 58, 61
- Parabrachial nucleus, 112
 connections, 55, 57, 64, 73, 86
 afferents to pontine reticular formation, 79
 basal forebrain-brainstem, 75
 locus coeruleus, 128
 spinoreticular pathways, 66
 muscle atonia, central mechanisms, 453
- Paracentral nuclei, projections of, 141
- Paracentral rostral intralaminar nucleus, 332
- Paradoxical sleep, 9, 386
- Parafascicular nuclei
 centromedian, *see* Centromedian-parafascicular nuclei
 striatal projections, 141
- Paragigantocellularis (PGCL) nucleus, 65
 afferents to pontine reticular formation, 79
 brainstem reticular projections, 102
 locus coeruleus afferents, 86, 87
- Paraleminiscal tegmental field (FTP), 62, 91, 459
- Parallel activation
 blockage of slow cortical oscillations by mesopontine PPT nucleus, 393
 Lateral geniculate local-circuit interneurons, 357
- Paramedian pontine reticular formation (PPRF), 417, 419, 420
 brainstem afferents to, 83
 superior colliculus and frontal eye field projections to, 426, 427
- Paraventricular area, locus coeruleus
 connections, 85
- Paraventricular hypothalamic nucleus
 connections, 73
- Parietal association cortex, 331
- Parietal cortex
 connections, 105, 133
 NB and diagonal band nuclei projections, 133
 plastic changes in thalamocortical system, 331
 set-dependent tasks, electrophysiological recordings with, 377
- Paroxysmal depolarizing shifts, seizures, 327
- Pars compacta, 57, 109, 111
- Pars reticulata, 604
- Parvalbumin, 48, 147
- Parvocellular neurons, 61, 386, 387
- Parvocellular nucleus, *see* Lateral tegmental field
- Passive sleep, 20–24
- Patterns of sleep, modeling, 532–533
- PB (peribrachial area), *see* Peribrachial area
- Pedunculo pontine/laterodorsal tegmental neurons (PPT/LTD), 359
 brainstem-thalamic neurons implicated in tonic electrical activation of cerebrum, 383
 cholinergic agonists and, 217
 cholinergic influences on REM sleep, 483–487
 cholinergic neurons in NB nucleus, 394
 connections
 brainstem efferents to thalamic nuclei, 93, 95
 glutamatergic neurons and, 55–58
 NB inputs, 89, 90
 SNr inhibitory projections, 85
 electrophysiological properties, intrinsic, 167–171
 evoked potential studies, 350
 humoral factors
 adenosine and, 564–565
 orexin neuronal projections, 602
 mesopontine cholinergic neurons, 388, 389, 390, 391
 modeling
 postulated steps in production of REM sleep episode, 524–528
 structural (Reciprocal Interaction) model of organization, 515–516
 PGO-on bursts, 400
 PGO-on cells, 397
 PGO waves, 405; *see also* Ponto-geniculo-occipital waves
 in REM sleep, 401
 transfer to thalamus, 405
 rate of tonic firing, 400
 REM-on and REM-off neuron interaction sites, 501
 serotonergic inhibition of cholinergic neurons, 497–498
 serotonin effects, 249
 spikes preceding LG-PGO file potential, 398
 types of neurons in, 57–58
- Pedunculo pontine tegmental (PPT) neurons
 brainstem cholinergic neuron currents, 212–213, 219, 220
 blockage of slow cortical oscillations, 393
 excitatory amino acids and, 253
 firing rates in sleep transitions, 392
 PGO waves, 403; *see also* Ponto-geniculo-occipital waves
 ablation, PGO suppression, 395, 396
 PGO-on cells, 399
 in REM sleep, 402
 thalamically projecting neurons, 388
 thalamic reticular neurons, dual types of responses, 363

- Pedunculopontine tegmental (PPT) nucleus, 111
 - cell types, 101–102
 - cholinergic influences on REM sleep, 483–487
 - cholinergic nuclei, 57
 - connections, 61, 62, 84
 - basal forebrain-brainstem, 74
 - brainstem afferents to, 84
 - brainstem efferents to thalamic nuclei, 93, 95, 97
 - brainstem reticular projections, 101
 - brainstem reticular projections to thalamic nuclei, 104
 - cholinergic projections, spinal and bulbar, 110–112
 - cholinergic projections to bulbar reticular formation, 112
 - cholinergic projections to PFTG, 106–110
 - thalamus, 99
- GABAergic influences on REM sleep, 509–511
- humoral factors, adenosine, 567
- intracellular studies, EEG activation, 362
- pulse train
 - blockage of slow cortical oscillations by mesopontine PPT nucleus, 393
 - ventrolateral nucleus activation by, 362
- REM-on and REM-off neuron interaction sites, 501
- serotonergic inhibition of cholinergic neurons, 494–495, 497–498
- spindles, 297
- structural (Reciprocal Interaction) model of organization, 515
- Pedunculopontine tegmental nucleus (PPT)-pars compacta, 57
- Peptide cells, somatosensory cortex, 148
- Peptide neurotransmitters, 58
 - immunohistochemistry, 48
 - locus coeruleus afferents, 86
 - neocortex, 147
 - tyrosine hydroxylase colocalization, 128
 - ventral tegmental area, 88
- Perforant path, 153
- Periaqueductal gray
 - connections, 94, 98, 99
 - dopaminergic, 132
 - tuberomammillary area afferents, 88
- GABAergic influences and REM sleep, 506–507
- nonreticular brainstem projections to abducens, 426, 427
- Peribrachial (PB) area, 367
 - brainstem PB-evoked responses, 356
- connections, 57, 60, 64, 72
 - afferents, 74
 - afferents to pontine reticular formation, 79
 - basal forebrain-brainstem, 74, 75
 - brainstem, 84, 93, 94, 95, 100, 103
 - to midbrain reticular formation, 69
- excitatory amino acids and, 253
- intracellular studies, excitatory responses, 352, 353, 356, 357
- Peribrachial (PB) area *contd.*
 - mesopontine cholinergic neurons, 388
 - PGO waves, 78, 409
 - PPT nucleus, 352
 - spindles, 298
 - thalamic reticular neurons, dual types of responses, 363, 367, 369, 370
- Peribrachial (PB) volley, 409
- Perigeniculate nucleus (PGN)
 - brainstem reticular projections, 103
 - peribrachial (PB-PG) axons, 367
 - PGO waves, 409
 - spindles, 297, 299
 - thalamic reticular neurons, 365
- Peripallidum area, evoked potential studies, 350
- Peripheral motoneurons, 474
- Persistent nonactivating sodium current, 189
- Pes pedunculus, 77
- Petit mal epilepsy, 327
- PET scans, 53, 54
- PGO, *see* Ponto-geniculo-occipital waves
- PGO-off cells, 400, 404, 405
- PGO-on cells, 397–401, 404, 405
 - burst, 395, 397, 400, 401
 - in PPT nucleus during REM sleep, 401
 - SNr inhibitory projections and, 85
- PHA-L as anterograde tracer, 40
- Pharmacology
 - adenosine, 562
 - antidepressants, monoamine system, 550–552
 - GABA and pontine reticular formation, 507–509
 - muscle atonia of REM sleep, 458–460
 - neuromodulation of REM sleep, 482
 - neuronal control of REM sleep, *see* Neuronal control of REM sleep
- Phase advance, in depression, 549, 559
- Phase-locked calcium potentials, and theta waves, 261
- Phase plane graphs, 528, 529, 535, 545–546
- Phase response curve, cholinergically induced onset of REM sleep, 557–559
- Phase shifts, fast (beta/gamma) oscillations, 264
- Phasic discharges
 - neuronal control of REM sleep, 476–477
 - oculomotor neurons, 418
- Phentolamine, 239
- Phenylephrine, 237, 242
- Phenylethanolamine-*N*-methyltransferase, 87
- Picrotoxin, 87
- Piperoxan, 239
- Pirenzepine, 217, 221
- Plasticity
 - augmenting or incremental responses, 330–335
 - excitatory amino acids and, 254
 - frequency-dependent, 148
 - following spindles, experimental model, augmenting responses, 335–343
 - potentiation of cortical responses following fast oscillation, 343

- POAH, 591–592
- Pons/pontine structures, *see also specific structures*
 gigantocellular fields, *see* Gigantocellular fields
 muscle atonia, central mechanisms, 453,
 458–459
 oculomotor system lesions, 419
 rostral, cholinergic neurons, 56, 382
- Pontine cat, 462–463, 475
- Pontine gigantocellular tegmental fields (pFTG),
 74, 116
 connections, 83
 afferents to pontine reticular formation,
 79, 80
 cell morphology and, 117–128
 locus coeruleus, 130
 mesopontine cholinergic projections to,
 106–110
 noncholinergic brainstem and spinal cord
 projections, 112–117
- neuron morphology, 118–119
 bifurcating axonal collaterals, organization
 of, 128
 cells sending axons to bulbar reticular
 formation, 119–123
 cells sending axons to ipsilateral MLF, 119
 cell size distribution, 118
 dendrites, 123–124
 general comments on morphology, 127
 pontobulbar reticular projections to
 abducens, 424
- Pontine gray, 105, 130
- Pontine lateral tegmental field (PFTL), 109
- Pontine nuclei
 plastic changes in thalamocortical system, 334
 connections of brainstem monoaminergic
 nuclei, intrinsic cell morphology and,
 117–128
- Pontine reticular formation (PRF)
 adrenergic receptors, 243–244
 brainstem afferents to, 83
 brainstem neuron currents
 norepinephrine-modulated, 243
 serotonin-modulated, 248–249
 brainstem reticular neuronal activity over REM
 sleep cycle, 467
 extracellular recordings, 464–467
 pontine cat, 462–463
 burst neurons, 422–423, 424
 cerebral activation, 383
 cholinergic influences on REM sleep, 483
 connections, 90–91
 afferents to, 78–82, 83
 to brainstem cholinergic nuclei, 78–82, 83
 brainstem efferents to, 93, 102
 locus coeruleus, 86, 130
 mesopontine cholinergic projections to
 PFTG, 106–110
 spinoreticular pathways, 66
 thalamic relay, 91, 98
 excitability, modulation of, 473
- Pontine reticular formation (PRF) *contd.*
 excitatory activity, 478
 GABAergic influences on REM sleep, 507–509
 gaze control, 437–438
 interactions of neurons in saccade generation,
 432–437
 lumbar alpha neuron activity during waking
 and sleep, 452
 motor control
 muscle atonia, central mechanisms, 452,
 454–458
 saccades, short-lead burst neurons, 420–422
 medial, *see* Medial pontine reticular
 formation
 muscarinic receptors, 217
 excitability, 473, 478
 neuron size heterogeneity, 62–63
 oculomotor afferents, lesion studies, 419, 420
 orexin neuronal projections, 602
 PGO-on cells, 398
 pontobulbar reticular projections to
 abducens, 424
 sleep state control schematic, 472
 structural (Reciprocal Interaction) model of
 organization, 514–515, 516–517
 superior colliculus and frontal eye field
 projections to, 426
 terminology, 61, 63
 tonic neurons, 429
- Pontine tegmentum
 connections, 62, 92, 105
 muscle atonia, central mechanisms, 452
- Pontis caudalis, *see* Caudal nucleus
- Pontobulbar connections
 afferents to pontine reticular formation, 80
 brainstem and spinal cord projections,
 106–117
- Pontobulbar gigantocellular tegmental fields,
 neuronal morphology, 117–129
 bifurcating axonal collaterals, organization
 of, 128
 bulbar FTG neurons, 124–127
 cell sending axons to ipsilateral bulbar
 reticular core, 125–127
 morphology, 124, 125
 cell size distribution, 118
 dendrites, 123–124
 pontine FTG neurons, 118–123
 cells sending axons to bulbar reticular
 formation, 119–123
 cells sending axons to ipsilateral MLF, 119
 morphology, 118–119
- Pontobulbar nuclei, noncholinergic projections
 to spinal cord and brainstem, 112–117
- Pontobulbar reticular formation, *see also* Bulbar
 reticular formation; Pontine reticular
 formation
 burst neurons, 422–423
 connections, 90–91
 excitatory activity, 478

- Ponto-geniculo-occipital (PGO) waves, 401
 antidepressants and, 551
 brainstem neurons, ponto(thalamo)cortical
 potential generation, 394–416
 brainstem genesis of PGO waves, 395–402
 cellular mechanisms, 402–409
 during natural sleep, 409–416
 brainstem reticular neuronal activity over REM
 sleep cycle, 467, 468, 469
 bulbothalamic neurons and, 386, 387
 cholinergic influences on REM sleep, 483, 484
 dorsal raphe nucleus neurons and, 176
 electrophysiological properties, intrinsic, 170
 GABAergic influences and REM sleep, 509–510
 historical developments and changing
 concepts, 10, 12, 16, 33
 intracellular studies, excitatory responses,
 353, 354
 locus coeruleus cooling and, 499
 mesopontine cholinergic neurons, 388, 390
 modulation of excitability in neuronal pools,
 experimental evidence for, 473, 474–475
 muscle atonia, central mechanisms, 455
 neuronal control of REM sleep, 476
 pontine cat preparation, 463
 PPT neuron firing rates, 392
 raphe system REM-off neurons and, 491–495
 REM sleep, 401, 402
 sleep state control schematic, 472
 SNr inhibitory projections and, 85
 stimulation of amygdala central nuclei
 and, 76
 structural (Reciprocal Interaction) model of
 organization, 515
 Positive feedback process, 478
 Positron emission tomography, 53, 54
 Posterior hypothalamus
 connections
 histaminergic, 133
 NB inputs, 89
 tuberomammillary area, 88
 Posterior parietal cortex recording,
 set-dependent tasks, 377
 Posterior thalamic complex, sensorimotor
 rhythms, 258–259
 Postsynaptic potentials, *see also* Excitatory
 postsynaptic potentials; Inhibitory
 postsynaptic potentials
 afferents to pontine reticular formation, 79,
 80, 81
 brainstem control of corticothalamic
 networks, 140
 electrophysiological methods, 54
 lumbar alpha neuron activity during waking
 and sleep, 451–452
 muscle atonia, 459
 pre-REM sleep changes, 469
 Potassium conductance
 acetylcholine and, 231, 234
 dorsal raphe nucleus neurons, 176, 177
 Potassium conductance *contd.*
 excitatory amino acids and, 250, 251, 253
 hippocampus, 234
 locus coeruleus, 240–242
 neocortex, 231
 norepinephrine and, 236, 237, 240–242
 thalamocortical neurons, 185–186, 187, 189
 Potassium currents, *see also* Electrophysiology,
 intrinsic properties; Neurotransmitter-
 modulated currents
 excitatory amino acids and, 253
 inwardly rectifying conductance, 217
 leak, 55, 148
 medial pontine reticular formation neurons,
 157, 162, 163, 164, 166
 norepinephrine and, 246
 serotonin and, 246–250
 slow oscillation, cellular basis of, 306
 Power spectral analysis, 565
 PPT, *see* Pediculopontine tegmental neurons
 PPT/LTD, *see* Pediculopontine/laterodorsal
 tegmental neurons
 Prazosin, 237, 242, 245
 Prearcuate frontal cortex, nonreticular brainstem
 projections to abducens, 426, 427
 Precentral gyrus, interhemispheric
 integration, 151
 Predorsal bundle (PDB), 426, 427
 Prefrontal cortex connections, 87
 dopaminergic, 132
 ventral tegmental area afferents, 88
 Preoptic-anterior hypothalamus
 humoral factors
 adenosine, 567
 GHRH-containing neurons, 591–592
 IL-1 β and, 587, 588
 posterior hypothalamus connections, 138
 Preoptic area
 connections
 locus coeruleus, 85
 substantia innominata neurons, 89
 tuberomammillary area afferents, 88
 ventral tegmental area afferents, 88
 convergent inputs onto single brainstem
 reticular neurons, 76
 convergent synaptic excitation of midbrain
 reticular neurons, 77
 GABAergic influences and REM
 sleep, 507
 locus coeruleus studies, retrograde
 labeling in, 86
 midbrain neuronal responses, 73
 raphe nuclei afferents, 87
 Prepositus hypoglossi (PH), 86, 114, 430
 abducens projections, 420
 gaze control, 438
 nonreticular brainstem projections to
 abducens, 424, 425, 426
 Prepositus medial vestibular nucleus complex,
 leaky integrator, 429

- Pre-REM sleep and transitions
 - brainstem reticular neuronal activity over REM sleep cycle, 468–469
 - bulbothalamic neurons and, 386, 387
 - mesopontine cholinergic neurons, 388
 - PGO waves, 403, 410, 411, 412, 413, 414, 415, 516
 - PPT neuron firing during wake-sleep cycle, 391
 - PPT neuron firing rates, 392
- Primary sensory areas, *see* Sensory cortex
- Primary somatosensory cortex, *see* Somatosensory cortex
- Primary visual cortex, *see* Visual cortex
- Priming, 375
- Probst's tract, 111, 112
- Procedural memory, 330
- Process S, 549, 560
- Procion yellow, 39
- Propranolol, 237
- Prostaglandin D2 system, 574–576, 587, 588
- Protein kinase A, 330
- Pulse trains
 - augmenting response, 336
 - intracellular studies, excitatory responses, 361
 - plastic changes in thalamocortical system, 339
 - cortical augmenting responses and, 340
 - repetitive callosal stimulation and, 343
 - potentiation of cortical responses following fast oscillations, 343
- Pulvinar-lateroposterior nucleus, 93, 97, 102
- Pulvinar nucleus, 388
 - acetylcholine effects, 229
 - cortical projections, 141
 - locus coeruleus efferents, 129
- Purkinje cells, 130, 242
- Putamen, 132, 135
- Pyramidal neurons
 - Golgi staining, 39
 - hippocampus
 - acetylcholine and, 235
 - trisynaptic loop, 153
 - intracortical connections, 149–150
 - neocortex, 146, 147–148
 - acetylcholine effects, 231, 232–233
 - excitatory amino acids and, 254
 - plastic changes in thalamocortical system, 337
 - slow oscillation, cellular basis of, 306, 307
 - and theta waves, 261
- Pyramidal tract, LDT and PPT neuron
 - distribution, 108
- Pyramidal cortex, 129, 132
- Q-like current, dorsal raphe nucleus, 247
- Quasi-intracellular recordings, 351
- Quiet sleep state, 10
- Quisqualate, 87, 250, 251, 254
- QX314, 187, 189, 192
- Raphe nuclei, 64, 65
 - connections
 - to brainstem monoaminergic nuclei, 87
 - LDT and PPT neuron distribution studies, 108, 109
 - serotonergic, 130–131
 - ventral tegmental area afferents, 88
 - GABAergic influences on of REM sleep
 - microdialysis, 502–503
 - microiontophoresis, 503–505
 - source of input to, 506–507
 - monoaminergic influences in REM sleep, 490
 - dorsal raphe discharge, inverse association with REM events, 490–495
 - dorsal raphe nucleus suppression and increases in REM sleep, 495–497
- Raphe nucleus centralis superior (CS), *see* Central superior raphe nucleus
- Raphe nucleus interpositus, 428, 429
- Raphe nucleus magnus, 79, 130, 132, 430
- Raphe nucleus pontis, 429, 430
- Raphe pallidus, 130, 132, 455
- Rapid eye movements
 - bulbothalamic neurons and, 386, 387
 - neuronal control of REM sleep, 474–475
- Rapid eye movement (REM) sleep, 55, 150
 - age of animal and, 156
 - brainstem reticular neuronal activity over REM sleep cycle, 469
 - bulbothalamic neurons and, 386, 387
 - corticothalamic activity, 380
 - dorsal raphe nucleus neurons and, 176
 - EEG activation during transition, 382
 - evoked potential studies, 350
 - extracellular recordings, 351
 - historical developments and changing concepts, 10–11; *see also* Historical developments and changing concepts
 - states of vigilance, 12, 13–17, 15–16
 - hypothalamus and, 73
 - mesopontine cholinergic neurons, 388
 - mesopontine cholinergic PPT neuron discharges, 390
 - muscle atonia, *see* Motor systems
 - PFTG neostigmine injections, 110
 - PGO-on burst neurons in, 401
 - PGO-on PPT cell with tonic discharge patterns, 399
 - PGO waves, 394, 395, 401, 403, 410, 412, 413, 414, 415, 516
 - PPT/LDT neuron firing in, 391, 392, 400
 - PPT/LDT nuclei stimulation, 359
 - SNr inhibitory projections and, 85
 - thalamocortical circuits and, 153
 - transition to, 383, 384
- Rebound bursts
 - medial pontine reticular formation neurons, 161, 164
 - TC cells, 400
- Rebound LTS, 355

- Rebound spikes
 - augmenting response, 336
 - plastic changes in thalamocortical system, 331, 338
- Reciprocal Interaction model, 513–520, 609
 - depression, 554
 - excitation of REM-off neurons by REM-on neurons, 517
 - inhibition of REM-on neurons by REM-off neurons, 517–518
 - inhibitory feedback of REM-off neurons, 518–520
 - and Lotka-Volterra equations, 526–530
 - postulated steps in production of REM sleep episode, 526–528
 - simple LV equations, 528–530
 - simple LV equations, limits of, 530
 - REM-on neurons and interaction with other elements in model, 514–517
- Recruitment
 - factors producing modulations of excitability, 478–480, 481
 - plastic changes in thalamocortical system, 334
 - primary and augmenting responses, 332
- Recurrent collaterals, 518
- Red nucleus, 62, 77, 92, 94
- Regular spiking neurons
 - cortical augmenting responses and, 340
 - slow oscillations, 309, 310
- Relaxed wakefulness, 15
- Relay cells, thalamic, *see* Thalamic relay neurons
- REM-off neurons, monoaminergic influences in REM sleep, 488–501
- REM-off/REM-on neuron interactions
 - Limit Cycle model, 543–545
 - modeling, *see* Reciprocal Interaction model
 - sites of, 501
- REM-on neurons
 - autoexcitation growth function, Limit Cycle model, 539–540
 - cholinergic influences on REM sleep, 485–487
 - muscle atonia, central mechanisms, 454
 - permissive disinhibitory role in REM sleep genesis, 490–501
 - serotonergic inhibition of cholinergic neurons, 497–498
- Reserpine, 354, 366, 403, 409
- Respiration
 - cholinergic influences on REM sleep, 483
 - neuronal control of REM sleep, 477
 - sleep state control schematic, 472
- RE-TC-RE loop, spindles, 293
- Reticularis gigantocellularis, *see* Lateral tegmental field
- Reticularis pontis caudalis (RPC), 63, 65, 78, 79, 156, 425, 439, 453
- Reticularis pontis oralis (RPO), 63, 65, 92, 156
 - afferents to pontine reticular formation, 78, 79
 - muscle atonia, 458, 458–459
 - neocortical projections of intralaminar thalamic neurons and brainstem excitation, 105
 - neuronal control of REM sleep, 476
- Reticulocortical system studies, 91–92
- Reticuloreticular connections, 78–79
 - brainstem afferents to, 83–84
 - feedback, recruitment within reticular pool, 480, 481
 - modulations of excitability, 478–480, 481
 - pontine reticular formation, 63, 78–79
- Reticulospinal pathways, 115, 116
 - afferents to pontine reticular formation, 80
 - bulbar, 113
 - eye-neck, 438, 439
- Retina, fast oscillations, 267
- Retinal error signal, 434, 435
- Retrograde tracing methods, 39–44
- Retrobulbar fields, 58, 132
- Retrospinal gyrus, 98
- Rhinal sulcus, 88, 336
- Rhombencephalon
 - brainstem afferents to midbrain and bulbar reticular formation, 82–85
 - and physiological functions, 478
 - spinoreticular pathways, 66
- Rhomboid nucleus, 105
- Rhythms, *see also* Oscillations; Synchronized oscillations
 - modeling, 520–526
 - mathematical characterization of oscillators, 522–526
 - phenomenology of, 520–522
 - nucleus basalis, 179
 - thalamocortical neuron electrophysiology, 182–184, 185
- Ripple rhythms, 324
 - origins of, 262–275, 276
 - seizures, 327
- Rostral brainstem, 61, 73
- Rostral interstitial nucleus of medial longitudinal fascicle (riMLF), 419
 - nonreticular brainstem projections to abducens, 426
 - omnipause neurons, 428
- Rostral intralaminar neurons, 98
- Rostral intralaminar nuclei, plastic changes in thalamocortical system, 335
- Rostral midbrain
 - brainstem afferents to, 83
 - cerebral activation, 382
 - histaminergic connections, 133
 - thalamic reticular neurons, dual types of responses, 363

- Rostral pontine reticular formation
 - brainstem efferents to thalamic nuclei, 97–98
 - cholinergic neurons, 56, 382
 - non-giant cell, afferents to pontine reticular formation, 78, 79
- Rostral reticular neurons, 62
 - amygdala projections to basal forebrain, 74
 - thalamic reticular neurons, 365
- Rostral thalamic reticular neurons, spindles, 281
- RPG (nucleus paragigantocellularis), *see* Paragigantocellularis nucleus
- RPO (reticularis pontis oralis), *see* Reticularis pontis oralis
- Rubrospinal tract, 455
- RX 781094, 239
- Saccades, 16, 403
 - motor system, *see* Motor systems
 - sleep state control schematic, 472
- Schaffer fibers, 153
- Scopolamine, 366, 371
 - acetylcholine effects, 228
 - PGO waves, 409
 - spindles, 298
 - thalamic reticular neuron dual response, 367
- Secondary depolarization, augmenting response, 336
- Seizures, 325, 327, 328
- Self-augmenting feedback process, 478
- Sensorimotor cortex
 - acetylcholine effects, 231
 - adrenergic receptors, 237, 245
- Sensorimotor rhythm, origins of, 257–259
- Sensorium commune, 4
- Sensory cortex
 - circuitry, 148
 - connections
 - cholinergic projections from NB and diagonal band nuclei, 134
 - thalamic projections, 141
 - evoked potential studies, 350
 - fast (beta/gamma) oscillations, 262, 263
- Sensory cranial nerves, spinoreticular pathways, 66
- Sensory neurons, modulation of excitability in neuronal pools, 473, 474–475
- Sensory nuclei, spinal cord
 - locus coeruleus efferents, 130
 - spinoreticular pathways, 66
- Sensory pathways, thalamic nuclei and, 141
- Sensory signals
 - cerebellar relays, 68
 - spinoreticular pathways, 66
 - substantia nigra pars reticulata firing rates, 85
 - thalamic relay, 93, 98, 99
- Septohippocampal system
 - dopaminergic connections, 132
 - theta rhythm origins, 259–262
- Septum, tuberomammillary area afferents, 88
- Sequential firing rate (SFR), 391
- Sequential mean frequency (SMF), 386, 388, 392
- Serotonin, 87
 - brainstem neurons, actions of, 246–250
 - cerebral cortex, 250
 - dorsal raphe nucleus, 247–248
 - facial motoneurons, 248–249
 - mesopontine cholinergic nucleus, 249
 - pontine reticular formation, 248–249
 - thalamus, 250
 - connections
 - histaminergic, 133
 - locus coeruleus, 86
 - dorsal raphe nucleus
 - electrophysiological properties, intrinsic, 175–179
 - sleep-wake cycle, 491–495
 - suppression of, 495–497
 - efferent connections, 130–132
 - IL-1 β and, 587, 588
 - immunohistochemistry, 44, 48
 - LG thalamic nucleus, 93
 - locus coeruleus afferents, 87
 - modeling, 518
 - LDT cholinergic neuron inhibition, 517
 - REM sleep in depression, 549–550
 - structural (Reciprocal Interaction) model of organization, 515
 - muscle atonia
 - other pontine structures and pharmacology of, 459
 - paragigantocellularis nucleus, 86
 - potassium conductance in cultured cells, 217
 - PPT/LDT nuclei, 57–58
 - raphe nuclei, 87
 - receptor types, 246–247
 - reticulocortical system studies, 92
 - suppression of serotonergic dorsal raphe neuronal activity, 495–497
 - thalamic nuclei, 95, 96
 - truncated, 44
- Set-dependent tasks in monkeys, 375–378
- Short-lead burst neurons (SBLNs), 420–422, 423
 - omnipause neurons, 428
 - state-dependent alterations in oculomotor system function, 441
- Signal transduction
 - adenosine, 576–583
 - cyclic AMP-mediated, 217, 246
 - cyclic GMP-mediated, 233
- Sleep, dual nature of, 9–10
- Sleep deprivation, 562
 - factors in sleepiness, 562
 - and PGO waves, 413
- Sleep factors, *see* Forebrain and humoral factors
- Sleep oscillation, fast (beta/gamma) oscillations, 265
- Sleep-promoting mechanisms, 20–30
 - active sleep, 24–30
 - passive sleep, 20–24

- Sleep-wake states, *see also* Non-REM sleep; REM sleep; Wakefulness/waking state
 - brainstem and basal forebrain neuronal activities controlling, 380; *see also* Neuronal activities, brainstem and basal forebrain structures
 - changing concepts, *see* Historical developments and changing concepts
 - control, modulation of excitability in neuronal pools, 470, 472–480
 - transitions, *see* Transitions/state changes
- Slow oscillations, 310, 312
 - abnormal oscillations during non REM sleep, 325
 - blockage by mesopontine PPT nucleus, 393
 - brainstem-thalamic neurons implicated in tonic electrical activation of cerebrum, 383
 - fast oscillations during depolarizing phase, 266, 267
 - neocortical, 305–327, 328
 - cellular basis of, 306–307, 310
 - delta spindles and fast oscillation grouping by slow oscillation, 318–324, 325
 - intracellular recording during natural NREM sleep, 310, 311, 312, 313
 - intracortical synchronization of, 311–314
 - synaptic reflection in thalamic and other structures, 314–318
 - ventrolateral nucleus neuron responsiveness, differential brainstem reticular effects on, 362
- Slow-wave activity (SWA)
 - IL-1 β and, 587, 588
 - TNF-alpha and, 590
- Slow-wave seizures, 327
- Slow-wave sleep (SWS), 98, 150, 562
 - brainstem-thalamic neurons implicated in tonic electrical activation of cerebrum, 384, 385, 386
 - corticothalamic arousal and inhibitory processes, 379, 380
 - fast (beta/gamma) oscillations and, 265, 271
 - historical developments and changing concepts, 9; *see also* Historical developments and changing concepts
 - hypothalamus and, 73
 - muscle atonia, central mechanisms, 455
 - PGO waves, 411
 - PPT neuron firing during wake-sleep cycle, 391
 - rhythms during, 276
 - states of vigilance, 12, 13–17
 - transitions, 55; *see also* Transitions/state changes
- Smooth pursuit, 429, 432
- Sodium action potentials
 - PGO-related, 413
 - spindles, 279
- Sodium conductance
 - excitatory amino acids and, 250, 251
 - serotonin and, 246
- Sodium currents
 - dorsal raphe nucleus neurons, 176, 177, 178
 - locus coeruleus, 174, 175
 - slow oscillation, cellular basis of, 306
 - thalamocortical neurons, 189
- Solitary tract nucleus, 111, 112
 - locus coeruleus connections, 85
 - muscle atonia, central mechanisms, 455
 - raphe nuclei afferents, 87
- Soma-dendritic (SD) profile, 39
- Soma size, 118–119, 124–127, 480, 481
 - BFTG neurons, 113
 - cortical neurogliaform cells, 147
 - medial pontine reticular formation neurons, 158–159
 - pontine reticular neurons, 62–63
 - PPT neurons, 57
 - terminology, 61
 - thalamic neurons, 141
 - and time of onset of depolarization, 480, 481
- Somatodendritic spikes, 334
- Somatosensory cortex
 - acetylcholine and, 234
 - excitatory and inhibitory circuits, 148
 - neocortical projections to brainstem, 76
 - primary
 - evoked potential studies, 350, 351
 - plastic changes in thalamocortical system, 331
 - primary and augmenting responses, 332
 - sensorimotor rhythms, 259
 - slow oscillation, cellular basis of, 306, 307
 - thalamocortical secondary excitation, 186
- Somatosensory evoked potentials, cognitive components, 373, 374
- Somatostatin, 592
 - immunohistochemistry, 48
 - neocortex, 147
- Somatostatin-like immunoreactivity, 48
- Spatial coding, burst neurons, 423
- Spike-and-wave (SW) complexes, 342
- Spike-bursts
 - augmenting response, 336
 - delta waves, 302
 - extracellular recordings, 352
 - intracellular studies, 359
 - PGO-on neurons, 395
 - PGO-related, 397, 401, 412
 - plastic changes in thalamocortical system, 339, 344
 - PPT neurons, 400
 - rebound, 296
 - seizures, 327
 - slow oscillations, synaptic reflection in thalamic and other structures, 314–315, 316, 317–318
 - spindles, 279, 282
 - thalamic neurons, 143–145
 - thalamic reticular neurons, 364, 400
 - thalamocortical neurons, 347

- Spikes**
 abnormal oscillations during non REM sleep, 325
 brainstem control of corticothalamic networks, 140
 low-threshold (LTS), 517
 PGO-on cells, 397, 398, 399
 PGO-related, 407, 413
 plastic changes in thalamocortical system, 331, 334, 338, 339
 cortical augmenting responses and, 340
 inactivation of, 339
 seizures, 328
 thalamic neurons, 143–145
- Spiking, slow oscillations, 309, 310**
- Spinal cord**
 connections
 afferents to locus coeruleus, 85
 BFTG bifurcating axonal collaterals, 128
 to brainstem cholinergic nuclei, 63–68
 cholinergic projections to PPT nucleus, 110–112
 locus coeruleus, 85, 86
 locus coeruleus efferents, 130
 mesopontine cholinergic and pontobulbar nuclei, 90–91, 106–117
 noncholinergic projections from pontobulbar reticular formation, 112–117
 pontine reticular neurons, 63
 serotonergic efferents, 132
 spinoparabrachial neurons, 63–68, 66, 70
 excitatory amino acids and, 254
 neocortical pyramidal neuron
 connections, 146
- Spinal motoneurons**
 cholinergic agents and, 212
 modulation of excitability in neuronal pools, experimental evidence for, 474
 muscle atonia, 446–452, 459
 neuronal control of REM sleep, 476
- Spindles, 14, 15, 256, 277–300**
 blockages by brainstem activating influences, 295–300
 brainstem-thalamic neurons implicated
 in tonic electrical activation of cerebrum, 383
 cellular basis of, 279–283
 cholinergic neurons in NB nucleus, 394
 chronology of spindles and other NREM rhythms, 277–279
 electrophysiology, 137
 mesopontine cholinergic neurons and, 389
 neocortex role in synchronizing and terminating, 290–294, 295, 296
 pacemaking, role of thalamic reticular neurons in genesis of, 284–290
 PGO waves, 410
 plastic changes in thalamocortical system, 330
 plasticity following, 335
- Spindles *contd.***
 reticular thalamic nucleus as pacemaker, 98
 sensorimotor rhythms versus, 259
 slow oscillation, cellular basis of, 306, 307
 slow oscillations, 316
 states of vigilance, 12, 13
 thalamic neurons, 143–145
 thalamic neurons in NREM sleep and brain-active states, 347
 thalamocortical neuron hyperpolarization-activated, 184
- Spiperone, 246, 250**
- Spontaneous firing modes during NREM sleep and brain active states, 346–347, 348**
- Spontaneous PGO waves, 403, 406, 409**
- Stages of sleep and transitions, 12–15**
- State, defined, 12**
- State changes, *see* Transitions/state changes**
- State-dependent alterations**
 oculomotor system, 441, 444–445
 reticular excitability, 470, 471
 thalamocortical systems, *see* Thalamocortical system, brainstem and state dependency of
- Stimulation effects**
 behavioral discrimination response, 350
 neuromodulation of REM sleep, 482
- Striatum**
 cholinergic agonists and, 217
 connections
 dopaminergic, 88, 132
 thalamic projections, 141
- Strychnine, 448**
- Substance P, 58, 61**
 immunohistochemistry, 48
 locus coeruleus afferents, 86
 spinoreticular pathways, 66
- Substance P-like immunoreactivity, 73**
- Substantia innominata (SI) connections, 73, 89**
 basal forebrain-brainstem, 74
 basal forebrain projections, 135
 orexin neuronal projections, 602
 ventral tegmental area afferents, 88
- Substantia nigra (SN)**
 connections, 58, 92, 112
 raphe nuclei afferents, 87
 ventral tegmental area afferents, 88
 DA neurons, orexin and, 604
- Substantia nigra pars compacta (SNc), 88, 132**
- Substantia nigra pars reticulata (SNr), 74, 84, 400, 405**
- Substantia nigra pars reticulata (SNr)-SC connection, 84, 85**
- Substantia nigra pars reticulata (SNr)-tectal pathway, 84–85**
- Subthreshold depolarizing currents, brainstem PB-evoked responses, 356**
- Superior cerebellar peduncle, LDT and PPT neuron distribution, 108**

- Superior colliculus, 94, 405
 - burst neurons, 423
 - connections, 58, 65, 74
 - convergent synaptic excitation of midbrain reticular neurons, 77
 - LDT and PPT neuron distribution, 108
 - locus coeruleus efferents, 129
 - spinoreticular pathways, 66, 68
 - substantia nigra pars reticulata connections, 84, 85
 - thalamic projections to midbrain reticular formation, 69, 71
- gaze control, 439
- interactions of neurons in saccade generation, 433–434
- neocortical pyramidal neuron
 - connections, 146
- omnipause neurons, 429
- projections to reticular formation, 426
- state-dependent alterations in oculomotor system function, 440
- Superior olive, 108, 427, 454
- Suprachiasmatic circadian oscillator, 524
- Suprachiasmatic nucleus, 73, 598
- Suprarhinal cortices, 132
- Suprasylvian gyrus, 149, 151, 342
- Sustained levels of discharge, recruitment within reticular pool, 480, 481
- Synaptic activity
 - brainstem-thalamic pathways, intracellular studies of excitatory responses, 355
 - diffuse modulatory systems, *see* Diffuse modulatory systems, targets of
 - extracellular recordings, 352
 - spindles, blockages, 295–300
 - plastic changes in thalamocortical system after repetitive stimulation, 339
 - spontaneous firing in NREM sleep and brain-active states, 346–347
 - thalamocortical neurons, intrinsic
 - electrophysiological properties, 191
- Synaptic convergence, 76–78, 88
- Synaptic reflection, slow oscillation, 314–318
- Synchronization, 181; *see also*
 - Electroencephalography, EEG-synchronized activity
 - acceleration synchronatrice*, 4
 - cortical rhythms, 149
 - modeling REM sleep in depression, 549
 - Synchronized oscillations, 255–344; *see also*
 - Electroencephalography, EEG-synchronized activity; Neuronal control of REM sleep
 - abnormal oscillations during NREM sleep, 325, 327–329
 - burst suppression, 327, 329
 - electrical seizures developing from, 325, 327, 328
 - brainstem reticular neuronal activity over REM sleep cycle, 462–480
 - cortical, locus coeruleus cooling and, 499, 500
- Synchronized oscillations *contd.*
 - delta waves, 300–305
 - cortical component, 304–305
 - thalamic component, 300–304
 - low-frequency rhythms during NREM sleep, 276–324
 - neocortical slow oscillation in NREM sleep and fast rhythm grouping, 305–327, 328
 - spindles, 277–300
 - thalamic and neocortical components of delta waves, 300–305
 - mesopontine cholinergic neurons and, 389
 - midbrain reticular noncholinergic neurons, 384
 - modeling REM sleep in depression, 547, 548
 - neocortical slow oscillation in NREM sleep and fast rhythm grouping, 305–327, 328
 - cellular basis of, 306–307, 310
 - grouping of delta spindles and fast oscillation by slow oscillation, 318–324, 325
 - intracellular recording during natural NREM sleep, 310, 311, 312, 313
 - intracortical synchronization of, 311–314
 - synaptic reflection in thalamic and other structures, 314–318
 - and neuronal plasticity, *see* Plasticity
 - physiological basis, 255–256
 - plastic changes in thalamocortical system
 - during sleep and waking oscillations, 329–344
 - augmenting or incremental responses, 330–335
 - plasticity following spindles, experimental model, augmenting responses, 335–343
 - potentiation of cortical responses following fast oscillation, 343
 - rhythms during active wake states and REM sleep, 256–276
 - alpha, 256–257
 - fast (beta/gamma) and ultrafast (ripple) rhythms, 262–276
 - sensorimotor, 257–259
 - theta, 259–262
 - spindles, 277–300
 - blockages by brainstem activating influences, 295–300
 - cellular basis of, 279–283
 - chronology of spindles and other NREM rhythms, 277–279
 - neocortex role in synchronizing and terminating, 290–294, 295, 296
 - pacemaking, role of thalamic reticular neurons in genesis of, 284–290
- Tectobulbospinal neurons (TBSNs), 66, 67
- Tectoreticular projections, 66

- Tectospinal tract, 113
 - Tegmental reticular nucleus of
 - Bechterew, 398
 - Tegmentoreticular tract
 - lateral, 111, 112
 - muscle atonia, central mechanisms, 450–453, 454, 456
 - Tegmentum, pontine, 62, 92, 105, 452
 - Telencephalon
 - brainstem modulatory system control, 375
 - dopaminergic connections, 132
 - muscarinic receptors, 217
 - REM sleep regulation, 478
 - Temperature
 - circadian rhythms, 561–562
 - cooling and locus coeruleus influences in REM sleep, 499–501
 - IL-1 β and, 589
 - thermoregulation, 477–478
 - Temporal coding, burst neurons, 423
 - Tetramethylbenzidine (TMB), 40–41, 42
 - Tetrodotoxin, 158, 162, 165, 166, 173, 174, 176, 179, 213, 216, 221, 243, 244
 - Thalamectomy, 337
 - Thalamic component of delta waves, 300–304, 360
 - Thalamic nuclei
 - augmenting response, 336, 337
 - connections, 60
 - central tegmental field projections, 62
 - convergent inputs onto single brainstem reticular neurons, 76
 - histaminergic, 133
 - locus coeruleus efferents, 129
 - parabigeminal nucleus projections, 58
 - serotonergic efferents, 131
 - diffuse modulatory systems
 - corticothalamic projections, 152–153
 - types and connections, 141
 - evoked potential studies, 350
 - excitatory amino acids and, 253
 - interhemispheric integration, 151
 - intracellular studies, excitatory
 - responses, 361
 - mesopontine neuron projections, 388
 - muscarinic activation, 215
 - NB cholinergic and GABAergic
 - projections, 394
 - neocortical pyramidal neuron
 - connections, 146
 - plastic changes in thalamocortical
 - system, 334
 - spindles, 285
- Thalamic relay neurons
 - excitatory amino acids and, 253
 - intracellular studies, excitatory
 - responses, 354
 - organization, 142, 143
 - PGO waves, 415
 - serotonin effects, 250
- Thalamic reticular neurons, 139
 - acetylcholine effects, 226, 229
- connections
 - basal forebrain-brainstem, 75
 - brainstem efferents to, 93, 98
 - brainstem reticular projections, 100
 - locus coeruleus efferents, 129
- corticothalamic synapse glutamate
 - receptors, 318
- diffuse modulatory systems
 - cell types and connections, 141–142
 - interactions with TC cells, 142–144, 145, 146
- dual response, 369, 370, 371
- electrophysiological properties, intrinsic, 194–196, 197, 198
- excitatory amino acids and, 253
- intracellular studies, 352
- NB cholinergic and GABAergic
 - projections, 394
- pacemaking, role in genesis of, 284–290
- plastic changes in thalamocortical system, 335
- slow oscillations, 317, 318
- spike bursts, 400
- spindles, 279, 280, 281, 282, 285, 286, 287, 289, 298
- types of thalamic neurons, 152
- Thalamic reticular nucleus
 - cholinergically evoked hyperpolarizations, 217
 - connections
 - basal forebrain projections, 134, 135, 137
 - brainstem reticular projections, 101, 103
 - diffuse modulatory systems, 143–145
 - slow cortical oscillations, blockage of, 393
 - spindles, blockages, 287, 295–300
- Thalamocortical activation
 - histaminergic connections, 133
 - hypothalamus and, 73
 - neuropeptides and, 58
- Thalamocortical neurons/networks
 - acetylcholine effects, 223–226, 227, 228
 - activation by neuronal activities in brainstem and forebrain, *see* Neuronal activities, brainstem and basal forebrain structures
 - brainstem projections to, 104, 105, 106
 - connections, 98
 - diffuse modulatory systems, 139, 140, 141; *see also* Diffuse modulatory systems, targets of cortical actions, 152–153
 - interactions with thalamic reticular cells, 142–144, 145, 147
 - disinhibition of, 352
 - electrophysiological properties, intrinsic, 181–191
 - firing modes, 180
 - high-voltage calcium current, 185–187, 188
 - hyperpolarization-activated cation current, 187, 189
 - low-threshold calcium current, 181–185
 - persistent nonactivating sodium current, 189
 - syaptic activities and, 191

- Thalamocortical neurons/networks *contd.*
- voltage and calcium dependent potassium conductances, 189–191
 - excitatory amino acids and, 253, 254
 - excitatory nature of, 106
 - extracellular recordings, 351, 352
 - intracellular studies, 357
 - PGO waves, 414; *see also* Ponto-geniculo-occipital waves
 - rebound bursts, 400
 - somatosensory cortical responses, 234
 - spindles, 296
 - thalamic reticular neurons and, 147–148
- Thalamocortical system, brainstem and state dependency of, 345–380
- cortical excitability during attentional tasks, 371, 373–380
 - differential alteration in two phases of inhibitory response during brain activation, 378–380
 - event-related potentials in humans, 373–375
 - neuronal recordings during set-dependent tasks in monkeys, 375–378
 - thalamic reticular neurons, dual types of responses, 363–371, 372
- thalamocortical neurons, 346–363
- evoked potential studies, 347–351
 - extracellular recordings, 351–352
 - intracellular studies, differential brainstem reticular effects on three phases of inhibitory responses, 361, 363
 - intracellular studies, excitatory responses, 352–361, 363
 - spontaneous firing modes during NREM sleep and brain active states, 346–347, 348
- Thalamocortical system oscillations, 256
- delta waves, 300–305, 383; *see also* Delta rhythms/waves
 - fast (beta/gamma) and ultrafast (ripple) rhythm, 262–275, 276
 - plasticity, 329–344
 - augmenting or incremental responses, 330–335
 - augmenting response, 336
 - delta waves, cortical component, 304–305
 - delta waves, thalamic component, 300–304
 - experimental model, augmenting responses, 335–343
 - potentiation of cortical responses following fast oscillation, 343
 - sensorimotor rhythms, 257–259
 - spindles, 280, 282–283, 286; *see also* Spindles
- Thalamocorticothalamic networks, 139, 277
- Thalamus, 139
- acetylcholine effects, 223–231
 - local interneurons, 229–231
 - thalamic reticular neurons, 226, 229
 - thalamocortical neurons, 223–226, 227, 228
- Thalamus *contd.*
- activation by neuronal activities in brainstem and forebrain, *see* Neuronal activities, brainstem and basal forebrain structures
 - adenosine and, 565
 - adrenergic receptors, 245
 - brainstem neuron currents
 - acetylcholine-modulated, 223–231
 - excitatory amino acid-modulated, 253, 254
 - norepinephrine-modulated, 245
 - serotonin-modulated, 250
 - cerebral activation, 382–383, 392
 - connections, 55
 - basal forebrain, 74, 75, 134–137
 - basal forebrain-brainstem, 75
 - to brainstem cholinergic nuclei, 68–72
 - brainstem efferents to, 92–106
 - brainstem reticular nuclei efferents to, 90
 - dual connections of brainstem cholinergic neurons, 106
 - locus coeruleus efferents, 129
 - pontine reticular neurons, 63
 - serotonergic efferents, 131
 - spinoreticular pathways, 66
 - diffuse modulatory systems, 141–145, 146
 - brainstem control of corticothalamic networks, 139, 140, 141
 - corticothalamic projections, 152–153
 - electrophysiology, 142–145, 146
 - types of neurons, transmitters, and connections, 141–142, 143, 144, 145
 - electrophysiological properties, intrinsic, 179–197, 198
 - local-circuit inhibitory cells, 191–194
 - thalamic reticular GABAergic neurons, 194–196, 197, 198
 - thalamocortical, 181–191
 - excitatory amino acids and, 253, 254
 - extracellular recordings, 351
 - fast (beta/gamma) oscillations, 263
 - intracellular studies, 354, 355, 361
 - mesopontine cholinergic PPT-LDT projections, 390
 - parallel activating pathways, 393
 - PGO waves, 76; *see also* Ponto-geniculo-occipital waves
 - plastic changes in thalamocortical system, 329
 - seizures, 327
 - sleep state control schematic, 472
 - synaptic reflection in, 314–318
 - wake-sleep transitions, 49
- Theophylline, 562–563
- Thermoregulation, 477–478
- Theta-like activity, cholinergic neurons in NB nucleus, 394
- Theta waves, 153, 256
- cholinergic influences on REM sleep, 484
 - nucleus basalis, 179
 - sleep state control schematic, 472
 - thalamic oscillations, 145

- Time course of depolarization, 478
- Time-resetting (*Zeitgeber*) inputs, 524
- TNF-alpha, 582, 589–590, 591
- Tracing techniques
 - historical developments and changing concepts, 5
 - methods, 39–44
- Transcriptional changes, sleep deprivation and, 562
- Transcriptional modulation, adenosine, 576–583
- Transection techniques, 6, 8
- Transgenic model, orexin actions, 608–609
- Transitional epoch (SD), PPT neuron firing rates, 392
- Transition period T, 468–469
- Transitions/state changes, 55
 - brainstem reticular neuronal activity over REM sleep cycle, 469
 - brainstem-thalamic neurons implicated in tonic electrical activation of cerebrum, 383, 384
 - bulbothalamic neurons and, 386, 387
 - changing concepts, *see* Historical developments and changing concepts
 - EEG activation during, 382
 - electrophysiology, 49
 - excitatory amino acids and, 253
 - evoked potentials, 349
 - factors producing modulations of excitability, 478–480, 481
 - locus coeruleus cooling and, 499
 - midbrain reticular noncholinergic neurons, 384
 - oscillator characterization, 524
 - PPT neuron firing rates, 392
 - slow oscillation during, 308, 310, 312
 - spindles, 277, 297
 - states of vigilance, 12, 13
- Trigeminal nerve and nuclei, 156
- deafferentiation, 352
- locus coeruleus efferents, 130
- LDT and PPT neuron distribution, 108
- mesencephalic nucleus, 60
- motor nuclei, 63
- muscle atonia, 475
 - central mechanisms, 453, 454
 - jaw closer motoneurons, 444–446, 474
 - spinoreticular pathways, 66
- Trigger input neurons, 422, 432–437
- Trisynaptic loop, hippocampus, 153
- Tuberomammillary area, 88, 133
- Tyrosine hydroxylase, 58, 61, 388, 396
 - cat brainstem, 59
 - immunohistochemistry, 45, 48
 - neuropeptide colocalization, 128
 - reticulocortical system studies, 92
 - thalamic nuclei, 93, 95, 96
- Ultradian rhythms, 520, 521
- Ultrafast ripple rhythms, 262–275, 276
- Vagus, 237
- Vasoactive intestinal peptide, 147
- Vasoconstriction, 86
- Vector burst neurons, 422, 423, 426, 441
- Ventral funiculus, 80, 113, 114, 115, 116
- Ventral tegmental area of mesencephalon
 - connections
 - to brainstem monoaminergic nuclei, 87–88
 - dopaminergic, 132
 - locus coeruleus efferents, 129
 - sensorimotor rhythms, 259
- Ventroanterior thalamic nucleus, 334
- Ventroanterior-ventrolateral nucleus
 - acetylcholine effects, 224
 - brainstem efferents to, 93, 94, 95
- Ventrobasal nucleus, 94, 223–224, 229
- Ventrolateral CL nuclei, spindles, 296
- Ventrolateral funiculus, 130
- Ventrolateral nucleus
 - acetylcholine effects, 224
 - activation by PPT pulse train, 362
 - augmenting response, 336
 - burst discharges, 347
 - connections, 72
 - convergent synaptic excitation of midbrain reticular neurons, 77
 - diffuse modulatory systems, 141
 - intracellular studies, excitatory responses, 362
 - plastic changes in thalamocortical system, 338, 339
 - spindles, 280
 - thalamocortical neuron electrophysiology, 191
- Ventrolateral preoptic area (VLPO), 561, 592–600
 - active control of sleep
 - and adenosine, 598–600
 - identification of sleep-active neurons, 592–595, 596
 - lesions and extended VLPO, 596–598
 - modeling, 600
 - relationship to other preoptic areas and SCN, 598
 - adenosine and, 575
 - GABAergic influences and REM sleep, 507
 - lesions and extended VLPO, 595–600
 - modeling, 600
 - sleep-active neurons, identification of, 592–595, 596
- Ventrolateral reticulospinal tract, 456
- Ventromedial nucleus
 - acetylcholine effects, 224
 - connections, 69, 72, 94, 95, 105
 - GHRH-containing neurons, 591
 - projections to, 382
 - recruiting systems, 332
- Ventroposterior thalamic (VP) nucleus, 95
 - connections, 93, 95, 105
 - primary and augmenting responses, 332

- Ventroposterolateral (VPL) thalamic nucleus
 - sensorimotor rhythms, 257, 258, 259
 - somatosensory cortical responses to stimulation, 234
- Very fast oscillations, 324, 327
- Vestibular nerve and nuclei, 113
 - abducens projections, 420
 - brainstem reticular neuronal activity over REM sleep cycle, 467
 - gaze control, 438
 - leaky integrator, 429
 - muscle atonia, central mechanisms, 455
 - nonreticular brainstem projections to abducens, 424, 425
 - spinoreticular pathway, 66
- Vestibuloocular system
 - neural integrator, 429
 - reflexes, 432
- Vigilance, 1, 55
 - centers for states of, 32
 - fast (beta/gamma) oscillations, 262–263
 - historical development of definitions, 11–20
 - NB inputs, 89
 - plastic changes in thalamocortical system, 329
 - synchronization of cortical rhythms, 149
 - thalamic nuclei and, 141
- Vigil coma, 22–23
- Visual association areas, slow oscillations, 311
- Visual cortex
 - acetylcholine effects, 231
 - alpha rhythms, 256, 257
 - brainstem reticular neuron projection studies, 91–92
 - evoked potential studies, 349, 350
 - excitatory amino acids and, 254
 - fast oscillations, 263, 266, 267
 - intracortical connections, 149
 - serotonergic efferents, 132
 - set-dependent tasks, 377
 - slow oscillations, 309
- Visual signals
 - cerebellar relays, 68
 - fast (beta/gamma) oscillations, 262
 - spinoreticular pathways, 66
- Visual thalamic relay, fast oscillations, 267
- Visual thalamus connections
 - brainstem efferents, 93
 - serotonergic efferents, 131
- Voltage dependency, spindles, 280–281
- Voltage-dependent currents
 - locus coeruleus pacemaker activity, 175
 - thalamocortical neurons, 189–191
- Wake-active neurons, adenosine and, 564
- Wakefulness/waking state
 - attentional task studies, 371, 373
 - brainstem and basal forebrain neuron control of, *see* Neuronal activities, brainstem and basal forebrain structures
 - cholinergic neurons in NB nucleus, 394
 - corticothalamic activity, 380
 - evoked potential studies, 350
 - extracellular recordings, 351
 - factors in sleepiness, 562
 - humoral factors
 - adenosine, 563, 565, 567–568, 565
 - adenosine sources, 565, 567–570
 - orexin/hypocretin, 606
 - interhemispheric integration and, 150
 - mesopontine cholinergic PPT neuron discharges, 390
 - PPT/LDT nuclei stimulation, 359
 - PPT neuron firing during wake-sleep cycle, 391
 - sleep-to-wake transition, 384; *see also* Transitions/state changes
 - states of vigilance, 12
 - thalamic reticular neurons, 364
 - thalamocortical circuits and, 153
- Wake/REM-on activity
 - cholinergic influences on REM sleep, 486, 487
 - serotonergic inhibition of cholinergic neurons, 497–498
- Wake-sleep continuum, PGO-on neurons in, 395, 397
- Wake-sleep cycle, PPT neuron firing during, 391
- Wake-sleep transitions, *see* Transitions/state changes
- Wheat germ agglutinin (WGA), 41–43, 47
- Yohimbine, 237, 238, 239, 242
- Zeitgeber*, 524
- Zinc, 251
- Zona incerta connections, 62
 - afferents to pontine reticular formation, 79
 - brainstem efferents to, 93, 98
 - brainstem reticular projections, 100, 102
 - locus coeruleus efferents, 129
 - thalamic projections to midbrain reticular formation, 68, 70, 72